1. GENERAL

X7005 is a wrought, age-hardenable aluminum-zinc-magnesium alloy developed recently for use in large structures where post-braze solution heat treatment is impractical. This high strength aluminum alloy has a high melting range and can be readily brazed, soldered or welded. Its high mechanical properties are maintained after brazing or welding without the need for solution heat treatment. The low quench sensitivity of this alloy requires only a moderate rate of cooling from brazing or soldering temperatures. Thus, severe distortions are avoided.

X7005 exhibits good corrosion and stress-corrosion cracking resistance, good mechanical properties at room and cryogenic temperatures and its fracture toughness appears to be excellent, (1)(2).

The alloy is considered to be experimental, at present, except for extrusions made by the producer.

1.01 Commercial Designation

X7005.

1.02 Alternate Designation

None.

1.03 Specifications

None.

1.04 Composition

Table 1.04.

TABLE 1.04

Source	Alcoa (1)	
	Percent	
	Min	Max
Chromium	0.06	0.20
Copper	-	0.10
Iron	-	0.35
Magnesium	1.0	1.8
Manganese	0.20	0.70
Silicon	-	0.35
Titanium	0.01	0.06
Zinc	4.2	5.0
Zirconium	0.06	0.20
Others Each	-	0.05
Total	-	0.15
Aluminum	Balance	

1.05 Heat Treatment

1.051 Anneal (O temper): Heat to 650 to 750F, hold several hours, furnace cool at 50F per hour to about 400F, air cool.

1.0511 Stabilizing anneal: Heat to 450F, hold 4 to 6 hours subsequent to full anneal treatment and air or furnace cool.

1.052 Thermal treatment: Optimum strength and resistance to stress-corrosion cracking are obtained by a thermal treatment resulting in the T53 or T63 temper. This thermal treatment practice was developed by Alcoa and is proprietary. Requests for licensing and disclosure of this practice should be directed to Alcoa, (1).

1.053 Brazing temperatures are sufficiently high to cause solution treatment during brazing of the alloy, and the alloy is relatively insensitive to rate of cooling from the braze temperature. Thus many assemblies can be air cooled after brazing and then artificially aged or natural aged to high strengths.

1.054 Temper designations for the alloy, Table 1.054.

TABLE 1.054

Source	(1)
Alloy	X7005
Temper	Description
F	As fabricated
O	Annealed
W	Solution heat treated
T6	Solution heat treat + artificial age by producer
T62	Solution heat treat + artificial age by user
T53(a)	Artificially aged following an elevated temperature fabricating process by producer
T63	Solution heat treat + artificial age by producer

(a) For extrusions and tubing

	Al
4.6	Zn
1.4	Mg
0.5	Mn
0.1	Zr
0.1	Cr
0.03	Ti

X7005

1.06 Hardness

1.07 Forms and Conditions Available

1.071 Sheet (O, F and T6 tempers).

1.072 Plate (O, F, T6 and T63 tempers).

1.073 Extrusions and tubing (O, T53, T6 and T63 tempers).

1.08 Melting and Casting Practice

1.09 Special Considerations

1.091 Thick sections, stressed in the short-transverse direction, are susceptible to stress-corrosion cracking at stresses as low as 25 percent of F_{ty}. Stress corrosion cracking resistance in the longitudinal and long-transverse directions, however, is of a high order for material stressed up to 75 percent of F_{ty}, (1).

1.092 Forming of alloy products in an artificially aged temper may produce residual stresses that can cause stress corrosion cracking, particularly if a sustained tension load is super-imposed upon the residual tension stress. It is recommended that when severe forming operations are required, that the alloy be formed in the O or W temper and then given the appropriate thermal treatment, (1).

1.093 In fillet-welded joints, residual welding stresses exerting tension across the edge of a plate may cause stress-corrosion cracking in the edges. Care should be taken in the design of such joints, (1).

2. PHYSICAL AND CHEMICAL PROPERTIES

2.01 Thermal Properties

2.011 Melting range. 1125 to 1195F, (1).

2.012 Phase changes

2.0121 Time-temperature-transformation diagrams

2.013 Thermal conductivity

O temper. 96.8 Btu ft per (hr sq ft F),

T63 temper. 87.1 Btu ft per (hr sq ft F), (1).

2.014 Thermal expansion

Fig. 2.014.

2.015 Specific heat

2.016 Thermal diffusivity

2.02 Other Physical Properties

2.021 Density. 0.101 lb per cu in; 2.8 gr per cu cm, (1).

2.022 Electrical properties

2.0221 Electrical conductivity at RT.

O temper, 43% IACS,

T63 temper, 38% IACS, (1).

2.023 Magnetic properties

The alloy is nonmagnetic, (1).

2.024 Emissivity

2.025 Damping capacity

	Al
4.6	Zn
1.4	Mg
0.5	Mn
0.1	Zr
0.1	Cr
0.03	Ti

X7005

2.03 Chemical Properties

2.031 General. In the aged tempers, the corrosion resistance of X7005 is comparable to that of 6061 and 5000 series of aluminum alloys and is superior to that of the 7000 series alloys such as 7075-T6 and 7079-T6. Susceptibility to exfoliation has been observed in the F and in the W tempers only, and it is recommended that the final product should receive a thermal treatment during or after fabrication to eliminate this characteristic, (1)(2).

2.032 Preliminary studies indicate that the corrosion resistance of brazed specimens, artificially aged after brazing, is good. Specimens naturally aged after brazing exhibit a slight reduction in corrosion resistance.

2.033 X7005 is anodic to the recommended brazing filler alloys and to most other aluminum alloys. Thus it generally will preferentially corrode to protect the filler metal and the dissimilar metal to which it is joined, when exposed to environments conducive to galvanic corrosion, (2).

2.034 Resistance to stress corrosion cracking of aged material is good when alloy is stressed up to 75 percent of F_{ty} in the longitudinal and transverse directions. Thick sections stressed in the short-transverse direction are susceptible to stress corrosion cracking at stresses as low as 25 percent of F_{ty}. (See also Section 1.09). Optimum strengths and stress corrosion crack resistance are obtained by a thermal treatment resulting in the T53 or T63 temper.

2.035 Preliminary studies on butt-welded T6 and T63 sheet and plate indicate that little problem with stress corrosion cracking is expected in these joints. In good electrolytes such as sea water, however, severe selective attack may occur in the heat affected zone adjacent to the weld. This can be avoided by post-weld aging joints, which are welded in the W or T63 temper, using the T63 aging practice.

2.04 Nuclear Properties

3. MECHANICAL PROPERTIES

3.01 Specified Mechanical Properties

3.011 AMS Specifications.
None.

3.012 Producer's tentative typical and expected minimum design properties of sheet, plate and extrusions, Table 3.012.

3.0213 Effect of long time aging at 250F on tensile properties of sheet, Fig. 3.0213.

3.0214 Effect of aging time at room temperature on tensile properties of sheet, Table 3.0214.

TABLE 3.0214

Source	(1)(2)		
Alloy	X7005		
Form	0.063 inch sheet		
Condition	Heated 1090F, 10 min, AC + natural age at RT		
Aging time	F_{tu}, ksi	F_{ty}, ksi	e(2 in), percent
None	28	12	26
3 days	42	21	22
1 week	45	24	22
1 month	49	27	21
3 months	52	30	21
6 months	54	32	21
to T63	52	44	13

3.022 Compression

3.0221 Compressive yield strength, see Table 3.012.

3.023 Impact

3.024 Bending.
Cold bend tests have indicated that the bend properties of plate and sheet in the T63 temper are similar to 6061-T6 bend properties.

3.0241 Suggested bend radii for plate and sheet in O and T63 tempers, Table 3.0241.

TABLE 3.0241

Source	(1)	
Alloy	X7005	
Form	Plate, sheet	
Condition	O	T63
Thickness - in	Approx. radii for 90° cold bend	
0.064	1/2 - 1 1/2t	1-2t
0.125	1- 1 1/2t	1 1/2-2 1/2t
0.187	1- 2t	2-3t
0.250	1- 2t	2 1/2-3 1/2t
0.375	2- 3t	3-4t
0.500	2- 3t	3-4t

TABLE 3.012

Source		Alcoa (1)						
Alloy		X7005						
Form		Extrusions				Sheet, plate		Extrusions
Condition		O	T53	T6	T63, T6351	T6	T63, T6351	T53
Thickness - in		-				≤ 0.250	0.250-3.00	-
		Typical				Minimum		Minimum
F_{tu},	-ksi, L	28	60	54	54	47	47	50
	T	28	60	54	54	47	47	46
F_{ty},	-ksi, L	12	53	46	46	38	38	44
	T	12	53	46	46	38	38	40
F_{cy},	-ksi L	-	-	-	-	39	38	42
	T	-	-	-	-	39	40	42
F_{su},	-ksi	17	32	32	32	29	27	27
F_{bru},	-ksi							
e/D = 1.5		-	-	-	-	70	70	70
e/D = 2.0		-	-	-	-	91	91	90
F_{bry},	-ksi							
e/D = 1.5		-	-	-	-	53	53	57
e/D = 2.0		-	-	-	-	61	61	70
e(2 in or 4D)	-percent	20	15	12	12	7	7	10

3.02 Mechanical Properties at Room Temperature

3.021 Tension. See also Table 3.012.

3.0211 Effect of natural aging on tensile properties of sheet and plate, Fig. 3.0211.

3.0212 Effect of natural aging on tensile properties of extrusions, Fig. 3.0212.

3.025 Torsion and shear

3.0251 Shear ultimate strength, see Table 3.012.

3.026 Bearing

3.0261 Bearing ultimate and yield strengths, see Table 3.012.

3.027 Stress concentration. See Section 3.037.

3.0271 Notch properties

3.0272 Fracture toughness
3.028 Combined properties

3.03 Mechanical Properties at Various Temperatures
3.031 Tension
3.0311 Stress-strain diagrams
3.0312 Effect of low temperatures on tensile properties of sheet, Fig. 3.0312.
3.032 Compression
3.033 Impact
3.034 Bending
3.035 Torsion and shear
3.036 Bearing
3.037 Stress concentration
3.0371 Notch properties
3.03711 Effect of low temperature on sharp notch strength of sheet and extrusions, Fig. 3.03711.
3.03712 Effect of low temperature on notch-strength-ratio for sheet and extrusions, Fig. 3.03712.
3.03713 Effect of low temperature on tear strength of sheet and extrusions, Fig. 3.03713.
3.03714 Results of tear tests on T6 sheet and T53 extrusions at room temperature and low temperatures, Table 3.03714.

TABLE 3.03714

Source			(1)			
Alloy			X7005			
Test			Tear tests (a)			
Form			0.063 in. T6 sheet and T53 extrusions			
			Energy required to			
Temp F	Temper	Dir	Initiate a crack	propagate a crack	Total energy	Unit propagation energy
			in-lb	in-lb	in-lb	in-lb/in^2
RT	T6	L	29	83	112	1290
RT	T6	T	36	82	118	1275
RT	T53	L	67	104	171	1040
RT	T53	T	64	84	148	840
-112	T53	L	40	59	99	590
-112	T53	T	40	37	77	375
-320	T53	L	27	59	86	590
-320	T53	T	28	37	65	375

(a) For tear test specimen used, See Fig. 3.03713.

3.0372 Fracture toughness
3.038 Combined properties

3.04 Creep and Creep Rupture Properties

3.05 Fatigue Properties
3.051 S-N curves for smooth and notched extrusions in various conditions, Fig. 3.051.
3.052 S-N flexural fatigue curve for sheet, Fig. 3.052.

3.06 Elastic Properties
3.061 Poisson's ratio
3.062 Modulus of elasticity
3.0621 Young's modulus. $E = 10.3 \times 10^3$ ksi, (1).
3.0622 Compression modulus. $E_c = 10.5 \times 10^3$ ksi, (1).
3.0623 Modulus of rigidity. $G = 3.9 \times 10^3$ksi, (1).

4. FABRICATION

4.01 Formability
4.011 General. Formability of the alloy in the T63 temper is reported to be similar to that of 6061-T6 as evaluated from 90° cold bend tests (see Section 3.024). Forming of artificially aged products may produce residual stresses that can cause stress corrosion cracking (see Section 1.092). Thus it is recommended that when severe forming is required the alloy should be formed in the O (annealed) or W (solution heat treated) temper and then given the appropriate thermal treatment. If severe forming is applied to material in the W Condition, it should be accomplished within 12 hours after solution heat treatment, (1).

4.012 Suggested bend radii for plate and sheet in O and T63 temper, see Table 3.0241.

4.02 Machining and Grinding

4.021 Machinability of this alloy is good. For high production work, high speed steel or preferably carbide-tipped cutting tools are recommended. Single point cutting tools of high speed steel should be ground 20 to 50 degree top rake, 10 to 20 degree side rake, 8 to 10 degree front and side clearance angles. High speeds and fine to medium feeds should be used. For rough lathe turning, cutting speeds of 500 to 1000 sfpm, feeds of 0.007 to 0.030 inch and depths of cut up to 0.25 inch can be employed. Cutting speeds of 600 to 1000 sfpm, feeds of 0.0002 to 0.010 inch and depth of cut of 0.002 to 0.010 inch can be used for finish lathe turning. In shaping, boring and planing operations a cutting speed equal to the maximum travel of the ram can be attained. The alloy can be cut dry, but a cutting fluid is recomended for good cooling and lubrication. Soluble oils are satisfactory for many operations. Carbon oils or kerosene mixed with lard oil, usually in equal parts, are also satisfactory. For heavy cuts and slow feeds, pure lard oil gives good results.
Cutting edges of tools should be kept sharp and free from grinding scratches, (2).

Al
4.6 Zn
1.4 Mg
0.5 Mn
0.1 Zr
0.1 Cr
0.03 Ti

X7005

4.03 Welding
4.031 General. This alloy can be readily welded, brazed or soldered, and will maintain high mechanical properties after welding or brazing without post-weld (or post-braze) solution heat treatment.
4.032 Fusion welding. Weldability by TIG and MIG fusion processes is excellent if X5180 filler wire is employed. After welding, the alloy will naturally age in several weeks to produce a stronger weld joint than any of the non-heat treatable aluminum alloys. Artificial aging, after welding, will further improve the weld strength, particularly the yield strength.
Welding procedures, joint preparation, machine settings and other welding variables are the same for X7005 as for other aluminum alloys. Precleaning procedures are the same as those employed for the other heat treatable alloys, (1).
4.0321 Average tensile strength (bead on) of butt-welded sheet joints, Table 4.0321.

TABLE 4.0321

Source	(1)	
Alloy	X7005 (X 5180 filler)	
Form	Butt-welded sheet joints	
Condition	T6 (before welding)	
	Postweld aged to T63	Natural age (3 months)
F_{tu}, -ksi	51	49
F_{ty}, -ksi	41	28
e(2 in) -percent	9	10.8
e(10 in) -percent	8.5	8.7

4.0322 The presence of zinc as a constituent in X7005 and in the filler metals requires that precautions be taken to provide adequate ventilation during shop or field welding operations.
4.033 Resistance welding. The alloy can be successfully spot, or stud welded by using machine schedules similar to those established for 7075 or X7106 alloys.
4.034 Brazing. The alloy is suitable for brazing by all brazing methods; furnace, dip, torch and the new vacuum fluxless brazing technique. It has good brazing characteristics, and high strength after brazing is obtained by natural or artificial aging. Brazing temperatures employed are sufficiently high to effect solution heat treatment during brazing. This alloy is relatively insensitive to rate of quenching. Thus many assemblies may be air cooled from brazing temperatures, (1)(2).

Al
4.6 Zn
1.4 Mg
0.5 Mn
0.1 Zr
0.1 Cr
0.03 Ti

X7005

Typical properties of sheet, air cooled from brazing temperatures, see Table 3.0214.

4.0341 The melting range of 1125 to 1195F for this alloy enables brazing to be accomplished with standard fluxes and fillers. For "dip brazing" in the recommended range of 1080 to 1100F, Alcoa No. 34 flux permits easy flow and good wetting of filler metals. Alcoa No. 33 and No. 53 fluxes are satisfactory for "furnace brazing". Alcoa No. 716 or No. 718 filler wires are recommended, (2).

4.0342 The alloy can be successfully brazed up to a temperature of 1120F. However, brazing times and temperatures should be kept as low as possible to minimize silicon penetration from the filler and to prevent excessive grain growth in the alloy, (1).

4.0343 Precleaning methods used for other heat treatable aluminum alloys are satisfactory for X7005. After brazing, the brazed joint must be thoroughly cleaned to remove all flux residue. Hot running water will wash off the major portion of the residue, (1).

4.0344 Recommended fillers and temperatures for brazing, Table 4.0344.

TABLE 4.0344

Source	(1)	
Alloy	X7005	
Brazing X7005 to	Filler *	Temperature range for brazing
X7005	4047 (No. 718)	1080-1100F
3003 or 1100	4047 (No. 718)	
No. 23 or 24 Brazing sheet	4045 (No. 714) or 4047 (No. 718)**	
No. 21 or 22 Brazing sheet	4343 (No. 713)	1100-1120F
No. 11 or 12 Brazing sheet	4343 (No. 713)	

* Use No. 34 flux for dip brazing; No. 33 or 53 flux for furnace

** Use No. 718 where additional filler is required.

4.035 Soldering. This alloy may be easily furnace soldered with Alcoa 805 or 806 solders and a reactive zinc chloride flux. A solution of 50 to 70 percent 66A flux in normal propyl alcohol is satisfactory for furnace soldering in the temperature range of 750-850F, (1).

4.0351 Tensile properties of sheet, furnace soldered, air cooled and aged, Table 4.0351.

TABLE 4.0351

Source	(1)		
Alloy	X7005		
Condition	Furnace soldered at 750F, 1 min, AC + age		
Aging treatment	F_{tu}, (ksi)	F_{ty}, (ksi)	e(2 in), (percent)
None	35	16	21
1 week at RT	48	25	20
1 month at RT	53	29	20
2 months at RT	54	30	20

4.04 Heat Treatment

4.041 If severe forming is required, it should be accomplished within 12 hours after solution heat treatment, see Section 4.011.

4.05 Surface Treatment

4.051 Alumilite finishes, including alumilite "hard coatings" can be applied to X7005 without difficulty. The annealed (O) temper requires a higher formation voltage than T6 or T63 tempers. Chromic acid anodize coatings and chemical conversion films may also be applied, (1).

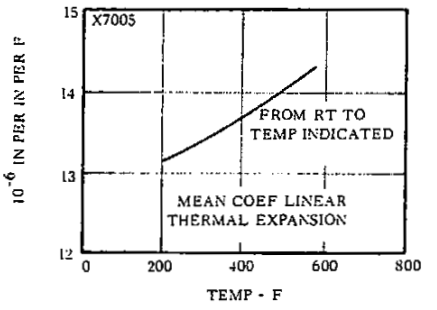


FIG. 2.014 THERMAL EXPANSION (1, p. 3)

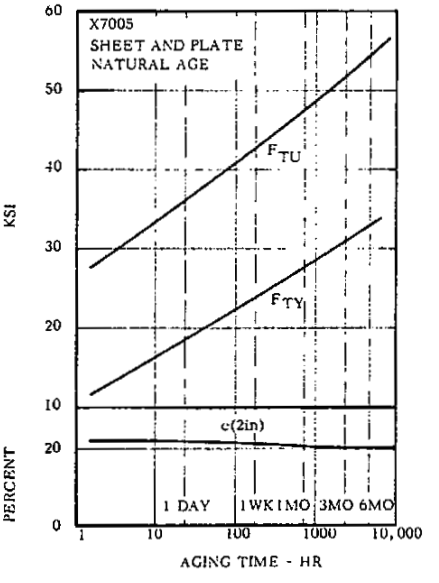


FIG. 3.0211 EFFECT OF NATURAL AGING ON TENSILE PROPERTIES OF SHEET AND PLATE (1)

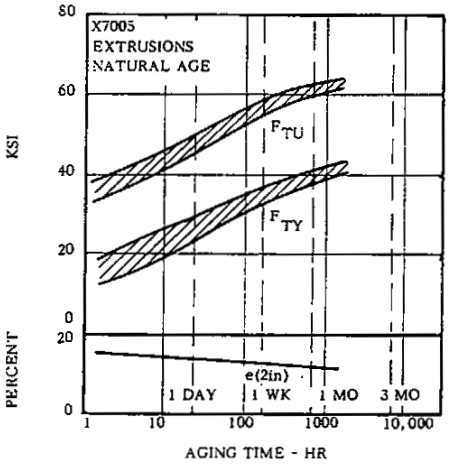


FIG. 3.0212 EFFECT OF NATURAL AGING ON TENSILE PROPERTIES OF EXTRUSIONS (1)

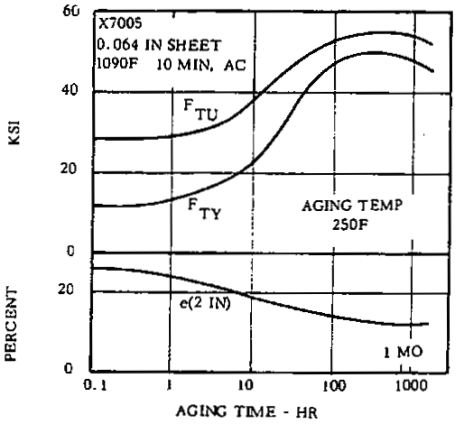


FIG. 3.0213 EFFECT OF LONG TIME AGING AT 250F ON TENSILE PROPERTIES OF SHEET (1)

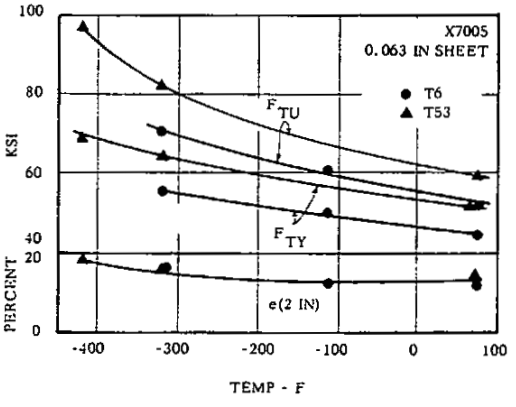


FIG. 3.0312 EFFECT OF LOW TEMPERATURES ON TENSILE PROPERTIES OF SHEET (4)(5)

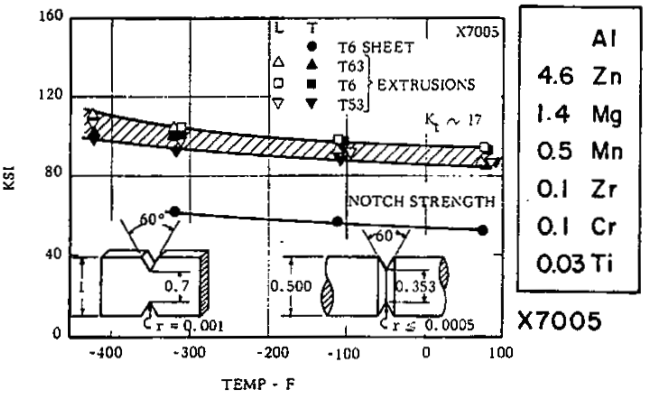


FIG. 3.03711 EFFECT OF LOW TEMPERATURE ON SHARP NOTCH STRENGTH OF SHEET AND EXTRUSIONS (1)(4)

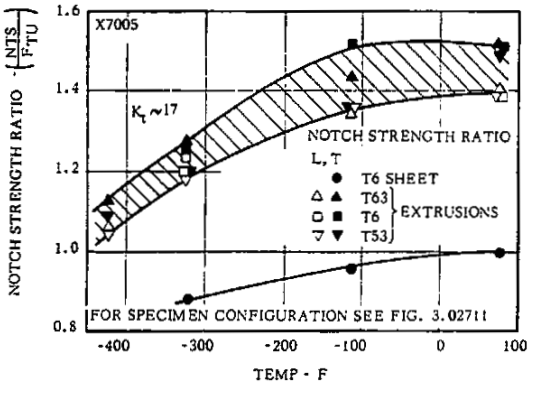


FIG. 3.03712 EFFECT OF LOW TEMPERATURE ON NOTCH STRENGTH RATIO FOR SHEET AND EXTRUSIONS (1)

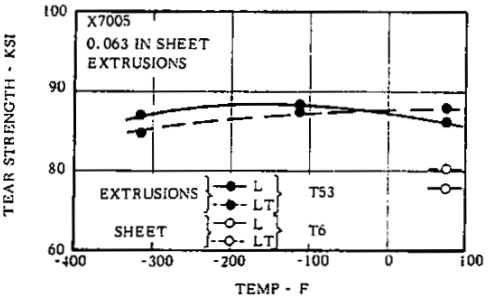
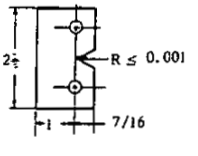


FIG. 3.03713 EFFECT OF LOW TEMPERATURES ON TEAR STRENGTH OF SHEET AND EXTRUSIONS (1)



	Al
4.6	Zn
1.4	Mg
0.5	Mn
0.1	Zr
0.1	Cr
0.03	Ti

X7005

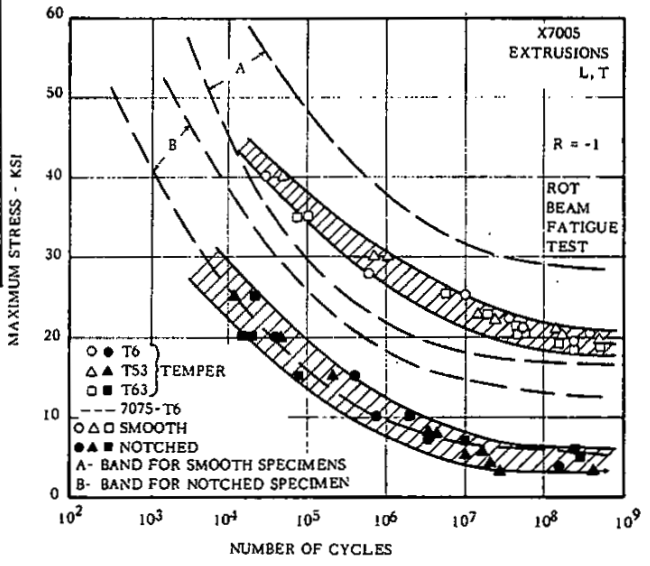


FIG. 3.051 S-N CURVE FOR SMOOTH AND NOTCHED EXTRUSION IN VARIOUS CONDITIONS (1)



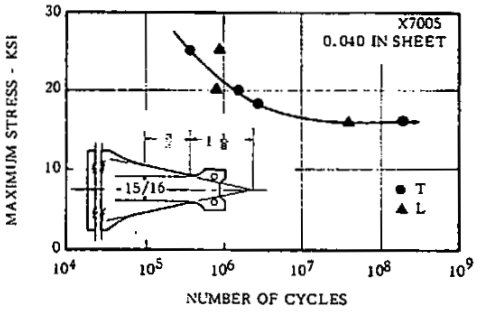


FIG. 3.052 S-N FLEXURAL FATIGUE CURVE FOR SHEET (1)

REFERENCES

1 Nuernberger, H. H., "Alcoa Aluminum Alloy X7005", Alcoa Green Letter, (Revised March 1965)

2 Alloy Digest, "Aluminum X7005", Filing Code: Al-151, Engineering Alloys Digest, Inc., (January 1966)

3 "A Review and Comparison of Alloys for Future Solid Propellant Rocket Motor Cases," DMIC Memorandum 184, Defense Metals Information Center, Battelle Memorial Institute, (November 15, 1963)

4 Anderson, W. A. et al., "Notch Sensitivity of Aluminum-Zinc-Magnesium Alloys at Cryogenic Temperatures", Proceedings, 1963 Cryogenic Engineering Conference, Advances in Cryogenic Engineering, Vol. 9, K.D. Timmerhaus (Editor), distributed by Plenum Press, New York, N. Y., (1964)

5 Kaufman, J. G. and Wanderer, E. T., "Aluminum for Cryogenic Applications", Machine Design, (November 11, 1965)

Code	Designation		Revised
Magnesium Alloys; Wrought, Not Heat Treatable (MgWN-3600)			
3601	Mg-3Al-1Zn	AZ31B	Jun 71
3602	Mg-1Zn-0.2Re	ZE10A	Mar 63
3603	Mg-6Al-1Zn	AZ61A	Mar 65

REVISED: MARCH 1977
AUTHOR: J. G. SESSLER

NONFERROUS ALLOYS

	Al
5	Si
1.3	Cu
0.5	Mg

355
C355

1. GENERAL

This heat treatable aluminum casting alloy is one of two alloys whose properties are primarily determined by its high silicon content in combination with magnesium. 355 and its high purity premium strength variety C 355 also contain copper which makes them stronger but less ductile and corrosion resistant than the other alloy of this group, 356. The general properties of these alloys are very similar. They are distinguished by exceptional castability and pressure tightness, high corrosion resistance and good weldability. 355 is available in the form of sand and permanent mold casting alloys, while C 355 is primarily a permanent mold casting. Data in the following paragraphs applies to 355 unless specifically noted C 355.

1.01 Commercial Designations

355 and C 355 (26).

1.02 Alternate Designations

ASTM B26 Sand castings, ASTM B108 Permanent mold castings, UNS A33550 (C 355) (30).

1.03 Specifications

Table 1.03.

1.04 Composition

Table 1.04.

1.05 Heat Treatment

1.051 Anneal (Stress relief) for dimensional stability. 650 to 750 F, 2 hr.

1.052 Solution heat treatment and artificial aging, Table 1.052.

1.06 Hardness

See also Tables 3.011 and 3.0212.

1.061 Quenching in boiling water followed by aging develops full hardening in all commercial sizes of 355 and C 355 castings.

1.062 Typical hardness values. (22)

355-T51	65 BHN
355-T6	80 BHN
355-T61	100 BHN
355-T7	85 BHN
355-T71	75 BHN

(500 kg. load, 10 mm. ball.)

1.07 Forms and Conditions Available

1.071 The 355 alloy is available as sand and permanent mold castings, usually without restrictions as to size, shape and section thickness.

1.072 The C 355 alloy is available primarily in the form of permanent mold castings as "premium strength" castings, with properties to be negotiated, depending upon casting design.

1.073 Conditions available, Table 1.073.

1.08 Melting and Casting Practice

These alloys can be melted and cast by all common aluminum alloy casting techniques without special considerations, see 4.01.

1.09 Special Considerations

2. PHYSICAL AND ENVIRONMENTAL EFFECTS

2.01 Thermal Properties

2.011 Melting range. 1015 - 1150F (8, p. 203).

2.012 Phase changes. Alloy is subject to precipitation.

2.0121 Time-temperature-transformation diagrams.

2.013 Thermal conductivity, Table 2.013.

2.014 Thermal expansion, Figure 2.014.

2.015 Specific heat. 0.23 Btu per (lb F), at 212F (15, p. 956).

2.016 Thermal diffusivity.

2.017 Solidification temperature range. 1160-1075F (23).

2.02 Other Physical Properties

2.021 Density. 0.098 lb per cu in, 2.71 gr per cu cm (22).

2.022 Electrical resistivity. Table 2.022.

2.0221 Electrical conductivity. (22). Percent IACS (as cast).

355	T51 Condition	43
	T6 Condition	39
	T61 Condition	37
	T62 Condition	38
	T7 Condition	42
	T71 Condition	39
C 355	T61 Condition	39

2.023 Magnetic properties. Alloy is nonmagnetic.

2.024 Emittance.

Emissivity in air at room temperature. 0.035 to 0.07 (16, p. 837).

2.025 Damping capacity.

2.03 Chemical Environment

2.031 Corrosion resistance. The general corrosion resistance of 355 and C 355 alloys is good, although they are inferior to that of 356 because of their higher copper content. These alloys are resistant to attack by rural, industrial and marine atmospheres.

2.032 These alloys exhibit a high resistance to stress corrosion and stress cracking.

2.033 Alloys are resistant to nitric, chromic and most organic acids. They are attacked by hydrochloric and sulfuric acids.

2.034 The alloys are resistant to ammonium hydroxide, but are attacked by sodium, potassium and calcium hydroxides.

2.035 Alloys are resistant to many salts such as sodium bicarbonate; sodium, potassium, calcium and magnesium chlorides; sulfates and nitrates. They are attacked by salts of heavy metals such as ferric chloride and nitrate, mercury salts, silver salts and tin salts (23) (24).

2.04 Nuclear Environment

3. MECHANICAL PROPERTIES

3.01 Specified Mechanical Properties

3.011 AMS specified mechanical properties for 355 alloy, Table 3.011.

3.012 AMS specified tensile properties for C 355 alloy, Table 3.012.

3.013 Aluminum Association mechanical property limits for sand and permanent mold castings of 355 alloy, Table 3.013.

3.014 Aluminum Association mechanical property limits for sand and permanent mold castings of C 355 alloy, Table 3.014.

3.015 Military specified tensile properties of specimens cut from castings, Table 3.015.

3.016 Producer's minimum mechanical properties for C 355 permanent mold castings, Table 3.016.

3.02 Mechanical Properties at Room Temperature

3.021 Tension.

3.0211 Stress-strain diagrams (tensile).

3.0212 Typical mechanical properties of cast test bars, Table 3.0212.

3.0213 Effect of diameter of cylindrical sand castings on tensile properties of specimens machined from the castings, Table 3.0213.

3.0214 Typical tensile properties of specimens cut from 355-T6 sand castings of different thicknesses, Table 3.0214.

3.0215 Typical tensile properties of specimens cut from C 355 premium strength sand castings, Table 3.0215.

3.022 Compression.

3.0221 Stress-strain diagrams (compression).

3.0222 AMS specified minimum mechanical property limits for 355 alloy, see Table 3.011.

3.0223 Producer's minimum mechanical properties for C 355 permanent mold castings, see Table 3.016.

3.0224 Typical mechanical properties of cast test bars, see Table 3.0212.

3.023 Impact.

3.024 Bending.

3.025 Torsion and shear.

3.0251 AMS specified minimum mechanical property limits for

	Al
5	Si
1.3	Cu
0.5	Mg

355
C355

355 alloy, see Table 3.011.

3.0252 Producer's minimum mechanical properties for C 355 permanent mold castings, see Table 3.016.

3.0253 Typical mechanical properties of cast test bars. see Table 3.0212.

3.0254 Typical values of shear strength for 355 and C 355 cast alloys, Table 3.0254.

3.026 Bearing.

3.027 Stress concentration.

3.0271 Notch properties.

3.0272 Fracture toughness.

3.028 Combined properties.

3.03 Mechanical Properties at Various Temperatures

3.031 Tension.

3.0311 Stress-strain diagrams (tensile).

3.0312 Effect of exposure and test temperature on tensile properties of 355 sand cast test bars in T51 Condition, Figure 3.0312.

3.0313 Effect of exposure and test temperature on tensile properties of 355 cast test bars in T7 and T71 Conditions, Figure 3.0313.

3.0314 Effect of exposure and test temperature on tensile properties of C 355 permanent mold, cast test bars in T61 Condition, Figure 3.0314.

3.0315 Tensile properties of 355-T6 alloy after long time exposure at test temperature, Figure 3.0315.

3.0316 Tensile properties of 355-T51 alloy after long time exposure at test temperature, Figure 3.0316.

3.0317 Tensile properties of 355-T71 alloy after long time exposure at test temperature, Figure 3.0317.

3.0318 Tensile properties of C 355-T61 alloy after long time exposure at test temperature, Figure 3.0318.

3.032 Compression.

3.0321 Stress-strain diagrams.

3.033 Impact.

3.034 Bending.

3.035 Torsion and shear.

3.036 Bearing.

3.037 Stress concentration.

3.0371 Notch properties.

3.0372 Fracture toughness.

3.038 Combined properties.

3.04 Creep and Creep-Rupture Properties

3.041 Creep and creep-rupture curves at 400 and 600F for 355 sand cast test bars in T51 Condition, Figure 3.041.

3.042 Creep and creep-rupture curves at 212 to 400F for 355 sand cast test bars in T71 Condition, Figure 3.042.

3.043 Creep and creep-rupture curves at 300 to 500F for C 355 permanent mold cast test bars, Figure 3.043.

3.05 Fatigue Properties

3.051 The fatigue properties of aluminum cast alloys vary greatly according to the quality of the casting. Values for permanent mold castings are usually somewhat higher than those obtained on sand castings. For design applications, allowance must be made for the effect of stress raisers. Typical fatigue data reported by alloy producers are given below.

3.052 Scatterbands for fatigue strength of heat treated 355 sand cast test bars, Figure 3.052.

3.053 Average stress range diagrams for heat treated 355 sand cast test bars. Figure 3.053.

3.054 Typical values of fatigue strength of cast test bars at room and elevated temperatures, Table 3.054.

3.055 Typical fatigue properties for sand and permanent mold castings in various conditions, Table 3.055.

3.056 Effect of porosity, sand holes and dross on fatigue properties of 355-T6 sand castings, Figure 3.056.

3.06 Elastic Properties

3.061 Poisson's ratio. 0.33 (15).

3.062 Modulus of elasticity. 10,200 ksi (27).

3.063 Modulus of rigidity. 3,800 ksi.

3.064 Tangent modulus.

3.065 Secant modulus.

4. FABRICATION

4.01 Casting

4.011 Melting of aluminum casting alloys is readily done by all common methods. Gas and oil fired furnaces are most common, and the low frequency induction furnace is also becoming widely used. The furnace may be the lift out refractory crucible type or it may be stationary or tilting. Special considerations in melting must be given to the ease with which aluminum combines with oxygen, hydrogen and common metallic materials. To prevent absorption of iron from cast iron tools, these should be coated by a protective material. Silicon pickup by reduction of firebrick used as hearth linings can be very harmful. High alumina linings reduce this difficulty.

4.012 Hydrogen readily dissolves in molten aluminum from moisture in all forms and from hydrocarbons. It is liberated during solidification causing harmful porosity. Gas absorption increases with increasing temperature of the molten aluminum and with increasing time held at temperature. Any increased contact surface between molten metal and hydrogen forming gases. particularly that caused by stirring, also increases gas absorption.

4.013 Dross forms as a result of oxidation and it may be trapped in the metal and cause defects in the casting, because its density is slightly higher than that of aluminum.

4.014 The oxide film on the aluminum melt, however, gives an excellent protection against further oxidation and gas absorption. On casting, the metal should flow steadily and for a minimum distance to maintain the oxide layer and thus avoid dross inclusions.

4.015 Gaseous or solid fluxes are generally used to remove hydrogen and dross from the melt. Flushing with gaseous fluxes, such as chlorine and nitrogen may be used for this purpose. Solid fluxes are introduced into the melt to form either a gas or a liquid protective coating on top of the melt after thoroughly stirring the metal. This liquid may be either inert or reactive. Generally, the metal is heated to 1250 to 1400F before adding flux. After fluxing, the melt must be allowed to settle for 10 to 20 minutes to allow the flux to float to the top, while the temperature of the liquid is adjusted to the pouring temperature.

4.016 355 and C 355 have excellent castability. These alloys also have excellent fluidity, low solidification shrinkage tendency, high resistance to hot cracking and good pressure tightness. The alloys are suitable for very intricate castings, containing thin and variable sections and sudden section changes.

4.017 Castings can be straightened in either the annealed or T4 Condition.

4.018 For a more complete discussion of fabrication and casting of aluminum alloys, see Reference (28).

4.02 Machining and Grinding. The machinability of this alloy is good, but it is inferior to that of the low silicon aluminum castings. The relatively large amount of silicon makes the alloy abrasive to carbon steel and high speed steel tools, while the alloy can be machined satisfactorily with cemented carbide tools. It will machine best if the speeds and cuts are reduced and the rake angles increased compared to those used for other aluminum alloys.

4.021 Cast alloys 355 and C 355 when machined properly yield curled or easily broken chips and results in good to excellent surface finish (28).

4.022 Grinding of aluminum alloys is accomplished with methods and equipment similar to those used for other metals, but grinding speeds are much higher than those used for ferrous alloys. Abrasive-belt grinding machines are commonly used.

4.023 For a more complete discussion of machining and grinding of aluminum alloys, see Reference (28).

4.03 Joining

4.031 General. In general, the welding techniques employed on aluminum alloy castings are similar to those used for wrought products. Sound welds of good quality can be ob-

tained with proper procedures. 355 and C 355 alloy castings are weldable by all common fusion methods such as gas, electric arc with flux and electric arc with inert gas. The alloys are also weldable with resistance welding techniques. Pressure welding, brazing and soldering are not recommended for these alloys; however, soldering can be accomplished using special techniques.

4.032 Castings containing gas porosity, dross, shrinkage or inclusions will have poor weldability and low weld properties.

4.033 A partial loss in mechanical properties occurs in welding of heat treated alloys such as 355 and C 355. Post-weld re-heatreatment will restore their original properties.

4.044 For selection of proper filler metals and more detailed information on joining of cast aluminum alloys, see Reference (29).

4.04 Surface Treating

4.051 General. The resistance of these alloys to normal atmospheric weathering is good, and protective castings are not usually required. The alloys can be anodized to provide increased resistance to corrosion and abrasion. Other surface finishes such as electroplating, porcelain enameling, and painting can be applied for special purposes if desired (28).

Source	(19)(20)(21)		(19) (20) (21)	
Alloy	355		C 355	
	Percent		Percent	
	Min.	Max.	Min.	Max.
Silicon	4.5	5.5	4.5	5.5
Copper	1.0	1.5	1.0	1.5
Magnesium	0.40	0.6	0.40	0.6
Iron	(a)	0.6	-	0.20
Manganese	(a)	0.5	-	0.10
Zinc	-	0.35	-	0.10
Chromium	-	0.25	-	-
Titanium	-	0.25	-	0.20
Other impurities each	-	0.05	-	0.05
Total	-	0.15	-	0.15
Aluminum	Balance		Balance	

(a) If iron exceeds 0.45 percent, manganese content shall not be less than one-half the iron content.

TABLE 1.04 CHEMICAL COMPOSITIONS.

Al
5 Si
1.3 Cu
0.5 Mg

355
C355

AMS	Alloy	Form	
4210F	355	Castings, Sand (T51 Cond.)	QQ-A-601, Alloy 355, Temp. T51
4212E	355	Castings, Sand (T6 Cond.)	QQ-A-601, Alloy 355, Temp. T6
4214D	355	Castings, Sand (T71 Cond.)	QQ-A-601, Alloy 355, Temp. T71
4280E	355	Castings, Permanent Mold (T71 Cond.)	QQ-A-596, Alloy 355, Temp. T71
4281C	355	Castings, Permanent Mold (T6 Cond.)	QQ-A-596, Alloy 355, Temp. T6
4215B	C355	Castings, Premium Grade	MIL-A-21180c, Alloy C355, Class 12

TABLE 1.03 SPECIFICATIONS.

Source	(8, p.212) (13, p.89, 90)			
Condition	Sand and/or permanent mold castings	ST WQ at 150-212 F (a)		Artificial Age
		Temp-F	Time-hr (b)	Temp-F	Time-hr (b)
T4	S.C. and P.M.C.	965-985	12	---	---
T51	S.C. and P.M.C.	---	-	430-450	7-9
T6	S.C.	970-990	12	300-320	3-5
T6	P.M.C.	970-990	8	300-320	3-5
T61	S.C.	965-985	12	300-320	8-10
T62	P.M.C.	970-990	8	330-350	14-18
T7	S.C.	970-990	12	430-450	3-5
T7	P.M.C.	970-990	12	430-450	7-9
T71	S.C.	970-990	12	465-485	4-6
T71	P.M.C.	970-990	8	465-485	4-6
C355-T61	P.M.C.	970-990	12	300-320	10-12

(a)212 F preferred.
(b)Exact time influenced by foundry variables and may have to be adjusted from experience.

TABLE 1.052 SOLUTION HEAT TREATMENT AND ARTIFICIAL AGING.

Al
5 Si
1.3 Cu
0.5 Mg

355
C355

Source	(8) (19)		
Alloy	355		C 355
Form	Sand castings	Permanent Mold Castings	
Condition	T6, T7, T51, T71	T6, T51, T62, T71	T6, T61

TABLE 1.073 CONDITIONS AVAILABLE.

Source		(22)
Alloy	Condition	Thermal Conductivity Btu ft per (hr sq ft F)
355	T51	96.8
	T6	82.3
	T6 (a)	87.1
	T61	84.7
	T62 (a)	84.7
	T7	94.4
	T71	87.1
C 355	T61	87.1

(a) Chill cast samples; all other samples cast in green sand molds.

TABLE 2.013 THERMAL CONDUCTIVITY.

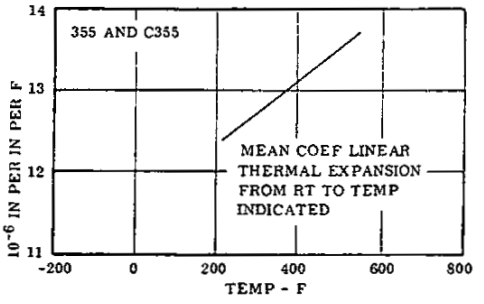


FIG. 2.014 THERMAL EXPANSION (22)

Source	(15, p. 956)	
Alloy	Condition	Electrical Resistivity, microhm-in
355	T51 Sand Cast	1.58
	T6 Sand Cast	1.88
	T61 Sand Cast	1.83
	T7 Sand Cast	1.61
	T6 Permanent Mold Cast	1.74

TABLE 2.022 ELECTRICAL RESISTIVITY.

Source	AMS(1) 7.p.62		AMS(2) 7.p.62		7.p.62		AMS(3) 7.p.62		AMS(5) 7.p.62	7.p.62		7.p.62		AMS(4) 7.p.62	
Alloy	355														
Form	Sand castings								Permanent mold castings						
Condition	T51		T6		T61	T7	T71		T51	T6		T62	T7	T71	
Specimen type	Cast test bars	From casting Avg(a)	Cast test bars	From casting Avg(a)	Cast test bars		Cast test bars	From casting Avg(a)	Cast test bars	Cast test bars	From casting Avg(a)	Cast test bars		Cast test bars	From casting Avg(a)
F_{tu}, min - ksi	25	18.75	32	24	36	35	30(b)	22.5	27	37	27.7	42	36	34	25.5
F_{ty}, min - ksi	18(b)	-	20	15	31	32	22(b)	-	22	23	17	37	27	27	20
e(2in), min-percent	-	-	2	-	-	-	-	-	-	1.5	-	-	-	-	-
e(4D), min-percent	-	-	-	0.5	-	-	-	0.25	-	-	0.4	-	-	-	-
F_{cy}, min - ksi	18(b)	-	21(b)	-	33	34	23(b)	-	22	23(b)	-	37	27	27	-
F_{su}, min - ksi	19(b)	-	24(b)	-	28	25	21(b)	-	22	26(b)	-	34	27	26	-
Hardness, BHN (500 kg, 10 mm)															
min	-	55	-	65	-	-	-	65	-	-	80	-	-	-	70
max	-	-	-	95	-	-	-	86	-	-	110	-	-	-	95

(a) Average values for at least 4, preferably 10 specimens.
(b) Alcoa only.

TABLE 3.011 AMS SPECIFIED MINIMUM MECHANICAL PROPERTY LIMITS FOR 355 ALLOY.

Source	AMS (17)	
Alloy	C355	
Form	Mold type not restricted	
Condition	Solution Treated and Aged (T6)	
Specimen Type	(a)	(b)
F_{tu}, min - ksi	35	37
F_{ty}, min - ksi	28	30
e(2 in) min - percent	2	1

(a) Specimen cut from casting.
(b) Cast specimen.

TABLE 3.012 AMS SPECIFIED TENSILE PROPERTIES FOR C355 ALLOY.

Source	(19) (24)							
Alloy	355 (a)							
Form	Sand Castings				Permanent Mold Castings			
Condition	T51	T6	T7	T71	T51	T6	T62	T71
F_{tu}, min-ksi	25.0	32.0	35.0	30.0	27.0	37.0	42.0	34.0
F_{ty}, min-ksi	-	20.0	-	-	-	-	-	-
e(2 in)min-percent	-	2.0	-	-	-	1.5	-	-

(a) Values represent properties obtained from separately cast test bars.

TABLE 3.013 ALUMINUM ASSOCIATION MECHANICAL PROPERTY LIMITS FOR SAND AND PERMANENT MOLD CASTINGS OF 355 ALLOY.

Source	(6)					
Alloy	C 355					
Form	Special mold, permanent mold or sand castings					
Condition	T61					
Specimen location in casting	Designated			Any		
Class	I	II(a)	III(a)	X	XI	XII
F_{tu}, min - ksi	41	44	50	41	37	35
F_{ty}, min - ksi	31	33	40	31	30	28
e, min - percent	3	3	5	3	1	1

(a) Obtainable only in a favorable casting configuration and must be negotiated with the foundry.

TABLE 3.015 MILITARY SPECIFIED TENSILE PROPERTIES OF SPECIMENS CUT FROM CASTINGS.

Al
5 Si
1.3 Cu
0.5 Mg

355
C355

Source	(19) (24)	
Alloy	C 355 (a)	
Form	Sand Castings	Permanent Mold Castings
Condition	T6	T61
F_{tu}, min - ksi	36.0	40.0
F_{ty}, min - ksi	25.0	-
e(2 in) min-percent	2.5	3.0

(a) Values represent properties obtained from separately cast test bars.

TABLE 3.014 ALUMINUM ASSOCIATION MECHANICAL PROPERTY LIMITS FOR SAND AND PERMANENT MOLD CASTINGS OF C 355 ALLOY.

Source	(7, p. 64) MIL(6)		
Alloy	C 355		
Form	Permanent mold castings		
Condition	T61		
Specimen	From castings		
Type	(a)	(b)	(c)
F_{tu}, min - ksi	37	41	44
F_{ty}, min - ksi	30	31	33
e(2 in), min -ksi	1	3	3
F_{cy}, min - ksi	30	-	-
Fsu, min - ksi	26	-	-

(a) Individually cast specimens.
(b) Cut from designated location in casting.
(c) Must be negotiated with foundry.

TABLE 3.016 PRODUCER'S MINIMUM MECHANICAL PROPERTIES FOR C355 PERMANENT MOLD CASTINGS.

Source	(8, p.197) (9, p.198)								
Alloy	355								C355
Form	Sand Castings				Permanent Mold Castings				
Specimen type	Cast test bars								
Condition	T51	T6	T7	T71	T51	T6	T62	T71	T61
F_{tu}, typ - ksi	28	35	38	35	30	42	45	36	46
F_{ty}, typ - ksi	23	25	36	29	24	27	40	31	34
e(2 in), typ - percent	1.5	3	0.5	1.5	2	4.0	1.5	3	6
F_{cy}, typ - ksi	24	26	38	30	24	27	40	31	36
F_{su}, typ - ksi	22	28	28	26	24	34	36	27	32
Hardness - BHN	65	80	85	75	75	90	105	85	100

TABLE 3.0212 TYPICAL MECHANICAL PROPERTIES OF CAST TEST BARS.

Source	(9, p. 58)									
Alloy	355									
Form	Sand cast cylindrical bar									
Condition	T51					T6				
Section thickness-in	Test bar 0.505	3/4	1 1/4	1 3/4	2 1/4	Test bar 0.505	3/4	1 1/4	1 3/4	2 1/4
F_{tu} - ksi	34.8	29.0	26.9	23.2	21.3	27.1	27.3	22.0	19.1	18.1
F_{ty} - ksi	23.4	23.0	22.2	20.8	20.8	-	24.6	20.3	18.8	17.7
e -percent	3.3	1.7	1.0	1.0	1.0	1.3	1.0	1.0	-	1.0

TABLE 3.0213 EFFECT OF DIAMETER OF CYLINDRICAL SAND CASTINGS ON TENSILE PROPERTIES OF SPECIMENS MACHINED FROM THE CASTINGS.

	Al
5	Si
1.3	Cu
0.5	Mg

355
C355

Source	(9, p.57)				
Alloy	355				
Form	Sand castings				
Condition	T6				
Section thickness-in	≤1/8	1/8 to 1/4	1/4 to 1/2	1/2 to 3/4	3/4 to 1
F_{tu} - ksi	36.5	36.0	36.0	35.5	33.0
F_{ty} - ksi	26.0	25.75	25.5	25.0	23.0
e(4D)- percent	4.5	4.0	4.0	3.5	3.5

TABLE 3.0214 TYPICAL TENSILE PROPERTIES OF SPECIMENS CUT FROM 355-T6 SAND CASTINGS OF DIFFERENT THICKNESSES

Source	(10, p. A)		
Alloy	C 355		
Form	Premium strength castings		
Condition	T61		
	(a)	(a)	(b)
F_{tu} - ksi	43	47	50
F_{ty} - ksi	34	36	38
e - percent	4	6	7

(a) Produced in all or part of casting (as desired)
(b) Must be negotiated with foundry

TABLE 3.0215 TYPICAL TENSILE PROPERTIES OF SPECIMENS CUT FROM C355 PREMIUM STRENGTH SAND CASTINGS

Source	(22)			
Alloy	355		C 355	
Type	Sand cast	Permanent mold	Sand cast	Permanent mold
Condition				
T51	22	-	-	-
T6	28	34	-	-
T61	36(a)	-	-	32
T7	28	-	-	-
T71	26	-	-	-
T62	-	36	-	-

(a) Estimated

TABLE 3.0254 TYPICAL VALUES OF SHEAR STRENGTH FOR 355 AND C 355 ALLOYS

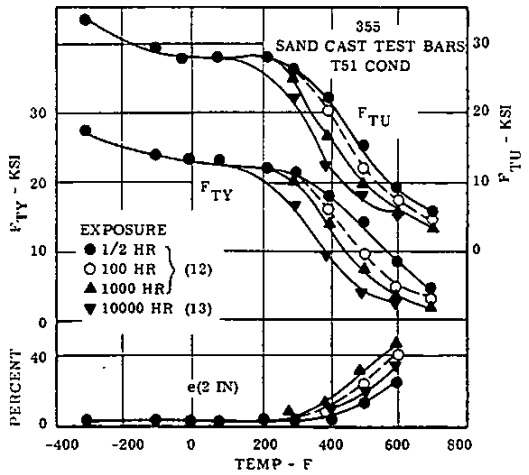


FIG. 3.0312 EFFECT OF EXPOSURE AND TEST TEMPERATURE ON TENSILE PROPERTIES OF 355 SAND CAST TEST BARS IN T51 CONDITION (12)(13, p. 104)

	Al
5	Si
1.3	Cu
0.5	Mg

355
C355

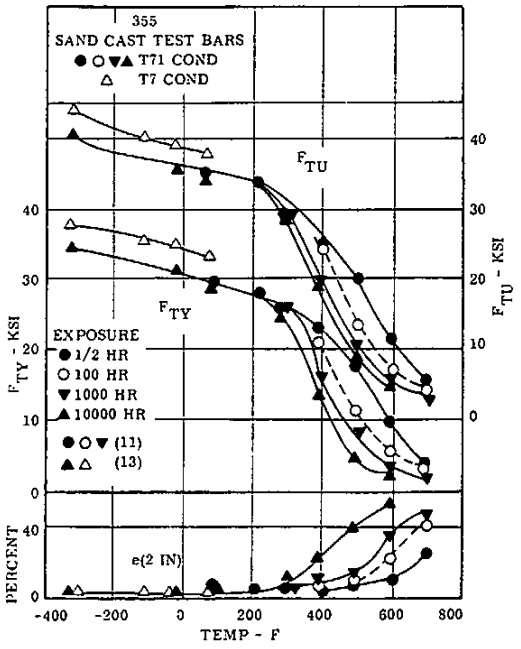


FIG. 3.0313 EFFECT OF EXPOSURE AND TEST TEMPERATURE ON TENSILE PROPERTIES OF 355 CAST TEST BARS IN T7 AND T71 CONDITIONS
(11) (13, p. 105, 109)

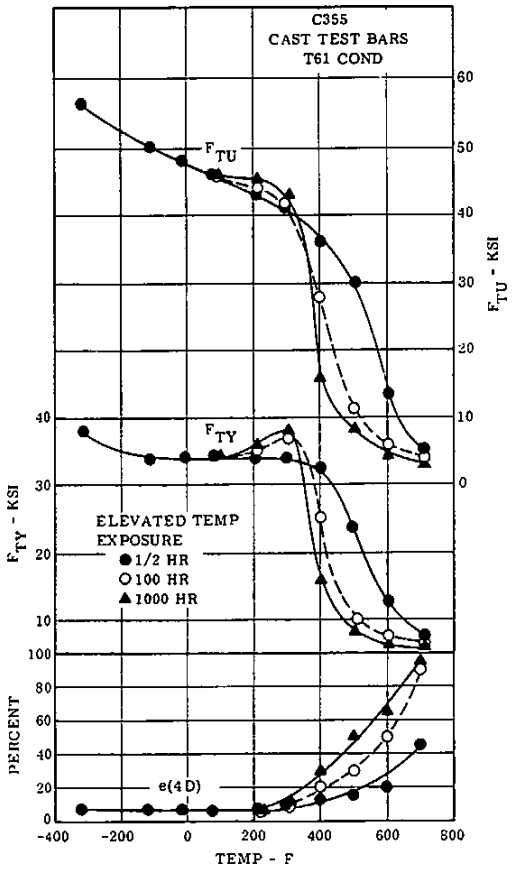


FIG. 3.0314 EFFECT OF EXPOSURE AND TEST TEMPERATURE ON TENSILE PROPERTIES OF C 355 PERMANENT MOLD CAST TEST BARS IN T61 CONDITION.
(10, p. 10)

	Al
5	Si
1.3	Cu
0.5	Mg

355
C355

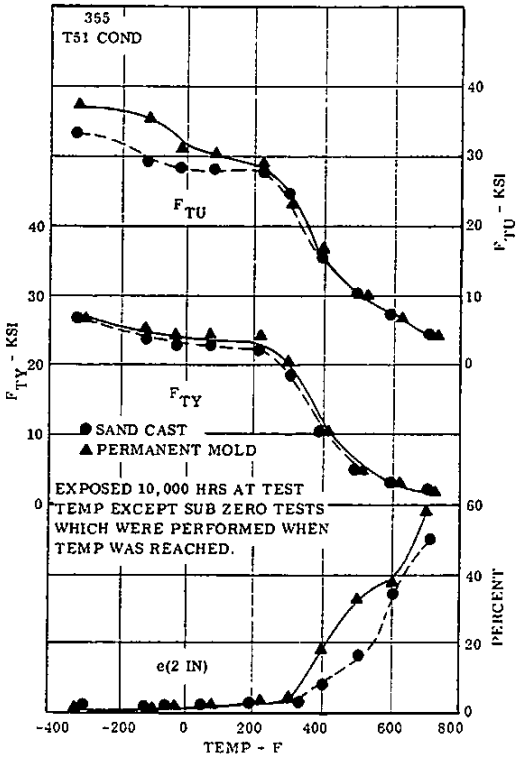


FIG. 3.0316 TENSILE PROPERTIES OF 355-T51 ALLOY AFTER LONG TIME EXPOSURE AT TEST TEMPERATURE.
(22)

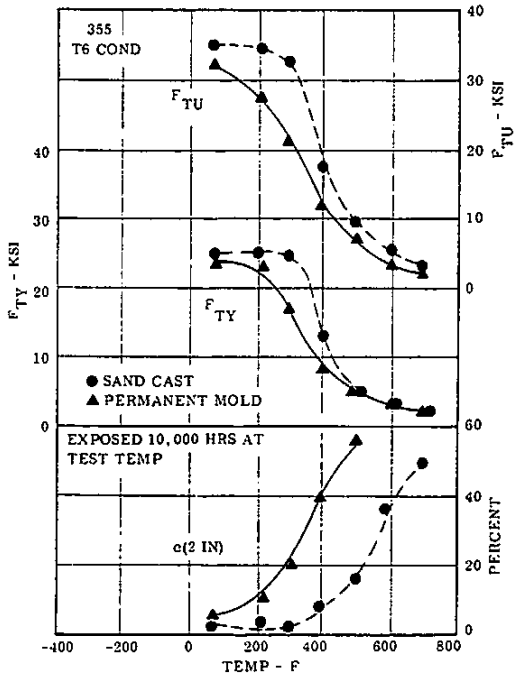


FIG. 3.0315 TENSILE PROPERTIES OF 355 - T6 ALLOY AFTER LONG TIME EXPOSURE AT TEST TEMPERATURE.
(22)

	Al
5	Si
1.3	Cu
0.5	Mg

355
C355

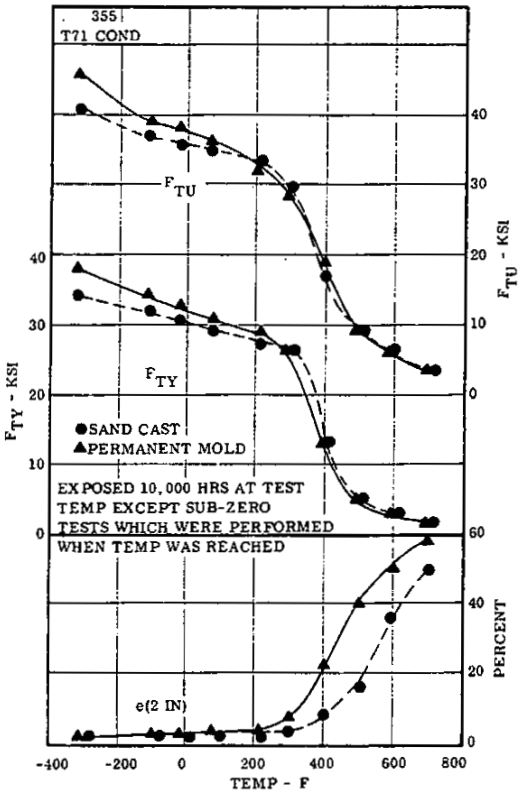


FIG. 3.0317 TENSILE PROPERTIES OF 355-T71 ALLOY AFTER LONG TIME EXPOSURE AT TEST TEMPERATURE. (22)

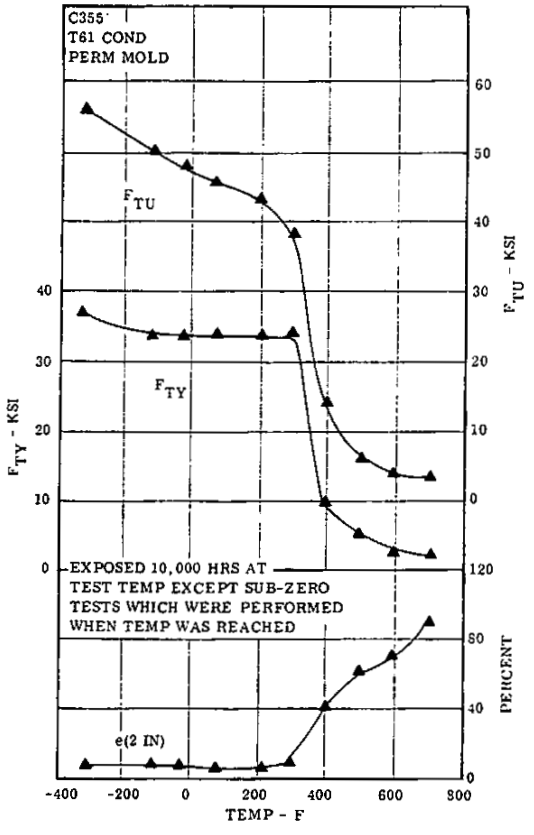


FIG. 3.0318 TENSILE PROPERTIES OF C355-T61 ALLOY AFTER LONG TIME EXPOSURE AT TEST TEMPERATURE. (22)

5	Al
1.3	Si
0.5	Cu
	Mg

355
C355

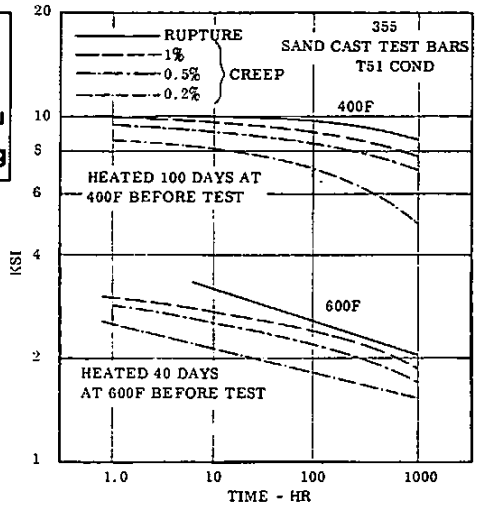


FIG. 3.041 CREEP AND CREEP RUPTURE CURVES AT 400 AND 600F FOR 355 SAND CAST TEST BARS IN T51 CONDITION.

(12)

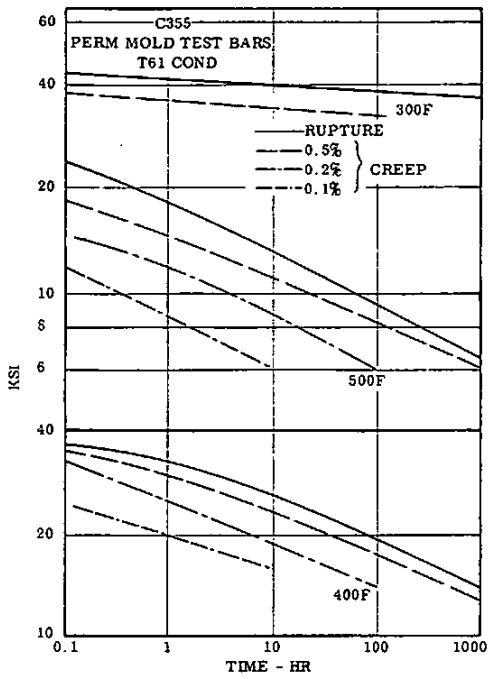


FIG. 3.043 CREEP AND CREEP RUPTURE CURVES AT 300 TO 500F FOR C 355 PERMANENT MOLD TEST BARS.

(10. p.B)

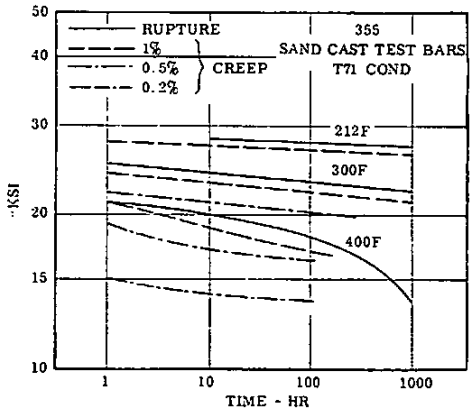


FIG. 3.042 CREEP AND CREEP RUPTURE CURVES AT 212 TO 400F FOR 355 SAND CAST TEST BARS IN T71 CONDITION.

(11)

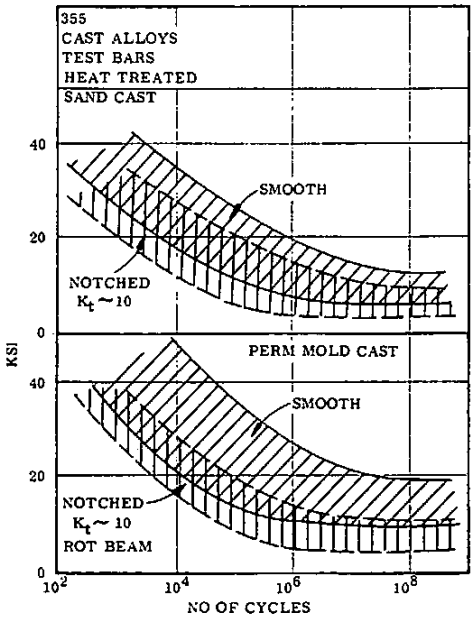


FIG. 3.052 SCATTERBANDS FOR FATIGUE STRENGTH OF HEAT TREATED CAST ALLOY TEST BARS. (9, p.59)

	Al
5	Si
1.3	Cu
0.5	Mg

355
C355

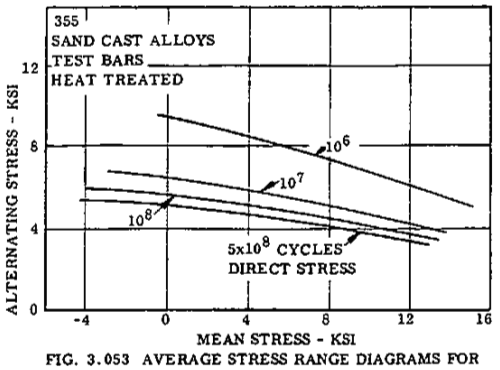


FIG. 3.053 AVERAGE STRESS RANGE DIAGRAMS FOR HEAT TREATED 355 SAND CAST TEST BARS. (8)

Source	(11) (10, p. B)									
Form	Cast test bars									
Alloy	Condition	Temp F	Method	Stress Ratio A	Stress Ratio R	Fatigue strength - ksi at cycles 10^5	10^6	10^7	10^8	$5x10^8$
355 (Sand cast)	T71	RT	Rot beam	∞	-1	21	15	12	11	10.5
		300				18	14	11	10	9.5
		400				17	13	9.5	7.5	7
		500				14	10	7	5	4.5
C355 (Permanent mold)	T61	RT	Rot beam			28	19	16	14.5	14
		300				27	18	13.5	12.5	12
		400				24	16.5	12	10	9
		500				18	11.5	7.5	5.5	5

TABLE 3.054 TYPICAL VALUES OF FATIGUE STRENGTH OF CAST TEST BARS AT ROOM AND ELEVATED TEMPERATURES.

Source	(22) (27)		
Alloy	355		C 355
Form	Sand Cast	Permanent Mold	Permanent Mold
Condition	Endurance Limit - ksi (500 x 10^6 cycles) (a)		
T51	8	-	-
T6	9	10	-
T7	10	-	-
T71	10	10	-
T62	-	10	-
T61	-	-	14
(a) R.R. Moore type rotating beam specimen.			

TABLE 3.055 TYPICAL FATIGUE PROPERTIES FOR SAND AND PERMANENT MOLD CASTINGS IN VARIOUS CONDITIONS

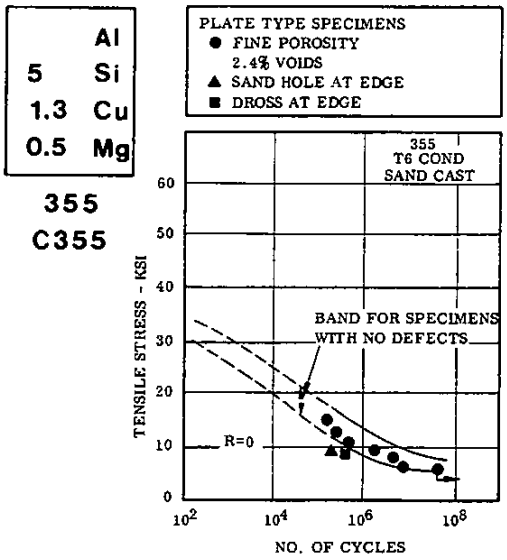


FIG. 3.056 EFFECT OF POROSITY, SAND HOLES AND DROSS ON FATIGUE PROPERTIES OF 355-T6 SAND CASTINGS.

REFERENCES

1. AMS 4210 F (Jan. 15, 1959).
2. AMS 4212 E (Jan. 15, 1959).
3. AMS 4214 D (Jan. 15, 1959).
4. AMS 4280 E (Jan. 15, 1959).
5. AMS 4281 C (Jan. 15, 1959).
6. MIL-C-21180 A (ASG).
7. Alcoa Structural Handbook (1958).
8. Alcoa Aluminum Handbook (1959).
9. Metals Handbook Supplement (1955).
10. Burton, C. L., "Premium Castings". Alcoa Green Letter (Supersedes GL159). Aluminum Company of America, Applications Engineering Division, New Kensington, Pennsylvania.
11. Alcoa Research Laboratories, "Data Sheet"(Sep. 9, 1957).
12. Alcoa Research Laboratories, "Data Sheet" (March 16, 1956).
13. Reynolds Metals Co., "The Aluminum Data Book - Aluminum Alloys and Mill Products" (1958).
14. Heimer, George J., "Time-Temperature Parameters and an Application to Rupture and Creep of Aluminum Alloys", NACA TN 3195 (June 1954).
15. American Society for Metals, "Metals Handbook", 8th Ed. (1961).
16. American Society for Metals, "Metals Handbook", 7th Ed. (1948).
17. AMS 4215 B (Jan. 15, 1962).
18. "Standards for Aluminum Sand and Permanent Mold Castings", 4th Ed., The Aluminum Association (July 1972).
19. "Aluminum Standards and Data - 1976", 5th Ed., The Aluminum Association (Jan. 1976).
20. ASTM B26-75, "Standard Specification for Aluminum-Alloy Sand Castings", American Society for Testing and Materials (1975).
21. ASTM B108-75, "Standard Specification for Aluminum-Alloy Permanent Mold Castings", American Society for Testing and Materials (1975).
22. "Aluminum - Properties, Physical Metallurgy and Phase Diagrams", Vol. 1, Edited by Kent R. Van Horn, American Society for Metals (1967).
23. Everhart, John L., "Aluminum Alloy Castings", Materials in Design Engineering, (Feb. 1958).
24. Materials Engineering, Materials Selector Issue, Vol. 66, No. 5 (Oct. 1967).
25. "Aluminum Construction Manual, Sec. 3, Engineering Data for Aluminum Structures", 2nd Ed., The Aluminum Association (1972).
26. "Standards for Aluminum Sand and Permanent Mold Castings", 6th Ed., The Aluminum Association (1975)
27. "Alcoa Aluminum Handbook", Aluminum Company of America (1962).
28. "Aluminum - Fabrication and Finishing", Vol. 3, Edited by K.R. Van Horn, American Society for Metals (1967).
29. "Welding Aluminum" American Welding Society, 6th Ed. (1972).
30. 1975 Annual Book of ASTM Standards, "Die-Cast Metals; Aluminum and Magnesium Alloys", Part 7 (July 1975).
31. Holt, M., "Some Factors Affecting Fatigue Strength of Aluminum Alloy Sand Castings", Aluminum Company of America (1954).

1. General

Aluminums 356.0 and A356.0 are heat-treatable, aluminum-silicon-magnesium casting alloys whose distinctive properties are primarily determined by their high silicon content in combination with magnesium. 356.0 is the conventional cast alloy, while castings of A356.0 are classified as "premium quality," guaranteed to meet specified high levels of mechanical properties. Premium quality results from advanced foundry practices and low impurity content, particularly iron. A356.0 exhibits higher tensile strength and ductility than does the 356.0 alloy.

Both 356.0 and A356.0 possess excellent castability, pressure tightness, and resistance to hot cracking. Fluidity is moderately high and the tendency toward shrinkage is low. Resistance to corrosion by salt spray is high. Weldability is acceptable by fusion techniques if proper procedures are employed.

356.0 and A356.0 have much in common with the aluminum casting alloy A357.0. The reader is therefore referred to the detailed discussions in the A357.0 chapter in this volume (Code 3109) for helpful information on most of the subjects covered in this chapter.

1.1 Commercial Designation

356.0 (UNS A03560); A356.0 (UNS A13560); Aluminum Alloy, Welding Wire (UNS A94008)

1.2 Alternate Designations

ASTM SG70A (356 alloy); ASTM SG70B (A356 alloy) (Ref. 27)

1.3 Specifications

1.3.1 [Table] AMS Specifications for 356.0 and A356.0 castings and applicable welding wire.

1.4 Composition

1.4.1 **General** Both 356.0 and A356.0 contain 6.5% to 7.5% Si and a maximum of 0.45% Mg.

The composition of A356.0 differs from that of 356.0 in that smaller amounts of other elements (particularly Fe) are allowed, and the minimum amount of Mg is 0.25% rather than 0.20%.

1.4.2 *[Table]* Composition specifications for 356.0 and A356.0.

1.4.3 Effect of element contents on tensile properties.

1.4.3.1 *[Table]* Composition, foundry practice, heat treatment, and properties of investment-cast test plates.

1.4.3.2 *[Table]* Composition, foundry practice, heat treatment, and properties of sand-cast test plates.

1.4.3.3 *[Figure]* Effect of magnesium content on the tensile properties of shell- investment castings.

Strength increases with increasing Mg content, while elongation decreases significantly.

1.4.3.4 *[Figure]* Effect of magnesium content on the tensile properties of sand- composite castings.

Strength increases with increasing Mg content, with a smaller relative decrease in elongation than occurs in shell-investment castings.

1.4.3.5 *[Figure]* Effect of iron content on the tensile properties of shell investment castings.

Strength is optimum with an Fe content of approximately 0.15 percent. Higher Fe content is detrimental to both strength and elongation.

1.4.3.6 *[Figure]* Effect of iron content on the tensile properties of sand composite castings.

Strength is optimum with an Fe content of approximately 0.15 percent. Higher Fe content is detrimental to both strength and elongation.

1.4.3.7 *[Table]* Composition and foundry practice of as-cast plates.

1.4.3.8 *[Figure]* Effect of titanium content on the grain sizes and quality indices of castings in three types of molds.

Titanium is added to these alloys as a grain refiner. The *Quality index, Q* is an empirical parameter which combines the benefits of higher ultimate tensile strength, F_{tu}, and higher elongation, e, as follows (Ref. 16):

$Q = F_{tu} + 21.8 \log (e)$ (ksi; e in percent)

Ti contents from 0.15 to 0.30 percent maximize the benefits of grain refinement for all three mold types.

1.4.3.9 *[Table]* Composition, foundry practice, and heat treatment of low-pressure-cast test components.

1.4.3.10 *[Figure]* Effect of strontium content on the tensile properties of low-pressure permanent mold castings.

Sr is added to these alloys to modify the structure of the strengthening silicon particles into a more-spherical shape (Ref. 65). At least 0.020 percent Sr is needed for any noticeable effect on tensile properties.

1.4.3.11 *[Figure]* Effect of strontium content on impact energy absorbed by unnotched bars from low-pressure permanent mold castings.

Improvement is seen for Sr contents above 0.010 percent.

This section produced with the support of NASA-Lewis Research Center.

© 1996 by Purdue Research Foundation, West Lafayette, Indiana 47907. All Rights Reserved. U.S. Government License. This material may be used, duplicated or disclosed by United States Government agencies without the payment of any royalty.

1.4.3.12 *[Figure]* Effect of strontium content on the quality indices of alloy as-cast in metal and sand molds.

For metal molds, Sr contents as high as 0.040 percent produce improvements in alloy quality, with and without Ti grain refinement. For sand molds, Sr contents above 0.020 percent do not produce additional improvement.

1.5 Heat Treatment

1.5.1 Basic temper designations

1.5.2 *[Table]* Typical Heat Treatment

Basic temper designations, applied to cast alloys	
F	As-cast
O	Annealed to improve ductility and dimensional stability
T	Heat-treated; applied to an alloy whose strength is stable within a few weeks of heat treatment; always followed by one or more digits to indicate quenching, and aging temperatures and times; standard heat-treat designations are
T4	Solutionized and quenched
T5	Artificially aged only
T6	Solutionized, quenched, and artificially aged
T7	Solutionized, quenched, and artificially overaged
Variations in thermal treatment practice are shown as the second and third digits in the standard designations (e.g. T61). There is no consistent convention for the assignment of temper designation variations except that the general practice for solution heat-treated alloys has been to assign tempers T6, T61, and T62 to an ascending order in strength (Ref. 67).	

1.5.3.1 *[Table]* Composition, foundry practice, and heat treatment.

Modifications to these typical heat treatments may be specified by users to produce properties required for specific applications.

1.5.3.2 *[Figure]* Effect of solution-treatment temperature on relative tensile properties of sand and permanent mold castings.

Full solutionizing occurs at a temperature of approximately 1020 F. Solutionizing at temperatures much above 1020 F results in a rapid loss of strength and elongation.

1.5.3.3 *[Figure]* Effect of solution-treatment temperature on variability of tensile properties of sand and permanent mold castings.

Solution-treatment temperatures above 1030 F significantly increase variability in tensile properties.

1.5.3.4 *[Figure]* Effect of solution-treatment time on tensile properties of shell investment castings.

Longer solution-treatment times produce an increase in elongation without decreasing strength.

1.5.3.5 *[Figure]* Effect of solution-treatment time on tensile properties of sand castings.

As with shell-investment castings, longer solution-treatment times produce an optimum combination of strength and ductility. Some yield strength loss is seen for treatment times of approximately 12 hours.

1.5.3.6 *[Table]* Composition, foundry practice, and heat treatment of sand and permanent-mold cast test bars.

1.5.3.7 *[Figure]* Effect of solution-treatment time on notched tensile strength of sand and permanent mold castings.

NTS increases with increasing solution-treatment time, up to 100 to 200 hours at a temperature of 340 F.

1.5.4 Quenching.

1.5.4.1 *[Figure]* Effect of quench water temperature on tensile properties of shell- investment castings.

A temperature of approximately 160 F is optimum for strength. Quench water temperature has little effect on the elongation of shell-investment castings.

1.5.4.2 *[Figure]* Effect of quench water temperature on tensile properties of sand castings.

Quenching in RT water produces the highest strength and elongation in sand castings. Significant loss in elongation occurs with boiling water.

1.5.4.3 *[Figure]* Effect of quench time on notched tensile strength of sand and permanent mold castings.

Quench time is the time required to cool the casting from its solutionizing temperature to approximately the quench temperature.Quench times longer than 100 seconds result in a rapid loss of NTS.

1.5.5 Delay time at room temperature.

1.5.5.1 *[Figure]* Effect of delay time between quench and the start of artificial aging on tensile properties of shell investment castings.

A 1-2 day delay time improves strength without significantly degrading elongation.

1.5.5.2 *[Figure]* Effect of delay time between quench and the start of artificial aging on tensile properties of sand castings.

A delay of 1/2 day causes a temporary drop in yield strength and a temporary increase in elongation. Little change in tensile properties is seen for delay times longer than one day.

1.5.6 Artificial aging.

1.5.6.1 *[Figure]* Effect of artificial aging time at 310 F on tensile properties of shell- investment castings.

Strength increases and elongation decreases with increasing aging time. The quality index calculated from these data (see 1.4.3.8 above for formula) of shell-investment castings is a maximum for aging times between 8 and 12 hours at this temperature.

1.5.6.2 *[Figure]* Effect of artificial aging time at 310 F on tensile properties of sand castings.

Aging times from approximately 4 to 6 hours produce the maximum quality index for sand castings, as calculated from these data.

1.5.6.3 *[Figure]* Effect of longer artificial aging times at 311 F and 340 F on tensile properties of sand and permanent mold castings.

After about 15 hours of aging, strength decreases rapidly and elongation remains low. After 30 hours elongation rises while strength remains at a very low level.

1.5.6.4 *[Table]* Composition, foundry practice, and heat treatment.

1.5.6.5 *[Figure]* Configurations of tensile and Charpy impact specimens.

1.5.6.6 *[Figure]* Effect of longer artificial aging times at 310 F on tensile properties of permanent mold castings. In these tests, strength peaked with aging times of 30 to 100 hours.

1.5.6.7 *[Figure]* Effect of longer artificial aging times at 310 F on Charpy impact energy absorbed and the ultimate-to-yield tensile strength ratio of permanent- mold castings.

The drop-off in these two measures indicates a loss of elongation with aging times longer than about 2 hours, reaching a minimum after 24 hours. This is consistent with the data in Figure 1.5.6.3.

1.5.6.8 *[Table]* Composition, foundry practice, and heat treatment of sand-cast test bars.

1.5.6.9 *[Figure]* Effect of aging temperature on tensile properties of sand and permanent-mold castings.

For 4 hours of aging, a temperature of approximately 375 F produces a desirable combination of strength and elongation.

1.5.6.10 *[Figure]* Effect of natural aging time on notched tensile strength of sand castings.

NTS stabilizes after approximately 24 hours at RT.

1.6 Hardness

1.6.1 Quenching in boiling water followed by aging develops full hardening in all commercial sizes of castings.

1.6.2 *[Table]* Desirable hardness ranges.

1.6.3 Effects of aging

1.6.3.1 *[Figure]* Effect of artificial aging temperature on hardness of sand and permanent mold castings.

For 4 hours of aging, maximum hardness is achieved with temperatures between 350 and 400 F. No significant difference was observed between the aging behaviors of permanent mold and sand cast alloys.

1.6.3.2 *[Figure]* Effect of natural aging time on hardness of sand and permanent mold castings.

Hardness stabilizes after approximately 24 hours at RT, with a 40-percent increase in the T4 condition and a 4-percent decrease in the T6 condition.

1.7 Forms and Conditions Available

1.7.1 356.0 is available in sand, permanent-mold, and centrifugal castings, usually with few restrictions as to shape, size, or section thickness.

1.7.2 A356.0 is available primarily in the form of permanent-mold premium-strength structural castings. A356.0 sand castings, however, are also produced as premium-grade castings.

1.7.3 Available heat treatment conditions (Ref. 14):

Available heat treatment conditions (Ref. 14):	
Sand-cast 356.0:	F, O, T4, T51, T6, T61, T7, T71
Permanent-mold cast 356.0:	F, O, T4, T51, T6, T61, T7, T71
Sand-cast A356.0:	F, O, T4, T6, T61
Permanent-mold cast A356.0:	F, O, T4, T6, T61

1.8 Melting and Casting Practice

1.8.1 General

1.8.1.1 356.0 and A356.0 have excellent castability characteristics, such as high fluidity, low tendency to shrink during solidification, high resistance to hot cracking, and good pressure tightness. These alloys are suitable for intricate castings containing thin sections and variable thicknesses (Ref. 29). For thin sections of castings, it may be necessary to use a mold coating to increase fluidity (Ref. 28).

1.8.1.2 The 356.0 alloy can be melted and cast using conventional aluminum-alloy practices, without any special considerations.

1.8.1.3 Premium-quality castings of the A356.0 alloy are guaranteed to meet a specified high level of mechanical properties, as measured using test bars cut from specified locations within the heat-treated casting (Ref. 18). Improved casting tech-

niques need to be employed in order to obtain these superior properties, including the following:

1. High-purity ingot, with low iron content.
2. Adequate de-gassing and proper melting.
3. Streamlined gating to avoid turbulence and aspiration of mold gases.
4. Sufficient number of risers to adequately feed the casting.
5. Liberal use of chills to control solidification rate and provide directional solidification.

Melting of premium quality ingots is normally performed in silicon-carbide crucibles (rather than in iron pots) to minimize the possibility of iron pickup. Iron skimming tools used for removing dross should be coated with a suitable refractory wash of clay or lime, or with a similar refractory sodium-silicate binder (Ref. 23).

For A356.0 castings, specific aluminum processing technologies are recommended to ensure that high-quality metal is fed to low-pressure casting stations (Ref. 55). Proper molten metal processing in the furnace and casting station produces clean, degassed, and highly-filtered metal. Once charged in the furnace, the molten metal should never cascade during the entire handling process. Metal should never be transferred out of the furnace by ladles or by normal pouring. Instead, the mold cavity should be counter-gravity poured.

1.8.1.4 *[Figure]* Effect of pouring temperature on grain size of 356 castings.

Pouring temperatures above 1200 F result in a rapid increase in grain size, an expected degradation in tensile strength, and an expected increase in elongation.

1.8.1.5 Fluxing procedures for premium quality castings are essentially the same as those used in normal aluminum melting practice (Ref. 26).

1.8.2 Filtering of molten metal.

1.8.2.1 *[Figure]* Schematic elevation view showing a typical installation of a ceramic filter in a mold.

Filtering of the melt to remove impurities is one of the special foundry practices necessary for the production of premium-quality castings.

1.8.2.2 *[Figure]* Effect of filtering on tensile properties of sand and metal mold castings.

Some benefits were found in all cases, with the most significant being an increase in elongation when the ingot contained foundry returns, with a higher probability of impurities.

1.8.2.3 *[Table]* Composition, foundry practice, and heat treatment of sand-cast test bars.

1.8.2.4 *[Figure]* Effect of filtering on variability of tensile properties of sand mold castings.

Filtering significantly reduces the variability in strength within a large population of tests, down to coefficients of variation from 2.3 to 3.6 percent. (COV = standard deviation / mean). Standard deviations in elongation were reduced approximately 0.5 percent in absolute value by filtering.

1.8.3 Strip casting.

1.8.3.1 *[Figure]* Schematic configuration of horizontal twin-roll strip caster.

Strip casting can produce a refinement in the structure of an alloy by increasing the cooling rate, with potential
benefits to both strength and ductility (Ref. 43).

1.8.3.2 *[Table]* Composition, foundry practice, and heat treatment of strip-cast sheet.

1.8.3.3 *[Figure]* Effect of roll speed and contact angle on tensile properties of strip castings.

Strength and elongation were relatively constant for roll speeds below 5 rpm and dropped significantly at higher roll speeds. (No roll diameter given in Ref. 43). After 4 hours of aging, tensile properties of strip castings were approximately equal to those of conventional sand castings (Fig. 1.5.6.2).

1.9 Special Considerations

A detailed discussion of special melting and casting procedures required for producing premium quality parts is given in Ref. 66.

2 Physical Properties and Environmental Effects

2.1 Thermal Properties

2.1.1 Melting ranges

356.0 Alloy	1035 F to 1135 F
A356.0 Alloy	1035 F to 1130 F

2.1.2 Phase changes: 356.0 and A356.0 alloys are subject to precipitation.

2.1.3 *[Table]* Thermal conductivity

2.1.4 *[Figure]* Mean coefficient of thermal expansion of 356 castings.

2.1.5 Specific heat: 0.23 Btu/lb/F at 212 F (Ref. 15)

2.1.6 Thermal diffusivity.

2.2 Other Physical Properties

2.2.1 Density: 0.097 lb/in.^{3} (2.68 g/cm^3).

2.2.2 Electrical properties.

2.2.2.1 *[Table]* Electrical resistivity and conductivity.

2.2.2.2 Electrical conductivity: See Table 2.2.2.1.

2.2.3 Magnetic properties: Alloys are non-magnetic.

2.2.4 Emittance: 0.035 to 0.070 at 77 F in air (Ref. 15).

2.2.5 Damping capacity.

2.3 Chemical Environments

2.3.1 General corrosion. The general corrosion and atmospheric weathering resistances of 356.0 and A356.0 are very good, being comparable to the resistances of pure aluminum. These alloys may be used in industrial and seacoast environments without protection (Ref. 20). They also exhibit excellent resistance to stress-corrosion cracking.

2.3.2 Electrolytic solution potential of 356.0-T6 (solution: 53 g NaCl + 3 g H_2O_2) versus N/10 Calomel Electrode: 0.82 v (Ref. 14).

2.3.3 These alloys are subject to corrosion when exposed to hydrazine or UDMH (unsymmetrical dimethyl hydrazine) in the presence of moisture. Initial corrosive attack is very severe, after which the rate of attack is reduced because of a gradual build-up of a passive film. Passivation in a 30-percent solution of UDMH for 2 hours at 170-180 F renders the surfaces resistant to attack by diluted UDMH at room temperature. Resistance is also obtained by sulfuric acid anodizing and, to a lesser extent, by chromic acid anodizing (Ref. 22).

2.3.4 Effect of sea water on fatigue resistance: See Figure 3.5.1.5.

2.4 Nuclear Environments

2.4.1 *[Table]* Effect of neutron radiation on tensile properties of cast test bars.

2.4.2 *[Table]* Effect of nuclear radiation at -420 F on tensile properties at -420 F.

2.4.3 *[Figure]* Typical effect of nuclear radiation at -420 F on room-temperature stress-strain curves of cast plates.

2.4.4 *[Table]* Effect of neutron radiation on tensile properties of A356.0 castings.

3 Mechanical Properties

3.1 Specified Mechanical Properties

3.1.1 *[Table]* AMS specifications for mechanical properties.

3.1.2 *[Table]* MIL-A-2118B specified tensile properties for specimens cut from castings of A356.0.

3.2 Mechanical Properties at Room Temperature

3.2.1 Tension-stress-strain diagrams-tension properties.

3.2.1.1 *[Table]* Composition, foundry practice, and heat treatment of investment-cast test bars.

3.2.1.2 *[Table]* Composition, foundry practice, and heat treatment of sand-cast test bars.

3.2.1.3 *[Figure]* Monotonic and cyclic tensile stress-strain curves for shell investment and sand castings.

A356.0 is a cyclic strain-hardening alloy. Stresses are the maximum measured during axial fatigue testing with an R-ratio of -1 (fully reversed) at approximately half-life. Sand castings, starting from a lower monotonic strength, hardened to the same strength as the shell-investment castings.

3.2.1.4 *[Figure]* Effect of dendrite arm spacing on tensile properties of shell investment and sand castings.

Dendrite arm spacings less than 0.0020 inch characterize an alloy with both higher strength and higher elongation.

3.2.1.5 *[Table]* Composition, foundry practice, and heat treatment of sand-cast test plates.

3.2.1.6 *[Figure]* Configuration of the Aluminum Association sand-cast test plates.

3.2.1.7 *[Figure]* Effect of dendrite arm spacing on tensile properties of sand cast test plates from at least six commercial foundries.

These round-robin tests by the Aluminum Association define the expected range of properties of sand casting components produced by a variety of commercial foundries in various thicknesses and distances from chills.

3.2.1.8 *[Figure]* Effect of dendrite arm spacing on tensile properties of sand-cast components from a commercial foundry following normal and modified melt processes.

These data illustrate the improvements in the properties of sand-cast components that can be achieved by a foundry through the development of special melting practices and the addition of custom-designed chills. Comparison is made with the Aluminum Association average properties shown in Figure 3.2.1.7.

3.2.1.9 *[Table]* Composition, foundry practice, and heat treatment of sand-cast automotive engine components.

3.2.1.10 *[Figure]* Effect of dendrite arm spacing on tensile properties of automotive engine component sand castings from a commercial foundry following conventional and improved low-pressure processes.

This improved low-pressure process described in Reference 55 uses heat-absorbing chill plates engineered and strategically located in the mold to promote rapid freezing and directional solidi-

fication. Casting soundness and microstructure are thereby improved. See also 1.8.1.3 for recommended casting processes. Significant improvements are demonstrated in the tensile properties of sand-cast components, compared with the Aluminum Association average properties shown in Figure 3.2.1.7.

3.2.1.11 *[Table]* Composition, foundry practice, and heat treatment of permanent-mold cast test plates.

3.2.1.12 *[Figure]* Configuration of the Aluminum Association permanent-mold cast test plates.

3.2.1.13 *[Figure]* Effect of dendrite arm spacing on tensile properties of permanent-mold cast test plates of 356.0 alloy from seven commercial foundries.

These round-robin tests by the Aluminum Association define the expected range of properties of components cast in permanent molds produced by a variety of commercial foundries in various thicknesses and distances from chills.

3.2.1.14 *[Figure]* Effect of exposure to elevated temperature on room temperature tensile properties of sand-cast test bars in T51 condition.

Exposure to temperatures above 300 F can cause a significant loss of strength and a gain in elongation, depending on the exposure time.

3.2.1.15 *[Figure]* Effect of exposure to elevated temperature on room temperature tensile properties of sand-cast test bars in T7 condition.

Exposure to temperatures above 250 F can cause a significant loss of strength and a gain in elongation, depending on the exposure time.

3.2.1.16 *[Table]* Composition, foundry practice, and heat treatment of directionally-solidified ingots.

3.2.1.17 *[Figure]* Effect of cooling rate and heat treatment on tensile properties of specimens cut from directionally-solidified water-chilled ingots. As expected, properties near the chill, where dendrite cell sizes are smallest, are superior to those farther from the chill.

3.2.2 Compression - stress-strain diagrams - compression properties.

3.2.2.1 *[Table]* Compression, shear, and bearing properties of 356.0 and A356.0.

3.2.3 Impact: See Figures 1.4.3.11 and 1.5.6.7.

3.2.4 Bending.

3.2.5 Torsion and shear: See Table 3.2.2.1 and Figure 1.5.6.10.

3.2.6 Bearing: See Table 3.2.2.1.

Stress concentrations.

3.2.7.1 Notch properties: See Table 2.4.2.

3.2.7.2 Fracture toughness

3.2.7.2.1 *[Figure]* Configurations of compact tensile (CT) specimens for fracture toughness and crack propagation tests.

3.2.7.2.2 *[Figure]* Effect of thickness on fracture toughness of compact tensile (CT) specimens from unchilled shell-investment and water-chilled sand castings.

Projection to a thickness of 1.3 inch is required for the tougher water-chilled sand-cast material, following the trend of the shell-investment material.

3.2.7.2.3 *[Figure]* Effect of dendrite arm spacing on plane-strain fracture toughness projected from K_Q test data for unchilled shell-investment and water-chilled sand castings.

Reducing dendrite arm spacing 0.0020 inch by rapid solidification increases fracture toughness by approximately 20 percent.

3.2.7.2.4 *[Figure]* Configurations of compact tensile (CT) and short rod (SR) specimens cut from directionally-solidified ingots for fracture toughness tests.

3.2.7.2.5 *[Figure]* Effect of cooling rate on fracture toughness of specimens cut from directionally-solidified water-chilled ingots.

Again, reducing dendrite cell size by rapid solidification increases fracture toughness.

3.2.8 Combined properties.

3.3 Mechanical Properties at Various Temperatures

3.3.1 Tension - stress-strain diagrams - tension properties

3.3.1.1 *[Figure]* Monotonic stress-strain curves for permanent-mold cast test bars at various temperatures after an exposure time of one hour.

3.3.1.2 *[Figure]* Effect of elevated temperature exposure on the tensile properties of sand and permanent-mold cast test bars.

In addition to these data, it was found that after exposure to temperatures above 400 F the properties of as-cast and heat-treated materials were similar.

3.3.1.3 *[Figure]* Classification of fracture appearance of tensile test specimens from sand and permanent-mold cast test bars after exposure and testing at elevated temperature.

3.3.1.4 *[Figure]* Effect of exposure and testing at elevated temperature on tensile properties of sand cast test bars in T51 condition.

3.3.1.5 *[Figure]* Effect of exposure and testing at elevated temperature on tensile properties of sand cast test bars in T6 condition.

3.3.1.6 *[Figure]* Effect of exposure and testing at elevated temperature on tensile properties of sand cast test bars in T7 condition.

3.3.1.7 *[Figure]* Effect of exposure and testing at elevated temperature on tensile properties of sand cast test bars in T61 condition.

3.3.1.8 *[Figure]* Effect of exposure and testing at elevated temperature on tensile properties of sand cast test bars in T6 and T7 conditions.

3.3.1.9 *[Figure]* Effect of low test temperature on tensile properties of permanent-mold cast test bars in T6 condition.

3.3.2 Compression

3.3.3 Impact.

3.3.4 Bending.

3.3.5 Torsion and shear.

3.3.6 Bearing.

3.3.7 Stress concentration.

3.3.8 Combined properties.

3.4 Creep and Creep-Rupture Properties

3.4.1 *[Figure]* Creep and creep-rupture curves from room temperature to 400 F for sand castings in T7 condition.

3.4.2 *[Figure]* Creep and creep-rupture curves at 300 F for permanent-mold castings in T61 condition.

3.5 Fatigue Properties

3.5.1 Conventional high-cycle fatigue.

3.5.1.1 *[Table]* Composition, foundry practice, and heat treatment of sand- and permanent-mold fatigue test bars.

3.5.1.2 *[Figure]* Configuration of CO_2 sand mold for casting cantilever specimens tested in rotating bending fatigue in Ono- and Krause-type machines.

3.5.1.3 *[Figure]* Effect of dendrite arm spacing on high-cycle fatigue strength at 10^7 cycles to failure.

Decreasing dendrite arm spacing by rapid cooling of the casting significantly increases long-life fatigue strength.

3.5.1.4 *[Table]* Composition, heat treatment, and tensile properties of sand cast plates for fatigue test specimens.

3.5.1.5 *[Figure]* Effect of exposure to ASTM artificial sea water on S-N curves for smooth specimens from sand cast plates.

Exposure times longer than 10 hours can significantly degrade long-life fatigue strength, by more than 50 percent for very long exposures and very long lives.

3.5.1.6 *[Table]* Characteristics of fatigue test materials.

3.5.1.7 *[Figure]* Effect of casting method on stress-fatigue life curves for smooth specimens from die-cast wheels and from direct-chill cast billets, with and without extrusion.

The larger elongation and smaller porosity produced by direct-chill casting and extended further by extrusion result in a significant increase in fatigue strength at all lives.

3.5.2 Low-cycle fatigue.

3.5.2.1 *[Figure]* Configurations of specimens for tensile and axial-fatigue tests of shell-investment and of water-chilled sand castings.

3.5.2.2 *[Figure]* Strain-fatigue life curves for smooth axial fatigue specimens from three shell-investment castings poured at different mold temperatures.

The test data shown in Figure 3.2.1.3 and Figures 3.5.2.2 to 3.5.3.2 were produced during a comprehensive round-robin research program conducted by the Society of Automotive Engineers Fatigue Design and Evaluation (SAEFDE) committee, with participation by six companies and the University of Iowa.

3.5.2.3 *[Figure]* Composite of strain-fatigue life curves for smooth axial fatigue specimens from three castings cooled at different rates, showing mean fatigue strength and mean-minus-2 standard deviations fatigue strength.

The latter is approximately 20 percent lower than the mean strength expressed in terms of maximum strain.

3.5.2.4 *[Figure]* Comparison of strain-fatigue life curves for smooth axial fatigue specimens from unchilled shell-investment castings and water-chilled sand castings.

Strain-cycling fatigue strength is also significantly increased by rapid solidification which reduces dendrite arm spacing and increases elongation.

3.5.2.5 *[Figure]* Effect of dendrite arm spacing on axial strain-cycling fatigue strength at 10^7 cycles to failure of smooth specimens from unchilled shell- investment castings and water-chilled sand castings.

Reducing dendrite arm spacing significantly increases long-life strength in strain-cycling fatigue, as was shown earlier for stress-cycling fatigue (see Fig. 3.5.1.3).

3.5.2.6 *[Figure]* Effect of tensile elongation on axial strain-cycling fatigue strength at 10^7 cycles to fail-

ure of smooth specimens from unchilled shell-investment castings and water-chilled sand castings.

Low-cycle fatigue strength increases rapidly with increasing tensile elongation.

3.5.2.7 *[Figure]* Effect of mean strain on axial strain-fatigue life behavior of smooth specimens from shell-investment castings.

Compared to strain-cycling fatigue life with zero mean strain (R-ratio = -1) tensile mean strains reduce fatigue life while compressive mean strains increase it, with relatively larger effects at longer lives.

3.5.3 Fatigue-crack propagation.

3.5.3.1 *[Figure]* Scatter bands of fatigue-crack growth rates at two R-ratios for CT specimens from three shell-investment castings and one water-chilled sand casting, containing data from several laboratories.

No consistent differences were found between the crack growth rates for the two types of castings.

3.5.3.2 *[Figure]* Effect of dendrite arm spacing on crack-propagation threshold stress intensity at two R-ratios and on projected plane-strain fracture toughness of shell-investment and water-chilled sand castings. Differences in threshold stress intensity are consistent with differences in fracture toughness, when analyzed on the basis of dendrite arm spacing.

3.6 Elastic Properties

3.6.1 Poisson's ratio: 0.33 (Ref. 15).

3.6.2 *[Figure]* Modulus of elasticity at various temperatures.

3.6.3 *[Figure]* Modulus of rigidity at various temperatures.

3.6.4 Tangent modulus.

3.6.5 Secant modulus.

4 Fabrication

4.1 Forming

4.1.1 Hot Isostatic Pressing (HIP)

4.1.1.1 *[Table]* Composition, heat treatment, and HIP treatment.

Hot isostatic pressing (HIP) can be used to form or bond materials at high temperatures with pressures acting on all surfaces simultaneously. The most widely-used pressurized gas is argon. Originally developed for the gas-pressure bonding of materials and powder compaction applications, HIP has been proven capable of healing micro-porosity in castings and thereby upgrading mechanical properties. HIP also makes possible the salvaging of castings that have been scrapped because of internal porosity (Refs. 58 and 67).

4.1.1.2 *[Figure]* Configurations of permanent steel molds and fracture toughness specimens used for testing the effects of hot isostatic pressing (HIP).

4.1.1.3 *[Figure]* Effect of hot isostatic pressing (HIP) on void fraction and tensile properties of test specimens as-cast in permanent steel molds.

Void fraction is dramatically reduced by HIP, both in mean value and standard deviation from the mean. This leads to increases in all mean tensile properties measured in the as-cast condition. Most significant are the increases in mean ultimate tensile strength and elongation. Both increases and decreases are found in the standard deviations of tensile properties.

4.1.1.4 *[Figure]* Effect of HIP on tensile properties of heat-treated test specimens.

4.1.2 Laser Shock Processing (LSP)

4.1.2.1 *[Table]* Composition, heat treatment, and laser shock treatment.

Laser shock processing (LSP) is an experimental technique in which laser-induced shock waves are used to alter the surface structure of a material, in a manner analogous to shot-peening. The first atomic layers of the material are vaporized. Sub-surface plastic deformation occurs which results in beneficial compressive residual stresses (Ref. 59). During fatigue cycling, these act as compressive mean stresses (or strains) which have the potential of increasing fatigue life (see Fig. 3.5.2.7).

4.1.2.2 *[Figure]* Configuration of notched fatigue test specimens loaded in three-point bending to test the effects of laser shock processing (LSP) on sand castings, showing overlapping impact areas at root of notch.

4.1.2.3 *[Figure]* Effect of laser shock processing (LSP) on stress-fatigue life curves for notched bar specimens from chilled sand castings.

Treatment by LSP increased mean fatigue strength by 30 to 50 percent, although the data exhibit large scatter.

4.1.3 Thixoforging

4.1.3.1 *[Table]* Preliminary comparison of tensile properties of thixoforged and conventionally-cast 356 alloys.

Thixoforging is a combination of forging and casting technologies which uses the physical state between solidus and liquidus temperatures to drastically reduce the material's flow stress and

thereby the required forming loads. Like a casting, near-perfect reproduction of complex die geometries is possible with thixoforging (Ref. 63).

4.2 Machining and Grinding

4.2.1 General. The machinability of these alloys is fair. Tool wear is greater for 356.0 and A356.0 than for 355 alloy because of their higher silicon content. Carbide cutting tools and lubricants such as lard oil and kerosene are recommended for general machining. For tapping of threads, pure lard oil is preferred.

4.3 Welding

4.3.1 General. A detailed discussion of the welding of aluminum castings is given in Reference 30. 356.0 and A356.0 alloys are readily weldable by GTA techniques. Gas welding, metal arc, carbon arc, and atomic hydrogen techniques have also been used, usually with a furnace for preheating. Foundry welding of small defects, etc., is usually performed with a filler metal of the same composition as the parent cast metal. For repair or assembly welding, 4043 filler metal is recommended in order to keep cracking sensitivity at a minimum (Ref. 30).

4.3.2 Temperatures exceeding 400 F during preheating or welding will affect the mechanical properties of heat-treated castings. After welding, however, the castings can be heat treated again to restore their properties. A general rule during welding is to keep the heat of welding concentrated in a narrow region.

4.3.3 Brazing of 356.0 and A356.0 is normally not recommended. It is possible, however, to braze these alloys by using special techniques (Ref. 31).

4.4 Heat Treatment

4.5 Surface Treatment

4.5.1 General. Because the resistance of these alloys to normal atmospheric weathering is good, protective coatings are not usually required. These alloys can be anodized to provide increased resistance to corrosion and abrasion. Other surface finishes such as electroplating, porcelain enameling, and painting can be applied for special purposes (Ref. 29).

References

1. AMS 4217G (June 1996)
2. AMS 4260E (November 1997)
3. AMS 4284F (October 1, 1989)
4. AMS 4285B (January 1, 1990))
5. AMS 4286D (July 1, 1984)
6. MIL-A-21180B (August 4, 1960 or latest revision).
7. Alcoa Structural Handbook (1958).
8. Alcoa Aluminum Handbook (1959).
9. Alcoa Research Laboratories, "Data Sheet" (August, 1957).
10. Alcoa Research Laboratories, "Data Sheet" (February, 1956).).
11. North American Aviation, Missile Development Division, "Materials Property Manual and Summary Report" (October, 1957).
12. Alcoa, Sales Development Division, "Premium Strength Structural Castings" (January, 1959).
13. Alcoa Research Laboratories, "Data Sheet" (December, 1956).
14. "The Aluminum Data Book," Reynolds Metals Company (1965).
15. ASM "Metals Handbook," American Society for Metals, Volume 1, 8th Edition (1961).
16. AMS 4218G (January, 1994).
17. Campbell, J.E., Aluminum Alloys for Cryogenic Service," ASTM Materials Research and Standards, Volume 4, No. 10 (October 1964).
18. Grube, K. R., Williams, D. N., and Ogden, H. R., "Premium-Quality Aluminum Castings, " DMIC Report 211, Battelle Memorial Institute (January 1965).
19. Shober, F. R., "The Effects of Nuclear Radiation on Structural Metals," DMIC Report 166, Battelle Memorial Institute (September 1961).
20. "Aluminum-Properties, Physical Metallurgy and Phase Diagrams," Volume 1 (Edited by K. R. VanHorn), American Society for Metals (1967).
21. Lombardo, J. J.,, Dixon, C. E., and Begley, J., "Cryogenic Radiation Effects on NERVA Structural Materials," *ASTM Preprint* No. 44 (June, 1966).
22. Nowak, J. J., "Preparation of Aluminum Alloys for UDMH Service," *Bell Aerosystems Company*, Report No. I-237 Revision A (October, 1962).

23. Colwell, D. L., "Melting Practice for Aluminum Die and Permanent Mold Castings," Modern Castings, Volume 39 (April, 1961).

24. Kangilaski, M., "The Effects of Neutron Radiation on Structural Materials," *REIC Report 45 to NASA*, Radiation Effects Information Center, Battelle Memorial Institute (June, 1967).

25. Graber, M. J., and Ronsick, J. H., "ETR Damage Surveillance Programs," *Progress Report* No. 1, IDO-16628 (1961).

26. Elijah, L. M., "Aluminum Alloy Fluxes," *Foundry*, (March, 1964), p. 88.

27. 1968 Book of Standards, Part 6, "Die-Cast Metals; Light Metals and Alloys" (October, 1968).

28. Flemings, M. C., Conrad, H. F., and Taylor, H. F., "Aluminum Alloys Fluidity Test," *AFS Transactions*, Volume 67 (1959), p. 496.

29. Aluminum, "Fabrication and Finishing" (Edited by K. R. VanHorn) Volume 3, American Society for Metals (1967).

30. "Welding Alcoa Aluminum", Aluminum Company of America (1958).

31. "Brazing Alcoa Aluminum," Aluminum Company of America (1959).

32. Oswalt, J. K., and Lii, Y., "Manufacturing Methods for Process Effects on Aluminum Casting Allowables," AFWAL TR 84-4117, Contract F33615-79-C-5116, Northrop Corp. (March 1985).

33. Pan, E. N., Hsieh, M. W., Jang, S.S., *et al.*, "Study of the Influence of Processing Parameters on the Microstructure and Properties of A356 Aluminum Alloy," *AFS Transactions*, Vol. 97, pp. 397-414 (1990).

34. Closset, B. M., "Modification and Quality of Low Pressure Aluminum Castings," *AFS Transactions*, Vol. 96, pp. 249-260 (1989).

35. Shivkumar, S., Keller, C., and Apelian, D., "Aging Behavior in Cast Al-Si-Mg Alloys," *AFS Transactions*,

35. Shivkumar, S., Keller, C., and Apelian, D., "Aging Behavior in Cast Al-Si-Mg Alloys," *AFS Transactions*, Vol. 98, pp. 905-911 (1990).

36. Shivkumar, S., Ricci, S., Jr., and Apelian, D., "Influence of Solution Parameters and Simplified Supersaturation Treatments on Tensile Properties of A356 Alloy," *AFS Transactions*, Vol. 98, pp. 913-922 (1990).

37. Shivkumar, S., Wang, L., and Keller, C., "Notched Tensile Properties of Heat-Treated A356 Castings, *AFS Transactions*, Vol. 103, pp. 705-709 (1995).

38. Din, T., and Campbell, J., "High Strength Aerospace Aluminum Casting Alloys: A Comparative Study," *Materials Science and Technology*, Vol. 12, pp. 644-650 (August 1996).

39. Takaai, T., Koga, M., Nakayama, Y., *et al.*, "Heat Treatment and Mechanical Properties of A356 Aluminum Casting Alloy," *Light Metals Processing and Applications*, Canadian Institute of Mining, Metallurgy, and Petroleum, pp. 713-720 (1993).

40. Brosnan, M., and Shivkumar, S., "Elevated-Temperature Tensile Properties and Fracture Behavior of A356 Castings," *AFS Transactions*, Vol. 103, pp. 727-737 (1995).

41. Tuttle, B. L., Keslinke, A., Twaróg, D., *et al.*, "Influence of Antimony on A356 Sr-Modified Aluminum Melts," *AFS Transactions*, Vol. 97, pp. 889-902 (1990).

42. Tuttle, B. L., Twarog, D., and Daniels, E., "The Effects of Trace Amounts of Antimony on the Structure and Properties of Aluminum Alloy A356.2," *AFS Transactions*, Vol. 99, pp. 7-16 (1991).

43. Essadiqi, E., Caron, S., Hamel, F. G., *et al.*, "Structure and Mechanical Properties of a Strip Cast Al-Si Alloy," *Light Metals 1990*, The Minerals, Metals, and Materials Society, pp. 963-966 (1990).

44. Stephens, R. E., Berns, H. D., Chernenkoff, R. A., *et al.*, "Low Cycle Fatigue of A356-T6 Cast Aluminum Alloy-A Round-Robin Test Program," *Fatigue and Fracture Toughness of A356 Cast Aluminum Alloy*, Society of Automotive Engineers, pp. 1-28 (1988).

45. Mahoney, B. J., and Stephens, R. I., "Fatigue and Fracture Toughness of Water-Chilled A356-T6 Cast Aluminum Alloy, *"Fatigue and Fracture Toughness of A356 Cast Aluminum Alloy*, Society of Automotive Engineers, pp. 71-92 (1988).

46. Stephens, R. I., "The SAE Round-Robin Fatigue Program with A356-T6 (Al7SiMg) Cast Aluminum Alloy, " *Advances in Fatigue Science and Technology*, Kluwer Academic Publishers (Dordrecht, The Netherlands), pp. 491-520 (1989). *AFS Transactions*, Vol. 98, pp. 913-922 (1990).

47. Stephens, R. I., "The Influence of Microstructure on the Fatigue Behavior of A356-T6 Cast Aluminum Alloy," *Basic Mechanisms in Fatigue of Metals*, Elsevier (Amsterdam), pp. 185-195 (1988).

48. Wigant, C. C., and Stephens, R. I., "Fatigue Crack Growth of A356-T6 Cast Aluminum Alloy," *Fatigue and Fracture Toughness of A356 Cast Aluminum Alloy*, Society of Automotive Engineers, pp. 49-60 (1988).

49. Wigant, C. C., and Stephens, R. I., "Fatigue Crack Growth Behaviour of A356-T6 Cast Aluminum Alloy *Fatigue '87: Papers Presented at the Third International a Conference on Fatigue and Fatigue Thresholds*, pp. 165-173 (1987).

50. Koh, S. K., and Stephens, R. I., "Fracture Toughness of A356-T6 Cast Aluminum Alloy," *Fatigue and Fracture Toughness of A356 Cast Aluminum Alloy*, Society of Automotive Engineers, pp. 61-69 (1988)

51. Cordes, T. S., Berns, H. D., Lingenfelser, D. J., *et al.*, A SWT Fatigue Mean Stress Model for A356-T6 Cast Aluminum Alloy, " Fatigue and Fracture Toughness of A356 Cast Aluminum Alloy, Society of Automotive Engineers, pp. 39-47 (1988).

52. Anon., *Special Report on the Mechanical Properties of Sand Cast Aluminum Alloy Test Casting*, Jobbing Foundry Division of the Aluminum Association, (1979).

53. Anon., *Special Report on the Mechanical Properties of Permanent Mold Aluminum Alloy Test Casting*, Jobbing Foundry Division of the Aluminum Association, (1986).

54 Kramer, T. E., and Coberly, E. D., "Aluminum Alloy Characteristics; The State of the Art," *Aluminum Conference: State of the Art*, Cast Metals Institute of the American Foundrymen's Society, pp. 7-21 (1979).

55. Hetke, A., and Gundlach, R. B., "Aluminum Casting Quality in Alloy 356 Engine Components," *AFS Transactions*, Vol. 102, pp. 367-380 (1994).

56. Honma, U., and Kitaoka, S., "Fatigue Strength and Mechanical Properties of Aluminum Alloy Castings of Different Structural Fineness, *Aluminum*, Vol. 60, pp. E 780-E 783, (Dec. 1984).

57. Czyryca, E. J., "Long-Life Corrosion Fatigue Crack Initiation in Cast A356-T6 Aluminum Alloy, " *Economic Implications of Mechanical Failure Prevention*, Vibration Institute (Willowbrook, IL), pp. 75-86 (1992).

58. Meyers, C. W., and Chou, J. -S., "Experimental Investigations of Deformation in HIPped A356 Aluminum Castings," *AFS Transactions*, Vol. 99, pp. 175-186 (1991).

59. Peyre, P., Fabbro, R., Merrien, P., *et al.*, "Laser Shock Processing of Aluminum Alloys, Application to High Cycle Fatigue Behaviour, *Materials Science and Engineering A210*, Elsevier, pp. 102-113 (1996).

60. Drouzy, M., Jacob, S., and Richard, M., "Interpretation of Tensile Results by Means of Quality Index and Probable Yield Strength," *AFS International Cast Metals Journal*, (June 1980).

61. AMS 4181B (July 1996).

62. Odegard, J. A., and Pedersen, Ketill, "Fatigue Properties of an A356 (AlSi7Mg) Aluminum Alloy for Automotive Applications-Fatigue Life Prediction," *Metal Matrix Composites*, Society of Automotive Engineers, pp. 25-32 (1994).

63. Tietmann, A., Bremer, T., Hirt, G., and Kopp, R., "Preliminary Results in Thixoforging Aluminum Wrought Alloys," *Processing of Semi-Solid Alloys and Composites*, The Minerals, Metals & Materials Society, pp. 170-179 (1993).

64. Scott, G. D., Cheney, B. A., and Granger, D. A., "Fracture Toughness and Tensile Properties of Directionally Solidified Aluminum Foundry Alloys," *Technology for Premium Quality Castings*, The Metallurgical Society/ AIME, pp. 123-149 (1988).

65. Dimayuga, F. C., "Modification of Al-Si Alloys Using Strontium, Sodium, and Antimony," *Molten Aluminum Processing*, American Foundrymen's Society, pp. 6-1 to 6-25 (1989).

66. Brown, W. F., and Spera, D. A., "Aluminum Alloy A357.0," *Aerospace Structural Metals Handbook*, Code 3109, Purdue University (1997).

67. MIL-H-6088G Amendment 1 (September 15, 1992).

68. *Aluminum and Aluminum Alloys.* ASM Specialty Handbook, J. R. Davis, ed., pp. 18-27, and 103-117 (1993).

69. AMS 4261D (July 1991)

Table 1.3.1 AMS Specifications for 356.0 and A356.0 castings and applicable welding wire.

AMS No.	Alloy	Form	Quality/Condition	UNS No.	Similar Specification	References
4181B	4008	Welding wire	Annealed	A94008	AWS A5.10, Class R-A356.0	61
4260E	356.0-T6	Castings, Investment	Radiographic	A03560		2
4261D	356.0-T51	Castings, Investment	Radiographic Precipitation Heat Treated	A03560		69
4286D	356.0-T51	Castings, Permanent Mold	Radiographic Precipitation Heat Treated	A03560	FED-QQ-A-596 Alloy 356, Temper T51	5
4285B	356.0-T6	Castings, Centrifugal	Radiographic Solution and Precipitation Heat Treated	A03560		4
4284F	356.0-T6	Castings, Permanent Mold	Radiographic Solution and Precipitation Heat Treated	A03560	FED-QQ-A-596 Alloy 356	3
4217G	356.0-T6	Castings,Sand	Solution and Precipitation Heat Treated	A03560		1
4218G	A356.0-T61P	Castings,Sand or Composite Permanent Mold and Investment	Solution and Precipitation Heat Treated	A13560	MIL-A-21180, Alloy A356.0, Class 12	16

Table 1.4.2 Composition specifications for 356.0 and A356.0

Alloy	356.0				A356.0	
Specifications	AMS 4217G AMS 4260E AMS 4261D AMS 4286D AMS 4181B		AMS 4284F AMS 4285B		AMS 4218G	
References	1, 2, 5, 61, 69		3, 4		6,16	
Designation	356.0-T6, -T51 4008		356.0-T6		356.0-T6P	
UNS	A03560 A94008		A03560		A13560	
Composition	Minimum	Maximum	Minimum	Maximum	Minimum	Maximum
Si	6.5	7.5	6.5	7.5	6.5	7.5
Mg	0.20	0.45	0.20	0.40	0.25	0.45
Ti	–	0.25	–	0.25	–	0.20
Fe	–	0.60	–	0.60	–	0.20
Cu	–	0.25	–	0.25	–	0.20
Zn	–	0.35	–	0.35	–	0.10
Mn	–	0.35	–	0.35	–	0.10
Be	–	0.0008[a]				
Other, each	–	0.05	–	0.05	–	0.05
Other, total	–	0.15	–	0.15	–	0.15
Al	Remainder		Remainder		Remainder	

[a] AMS 4181B only

Table 1.4.3.1 Composition, foundry practice, heat-treatment, and properties of investment-cast test plates (Ref. 32)

Alloy	A356.0-T6			
Form	3-inch x 10-inch x 1/10-inch Thick Shell Investment Casting			
Foundry Practice	100 percent Ingot, Melt at 1350 F + (95%N + 5 % Freon) Degas + 1320 F Pour Into 1000 F Mold			
Composition	Base: 0.36 Mg, 0.04 Fe			
Heat Treat	1000 F 18 hr + WQ + 12-24 hr at RT + 310 F 5 hr			
Tensile Properties	F_{tu} (ksi)	F_{ty} (ksi)	e (percent)	Hardness (RE)
n = 10: Mean Standard Dev.	41.7 0.7	32.3 1.1	7.2 0.7	87 1.7
Plate Surface DAS Range	1.8 - 2.5 mils			

Table 1.4.3.2 Composition, foundry practice, heat-treatment, and properties of sand-cast test plates (Ref. 32)

Alloy	A356.0-T6			
Form	3-inch x 10-inch x 3/4-inch Thick Sand Composite Casting			
Foundry Practice	AFS 60 Bank Sand With 0.8 Percent Binder, Chills in Both Cope and Drag, Two Risers, Steel Wool and Screens in Well of Sprue, 60 percent Ingot, 40 percent returns, 3000-lb Melt + (90%N + 10% Chlorine) Degas + 1375 F Pour Into RT Mold			
Composition	Base: 0.38 Mg, 0.10 - 0.12 Fe			
Heat Treat	1000 F 18 hr + 40 F WQ + 12-24 hr at RT + 310 F 8 hr			
Tensile Properties	F_{tu} (ksi)	F_{ty} (ksi)	e (percent)	Hardness (RE)
n = 10: Mean Standard Dev.	41.9 1.7	32.4 0.3	6.4 1.2	88 1.7
Plate Surface DAS Range	0.9 - 1.1 mils			

Table 1.4.3.7 Composition, foundry practice of as-cast test plates (Ref. 33)

Alloy	A356.0
Form	2-inch D x 8.3-inch Long Cylinders In Cast Iron Mold 0.83-inch D x 7.9-inch Long Cylinders In Green or Furan Sand Molds
Foundry Practice	26-lb and 400-lb Melts + N2 Degas 15-20 Min at 1310 F Series B: 100 percent Virgin Ingot Series D: 100 percent Virgin Ingot or 100 percent Returns + 0.02 Sr With and Without Ceramic Foam Filters
Composition	Series B: 7.1 Si, 0.27 Mg, 0.02-0.31 Ti, 0.005 Mn, 0.12 Fe, 0.02 Zn Series D: 6.6 Si, 0.22 Mg, 0.17 Ti, 0.014 Mn, 0.08 Fe, 0.02 Zn
Heat Treat	None

Table 1.4.3.9 Composition, foundry practice, and heat-treatment of low-pressure-cast test components (Ref. 34)

Alloy	A356.0 and A356.0-T6
Form	12-inch x 7-inch x 4-inch Thick U-Shaped Components
Foundry	Pre-Heated Low-Pressure Molds 400-lb Melt Without Degas 4 Series of 15 to 30 Castings Each; Specimens Cut from Randomly Selected Castings
Composition	7.4 Si, 0.09 Fe, 0.006 Cu, 0.005 Mn, 0.42 Mg, 0.016 Zn, 0.07 Ti, 0-0.024 Sr
Heat Treat	One Lot As-Cast; One Lot 1000 F 13 hr + 77 F WQ + 310 F 8 hr

Table 1.5.2 Typical heat Treatments

Alloy and condition	Method of casting [a]	Solution heat treatment			Artifical aging		Ref.
		Temp (F)	Time (hr)	Quench	Temp (F)	Time (hr)	
356.0-F	S or PM	None	None	None	None	None	
356.0-O	S or PM	650	2	None	None	None	14
356.0-T4	S or PM	980 - 1025	6 - 24	Water	None	None	67
356.0-T51	S or PM	None	None	None	430 - 450	6 - 12	67
356.0-T51	S or PM	None	None	None	440	7 - 9	68
356.0-T6	S	1000	12	Water	310	3 - 5	68
356.0-T6	PM	1000	4 - 12	Water	310	2 - 5	68
356.0-T6	S or PM	980 - 1025	6 - 24	Water	300 - 320	1 - 6	67
356.0-T61	S or PM	980 - 1025	6 - 24	Water	300 - 320	6 - 10	67
356.0-T7	S	1000	12	Water	400	3 - 5	68
356.0-T7	PM	1000	4 - 12	Water	440	7 - 9	68
356.0-T71	S	1000	10 - 12	Water	475	3	68
356.0-T71	PM	1000	4 - 12	Water	475	3 - 6	68
A356.0-F	S or PM	None	None	None	None	None	
A356.0-O	S or PM	650	2	None	None	None	14
A356.0-T4	S or PM	980 - 1025	6 - 24	Water	None	None	67
A356.0-T6	S	1000	12	Water	310	3 - 5	68
A356.0-T6	S or PM	980 - 1025	6 - 24	Water	300 - 320	1 - 6	67
A356.0-T61	PM	1000	6 - 12	Water	RT 310	8 (min) 6 - 12	68
A356.0-T61	S or PM	980 - 1025	6 - 24	Water	300 - 320	6 - 10	67

[a] S = sand casting; PM = permanent-mold casting

Table 1.5.3.1 Composition, foundry practice, and heat treatment (Refs. 35 and 36)

Alloy	A356.2			
Form	Sand and Permanent-Mold Cast Test Bars			
Composition	Sand Castings		Permanent Mold Castings	
Element	Unmodified	Sr-Modified	Unmodified	Sr-Modified
Si	7.19	7.10	6.90	6.83
Mg	0.40	0.39	0.41	0.42
Fe	0.09	0.10	0.11	0.09
Ti	0.16	0.17	0.15	0.17
Sr	0.002	0.022	0.003	0.023
P	–	–	0.0013	0.0014
Sb	–	–	0.0059	0.0034
Cr	0.0012	0.0017	0.0022	0.0013
Ni	0.0028	0.0048	0.0053	0.0050
Cu	0.001	0.001	0.022	0.014
Foundry Practice	100 percent Virgin Melt at 1360 +/- 20 F (Sand Mold) or 1400 +/- 20 F (Permanent Mold) + Grain Refinement + N2 Degas + Ceramic Foam Filter			
Heat Treatment	T6: Sand Mold: 1022 F, 100 min; WQ, 140 F; RT, 0 to 72 hr; 293 F to 394 F, 0 to 100 hr Permanent Mold: 1022 F, 50 min; WQ, 140 F; RT, 0 to 72 hr; 293 F to 394 F, 0 to 100 hr T4: Same solution treatment and quench as T6; no artifical aging			

Notes: Radiograph all specimens: reject for visible defects

Table 1.5.3.6. Composition, foundry practice, and heat treatment (Refs. 37 and 40)

Alloy	A356.2 As-Cast and -T6		
Form	Sand and Permanent-Mold Cast Test Bars		
Composition	Sand Castings		Permanent Mold Casting
Element	Unmodified	Sr-Modified	Sr-Modified
Si	6.65	6.67	7.20
Mg	0.37	0.39	0.41
Fe	0.07	0.08	0.09
Ti	0.12	0.11	0.13
Sr	0.001	0.020	0.025
P	0.01	0.01	0.02
Mn	0.03	0.02	0.02
Microstructure	Sand Castings		Permanent Mold Casting
Parameter	Unmodified	Sr-Modified	Sr-Modified
DAS (10^{-4} in.)	15 - 19	16 - 19	9 - 12
Grain Size (in.)	0.035	0.034	0.009
Porosity (percent)	0.13	0.85	0.02
Relative Pore Area			
Average	1.0	3.2	0.05
Max	5.5	21.7	0.28
Pore Aspect Ratio	3.1	3.4	3.9
Foundry Practice	100 percent Virgin Melt at 1370 +/- 20 F (Sand Mold) or 1400 +/- 20 F (Permanent Mold) + Ti Grain Refinement + N_2 De-Gas + Ceramic Foam Filter		
Heat Treatment	Sand Mold: 1020 F, 2 to 200 hr; WQ, 140-160 F; RT, 24 hr; 310 F, 4 hr Permanent Mold: 1020 F, 2 to 200 hr; WQ, 140-160 F; RT, 24 hr; 340 F, 4 hr		
As-Cast Tensile Properties at RT			
F_{tu} (ksi)	23.9	24.4	28.7
F_{ty} (ksi)	14.6	14.5	14.6
e (percent)	4.7	6.1	7.4
Heat-Treated T6 Tensile Properties at RT			
F_{tu} (ksi)	39.6	43.5	45.4
F_{ty} (ksi)	32.5	30.8	35.5
e (percent)	2.8	9.3	7.6

Notes: Radiograph all specimens; reject for visible defects; ASTM B-108 test bars

Table 1.5.6.4. Composition, foundry practice, and heat treatment (Ref. 38)

Alloy	A356.0
Form	Metal Mold Cast Ingot
Composition	7.09 Si, 0.30 Mg, 0.08 Fe, 0.01 Ni, --- Zn, 0.09 Ti, 76 ppm Sr
Foundry Practice	Melt at 1292 F + Metal Mold at 302 F + Cooling at 7 to 30 F/s
Heat Treatment	1057 F, 0+ min; WQ; (311F, 0 to 200 hr

Table 1.5.6.8. Composition, foundry practice, and heat treatment (Ref. 39)

Alloy	A356.0
Form	Sand Cast Test Bars
Composition	7.04 Si, 0.39 Mg, 0.031 Cu, 0.32 Fe, 0.23 Mn, 0.00 Ni, 0.025 Zn, 0.001 Pb, 0.027 Ti
Foundry Practice	Melt at 1200 F 30 min to De-Gas + 1400 F 1 min + 1200 F Pour AFS 60 Silica Sand + Pepset 5000 Binder + Ceramic Foam Filter + Aluminum Block Chills
Heat Treatment	1000 F, 8 hr; WQ; 350 F and 420 F, 4 hr

Table 1.6.2 Desirable Hardness Ranges [a]

AMS	Alloy	Form	Hardness Range	Ref.
4181B	4008	Welding wire	–	61
4217G	356.0-T6	Castings	65 to 95 HB/10/500 or 70 to 100 HB/10/1000	1
4260E	356-T6	Castings, investment		2
4261D	356-T51	Castings, investment		69
4284F	356.0-T6	Castings, permanent mold	65 to 95 HB/10/500 or 70 to 100 HB/10/1000	3
4285B	356.0-T6	Castings, centrifugal		4
4286D	356.0-T51	Castings, permanent mold	50 HB/10/500, min or 55 HB/10/1000, min	5
4281G	A356.0-T6P	Castings	70 to 105 HB/10/500 or 75 to 110 HB/10/1000	16

[a] Castings not to be rejected for out-of-range hardness if tensile property requirements are met

Table 1.8.2.3. Composition, foundry practice, and heat treatment of sand-cast test bars (Refs. 41 and 42)

Alloy	A356.2-T6
Form	Sand Cast Test Bars
Composition	7.12 Si, 0.36 Mg, 0.11 Fe, 0.01 Zn, 0.11 Ti
Foundry Practice	100 percent Virgin Melt at 1300 F + Grain Refiner + Modifier, 30-50 min, N_2 De-Gas + 1360 F Sample + 1300 F Sample + 1250 F Sample + Pour Sand Molds With and Without 2x2x3/4 inch Reticulated Ceramic Foam Filter
Heat Treatment	1000 F, 12 hr; WQ; 320 F, 4 hr; AC

Table 1.8.3.2. Composition, foundry practice, and heat treatment of strip-cast sheet (Ref. 43)

Alloy	A356.0 As-Cast and T6 Heat-Treated
Form	Strip-Cast Sheet
Composition	7.39 Si, 0.48 Mg, 0.33 Fe, 0.24 Zn, 0.14 Mn, 0.19 Cu
Foundry Practice	See Figure 1.8.3.1
Heat Treatment	1000 F, 12 hr; WQ; RT, 48 hr; 310 F, 4 hr Cast strip 0.12 to 0.20-in. thick x 3.9-in wide

Table 2.1.3. Thermal conductivity at RT of 356.0 and A356.0 (Refs. 14 and 20)

Alloy and Condition	Btu-ft/ (hr-sq. ft.-F)
356.0 -T51	97
356.0 - T6	87
356.0 -T6[a]	92
356.0 -T7	90
A356.0 -T6	87

[a] Chill-cast samples; all other samples cast in green-sand molds

Table 2.2.2.1. Electrical resistivity at RT and conductivity (Refs. 14 and 15)

Alloy and Condition	Resistivity (Ref. 15) (micro-ohm-inch)	Conductivity (Ref. 14) (percent IACS)
356.0-T51	1.60	43
356.0-T6	1.74	39
356.0-T7	1.70	40
A356.0-T6	–	40

Table 2.4.1. Effect of neutron radiation on tensile properties of 356.0 cast test bars (Refs. 19 and 24)

Irradiation Temperature (F)	Integrated Neutron Flux (a) ($n\ cm^{-2}$)	F_{tu} (ksi)		F_{ty} (ksi)		e (2 inches) (percent)	
		A	B	A	B	A	B
–	2.4×10^{20}	32.4	44.3	24.1	42.4	2.7	0.4
–	7.2×10^{20}	32.4	54.0	24.1	51.0	2.7	0.9
–	2.6×10^{21}	32.4	45.0	24.1	36.0	2.7	1.5
120	2.04×10^{19}	33.1	36.7	26.0	29.1	4.0	6.0
120	1.22×10^{20}	33.1	42.0	26.0	33.5	4.0	6.0
120	5.59×10^{20}	33.1	45.1	26.0	42.5	4.0	6.0
120	9.84×10^{20}	33.1	54.4	26.0	52.1	4.0	3.0

(a) Fast neutrons.
A - Not irradiated
B - Irradiated

Table 2.4.2. Effect of nuclear radiation at -420 F on tensile properties of A356.0-T6 cast plate at -420 F (Ref. 21)

Test	Pre and Post Irradiation Data at -420				
Property	Specimen Type (b)	Control (average)	Irradiated (average) (a)	Change	Percent Change
F_{tu} (ksi)	L	44.7	52.8	+ 8.1	+ 18 (c)
F_{ty} percent	L	31.0	42.8	+ 11.8	+ 38 (c)
- 0.1 percent	L	1.5	1.4	- 0.1	- 7
RA (ksi)	L	2.8	0.8	- 2.0	- 72 (c)
F_{su} (ksi)	L	50.4	45.6	- 4.8	- 10 (c)
Notch Strength (ksi) (K_t = 6.3)	L	39.7	43.2	+ 3.5	+ 9
Notch/Unnotch Strength Ratio (d)	L	0.89	0.82	–	–

(a) Irradiated at 5 x 10^{16} nvt (E> 1.0 MeV) in liquid hydrogen.
(b) L = longitudinal specimen
(c) Statistically significant change; probability > 0.90.
(d) Notch specimen geometry:
Width = 1.0 inch
Notched Radius = 0.005 inch
Notched Depth = 30 percent
Notched Angle = 60 degrees
Thickness = 0.063 inch

Table 2.4.4. Effect of neutron radiation on tensile properties of A356.0 (Ref. 25)

Irradiation Temperature (F)	Test Temp (F)	Fast Neutron Flux (a) (n cm^{-2})	F_{tu} (ksi)		F_{ty} (ksi)		e (2 inches) (percent)	
			A	B	A	B	A	B
120	RT	2.0 x 10^{19}	33.1	36.7	26	29.1	4	6
120	RT	1.2 x 10^{20}	33.1	42.0	26	33.5	4	6
120	RT	5.6 x 10^{20}	33.1	45.9	26	42.4	4	6
120	RT	9.8 x 10^{20}	33.1	54.4	26	52.1	4	3

(a) Energy greater than 1.0 MeV
A not irradiated
B Irradiated

Table 3.1.1. AMS specifications for mechanical properties (a)

AMS	Alloy	Form	F_{tu} (ksi)	F_{ty} (ksi)	e (percent)	Ref.
4181B	4008	Welding wire	–	–	–	61
4217G	356.0-T6	Castings Separately cast specimens: min.: Specimens integrally cast or cut from castings, min. average of at least 4; preferably 10:	 30.0 22.5	 20.0 15.0	 3.0 0.7	1
4260E	356-T6	Castings, investment Separately cast specimens: min.: Specimens integrally cast or cut from castings, min. average of at least 4; preferably 10:	 33.0 25.0	 22.0 16.5	 3.0 1.0	2
4284F	356.0-T6	Castings, permanent mold Separately cast specimens: min.: Specimens cut from castings, min.:	 33.0 24.75	 22.0 16.5	 3.0 0.7	3
4285B	356.0-T6	Castings, centrifugal Separately cast specimens: min.: Specimens cut from castings, min.:	 33.0 24.8	 22.0 16.5	 3.0 1.0	4
4286D	356.0-T51	Castings, permanent mold Separately cast specimens: min.: Specimens integrally cast or cut from castings, min. average of at least 4; preferably 10:	 25.0 18.8	 – –	 – –	5
4218G	A356.0-T6P	Castings Separately cast specimens: min.: Specimens integrally cast, min: Specimens cut from any area of castings min. of at least 2:	 33.0 32.0 32.0	 27.0 22.0 22.0	 3.0 2.0 2.0	16

(a) Specimens conforming to ASTM B557 or ASTM B557M

Table 3.1.2. MIL-A-21180B specified tensile properties for specimens cut from castings of A356.0 (Ref. 6)

Form	Special Mold, Permanent Mold, or Sand Mold with Chills					
Condition	T61					
Location of Castings	Designated Area			Any Area		
Class	1	2 (a)	3 (a)	10	11	12
$F_{tu\ min}$ (ksi)	38.0	40.0	45.0	38.0	33.0	32.0
$F_{ty,\ min}$ (ksi)	28.0	30.0	34.0	28.0	27.0	22.0
e_{min} (percent)	5.0	3.0	3.0	5.0	3.0	2.0

(a) Obtainable only in favorable casting configurations and must be negotiated with the foundry.

Table 3.2.1.1. Composition, foundry practice, and heat treatment (Ref. 44)

Alloy		A356.0-T6	
Form		Investment-Mold Cast Test Bars: Near-Net-Shape	
Composition		7.15 Si, 0.36 Mg, 0.009 Cu, 0.031 Fe, 0.008 Mn, 0.009 Zn, 0.05 Ti	
Foundry Practice		Melt at 1300 F + Pour + Investment Mold Temperatures: Casting X, RT; Casting Y, 1000 F; Casting Z, 1800 F	
Heat Treatment		MIL-A-21180,T6	
Casting	X	Y	Z
DAS (10^{-4} in.)	13	24	26
Tensile Properties			
E (10^3 ksi)	10.1	10.1	10.3
F_{tu} (ksi)	41.1	38.6	36.6
F_{ty} (ksi)	33.3	32.5	31.5
e (percent)	3.5	1.8	1.7
RA (percent)	5.7	3.0	2.9

Notes: Tensile specimens machined from cast bars

Table 3.2.1.2. Composition, foundry practice, and heat treatment (Ref. 44)

Alloy	A356.0-T6
Form	Sand-Mold Cast Test Bars: Near-Net-Shape
Composition	7.0 Si, 0.36 Mg, 0.04 Cu, 0.11 Fe, <0.01 Mn, 0.01 Zn, 0.15 Ti, <0.01 Cr, <0.01 Ni, < 0.01 Sn
Foundry Practice	Melt at 1310 F + Pour + Sand-Mold Casting W + Internal Cold-Water Chill Tube
Heat Treatment	MIL-A-21180,T6; 990 F, 12 hr
Casting	W
DAS (10^{-4} in.)	12
Tensile Properties	
E (10^3 ksi)	9.9
F_{tu} (ksi)	38.9
F_{ty} (ksi)	21.2
e (percent)	9.2
RA (percent)	8.5

Notes: Tensile specimens machined from cast bars

Table 3.2.1.5. Composition, foundry practice, and heat treatment (Ref. 52)

Alloy	A356.0-T6
Form	Sand-Mold Cast Test Plates
Composition	6.7-7.15 Si, 0.23-0.35 Mg, 0.01-0.19 Cu, 0.10-0.17 Fe, 0.01-0.07 Zn, 0.10-0.16 Ti
Foundry Practice	1350 F-1380 F Pour
Heat Treatment	T6

Note: Radiographic Quality Level AA-CS-M5-71: AA all plate sections

Table 3.2.1.9. Composition, foundry practice, and heat treatment (Ref. 55)

Alloy	A356.0-T6
Form	Sand-Cast Automotive Engine Components: Blocks and Heads
Composition	
Unmodified:	7.01 Si, 0.36 Mg, <0.01 Cu, 0.11 Fe, 0.01 Zn, 0.07 Ti, 0.01 Mn,<0.01 Cr, <0.01 Ni, <0.01 Sn, <0.01 Pb, 0.003 P, <0.01 Sb, 0.001 Na, <0.001 Sr
Sr-Modified:	6.25 Si, 0.38 Mg, <0.01 Cu, 0.07 Fe, 0.01 Zn, 0.08 Ti, 0.04 Mn,<0.01 Cr, <0.01 Ni, <0.01 Sn, <0.01 Pb, 0.002 P, <0.01 Sb, 0.004 Na, 0.010 Sr
Foundry Practice	De-Gassed + Highly Filtered + Counter-Gravity Poured;Conventional low-pressure casting, and improved low-pressure process (ILP): Chill plate insert in mold engineered to produce rapid, controlled directional solidification
Heat Treatment	T6

Note: Brinell hardness: 81.8 to 98.1 HB500

Table 3.2.1.11 Composition, foundry practice, and heat treatment (Ref. 53)

Alloy	356.0-T6
Form	Permanent-Mold Cast Test Plates
Composition	6.84-7.48 Si, 0.28-0.44 Mg, 0.00-0.15 Cu, 0.34-0.53 Fe, 0.00-0.14 Zn, 0.08-0.15 Ti, 0.00-0.20 Mn
Foundry Practice	1360 F-1540 F Pour
Heat Treatment	T6

Note: Radiographic Quality Level AA-CS-M5-71: AA all plate sections

Table 3.2.1.16. Composition, foundry practice, and heat treatment (Ref. 64)

Alloy	A356.0-T5, - T6, and T7
Form	Directionally-solidified Ingots, 3-inch x 3-inch x 9-inch High
Composition	7.15 Si, 0.38 Mg, 0.08 Fe, 0.138 Ti, 0.0013 B
Foundry Practice	Melt in 50-lb Capacity Clay-graphite Crucible 1320 F + De-Gas Ar-10 percent Cl2 + Plaster Mold at 1420 F + Water-Chilled Copper Base + Top Insulation
Heat Treatment	
T5	Age 8 hr at 440 F
T6	Solutionize 12 hr at 1000 F; RT Age 8 hr: age 3 hr at 310 F
T7	Solutionize 12 hr at 1000 F; Age 8 hr at 440 F

Note: Specimen blanks sliced parallel to bottom chill for properties at different cooling rates

Table 3.2.2.1. Compression, shear, and bearing propertries of 356.0 and A356.0 cast test bars (Refs. 7, 8, and 69)

Alloy	356.0						A356.0
Mold	Sand				Permanent		Permanent
Condition	T51	T6	T7	T71	T6	T7	T61
$F_{cy,\ min}$ (ksi)	17	20	27	19	22	21	27
$F_{cy,\ typ}$ (ksi)	21	25	31	22	27	24	32
$F_{su,\ min}$ (ksi)	17	25	21	17	25	22	23
$F_{su,\ typ}$ (ksi)	20	26	24	20	30	25	28
$F_{bru,\ min}$ (ksi) (e/D = 2.0)	48	63	65	52	59	52	–
$F_{bru,\ min}$ (ksi) (e/D = 2.0)	32	40	52	36	40	38	–

Table 3.5.1.1. Composition, foundry practice, and heat treatment (Ref. 56)

Alloy	A356.0-T6		
Form	Sand-Cast and Permanent-Mold Rotating Bending Fatigue Test Bars		
Composition	7 Si, 0.3 Mg, Ti		
Foundry Practice	(1310 F) Melt		
Mold Type	Permanent	Permanent	CO_2 Sand
Mold Preheat (F)	300 F	660 F	–
Cooling Rate (F/s)	4.7	2.6	0.3
DAS (10^{-4} in.)	20	32	66
Heat Treatment	970 F, 8 hr; 320 F, 6 hr		

Table 3.5.1.4. Composition, heat treatment, and tensile properties (Ref. 57)

Alloy	A356.0-T6
Form	Wedge-Shaped Sand Castings 2.5-in. x 14-in. x 14-in.
Composition	7.3 Si, 0.12 Fe, 0.41 Mg, 0.02 Zn, 0.04 Ti, nil Mn
Heat Treatment	T6; Average Rockwell B Hardness 21
Tensile Properties	F_{tu} 32.9 ksi; F_{ty} 21.2 ksi; e 2.5 percent; RA 2 percent

Notes: Laboratory air fatigue specimens: 0.250-inch D test section
Sea water fatigue specimens: 0.500-inch D test section

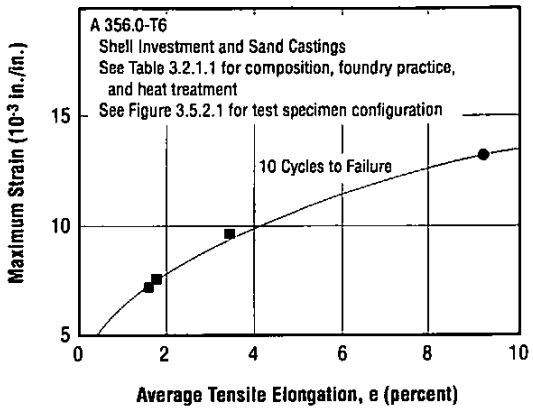


Figure 3.5.2.6 Effect of tensile elongation on axial strain-cycling fatigue strength at 10 cycles to failure of smooth specimens from unchilled shell investment castings and water-chilled sand castings (Refs. 44–47)

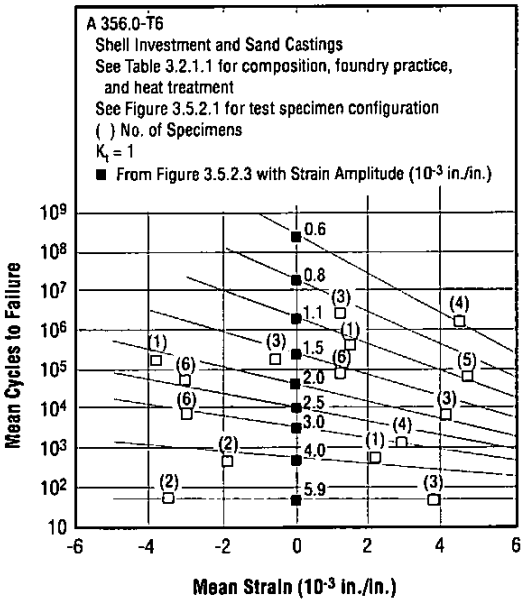


Figure 3.5.2.7 Effect of mean strain on axial strain-fatigue life behavior of smooth specimens from shell-investment castings (calculated from data in Ref. 51)

Table 3.5.1.6. Chacteristic of fatigue test materials (Ref.62)

Alloy		A357.0-T6 Sand-Cast	
Form:	Die-cast wheels (low pressure)	Direct-chill cast billets without extrusion	Direct-chill cast billets with extrusion before HT
Grain Size: (10^{-4} in.)	98	138	Longitudinal: 1575 Transverse 394
DAS (10^{-4} in.)	9	8	---
Porosity (percent)	1.0	0.0	0.0
F_{tu} (ksi):	41.8	45.7	43.5
F_{ty} (ksi):	32.2	33.4	31.9
e (percent):	6	16	20

Note: Direct-chill casting is a semi-continuous process

Table 4.1.1.1. Composition, heat treatment, and HIP treatment (Ref. 58)

Alloy	A356.0
Form.	Steel Permanent Mold Castings 1.5-in. D x 8-in
Composition	6.6 Si, 0.15 Fe, 0.38 Mg, 0.02 Zn, 0.17 Ti, 0.00 Mn, 0.04 Sb, 0.01 Cu,0.01 Cr
Heat Treatment	None
HIP Treatment	970 F + 15 ksi, 2 hr

Table 4.1.2.1. Composition, heat treatment, and laser shock treatment (Ref. 59)

Alloy	A356.0
Form	Steel Permanent Mold Castings 1.5-in. D x 8-in.
Composition	7.05 Si, 0.2 Fe, 0.33 Mg, 0.03 Zn, 0.15 Ti, 0.03 Mn, 0.05 Cu
Heat Treatment	900 F, 6 hr; WQ 70 F; 320 F, 6 hr
Laser Shock Treatment	14.8 GW/in^2; 5 impacts 0.0024-in. square, or 3 elliptical impacts; 50 percent overlap; 1 repetition

Table 4.1.3.1. Preliminary comparison of tensile properties of thixoforged and conventionally-cast 356 aloys (Ref. 63)

Property	Convential Casting (typical)	Trixoforged Complex Part (a)	Change (percent)
Ultimate Tensile Strength, Ftu (ksi)	49.3	43.5	-12
Tensile Yield Strength, Fty (ksi)	40.6	37.1	-9
Elongation, e (percent)	9.0	11.4	+27

(a) Ribbed plate 6.9 x 10.4 in.; thicknesses from 0.4 to 1.0 in.

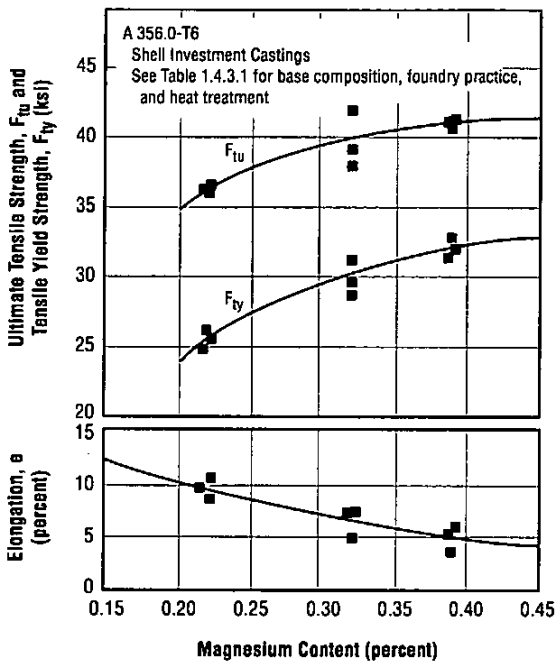


Figure 1.4.3.3 Effect of magnesium content on the tensile properties of shell investment castings (Ref. 32)

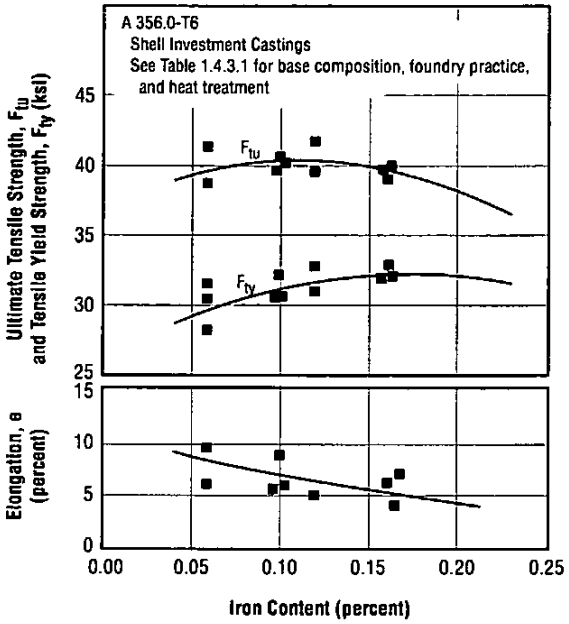


Figure 1.4.3.5 Effect of iron content on the tensile properties of shell investment castings (Ref. 32)

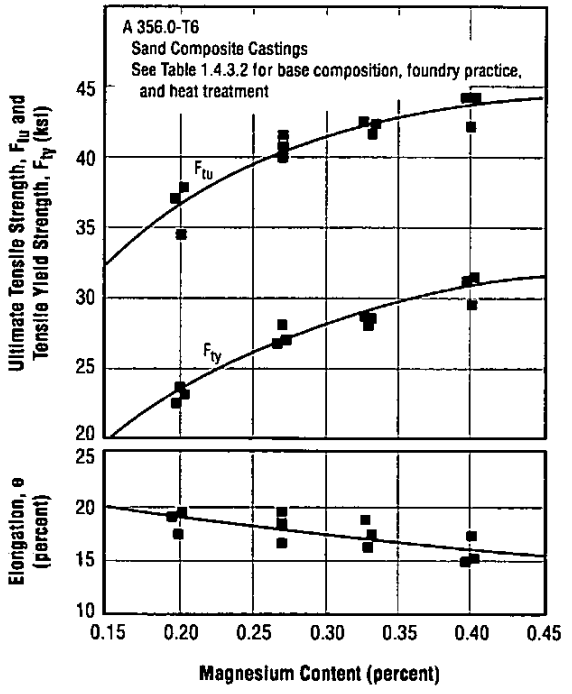


Figure 1.4.3.4 Effect of magnesium content on the tensile properties of sand composite castings (Ref. 32)

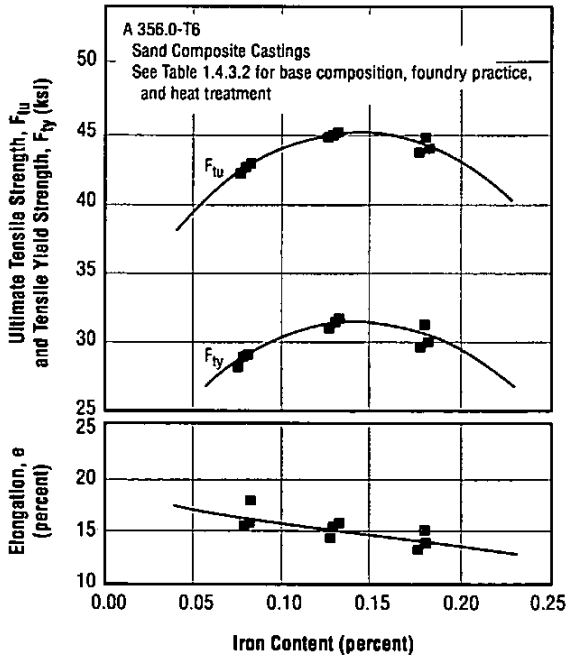


Figure 1.4.3.6 Effect of iron content on the tensile properties of sand composite castings (Ref. 32)

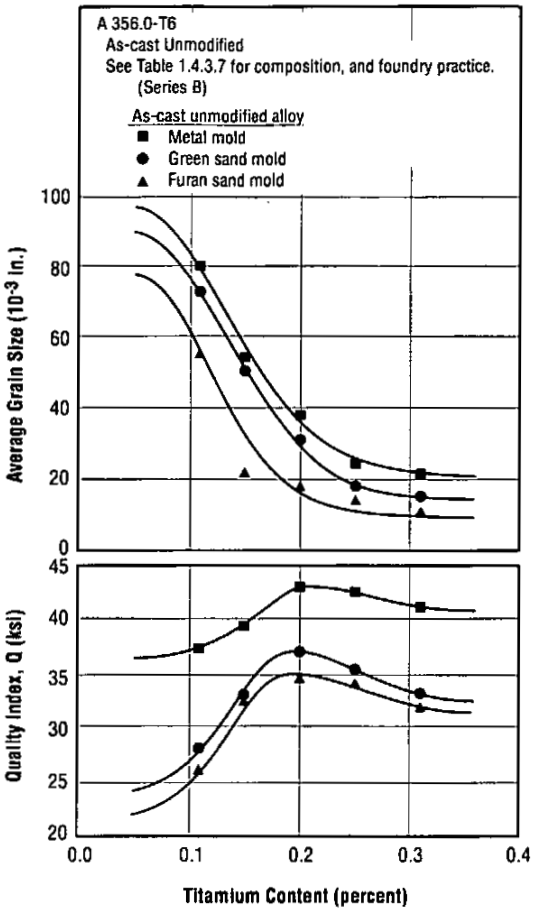


Figure 1.4.3.8 Effect of titanium content on the grain sizes and quality indicies of castings in three types of molds (Ref. 33)

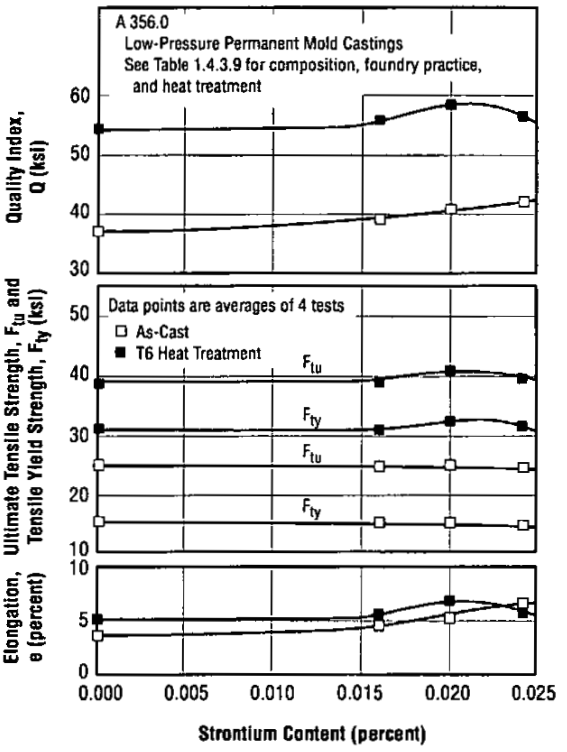


Figure 1.4.3.10 Effect of strontium content on the tensile properties of low-pressure permanent mold castings (Ref. 34)

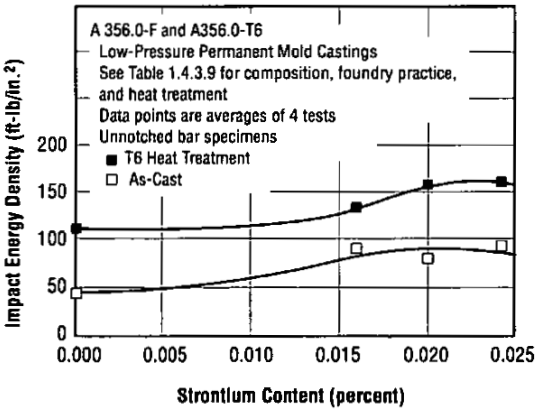


Figure 1.4.3.11 Effect of strontium content on impact energy absorbed by unnotched bars from low-pressure permanent mold castings (Ref. 34)

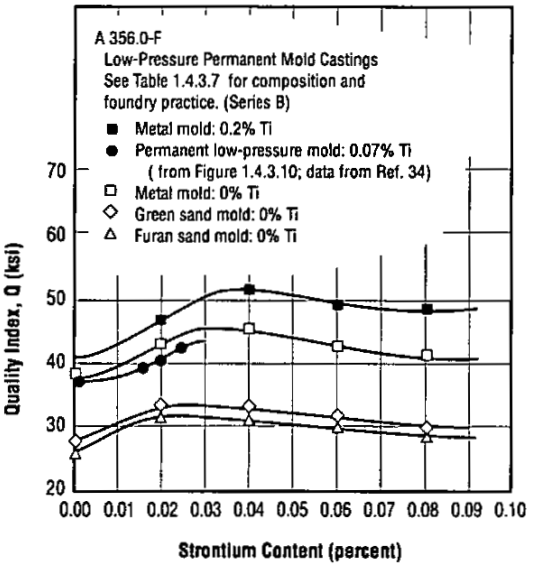


Figure 1.4.3.12 Effect of strontium content on the quality indices of alloy as-cast in metal and sand molds (Ref. 33)

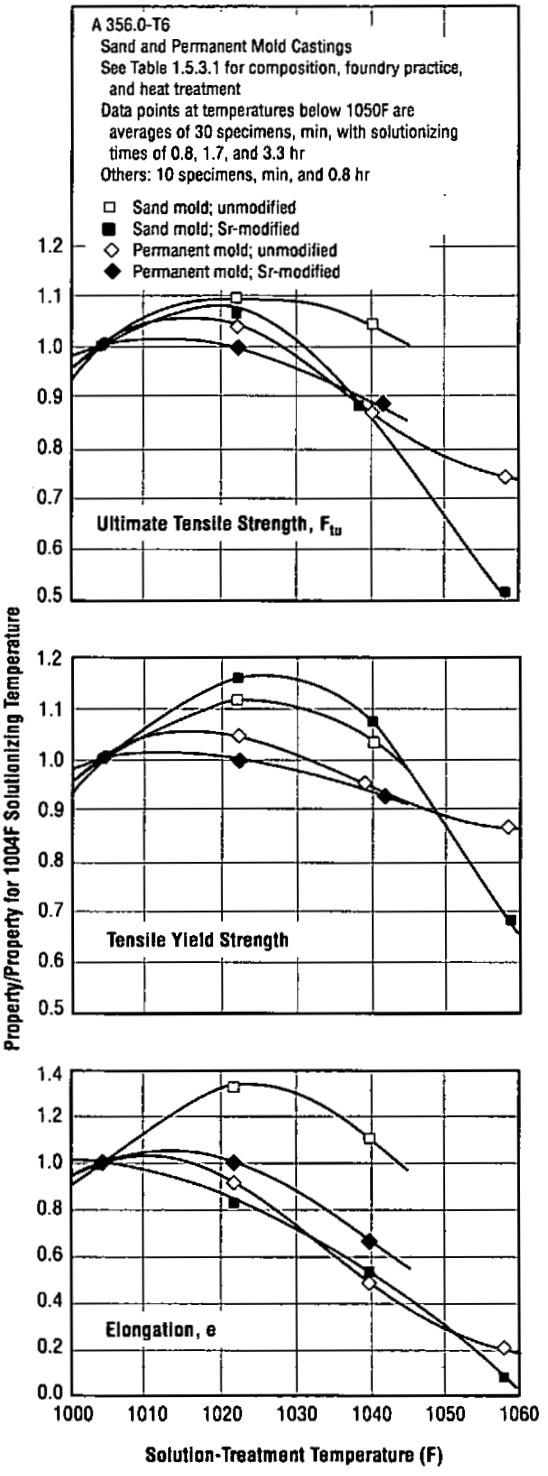


Figure 1.5.3.2 Effect of solution-treatment temperature on relative tensile properties of sand and permanent mold castings (Ref. 36)

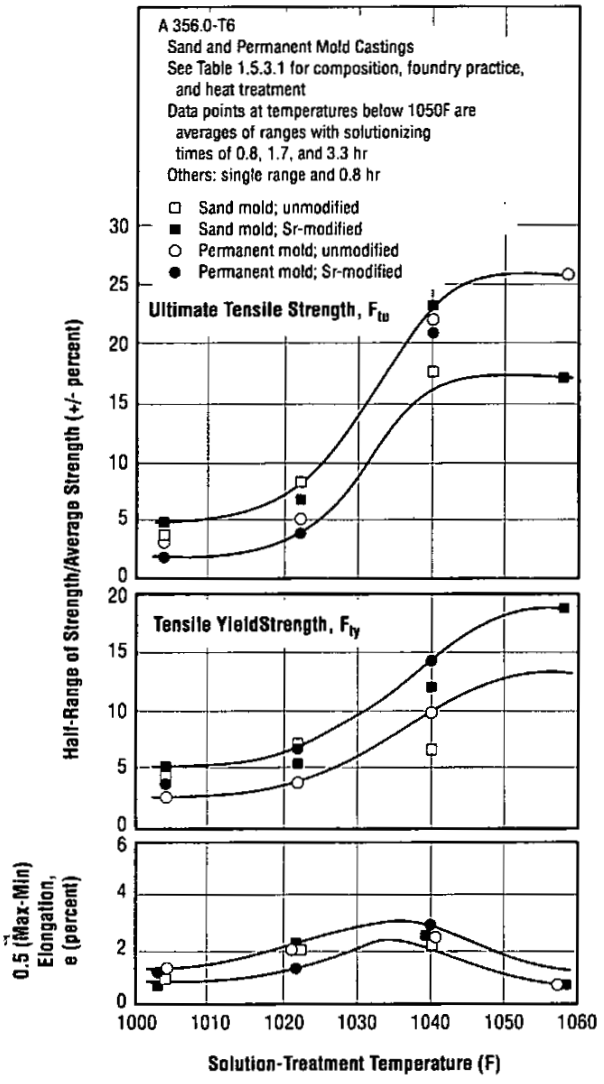


Figure 1.5.3.3 Effect of solution-treatment temperature on variability of tensile properties of sand and permanent mold castings (Ref. 36)

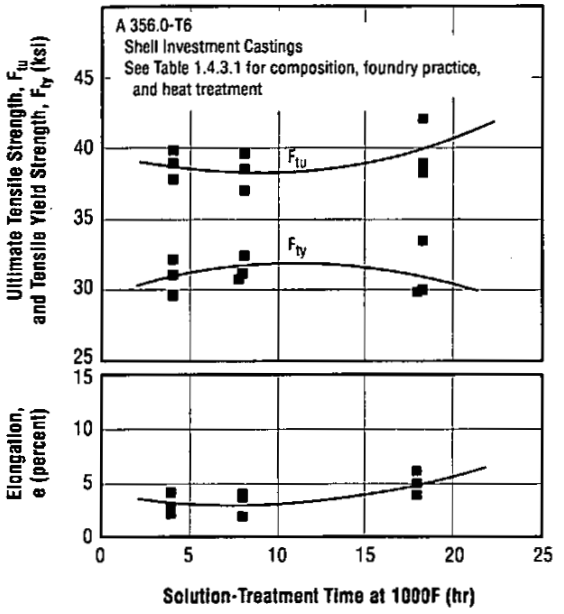


Figure 1.5.3.4 Effect of solution-treatment time on tensile properties of shell investment castings (Ref. 32)

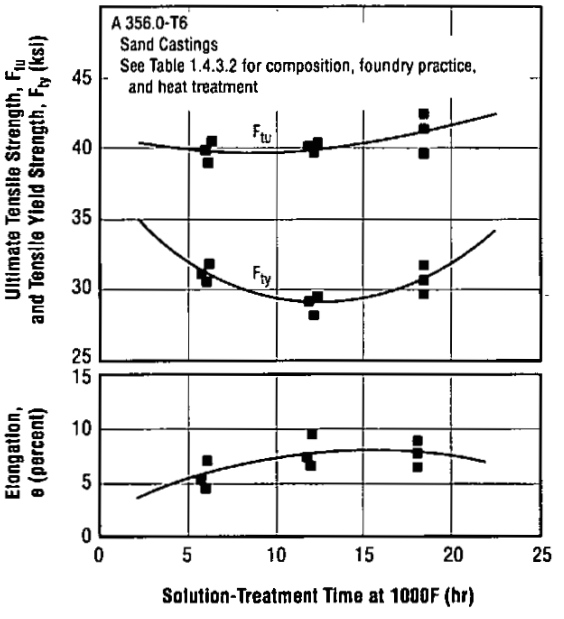


Figure 1.5.3.5 Effect of solution-treatment time on tensile properties of sand castings (Ref. 32)

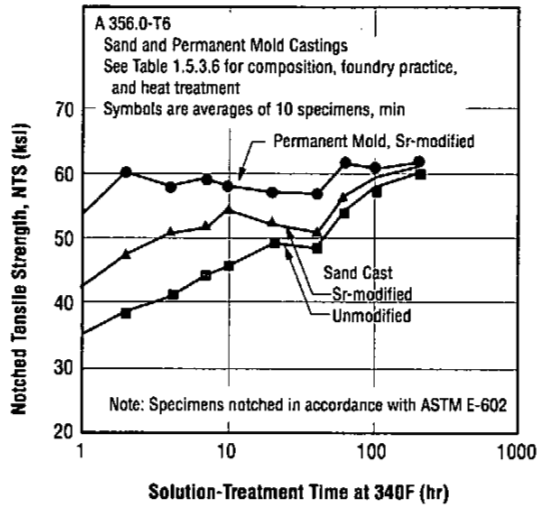


Figure 1.5.3.7 Effect of solution-treatment time on notched tensile strength of sand and permanent mold castings (Ref. 37)

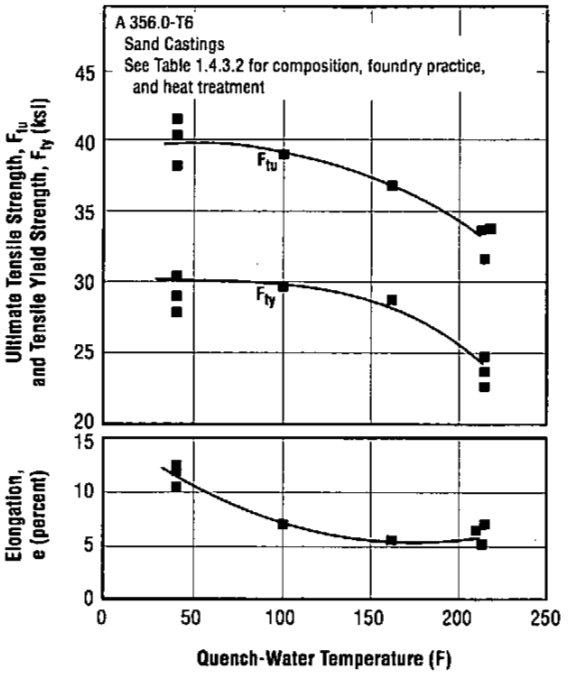


Figure 1.5.4.2 Effect of quench-water temperature on tensile properties of sand castings (Ref. 32)

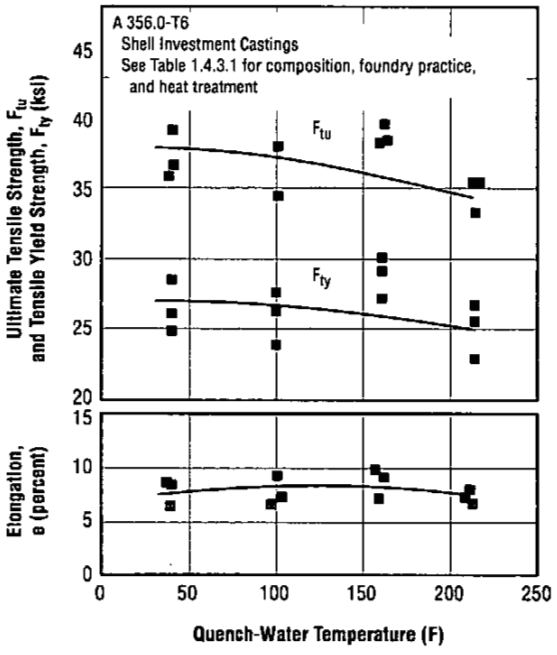


Figure 1.5.4.1 Effect of quench-water temperature on tensile properties of shell investment castings (Ref. 32)

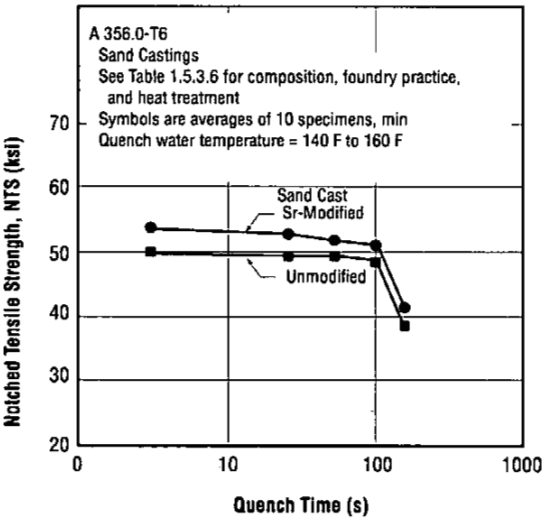


Figure 1.5.4.3 Effect of quench time on notched tensile strength of sand castings (Ref. 37)

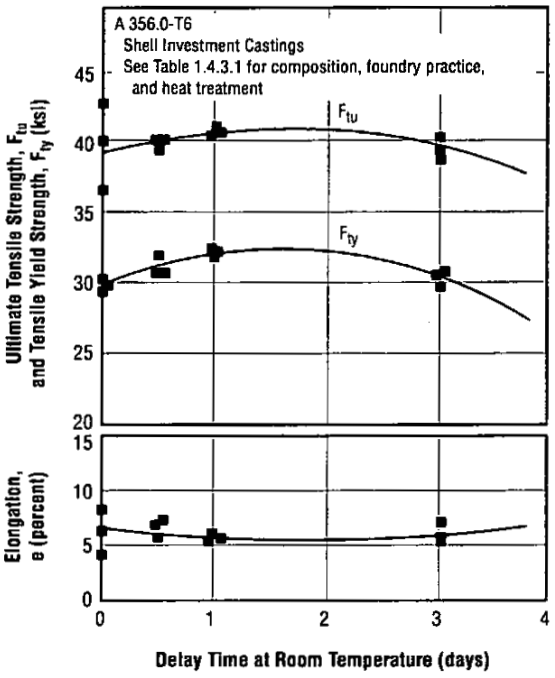


Figure 1.5.5.1 Effect of delay time between quench and the start of artificial aging on tensile properties of shell investment castings (Ref. 32)

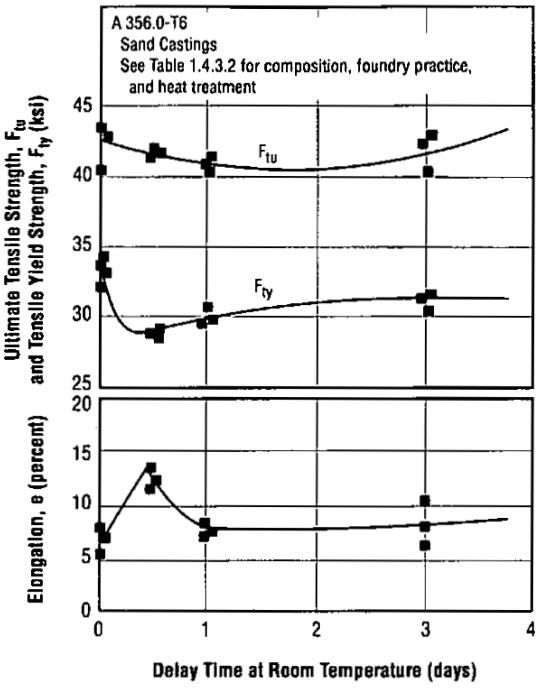


Figure 1.5.5.2 Effect of delay time between quench and the start of artificial aging on tensile properties of sand castings (Ref. 32)

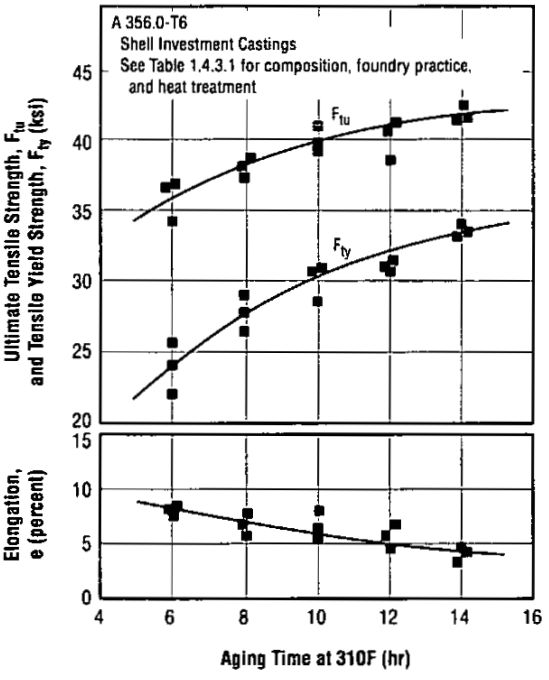


Figure 1.5.6.1 Effect of artificial aging time at 310 F on tensile properties of shell investment castings (Ref. 32)

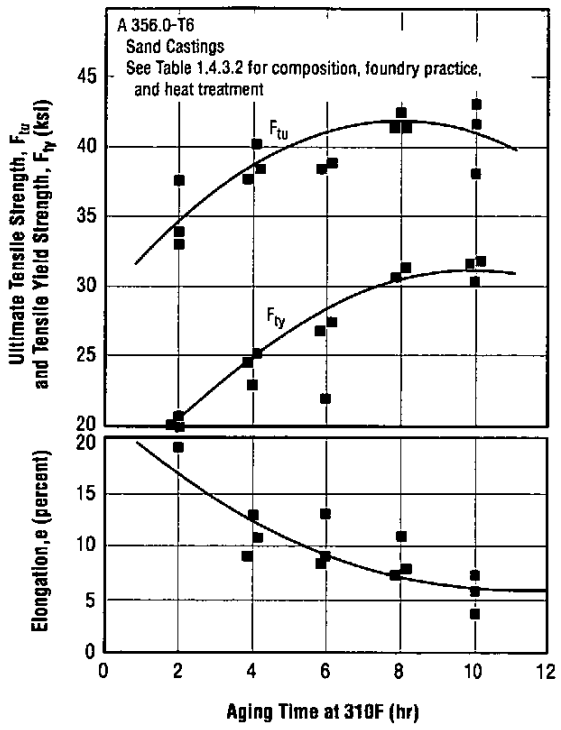


Figure 1.5.6.2 Effect of artificial aging time at 310 F on tensile properties of sand castings (Ref. 32)

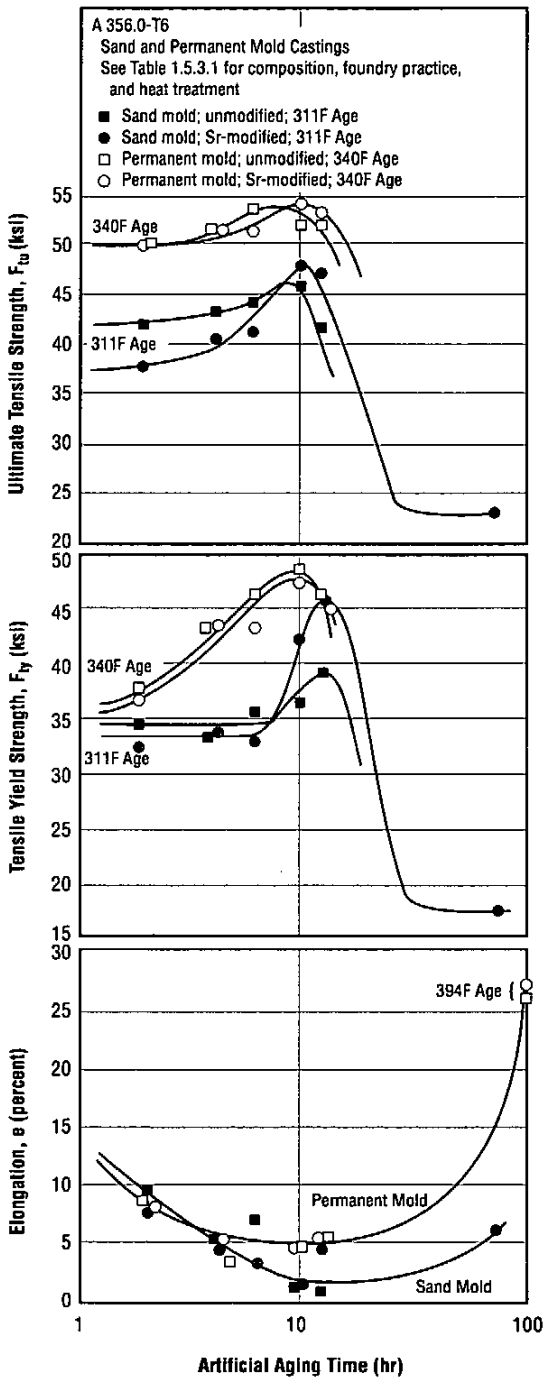


Figure 1.5.6.3 Effect of longer artificial aging times at 311 F and 340 F on tensile properties of sand and permanent mold castings (Ref. 35)

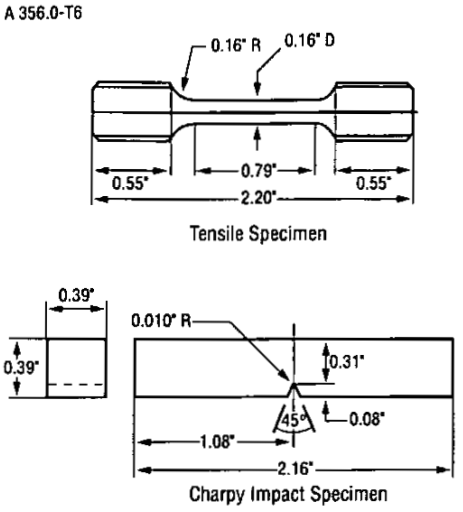


Figure 1.5.6.5 Configurations of tensile and Charpy impact specimens (Ref. 38)

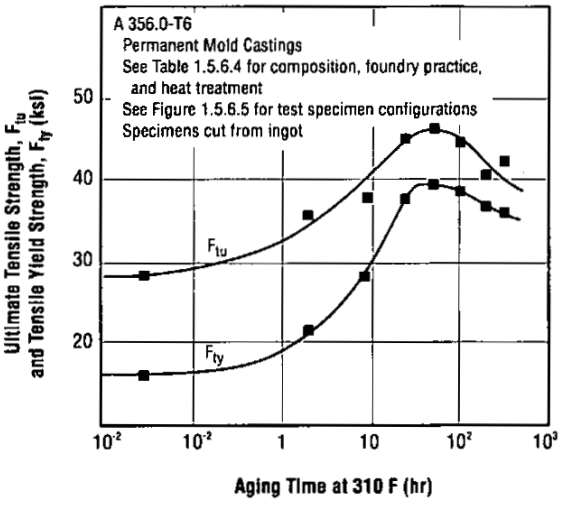


Figure 1.5.6.6 Effect of longer aging times at 310 F on tensile properties of permanent mold castings (Ref. 38)

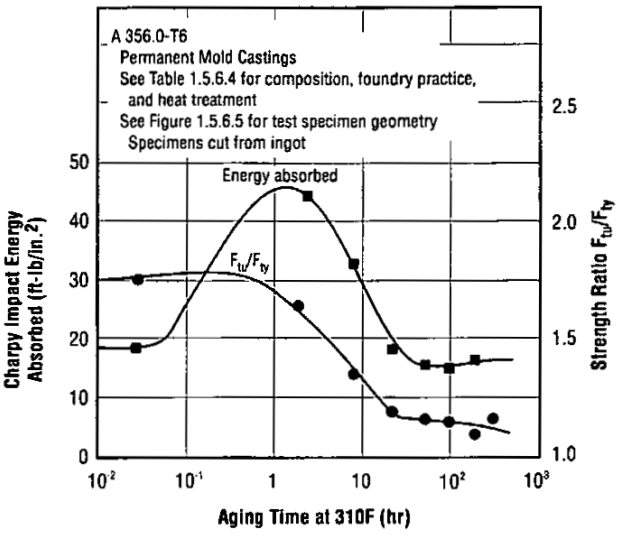


Figure 1.5.6.7 Effect of longer aging times at 310 F on Charpy impact energy absorbed and the ultimate-to-yield tensile strength ratio of permanent-mold castings (Ref. 38)

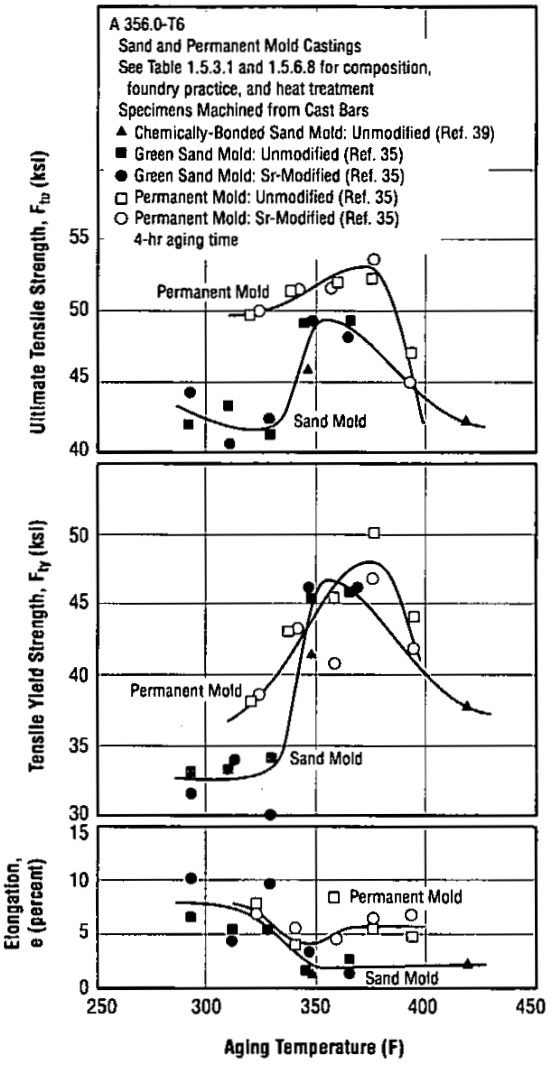


Figure 1.5.6.9 Effect of aging temperature on tensile properties of sand and permanent-mold castings (Refs. 35, 39)

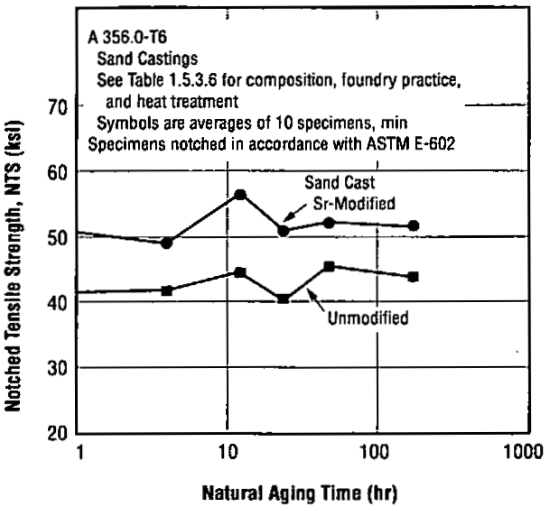


Figure 1.5.6.10 Effect of natural aging time on notched tensile strength of sand castings (Ref. 37)

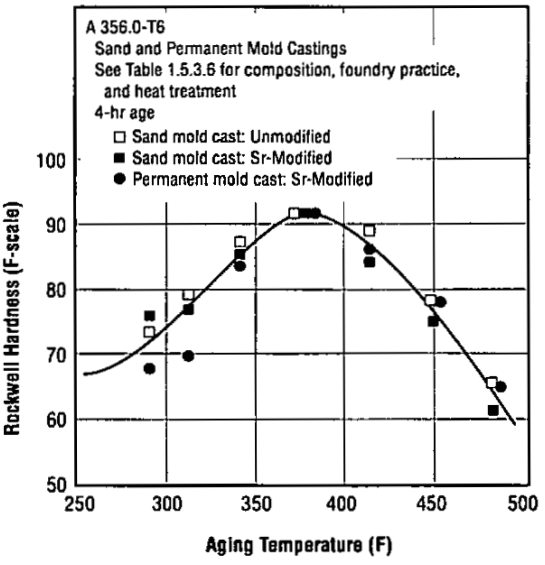


Figure 1.6.3.1 Effect of artificial aging temperature on hardness of sand and permanent mold castings (Ref. 40)

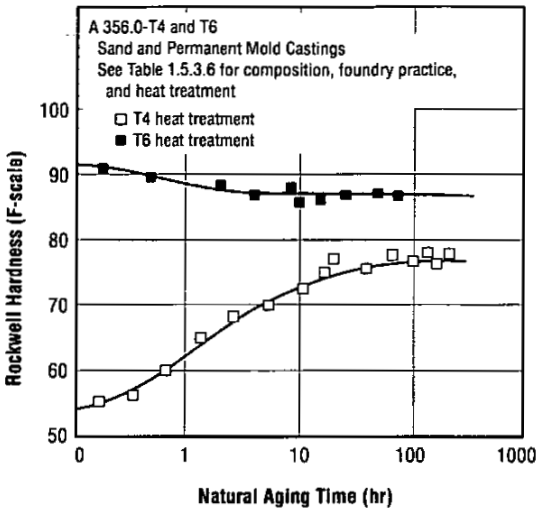


Figure 1.6.3.2 Effect of natural aging time on hardness of sand and permanent mold castings (Ref. 35)

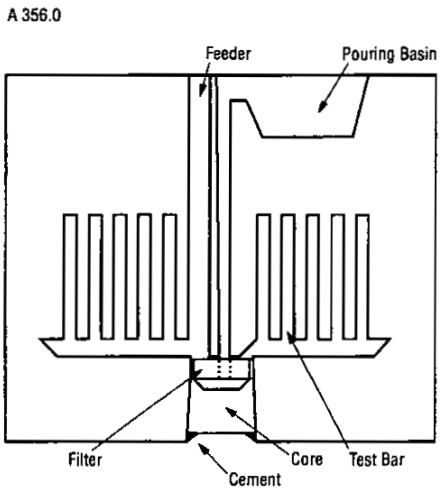


Figure 1.8.2.1 Schematic elevation view showing a typical installation of a ceramic filter in a mold (Ref. 39)

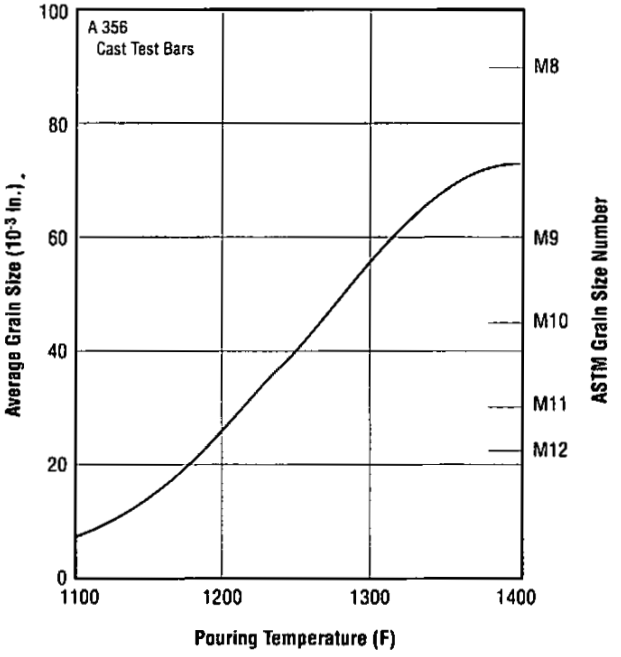


Figure 1.8.1.4 Effect of pouring temperature on grain size of 356 castings (Ref. 18)

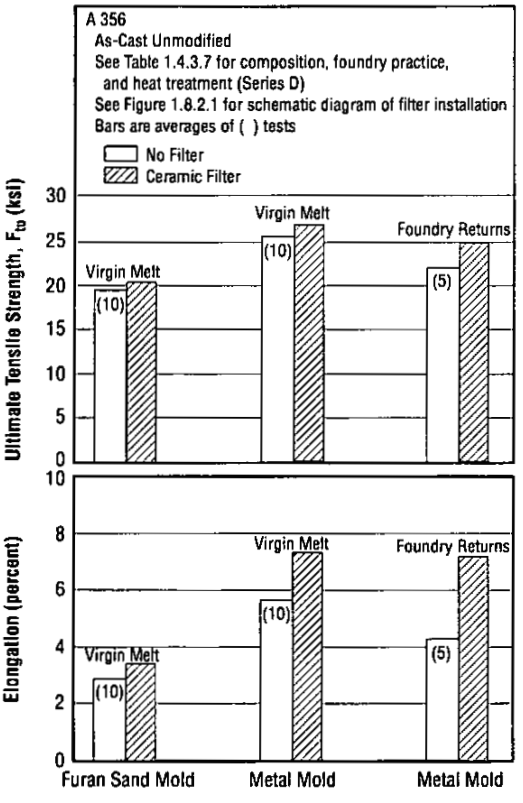


Figure 1.8.2.2 Effect of filtering on tensile properties of sand and metal mold castings (Ref. 33)

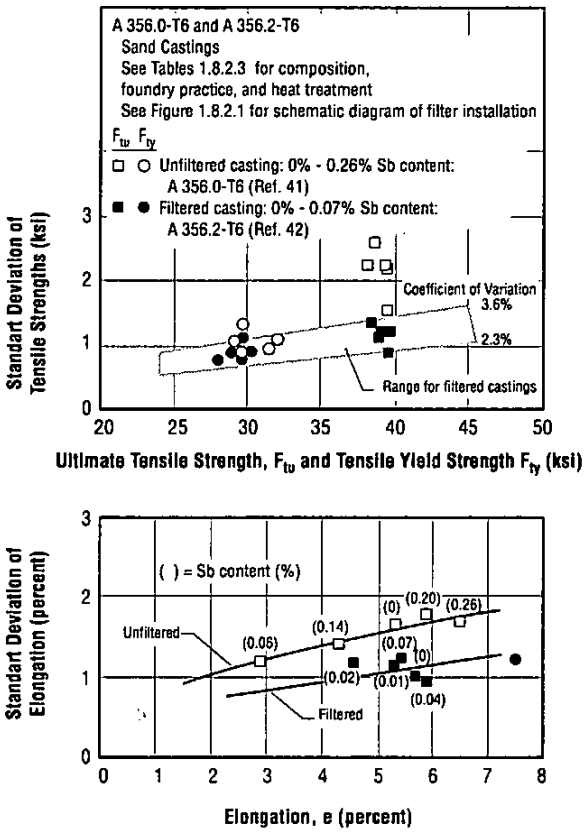


Figure 1.8.2.4 Effect of variability of tensile properties of sand mold castings (Refs. 41, 42) Note: Tensile testing conducted in accordance with ASTM B-557-84 procedures.

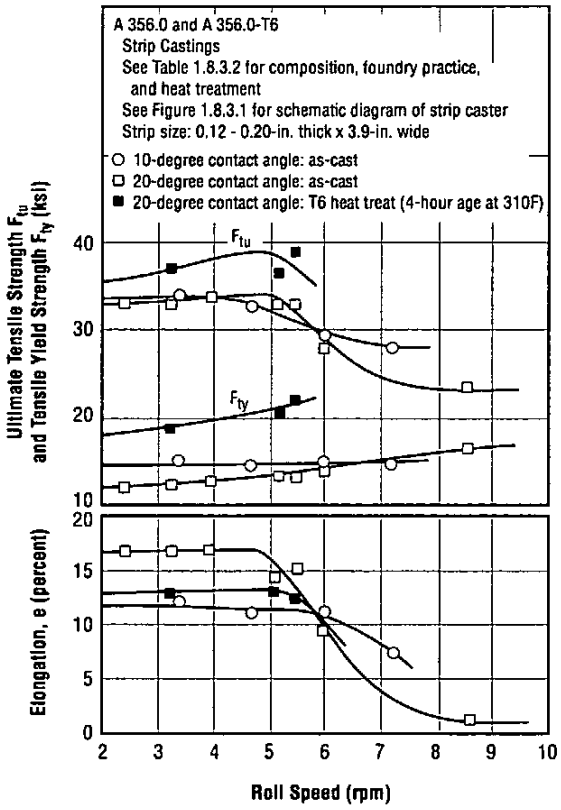


Figure 1.8.3.3 Effect of roll speed and contact angle on tensile properties of strip castings (Ref. 43)

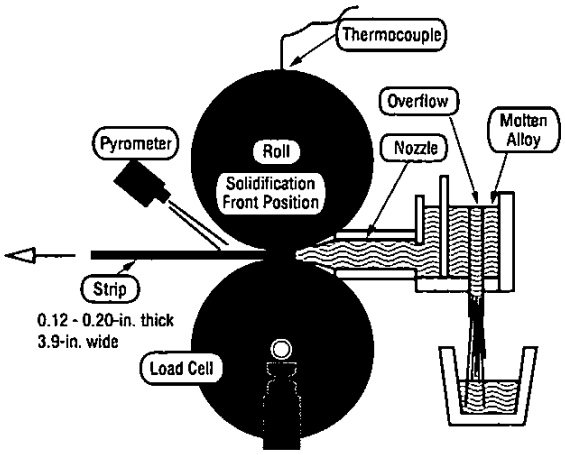


Figure 1.8.3.1 Schematic confguration of horizontal twin-roll strip caster (Ref. 43)

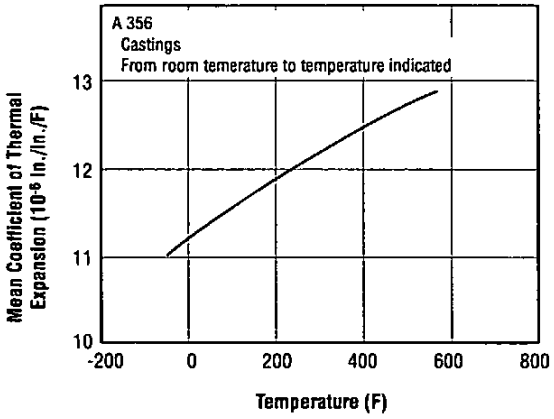


Figure 2.1.4 Mean coefficient of thermal expansion of 356 castings (Ref. 8)

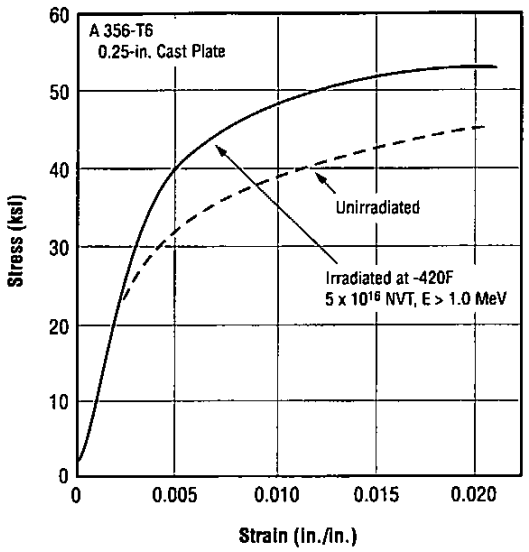


Figure 2.4.3 Typical effect of nuclear radiation at -420F on room-temperature stress-strain curves of cast plates (Ref. 21)

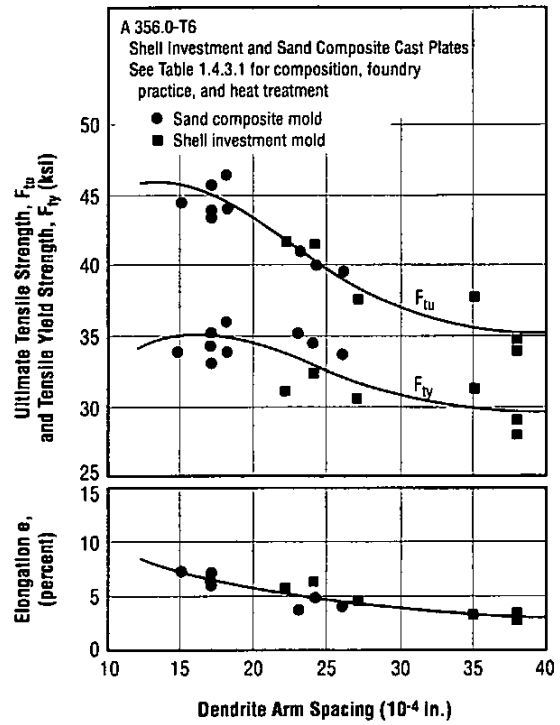


Figure 3.2.1.4 Effect of dendrite arm spacing on tensile properties of shell investment and sand castings (Ref. 32)

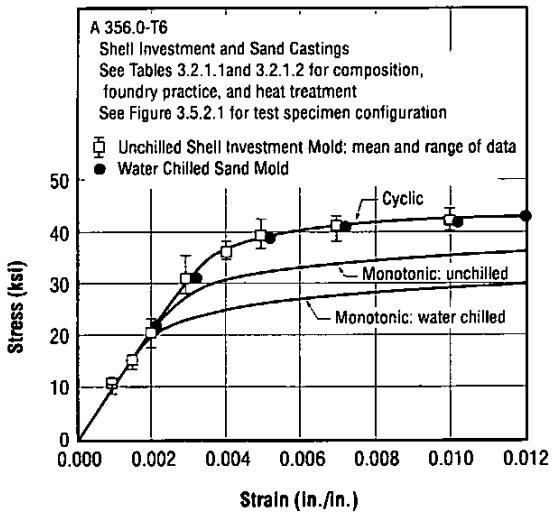
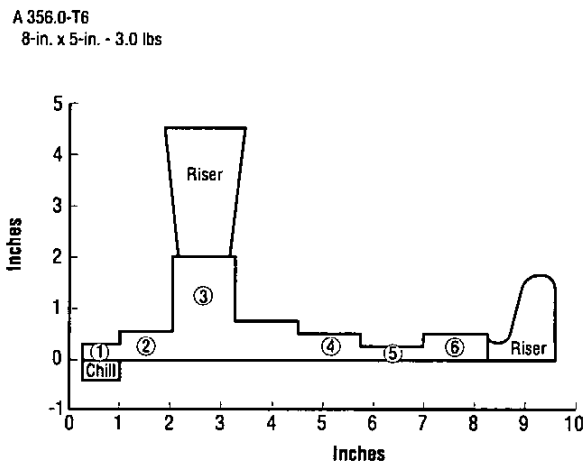


Figure 3.2.1.3 Monotonic and cyclic tensile stress-strain curves for shell investment and sand castings (Refs. 44, 45)



Location	Section Thickness (in.)	Description
1	1/4	Chilled Area
2	1/2	Adjacent to Chilled Area
3	2	Gate and Riser Area
4	1/2	Typical Section
5	1/4	Typical Section
6	1/2	Gate and Riser Area
—	0.505	Separately Cast Bar

Figure 3.2.1.6 Configuration of the Aluminum Association sand-test cast plates (Ref. 52)

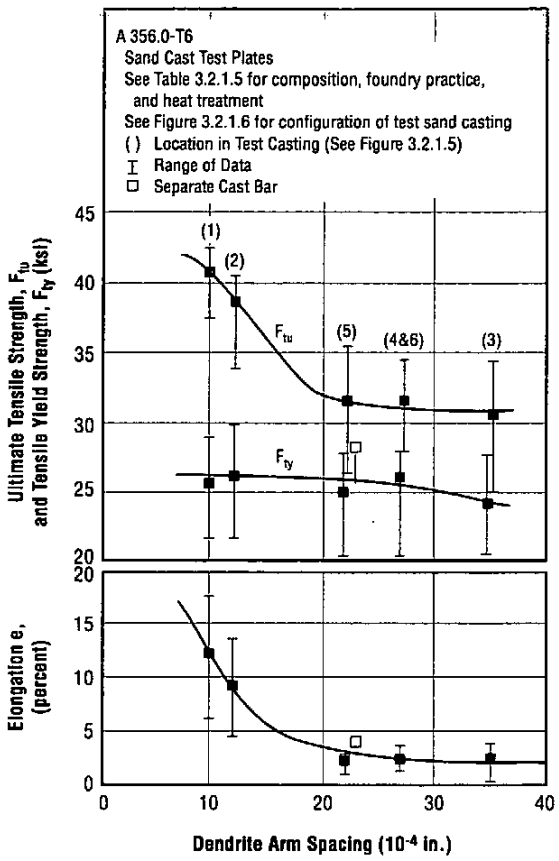


Figure 3.2.1.7 Effect of dendrite arm spacing on tensile properties of sand cast test plates from at least six commercial foundries (Ref. 52)

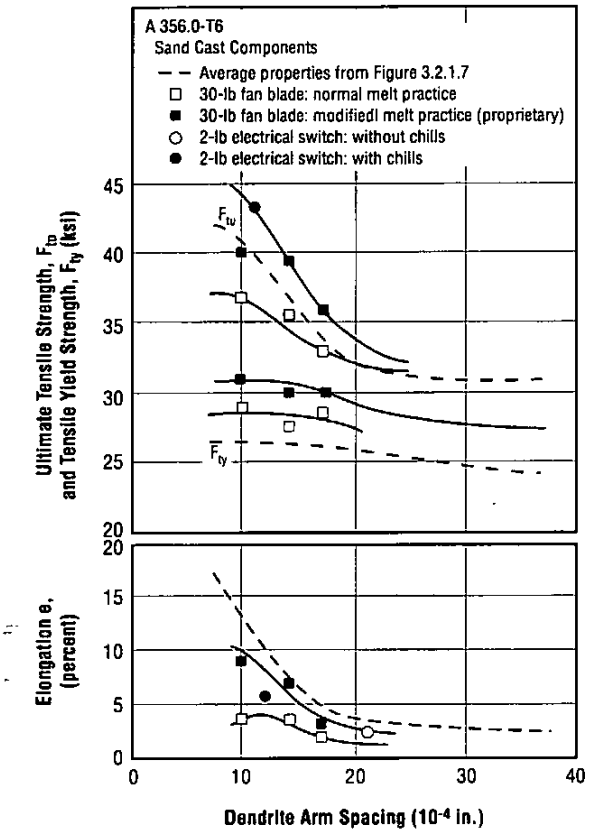


Figure 3.2.1.8 Effect of dendrite arm spacing on tensile properties of sand cast components from a commercial foundry following normal and modified melt processes (Ref. 54)

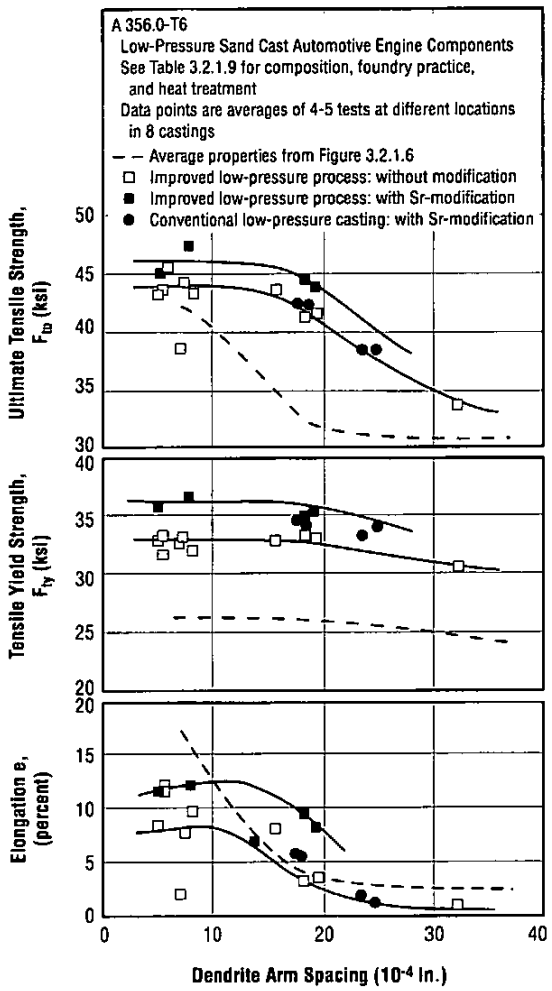
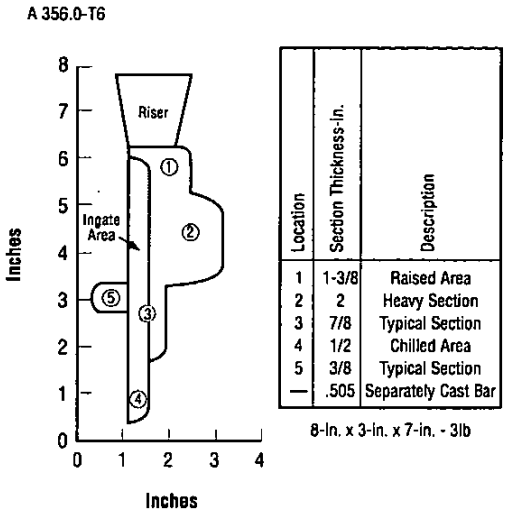


Figure 3.2.1.10 Effect of dendrite arm spacing on tensile properties of automotive engine component sand castings from a commercial foundry following conventional and improved low-pressure processes (Ref. 55)



Location	Section Thickness-in.	Description
1	1-3/8	Raised Area
2	2	Heavy Section
3	7/8	Typical Section
4	1/2	Chilled Area
5	3/8	Typical Section
—	.505	Separately Cast Bar

Figure 3.2.1.12 Configuration of the Aluminum Association permanent-mold cast plates (Ref. 53)

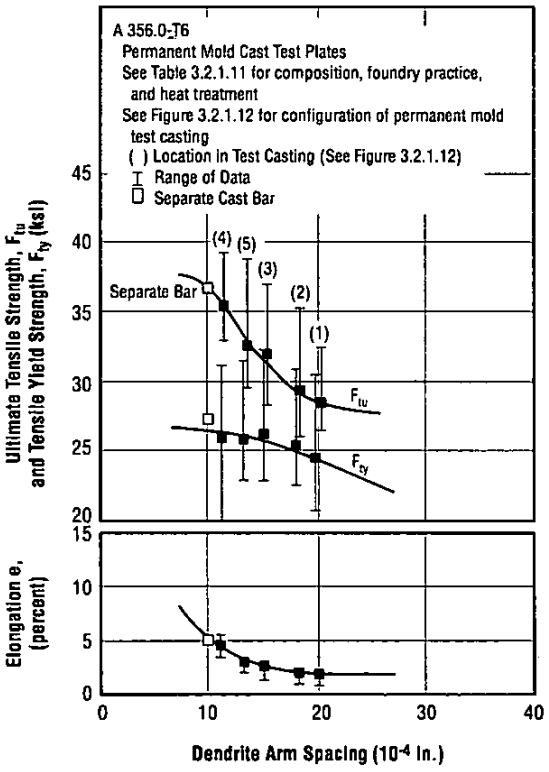


Figure 3.2.1.13 Effect of dendrite arm spacing on tensile properties of permanent-mold cast test plates from seven commercial foundries (Ref. 53)

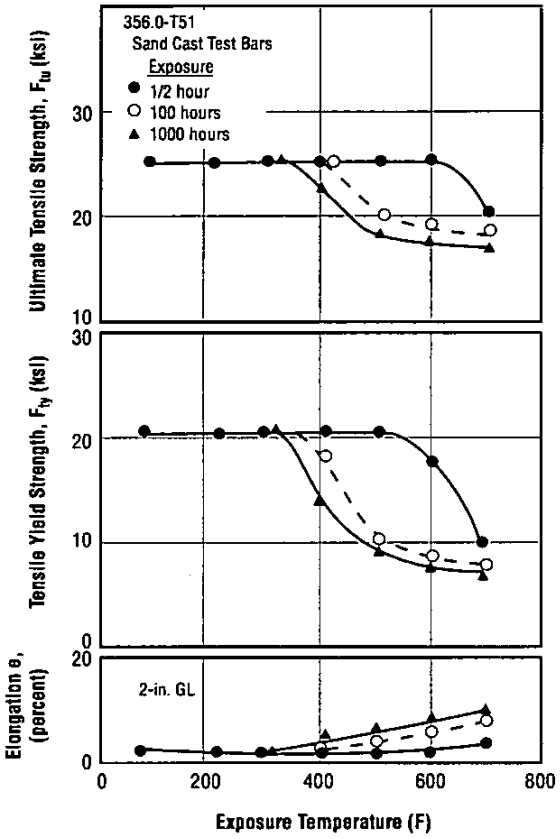


Figure 3.2.1.14 Effect of exposure to elevated temperature on room temperature tensile properties of sand-cast test bars in T51 condition (Ref. 10)

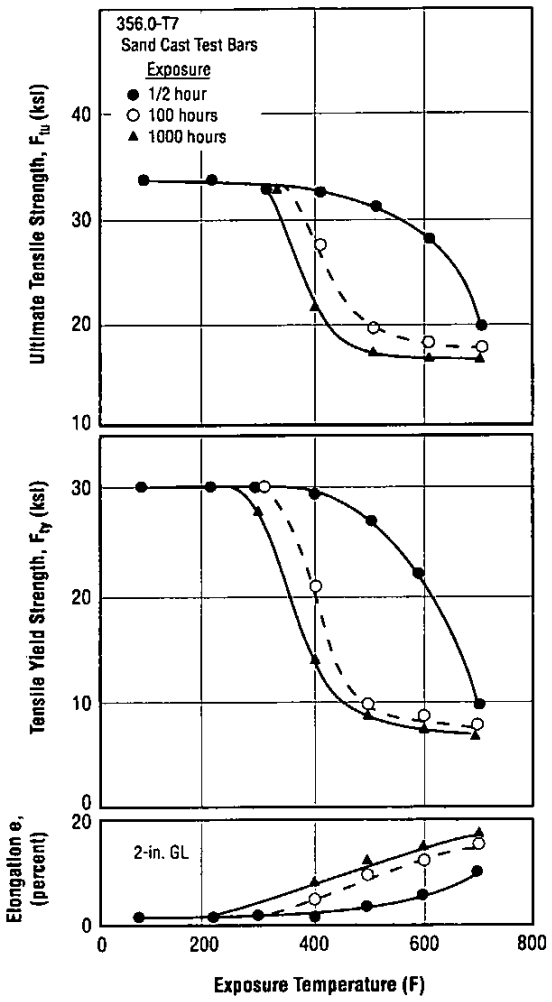


Figure 3.2.1.15 Effect of exposure to elevated temperature on room temperature tensile properties of sand cast test bars in T7 condition (Ref. 9)

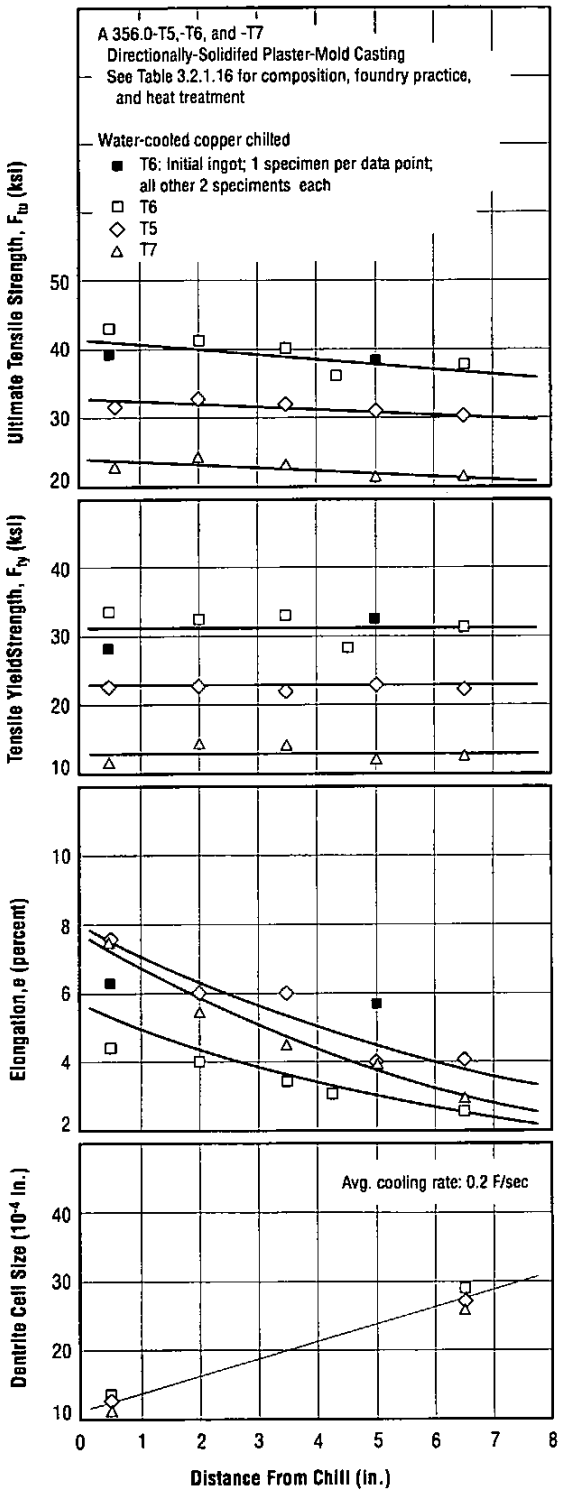
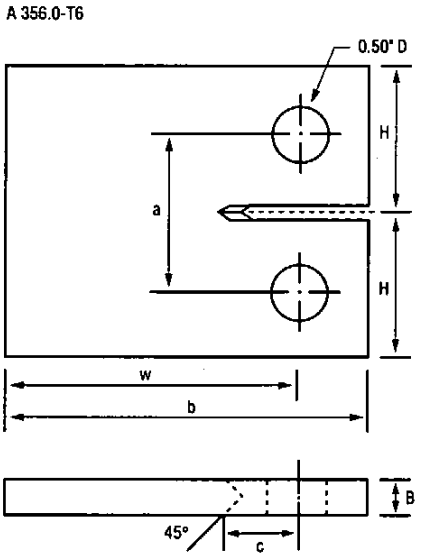


Figure 3.2.1.17 Effect of cooling rate and heat treatment on tensile properties of specimens cut from directionally-solidified water-chilled ingots (Ref 64).



Specimen Type	Casting	B	H	W	a	b	c
Fracture toughness	W	0.36	1.68	2.80	–	3.50	0.78
		0.75	1.68	2.80	–	3.50	0.78
	X, Y, Z	0.36	1.37	2.29	–	2.94	0.75
		0.80	1.32	2.20	–	2.76	0.99
Crack propagation	W	0.36	1.68	2.80	–	3.50	0.78
	X, Y, Z	0.36	1.37	2.80	1.54	3.50	0.78

Figure 3.2.7.2.1 Configurations of compact tensile (CT) specimens for fracture toughness and crack propagation tests (Refs. 45, 50)

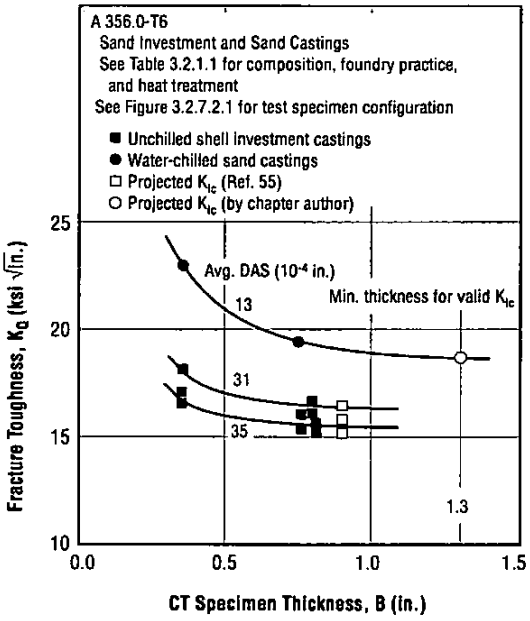


Figure 3.2.7.2.2 Effect of thickness on fracture toughness of compact tensile (CT) specimens from unchilled shell investment and water-chilled sand castings (Refs. 45, 50)

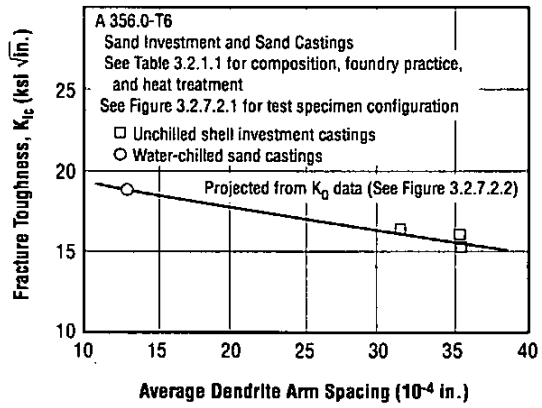


Figure 3.2.7.2.3 Effect of dendrite arm spacing on plane-strain fracture toughness projected from K_Q test data for unchilled shell investment and water-chilled sand castings

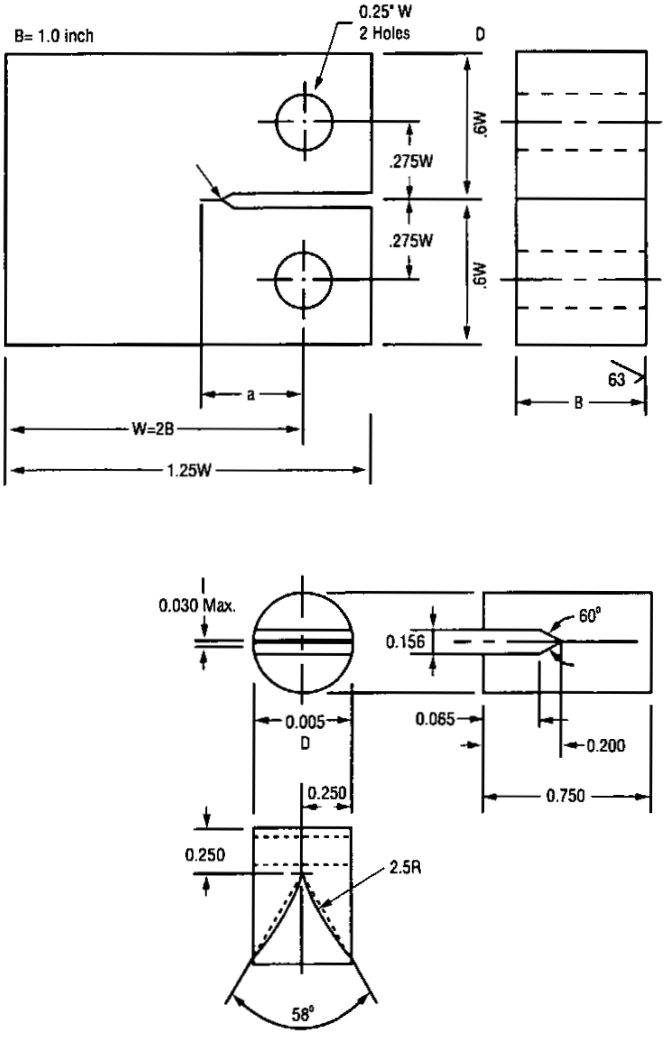


Figure 3.2.7.2.4 Configurations of compact tensile (CT) and short rod (SR) specimens for fracture toughness tests (Refs. 64)

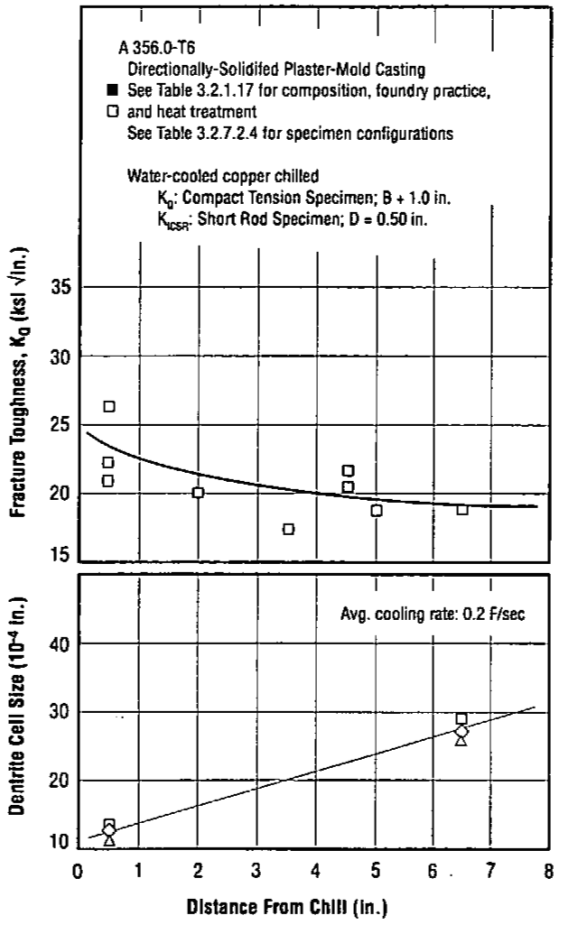


Figure 3.2.7.2.5 Effect of cooling rate on fracture toughness of specimens cut from directionally-solidified water-chilled ingots (Ref 64).

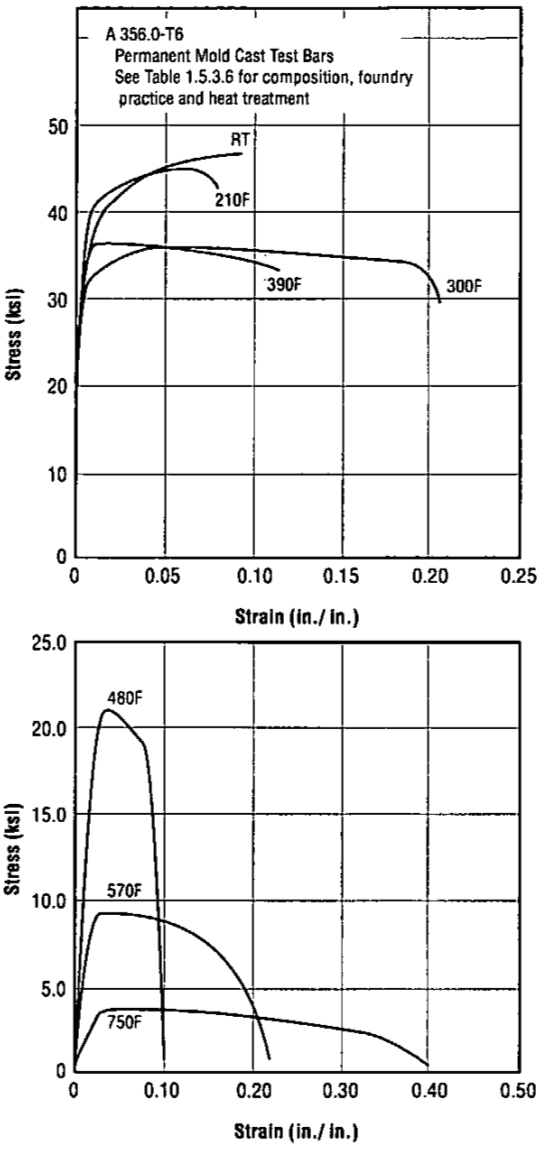


Figure 3.3.1.1 Monotonic stress-strain curves for permanent-mold cast test bars at various temperatures after an exposure time of one hour (Ref. 40)

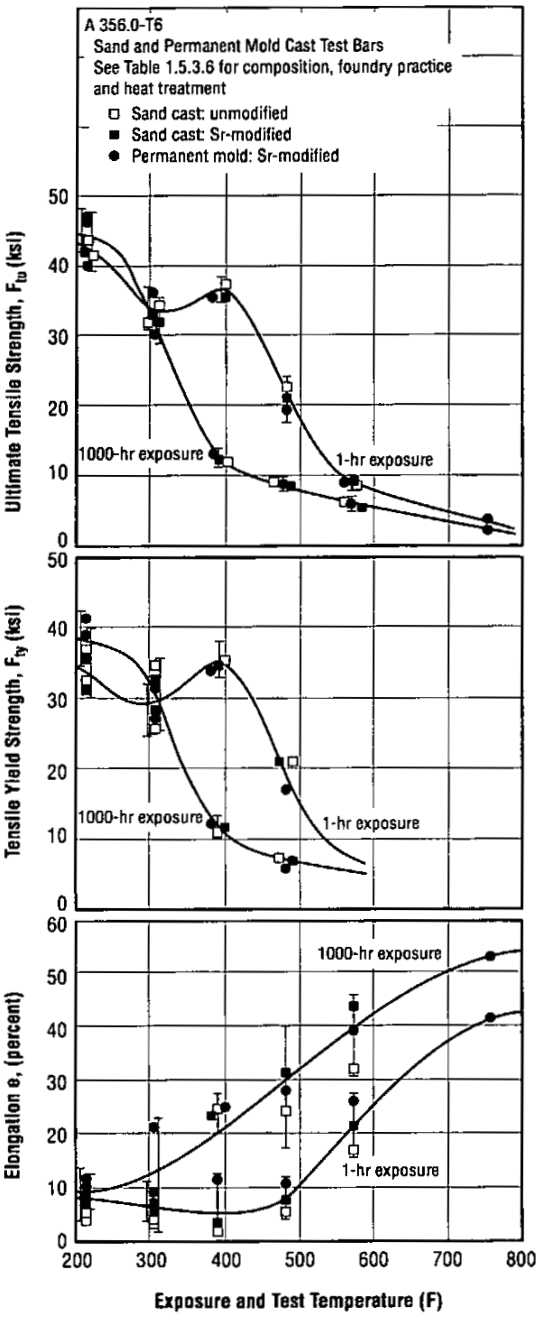
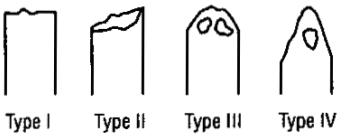


Figure 3.3.1.2 Effect of elevated temperature exposure on the tensile properties of sand and permanent-mold cast test bars (Ref. 40)

A 356.0-T6
Sand and Permanent Mold Cast Test Bars
See Table 1.5.3.6 for composition, foundry practice and heat treatment



Tempreature (F)	1 hr. Exposure			1000 hr. Exposure		
	SCU	SCM	PM	SCU	SCM	PM
210	I	I	I	I	I	I
300	I	I	I	I	I	II
390	I	I	II	II	II	II
480	II	II	III	II	II	III
570	II	II	IV	III	III	IV
750			IV			IV

SCU= sand cast, unmodified; SCM= sand cast, modified; PM= permanent mold.

Figure 3.3.1.3 Classification of fracture appearance of tensile test specimens from sand and permanent-mold cast test bars after exposure and testing at elevated temperature (Ref. 40)

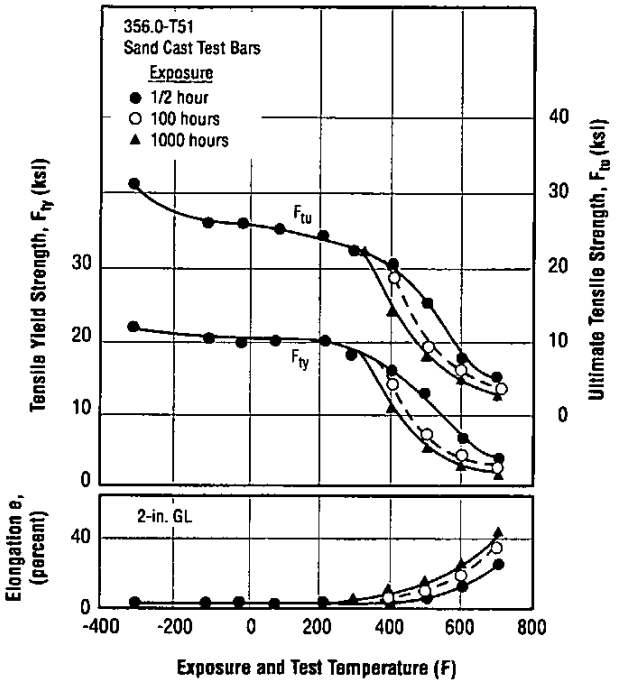


Figure 3.3.1.4 Effect of exposure and testing at elevated temperature on tensile properties of sand cast test bars in T51 condition (Ref. 10)

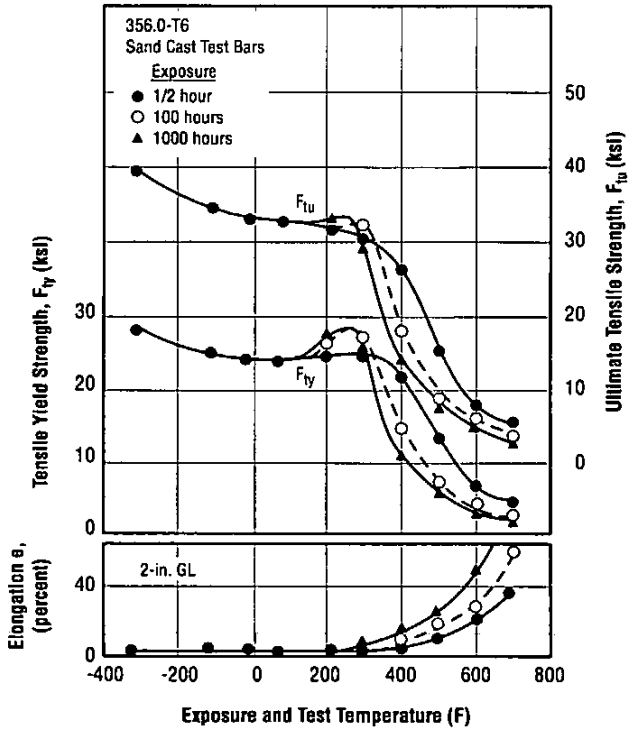


Figure 3.3.1.5 Effect of exposure and testing at elevated temperature on tensile properties of sand cast test bars in T6 condition (Ref. 13)

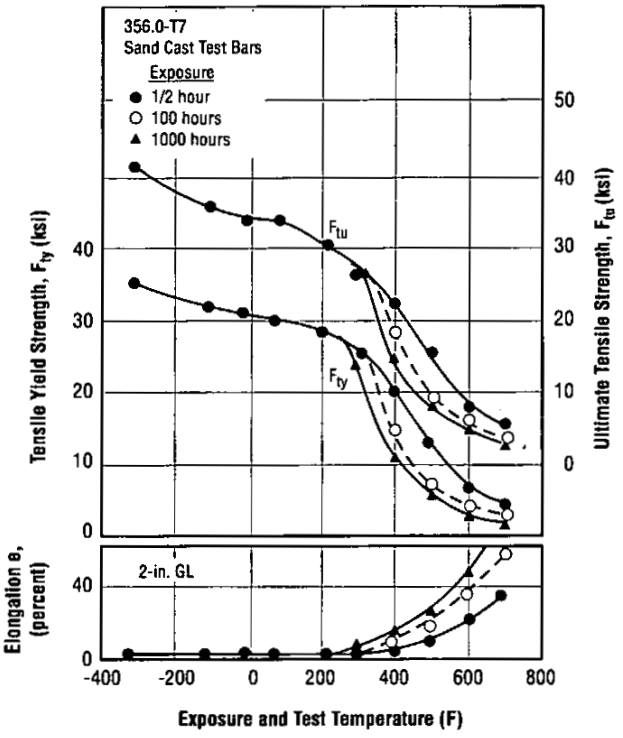


Figure 3.3.1.6 Effect of exposure and testing at elevated temperature on tensile properties of sand cast test bars in T7 condition (Ref. 9)

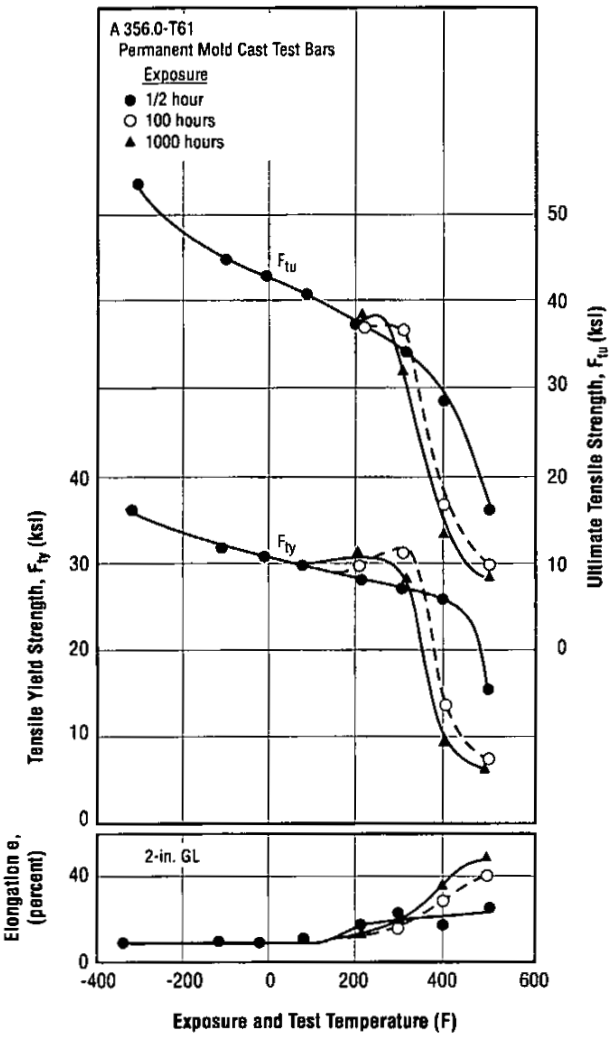


Figure 3.3.1.7 Effect of exposure and testing at elevated temperature on tensile properties of permanent-mold cast test bars in T61 condition (Ref. 12)

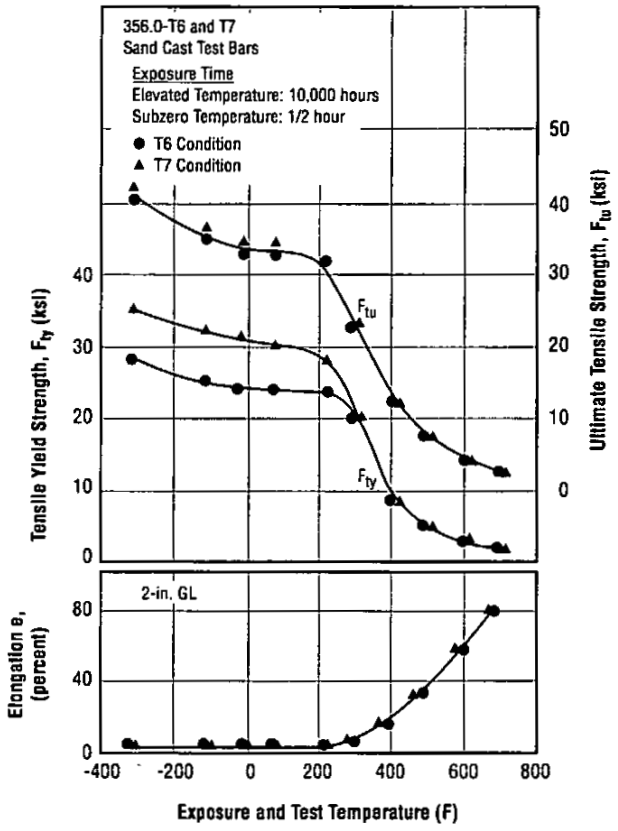


Figure 3.3.1.8 Effect of exposure and test temperature on tensile properties of sand cast test bars in T6 and T7 condition (Ref. 20)

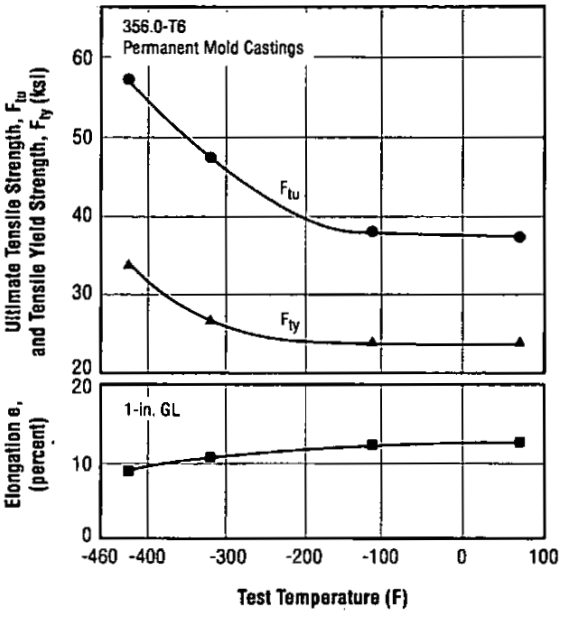


Figure 3.3.1.9 Effect of low test temperature on tensile properties of permanent mold castings in T6 condition (Ref. 17)

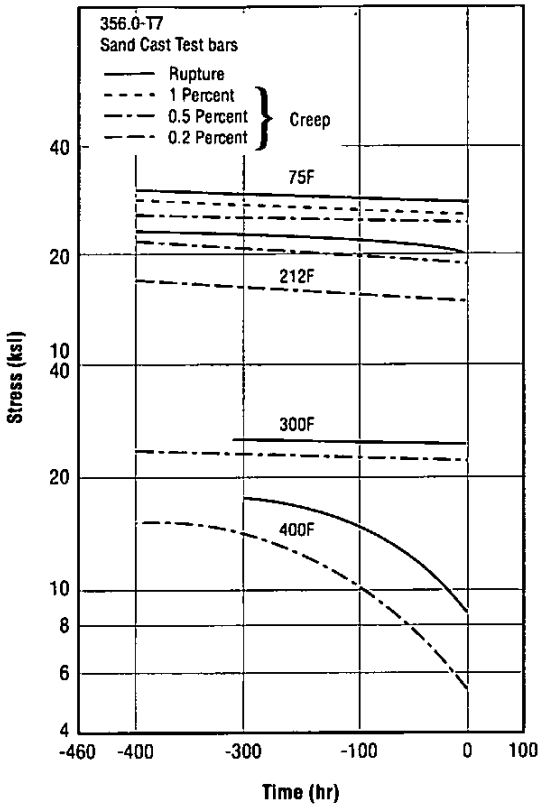
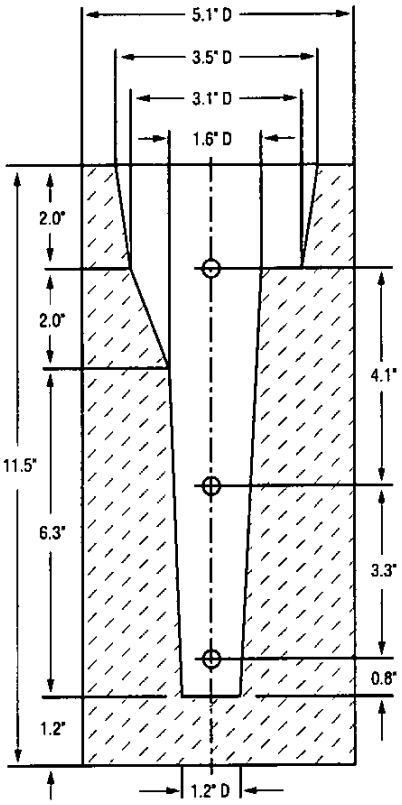


Figure 3.4.1 Creep and creep-rupture curves from room temperature to 400F for sand cast test bars in T7 condition (Ref. 9)



All dimensions in inches

Figure 3.5.1.2 Configuration of CO_2 sand mold for casting cantilever specimens tested in rotating bending fatigue in Ono- and Krause-type machines (Ref. 56)

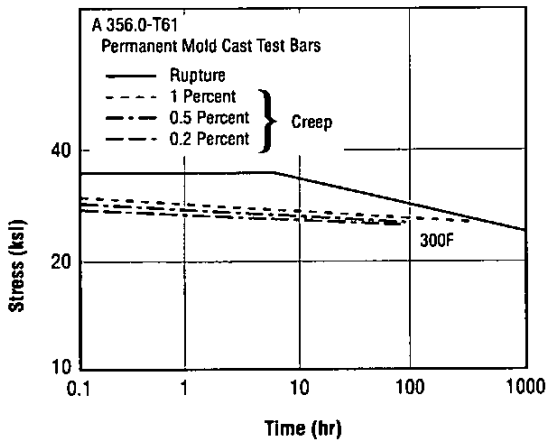


Figure 3.4.2 Creep and creep-rupture curves at 300F for permanent mold cast test bars in T61 condition (Ref. 12)

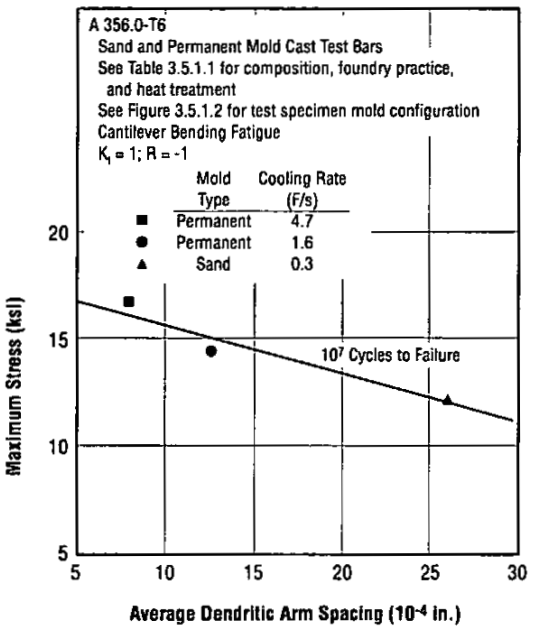


Figure 3.5.1.3 Effect of dendrite arm spacing on high-cycle fatigue strength at 10^7 cycles to failure (Ref. 56)

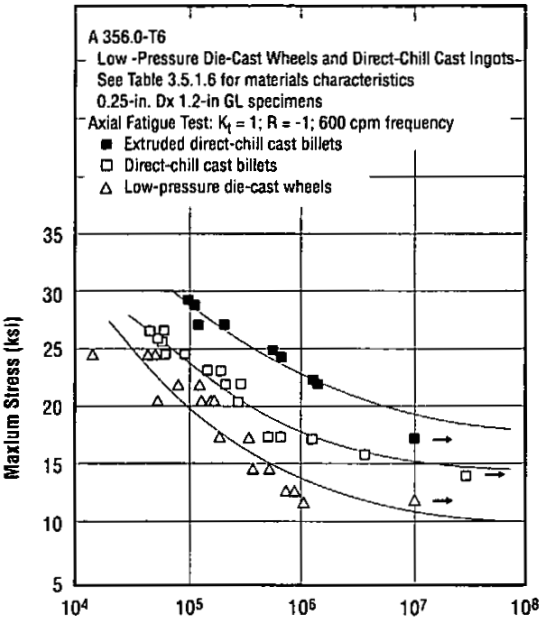


Figure 3.5.1.7 Effect of casting method on stress-fatigue life curves for smooth specimens from die-cast wheels and from direct-chill cast billets, with and without extrusions (Ref. 62)

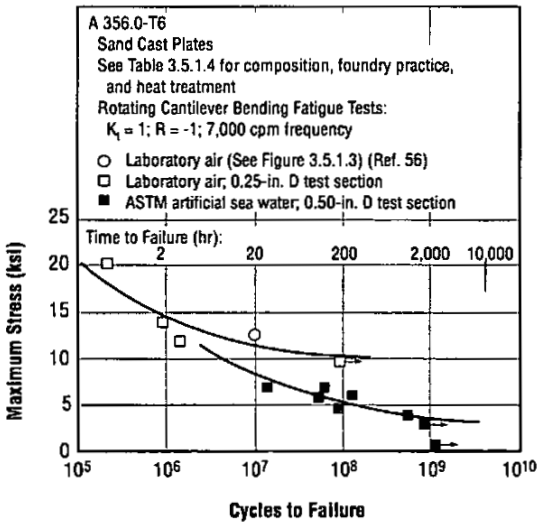


Figure 3.5.1.5 Effect of exposure to ASTM artificial sea water on S-N curves for smooth specimens from sand cast plates (Ref. 57)

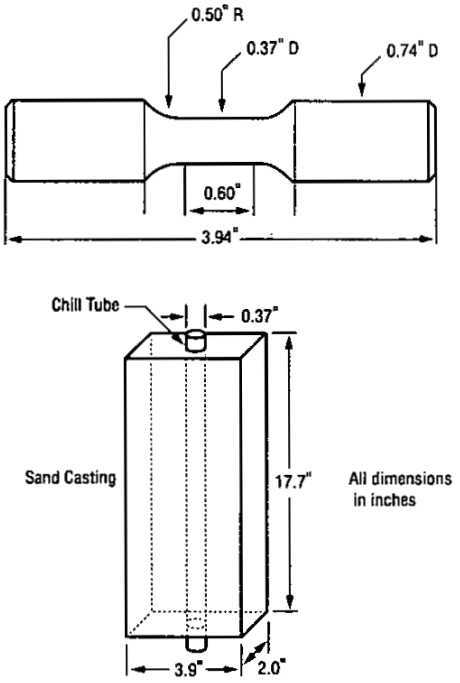


Figure 3.5.2.1 Configurations of specimens for tensile and axial-fatigue tests and configuration of water-chilled sand castings (Refs. 44, 45)

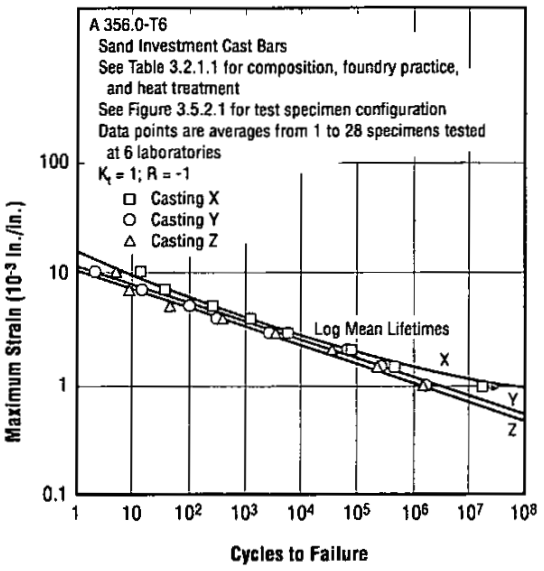


Figure 3.5.2.2 Strain-fatigue life curves for smooth axial fatigue specimens from three castings poured at different mold temperatures (Refs. 44, 46, 47)

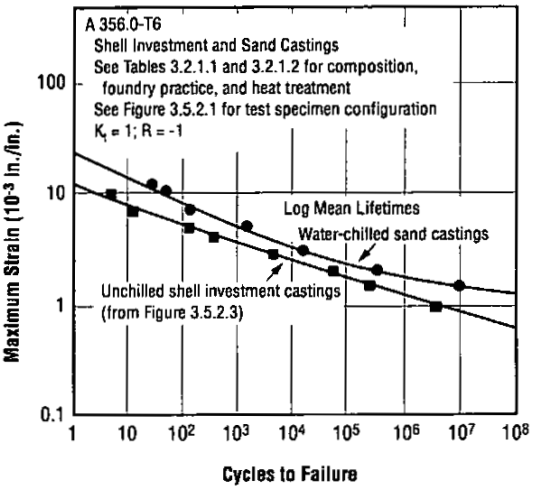


Figure 3.5.2.4 Comparison of strain-fatigue life curves for smooth axial fatigue specimens from unchilled shell-investment castings and water-chilled sand castings (Ref. 45)

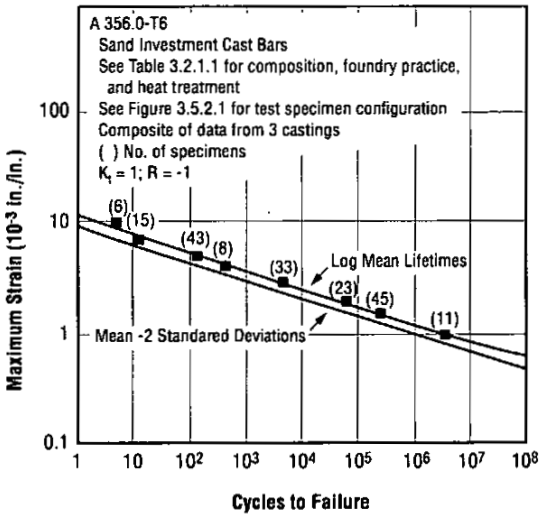


Figure 3.5.2.3 Composite of strain-fatigue life curves for smooth axial fatigue specimens from three shell investment castings poured at different mold temperatures, showing mean fatigue strength and mean-minus-2 standard deviations fatigue strength (Refs. 44, 46, 47)

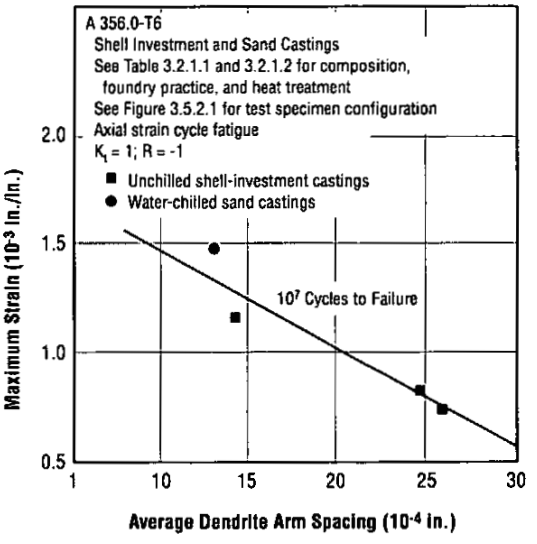


Figure 3.5.2.5 Effect of dendrite arm spacing on axial strain-cycling fatigue strength at 10^7 cycles to failure of smooth specimens from unchilled shell-investment castings and water-chilled sand castings (Refs. 44-47)

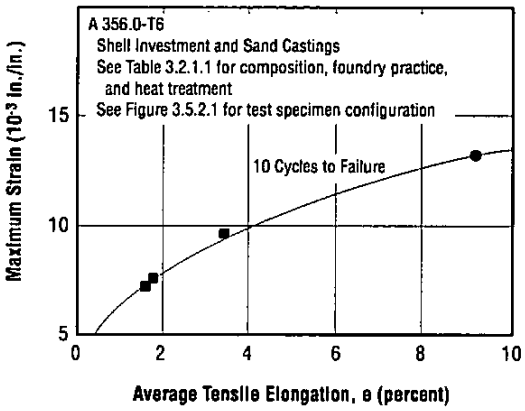


Figure 3.5.2.6 Effect of tensile elongation on axial strain-cycling fatigue strength at 10 cycles to failure of smooth specimens from unchilled shell investment castings and water-chilled sand castings (Refs. 44-47)

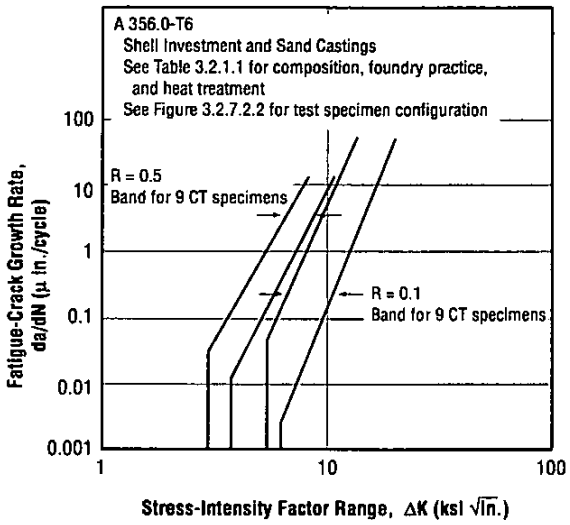


Figure 3.5.3.1 Scatter bands of fatigue-crack growth rates at two R-ratios for CT specimens from three shell-investment castings and one water-chilled sand casting, containing data from several laboratories (Refs. 45-49)

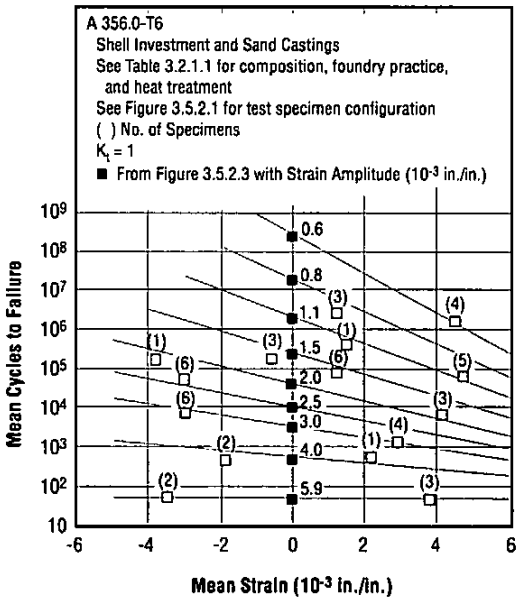


Figure 3.5.2.7 Effect of mean strain on axial strain-fatigue life behavior of smooth specimens from shell-investment castings (calculated from data in Ref. 51)

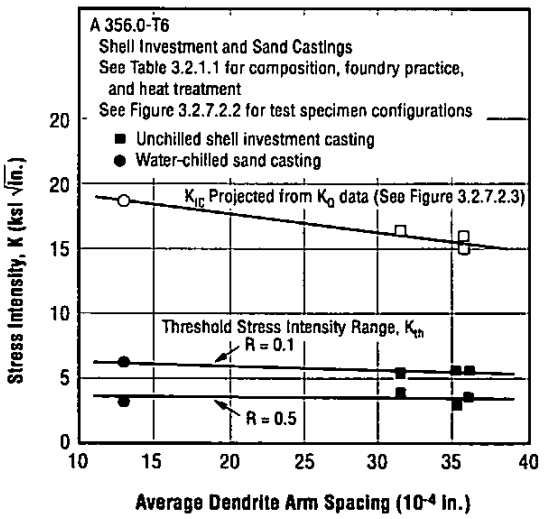


Figure 3.5.3.2 Effect of dendrite arm spacing on crack-propagation threshold stress intensity at two R-ratios and on projected plane-strain fracture toughness of shell-investment and water-chilled sand castings (Refs. 45-49)

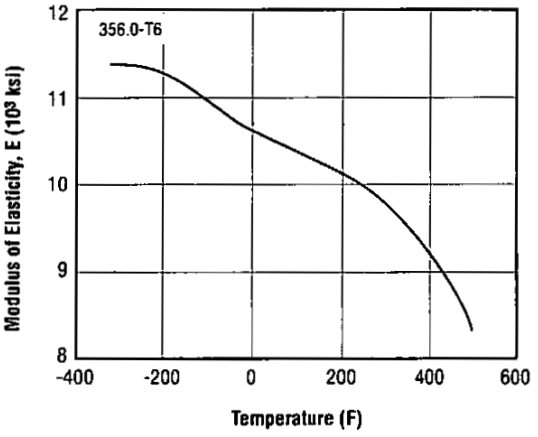


Figure 3.6.2 Modulus of elasticity at various temperatures (Ref. 11)

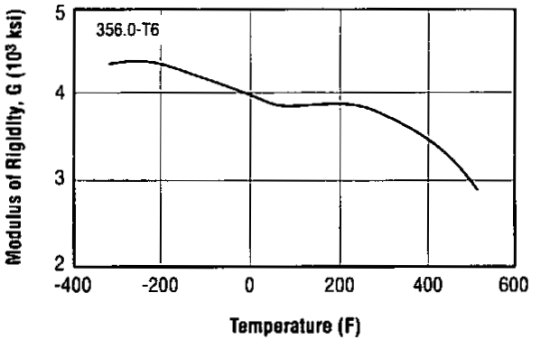


Figure 3.6.3 Modulus of rigidity at various temperatures (Ref. 11)

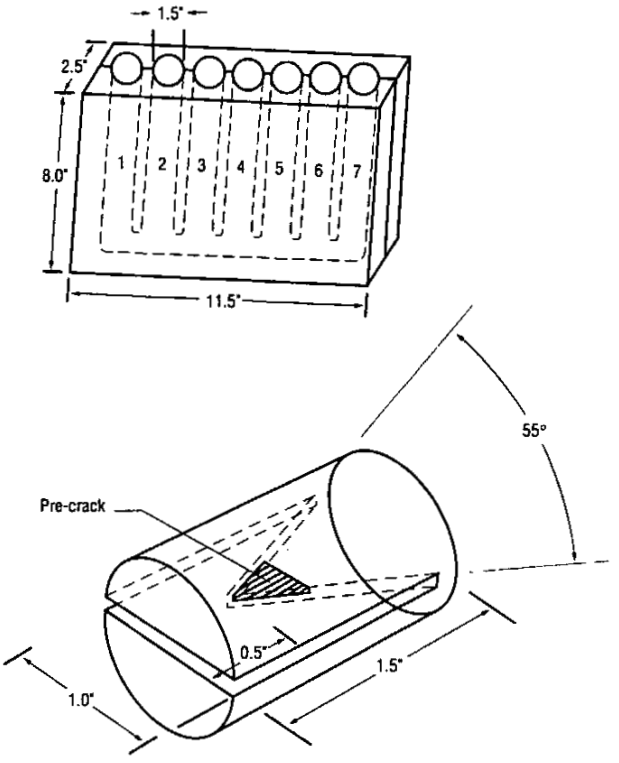


Figure 4.1.1.2 Configurations of permanent steel molds and fracture toughness specimens used for testing the effects of hot isostatic pressing (HIP) (Ref. 58)

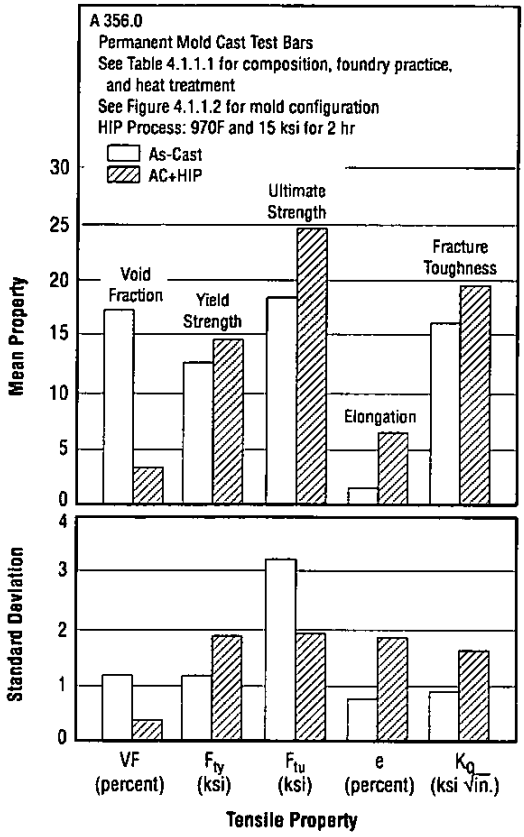


Figure 4.1.1.3 Effect of hot isostatic pressing (HIP) on void fraction and tensile properties of test specimens as-cast in permanent steel molds (Ref. 58)

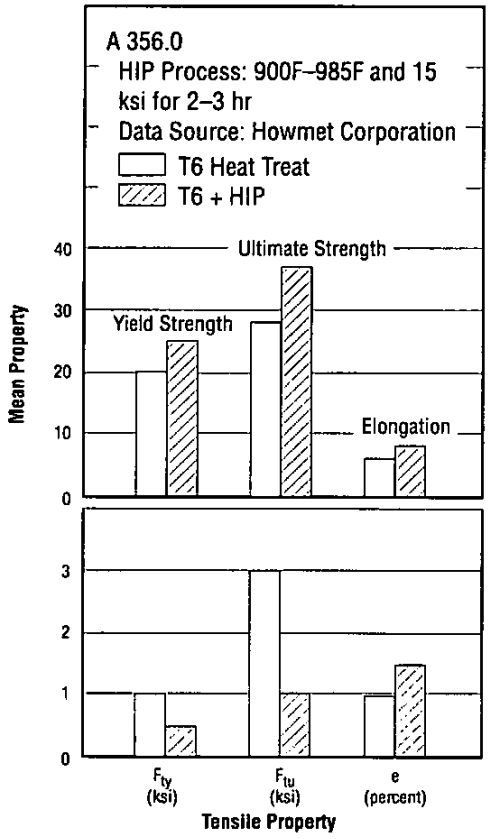


Figure 4.1.1.4 Effect of hot isostatic pressing (HIP) on tensile properties of test specimens heat-treated to the T6 conditionin (Ref. 68)

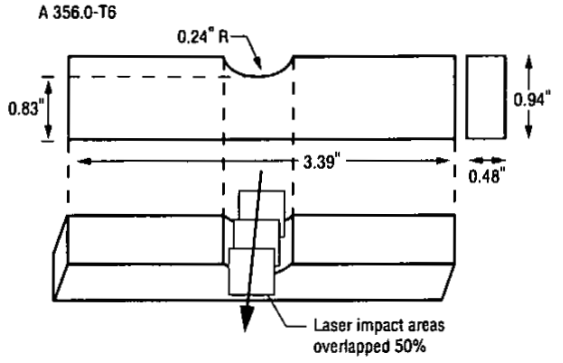


Figure 4.1.2.2 Configuration of notched fatigue test specimens loaded in three-point bending to test the effects of laser shock processing (LSP) on sand castings, showing overlapping impact areas at root of notch (Ref. 59)

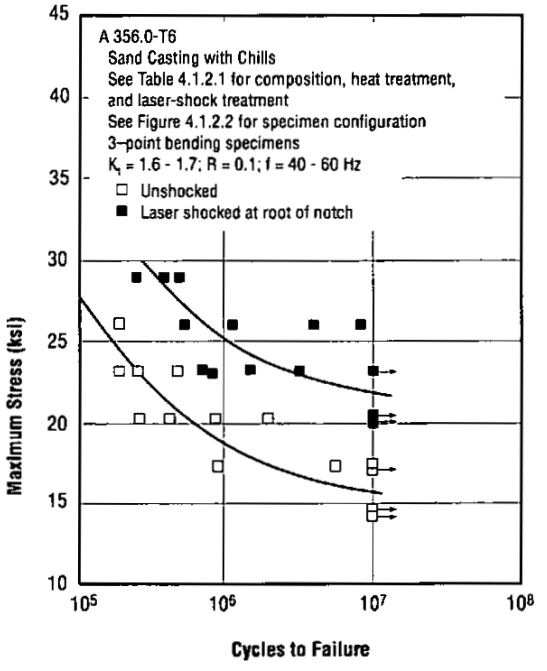


Figure 4.1.2.3 Effect of laser shock processing (LSP) on stress-fatigue life curves for notched bar specimens from chilled sand castings (Ref. 59)

This page is blank.

REVISED: DECEMBER 1969

NONFERROUS ALLOYS

AUTHOR: JOHN G. SESSLER

Al
7 Si
0.3 Mg

356, A356

1. GENERAL

Aluminums 356 and A356 are heat treatable aluminum-silicon-magnesium casting alloys whose properties are primarily determined by a high silicon content in combination with magnesium. 356 is the conventional cast alloy, while castings of A356 are classified as premium quality castings, which are guaranteed to meet a specified high level of mechanical properties. Premium quality results from low impurity content (lower amount of iron) and advanced foundry practices.

Both 356 and A356 possess excellent castability, pressure tightness, and resistance to hot cracking. Fluidity is good and the tendency toward shrinkage is low. Resistance to corrosion by salt spray is high. Weldability is good by fusion techniques if proper procedures are employed. A356 exhibits higher tensile strength and ductility than does the 356 alloy.

356 is available in the form of sand and permanent mold castings, while A356 is primarily a permanent mold casting alloy. Data in the following sections apply to 356 unless specifically noted A356.

1.01 Commercial Designation

356
A356

1.02 Alternate Designation

ASTM SG70A (356 alloy).
ASTM SG70B (A356 alloy) (37).

1.03 Specifications

Table 1.03.

TABLE 1.03

AMS	Alloy	Form	Similar Specification*
4217D	356-T6	Castings, sand	QQ-A-601, Class 3M
4260B	356-T6	Castings, investment	
4261	356-T51	Castings, investment	
4284D	356-T6	Castings, permanent mold	QQ-A-596, Class B
4285	356-T6	Castings, centrifugal	
4286A	356-T51	Castings, permanent mold	
4218B	A356	Castings, premium grade	MIL-A-21180B

* Military or Federal specification.

1.04 Composition

Table 1.04.

TABLE 1.04

Source	AMS (1)(2)(3)(4)(5)		MIL (6), AMS (19)	
Alloy	356		A356	
	Percent		Percent	
	Minimum	Maximum	Minimum	Maximum
Copper	-	0.20	-	0.20
Magnesium	0.20	0.40	0.20	0.40
Manganese	-	0.30	-	0.10
Iron	-	0.60	-	0.20
Silicon	6.5	7.5	6.5	7.5
Zinc	-	0.30	-	0.10
Titanium	-	0.20	-	0.20
Other impurities				
each	-	0.05	-	0.05
total	-	0.15	-	0.15
Aluminum	Balance		Balance	

1.05 Heat Treatment

1.051 Anneal (stress relieve) for dimensional stability. 650F, 2 hours, air cool (17).

1.052 Solution treatment and artificial aging, Table 1.052.

TABLE 1.052

Source	(17)				
Data	Typical Heat Treatment				
		Solution Heat Treatment		Artificial Aging	
Alloy and Condition	Method of Casting	Temp F (a)	Time Hours (b)	Quench (c)	Temp F (a)	Time Hours (d)
356-T6	Sand	1000	12	Water	310	3-5
356-T7	Sand	1000	12	Water	400	3-5
356-T51	Sand	-	-	-	440	7-9
356-T71	Sand	1000	12	Water	475	2-4
356-T6	Permanent Mold	1000	8	Water	310	3-5
356-T7	Permanent Mold	1000	8	Water	440	7-9
A356-T6	Sand	1000	12	Water	310	2-5
A356-T6	Permanent Mold	1000	8	Water	310	3-5
A356-T61	Permanent Mold	1000	8-10	Water	320	8-10

(a) Variation of temperature in furnace should not exceed plus or minus 10F.
(b) Soaking time required for average casting. Time can be decreased or may have to be increased as demonstrated by experience.
(c) Water temperature from 150 to 212F. 212F is preferred to minimize distortion.
(d) Exact time is best established by experience to obtain typical properties.

1.06 Hardness

(see Tables 3.011 and 3.0212)

1.061 Quenching in boiling water followed by aging develops full hardening in all commercial sizes of castings.

1.062 Hardness of sand and permanent mold castings, Table 1.062.

TABLE 1.062

Source		(27)	(31)	(8)
Alloy	Form	Hardness, BHN** (500 kg, 10mm ball)		
356-T51	Sand Cast	60	60	60
356-T71	Sand Cast	-	-	60
356-T6	Sand Cast	70	70	70
356-T7	Sand Cast	75	-	75
356-T6	PM Cast*	80	-	80
356-T7	PM Cast	70	-	70
A356-T61	PM Cast	90	80	90

* PM - Permanent mold
** Hardness values determined from standard 1/2 inch diameter test specimens, individually cast in green sand or permanent molds.

1.07 Forms and Conditions Available

1.071 356 is available in sand, permanent mold, and centrifugal castings, usually without any restrictions as to shape, size, or section thickness.

1.072 A356 is available primarily in the form of permanent mold "premium strength structural castings" with properties to be negotiated with producer. Sand castings, however, are also produced as premium grade castings.

1.073 Conditions available, Table 1.073.

TABLE 1.073

Source	(17)	
Alloy	Form	Conditions Available
356	Sand Cast	F, T51, T6, T7, T71
	Permanent Mold	F, T51, T6, T7
A356	Sand Cast	T6
	Permanent Mold	T6, T61

1.08 Melting and Casting Practice

1.081 The 356 alloy can be melted and cast using conventional aluminum alloy practices without any special considerations.

1.082 Premium quality castings of the A356 alloy are guaranteed to meet a specified high level of mechanical properties as measured by using test bars cut from specified locations within the heat treated casting (24). To obtain these superior properties, improved casting techniques

	Al
7	Si
0.3	Mg

356, A356

need to be employed, which include:
1) The use of high purity ingot (low iron content).
2) Adequate degassing and proper melting.
3) Streamlined gating design to avoid turbulence and aspiration of mold gases.
4) The use of a sufficient number of risers to adequately feed the casting.
5) Liberal use of chills to control solidification rate and provide directional solidification.
6) The use of proper heat treatment to develop maximum properties.

1.083 Melting of premium quality ingots is normally performed in silicon carbide crucibles (rather than in iron pots) to minimize the possibility of iron pickup. Iron skimming tools used for dross removal should be coated with a suitable refractory wash of clay, lime or with a similar refractory sodium-silicate binder (33).

1.084 Effect of pouring temperature on grain size, Figure 1.084.

1.085 Fluxing procedures for premium quality castings are essentially the same as those used in normal aluminum melting practice (36).

1.086 A more detailed discussion of melting and casting procedures for premium quality parts is given in Reference 24.

1.09 Special Considerations

1.091 (See 1.082 for special considerations concerning premium quality castings of A356 alloy.)

2. PHYSICAL AND CHEMICAL PROPERTIES

2.01 Thermal Properties

2.011 Melting range.
356 alloy 1035 to 1135F
A356 alloy 1035 to 1130F (17).

2.012 Phase changes. Alloys are subject to precipitation.

2.0121 Time-temperature-transformation diagrams.

2.013 Thermal conductivity, Table 2.013.

TABLE 2.013

Source	(17) (27)	
Alloy	Condition	Thermal Conductivity at Room Temperature, Btu ft per(hr sq ft F)
356	T51	97
	T6	87
	T6*	92
	T7	90
A356	T6	87

* Chill cast samples - all other samples cast in green sand molds.

2.014 Thermal expansion, Figure 2.014.

2.015 Specific heat, 0.23 Btu per (lb F) at 212F (18).

2.016 Thermal diffusivity.

2.02 Other Physical Properties

2.021 Density, 0.097 lb per cu in; 2.68 gr per cu cm (17).

2.022 Electrical properties.

2.0221 Electrical resistivity, Table 2.0221.

TABLE 2.0221

Source	(18, p. 957)
Condition	Electrical Resistivity at Room Temperature; Microhm Inch
T51	1.60
T6	1.74
T7	1.70

2.0222 Electrical conductivity (percent of IACS)
356-T51 43
356-T6 39
356-T7 40
A356-T6 40 (17).

2.023 Magnetic properties. Alloys are nonmagnetic.

2.024 Emittance, 0.035 to 0.07 at 77F in air (18).

2.025 Damping capacity.

2.03 Chemical Properties

2.031 General. The general corrosion and atmospheric weathering resistance of 356 and A356 is very good, comparable to pure aluminum in this respect. The alloys may be used in industrial and seacoast atmospheres without protection (27). They also exhibit excellent resistance to stress-corrosion cracking. There are no known instances of failure by stress corrosion in service applications or in laboratory tests employing 3.5 percent NaCl alternate immersion.

2.032 Electrolytic solution potential versus N/10 Calomel Electrode (solution: 53 gr NaCl + 3 gr H_2O_2). 356-T6 (sand-cast) 0.82 volt (17).

2.033 These alloys are subject to corrosion when exposed to hydrazine or UDMH (unsymmetrical dimethyl hydrazine) in the presence of moisture. Initially corrosive attack is very severe with a gradual build up of a passive film, after which the rate of attack is reduced. Passivation in a 30 percent solution of UDMH for 2 hours at 170-180F renders the surfaces resistant to attack by diluted UDMH at room temperature. Resistance is also obtained by sulfuric acid anodizing and, to a lesser extent, by chromic acid anodizing (32).

2.04 Nuclear Properties

2.041 Effect of neutron radiation on tensile properties of cast test bars, Table 2.041.

TABLE 2.041

Source	(25) (34)						
Alloy	356						
Irradiation Temperature F	Integrated Neutron Flux n cm^{-2} *	F_{tu} ksi		F_{ty} ksi		e(2 inches) percent	
		A	B	A	B	A	B
-	2.4×10^{20}	32.4	44.3	24.1	42.4	2.7	0.4
-	7.2×10^{20}	32.4	54.0	24.1	51.0	2.7	0.9
-	2.6×10^{21}	32.4	45.0	24.1	36.0	2.7	1.5
120	2.04×10^{19}	33.1	36.7	26.0	29.1	4.0	6.0
120	1.22×10^{20}	33.1	42.0	26.0	33.5	4.0	6.0
120	5.59×10^{20}	33.1	45.1	26.0	42.5	4.0	6.0
120	9.84×10^{20}	33.1	54.4	26.0	52.1	4.0	3.0

* Fast neutrons.
A - Not irradiated
B - Irradiated

2.042 Comparison of mechanical properties before and after nuclear radiation at -420F, Table 2.042.

TABLE 2.042

Source	(30)				
Alloy	A356-T6 Cast Plate				
Test	Pre and Post Irradiation Data at -420F				
Property	Specimen Type (b)	Control (average)	Irradiate (average) (a)	Change	Percent Change
F_{tu} -ksi	L	44.7	52.8	+ 8.1	+18 (c)
F_{ty} -ksi	L	31.0	42.8	+11.8	+38 (c)
e -percent	L	1.5	1.4	- 0.1	- 7
RA -percent	L	2.8	0.8	- 2.0	-72 (c)
F_{su} -ksi	L	50.4	45.6	- 4.8	-10 (c)
Notch Strength - ksi (K_t = 6.3)	L	39.7	43.2	+ 3.5	+ 9
Notch/Unnotch Strength ratio (d)	L	0.89	0.82	-	-

(a) Irradiated at 5×10^{16} nvt (E>1.0 Mev) in liquid hydrogen.
(b) L = longitudinal specimen
(c) Statistically significant change; probability>0.90.
(d) Notch specimen geometry:
Width = 1.0
Notch Radius = 0.005
Notch Depth = 30 percent
Notch Angle = 60 degrees
Thickness = 0.063

2.043 Effect of nuclear radiation at -420F on stress-strain curves of plate (typical), Figure 2.043.

2.044 Effect of neutron radiation on tensile properties of A356 castings, Table 2.044.

TABLE 2.044

Source	(35)							
Alloy	A356							
Irradiation Temperature F	Test Temp F	Fast Neutron Flux ($n\ cm^{-2}$)*	F_{tu} ksi		F_{ty} ksi		e (2 inches) percent	
			A	B	A	B	A	B
120	RT	2.0×10^{19}	33.1	36.7	26	29.1	4	6
120	RT	1.2×10^{20}	33.1	42.0	26	33.5	4	6
120	RT	5.6×10^{20}	33.1	45.9	26	42.4	4	6
120	RT	9.8×10^{20}	33.1	54.4	26	52.1	4	3

* Energy greater than 1.0 MeV
A not irradiated
B irradiated

3. MECHANICAL PROPERTIES

3.01 Specified Mechanical Properties

3.011 AMS and producer's specified mechanical properties for 356 alloy, Table 3.011.

TABLE 3.011

Source	(7, p.62)	(7, p. 62) (1)		(7, p.62)		(5)		(7, p. 65) (3)		(7, p.65)	(2) (4)	
Alloy	356											
Form	Sand Castings					Permanent Mold Castings					Investment and Centrifugal Castings	
Condition	T51	T6		T7	T71	T51		T6		T7	T6	
Specimen	Cast Test Bars	Cast Test Bars	From Castings Average*	Cast Test Bars		Cast Test Bars	From Castings Average*	Cast Test Bars	From Castings Average*	Cast Test Bars	Cast Test Bars	From Castings Average*
F_{tu}, min -ksi	23	30	22.5	31	25	25	18.8	33	24.75	29	33	24.75
F_{ty}, min -ksi	16	20	15.0	26	18	-	-	22	16.5	21	22	16.5
e(2 in), min - percent	-	3	-	-	3	-	-	3	-	4	3	-
e(4 D), min - percent	-	-	0.7	-	-	-	-	-	0.7	-	-	0.7
F_{cy}, min -ksi	17	20	-	27	19	-	-	22	-	21	-	-
F_{su}, min -ksi	17	25	-	21	17	-	-	25	-	22	-	-
F_{bru}, min (e/D = 2.0) -ksi	48	63	-	65	52	-	-	59	-	52	-	-
F_{bry}, min (e/D = 2.0) -ksi	32	40	-	52	36	-	-	40	-	38	-	-
Hardness, BHN (500 kg, 10 mm) min	-	-	65.0	-	-	-	65.0	-	65.0	-	-	65.0
max	-	-	95.0	-	-	-	-	-	95.0	-	-	95.0

* Average values for at least 4, preferably 10, specimens.

3.012 Producer's specified properties for A356 alloy, Table 3.012.

TABLE 3.012

Source	(7, p. 65) MIL (6)		
Alloy	A356		
Form	Permanent Mold Castings		
Condition	T61		
Specimen Type	From Castings		
	(a)	(b)	(c)
F_{tu}, minimum -ksi	33	38	40
F_{ty}, minimum -ksi	27	28	30
e(2 inches) minimum - percent	3	5	3
F_{cy}, minimum -ksi	27	-	-
F_{su}, minimum -ksi	23	-	-

(a) Individually cast specimen.
(b) Cut from designated location in casting.
(c) Must be negotiated with foundry.

3.013 AMS specified tensile properties for A356 alloy, Table 3.013.

TABLE 3.013

Source	AMS (19)	
Alloy	A356	
Form	Type of Mold Not Restricted	
Condition	Solution and Precipitation Heat Treated	
Specimen Type	(a)	(b)
F_{tu}, minimum -ksi	32	33
F_{ty}, minimum -ksi	22	27
e(2 inches) minimum - percent	2	3

(a) Specimen cut from any area of casting.
(b) Cast specimen.

3.014 MIL-A-21180B specified tensile properties for specimens cut from castings of A356, Table 3.014.

TABLE 3.014

Source	MIL-A-21180B (6)					
Alloy	A356					
Form	Special Mold, Permanent Mold, or Sand Mold With Chills					
Condition	T61					
Location in Casting	Designated Area			Any Area		
Class	1	2*	3*	10	11	12
F_{tu}, minimum - ksi	38.0	40.0	45.0	38.0	33.0	32.0
F_{ty}, minimum - ksi	28.0	30.0	34.0	28.0	27.0	22.0
e, minimum - percent	5.0	3.0	3.0	5.0	3.0	2.0

* Obtainable only in favorable casting configurations and must be negotiated with the foundry.

3.02 Mechanical Properties at Room Temperature

3.021 Tension.

3.0211 Stress-strain diagrams (see Figure 2.043).

3.0212 Typical mechanical properties of 356 cast test bars at room temperature, Table 3.0212.

TABLE 3.0212

Source	(8) (27)						
Alloy	356				A356		
Form	Sand Cast				Permanent Mold Cast		
Specimen	Cast Test Bars						
Condition	T51	T6	T7	T71	T6	T7	T61
F_{tu} -ksi	25	33.0	34	28.0	37	32	41
F_{ty} -ksi	20	24.0	30	21.0	27	24	30
e(2 inches)-percent	2	3.5	2	3.5	5	6	10
F_{cy} -ksi	21	25.0	31	22.0	27	24	32
F_{su} -ksi	20	26.0	24	20.0	30	25	28
Hardness,* BHN	60	70.0	75	60.0	80	70	90

* 500 kg load 10 mm ball.

3.0213 Effect of diameter of cylindrical 356-T6 castings on tensile properties, Table 3.0213.

Al
7 Si
0.3 Mg

356, A356

Al
7 Si
0.3 Mg

TABLE 3.0213

Source		(9, p. 58)								
Alloy		356								
Form		Sand Cast								
Condition		T51				T6				
Section Thickness-Inches		Test Bar 0.505	3/4	1 1/4	1 3/4	Test Bar 0.505	3/4	1 1/4	1 3/4	2 1/4
F_{tu}	-ksi	27.2	21.9	17.15	14.4	34.1	28.3	23.0	19.4	15.1
F_{ty}	-ksi	-	16.7	13.45	12.7	24.3	23.0	22.5	-	-
e	-percent	1.6	1.5	1.3	1.2	4.6	2.0	1.0	0.7	0.5

356, A356 3.0214 Typical tensile properties of specimens cut from 356-T6 sand and permanent mold castings of different thickness, Table 3.0214.

TABLE 3.0214

Source		(9, p. 57)									
Alloy		356									
Form		Sand Cast					Permanent Mold Cast				
Condition		T6									
Section thickness-inches		≤ 1/8	1/8 to 1/4	1/4 to 1/2	1/2 to 3/4	3/4 to 1.0	≤ 1/8	1/8 to 1/4	1/4 to 1/2	1/2 to 3/4	3/4 to 1.0	1.0 to 1.5
F_{tu}	-ksi	37.0	35.5	34.0	32.5	31.0	43.0	42.0	40.0	37.0	37.0	36.0
F_{ty}	-ksi	25.5	24.5	23.5	22.5	21.5	31.0	30.0	30.0	29.0	28.0	28.0
e(4D)	- percent	5.0	4.5	4.0	3.5	3.0	-	-	-	-	-	-
e(2 inches)	- percent	-	-	-	-	-	6.0	5.0	4.0	2.0	2.0	1.25

3.0215 Typical tensile properties of specimens cut from premium strength A356 castings, Table 3.0215.

TABLE 3.0215

Source		(14, p. 4)		
Alloy		A356		
Form		Premium Strength Castings		
Condition		T61		
Specimen Type		From Castings		
		(a)	(a)	(b)
F_{tu}	-ksi	41	43	45
F_{ty}	-ksi	31	33	35
e	-percent	8	9	6

(a) Produced in either all or part of castings.
(b) Must be negotiated with foundry.

3.0216 Effect of exposure to elevated temperature on tensile properties of sand cast test bars in T51 condition, Figure 3.0216.

3.0217 Effect of exposure to elevated temperature on tensile properties of sand cast test bars in T7 condition, Figure 3.0217.

3.0218 Effect of iron content on properties of A356-T6 sand castings, Table 3.0218.

TABLE 3.0218

Source	(28)						
Alloy	A356-T6						
Type	Sand Castings (without chills)						
Iron Content percent	Room Temperature Tensile (a)			Charpy-V Impact (ft-lbs)			Notch to Unnotched Strength Ratio
	F_{tu} ksi	F_{ty} ksi	e(2 inches) percent	75F	-320F	-450F	(-320F) (b)
0.13	37.3	24.4	7.5	2.8	2.0	2.4	1.14
0.01	37.4	23.5	12.4	5.0	5.0	5.2	1.22

(a) Machined cast test bars.
(b) K_t = 6 for notched tensile samples.

3.0219 Effect of iron content and section thickness on tensile properties of 356 and A356 castings, Table 3.0219.

TABLE 3.0219

Source	(29)			
Condition	T6			
Section Thickness (inches)	Test Data		356 (0.34 Fe)	A356 (0.18 Fe)
1 1/4	F_{tu}	-ksi	28.14	32.99
	F_{ty}	-ksi	20.52	25.71
	e	-percent	4.0	4.4
3/4	F_{tu}	-ksi	28.80	34.11
	F_{ty}	-ksi	21.37	26.85
	e	-percent	4.0	5.1
3/8	F_{tu}	-ksi	30.64	35.34
	F_{ty}	-ksi	22.11	26.91
	e	-percent	4.0	5.6

3.022 Compression (see Tables 3.0212, 3.011 and 3.012).
3.0221 Stress-strain diagrams.
3.023 Impact (see Table 3.0218).
3.024 Bending.
3.025 Torsion and shear (see Tables 3.0212, 3.011 and 3.012).
3.026 Bearing (see Table 3.011).
3.027 Stress concentration.
3.0271 Notch properties (see Tables 2.042 and 3.0218).
3.0272 Fracture toughness.
3.028 Combined properties.

3.03 Mechanical Properties at Various Temperatures
3.031 Tension.
3.0311 Stress-strain diagrams.
3.0312 Effect of exposure and test temperature on tensile properties of sand cast test bars in T51 condition, Figure 3.0312.
3.0313 Effect of exposure and test temperature on tensile properties of sand cast test bars in T6 condition, Figure 3.0313.
3.0314 Effect of exposure and test temperature on tensile properties of sand cast test bars in T7 Condition, Figure 3.0314.
3.0315 Effect of exposure and test temperature on tensile properties of A356 permanent mold cast test bars in T61 condition, Figure 3.0315.
3.0316 Effect of test temperature on tensile properties of permanent mold castings in T6 and T7 conditions, Figure 3.0316.
3.0317 Effect of test temperature on tensile properties of sand castings in T6 and T7 conditions, Figure 3.0317.
3.0318 Effect of low temperatures on tensile properties of T6 castings, Figure 3.0318.
3.032 Compression.
3.0321 Stress-strain diagrams.
3.033 Impact.

	Al
7	Si
0.3	Mg

356, A356

3.034 Bending.
3.035 Torsion and shear.
3.036 Bearing.
3.037 Stress concentration.
3.0371 Notch properties.
3.0372 Fracture toughness.
3.038 Combined properties.

3.04 Creep and Creep Rupture Properties

3.041 Creep and creep rupture curves at room temperature to 400F for sand cast test bars in T7 condition, Figure 3.041.

3.042 Creep and creep rupture curves at 300F for A356 permanent mold cast test bars in T61 condition, Figure 3.042.

3.05 Fatigue Properties

3.051 Typical fatigue strength of cast test bars at room temperature, Table 3.051.

TABLE 3.051

Source	(8, p. 197) (10) (14, p. B)									
Form	Cast Test Bars-Room Temperature									
Alloy	Condition	Method	Stress Ratio A	Stress Ratio R	Stress Concentration	Fatigue Strength - ksi at Cycles 10^5	10^6	10^7	10^8	$5x10^8$
356 Sand cast	T51	Rot Beam	∞	-1	Smooth K_t=1	-	-	-	-	8.0
	T6					-	-	-	-	8.5
	T7					21	14.5	10.5	9.5	9.5
	T71					-	-	-	-	8.5
356 Perm Mold	T6					-	-	-	-	13.0
	T7					-	-	-	-	11.0
A356	T61					29	23.0	17.0	14.0	13.0

3.052 Endurance limit.
356-T6 13.0 ksi
A356-T61 13.0 ksi (27)
(Based on R. R. Moore rotating beam tests; 5.0×10^8 cycles.)

3.06 Elastic Properties

3.061 Poisson's ratio, 0.33 (18).

3.062 Modulus of elasticity at various temperatures, Figure 3.062.

3.063 Modulus of rigidity at various temperatures, Figure 3.063.

4. FABRICATION

4.01 Formability
(see also Section 1.08)

4.011 General. 356 and A356 have excellent castability characteristics such as high fluidity, low solidification shrinkage tendencies, high resistance to hot cracking and good pressure tightness. These alloys are suitable for intricate castings containing thin sections and variable thicknesses (39).

4.012 Melting of these alloys is discussed in Section 1.08.

4.013 Hydrogen readily dissolves in molten aluminum from moisture in all forms and from hydrocarbons. It is liberated during solidification and can cause harmful porosity. Gas absorption increases with increasing temperature of the molten aluminum and with increasing time at temperature. Absorption of gas is also increased when the contact surface between molten metal and hydrogen forming gases is made larger.

4.014 Dross forms as a result of oxidation, and it may be trapped in the metal, causing defects in the casting because its density is slightly higher than the density of aluminum. The oxide film on the aluminum melt, however, gives an excellent protection against further oxidation and gas absorption. On casting, the metal should flow steadily and for a minimum distance to maintain the oxide layer and thus avoid dross inclusions.

4.015 Gaseous or solid fluxes are generally used to remove hydrogen and dross from the melt. Flushing with gaseous fluxes, such as chlorine or nitrogen, may be used for this purpose. Solid fluxes are introduced into the melt to form a gas or liquid protective coating on top of the melt. Generally the metal is heated to 1250-1400F before adding flux. After fluxing, the melt should be allowed to settle for 10 to 20 minutes to allow the flux to float to the top, while the temperature of the liquid is adjusted to the pouring temperature.

4.016 For thin sections of castings, it may be necessary to use a mold coating to increase fluidity. Hexachlorethane has been found to be effective in this respect. For example, it was reported that by spraying the mold with a saturated solution of hexachlorethane in ether, the fluidity of 356 alloy was increased 86 percent at 1320F and 96 percent at 1250F (38).

4.02 Machining and Grinding

4.021 General. The machinability of these alloys is fair. Tool wear is greater for these alloys than for 355 alloy because of the higher silicon content. Carbide cutting tools and lubricants such as lard oil and kerosene are recommended for general machining. For tapping, pure lard oil is preferred.

4.03 Welding

4.031 General. These alloys are readily weldable by GTA techniques. Gas welding, metal arc, carbon arc, and atomic hydrogen techniques have also been used, usually with a furnace for preheating. Foundry welding of small defects, etc., usually employs filler metal of the same composition as the parent cast metal. For repair or assembly welding, 4043 filler metal is recommended to keep cracking sensitivity at a minimum (40).

4.032 Temperatures exceeding 400F during preheating or welding will affect the mechanical properties of heat treated castings. After welding, however, the castings can be reheat treated to restore their properties. A general rule during welding is to keep the heat of welding concentrated in a narrow region.

4.033 A more detailed discussion of the welding of aluminum castings is given in Reference 40.

4.034 Brazing of 356 and A356 is not normally recommended. However, it is possible to braze these alloys with special techniques (41).

4.04 Heat Treatment

4.05 Surface Treatment

4.051 General. The resistance of these alloys to normal atmospheric weathering is good, and protective coatings are not usually required. These alloys can be anodized to provide increased resistance to corrosion and abrasion. Other surface finishes such as electroplating, porcelain enameling, and painting can be applied for special purposes if desired (39).

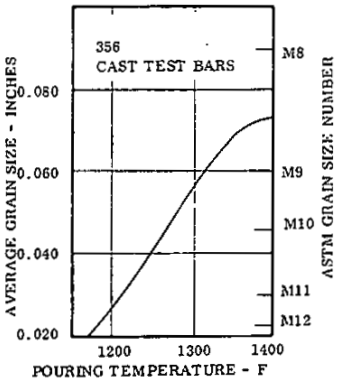


FIG. 1.084 EFFECT OF POURING TEMPERATURE ON GRAIN SIZE. (26)

	Al
7	Si
0.3	Mg

356, A356

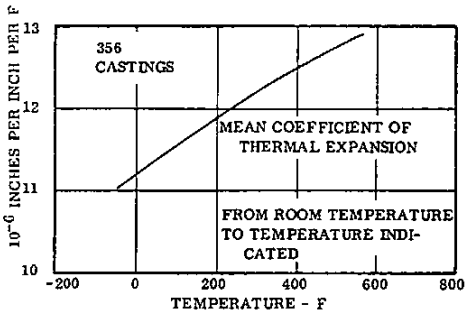


FIG. 2.014 THERMAL EXPANSION. (8, p. 205)

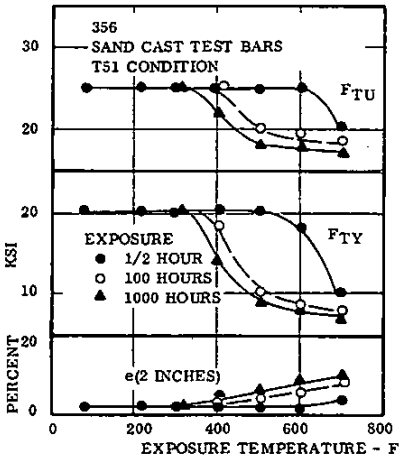


FIG. 3.0216 EFFECT OF EXPOSURE TO ELEVATED TEMPERATURE ON ROOM TEMPERATURE TENSILE PROPERTIES OF SAND CAST TEST BARS IN T51 CONDITION. (12)

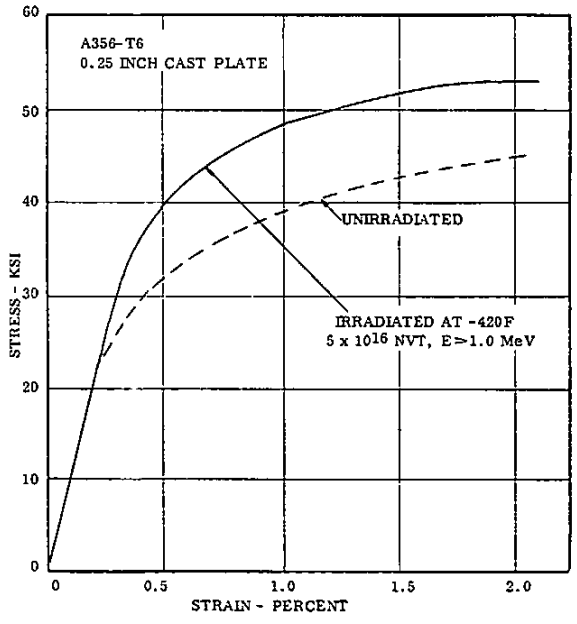


FIG. 2.043 EFFECT OF NUCLEAR RADIATION AT -420F ON STRESS-STRAIN CURVES OF PLATE (TYPICAL). (30)

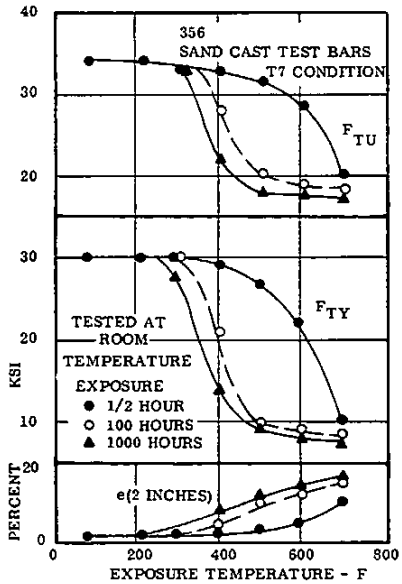


FIG. 3.0217 EFFECT OF EXPOSURE TO ELEVATED TEMPERATURE ON ROOM TEMPERATURE TENSILE PROPERTIES OF SAND CAST TEST BARS IN T7 CONDITION. (10)

	Al
7	Si
0.3	Mg

356, A356

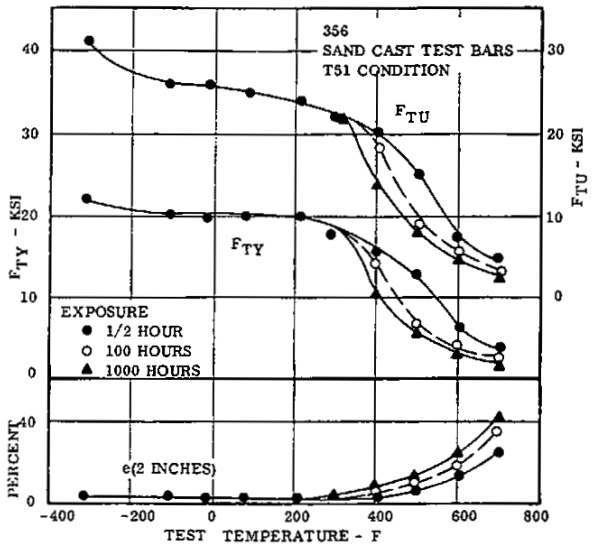


FIG. 3.0312 EFFECT OF EXPOSURE AND TEST TEMPERATURE ON TENSILE PROPERTIES OF SAND CAST TEST BARS IN T51 CONDITION. (12)

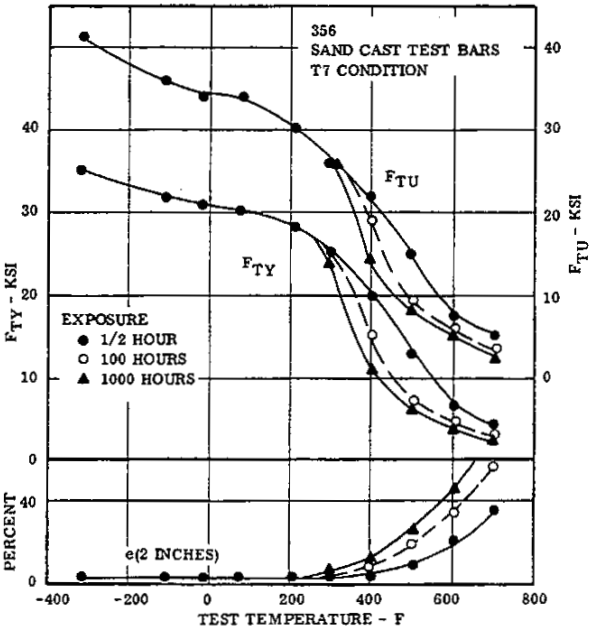


FIG. 3.0314 EFFECT OF EXPOSURE AND TEST TEMPERATURE ON TENSILE PROPERTIES OF SAND CAST TEST BARS IN T7 CONDITION. (10)

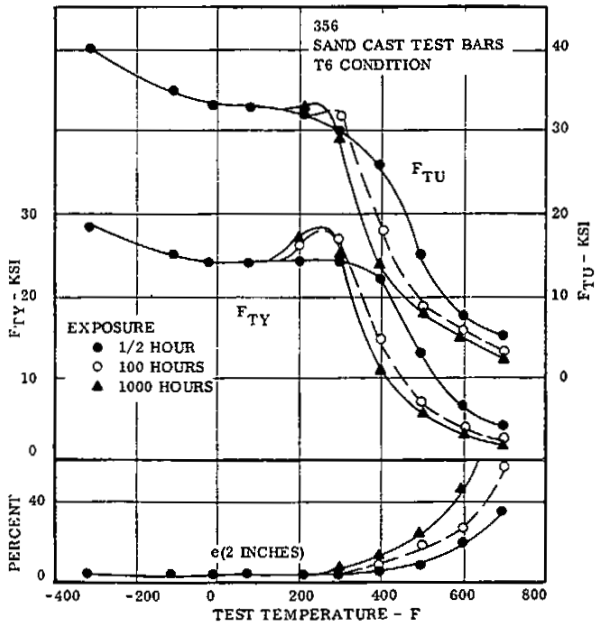


FIG. 3.0313 EFFECT OF EXPOSURE AND TEST TEMPERATURE ON TENSILE PROPERTIES OF SAND CAST TEST BARS IN T6 CONDITION. (16)

Al
7 Si
0.3 Mg

356, A356

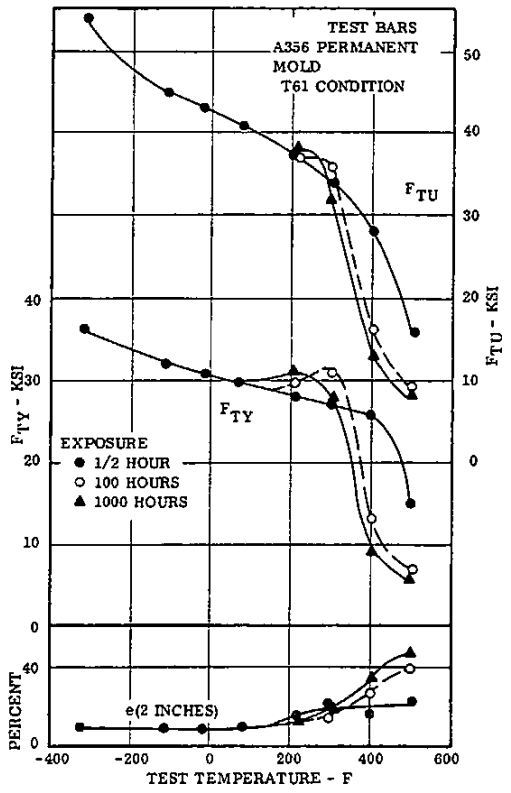


FIG. 3.0315 EFFECT OF EXPOSURE AND TEST TEMPERATURE ON TENSILE PROPERTIES OF A356 PERMANENT MOLD CAST TEST BARS IN T61 CONDITION. (14, p. B)

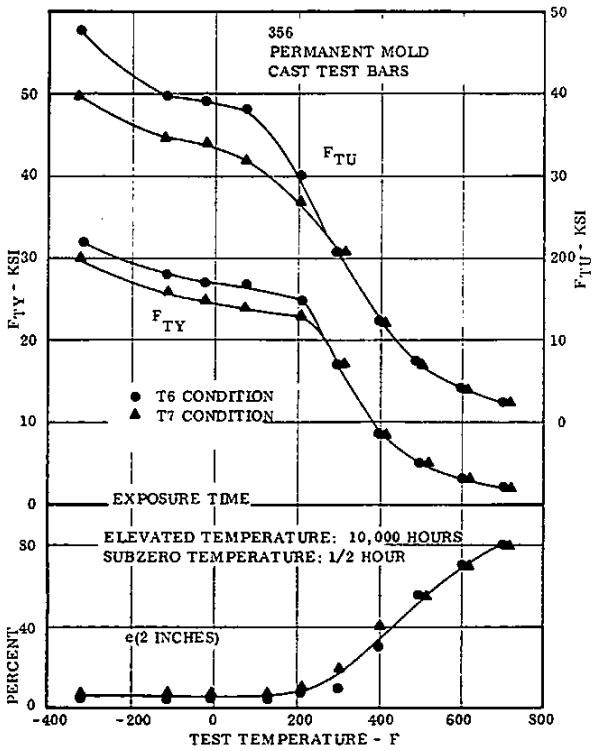


FIG. 3.0316 EFFECT OF TEST TEMPERATURE ON TENSILE PROPERTIES OF PERMANENT MOLD CASTINGS IN T6 AND T7 CONDITIONS. (27)

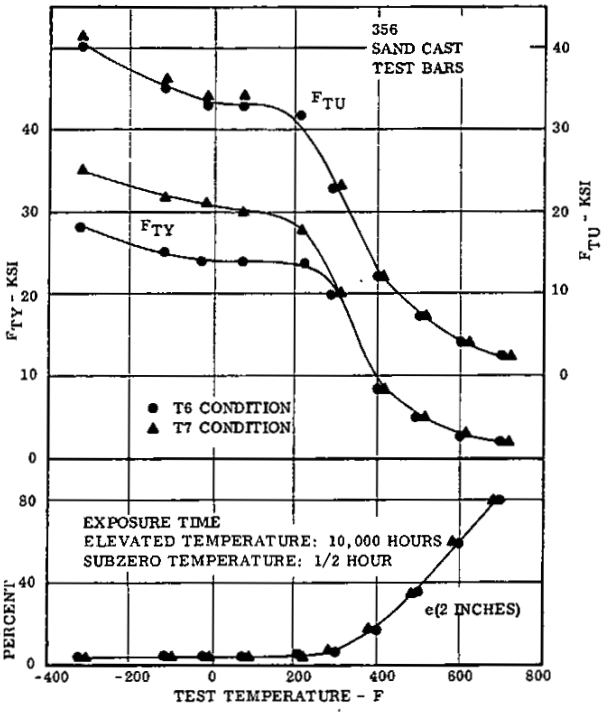


FIG. 3.0317 EFFECT OF TEST TEMPERATURE ON TENSILE PROPERTIES OF SAND CASTINGS IN T6 AND T7 CONDITIONS. (27)

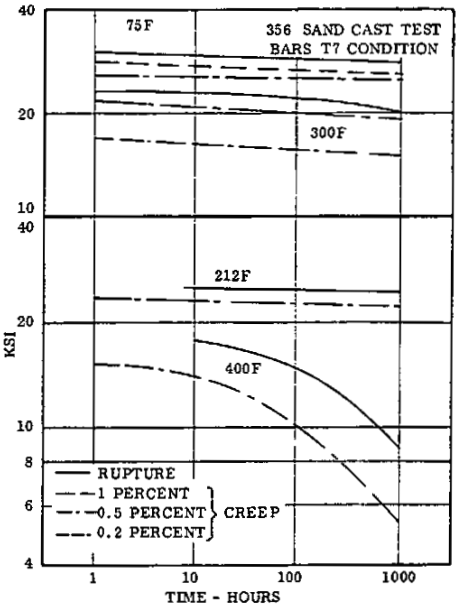


FIG. 3.041 CREEP AND CREEP RUPTURE CURVES AT ROOM TEMPERATURE TO 400F FOR SAND CAST TEST BARS IN T7 CONDITION. (10)

	Al
7	Si
0.3	Mg

356, A356

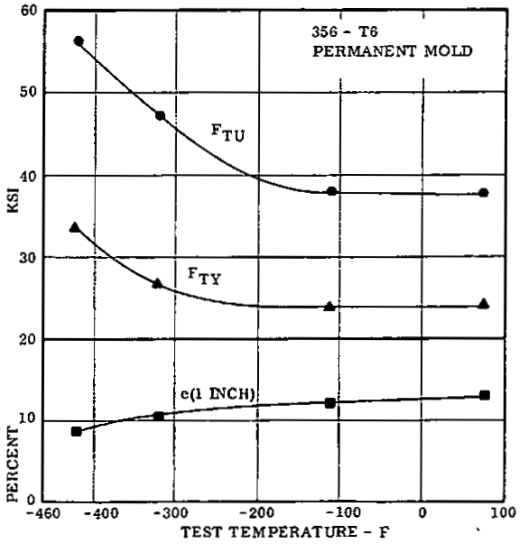


FIG. 3.0318 EFFECT OF LOW TEMPERATURE ON TENSILE PROPERTIES OF T6 CASTINGS. (22)

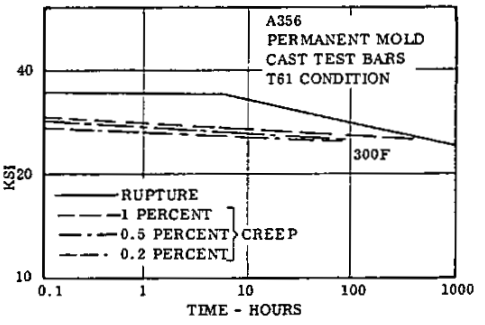


FIG. 3.042 CREEP AND CREEP RUPTURE CURVES AT 300F FOR A356 PERMANENT MOLD CAST TEST BARS IN T61 CONDITION. (14, p. B)

	Al
7	Si
0.3	Mg

356, A356

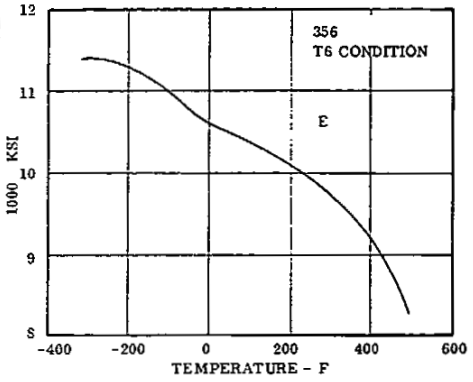


FIG. 3.062 MODULUS OF ELASTICITY AT VARIOUS TEMPERATURES. (13, p. 1-2-2.2)

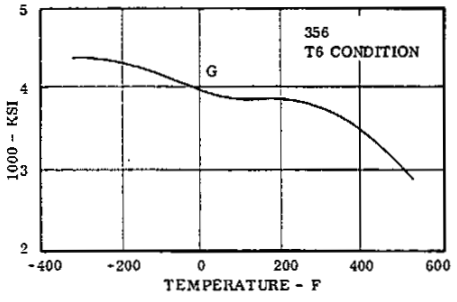


FIG. 3.063 MODULUS OF RIGIDITY AT VARIOUS TEMPERATURES. (13, p. 1-2-2.2)

REFERENCES

1. AMS 4217D (June 15, 1959).
2. AMS 4260B (November 1, 1967).
3. AMS 4284D (January 15, 1959).
4. AMS 4285 (May 1, 1954).
5. AMS 4286A (August 15, 1958).
6. MIL-A-21180B (August 4, 1960).
7. Alcoa Structural Handbook (1958).
8. Alcoa Aluminum Handbook (1959).
9. ASM Metals Handbook Supplement (1955).
10. Alcoa Research Laboratories, "Data Sheet" (August, 1957).
11. Alcoa Aluminum Handbook (1957).
12. Alcoa Research Laboratories, "Data Sheet" (February, 1956).
13. North American Aviation, Missile Development Division, "Materials Property Manual and Summary Report" (October, 1957).
14. Alcoa, Sales Development Division, "Premium-Strength Structural Castings" (January, 1959).
15. ARTC-10-1955, Aircraft Industries Association.
16. Alcoa Research Laboratories, "Data Sheet" (December, 1956).
17. "The Aluminum Data Book," Reynolds Metals Company (1965).
18. ASM "Metals Handbook," American Society for Metals, Volume 1, 8th Edition (1961).
19. AMS 4218B (January 31, 1964).
20. AMS 4261 (June 30, 1964).
21. Alloy Digest, "Aluminum 356, Heat Treatable Aluminum Casting Alloy," Filing Code: Al-21, Engineering Alloy Digest, Incorporated (October 1954).
22. Campbell, J. E., "Aluminum Alloys for Cryogenic Service," ASTM Materials Research and Standards, Volume 4, No. 10 (October 1964).
23. Everhart, J. L., "Aluminum Alloy Castings," Materials in Design Engineering, Manual No. 146 (February, 1958).
24. Grube, K. R., Williams, D. N., and Ogden, H. R., "Premium-Quality Aluminum Castings," DMIC Report 211, Battelle Memorial Institute (January, 1965).
25. Shober, F. R., "The Effect of Nuclear Radiation on Structural Metals," DMIC Report 166, Battelle Memorial Institute (September, 1961).
26. Meier, J. W., and Couture, A., "Aluminum Alloy Test Bar Casting Temperature Effect on Properties," Transactions, American Foundrymen's Society, Volume 68 (1960) p. 670.
27. "Aluminum-Properties, Physical Metallurgy and Phase Diagrams," Volume 1 (Edited by K. R. VanHorn), American Society for Metals (1967).
28. Williams, D. N., Wood, R. A., and Ogden, H. R., "Improving Low Temperature Aluminum Casting Properties," Modern Castings (January, 1963).
29. Bailey, W. A., and Bossing, E. N., "High Strength Aluminum Alloy Airframe Castings," Modern Castings (October 1961).
30. Lombardo, J. J., Dixon, C. E., and Begley, J., "Cryogenic Radiation Effects on NERVA Structural Materials," ASTM Preprint No. 44 (June, 1966).
31. "SAE Handbook, Standards, Information Reports, Recommended Practices," SAE, Incorporated (1965).
32. Nowak , J. J., "Preparation of Aluminum Alloys for UDMH Service," Bell Aerosystems Company, Report No. I-237 Revision A (October, 1962).
33. Colwell, D. L., "Melting Practice for Aluminum Die and Permanent Mold Castings," Modern Castings, Volume 39 (April, 1961).
34. Kangilaski, M., "The Effects of Neutron Radiation on Structural Materials," REIC Report No. 45 to NASA, Radiation Effects Information Center, Battelle Memorial Institute (June, 1967).
35. Graber, M. J., and Ronsick, J. H., "ETR Damage Surveillance Programs," Progress Report No. 1, IDO-16628 (1961).
36. Elijah, L. M., "Aluminum Alloy Fluxes," Foundry (March, 1964) p. 88.
37. 1968 Book of ASTM Standards, Part 6, "Die-Cast Metals; Light Metals and Alloys" (October, 1968).
38. Flemings, M. C., Conrad, H. F., and Taylor, H. F., "Aluminum Alloys Fluidity Test," Transactions, American Foundrymen's Society, Volume 67 (1959), p. 496.
39. Aluminum, "Fabrication and Finishing" (Edited by K. R. VanHorn) Volume 3, American Society for Metals (1967).
40. "Welding Alcoa Aluminum," Aluminum Company of America (1958).
41. "Brazing Alcoa Aluminum," Aluminum Company of America (1959).

	Al
4.5	Cu
1	Mn
1	Si
0.5	Mg

2014, Clad 2014

3.023 Impact (see 3.033).
3.024 Bending.
3.025 Torsion and shear (see 3.035).
3.0251 Shear ultimate strength of hand forgings, Table 3.0251.
3.026 Bearing (see also 3.036).
3.0261 Bearing property reductions for thick plate, Table 3.0261.
3.0262 Pin bearing strength of plate in the T651 Condition, Table 3.0262.
3.0263 Bearing strength of hand forgings, Table 3.0263.
3.027 Stress concentration.
3.0271 Notch properties.
3.02711 Strength of sheet containing shallow cracks, Figure 3.02711.
3.0272 Fracture toughness (see Appendix C).
3.02721 Results of fracture toughness tests on plate in the T651 Condition, Table 3.02721.
3.02722 Plane strain fracture toughness for various thicknesses of T651 plate, Table 3.02722.
3.02723 Plane strain fracture toughness of hand forgings and extrusions, Table 3.02723.
3.02724 Plane strain fracture toughness of plate tested in several directions, Table 3.02724.
3.028 Combined properties.

3.03 Mechanical Properties at Various Temperatures
3.031 Tension.
3.0311 Stress-strain diagrams (see also 3.0211).
3.03111 Stress-strain curves for alloy in T6 Condition at various temperatures, Figure 3.03111.
3.03112 Stress-strain curves for clad sheet in T6 Condition at room and elevated temperatures, Figure 3.03112.
3.03113 Stress-strain curves for sheet in T6 Condition at low temperatures, Figure 3.03113.
3.0312 Typical tensile properties at various temperatures for alloy in T6 Condition, Figure 3.0312.
3.0313 Effect of exposure and test temperature on tensile properties of alloy in T6 Condition, Figure 3.0313.
3.0314 Effect of exposure and test temperature on tensile properties of clad sheet in T6 Condition, Figure 3.0314.
3.0315 Effect of low test temperature on tensile properties of sheet and bar in T6 Condition, Figure 3.0315.
3.03151 Mechanical properties of bar at low temperatures, Table 3.03151.
3.0316 Effect of low temperatures on tensile properties and hardness of forgings in T6 Condition, Figure 3.0316.
3.0317 Effect of test temperature on F_{tu}, F_{ty} and F_{cy} of clad sheet in T6 Condition, Figure 3.0317.
3.0318 Effect of exposure on room temperature tensile properties of T6 forged rod, Figure 3.0318.
3.0319 Effect of exposure on room temperature tensile properties of T6 rolled and drawn rod, Figure 3.0319.
3.032 Compression (see also 3.0317).
3.0321 Stress-strain diagrams.
3.03211 Stress-strain curves in compression for clad sheet in T6 Condition at room and elevated temperatures, Figure 3.03211.
3.0322 Effect of exposure and test temperature on compressive yield strength of clad sheet in T6 Condition, Figure 3.0322.
3.033 Impact.
3.0331 Effect of low temperatures on Charpy V impact properties of plate, Figure 3.0331.
3.034 Bending (see 3.024).
3.035 Torsion and shear.
3.0351 Effect of exposure and test temperature on shear strength of clad sheet in T6 Condition, Figure 3.0351.
3.0352 Effect of low temperature on shear strength of sheet in T6 Condition, Figure 3.0352.
3.0353 Effect of test temperature on F_{bru}, F_{bry} and F_{su} of clad sheet in T6 Condition, Figure 3.0353.
3.036 Bearing (see also 3.0353).
3.0361 Effect of exposure and test temperature on bearing properties of clad sheet in T6 Condition, Figure 3.0361.
3.037 Stress concentration.
3.0371 Notch properties.
3.03711 Effect of low test temperatures on notched and smooth sheet in T6 Condition, Figure 3.03711.
3.03712 Effect of low temperature on tensile and sharp notch properties of sheet in T6 Condition, Figure 3.03712.
3.03713 Effect of low test temperature on notch strength and fracture toughness of sheet in T6 Condition, Figure 3.03713.
3.03714 Effect of low temperature on tensile and notch properties of sheet in the T6 Condition, Figure 3.03714.
3.0372 Fracture toughness (see also 3.03713). (See Appendix C.)
3.03721 Fracture test data for thin walled cylinders tested at -320 F, Table 3.03721.
3.038 Combined properties.

3.04 Creep and Creep Rupture Properties
3.041 Creep and creep rupture curves for alloy in T6 Condition 212-600 F, Figure 3.041.
3.042 Short time total strain curves for clad sheet in T6 Condition at 300 to 600 F, Figure 3.042.
3.043 Isochronous stress-strain curves in tension for alloy in T6 Condition at 400 F, Figure 3.043.

3.05 Fatigue Properties
3.051 Typical fatigue strength of alloy in T4 and T6 Conditions, Table 3.051.
3.052 Average stress range diagrams for bar and extrusions in T6 Condition, Figure 3.052.
3.053 Stress range diagrams for smooth and notched bar in T6 Condition, Figure 3.053.
3.054 Scatter band of fatigue data for smooth and notched hand forged bar in T6 Condition, Figure 3.054.
3.055 S-N curves for alloy tested in air and in simulated sea water, Figure 3.055.

	Al
4.5	Cu
1	Mn
1	Si
0.5	Mg

2014, Clad 2014

3.056 Effect of strain cycling on fatigue life in T6 bar, Figure 3.056.

3.057 Effect of low temperature on smooth and notched fatigue strength in sheet, Figure 3.057.

3.058 Effect of low temperatures on strain cycle fatigue of bar, Figure 3.058.

3.059 Scatter band for fatigue crack growth data for sheet, Figure 3.059.

3.0510 Scatter band for fatigue crack growth data for hand forgings, Figure 3.0510.

3.0511 Scatter band for fatigue crack growth data for forgings, Figure 3.0511.

3.06 Elastic Properties
(See also Table 3.03151.)

3.061 Poisson's ratio (elastic and plastic), Table 3.061.

3.062 Modulus of elasticity, E.

3.0621 Bare products,
Condition O, T4 and T6; E = 10.6×10^3 ksi,
Clad products,
Condition O, T3, T4 and T6; E = 10.5×10^3 ksi (13).

3.0622 Effect of temperature on E and E_c, Figure 3.0622.

3.0623 Compression modulus, E_c is approximately 2 percent higher than tension modulus, E (13).

3.0624 Elastic moduli in tension and compression for hand forgings tested in several directions, Table 3.0624.

3.063 Modulus of rigidity.

3.0631 Design value at RT. G = 4.0×10^3 ksi (5).

3.064 Tangent modulus.

3.0641 Typical tangent modulus curves for clad sheet at room temperature, Figure 3.0641.

3.0642 Tangent modulus curves in compression for clad sheet in T6 Condition at room and elevated temperatures, Figure 3.0642.

3.0643 Typical tangent modulus curves for extrusions and rolled products at room temperature, Figure 3.0643.

3.065 Secant modulus.

4. FABRICATION
(See also 2024 alloy.)

4.01 Forming

4.011 General. The alloy exhibits good forming characteristics, superior to alloys such as 7075 but inferior to 6061 alloy. In the O Condition, its formability is comparable to 2024-O, and the W Condition is slightly better than 2024-W.

4.012 Forming operations may be performed in the freshly quenched (W) Condition and maximum formability is attained immediately after quenching within about 20 minutes. If refrigeration is used the following maximum holding times are suggested:

RT	20 minutes
32 F	24 hours
20 F	3 days
Zero F	7 days

4.0121 For mild operations, the alloy can be formed in the T3 or T4 Conditions, but this involves die allowances for "springback" and general inconvenience as compared with forming in the W Condition.

4.0122 Material in T6 Condition has very limited formability at room temperature and is comparable to 7075-T6. Hot forming at 350–700 F may be used to advantage for T6 Condition but time at temperature should be limited to the values given in Figure 4.0122.

4.01221 Maximum time at various temperatures for hot forming sheet in T-6 condition, Figure 4.01221.

4.0123 Hot forming in W or T4 Conditions is permissible only if subsequently aged to T6 Condition and offers little advantage over hot forming in T6 Condition.

4.013 Forging.

4.0131 The 2014 alloy is widely used as a forging alloy and it has forging characteristics superior to 7075 or 7079 alloys. Starting temperature 875 F maximum, finishing temperature 600 F minimum. Maximum temperature should not be exceeded to prevent hot shortness, particularly in hammer forging.

4.014 Bending.

4.0141 Approximate bend radii for 90 degree cold bend, Table 4.0141.

4.02 Machining and Grinding

4.021 This alloy is readily machined in all conventional machining operations. Best machinability is obtained in the hardest temper. In the softer tempers, alloy tends to be somewhat gummy.

4.022 Typical grinding operations use a wheel of type A46KV at a speed of 6000 feet per minute and table speed of 60 feet per minute. A down feed of about 0.001 inch per pass will give a rough finish. A fine finish is produced at 0.0005 inch per pass. A water base emulsion is used as the grinding fluid.

4.023 Removal of material by either electro-chemical milling (ECM) or chemical milling may be successfully accomplished.

4.03 Joining

4.031 General. The heat treatable alloys, such as 2014, are slightly more difficult to weld than the nonheat treatable aluminum alloys. However, with proper precautions, refined techniques and close control of variables, the 2014 alloy is satisfactorily welded by both fusion and resistance techniques.

4.032 Fusion welding is usually accomplished by GTA or GMA welding methods using 4043 or 2319 aluminum alloy filler wire when required. Generally, the alloy is used in the "as welded" condition, with the weld joint about twice the thickness of the base metal to compensate for the lower strength in this condition. Stress corrosion tests have indicated that "as welded" joints have superior corrosion resistance to joints aged after welding. The strength of welded joints is apparently reduced

	Al
4.5	Cu
1	Mn
1	Si
0.5	Mg

2014, Clad 2014

by porosity and mismatch of parts and these factors should be held to a minimum wherever possible. Strength of joints may also be impaired by repair welding.

4.0321 Effect of welding speed on tensile strength of GTA welds, Figure 4.0321.

4.0322 Combined effect of porosity and mismatch for GTA welded sheet, Figure 4.0322.

4.0323 Effect of cryogenic temperatures on tensile properties of weldments and parent metal sheet in T6 Condition, Figure 4.0323.

4.0324 S-N fatigue curves for GTA butt-welded sheet at room and cryogenic temperatures, Figure 4.0324.

4.033 Resistance welding of 2014 alloy is successfully accomplished but requires special practices. Spot welds are best made in heat treated material. Spot welding of annealed material is not recommended. Corrosion resistance of clad material is good but resistance of bare material is poor.

4.034 Brazing and soldering of 2014 products are not recommended.

4.04 Surface Treatment

4.041 Alloy is available as Alclad sheet and plate which have a high resistance to surface corrosion and which may be used without additional protective coatings for many applications (47) (48).

4.042 A wide variety of surface treatments may be employed to protect and improve surface appearance. These include mechanical, chemical and electrochemical finishes and organic, porcelain and paint coatings. Detailed information on surface protection is available from the producers of aluminum alloys (47) (48).

REFERENCES

1. AMS 4014B
AMS 4028D
AMS 4029E
AMS 4121D
AMS 4134A
AMS 4135K
AMS 4153F
(Available from Society of Automotive Engineers, Inc.)
2. "The Aluminum Data Book", Reynolds Metal Co. (1958).
3. "Standards for Aluminum Mill Products", Eighth Edition, Aluminum Association (1965).
4. "Aluminum Handbook", Aluminum Co. of America (1962).
5. "Metallic Materials & Elements for Flight Vehicle Structures", Military Handbook – 5, Dept. of Defense, FSC 1500 (August 1962).
6. "Data Sheet", Aluminum Co. of America, Research Laboratories (August 29, 1957).
7. "Tensile Stress-Strain Curves for 2014-T6", Aluminum Co. of America, Research Laboratories (September 26, 1958).
8. Miller, D. E., "Determining Physical Properties of Ferrous and Non-Ferrous Structural Sheet Materials at Elevated Temperatures", AFTR 6517, Pt. 3 (December 1953).
9. Howell, F. M., Stickley, G. W., "Isochronous Stress-Strain Curves for Several Heat-Treated Wrought Aluminum Alloys at 300 and 400 F", Alcoa Research Laboratories, Mechanical Testing Div. (April 29, 1958).
10. Van Echo, J. A., Wirth, W. F., Simmons, W. F., "Short-Time Creep Properties of Structural Sheet Materials for Aircraft & Missiles", AFTR 6731, Pt. III (May 1955).
11. Lazan, B. J., Blatherwick, A. A., "Fatigue Properties of Aluminum Alloys at Various Direct Stress Ratios", WADC TR 52-307, Pt. II (December 1952).
12. Howell, F. M., Miller, D. E., "Axial-Stress Fatigue Strengths of Several Structural Aluminum Alloys", ASTM Proceedings, Vol. 55 (1955).
13. "Metals Handbook", American Society for Metals, 8th Edition (1961).
14. "Metals Handbook", American Society for Metals, 7th Edition (1948).
15. "Aluminum Sheet & Plate, General Information, Mechanical Properties, Physical Properties", Aluminum Co. of America, Product Data (December 1, 1961).
16. "Data Sheet", General Electric Co. (April 26, 1957).
17. "Sheet & Plate Product Information", 2nd Edition, Kaiser Aluminum Corp. (1958).
18. "Structural Handbook", Aluminum Co. of America (1960).
19. "Compilation of Materials Research Data – 4th Quarterly Progress Report – Phase I", General Dynamics Astronautics, Rep. AE 62-0138-3 (March 1962).
20. "Phase II – Cryogenic Properties of 2014-T6 and A-286", Bell Aerosystems Co., BLR61-35(M) Rev. A (June 29, 1962).
21. Christian, J. L., "Physical and Mechanical Properties of Pressure Vessel Materials for Applications in a Cryogenic Environment", ASD-TDR-62-258 (March 1962).
22. "Index of Specifications and Standards", Part I, Alphabetical Listing, Department of Defense (September 1964).
23. "Light Metals and Alloys", ASTM Standards, Part 6 (October 1965).
24. Materials in Design Engineering, Materials Selector Issue (Mid-October 1965).
25. Sprowls, D. O., Brown, R. H., "Stress Corrosion of Aluminum", Metal Progress, Vol. 81, No. 4 (April 1962).
26. Terry, E. L., McClaren, S. W., "Biaxial Stress and Strain Data on High Strength Alloys for Design of Pressurized Components", Chance-Vought Corp., ASD-TDR-62-401 (1962).
27. Bockrath, G. E., Glassco, J. B., "Fracture Toughness of High Strength Sheet Metal", Douglas Missile & Space Systems Div. (March 1963).
28. Military Specification, MIL-H-6088 C (October 15, 1962).

	Al
4.5	Cu
1	Mn
1	Si
0.5	Mg

2014, Clad 2014

REFERENCES (Continued)

29. Schwartzberg, F. R., et al., "Cryogenic Materials Data Handbook", Martin Co. Denver, ML-TDR-64-280 (August 1964).
30. "The Aluminum Data Book", Reynolds Metals Co. (1965).
31. Belton, J. H., et al., "Materials for Use at Liquid Hydrogen Temperatures", ASTM-STP 287 (1960).
32. Hanson, M. P., et al., "Sharp Notch Behavior of Some High Strength Aluminum Alloys & Welded Joints at 75, -320, and -423 F, ASTM STP 287 (1960).
33. Lucas, W. R., Cataldo, C. E., "Some Low Temperature Properties of Aluminum Alloy Weldments", ASTM-STP-287 (1960).
34. "Report on the Elevated Temperature Properties of Aluminum & Magnesium Alloys", ASTM-STP 291 (October 1960).
35. Paul, D. A., Wang, O. Y., "Fatigue Behavior of 2014-T6, 7075-T6 and 7079-T6 Aluminum Alloy Regular Hand Forgings", WADC-TR-59-591 (1960).
36. Austin, C. W., "Rotating-Beam Fatigue & Corrosion Fatigue Properties of Aluminum & Magnesium Alloys", Rpt. No. DS-TN-169, Army Ballistic Missile Agency (February 1958).
37. Smith, R. W., et al., "Fatigue Behavior of Materials Under Strain Cycling in Low & Intermediate Life Range", NASA Lewis Research Center, NASA TN D-1574 (1963).
38. Birch, W. L., "Fusion Welding of 2014 Aluminum Alloys", Bell Lab Report BLR 61-41 (M), Bell Aerosystems Co. (1961).
39 Bandelin, B. G., "Evaluation of the Combined Effects of Porosity & Mismatch on Weld Strength of 2014-T6 Aluminum Alloy", Martin Co. (1964).
40. "Aluminum – Fabrication and Finishing", Vol. III, Edited by K. R. Van Horn, American Society for Metals (1967).
41. "Aluminum Standards and Data", Fifth Edition, The Aluminum Association, Inc. (1976).
42. Shreir, L. L., "Corrosion", Vol. I, Sect. 4.1, John Wiley & Sons (1963).
43. Aziz, P. M., Goddard, H. P., "Corrosion" (1959).
44. Pierce, W. S., "Effects of Surface and Through Cracks on Failure of Pressurized Thin Walled Cylinders of 2014-T6 Aluminum", NASA TN D-6099 (Nov. 1970).
45. Nachtigall, A. J., Klima, S. J., Freche, J. C., "Fatigue of Liquid Rocket Engine Metals at Cryogenic Temperatures to -452 F", NASA TN D-4274 (December 1967).
46. Reid, R. J., Jones, A. H., Green, S. J., "Characterization of 2014-T651 Aluminum Alloy", AMMRC CTR 74-68, Army Materials and Mechanics Research Center (November 1974).
47. Sessler, J. G., Weiss, V. W., "Materials Data Handbook – Aluminum Alloy 2014", NASA-CR-84454, Syracuse University Research Institute (April 1966).
48. Muraca, R. F., Whittick, J. S., "Materials Data Handbook – Aluminum Alloy 2014", 2nd Edition, NASA-CR-123779, Accession No. N72-31535, Western Applied Research & Development, Inc. (May 1972).
49. Nachtigall, A. J., "Strain Cycling Fatigue Behavior of Ten Structural Metals Tested in Liquid Helium (4 K), in Liquid Nitrogen (78 K), and in Ambient Air (300 K)", NASA TN D-7532, NASA Lewis Research Center (February 1974).
50. Wygouik, R. H., "Compilation of Fracture Mechanics Data", Alcoa AF Contract F33-615-73-C-5051 (June 1973).
51. Brownhill, D. J., Babilon, C. F., Nordmark, G. E., Sprowls, D. O., "Mechanical Properties Including Fracture Toughness & Fatigue, Corrosion Characteristics & Fatigue Crack Propagation Rates of Stress-Relieved Aluminum Alloy Hand Forgings", AFML TR 70-10 (February 1970).
52. Brown, W. F., Jr., Unpublished data from NASA-Lewis Lab. (1974).
53. Damage Tolerant Design Handbook HB01 MCIC (January 1975), Figs. NAA3 and NAA4.
54. Sprowls, D. O., Shumaker, M. B., Walsh, J. D., Coursen, J. W., "Evaluation of Stress Corrosion Cracking Susceptibility Using Fracture Mechanics Techniques", Alcoa NASA Contract NAS8-21487, Final Report, Part I (May 1973).
55. "Military Standardization Handbook, Metallic Materials and Elements for Aerospace Vehicle Structures", MIL-HDBK-5C, FSC 1560, 15 September 1976.

ADDITIONAL BIBLIOGRAPHY
References (Not Used)

1. Orange, T. W., "Fracture Toughness of Wide 2014-T6 Aluminum Sheet at -320 F", NASA TN D-4017 (1967).
2. Czyryca, E. J., Vassilaros, M. G., "Engineering Properties of Structural Aluminum Alloys – A Handbook", Report No. 3571, Naval Ship Research & Development Center (June 1972).
3. Kaufman, J. G., Brownhill, D. J., Davies, R. E., Babilow, C. F., "New Data on the Moduli of Elasticity of Aluminum Alloys", ASTM Journal of Materials, Vol. 6, No. 4 (December 1971).
4. Ezra, A. A., "Advances in the Theory of Explosive Metalworking", ASTM Journal of Materials, Vol. 4, No. 2 (June 1969).
5. Haynie, F. H., Boyd, W. K., "Stress Corrosion Cracking of Aluminum Alloys", DMIC Report 228, Battelle Memorial Institute (July 1966).
6. Evans, R. M., Maykuth, D. J., "Weldability of High Strength Aluminum Alloys", DMIC Memorandum 216, Battelle Memorial Institute (August 1966).
7. Klima, S. J., Freche, J. C., "Ultrasonic Detection and Measurement of Fatigue Cracks in Notched Specimens", NASA TN D-4782 (September 1968).
8. Marschall, C. W., Maringer, R. E., "Stress Relaxation as a Source of Dimensional Instability", ASTM Journal of Materials (June 1971).

Alloy	2014	
Source	(1)	
AMS	Condition	Form
4014B	T651	Plate
4028D	O	Sheet and Plate (bare)
4029E	T6	Sheet (bare)
	T651	Plate (bare)
4121D	T6	Bar, Rods, Wire (rolled, drawn or cold finished)
4133	T6	Forgings
4134A	T4	Die Forgings and Forging Stock
4135K	T6	Die Forgings, Hand Forgings and Forging Stock
4153F	T6	Extrusions

	Al
4.5	Cu
1	Mn
1	Si
0.5	Mg

2014,
Clad 2014

TABLE 1.031 AMS SPECIFICATIONS

Alloy	2014		
Form	Military	Federal	ASTM
Sheet and Plate (bare)	-	QQA-250d	B209
Bar, Rod, Wire (rolled or cold finished)	-	QQ-A-225/4c	B211
Bar, Rod, Wire, Shapes (extruded)	-	QQ-A-200/2D	B221
Tube, seamless (extruded)	-	-	B241
Tube, seamless (drawn)	-	-	B210
Forgings and Forging Stock	MIL-A-22771	QQ-A-367g	B247
Impact extrusions	MIL-A-12545	-	-
Sheet and Plate (Alclad)	-	QQ-A-250/3E	B209
Structural shapes (rolled or extruded)	- MIL-A-25994	- -	- B308

TABLE 1.032 SIMILAR SPECIFICATIONS

Alloy	2014		2014		6003		6053	
Source	AMS (1)		(41)		(41)		(41)	
	Core		Core		Cladding		Cladding	
	Percent		Percent		Percent		Percent	
	Min.	Max.	Min.	Max.	Min.	Max.	Min.	Max.
Copper	3.90	5.00	3.9	5.0	-	0.10	-	0.10
Magnesium	0.20	0.80	0.20	0.8	0.8	1.5	1.1	1.4
Manganese	0.40	1.20	0.40	1.2	-	0.8	-	-
Iron	-	1.00	-	0.7	-	0.6	-	0.35
Silicon	0.50	1.20	0.50	1.2	0.35	1.0	-	(a)
Zinc	-	0.25	-	0.25	-	0.20	-	0.10
Chromium	-	0.10	-	0.10	-	0.35	0.15	0.35
Titanium	-	0.15	(b)	0.15	-	0.10	-	-
Other Impurities								
each	-	0.05	-	0.05	-	0.05	-	0.05
total	-	0.15	-	0.15	-	0.15	-	0.15
Aluminum	Remainder		Remainder		Remainder		Remainder	

(a) Silicon 45 to 65 percent of magnesium content.
(b) Zirconium + titanium 0.20 percent maximum.

TABLE 1.04 COMPOSITION

	Al
4.5	Cu
1	Mn
1	Si
0.5	Mg

2014,
Clad 2014

Source	(28)
Alloy	2014
Data	Maximum quench delay times (a)
Nominal thickness	Maximum time, seconds
≤ 0.016 in	5
0.017 to 0.032 in	7
0.033 to 0.091 in	10
≥ 0.091 in	15

(a) For immersion type quenching after solution treatment

TABLE 1.0521 MAXIMUM ALLOWABLE QUENCH DELAY TIMES

Source	(13)(24)	
Alloy	2014	
Condition	Brinell scale	Rockwell scale
O	45	H87-98
T4	105	B65-73
T6	135	B80-86

TABLE 1.061 TYPICAL HARDNESS VALUES AT ROOM TEMPERATURES

Source	(41)
Temperature	R. T.
Condition	Thermal Conductivity-Btu-ft. per (hr. sq. ft. F)
O	111.6
T4	77.5
T6	89.2

TABLE 2.013 THERMAL CONDUCTIVITY

Source	(41)
Alloy	2014 and Clad 2014
Product	Available tempers
Bare sheet and plate	O, T3, T4, T451, T6, T651
Clad sheet and plate	O, T3, T4, T451, T6, T651
Wire, rod, bar (rolled or CF)	O, T4, T451, T6, T651
Rod, bar, shapes, tube (extruded)	O, T4, T4510, T4511, T6, T6510, T6511
Drawn tube	O, T4, T6
Forgings	T4, T6, T652

TABLE 1.073 CONDITIONS AVAILABLE

Source	(41)
Condition	Electrical Resistivity at 68F - Microhm inch
O	1.34
T4	2.01
T6	1.69

TABLE 2.0221 ELECTRICAL RESISTIVITY

Source	(25)		
Alloy	2014 - T6		
Form	0.063 in sheet		
Test Data	Resistance to stress corrosion		
Environment	Exposure (days)	Average loss in F_{tu}, percent Unstressed	Stressed 75% of F_{ty}
Inland industrial	365	7	7
Sea coast	365	18	28
3.5% NaCl (alternate immersion)	84	42	55

TABLE 2.033 RESISTANCE TO STRESS CORROSION IN VARIOUS ENVIRONMENTS

Alloy	2014-T6				
Source	(25)				
Test Data	SCR-Highest Sustained Tensile Stress Without Failure, ksi				
Test Direction	Plate	Bar	Extruded Shapes 0.25-1 in.	Extruded Shapes 1.25-2 in.	Hand Forgings
L	45	45	50	45	30
T	30	-	27	22	25
ST	7	15	-	7	7
Test Environment: 3.5 percent NaCl, alternate immersion, 12 weeks SCR - Stress corrosion resistance					

TABLE 2.0331 STRESS CORROSION RESISTANCE OF PLATE, BAR, SHAPES AND FORGINGS IN ALTERNATE IMMERSION TESTS

Source	(13)
Environment	Aqueous Solution of 53 gr. NaCl and 3 gr. H_2O per Liter
Test Data	Electrode Potentials vs 0.1 N Calomel at 25°C
2014-T4	0.69 volt
2014-T6	0.78 volt
Alclad 2014	0.83 volt
Al(99.5 + %)	0.85 volt

TABLE 2.0332 ELECTRODE POTENTIALS OF ALLOY IN VARIOUS CONDITIONS

Al
4.5 Cu
1 Mn
1 Si
0.5 Mg

2014, Clad 2014

Alloy	2014								
Source	(51 - Tables 26 to 29)								
Form	Hand Forgings								
Condition	T652								
Size - (inch)	2 x 8								
Direction	L	LT	ST	L	LT	LT	ST	ST	ST
Exposure stress percent F_{ty} (a)	O	O	O	75	75	50	37	25	12
Range of failure time - days (c)	-	-	-	NF 182	8 to 64	NF 182	NF 84	NF 84	NF 84
Reduction in (b) F_{tu} - percent	5	1	8	8	-	29	21	17	9

(a) Initial stress under constant displacement. Alternate immersion-10 minutes in 3½ percent NaCl and 50 minutes in air. Tests at ambient lab conditions.
(b) Retained F_{tu} following alternate immersion with or without stress.
(c) NF - no failure indicated.

TABLE 2.0333 RESULTS OF ALTERNATE IMMERSION STRESS CORROSION TESTS ON 2 x 8 INCH HAND FORGINGS

Alloy	2014								
Source	(51 - Table 26 to 29)								
Condition	T652 (Hand Forgings)								
Size-(inch)	6 x 24								
Direction	L	LT	ST	L	LT	LT	ST	ST	ST
Exposure stress percent F_{ty} (a)	O	O	O	75	75	50	37	25	12
Range of failure time - days	-	-	-	NF 182	23 to 113	NF 182	4 to 5	10 to 21	NF 84
Reduction in F_{tu} - percent	5	18	20	6	27	-	-	-	23

(a) See Table 2.0233 for details.

TABLE 2.0334 RESULTS OF ALTERNATE IMMERSION STRESS CORROSION TESTS ON 6 x 24 INCH HAND FORGINGS

Source	(41)				
Alloy	2014				
Form	Bar, Wire	Extruded bar tube, shapes	Drawn tube	Sheet and plate	
Condition	0				
Thickness - in	≤8.00 dia	All	All	0.020 to 0.499	0.500 to 1.000
F_{tu}, max -ksi	35	30	32	32	32
F_{ty}, max -ksi	-	18	16	16	-
e, min-percent	12	12	-	16	10

TABLE 3.011 ALUMINUM ASSOCIATION MECHANICAL PROPERTY LIMITS FOR VARIOUS PRODUCTS IN THE 0 CONDITION

	Al
4.5	Cu
1	Mn
1	Si
0.5	Mg

2014, Clad 2014

Alloy	2014 (Bare)					
Source	(41)					
Form	Flat Sheet		Coiled Sheet	Sheet & Plate	Sheet	
Condition	T3		T4	T42	T6 & T62	
Thickness, (inch)	0.020-0.039	0.040-0.249	0.020-0.249	0.020-1.000	0.020-0.039	0.040-0.249
F_{tu}(min.) - (ksi)	59.0	59.0	59.0	58.0	64.0	66.0
F_{ty}(min.) - (ksi)	35.0	36.0	35.0	34.0	57.0	58.0
e(2in.) - percent (min.)	14	14	14	14	6	7

TABLE 3.012 ALUMINUM ASSOCIATION MECHANICAL PROPERTY LIMITS FOR BARE SHEET AND PLATE IN THE T3, T4, T42, T6 and T62 CONDITIONS

Alloy	2014 (Bare)									
Source	(41)									
Form	Plate				Plate					
Condition	T451				T62 & T651					
Thickness, inch	0.250-0.499	0.500-1.000	1.001-2.000	2.001-3.000	0.250-0.499	0.500-1.000	1.001-2.000	2.001-2.500	2.501-3.000	3.001-4.000
F_{tu}(min.) - ksi	58.0	58.0	58.0	57.0	67.0	67.0	67.0	65.0	63.0	59.0
F_{ty}(min.) - ksi	36.0	36.0	36.0	36.0	59.0	59.0	59.0	58.0	57.0	55.0
e(2 in.) - percent (min.)	14	14	12	8	7	6	4	2	2	1

TABLE 3.0121 ALUMINUM ASSOCIATION MECHANICAL PROPERTY LIMITS FOR BARE PLATE IN THE T451, T62 and T651 CONDITIONS

Alloy	Alclad 2014									
Source	(41)									
Form	Flat Sheet			Coiled Sheet				Sheet		
Condition	T3			T4				T6 & T62		
Thickness, inch	0.020-0.024	0.025-0.039	0.040-0.249	0.020-0.024	0.025-0.039	0.040-0.128	0.129-0.249	0.020-0.024	0.025-0.039	0.040-0.249
F_{tu}(min.) - ksi	54.0	55.0	57.0	54.0	55.0	57.0	57.0	62.0	63.0	64.0
F_{ty}(min.) - ksi	33.0	34.0	35.0	31.0	32.0	34.0	34.0	54.0	55.0	57.0
e(2in.) - percent (min.)	14	14	15	14	14	15	15	7	7	8

TABLE 3.0122 ALUMINUM ASSOCIATION MECHANICAL PROPERTY LIMITS FOR ALCLAD SHEET IN THE T3, T4, T6 AND T62 CONDITIONS

Alloy	Alclad 2014									
Source	(41)									
Form	Plate				Plate					
Condition	T451				T62 & T651					
Thickness, inch	0.250-0.499	0.500-1.000	1.001-2.000	2.001-3.000	0.250-0.499	0.500-1.000	1.001-2.000	2.001-2.500	2.501-3.000	3.001-4.000
F_{tu}(min.) - ksi	57.0	58.0	58.0	57.0	64.0	67.0	67.0	65.0	63.0	59.0
F_{ty}(min.) - ksi	36.0	36.0	36.0	36.0	57.0	59.0	59.0	58.0	57.0	55.0
e(2in.) - percent (min.)	15	14	12	8	8	6	4	2	2	1

TABLE 3.0123 ALUMINUM ASSOCIATION MECHANICAL PROPERTY LIMITS FOR ALCLAD PLATE IN THE T451, T62 and T651 CONDITIONS

Al	
4.5	Cu
1	Mn
1	Si
0.5	Mg

2014, Clad 2014

Alloy	2014					
Source	(41)					
Form	Alclad Sheet and Plate					
Condition	T42					
Thickness, inch	0.020-0.024	0.025-0.039	0.040-0.128	0.129-0.249	0.250-0.499	0.500-1.000
F_{tu}(min.)- ksi	54.0	55.0	57.0	57.0	57.0	58.0
F_{ty}(min.)- ksi	31.0	32.0	34.0	34.0	34.0	34.0
e(2 in.)- percent (min.)	14	14	15	15	15	14

TABLE 3.0124 ALUMINUM ASSOCIATION MECHANICAL PROPERTY LIMITS FOR ALCLAD SHEET AND PLATE IN THE T42 CONDITION

Alloy	2014	
Source	(41)	
Form	Wire, Rod & Bar (b)	
Condition	T4, T42, T451	T6, T62, T651
Diameter, inch (a)	≤ 8.000	≤ 8.000
F_{tu} (min.) - ksi	55.0	65.0
F_{ty} (min.) - ksi	32.0	55.0
e(2 in. or 4D) min.-percent	16	8
(a) Diameter or least distance between faces		
(b) Rolled or cold finished		

TABLE 3.013 ALUMINUM ASSOCIATION MECHANICAL PROPERTY LIMITS FOR COLD FINISHED WIRE, ROD AND BAR

Alloy	2014								
Source	(41)								
Form	Extruded Wire, Rod, Bar and Shapes								
Condition	T4, T4510 T4511	T42	T6, T6510, T6511				T62		
Area-in.^{2}	All	All	All	All	≤ 25	25-32	All	≤ 25	25-32
Thickness, in.	All	All	≤ 0.499	0.500-0.749	≥ 0.750	≥ 0.750	≤ 0.749	≥ 0.750	≥ 0.750
F_{tu}(min.)-ksi	50.0	50.0	60.0	64.0	68.0	68.0	60.0	60.0	60.0
F_{ty}(min.)-ksi	35.0	29.0	53.0	58.0	60.0	58.0	53.0	53.0	53.0
e(2 in.)-percent (min.)	12	12	7	7	7	6	7	7	6

TABLE 3.014 ALUMINUM ASSOCIATION MECHANICAL PROPERTY LIMITS FOR EXTRUDED WIRE, ROD, BAR AND SHAPES

Alloy	2014							
Source	(41)							
Form	Drawn Tube							
Condition	T4, T42				T6, T62			
Wall Thickness, in.	0.018 to 0.024	0.025 to 0.049	0.050 to 0.259	0.260 to 0.500	0.018 to 0.024	0.025 to 0.049	0.050 to 0.259	0.260 to 0.500
F_{tu}(min.)-ksi	54	54	54	54	65	65	65	65
F_{ty}(min.)-ksi	30	30	30	30	55	55	55	55
e(2 in. or 4D)								
A percent (min.)	10	12	14	16	7	7	8	9
B percent (min.)	-	10	10	12	-	6	7	8
A - Elongation for a full section specimen								
B - Elongation for a cut-out specimen								

TABLE 3.015 ALUMINUM ASSOCIATION MECHANICAL PROPERTY LIMITS FOR DRAWN TUBE

	Al
4.5	Cu
1	Mn
1	Si
0.5	Mg

2014, Clad 2014

Alloy	2014								
Source	(41)								
Form	Extruded Tube								
Condition	T4, T4510 T4511	T42	T6, T6510, T6511				T62		
Area-in.^{2}	All	All	All	All	≤25	25-32	All	≤25	25-32
Wall Thickness, in.	All	All	≤0.499	0.500-0.749	≥0.750	≥0.750	≤0.749	≥0.750	≥0.750
F_{tu}(min.)-ksi	50.0	50.0	60.0	64.0	68.0	68.0	60.0	60.0	60.0
F_{ty}(min.)-ksi	35.0	29.0	53.0	58.0	60.0	58.0	53.0	53.0	53.0
e(2 in. or 4D)-percent(min.)	12	12	7	7	7	6	7	7	6

TABLE 3.016 ALUMINUM ASSOCIATION MECHANICAL PROPERTY LIMITS FOR EXTRUDED TUBE

Alloy	2014									
Source	(41)									
Form	Die Forgings									
Condition	T4		T6							
Thickness, in.	≤4		≤1		>1 thru 2		>2 thru 3		>3 thru 4	
Orientation	A	B	A	B	A	B	A	B	A	B
F_{tu}(min.)-ksi	55.0	-	65.0	64.0	65.0	64.0	65.0	63.0	63.0	63.0
F_{ty}(min.)-ksi	30.0	-	56.0	55.0	56.0	55.0	55.0	54.0	55.0	54.0
e(2 in. or 4D) percent(min.)	11	-	6	3	6	2	6	2	6	2
Brinell Hardness(a)	100	-	125	-	125	-	125	-	125	-

A Specimen axis parallel to direction of grain flow
B Specimen axis not parallel to direction of grain flow
(a) 500 kg load - 10 mm ball

TABLE 3.017 ALUMINUM ASSOCIATION MECHANICAL PROPERTY LIMITS FOR DIE FORGINGS

Alloy	2014										
Source	(41)										
Form	Hand Forgings										
Condition	T6										
Thickness, in.	≤2.000		2.001 - 3.000			3.001 - 4.000			4.001 - 5.000		
Orientation	L	T	L	T	ST	L	T	ST	L	T	ST
F_{tu} (min.)-ksi	65.0	65.0	64.0	64.0	62.0	63.0	63.0	61.0	62.0	62.0	60.0
F_{ty} (min.)-ksi	56.0	56.0	56.0	55.0	55.0	55.0	55.0	54.0	54.0	54.0	53.0
e(2 in. or 4D) percent (min.)	8	3	8	3	2	8	3	2	7	2	1

TABLE 3.018 ALUMINUM ASSOCIATION MECHANICAL PROPERTY LIMITS FOR T6 HAND FORGINGS UP TO 5 INCHES THICK

Alloy	2014								
Source	(41)								
Form	Hand Forgings								
Condition	T6								
Thickness, in.	5.001 - 6.000			6.001 - 7.000			7.001 - 8.000		
Orientation	L	T	ST	L	T	ST	L	T	ST
F_{tu}(min.)-ksi	61.0	61.0	59.0	60.0	60.0	58.0	59.0	59.0	51.0
F_{ty}(min.)-ksi	53.0	53.0	53.0	52.0	52.0	52.0	51.0	51.0	51.0
e(2 in. or 4D) percent (min.)	7	2	1	6	2	1	6	2	1

TABLE 3.0181 ALUMINUM ASSOCIATION MECHANICAL PROPERTY LIMITS FOR T6 HAND FORGINGS 5 INCHES TO 8 INCHES THICK

	Al
4.5	Cu
1	Mn
1	Si
0.5	Mg

2014, Clad 2014

Alloy	2014										
Source	(41)										
Form	Hand Forgings										
Condition	T652										
Thickness, in.	≤ 2.000		2.001 - 3.000			3.001 - 4.000			4.001 - 5.000		
Orientation	L	T	L	T	ST	L	T	ST	L	T	ST
F_{tu}(min.)-ksi	65.0	65.0	64.0	64.0	62.0	63.0	63.0	61.0	62.0	62.0	60.0
F_{ty}(min.)-ksi	56.0	56.0	56.0	55.0	52.0	55.0	55.0	51.0	54.0	54.0	50.0
e(2 in. or 4D) percent(min.)	8	3	8	3	2	8	3	2	7	2	1

TABLE 3.0182 ALUMINUM ASSOCIATION MECHANICAL PROPERTY LIMITS FOR T652 HAND FORGINGS UP TO 5 INCHES THICK

Alloy	2014								
Source	(41)								
Form	Hand Forgings								
Condition	T652								
Thickness in.	5.001 - 6.000			6.001 - 7.000			7.001 - 8.000		
Orientation	L	T	ST	L	T	ST	L	T	ST
F_{tu}(min.)-ksi	61.0	61.0	59.0	60.0	60.0	58.0	59.0	59.0	57.0
F_{ty}(min.)-ksi	53.0	53.0	50.0	52.0	52.0	49.0	51.0	51.0	48.0
e(2 in. or 4D) percent(min.)	7	2	1	6	2	1	6	2	1

TABLE 3.0183 ALUMINUM ASSOCIATION MECHANICAL PROPERTY LIMITS FOR T652 HAND FORGINGS 5 INCHES TO 8 INCHES THICK

Source	(41)						
Alloy	Wrought products						
Form	2014			Clad 2014			
Condition	0	T4*	T6**	0	T3	T4*	T6**
F_{tu}, typ - ksi	27	62	70	25	63	61	68
F_{ty}, typ - ksi	14	42	60	10	40	37	60
F_{su}, typ - ksi	18	38	42	18	37	37	41
e, typ-percent	18	20	13	21	20	22	10
Hardness, BHN	45	105	135	-	-	-	-

*Also T451
**Also T651

TABLE 3.0213 TYPICAL MECHANICAL PROPERTIES AT ROOM TEMPERATURE

Alloy	2014								
Source	(51 - Table 2)								
Form	Hand Forgings								
Size - in.	2 x 8			4 x 8			6 x 24		
Direction	L	LT	ST	L	LT	ST	L	LT	ST
F_{cy} - ksi	69	70	69	66	65	69	58	62	59

TABLE 3.0222 COMPRESSIVE YIELD STRENGTH FOR HAND FORGINGS TESTED IN SEVERAL DIRECTIONS

	Al
4.5	Cu
1	Mn
1	Si
0.5	Mg

2014, Clad 2014

Alloy	2014								
Source	(51, Table 2)								
Form	Hand Forgings								
Condition	T652								
Size - in.	2 x 8			4 x 8			6 x 24		
Direction	L	LT	ST	L	LT	ST	L	LT	ST
F_{su} - ksi	44	44	-	40	41	40	43	39	39

TABLE 3.0251 SHEAR ULTIMATE STRENGTH OF HAND FORGINGS

Source	(55)
Thickness, inches	Bearing Property Reduction, percent 1.001–6.000
F_{bru} (e/D = 1.5)	15
F_{bru} (e/D = 2.0)	10
F_{bry} (e/D = 1.5)	5

TABLE 3.0261 BEARING PROPERTY REDUCTIONS FOR THICK PLATE WHERE THE STRESS CONDITION APPROXIMATES THE LONGITUDINAL OR LONG-TRANSVERSE EDGE-WIRE ORIENTATIONS

Alloy	2014 - T651		2 in. rolled plate (a)		
Source	(46)				
Pin Diameter (inch)	Edge Distance (in.)	e/D ratio (approx.)	Plate Thickness (in.)	Bearing Strength F_{bru} (ksi)	Bearing Yield Strength F_{bry} (ksi)
0.2503	0.501	2	0.152	152.6	109.2
	0.501	2	0.1252	140.4	106.9
	0.501	2	0.103	147.6	109.1
	0.375	1.5	0.150	109.2	98.5
	0.375	1.5	0.1226	102.8	94.6
	0.375	1.5	0.095	109.5	98.9
(a) All specimens taken in rolling direction.					

TABLE 3.0262 PIN BEARING STRENGTH OF ALLOY PLATE IN THE T651 CONDITION

Alloy	2014							
Source	(51, Table 2)							
Form	Hand Forgings							
Condition	T652							
Size - in.	2 x 8		4 x 8		5 x 10		6 x 24	
Direction	L	LT	L	LT	L	LT	L	LT
F_{bru} - ksi (e/D = 1.5)	101	101	89	91	93	89	90	86
F_{bry} - ksi (e/D = 1.5)	88	89	86	87	83	84	81	80
F_{bru} - ksi (e/D = 2)	123	130	124	122	117	123	118	118
F_{bry} - ksi (e/D = 2)	102	100	103	102	95	99	100	99

TABLE 3.0263 BEARING STRENGTH OF HAND FORGINGS

Al
4.5 Cu
1 Mn
1 Si
0.5 Mg

2014, Clad 2014

Alloy	2014-T651 2 in. Rolled Plate (a)				
Source	(46)				
Specimen Type	ASTM Compact Tension Fracture Toughness (b)				
Specimen Description	Initial Fatigue Load A - max. lbs. B - min. lbs.	Fatigue Cycles	Average Fatigue Crack Length in.	Loading Rate lbs/sec	K_{IC} ksi $\sqrt{in.}$
Straight Cut	A = 990 B = 110	26,000	0.085	16	24.3
Chevron	A = 1010 B = 100	72,000	0.077	17	25.6
Chevron	A = 1000 B = 100	76,000	0.107	16	23.5
Chevron	A = 1000 B = 100	64,000	0.098	154	25.1
Chevron	A = 1100 B = 150	57,500	0.113	154	25.5
Chevron	A = 1020 B = 100	98,000	0.071	166	23.7

(a) All specimens were taken in the rolling direction.
(b) Tests conducted according to ASTM E399-72. Specimens were 0.625 inches thick.

TABLE 3.02721 RESULTS OF FRACTURE TOUGHNESS TESTS ON PLATE IN THE T651 CONDITION

Alloy	2014										
Source	(50)										
Condition	T651										
Form	Plate										
Thickness-in.	1	1.5				1.75		2.5	5		
Direction	TL	TL	LT	LS	TS	LT	TL	LT	LT	TL	SL
F_{ty} - ksi	66	63	67	67	63	68	66	64	59	58	55
K_{IC} - ksi $\sqrt{in.}$	20	19	19	24	22	22	23	24	22	19	18

TABLE 3.02722 PLANE STRAIN FRACTURE TOUGHNESS FOR VARIOUS THICKNESSES OF T651 PLATE

Alloy	2014									
Source	(51, Table 22)									
Condition	T652								T8510	
Form	Hand Forgings								Extrusions	
Size-in.	2 x 8		4 x 16			5 x 20			-	
Direction	LT	TL	LT	TL	SL	LT	TL	SL	LT	TL
F_{ty} - ksi	67	65	62	59	67	61	57	56	-	-
K_{IC} - ksi in.	25	19	34	23	19	29	20	18	29	18

TABLE 3.02723 PLANE STRAIN FRACTURE TOUGHNESS OF HAND FORGINGS AND EXTRUSIONS

Alloy	2014				
Source	(54, Table 9)		(52)		
Condition	T651				
Form	Plate				
Thickness-in.	2.0		1.8.		
Direction	LT	SL	LT	LS	SL
F_{ty}-ksi	64	60	66	66	63
K_{IC}-ksi $\sqrt{in.}$	23	19	20	23	17

TABLE 3.02724 PLANE STRAIN FRACTURE TOUGHNESS OF PLATE TESTED IN SEVERAL DIRECTIONS

	Al
4.5	Cu
1	Mn
1	Si
0.5	Mg

2014,
Clad 2014

Alloy	2014		
Source	(49)		
Form	1.0 in. Bar Stock		
Condition	T6		
Test Temperature, F	80F	-320F	-452F
F_{tu} - ksi	77.5	86.1	118.5
F_{ty} - ksi	70.4	75.5	102.5
Tensile Ductility, D(a)	0.38	0.26	0.016
Modulus of Elasticity, E(b)	10.78	11.86	11.92
Poisson's Ratio, μ	0.321	0.337	0.335
(a) $D = \ln \frac{100}{100-RA}$			
(b) 1000 ksi			

TABLE 3.03151 MECHANICAL PROPERTIES OF BAR AT LOW TEMPERATURES

Alloy	2014-T6				
Source	(44)				
Specimen	Thin-Walled Cylinders (c)				
	Specimen Thickness t(in.)	Crack Depth a(in.)	Crack Length 2c(in.)	Fracture Stress σ_H (ksi)	Apparent Fracture Toughness K_Q(ksi$\sqrt{in.}$)
Outside - surface crack	0.061	0.025	0.096	85.3	23.5
		0.040	0.100	80.7	23.1
		0.050	0.114	74.1	22.8
		0.025	0.140	80.7	24.0
		0.039	0.240	72.9	27.3
		0.042	0.240	66.9	25.0
		0.041	0.300	61.3	23.6
		0.047	0.340	56.0	22.8
		0.044	0.370	58.4	23.1
		0.060	0.380	49.9(a)	18.0(b)
		0.041	0.450	55.5	22.0
		0.024	0.500	73.7	23.5
		0.039	0.955	46.9	18.4
		0.034	1.000	47.9	17.4
Inside - surface crack	0.061	0.022	0.442	73.9	22.8
	0.061	0.042	0.985	46.8	17.3
No crack	0.060	0	0	90.2	-
Through the thickness crack	0.062	0.062	0.154	66.0	-
	0.062	0.062	0.481	40.2	-
	0.061	0.061	1.012	23.6	-
(a) Leakage occurred at 41.0 ksi (b) Computed using stress at leakage (c) Tested at -320F					

TABLE 3.03721 FRACTURE TEST DATA FOR THIN WALLED CYLINDERS TESTED AT -320F

	Al
4.5	Cu
1	Mn
1	Si
0.5	Mg

2014, Clad 2014

Source	(5, p. 78)(6)(18, p. 83)								
Form	All								
Temp RT	Method	Stress Ratio		Stress Concentration	Fatigue Strength - ksi at Cycles				Ref
Condition		A	R		10^5	10^6	10^7	10^8	$5x10^8$	
T4	Rot beam	∞	-1	Smooth K = 1	42	34	27	22	20	(18)
T6				Smooth K = 1	39	30	24	19	18	(6)
				Notched K = 8	21	14	10	9	9	(5)

TABLE 3.051 TYPICAL FATIGUE STRENGTH OF ALLOY IN T4 AND T6 CONDITIONS

Source	(26)	
Alloy	2014-T6	
Property	Poisson's Ratio (elastic and plastic values)	
Form	0.125 in sheet (a)	
Grain Direction	μ, elastic	μ, plastic
Longitudinal	0.33	0.48
Transverse	0.27	0.52

(a) Purchased in the form of clad, heat treated sheet. Cladding removed prior to testing

TABLE 3.061 POISSON'S RATIO

Alloy		2014	
Source		(51, Table 21)	
Form		Hand Forgings (a)	
Condition		T652	
Direction	L	LT	ST
E_T - 1000 ksi	10.40	10.49	10.40
E_C - 1000 ksi	10.74	10.89	10.75
(a) Average values from 2 to 6 inch thick sections.			

TABLE 3.0624 ELASTIC MODULI IN TENSION AND COMPRESSION FOR HAND FORGINGS TESTED IN SEVERAL DIRECTIONS

Source	(3)			
Alloy	2014			
Data	Approximate bend radii for 90 degree cold bend (a)			
Form	Sheet			
Thickness-in	1/16	1/8	1/4	1/2
0	0	0	0 - 1t	3 - 5t
T3	2 - 4t	3 - 5t	4 - 6t	5.5- 8t
T4	2 - 4t	3 - 5t	4 - 6t	5.5- 8t
T6	3 - 5t	4 - 6t	6 -10t	8 -11t

(a) Radii for various thickness sheet in terms of thickness, t

TABLE 4.0141 APPROXIMATE BEND RADII FOR 90 DEGREE COLD BEND

	Al
4.5	Cu
1	Mn
1	Si
0.5	Mg

2014,
Clad 2014

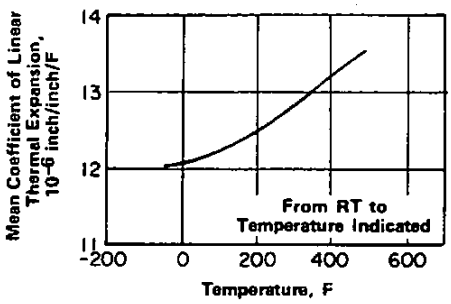


FIGURE 2.014. THERMAL EXPANSION (4, p. 35)

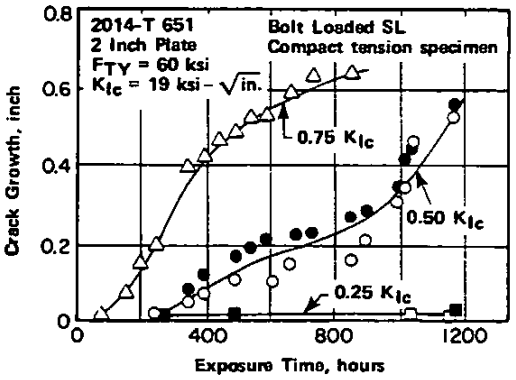


FIGURE 2.0335. CRACK GROWTH OF PLATE IN A SALT-DICHROMATE-ACETATE SOLUTION (3.5% NaCl+0.02M $Na_2Cr_2O_7$+0.07M $NaC_2H_3O_2$+ $HC_2H_3O_2$ TO PH OF 4) (54, Fig. 35)

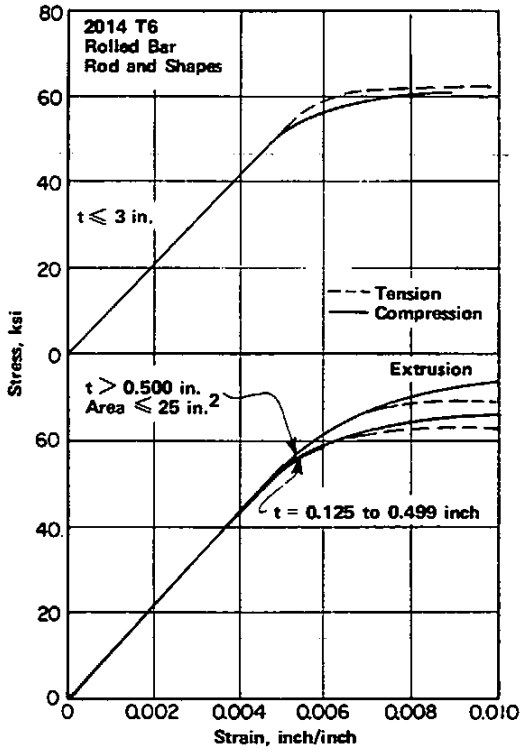


FIGURE 3.02111. STRESS-STRAIN CURVES IN TENSION AND COMPRESSION FOR BAR AND EXTRUSIONS IN T6 CONDITION (5, p. 86, 88)

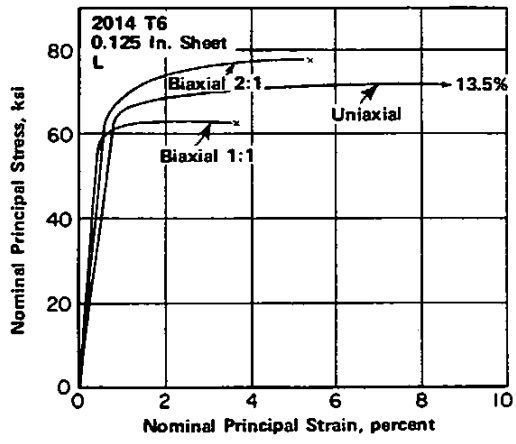


FIGURE 3.02112. TYPICAL UNIAXIAL AND BI-AXIAL STRESS-STRAIN CURVES FOR SHEET IN T6 CONDITION (26)

	Al
4.5	Cu
1	Mn
1	Si
0.5	Mg

2014,
Clad 2014

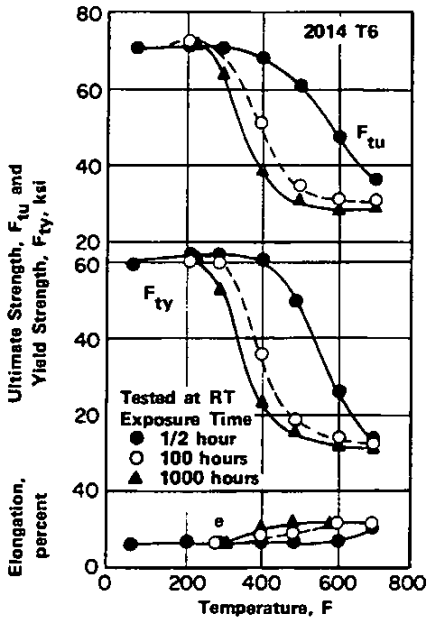


FIGURE 3.0212. EFFECT OF EXPOSURE TO ELEVATED TEMPERATURE ON ROOM TEMPERATURE TENSILE PROPERTIES OF ALLOY IN T6 CONDITION (6)

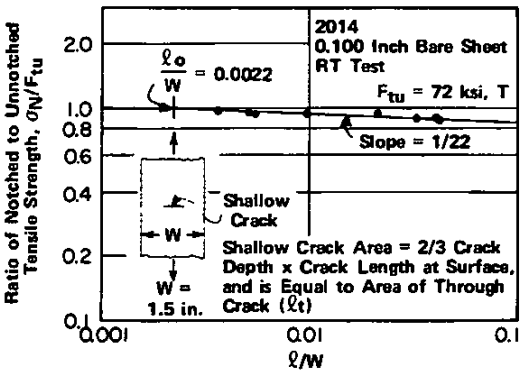


FIGURE 3.02711. RATIO OF NOTCHED TO UNNOTCHED TENSILE STRENGTH OF SHEET CONTAINING SHALLOW CRACKS (27)

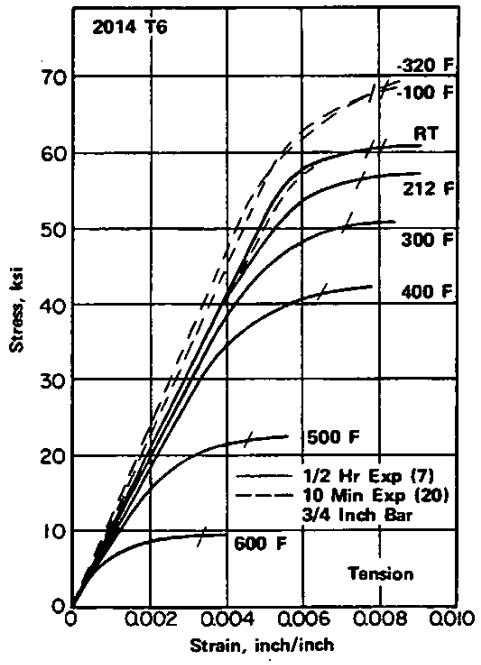


FIGURE 3.03111. STRESS STRAIN CURVES FOR ALLOYS IN T6 CONDITION AT VARIOUS TEMPERATURES (20, p. 12-18)

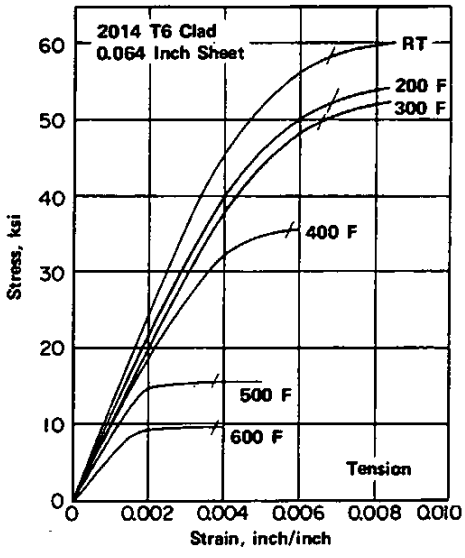


FIGURE 3.03112. STRESS-STRAIN CURVES FOR CLAD SHEET IN T6 CONDITION AT ROOM AND ELEVATED TEMPERATURES (8, p. 115-120)

	Al
4.5	Cu
1	Mn
1	Si
0.5	Mg

2014,
Clad 2014

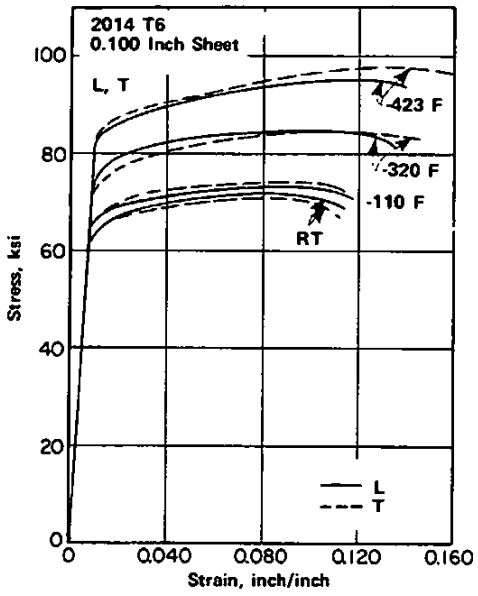


FIGURE 3.03113. STRESS-STRAIN CURVES FOR SHEET IN T6 CONDITION AT LOW TEMPERATURES (29)

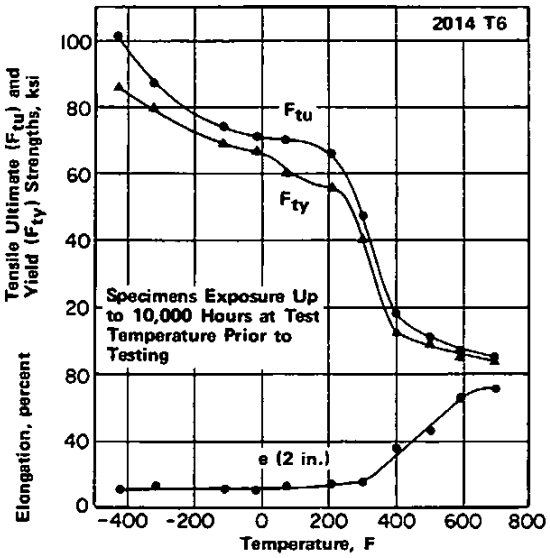


FIGURE 3.0312. TYPICAL TENSILE PROPERTIES AT VARIOUS TEMPERATURES FOR ALLOY IN T6 CONDITION (30)

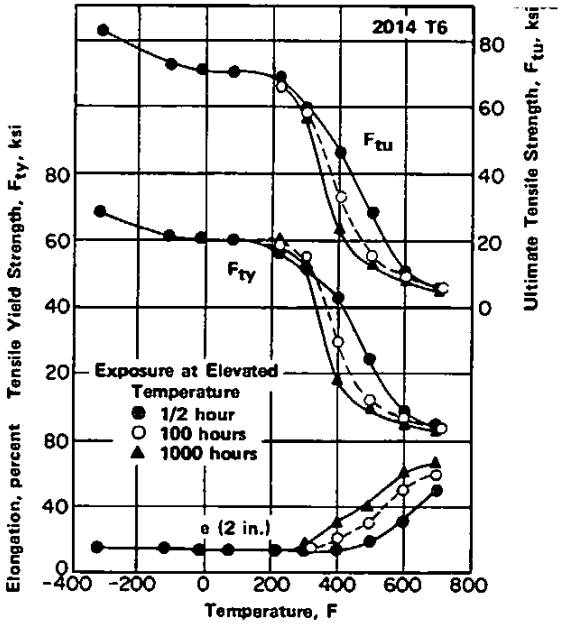


FIGURE 3.0313. EFFECT OF EXPOSURE AND TEST TEMPERATURE ON TENSILE PROPERTIES OF ALLOY IN T6 CONDITION (6)

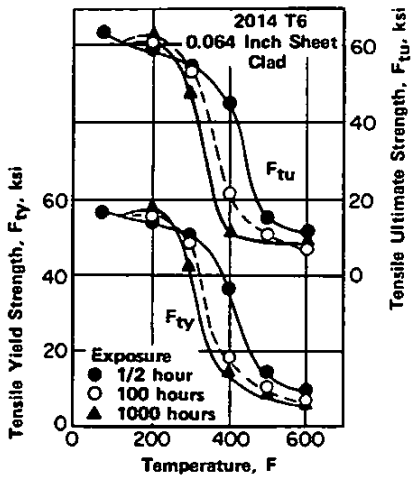


FIGURE 3.0314. EFFECT OF EXPOSURE AND TEST TEMPERATURE ON TENSILE PROPERTIES OF CLAD SHEET IN T6 CONDITION (8, p. 91)

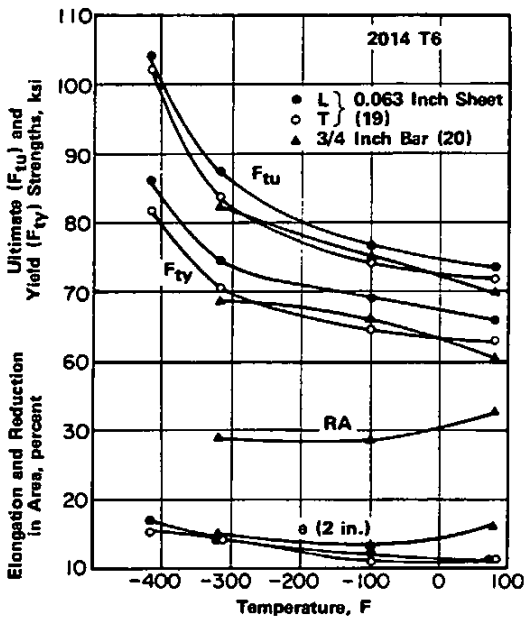
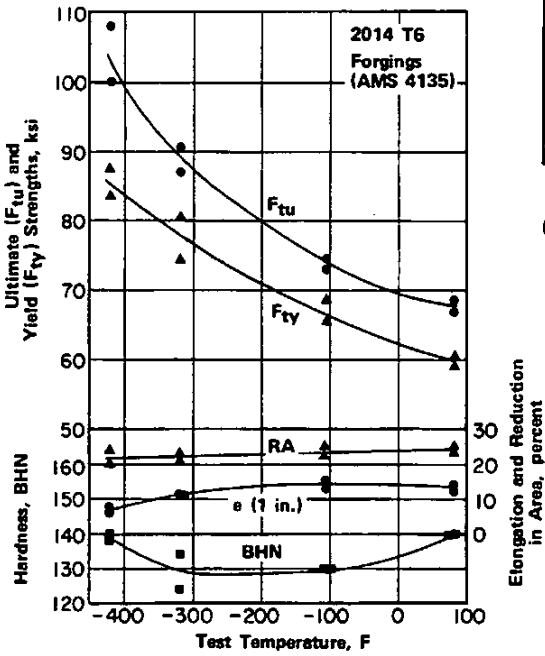


FIGURE 3.0315. EFFECT OF LOW TEST TEMPERATURES ON TENSILE PROPERTIES OF SHEET AND BAR IN T6 CONDITION (19, p. 14) (20, p. 8)



Al	
4.5	Cu
1	Mn
1	Si
0.5	Mg

2014, Clad 2014

FIGURE 3.0316. EFFECT OF LOW TEMPERATURES ON TENSILE PROPERTIES AND HARDNESS OF FORGINGS IN THE T6 CONDITION (31)

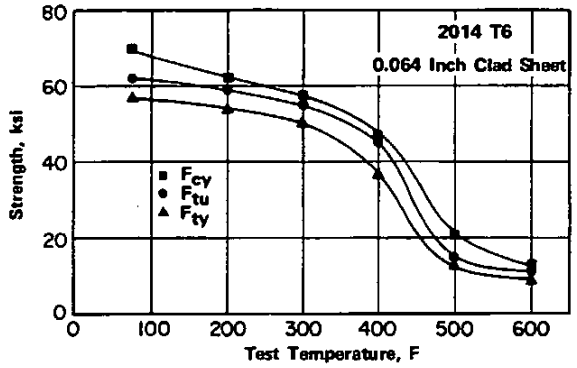


FIGURE 3.0317. EFFECT OF TEST TEMPERATURE ON STRENGTH, F_{TU}, F_{TY} AND F_{CY}, OF CLAD SHEET IN T6 CONDITION (8)

	Al
4.5	Cu
1	Mn
1	Si
0.5	Mg

2014,
Clad 2014

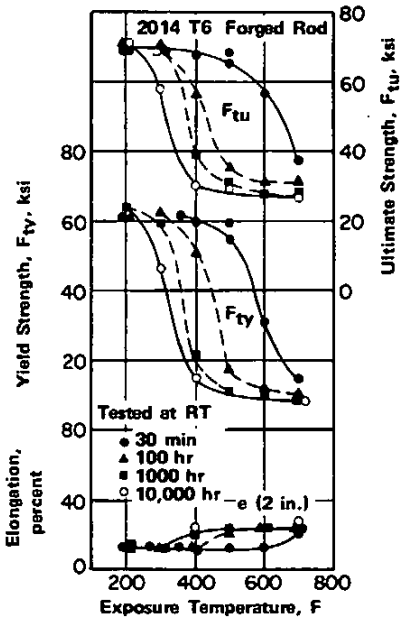


FIGURE 3.0318. EFFECT OF EXPOSURE ON ROOM TEMPERATURE TENSILE PROPERTIES OF T6 FORGED ROD (34)

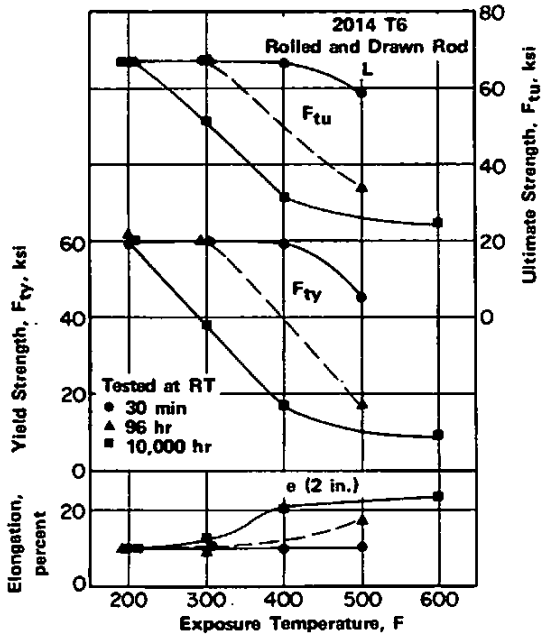


FIGURE 3.0319. EFFECT OF EXPOSURE ON ROOM TEMPERATURE TENSILE PROPERTIES OF T6 ROLLED AND DRAWN ROD (34)

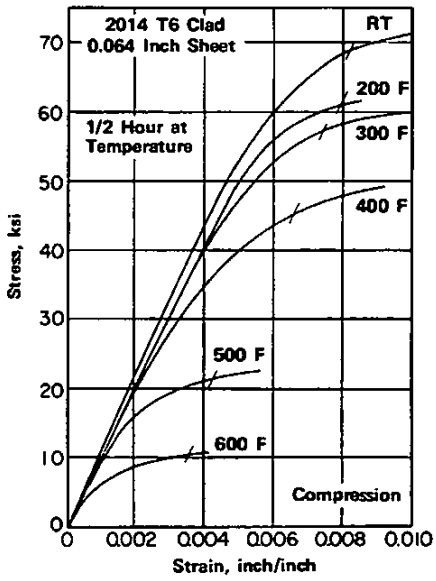


FIGURE 3.03211. STRESS-STRAIN CURVES IN COMPRESSION FOR CLAD SHEET IN T6 CONDITION AT ROOM AND ELEVATED TEMPERATURES (8, p. 121-126)

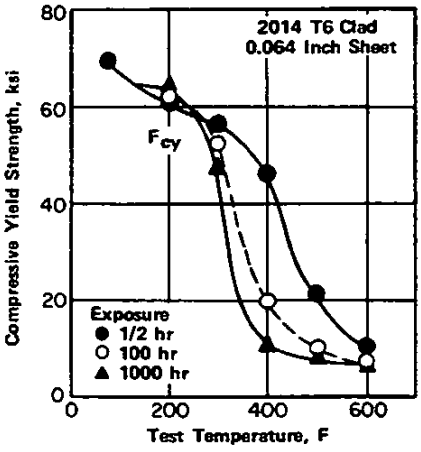


FIGURE 3.0322. EFFECT OF EXPOSURE AND TEST TEMPERATURE ON COMPRESSIVE YIELD STRENGTH OF CLAD SHEET IN T6 CONDITION (8, p. 92)

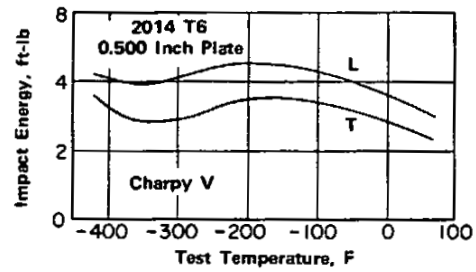


FIGURE 3.0331. EFFECT OF LOW TEMPERATURES ON CHARPY V IMPACT PROPERTIES OF PLATE (29)

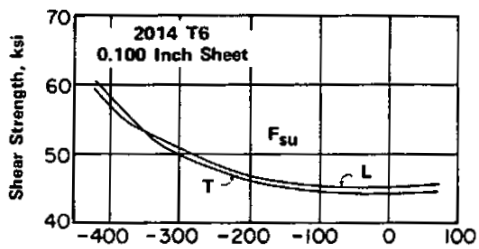


FIGURE 3.0352. EFFECT OF LOW TEMPERATURE ON SHEAR STRENGTH OF SHEET IN T6 CONDITION (29)

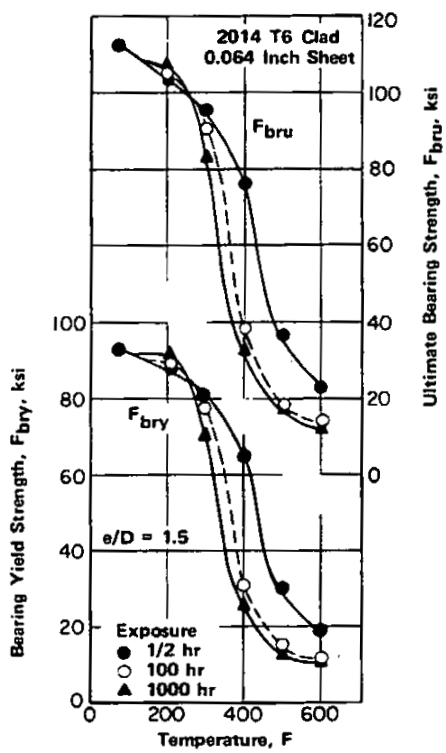


FIGURE 3.0361. EFFECT OF EXPOSURE AND TEST TEMPERATURE ON BEARING PROPERTIES OF CLAD SHEET IN T6 CONDITION (8, p. 93)

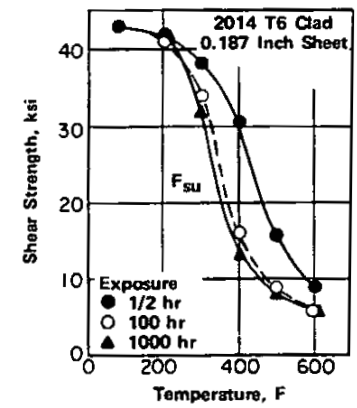


FIGURE 3.0351. EFFECT OF EXPOSURE AND TEST TEMPERATURE ON SHEAR STRENGTH OF CLAD SHEET IN T6 CONDITION (8, p. 95)

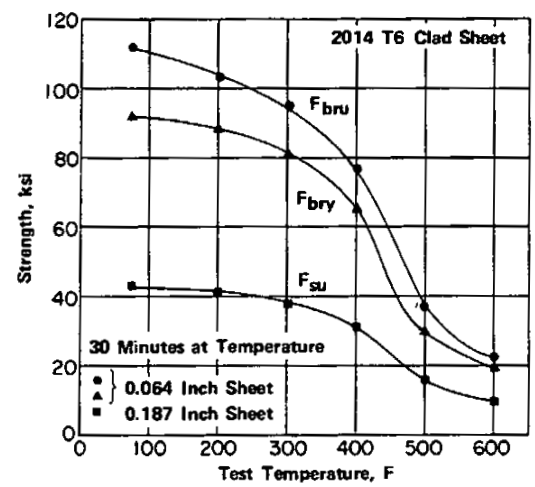


FIGURE 3.0353. EFFECT OF TEST TEMPERATURE ON F_{BRU}, F_{BRY} AND F_{SU} OF CLAD SHEET IN T6 CONDITION (8)

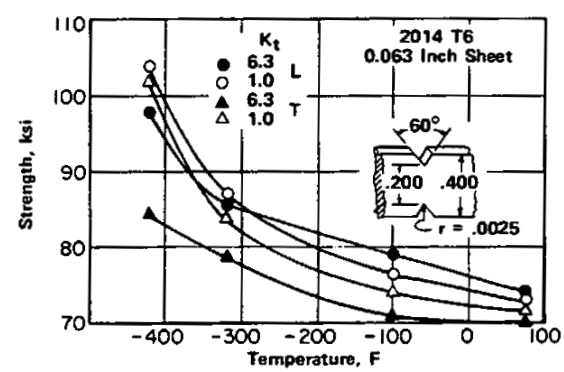


FIGURE 3.03711. EFFECT OF LOW TEST TEMPERATURES ON NOTCHED AND SMOOTH SHEET IN T6 CONDITION (19, p. 14)

	Al
4.5	Cu
1	Mn
1	Si
0.5	Mg

2014,
Clad 2014

	Al
4.5	Cu
1	Mn
1	Si
0.5	Mg

2014,
Clad 2014

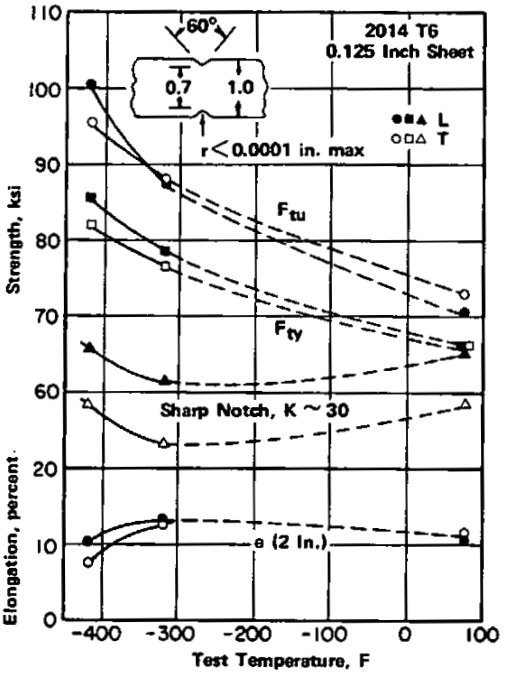


FIGURE 3.03712. EFFECT OF LOW TEMPERATURES ON TENSILE AND SHARP NOTCH PROPERTIES OF SHEET IN T6 CONDITION (32)

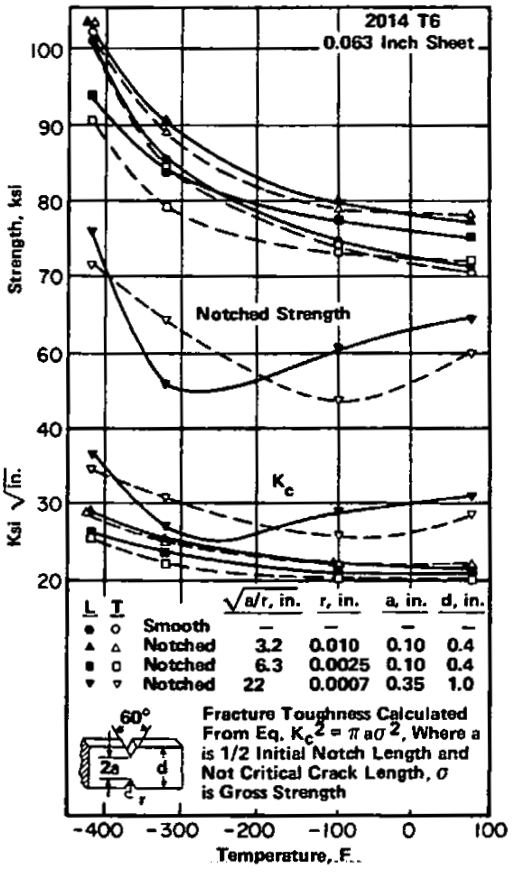


FIGURE 3.03713. EFFECT OF LOW TEST TEMPERATURES ON NOTCH STRENGTH AND FRACTURE TOUGHNESS OF SHEET IN T6 CONDITION (21, p. 190-195)

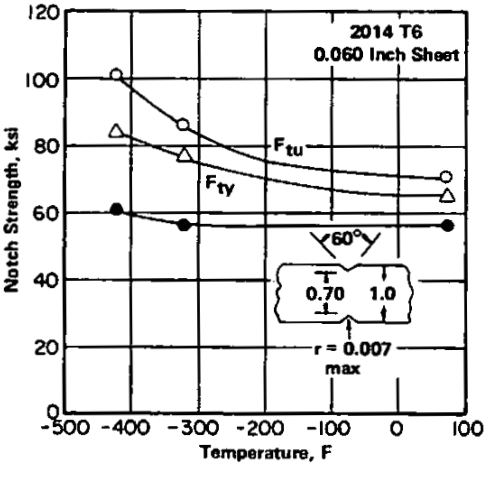


FIGURE 3.03714. EFFECT OF LOW TEMPERATURES ON TENSILE AND NOTCH PROPERTIES OF SHEET IN THE T6 CONDITIONS (45)

	Al
4.5	Cu
1	Mn
1	Si
0.5	Mg

2014,
Clad 2014

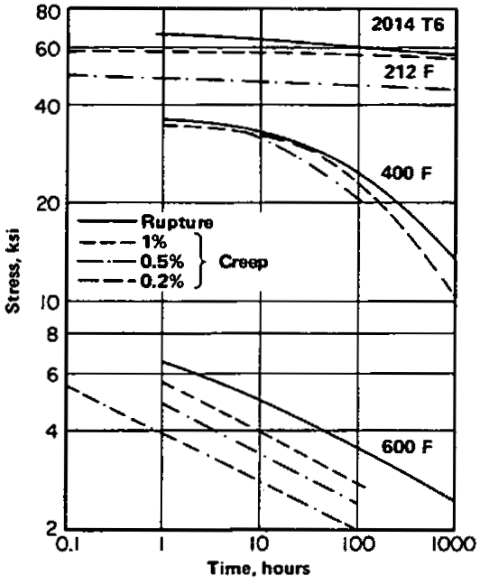


FIGURE 3.041. CREEP AND CREEP RUPTURE CURVES FOR ALLOY IN T6 CONDITION AT 212 TO 600 F (6)

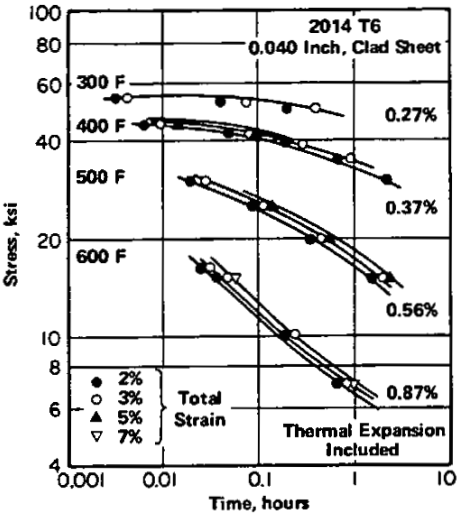


FIGURE 3.042. SHORT TIME TOTAL STRAIN CURVES FOR CLAD SHEET IN T6 CONDITION AT 300 TO 600 F (10, p. 33, 34)

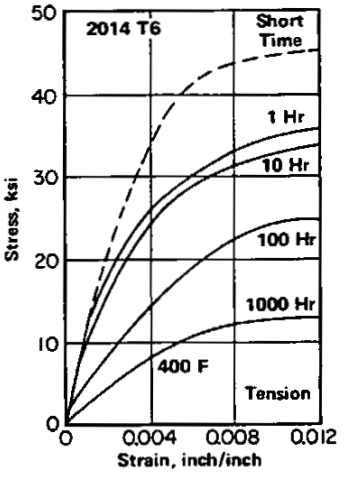


FIGURE 3.043. ISOCHRONOUS STRESS-STRAIN CURVES IN TENSION FOR ALLOY IN T6 CONDITION AT 400 F (9, Fig. 1)

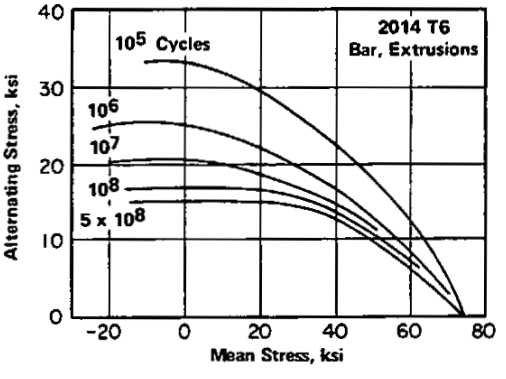


FIGURE 3.052. AVERAGE STRESS RANGE DIAGRAMS FOR BAR AND EXTRUSIONS IN T6 CONDITION (12, p. 966)

	Al
4.5	Cu
1	Mn
1	Si
0.5	Mg

2014,
Clad 2014

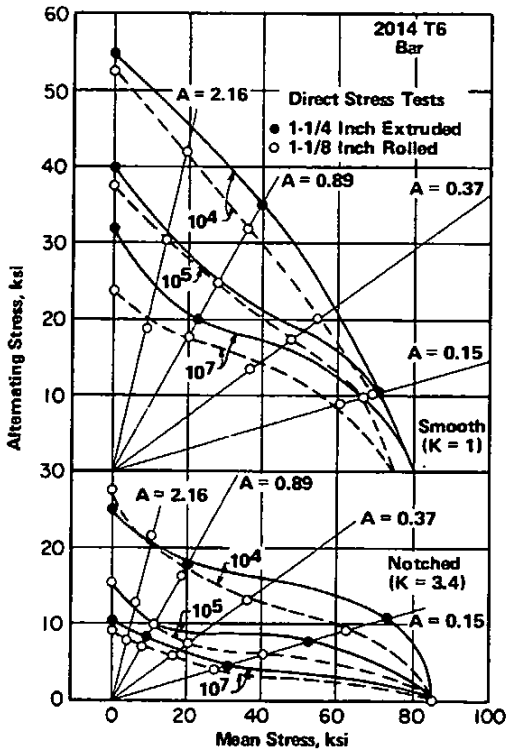


FIGURE 3.053. STRESS RANGE DIAGRAMS FOR SMOOTH AND NOTCHED BAR IN T6 CONDITION (11)

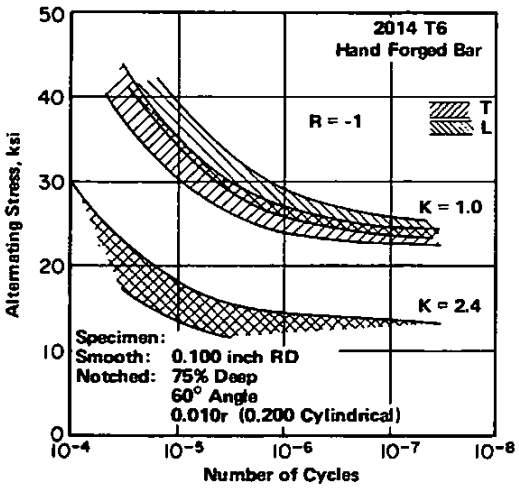


FIGURE 3.054. SCATTER BAND OF FATIGUE DATA FOR SMOOTH AND NOTCHED HAND FORGED BAR IN T6 CONDITION (35)

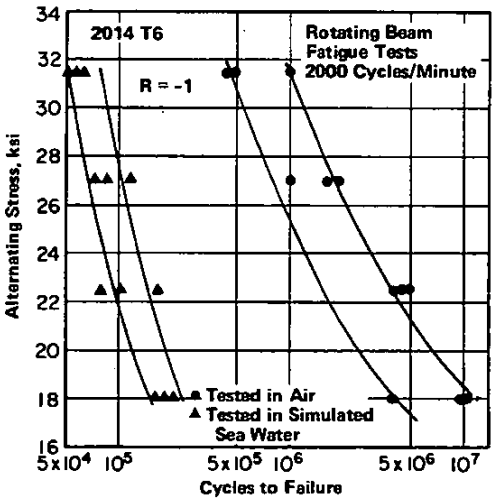


FIGURE 3.055. S-N CURVES FOR ALLOY TESTED IN AIR AND IN SIMULATED SEA WATER (36)

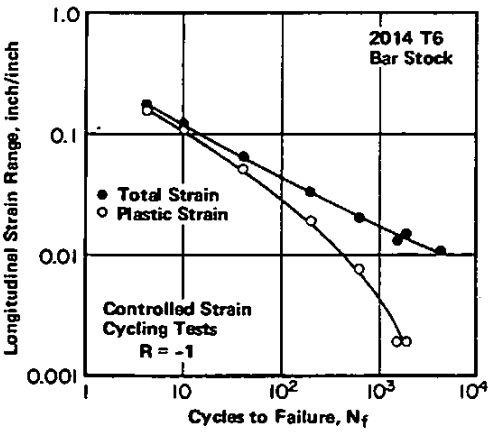


FIGURE 3.056. EFFECT OF STRAIN CYCLING ON FATIGUE LIFE OF T6 BAR (37)

	Al
4.5	Cu
1	Mn
1	Si
0.5	Mg

2014,
Clad 2014

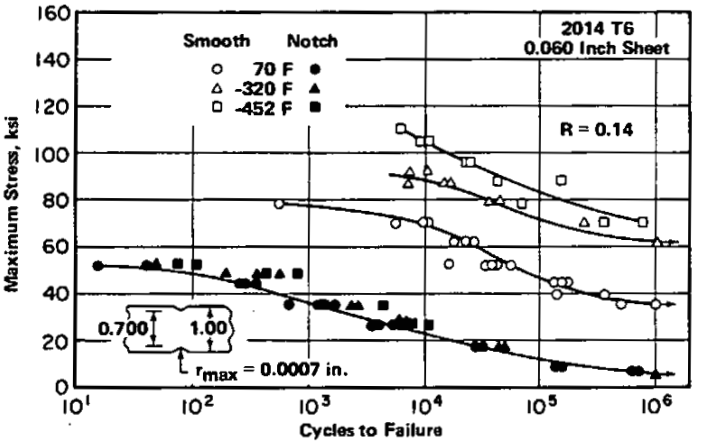


FIGURE 3.057. EFFECT OF LOW TEMPERATURE ON SMOOTH AND NOTCHED FATIGUE STRENGTH OF SHEET (45)

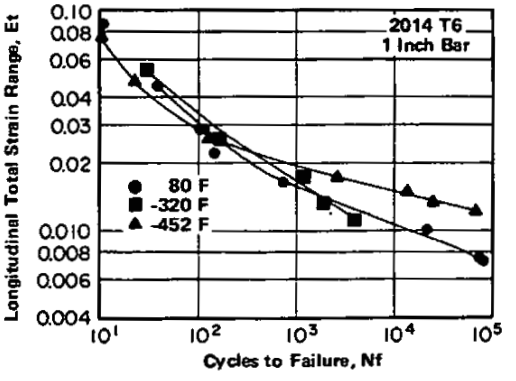


FIGURE 3.058. EFFECT OF LOW TEMPERATURE ON STRAIN CYCLE FATIGUE OF BAR (49)

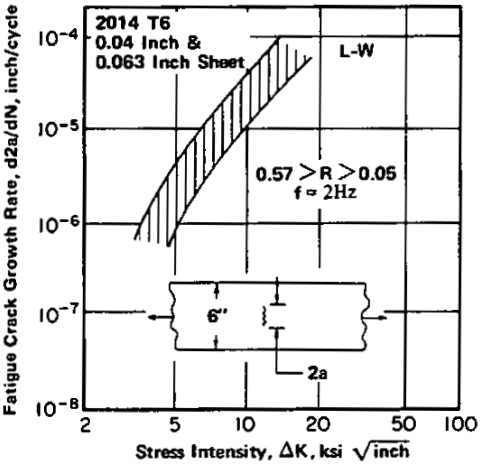


FIGURE 3.059. SCATTER BAND FOR FATIGUE CRACK GROWTH DATA FOR SHEET (53, Figs. NAA3 & NAA4)

	Al
4.5	Cu
1	Mn
1	Si
0.5	Mg

2014,
Clad 2014

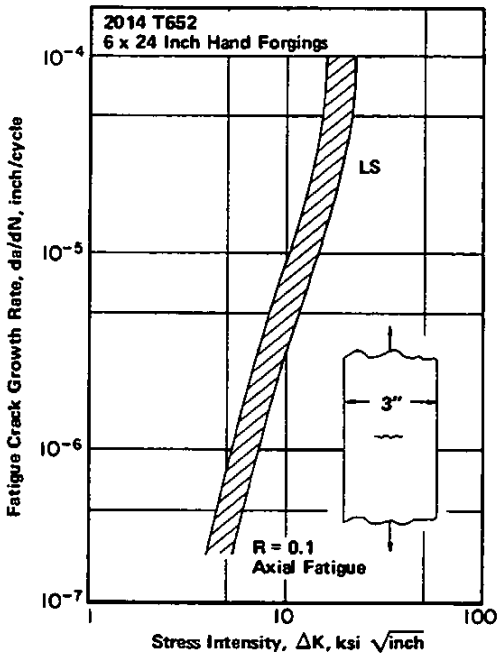


FIGURE 3.0510. SCATTER BAND FOR FATIGUE CRACK GROWTH DATA FOR FORGINGS (51, p. 67)

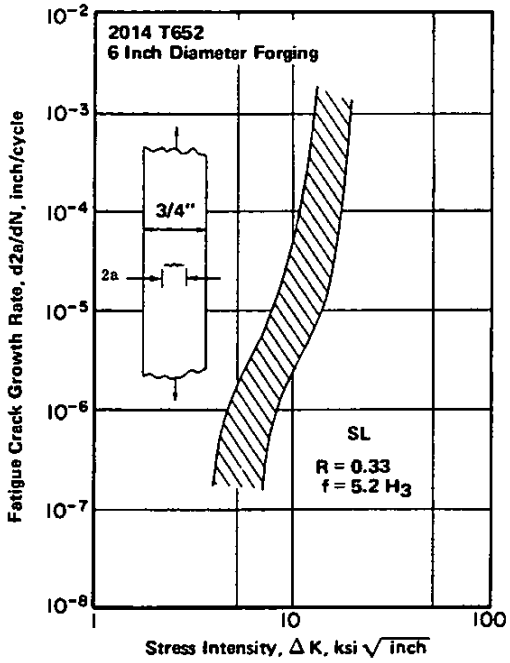


FIGURE 3.0511. SCATTER BAND FOR FATIGUE CRACK GROWTH DATA FOR FORGING (53, Fig. NAA6)

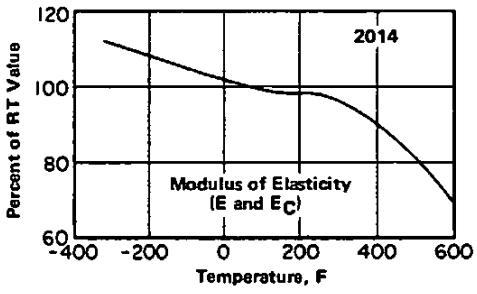


FIGURE 3.0622. EFFECT OF TEMPERATURE ON E AND E_C (5)

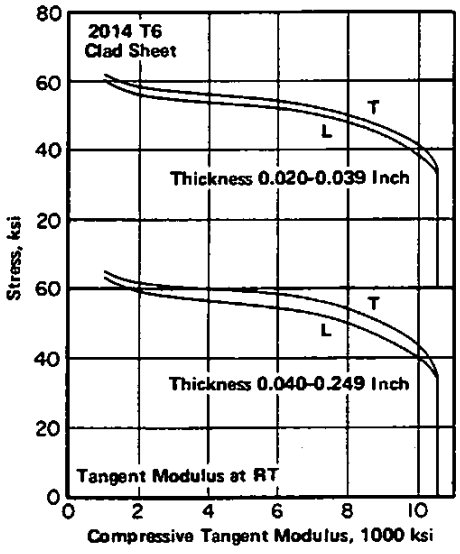


FIGURE 3.0641. TYPICAL TANGENT MODULUS CURVES FOR CLAD SHEET AT ROOM TEMPERATURE (5)

	Al
4.5	Cu
1	Mn
1	Si
0.5	Mg

2014,
Clad 2014

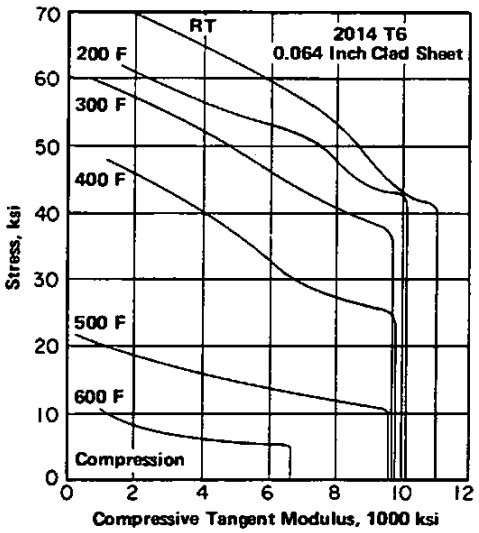


FIGURE 3.0642. TANGENT MODULUS CURVES IN COMPRESSION FOR CLAD SHEET IN T6 CONDITION AT ROOM AND ELEVATED TEMPERATURES (8, p. 183-188)

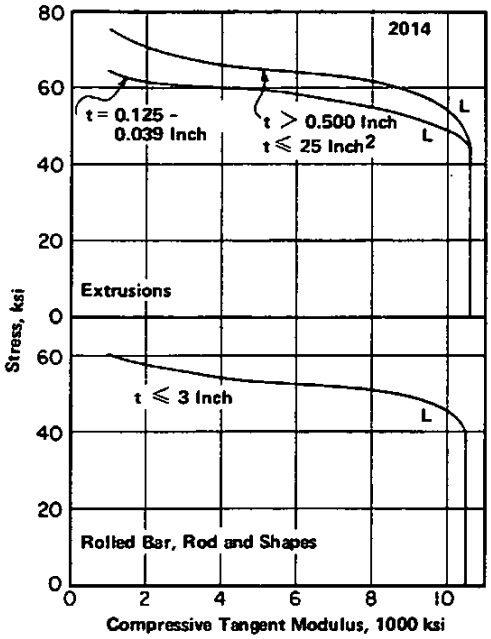


FIGURE 3.0643. TYPICAL TANGENT MODULUS CURVES FOR EXTRUSIONS AND ROLLED PRODUCTS AT ROOM TEMPERATURE (5)

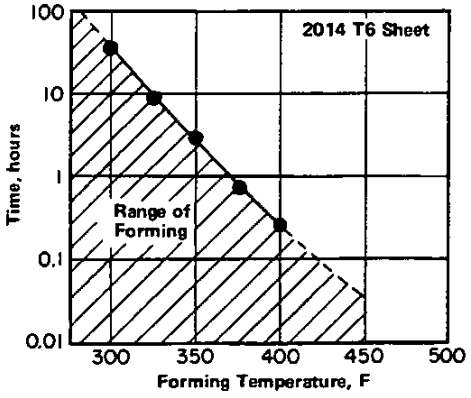


FIGURE 4.0122. MAXIMUM TIME AT VARIOUS TEMPERATURES FOR HOT FORMING SHEET IN T6 CONDITION (17, p. 133)

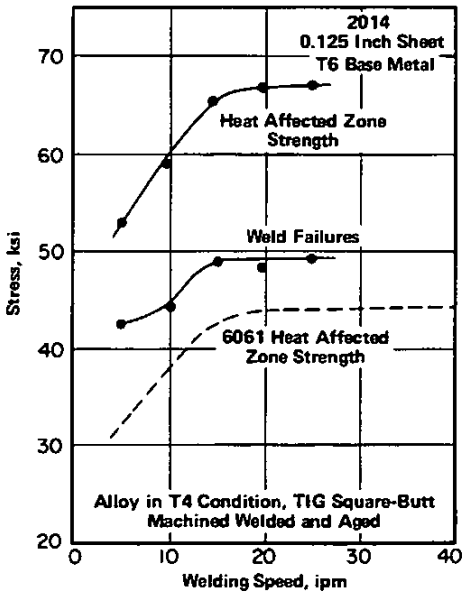


FIGURE 4.0321. EFFECT OF WELDING SPEED ON TENSILE STRENGTH OF GTA WELDS (38)

	Al
4.5	Cu
1	Mn
1	Si
0.5	Mg

2014,
Clad 2014

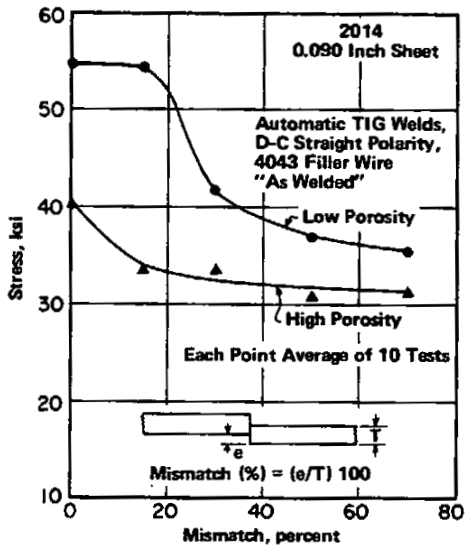


FIGURE 4.0322. COMBINED EFFECT OF POROSITY AND MISMATCH FOR GTA WELDED SHEET (39)

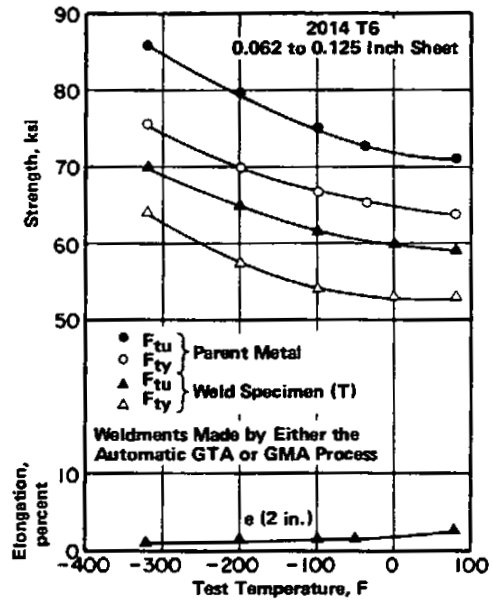


FIGURE 4.0323. EFFECT OF CRYOGENIC TEMPERATURES ON TENSILE PROPERTIES OF WELDMENTS AND PARENT METAL SHEET IN T6 CONDITION (33)

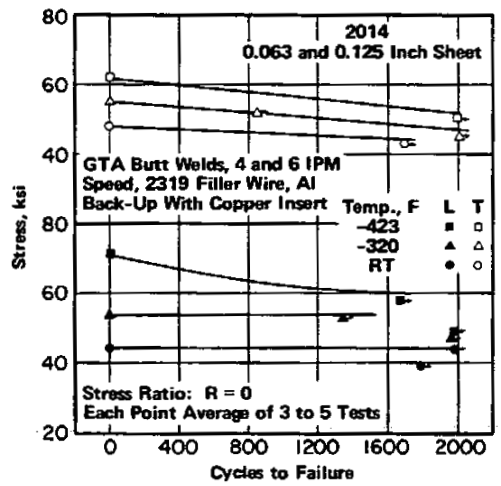


FIGURE 4.0324. S-N FATIGUE CURVES FOR GTA BUTT-WELDED SHEET AT ROOM AND CRYOGENIC TEMPERATURES (21)

Al
4.5 Cu
1.5 Mg
0.6 Mn
2024

Alloy	2024
Condition	Thermal Conductivity, Btu ft/(hr ft^2 F)
0	111.7
T3, T36, T351, T361, T4	70.0
T6, T81, T851, T861	88.5

TABLE 2.0131. THERMAL CONDUCTIVITY AT ROOM TEMPERATURE FOR VARIOUS HEAT-TREATED CONDITIONS (16) (19)

Alloy	2024		
Condition	Resistivity, Microhm inch	Conductivity, Megohms/in.^{3}	Conductivity, percent IACS
0	1.37	0.730	49.6
T3, T36, T351, T361, T4	2.29	0.437	29.7
T6, T81, T851, T861	1.77	0.565	38.4

TABLE 2.022. ELECTRICAL PROPERTIES (16) (19)

Alloy	2024			
Form	2.5-inch Thick Plate			
Condition	Orientation	Stress, ksi	Time to SC Failure, days(a)	Loss in F_{tu}, percent(a)
T851	L	0	—	15
T851	L	45	—	14
T851	ST	0	—	42
T851	ST	46	—	35
T851	ST	27	—	42
T351	L	0	—	15
T351	L	45	—	20
T351	T	0	—	37
T351	T	46	25	—
T351	T	27	67	—

(a) Tensile specimens, 0.125-in. diam. x 2 in. long, exposed to alternate immersion in 3.5 percent aqueous sodium chloride solution, 10 minutes in solution and 50 minutes in air each hour, at given stresses until stress corrosion failure or for 84 days. Specimens that did not fail within 84 days were then tensile tested to determine loss of strength.

TABLE 2.0311. EFFECTS OF HEAT-TREAT CONDITION, ORIENTATION, AND STRESS ON TIME TO STRESS-CORROSION FAILURE OR ON LOSS OF TENSILE STRENGTH DUE TO ALTERNATE IMMERSION IN 3.5 PERCENT SODIUM CHLORIDE SOLUTION (14)

Alloy	2024				
			Rolled	Extruded Shapes	
Condition	Orientation	Plate(a)	Rod & Bar(a)	0.25-1 inch(a)	1.25-2 inch(a)
T3, T4	L	35	30	>50	>50
T3, T4	T	20	—	37	18
T3, T4	ST	7	10	—	7
T6, T8	L	>50	>47	>60	>60
T6, T8	T	>50	—	50	50
T6, T8	ST	43	>43	—	16

(a) Numbers indicate highest sustained tensile stress (ksi) at which test specimens did not fail in 84-day test duration in aqueous 3.5 percent sodium chloride alternate-immersion test (10 minutes in solution and 50 minutes in air).

TABLE 2.0312. RESISTANCE TO STRESS CORROSION OF VARIOUS PRODUCT FORMS, HEAT TREAT-CONDITIONS, AND ORIENTATIONS (29)

Alloy	2024-T4			
Form	0.063-inch Thick Sheet			
	Exposure,	Percent Failed	Average Loss of F_{tu}, percent	
Environment	days	in SC	Unstressed[a]	Stressed[a]
3.5% NaCl[b]	84	0	33	40
Seacoast	365	0	16	20
Industrial	365	0	6	9

(a) Half of the specimens unstressed and other half stressed at 75 percent of F_{ty}.
(b) Alternate immersion: 10 minutes in aqueous NaCl solution and 50 minutes in air.

TABLE 2.0313. SUMMARY OF THE EFFECTS OF EXPOSURES TO VARIOUS ENVIRONMENTS ON STRESS-CORROSION BEHAVIOR AND LOSS OF TENSILE STRENGTH OF NUMEROUS SHEET SPECIMENS (BOTH LONGITUDINAL AND TRANVERSE) (28)

Al
4.5 Cu
1.5 Mg
0.6 Mn
2024

Alloy	2024-T852			
Form	3 x 18 x 35-inch Forged Block			
Orientation	Environment	K_{Ic}, ksi$\sqrt{in.}$	K_{Iscc}, ksi$\sqrt{in.}$	K_{Iscc}/K_{Ic}
LT[a]	FTSRW[d]	28.0	22.5	0.80
LS[b]	FTSRW[d]	--	20.0	--
TL[c]	FTSRW[d]	27.0	20.5	0.76
LT[a]	SCS[e]	37.0	28.0	0.76

(a) Longitudinal loading – transverse fracture direction.
(b) Longitudinal loading – short-transverse fracture direction.
(c) Transverse loading – longitudinal fracture direction.
(d) Artificial fuel tank sump residue water (B-1 bomber).
(e) Metal cleaning solvent.

TABLE 2.0314. COMPARISON OF K_{Ic} AND K_{Iscc} OF FORGINGS (25)

Alloy	2024				
Condition	Form	Thickness, inches	F_{ty}, ksi (Min)	F_{tu}, ksi (Min)	Elongation, e, (2 inch or 4D), percent, (Min)
O	Sheet & Plate	0.010-0.499	14.0 (Max)	32.0 (Max)	12
		0.500-1.750	--	32.0 (Max)	12
T3	Flat Sheet	0.008-0.009	42.0	63.0	10
		0.010-0.020	42.0	63.0	12
		0.021-0.128	42.0	63.0	15
		0.129-0.249	42.0	64.0	15
T361	Flat Sheet & Plate	0.020-0.062	50.0	67.0	8
		0.063-0.249	51.0	68.0	9
		0.250-0.499	49.0	66.0	9
		0.500	49.0	66.0	10
T4	Coiled Sheet	0.010-0.020	40.0	62.0	12
		0.021-0.249	40.0	62.0	15
T351	Plate	0.250-0.499	42.0	64.0	12
		0.500-1.000	42.0	63.0	8
		1.001-1.500	42.0	62.0	7
		1.501-2.000	42.0	62.0	6
		2.001-3.000	42.0	60.0	4
		3.001-4.000	41.0	57.0	4
T42	Sheet & Plate	0.010-0.020	38.0	62.0	12
		0.021-0.249	38.0	62.0	15
		0.250-0.499	38.0	62.0	12
		0.500-1.000	38.0	61.0	8
		1.001-1.500	38.0	60.0	7
		1.501-2.000	38.0	60.0	6
		2.001-3.000	38.0	58.0	4
T62	Sheet & Plate	0.010-0.499	50.0	64.0	5
		0.500-3.000	50.0	63.0	5
T72	Sheet	0.010-0.249	46.0	60.0	5
T81	Flat Sheet	0.010-0.249	58.0	67.0	5
T851	Plate	0.250-0.499	58.0	67.0	5
		0.500-1.000	58.0	66.0	5
		1.001-1.499	57.0	66.0	5
T861	Flat Sheet & Plate	0.020-0.062	62.0	70.0	3
		0.063-0.249	66.0	71.0	4
		0.250-0.499	64.0	70.0	4
		0.500	64.0	70.0	4

TABLE 3.011. ALUMINUM ASSOCIATION MECHANICAL-PROPERTY LIMITS FOR SHEET AND PLATE (16)

Al
4.5 Cu
1.5 Mg
0.6 Mn
2024

Alloy	2024				
Form	Drawn Table				
	Wall	F_{ty}, ksi	F_{tu}, ksi	e, (2 inch or 4D), (Min)	
Condition	Thickness, inch	(Min)	(Min)	Full Section	Cut-out Spec
0	0.018-0.500	15.0 (Max)	32.0 (Max)	--	--
T3	0.018-0.024	42.0	64.0	10	--
	0.025-0.049	42.0	64.0	12	10
	0.050-0.259	42.0	64.0	14	10
	0.260-0.500	42.0	64.0	16	12
T42	0.018-0.024	40.0	64.0	10	--
	0.025-0.049	40.0	64.0	12	10
	0.050-0.259	40.0	64.0	14	10
	0.260-0.500	40.0	64.0	16	12

TABLE 3.012. ALUMINUM ASSOCIATION MECHANICAL-PROPERTY LIMITS FOR DRAWN TUBE (16)

Alloy	2024				
Form	Drawn Table				
Condition	Wall Thickness, inches	Area, in.^{2}	F_{ty}, ksi (Min)	F_{tu}, ksi (Min)	Elongation, e, (2 inch or 4D), percent, (Min)
0	All	All	19.0 (Max)	35.0 (Max)	12
T3, T3510, & T3511	Up Thru 0.249	All	42.0	57.0	10
	0.250-0.749	All	44.0	60.0	10
	0.750-1.499	All	46.0	65.0	10
	1.500 and Over	Up Thru 25	48.0	70.0	10
	1.500 and Over	25-32	46.0	68.0	8
T42	Up Thru 0.749	All	38.0	57.0	12
	0.750-1.499	All	38.0	57.0	10
	1.500 and Over	Up Thru 25	38.0	57.0	10
	1.500 and Over	25-32	38.0	57.0	8
T81, T8510 & T8511	0.050-0.249	All	56.0	64.0	4
	0.250-1.499	All	58.0	66.0	5
	1.500 and Over	Up Thru 32	58.0	66.0	5

TABLE 3.013. ALUMINUM ASSOCIATION MECHANICAL-PROPERTY LIMITS FOR EXTRUDED TUBE (16)

Alloy	2024				
Form	Extruded Wire, Rod, Bar, and Shapes				
Condition	Diameter or Thickness, inches	Area, in.^{2}	F_{ty}, ksi (Min)	F_{tu}, ksi (Min)	Elongation, e, (2 inch or 4D), percent, (Min)
0	All	All	19.0 (Max)	35.0 (Max)	12
T3, T3510, & T3511	Up Thru 0.249	All	42.0	57.0	12
	0.250-0.749	All	44.0	60.0	12
	0.750-1.499	All	46.0	65.0	10
	1.500 and Over	Up Thru 25	52.0	70.0	10
	1.500 and Over	25-32	48.0	68.0	8
T42	Up Thru 0.749	All	38.0	57.0	12
	0.750-1.499	All	38.0	57.0	10
	1.500 and Over	Up Thru 25	38.0	57.0	10
	1.500 and Over	25-32	38.0	57.0	8
T81, T8510, & T8511	0.050-0.249	All	56.0	64.0	4
	0.250-1.499	All	58.0	66.0	5
	1.500 and Over	Up Thru 32	58.0	66.0	5

TABLE 3.014. ALUMINUM ASSOCIATION MECHANICAL-PROPERTY LIMITS FOR EXTRUDED WIRE, ROD, BAR, AND SHAPES (16)

Alloy	2024			
Form	Rolled Wire, Rod, and Bar			
Condition	Diameter or Thickness, inches	F_{ty}, ksi (Min)	F_{tu}, ksi (Min)	Elongation, e, (2 inch or 4D), percent, (Min)
0	Up Thru 8.000	--	35.0 (Max)	16
T36	Up Thru 0.375	52.0	69.0	10
T4	Up Thru 0.499	45.0	62.0	10
	0.500-4.500	42.0	62.0	10
	4.501-6.500	40.0	62.0	10
	6.501-8.000	38.0	58.0	10
T42	Up Thru 6.500	40.0	62.0	10
T351	0.500-6.500	45.0	62.0	10
T6	Up Thru 6.500	50.0	62.0	5
T62	Up Thru 6.500	46.0	60.0	5
T851	0.500-6.500	58.0	66.0	5

TABLE 3.015. ALUMINUM ASSOCIATION MECHANICAL-PROPERTY LIMITS FOR ROLLED WIRE, ROD, AND BAR (16)

Al
4.5 Cu
1.5 Mg
0.6 Mn
2024

Alloy	2024-T4
Form	Cold-Heading Wire and Rod, 0.063-1.000 inch Diameter
F_{ty}, ksi (Min)	40.0
F_{tu}, ksi (Min)	62.0
Elongation, e, (2 inch or 4D), percent (Min)	10
F_{su}, ksi	37.0

TABLE 3.016. ALUMINUM ASSOCIATION MECHANICAL-PROPERTY LIMITS FOR COLD-HEADING WIRE AND ROD (16)

Alloy	2024			
	F_{ty},	F_{tu},	Elongation, e, (2 inch), percent	
Condition	ksi	ksi	1/16 inch thick	1/2 inch diameter
0	11	27	20	22
T3	50	70	18	–
T4, T351	47	68	20	19
T361, T36	57	72	13	–
T6	57	69	10	–
T81, T851	65	70	6	–
T86	71	75	6	–

TABLE 3.0214. TYPICAL TENSILE PROPERTIES FOR VARIOUS HEAT-TREATED CONDITIONS (16) (26)

Alloy	2024								
Form	2.5- inch Thick Plate								
Orientation	Longitudinal			Transverse			Short Transverse		
Condition	F_{ty}, ksi	F_{tu}, ksi	Elongation, e, (4D), percent	F_{ty}, ksi	F_{tu}, ksi	Elongation, e, (4D), percent	F_{ty}, ksi	F_{tu}, ksi	Elongation, e, (4D), percent
T351	53.9	70.7	12.0	47.4	68.2	17.4	43.0	57.2	3.5
T851	60.0	67.2	8.0	63.3	69.5	7.2	62.0	64.5	1.0

TABLE 3.0215. TENSILE PROPERTIES OF PLATE IN DIFFERENT ORIENTATIONS AND HEAT-TREAT CONDITIONS (14)

Alloy	2024-T852								
Form	Hand Forgings								
Orientation	Longitudinal			Transverse			Short Transverse		
Forging Section, inches	F_{ty}, ksi	F_{tu}, ksi	Elongation, e, (2 inch), percent	F_{ty}, ksi	F_{tu}, ksi	Elongation, e, (2 inch), percent	F_{ty}, ksi	F_{tu}, ksi	Elongation, e, (2 inch), percent
2 x 8	67.2	72.4	5.0	71.2	76.4	7.0	–	–	–
4 x 8	61.7	67.8	7.5	64.2	70.8	5.5	–	–	–
5 x 5	63.9	70.2	9.0	61.1	66.5	3.5	58.1	67.0	3.5
5 x 20	56.9	65.5	8.0	56.9	63.3	3.0	55.3	61.9	3.0
6 x 12	58.5	66.5	9.0	59.9	66.8	2.0	54.5	64.2	2.5

TABLE 3.0216. TENSILE PROPERTIES OF HAND FORGINGS IN DIFFERENT SIZES AND ORIENTATIONS (9)

Al
4.5 Cu
1.5 Mg
0.6 Mn
2024

Alloy	2024-T852		
Form	Hand Forgings		
Property	Compressive Yield Strength, F_{cy}, ksi		
Forging Section, inches	Longitudinal	Transverse	Short Transverse
2 x 8	70.1	64.1	–
4 x 8	62.5	60.6	–
5 x 5	64.8	62.2	67.7
5 x 20	56.0	60.6	60.7
6 x 12	59.1	63.2	63.3

TABLE 3.0222. COMPRESSIVE YIELD STRENGTH OF HAND FORGINGS IN DIFFERENT SIZES AND ORIENTATIONS (9)

Alloy	2024
Condition	Shear Strength, F_{su}, ksi
O	18
T3, T4, T351, T6	41
T36, T361	42
T81, T851	43
T86	45

TABLE 3.0251. TYPICAL SHEAR STRENGTH FOR VARIOUS HEAT-TREATED CONDITIONS (16) (26)

Alloy	2024-T852		
Form	Hand Forgings		
Property	Shear Strength, F_{su}, ksi		
Forging Section, inches	Longitudinal	Transverse	Short Transverse
2 x 8	42.7	41.8	–
4 x 8	40.5	39.5	38.6
5 x 5	40.8	40.7	39.6
5 x 20	38.8	38.0	37.0
6 x 12	39.6	38.4	37.4

TABLE 3.0252. SHEAR STRENGTH OF HAND FORGINGS IN VARIOUS SIZES AND ORIENTATIONS (9)

Alloy		2024-T852			
Form		Hand Forgings			
Property		Bearing Yield Strength, F_{bry}, ksi		Bearing Ultimate Strength, F_{bru}, ksi	
Forging Section, inches	Specimen Orientation	e/d=1.5	e/d=2.0	e/d=1.5	e/d=2.
2 x 8	L	95.5	116.3	97.7	133.1
	T	89.5	114.2	94.5	125.9
4 x 8	L	82.5	100.5	91.9	117.9
	T	82.8	101.0	88.8	119.4
5 x 5	L	89.9	105.1	93.5	125.2
	T	84.4	101.1	89.1	121.6
5 x 20	L	79.3	94.4	83.6	112.6
	T	82.5	98.0	84.9	114.6
6 x 12	L	82.4	100.5	84.7	117.1
6 x 12	T	81.4	95.7	85.7	113.4

TABLE 3.0261. BEARING PROPERTIES OF HAND FORGINGS IN VARIOUS SIZES AND ORIENTATIONS (9)

Alloy	2024-T851				
Form	Plate				
Plate Thickness, inches	Notched Specimen Diameter, inches	Specimen Orientation	Notch Tensile Strength, (NTS), ksi	F_{tu}, ksi	F_{ty}, ksi
1-3/8	1/2	T	71.5	71.2	64.8
1-3/8	1-1/16	T	51.0	71.2	64.8
6.0	1/2	ST	40.5	67.7	59.9
6.0	1-1/16	ST	29.0	67.7	59.9

TABLE 3.02712. EFFECTS OF SPECIMEN SIZE AND ORIENTATION ON SHARP-NOTCH TENSILE STRENGTH (34)

Alloy	2024-T851	
Form	Plate	
Plate Thickness, inches	Specimen Orientation	K_{Ic}, ksi$\sqrt{in.}$
1.00	L-T	20.9
	T-L	18.7
1.37	L-T	22.8
	T-L	19.6

TABLE 3.02721. FRACTURE TOUGHNESS FOR VARIOUS PLATE THICKNESSES AND ORIENTATIONS (35)

Alloy	2024	
Form	2.5-inch Thick Plate	
Orientation	Longitudinal (L-T)	Short Transverse (S-L)
Condition	K_{Ic}, ksi$\sqrt{in.}$	K_{Ic}, ksi$\sqrt{in.}$
T351	29.6	21.0
T851	25.3	16.7

TABLE 3.02723. FRACTURE TOUGHNESS OF PLATE IN VARIOUS LOADING ORIENTATIONS AND HEAT-TREATED CONDITIONS (14)

Al
4.5 Cu
1.5 Mg
0.6 Mn
2024

Alloy	2024-T852		
Form	Hand Forgings		
Property	K_{Ic}, ksi$\sqrt{in.}$		
Forging Section, inches	Longitudinal	Transverse	Short Transverse
2 x 8	24.2	21.5	–
3 x 12	23.0	17.7	–
4 x 16	27.3	–	15.6
5 x 20	27.1	17.6	15.9
6 x 24	29.9	16.6	16.2

TABLE 3.02724. FRACTURE TOUGHNESS OF HAND FORGINGS IN VARIOUS SIZES AND ORIENTATIONS (9)

Alloy	2024
Condition	Fatigue Limit for 5×10^8 cycles, ksi(a)
0	13
T36, T6, T81, T851, T86	18
T3, T4, T351	20

(a) Rotating beam, R= -1, smooth specimens.

TABLE 3.052. TYPICAL FATIGUE LIMITS FOR VARIOUS HEAT-TREATED CONDITIONS (16) (26)

Alloy	2024-T852	
Form	Hand Forgings	
Property	Modulus of Elasticity, 10^3 ksi	
Orientation	Tension	Compression
Longitudinal	10.49	10.75
Transverse	10.50	10.79
Short Transverse	10.45	10.75

TABLE 3.0622. STATIC MODULUS OF ELASTICITY OF HAND FORGINGS IN TENSION AND COMPRESSION AT ROOM TEMPERATURE (9)

Alloy	2024					
Form	Sheet and Plate					
Condition	0	T3	T361	T4	T81	T861
Thickness, inch	Bend Radii Expressed in Terms of Thickness, t					
1/64	0	2.5t	3t	2.5t	4.5t	5t
1/32	0	3t	4t	3t	5.5t	6t
1/16	0	4t	5t	4t	6t	7t
1/8	0.5t	5t	6t	5t	7.5t	8.5t
3/16	1t	5t	6t	5t	8t	9.5t
1/4	1t	6t	8t	6t	9t	10t
3/8	2.5t	7t	8.5t	7t	10t	11.5t
1/2	4t	7.5t	9.5t	7.5t	10.5t	11.5t

TABLE 4.011. APPROXIMATE MINIMUM BEND RADII FOR 90 DEGREE COLD BEND FOR VARIOUS THICKNESSES AND HEAT-TREATED CONDITIONS (33)

Al
4.5 Cu
1.5 Mg
0.6 Mn
2024

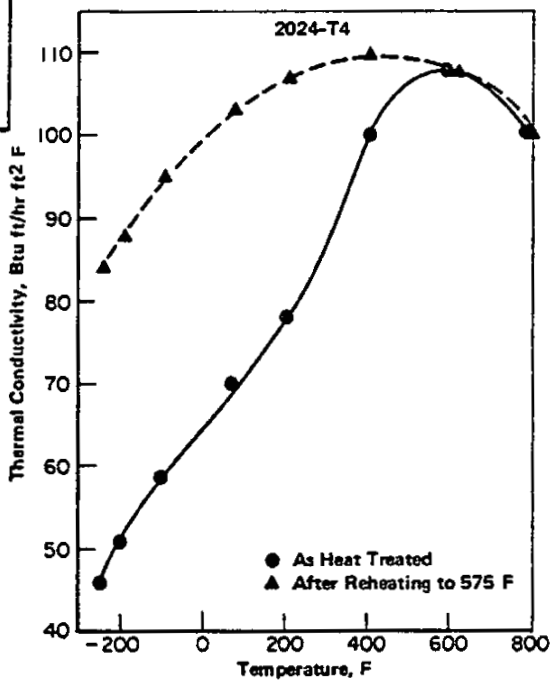


FIGURE 2.0132. EFFECT OF TEMPERATURES ON THERMAL CONDUCTIVITY (21)

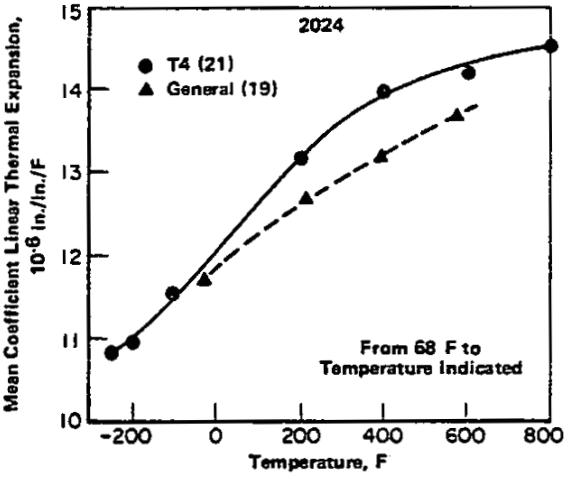


FIGURE 2.0142. EFFECT OF TEMPERATURE ON THERMAL EXPANSION (19) (21)

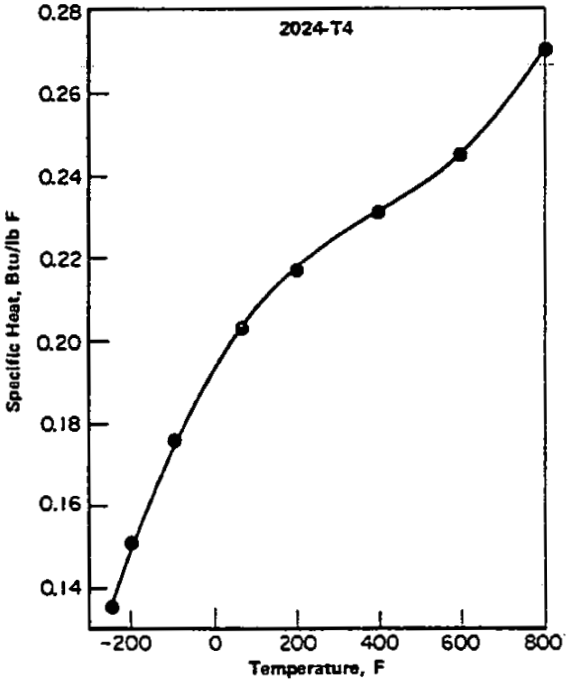


FIGURE 2.0151. EFFECT OF TEMPERATURE ON SPECIFIC HEAT (21)

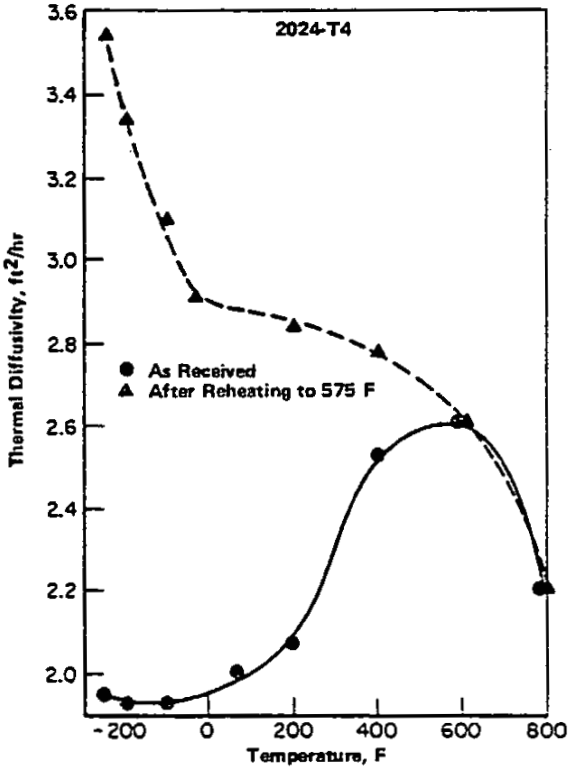


FIGURE 2.0161. EFFECT OF TEMPERATURE ON THERMAL DIFFUSIVITY (21)

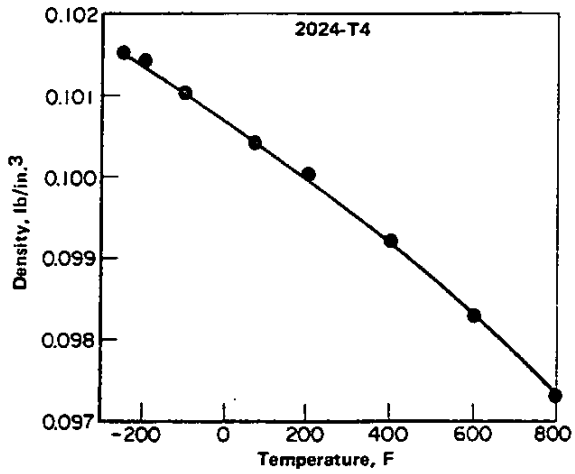


FIGURE 2.0211. EFFECT OF TEMPERATURE ON DENSITY (21)

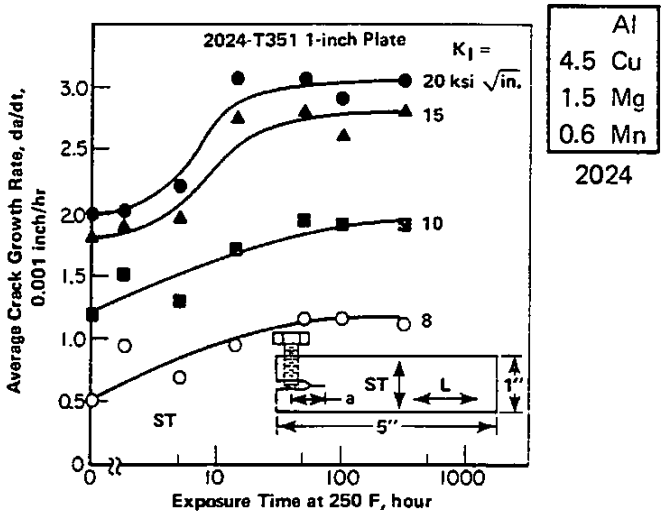


FIGURE 2.0315. EFFECTS OF PRIOR EXPOSURES AT 250 F ON STRESS-CORROSION CRACK-GROWTH RATE AT VARIOUS INITIAL LEVELS OF STRESS INTENSITY (K_I) IN DOUBLE CANTILEVER BEAM SPECIMENS LOADED IN THE SHORT TRANSVERSE (ST) DIRECTION AND INTERMITTENTLY EXPOSED 10 MIN. OF EACH HOUR IN SOLUTION AND 50 MIN. IN AIR TO 3.5 PERCENT AQUEOUS SODIUM CHLORIDE SOLUTION AT ROOM TEMPERATURE (4)

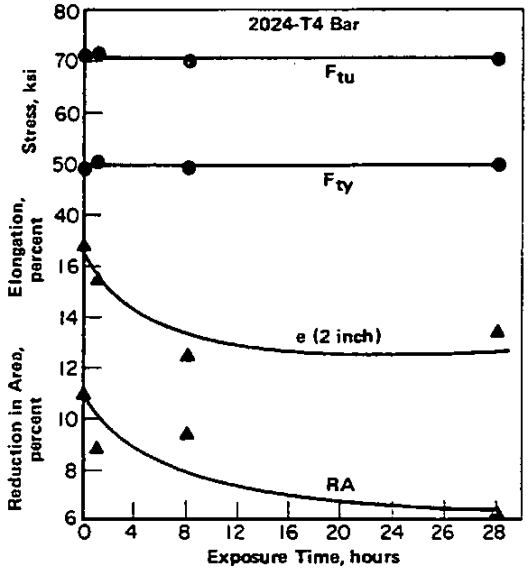


FIGURE 2.0316. EFFECTS OF EXPOSURES OF SMOOTH UNSTRESSED SPECIMENS TO SALT SPRAY AT 95 F (20 PERCENT NaCl IN DEIONIZED WATER) ON TENSILE PROPERTIES AT ROOM TEMPERATURE (2)

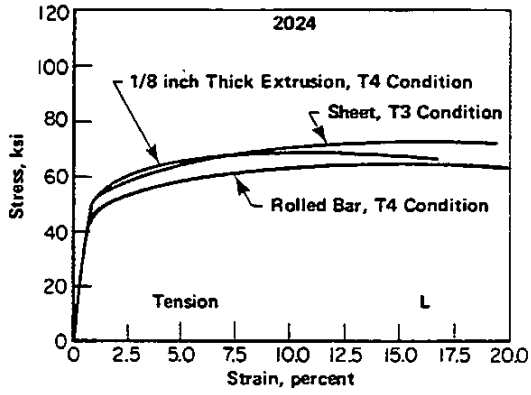


FIGURE 3.0211. COMPLETE TENSILE STRESS STRAIN CURVES FOR VARIOUS FORMS AND CONDITIONS (12)

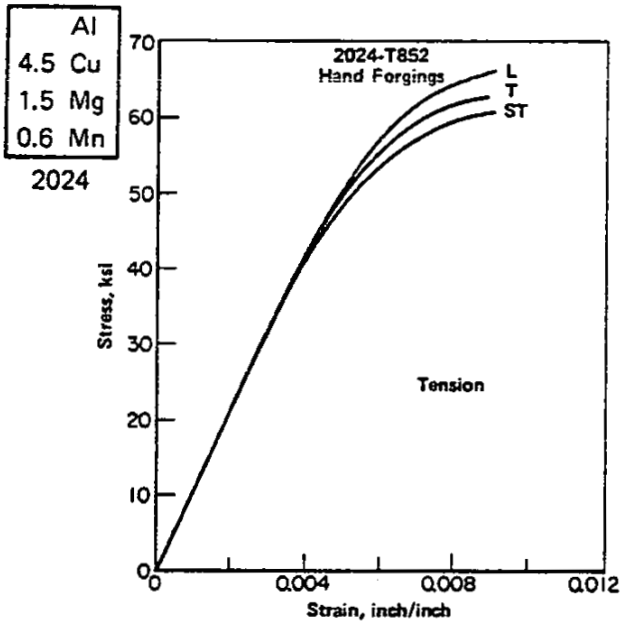


FIGURE 3.0212. TENSILE STRESS-STRAIN CURVES FOR HAND FORGINGS IN VARIOUS ORIENTATIONS, LONGITUDINAL (L), TRANSVERSE (T), AND SHORT TRANSVERSE (ST) (9)

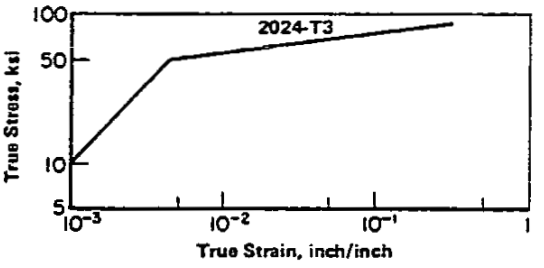


FIGURE 3.0213. TRUE-STRESS, TRUE-STRAIN CURVE (32)

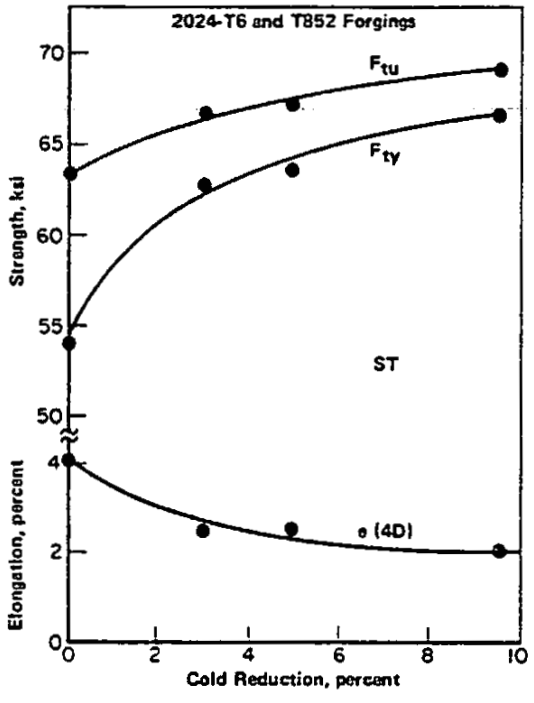


FIGURE 3.0217. EFFECTS OF COLD REDUCTION BETWEEN SOLUTION TREATMENT AND ARTIFICIAL AGING ON THE SHORT-TRANSVERSE TENSILE PROPERTIES OF FORGINGS (31)

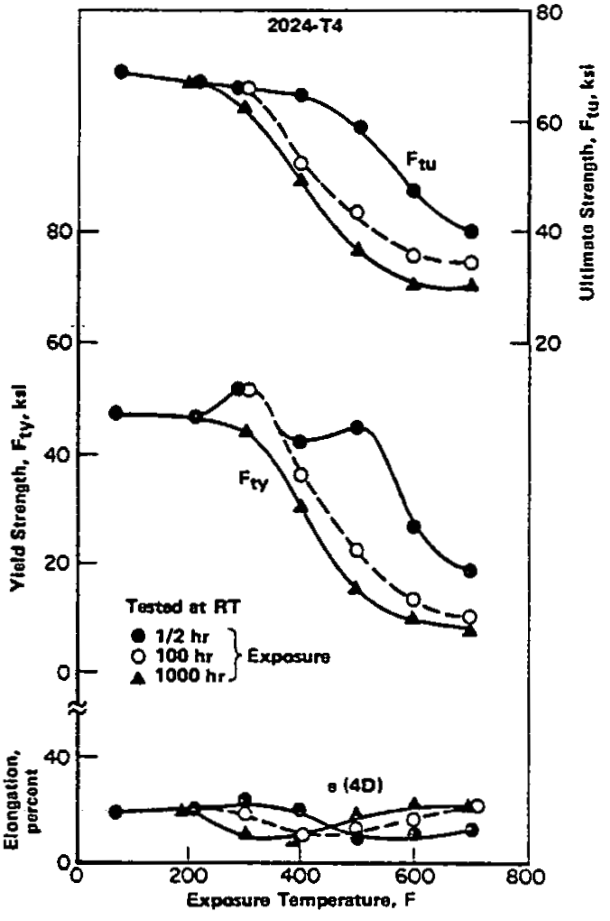


FIGURE 3.0218. EFFECTS OF EXPOSURES TO ELEVATED TEMPERATURES ON ROOM-TEMPERATURE TENSILE PROPERTIES OF ALLOY IN T4 CONDITION (38)

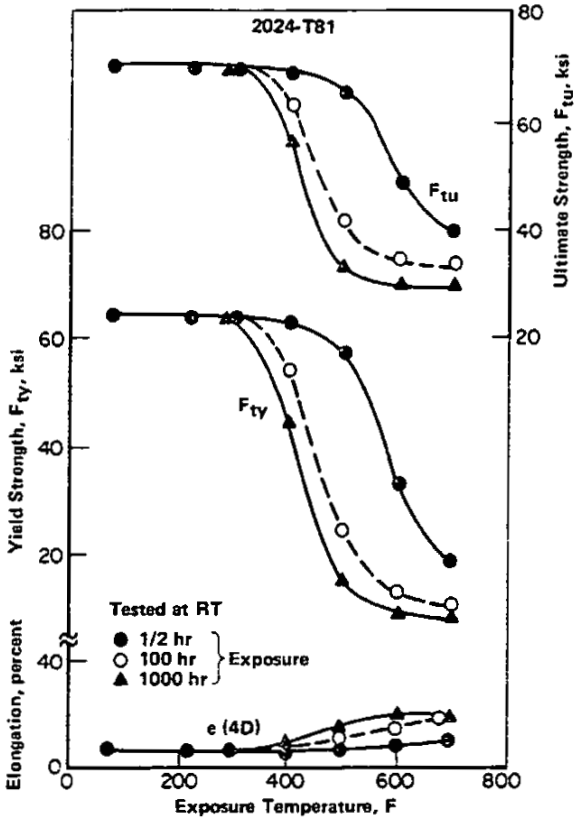


FIGURE 3.0219. EFFECTS OF EXPOSURES TO ELEVATED TEMPERATURES ON ROOM-TEMPERATURE TENSILE PROPERTIES OF ALLOY IN T81 CONDITION (39)

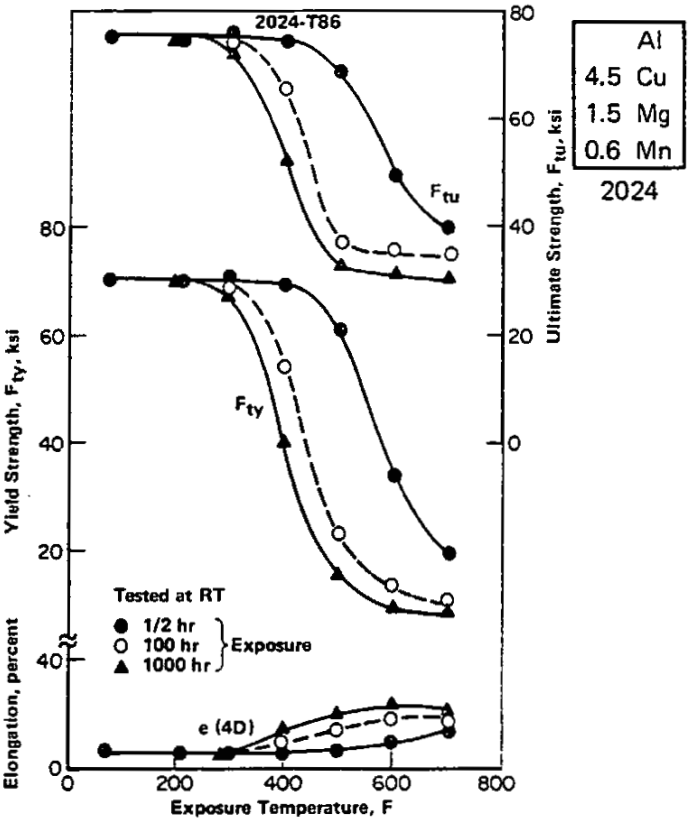


FIGURE 3.02110. EFFECTS OF EXPOSURES TO ELEVATED TEMPERATURES ON ROOM-TEMPERATURE TENSILE PROPERTIES OF ALLOY IN T86 CONDITION (40)

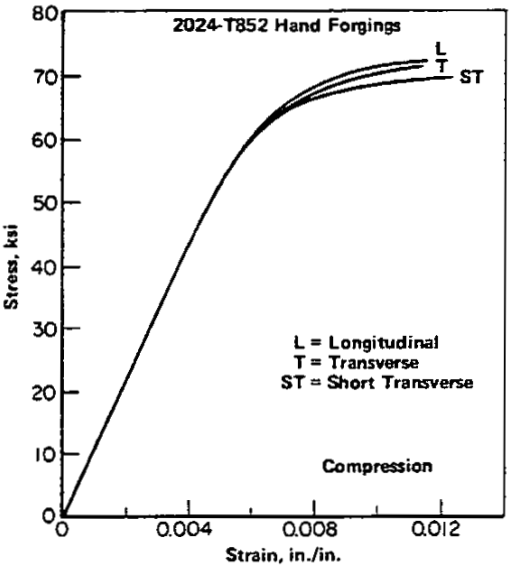


FIGURE 3.0221. COMPRESSIVE STRESS-STRAIN CURVES FOR HAND FORGINGS IN DIFFERENT ORIENTATIONS (9)

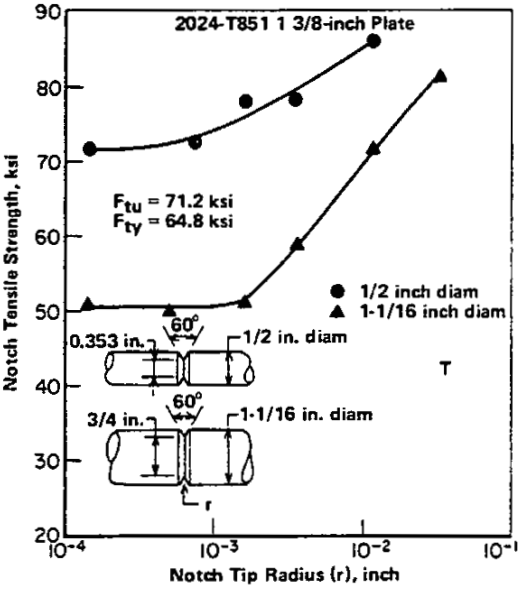


FIGURE 3.02711. EFFECTS OF SPECIMEN SIZE AND NOTCH-TIP RADIUS ON NOTCH TENSILE STRENGTH (34)

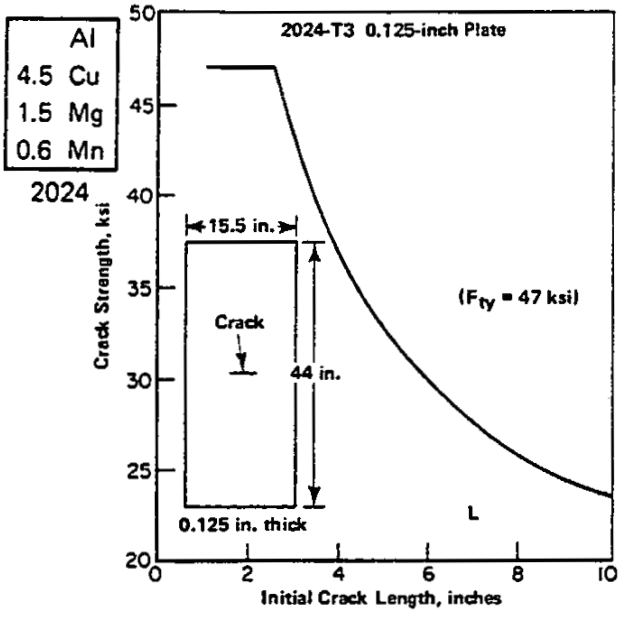


FIGURE 3.02713. EFFECT OF LENGTH OF CENTER CRACK ON CRACK STRENGTH OF 0.125-INCH PLATE (15)

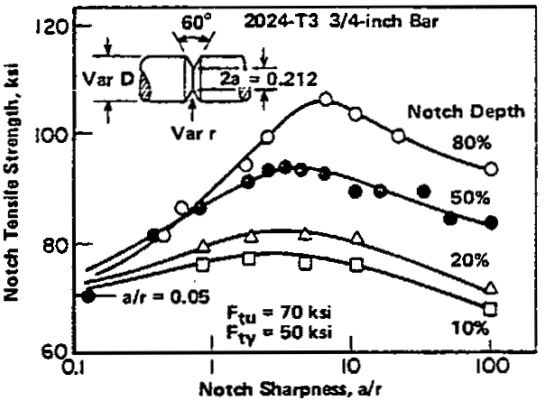


FIGURE 3.02714. EFFECTS OF NOTCH SHARPNESS AND DEPTH ON NOTCH TENSILE STRENGTH OF BAR IN T3 CONDITION (41)

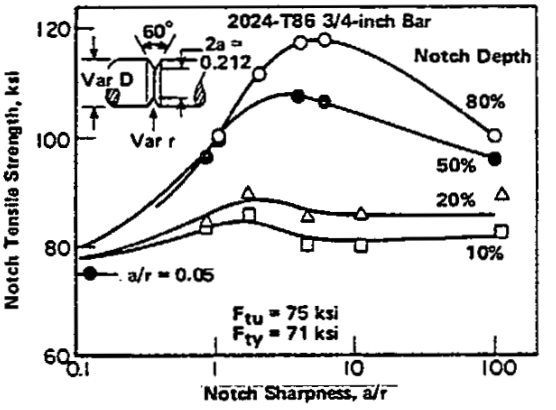


FIGURE 3.02715. EFFECTS OF NOTCH SHARPNESS AND DEPTH ON NOTCH TENSILE STRENGTH OF BAR IN T86 CONDITION (41)

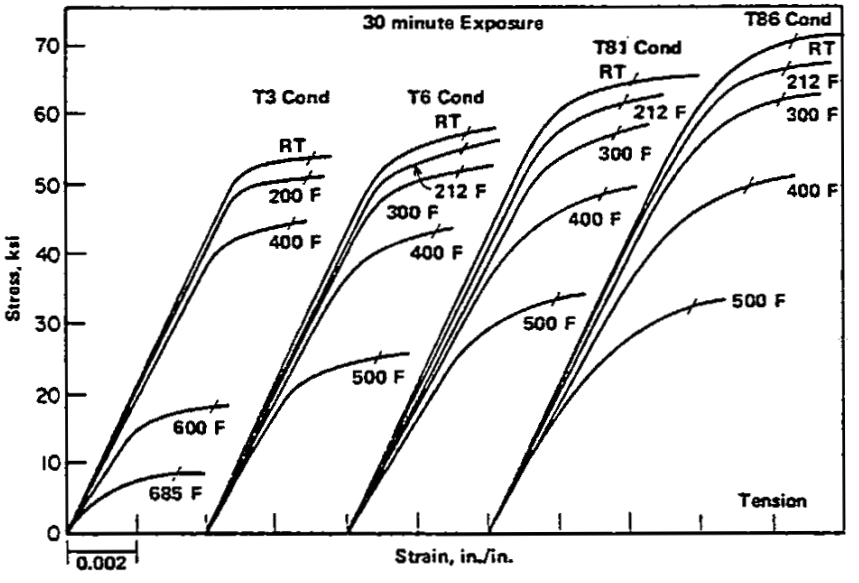


FIGURE 3.0311. STRESS-STRAIN CURVES AT VARIOUS TEMPERATURES FOR SHEET AND PLATE IN T3, T6, T81, AND T86 CONDITIONS (42)

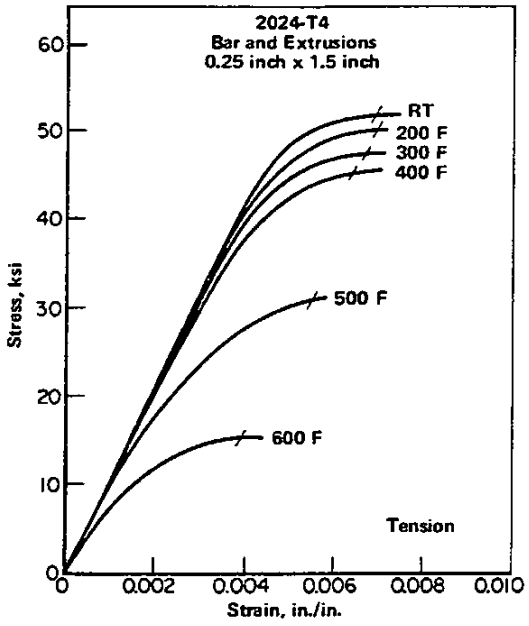
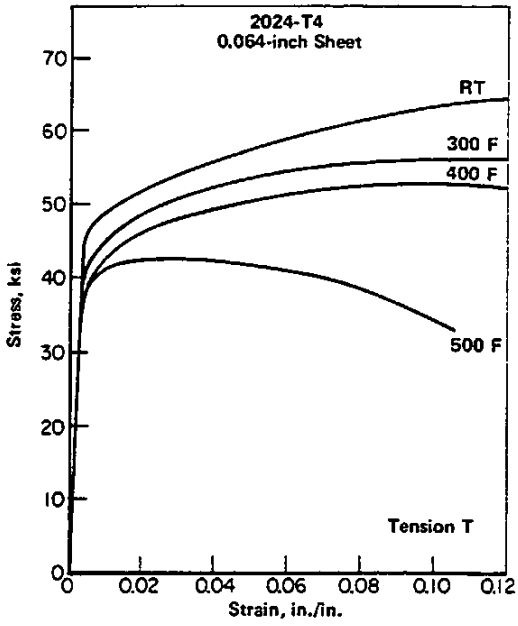


FIGURE 3.0312. STRESS-STRAIN CURVES AT VARIOUS TEMPERATURES FOR BAR AND EXTRUSIONS IN T4 CONDITION (43)



Al
4.5 Cu
1.5 Mg
0.6 Mn
2024

FIGURE 3.0313. COMPLETE STRESS-STRAIN CURVES AT VARIOUS TEMPERATURES FOR SHEET IN T4 CONDITION (44)

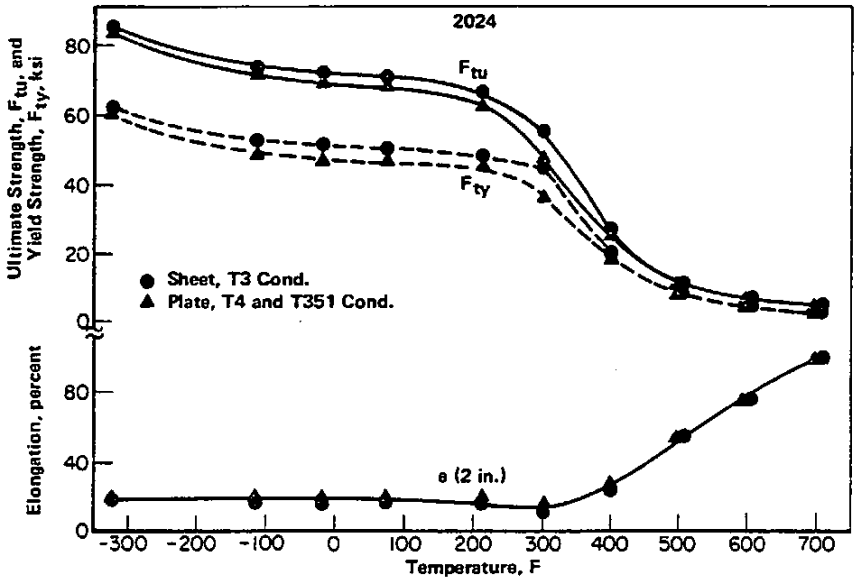


FIGURE 3.0314. EFFECTS OF TEMPERATURES FROM -320 TO 700 F ON TENSILE PROPERTIES OF SHEET AND PLATE AFTER 10,000 HOURS' EXPOSURE TIME AT TEMPERATURE (16) (26)

Al
4.5 Cu
1.5 Mg
0.6 Mn

2024

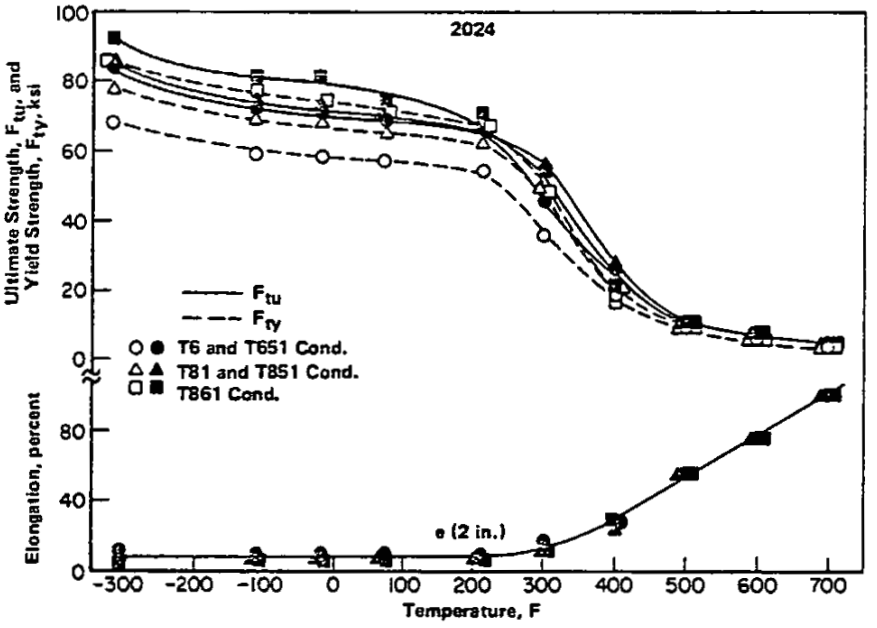


FIGURE 3.0315. TYPICAL TENSILE PROPERTIES AT TEMPERATURES FROM -320 TO 700 F FOR WROUGHT PRODUCTS IN SEVERAL HEAT-TREATED CONDITIONS AFTER 10,000 HOURS' EXPOSURE TIME AT TEMPERATURE (16) (26)

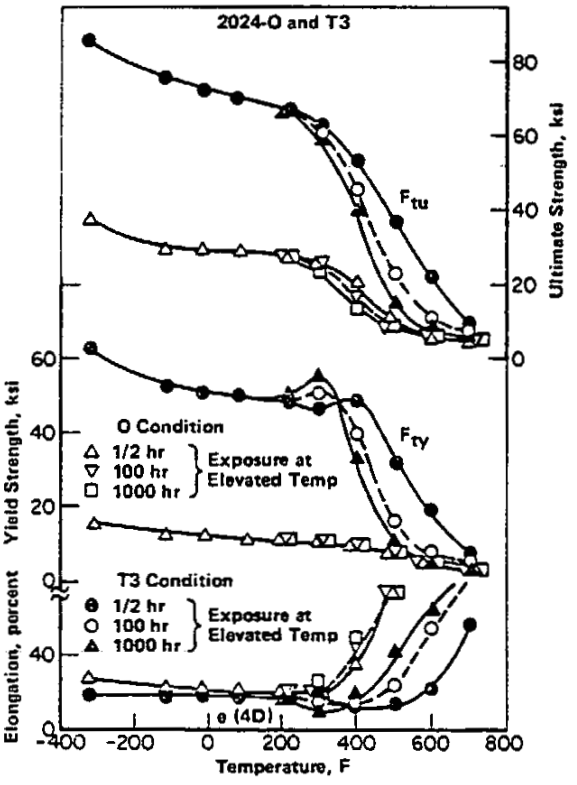


FIGURE 3.0316. EFFECTS OF TEMPERATURE AND EXPOSURE TIME AT TEMPERATURE ON TENSILE PROPERTIES OF ALLOY IN O AND T3 CONDITIONS (45) (46)

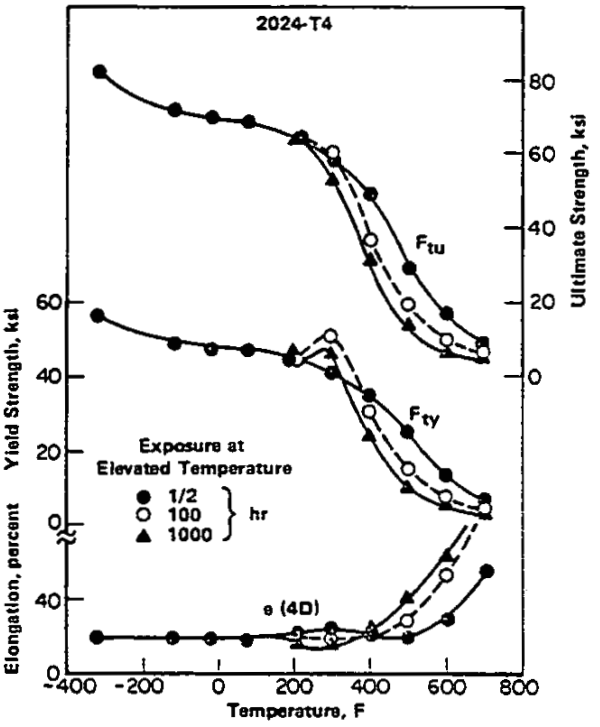


FIGURE 3.0317. EFFECTS OF TEMPERATURE AND EXPOSURE TIME AT TEMPERATURE ON TENSILE PROPERTIES OF ALLOY IN T4 CONDITION (38)

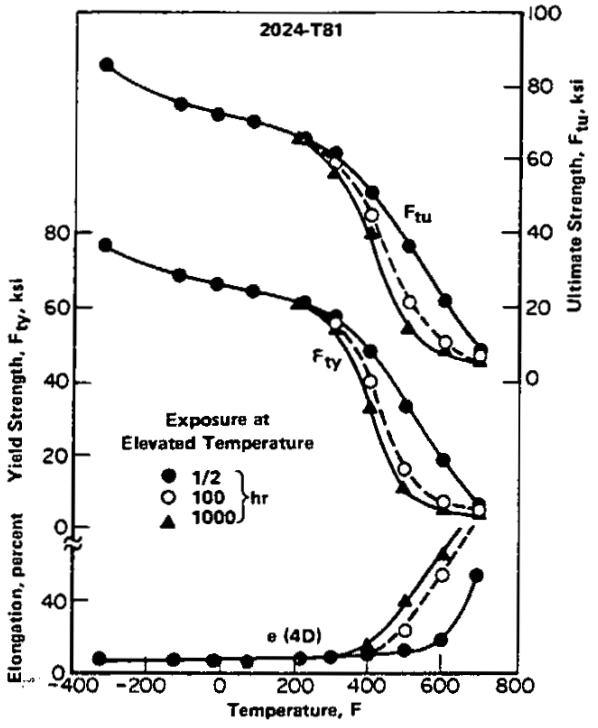


FIGURE 3.0318. EFFECTS OF TEMPERATURE AND EXPOSURE TIME AT TEMPERATURE ON TENSILE PROPERTIES OF ALLOY IN T81 CONDITION (39)

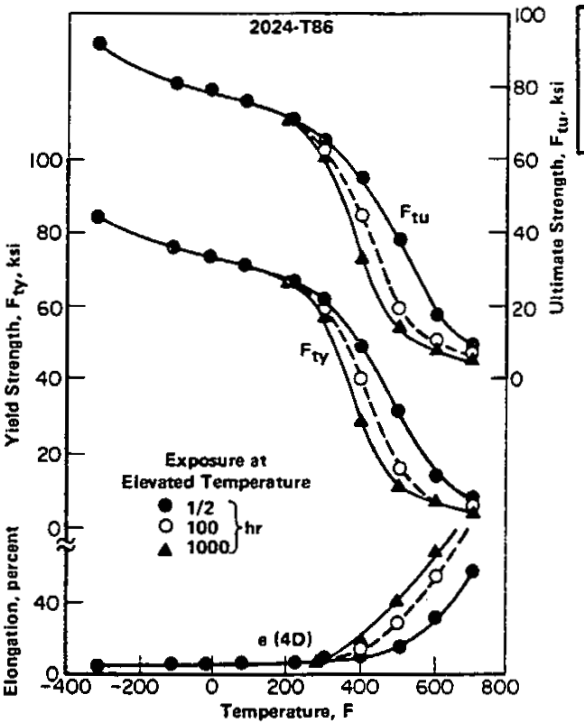


FIGURE 3.0319. EFFECTS OF TEMPERATURE AND EXPOSURE TIME AT TEMPERATURE ON TENSILE PROPERTIES OF ALLOY IN T86 CONDITION (40)

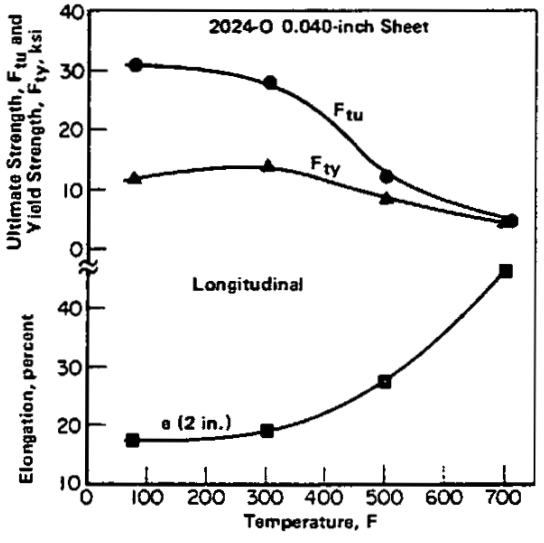


FIGURE 3.03110. EFFECTS OF TEMPERATURES FROM 75 TO 700 F ON TENSILE PROPERTIES OF ANNEALED SHEET (3)

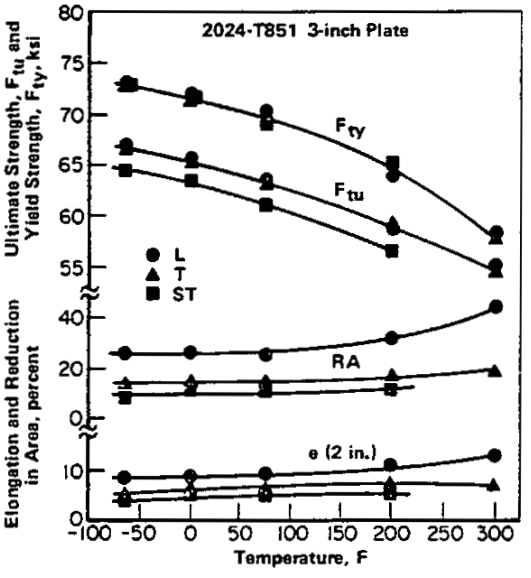


FIGURE 3.03111. EFFECTS OF TEMPERATURES FROM -65 TO 300 F AND OF LOADING ORIENTATION ON TENSILE PROPERTIES OF PLATE IN THE T851 CONDITION (8)

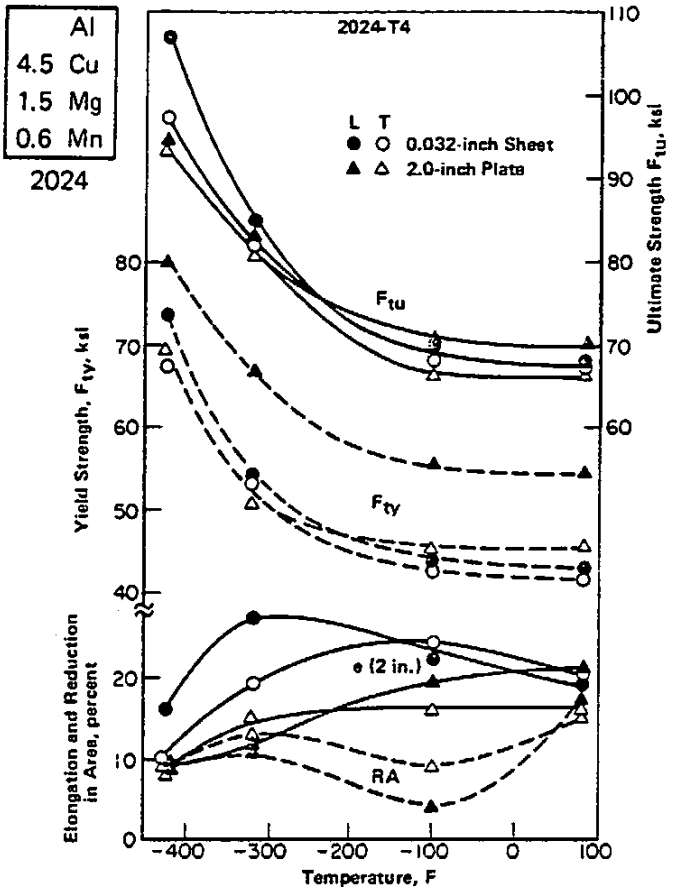


FIGURE 3.03112. EFFECTS OF TEMPERATURES FROM -423 TO 78 F ON TENSILE PROPERTIES OF SHEET AND PLATE IN THE T4 CONDITION (10)

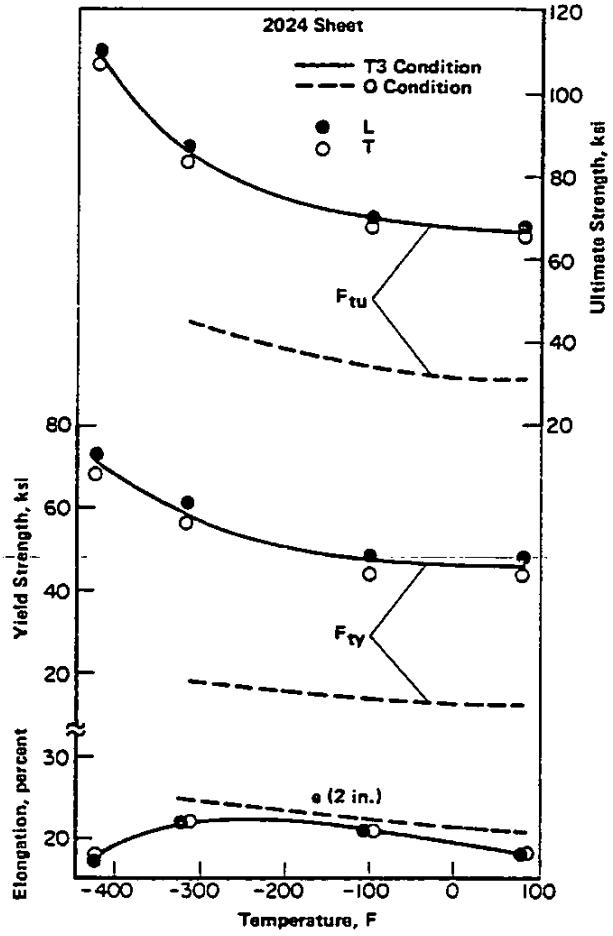


FIGURE 3.03113. EFFECTS OF TEMPERATURES FROM -423 TO 78 F ON TENSILE PROPERTIES OF SHEET IN THE T3 AND O CONDITIONS (10)

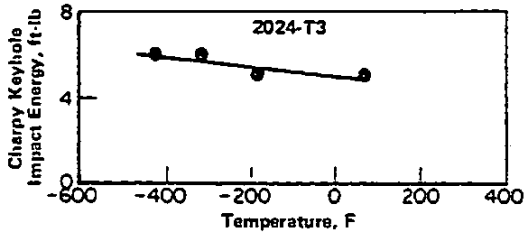


FIGURE 3.0331. EFFECT OF LOW TEST TEMPERATURES ON IMPACT STRENGTH OF ALLOY IN T3 CONDITION (47)

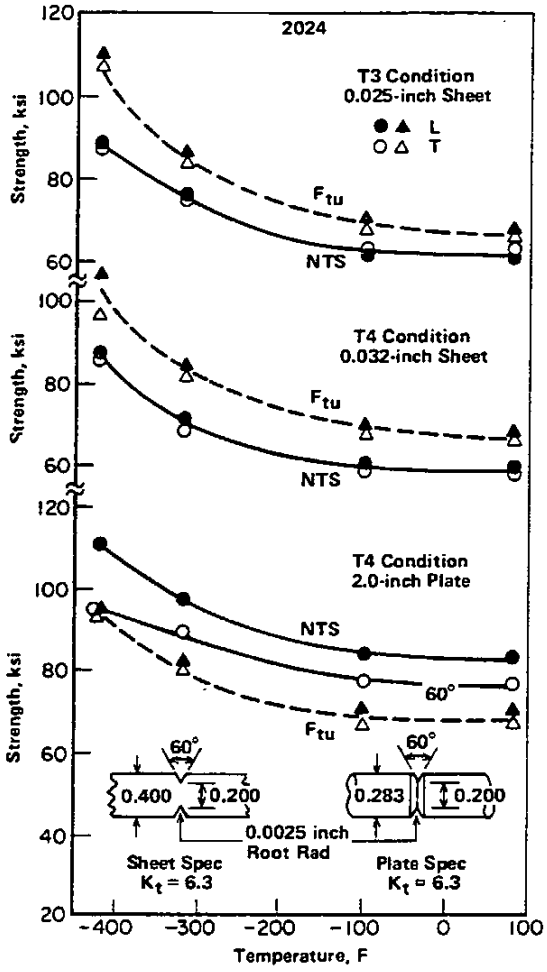


FIGURE 3.03711. COMPARISON OF LOW-TEMPERATURE NOTCH TENSILE STRENGTH AND ULTIMATE TENSILE STRENGTH OF SHEET AND PLATE IN T3 AND T4 CONDITIONS (10)

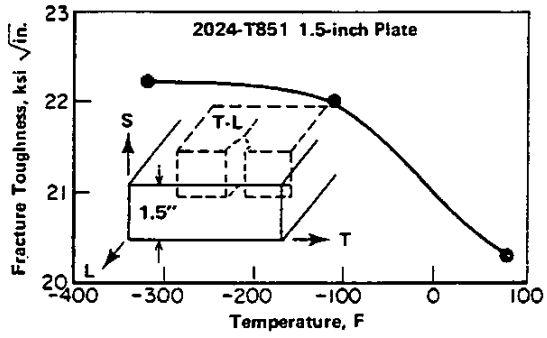
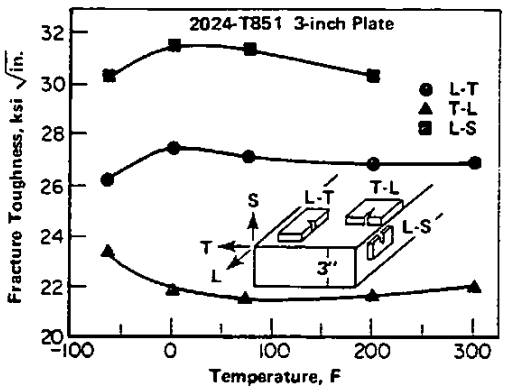


FIGURE 3.03722. EFFECTS OF TEMPERATURES FROM 75 TO -320 F ON FRACTURE TOUGHNESS (24)



Al
4.5 Cu
1.5 Mg
0.6 Mn

2024

FIGURE 3.03721. EFFECTS OF TEMPERATURES FROM -65 TO 300 F AND OF LOADING ORIENTATION ON FRACTURE TOUGHNESS (8)

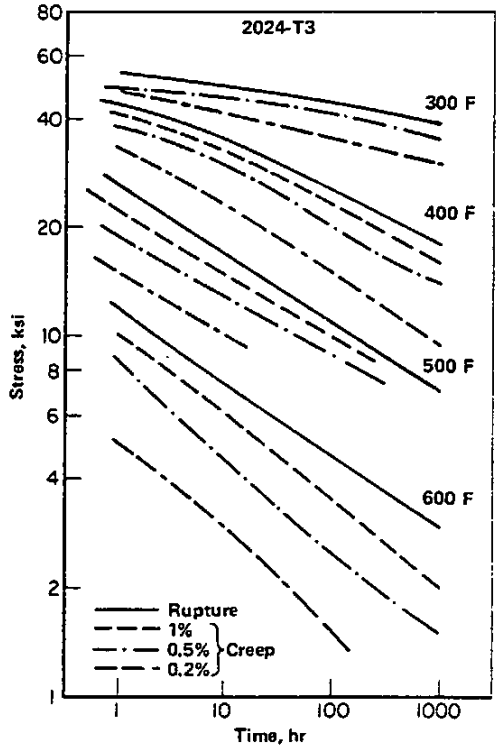


FIGURE 3.041. CREEP AND CREEP-RUPTURE CURVES AT 300 TO 600 F FOR ALLOY IN T3 CONDITION (45)

Al
4.5 Cu
1.5 Mg
0.6 Mn
2024

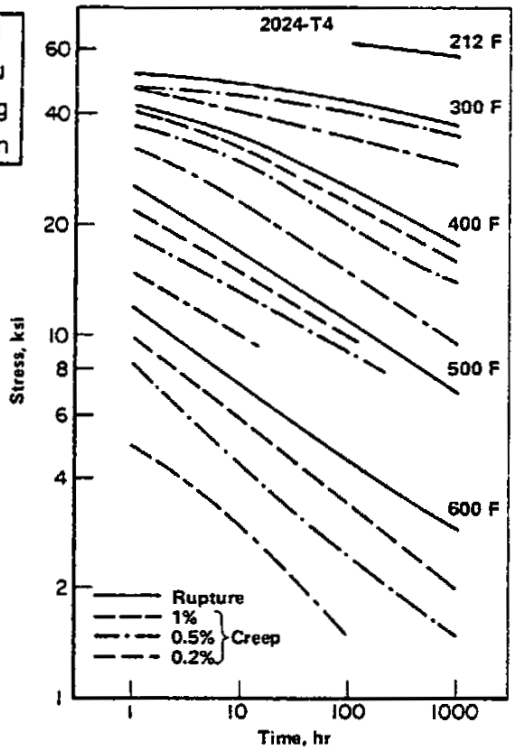


FIGURE 3.042. CREEP AND CREEP-RUPTURE CURVES AT 212 TO 600 F FOR ALLOY IN T4 CONDITION (38)

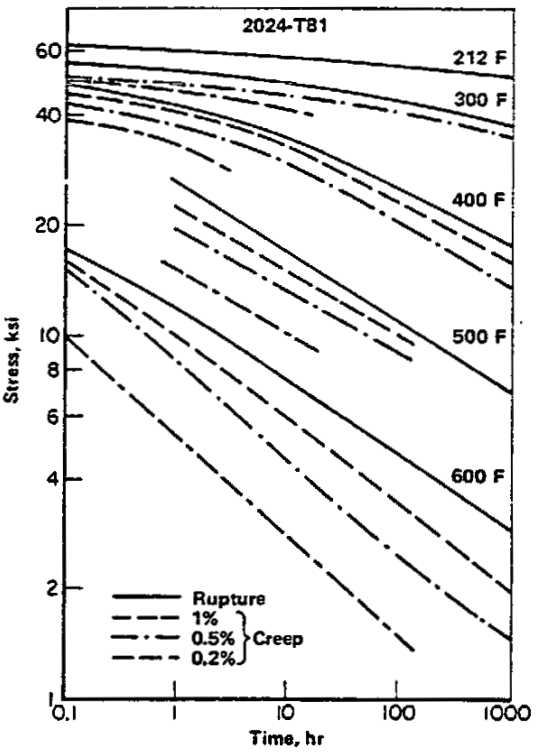


FIGURE 3.043. CREEP AND CREEP-RUPTURE CURVES AT 212 TO 600 F FOR ALLOY IN T81 CONDITION (39)

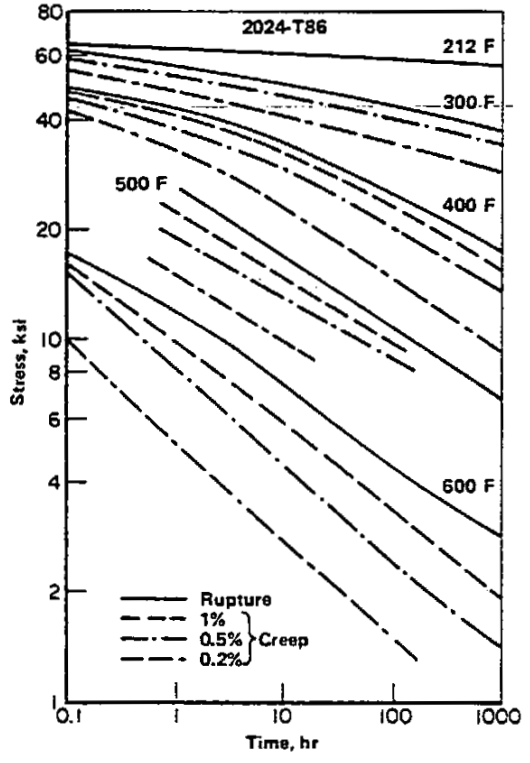


FIGURE 3.044. CREEP AND CREEP-RUPTURE CURVES AT 212 TO 600 F FOR ALLOY IN T86 CONDITION (40)

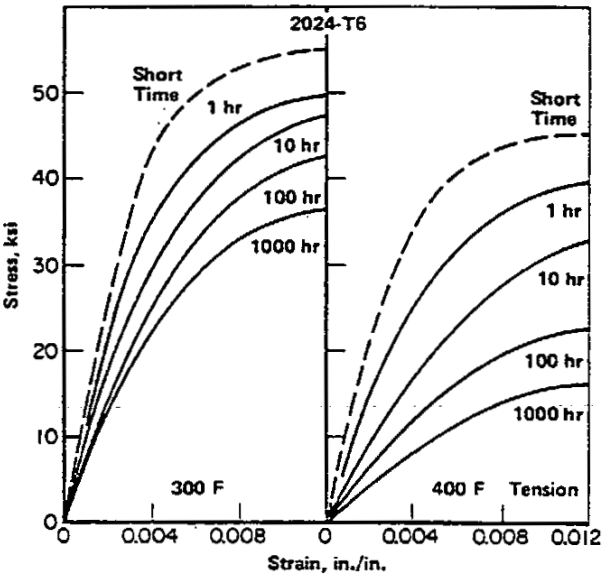


FIGURE 3.045. ISOCHRONOUS STRESS-STRAIN CURVES IN TENSION AT 300 AND 400 F FOR ALLOY IN T6 CONDITION (48)

Al
4.5 Cu
1.5 Mg
0.6 Mn
2024

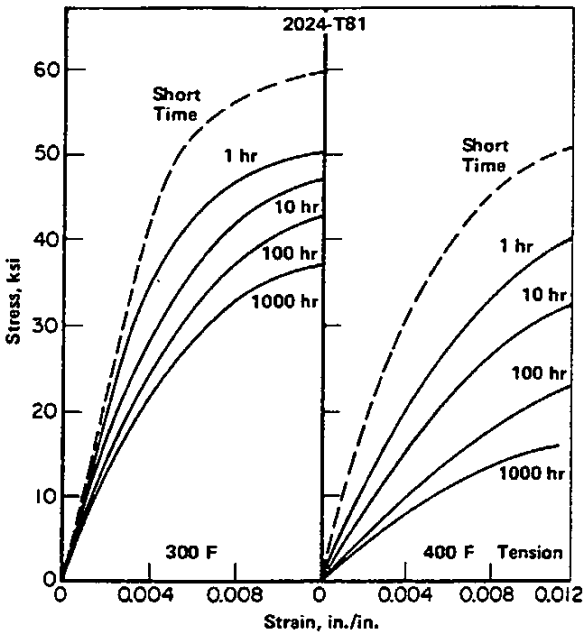


FIGURE 3.046. ISOCHRONOUS STRESS-STRAIN CURVES IN TENSION AT 300 AND 400 F FOR ALLOY IN T81 CONDITION (48)

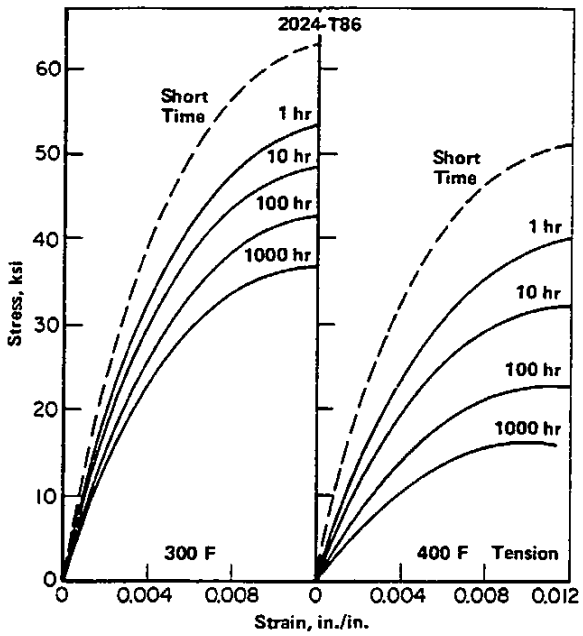


FIGURE 3.047. ISOCHRONOUS STRESS-STRAIN CURVES IN TENSION AT 300 AND 400 F FOR ALLOY IN T86 CONDITION (48)

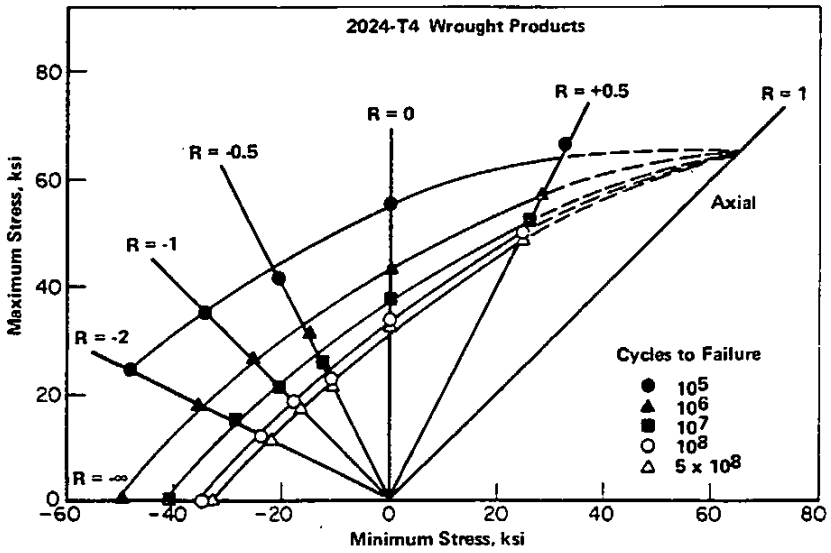


FIGURE 3.051. MODIFIED GOODMAN DIAGRAM SHOWING FATIGUE PROPERTIES OF WROUGHT PRODUCTS IN T4 CONDITION (27)

Al
4.5 Cu
1.5 Mg
0.6 Mn
2024

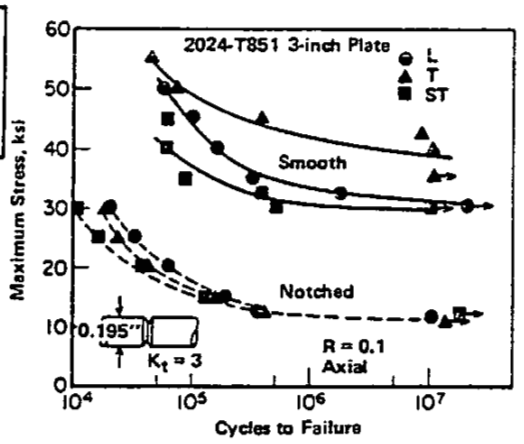


FIGURE 3.053. AXIAL FATIGUE PROPERTIES OF SMOOTH AND NOTCHED SPECIMENS TAKEN FROM PLATE IN DIFFERENT ORIENTATIONS (8)

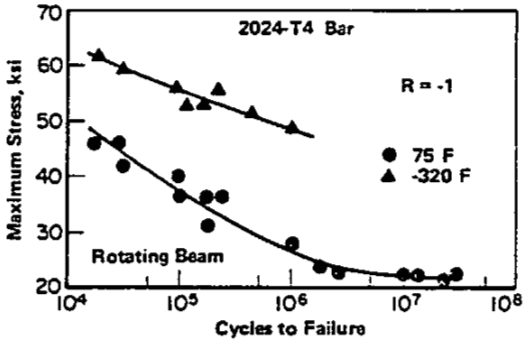


FIGURE 3.054. ROTATING BEAM FATIGUE LIFE OF BAR AT ROOM TEMPERATURE AND -320 F (11)

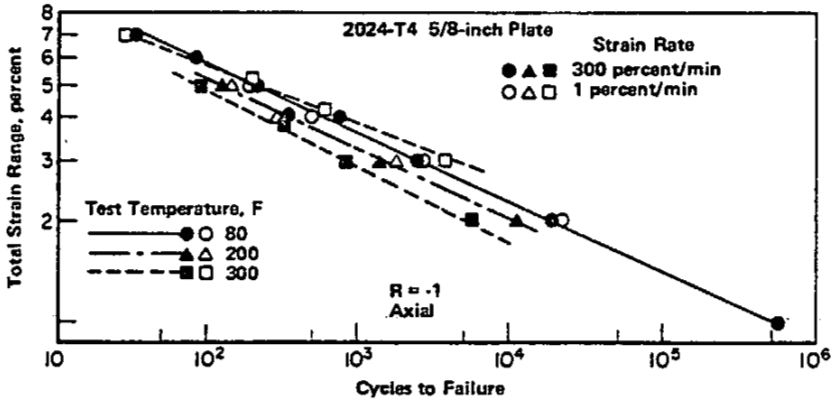


FIGURE 3.055. EFFECTS OF TOTAL STRAIN RANGE PER CYCLE, TEMPERATURE, AND STRAIN RATE ON FATIGUE LIFE (18)

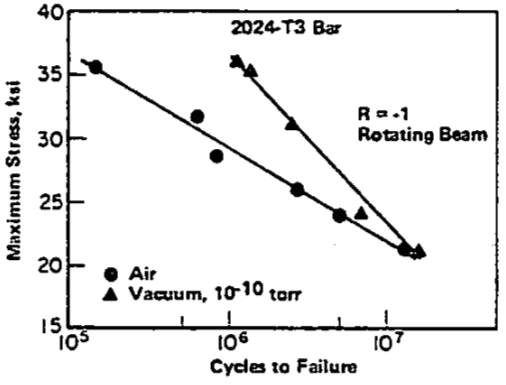


FIGURE 3.056. EFFECTS OF VACUUM VERSUS AIR ENVIRONMENT ON THE ROTATING-BEAM FATIGUE PROPERTIES OF SMOOTH SPECIMENS (5)

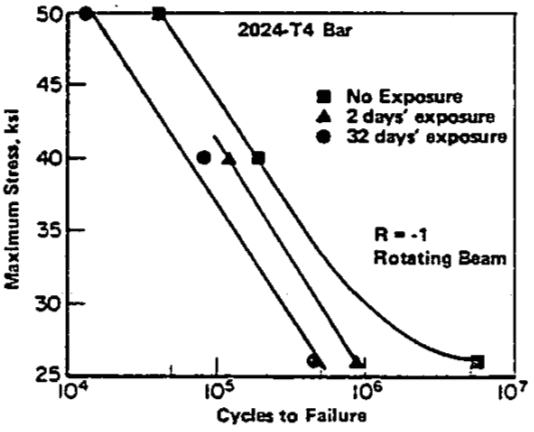


FIGURE 3.057. EFFECTS OF PRIOR EXPOSURE TO SALT SPRAY AT 95 F (20 PERCENT NaCl IN DEIONIZED WATER) ON ROTATING-BEAM FATIGUE PROPERTIES OF SMOOTH SPECIMENS AT ROOM TEMPERATURE (2)

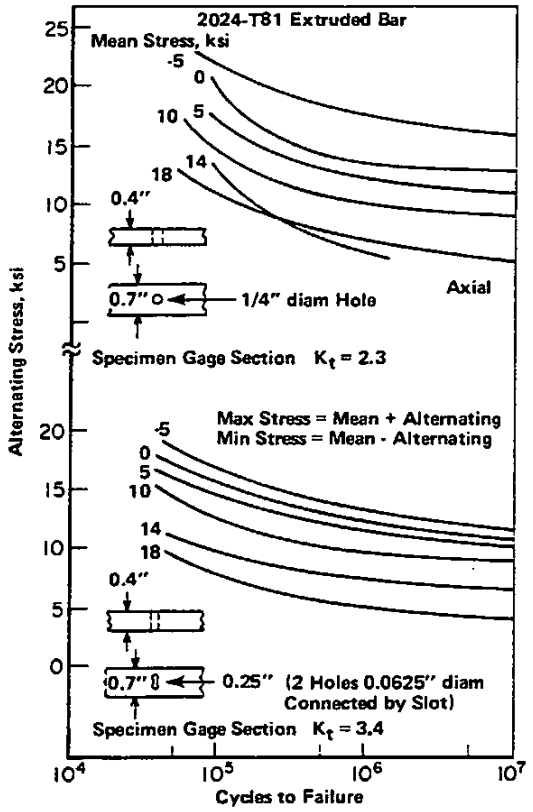
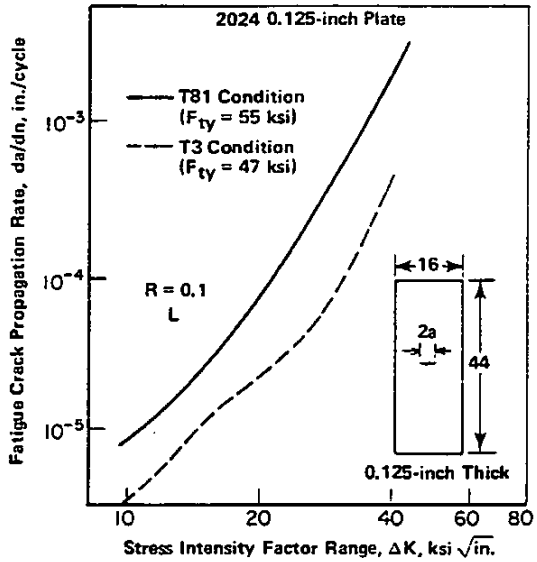


FIGURE 3.058. EFFECTS OF VARIATIONS IN MEAN STRESS ON AXIAL FATIGUE PROPERTIES OF NOTCHED SPECIMENS (6)



Al
4.5 Cu
1.5 Mg
0.6 Mn

2024

FIGURE 3.059. FATIGUE-CRACK PROPAGATION RATE AS A FUNCTION OF STRESS-INTENSITY-FACTOR RANGE IN 0.125 INCH PLATE IN TWO HEAT-TREATED CONDITIONS (15)

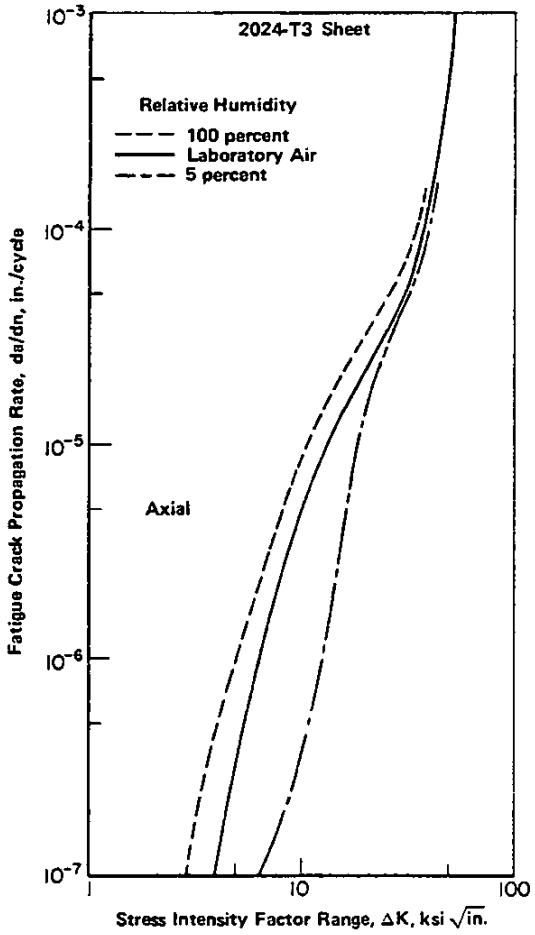


FIGURE 3.0510. FATIGUE-CRACK GROWTH RATE AS A FUNCTION OF STRESS-INTENSITY-FACTOR RANGE IN AIR ENVIRONMENTS WITH VARIOUS RELATIVE HUMIDITIES (30)

Al
4.5 Cu
1.5 Mg
0.6 Mn

2024

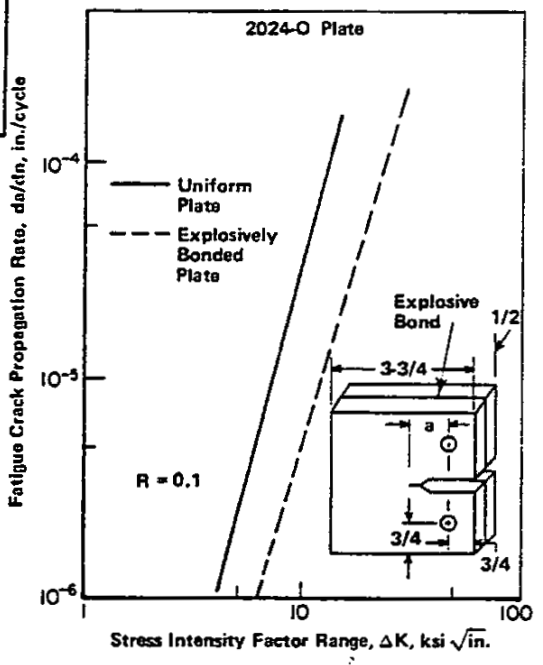


FIGURE 3.0511. FATIGUE-CRACK PROPAGATION RATE AS A FUNCTION OF STRESS-INTENSITY-FACTOR RANGE IN EXPLOSIVELY BONDED PLATE COMPARED WITH UNIFORM PLATE IN THE ANNEALED CONDITION (7)

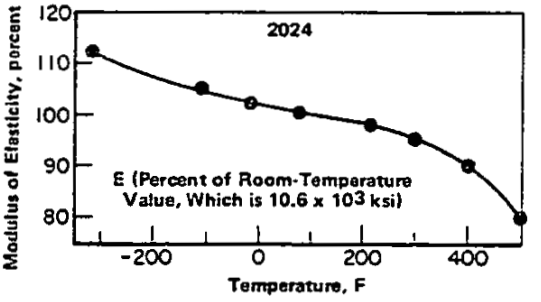


FIGURE 3.0623. EFFECT OF TEMPERATURE ON MODULUS OF ELASTICITY RELATIVE TO ROOM-TEMPERATURE VALUE (20)

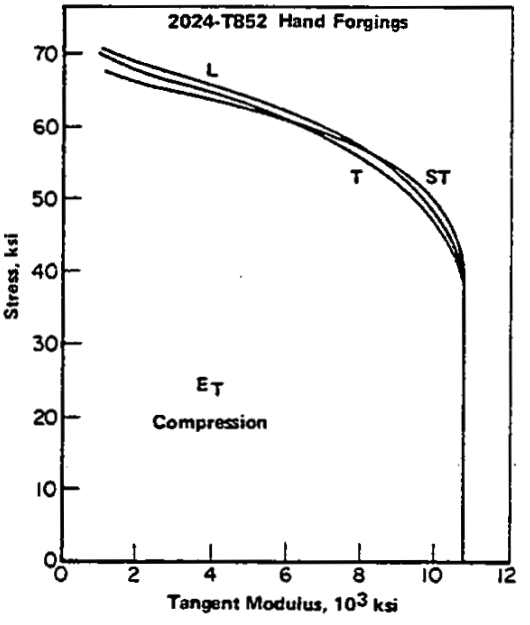


FIGURE 3.0641. TANGENT MODULUS CURVES FOR HAND FORGINGS IN DIFFERENT ORIENTATIONS (9)

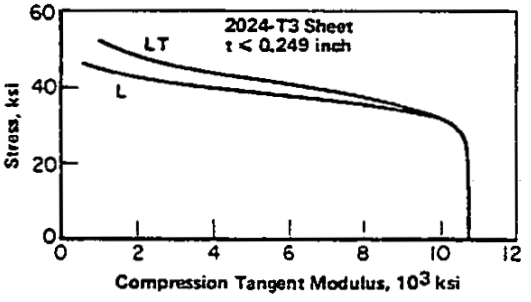


FIGURE 3.0642. TYPICAL COMPRESSIVE TANGENT-MODULUS CURVES FOR 2024-T3 ALUMINUM ALLOY AT ROOM TEMPERATURE (49)

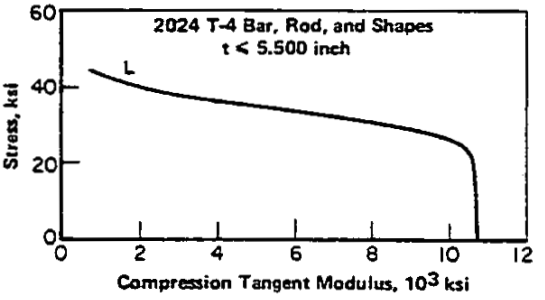


FIGURE 3.0643. TYPICAL COMPRESSIVE TANGENT-MODULUS CURVES FOR 2024-T4 ALUMINUM ALLOY AT ROOM TEMPERATURE (49)

	Al
4.5	Cu
1.5	Mg
0.6	Mn

CLAD 2024

1. GENERAL
In order to improve the corrosion resistance of 2024 sheet, strip and plate it is clad with high purity (99.3%+) aluminum (1230). This imparts to Clad 2024 a corrosion resistance equal to that of pure aluminum, unless it is overheated. The cladding reduces the strength of 2024 by about 5 percent. In most respects Clad 2024 behaves in the same manner as bare 2024, sheet, strip and plate.

1.01 Commercial Designation. Clad 2024.

1.02 Alternate Designations. Alclad 2024. Clad 24 S (obsolete).

1.03 Specifications. Table 1.03.

TABLE 1.03

AMS	Form	Military
4034	Plate,(T351 Cond)	
4036	Clad one side sheet (T3 Cond), plate (T4 Cond)	
4040 E	Sheet, plate (0 Cond)	
4041 F	Sheet, (T3 Cond) plate, (T4 Cond)	
4042 E	Sheet, plate, (T36 Cond)	
-	Sheet, plate (T6, T81, T86 Cond)	MIL-A-8705

1.04 Composition. Table 1.04.

TABLE 1.04

Source	AMS (1)			
	Core		Cladding(*)	
	Percent		Percent	
	Min	Max	Min	Max
Copper	3.8	4.9	-	0.10
Magnesium	1.2	1.8	-	-
Manganese	0.30	0.9	-	0.05
Iron	-	0.50	-	0.7
Silicon	-	0.50	-	
Zinc	-	0.25	-	0.10
Chromium	-	0.10	-	-
Other Impurities				
each	-	0.05	-	0.05
total	-	0.15	-	0.15
Aluminum	Balance		99.3	

* The nominal cladding thickness is between 5 and 1.5 percent of the total thickness on each side, depending on the total thickness of the product

1.05 Heat Treatment. Clad 2024 is heat treated under the same conditions as 2024, but the shortest heat treatment time consistant with securing the required properties should be used. Prolonged heating or repeated reheat treatments which cause diffusion of alloying elements into the coating and impair the resistance to corrosion should be avoided. See 4.043.

1.06 Hardenability. See 2024.

1.07 Forms and Conditions Available

1.071 Alloy is available in the full commercial range of sizes for sheet and plate.

1.072 Conditions available, Table 1.072.

TABLE 1.072

Source	(3, p. 32-34)
Form	Condition
Sheet	0, T3, T36, T4, T42, T6, T81, T851, T86
Plate	0, T36, T351, T4, T42, T6, T81, T851, T86

1.08 Melting and Casting Practice. Clad sheet is produced today exclusively by rolling a sandwich, rather than by casting.

1.09 Special Considerations. See 2024 also. Prolonged heating or repeated reheat treatments of clad material will cause diffusion of alloying elements into the cladding and impair its resistance to corrosion.

2. PHYSICAL AND CHEMICAL PROPERTIES

2.01 Thermal Properties. See 2024 also.

2.011 Thermal conductivity. T3 and T4 Conditions, 70.2 Btu ft per (hr sq ft F). T6 Condition, 84.7 Btu ft per (hr sq ft F).

2.012 Thermal expansion from RT to 212 F, 12.6x10^{-6} in per in per F.

2.013 Specific heat. 0.23 Btu per (lb F).

2.03 Chemical Properties

2.031 Corrosion resistance

2.0311 The general corrosion resistance of clad material is considerably superior to that of bare metal as the cladding possesses an inherent corrosion resistance comparable to that of pure aluminum. Since the cladding is more anodic than the core material, the core is protected even when it is exposed.

2.0312 The corrosion resistance is impaired by copper diffusion into the cladding during heating and heat treating for times exceeding the required minimum time or repeated heat treating.

2.032 Oxidation resistance. See 2024.

3. MECHANICAL PROPERTIES. See 2024 also and deduct 3 to 10 percent from strength values, depending on thickness of cladding.

3.01 Specified Mechanical Properties

3.011 Aluminum Association specified mechanical properties for clad sheet and plate in 0 Condition, Table 3.011.

TABLE 3.011

Source	(2, p. 32)				
Alloy	Al-4.5Cu-1.5Mg-0.6Mn				
Form	Sheet, Plate				
Condition	0 *				
Thickness - in	0.008 to 0.009	0.010 to 0.032	0.033 to 0.062	0.063 to 0.499	0.500 to 1.750
F_{tu}, max - ksi	30	30	30	32	32
F_{ty}, max - ksi	14	14	14	14	-
e(2 in), min-percent	7	8	10	12	8

* For all standard widths and clad thickness.

3.012 Aluminum Association specified mechanical properties for clad sheet in T3 Condition and clad sheet and plate in T36 Condition. Table 3.012.

3.013 Aluminum Association specified mechanical properties for clad coiled sheet in T4 Condition, clad plate in T4 and T357 Condition and clad sheet and plate in T42 and T6 Condition, Table 3.013.

3.014 Aluminum Association specified mechanical properties for clad sheet and plate in T81 and T851 Condition and T86 Condition up to width of 48 inches, Table 3.014.

3.015 Aluminum Association specified mechanical properties for clad sheet and plate in T86 Condition over 48 inches width, Table 3.015.

3.02 Mechanical Properties at Room Temperature. See 3.03 also.

3.021 Stress strain curves in tension and compression for sheet in T3 and T36 Conditions, Fig. 3.021.

3.022 Effect of stretching on tensile and compressive yield strengths of sheet in the T4 Condition, Fig. 3.022.

3.03 Mechanical Properties at Various Temperatures

3.031 Short time tension properties

3.0311 Stress strain curves for sheet in T3 Condition at room and elevated temperatures, Fig. 3.0311.

3.0312 Stress strain curves for sheet in T81 and T86 Conditions at room and elevated temperatures, Fig. 3.0312.

3.0313 Effect of exposure and test temperature on tensile properties of sheet in T3 Condition, Fig. 3.0313.

3.0314 Effect of exposure and test temperature on tensile properties of sheet in T81 Condition, Fig. 3.0314.

3.0315 Effect of exposure and test temperature on tensile properties of sheet in T86 Condition, Fig. 3.0315.

Al
4.5 Cu
1.5 Mg
0.6 Mn

CLAD 2024

TABLE 3.012

Source	(2, p. 32, 33)														
Alloy	Al-4.5Cu-1.5Mg-0.6Mn														
Form	Flat sheet					Flat sheet and plate*									
Condition	T3					T36									
Width - in	All					≤ 48			> 48 ≤ 60				> 60		
Clad thickness - %	5	5	5	2 1/2	1 1/2	5	2 1/2	1 1/2	5	2 1/2	1 1/2	1 1/2	2 1/2	1 1/2	
Thickness - in	0.008 to 0.009	0.010 to 0.020	0.021 to 0.062	0.063 to 0.249	0.188 to 0.249	0.020 to 0.062	0.063 to 0.499	0.188 to 0.499	0.020 to 0.062	0.063 to 0.499	0.188 to 0.249	0.250 to 0.499	0.063 to 0.499	0.188 to 0.249	0.250 to 0.499
F_{tu}, min -ksi	58	59	59	62	63	62	66	67	61	65	66	66	64	65	65
F_{ty}, min -ksi	39	39	39	40	41	48	50	51	47	49	50	49	48	49	48
e(2 in) min - percent	10	12	15	15	15	8	9	9	8	9	9	9	9	9	9

* For plate 0.500 in or over in thickness the clad has been removed to prepare specimens and therefore the properties are for core material only. The actual composite properties would be slightly lower. For values see 2024.

TABLE 3.013

Source	(2, p. 33, 34)														
Alloy	Al-4.5Cu-1.5Mg-0.6Mn														
Form	Coiled sheet			Plate*		Sheet and plate*							Sheet and plate		
Condition	T4			T4, T351		T42							T6		
Width - in	All			All		All							All		
Clad thickness-%	5	5	2 1/2	2 1/2	1 1/2	5	5	5	2 1/2	1 1/2	2 1/2	1 1/2	5	2 1/2	1 1/2
Thickness - in	0.010 to 0.020	0.021 to 0.062	0.068 to 0.128	0.250 to 0.499	0.250 to 0.499	0.008 to 0.009	0.010 to 0.020	0.021 to 0.062	0.063 to 0.249	0.188 to 0.249	0.250 to 0.499	0.250 to 0.499	0.010 to 0.062	0.063 to 0.499	0.188 to 0.499
F_{tu}, min -ksi	58	58	61	62	63	55	56	56	59	60	62	63	60	62	62
F_{ty}, min -ksi	37	37	38	40	40	34	34	34	36	37	38	38	47	49	49
e(2 in) min-percent	12	15	15	12	12	10	12	15	15	15	12	12	5	5	5

* See footnote for Table 3.012.

TABLE 3.014

Source	(2, p. 34)												
Alloy	Al-4.5Cu-1.5Mg-0.6Mn												
Form	Flat sheet and plate*												
Condition	T81 and T851			T86									
Width - in	All			≤ 30					> 30 ≤ 48				
Clad thickness - %	5	2 1/2	1 1/2	5	2 1/2	1 1/2	2 1/2	1 1/2	5	2 1/2	1 1/2	2 1/2	1 1/2
Thickness - in	0.010 to 0.062	0.063 to 0.499	0.188 to 0.499	0.020 to 0.062	0.063 to 0.249	0.188 to 0.249	0.250 to 0.499	0.250 to 0.499	0.020 to 0.062	0.063 to 0.249	0.188 to 0.249	0.250 to 0.499	0.250 to 0.499
F_{tu}, min -ksi	62	65	66	66	70	71	70	71	66	70	71	69	70
F_{ty}, min -ksi	54	56	57	62	66	67	65	66	62	65	66	64	65
e(2 in) min-percent	5	5	5	3	4	4	4	4	3	4	4	4	4

* See footnote for Table 3.012.

TABLE 3.015

Source	(2, p. 34)								
Alloy	Al-4.5Cu-1.5Mg-0.6Mn								
Form	Flat sheet and plate*								
Condition	T86								
Width - in	> 48 ≤ 60					> 60			
Clad thickness-%	5	2 1/2	1 1/2	2 1/2	1 1/2	2 1/2	1 1/2	2 1/2	1 1/2
Thickness - in	0.020 to 0.062	0.063 to 0.249	0.188 to 0.249	0.250 to 0.499	0.250 to 0.499	0.063 to 0.249	0.188 to 0.249	0.250 to 0.499	0.250 to 0.499
F_{tu}, min -ksi	64	69	70	68	69	69	70	68	69
F_{ty}, min -ksi	58	65	66	63	64	64	65	62	63
e(2 in) min-percent	3	4	4	4	4	4	4	4	4

* See footnote for Table 3.012.

3.032 Short time properties other than tension

3.0321 Stress strain curves in compression for sheet in T3 Condition at room and elevated temperatures, Fig. 3.0321.

3.0322 Stress strain curves in compression for sheet in T81 and T86 Conditions at room and elevated temperatures, Fig. 3.0322.

3.0323 Effect of exposure and test temperature on compressive yield strength of sheet in T3, T81 and T86 Conditions, Fig. 3.0323.

3.0324 Effect of exposure and test temperature on shear strength of sheet in T3, T81 and T86 Conditions, Fig. 3.0324.

3.0325 Effect of exposure and test temperature on bearing properties of sheet in T3 Condition, Fig. 3.0325.

3.0326 Effect of exposure and test temperature on bearing properties of sheet in T81 and T86 Conditions, Fig. 3.0326.

3.033 Static stress concentration effects

3.04 Creep and Creep Rupture Properties. See 2024.

3.041 Short time total strain curves for sheet in T81 Condition at 300 to 600 F, Fig. 3.041.

3.042 Short time total strain curves for sheet in T86 Condition at 300 to 600 F, Fig. 3.042.

3.05 Fatigue Properties. See 2024 also.

3.051 Fatigue strength of alloy in various Conditions, Table 3.051.

3.06 Elastic Properties. See 2024 also.

3.061 Clad aluminum alloys have two separate modulus values. The initial, or primary, modulus is substantially the same as that of the core material. It applies up to stresses near the yield strength of the cladding. Above this point the material exhibits a secondary modulus up to the elastic limit of the core material. The secondary modulus is from

TABLE 3.051

Source	(3, p. 142)								
Form	Sheet								
Condition	Temp F	Method	Stress Ratio		Fatigue Strength - ksi at Cycles				
			A	R	10^5	10^6	10^7	10^8	$5x10^8$
T3	RT	Rot beam	∞	-1	32	20	15	13	12.5
T36					32	20.5	16	13.5	13.5
T81					27.5	17	14.5	13.5	13.5
T86					32	19	14.5	13.5	13.0

3 to 20 percent lower depending upon the cladding thickness.

3.062 Modulus of elasticity in tension and compression for sheet in T3 Condition at room and elevated temperatures, Fig. 3.062.

3.063 Tangent modulus curves in compression for sheet in T3 Condition, Fig. 3.063.

3.064 Tangent modulus curves in compression for sheet in T81 and T86 Conditions at room and elevated temperatures, Fig. 3.064.

4. FABRICATION

In most respects this material performs in much the same manner as its core material, 2024. Exceptions are listed below.

4.01 Forming and Casting. The alloy has forming properties slightly superior to those of 2024.

4.03 Welding

4.031 Resistance welding of clad sheet in the heat treated conditions can be performed with special practices and over a narrow range of machine settings without reduction in corrosion resistance.

4.04 Heating and Heat Treating

4.041 Heat treating and reheat treating of clad material should be as fast and as short as necessary to obtain the specified properties. This requires a number of provisions during heat treating which are listed below (MIL-H-6088B(ASG).

4.042 When solution treating clad material, the load and its distribution should permit heating within a minimum time. This includes the fact that a furnace charge should contain material of nearly equal thickness.

4.043 The soaking time should be as close as possible to the specified minimum time to prevent copper diffusion to the surface and decrease in corrosion resistance. Maximum soaking times for solution treating clad material, Table 4.043.

TABLE 4.043

Source	(12)	
Thickness - in	Maximum Soaking Time - min	
	Salt Bath	Air Furnace*
≤ 0.016	15**	25
0.017 to 0.020	20	30
0.021 to 0.032	25	35
0.033 to 0.063	30	40
0.064 to 0.090	35	45
0.091 to 0.125	40	50
0.126 to 0 250	45	60
0.251 to 0.500	55	70
0.501 to 1.000	70	100
1.001 to 1.500	100	130
1.501 to 2.000	115	160
2.001 to 2.500	130	190
2.501 to 3.000	160	220
3.001 to 3.500	175	250
3.501 to 4.000	190	280

* Total time in furnace when no load thermocouple is used should not exceed indicated times by more than 35 min if thickness is 0.102 in maximum and 60 min if thickness is greater than 0.102 in

** Times less than 20 min may not yield full solution treatment.

4.044 Spray quenching can be substituted for water quenching provided that the test for intergranular corrosion is passed.

4.045 Resolution treating of clad aluminum alloys is limited to the following number of times: Thicknesses to 0.125 in maximum, once, thicknesses over 0.125 in, twice.

4.046 Regarding possible damage by improper heat treating and its detection, clad material differs from bare sheet in the following respects: In addition to the various damages possible in 2024, diffusion of copper should be tested by microscopic examination at 100 to 1000 X. To test for intergranular corrosion the cladding should be removed from both sides.

	Al
4.5	Cu
1.5	Mg
0.6	Mn

CLAD 2024

4.05 Surface Treating

4.051 The cladding protects the core by galvanic action and Clad 2024, therefore, is subject to surface treating in much the same manner as pure aluminum (1100).

4.052 Anodizing is the most popular type of surface treatment for additional corrosion protection.

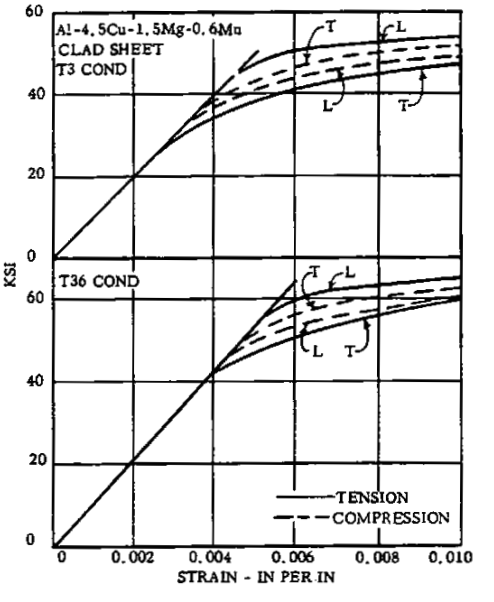


FIG. 3.021 STRESS STRAIN CURVES IN TENSION AND COMPRESSION FOR SHEET IN T3 AND T6 CONDITIONS (9)

	Al
4.5	Cu
1.5	Mg
0.6	Mn

CLAD 2024

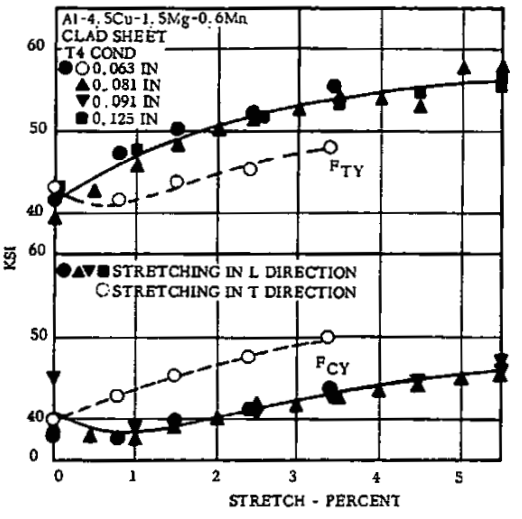


FIG. 3.022 EFFECT OF STRETCHING ON TENSILE AND COMPRESSIVE YIELD STRENGTHS OF SHEET IN T4 CONDITION

(9)

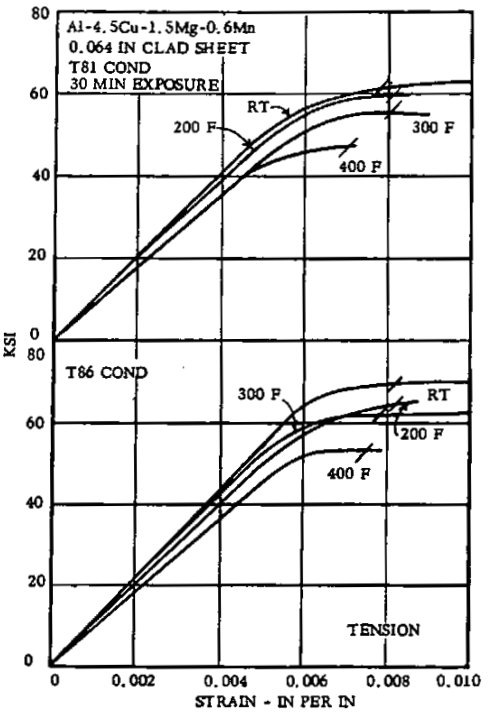


FIG. 3.0312 STRESS STRAIN CURVES FOR SHEET IN T81 AND T86 CONDITIONS AT ROOM AND ELEVATED TEMPERATURES

(5, p. 133-136, 145-148)

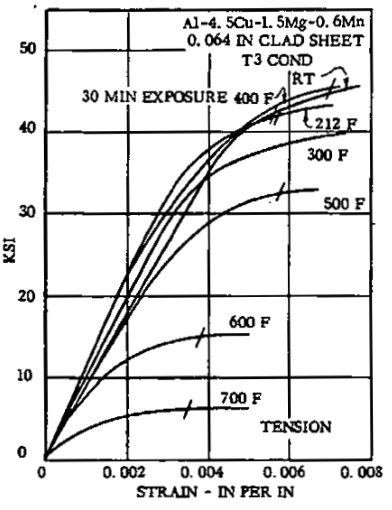


FIG. 3.0311 STRESS STRAIN CURVES FOR SHEET IN T3 CONDITION AT ROOM AND ELEVATED TEMPERATURES

(8, p. 1-7)

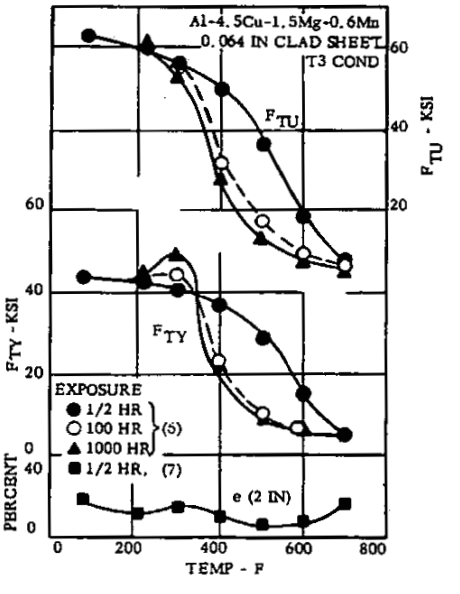


FIG. 3.0313 EFFECT OF EXPOSURE AND TEST TEMPERATURE ON TENSILE PROPERTIES OF SHEET IN T3 CONDITION

(c, p. 96)(7, p. 29)

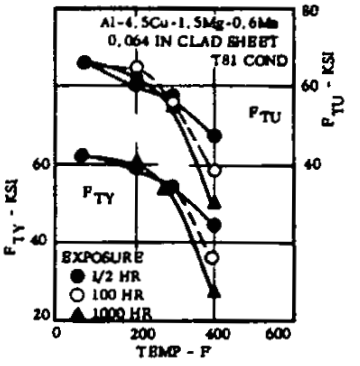
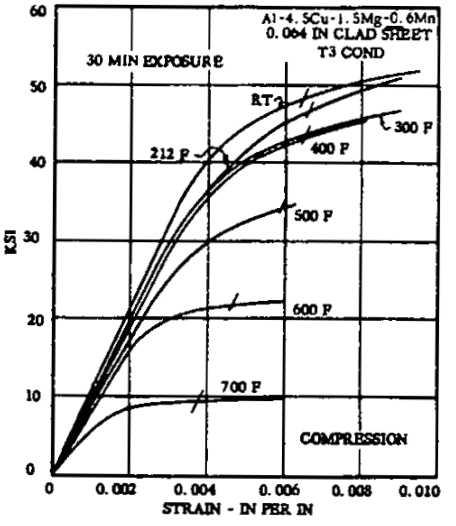


FIG. 3.0314 EFFECT OF EXPOSURE AND TEST TEMPERATURE ON TENSILE PROPERTIES OF SHEET IN T81 CONDITION (5, p. 42)



Al	
4.5	Cu
1.5	Mg
0.6	Mn

CLAD 2024

FIG. 3.0321 STRESS STRAIN CURVES IN COMPRESSION FOR SHEET IN T3 CONDITION AT ROOM AND ELEVATED TEMPERATURES (8, p. 8-14)

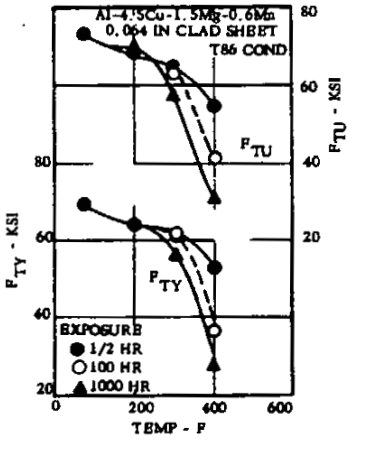


FIG. 3.0315 EFFECT OF EXPOSURE AND TEST TEMPERATURE ON TENSILE PROPERTIES OF SHEET IN T86 CONDITION (5, p. 44)

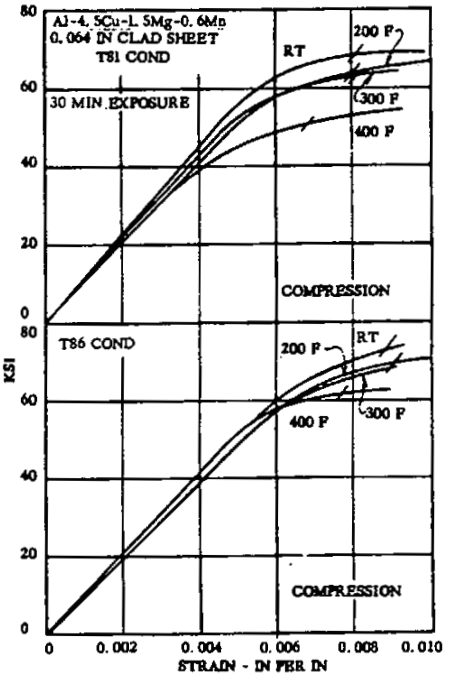


FIG. 3.0322 STRESS STRAIN CURVES IN COMPRESSION FOR SHEET IN T81 AND T86 CONDITIONS AT ROOM AND ELEVATED TEMPERATURES (5, p. 137-140, 149-152)

Al	
4.5	Cu
1.5	Mg
0.6	Mn

CLAD 2024

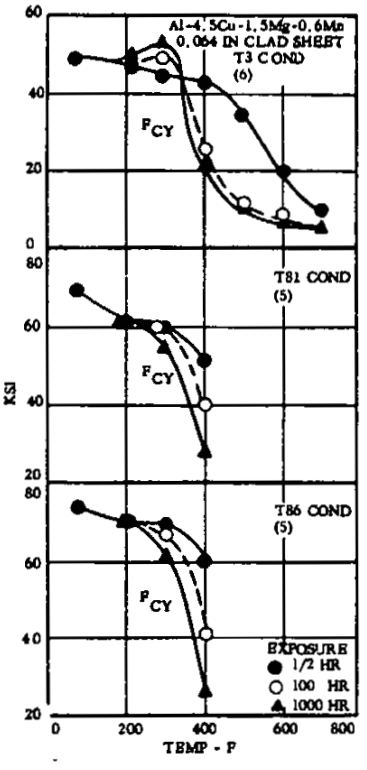


FIG. 3.0323 EFFECT OF EXPOSURE AND TEST TEMPERATURE ON COMPRESSIVE YIELD STRENGTH OF SHEET IN T3, T81 AND T86 CONDITIONS
(5, p. 42, 44)(6, p. 97)

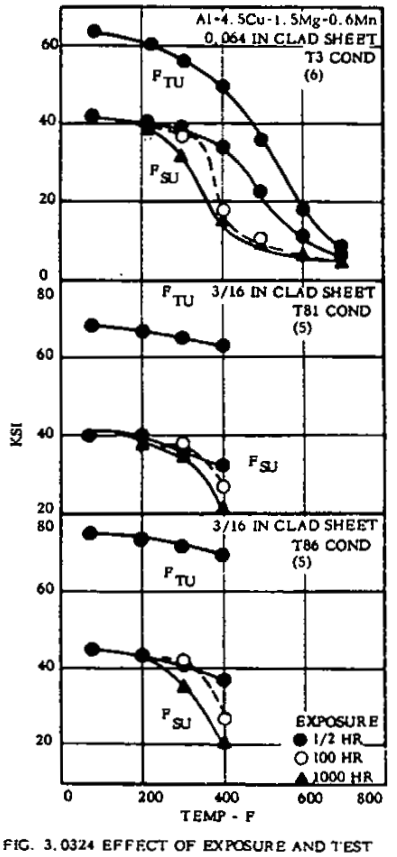


FIG. 3.0324 EFFECT OF EXPOSURE AND TEST TEMPERATURE ON SHEAR STRENGTH OF SHEET IN T3, T81 AND T86 CONDITIONS
(5, p. 42, 44)(6, p. 96, 99)

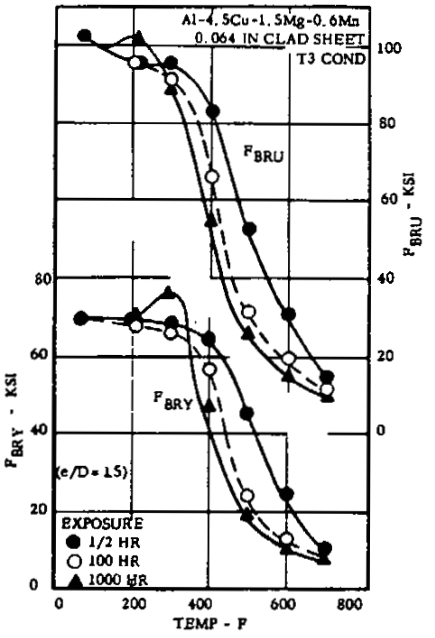


FIG. 3.0325 EFFECT OF EXPOSURE AND TEST TEMPERATURE ON BEARING PROPERTIES OF SHEET IN T3 CONDITION

(6, p. 98)

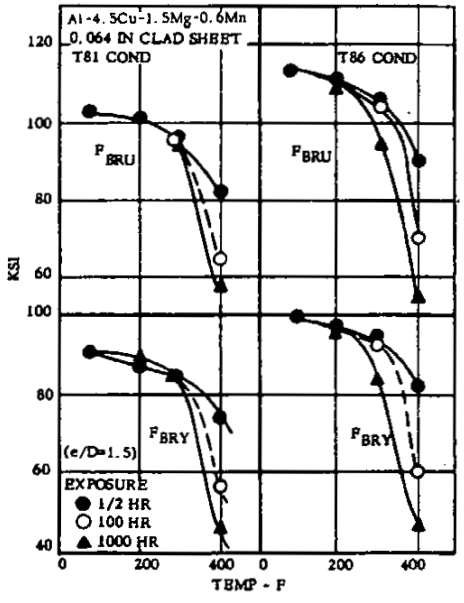
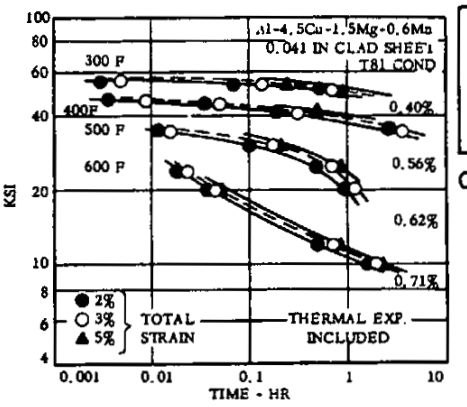


FIG. 3.0326 EFFECT OF EXPOSURE AND TEST TEMPERATURE ON BEARING PROPERTIES OF SHEET IN T81 AND T86 CONDITIONS

(5, p. 98, 102)



Al	
4.5	Cu
1.5	Mg
0.6	Mn

CLAD 2024

FIG. 3.041 SHORT TIME TOTAL STRAIN CURVES FOR SHEET IN T81 CONDITION AT 300 TO 600 F

(11, p. 33, 34)

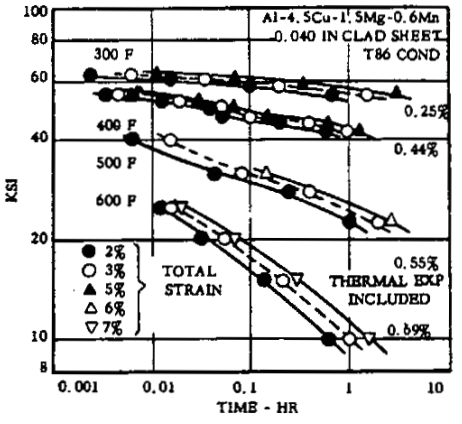


FIG. 3.042 SHORT TIME TOTAL STRAIN CURVES FOR SHEET IN T86 CONDITION AT 300 TO 600 F

(10, p. 38-41)

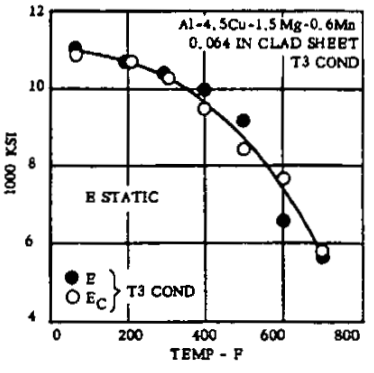


FIG. 3.062 MODULUS OF ELASTICITY IN TENSION AND COMPRESSION FOR SHEET IN T3 CONDITION AT ROOM AND ELEVATED TEMPERATURES (6, p. 96, 97)

	Al
4.5	Cu
1.5	Mg
0.6	Mn

CLAD 2024

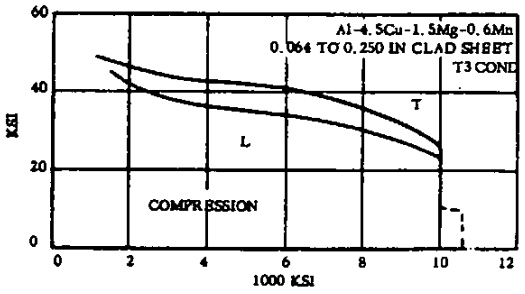


FIG. 3.063 TANGENT MODULUS CURVES IN COMPRESSION FOR SHEET IN T3 CONDITION (4, p. 84)

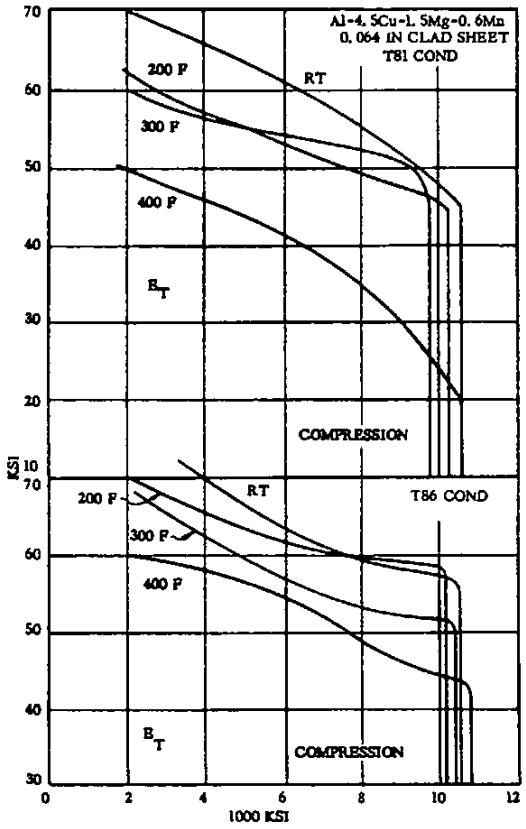


FIG. 3.064 TANGENT MODULUS CURVES IN COMPRESSION FOR SHEET IN T81 AND T86 CONDITIONS AT ROOM AND ELEVATED TEMPERATURES (5, p. 189-196)

REFERENCES

1 AMS 4034, (June 30, 1960);
AMS 4036, (Jan. 15, 1961)
AMS 4040 E, (Apr. 15, 1958)
AMS 4041 F, (Aug. 15, 1958)
AMS 4042 E, (Aug. 15, 1958)

2 The Aluminum Association, "Standards for Wrought Aluminum Mill Products", (Aug. 1961)

3 Reynolds Metals Co., "The Aluminum Data Book, Aluminum Alloys and Mill Products", Tbl. 55, (1958)

4 ANC-5, "Strength of Metal Aircraft Elements", (Mar. 1955)

5 Miller, D. E., "Determination of Physical Properties of Ferrous and Nonferrous Structural Sheet Materials at Elevated Temperatures", WADC AF TR No. 6517, Pt. 3, (June 1954)

6 Doerr, D. D., "Determination of Physical Properties of Ferrous and Nonferrous Structural Sheet Materials at Elevated Temperatures", WADC AF TR No. 6517, Pt. 1, (Dec. 1951)

7 Miller, D. E., "Determination of Physical Properties of Ferrous and Nonferrous Structural Sheet Materials at Elevated Temperatures", WADC AF TR No. 6517, Pt. 5, (Dec. 1957)

8 Doerr, D. D., "Determination of Physical Properties of Ferrous and Nonferrous Structural Sheet Materials at Elevated Temperatures", WADC AF TR No. 6517, Pt. 1, Sup. 1, (Feb. 1953)

9 Klinger, L. J. and Sachs, G., "Dependence of the Stress-Strain Curves of Cold Worked Metals Upon the Testing Direction", J. Aer. Sci., Vol. 15, p. 151, (1948)

10 Van Echo, J. A., Page, L. C., Summers, W. F. and Gross, H. C., "Short-Time Creep Properties of Structural Sheet Materials for Aircraft", WADC AF TR No. 6731, Pt. 1, (Dec. 1951)

11 Van Echo, J. A., Wirth, W. F. and Simmons, W. F., "Short-Time Creep Properties of Structural Sheet Materials for Aircraft and Missiles", WADC AF TR 6731, Pt. III, (May 1955)

12 MIL H-6088 B (ASG) Amendment 1 - Mil. Spec., "Heat Treatment of Aluminum Alloys", (Jan. 27, 1959)

NONFERROUS ALLOYS

RELEASED: JUNE 1977
AUTHOR: J. G. SESSLER

	Al
3.3	Cu
1.5	Mg
0.4	Mn

2048 Al

1. GENERAL

Aluminum alloy 2048 is a recently developed high strength alloy designed to exhibit improved fracture toughness and thermal stability at moderately elevated temperatures with only minor reduction in mechanical properties. Fracture toughness of this alloy is significantly higher than that of 2024 (the alloy from which it was derived) in the T851 Condition. Improved toughness is obtained by reduced copper content and by close control of both composition and thermal processing to reduce the amounts of second-phase particles which then yields a more homogeneous structure, (1)(4).

Conventional processing of the alloy results in material in the T851 Condition. To date, there appears to be no significant improvement in fatigue resistance nor in resistance to stress corrosion cracking in the T851 Condition as compared to 2024 - T851. However, the 2048 alloy is currently being evaluated to determine the effect of thermomechanical processing (TMP) on fatigue and stress corrosion, (4).

In this chapter, the information presented is limited to the T851 Condition only.

1.01 Commercial Designation
Aluminum alloy 2048, 2048 - T851.

1.02 Alternate Designation
None.

1.03 Specifications

1.04 Composition
Table 1.04.

1.05 Heat Treatment.

1.051 General. The heat treatment of this alloy is performed by the producer. The T851 Condition is obtained by solution treatment plus stress-relieved by stretching to produce a specified amount of permanent set, followed by artificial aging. Detailed information on heat treating procedure is available from the producer of the alloy.

1.06 Hardness.

1.07 Forms and Conditions Available.
Conventionally processed material is available as 3 inch plate in the T851 Condition. Data for other gages of sheet and plate are currently being obtained and evaluated, (6).

1.08 Melting and Casting Practice.
(See 2024).

1.09 Special Considerations.
(See 2024).

2. PHYSICAL AND ENVIRONMENTAL EFFECTS

2.01 Thermal Properties.
2.011 Melting Range. 935-1180F (approx.).
2.012 Phase Changes. Alloy is subject to precipitation hardening.
2.0121 Time-temperature-transformation diagrams.
2.013 Thermal Conductivity. 91.96 Btu-ft per (hr sq ft F) at RT, (6).
2.014 Thermal Expansion. 68-350F 12.9×10^{-6} in/in/F, (2).
70-220F 13.05×10^{-6} in/in/F, (6).
2.015 Specific Heat. 0.225 Btu per (lbF), (6).
2.016 Thermal Diffusivity.

2.02 Other Physical Properties.
2.021 Density. 0.0994 lb per cu in. 2.748 gr per cu cm, at 68F, (6).
2.022 Electrical Properties.
2.0221 Electrical Conductivity. 42 percent IACS, (6).
2.0222 Electrical Resistivity. 1.586 micro-ohm-in, (6).
2.023 Magnetic Properties. Alloy is nonmagnetic.
2.024 Emmitance.
2.025 Damping Capacity.

2.03 Chemical Environment
2.031 Stress corrosion. Seven specimens were tested for stress corrosion crack resistance in 4 point bend tests by alternate immersion in 3.5 percent sodium chloride solution at room temperature. Stress applied was 80 percent of the tensile yield strength of the material. The stress corrosion bend specimens were 5 inches by 0.5 inches and 0.050 inch thick. No cracks were observed in any of the specimens after 1000 hrs exposure, (2).
2.032 Results of stress corrosion tests with double cantilever bend (DCB) specimens taken from plate, Figure 2.032.

2.04 Nuclear Environment.

3. MECHANICAL PROPERTIES

3.01 Specified Mechanical Properties.
3.011 Tentative minimum mechanical properties for plate, Table 3.011.

3.02 Mechanical Properties at Room Temperature.
3.021 Tension.
3.0211 Stress-strain diagrams.
3.02111 Typical tensile stress-strain curves for plate (longitudinal), Figure 3.02111.
3.02112 Typical tensile stress-strain curves for plate (transverse), Figure 3.02112).
3.0212 Room temperature mechanical properties of plate, Table 3.0212.
3.0213 Effect of 1000 hour exposure at 400F on room temperature properties of plate, Table 3.0213.
3.022 Compression.
3.0221 Stress-strain diagrams.
3.02211 Typical compressive stress-strain curves for plate (longitudinal), Figure 3.02211.
3.02212 Typical compressive stress-strain curves for plate (transverse), Figure 3.02212.
3.0222 Room temperature compressive yield strength of plate, see Table 3.0212.
3.023 Impact.
3.0231 V-notch Charpy. L 7.6 ft-lb. T 4.5 ft-lb, (1).
3.024 Bending.
3.025 Torsion and Shear.
3.0251 Room temperature shear strength of plate, see Table 3.0212
3.026 Bearing.
3.027 Stress Concentration.
3.0271 Notch Properties.
3.0272 Fracture toughness. (See Appendix C).
3.02721 Results of slow bend fracture toughness tests on plate, Table 3.02721.
3.02722 Tentative minimum fracture toughness values for plate, see Table 3.011.
3.02723 Room temperature fracture toughness of plate, Table 3.02723.
3.028 Combined properties.

3.03 Mechanical Properties at Various Temperatures.
3.031 Tension.
3.0311 Stress-strain diagrams, see Figures 3.02111 and 3.02112
3.0312 Tensile properties of plate at room and elevated temperatures, Figure 3.0312.
3.0313 Tensile properties of plate at room and elevated temperatures, Figure 3.0313.
3.032 Compression.
3.0321 Stress-strain diagrams, see Figures 3.02211 and 3.02212.
3.0322 Compressive properties of plate at room and elevated temperatures, Figure 3.0322.
3.033 Impact.
3.034 Bending.
3.035 Torsion and Shear.
3.036 Bearing.
3.037 Stress Concentration.
3.0371 Notch Properties.
3.0372 Fracture toughness. (See Appendix C).
3.03721 Fracture toughness of plate at 200 and 400F, Table 3.03721
3.038 Combined Properties.

Al
3.3 Cu
1.5 Mg
0.4 Mn

2048 Al

3.04 Creep and Creep-Rupture Properties.

3.041 Stress-rupture and plastic deformation curves for plate, Figure 3.041.

3.05 Fatigue Properties.

3.051 Scatterband of fatigue data for smooth specimens at room and elevated temperatures, Figure 3.051.

3.052 Scatterband of fatigue data for notched specimens at room and elevated temperatures, Figure 3.052.

3.06 Elastic Properties.

3.061 Poisson's ratio.

3.062 Modulus of elasticity.

3.0621 Tensile modulus of elasticity at room and elevated temperatures, Figure 3.0621.

3.0622 Compressive modulus of elasticity at room and elevated temperatures, Figure 3.0622.

3.063 Modulus of rigidity.

3.064 Tangent modulus.

3.0641 Typical tangent modulus curves for plate (longitudinal), Figure 3.0641.

3.0642 Typical tangent modulus curves for plate (transverse), Figure 3.0642.

4. FABRICATION

4.01 Forming. (See also 2024).

4.011 Forming operations on plate is best accomplished in the O Condition with subsequent heat treatment.

4.02 Machining and Grinding. (See also 2024).

4.021 General. This alloy is rated as having good machinability in the annealed condition and very good to excellent machinability in heat treated conditions.

4.03 Joining. (See also 2024).

4.031 General. Heat treatable aluminum alloys, such as 2048, generally exhibit poor weldability. Fusion welding, although not usually recommended, can be accomplished using inert gas methods. Resistance welding of the alloy in heat treated conditions is possible, using special techniques. Brazing and soldering are not recommended.

4.04 Surface Treating. (See also 2024 and 2124).

4.041 The medium or atmosphere for solution treating may be molten salt, air or controlled atmospheres. Solution treat temperature should be controlled within ±10F.

4.042 Anodizing of the surfaces will improve the corrosion resistance of this alloy. Pretreatments include chemical or mechanical cleaning. Anodizing should be followed by sealing.

4.043 Scratching of surfaces should be avoided during handling of this alloy.

Source	(1)	
Element	Percent Min	Max
Copper	2.8	3.8
Magnesium	1.2	1.8
Manganese	0.20	0.60
Zinc	-	0.25
Iron	-	0.20
Silicon	-	0.15
Titanium	-	0.10
Other (Total)	-	0.15
Aluminum	Balance	

TABLE 1.04 CHEMICAL COMPOSITION

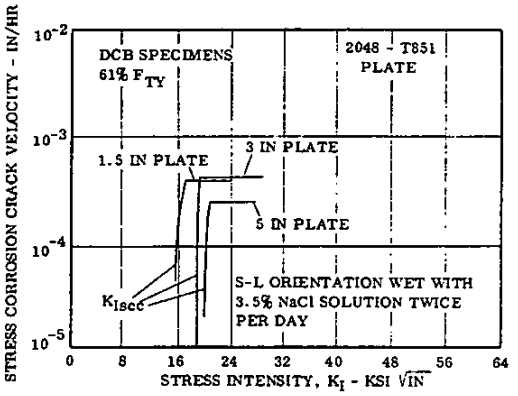


FIG. 2.032 RESULTS OF STRESS CORROSION TESTS WITH DOUBLE CANTILEVER BEND (DCB) SPECIMENS TAKEN FROM PLATE. (6)

Source	(6)		
Alloy	2048		
Form	Plate - 3 in thick		
Condition	T851		
Orientation	L	T	ST
Ftu, min - ksi	62	62	60
Fty, min - ksi	56	56	54
e(in 4D) - percent	6	5	2.5
K_{IC} - ksi $\sqrt{in}$	33	30	24

TABLE 3.011 TENTATIVE MINIMUM MECHANICAL PROPERTIES FOR PLATE.

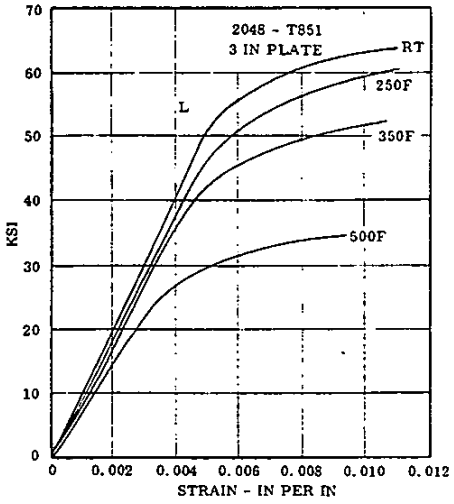


FIG. 3.02111 TYPICAL TENSILE STRESS-STRAIN CURVES FOR PLATE (LONGITUDINAL) (2)

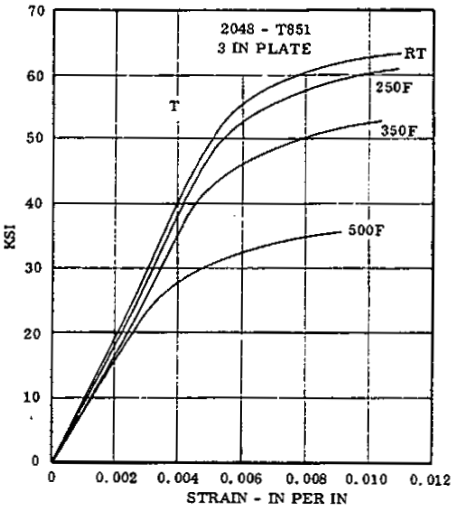


FIG. 3.02112 TYPICAL TENSILE STRESS-STRAIN CURVES FOR PLATE (TRANSVERSE). (2)

Source	(5)					
Alloy	2048					
Form	3 inch Plate					
Condition	T851					
Exposure	Tested at Room Temp (a) (No prior E. T. Exposure)			Tested at Room Temp (a) (After 1000 HR at 400F)		
Orientation	L	T	ST	L	T	ST
Ftu, ksi	68.0	68.4	65.5	47.9	48.0	44.7
Fty, ksi	62.3	62.1	59.1	33.4	33.8	31.7
e - percent	7.0	6.1	4.7	7.6	6.6	4.7
RA, (1 inch) - percent	15.7	11.1	10.8	13.7	10.6	4.3

(a) Average of 3 tests.

TABLE 3.0213 EFFECT OF 1000 HOURS EXPOSURE AT 400F ON ROOM TEMPERATURE TENSILE PROPERTIES OF PLATE.

Al
3.3 Cu
1.5 Mg
0.4 Mn

2048 Al

Source	(1)		
Alloy	2048		
Form	Plate - 3 in thick (a)		
Condition	T851		
Orientation	L	T	ST
Ftu, ksi	66.3	67.4	67.1
Fty, ksi	60.4	60.9	58.9
e, percent (in 2 inch)	8.3	7.2	6.3
RA, percent	15.7	11.7	9.4
Fcy, ksi	60.9	60.6	-
Fsu, ksi (b)	39.3	39.2	-

(a) Values are averages of triplicate tests except as otherwise indicated.
(b) Double-shear pin-type specimens; average of 4 tests in each direction.

TABLE 3.0212 ROOM TEMPERATURE MECHANICAL PROPERTIES OF PLATE.

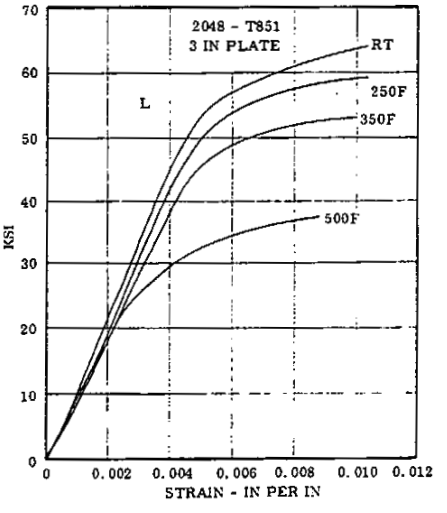


FIG. 3.02211 TYPICAL COMPRESSIVE STRESS-STRAIN CURVES FOR PLATE (LONGITUDINAL). (2)

Al
3.3 Cu
1.5 Mg
0.4 Mn

2048 Al

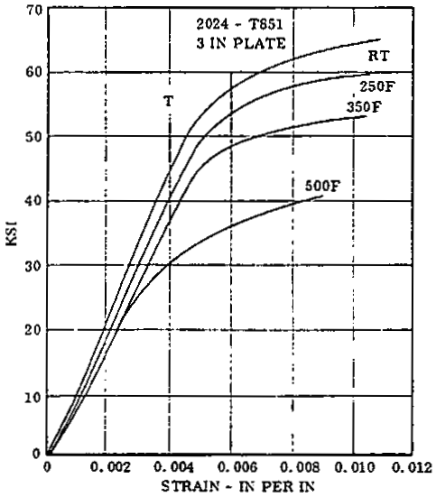


FIG. 3.02212 TYPICAL COMPRESSIVE STRESS-STRAIN CURVES FOR PLATE (TRANSVERSE). (2)

Source	(2)			
Alloy	2048-T851 (a) (b)			
Form	3 in Plate			
Orientation	a (in)	P (lbs)	$f\left(\frac{a}{w}\right)$	K_{IC} (ksi$\sqrt{in}$) (c)
T-L	0.903	4500	2.294	29.20
T-L	0.936	4100	2.410	27.95
T-L	0.946	4350	2.448	30.12
T-L	0.942	4300	2.433	29.59
T-L	0.911	4350	2.321	28.56
T-L	0.916	4425	2.339	29.27
			Average	29.12
L-T	0.876	4925	2.205	30.72
L-T	0.903	4950	2.294	32.12
L-T	0.918	4900	2.346	32.52
L-T	0.947	5075	2.452	35.19
L-T	0.880	4880	2.218	30.61
L-T	0.920	4950	2.353	32.94
			Average	32.35

(a) All tests were chevron-notched slow bend fracture toughness tests. ASTM Method E-399-72. Specimens were precracked and tested under 3 point bend loading.
(b) W = 2.00 inches
T = 1.00 inches
Span = 8.0 inches
(c) These values meet ASTM E-399-72 criteria.

TABLE 3.02721 RESULTS OF SLOW BEND FRACTURE TOUGHNESS TESTS ON PLATE.

Source	(5)				
Alloy	2048				
Form	3 in Plate				
Condition	T-851				
Orientation	Width (in)	Thickness (in)	a/w	P_{max}/P_Q	K_{IC} (ksi$\sqrt{in}$) (a)
L-T	2.8	1.4	0.484	1.06	37.0
L-T	2.8	1.4	0.466	1.07	35.8
L-T	1.75	0.875	0.486	1.06	34.4
L-T	1.75	0.875	0.563	1.05	34.9
L-T	1.75	0.875	0.491	1.06	34.8
T-L	2.8	1.4	0.475	1.01	31.4
T-L	2.8	1.4	0.476	1.01	31.2
T-L	2.8	1.4	0.475	1.02	31.2
T-L	1.75	0.875	0.492	1.00	29.3
T-L	1.75	0.875	0.500	1.02	31.3
T-L	1.75	0.875	0.500	1.05	30.7
T-L	1.5	0.75	0.506	1.07	31.0
T-L	1.5	0.75	0.507	1.02	28.0
T-L	1.5	0.75	0.496	1.02	31.7
S-L	1.75	0.875	0.499	1.03	27.5
S-L	1.75	0.875	0.497	1.05	26.9
S-L	1.75	0.875	0.506	1.05	25.4

(a) ASTM E-399-72 compact tension.

TABLE 3.02723 ROOM TEMPERATURE FRACTURE TOUGHNESS OF PLATE.

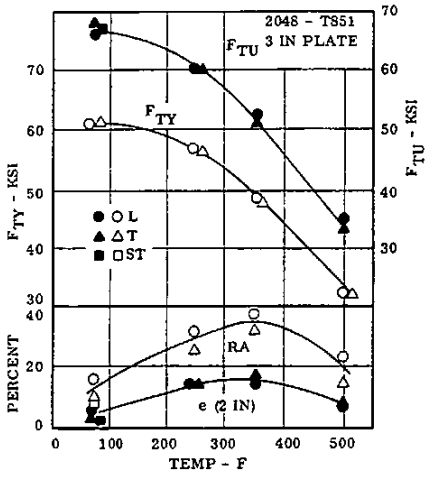


FIG. 3.0312 TENSILE PROPERTIES OF PLATE AT ROOM AND ELEVATED TEMPERATURES. (1)

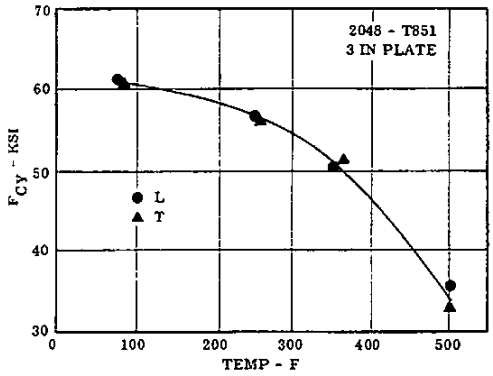


FIG. 3.0322 COMPRESSIVE PROPERTIES OF PLATE AT ROOM AND ELEVATED TEMPERATURES. (1)

Al
3.3 Cu
1.5 Mg
0.4 Mn

2048 Al

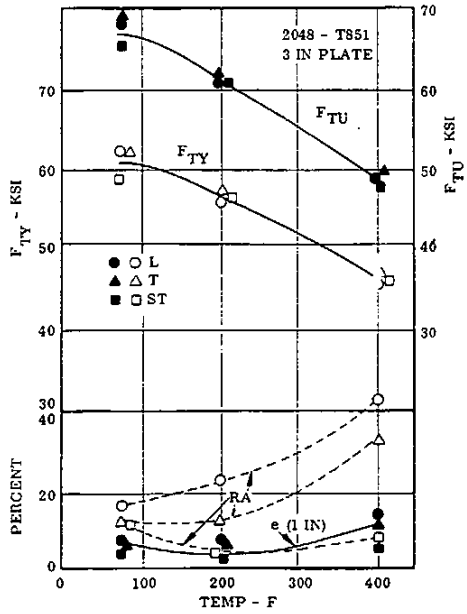


FIG. 3.0313 TENSILE PROPERTIES OF PLATE AT ROOM AND ELEVATED TEMPERATURES. (5)

Al
3.3 Cu
1.5 Mg
0.4 Mn

2048 Al

Source	(5)					
Alloy	2048					
Form	3 in Plate					
Condition	T851					
Orientation	Width (in)	Thickness (in)	a/w	Test Temp-F	Pmax/Pq	K_{IC} (ksi $\sqrt{in}$) (a)
L-T	2.8	1.4	0.481	200	1.06	36.9
L-T	2.8	1.4	0.489	200	1.05	37.0
L-T	2.8	1.4	0.482	200	1.05	37.0
T-L	2.8	1.4	0.486	200	1.04	32.1
T-L	2.8	1.4	0.489	200	1.05	31.0
T-L	2.8	1.4	0.477	200	1.04	31.5
S-L	2.5	1.25	0.521	200	1.03	25.6
S-T	2.5	1.25	0.533	200	1.01	28.3
T-L	2.8	1.4	0.475	400	1.05	31.1
S-L	2.5	1.25	0.528	400	1.05	30.7
S-T	2.5	1.25	0.508	400	1.05	32.3

(a) ASTM E-399-72 compact tension.

TABLE 3.03721 FRACTURE TOUGHNESS OF PLATE AT 200 AND 400F.

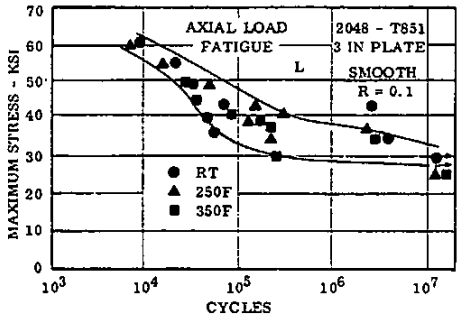


FIG. 3.051 SCATTERBAND OF FATIGUE DATA FOR SMOOTH SPECIMENS AT ROOM AND ELEVATED TEMPERATURES. (2)

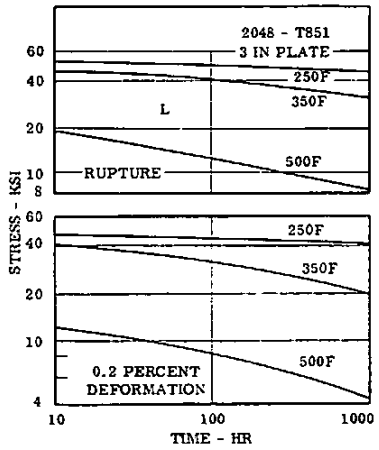


FIG. 3.041 STRESS-RUPTURE AND PLASTIC DEFORMATION CURVES FOR PLATE. (1)

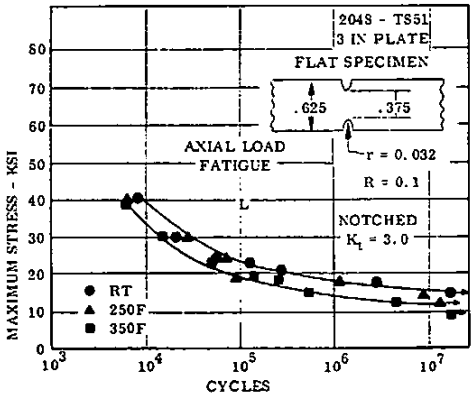


FIG. 3.052 SCATTERBAND OF FATIGUE DATA FOR NOTCHED SPECIMENS AT ROOM AND ELEVATED TEMPERATURES. (2)

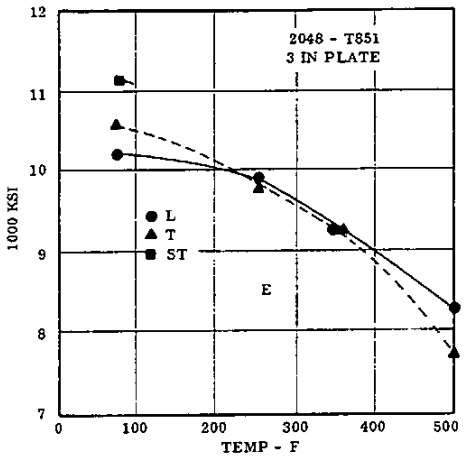
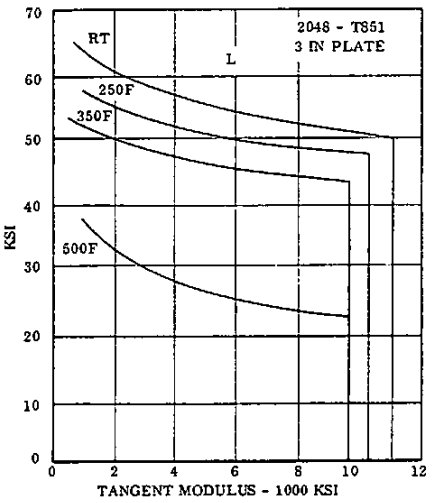


FIG. 3.0621 TENSILE MODULUS OF ELASTICITY AT ROOM AND ELEVATED TEMPERATURES. (1)



Al
3.3 Cu
1.5 Mg
0.4 Mn

2048 Al

FIG. 3.0641 TYPICAL TANGENT MODULUS CURVES FOR PLATE (LONGITUDINAL).

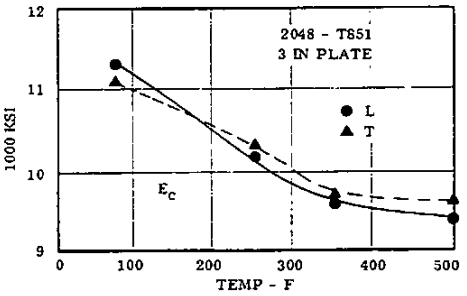


FIG. 3.0622 COMPRESSIVE MODULUS OF ELASTICITY AT ROOM AND ELEVATED TEMPERATURES. (1)

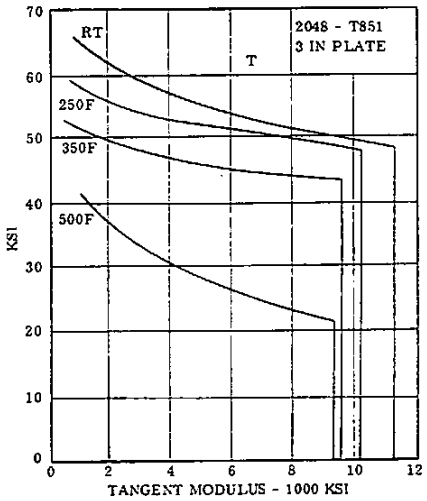


FIG. 3.0642 TYPICAL TANGENT MODULUS CURVES FOR PLATE (TRANSVERSE). (2)

	Al
3.3	Cu
1.5	Mg
0.4	Mn

2048 Al

REFERENCES

1. "Mechanical-Property Data X-2048-T851 Aluminum Alloy", Data Sheet F33615-72-1280; Prepared by Battelle Memorial Institute, Columbus, Ohio; Issued by Air Force Materials Laboratory (October 1972).
2. Deel, O. L., Ruff, P. E. and Mindlin, H., "Engineering Data on New Aerospace Structural Materials", Data Sheet F33615-72-C-1280; Battelle Memorial Institute, Columbus, Ohio, Technical Report AFML-TR-73-114 (June 1973).
3. Thompson, D. S., Levy, S. A., Spangler, G. E. and Benson, D.K., "Program to Improve Fracture Toughness and Fatigue Resistance of Aluminum Sheet and Plate for Aircraft Applications", Reynolds Metals Company, AFML-TR-73-247, Vol. I (September 1973).
4. Thompson, D. S. and Zinkham, R. E., "Program to Improve the Fracture Toughness and Fatigue Resistance of Aluminum Sheet and Plate for Aircraft Applications", Reynolds Metals Company, AFML-TR-73-247, Vol. II (September 1974).
5. Petrak, G. J., "Fracture Related Properties of X-2048-T851 Plate Including Specimen Size Effects on K_{IC}", Dayton University, AFML-TR-74-261 (December 1974).
6. Levy, S. A., Thompson, D. S. and Spangler, G. E., "2048 Update, Conventional and Thermomechanical Aging" Metals Engineering Quarterly (May 1975).

	Al
2.7	Cu
2.3	Li
0.12	Zr

2090 Al

1 **GENERAL**

This alloy was developed in the late 1970's in response to the desire for lighter aerospace structures following a steep rise in fuel prices. The 2090 alloy has approximately 8 percent lower density and a 10 percent higher elastic modulus than either 2024 or 7075, which it was designed to replace. Initially, it was hoped that direct substitution would be possible, with little change in aircraft fabrication procedures. Properly processed sheet products and other thin sections have strength and toughness combinations approaching those of 7075, coupled with lower fatigue crack growth rates. However, as the development programs progressed several important limitations were revealed (see 1.09) which indicate that direct substitution is possible in only limited applications.

At present 2090 is offered in two groups of tempers, a high-strength and relatively low toughness substitute for 7075-T6, and a medium-strength, damage-tolerant substitute for 2024-T3. Various tempers have been developed within these groups, most of which are not available. In most cases the heat treating and processing schedules are proprietary.

Two major aluminum producers offer the alloy in sheet and plate. Only one producer offers extrusions. Forgings have been made but their poor properties, compared with conventional aluminum alloys, have discouraged production.

1.01 **Commercial Designation**

2090.

1.02 **Alternate Designation**

None.

1.03 **Specifications**

An AMS for 2090-T83 is in preparation for issue in 1990.

1.031 Many of the tempers identified in the literature are experimental designations used by the producers, e.g., T8E41. Many of these are not yet registered. (See 3.011.)

1.04 **Composition**

1.041 Registered composition limits for alloy 2090, Table 1.041.

1.05 **Heat Treatment**

See 1.096 for health and safety considerations.

Salt bath heat treatment has been reported to have no additional safety problems if melting is avoided. (See 1.081.)

T81 temper: Solution heat treat 986 F for 1 hr, water quench, cold work 6%, age 24 hr at 374 F (13).

T83: Solution heat at 1020 F, water quench, 6% cold work, age 24 hr at 60 F.

Extended times at solution heat treatment temperatures may result in the loss of some lithium from the surface layers of the product.

1.06 **Hardness**

In addition to varying with time and aging temperature, the hardness of this alloy is markedly sensitive to the degree of cold work between quenching and aging.

1.061 Rockwell B hardness versus aging time at temperatures in the range 320 F to 455 F, Figure 1.061.

1.062 Rockwell B and E hardness of 2090 sheet in -T3 and -T8 condition, Table 1.062.

1.063 Maximum hardnesses in a superplastically formed component, Table 1.063.

1.064 Aging curves for a superplastically formed component at 320 F, Figure 1.064.

1.065 Aging curves for a superplastically formed component at 350 F, Figure 1.065.

1.066 Aging curves for a superplastically formed component at 375 F, Figure 1.066.

1.07 **Forms and Conditions Available**

All forms are available only from the producer. Sheet, 0.02 to 0.249 inch thick, bare and clad (9,14). Plate, 0.25 to 1.5 inch thick. Extrusions, in shapes producible from a 16-inch diameter billet (9).

1.08 **Melting and Casting Practices**

1.081 The presence of lithium in alloy 2090 complicates melting practices. It destroys the protective nature of the oxide film formed on molten aluminum, and causes rapid oxidation, with enhanced likelihood of oxide inclusions being entrapped in the alloy. The risk of explosions, particularly in the presence of moisture or rust, is high. Lithium also increases the rate of attack of the melt on refractories normally used to contain molten aluminum. Care should be taken to ensure that fluxes and salts are compatible with the molten alloy.

As lithium is a contaminant in most conventional alloys, scrap must be segregated to prevent its entry into the scrap cycle of conventional alloys (3).

1.09 **Special Considerations**

1.091 Commercial 2090 has an unrecrystallized grain structure. This structure is associated with the highest combination of strength and (LT and TL) toughness. However, this product possesses a high degree of anisotropy with the tensile strength at 45° to the rolling direction being about 15 to 20 percent lower than the strength in the longitudinal or transverse directions. This requires special design considerations.

1.092 The alloy possesses a pronounced laminar microstructure which results in low short-transverse tensile ductility and poor toughness for the SL and ST crack orientations. This laminar structure also can cause delaminations during shearing sheet or thin extruded sections. Spalling may also be encountered during machining.

1.093 In order to develop peak strength, the alloy requires more deformation after solution heat treatment than the conventional aluminum alloys. From 5 to 8 percent cold work is necessary to develop peak strength and toughness in aged 2090. In

	Al
2.7	Cu
2.3	Li
0.12	Zr

2090 Al

some fabrication processes such as forging, this may be impossible.

1.094 The alloy ages at moderately elevated service temperatures with significant increases in strength coupled with substantially reduced fracture toughness and a change in fracture mode from transgranular to intergranular.

1.095 The scrap from Al-Li alloys is a contaminant to the normal aluminum scrap cycle and must be segregated.

1.096 Health. Lithium compounds are poisonous if ingested, and these may be formed during melting or chemical processing. Carbonates or oxides that are formed on metal surfaces at high temperatures react with atmospheric moisture, perspiration, or water, to form caustic compounds that may cause mild chemical burns. Care should be taken in handling 2090 components that have previously been heated to high temperatures.

The fines generated during grinding, machining, forging, welding or melting are potentially irritating to the mucous membranes. The degree of irritation varies markedly between individuals (3).

1.097 Safety. See melting and casting, 1.081.

2 PHYSICAL AND CHEMICAL PROPERTIES

2.01 Thermal Properties

2.011 Melting range: 1042 to 1054 F (48).

2.012 Phase changes: alloy is subject to precipitation.

2.0121 Time-temperature-transformation diagrams.

2.013 Thermal conductivity: 48.2–53.4 Btu-ft/hr-ft-F (0.834–0.924 J/sec-cm^2-C/cm) (48).

2.014 Thermal expansion. Linear coefficient of thermal expansion: at 68 to 212 F: 9 x 10^{-6} in./in./F (48).

2.015 Specific heat. Specific heat at 212 F: 0.2873 Btu/lb-F (48).

2.016 Thermal diffusivity.

2.02 Other Physical Properties

2.021 Density: 0.093 lb/in.^{3}, 2.59 gm/cm^3 (1); 2.57 gm/cm^3 (48).

2.022 Electrical properties.

2.0221 Electrical conductivity. The electrical conductivity of 2090 is markedly less than conventional alloys. Sheet in solution heat treated condition (T3): 15.5–16.5% IACS; after stretching and aging to T8: 18.0–19.0% IACS (34).

2.023 Magnetic properties. Alloy is nonmagnetic.

2.024 Emissivity.

2.025 Damping capacity.

2.03 Chemical Environments

2.031 General corrosion.

2.0311 Exfolidation corrosion of 2090-T83 plate, Table 2.0311.

2.0312 Exfoliation of 2090 plate, Table 2.0312.

2.0313 Corrosion test comparison, 2090 plate, Table 2.0313.

2.0314 Accelerated corrosion tests of 0.5 inch plate of 2090, Table 2.0314.

2.032 Stress corrosion.

2.0321 Stress corrosion of 2090-T83 plate, effect of composition, Table 2.0321.

2.0322 Stress corrosion of 2090-T83 extrusion, effect of aging, Table 2.0322.

2.0323 Time to failure for 2090 1.5-inch plate in various environments, Table 2.0323.

2.0324 Stress corrosion data (time to failure) for 2090 sheet, Table 2.0324.

2.0325 Crevice corrosion of 2090 sheet, Table 2.0325.

2.0326 Stress corrosion crack growth rate for 2090 T-X extrusions in 3.5% NaCl, Figure 2.0326.

2.0327 Stress corrosion results for 2090-T81 plate in various environments, Table 2.0327.

2.0328 Stress corrosion crack growth rates in 3.5% NaCl for 2090-T81 and 7075-T61 plate tested in the SL direction, Figure 2.0328.

2.033 Alloy has been reported to react more than conventional alloys when impacted in liquid oxygen.

2.034 Hydrogen embrittlement.

2.0341 Effect of hydrogen charging on the mechanical properties of 2090 plate, Table 2.0341.

2.0342 Effect of hydrogen charging on the strength of 2090-T83 0.5-inch plate, Figure 2.0342.

2.0343 Effect of hydrogen charging on the fracture strain of 2090-T83 0.5-inch plate, Figure 2.0343.

2.04 Nuclear Environments

3 MECHANICAL PROPERTIES

3.01 Specified Mechanical Properties

3.011 Aluminum Association registered tempers, Table 3.011.

3.02 Mechanical Properties at Room Temperature

3.021 Tension.

3.0211 Stress strain curve for 2090-T83 sheet, Figure 3.0211.

3.0212 Tensile properties of 2090-T83 plate from two sources, Table 3.0212.

3.0213 Tensile properties of various 2090 product forms in the -T6 and underaged tempers, Table 3.0213.

3.0214 Tensile properties of 2090-T83 extrusion, Table 3.0214.

3.0215 Tensile properties of 2090-T3 sheet, Table 3.0215.

3.0216 Tensile properties of 2090-T31 and -T83 sheet, Table 3.0216.

3.0217 Tensile properties of 2090-T83 sheet, Table 3.0217.

3.0218 Tensile properties of superplastically formed 2090-T6 sheet, Table 3.0218.

3.0219 Strength-ductility relationships for 0.090-inch 2090 sheet in various tempers, Figure 3.0219.

3.02110 Yield strength as a function of orientation to the rolling direction for 2090-T83 and 7075-T6 sheet, Figure 3.02110.

3.02111 Yield strength as a function of stretching and aging at 375 F, Figure 3.02111.

3.02112 Yield strength and elongation as a function of cold work before aging in 2090-T6 hand forgings, Figure 3.02112.

3.02113 Transverse yield strength as a function of cold work before aging in 2090 extrusions, Figure 3.02113.

3.02114 Tensile properties as a function of cold work (rolling) before aging in 2090 sheet, Figure 3.02114.

3.02115	Effect of exposure at 150 F on the tensile properties of 2090 plate and extrusion. (See also Table 3.027211), Table 3.02115.
3.02116	Effect of exposure at 200 F on the tensile properties of 2090 sheet. (See also 3.02727), Figure 3.02116.
3.022	Compression.
3.0221	Compressive yield strength of 2090-T83 sheet, Table 3.0221.
3.0222	Proposed compressive yield design allowables for 2090-T83 sheet, Table 3.0222.
3.0223	Compressive stress-strain and tangent modulus curves for 2090-T83 sheet, Figure 3.0223.
3.023	Impact.
3.0231	Charpy-V results for 2090 plate cold worked various amounts and aged to equivalent strength, Table 3.0231.
3.024	Bending. Minimum bend radii for design, in multiples of sheet thickness (longitudinal direction): as quenched (W temper) = 1.5; -T3 = 3.0; -T6 = 5.0; -T8 = 5.5 (46).
3.025	Torsion and shear.
3.0251	Shear strength of 2090-T83 sheet, Table 3.0251.
3.0252	Design allowable shear strength for 2090-T83 sheet, F_{su} is 37 ksi (1).
3.026	Bearing.
3.0261	Bearing properties of 2090-T83 sheet, Table 3.0261.
3.0262	Proposed design allowable bearing strengths for 2090-T83 sheet, Table 3.0262.
3.027	Stress concentration.
3.0271	Notch properties.
3.0272	Fracture toughness. In most semi-fabricated forms, the alloy possesses a laminar structure with the planes being parallel to the surface and extending in the major working direction. This structure results in irregular crack paths for cracks orientated normal to the layers. For crack orientations parallel to the layers (SL and ST), the fracture toughness is relatively low, as might be expected (Table 3.02728). As illustrated previously (Figure 3.02110), the unrecrystallized product exhibits a texture resulting in a substantial decrease in the yield strength at 45 degrees to the rolling direction. The fracture toughness with this crack orientation (TL + 45) appears slightly higher than for the LT and TL orientations (Table 3.02728). Extended exposure at 150 F results in increases in yield strength (see Table 3.02115) and substantial reduction in fracture toughness (Table 3.027211). Fracture toughness of sheet products in aluminum alloys is frequently measured using ASTM E561 Practice for R-Curve Determination. Two measures of toughness are obtained from the load versus crack opening displacement record. The first, K_C, is described in ASTM B646, and is determined from the maximum load in the test record, and the corresponding crack length at the maximum load. The second, $K_{apparent}$ ($K_{app.}$) is not described in ASTM B646, but is widely used in the aircraft industry. It is calculated from the maximum load, and the initial crack length. On the same test, $K_{app.}$ values are always less than or equal to K_C values. These K values are geometry dependent, and may be useful only for comparative purposes.
3.02721	Fracture toughness values for 2090 sheet, Table 3.02721.
3.02722	Fracture toughness of damage tolerant 2090 sheet, Table 3.02722.
3.02723	Fracture toughness of 2090-T83 sheet, Table 3.02723.
3.02724	Fracture toughness of production 2090 sheet as a function of strength level, Figure 3.02724.
3.02725	Fracture toughness of 2090 peak-aged sheet, Table 3.02725.
3.02726	Fracture toughness of various 2090 forms, Table 3.02726.
3.02727	Effect of exposure for 0 to 6 weeks at 200 F on the unit propagation energy in a Kahn test for 2090 sheet, Figure 3.02727.
3.02728	Plane-strain fracture toughness for plate and extrusions from a cooperative test program, Table 3.02728.
3.02729	Plane-strain fracture toughness of 2090-T83 plate for several crack orientations, Figure 3.02729.
3.027210	Plane-strain fracture toughness of 0.5-inch 2090-T83 plate, Table 3.027210.
3.027211	Effect of exposure at 150 F on the fracture toughness of 2090 plate and extrusion, Table 3.027211.
3.03	**Mechanical Properties at Various Temperatures** (See also 4.031.)
3.031	Tension.
3.0311	Tensile properties of 2090-T83 sheet at room and cryogenic temperatures, Table 3.0311.
3.0312	Tensile properties of 0.25-inch 2090-T62 and -T83 plate as a function of temperature, Figure 3.0312.
3.0313	Effect of low test temperatures on the short transverse tensile strength of 2090-T81 plate, Figure 3.0133.
3.0314	Tensile properties of 2090-T6 sheet, Table 3.0314.
3.032	Compression.
3.033	Impact.
3.034	Bending.
3.035	Torsion and shear.
3.036	Bearing.
3.037	Stress concentration.
3.0371	Notch properties.
3.0372	Fracture toughness.
3.03721	R curves for 2090-T83 sheet at ambient and liquid nitrogen temperatures, Figure 3.03721.
3.03722	Effect of low test temperatures on the tensile yield strength and plane-strain fracture toughness of 2090-T81 plate, Figure 3.03722.
3.03723	Kahn tear test toughness (LT) of 2090-T6 and -T81 at ambient and cryogenic temperatures, Table 3.03723.
3.038	Combined properties.
3.04	**Creep and Creep Rupture Properties**
3.05	**Fatigue Properties**
3.051	Conventional fatigue properties.
3.0511	Fatigue life of 2090-T83 0.5-inch plate in fully reversed bending, Figure 3.0511.
3.052	Fatigue crack propagation. Fatigue crack propagation rates of 2090 and other Al-Li alloys in tension loading appear to be lower than those of the 2XXX and 7XXX alloys. This advantage is in part due to crack tip shielding associated with irregular crack paths and the resulting roughness induced crack closure forces acting on relatively

Al
2.7 Cu
2.3 Li
0.12 Zr

2090 Al

	Al
2.7	Cu
2.3	Li
0.12	Zr

2090 Al

long cracks, but these forces are absent or greatly reduced for very short cracks (Figure 3.0524). The downside of this behavior is the relatively poor performance of Al-Li alloys in compression-dominated, variable amplitude spectra loading. This is illustrated by the reinitiation of cracks at crack tip stress intensity threshold values (K_{th}) when compression loads are applied (Figure 3.0525). Crack orientation effects are pronounced in this alloy with the SL and LT + 45-degree orientations showing the highest growth rates and the lowest K_{th} values (Figure 3.0523). Overaging for long times at 325 F leads to an increase in fatigue crack growth rates (Figure 3.0524).

3.0521 Fatigue crack growth curves for 0.5-inch 2090-T83 plate showing the effect of heterogeneity, Figure 3.0521.

3.0522 Fatigue crack growth rate for 0.5-inch 2090-T83 plate in air and in 3.5% NaCl, Figure 3.0522.

3.0523 Fatigue crack growth rates for 2090-T83 plate showing the effects of crack orientation and K_{th} values, Figure 3.0523.

3.0524 Fatigue crack growth rates for long and very short cracks in 2090 0.5-inch plate, showing the effects of aging time, Figure 3.0524.

3.0525 Crack growth at a constant value of $K = \Delta K_{th}$, following various compression overloads, Figure 3.0525.

3.0526 Fatigue crack growth rate of 2090-T83 0.5-inch plate in humid air, Figure 3.0526.

3.06 **Elastic Properties**

3.061 Elastic moduli of 2090-T83 plate, Table 3.061.

3.062 Elastic moduli of 2090-T83 sheet for several testing directions, Table 3.062.

3.063 Anisotropy of Young's Modulus in 2090-T83 sheet, Figure 3.063.

3.064 Anisotropy of Young's Modulus in 2090-T83 sheet, effect of aging at 325 F, Figure 3.064.

3.065 Anisotropy of Young's Modulus in 2090-T83 sheet and extrusion, effect of thickness, Figure 3.065.

3.066 Anisotropy of Poisson's Ratio in 2090-T83 plate, Figure 3.066.

3.067 Anisotropy of shear modulus in 2090 sheet, effect of aging at 325 F (163 C), Figure 3.067.

4 FABRICATION

4.01 **Forming**

An advantage of 2090 is that it is relatively stable in the solution-heat-treated and quenched condition. Unlike 2024, it can be stored at room temperature for up to a year before forming. It has good ductility, but less than 2024-O temper, and can be low-temperature aged to final properties without the need for high temperature heat treatment and consequent distortion.

4.011 Flow stress versus strain rate for 2090 sheet superplastically formed at 985 F, Figure 4.011.

4.02 **Machining and Grinding**

For health hazards associated with fines, see 1.091 above.

4.03 **Joining**

4.031 Welding. There has been only a limited amount of welding experience with the 2090 alloy. Data are available for variable polarity plasma arc (VPPA) gas-tungsten-arc (GTA), and electron beam welds in both sheet and plate (49). Acceptable fillers have been reported as 4043, 4047, 4245, 2319 and 5556, with 2319 and 5556 having the least hot cracking susceptibility (49). As-welded (VPPA) tensile properties can be considerably improved by solution treating and aging to the T62 condition with a joint efficiency of essentially 100 percent at room temperature and about 80 percent at -423 F (Table 4.0312). It is important that the surface of material to be welded is free of contaminants. This can be assured either by hand scraping or milling to remove about 0.01-inch of surface material. Moisture should be minimized as in the welding of any aluminum alloy.

4.0312 Tensile properties of VPPA-welded 2090-T83 sheet at low temperatures for several post-weld heat treatments, Table 4.0312.

4.0313 Tensile properties of 2090-T83 sheet welded by VPPA and GTA processes, Table 4.0313.

4.0314 Comparison of parent metal and weld metal tensile properties for 2090 sheet and 2219 plate, Table 4.0314.

4.0315 Tensile properties at cryogenic temperatures for 2090-T83 sheet welds, Table 4.0315.

4.0316 Fracture toughness as a function of low temperatures for parent metal and VPPA welds, Figure 4.0316.

4.0317 Tensile properties of welded and unwelded 2090-T83 plate as a function of temperature, Table 4.0317.

4.04 **Surface Treatment**

No difficult problems are reported in anodizing, surface treating, or chemical milling 2090 components.

REFERENCES

1 Minutes, Military Handbook 5 Committee, 77th Meeting (1989).

2 Aluminum Association Registered Temper Designations (August, 1989).

3 Aluminum Association Publication T4, "The Safety, Health and Recycling Aspects of Aluminum-Lithium Alloys", The Aluminum Association, Washington, DC.

4 Colvin, E. L., "Exfoliation and Stress Corrosion Cracking Performance of Al-Li Alloys", p 237 in "Aluminum Lithium Alloys, Design, Development and Applications Update", Symposium Proceedings, ASM International, Los Angeles, CA, R. J. Kar, S. P. Agrawal, and W. E. Quist, Eds. (March, 1987).

5 Waldman, J., Mahapatra, R., and Neu, C., "Aluminum Lithium Alloys for Navy Aircraft", p 341 in "Aluminum Lithium Alloys, Design, Development and Applications Update", Symposium Proceedings, ASM International, Los Angeles, CA, R. J. Kar, S. P. Agrawal, and W. E. Quist, Eds. (March, 1987).

6 Reynolds, M. J., Henshall, C. A., and Wadsworth, J., "Superplastic Forming Characteristics and Properties of Aluminum Lithium Alloys", p 387 in "Aluminum Lithium Alloys, Design, Development and Applications Update", Symposium Proceedings, ASM International, Los Angeles, CA, R. J. Kar, S. P. Agrawal, and W. E. Quist, Eds. (March, 1987).

7 Quist, W. E., Hyman, M., Gane, D. H., and Badger, D. V., "Forming Characteristics of Aluminum Lithium Alloys", p 401 in "Aluminum Lithium Alloys, Design, Development and Applications Update", Symposium Proceedings, ASM International, Los Angeles, CA, R. J. Kar, S. P. Agrawal, and W. E. Quist, Eds. (March, 1987).

8 Venkatesware, K. T., Yu, R. W., and Ritchie, R. O., "Mechanisms of Fatigue Crack Propagation in Commercial Aluminum Lithium Alloys", p 173 in "Aluminum Lithium Alloys, Design, Development and Applications Update", Symposium Proceedings, ASM International, Los Angeles, CA, R. J. Kar, S. P. Agrawal, and W. E. Quist, Eds. (March, 1987).

9 Bretz, P. E., "Alithalite Alloys: 1987 Update", p 1 in "Aluminum Lithium Alloys, Design, Development and Applications Update", Symposium Proceedings, ASM International, Los Angeles, CA, R. J. Kar, S. P. Agrawal, and W. E. Quist, Eds. (March, 1987).

10 Dorward, R. C., "Al-Li Development at Kaiser Aluminum", p 155 in "Aluminum Lithium Alloys, Design, Development and Applications Update", Symposium Proceedings, ASM International, Los Angeles, CA, R. J. Kar, S. P. Agrawal, and W. E. Quist, Eds. (March, 1987).

11 Blackburn, L., Casada, W., Colvin, G., Shiftler, G., and Starke, E., "The Effect of Processing on the Strength and Fracture Behavior of Aluminum Lithium Alloys", p 187 in "Aluminum Lithium Alloys, Design, Development and Applications Update", Symposium Proceedings, ASM International, Los Angeles, CA, R. J. Kar, S. P. Agrawal, and W. E. Quist, Eds. (March, 1987).

12 Monhaghegh, M., Zafari, F., Pada, C. S., and Lin, F., "Property Trends for 2091 and 2090 Sheet", p 237 in "Aluminum Lithium Alloys, Design, Development and Applications Update", Symposium Proceedings, ASM International, Los Angeles, CA, R. J. Kar, S. P. Agrawal, and W. E. Quist, Eds. (March, 1987).

13 Glazer, J., and Morris, J. W., "The Strength-Toughness Relationships at Cryogenic Temperatures in Aluminum Lithium Alloy Plate", p 1471 in "Aluminum-Lithium Alloys", Proc. Fifth International Al-Li Conference, Williamsburg, VA, T. H. Sanders and E. A. Starke, Eds., Materials and Component Engineering Publications, Ltd., Birmingham, UK (March, 1989).

14 Kaiser Aluminum and Chemical Corporation, Data Sheets on 2090 Alloy (January, 1988).

15 Pao, P. S., Imam, M. A., Cooley, L. A., and Yoder, G. R., "Corrosion Fatigue Crack Growth in Al-Li Alloy 2090", p 1125 in "Aluminum-Lithium Alloys", Proc. Fifth International Al-Li Conference, Williamsburg, VA, T. H. Sanders and E. A. Starke, Eds., Materials and Component Engineering Publications, Ltd., Birmingham, UK (March, 1989).

16 Tobler, R. L., Han, J. K., Ma, L., Walsh, R. P., and Reed, R. P., "Tensile, Fracture, and Fatigue Properties of Notched Aluminum Alloy Sheets at Liquid Nitrogen Temperatures", p 1115 in "Aluminum-Lithium Alloys", Proc. Fifth International Al-Li Conference, Williamsburg, VA, T. H. Sanders and E. A. Starke, Eds., Materials and Component Engineering Publications, Ltd., Birmingham, UK (March, 1989).

17 Yoder, G. R., Pao, P. S., Imam, M. A., and Cooley, L. A., "Micromechanisms of Fatigue Fracture in Al-Li Alloy 2090", p 103 in "Aluminum-Lithium Alloys", Proc. Fifth International Al-Li Conference, Williamsburg, VA, T. H. Sanders and E. A. Starke, Eds., Materials and Component Engineering Publications, Ltd., Birmingham, UK (March, 1989).

18 Rioja, R. J., Bretz, P. E., Sawtell, R. R., Hunt, W. H., and Ludwiczac, E. A., "Aluminum Alloys: Their Physical and Mechanical Properties", EMAS Ltd., Warley, UK, E. A. Starke and T. H. Sanders, Eds. (1986).

19 Crookes, R., and Mitchell, M. R., "The Fracture of 2090 Plate in Bending Fatigue", p 1023 in "Aluminum-Lithium Alloys", Proc. Fifth International Al-Li Conference, Williamsburg, VA, T. H. Sanders and E. A. Starke, Eds., Materials and Component Engineering Publications, Ltd., Birmingham, UK (March, 1989).

20 Venkateswara Rao, K. T., Piascik, R. S., Gangloff, R. P., and Ritchie, R. O., "Fatigue Crack Propagation in Aluminum Lithium Alloys", p 955 in "Aluminum-Lithium Alloys", Proc. Fifth International Al-Li Conference, Williamsburg, VA, T. H. Sanders and E. A. Starke, Eds., Materials and Component Engineering Publications, Ltd., Birmingham, UK (March, 1989).

21 Rooney, W. D., Papazian, J. M., Balmuth, E. S., Davis, R. C., and Adler, P. N., "Elastic Anisotropy in Al-Li Alloys", p 799 in "Aluminum-Lithium Alloys", Proc. Fifth International Al-Li Conference, Williamsburg, VA, T. H. Sanders and E. A. Starke, Eds., Materials and Component Engineering Publications, Ltd., Birmingham, UK (March, 1989).

22 Bretz, P. E., "Low Density Aluminum Technology", p 74 in "Aluminum-Lithium, Development, Application, and Superplastic Forming", Proc. ASM Symposium, Los Angeles, CA, S. P. Agrawal and R. J. Kar, Eds., ASM, Metals Park, OH (1986).

23 Cassada, W. A., Shiflet, G. J., and Starke, E. A., "The Precipitation, Deformation, and Fracture Behavior of Aluminum-Lithium Alloys", p 2 in "Aluminum-Lithium, Development, Application, and Superplastic Forming", Proc. ASM Symposium, Los Angeles, CA, March, 1986, S. P. Agrawal and R. J. Kar, Eds., ASM, Metals Park, OH (1986).

24 Glazer, J., and Morris, J. W., "Thermomechanical Processing of Two Phase Al-Cu-Li-Zr Alloys", p 191 in "Aluminum-Lithium Alloys 3", Proc. Symposium, The Institute of Metals, Oxford, UK, July, 1985, C. Baker, P. J. Gregson, S. J. Harris, and C. J. Peel, Eds., The Institute of Metals, London (1986).

	Al
2.7	Cu
2.3	Li
0.12	Zr

2090 Al

	Al
2.7	Cu
2.3	Li
0.12	Zr

2090 Al

25 Skillingberg, M. H., and Ashton, R. F., "Processing and Performance of Al-Li-Cu-X Extrusions", p C3-179 in "4th International Aluminum-Lithium Conference", Conference Proceedings, June, 1987, Paris, France, G. Champier, B. Dubost, D. Miannay, and L. Sabetay, Eds., Journal de Physique, Les Ulis, France (1987).

26 Papazian, J. M., Bott, G. G., and Shaw, P., "Influence of Forming in the T3 Condition on Properties of 2090-T8X, 2091-T8X, and 8090-T8X", p C3-231 in "4th International Aluminum-Lithium Conference", Conference Proceedings, June, 1987, Paris, France, G. Champier, B. Dubost, D. Miannay, and L. Sabetay, Eds., Journal de Physique, Les Ulis, France (1987).

27 Lippold, J. C., "Weldability of Commercial Aluminum-Lithium Alloys", p 1365 in "Aluminum-Lithium Alloys", Proc. Fifth International Al-Li Conference, Williamsburg, VA, March, 1989, T. H. Sanders and E. A. Starke, Eds., Materials and Component Engineering Publications, Ltd., Birmingham, UK (1989).

28 Zacharia, T., David, S. A., Vitek, J. M., and Martukanitz, R. P., "Weldability and Microstructure Characterization of Al-Li Alloys", p 1387 in "Aluminum-Lithium Alloys", Proc. Fifth International Al-Li Conference, Williamsburg, VA, March, 1989, T. H. Sanders and E. A. Starke, Eds., Materials and Component Engineering Publications, Ltd., Birmingham, UK (1989).

29 Kramer, L. S., Heubaum, F. H., and Pickens, J. R., "The Weldability of High-Strength Al-Cu-Li Alloys", p 1415 in "Aluminum-Lithium Alloys", Proc. Fifth International Al-Li Conference, Williamsburg, VA, March, 1989, T. H. Sanders and E. A. Starke, Eds., Materials and Component Engineering Publications, Ltd., Birmingham, UK (1989).

30 Marsico, T. A., and Kossowsky, R., "Physical Properties of Laser-Welded Aluminum-Lithium Alloy 2090", p 1447 in "Aluminum-Lithium Alloys", Proc. Fifth International Al-Li Conference, Williamsburg, VA, March, 1989, T. H. Sanders and E. A. Starke, Eds., Materials and Component Engineering Publications, Ltd., Birmingham, UK (1989).

31 Griffee, C. C., Jensen, G. A., and Reinhart, T. L., "Factors Influencing the Quality and Properties of Aluminum Alloy Welds", p 1425 in "Aluminum-Lithium Alloys", Proc. Fifth International Al-Li Conference, Williamsburg, VA, March, 1989, T. H. Sanders and E. A. Starke, Eds., Materials and Component Engineering Publications, Ltd., Birmingham, UK (1989).

32 Pao, P. S., Cooley, L. A., Imam, M. A., and Yoder, G. R., "Fatigue Crack Growth in 2090 Al-Li Alloy", pp 1455 to 1460, Scripta Metallurgica, Vol 23, No. 8.

33 Buscemi, C. D., and Chin, E.S.C., "Characterization of X2090 Al-Li Alloy", Report MTL-TR-88-26, U.S. Army Laboratory Command, Materials Technology Laboratory, Watertown, Mass. (September, 1988).

34 Dorward, R. C., Kaiser Aluminum and Chemical Corp., Pleasanton, CA, personal communication.

35 Kaiser Aluminum and Chemical Corp., Data Sheets, Vol 2 (1988).

36 Moran, J. P., and Stoner, G. E., "Solution Chemistry Effects on the Stress Corrosion Behavior of Alloy 2090 and 2034", p 1187 in "Aluminum-Lithium Alloys", Proc. Fifth International Al-Li Conference, Williamsburg, VA, March, 1989, T. H. Sanders and E. A. Starke, Eds., Materials and Component Engineering Publications, Ltd., Birmingham, UK (1989).

37 Bavarian, B., Becker, J., Parikh, S. N., and Zamanzadeh, M., "Localized Corrosion of 2090 and 2091 Al-Li Alloy", p 1227 in "Aluminum-Lithium Alloys", Proc. Fifth International Al-Li Conference, Williamsburg, VA, March, 1989, T. H. Sanders and E. A. Starke, Eds., Materials and Component Engineering Publications, Ltd., Birmingham, UK (1989).

38 Colvin, E. L., and Murtha, S. J., "Exfoliation Corrosion Testing of Al-Li Alloys 2090 and 2091", p 1251 in "Aluminum-Lithium Alloys", Proc. Fifth International Al-Li Conference, Williamsburg, VA, March, 1989, T. H. Sanders and E. A. Starke, Eds., Materials and Component Engineering Publications, Ltd., Birmingham, UK (1989).

39 Meletis, E. I., and Huang, W., "Pre-Exposure Embrittlement in Al-Li-Cu-Zr Alloys", p 1309 in "Aluminum-Lithium Alloys", Proc. Fifth International Al-Li Conference, Williamsburg, VA, March, 1989, T. H. Sanders and E. A. Starke, Eds., Materials and Component Engineering Publications, Ltd., Birmingham, UK (1989).

40 Shin, K. S., Kim, S. S., and Lee, E. W., "Hydrogen Embrittlement of a 2090 Al-Li Alloy", p 1319 in "Aluminum-Lithium Alloys", Proc. Fifth International Al-Li Conference, Williamsburg, VA, March, 1989, T. H. Sanders and E. A. Starke, Eds., Materials and Component Engineering Publications, Ltd., Birmingham, UK (1989).

41 Rivet, F. C., and Swanson, R. E., "Influence of Dissolved Hydrogen on Aluminum-Lithium Alloy Fracture Behavior", p 1329 in "Aluminum-Lithium Alloys", Proc. Fifth International Al-Li Conference, Williamsburg, VA, March, 1989, T. H. Sanders and E. A. Starke, Eds., Component Engineering Publications, Ltd., Birmingham, UK (1989).

42 Griffee, C. C., Jensen, G. A., and Reinhart, T. L., "Factors Influencing the Quality and Properties of Al-Li Alloy Welds", p 1425 in "Aluminum-Lithium Alloys", Proc. Fifth International Al-Li Conference, Williamsburg, VA, March, 1989, T. H. Sanders and E. A. Starke, Eds., Materials and Component Engineering Publications, Ltd., Birmingham, UK (1989).

43 Kerr, J. R., and Merino, R. E., "Cryogenic Properties of VPPA Welded Aluminum-Lithium Alloys", p 1491 in "Aluminum-Lithium Alloys", Proc. Fifth International Al-Li Conference, Williamsburg, VA, March, 1989, T. H. Sanders and E. A. Starke, Eds., Materials and Component Engineering Publications, Ltd., Birmingham, UK (1989).

44 Venkateswara Rao, K. T., and Ritchie, R. O., "Influence of Extrinsic Crack Deflection and Delamination Mechanisms on the Cryogenic Toughness of Al-Li Alloy 2090; Behavior in Plate

(T81) vs. Sheet (T83) Material", p 1501 in "Aluminum-Lithium Alloys", Proc. Fifth International Al-Li Conference, Williamsburg, VA, March, 1989, T. H. Sanders and E. A. Starke, Eds., Materials and Component Engineering Publications, Ltd., Birmingham, UK (1989).

45 Verzasconi, S. L., and Morris, J. W., "Cryogenic Mechanical Properties of Low Density Superplastically Formable Al-Li Alloys", p 1523 in "Aluminum-Lithium Alloys", Proc. Fifth International Al-Li Conference, Williamsburg, VA, March, 1989, T. H. Sanders and E. A. Starke, Eds., Materials and Component Engineering Publications, Ltd., Birmingham, UK (1989).

46 Tuegel, E. J., Vasey-Glandon, V. M., Pruitt, M. O., and Sankaran, K. K., "Forming of Aluminum Lithium Sheet for Fighter Aircraft Applications"; p 1597 in "Aluminum-Lithium Alloys", Proc. Fifth International Al-Li Conference, Williamsburg, VA, March, 1989, T. H. Sanders and E. A. Starke, Eds., Materials and Component Engineering Publications, Ltd., Birmingham, UK (1989).

47 Huang, J. C., and Ardell, A. J., "Microstructural Development in Two Al-Li-Cu Alloys", p 455 in "Aluminum-Lithium Alloys 3", Proc. Symposium The Institute of Metals, Oxford, UK, July, 1985, C. Baker, P. J. Gregson, S. J. Harris, and C. J. Peel, Eds., The Institute of Metals, London (1986).

48 Spiropoulos, P. T., "Thermomechanical Processing of an Al Alloy 2090 for Grain Refinement and Superplasticity", Thesis, December, 1987, Naval Postgraduate School, Monterey, CA (1987).

49 Bucci, R. J., Malcom, R. C., Colvin, E. L., Murtha, S. J., and James, R. S., "Cooperative Test Program for the Evaluation of Engineering Properties of Al-Li Alloy 2090-TX Sheet, Plate, and Extrusion Products", Aluminum Co. of America, NSWC-TR 89-06 (September 15, 1989).

Al
2.7 Cu
2.3 Li
0.12 Zr

2090 Al

Alloy	2090	
	Percent	
Element	Min	Max
Si	–	0.10
Fe	–	0.12
Cu	2.4	3.0
Mn	–	0.05
Mg	–	0.25
Cr	–	0.05
Zn	–	0.10
Li	1.9	2.6
Zr	0.08	0.15
Ti	–	0.15
Others		
Each	–	0.05
Total	–	0.15

TABLE 1.041. REGISTERED COMPOSITION LIMITS FOR ALLOY 2090 (2)

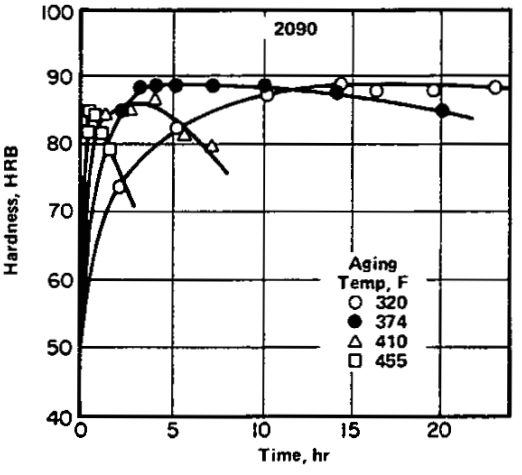


FIGURE 1.061. ROCKWELL B HARDNESS VERSUS AGING TIME AT TEMPERATURES IN THE RANGE 320 F TO 455 F (47)

	Al
2.7	Cu
2.3	Li
0.12	Zr

2090 Al

Alloy	2090		
Form	Sheet		
Gauge	0.063 in. and 0.10 in.		
Temper	-T3	Stretch,	-T8
Hardness	Rockwell E	percent	Rockwell B
	87.2	0	76.6
	95.1	1	84.7
	91.7	2.25	82.1
	95.3	3	85.5
	92.1	3.5	83.3
	90.5	5	85.9

TABLE 1.062. ROCKWELL B AND E HARDNESS OF 2090 SHEET IN -T3 AND -T8 CONDITION (34)

Alloy	2090					
Temper	T6					
Form	Superplastically Formed Sheet					
Aging Temperature, F	320		350		375	
Thickness, in.	Maximum Hardness, HRB	Time, hr	Maximum Hardness, HRB	Time, hr	Maximum Hardness, HRB	Time, hr
0.02	70	128	64	64	66	8
0.03	68	128	65	128	67	8–16
0.045	74	128	69	64	75	8–16
0.075	80	128	75	128	79	16
0.075 (Flange, as-received)	79	32	74	64	75	2–4

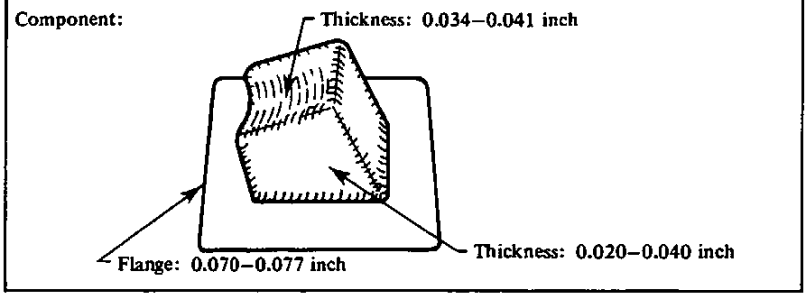


TABLE 1.063. MAXIMUM HARDNESS IN A SUPERPLASTICALLY FORMED COMPONENT (6)

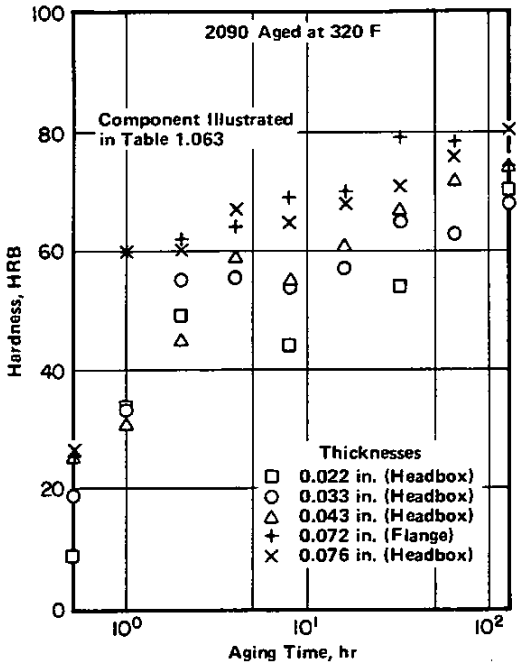
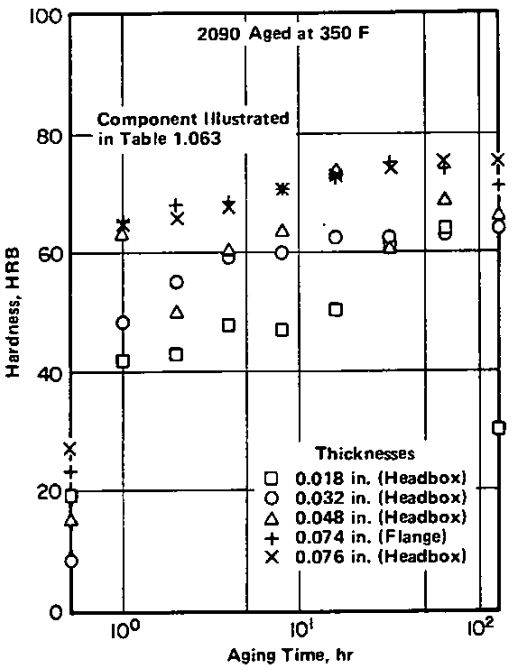


FIGURE 1.064. AGING CURVES FOR A SUPERPLASTICALLY FORMED COMPONENT AT 320 F (6)



Al	
2.7	Cu
2.3	Li
0.12	Zr

2090 Al

FIGURE 1.065. AGING CURVES FOR A SUPERPLASTICALLY FORMED COMPONENT AT 350 F (6)

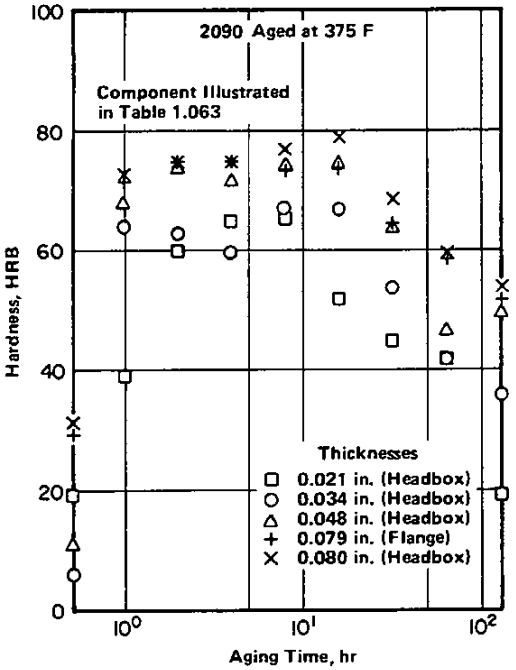


FIGURE 1.066. AGING CURVES FOR A SUPERPLASTICALLY FORMED COMPONENT AT 375 F (6)

Al
2.7 Cu
2.3 Li
0.12 Zr

2090 Al

Alloy			2090				
Temper			T83				
Form			Plate				
Composition, weight percent			Thickness,	Corrosion Exposure			
				EXCO[a]	MASTMAASIS[b]	Point Judith	
Li	Cu	Zr	in.	2 days	2 weeks	Months	Rating
2.2	2.5	0.12	0.25	EB[c]	p[c]	22	N[c]
2.2	3.0	0.12	0.25	EC	p	22	N
2.5	2.5	0.12	0.25	EC	p	22	N
2.5	3.0	0.12	0.25	EC	p	22	N
2.2	2.5	0.12	1.0	EA	p	22	N
2.2	3.0	0.12	1.0	EA	p	22	N
2.5	2.5	0.12	1.0	EA	p	22	N
2.5	3.0	0.12	1.0	EA	p	22	N

Note: These samples represent efforts to study the effects of composition variation on the properties of 2090. The panels have suffered no exfoliation in either MASTMAASIS or the Point Judith seacoast atmosphere, but EXCO attacked the 0.25 inch thick plate severely. Composition did not influence the results; the difference in EXCO ratings was probably caused by a more directional grain structure in the thinner plate.

(a) Total immersion in 4N, NaCl + 0.5N, KNO_3 + 0.1N, HNO_3 solution for 48 hours – ASTM Method G34-86.
(b) Exposure to acetic acid acidified salt spray, ASTM Method G85, Annex 2.
(c) Ratings according to ASTM Method G34-72: p = pitting and E = exfoliation; severity is denoted by the letter A, B, or C in increasing severity.

TABLE 2.0311. EXFOLIATION CORROSION OF 2090-T83 PLATE (4)

Alloy			2090					
Composition, weight percent					Corrosion Exposure			
				Temper,	EXCO[a],	MASTMAASIS[b],	Point Judith	
Li	Cu	Zr	Product	hr/temp, F	2 days	2 weeks	Months	Rating
2.0	3.0	0.12	1-in. Thick	-T3	N[c]	–	30	N
				8/300 (U)	EA	–	30	N
				16/325 (U)	N	–	30	N
				48/325 (O)	EB	–	30	N

Note: (U) underaged, (P) near peak-aged, (O) overaged.

(a) Total immersion in 4N, NaCl + 0.5N, KNO_3 + 0.1N, HNO_3 solution for 48 hours – ASTM Method G34-86.
(b) Exposure to acetic acid acidified salt spray, ASTM Method G85, Annex 2.
(c) Ratings according to ASTM Method G34-72: p = pitting, and E = exfoliation; severity is denoted by the letter A, B, or C in increasing severity.

TABLE 2.0312. EXFOLIATION OF 2090 PLATE (4)

Alloy			2090					
Temper			T83					
Form			Plate					
Composition				Gauge,	Temper,	EXCO[a],	MAST.[b],	Point Judith
Li	Cu	Zr	Product	in.	hr/F	4 day	4 week	Rating, mo
Alloy 2090			Plate	0.5	T81	ED,ED[c]	P,P	N (24)
			Extrusion	0.4	T83	ED,ED	P,P	N (24)
2.2	2.5	0.12	Plate	0.25	24/325	ED	P	N (48)
2.2	3.0	0.12	Plate	0.25	24/325	ED	P	N (48)
2.5	2.5	0.12	Plate	0.25	24/325	ED	P	N (48)
2.5	3.0	0.12	Plate	0.25	24/325	ED	P	N (48)
2.2	2.5	0.12	Plate	1	24/325	EA	P	EA (48)
2.2	3.0	0.12	Plate	1	24/325	EA	P	EA (48)
2.5	2.5	0.12	Plate	1	24/325	EA	P	EA (48)
2.5	3.0	0.12	Plate	1	24/325	EC	P	EA (48)

Note: The 0.5 inch plate and the extrusion were produced as part of the Navy sponsored cooperative test program. The 0.25 inch and 1 inch plates were cast as small ingots and rolled at the Alcoa Technical Center as part of the 2090 development program.

(a) Total immersion in 4N, NaCl + 0.5N, KNO_3 + 0.1N, HNO_3 solution for 48 hours – ASTM Method G34-86.
(b) Exposure to acetic acid acidified salt spray, ASTM Method G85, Annex 2.
(c) Ratings according to ASTM Method G34-72: P = pitting, and E = exfoliation; severity is denoted by the letter A, B, C, or D in increasing severity.

TABLE 2.0313. CORROSION TEST COMPARISON, 2090 PLATE (38)

Alloy	2090					
Temper	T83					
Form	Plate					
		EXCO[a],	MASTMAASIS[b]			Point Judith
Condition	Plane	4 day	Wet	Dry	Asset	Rating, mo
As-Received	T/2	ED[d]	P[c]			N (24)
(T83)	T/10	ED[d]	P	P	P	N (24)
As-Quenched	T/2	EB	EA	ED	EC	ED (24)
(212 F Water)	T/10	EC	EA	ED	EC	ED (24)
As-Quenched	T/2	EA	EA	EB	EC	EC (24)
(68 F Water)	T/10	EA	EA	EC	EC	ED (24)

(a) Total immersion in 4N, NaCl + 0.5N, KNO_3 + 0.1N, HNO_3 solution for 48 hours – ASTM Method G34-86.
(b) Exposure to acetic acid acidified salt spray, ASTM Method G85, Annex 2.
(c) Ratings according to ASTM Method G34-72: P = pitting and E = exfoliation; severity is denoted by the letter A, B, C, or D in increasing severity.
(d) Specimens removed from test after 2 days.

TABLE 2.0314. ACCELERATED CORROSION TESTS OF 0.5-INCH PLATE OF 2090 (38)

Al
2.7 Cu
2.3 Li
0.12 Zr

2090 Al

Al
2.7 Cu
2.3 Li
0.12 Zr

2090 Al

Alloy		2090							
Temper		T83							
Form		1-inch Plate							
Composition, weight percent		Alternate Immersion[a]				Point Judith, Rhode Island			
		25 ksi		35 ksi		25 ksi		35 ksi	
Li	Cu	F/N[b]	Days	F/N	Days	F/N	Days	F/N	Days
2.5	3.0	0/3	–	3/3	3,3,5	0/3	–	2/3	367,367
2.2	3.0	0/3	–	1/3	9	0/3	–	1/3	966
2.5	2.5	1/3	5	3/3	3,3,3	0/3	–	3/3	367,839 966
2.2	2.5	0/3	–	3/3	3,9,9	0/3	–	0/3	–

(a) ASTM G47 test; ASTM G44 solution.
(b) Number of specimens failed/number exposed.

TABLE 2.0321. STRESS CORROSION OF 2090-T83 PLATE, EFFECT OF COMPOSITION (4)

Alloy	2090						
Temper	T83						
Form	Extrusion						
Test	Alternate Immersion[a]						
Aging Treatment, hr at 325 F	Stress, ksi (L)	25 ksi		35 ksi		45 ksi	
		F/N	Days	F/N	Days	F/N	Days
10	64.4	4/6	10,19,28,28	3/6	9,15,28	6/6	3,3,3,5,5,6
18	72.8	0/6	–	0/6	–	2/6	20,25
24	73.2	0/6	–	0/6	–	1/6	4
36	74.2	0/6	–	0/6	–	1/6	12
Note: All aged conditions survived 30 days at 15 ksi.							

(a) ASTM G47 test method; ASTM G44 solution.

TABLE 2.0322. STRESS CORROSION OF 2090-T83 EXTRUSION, EFFECT OF AGING (4)

Alloy	2090		
Form	Plate		
Times to Failure (days) After NaCl Immersion for 6 Days[a]			
Environment		Alloy 2024	Alloy 2090UA[b]
Lab Air (≈50% R.H.)		>60[c]	0.6 ± 0.1[d]
Lab Air (≈100% R.H.)		5 ± 1	–
CO_2-Free Air (≈100% R.H.)		>60	>60
Times to Failure (days) Under Constant Immersion			
Added Species[e]	Alloy 2024	Alloy 2090UA	Alloy 2090PA[f]
None	>60	>30	>30
LiCl	>60	16.0 ± 3.0[d]	10.7 ± 2.7
Li_2CO_3	5.7 ± 1.5	1.0 ± 0.3	1.70 ± 0.1
Na_2CO_3	>60	>60	>60

(a) Naturally aerated 3.5% NaCl in distilled water; specimens stressed to 35 ksi in the environments listed.
(b) UA = underaged.
(c) "> X" = test ended after X days, with no failures.
(d) Mean ± standard deviation.
(e) All environments have aerated 3.5 w/o NaCl as their base, with 0.1 M of the listed species added. The exception is LiCl, where 0.2 M LiCl was added to 2.6 w/o NaCl, in an effort to keep Cl^- and Li^+ concentrations consistent with Li_2CO_3. All initial pH = 10. Chemicals were all reagent grade.
(f) PA = peak aged.

TABLE 2.0323. TIME TO FAILURE FOR 2090 1.5-INCH PLATE IN VARIOUS ENVIRONMENTS (36)

Al	
2.7	Cu
2.3	Li
0.12	Zr

2090 Al

Alloy	2090			
Environment	3.5% NaCl, Alternate Immersion[a]			
Specimen-Heat Treat	Stress Method	Induced Stress	Hours in Solution	Condition
2090-T3	U-bend[b]	36.2	428	Severe exfoliation and pitting; no IG[c]
2090-T3	U-bend	33.6	240	Exfoliation, no IG nor SCC
2090-T3	U-bend	36.2	240	Exfoliation, no IG
2090-T8	U-bend	40.6	91	Heavily pitted, heavy IG
2090-T8	U-bend	43.5	48	24 hrs crack 0.012-in. deep 48 hrs crack 0.02-in. deep Also heavily pitted
2090-T8	U-bend	45.7	18	IG, SCC[d], delamination, pitting
2090-T8	U-bend	43.5	10	Mainly pitting, no IG nor SCC

(a) ASTM G47.
(b) U-bend = U-bend specimen in the longitudinal direction.
(c) IG = intergranular cracking.
(d) SCC = stress corrosion cracking (cracking initiated at the stressed edge).

TABLE 2.0324. STRESS CORROSION DATA (TIME TO FAILURE) FOR 2090 SHEET (37)

Alloy	2090	
Environment	3.5% NaCl, Alternate Immersion[a]	
Crevice Corrosion Test		
Specimen-Heat Treat	Hours in Solution	Condition
2090-T8	336	In O_2-depleted area, severe pitting similar to 2024, no delamination
2024-T3	336	In O_2-depleted area, severe pitting

(a) ASTM G47.

TABLE 2.0325. CREVICE CORROSION OF 2090 SHEET (37)

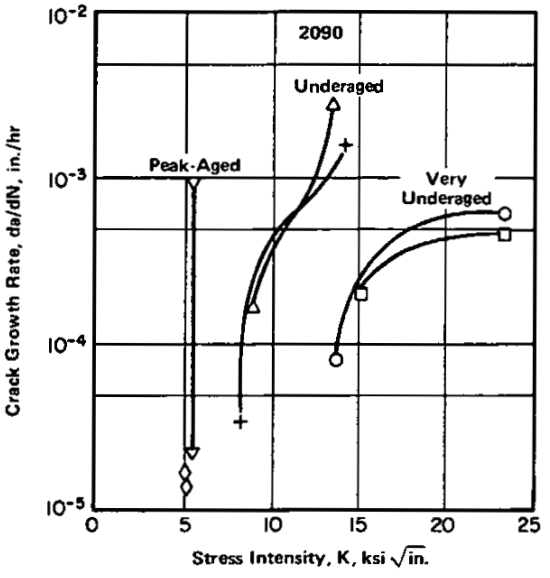


FIGURE 2.0326. STRESS CORROSION CRACK GROWTH RATE FOR 2090 T-X EXTRUSIONS IN 3.5% NaCl (10)

Al
2.7 Cu
2.3 Li
0.12 Zr

2090 Al

Alloy	2090								
Temper	T81								
Form	Plate								
Test Type	1/8-inch Diameter Tension								
Thickness, in.	0.5	1.5							
Direction	T	ST							
Environment	(a)	(a)			(b)			(c)	
Exposure Stress, ksi	60	20	25	35	15	25	35	25	35
Exposure Time, days	30	30	30	30	120	120	120	150	150
No. Failed/No. Tests	0/5	0/5	4/5	5/5	0/5	4/5	5/5	0/5	1/5
Failure Time Range, days	–	–	1–10	2–9	–	13–19	13	–	105

(a) 3.5% NaCl alternate immersion per ASTM G44.
(b) Seacoast, Point Judith, RI.
(c) Mild industrial inland, New Kingsington, PA.

TABLE 2.0327. STRESS CORROSION RESULTS FOR 2090-T81 PLATE IN VARIOUS ENVIRONMENTS (49)

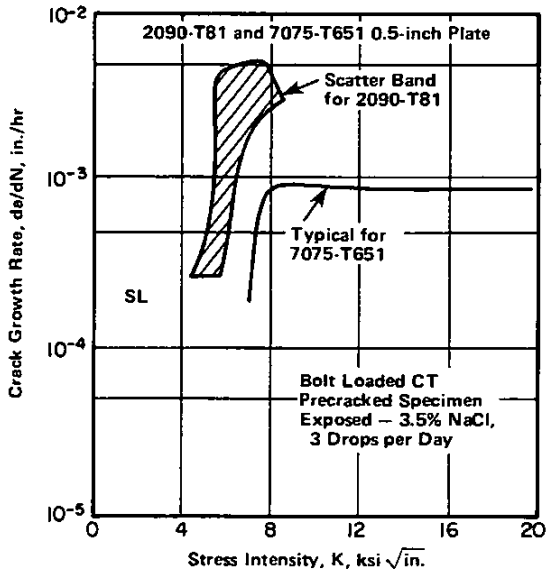


FIGURE 2.0328. STRESS CORROSION CRACK GROWTH RATES IN 3.5% NaCl FOR 2090-T81 AND 7075-T651 PLATE TESTED IN THE SL DIRECTION (49)

Alloy	2090				
Form	Plate				
Temper	Condition	F_{ty}, ksi	F_{tu}, ksi	Elongation, percent	Percent Loss in Elongation
T6	Charged	70.9	71.8	6.3	36
	Uncharged	73.2	79.8	9.8	–
Overaged	Charged	49.6	57.7	3.9	65
	Uncharged	56.6	66.0	11	–
Tensile specimens chemically polished and cathodically charged in 0.1N HCl, pH = 1 or 0.5N H_2SO_4 at -2000 mV.					

TABLE 2.0341. EFFECT OF HYDROGEN CHARGING ON THE MECHANICAL PROPERTIES OF 2090 PLATE (39)

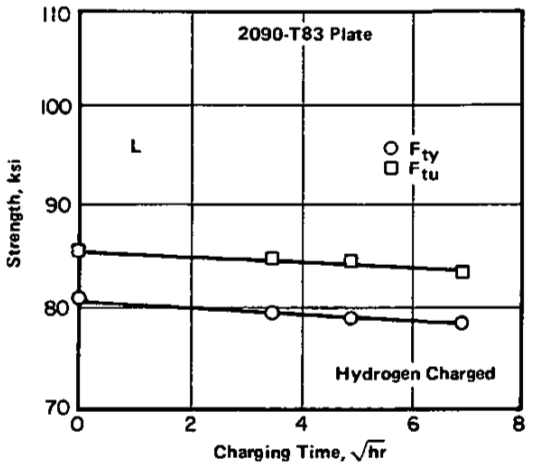
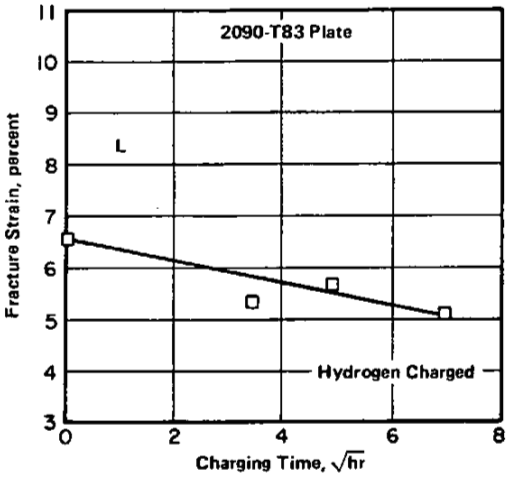


FIGURE 2.0342. EFFECT OF HYDROGEN CHARGING ON THE STRENGTH OF 2090-T83 0.5-INCH PLATE (40)



	Al
2.7	Cu
2.3	Li
0.12	Zr

2090 Al

FIGURE 2.0343. EFFECT OF HYDROGEN CHARGING ON THE FRACTURE STRAIN OF 2090-T83 0.5-INCH PLATE (40)

Alloy	2090					
				Minimums		Elongation,
Condition	Form	Thickness, in.	Direction	F_{tu}, ksi	F_{ty}, ksi	percent in 2 in.
0	Sheet	0.032–0.249	–	31.0 max	28.0 max	11
T3	Sheet	0.032–0.249	–	46.0	31.0	6
T31	Sheet	0.032–0.249	–	42.0	28.0	11
				55.0 max	42.0 max	–
T81	Plate	0.500–1.5	L	75.0	70.0	4
			T	75.0	68.0	3
T83	Sheet	0.032–0.125	L	77.0	70.0	3
			T	73.0	66.0	5
		0.126–0.249	L	75.0	70.0	4
			T	73.0	66.0	5
T84	Sheet	0.032–0.249	L	72.0	66.0	3
			T	69.0	60.0	5
T86	Extrusion	Up to 0.124	L	77.0	71.0	4
		0.125–0.249	L	77.0	72.0	4
		0.250–0.499	L	78.0	72.0	5
			T	75.0	70.0	3

TABLE 3.011. ALUMINUM ASSOCIATION REGISTERED TEMPERS (2)

	Al
2.7	Cu
2.3	Li
0.12	Zr

2090 Al

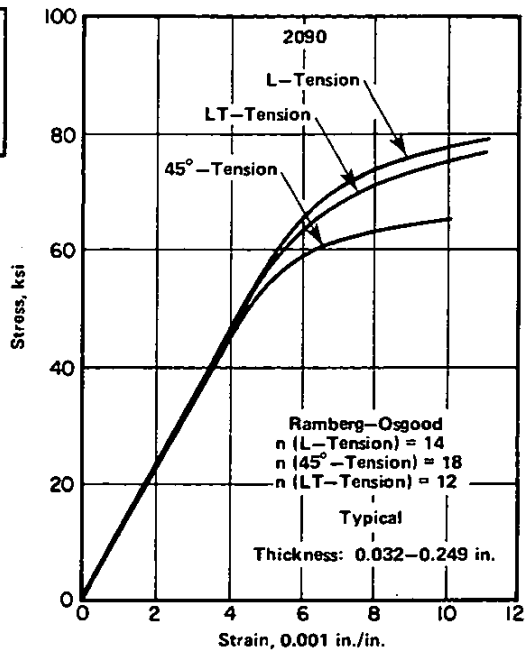


FIGURE 3.0211. STRESS STRAIN CURVE FOR 2090-T83 SHEET (1)

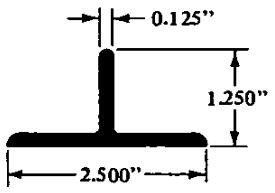
Alloy	2090				
Form	0.5 inch Plate				
Temper	T83				
Source	(5)		(8)		
Orientation	L	T	L	T	45 Degree
F_{tu}, ksi	85	85	85	84	75
F_{ty}, ksi	75	80	80	80	67
Elongation, percent	7.6	6.2	9.3	5.4	11

TABLE 3.0212. TENSILE PROPERTIES OF 2090-T83 PLATE FROM TWO SOURCES (5,8)

Alloy	2090				
Form	Thickness or Shape	Temper	F_{tu}, ksi	F_{ty}, ksi	Elongation, percent
Sheet	0.12 in.	T6	78.3	70.3	5
		Underaged	66.0	55.1	7
Plate	0.79 in.	T6	76.9	70.3	6
Extrusion	L-Shape	T6	81.9	74.7	6
	1 x 5 x 6 in.	Underaged	68.2	55.1	8
Hand Forging	3 x 6 in.	T6	74.7	60.2	5
Die Forging	Complex	T6	68.2–79.8	50.0–70.3	2–8

TABLE 3.0213. TENSILE PROPERTIES OF VARIOUS 2090 PRODUCT FORMS IN THE -T6 AND UNDERAGED TEMPERS (10)

Alloy		2090		
Temper		T83		
Form		Extrusion		
Lot		F_{tu}, ksi	F_{ty}, ksi	Elongation, percent
1	Rear[a]	85.6	79.7	6.0
	Front	82.7	78.0	6.5
2	Rear	88.3	82.2	5.5
	Front	87.0	81.3	5.5



(a) Front and rear denote initial and final sections of extrusion length from a billet.

TABLE 3.0214. TENSILE PROPERTIES OF 2090-T83 EXTRUSION (9)

Al
2.7 Cu
2.3 Li
0.12 Zr

2090 Al

Alloy	2090			
Form	Sheet			
Temper	T3			
Thickness/ Lot	Test Direction	F_{tu}, ksi	F_{ty}, ksi	Elongation, percent in 2 in.
0.090 in.				
A	Longitudinal	39.9	25.3	18.8
	Transverse	44.1	26.4	19.0
B	Longitudinal	46.9	31.2	18.8
	Transverse	46.9	29.5	19.3
0.125 in.				
C	Longitudinal	48.4	32.8	11.5
	Transverse	48.4	30.6	16.5

TABLE 3.0215. TENSILE PROPERTIES OF 2090-T3 SHEET (35)

Alloy	2090						
Form	Sheet						
Temper		F_{tu}, ksi		F_{ty}, ksi		Elongation, percent in 2 in.	
T83	Orientation	T	L	T	L	T	L
	0.125 in.						
	Process 2[a]	80.3	84.3	73.8	81.0	6.7	4.1
	Process 1	79.1	82.2	71.3	75.9	6.6	4.8
	Lot Average	79.5	82.6	72.6	77.4	6.3	4.5
	0.063 in.						
	Lot Average	78.2	80.5	71.3	73.5	6.1	5.0
T31	Lot A	63.9	63.5	49.8	54.2	12.0	5.9
	Lot B	64.8	63.2	51.8	54.5	10.1	5.8
	Lot C	67.2	68.4	53.3	60.8	10.8	5.0

(a) Processes 1 and 2 not specified in (35).

TABLE 3.0216. TENSILE PROPERTIES OF 2090-T31 AND -T83 SHEET (35)

Alloy	2090			
Temper	T83			
Form	Sheet			
		Tensile Strength		Elongation,
Thickness, in.	Orientation	F_{tu}, ksi	F_{ty}, ksi	percent
0.090	L	83.9	77.2	5.5
	T	80.5	74.3	7.5
0.144	L	83.1	76.6	6.0
	T	79.3	72.8	9.0
0.190	L	82.1	76.2	6.5
	T	78.7	72.4	9.0

TABLE 3.0217. TENSILE PROPERTIES OF 2090-T83 SHEET (9)

	Al
2.7	Cu
2.3	Li
0.12	Zr

2090 Al

Alloy	2090			
Form	Sheet (Superplastically Formed)(a)			
Temper	T6			
Area(b)	Thickness, in.	F_{ty}, ksi	F_{tu}, ksi	Elongation, percent
A	0.028	48.1	63.5	8.9
B	0.028	49.2	65.1	8.5
C	0.032	46.2	62.6	9.7
D	0.042	46.0	58.9	12.9
E	0.025	46.3	62.1	11.2
F	0.027	44.8	61.7	12.5
G	0.034	43.2	58.6	8.5
Flange	0.073	46.5	65.5	7.8
Unformed Sheet	0.074	44.5	60.1	8.9

(a) For illustration of component, see Table 1.063.
(b) Areas on drawn sidewall: A, E, F, G; areas on bottom: B, C, and D.

TABLE 3.0218. TENSILE PROPERTIES OF SUPERPLASTICALLY FORMED 2090-T6 SHEET (6)

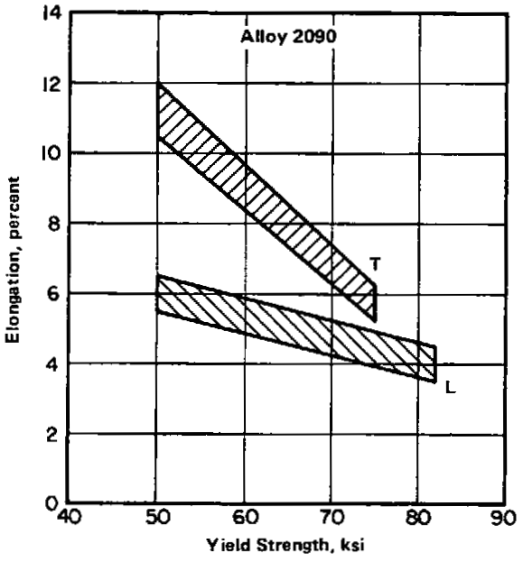


FIGURE 3.0219. STRENGTH-DUCTILITY RELATIONSHIPS FOR 0.090-INCH 2090 SHEET IN VARIOUS TEMPERS (35)

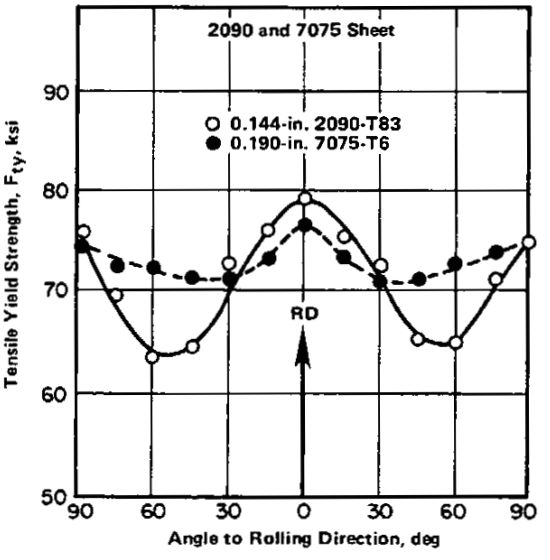


FIGURE 3.02110. YIELD STRENGTH AS A FUNCTION OF ORIENTATION TO THE ROLLING DIRECTION FOR 2090-T83 AND 7075-T6 SHEET (49)

	Al
2.7	Cu
2.3	Li
0.12	Zr

2090 Al

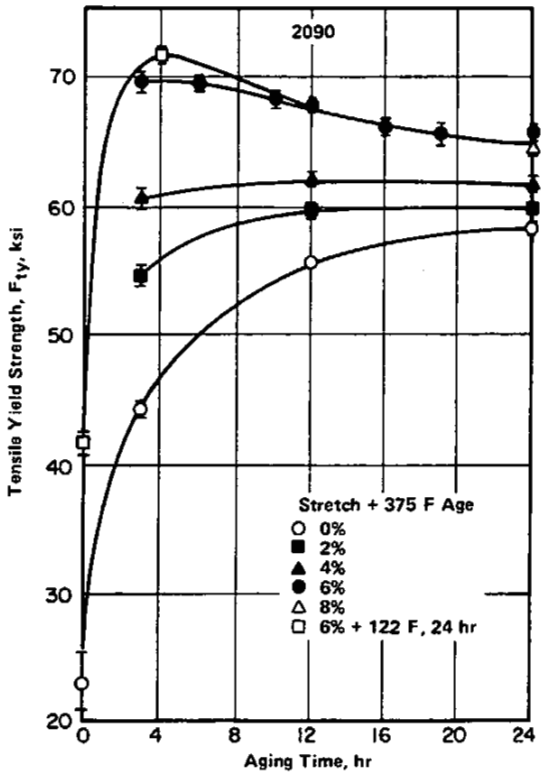


FIGURE 3.02111. YIELD STRENGTH AS A FUNCTION OF STRETCHING AND AGING AT 375 F (11)

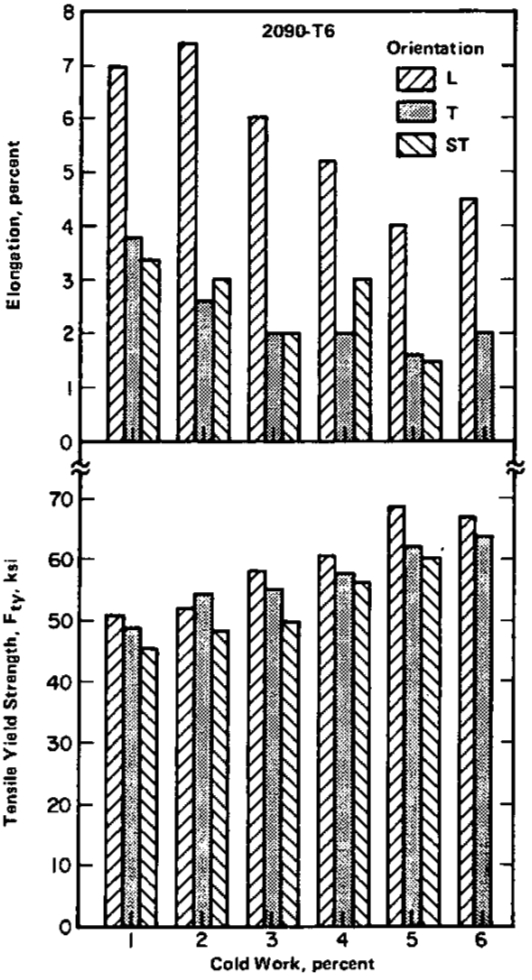


FIGURE 3.02112. YIELD STRENGTH AND ELONGATION AS A FUNCTION OF COLD WORK BEFORE AGING IN 2090-T6 HAND FORGINGS (11)

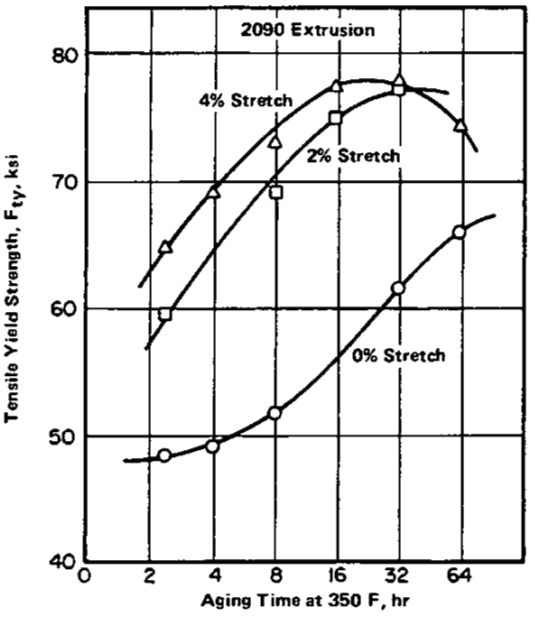


FIGURE 3.02113. TRANSVERSE YIELD STRENGTH AS A FUNCTION OF COLD WORK BEFORE AGING IN 2090 EXTRUSIONS (11)

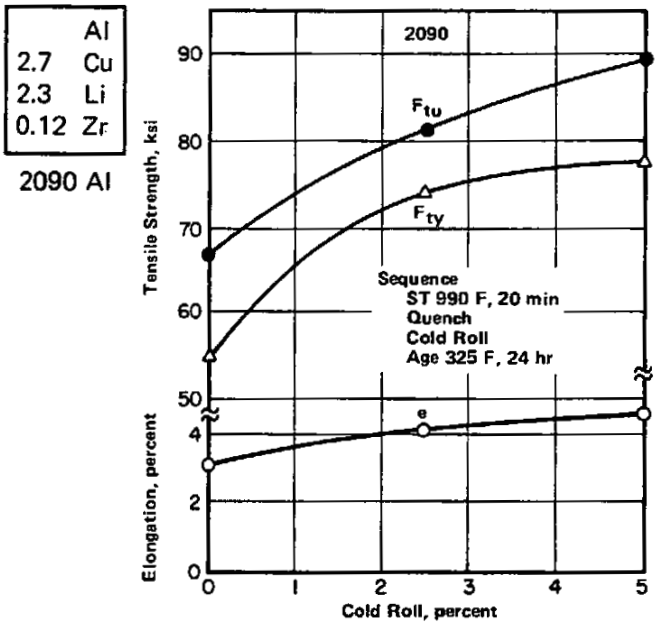


FIGURE 3.02114. TENSILE PROPERTIES AS A FUNCTION OF COLD WORK (ROLLING) BEFORE AGING IN 2090 SHEET (7)

Alloy	2090		
Form	Plate and Extrusion		
Temper	T8		
Orientation	F_{tu}, ksi	F_{ty}, ksi	Elongation, percent
As-Received			
Plate			
L	84.2	78.0	6.6
LT	82.1	76.1	8.5
Extrusion			
LX	82.3	78.0	6
TX	70.6	66.3	11
After 1000 hr at 150 F			
Plate			
L	88.8	82.6	2.5
LT	88.6	80.6	6
Extrusion			
LX	86.1	82.9	1.5
TX	80.6	75.9	5

TABLE 3.02115. EFFECT OF EXPOSURE AT 150 F ON THE TENSILE PROPERTIES OF 2090 PLATE AND EXTRUSION (SEE ALSO TABLE 3.02727) (33)

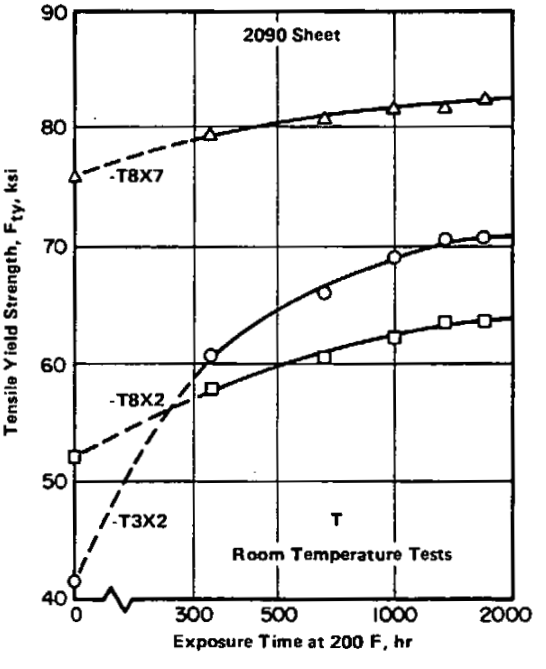


FIGURE 3.02116. EFFECT OF EXPOSURE AT 200 F ON THE TENSILE PROPERTIES OF 2090 SHEET (SEE ALSO 3.02727) (34)

Alloy	2090	
Temper	T83	
Form	Sheet	
Thickness, in.	Orientation	Compressive Yield Stress, F_{cy}, ksi
0.090	L	77
	T	81.4
0.144	L	73.9
	T	78.7
0.190	L	74.5
	T	78.2

TABLE 3.0221. COMPRESSIVE YIELD STRENGTH OF 2090-T83 SHEET (9)

Alloy	2090			
Product Form		Compressive Yield Strength, F_{cy}, ksi		
Sheet Thickness, in.	Temper	L	45 Degree	LT
0.032–0.125	T83	67	58	71
0.125–0.249	T83	63	60	71

TABLE 3.0222. PROPOSED COMPRESSIVE YIELD DESIGN ALLOWABLES FOR 2090-T83 SHEET (1)

Al	
2.7	Cu
2.3	Li
0.12	Zr

2090 Al

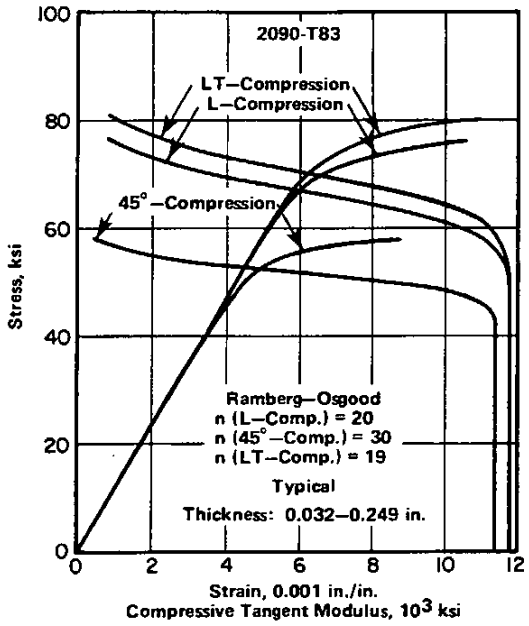


FIGURE 3.0223. COMPRESSIVE STRESS-STRAIN AND TANGENT MODULUS CURVES FOR 2090-T83 SHEET (1)

Alloy	2090			
Temper	Various			
Form	Plate			
Orientation			L-T	L
Cold Work (Stretch), percent	Aging Temperature, F	Aging Time, hr	Charpy Values, in.-lb/in.^{2}	F_{ty}, ksi
0	347	36	135	60.3
3	297	24	520	59.6
7	250	60	600	61.8

TABLE 3.0231. CHARPY V RESULTS FOR 2090 PLATE COLD WORKED VARIOUS AMOUNTS AND AGED TO EQUIVALENT STRENGTH (23)

	Al
2.7	Cu
2.3	Li
0.12	Zr

2090 Al

Alloy	2090	
Temper	T83	
Form	Sheet	
Thickness, in.	Orientation	Ultimate Shear Strength, F_{su}, ksi
0.090	L	41.6
	T	43.9
0.144	L	41.1
	T	44.3
0.190	L	41.9
	T	44.2

TABLE 3.0251. SHEAR STRENGTH OF 2090-T83 SHEET (9)

Alloy	2090			
Temper	T83			
Form	Sheet			
		Bearing		
		F_{bu}, ksi		F_{by}, ksi	
Thickness, in.	Orientation	e/D = 1.5	e/D = 2.0	e/D = 1.5	e/D = 2.0
0.090	L	116.3	145.8	98.6	113
	T	115.3	148.8	98.1	121.4
0.144	L	110.7	146.3	99.2	117.1
	T	114.1	141.2	99.7	119.2
0.190	L	112.7	147.3	99.2	111.7
	T	115.6	144.7	101	117.7

TABLE 3.0261. BEARING PROPERTIES OF 2090-T83 SHEET (9)

Alloy		2090	
Dry Pin Bearing Values		F_{bry}, ksi	
Product Form	Temper	e/D = 1.5	e/D = 2.0
Sheet 0.032–0.249 in.	T83	100	126

TABLE 3.0262. PROPOSED DESIGN ALLOWABLE BEARING STRENGTHS FOR 2090-T83 SHEET (1)

Alloy	2090									
Temper	T83									
Form	0.053-inch Sheet									
Test Method	R Curves by ASTM E561 With Analysis by ASTM B646									
Specimen Type	M(T) W = 16 in. 4 in. Crack		M(T) W = 6 in. 2 in. Crack		M(T) W = 6 in. 1.5 in. Crack		M(T) W = 4 in. 1.5 in. Crack		C(T) W = 14 in.	
Orientation	LT	TL	LT	TL	LT	TL	LT	TL	LT	TL
No. of Tests	4	3	1	1	1	1	2	2	1	1
K_c Avg., ksi $\sqrt{in.}$	49	32	46	27	–	–	38	32	46	43
K_c Spread	42–59	30–35	–	–	–	–	36–40	23–41	–	–
K_{app}, ksi $\sqrt{in.}$(a)	43	31	27	30	38	37	36	27	–	–
K_{app} Spread	38–50	28–33	–	–	–	–	37–37	23–32	–	–

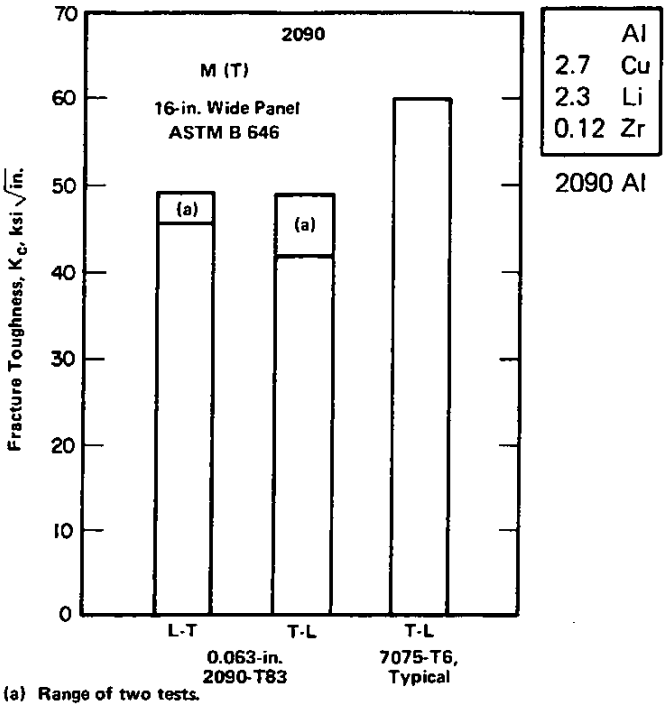
(a) Based on original crack length.

TABLE 3.02721. FRACTURE TOUGHNESS VALUES FOR 2090 SHEET (49, TABLE A6)

Alloy	2090			
Form	Sheet			
Temper	T31			
Gauge	0.090 inch			
Orientation	L-T		T-L	
Lot No.	K_c[a], ksi $\sqrt{in.}$	K_{app}, ksi $\sqrt{in.}$	K_c, ksi $\sqrt{in.}$	K_{app}, ksi $\sqrt{in.}$
A[b]	86.1	65.1	92.7	69.7
	106.3	77.8	–	–
(c)	104.8	77.6	–	–
(d)	97.1	61.9	–	–
(e)	109.1	69.8	–	–
B	89.4	66.9	94.6	69.3
	91.3	69.1	–	–
C	83.3	69.1	94.7	71.6
	88.0	64.2	–	–

(a) See 3.0272 for a discussion of test methods.
(b) Determined on 16 inch wide panel to ASTM E561 and B646, tested at full thickness.
(c) Machined to 0.049 inch at mid thickness.
(d) Machined to 0.039 inch from one side.
(e) Machined to 0.036 inch from one side.

TABLE 3.02722. FRACTURE TOUGHNESS OF DAMAGE TOLERANT 2090 SHEET (35)



(a) Range of two tests.

FIGURE 3.02723. FRACTURE TOUGHNESS OF 2090-T83 SHEET (22)

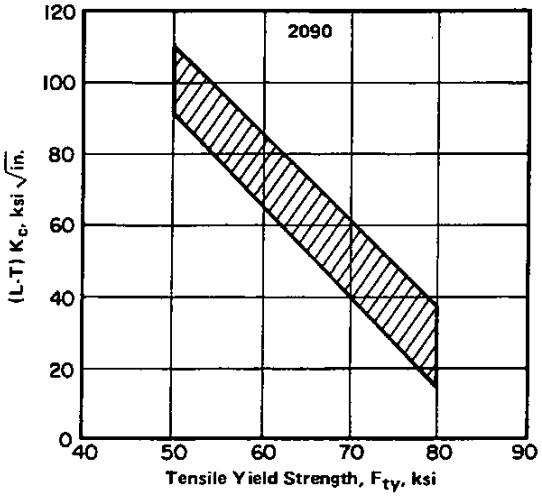


FIGURE 3.02724. FRACTURE TOUGHNESS OF PRODUCTION 2090 SHEET AS A FUNCTION OF STRENGTH LEVEL (35)

Alloy	2090	
Form	Sheet	
Temper	T8	
Orientation L-T	ksi $\sqrt{in.}$	
Thickness, in.	K_c[a]	K_{app}[a]
0.063	44.1	40.0
0.063	53.0	
0.063	38.0	
0.125 (Process 1)	38.3	35.9
0.125 (Process 2)	35.9	33.4

(a) See 3.0272 for discussion of test methods.

TABLE 3.02725. FRACTURE TOUGHNESS OF 2090 PEAK-AGED SHEET (35)

	Al
2.7	Cu
2.3	Li
0.12	Zr

2090 Al

Alloy	2090		
Thickness	0.5 inch		
Orientation	L-T		
Form	Thickness or Section, in.	Temper	Toughness, K_{Ic} or K_Q, ksi $\sqrt{in.}$(a)
Sheet	0.12	T6	50
Sheet	0.12	Underaged	100
Plate	0.8	T6	31.8
Extrusion	L Shape, 1 x 5 x 6	T6	18.2
Extrusion	L Shape, 1 x 5 x 6	Underaged	31.8

(a) Determined by ASTM E399.

TABLE 3.02726. FRACTURE TOUGHNESS OF VARIOUS 2090 FORMS (10)

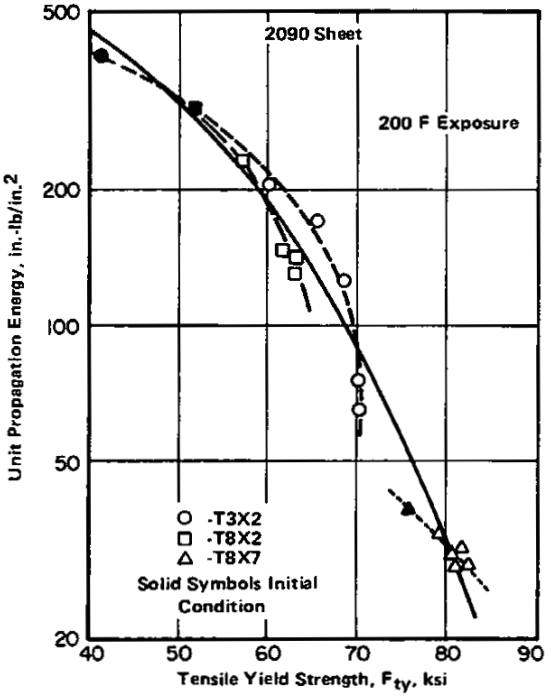


FIGURE 3.02727. EFFECT OF EXPOSURE FOR 0 TO 6 WEEKS AT 200 F ON THE UNIT PROPAGATION ENERGY IN A KAHN TEST FOR 2090 SHEET (34)

Alloy	2090							
Temper	T81						T86	
Form	0.5 inch Plate			1.5 inch Plate			Extrusion(a)	
Orientation	L-T	T-L	T-L + 45	T-L	S-L	S-T	L-T	T-L
K_{Ic} Avg., ksi $\sqrt{in.}$(b)	29	29	35	25	12	9	24	19
s, ksi(c)	2.4	4.0	–	2.8	–	1.4	2.7	2.8
Spread	26–31	26–31	–	23–27	7–17	8–10	19–29	14–22
No. of Tests	9	30	(d)	17	2	5	24	26

(a) T shaped extrusion with 0.75 inch thick test area.
(b) $P_{max}/PQ < 1.2$ but crack straightness requirement not always met.
(c) Sample standard deviation.
(d) Not given.

TABLE 3.02728. PLANE-STRAIN FRACTURE TOUGHNESS FOR PLATE AND EXTRUSIONS FROM A COOPERATIVE TESTING PROGRAM (49, TABLES 21, B5 AND B6)

Al
2.7 Cu
2.3 Li
0.12 Zr
2090 Al

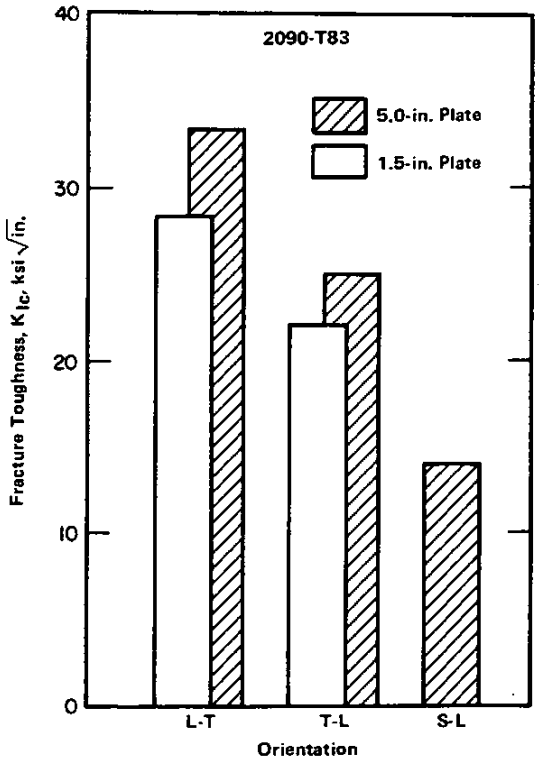


FIGURE 3.02729. PLANE-STRAIN FRACTURE TOUGHNESS OF 2090-T83 PLATE FOR SEVERAL CRACK ORIENTATIONS (22)

Alloy	2090
Form	Plate
Thickness	0.5 inch
Temper	T83
Orientation	Toughness, K_{Ic}, ksi $\sqrt{in.}$
L-T	31.8
T-L	21.8
L + 45/T + 45	25.5

TABLE 3.027210. PLANE-STRAIN FRACTURE TOUGHNESS OF 0.5-INCH 2090-T83 PLATE (8)

Alloy	2090
Form	Plate and Extrusion
Temper	T8
Orientation	Fracture Toughness, K_Q, ksi$\sqrt{in.}$
As-Received Plate (0.5 in.)	
T-L	29.7
L-T	30.2
Extrusion (0.125-in., T-Shape)	
T-L	32
After 1000 hr at 150 F	
Plate (0.5 in.)	
T-L	12.5
L-T	13.7
Extrusion (0.125-in., T-Shape)	
T-L	11.1

TABLE 3.027211. EFFECT OF EXPOSURE AT 150 F ON THE FRACTURE TOUGHNESS OF 2090 PLATE AND EXTRUSION (SEE TABLE 3.02115 FOR TENSILE PROPERTIES) (33)

Al
2.7 Cu
2.3 Li
0.12 Zr

2090 Al

Alloy	2090			
Form	Sheet			
Temper	T83			
Temperature, F	F_{ty}, ksi	F_{tu}, ksi	Elongation, percent	Modulus, ksi x 10^3
70	70.7	76.6	12.0	11.19
	70.6	76.4	12.1	10.27
-323	80.0	92.4	10.5	–
	79.8	93.2	11.1	11.15

TABLE 3.0311. TENSILE PROPERTIES OF 2090-T83 SHEET AT ROOM AND CRYOGENIC TEMPERATURES (16)

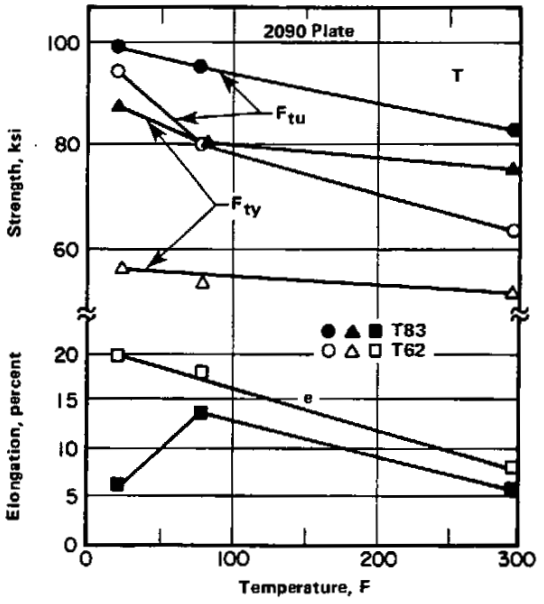


FIGURE 3.0312. TENSILE PROPERTIES OF 0.25-INCH 2090-T62 AND -T83 PLATE AS A FUNCTION OF TEMPERATURE (43)

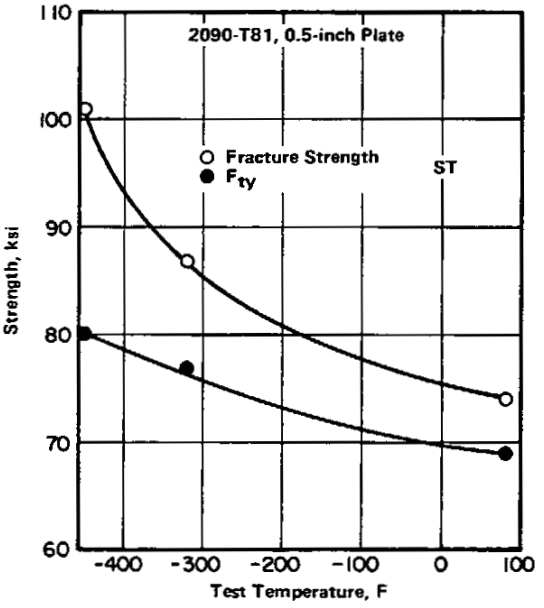


FIGURE 3.0313. EFFECT OF LOW TEST TEMPERATURES ON THE SHORT TRANSVERSE TENSILE STRENGTH OF 2090-T81 PLATE (13)

Alloy	2090				
Form	Sheet				
Temper	T6				
Material	Temp, F	Yield Strength, ksi	Tensile Strength, ksi	Total Elongation, percent	Reduction in Area, percent
2090-T6	63	49	62	5	8
	-320	55	77	15	15

TABLE 3.0314. TENSILE PROPERTIES OF 2090-T6 SHEET (45)

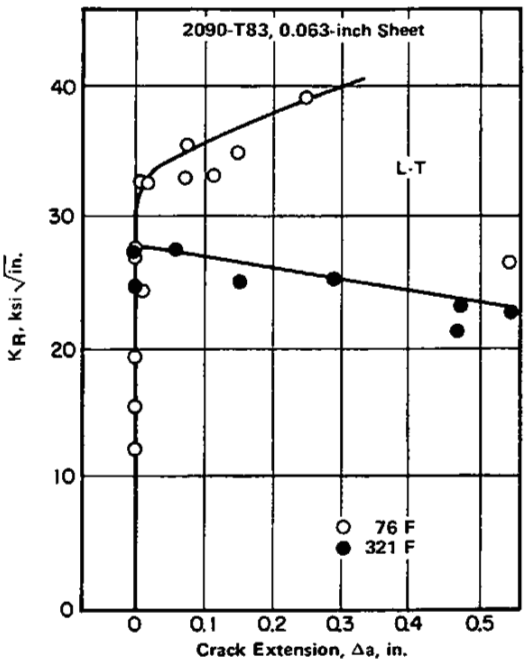
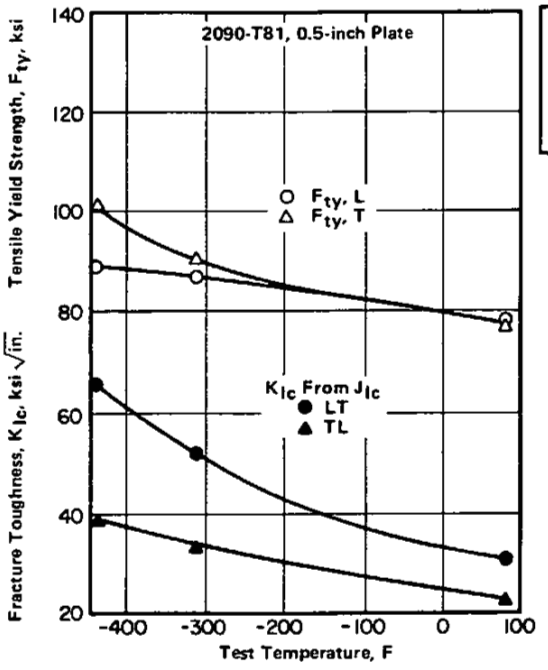


FIGURE 3.03721. R CURVES FOR 2090-T83 SHEET AT AMBIENT AND LIQUID NITROGEN TEMPERATURES (44)



Al
2.7 Cu
2.3 Li
0.12 Zr

2090 Al

FIGURE 3.03722. EFFECT OF LOW TEST TEMPERATURES ON THE TENSILE YIELD STRENGTH AND PLANE-STRAIN FRACTURE TOUGHNESS OF 2090-T81 PLATE (13)

Alloy	2090				
Form	0.5-inch Plate Machined to 0.063-inch at T/4 for Testing				
Temper	T6 and T81				
Material	Test Temp, F	UIE(a), in.-lb/in.^{2}	UPE(b), in.-lb/in.^{2}	Tear Strength, ksi	Tear Yield Ratio
2090-T6	80	144	89	54	1.10
	-320	131	63	57	1.04
2090-T81	80	220	137	65	0.98
	-320	258	218	75	0.98

(a) UIE = unit initiation energy.
(b) UPE = unit propagation energy.

TABLE 3.03723. KAHN TEAR TEST TOUGHNESS (LT) OF 2090-T6 AND -T81 AT AMBIENT AND CRYOGENIC TEMPERATURES (45)

	Al
2.7	Cu
2.3	Li
0.12	Zr

2090 Al

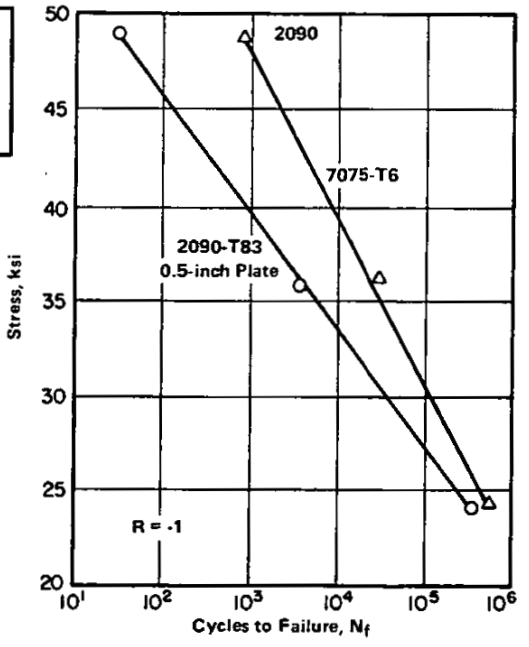


FIGURE 3.0511. FATIGUE LIFE OF 2090-T83 0.5-INCH PLATE IN FULLY REVERSED BENDING (19)

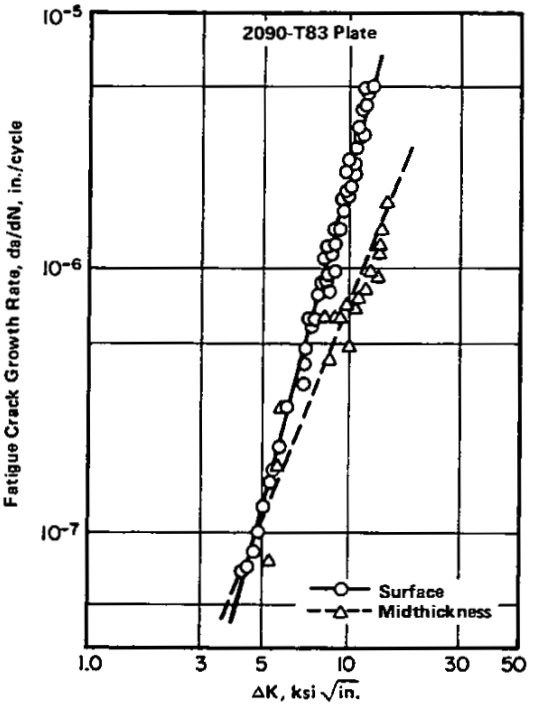


FIGURE 3.0521. FATIGUE CRACK GROWTH RATE CURVES FOR 0.5-INCH 2090-T83 PLATE SHOWING THE EFFECT OF HETEROGENEITY (32)

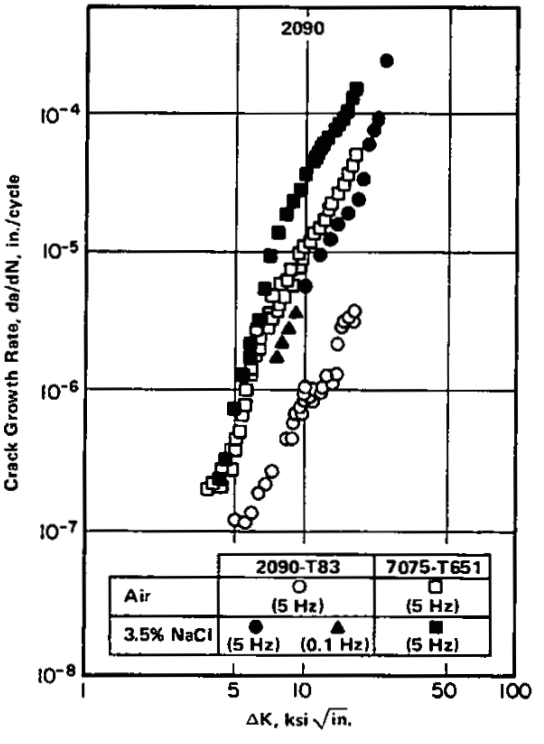


FIGURE 3.0522. FATIGUE CRACK GROWTH RATE FOR 0.5-INCH 2090-T83 PLATE IN AIR AND IN 3.5% NaCl (15)

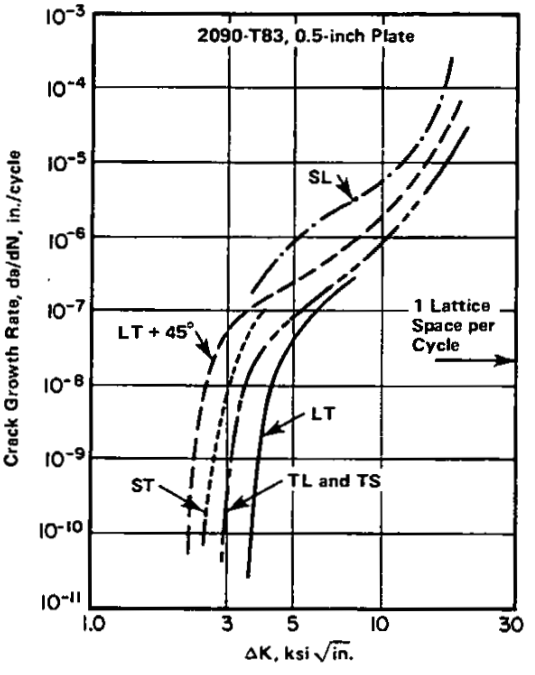


FIGURE 3.0523. FATIGUE CRACK GROWTH RATES FOR 2090-T83 PLATE SHOWING THE EFFECTS OF CRACK ORIENTATION AND K_{th} VALUES (8)

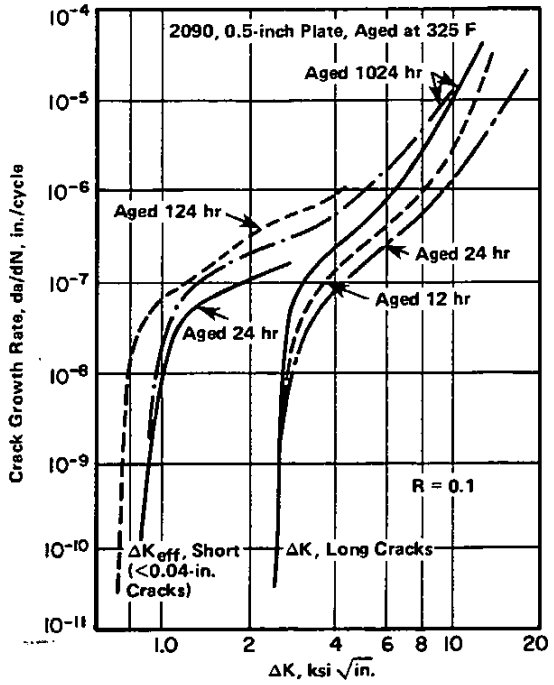


FIGURE 3.0524. FATIGUE CRACK GROWTH RATES FOR LONG AND VERY SHORT CRACKS IN 2090 0.5-INCH PLATE, SHOWING THE EFFECTS OF AGING TIME (8)

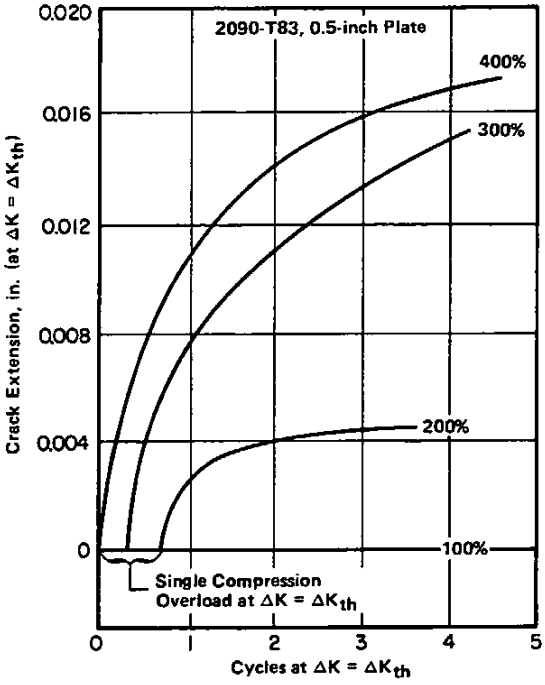


FIGURE 3.0525. CRACK GROWTH AT A CONSTANT VALUE OF $\Delta K = \Delta K_{th}$, FOLLOWING VARIOUS COMPRESSION OVERLOADS (8)

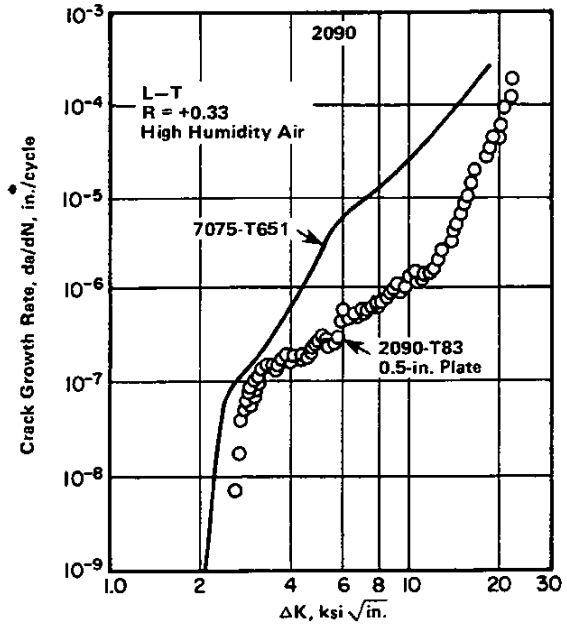


FIGURE 3.0526. FATIGUE CRACK GROWTH RATE OF 2090-T83 0.5-INCH PLATE IN HUMID AIR (5)

Alloy	2090	
Form	Plate	
Temper	T83	
	Modulus	
Orientation	Tension, ksi x 10^3	Compression, ksi x 10^3
L	11.5	12.0
T	11.6	12.1

TABLE 3.061. ELASTIC MODULI OF 2090-T83 PLATE (5)

	Al
2.7	Cu
2.3	Li
0.12	Zr

2090 Al

Alloy	2090							
Form	Sheet							
Temper	T83							
Source	(9)						(1)	
Thickness, in.	0.090		0.144		0.190		0.032–0.249	
Orientation	L	T	L	T	L	T	L & T	T + 45
Tension, 1000 ksi	11.3	11.4	11.3	11.4	11.2	11.3	11.5	11
Compression, 1000 ksi	11.7	11.7	11.6	11.8	11.6	11.8	11.8	11.4

TABLE 3.062. ELASTIC MODULI OF 2090-T83 SHEET FOR SEVERAL TESTING DIRECTIONS (1,9)

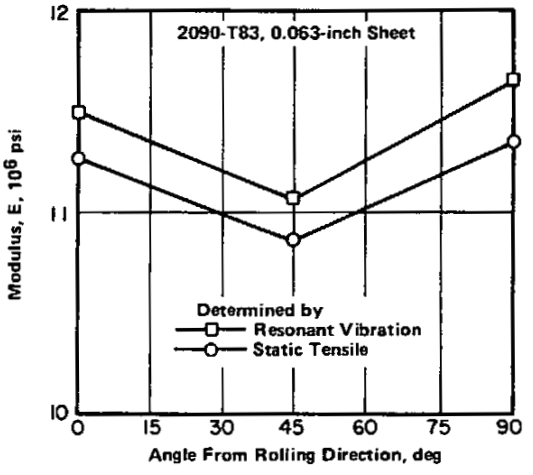


FIGURE 3.063. ANISOTROPY OF YOUNG'S MODULUS IN 2090-T83 SHEET (21)

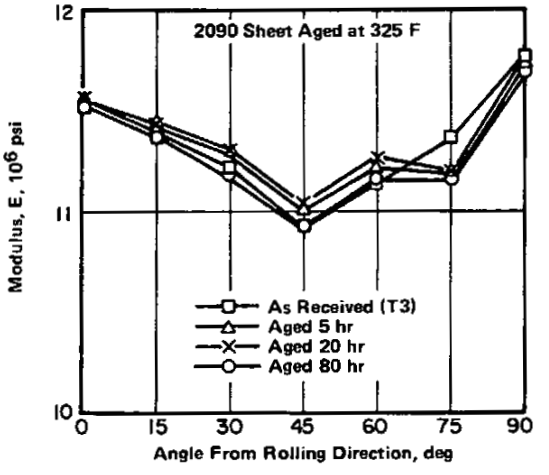


FIGURE 3.064. ANISOTROPY OF YOUNG'S MODULUS IN 2090-T83 SHEET, EFFECT OF AGING AT 325 F (21)

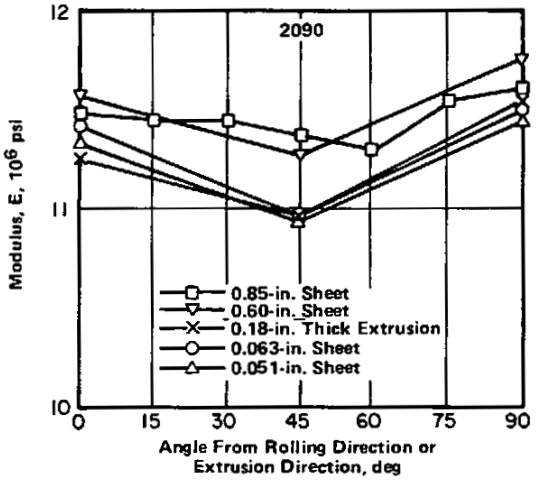


FIGURE 3.065. ANISOTROPY OF YOUNG'S MODULUS IN 2090-T83 SHEET AND EXTRUSION, EFFECT OF THICKNESS (21)

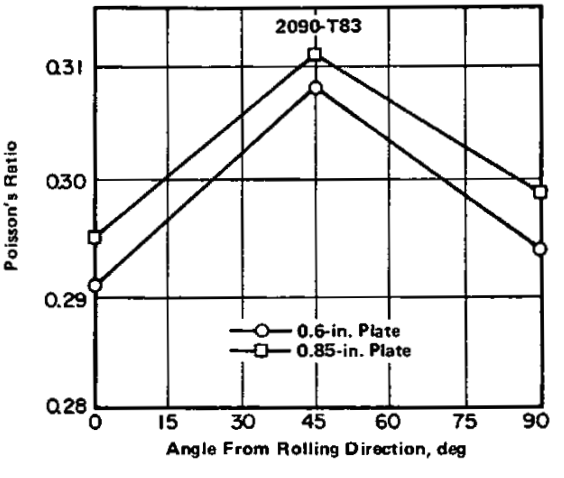


FIGURE 3.066. ANISOTROPY OF POISSON'S RATIO IN 2090-T83 PLATE (21)

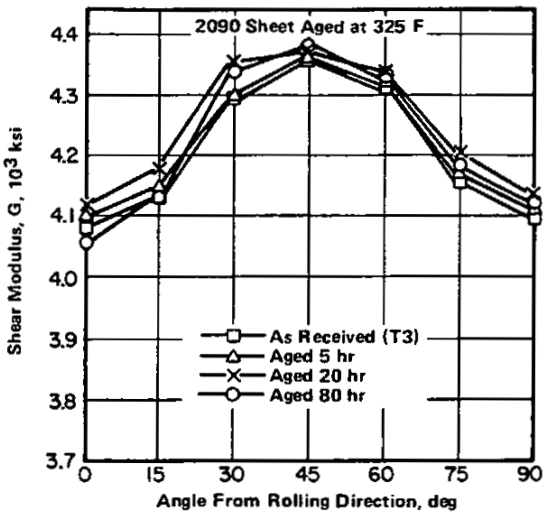


FIGURE 3.067. ANISOTROPY OF SHEAR MODULUS IN 2090 SHEET, EFFECT OF AGING AT 325 F (21)

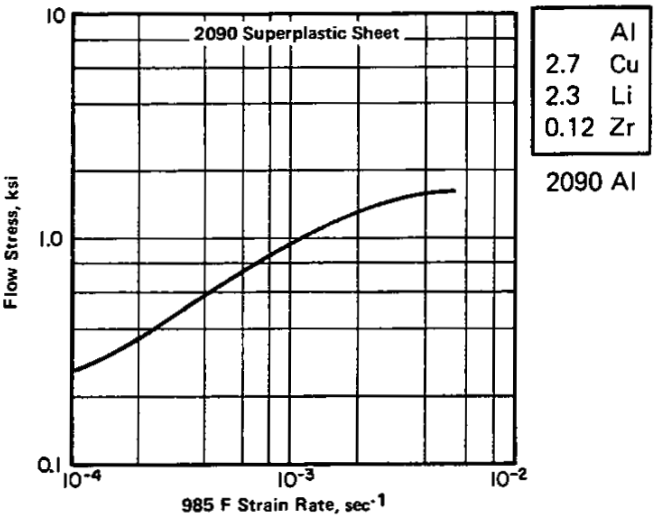


FIGURE 4.011. FLOW STRESS VERSUS STRAIN RATE FOR 2090 SHEET SUPERPLASTICALLY FORMED AT 985 F (46)

Alloy	2090									
Temper	T62[a]		T83							
Form	0.25-in. Sheet		0.25-in. Sheet							
Welding	None	None	Variable Polarity Plasma Arc With EB2319 Filler, Welds Machined Flush							
Post-Weld Treat	None	None	None			T62			30 hr 324 F	
Test Temperature, F	R.T.	-423	R.T.	-320	-423	R.T.	-320	-423	R.T.	-423
F_{tu}, ksi	60	98	40	55	65	60	66	80	47	61
F_{ty}, ksi	49	56	20	29	29	50	55	58	38	38
Elongation, percent	8	22	9	11	10	9	8	8	4	3

(a) 1000 F, WQ + 325 F, 30 hr.

TABLE 4.0312. TENSILE PROPERTIES OF VPPA-WELDED 2090-T83 SHEET AT LOW TEMPERATURES FOR SEVERAL POST-WELD HEAT TREATMENTS (43, FIG. 4–7)

Alloy	2090-T83						
Specimen Machining	Welds Machined Flat					Tested as Welded	
Weld Process[a]	Variable Polarity Plasma Arc				GTA	VPPA	
Thickness, in.	0.12	0.12	0.21	0.32[b]	0.12	0.12	0.21
Postweld Heat Treat.	None	T62	None	None	None	None	None
Failure Location	Weld	HAZ	Weld	Weld	Weld	Weld	Weld
F_{tu}, ksi	35	64	37	36	36	45	42
F_{ty}, ksi	22	48	21	22	23	26	25
Elongation, percent	4.2	10	7	6	4.3	4	4

(a) Filler ER2319, except as noted; all welds vertical.
(b) Horizontal weld.

TABLE 4.0313. TENSILE PROPERTIES OF 2090-T83 SHEET WELDED BY VPPA AND GTA PROCESSES (42, TABLES 2 AND 3)

	Al
2.7	Cu
2.3	Li
0.12	Zr

2090 Al

Alloy	2090		2219	
Temper	T83		T851	
Form	0.25-in. Sheet		0.75-in. Plate	
Weld	None	VPPA[a]	None	VPPA
F_{tu}, ksi	84	42	68	40
F_{ty}, ksi	78	25	55	18
Elongation, percent	6	9	9	18

(a) Variable Polarity Plasma Arc with EB2319 filler.

TABLE 4.0314. COMPARISON OF PARENT METAL AND WELD METAL TENSILE PROPERTIES FOR 2090 SHEET AND 2219 PLATE (43, TABLE 2)

Alloy	2090
Temper	T83
Form	0.125-in. Sheet
Welds	Variable Polarity Plasma Arc With EB2319 Filler
Test Temperature, F	-423
F_{tu}, ksi	60
F_{ty}, ksi	37
Elongation, percent	2.4

TABLE 4.0315. TENSILE PROPERTIES AT CRYOGENIC TEMPERATURE FOR 2090-T83 SHEET WELDS (42, TABLE 5)

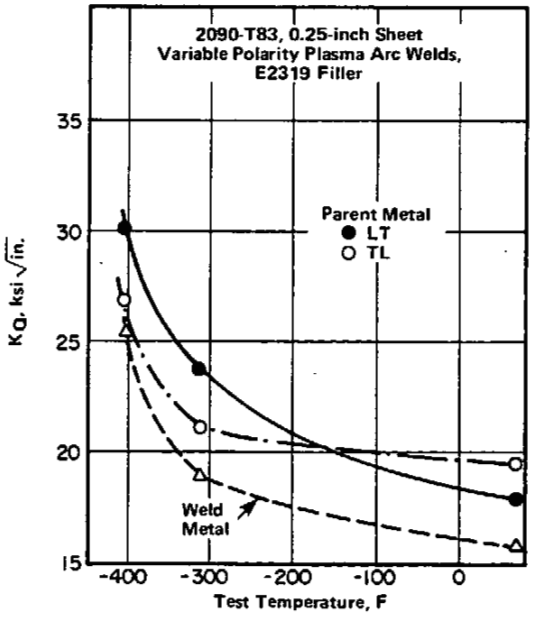


FIGURE 4.0316. FRACTURE TOUGHNESS AS FUNCTION OF LOW TEMPERATURES FOR PARENT METAL AND VPPA WELDS (43, FIGURE 3)

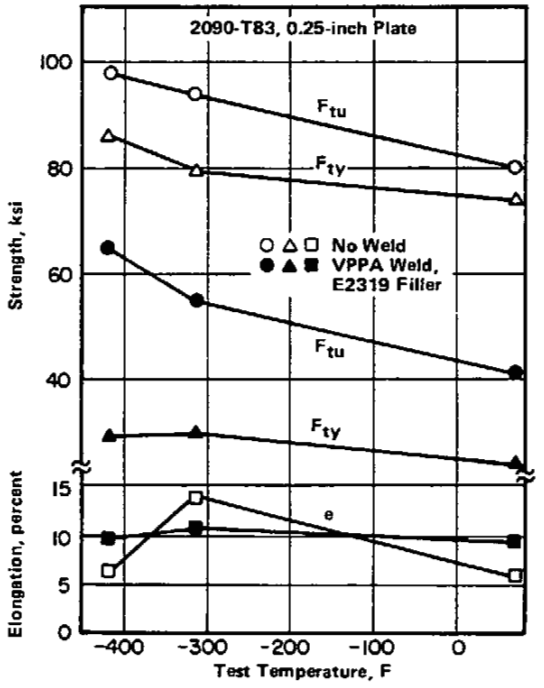


FIGURE 4.0317. TENSILE PROPERTIES OF WELDED AND UNWELDED 2090-T83 PLATE AS A FUNCTION OF TEMPERATURE (43)

Al
4.4 Cu
1.5 Mg
0.6 Mn

2124 Al

1 **GENERAL**

Alloy 2124 is one of a series of premium aluminum alloys which were developed as a result of studies into the micromechanisms of fracture in high strength aluminum compositions (34)(35). It is essentially 2024 with close controls on the content of Fe and Si. These elements were shown to form second phase particles which contributed to void formation at low average matrix strains but did not contribute significantly to the strength. Composition control coupled with special processing minimizes the deleterious influence of these phases by reducing their size and controlling their distribution with a resulting increase in fracture toughness and uniformity of fracture properties particularly in the short transverse direction. These improvements have been accomplished with no loss in other properties. The alloy is normally produced in plate form in the T851 condition in a thickness range up to 6 inch. The T351 condition is also available but no minimum mechanical properties have been published for this temper. It would be expected to have a lower strength than T851 but a higher toughness.

1.01 Commercial Designation

2124 aluminum alloy, 2124-T851.

1.02 Alternate Designations

UNS A92124.

1.03 Specifications

Federal specification: QQ-A-250/29, AMS 4101, and ASTM-B209.

1.04 Composition

Chemical composition, Table 1.04.

1.05 Heat Treatment

See also 2024-T851 plate.

1.051 General. The solution treatment and artificial aging practices applicable to 2124 plate are the same as those specified in MIL-H-6088 F for 2024 plate (4).

1.052 Anneal.

1.0521 Anneal heat treated material to 0 condition, 745 to 770 F, 2 hr, furnace cool 50 F per hour maximum to 500 F, maximum. The rate of subsequent cooling is not critical (4).

1.053 Solution treat.

1.0531 Heat 910 to 930 F, 20 min. to 4-1/2 hr depending on thickness. Quench by total immersion in sufficient cold water so as not to raise water temperature above 100 F (4).

1.0532 Recommended soaking times required for solution treating plate, Table 1.0532.

1.054 Stretch to T351 condition, subsequent to solution treat (4).

1.0541 Plate. Stretch 1-1/2 to 3 percent. No straightening is permitted after stretching.

1.055 Artificial age 2124 in T351 condition to T851 condition.

1.0551 Plate. Heat 365 to 385 F, 12 hr. The time at temperature depends on the time required for the load to reach temperature. Time shown (see Table 1.0532) is based on rapid heating with soaking time measured from the time the load reaches within 10 F of the applicable temperature (4).

1.06 Hardness

See Section 1.092.

1.07 Forms and Conditions Available

1.071 Alloy is available in the form of plate in the T851 or T351 condition up to 6 inch in thickness.

1.08 Melting and Casting Practice

The alloy is not a casting alloy.

1.09 Special Considerations

1.091 Hydrogen embrittlement. The naturally aged tempers T-4 and T-3 and the incompletely aged conditions can be embrittled by severe hydrogen charging conditions. This embrittlement was reported as associated with homogeneous coherent precipitates within the matrix which tend to produce planar slip. The observed effects of hydrogen in this alloy are considerably less than in 7075 (24)(27). While the effects of hydrogen on aluminum alloys are of no direct practical importance they may be related to the stress corrosion mechanism.

1.0911 Effect of hydrogen charging on the tensile ductility of 2124 in several aged conditions, Table 1.0911.

1.092 Slack quenching. To achieve full hardness and strength, very rapid cooling from the solution treated condition is necessary. Plate is normally spray quenched on both top and bottom surfaces as it leaves the solution treating furnace. If the spray quench process is in some way defective, the cooling rate will be insufficient and soft spots will be produced in the plate. These will not normally be detected by samples taken from the plate ends since water run-off adequately cools these regions. The soft areas may show as a dark discoloration after anodizing and will exhibit higher than normal electrical conductivity. The effects of deficiencies in the spray quench system will be most pronounced in the heavier plate gages (> 2 inch thickness). Normally quenched heavy plate exhibits a relatively mild tensile strength, hardness, and electrical conductivity gradient through its thickness (Figure 1.0921) which can be drastically altered by deficient spray quenching (Figure 1.0922).

MIL-H-6088 F (4) provides specifications for qualification of the spray quenching process used for aluminum alloys. Essentially the qualification process is based on sampling the transverse tensile properties from a single run of a 2000 or a 7000 (preferably 7075) alloy of maximum thickness to be run on the line. Tensile samples are required from each end of the plate as well as from the center third of the quenched length. These samples

Al
4.4 Cu
1.5 Mg
0.6 Mn
2124 Al

where possible should be selected to represent both center thickness and near-surface properties. For specific details reference should be made to MIL-H-6088 F.

The following discussion will refer to the top and the bottom of a 5-1/2-inch plate which had deficient spray cooling on its bottom surface which caused specimens taken from sections near the bottom of the plate to be softer than those taken from sections near the top. As might be expected, compression and bearing strength (Tables 1.0923 and 1.0924) values show that the softer portions of the plate have considerably reduced strength properties. Stress corrosion tests on these bottom specimens (75 percent F_{ty} alternate immersion 10 min. in 3.5 percent NaCl + 50 min. in air for 600 hr) indicated no stress corrosion problem was associated with the slack quenching of this plate (29). Precracked LT specimens from the top and bottom of the plate did not fail in 2000 hr when subjected to an initial $K_I = 22$ ksi$\sqrt{\text{in.}}$ (29). Crack growth resistance curves revealed a somewhat higher resistance for the bottom specimens (29) as might be expected from their lower yield strength. Constant amplitude fatigue crack-growth rates (Figure 1.0925) and spectrum-growth rates (Figure 1.0926) appeared to be somewhat higher for the softer specimens.

Fatigue specimens containing a small hole (notched specimens) were cut from various positions in relation to the plate thickness and subjected to either constant amplitude fatigue or to a selected spectrum. The results (Figures 1.0927 and 1.0928) show increasing fatigue strength with increasing hardness and decreasing electrical conductivity. Constant amplitude tests on smooth specimens revealed no definite effect on hardness (29).

Both hardness and electrical conductivity are sensitive to slack quenching (Figures 1.0929 and 1.09210). However, electrical conductivity is also sensitive to changes in composition which may result in different relations between tensile strength and conductivity for different lots of the alloy. While hardness measurements appear to be a more reliable index of tensile strength, it is not possible to explore the surfaces of large plates with standard Rockwell or Brinell testers; miniature units requiring special calibrations must be used. Considering these facts, the U.S. Air Force (ASD) has recommended (29) that an indication of proper quenching requires that all conductivity readings on one side of a plate not vary by more than 2 percent IACS. MIL-H-6088 F specifies 2.5 percent IACS variation. While these specifications provide a reasonable and relatively easy method of quality control, the presently available information is not sufficient to establish whether this variation of conductivity will always represent the same variation in tensile strength from lot to lot of the same nominal alloy composition.

1.0921 Variation of hardness, tensile strength, and electrical conductivity through the thickness of normally quenched 2124-T851 plate, Figure 1.0921.

1.0922 Variation of hardness, tensile strength, and electrical conductivity through the thickness of slack quenched 2124-T851 plate, Figure 1.0922.

1.0923 Hardness, electrical conductivity, and compression strength of specimens taken from a slack quenched 2124-T851 plate, Table 1.0923.

1.0924 Hardness, electrical conductivity, and bearing strength of slack quenched 2124-T851 plate, Table 1.0924.

1.0925 Fatigue crack propagation rate for specimens cut from near the top and near the bottom of a slack quenched 2124-T851 plate, Figure 1.0925.

1.0926 Fatigue crack growth as a function of K_{max} in a fighter spectrum loading for specimens taken from a normal hardness region and a soft region in a 5-1/2-inch slack quenched 2124-T851 plate, Figure 1.0926.

1.0927 Notched fatigue life for specimens cut from 2124-T851 slack quenched plate as a function of hardness and electrical conductivity, Figure 1.0927.

1.0928 Flights to failure under the Falstaff fatigue spectrum as a function of hardness and electrical conductivity for notched specimens cut from slack quenched 2124-T851 plate, Figure 1.0928.

1.0929 Tensile strength properties as a function of hardness for slack quenched and normal quenched 2124-T851 plates, Figure 1.0929.

1.09210 Tensile strength properties as a function of electrical conductivity for slack quenched and normal quenched 2124-T851 5-1/2-inch plates, Figure 1.09210.

1.093 Directionality. The mechanical anisotropy in this and other high-strength aluminum alloys results in stress corrosion resistance which is substantially poorer for stressing in the short transverse direction than in the longitudinal and long transverse directions (e.g., Table 2.0321). An anisotropy of plane strain fracture toughness is also observed with the K_{Ic} values, on the average, being highest for the LT direction, lower for the TL direction, and lowest for the SL direction (e.g., Table 3.02721). Considerable scatter characterizes the fatigue crack-growth data (see Section 3.052) which could define a directionality effect. On balance there appears to be no practical difference between the LT and TL directions. The SL and ST directions appear to have slightly higher growth rates than the LT and TL directions, particularly in a 3.5 percent salt solution. As might be expected the TS and LS exhibit rapidly decreasing rates as the crack deepens (see Figures 3.05219 and 3.052110).

1.094 Effects of reheat treatment. The corrosion resistance of this alloy can be reduced by reheat

Al
4.4 Cu
1.5 Mg
0.6 Mn

2124 Al

treatments which involve solution temperatures and/or aging temperatures below those recommended. If such a reheat treatment has occurred, the alloy should be resolution treated using a longer than average soaking time and a temperature within 5 F of the maximum range. Solution treatment above the maximum may produce eutectic melting and possible blistering. Such overheated material will have inferior properties which may not be recoverable (4).

2 PHYSICAL AND CHEMICAL PROPERTIES

2.01 Thermal Properties

2.011 Melting range, 935 to 1180 F (approximately), based on typical composition (3).

2.012 Phase changes. Alloy is subject to precipitation hardening below 775 F.

2.0121 Time-temperature-transformation diagrams.

2.013 Thermal conductivity:
87.5 Btu ft per (hr ft^2 F) at 77 F (3)
87.12 Btu ft per (hr ft^2 F) at 100 F (1)
91.9 Btu ft per (hr ft^2 F) at 300 F (1).

2.014 Thermal expansion, Figure 2.014.

2.015 Specific heat, Figure 2.015.

2.016 Thermal diffusivity.

2.02 Other Physical Properties

2.021 Density:
0.100 lb per $in.^3$, 2.77 gr per cm^3 at 68 F
0.099 lb per $in.^3$, 2.74 gr per cm^3 at 300 F
0.098 lb per $in.^3$, 2.72 gr per cm^3 at 500 F
0.097 lb per $in.^3$, 2.70 gr per cm^3 at 700 F.

2.022 Electrical properties.

2.0221 Electrical conductivity, T851 condition typically 39.3 percent IACS (see also Section 1.092) (7).

2.023 Magnetic properties, alloy is nonmagnetic.

2.024 Emissivity.

2.025 Damping capacity.

2.03 Chemical Environments

2.031 General corrosion. The resistance to atmospheric corrosion including exfoliation is essentially equal to that of 2024 in comparable tempers. Tests conducted in the seacoast atmosphere at Point Judith, Rhode Island, have not produced exfoliation in a period of 8 years (1).

2.032 Stress corrosion. Resistance to stress corrosion has been determined using alternate immersion in 3.5 percent NaCl and by slow strain rate testing. A statistical summary of the results of SCC tests by alternate immersion in 3.5 percent NaCl (Table 2.0321) shows that the threshold for the L and LT direction of 2124-T851 plate is $\geq 0.75\ F_{ty}$ and for the ST direction is $\geq 0.50\ F_{ty}$. The results for both bend and tension tests of 2124-T851 plate subject to alternate immersion in 3.5 percent NaCl (Table 2.0322) are in agreement with these threshold values. The SCC resistance determined by alternate immersion (Figure 2.0323) or by seacoast exposure (Table 2.0324) shows the SCC resistance in the ST direction decreases with decreasing plate thickness. Similar effects of thickness are also observed in slow strain rate tests in 3.5 percent NaCl (Figure 2.0325). Both alternate immersion tests (23) and slow strain rate tests (Figures 2.0326 and 2.0327) show that the underaged conditions are considerably more susceptible to SCC in chloride solutions than the fully aged temper.

2.0321 Smooth bar stress corrosion thresholds for 2124-T851 plate by alternate immersion in 3.5 percent NaCl solution (ASTM G-47), Table 2.0321.

2.0322 Results of alternate immersion tests in 3.5 percent NaCl on 2124-T851 plate stressed in bending or tension at various percentages of the yield strength, Table 2.0322.

2.0323 Effect of exposure of plate of various thicknesses to 3.5 percent NaCl solution, Figure 2.0323.

2.0324 Results of exposure to seacoast atmosphere on 2124-T851 specimens from three lots with different thicknesses, Table 2.0324.

2.0325 Effect of strain rate on tensile properties in air and in 3.5 percent NaCl for two thickness 2124-T851 plates from different lots, Figure 2.0325.

2.0326 Effect of age time on several measures of relative performance for 2124-T351 plate tested at a slow strain rate in corrosion cell containing oxygen saturated 1M $AlCl_3$ pH-2, Figure 2.0326.

2.0327 Effect of strain rate on the reduction in tensile strength of 2124-T851 and 2124-T351 plate tested in corrosion cell containing oxygen saturated 3.5 percent NaCl or 1M $AlCl_3$, Figure 2.0327.

2.033 K_{Iscc} testing. Various specimen types have been used to investigate the resistance to crack growth in fatigue precracked specimens subjected to a steady load in 3.5 percent NaCl solution. Tests on a 2-inch plate using bolt loaded specimens and compact tension specimens (Table 2.0331) did not reveal any crack growth in LT, TL, SL, and ST specimens after 30 days alternate immersion in 3.5 percent NaCl. Various K_{Ii}/K_{Ic} levels were used. The highest were as follows: LT and TL 0.9, SL 0.87, and ST 0.82. However, the same investigator employing the same alternate immersion conditions reported crack growth in SL surface flawed specimens for $K_{Ii}/K_{Ic} = 0.65$ but no crack growth in center cracked specimens for $K_{Ii}/K_{Ic} = 0.95$ (Table 2.0332). This discrepancy may be associated with the presence of bending in these very short (2 inch) SL specimens. A K_{Iscc} of about 14 ksi$\sqrt{in.}$ was reported for alternate immersion in 3.5 percent NaCl for SL specimens from 1-inch plate (Figure 2.0333). A K_{Iscc} value of about 23 ksi$\sqrt{in.}$ in the SL direction and about 27 ksi$\sqrt{in.}$ in the LT direction was reported for a 3-inch plate tested in fuel tank sump water (Table 2.0334).

Sustained load (0.6 K_{Ic}) tests in air at 300 F using C(T) specimens from a 2-inch 2124-T851

Al
4.4 Cu
1.5 Mg
0.6 Mn

2124 Al

plate showed completely intergranular fracture. Cracks develop initially at large second phase particles ($CuMgAl_2$) at or near grain boundaries which then crack at triple points. Voids form from the cracked particles and the accompanying slip in the matrix imposes shear stresses on the boundaries which slide resulting in a linking of small voids leading to boundary separation. (11).

2.0331. Results of alternate immersion tests in 3.5 percent NaCl on 2124-T851 plate using compact specimens loaded to various K_{1i}/K_{Ic} levels, Table 2.0331.

2.0332 Results of alternate immersion tests in 3.5 percent NaCl on 2124-T851 plate tested using surface flawed and center cracked specimens representing several crack orientations, Table 2.0332.

2.0333 Crack propagation rate as a function of applied stress intensity for 2124-T851 plate subjected to alternate immersion in 3.5 percent NaCl solution, Figure 2.0333.

2.0334 Stress corrosion crack growth stress intensity threshold of plate from the B-1 program tested in fuel tank sump water, Table 2.0334.

2.0335 Composition of fuel tank sump residue water used in certain stress corrosion and fatigue crack propagation tests in the B-1 program, Table 2.0335.

2.034 Fatigue crack growth. Limited test data indicate the fatigue crack-growth rates at 5.2 Hz are essentially the same in dry air, humid air, and salt fog (see Figure 3.05212). The lack of humidity effect is supported by results from two investigations which did not test the same plate thickness (compare Figures 3.0526 and 3.0527). Tests in low humidity air (10 percent R.H.) show higher growth rates for a cycle frequency of 1 Hz than one of 6 Hz (see Figure 3.0524) and suggest that humidity effects might be observed at very slow cycle frequencies. However, these results are in contrast with data which show the same growth rates for tests at 1 Hz in fuel tank sump water as observed at 6 Hz in low humidity air (see Figure 3.05211). The available data (see Figures 3.05217 to 3.052112) show a consistently higher growth rate in 3.5 percent NaCl solution than in laboratory air at a cycle rate of 5 Hz.

3 MECHANICAL PROPERTIES

3.01 Specified Mechanical Properties

3.011 Aluminum Association mechanical properties for plate, Table 3.011.

3.012 Design mechanical properties for 2124-T851 plate, Table 3.012.

3.013 AMS specified tensile properties for 2124-T851 plate, Table 3.013.

3.014 Specified plane strain fracture toughness minima and corresponding acceptance criteria based on a sharp notch to tensile strength ratio, Table 3.014.

3.015 AMS specified plane strain fracture toughness for 2124-T851 plate, Table 3.015.

3.02 Mechanical Properties at Room Temperature

3.021 Tension – stress/strain diagrams – tension properties.

3.0211 Typical tensile stress-strain curves for 4-inch thick plate, Figure 3.0211.

3.0212 Typical tensile properties of 2124-T851 plate, Table 3.0212.

3.0213 Tensile properties as a function of distance from surface of 2124-T851 condition thick plates, Figure 3.0213.

3.0214 Typical tensile properties of 2-inch and 3-inch thick 2124-T851 plate from the B-1 program, Table 3.0214.

3.0215 Effect of 1000 hr exposure at elevated temperatures on retained room temperature tensile properties of 2124-T851 plate, Figure 3.0215.

3.022 Compression.

3.0221 Typical compression stress-strain curves for 4-inch thick 2124-T851 plate, Figure 3.0221.

3.0222 Typical compression, shear, and bearing properties of 2124-T851 plate, Table 3.0222.

3.023 Impact.

3.024 Bending.

3.025 Torsion and shear (see Tables 3.012 and 3.0222).

3.026 Bearing (see Tables 3.012 and 3.0222).

3.027 Stress concentration.

3.0271 Notch properties.

3.0272 Fracture toughness.

3.02721 Plane strain fracture toughness results for LT, TL, and SL orientations of plate obtained from many tests made by two producers, Table 3.02721.

3.02722 Plane strain fracture toughness of a 2-inch and 3-inch plate from the B-1 program, Table 3.02722.

3.02723 Scatterbands for relation between sharp-notch strength to yield strength ratio and plane strain fracture toughness determined using two notch specimen diameters for 2124-T851 plate having thicknesses from 1.57 to 6 inch and tested in the LT, TL, and SL orientations with specimens located at plate center and mid thickness, Figure 3.02723.

3.028 Combined properties.

3.03 Mechanical Properties at Various Temperatures

3.031 Tension – stress/strain diagrams – tension properties.

3.0312 Effect of test temperature and exposure time on tensile properties of 2124-T851 plate, Figure 3.0312.

3.0313 Effect of temperature and testing direction on tensile properties of 2124-T851 plate, Figure 3.0313.

3.0314 Effect of temperature on tensile properties of 2124-T851 plate, Figure 3.0314.

3.033 Impact.

3.034 Bending.

3.035 Torsion and shear.

3.036 Bearing.

3.037 Stress concentration.

3.0371 Notch properties.

3.0372 Fracture toughness.

3.03721 Plane strain fracture toughness of plate at room temperature and 250 F, Table 3.03721.

3.03722 Effect of temperature on plane strain fracture toughness of two lots of 2124-T851 plate, Figure 3.03722.

3.04 Creep and Creep-Rupture Properties

3.041 Creep and creep-rupture curves at temperatures from 75 to 600 F for 2124-T851 plate, Figure 3.041.

3.05 Fatigue

3.051 Smooth and notch fatigue.

3.0511 Cycles to crack initiation as a function of nominal maximum fatigue stress for specimens with carefully polished notches, Figure 3.0511.

3.0512 Axial load fatigue curves for longitudinal smooth and notched (K_t = 3) specimens from 2124-T851 plate, Figure 3.0512.

3.0513 Axial load fatigue curves for transverse smooth and notched (K_t = 3) specimens from 2124-T851 plate, Figure 3.0513.

3.0514 Axial load fatigue curve for notched (K_t = 5) specimens from 4- to 6-inch 2124-T851 plate, Figure 3.0514.

3.0515 Rotating bending fatigue curves for smooth specimens from 4-inch 2124-T851 plate, Figure 3.0515.

3.0516 Rotating bending fatigue curves for sharply notched specimens from 2124-T851 4-inch plate, Figure 3.0516.

3.0517 Effect of salt fog on axial load fatigue life of smooth and notched (K_t = 3) specimens from 2124-T851 plate, Figure 3.0517.

3.052 Fatigue crack-growth rates. Fatigue crack-growth rate data are available which illustrate the effects of directionality, cycle frequency, corrosive environments, test temperature, and R ratio. The effects of directionality are discussed in Section 1.093 and cycle frequency effects and corrosive environments are discussed in Section 2.034. As might be expected, the fatigue crack-growth rates increase with increasing testing temperature (see Figures 3.05214 to 3.05216). The effect of R ratio is also as expected, with growth rates increasing particularly at the higher ΔK values as R increases (see Figures 3.0527 to 3.0529). Threshold (ΔK_{th}) values as a function of R ratio for 2124-T851 plate in 95 percent RH air at 30 to 35 Hz (Table 3.052113) show the expected trend of reduced ΔK_{th} with increasing R ratio. The threshold value for T-4 sheet appears to be increased substantially for tests at -320 F (Figure 3.05213) as compared with the estimates from room temperature tests (Figure 3.0522).

3.0521 Typical fatigue crack-growth data for 2-inch plate in various environments, Figure 3.0521.

3.0522 Fatigue crack-growth rates for 2124 sheet in T4 condition, Figure 3.0522.

3.0523 Fatigue crack-growth rates for 2124-T851 plate from the B-1 program at several R ratios in low humidity air, Figure 3.0523.

3.0524 Fatigue crack-growth rates for 2124-T851 plate from the B-1 program for two loading frequencies in low humidity air, Figure 3.0524.

3.0525 Fatigue crack-growth rates at R = 0.33 for 4.5-inch plate, Figure 3.0525.

3.0526 Fatigue crack-growth rates at low ΔK values for 2124-T851 plate tested at two R ratios and thicknesses of 0.375, 0.75, and 1.5 inch, Figure 3.0526.

3.0527 Fatigue crack-growth rates for 2124-T851 plate tested in high humidity air at R = 0.1, Figure 3.0527.

3.0528 Fatigue crack-growth rates for 2124-T851 plate tested in high humidity air at R = 0.25, Figure 3.0528.

3.0529 Fatigue crack-growth rates for 2124-T851 plate tested in high humidity air at R = 0.5, Figure 3.0529.

3.05210 Fatigue crack-growth rates for two thicknesses of plate tested in high humidity air, Figure 3.05210.

3.05211 Fatigue crack-growth rates for 2124-T851 plate from the B-1 program tested in low humidity air and in sump water, Figure 3.05211.

3.05212 Typical fatigue crack-growth rates for 2-inch 2124-T851 plate in various environments, Figure 3.05212.

3.05213 Fatigue crack-growth rates approaching zero for 2124 sheet in the T4 condition at -320 F, Figure 3.05213.

3.05214 Fatigue crack-growth rates for plate tested in the LT direction at cryogenic and elevated temperature, Figure 3.05214.

3.05215 Fatigue crack-growth rates for 2124-T851 plate at room and elevated temperatures, Figure 3.05215.

3.05216 Fatigue crack-growth rates for 2124-T851 plate at low temperatures, Figure 3.05216.

3.05217 Fatigue crack-growth rates for 2124-T851 plate in air and 3.5 percent NaCl for LT direction, Figure 3.05217.

3.05218 Fatigue crack-growth rates for 2124-T851 plate in air and in 3.5 percent NaCl for TL direction, Figure 3.05218.

3.05219 Fatigue crack-growth rates for 2124-T851 plate in air and in 3.5 percent NaCl for TS direction, Figure 3.05219.

3.052110 Fatigue crack-growth rates for 2124-T851 plate in air and in 3.5 percent NaCl for LS direction, Figure 3.052110.

3.052111 Fatigue crack-growth rates for 2124-T851 plate in air and in 3.5 percent NaCl for ST direction, Figure 3.052111.

3.052112 Fatigue crack-growth rates for 2124-T851 plate in air and in 3.5 percent NaCl for SL direction, Figure 3.052112.

3.052113 Fatigue crack growth threshold for 2124-T851 plate in high humidity air at several R ratios, Table 3.052113.

3.06 Elastic Properties

3.061 Poisson's ratio, 0.33 at room temperature.

3.062 Modulus of elasticity.

3.0621 Modulus of elasticity at low and elevated temperatures, Figure 3.0621.

3.0622 Tensile and compressive modulus of elasticity, Table 3.0622.

3.063 Modulus of rigidity.

3.064 Tangent modulus.

3.0641 Tangent modulus curves for 2124-T851 plate, Figure 3.0641.

Al
4.4 Cu
1.5 Mg
0.6 Mn

2124 Al

Al
4.4 Cu
1.5 Mg
0.6 Mn

2124 Al

4 **FABRICATION**

4.01 Forming
(See also 2024.)

4.011 Forming of plate is preferably accomplished in the 0 condition with subsequent heat treatment (8).

4.02 Machining and Grinding
(See also 2024.)

4.021 General. The alloy is considered to have good machinability in the 0 condition and good to excellent machinability in the T851 condition.

4.03 Joining
(See 2024.)

4.04 Surface Treatment
(See also 2024.)

REFERENCES

1 Hart, R. M., "Aluminum Alloy 2124 Plate", Aluminum Company of America, Alcoa Technical Center (April 1, 1982).

2 Alcoa Alloy 2124-T851 Plate and 2024-T851 Forgings, Aerospace Technical Information Bulletin, Alcoa (not dated), deleted from this revision.

3 Aluminum Standards and Data, 1974-1975, 4th edition and 7th edition, Aluminum Association, N.Y. (1982).

4 Military Specification, Heat Treatment of Aluminum Alloys, MIL-H-6088 F (July 21, 1981).

5 Federal Specification, Aluminum Alloy 2124 Plate, QQ-A 250/29.

6 Babilon, C. F., Wygonik, R. H., Nordmark, G. E., and Lifka, B. W., "Mechanical Properties, Fracture Toughness, Fatigue, Environmental Fatigue Crack Growth Rates and Corrosion Characteristics of High Toughness Aluminum Alloy Forgings, Sheet and Plate", Aluminum Company of America, AFML-TR-73-83 (March 1973).

7 Thompson, D. S., Levy, S. A., Spangler, G.E., and Benson, D. K., "Program to Improve the Fracture Toughness and Fatigue Resistance of Aluminum Sheet and Plate for Aircraft Applications", Reynolds Metals Co., AFML-TR-73-247, Vol. I (September 1973).

8 "Aluminum, Vol. III Fabrication and Finishing", Edited by K. R. Van Horn, American Society for Metals (1967).

9 Fudge, K. A. and Jones, R. E., "Engineering Design Data for Aluminum Alloy 2124-T851 Thick Plate", University of Dayton Research Institute, AFML-TR-73-310 (January 1974).

10 Pionke, L. J. and Linback, R. K., "Fracture Mechanics Data for 2024-T851 Aluminum", McDonnell Douglas Astronautics Co., NASA-CR-141695 (October 25, 1974).

11 Kaufman, J. G. and Low, J. R. Jr., "The Micromechanism of Sustained Load Crack Growth in Al-Cu Alloys 2124 and 2219 at 300 F", 2nd International Conference on Mechanical Behavior (Special Volume) ASM (1978).

12 Cervay, R. R., "Temperature Effect on the Mechanical Properties of Aluminum Alloy 2124-T851", University of Dayton Research Institute, AFML-TR-75-208 (1975).

13 Ruschaw, J. J., "Complete Fatigue Crack Growth Rate Curves for Aluminum Alloy 2124-T851 Including Typical Crack Growth Models", University of Dayton Research Institute, TR-78-155 (1978).

14 Humphries, T. S. and Nelson, E. E., "Seacoast Stress Corrosion Cracking of Aluminum Alloys", NASA TM 82393 (January 1981).

15 Kaufman, J. G., Sha, G. T., Kohm, R. F., and Bucci, R. J., "Notch Yield Ratio as a Quality Control Index for Plane Strain Fracture Toughness", Cracks and Fracture ASTM STP 601, ASTM (1976) p 169.

16 Schwartzenberg, F. R. and Schepic, J. A., "Environmental Effects on Aluminum Fracture", Martin Marietta Corp., NASA CR 135182 (August 1976).

17 Kung, C. Y. and Fine, M. E. "Fatigue Crack Initiation and Microcrack Growth in 2024-T4 and 2124-T4 Aluminum Alloys", Metallurgical Transactions A, Vol. 10A (May 1979) p 603.

18 Vgianski, G. M., Johnson, C. E., Thompson, O. S., and Gillespie, E. H., "Slow Strain Rate Stress Corrosion Testing of Aluminum Alloys", Stress Corrosion Cracking – The Slow Strain Rate Technique, ASTM STP 665, ASTM (1979) p 254.

19 Fine, M. E., "Relation of Microstructure to Fatigue Crack Properties in Aluminum Base Alloys", Department of Materials Science and Engineering, Northwestern University, AFOSR-TR-78-1518 (November 30, 1978).

20 Bucci, R. J., "Selecting Aluminum Alloys to Resist Failure by Fracture Mechanisms", Engineering Fracture Mechanics, Vol. 12, p 407.

21 Harmsworth, C. L. and Petrak, G. J., "An Investigation of Improperly Quenched (Soft) Aluminum Plate", AFML-TR-79-2405 (1979).

22 Speidel, M. O., "Design Against Environment Fracture", Mechanical Behavior of Materials, Proceedings of the 3rd International Conference, Cambridge, England, Vol. 1, Pergamon Press (August 1979) p 109.

23 Maitra, Shantanu, "Determination of Stress Corrosion Cracking Resistance of Al-Cu-Mg Alloys by Slow Strain Rate and Alternate Immersion Testing, Corrosion, Vol. 37 (February 1981) p 98.

24 Hardwick, D. A., Taheri, M., Thompson, A. W., and Bernstein, I. M., "Hydrogen Embrittlement in a 2000 Series Aluminum Alloy", Metallurgical Transactions A, Vol. 13A (February 1982) p 235 (see reference 27 also).

25 Ferguson, R. R. and Berryman, R. C., "Fracture Mechanics Evaluation of B-1 Materials – Vol. II", Rockwell International B-1 Division, AFML-TR-76-137 (1976).

26 Ferguson, R. R. and Berryman, R. C., "Fracture Mechanics Evaluation of B-1 Materials – Vol. I", Rockwell International B-1 Division, AFML-TR-76-137 (1976).

27 Thompson, A. W. and Bernstein, I. M., "The Role of Hydrogen in Stress Corrosion Cracking of High Strength Aluminum Alloys", Carnegie-Mellon University, AFOSR-TR-81-0403 (December 1980) (see reference 24 also).

28 Kaufman, J. G. and Collis, S. F., "A Fracture Toughness Data Bank", Journal of Testing and Evaluation, Vol. 9 (March 1981) p 121.

29 Petrak, G. J. and Gunderson, A. W., "Complication of Mechanical Property Data for Improperly Quenched (Soft) Aluminum Plate", AFML-TR-81-4023 (1981).

30 Petrak, G. J. and Ruschaw, J. J., "Fatigue and Fatigue Crack Growth Characteristics of Improperly Quenched (Substrength) Aluminum", Engineering Fracture Mechanics, Vol. 15, No. 2 (1981) p 143.

31 McKittrick, J., Liaw, P. K., Kwun, S. I., and Fine, M. E., "Threshold for Fatigue Microcrack Propagation in Some Aluminum Alloys", Metallurgical Transactions A, Vol. 12A (August 1981) p 1535.

32 Ruff, Paul E. and Smith, S. H., "Development of MIL-HDBK Design Allowable Properties and Fatigue Crack Propagation Data for Several Aerospace Materials", Battelle Columbus Laboratories, AFML-TR-77-162 (1977).

33 SAE-AMS Specification, AMS 4101 (July 15, 1978).

34 Tanaka, J. P., Pampillo, C. A., and Low, J. R. Jr., "Fractographic Analysis of Low Energy Fracture of an Aluminum Alloy", Review of Developments in Plane Strain Fracture Toughness Testing, Edited by W. F. Brown, Jr., ASTM STP 463 (1970) p 191.

35 Low, J. R. Jr., VanStone, R. H., and Merchant, R. H., "An Investigation of Plastic Fracture in Aluminum Alloys", NASA Research Grant NGR 39-087-003 (May 1972) ASTM STP 556 (1974) p 93.

Alloy	2124	
	Percent	
Composition	Min	Max
Cu	3.8	4.9
Mg	1.2	1.8
Mn	–	0.9
Fe	–	0.25
Zn	–	0.20
Si	–	0.20
Zr+Ti	–	0.20(a)
Ti	–	0.15
Cr	–	0.10
Other		
Each	–	0.05
Total	–	0.15
Al	Balance	

(a) AMS only.

TABLE 1.04. CHEMICAL COMPOSITION (1,3,5,33)

Al
4.4 Cu
1.5 Mg
0.6 Mn

2124 Al

Alloy	2124	
	Minimum Soaking Time, min	
Thickness, inch	Salt Bath	Air Furnace
0.251 to 0.500	45	60
0.501 to 1.000	60	90
1.001 to 1.500	90	120
1.501 to 2.000	105	150
2.001 to 2.500	120	180
2.501 to 3.000	150	210
3.001 to 3.500	165	240
3.501 to 4.000	180	270
4.001 to 4.500	195	300

TABLE 1.0532. RECOMMENDED SOAKING TIMES REQUIRED FOR SOLUTION TREATING PLATE (4)

Alloy	2124		
Form	0.21-inch diam x 1-inch Gage Length Plate		
Condition	914 F, 20 min, WQ + Age + Hydrogen Charge(a)		
		Mean, RA percent	
Age	F_{ty}, ksi(b)	No H_2	H_2
T3 (2% Strain + RT, 50 hr)	39	33	27
T4 (RT, 50 hr)	47	29	22
T8 (2% Strain + RT, 9 hr)	51	30	25
T3 + 374 F, 3 hr	50	30	30
UT (374 F, 4 hr)	32	24	18
σT (374 F, 24 hr)	46	31	31
T6 (374 F, 9 hr)	51	25	25

(a) Charging conditions: cathodically charged in pH = 1 HCl solution under potentiostatic control at -1500 mv vs standard calomel electrode while being plastically strained at about 1×10^{-6} per second.
(b) No H_2.

TABLE 1.0911. EFFECT OF HYDROGEN CHARGING ON TENSILE DUCTILITY OF 2124 IN SEVERAL AGED CONDITIONS (24)

Al
4.4 Cu
1.5 Mg
0.6 Mn
2124 Al

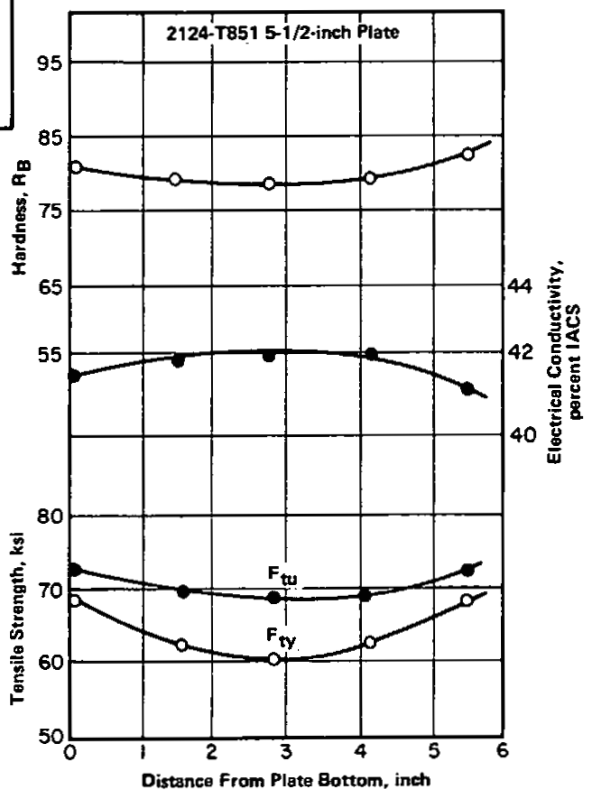


FIGURE 1.0921. VARIATION OF HARDNESS, TENSILE STRENGTH, AND ELECTRICAL CONDUCTIVITY THROUGH THE THICKNESS OF NORMALLY QUENCHED 2124-T851 PLATE (21)

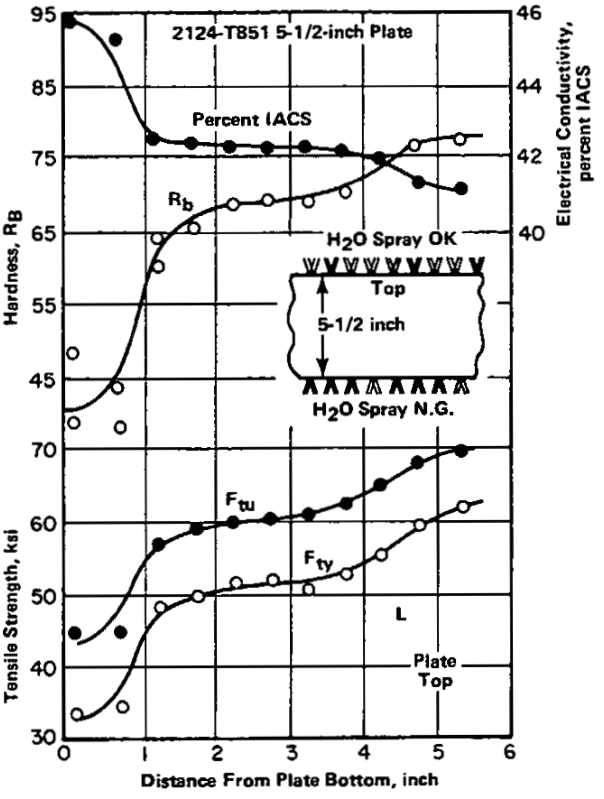


FIGURE 1.0922. VARIATION OF HARDNESS, TENSILE STRENGTH, AND ELECTRICAL CONDUCTIVITY THROUGH THE THICKNESS OF SLACK QUENCHED 2124-T851 PLATE (21)

Alloy	2124-T851	
Form	5-1/2-inch Plate	
Condition	Slack Quenched	
Specimen Location	Near Plate Top	Near Plate Bottom
Hardness, R_B	80.3	50.9
Electrical Conductivity, percent IACS	40.6	45
Compressive Yield Strength (F_{cy}), ksi	62.4	27.6

TABLE 1.0923. HARDNESS, ELECTRICAL CONDUCTIVITY, AND COMPRESSION STRENGTH OF SPECIMENS TAKEN FROM A SLACK QUENCHED 2124-T851 PLATE (29)

Alloy	2124-T851	
Form	5-1/2-inch Plate	
Condition	Slack Quenched	
Specimen Location	Near Plate Top	Near Plate Bottom
Hardness, R_B	77	56.8
Electrical Conductivity, percent IACS	40.7	43.9
Bearing Yield Strength (F_{bry}), ksi	98.4	68.3
Bearing Ultimate Strength (F_{bru}), ksi	130.7	101.0

TABLE 1.0924. HARDNESS, ELECTRICAL CONDUCTIVITY, AND BEARING STRENGTH OF SLACK QUENCHED 2124-T851 PLATE (29)

Al
4.4 Cu
1.5 Mg
0.6 Mn

2124 Al

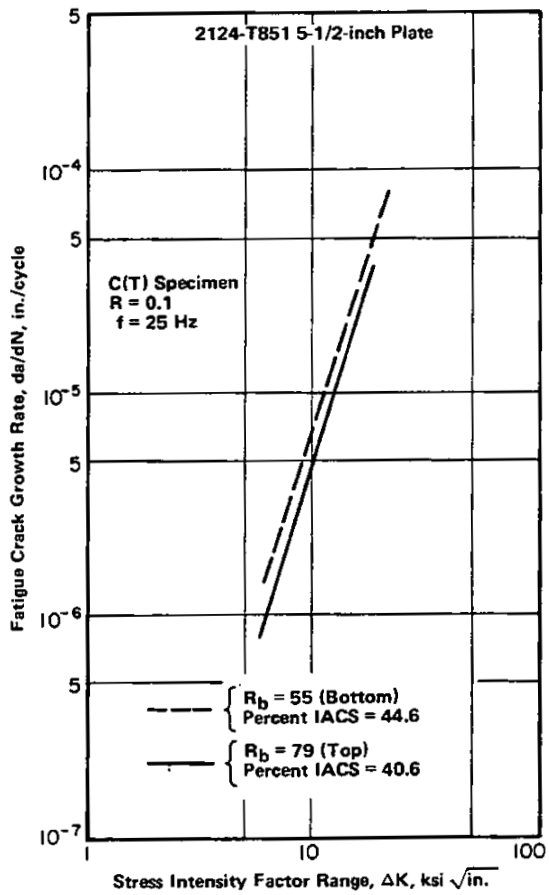


FIGURE 1.0925. FATIGUE CRACK PROPAGATION RATE FOR SPECIMENS CUT FROM NEAR THE TOP AND NEAR THE BOTTOM OF A SLACK QUENCHED 2124-T851 PLATE (21)

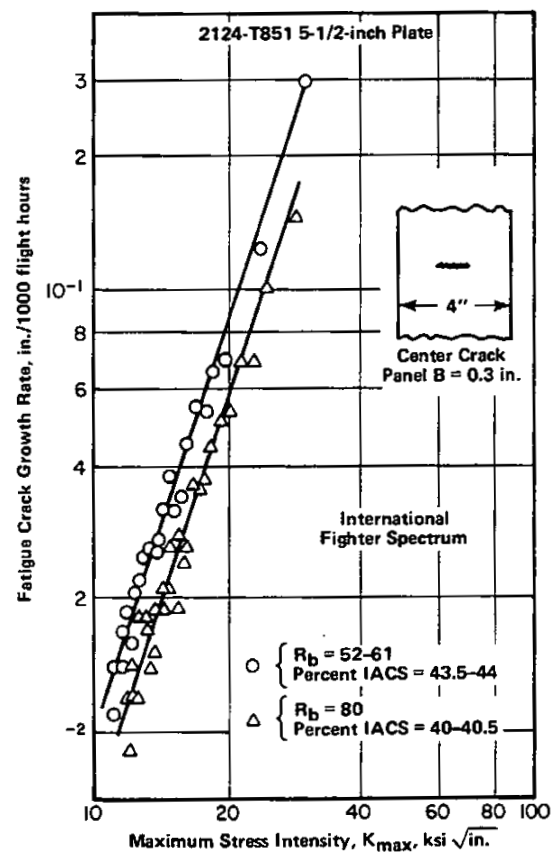


FIGURE 1.0926. FATIGUE CRACK GROWTH AS FUNCTION OF K_{MAX} IN A FIGHTER SPECTRUM LOADING FOR SPECIMENS TAKEN FROM A NORMAL HARDNESS REGION AND A SOFT REGION IN A 5-1/2-INCH SLACK QUENCHED 2124-T851 PLATE (29, 30)

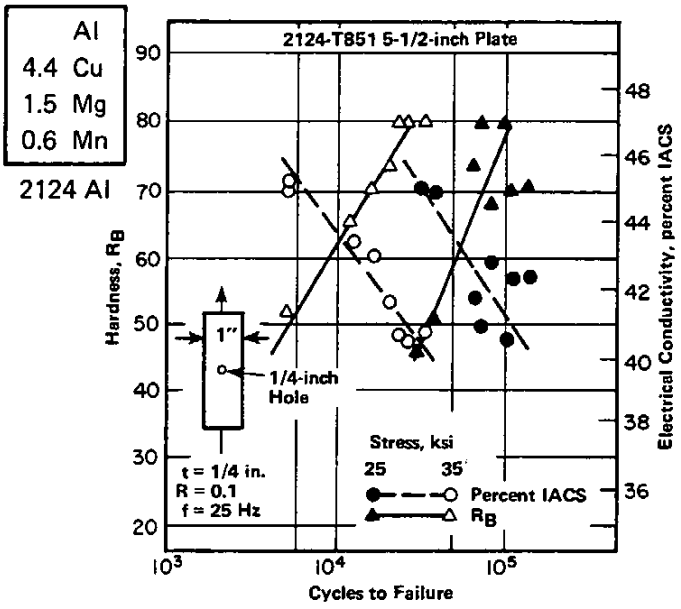


FIGURE 1.0927. NOTCHED FATIGUE LIFE FOR SPECIMENS CUT FROM 2124-T851 SLACK QUENCHED PLATE AS A FUNCTION OF HARDNESS AND ELECTRICAL CONDUCTIVITY (21)

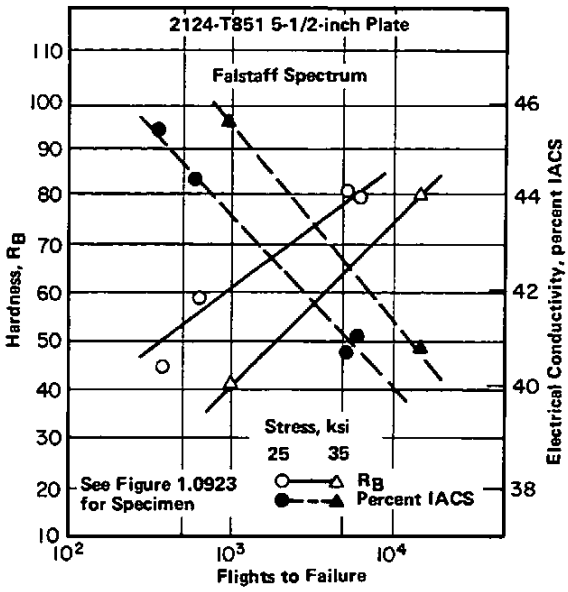


FIGURE 1.0928. FLIGHTS TO FAILURE UNDER THE FALSTAFF FATIGUE SPECTRUM AS A FUNCTION OF HARDNESS AND ELECTRICAL CONDUCTIVITY FOR NOTCHED SPECIMENS CUT FROM SLACK QUENCHED 2124-T851 PLATE (30)

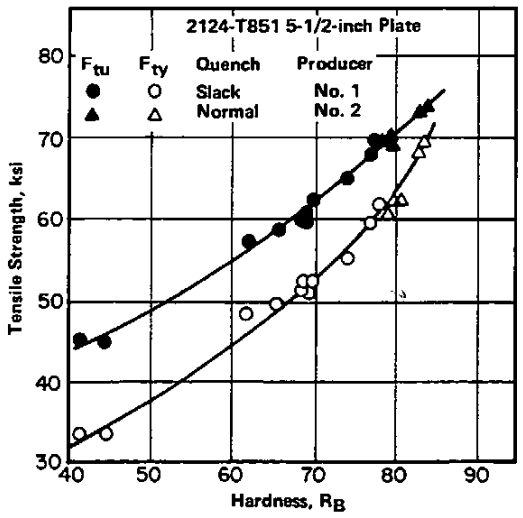


FIGURE 1.0929. TENSILE STRENGTH PROPERTIES AS A FUNCTION OF HARDNESS FOR SLACK QUENCHED AND NORMAL QUENCHED 2124-T851 PLATES (29)

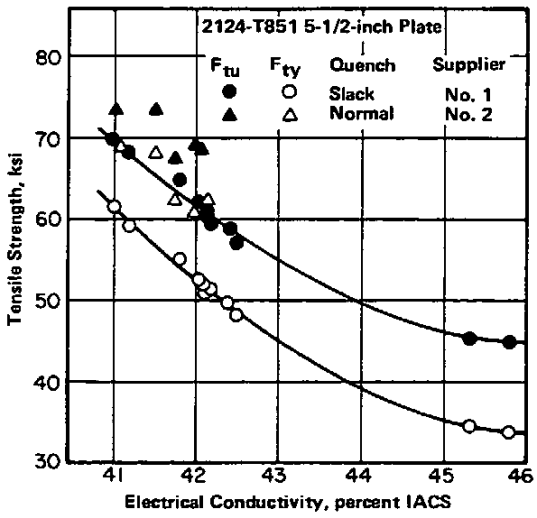


FIGURE 1.09210. TENSILE STRENGTH PROPERTIES AS A FUNCTION OF ELECTRICAL CONDUCTIVITY FOR SLACK QUENCHED AND NORMAL QUENCHED 2124-T851 5-1/2-INCH PLATES (29)

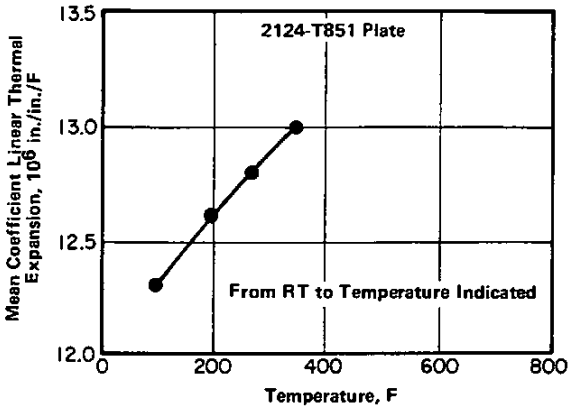


FIGURE 2.014. THERMAL EXPANSION (1)

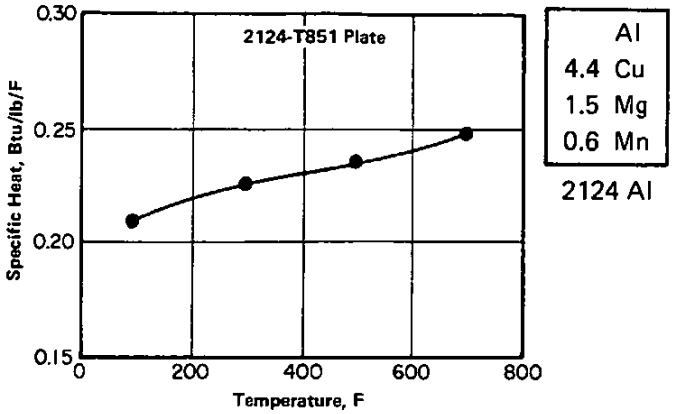


FIGURE 2.015. SPECIFIC HEAT (1)

Alloy	2124-T851		
Form	Rolled Plate		
Direction	L	LT	ST
Threshold(a)	≥0.75 F_{ty}	≥0.75 F_{ty}	≤0.50 F_{ty}

(a) Thresholds established by tests on a minimum of 10 random lots with results representing 90 percent probability with 95 percent confidence.

TABLE 2.0321. SMOOTH BAR STRESS CORROSION THRESHOLDS FOR 2124-T851 PLATE BY ALTERNATE IMMERSION IN 3.5 PERCENT NaCl SOLUTION (ASTM G-47) (20)

Alloy	2124-T851					
Form	2-inch Plate					
Direction and Specimen Type(f)	L and T(a) Bend(c)	ST(b) Bend(c)	ST Bend	ST Bend	ST Tension(d)	ST Tension
Environment	3.5 percent NaCl 50 min in Solution + 10 min in Air					
Fty, percent	46 to 92	49	66	82 to 98	35 to 65	70 to 78
Time, days	30	30	30	10 to 30	30	9
Result(e)	SP, GC No SCC	SP, GC No SCC	SP, GC IGC 0.020 inch	SP, GC IGC ~1/16 inch	SP, GC No SCC	Failure

(a) F_{tu} = 72 ksi (L & T), F_{ty} = 66 ksi (L & T), RA = 20 percent (L), RA = 16 percent T.
(b) F_{tu} = 67 ksi (ST), F_{ty} = 61 ksi (ST), RA = 1.0 percent (ST).
(c) L and T bends: L = 5 inch, W = 3/4 inch, t = 1/8 inch and ST beam: L = 2 inch, W = 3/8 inch, t = 1/16 inch.
(d) ST tensiles gage section: L = 1/2 inch, W = 3/4 inch, t = 1/8 inch.
(e) SP = surface pits: GC = general corrosion; and IGC = intergranular cracks (SCC).
(f) Bend specimens were four point loaded and tension specimens were pin loaded.

TABLE 2.0322. RESULTS OF ALTERNATE IMMERSION TESTS IN 3.5 PERCENT NaCl ON 2124-T851 PLATE STRESSED IN BENDING OR TENSION AT VARIOUS PERCENTAGES OF THE YIELD STRENGTH (16)

Al
4.4 Cu
1.5 Mg
0.6 Mn

2124 Al

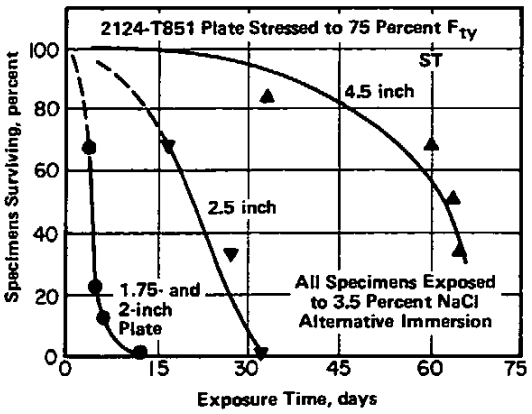


FIGURE 2.0323. EFFECT OF EXPOSURE OF PLATE OF VARIOUS THICKNESSES TO 3.5 PERCENT NaCl SOLUTION (6)

Alloy	2124-T851								
Form	Plate								
Exposure	Stressed (ST) Tensile Specimens 120 to 130 ft From Mean High Tide at KSC[a], Max Time = 38 Months								
Thickness, inch	2[b]			2.5[c]			3.9[d]		
Applied Stress F_{ty}, percent	0	50	75	0	50	75	0	50	75
Failures[e]	0/2	0/5	1/5(5)	0/2	0/4	4/5 (4.5.5.12)	0/2	0/5	0/5
Loss in F_{tu} (Avg), percent	16	33	42	5	22	–	14	29	44

(a) KSC refers to Kennedy Space Center.
(b) Lot 1: F_{tu} = 67 ksi and F_{ty} = 61 ksi.
(c) Lot 2: F_{tu} = 62 ksi and F_{ty} = 59 ksi.
(d) Lot 3: F_{tu} = 61 ksi and F_{ty} = 57 ksi.
(e) No. failed/no. exposed (failure times, months).

TABLE 2.0324. RESULTS OF EXPOSURE TO SEACOAST ATMOSPHERE ON 2124-T851 SPECIMENS FROM THREE LOTS WITH DIFFERENT THICKNESSES (14)

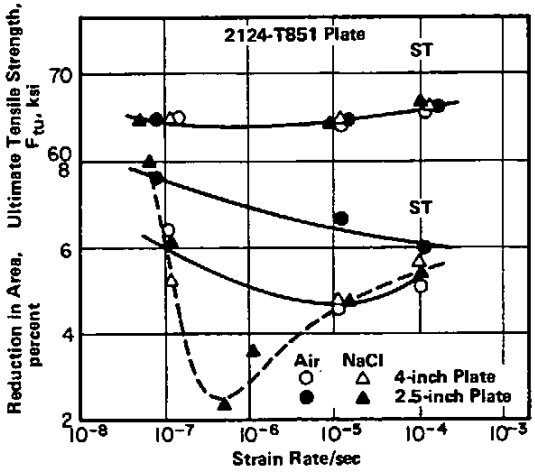


FIGURE 2.0325. EFFECT OF STRAIN RATE ON TENSILE PROPERTIES IN AIR AND IN 3.5 PERCENT NaCl FOR TWO THICKNESS 2124-T851 PLATES FROM DIFFERENT LOTS (18)

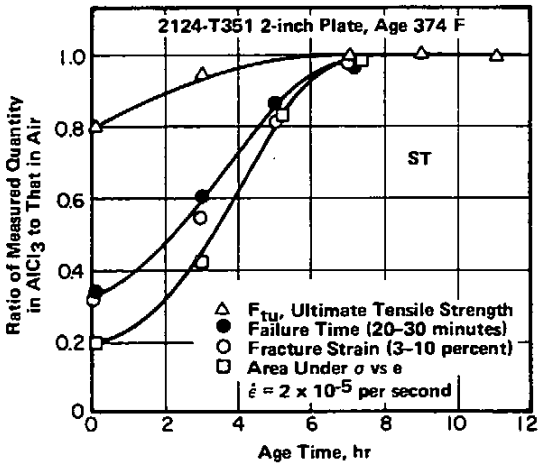


FIGURE 2.0326. EFFECT OF AGE TIME ON SEVERAL MEASURES OF RELATIVE PERFORMANCE FOR 2124-T351 PLATE TESTED AT A SLOW STRAIN RATE IN CORROSION CELL CONTAINING OXYGEN SATURATED 1M $AlCl_3$, pH-2 (23)

Al
4.4 Cu
1.5 Mg
0.6 Mn
2124 Al

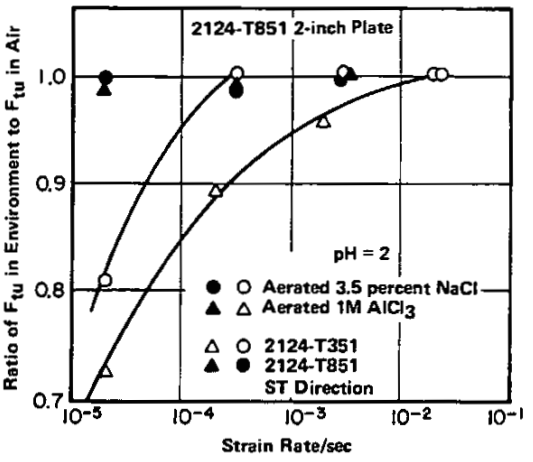


FIGURE 2.0327. EFFECT OF STRAIN RATE ON REDUCTION IN TENSILE STRENGTH OF 2124-T851 AND 2124-T351 PLATE TESTED IN CORROSION CELL CONTAINING OXYGEN SATURATED 3.5 PERCENT NaCl OR 1M $AlCl_3$ (23)

Alloy	2124-T851					
Form	2-inch Plate					
Environment	30-Day Alternate Immersion in 3.5 percent NaCl 50 min in Solution + 10 min in Air					
Specimen		MCW_b[a]			C(T)[b]	
Direction	LT	TL	SL	ST	SL	ST
K_{Ii}/K_{Ic}	0.6 to 0.9	0.6 to 0.9	0.41 to 0.70	0.36 to 0.73	0.65 to 0.87	0.75 to 0.82
K_{Ic}, ksi$\sqrt{in.}$[c]	28	26	23	23	23	23
Results	No Failures After 30 Days and No Compliance Change on any Specimen. No Evidence of SCC on Fractured Surfaces.					

(a) Bolt loaded compact specimens: W = 1.6 inch, $\alpha/W = 0.4$, B = 0.5 inch.
(b) Specimens dead weight loaded.
(c) E 399-81 C(T) specimen: W/B = 3.2, B = 0.5 inch.

TABLE 2.0331. RESULTS OF ALTERNATE IMMERSION TESTS IN 3.5 PERCENT NaCl ON 2124-T851 PLATE USING COMPACT SPECIMENS LOADED TO VARIOUS K_{Ii}/K_{Ic} LEVELS (16)

Alloy	2124-T851						
Form	2-inch Plate[e]						
Environment	30-Day Alternate Exposure in 3.5 percent NaCl, 50 min in Solution + 10 min in Air						
Direction	LS and TS	LT	SL		SL		
Specimen Type	PS[a]	PS	PS		MT[b]		
Flaw Size[a], inch	0.165 <a< 0.330	0.116 <a< 0.169	0.286	0.306	0.72	1.03	1.10
Q	1.36 <Q< 1.59	1.22 <Q< 1.39	1.59	1.66	–	–	–
Stress, ksi	33	39	13	18	11	14	13
K_{Ii}/K_{Ic}[f]	–	0.61	0.48	0.65	0.93	0.95	>1
Result	No SCC	No SCC	No SCC	SCC[c]	No SCC	No SCC	SCC[d]

(a) Surface flaw specimen: W = 3 inch and B = 1/2 inch.
(b) Center crack specimen: W = 3.5 inch and B = 1/2 inch.
(c) $\Delta a = 0.04$ inch.
(d) $\Delta a = 0.1$ inch.
(e) For tensile properties see Table 2.0322.
(f) For K_{Ic} see Table 2.0331.

TABLE 2.0332. RESULTS OF ALTERNATE IMMERSION TESTS IN 3.5 PERCENT NaCl ON 2124-T851 PLATE TESTED USING SURFACE FLAWED AND CENTER CRACKED SPECIMENS REPRESENTING SEVERAL CRACK ORIENTATIONS (16)

Al
4.4 Cu
1.5 Mg
0.6 Mn

2124 Al

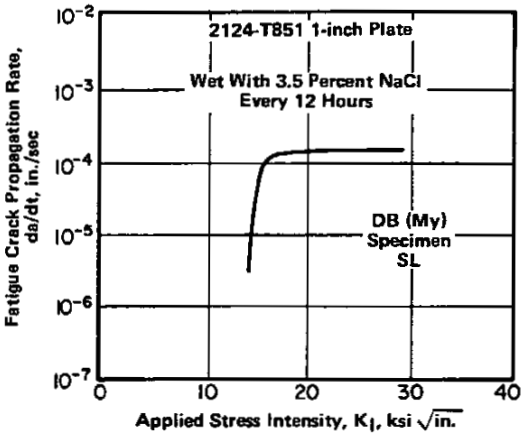


FIGURE 2.0333. CRACK PROPAGATION RATE AS A FUNCTION OF APPLIED STRESS INTENSITY FOR 2124-T851 PLATE SUBJECTED TO ALTERNATE IMMERSION IN 3.5 PERCENT NaCl SOLUTION (22)

Alloy	2124-T851					
Form	3-inch Plate					
Environment	Fuel Tank Sump Residue Water(a)					
Direction	LT			SL		
	Total Test Time, hr	Total Crack Growth, inch	K_{Iscc}, ksi $\sqrt{in.}$	Total Test Time, hr	Total Crack Growth, inch	K_{Iscc}, ksi $\sqrt{in.}$
	1,172	0.02	28	2,177	0.17	26
	1,172	0.015	27	906	0.19	21
	906	0.01	25	906	0.06	21

(a) See Table 2.0335 for composition.

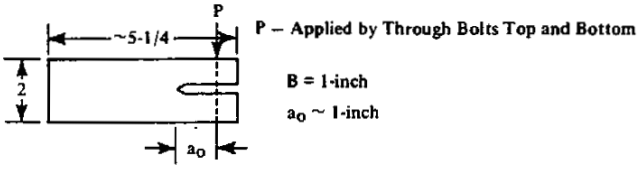


TABLE 2.0334. STRESS CORROSION CRACK GROWTH STRESS INTENSITY THRESHOLD OF PLATE FROM THE B-1 PROGRAM TESTED IN FUEL TANK SUMP WATER (25)

Sump Tank Water Composition, ppm	
$CaCl_2$	50
$CdCl_2$	1,000
$MgCl_2$	50
NaCl	100
ZnCl	10
PbCl	1
$CrCl_3 \cdot H_2O$	1
$CuCl_3 \cdot 2H_2O$	1
$FeCl_3$	5
$MnCl_2 \cdot 4H_2O$	5
$NiCl_2 \cdot 6H_2O$	1
Distilled Water	Remainder

TABLE 2.0335. COMPOSITION OF FUEL TANK SUMP RESIDUE WATER USED IN CERTAIN STRESS CORROSION AND FATIGUE CRACK PROPAGATION TESTS IN THE B-1 PROGRAM (16)

Alloy		2124-T851(a)(b)				
Form		Plate				
Thickness, inch		1.500 to 2.000	2.001 to 3.000	3.001 to 4.000	4.001 to 5.000	5.001 to 6.000
F_{tu} (Min), ksi	L	66.0	65.0	65.0	64.0	63.0
	T	66.0	65.0	65.0	64.0	63.0
	ST	64.0	63.0	62.0	61.0	58.0
F_{ty} (Min), ksi	L	57.0	57.0	56.0	55.0	54.0
	T	57.0	57.0	56.0	55.0	54.0
	ST	55.0	55.0	54.0	53.0	51.0
e (2 inch or 4D),	L	6	6	5	5	5
percent (Min)	T	5	4	4	4	4
	ST	1.5	1.5	1.5	1.5	1.5

(a) For stress relieved tempers, characteristics and properties other than those specified may differ somewhat from the corresponding characteristics and properties of material in the basic temper.
(b) Type of specimen used depends on thickness of material.

TABLE 3.011. ALUMINUM ASSOCIATION MECHANICAL PROPERTIES FOR PLATE (3)

Alloy		2124-T851									
Form		Plate									
Thickness, inch		1.000 to 1.500	1.501 to 2.000		2.001 to 3.000		3.001 to 4.000		4.001 to 5.000		5.001 to 6.000	
Basis		S(c)	A	B	A	B	A	B	A	B	A	B
F_{tu}, ksi	L	66	66	68	65	68	65	67	64	66	63	65
	LT	66	66	68	65	68	65	67	64	66	63	65
	ST	64(a)	64	66	63	64	62	63	61	62	58	59
F_{ty}, ksi	L	57	57	61	57	61	56	60	55	58	54	56
	LT	57	57	61	57	61	56	60	55	58	54	56
	ST	55(a)	55	59	55	59	54	57	53	55	51	53
F_{cy}, ksi	L	57	57	61	56	60	55	59	53	56	52	54
	LT	57	57	61	57	61	56	60	55	58	54	56
	ST	–	57	61	58	62	57	61	57	60	56	58
F_{su}, ksi	L	–	38	39	38	39	38	39	37	38	37	38
	LT	–	38	39	38	39	38	39	37	38	37	38
	ST	–	36	37	36	37	36	37	35	36	35	36
F_{bru}, ksi												
(e/D = 1.5)		–	97	100	96	100	96	99	94	97	93	96
(e/D = 2.0)		–	126	130	125	130	125	128	123	126	121	125
F_{bry}, ksi												
(e/D = 1.5)		–	79	84	80	85	80	85	79	84	79	82
(e/D = 2.0)		–	91	98	92	99	92	99	92	97	91	95
e, percent	L	6	6	–	6	–	5	–	5	–	5	–
	LT	5(b)	5	–	4	–	4	–	4	–	4	–
	ST	1.5(a)	1.5	–	1.5	–	1.5	–	1.5	–	1.5	–

(a) Short transverse values applicable to 1.500 inch (38.1 mm) thickness only.
(b) The above table is in agreement with MIL-HDBK-5 Table 3.2.5.0(b), except for the LT elongation shown for the 1.000 to 1.500 inch (25.4-38.1 mm) thickness range. The 5 percent value is accepted by federal and industry specifications such as QQ-A-250/29 and ASTM B209.
(c) Specification values.

TABLE 3.012. DESIGN MECHANICAL PROPERTIES FOR 2124-T851 PLATE (1)

Alloy	2124-T851														
Form	Plate														
Thickness, inch	1-1/2 to 2			>2 to 3			>3 to 4			>4 to 5			>5 to 6		
Direction	L	LT	ST	L	LT	ST	L	LT	ST	L	LT	ST	L	LT	ST
F_{tu}, ksi	66	66	64	65	65	63	65	65	64	64	64	61	63	63	58
F_{ty}, ksi	57	57	55	57	57	55	56	56	52	55	55	53	54	54	51
e (2 inch or 4D), percent	6	5	1.5	6	4	1.5	5	4	1.5	5	4	1.5	5	4	1.5

TABLE 3.013. AMS SPECIFIED TENSILE PROPERTIES FOR 2124-T851 PLATE (33)

Al
4.4 Cu
1.5 Mg
0.6 Mn
2124 Al

Al
4.4 Cu
1.5 Mg
0.6 Mn

2124 Al

Alloy	2124-T851		
Form	Plate		
Thickness (t), inch	$1.5 \leq t < 5.0$		
Direction	LT	TL	SL
K_{Ic}, ksi$\sqrt{in.}$ (Min)	24	20	18
Notch/F_{ty}[a] Ratio	1.01	0.83	0.69

(a) Based on 1-1/16-inch diameter sharp notch specimen (see Figure 3.02723).

TABLE 3.014. SPECIFIED PLANE STRAIN FRACTURE TOUGHNESS MINIMA AND CORRESPONDING ACCEPTANCE CRITERIA BASED ON A SHARP NOTCH TO TENSILE STRENGTH RATIO (1)

Alloy	2124-T851		
Form	Plate		
Thickness, inch	1-1/2 to 6 inch		
Direction	LT	TL	SL
K_{Ic}, ksi$\sqrt{in.}$ (Min)	24	20	18

TABLE 3.015. AMS SPECIFIED PLANE STRAIN FRACTURE TOUGHNESS FOR 2124-T851 PLATE (21)

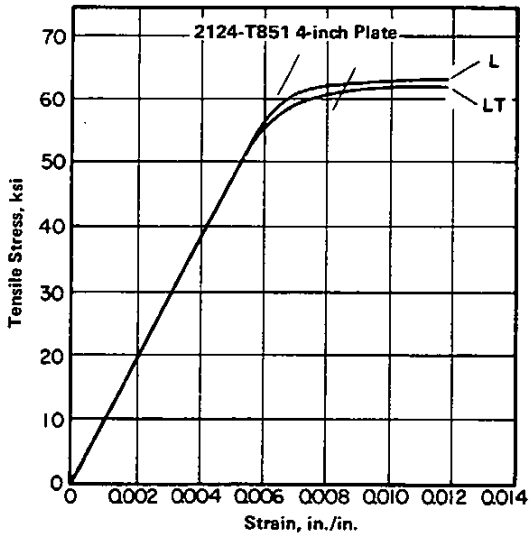


FIGURE 3.0211. TYPICAL TENSILE STRESS-STRAIN CURVES FOR 4-INCH THICK PLATE (1)

Alloy		2124-T851									
Form		Plate									
Producer[a]		A	B	C	A	A	B	A	C	A	C
Thickness, inch		1.75	2.04	2.00	2.5	3.5	4.00	4.5	4.5	5.5	6.00
F_{tu}, ksi	L	72.0	70.8	71.5	71.5	70.3	70.2	70.2	67.8	68.2	65.2
	T	71.5	70.9	71.1	70.7	69.9	69.7	69.4	67.5	67.5	64.6
	ST	70.4	68.2	68.2	69.2	68.5	65.9	65.6	64.1	63.6	60.6
F_{ty}, ksi	L	67.0	65.4	66.2	65.4	63.9	65.5	63.4	59.8	61.1	57.1
	T	65.7	65.2	65.4	64.2	62.7	64.2	61.4	58.5	59.3	55.0
	ST	65.3	62.7	64.9	63.5	61.4	60.2	59.8	57.3	57.5	54.8
e (2 inch or 4D), percent	L	10.0	8.5	9.5	9.0	9.0	6.5	8.0	8.0	8.0	8.0
	T	8.0	7.0	8.0	7.0	7.0	5.5	6.0	8.0	7.0	7.0
	ST	3.1	4.7	3.1	3.0	4.0	4.0	3.0	2.5	2.5	3.5
RA, percent	L	25	22	25	22	21	10	19	13	16	18
	T	18	26	15	14	13	11	11	11	10	9
	ST	8	8	9	6	6	6	3	5	4	2

(a) Producer: A – Alcoa; B – Kaiser; C – Reynolds.

TABLE 3.0212. TYPICAL TENSILE PROPERTIES OF 2124-T851 PLATE (6)

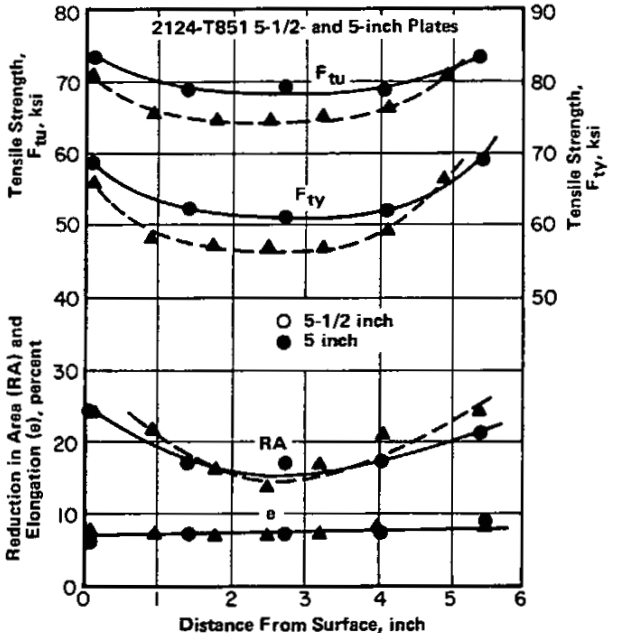


FIGURE 3.0213. TENSILE PROPERTIES AS A FUNCTION OF DISTANCE FROM SURFACE OF 2124-T851 CONDITION THICK PLATES (29)

Al
4.4 Cu
1.5 Mg
0.6 Mn

2124 Al

Alloy	2124-T851				
Form	Plate				
Thickness	2 inch		3 inch		
Supplier	A		B		
Test Direction	L	T	L	T	ST
F_{tu}, ksi	71	71	72	73	69
F_{ty}, ksi	65	66	65	67	63
e, percent	8	7	8	8	4
RA, percent	–	–	16	19	9

TABLE 3.0214. TYPICAL TENSILE PROPERTIES OF 2-INCH AND 3-INCH THICK 2124-T851 PLATE FROM THE B-1 PROGRAM (26)

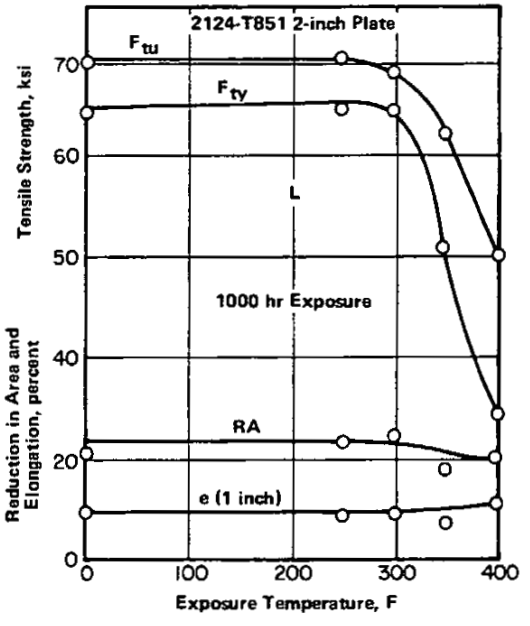


FIGURE 3.0215. EFFECT OF 1000 HR EXPOSURE AT ELEVATED TEMPERATURES ON RETAINED ROOM TEMPERATURE TENSILE PROPERTIES OF 2124-T851 PLATE (12)

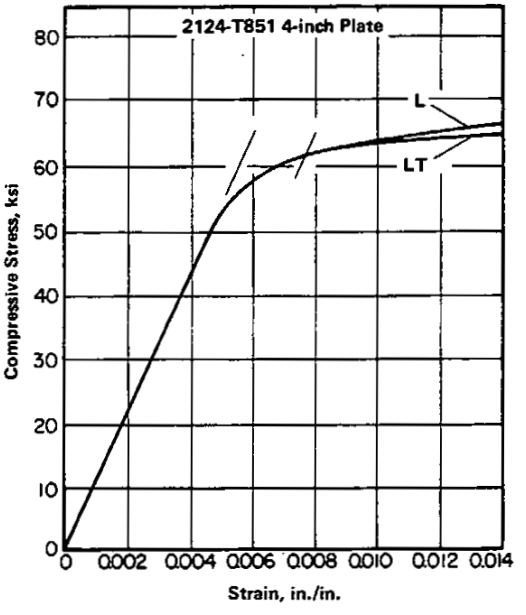


FIGURE 3.0221. TYPICAL COMPRESSION STRESS-STRAIN CURVES FOR 4-INCH THICK 2124-T851 PLATE (1)

Al
4.4 Cu
1.5 Mg
0.6 Mn

2124 Al

Alloy		2124-T851									
Form		Plate									
Producer[a]		A	C	B	A	A	B	A	C	A	C
Thickness, inch		0.75	2.00	2.04	2.5	3.5	4.00	4.5	4.5	5.5	6.00
F_{cy}, ksi	L	66.7	65.2	63.4	63.9	62.9	63.1	61.1	57.3	58.3	52.1
	T	67.0	66.7	65.7	66.0	63.7	64.2	62.9	58.1	60.1	56.0
	ST	68.0	68.0	66.2	66.7	64.9	65.7	64.2	62.4	61.6	58.5
F_{su}, ksi	L	41.9	41.2	41.2	40.9	40.7	40.7	40.5	39.1	40.0	38.2
	T	42.1	41.2	41.2	41.0	40.7	40.7	40.5	39.3	40.0	38.0
	ST	39.8	39.1	39.6	39.6	39.1	38.7	38.9	36.8	38.4	36.4
F_{bru}, ksi	L	107.5	108.1	105.7	106.4	104.9	103.7	103.8	100.9	101.7	96.5
(e/D = 1.5)[b]	T	107.2	107.4	105.4	106.6	105.5	103.4	105.4	100.9	102.5	97.4
	ST	–	–	–	–	–	–	–	–	–	–
F_{bru}, ksi	L	139.5	139.1	138.3	138.3	136.2	133.8	135.0	131.2	131.5	125.3
(e/D = 2.0)[b]	T	139.1	138.1	136.3	137.0	135.4	135.6	135.7	130.4	132.0	126.5
	ST	–	–	–	–	–	–	–	–	–	–
F_{bry}, ksi	L	94.8	96.5	92.0	93.0	91.3	94.3	93.3	85.2	90.3	83.8
(e/D = 1.5)[b]	T	94.1	95.5	92.8	92.1	92.0	91.8	93.0	86.4	88.6	84.1
	ST	–	–	–	–	–	–	–	–	–	–
F_{bry}, ksi	L	109.8	107.2	105.8	108.7	107.1	106.3	107.1	98.4	103.7	97.0
(e/D = 2.0)[b]	T	108.8	109.0	106.4	105.1	104.6	106.3	105.8	97.8	105.1	94.1
	ST	–	–	–	–	–	–	–	–	–	–

(a) Producer: A – Alcoa; B – Kaiser; C – Reynolds.
(b) Specimens and fixtures cleaned ultrasonically.

TABLE 3.0222. TYPICAL COMPRESSION, SHEAR, AND BEARING PROPERTIES OF 2124-T851 PLATE (6)

Alloy	2124-T851		
Form	1.5- to 6-inch Plate[a]		
Crack Orientation	LT	TL	SL
Number of Tests	138	145	135
Average K_{Ic}, ksi$\sqrt{in.}$	30	25.3	21.4
Standard Deviation, ksi$\sqrt{in.}$	2.7	2.2	2.0
Skewness Coefficient	+0.4	+0.5	-0.2
Min Value, ksi$\sqrt{in.}$	24	21.1	17
A - Value[b], ksi$\sqrt{in.}$	22.9 to 23.9	19.4 to 20.4	16.2 to 15.9
B - Value, ksi$\sqrt{in.}$	26.0 to 26.2	21.9 to 22.1	18.4 to 18.4

(a) Data from two producers November 1975 to August 1978.
(b) Lower limt based on normal distribution and upper limit based on Pearson type III function using skewness.

TABLE 3.02721. PLANE STRAIN FRACTURE TOUGHNESS RESULTS FOR LT, TL, AND SL ORIENTATIONS OF PLATE OBTAINED FROM MANY TESTS MADE BY TWO PRODUCERS (28)

Alloy	2124-T851				
Form	Plate				
Thickness, inch	2[a]		3[b]		
Supplier	A		B		
Crack Orientation	LT	TL	LT	TL	ST
K_{Ic}, ksi$\sqrt{in.}$	24	23	29	24	24
K_{Ic}^2/σ_{ys}^2, inch[c]	0.14	0.12	0.20	0.13	0.15

(a) Compact specimen: B = 0.75 and W/B = 2.7.
(b) Compact specimens: $0.62 < B < 0.75$ and $3.23 < W/B < 3.33$.
(c) See Table 3.0214 for tensile properties.

TABLE 3.02722. PLANE STRAIN FRACTURE TOUGHNESS OF A 2-INCH AND 3-INCH PLATE FROM THE B-1 PROGRAM (26)

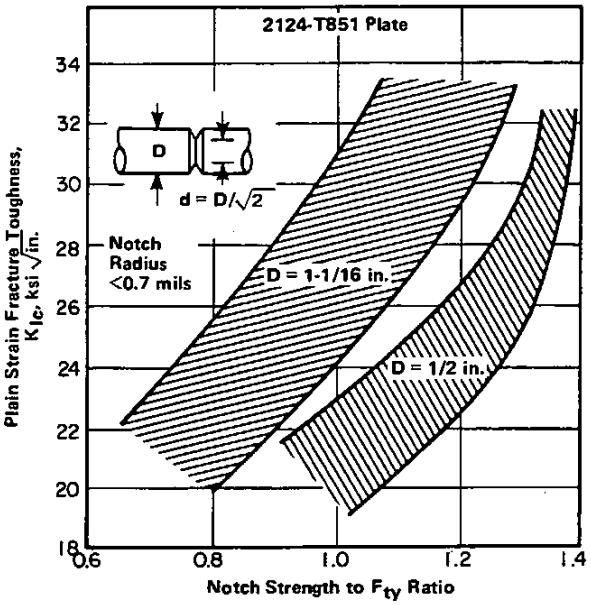


FIGURE 3.02723. SCATTERBANDS FOR RELATION BETWEEN SHARP-NOTCH STRENGTH TO YIELD STRENGTH RATIO AND PLANE STRAIN FRACTURE TOUGHNESS DETERMINED USING TWO NOTCH SPECIMEN DIAMETERS FOR 2124-T851 PLATE HAVING THICKNESS FROM 1.57 TO 6 INCH AND TESTED IN LT, TL, AND SL ORIENTATIONS WITH SPECIMENS LOCATED AT PLATE CENTER AND MID THICKNESS (15)

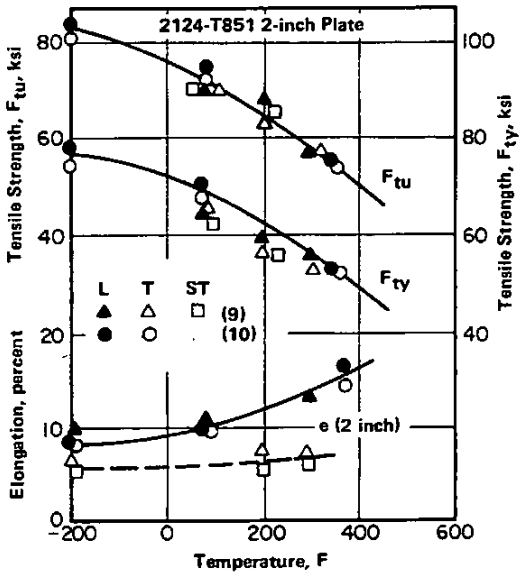


FIGURE 3.0313. EFFECT OF TEMPERATURE AND TESTING DIRECTION ON TENSILE PROPERTIES OF 2124-T851 PLATE (9, 10)

Al
4.4 Cu
1.5 Mg
0.6 Mn

2124 Al

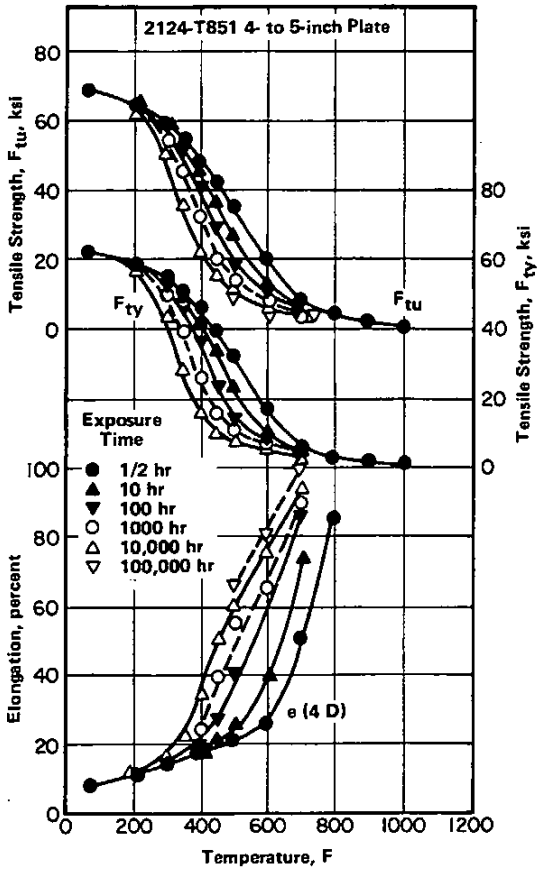


FIGURE 3.0312. EFFECT OF TEST TEMPERATURE AND EXPOSURE TIME ON TENSILE PROPERTIES OF 2124-T851 PLATE (1)

Al
4.4 Cu
1.5 Mg
0.6 Mn
2124 Al

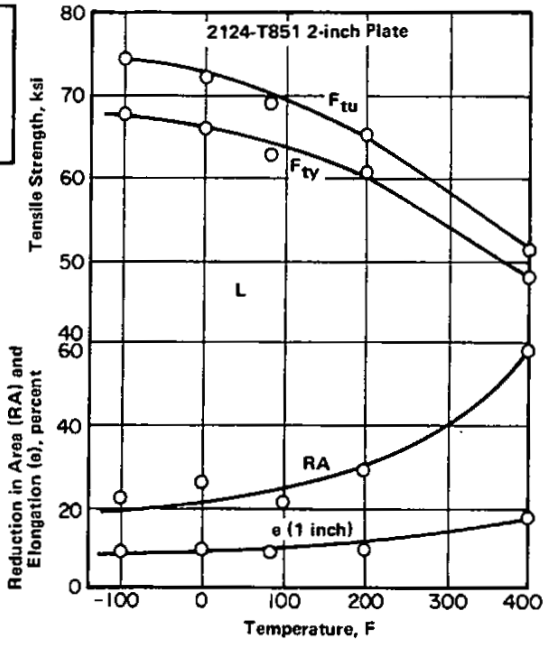


FIGURE 3.0314. EFFECT OF TEMPERATURE ON TENSILE PROPERTIES OF 2124-T851 PLATE (12)

Alloy	2124-T851					
Form	2-1/2 inch Plate					
Orientation	TL		LT		ST	
Temp. F	RT	250	RT	250	RT	250
K_{Ic}, ksi$\sqrt{in.}$	27	27	32	33	25	25

TABLE 3.03721. PLANE STRAIN FRACTURE TOUGHNESS OF PLATE AT ROOM TEMPERATURE AND 250 F (9)

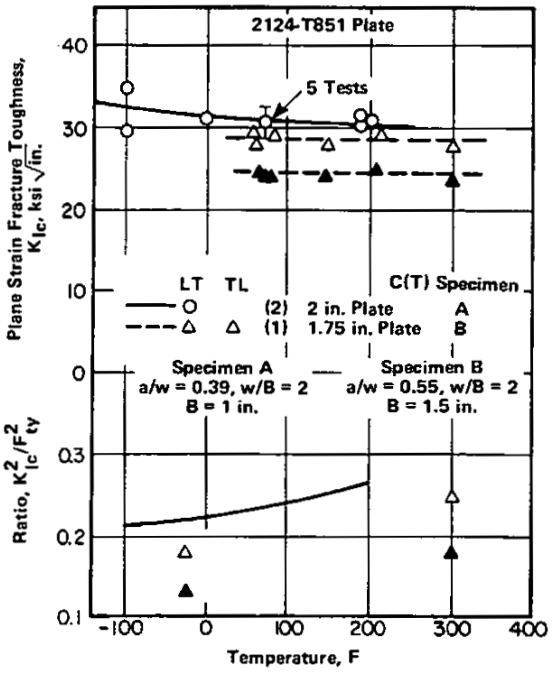


FIGURE 3.03722. EFFECT OF TEMPERATURE ON PLANE STRAIN FRACTURE TOUGHNESS OF TWO LOTS OF 2124-T851 PLATE (12)

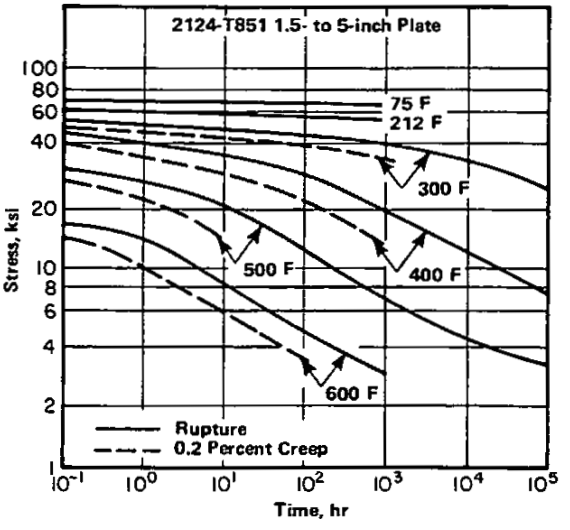


FIGURE 3.041. CREEP AND CREEP-RUPTURE CURVES AT TEMPERATURES FROM 75 TO 600 F FOR 2124-T851 PLATE (1)

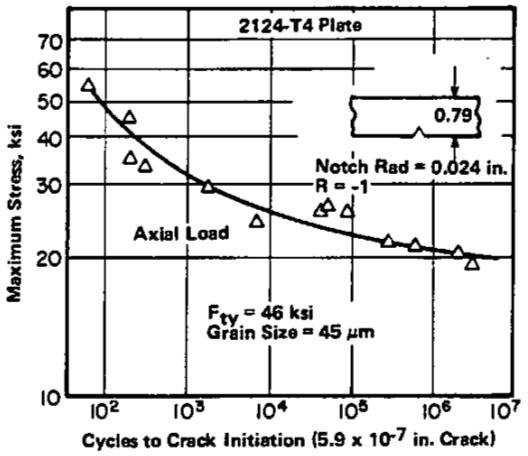


FIGURE 3.0511. CYCLES TO CRACK INITIATION AS A FUNCTION OF NOMINAL MAXIMUM FATIGUE STRESS FOR SPECIMENS WITH CAREFULLY POLISHED NOTCHES (19)

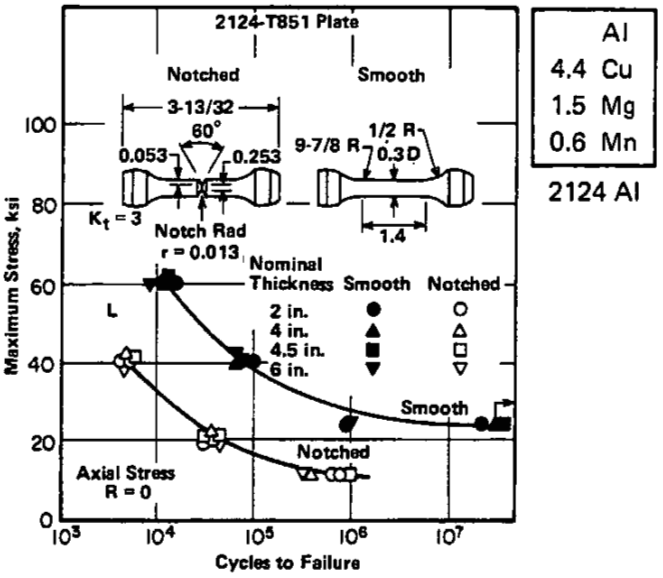


FIGURE 3.0512. AXIAL-LOAD FATIGUE CURVES FOR LONGITUDINAL SMOOTH AND NOTCHED (K_t = 3) SPECIMENS FROM 2124-T851 PLATE (6)

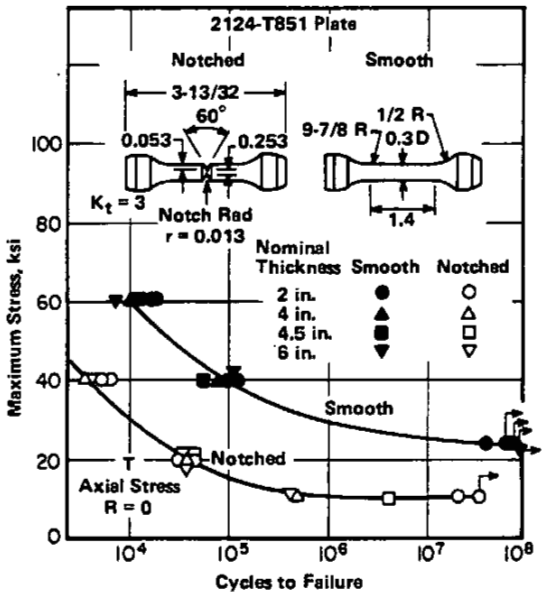


FIGURE 3.0513. AXIAL-LOAD FATIGUE CURVES FOR TRANSVERSE SMOOTH AND NOTCHED (K_t = 3) SPECIMENS FROM 2124-T851 PLATE (6)

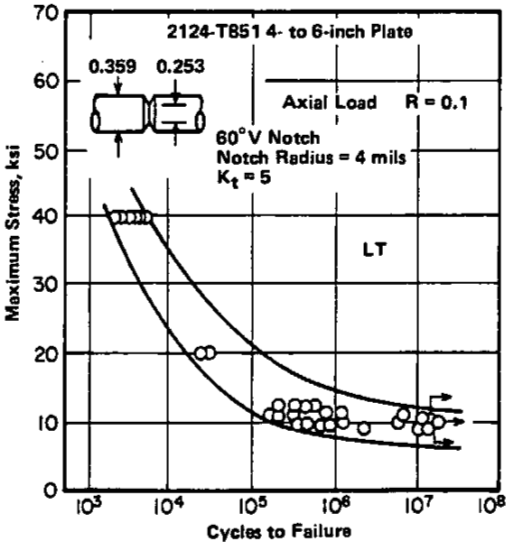


FIGURE 3.0514. AXIAL-LOAD FATIGUE CURVE FOR NOTCHED (K_t = 5) SPECIMENS FROM 4- TO 6-INCH 2124-T851 PLATE (1)

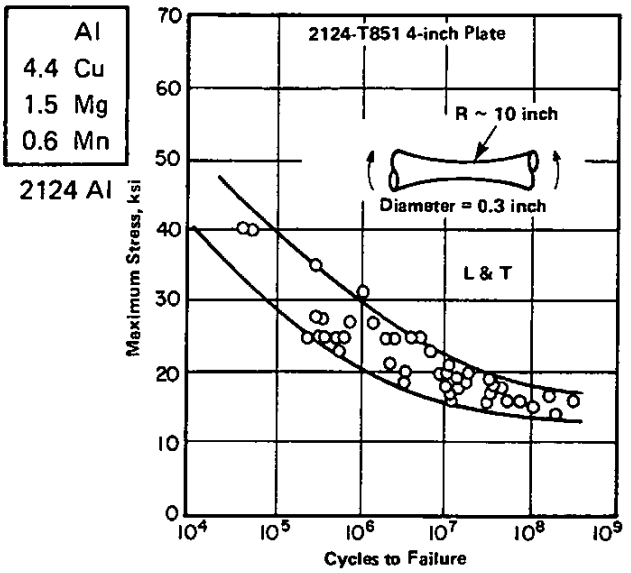


FIGURE 3.0515. ROTATING BENDING FATIGUE CURVES FOR SMOOTH SPECIMENS FROM 4-INCH 2124-T851 PLATE (1)

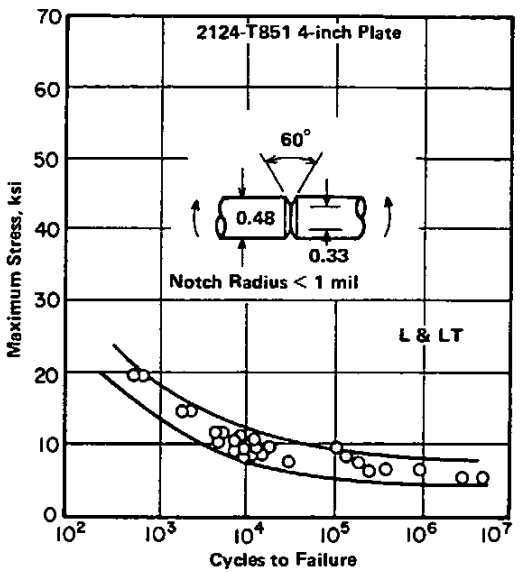


FIGURE 3.0516. ROTATING BENDING FATIGUE CURVES FOR SHARPLY NOTCHED SPECIMENS FROM 2124-T851 4-INCH PLATE (1)

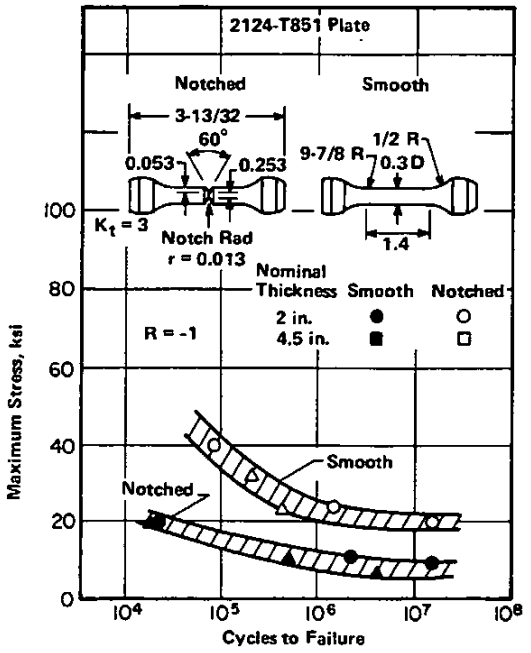


FIGURE 3.0517. EFFECT OF SALT FOG ON AXIAL LOAD FATIGUE LIFE OF SMOOTH AND NOTCHED (K_t = 3) SPECIMENS FROM 2124-T851 PLATE (6)

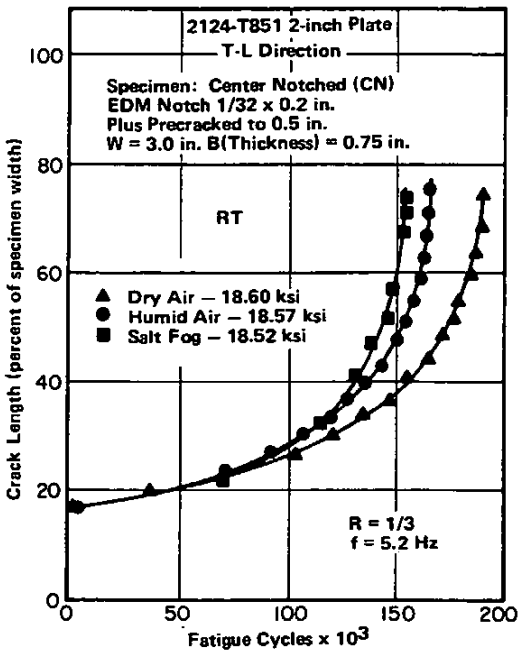


FIGURE 3.0521. TYPICAL FATIGUE CRACK-GROWTH DATA FOR 2-INCH PLATE IN VARIOUS ENVIRONMENTS (6)

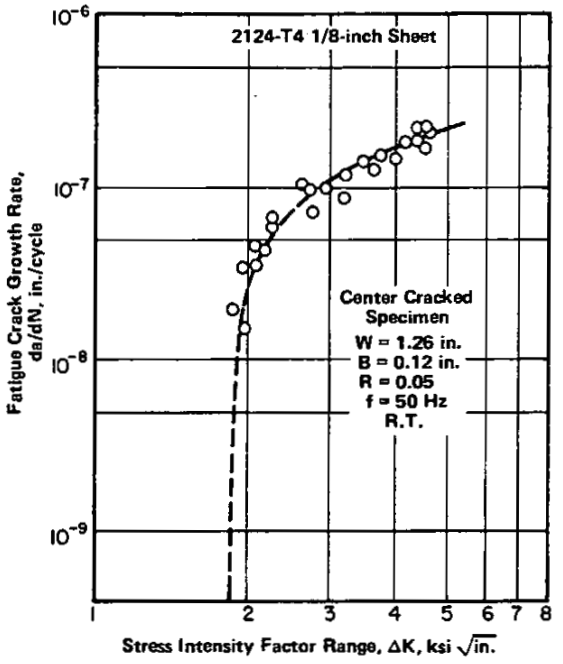


FIGURE 3.0522. FATIGUE CRACK-GROWTH RATES FOR 2124-SHEET IN T4 CONDITION (31)

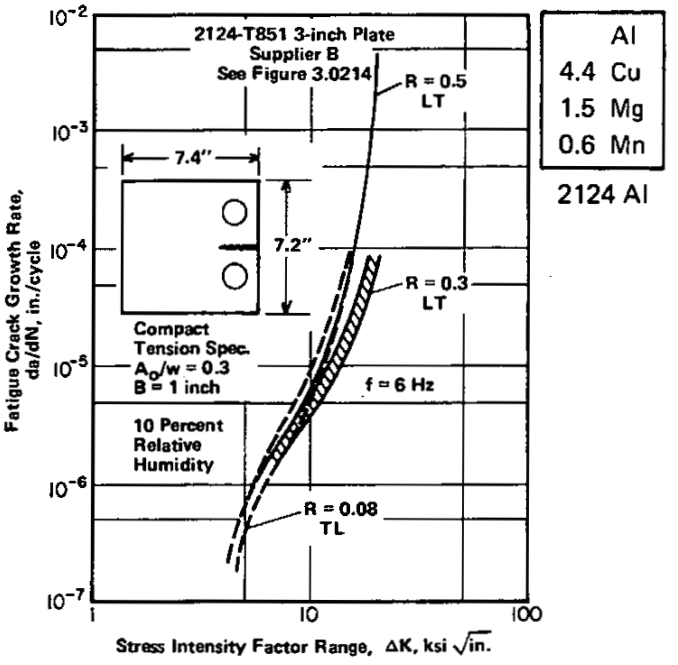


FIGURE 3.0523. FATIGUE CRACK-GROWTH RATES FOR 2124-T851 PLATE FROM THE B-1 PROGRAM AT SEVERAL R RATIOS IN LOW HUMIDITY AIR (25)

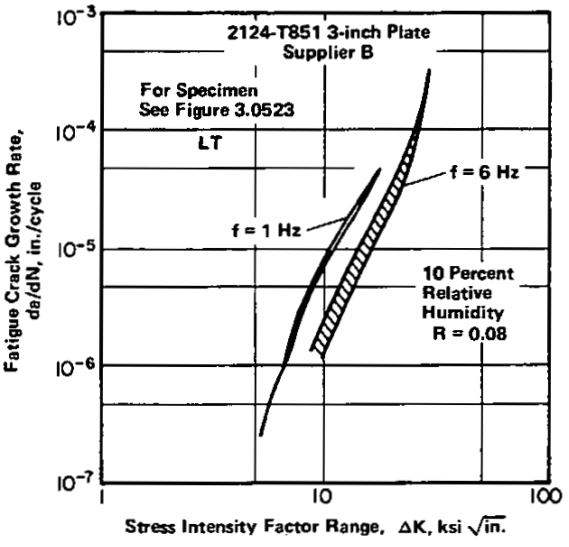


FIGURE 3.0524. FATIGUE CRACK-GROWTH RATES FOR 2124-T851 PLATE FROM THE B-1 PROGRAM FOR TWO LOADING FREQUENCIES IN LOW HUMIDITY AIR (25)

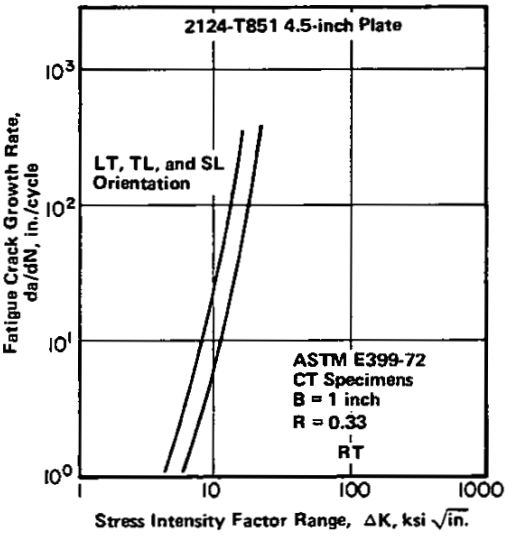


FIGURE 3.0525. FATIGUE CRACK-GROWTH RATES AT R = 0.33 FOR 4.5-INCH PLATE (6)

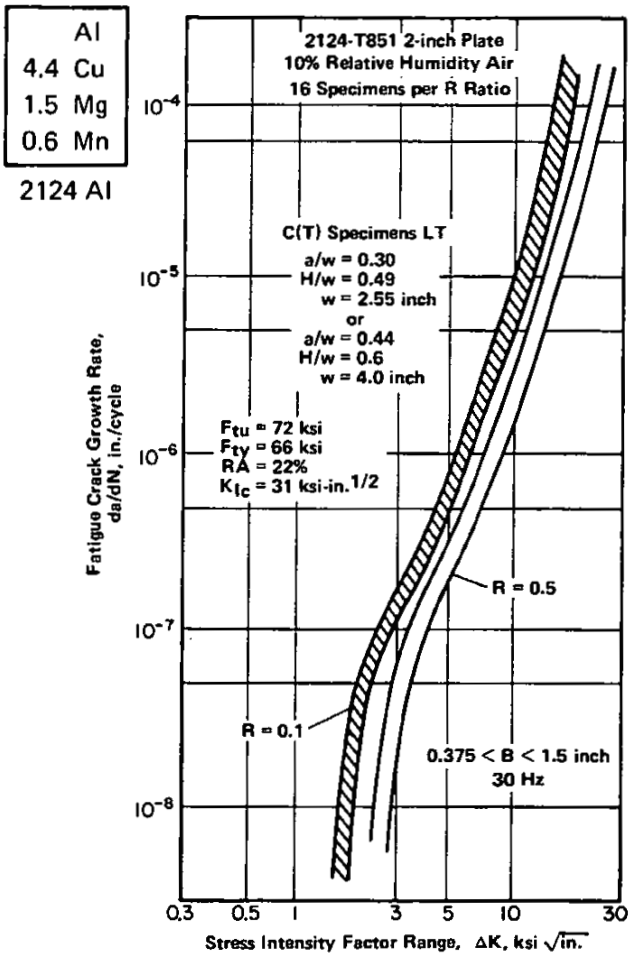


FIGURE 3.0526. FATIGUE CRACK-GROWTH RATES AT LOW ΔK VALUES FOR 2124-T851 PLATE TESTED AT TWO R RATIOS AND THICKNESSES OF 0.375, 0.75, AND 1.5 INCH (13)

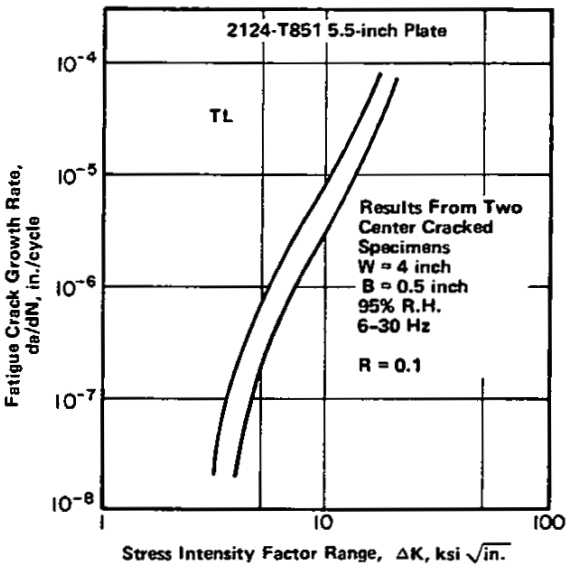


FIGURE 3.0527. FATIGUE CRACK-GROWTH RATES FOR 2124-T851 PLATE TESTED IN HIGH HUMIDITY AIR AT R = 0.1 (32)

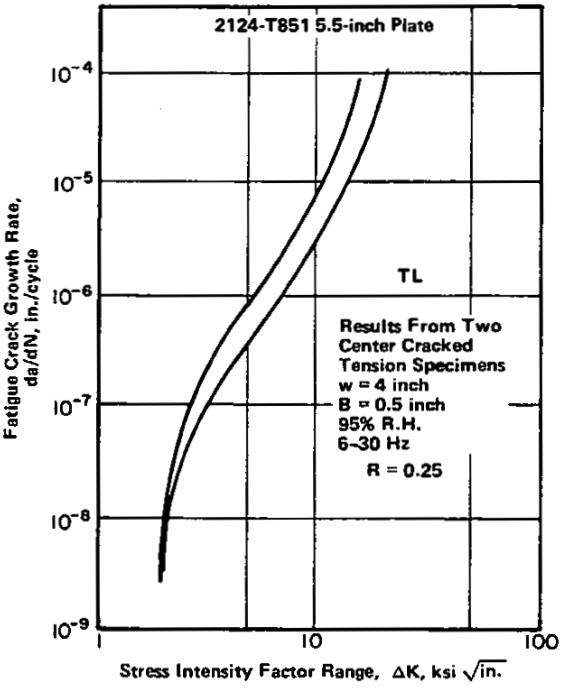


FIGURE 3.0528. FATIGUE CRACK-GROWTH RATES FOR 2124-T851 PLATE TESTED IN HIGH HUMIDITY AIR AT R = 0.25 (32)

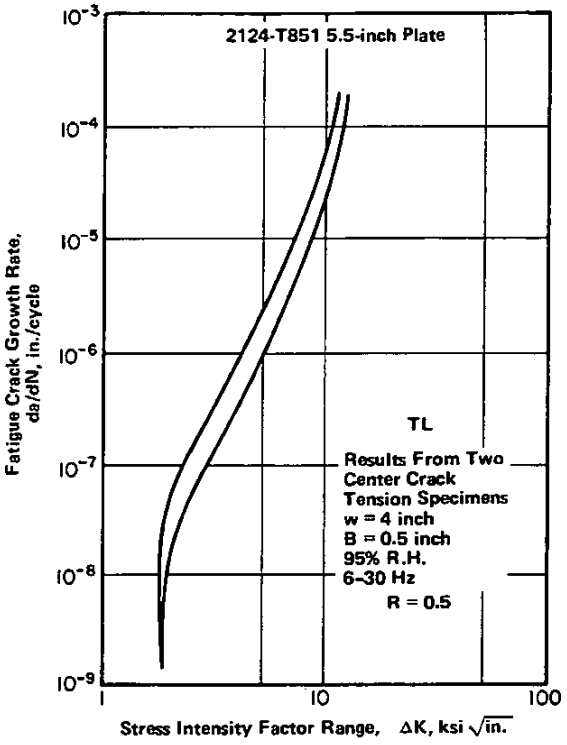


FIGURE 3.0529. FATIGUE CRACK-GROWTH RATES FOR 2124-T851 PLATE TESTED IN HIGH HUMIDITY AIR AT R = 0.5 (32)

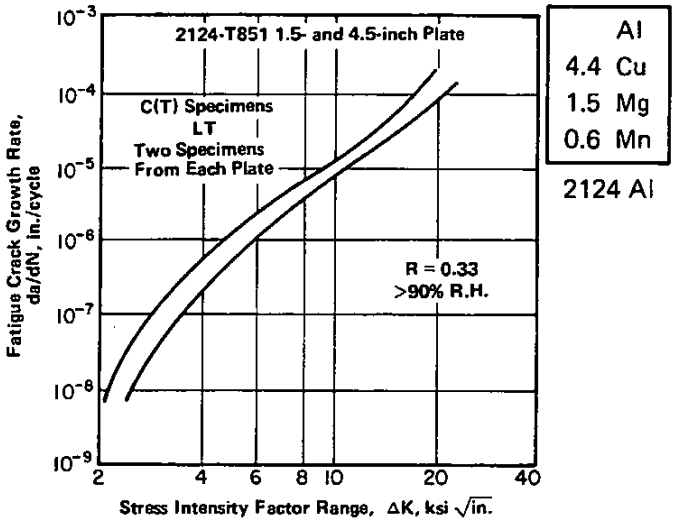


FIGURE 3.05210. FATIGUE CRACK-GROWTH RATES FOR TWO THICKNESSES OF PLATE TESTED IN HIGH HUMIDITY AIR (1)

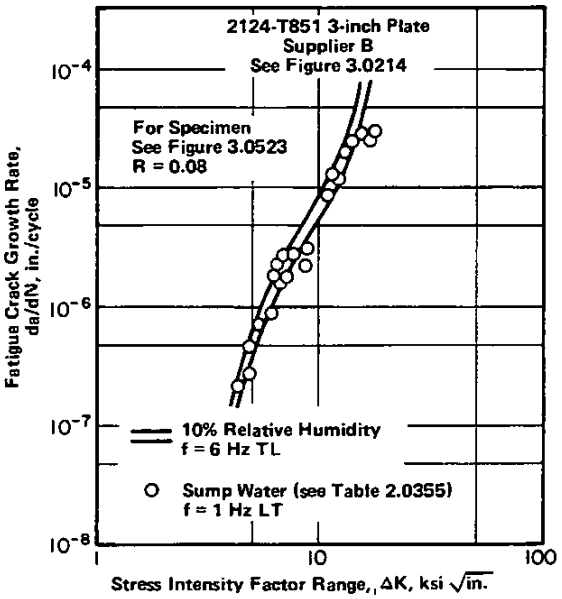


FIGURE 3.05211. FATIGUE CRACK-GROWTH RATES FOR 2124-T851 PLATE FROM THE B-1 PROGRAM TESTED IN LOW HUMIDITY AIR AND IN SUMP WATER (25)

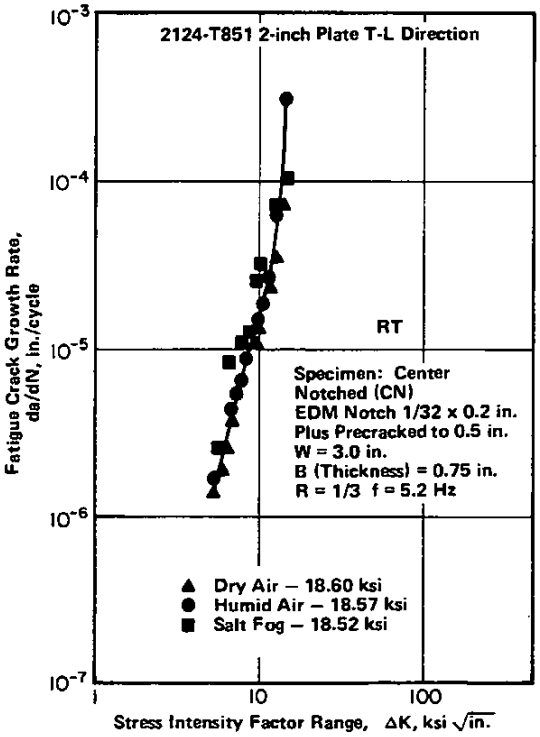


FIGURE 3.05212. TYPICAL FATIGUE CRACK-GROWTH RATES FOR 2-INCH 2124-T851 PLATE IN VARIOUS ENVIRONMENTS (6)

Al
4.4 Cu
1.5 Mg
0.6 Mn
2124 Al

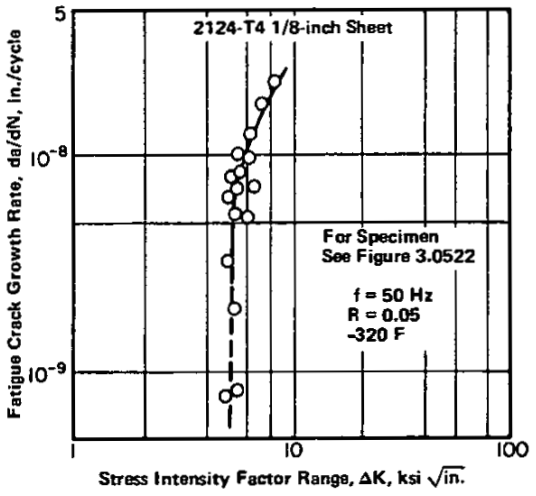


FIGURE 3.05213. FATIGUE CRACK-GROWTH RATES APPROACHING ZERO FOR 2124-SHEET IN THE T4 CONDITION AT -320 F (31)

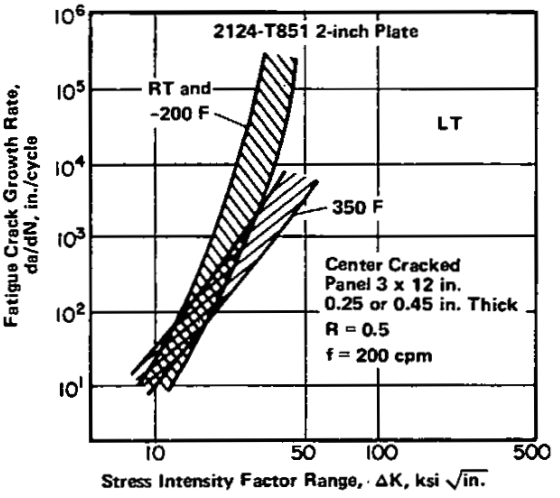


FIGURE 3.05214. FATIGUE CRACK-GROWTH RATES FOR PLATE TESTED IN THE LT DIRECTION AT CRYOGENIC AND ELEVATED TEMPERATURE (10)

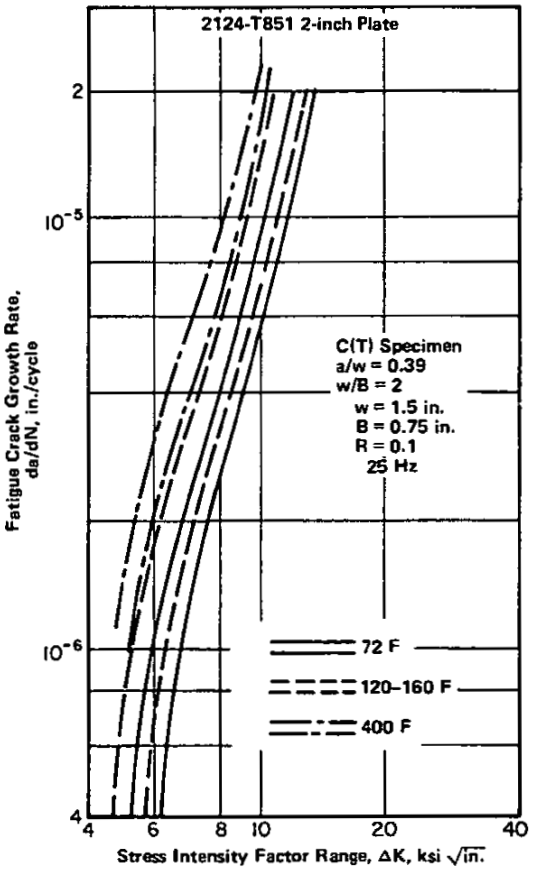


FIGURE 3.05215. FATIGUE CRACK-GROWTH RATES FOR 2124-T851 PLATE AT ROOM AND ELEVATED TEMPERATURES (12)

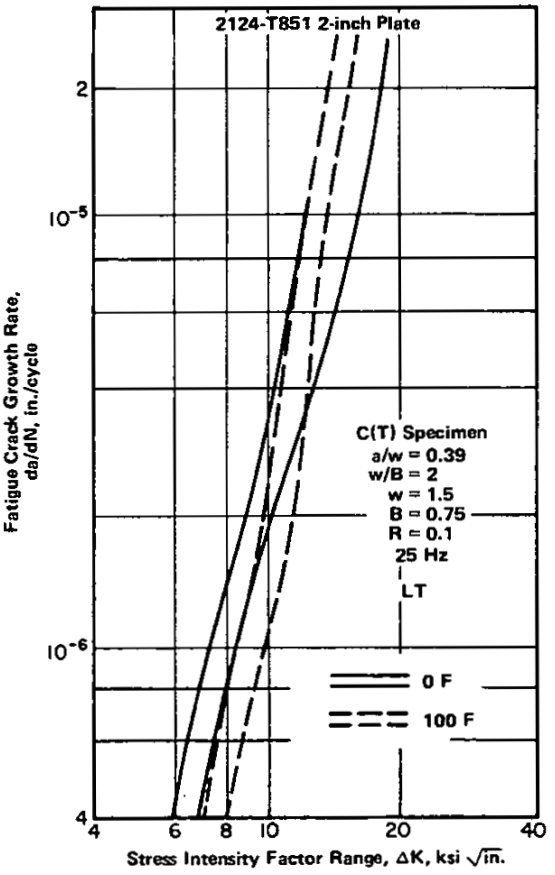


FIGURE 3.05216. FATIGUE CRACK-GROWTH RATES FOR 2124-T851 PLATE AT LOW TEMPERATURES (12)

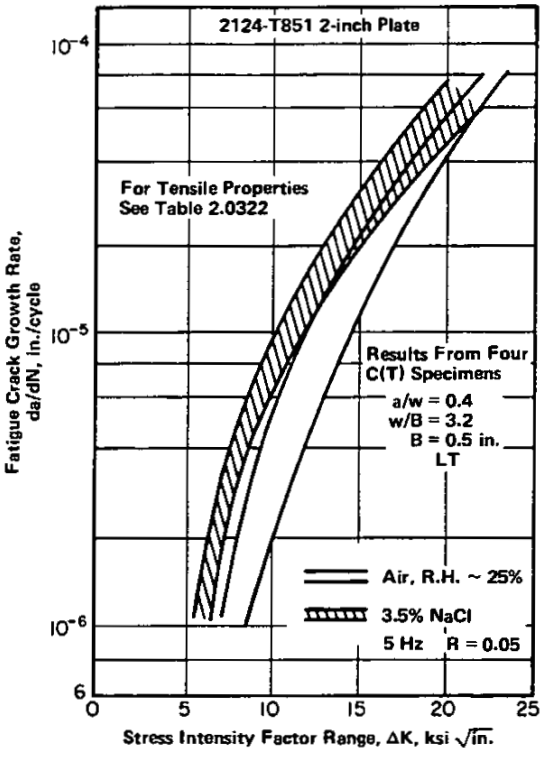


FIGURE 3.05217. FATIGUE CRACK-GROWTH RATES FOR 2124-T851 PLATE IN AIR AND 3.5 PERCENT NaCl FOR LT DIRECTION (16)

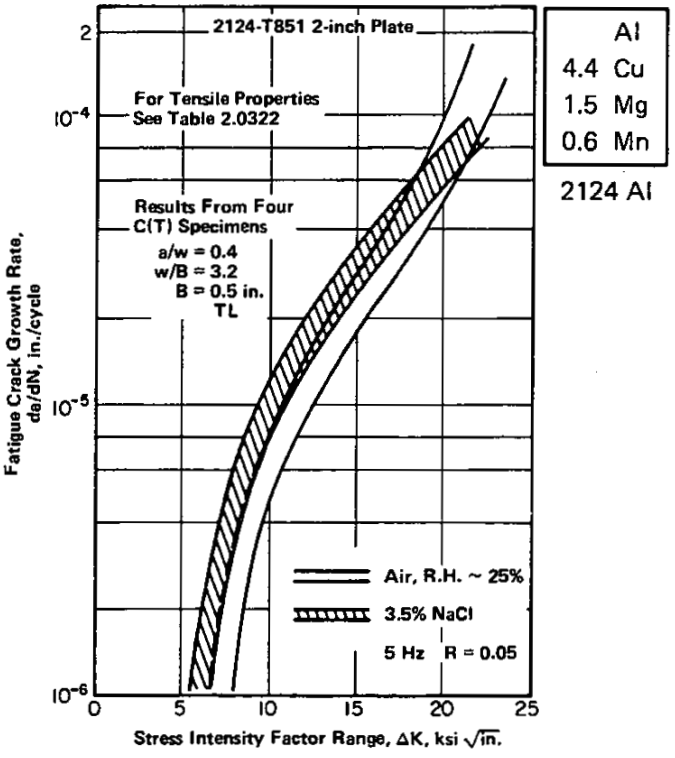


FIGURE 3.05218. FATIGUE CRACK-GROWTH RATES FOR 2124-T851 PLATE IN AIR AND IN 3.5 PERCENT NaCl FOR TL DIRECTION (16)

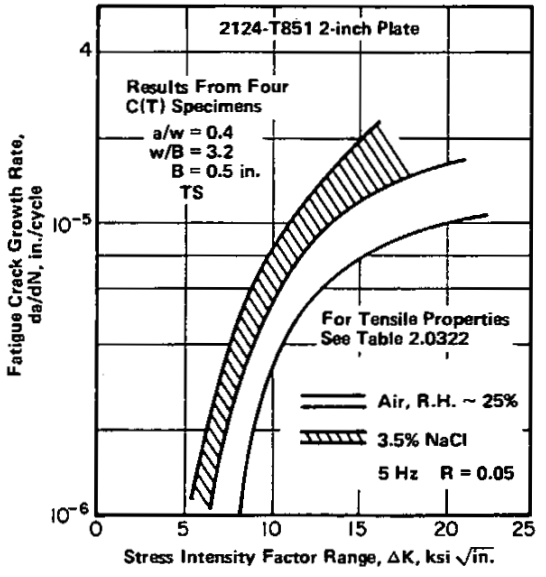


FIGURE 3.05219. FATIGUE CRACK-GROWTH RATES FOR 2124-T851 PLATE IN AIR AND IN 3.5 PERCENT NaCl FOR TS DIRECTION (16)

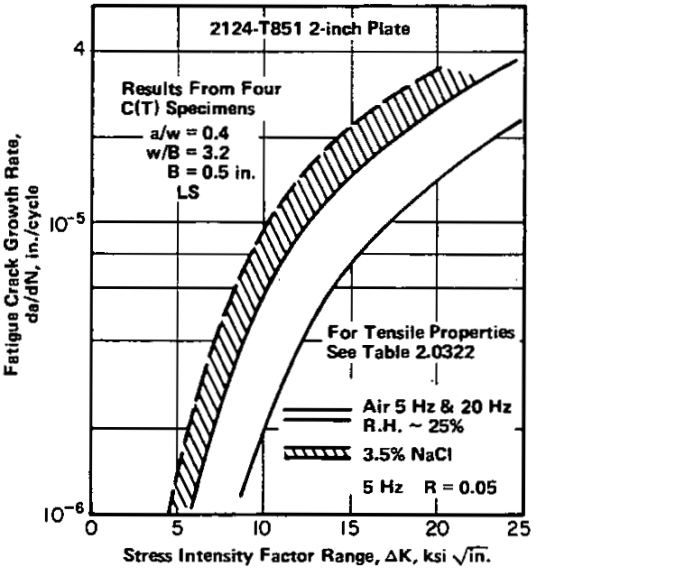


FIGURE 3.052110. FATIGUE CRACK-GROWTH RATES FOR 2124-T851 PLATE IN AIR AND IN 3.5 PERCENT NaCl FOR LS DIRECTION (16)

Al
4.4 Cu
1.5 Mg
0.6 Mn
2124 Al

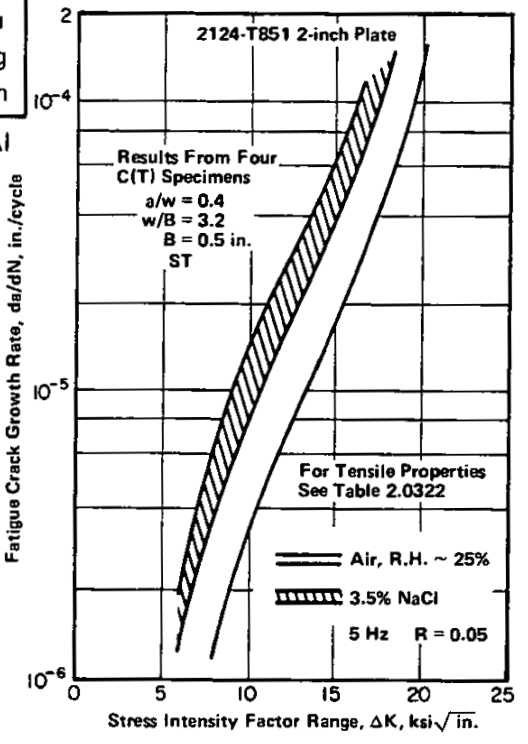


FIGURE 3.052111. FATIGUE CRACK-GROWTH RATES FOR 2124-T851 PLATE IN AIR AND IN 3.5 PERCENT NaCl FOR ST DIRECTION (16)

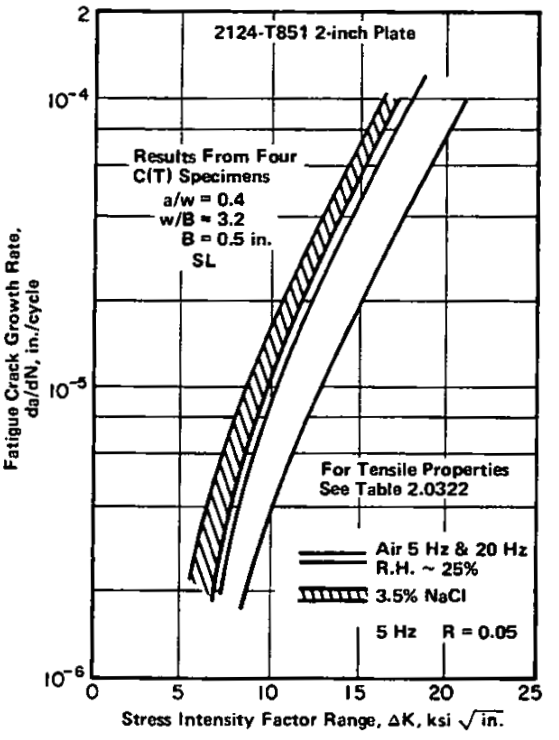


FIGURE 3.052112. FATIGUE CRACK-GROWTH RATES FOR 2124-T851 PLATE IN AIR AND IN 3.5 PERCENT NaCl FOR SL DIRECTION (16)

Alloy	2124-T851		
Form	5.5-inch Plate		
Direction	TL		
Location	Plate Center		
Specimen	Center Crack Tension M(T) W = 4 inch B = 0.5 inch with 4 Cracks Spaced ~8 inch Apart		
Environment	95 percent RH Air		
Frequency	30 to 35 Hz		
R Ratio	0.1	0.25	0.50
ΔK_{th}, ksi$\sqrt{in.}$(a)	2.8	2.0	1.4

(a) Lowest of observations on all cracks.

TABLE 3.052113. FATIGUE CRACK GROWTH THRESHOLD FOR 2124-T851 PLATE IN HIGH HUMIDITY AIR AT SEVERAL R RATIOS (32)

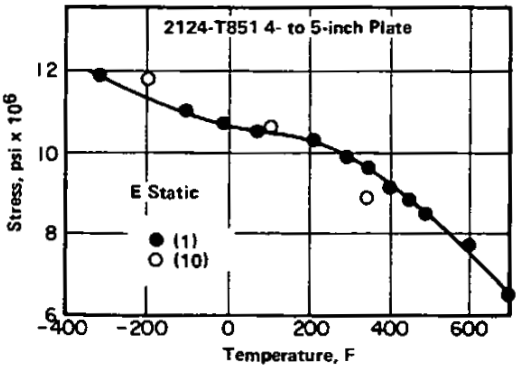


FIGURE 3.0621. MODULUS OF ELASTICITY AT LOW AND ELEVATED TEMPERATURES (1,10)

Al
4.4 Cu
1.5 Mg
0.6 Mn

2124 Al

Alloy	2124-T851					
Form	Plate					
	Tensile Modulus, 10^3 ksi			Compressive Modulus, 10^3 ksi		
Thickness, inch	L	T	ST	L	T	ST
1.750	10.49	10.48	10.05	10.90	11.02	10.84
2.500	10.45	10.50	10.35	10.98	10.84	10.81
3.500	10.39	10.38	10.47	10.84	10.94	10.87
4.500	10.37	10.59	10.45	10.77	11.04	10.84
5.500	10.55	10.53	10.47	10.85	10.90	10.86
Average	10.45	10.50	10.36	10.87	10.95	10.84

TABLE 3.0622. TENSILE AND COMPRESSIVE MODULUS OF ELASTICITY (6)

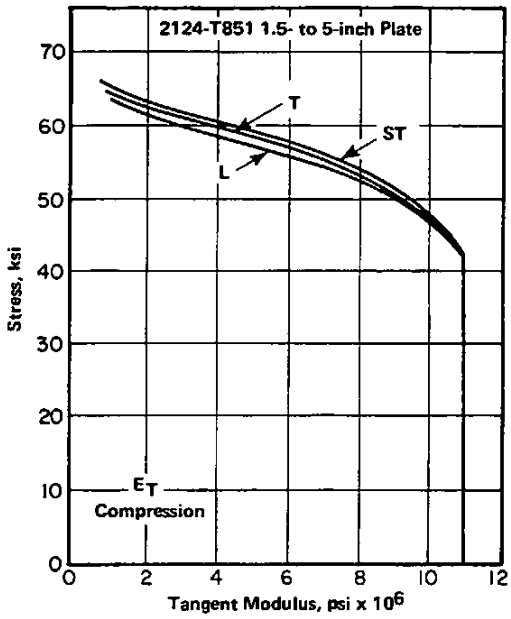


FIGURE 3.0641. TANGENT MODULUS CURVES FOR 2124-T851 PLATE (6)

Al
6.3 Cu
0.3 Mn
0.18 Zr
0.10 V
0.06 Ti

2219
CLAD 2219

1. GENERAL
The alloy was developed in 1954 to provide for applications at temperatures up to 600F. In the solution heat treated and aged condition this alloy exhibits typical mechanical properties in the 500-600F temperature range superior to those of any other commercially available aluminum alloy. The weldability of the alloy is excellent. Mechanical properties of welded and unwelded 2219 at temperatures down to -423F are also excellent. It is available in all wrought products, sheet, strip, plate and clad with 7072. Due to its low directionality tendencies it is well suited for forgings, (9).

1.01 Commercial Designations
2219, Clad 2219, (X2219 and Clad X2219, obsolete)

1.02 Alternate Designation
None.

1.03 Specifications
Table 1.03.

TABLE 1.03

AMS	FORM	CONDITION	MILITARY	ASTM
4031	Sheet and Plate	O	MIL-A-8920A	B209-64
	Sheet and Plate	F, T31, T351	MIL-A-8920A	B209-64
	Sheet and Plate	T37, T62, T81	MIL-A-8920A	B209-64
	Sheet and Plate	T851, T87	MIL-A-8920A	B209-64
4143	Forgings	T6	QQ-A-367F	B247-64
	Forgings	T852, T87	QQ-A-367F	—
—	Bar, rod, shapes	O, T62	—	B221-64
—	(tube extruded)	T8510, T8511	—	B221-64

1.04 Composition
1.041 Core material, Table 1.041.

TABLE 1.041

Source	AMS (8)	
	Percent	
	Min	Max
Copper	5.8	6.8
Iron	-	0.30
Magnesium	-	0.02
Manganese	0.20	0.40
Silicon	-	0.20
Titanium	0.02	0.10
Vanadium	0.05	0.15
Zinc	-	0.10
Zirconium	0.10	0.25
Others - Each	-	0.05
- Total	-	0.15
Aluminum	Balance	

1.042 Cladding, Table 1.042.

TABLE 1.042

Source	(11)	
Clad Alloy	7072 Alum. (a)	
	Percent	
	Min	Max
Zinc	0.8	1.3
Silicon + Iron	-	0.7
Manganese	-	0.1
Copper	-	0.1
Magnesium	-	0.1
Others		
Each	-	0.05
Total	-	0.15
Aluminum	Balance	

(a) The nominal cladding thickness per side is 10 percent of the total thickness of the composite if the latter is below 0.040 inch and 5 percent for a total thickness of composite products of 0.040 inch to 0.099 inch. For a total thickness of 0.100 inch or more the nominal cladding thickness on each side is 2.5 percent, (Ref. 3.3)

1.05 Heat Treatment
1.051 Anneal
1.0511 Heat treated conditions to O Condition. 750 to 775F, 2 to 3 hours, cool at 50F per hour down to 500F, (9).
1.0512 Intermediate anneal during repeated cold working O Condition. 650F, 30 minutes maximum. The same annealing treatment can be applied to heat treated material if only moderate forming is to be performed, (2).
1.052 Solution treat. 990 to 1010F, 20 minutes to 4 1/2 hours, depending on thickness and equipment, followed by an immediate cold water quench, (9). Maximum allowable quench delay times, Table 1.052.

TABLE 1.052

Source	(23)
Data	Max allowable quench delay times
Nominal thickness, inch	Max time, seconds
≤ 0.016	5
0.017 to 0.031	7
0.032 to 0.090	10
≥ 0.091	15

1.0521 If solution treatment is performed by supplier it is designated T4.
1.0522 If solution treatment is performed by user it is designated T42.
1.053 Modification of T4 by cold working, (9).
1.0531 T4 and stretch for sheet and drawn tube to T31.
1.0532 T4 and stretch 1.5 to 3% for plate to T351.
1.0533 T4 and stretch 1 to 3% for rod and bar to T351.
1.0534 T4 and cold work 2.5% for forgings to T352.
1.0535 T4 and stretch 1% for extrusions to T3511, T3510.
1.0536 T4 and cold work approximate 8% for sheet, plate and forgings to T37.
1.054 Modification of T4 by aging, (9).
1.0541 T4 and age 375F, 26 hours for forgings to T6.
1.0542 T4 and age 375F, 36 hours (18 hours for clad 2219) for sheet, plate, extrusions, drawn tube, rod and bar, to T62.
1.055 Modification of T3 by aging, (9).
1.0551 T31 and age 350F, 18 hours for sheet to T81.
1.0552 T31 and age 375F, 18 hours for drawn tube to T81.
1.0553 T351 and age 350F, 18 hours for plate to T851.
1.0554 T351 and age 375F, 18 hours for rod and bar to T851.
1.0555 T351 and age 350F, 18 hours for forgings to T832.
1.0556 T351 and age 357F, 18 hours for extrusions to T8511, T8510.
1.0557 T37 and age 325F, 24 hours for sheet, plate and hand forgings to T87.
1.056 Natural aging from T4.
1.0561 Effect of natural aging time on tensile properties of alloy in T4 Condition, Fig. 1.0561.

1.06 Hardness
1.061 Typical hardness values for various tempers sheet and plate, Table 1.061.

TABLE 1.061

Source	(9)				
Alloy	2219				
Form	Bare Sheet and Plate				
Condition	T31, T351	T37	T62	T81, T851	T87
BHN, typ 500 Kg load 10mm ball	96	110	113	123	128

1.07 Forms and Conditions Available
1.071 The alloy can be supplied in form of bar and clad sheet, strip and plate, bar, wire, forgings, tubing and extrusions in the full range of commercial sizes, (6).

Al
6.3 Cu
0.3 Mn
0.18 Zr
0.10 V
0.06 Ti

2219
CLAD 2219

1.072 Conditions available. Table 1.072.

TABLE 1.072

Source	(10)
Alloy	2219, Clad 2219
Form	Conditions Available
Sheet, plate-bare	O, T31, T351, T37, T62, T81, T851, T87
Sheet, plate-clad	O, T31, T351, T37, T62, T81, T851, T87
Wire, rod and bar	T851
Extruded rod, bar, shapes and tubes	O, T31, T3510, T3511, T62, T81, T8510, T8511
Hand forgings, die	T6
Rolled ring	T6

1.073 Components of clad plate and sheet. Table 1.073.

TABLE 1.073

Source	(10)		
Alloy	Clad 2219		
Cladding	7072		
Thickness - in	≥0.039	0.040 to 0.099	<0.100
Cladding thickness per side-%			
Nominal	10	5	2 1/2
Min-avg	8	4	2

1.08 Melting and Casting Practice

1.081 The impure ore (bauxite) is converted into pure aluminum oxide (alumina) by a series of chemical processes. Oxygen is removed from the alumina by smelting in carbon-lined electric furnaces (reduction pots). Pure molten aluminum is deposited at the bottom of the pot and is siphoned off periodically to form "pigs" and "sows". A separate furnace operation is used to form "alloy pig" from the pure aluminum by the addition of the desired alloying elements. This alloy metal is cast into ingots for further processing.

1.09 Special Considerations

1.091 Solution treating temperature should be closely controlled as higher temperatures may cause solid solution grain boundary melting or eutectic melting which cannot be repaired by subsequent heat treatment. Lower temperatures may result in a loss in hardening potential.

1.092 Rapid quenching after solution treatment is important because of possible precipitation which results in reduced corrosion resistance on slow cooling from the solution treat temperature.

1.093 Reheat treatment of clad material should be done carefully because copper tends to diffuse through the cladding to the surface, thereby decreasing corrosion resistance.

2. PHYSICAL AND CHEMICAL PROPERTIES

2.01 Thermal Properties

2.011 Melting range. 1010 to 1190F, (1).

2.012 Phase changes. Alloy is subject to precipitation hardening.

2.0121 Time-temperature-transformation diagrams.

2.013 Thermal conductivity at room temperature.
99 Btu ft per (hr sq ft F), O Condition
65 Btu ft per (hr sq ft F), T31, T37, T42 Conditions.
72 Btu ft per (hr sq ft F), T6, T62, T81, T87 Conditions, (9).

2.014 Thermal expansion, Fig. 2.014.

2.015 Specific heat at 212F, 0.23 Btu per (lb F), (9).

2.016 Thermal diffusivity

2.02 Other Physical Properties

2.021 Density, Fig. 2.021.

2.022 Electrical resistivity at room temperature. O Condition, 1.54 microhm-in; T31, T37, T42 Condition, 2.42 microhm-in, (9). Varies with chemical composition.

2.023 Magnetic properties. Alloy is nonmagnetic.

2.024 Emissivity

2.025 Damping capacity

2.026 Crystal structure. fcc.

2.03 Chemical Properties

2.031 Corrosion resistance. The alloy has about the same degree of resistance to atmospheric corrosion as other Al-Cu alloys, (see 2014 and 2024). When aged to T81 or T87 temper, the resistance to corrosion or stress corrosion cracking is similar to that of 2024-T6 and is considerably superior to 2014-T6. Corrosion characteristics of naturally aged tempers, T31 and T37 are similar to those of 2024-T3. For sheet thicknesses of 0.064 inch and greater, the corrosion resistance of the artificially aged tempers is superior to that of naturally aged tempers, (12).

2.0311 Effect of salt spray corrosion on tensile properties of sheet in various tempers, Fig. 2.0311.

2.04 Nuclear Properties

3. MECHANICAL PROPERTIES

3.01 Specified Mechanical Properties

3.011 AMS specified mechanical properties for sheet and plate, Table 3.011.

TABLE 3.011

Source		(8)			
Alloy		2219			
Form		Sheet and Plate			
Condition		O		Solution and precipitation heat treatment	
Thickness - in		0.040 to 0.499	0.499 to 2.00	0.040 to 1.000	1.000 to 2.000
F_{tu},	-min-ksi*	30	30	54	56
F_{ty},	-min-ksi*	16	-	36	36
e(2 in)	-min-%	12		6	6

* Maximum for O Condition

3.012 AMS specified mechanical properties for forgings, Table 3.012.

TABLE 3.012

Source	(8)						
Alloy	2219						
Form	Die forgings		Hand forgings			Rolled rings	
Condition	T6						
Thickness - in	≤ 4.00		≤4.00		2.375 to 4.00*	≤2.5	
Direction	L	T	L	T	ST	Tang.	Axial
F_{tu}, -min*-ksi	58	53	58	55	53	56	55
F_{ty}, -min*-ksi	38	35	40	37	35	40	37
e(2 in) -min -%	7	3	6	4	2	6	4

* Applicable only for thickness range shown.

Al
6.3 Cu
0.3 Mn
0.18 Zr
0.10 V
0.06 Ti

2219
CLAD 2219

3.013 Aluminum Association mechanical property limits for sheet and plate, Table 3.013.

TABLE 3.013

Source	(10)							
Alloy	2219							
Form	Sheet and plate							
Condition	O	T31	T31, T351	T37	T62	T81	T81, T851	T87
Width - in	All							
Thickness - in	0.020-2.000	0.020-0.249	0.250-6.000	0.020-5.000	0.020-2.000	0.020-0.249	0.250-6.000	0.020-5.000
F_{tu}, -min*-ksi	32.0	46.0	46.0-39.0	49.0-43.0	54	59.0-61.0	61.0-54.0	63.0-57.0
F_{ty}, -min*-ksi	16.0	29.0-28.0	28.0-25.0	38.0-34.0	36	44.0	44.0-41.0	50.0-47.0
e(2 in), -min -%	12	8-10	10-8	6-4	6	6	6-4	5-3

* Maximum for O Condition

3.014 Aluminum Association mechanical property limits for clad sheet and plate, Table 3.014.

TABLE 3.014

Source	(10)							
Alloy	Clad 2219							
Form	Clad sheet and plate							
Condition	O	T31	T31, T351	T37	T62	T81	T81, T851	T87
Width-in	All							
Thickness-in	0.040-2.000	0.040-0.249	0.250-0.499	0.040-0.499	0.040-0.499	0.040-0.249	0.250-0.499	0.040-0.499
F_{tu}, -min*-ksi	32.0	42.0-44.0	44	45.0-47.0	47.0-51.0	55.0-58.0	58.0	57.0-59.0
F_{ty}, -min*-ksi	16.0	25.0-26.0	26	34.0-35.0	32.0-34.0	40.0-42.0	42.0	46.0-48.0
e(2 in), -min- %	12	10	10	6	6	6	6	5

* Maximum for O Condition

3.015 Aluminum Association mechanical property limits for rolled or cold finished wire, rod and bar and extruded rod, bar, shapes and tubes, Table 3.015.

TABLE 3.015

Source	(10)							
Alloy	2219							
Form	Rolled or CF wire, rod and bar		Extruded rod, bar, shapes and tube					
Condition	T851		O	T31, T3510, T3511		T62		T81, T8510, T8511
Area - sq in	-		All	≤ 25		≤ 25	≤ 32	≤ 25
Thickness or Dia - in	0.500 - 2.000	2.001 - 4.000	All	≤ 0.499	0.500-2.999	≤0.999	≥ 1.000	≤ 2.999
F_{tu}, -min*-ksi	58	57	32	42	45	54		58
F_{ty}, -min*-ksi	40	39	18	26	27	36		42
e(in) -min -%	4	4	12	14	14	6		6

* Maximum for O Condition

3.016 Aluminum Association mechanical property limits for die forgings, hand forgings and rolled rings, Table 3.016.

TABLE 3.016

Source	(10)										
Alloy	2219										
Form	Die forgings		Hand forgings						Rolled rings		
Condition	T6		T6			T852			T6		
Thickness - in	≤4.00		≤ 4.00						≤ 2.500		
Direction	L	T	L	LT	ST	L	LT	ST	Tang.	Axial	Radial
F_{tu}, -min-ksi	58	56	58	55	53	62	62	60	56	55	53
F_{ty}, -min-ksi	38	36	40	37	35	50	49	46	40	37	35
e(2 in) -min-%	10	4	6	4	2	6	4	3	6	4	2

3.02 Mechanical Properties at Room Temperature

3.021 Tension

3.0211 Stress-strain diagrams. (See 3.0311).

3.0212 Typical tensile properties, Table 3.0212.

TABLE 3.0212

Source	(9)											
Alloy	2219											
Form	Sheet and plate											
Condition	O	T42	T31, T351		T37		T62		T81, T851		T87	
Direction	T	T	L	T	L	T	L	T	L	T	L	T
F_{tu}, typ -ksi	25	50	52	52	56	56	58	58	66	66	68	68
F_{ty}, typ -ksi	11	25	36	34	45	44	40	40	50	50	56	56
e(2 in), typ -%	18	20	20	16	12	10	10	10	10	10	10	10

	Al
6.3	Cu
0.3	Mn
0.18	Zr
0.10	V
0.06	Ti

2219
CLAD 2219

3.0213 Effect of exposure to elevated temperatures on tensile properties of forged rod in T6 Condition, Fig. 3.0213.
3.0214 Effect of exposure to elevated temperatures on tensile properties of plate in T6 Condition, Fig. 3.0214.
3.0215 Effect of exposure on tensile properties of plate in T62 Condition, Fig. 3.0215.
3.0216 Effect of exposure on tensile properties of sheet and plate in T81 and T851 Condition, Fig. 3.0216.
3.0217 Effect of exposure on tensile properties of plate in T87 Condition, Fig. 3.0217.
3.022 Compression
3.0221 Stress-strain diagrams
3.0222 Typical compressive yield strength, Table 3.0222.

TABLE 3.0222

Source	(9)					
Alloy	2219					
Form	Sheet and plate					
Condition	T62		T81, T851		T87	
Direction	L	T	L	T	L	T
F_{cy}, typ - ksi	44	44	53	54	57	60

3.023 Impact. See 3.033.
3.024 Bending
3.025 Torsion and shear
3.0251 Typical ultimate shear strength, Table 3.0251.

TABLE 3.0251

Source	(9)		
Alloy	2219		
Form	Sheet and plate		
Condition	T62	T81, T851	T87
F_{su}, typ. - ksi	36	38	40

3.026 Bearing
3.0261 Typical bearing properties, Table 3.0261.

TABLE 3.0261

Source	(9)					
Alloy	2219					
Form	Sheet and plate					
Condition	T62		T81, T851		T87	
e/D	1.5	2.0	1.5	2.0	1.5	2.0
F_{bru}, typ. - ksi	90	120	96	125	100	131
F_{bry}, typ. - ksi	67	80	76	87	80	90

3.027 Stress concentration. See 3.037.
3.0271 Notch properties
3.0272 Fracture toughness
3.028 Combined properties

3.03 Mechanical Properties at Various Temperatures
3.031 Tension
3.0311 Stress-strain diagrams
3.03111 Stress-strain curves for alloy in T6 Condition at room and elevated temperatures, Fig. 3.03111.
3.03112 Stress-strain curves for T62 sheet at low temperatures, Fig. 3.03112.
3.03113 Stress-strain curves for T81 sheet at low temperatures, Fig. 3.03113.
3.03114 Stress-strain curves for T87 sheet at low temperatures, Fig. 3.03114.
3.0312 Exposure time effect on tensile properties
3.03121 Effect of exposure and test temperature on tensile properties of alloy in T6 Condition, Fig. 3.03121.
3.03122 Effect of test temperature and exposure time on tensile properties of plate in T6 Condition, Fig. 3.03122.
3.03123 Effect of test temperature and exposure time on tensile properties of sheet and plate in T81 and T851 Condition, Fig. 3.03123.
3.03124 Effect of test temperature and exposure time on tensile properties of plate in T87 Condition, Fig. 3.03124.
3.03125 Effect of test temperature and exposure time on tensile properties of forgings in T6 Condition, Fig. 3.03125.
3.0313 Effect of test temperature on minimum tensile properties of alloy in T62 and T81 Conditions, Fig. 3.0313.
3.0314 Effect of test temperature on tensile properties of alloy in T6 and T62 Conditions, Fig. 3.0314.
3.0315 Effect of low temperature on tensile properties of sheet in T62 Condition, Fig. 3.0315.
3.0316 Effect of low temperature on tensile properties of sheet in T81 Condition, Fig. 3.0316.
3.0317 Effect of low temperature on tensile properties of sheet and plate in T87 Condition, Fig. 3.0317.
3.0318 Effect of elevated temperature on the tensile properties of sheet in T81 Condition, Fig. 3.0318.
3.0319 Effect of test temperature on tensile properties of extrusion in T6 Condition, Fig. 3.0319.
3.032 Compression
3.0321 Stress-strain diagrams
3.0322 Effect of test temperature on compressive yield stress of sheet and plate in the T62 Condition, Fig. 3.0322.
3.033 Impact
3.0331 Effect of low temperature on impact strength of plate in T87 Condition, Fig. 3.0331.
3.034 Bending
3.035 Torsion and shear
3.0351 Effect of test temperature on shear strength of sheet and plate in T62 Condition, Fig. 3.0351.
3.0352 Effect of low temperature on shear strength of sheet in various conditions, Fig. 3.0352.
3.036 Bearing
3.0361 Effect of test temperature on bearing properties of sheet in T31 and T81 Conditions, Fig. 3.0361.
3.037 Stress concentration
3.0371 Notch properties
3.03711 Effect of low temperature on tensile and notch properties of alloy in T87 Condition, Fig. 3.03711.
3.03712 Effect of stress concentration factor on low temperature notch strength of sheet and plate, Fig. 3.03712.
3.0372 Fracture toughness
3.03721 Effect of test temperature on net fracture strength of T81 sheet, Fig. 3.03721.
3.038 Combined properties

3.04 Creep and Creep Rupture Properties
3.041 Creep rupture curves for extrusion in T6 Condition at 400 and 600F, Fig. 3.041.
3.042 Creep and creep rupture curves for plate and forging in T6, T87 and T851 Conditions at room temperature, Fig. 3.042.
3.043 Creep and creep rupture curves for plate and forgings in T6, T62, T87 and T851 Conditions at 300F, Fig. 3.043.
3.044 Creep and creep rupture curves for forgings in T6 Condition from 400F to 700F, Fig. 3.044.
3.045 Creep and creep rupture curves for plate in T62, T851, and T87 Conditions from 400F to 700F, Fig. 3.045.
3.046 Creep and creep rupture curves for sheet in T81 Condition from 300F to 600F, Fig. 3.046.
3.047 Creep curves for clad sheet in T6 Condition at 400F, Fig. 3.047.
3.048 Creep curves for clad sheet in T6 Condition at 500F, Fig. 3.048.
3.049 Creep curves for clad sheet in T6 Condition at 600F, Fig. 3.049.

3.05 Fatigue Properties
3.051 Fatigue strength of alloy in T6 Condition at room and elevated temperatures, Table 3.051.

TABLE 3.051

Source	(3)							
Alloy	2219							
Form	Forged rod							
Condition	T6							
Temp - F	Method	Stress Ratio		Fatigue Strength - ksi at Cycles				
		A	R	10^5	10^6	10^7	10^8	5×10^8
RT	Rot Beam	∞	-1	30	25	21	18.5	17.5
300				27	22	17.5	14.5	13.5
400				25	20	15	12	11
500				22	17	12	9	8
600				18	13	9	7	6.5

3.052 Fatigue strength of extrusion in T6 Condition at 400 and 600F, Table 3.052.

TABLE 3.052

Source	(5)						
Alloy	2219						
Form	Extrusion						
Condition	T6						
Thickness-in	Temp-F	Method	Stress Ratio		Fatigue Strength-ksi at Cycles		
			A	B	10^5	10^6	10^7
1 1/2	400	Direct stress	+1	0	36	28	22
	600				25	20	14
1/8	600				25	20	16

3.053 Fatigue limit in rotating beam tests at 5×10^8 cycles, Table 3.053.

TABLE 3.053

Source	(9)	
Alloy	2219	
Form	Sheet and plate	
Condition	T62, T81, T851, T87	
Temp - F	Method	Fatigue limit-5×10^8 cycles
RT	Rot beam	15 ksi

3.054 S-N curves for smooth and notched specimens of plate in T81 Condition, Fig. 3.054.

3.055 S-N curves for forgings in T6 Condition at 400 and 600F, Fig. 3.055.

3.056 S-N curves for sheet in T87 Condition at room temperature and low temperatures, Fig. 3.056.

3.06 Elastic Properties

3.061 Poisson's ratio

3.062 Modulus of elasticity

3.0621 Modulus of elasticity for all Conditions at room temperature, $E = 10.6 \times 10^3$ ksi, (9).

3.0623 Modulus of elasticity at various temperatures for forgings in T6 Condition, Fig. 3.0623.

3.0624 Modulus of elasticity at various temperatures for sheet and plate in various Conditions, Fig. 3.0624.

3.0625 Modulus of elasticty at low temperature of sheet in T81 Condition, Fig. 3.0625.

3.063 Modulus of rigidity

3.0631 Design value of modulus of rigidity at room temperature for sheet and plate, $G = 4.0 \times 10^3$ ksi, (9).

4. FABRICATION

4.01 Formability

4.011 General. The alloy exhibits equal or superior formability characteristics to 2024 and 7075 for comparable tempers, (22).

4.012 Forging. Forgings are made using either the open die or closed die methods and by impact or pressure. Small runs are made using the hand forging open die techniques. Hand forgings over a ton in weight can be made.

4.013 Cold forming. The formability of the alloy in sheet and plate is directly related to the temper strength and ductility. Suggested minimum bend radii of sheet and plate in various tempers, Table 4.013.

Al
6.3 Cu
0.3 Mn
0.18 Zr
0.10 V
0.06 Ti

2219
CLAD 2219

4.02 Machining and Grinding

4.021 The alloy has good machining qualities in the annealed state. Since most of the machining is done in the heat treated conditions, lathe tools should be ground to 10-20° side rake and 8-10° clearance. Parting tools should have a 15-20° top rake with a 4-5° side rake. Planer and shaper tools for roughing cuts should have a 12-15° top rake, 32-38° side rake and a 8-10° front and side clearance. Finishing tools should have a 45-50° top rake, 50-60° side rake, 8-10° front clearance and little or no side clearance. Twist drills should have larger spiral angles than standard, highly polished deep flutes, narrow bands, and up to 18° lip clearance. Threading taps should have highly polished flutes and should be under cut. Spiral fluted taps are usually better than straight fluted. The rake angles should be increased to 12-18°. Soluble oil emulsions, kerosene, and kerosene-lard oil mixtures are recommended for most machining operations, but high viscosity lubricants are recommended for tapping operations, (22).

4.03 Welding

4.031 General. The alloy can be satisfactory welded by fusion and resistance welding techniques. Brazing, gas welding and soldering are not considered suitable techniques for joining the alloy, (9).

4.032 Fusion welding. Fusion welding of the alloy using 2319 alloy filler and the inert gas metal arc welding process has been found to be superior to any other heat treatable alloy of similar strength. The alloy is very similar to 6061 using 4043 filler with respect to ease of welding. Direct fusion welds are entirely practicable without the use of filler metal, (9).

TABLE 4.013

Source	(9)									
Alloy	2219									
Form	Sheet and plate									
Thickness - in Condition	Minimum bend radii for 90° cold bends									
	1/64	1/32	1/16	1/8	3/16	1/4	3/8	1/2	3/4	1
0	0		1/2 - 1 1/2t			1-2t		2-3t		3-4t
T42	0-1t		1-2t		1 1/2-2 1/2t		2-3t	2 1/2-3 1/2t	3-4t	3 1/2-4 1/2t
T31	1/2 - 1 1/2t	1 - 2t	1 1/2-2 1/2t	1 1/2 - 3t	2-4t		2 1/2-4t	3-5t		
T37	1/2 - 1 1/2t	1 - 2t	1 1/2-3t	2 1/2 - 4t	3 - 4 1/2t	3 1/2-5t	4-6t	5-7t		
T62, T81	2 - 3 1/2t	2 1/2 - 4t	3-5t	4-6t		5-7t		6-9t		
T87	2 1/2 - 4t	3- 5t	4-6t	5-7t	5 1/2-8t	6-9t	7-10t	8-11t		

4.0321 Welds in the alloy have high tensile efficiency and good ductility following a post weld heat treatment. Typical mechanical properties of butt welds, Table 4.0321.

TABLE 4.0321

Source	(9)			
Alloy	2219			
Form	Butt welded sheet and plate			
Condition	T81, T87	T31	-	-
After welding	As welded	Aged to T81 or T87	Reheat and Aged to T62	Reheat, shot peened and aged to T81
F_{tu}, typ-ksi	41	45	57	63
F_{ty}, typ-ksi	30	39	39	49
e(2in) type-%	3	2	8	8

Al	
6.3	Cu
0.3	Mn
0.18	Zr
0.10	V
0.06	Ti

2219
CLAD 2219

4.033 Resistance welding. The alloy can be successfully spot and seam welded using machine schedules similar to those established for 2014 and 2024 alloys. Conventional pre-cleaning practices are used. Shear strength of resistance welds is in the same range as obtained with 2014 and 2024 alloys. (9).

4.04 Heat Treatment

4.05 Surface Treatment

4.051 The same techniques used for anodizing, hard coating, and producing conversion coatings on 2024 and 2014 can be used on this alloy. (9).

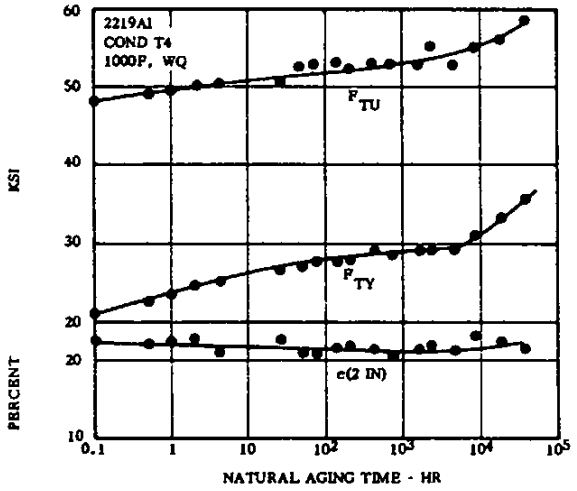


FIG. 1.0561 EFFECT ON NATURAL AGING TIME ON TENSILE PROPERTIES OF ALLOY IN T4 CONDITION (9, p. 26)

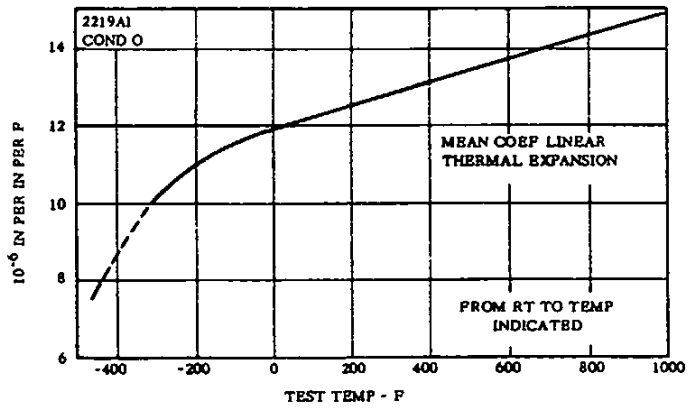


FIG. 2.014 THERMAL EXPANSION (11)

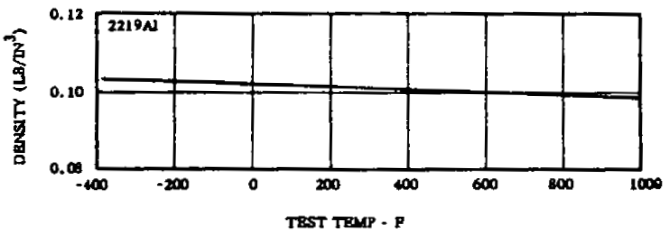


FIG. 2.021 DENSITY (11)

	Al
6.3	Cu
0.3	Mn
0.18	Zr
0.10	V
0.06	Ti

2219
CLAD 2219

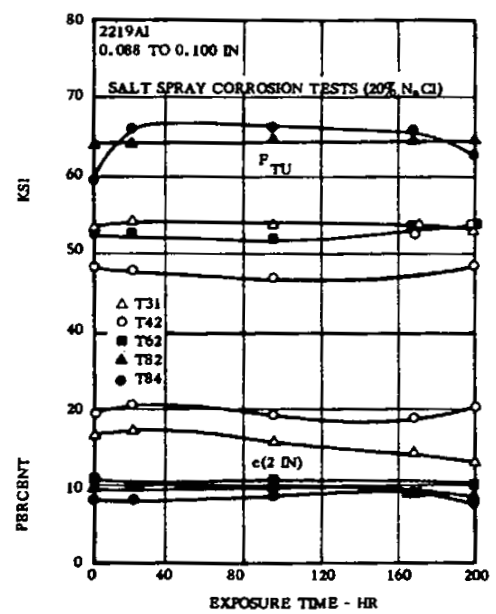


FIG. 2.0311 EFFECT OF SALT SPRAY CORROSION ON TENSILE PROPERTIES OF SHEET IN VARIOUS TEMPERS

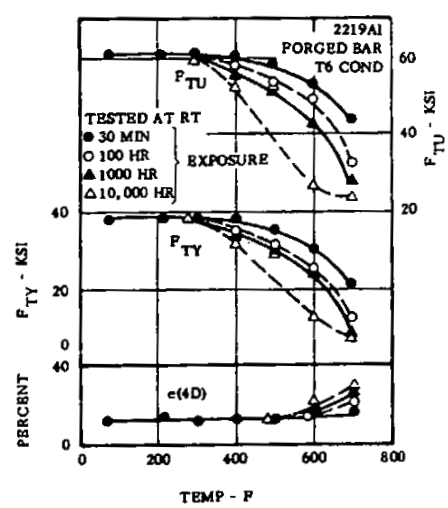


FIG. 3.0213 EFFECT OF EXPOSURE TO ELEVATED TEMPERATURES ON TENSILE PROPERTIES OF FORGED ROD IN T6 CONDITION (3)

Al
6.3 Cu
0.3 Mn
0.18 Zr
0.10 V
0.06 Ti

2219
CLAD 2219

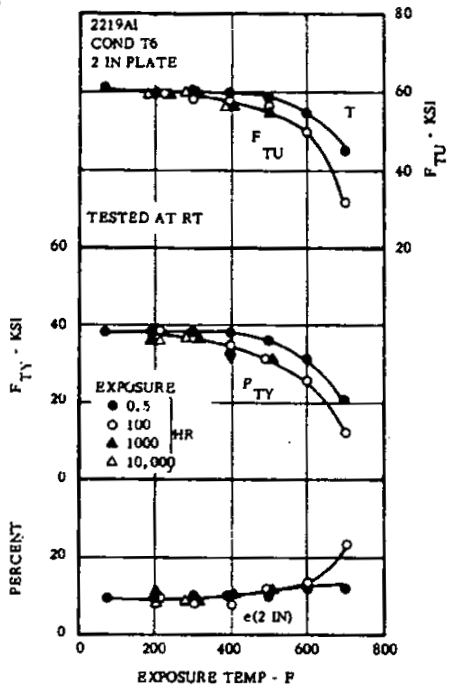


FIG. 3.0214 EFFECT OF EXPOSURE ON TENSILE PROPERTIES OF PLATE IN T6 CONDITION (13)

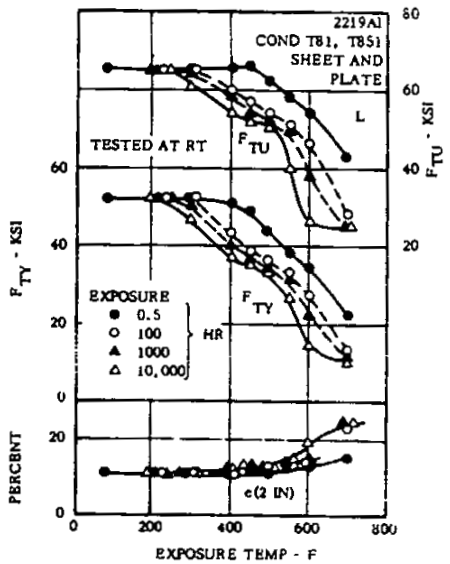


FIG. 3.0216 EFFECT OF EXPOSURE ON TENSILE PROPERTIES OF SHEET AND PLATE IN T81 AND T851 CONDITION (9, p. 15)

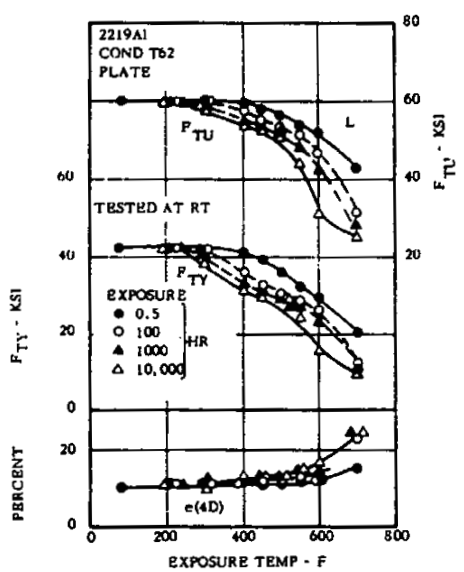


FIG. 3.0215 EFFECT OF EXPOSURE ON TENSILE PROPERTIES OF PLATE IN T62 CONDITION (9, p. 14)

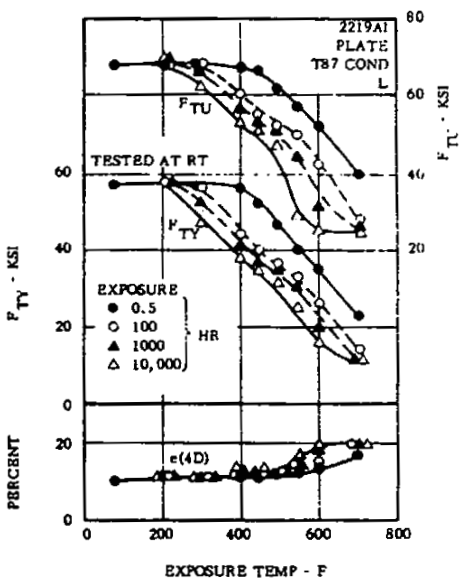


FIG. 3.0217 EFFECT OF EXPOSURE ON TENSILE PROPERTIES OF PLATE IN T87 CONDITION (9, p. 17)

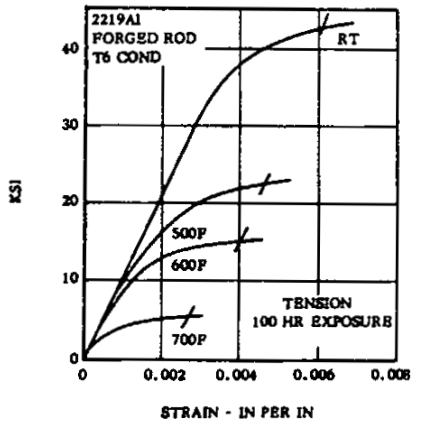
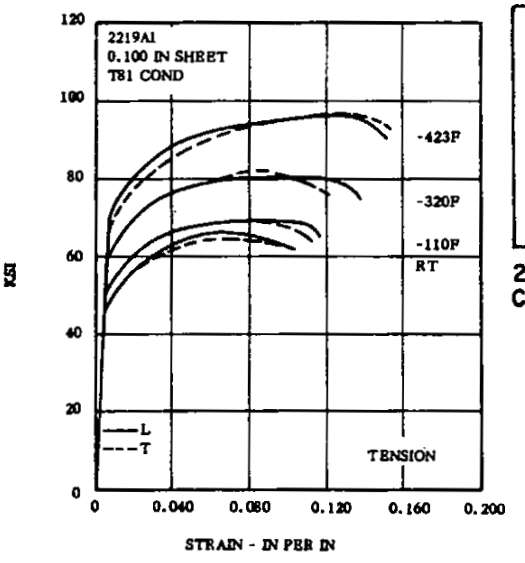


FIG. 3.03111 STRESS-STRAIN CURVES FOR ALLOY IN T6 CONDITION AT ROOM AND ELEVATED TEMPERATURES (4, p. 144)



Al
6.3 Cu
0.3 Mn
0.18 Zr
0.10 V
0.06 Ti

2219
CLAD 2219

FIG. 3.03113 STRESS-STRAIN CURVES FOR T81 SHEET AT LOW TEMPERATURES (14, p. A.5.h-2, A-5.h-3)

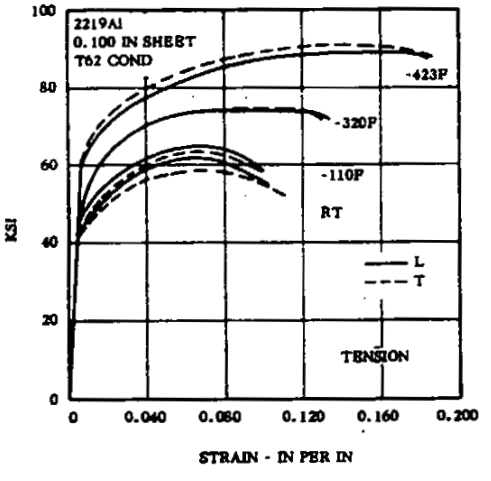


FIG. 3.03112 STRESS-STRAIN CURVES FOR T62 SHEET AT LOW TEMPERATURES (14, p. A.5.h, A.5.h-1)

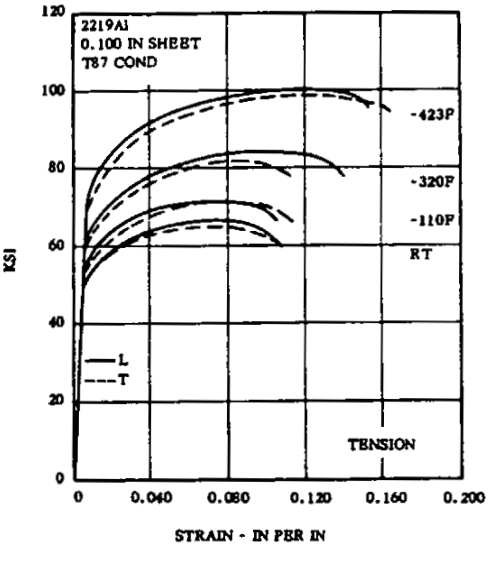


FIG. 3.03114 STRESS-STRAIN CURVES FOR T87 SHEET AT LOW TEMPERATURES (14, p. A.5.h-4, A.5.h-5)

Al
6.3 Cu
0.3 Mn
0.18 Zr
0.10 V
0.06 Ti

2219
CLAD 2219

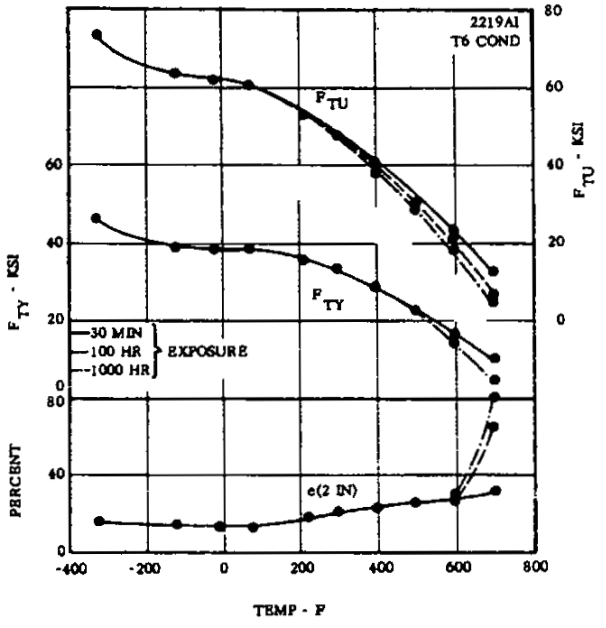


FIG. 3.03121 EFFECT OF EXPOSURE AND TEST TEMPERATURE ON TENSILE PROPERTIES OF ALLOY IN T6 CONDITION (3)

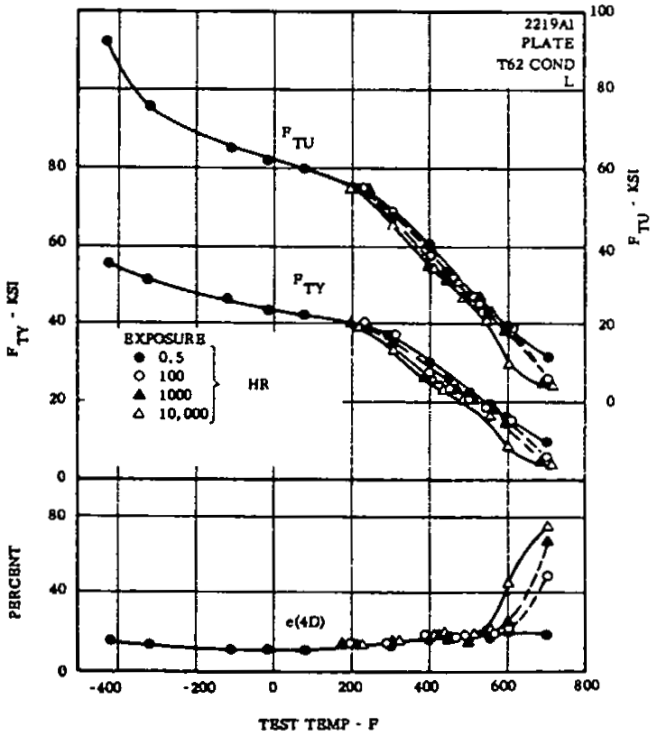


FIG. 3.03122 EFFECT OF TEST TEMPERATURE AND EXPOSURE TIME ON TENSILE PROPERTIES OF PLATE IN T6 CONDITION (9, p. 14)

Al
6.3 Cu
0.3 Mn
0.18 Zr
0.10 V
0.06 Ti

2219
CLAD 2219

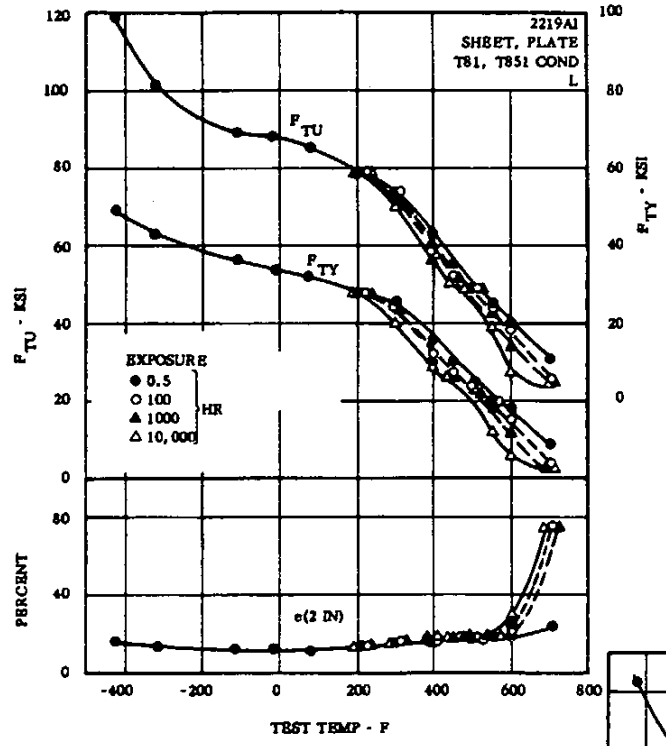


FIG. 3.03123 EFFECT OF TEST TEMPERATURE AND EXPOSURE TIME ON TENSILE PROPERTIES OF SHEET AND PLATE IN T81 AND T851 CONDITION (9, p.15)

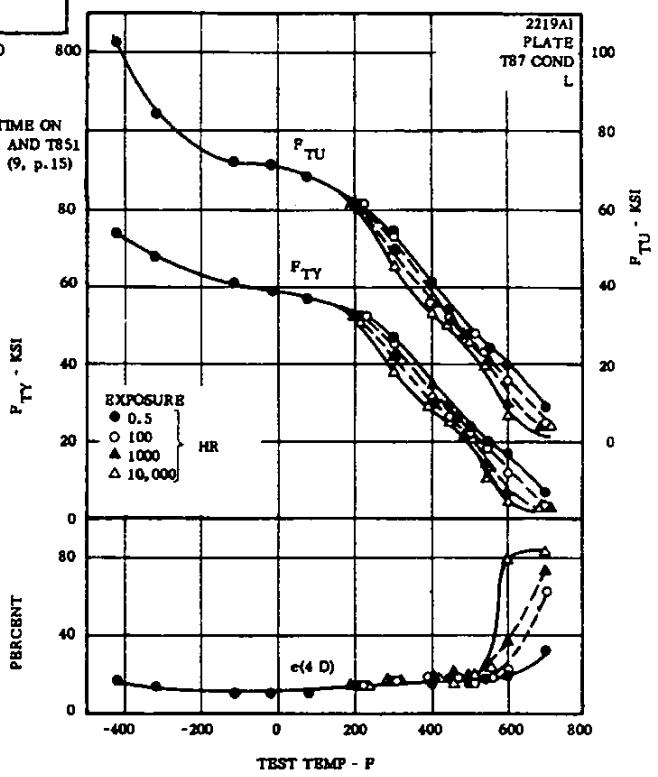


FIG. 3.03124 EFFECT OF TEST TEMPERATURE AND EXPOSURE TIME ON TENSILE PROPERTIES OF PLATE IN T87 CONDITION (9, p.17)

Al
6.3 Cu
0.3 Mn
0.18 Zr
0.10 V
0.06 Ti

2219
CLAD 2219

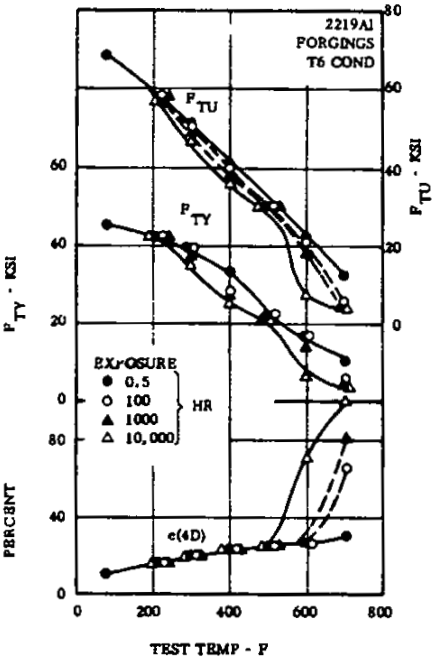


FIG. 3.0312S EFFECT OF TEST TEMPERATURE AND EXPOSURE TIME ON TENSILE PROPERTIES OF FORGINGS IN T6 CONDITION (9,p.18)

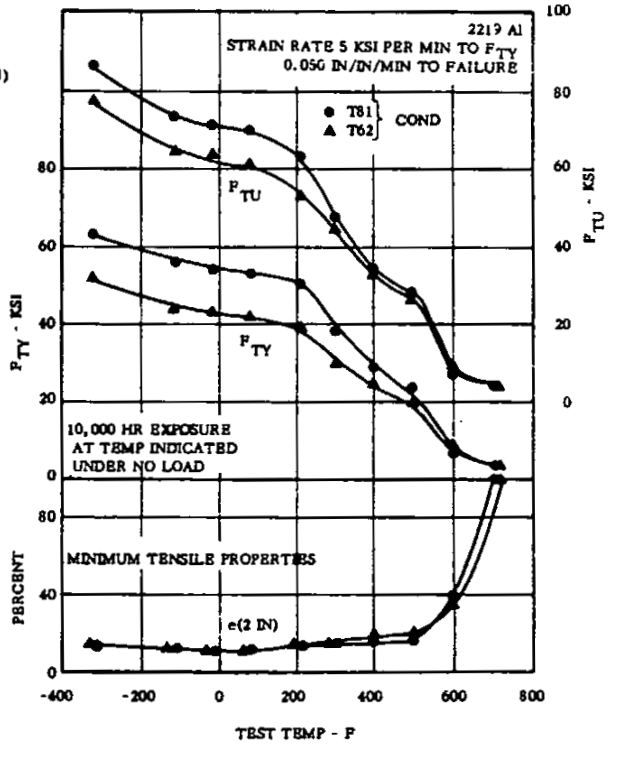


FIG. 3.0313 EFFECT OF TEST TEMPERATURE ON MINIMUM TENSILE PROPERTIES OF ALLOY IN T62 AND T81 CONDITIONS (11, p. 30)

	Al
6.3	Cu
0.3	Mn
0.18	Zr
0.10	V
0.06	Ti

2219
CLAD 2219

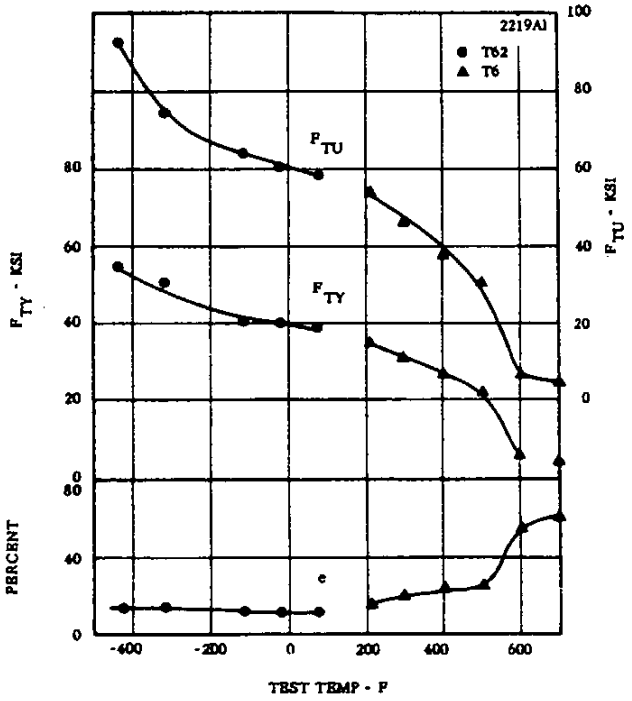


FIG. 3.0314 EFFECT OF TEST TEMPERATURE ON TENSILE PROPERTIES OF ALLOY IN T6 AND T62 CONDITION (15, p. 45, 49)

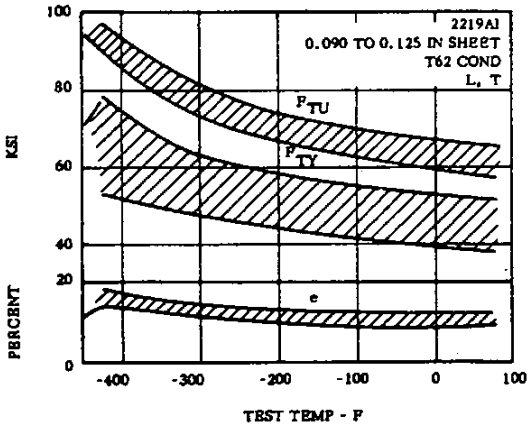


FIG. 3.0315 EFFECT OF LOW TEMPERATURE ON TENSILE PROPERTIES OF SHEET IN T62 CONDITION (14, p. A. 5. A, A. 5. b, A. 5c, A. 5c-1)

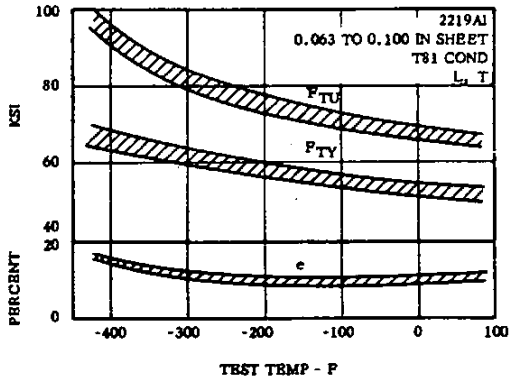


FIG. 3.0316 EFFECT OF LOW TEMPERATURE ON TENSILE PROPERTIES OF SHEET IN T81 CONDITION (14, p. A. 5a-1, A. 5. b-1, A. 5b-2, A. 5c-2, A. 5c-3)

Al
6.3 Cu
0.3 Mn
0.18 Zr
0.10 V
0.06 Ti

2219
CLAD 2219

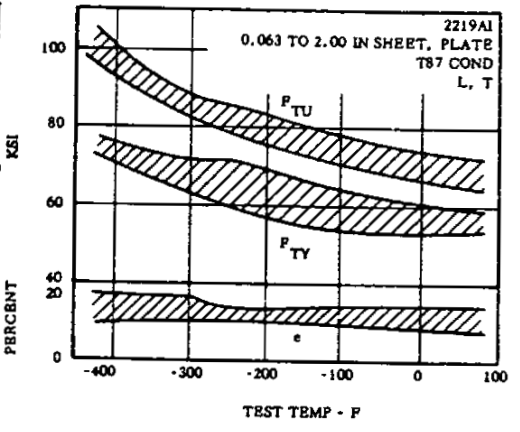


FIG. 3.0317 EFFECT OF LOW TEMPERATURE ON TENSILE PROPERTIES OF SHEET AND PLATE IN T87 CONDITION (14, p. A.5a-2, A.5b-3, A.5c-4)

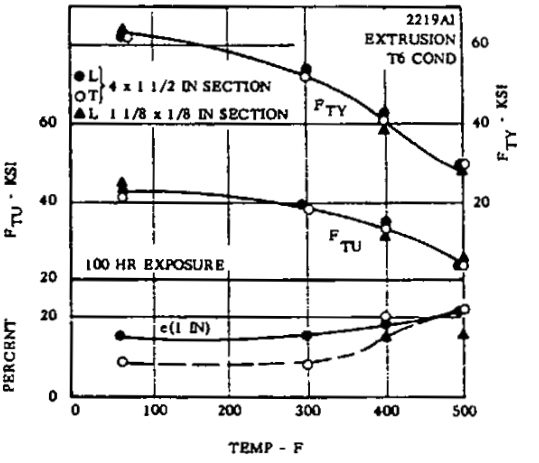


FIG. 3.0319 EFFECT OF TEST TEMPERATURE ON TENSILE PROPERTIES OF EXTRUSION IN T6 CONDITION (5, p. 8, 9)

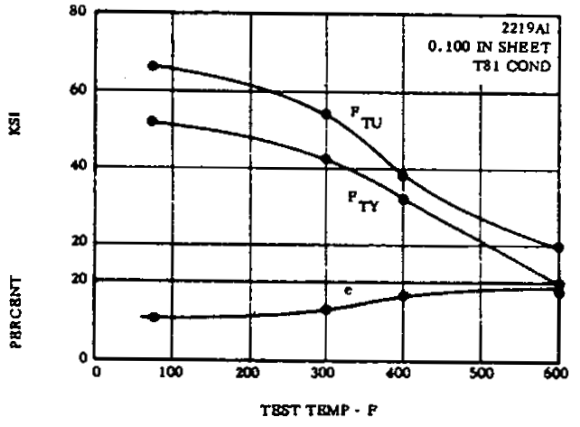


FIG. 3.0318 EFFECT OF ELEVATED TEMPERATURE ON THE TENSILE PROPERTIES OF SHEET IN T81 CONDITION (16)

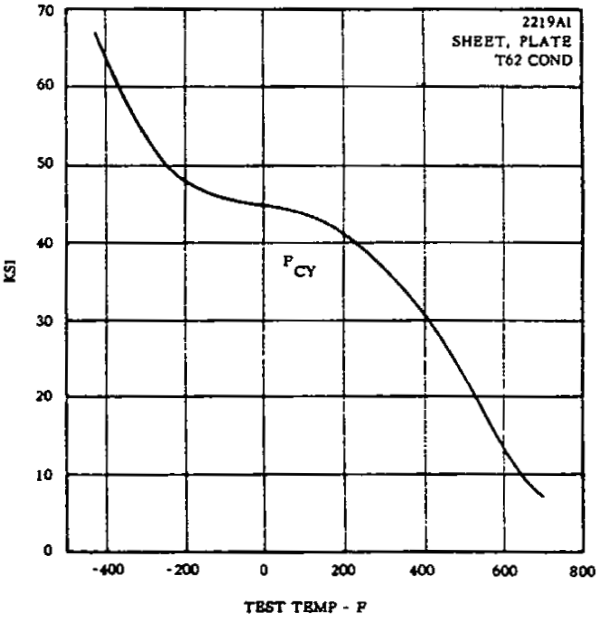


FIG. 3.0322 EFFECT OF TEST TEMPERATURE ON COMPRESSIVE YIELD STRESS OF SHEET AND PLATE IN THE T62 CONDITION (17)

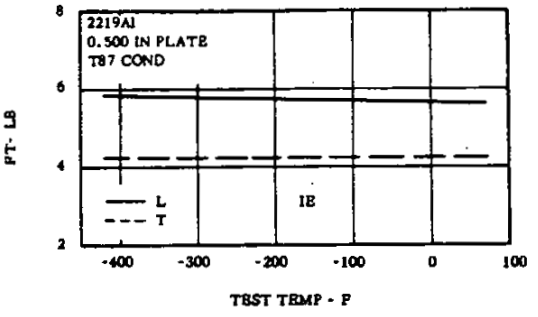
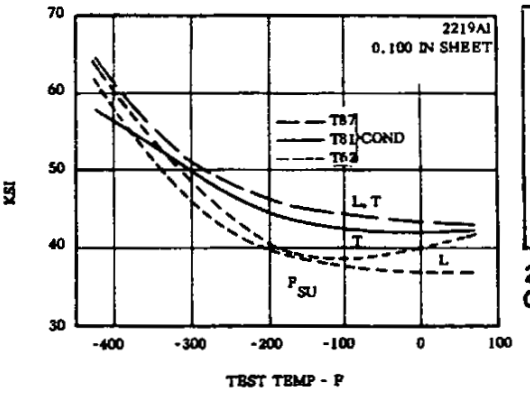


FIG. 3.0331 EFFECT OF LOW TEMPERATURE ON IMPACT STRENGTH OF PLATE IN T87 CONDITION (14, p. A.5.j)



Al
6.3 Cu
0.3 Mn
0.18 Zr
0.10 V
0.06 Ti

2219
CLAD 2219

FIG. 3.0352 EFFECT OF LOW TEMPERATURE ON SHEAR STRENGTH OF SHEET IN VARIOUS CONDITIONS (14, p. A.5p, A.5.p)

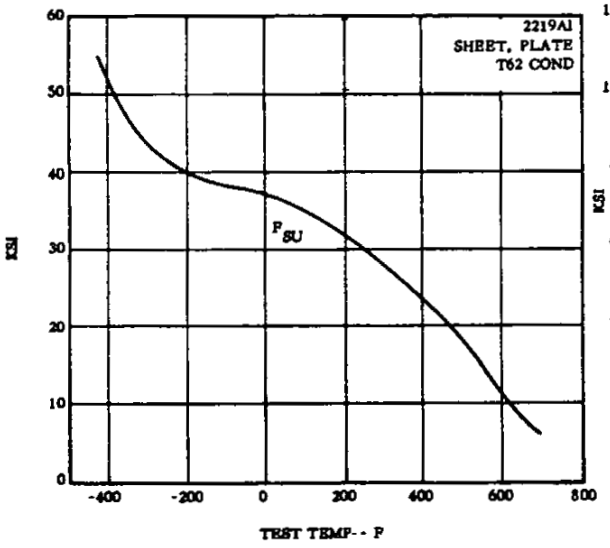


FIG. 3.0351 EFFECT OF TEST TEMPERATURE ON SHEAR STRENGTH OF SHEET AND PLATE IN T62 CONDITION (17)

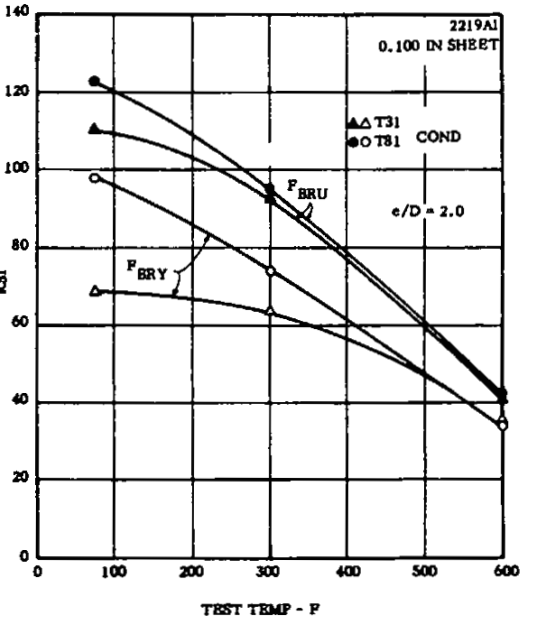


FIG. 3.0361 EFFECT OF TEST TEMPERATURE ON BEARING PROPERTIES OF SHEET IN T31 AND T81 CONDITIONS (16)

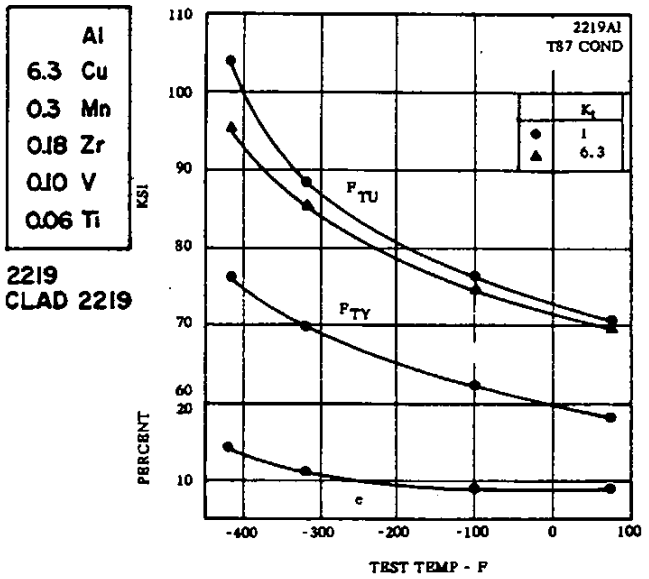


FIG. 3.03711 EFFECT OF LOW TEMPERATURE ON TENSILE AND NOTCH PROPERTIES OF ALLOY IN T87 CONDITION (18)

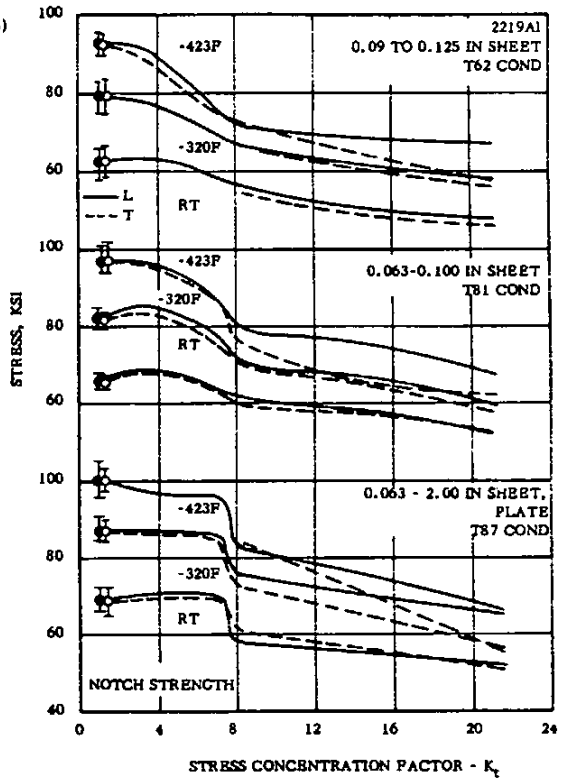


FIG. 3.03712 EFFECT OF STRESS CONCENTRATION FACTOR ON LOW TEMPERATURE NOTCH STRENGTH OF SHEET AND PLATE (14, p. A.5.e)

Al
6.3 Cu
0.3 Mn
0.18 Zr
0.10 V
0.06 Ti

2219
CLAD 2219

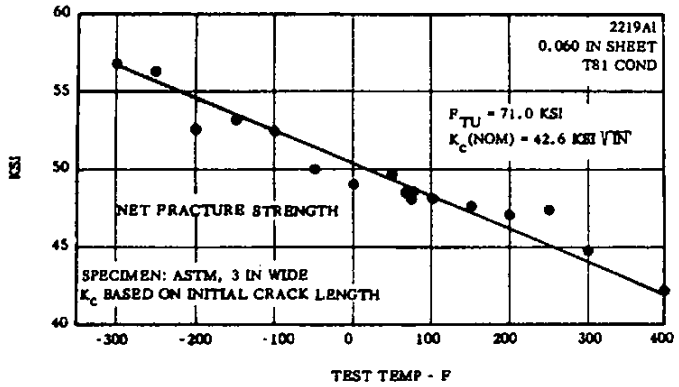


FIG. 3.03721 EFFECT OF TEST TEMPERATURE ON NET FRACTURE STRENGTH OF T81 SHEET

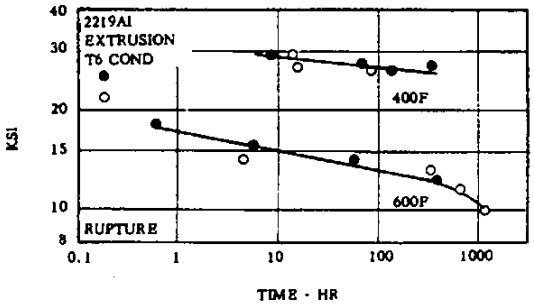


FIG. 3.041 CREEP RUPTURE CURVES FOR EXTRUSION IN T6 CONDITION AT 400 AND 600F (5, p. 13)

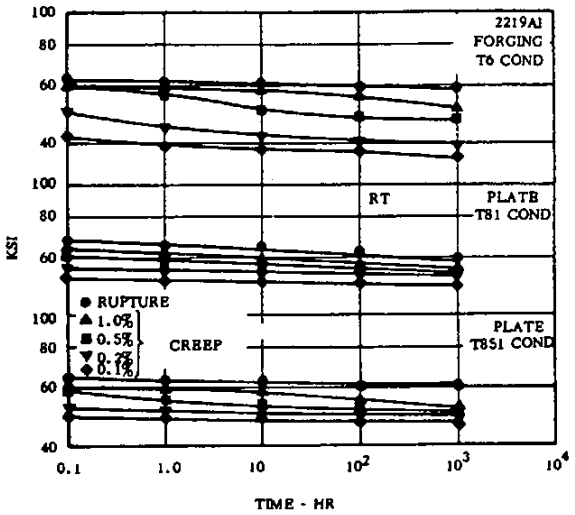


FIG. 3.042 CREEP AND CREEP RUPTURE CURVES FOR PLATE AND FORGING IN T6, T87 AND T851 CONDITIONS AT ROOM TEMPERATURE (9, p. 16, 17, 18)

Al
6.3 Cu
0.3 Mn
0.18 Zr
0.10 V
0.06 Ti

2219
CLAD 2219

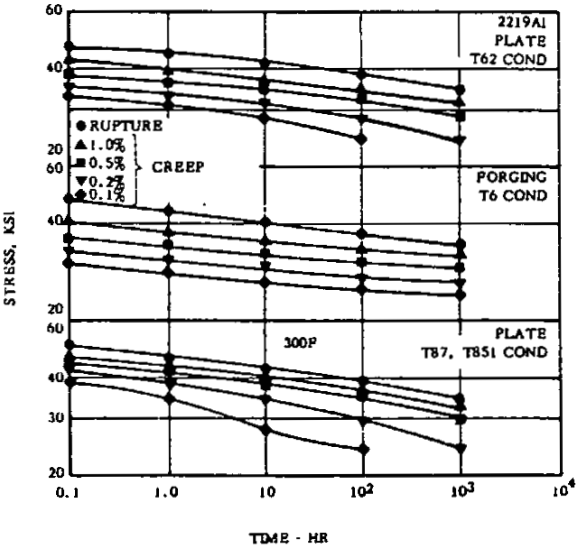


FIG. 3.043 CREEP AND CREEP RUPTURE CURVES FOR PLATE AND FORGING IN T6, T62, T87 AND T851 CONDITIONS AT 300F (9, p. 14, 16, 17, 18)

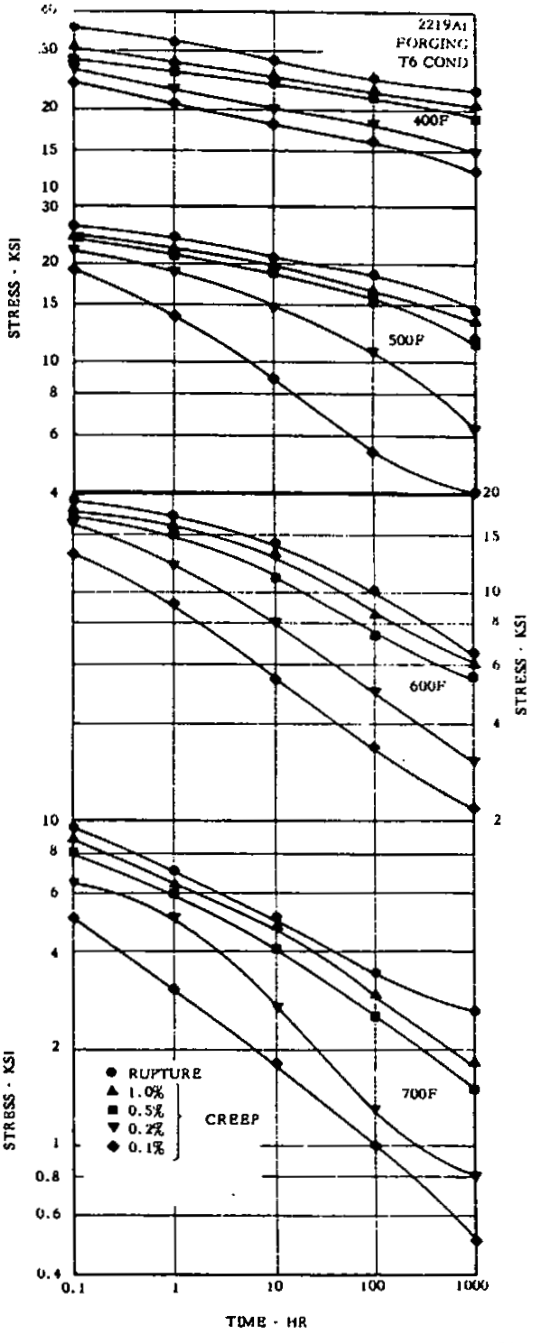


FIG. 3.044 CREEP AND CREEP RUPTURE CURVES FOR FORGINGS IN T6 CONDITION FROM 400F TO 700F (9, p. 18)

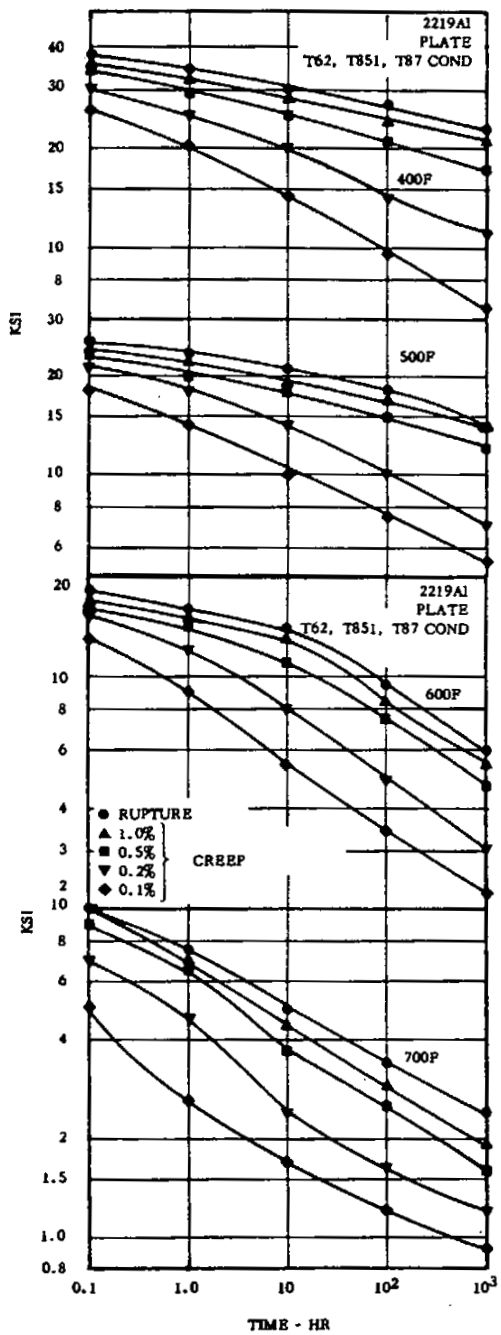
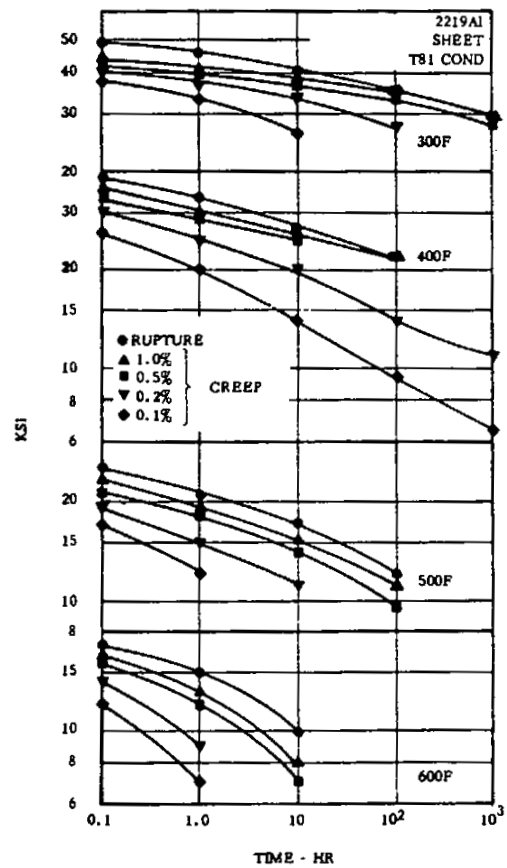


FIG. 3.045 CREEP AND CREEP RUPTURE CURVES FOR PLATE IN T62, T851 AND T87 CONDITIONS FROM 400F TO 700F (9, p. 14, 16, 17)



Al
6.3 Cu
0.3 Mn
0.18 Zr
0.10 V
0.06 Ti

2219
CLAD 2219

FIG. 3.046 CREEP AND CREEP RUPTURE CURVES FOR SHEET IN T81 CONDITION FROM 300F TO 600F (9, p. 15)

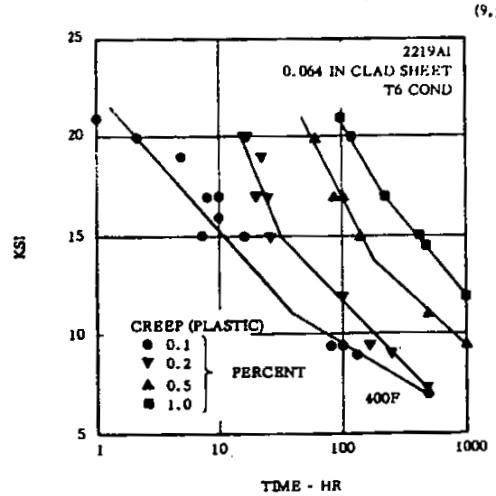


FIG. 3.047 CREEP CURVES FOR CLAD SHEET IN T6 CONDITION AT 400F (19)

Al
6.3 Cu
0.3 Mn
0.18 Zr
0.10 V
0.06 Ti

2219
CLAD 2219

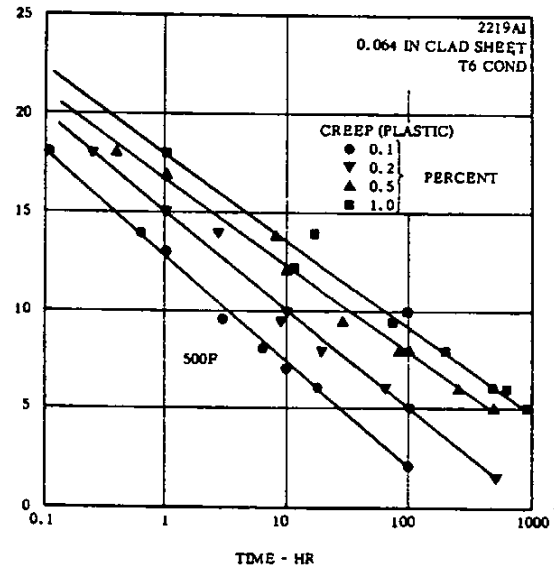


FIG. 3.048 CREEP CURVES FOR CLAD SHEET IN T6 CONDITION AT 500F (19)

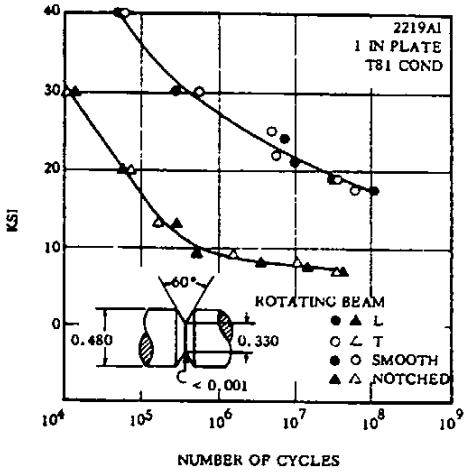


FIG. 3.054 S-N CURVES OF SMOOTH AND NOTCHED SPECIMENS OF PLATE IN T81 CONDITION (9, p. 22)

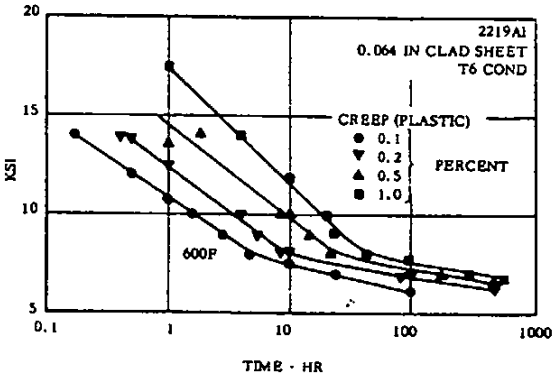


FIG. 3.049 CREEP CURVES FOR CLAD SHEET IN T6 CONDITION AT 600F (19)

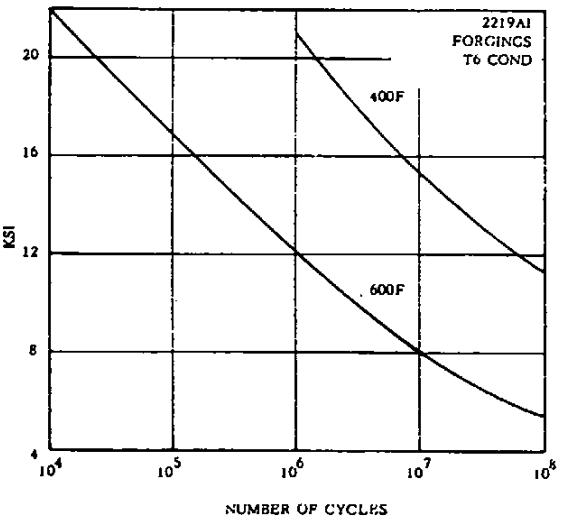


FIG. 3.055 S-N CURVES FOR FORGINGS IN T6 CONDITION AT 400 AND 600F (20)

	Al
6.3	Cu
0.3	Mn
0.18	Zr
0.10	V
0.06	Ti

2219
CLAD 2219

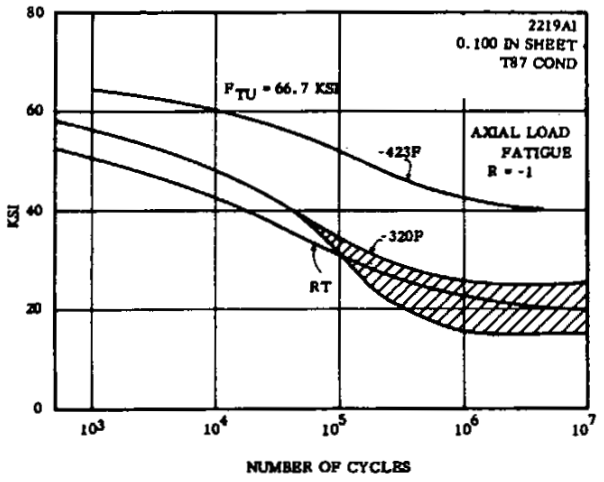


FIG. 3.056 S-N CURVES FOR SHEET IN T87 CONDITION AT ROOM TEMPERATURE AND LOW TEMPERATURES (14, p. A.5.0)

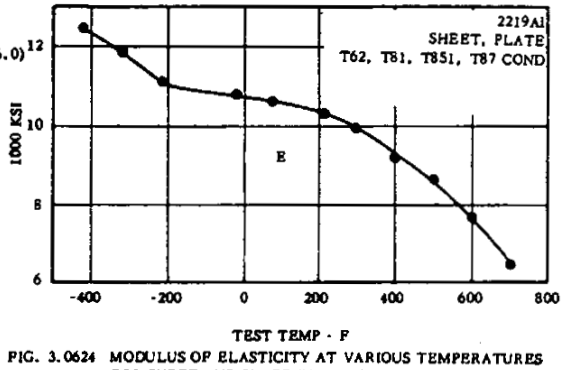


FIG. 3.0624 MODULUS OF ELASTICITY AT VARIOUS TEMPERATURES FOR SHEET AND PLATE IN VARIOUS CONDITIONS (9, p. 14-17)

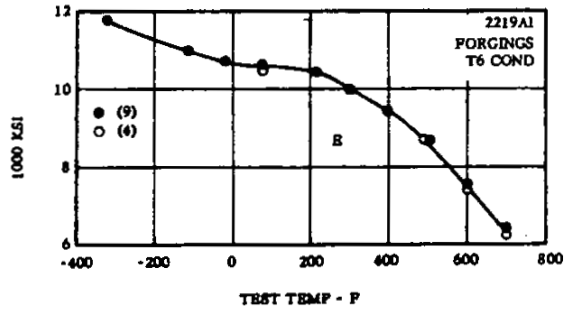


FIG. 3.0623 MODULUS OF ELASTICITY AT VARIOUS TEMPERATURES FOR FORGINGS IN T6 CONDITION (4, p. 144)(9, p. 18)

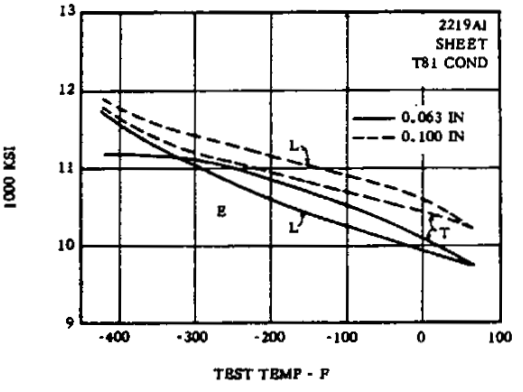


FIG. 3.0625 MODULUS OF ELASTICITY AT LOW TEMPERATURE OF SHEET IN T81 CONDITION (14, p. A.51, A.5.1-1)

	Al
6.3	Cu
0.3	Mn
0.18	Zr
0.10	V
0.06	Ti

2219
CLAD 2219

REFERENCES

1 Aluminum Co. of America, "Aluminum Sheet and Plate General Information, Mechanical and Physical Properties", Product Data, Sec. AC2A, (Dec. 1, 1961)

2 Aluminum Co. of America, "Alcoa Alloy 2219", Development Div., (Mar. 28, 1959)

3 Aluminum Co. of America, Research Laboratories, Data Sheet, (May 24, July 25, 1957)

4 Achbach, W.P., Favor, R.J. and Hyler, W.S., "Material-Property-Design Criteria for Metals", WADC TR 55-150, Part VI, (Oct. 1955)

5 Hendricks, P.L., "Metallurgical Investigation of Aluminum Alloy X-2219-T6", WADC TN 58-57, (June 1958)

6 Guy, D.M., Jr., "Personal Letter", Aluminum Co. of America, (May 28, 1959)

7 Brennecke, M. W., "Welding Characteristics of X-2219 Alloy", Aluminum Co. of America, Research Laboratories, Rep. No. 2-58-11a, (May 15, 1958)

8 AMS 4031, (June 30, 1962)
AMS 4143, (Feb. 15, 1965)

9 Mayer, L.W., "Aluminum Alloy 2219", Alcoa Green Letter, (Nov. 1963)

10 "Standards for Aluminum Mill Products", Aluminum Association, (Sept. 1965)

11 "Alcoa Aluminum Handbook", Aluminum Co. of America, (1962)

12 Nock, J. A. et al, "A New High Strength Aluminum Alloy ", Metal Progress, Vol. 80, No.2, (Sept. 1961)

13 "The Elevated Temperature Properties of Aluminum and Magnesium Alloys", ASTM STP 291, (1960)

14 Schwartzberg, F.R. et al, "Cryogenic Materials Data Handbook", ML-TDR-64-280, August 1964 and Progress Rep. No. 1, (Feb. 1965)

15 "The Aluminum Data Book", Reynolds Metals Co., (1965)

16 "Summary Information Regarding Aluminum Alloy 2219", Martin-Denver Evaluation Report No. 1, MI-64-44, (Nov. 1961)

17 "Materials Properties Data Book", Report No. 2275 to AEC-NASA, Nerva Program, Aerojet-General Corp. (Revised July 1964)

18 Christian, J.L. et al, "Structural Alloys for Cryogenic Service", Metal Progress, Vol. 83, No. 3, (March 1963)

19 Mahorter, R.G., Jr. and Emmons, W.F., "A Study of Creep Resistance, Formability and Heat Treatment of Clad X-2219-T6 Aluminum Alloy", Report No. NAMC-AML-AE 1100, Naval Air Materials Center, (August 1959)

20 Dix, E.H., Jr., "Aluminum Alloys for Elevated Temperature Applications", ASME Paper No. 56-AV-8, (1956)

21 Kaiser Aluminum and Chemical Sales, Inc., "Alloy Technical Data", (March 15, 1964)

22 Alloy Digest, "Aluminum 2219", Filing Code Al-96, (Oct. 1960)

23 Military Specification, "Heat Treatment of Aluminum Alloys", MIL-H-6088C, (October 15, 1962)

NONFERROUS ALLOYS

	Al
2.5	Cu
1.5	Mg
1.2	Ni
1.0	Fe
0.2	Si
0.1	Ti

2618

1. GENERAL

The 2618 aluminum alloy is a wrought alloy which responds to an age-hardening heat treatment. This alloy, originally developed for forging applications, has been used primarily in this form in the aircraft industry. It exhibits medium strength and ductility, fair resistance to general corrosion, and has good elevated temperature properties. Optimum composition and heat treating methods promote a high resistance to intercrystalline corrosion. The formability and machinability of the alloy are good.
Room temperature strength of this alloy is better than 2014-T6 but slightly lower than 7075-T6.
The 2618 alloy is presently used for large aircraft engine components and compressor blades. It is being considered for structural applications in supersonic aircraft as forged gas-turbine engine impellers, spacer rings, pistons and structural forgings. This alloy is available in wrought forms (1)(2)(8)(15).

1.01 Commercial Designation
Al 2618

1.02 Alternate Designations
Hiduminium RR, 58 (British)
AU2GN (French)

1.03 Specifications
1.031 Foreign, British Aircraft DTD 5070A
1.032 AMS and Federal Specifications, Table 1.032.

TABLE 1.032

AMS	Form	Federal
4132A	Die forgings, rolled rings, hand forgings, and forging stock (Condition T61)	QQ-A-367

1.04 Composition
Table 1.04

TABLE 1.04

Source	(1)(5)	
	Percent	
	Min	Max
Copper	1.9	2.7
Iron	0.9	1.3
Magnesium	1.3	1.8
Nickel	0.9	1.2
Silicon	-	0.25
Titanium	0.04	0.10
Other	-	
Each	-	0.05
Total		0.15
Aluminum	Balance	

1.05 Heat Treatment
1.051 All forms. Anneal 775F, 2 to 3 hours, furnace cool 50F per hour to 500F, air cool (5).
1.052 Forgings and rolled rings.
1.0521 Solution treatment, 975 to 995F, hold for 6 hours minimum at temperature, boiling water quench (BWQ) to age condition T4 (1)(5).
1.0522 Age condition T4 385 to 395F, 20 hours to condition T61, (4)(5).
1.053 Sheet (DTD 5070A).
1.0531 Solution treatment and age. 975 to 985F, hold for 5 minutes to 1 hour at temperature (depending on gauge), cold water quench:
Age 365 to 385F, 10 to 30 hours (12). Sheet should be quenched in water not exceeding 104F and sheet 0.028 inch thick or less should only be solution treated once (2).

1.06 Hardness

1.07 Forms and Conditions Available
1.071 This alloy has been available in the past in all wrought forms, such as clad and unclad sheet, plates, extrusions, and forgings (2)(8). Current producer production is generally limited to forging forms (1)(4).

1.08 Melting and Casting Practice

1.09 Special Considerations

2. PHYSICAL AND CHEMICAL PROPERTIES

2.01 Thermal Properties
2.011 Melting range.
2.012 Phase changes.
2.0121 Time-temperature-transformation diagrams.
2.013 Thermal conductivity. 82.1 Btu ft per (hr sq ft F) (2).
2.014 Thermal expansion. Figure 2.014.
2.015 Specific heat. 0.22 Btu per (lb F) (2).
2.016 Thermal diffusivity.

2.02 Other Physical Properties
2.021 Density. 0.0999 lb per cu in 2.76 gr per cu cm (2).
2.022 Electrical properties:
Condition O 1.44 microhm-inch at RT
Condition T61 2.60 microhm-inch at RT
2.023 Magnetic properties. This alloy is non-magnetic.
2.024 Emissivity.
2.025 Damping capacity.

2.03 Chemical Properties
2.031 Tests on 2618-T61 forging material indicate the alloy is susceptible to stress corrosion cracking in the transverse grain directions. Longitudinal bend specimens stressed to 75 percent of their yield strength did not fail after 12 weeks of alternate immersion testing in 3 1/2 percent NaCl solution, 10 minute immersion and 50 minute air dry. However, approximately half of the long transverse specimens stressed to 75 percent yield strength failed over the time period of 4 to 8 days while the remainder did not fail within the 12 week period, and all the short transverse specimens stressed to 75 percent yield strength failed over the period of 4 to 20 days (17).

	Al
2.5	Cu
1.5	Mg
1.2	Ni
1.0	Fe
0.2	Si
0.1	Ti

2618

2.04 Nuclear Properties

3. MECHANICAL PROPERTIES

3.01 Specified Mechanical Properties

3.011 AMS specified mechanical properties, Table 3.011.

TABLE 3.011

Source	(1)				
Alloy	Al-2.5Cu-1.5Mg-1.2Ni-1.0Fe-0.2Si-0.1Ti				
Condition	T61				
Form	Die Forgings (≤4 In)			Rolled Rings (≤4 In)	
	From Stock (a)	From Forgings			
		L	T	Tangential	Axial
F_{tu} (min) - Ksi	58	58	55	55	55
F_{ty} (min) - Ksi	48	48	45	41	44
e (4D) (min) - Percent	6	4	4(b)	6	5
Hardness (min) BHN (500 Kg), (10 mm ball)	115	115			

(a) Stock representative of the forging

(b) Diameter > 0.25 with axis in plane parallel to parting plane

3.012 Producer's guaranteed mechanical properties, Table 3.012.

TABLE 3.012

Source	(5)				
Alloy	Al-2.5Cu-1.5Mg-1.2Ni-1.0Fe-0.2Si-0.1Ti				
Condition	T61				
Form	Hand Forgings ≤ 16 square inch section			Rolled Rings ≤ 2 1/2 inch radial thickness	
Direction	L	LT	ST	Tangential	Axial
F_{tu} (min) - Ksi	58	55	52	55	55
F_{ty} (min) - Ksi	45	42	42	41	41
e(4D) (min) Percent	7	5	4	6	5

3.02 Mechanical Properties at Room Temperature

3.021 Tension.

3.0211 Stress strain diagrams, see 3.0311.

3.0212 Tensile properties of clad sheet, Table 3.0212.

TABLE 3.0212

Source	(2)	
Alloy	Al-2.5Cu-1.5Mg-1.2Ni-1.0Fe-0.2Si-0.1Ti	
Form	Clad Sheet	
Condition	CR + 977 to 995F, 1 Hr, WQ (Cold), flattened + 392F, 20 Hr	
Direction	T	L
F_{tu}, -ksi	57.5	58.0
F_{ty}, (0.1 percent)-ksi	49.0	50.5
e (2 in)-percent	6.0	7.0
E, 10^3 ksi	10.5	10.5

3.0213 Effect of exposure time and temperature on room temperature tensile properties of forged bar, Figure 3.0213.

3.0214 Effect of elevated temperature exposure and exposure time on tensile properties of forging, Figure 3.0214.

3.022 Compression.

3.0221 Stress-strain curve for clad sheet in compression, Figure 3.0221.

3.0222 Compressive properties of clad sheet, Table 3.0222.

TABLE 3.0222

Source	(2)	
Alloy	Al-2.5Cu-1.5Mg-1.2Ni-1.0Fe-0.2Si-0.1Ti	
Form	Clad Sheet	
Condition	CR + 986F, 1 Hr, WQ (Cold); Flattened + 392F, 20 Hr	
Direction	T	L
F_{cy}, (0.1 percent) ksi	52.0	51.0
(0.3 percent) ksi	53.5	53.0
E_c, 10^3 x ksi	10.5	10.5

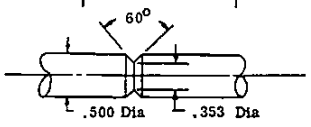
	Al
2.5	Cu
1.5	Mg
1.2	Ni
1.0	Fe
0.2	Si
0.1	Ti

2618

3.023 Impact.
3.024 Bending.
3.025 Torsion and shear.
3.0251 Effect of thickness and heat treatment on shear stress of forged bar, Figure 3.0251.
3.0252 Effect of thickness and heat treatment on shear stress of forged bar, Figure 3.0252.
3.026 Bearing, see 3.036.
3.027 Stress concentration.
3.0271 Notch properties.
3.02711 Effect of specimen cross section location on sharp notch strength ratio of forged alloy, Figure 3.02711.
3.02712 Typical notch strength properties of alloy plate, Table 3.02712.

TABLE 3.02712

Source	(18)	
Alloy	Al-2.5Cu-1.5Mg-1.2Ni-1.0Fe-0.2Si-0.1Ti	
Form	Plate	
Nominal Thickness	1.356	
Condition	2618-T651	
Direction	L	T
F_{tu} - Ksi	62.4	61.1
F_{ty} - Ksi	57.6	54.6
Notch Strength	81.2	83.2



Notch-Root Radius $\leq$ 0.0005, $K_t \geq$ 16

3.0272 Fracture toughness.
3.028 Combined properties.

3.03 Mechanical Properties at Various Temperatures
3.031 Tension.
3.0311 Stress-strain diagrams.
3.03111 Stress-strain curves at elevated temperature for clad sheet, Figure 3.03111.
3.03112 Typical tensile stress-strain curves at elevated temperature for several forgings, Figure 3.03112.
3.0312 Clad sheet.
3.03121 Effect of elevated temperature and short exposure time on tensile properties of clad sheet, Figure 3.03121.
3.03122 Effect of elevated test temperature and exposure time on tensile properties of clad sheet, Figure 3.03122.
3.03123 Effect of elevated test temperature and exposure time on tensile properties of clad sheet, Figure 3.03123.
3.03124 Effect of test temperature on tensile properties of clad sheet, Figure 3.03124.
3.0313 Extruded bar.
3.03131 Effect of test temperature on tensile properties of extruded bar, Figure 3.03131.
3.0314 Forgings.
3.03141 Effect of test temperature on average tensile properties of several forgings, Figure 3.03141.
3.03142 Effect of elevated test temperature and exposure time on tensile properties of forging, Figure 3.03142.
3.03143 Effect of elevated temperature on tensile properties of hand forged billets, Figure 3.03143.
3.03144 Typical tensile properties of forging at various temperatures, Figure 3.03144.
3.0315 Bar.
3.03151 Effect of elevated temperatures and exposure time on tensile properties of bar, Figure 3.03151.
3.032 Compression.
3.0321 Stress-strain diagrams.
3.03211 Typical compressive stress-strain curves at elevated temperature for several forgings, Figure 3.03211.
3.0322 Effect of elevated temperature on average compressive yield properties of several forgings, Figure 3.0322.
3.0323 Effect of elevated temperature and exposure time on compressive yield properties of forgings, Figure 3.0323.
3.033 Impact.
3.034 Bending.
3.035 Torsion and shear.
3.0351 Effect of elevated temperature on average shear strength of several forgings, Figure 3.0351.
3.036 Bearing.
3.0361 Effect of elevated temperature on average bearing properties of several forgings, Figure 3.0361.
3.037 Stress concentration.
3.0371 Notch properties.
3.03711 Crack strength of clad sheet at -110, 80 and 250F for various crack lengths, Figure 3.03711.
3.03712 Elevated temperature sharp notch strength ratio of forging for various cross-section locations, Figure 3.03712.
3.0372 Fracture toughness.
3.038 Combined properties.

3.04 Creep and Creep Rupture Properties
3.041 Creep curves for clad sheet at elevated temperature, Figure 3.041.
3.042 Creep and creep rupture curves for rod at elevated temperatures, Figure 3.042.
3.043 Creep and creep rupture curves for bar at 400 and 600F, Figure 3.043.
3.044 Creep and creep rupture curves for forged bar at elevated temperatures, Figure 3.044.
3.045 Creep and creep rupture curves for forging at elevated temperatures, Figure 3.045.

3.05 Fatigue Properties
3.051 Sheet.
3.052 Extruded bar.
3.053 Forging.
3.0531 Axial load fatigue strength for smooth longitudinal specimens from several forged billets, Figure 3.0531.
3.0532 Axial load fatigue strength for smooth long-transverse specimens from several forged billets, Figure 3.0532.
3.0533 Axial load fatigue strength for notched longitudinal specimens from several forged billets, Figure 3.0534.
3.0534 Axial load fatigue strength for notched long-transverse specimens from several forged billets, Figure 3.0535.
3.0535 Rotating beam fatigue strength for smooth and notched longitudinal specimens from forged billets, Figure 3.0535.
3.0536 Rotating beam fatigue strength for smooth and notched longitudinal specimens from forged billets, Figure 3.0536.
3.0537 Rotating beam fatigue strength for smooth and notched longitudinal specimens from forged billet tested at 250F, Figure 3.0537.
3.0538 Rotating beam fatigue strength for smooth and notched longitudinal specimens from forged billets tested at 400F, Figure 3.0538.

3.06 Elastic Properties
3.061 Poisson's ratio, 0.35 (2).
3.062 Modulus of elasticity, see Tables 3.0212 and 3.0222.
3.0621 Modulus of elasticity at room and elevated temperature for forged bar, Figure 3.0621.
3.0622 Effect of test temperature on modulus of elasticity in compression, Figure 3.0622.

	Al
2.5	Cu
1.5	Mg
1.2	Ni
1.0	Fe
0.2	Si
0.1	Ti

2618

4. FABRICATION

4.01 Formability

4.011 The alloy has good formability.

4.012 Hot forging. 970F and then forge within the temperature range of 970 to 900F down to 660F.

4.013 Cold work. All cold work should be done in the annealed or solution treated condition (2).

4.02 Machining

4.021 The machinability of this alloy is good and best results are obtained in the fully aged condition. Care must be taken if the alloy is machined in the quenched or annealed condition. Because of its softness in this condition it has a tendency to build up on the cutting edges. High carbon steel tools are recommended at low speeds and give a satisfactory result, while high speed steel should be used for large scale operations (2).

4.022 For continuous cuts, free from vibrations, single point turning tools of plain high carbon or high speed steel should be ground to:

35 to 80 degree	cutting angle,
30 to 53 degree	top rake,
7 to 10 degree	front clearance,
10 to 20 degree	side rake,
7 to 10 degree	side clearance.

Cemented carbide tipped tools should be ground to:

60 to 80 degree	cutting angle,
5 to 30 degree	top rake,
6 to 10 degree	front clearance,
5 to 10 degree	side rake,
6 to 10 degree	side clearance.

High speed steel milling cutters should be ground to:

50 to 60 degree	cutting angle,
25 to 35 degree	top rake,
3 to 7 degree	primary clearance,
7 to 12 degree	secondary angle,
10 to 50 degree	helix, and coarse tooth spacing (2)

4.023 More detailed machinability information can be obtained from the Air Force Machinability Data Center-Area Telephone Code 513-271-9510.

4.03 Welding

4.031 Al 2618 is weldable with special techniques. It is unsuited for fusion welding, but can be resistance welded (2,7).

4.04 Heat Treatment

4.05 Surface Treatment

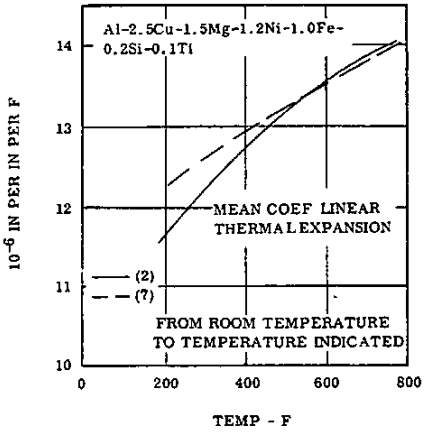


FIG. 2.014 THERMAL EXPANSION (2)(7)

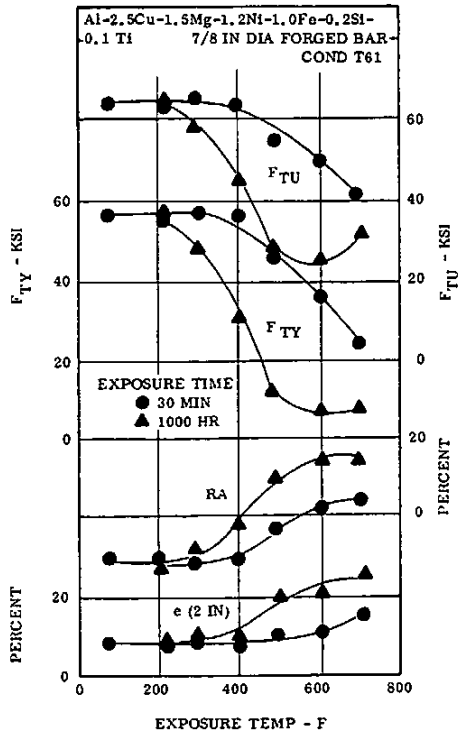


FIG. 3.0213 EFFECT OF EXPOSURE TIME AND TEMPERATURE ON ROOM TEMPERATURE TENSILE PROPERTIES OF FORGED BAR. (13)

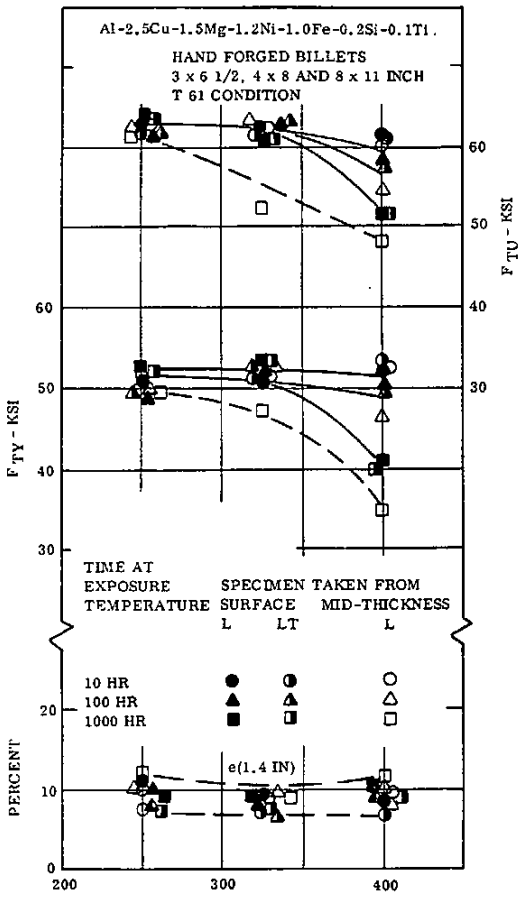


FIG. 3.0214 EFFECT OF ELEVATED TEMPERATURE EXPOSURE AND EXPOSURE TIME ON TENSILE PROPERTIES OF FORGINGS. (17)

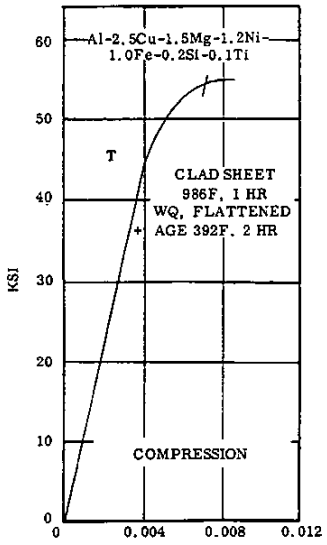


FIG. 3.0221 STRESS-STRAIN CURVE FOR CLAD SHEET IN COMPRESSION (7, p. 55)

	Al
2.5	Cu
1.5	Mg
1.2	Ni
1.0	Fe
0.2	Si
0.1	Ti

2618

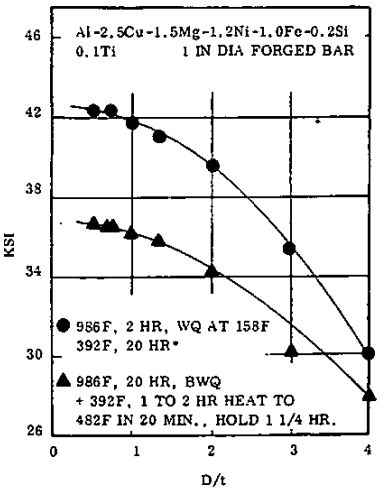


FIG. 3.0251 EFFECT OF THICKNESS AND HEAT TREATMENT ON SHEAR STRESS OF FORGED BAR (7, p. 20)

	Al
2.5	Cu
1.5	Mg
1.2	Ni
1.0	Fe
0.2	Si
0.1	Ti

2618

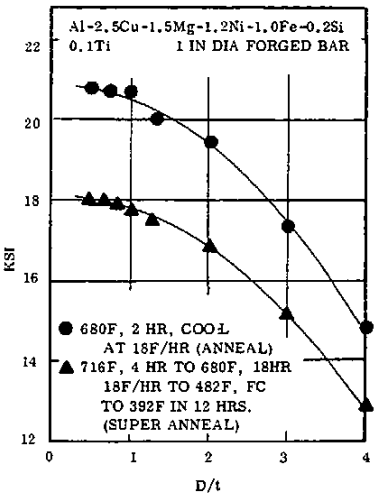


FIG. 3.0252 EFFECT OF THICKNESS AND HEAT TREATMENT ON SHEAR STRESS OF FORGED BAR (7, p. 21,22)

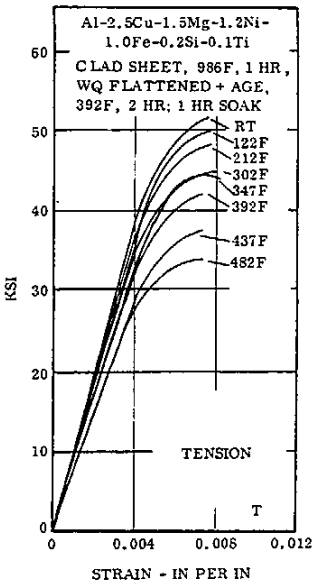


FIG. 3.03111 STRESS-STRAIN CURVES AT ELEVATED TEMPERATURES FOR CLAD SHEET (7, p. 53, 54)

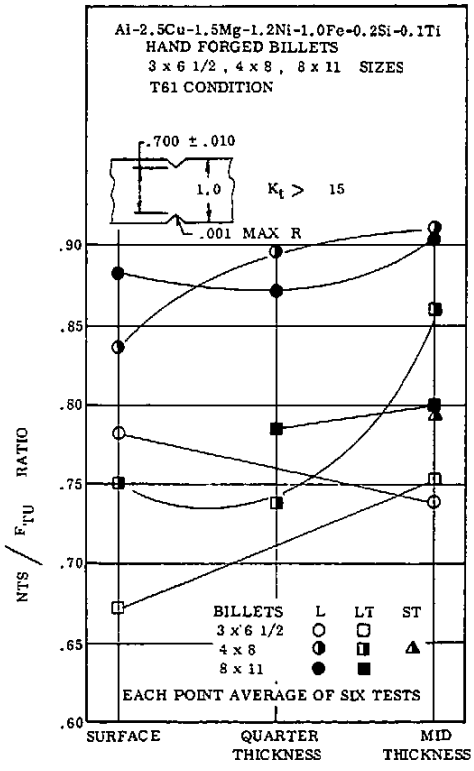


FIG. 3.02711 EFFECT OF SPECIMEN CROSS-SECTION LOCATION ON SHARP NOTCH STRENGTH RATIO OF FORGING. (17)

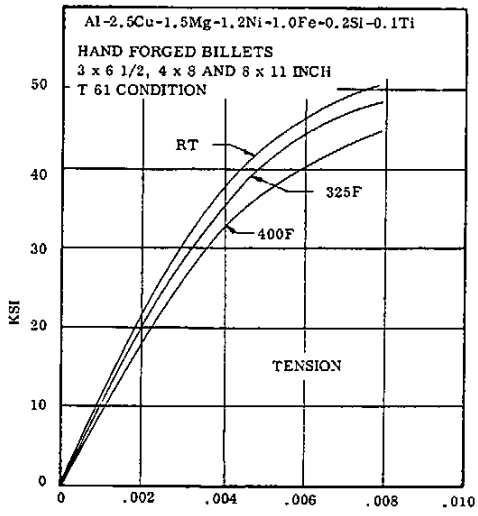


FIG. 3.03112 TYPICAL TENSILE STRESS-STRAIN CURVES AT ELEVATED TEMPERATURE FOR SEVERAL FORGINGS. (17)

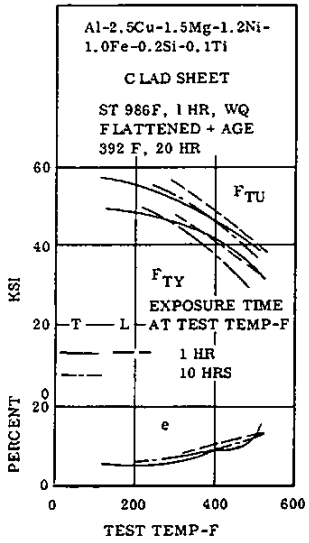


FIG. 3.03121 EFFECT OF ELEVATED TEMPERATURE AND SHORT EXPOSURE TIME ON TENSILE PROPERTIES OF CLAD SHEET (7, p.47, 148)

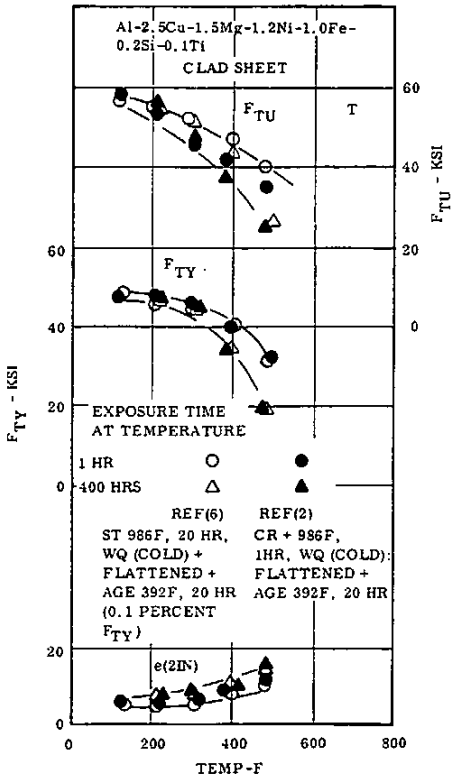


FIG. 3.03122 EFFECT OF ELEVATED TEST TEMPERATURE AND EXPOSURE TIME ON TENSILE PROPERTIES OF CLAD SHEET. (2)(6)

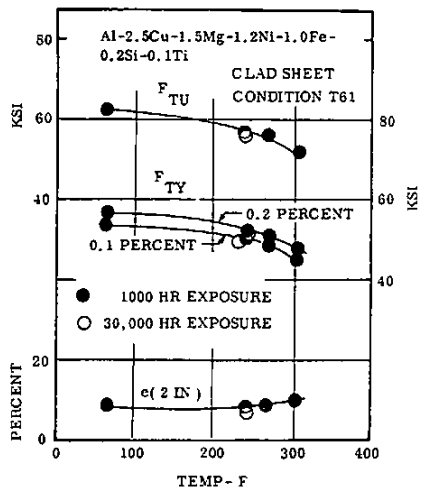


FIG. 3.03123 EFFECT OF ELEVATED TEST TEMPERATURE AND LONG EXPOSURE TIME ON TENSILE PROPERTIES OF CLAD SHEET. (8)

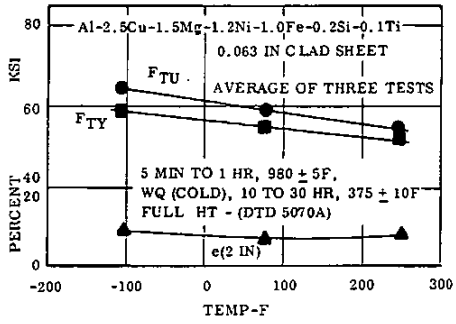


FIG. 3.03124 EFFECT OF TEST TEMPERATURE ON TENSILE PROPERTIES OF CLAD SHEET (12)

	Al
2.5	Cu
1.5	Mg
1.2	Ni
1.0	Fe
0.2	Si
0.1	Ti

2618

	Al
2.5	Cu
1.5	Mg
1.2	Ni
1.0	Fe
0.2	Si
0.1	Ti

2618

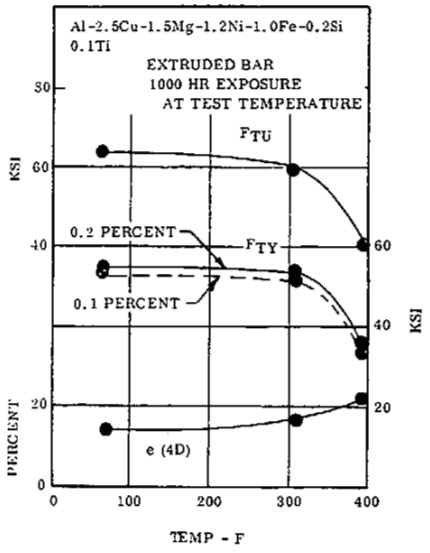


FIG. 3.03131 EFFECT OF TEST TEMPERATURE ON TENSILE PROPERTIES OF EXTRUDED BAR. (8)

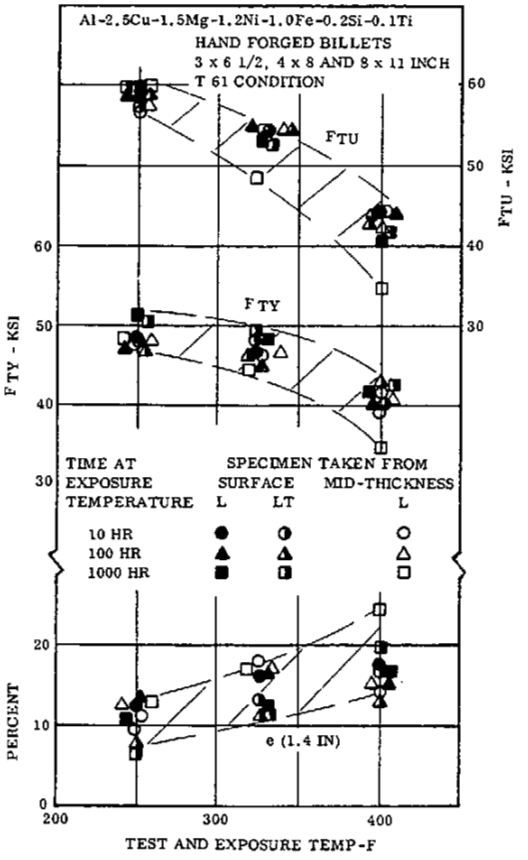


FIG. 3.03142 EFFECT OF ELEVATED TEST TEMPERATURE AND EXPOSURE TIME ON TENSILE PROPERTIES OF FORGINGS. (17)

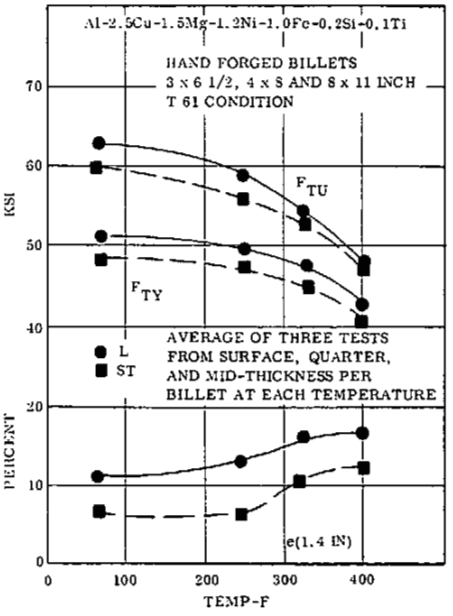


FIG. 3.03141 EFFECT OF TEST TEMPERATURE ON AVERAGE TENSILE PROPERTIES OF SEVERAL FORGINGS. (17)

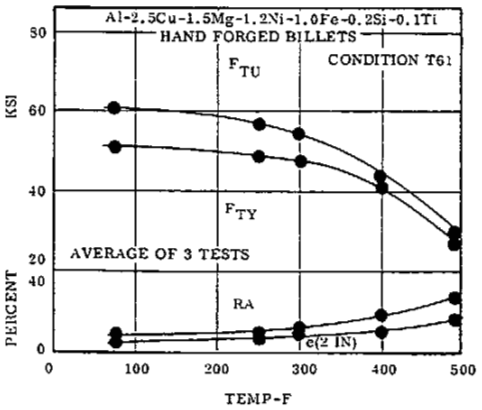


FIG. 3.03143 EFFECT OF ELEVATED TEMPERATURE ON TENSILE PROPERTIES OF HAND FORGED BILLETS. (11)(14)

	Al
2.5	Cu
1.5	Mg
1.2	Ni
1.0	Fe
0.2	Si
0.1	Ti

2618

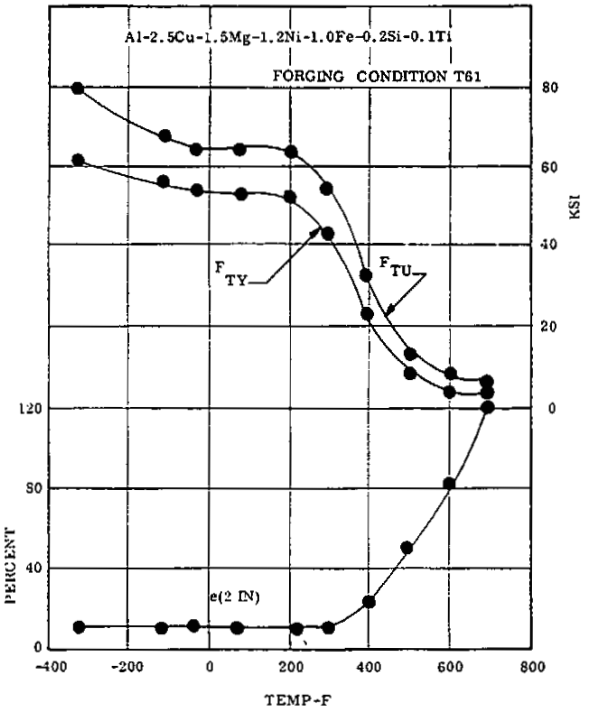


FIG. 3.03144 TYPICAL TENSILE PROPERTIES OF FORGING AT VARIOUS TEMPERATURES (4)

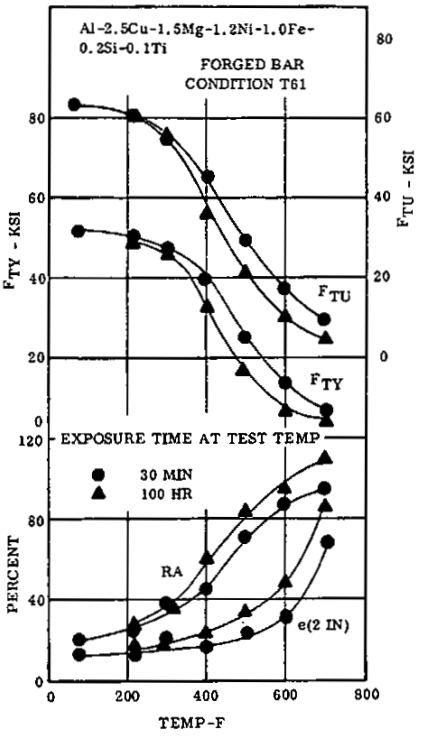


FIG. 3.03151 EFFECT OF ELEVATED TEMPERATURES AND EXPOSURE TIME ON TENSILE PROPERTIES OF BAR. (13)

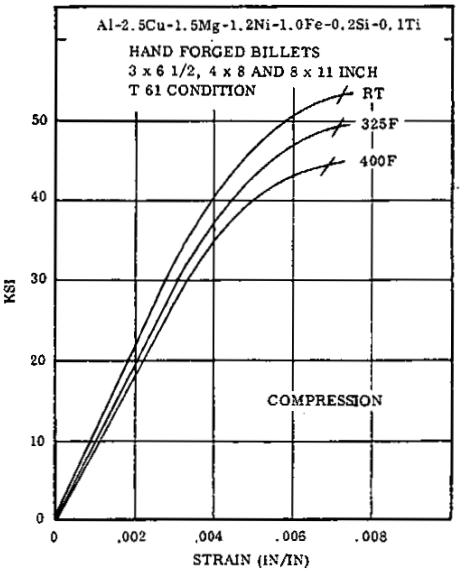


FIG. 3.03211 TYPICAL COMPRESSIVE STRESS - STRAIN CURVES AT ELEVATED TEMPERATURE FOR SEVERAL FORGINGS. (17)

	Al
2.5	Cu
1.5	Mg
1.2	Ni
1.0	Fe
0.2	Si
0.1	Ti

2618

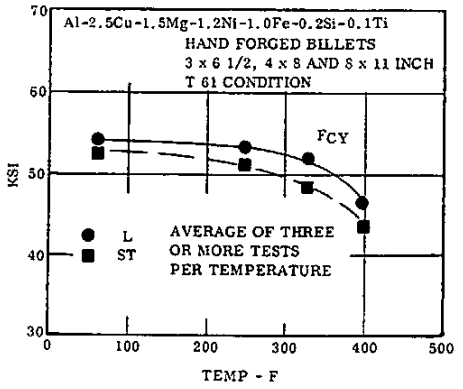


FIG. 3.0322 EFFECT OF ELEVATED TEMPERATURE ON AVERAGE COMPRESSIVE YIELD PROPERTIES OF SEVERAL FORGINGS. (17)

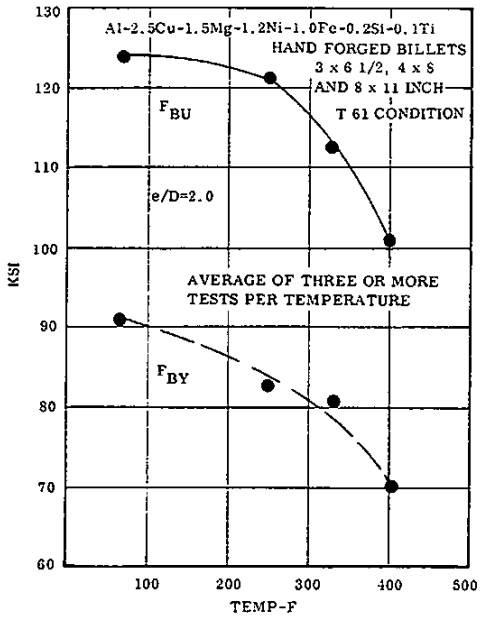


FIG. 3.0361 EFFECT OF ELEVATED TEMPERATURE ON AVERAGE BEARING PROPERTIES OF SEVERAL FORGINGS. (17)

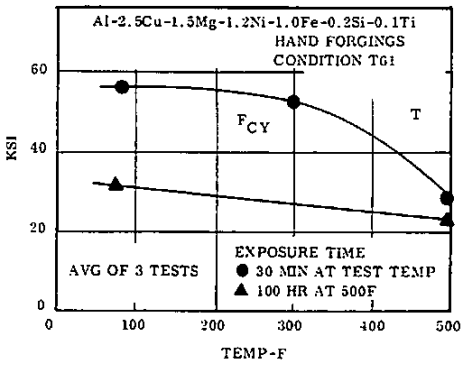


FIG. 3.0323 EFFECT OF ELEVATED TEMPERATURE AND EXPOSURE TIME ON COMPRESSIVE YIELD STRENGTH OF FORGINGS (11)(14)

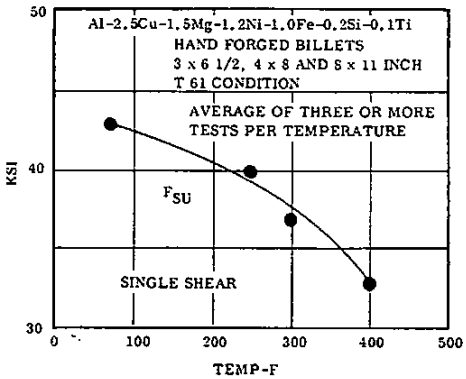


FIG. 3.0351 EFFECT OF ELEVATED TEMPERATURE ON AVERAGE SHEAR STRENGTH OF SEVERAL FORGINGS. (17)

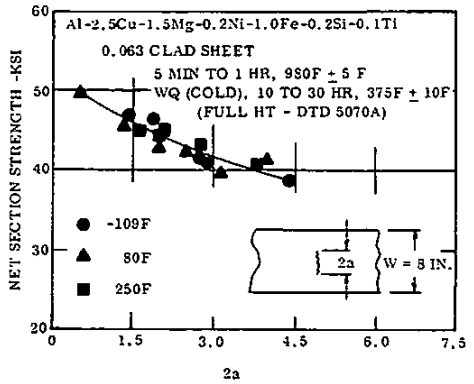


FIG. 3.03711 CRACK STRENGTH OF CLAD SHEET AT -109, 80 AND 250F FOR VARIOUS CRACK LENGTHS. (12)

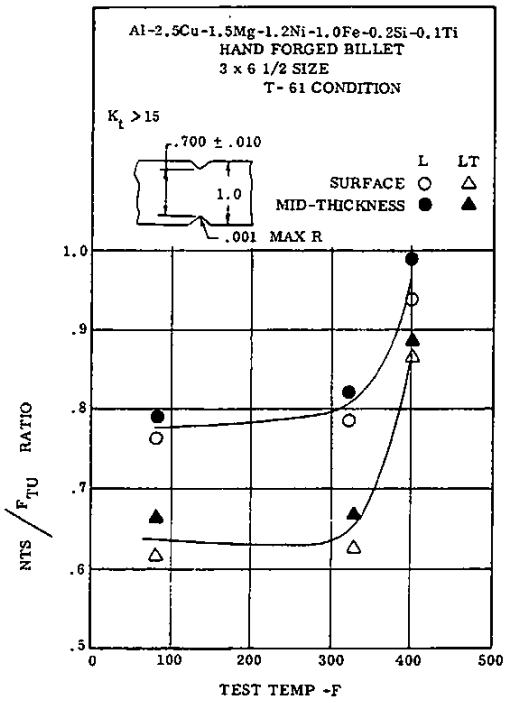
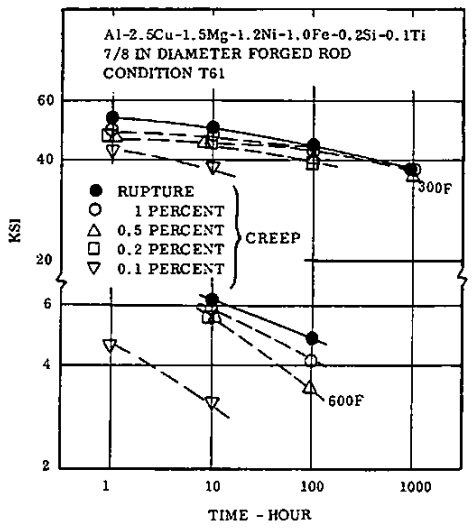


FIG. 3.03712 ELEVATED TEMPERATURE SHARP NOTCH STRENGTH RATIO OF FORGING FOR VARIOUS CROSS-SECTION LOCATIONS. (17)



Al	
2.5	Cu
1.5	Mg
1.2	Ni
1.0	Fe
0.2	Si
0.1	Ti

2618

FIG. 3.042 CREEP AND CREEP RUPTURE CURVES FOR ROD AT ELEVATED TEMPERATURE (13)

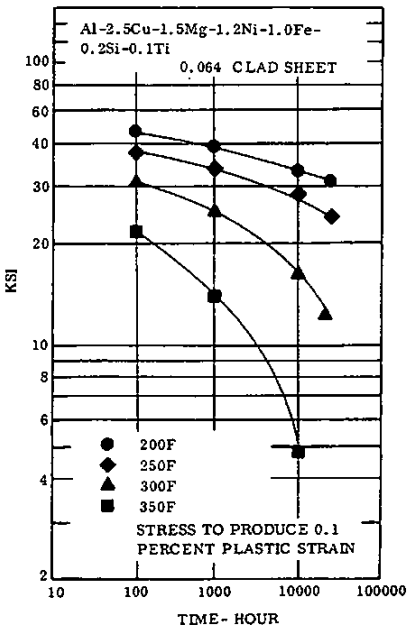


FIG. 3.041 CREEP CURVES FOR CLAD SHEET AT ELEVATED TEMPERATURE. (16)

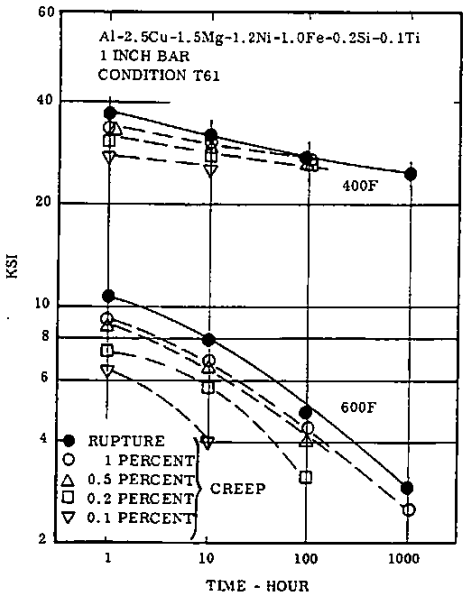


FIG. 3.043 CREEP AND CREEP RUPTURE PROPERTIES FOR BAR AT 400 AND 600F (13)

	Al
2.5	Cu
1.5	Mg
1.2	Ni
1.0	Fe
0.2	Si
0.1	Ti

2618

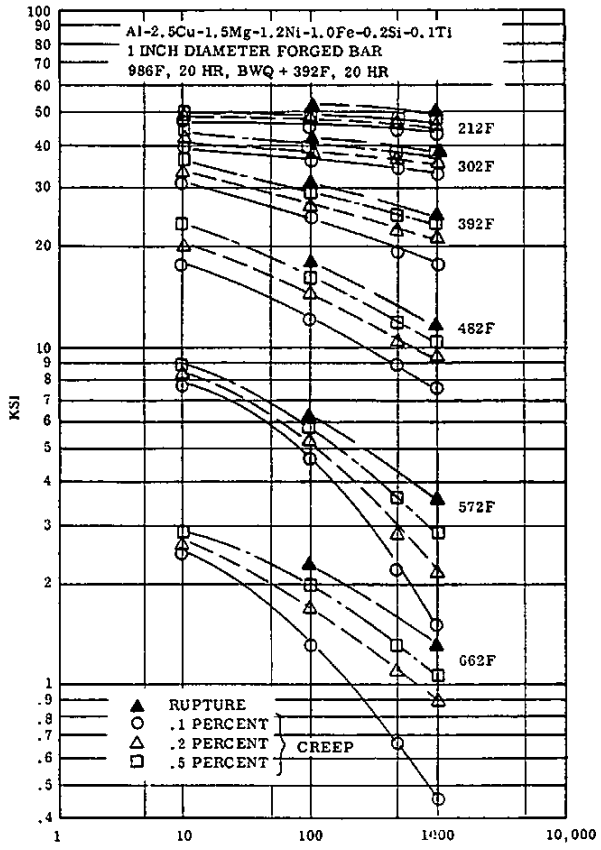


FIG. 3.044 CREEP AND CREEP RUPTURE PROPERTIES AT ELEVATED TEMPERATURES FOR FORGED BAR. (16)

	Al
2.5	Cu
1.5	Mg
1.2	Ni
1.0	Fe
0.2	Si
0.1	Ti

2618

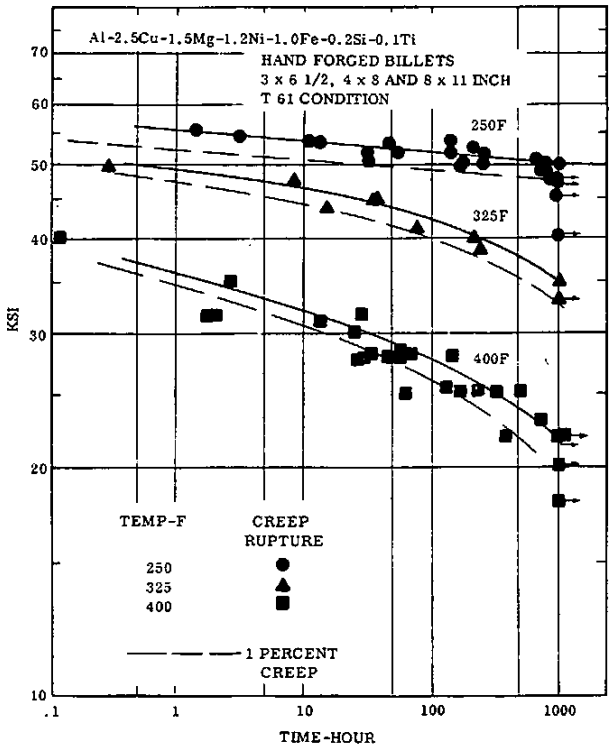


FIG. 3.045 CREEP AND CREEP RUPTURE CURVES FOR FORGING AT ELEVATED TEMPERATURES. (17)

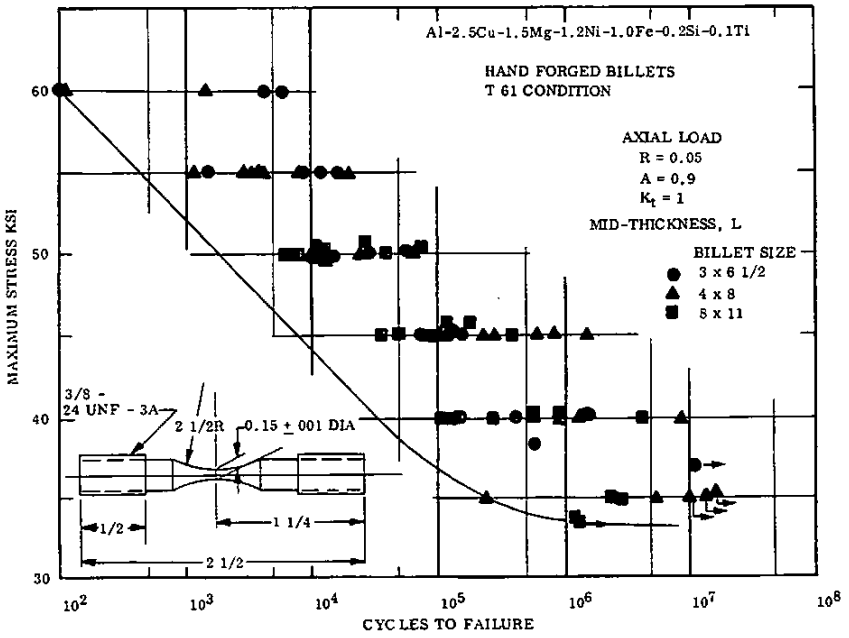


FIG. 3.0531 AXIAL LOAD FATIGUE STRENGTH FOR SMOOTH LONGITUDINAL SPECIMENS FROM SEVERAL FORGED BILLETS. (17)

	Al
2.5	Cu
1.5	Mg
1.2	Ni
1.0	Fe
0.2	Si
0.1	Ti

2618

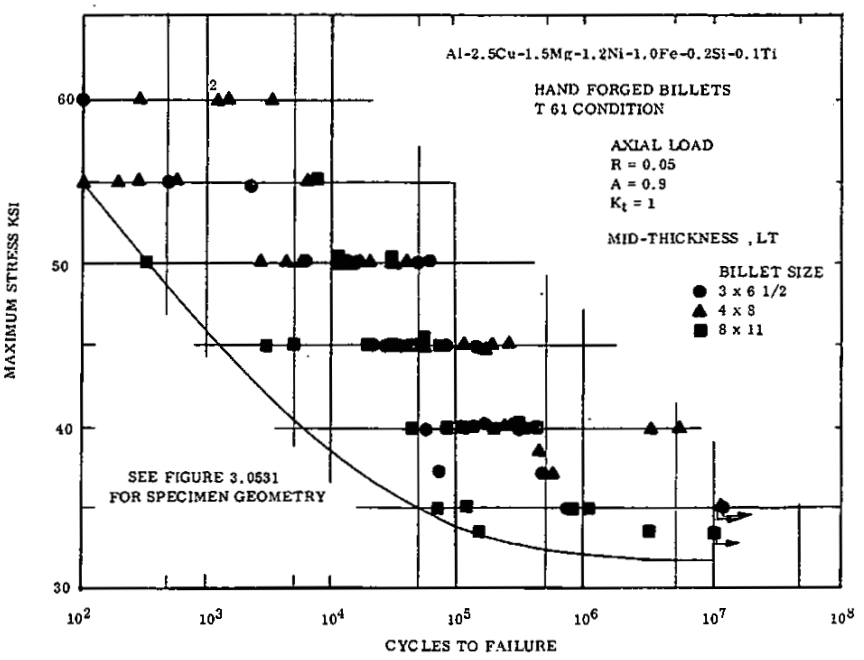


FIG. 3.0532 AXIAL LOAD FATIGUE STRENGTH FOR SMOOTH LONG-TRANSVERSE SPECIMENS FROM SEVERAL FORGED BILLETS. (17)

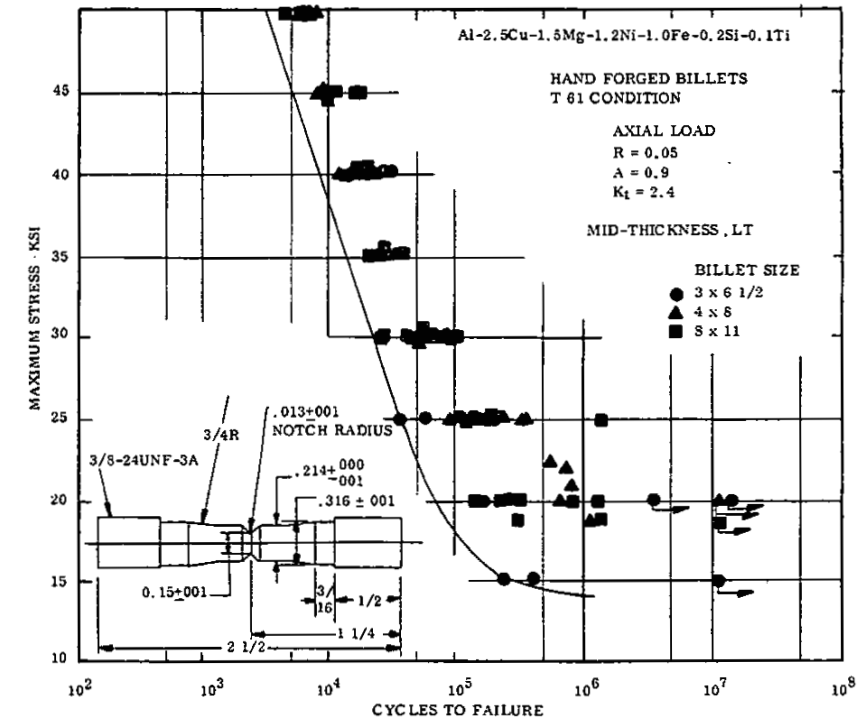


FIG. 3.0533 AXIAL LOAD FATIGUE STRENGTH FOR NOTCHED LONGITUDINAL SPECIMENS FROM SEVERAL FORGED BILLETS. (17)

	Al
2.5	Cu
1.5	Mg
1.2	Ni
1.0	Fe
0.2	Si
0.1	Ti

2618

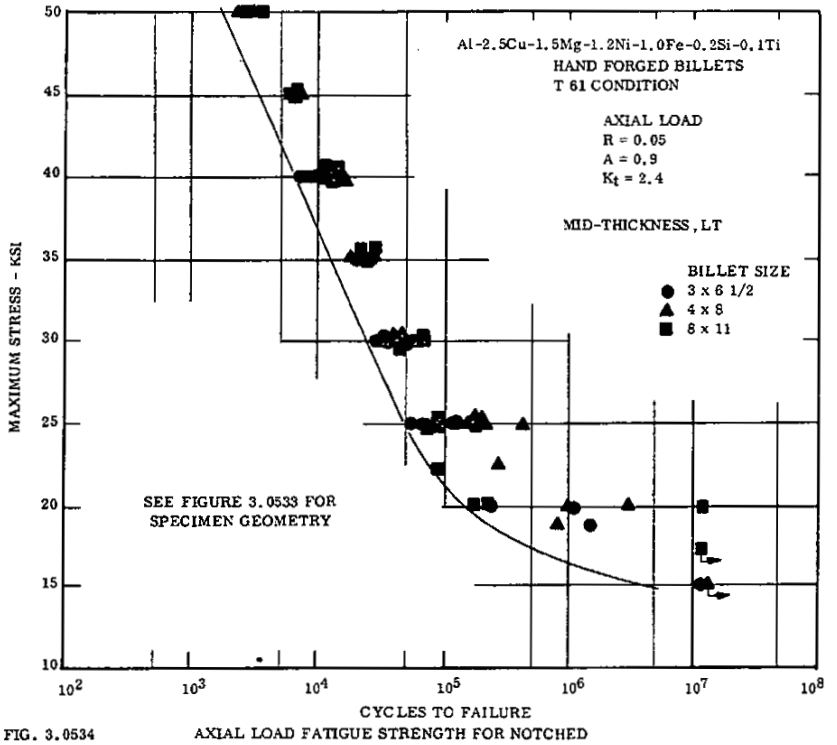
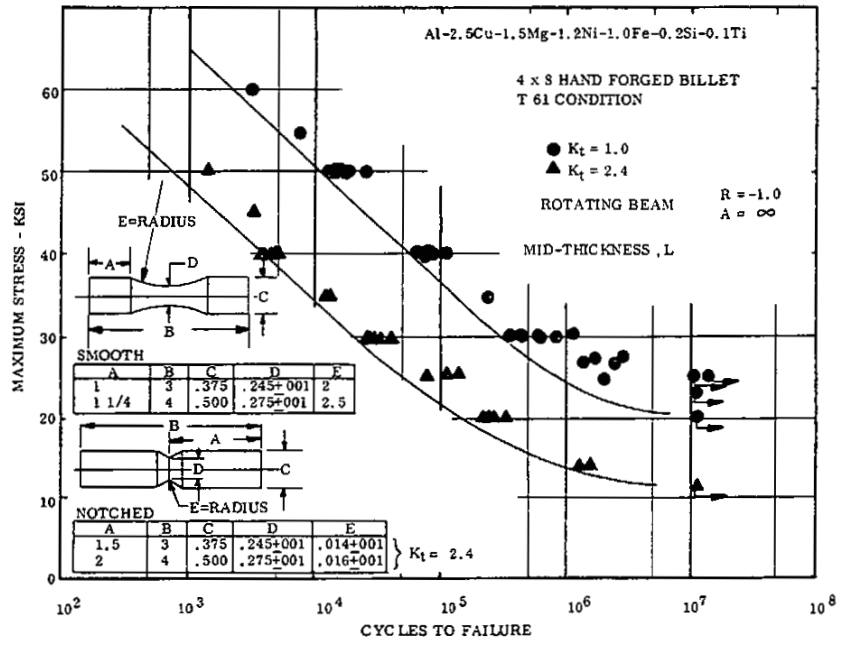


FIG. 3.0534 AXIAL LOAD FATIGUE STRENGTH FOR NOTCHED LONG-TRANSVERSE SPECIMENS FROM SEVERAL FORGED BILLETS. (17)



SMOOTH A	B	C	D	E
1	3	.375	.245±001	2
1 1/4	4	.500	.275±001	2.5

NOTCHED A	B	C	D	E
1.5	3	.375	.245±001	.014±001
2	4	.500	.275±001	.016±001

FIG. 3.0535 ROTATING BEAM FATIGUE STRENGTH FOR SMOOTH AND NOTCHED LONGITUDINAL SPECIMENS FROM FORGED BILLETS. (17)

	Al
2.5	Cu
1.5	Mg
1.2	Ni
1.0	Fe
0.2	Si
0.1	Ti

2618

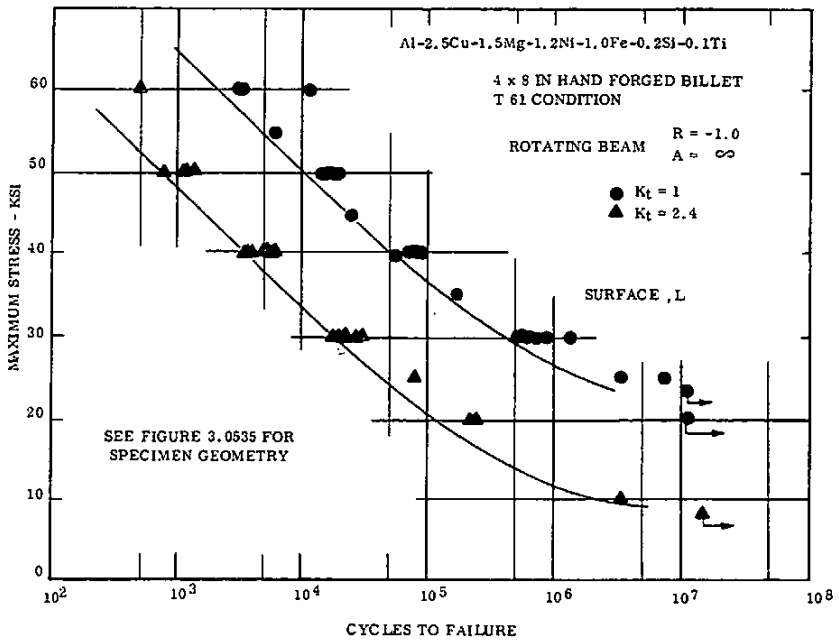


FIG. 3.0536 ROTATING BEAM FATIGUE STRENGTH FOR SMOOTH AND NOTCHED LONGITUDINAL SPECIMENS FROM FORGED BILLET. (17)

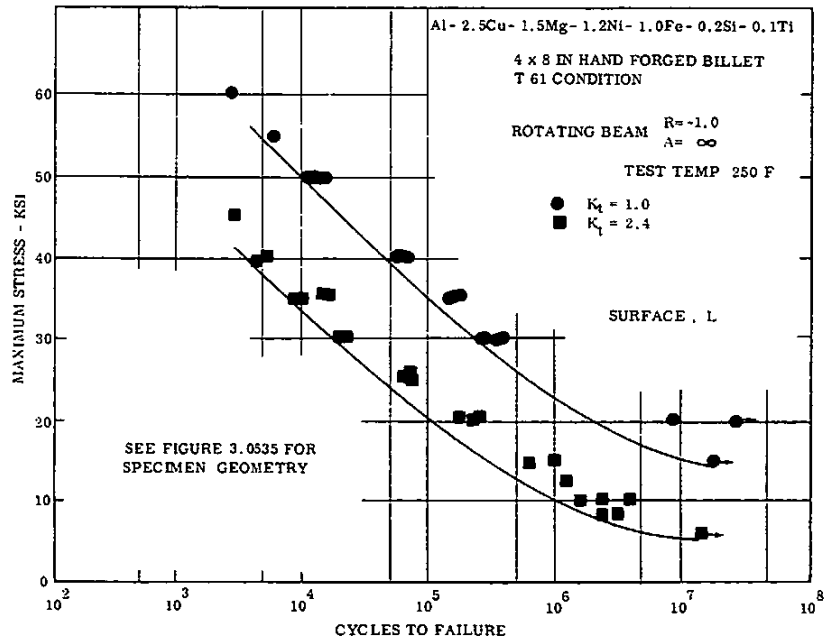


FIG. 3.0537 ROTATING BEAM FATIGUE STRENGTH FOR SMOOTH AND NOTCHED LONGITUDINAL SPECIMENS FROM FORGED BILLET TESTED AT 250F. (17)

	Al
2.5	Cu
1.5	Mg
1.2	Ni
1.0	Fe
0.2	Si
0.1	Ti

2618

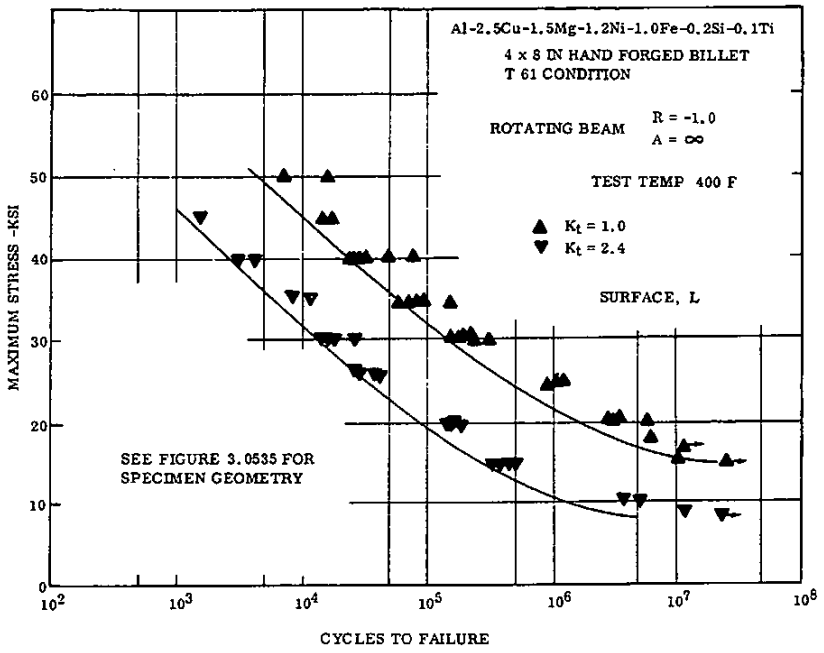


FIG. 3.0538 ROTATING BEAM FATIGUE STRENGTH FOR SMOOTH AND NOTCHED LONGITUDINAL SPECIMENS FROM FORGED BILLET TESTED AT 400F. (17)

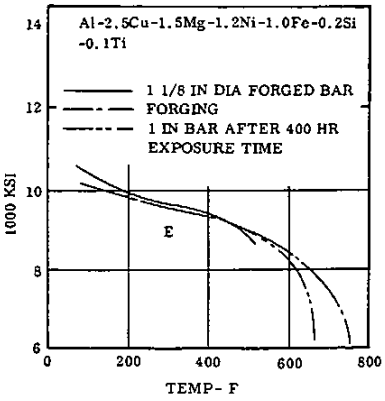


FIG. 3.0621 MODULUS OF ELASTICITY AT ROOM AND ELEVATED TEMPERATURE FOR FORGED BAR (7)

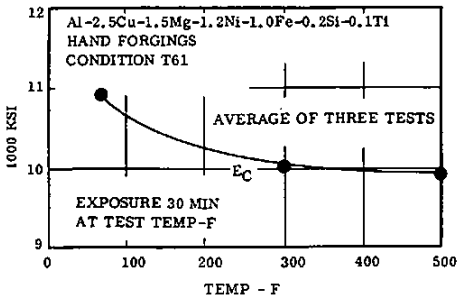


FIG. 3.0622 EFFECT OF TEST TEMPERATURE ON MODULUS OF ELASTICITY IN COMPRESSION. (14)

	Al
2.5	Cu
1.5	Mg
1.2	Ni
1.0	Fe
0.2	Si
0.1	Ti

2618

REFERENCES

1. AMS 4132A (January 15, 1962)
2. Aluminum 2618, Alloy Digest, Filing Code: Al-76 (February 1959)
3. Siegrist, F.L., "How to do More with Wrought Aluminum Alloys", Metal Progress, Vol. 82, No 4 (October 1962)
4. Aluminum Standards and Data, 1968-69, The Aluminum Association, First Edition (April 1968)
5. Alcoa Aluminum Handbook, Aluminum Company of America (1967)
6. Hiduminium, RR .58 Alloy Digest, Filing Code: Al-34 (November 1955)
7. "Hiduminium Elevated Temperature Alloys", High Duty Alloys Ltd. (1956)
8. Doyle, W.M., "Hiduminium RR .58", High Alloys Ltd. England (September 1964)
9. Fell, E.A. and Doyle, W.M., "The Effect of Intermediate Cold Work on the Structure of Hiduminium R.R. 58 Alloy Sheet", Journal of the Institute of Metals, Vol. 93 (1964-65)
10. "Standards for Aluminum Mill Products 1966", The Aluminum Association, Eighth Edition (September 1965)
11. "General Materials Information, Phase I - Material Data", Progress Report No. 1, Northrop Corporation, Norair Division (June 30, 1961)
12. Figge, I.E., "Residual Strength of Alloys Potentially Useful in Supersonic Aircraft", NASA TN-D-2613 (November 1964)
13. Voorhees, R. H. and Freeman, J.W., "Report on the Elevated-Temperature Properties of Aluminum and Magnesium Alloys", ASTM STP No. 291 (1960)
14. Kuschell, K.E., "Room and Elevated Temperature Properties of Aluminum Forging Alloy 2618-T61", Northrop Aircraft Inc. (April 1960)
15. "Properties and Applications of Wrought Aluminum Alloys", Metal Progress, Vol. 82, No. 4 (October 1962)
16. Private correspondance between Dr. W.M. Doyle, Technical Director, High Duty Alloys, Ltd, Slough Bucks, England, and the Mechanical Properties Data Center (June 13, 1968)
17. Lumm, J.A., "Mechanical Properties of 2618 Aluminum Alloy", Technical Report, AFML-TR-66-235, North American Aviation, Inc. (July 1966)
18. Kaufman, J.G., Holt, Marshall, "Fracture Characteristics of Aluminum Alloys", Alcoa Research Laboratory, Technical Paper #18, 1965 Aluminum Company of America
19. Roake, D.P., Gunn, N.J.F., Ballett, J.T., Bradshaw, F.J., "Crack Propagation in Fatigue. Some Experiments with DTD 5070A, Aluminum Alloy Sheet", (October 1964), Royal Aircraft Establishment Technical Report, 64025
20. Gunn, N.J.F., "Fatigue Cracking Rates and Residual Strength of Eight Aluminum Sheet Alloys" (October 1964) Royal Aircraft Establishment Technical Report, 64024

1 General

Aluminum alloy 6013 is a relatively new heat-treatable alloy of medium strength which derives its heat-treat response from the precipitation of magnesium-silicon and magnesium-silicon-copper-aluminum phases.

It is primarily available as sheet, but other forms may become available as development progresses.

In the peak-aged T6 condition, it appears to be similar in yield strength, fracture toughness, and fatigue resistance to 2024-T3 sheet, but it has better corrosion resistance and lower density. These properties have made it a candidate for aircraft skins and other aerospace and automotive components.

In the solution-heat-treated (SHT) and naturally aged condition, T4, it has better stretch forming characteristics than 2024-O and can withstand greater deformation before fracturing. As the alloy hardens little during natural aging beyond the first two weeks, it can be supplied in the T4 condition and stored for months before forming. This property, and the good stretch formability, may in some cases preclude the need for in-plant SHT of O-temper materials and improve the economics of manufacturing.

It has been implied (Ref. 1), because of the superior corrosion resistance, that the alloy can be used in the bare condition instead of as clad 2024 sheet; however, this substitution must be examined on a case-by-case basis. Unclad alloy 6013 has a tendency to corrode intergranularly, with expected deterioration in fatigue resistance, ductility, and strength; and clad 6013 should be considered in cases where corrosion resistance is important (see Section 2.3.1).

1.1 Commercial Designation

6013 (UNS A96013).

1.2 Alternate Designation

1.3 Specifications

1.3.1 *[Table]* AMS specifications for 6013 alloy sheet.

1.4 Composition

1.4.1 *[Table]* AMS specified composition.

1.5 Heat Treatment

1.5.1 T Tempers. Solution heat treatment: soak 20 to 30 minutes at 1040 to 1060F, cold water quench, naturally age (room temperature) for 2 weeks to T4 temper. Artificially age T4 material at 375F for 4 hours to T6 temper (Ref. 1). Similar heat treatments can be used by the fabricator to produce T42 and T62 tempers from annealed sheet. Slower quench rates following solution heat treatment will reduce mechanical properties (Ref. 18). Glycol quenching will significantly lower tensile properties (see Figs. 3.2.1.5-3.2.1.8). Water mist quenching results in strengths below specified minima.

1.5.1.1 *[Table]* AMS specified heat treatments for sheet.

1.5.1.2 *[Figure]* Rockwell B hardness of 6013 sheet as a function of aging time at three different temperatures.

1.5.2 Annealing. Soak at 775F for 2 to 3 hours, cool at 50F per hour to 500F. The subsequent cooling rate is unimportant (Ref. 1).

Al
0.90
Mg
0.80 Si
0.85 Cu

1.5.3 Post-weld Heat Treatment. A solution heat treatment temperature of 1000F maximum is recommended instead of the above 1040 to 1060F in order to avoid melting of the filler metal (Ref. 1). As with most aluminum alloys during welding, chemical segregation within the weld metal or the heat-affected zone (HAZ) may lower the melting temperature.

1.6 Hardness (see also Figure 1.5.4)

1.6.1 *[Table]* Hardness of 6013 sheet of O, T4, T6, and T62 tempers.

1.7 Forms and Conditions Available

6013 is currently available as sheet, but probably only from the producer. Forgings, extrusions, plate, rod, and wire will probably become available on special order.

1.8 Melting and Casting Practices

This alloy is supplied in the wrought form and is not recommended for foundry applications.

1.9 Special Considerations

Although recommended as a substitute for 2024-T3 sheet, 6013-T6 is more susceptible to intergranular corrosion (IGC) below sheet gauges of approximately 0.063 in. Above this gauge, both alloys may suffer IGC due to slower achievable quench rates. This can have a greater effect on ductility and fatigue resistance than pitting or general corrosion (see Section 2.3.1).

An advantage of this alloy over 2024 is that the T4 temper is much more stable at room temperature than the W temper of 2024. The latter requires refrigeration to maintain formability for a few days, but 6013-T4 is still relatively formable after months at ambient temperatures.

Additionally, the T4 sheet has similar formability to 2024-O sheet; and after forming can be aged to peak strength at relatively low temperatures. The 2024-O sheet requires solution heat treatment, quenching, and aging after forming, with consequent distortion of the formed part (see Section 4.1).

© 1992 by Purdue Research Foundation, West Lafayette, Indiana 47907. All Rights Reserved. U.S. Government License. This material may be used, duplicated or disclosed by United States Government agencies without the payment of any royalty.

Sensitivity to grain growth has been reported (19) for naturally aged material strained from 2 to 13 percent prior to resolution heat treatment. This grain growth resulted in a decrease in yield strength. Backside cracking during fillet welding was increased for sheet which was strained prior to resolution heat treatment and cracking was also observed in full penetration welds using 4043 filler. Resolution heat treatment should not be used after forming of 6013.

2 Physical and Chemical Properties

2.1 Thermal Properties

2.1.1 Melting Range. The alloy commences to melt at 1075F (Ref. 2) or 1080F (Ref. 10); however, this temperature is dependent on the homogeneity of the structure, the exact composition, and the heating rate.

2.1.2 Phase Changes. The alloy is subject to precipitation, but the solid matrix is always face centered cubic.

2.1.2.1 Time temperature transformation diagrams.

2.1.3 Thermal Conductivity at Room Temperature.

2.1.3.1 *[Table]* Thermal conductivity at room temperature.

2.1.4 Thermal Expansion.

68F to 212F 13.0 x 10^{-6} in./in./deg. F (Ref. 2)
13.1 x 10^{-6} in./in./deg. F (Ref. 10)

2.1.5 Specific Heat.

0.23 BTU/lb. deg. F at 212F

2.1.6 Thermal Diffusivity.

2.2 Other Physical Properties

2.2.1 Density.

0.098 lbs/cu in. (2.715 g/cc) (Ref. 2)

2.2.2 Electrical Properties.

2.2.2.1 *[Table]* Electrical conductivity.

2.2.3 Magnetic Properties. Alloy is non-magnetic.

2.3 Chemical Environments

2.3.1 General Corrosion. The alloy has relatively good corrosion resistance compared with other age hardening aluminum alloys, but because of the significant copper content it suffers slightly more intergranular corrosion in the T6 temper than does 6061. Tests in which this slightly increased pitting corrosion has been reported (Ref. 2) include 5 percent salt spray at 95F, total immersion in shallow sea water, MASTMAASIS (ASTM G 85 Annex A3), pine wood contact at 195F, and seacoast and semi-industrial atmospheres. In these tests specimens of 0.120-in. sheet did not show increased sensitivity to these environments when heated to 180, and 250F for 50 hours prior to exposure (Ref. 3).

In contrast to the above mentioned results in marine environments, seacoast exposure of T6 sheet at Daytona Beach produced significant pitting corrosion coupled with intergranular corrosion (IGC) similar to that developed in SWAACT (sea water acetic acidified corrosion test) or TOA (type of attack) tests (Refs. 9, 11). In the Daytona Beach tests large losses in elongation were observed for the thinner sheet gages, and a corresponding large loss in strength occurred for the thinnest gage (0.032 in.) (Figure 2.3.1.1). This type of thickness effect would be expected as a result of the pitting and IGA and may explain why no such losses were noted for the thicker sheet reported in Ref. 2. IGC has been reported in ASTM G 85 salt fog tests (Ref. 1). For 0.032-in. sheet complete perforation due to IGC occurred during a 7-day exposure in SWAACT tests (Ref. 11).

The Daytona Beach tests included 6061-T6 and 2024-T3. A comparison of the results for 0.063-in. sheet is shown in Figure 2.3.1.2. It will be noted that both 6013 and 6061 behave similarly while 2024 shows losses in both strength and elongation. Bare and clad 6013-T6 and 2024-T3 are compared in Figure 2.3.1.3. Cladding effectively protects both alloys for the 12 month exposures.

2.3.1.1 *[Figure]* Effect of seacoast exposure on retained tensile properties of 6013-T6 sheet of several thicknesses.

2.3.1.2 *[Figure]* Effect of seacoast exposure on retained tensile properties of 6013-T6, 6061-T6, and 2024-T3 sheet.

2.3.1.3 *[Figure]* Effect of seacoast exposure on retained tensile properties of bare and clad 6013-T6 and 2024-T6 sheet.

2.3.2 Stress Corrosion.

The SCC resistance of 6013 has been reported (Ref. 1) to be equal to that of 6061 which is essentially immune. Tests on 144 specimens of plate and extrusions resulted in no failure when stressed to 75 percent of F_{ty} and exposed for one year to alternate immersion in 3.5 percent NaCl solution and to seacoast environment at Point Judith, RI, for two years (Ref. 2).

2.4 Nuclear Properties

3 Mechanical Properties

3.1 Specified Mechanical Properties

3.1.1 *[Table]* Aluminum Association specified minimum tensile properties.

3.1.2 *[Table]* AMS specified tensile properties for sheet.

3.1.3 *[Table]* Design mechanical properties for 6013-T6 sheet.

3.2 Mechanical Properties at Room Temperature

3.2.1 Tension.

3.2.1.1 *[Figure]* Tensile stress-strain curves for 6013-T6 sheet.

3.2.1.2 *[Figure]* True stress, true strain tensile curve for 6013-T4 sheet.

3.2.1.3 *[Figure]* Load-displacement curve for a longitudinal tensile test of 0.08-in. thick 6013-T4 sheet.

3.2.1.4 *[Figure]* Load-displacement curve for a long-transverse tensile test of 0.08-in. thick 6013-T4 sheet.

3.2.1.5 *[Figure]* Load-displacement curve for a longitudinal tensile test of 0.08-in. thick 6013-T6 sheet.

3.2.1.6 *[Figure]* Load-displacement curve for a long-transverse tensile test of 0.08-in. thick 6013-T6 sheet.

3.2.1.7 *[Figure]* Load-displacement curve for a longitudinal tensile test of 36% PAG (glycol) quenched 0.08-in. thick 6013-T6 sheet.

3.2.1.8 *[Figure]* Load-displacement curve for a long-transverse tensile test of 36% PAG (glycol) quenched 0.08-in. thick 6013-T6 sheet.

3.2.1.9 Directionality of tensile properties.

3.2.1.9.1 *[Figure]* Tensile properties of 0.063-in. thick sheet as a function of the angle between the rolling direction and the tensile axis.

3.2.2 Compression.

3.2.2.1 *[Figure]* Compression stress-strain curves for 6013-T6 sheet at room temperature (Ref. 2).

3.2.3 Impact.

3.2.4 Bending, see Table 4.1.1

3.2.5 Torsion and Shear, see Table 3.1.3

3.2.6 Bearing, see Table 3.1.3

3.2.7 Stress Concentration.

3.2.7.1 Fracture toughness. As this alloy has been made largely in thin sections, little plane-strain fracture toughness data could be found (Table 3.2.7.1.1).

Most toughness measurements have been plane-stress fracture toughness, K_c, which is usually measured using the specimen described in ASTM E 561 and analysis described in ASTM B 646 (see Figure 3.2.7.1.3 and Table 3.2.7.1.2).

The $K_{apparent}$ in Fig. 3.2.7.1.3 refers to values measured using specimens described in ASTM E 561 but using the original crack length in calculating the K values. This presumably could give conservative results. However, it is likely that the $K_{apparent}$ values are relatively insensitive to the material's fracture toughness due to the small specimen size. Thus a valid K_c value for 6013-T6 would require a specimen width of over 15.75 in. None of the data reported here were obtained from specimens having a width exceeding 9.5 in.

3.2.7.1.1 *[Table]* Comparison of the plane-strain fracture toughness of 6013-T6 plate with 6061-T651 and 2024-T351.

3.2.7.1.2 *[Table]* Fracture toughness of 6013-T6 sheet in comparison with 2024-T3 and 6061-T6.

3.2.7.1.3 *[Figure]* Fracture toughness of 6013-T6 sheet of various gauges.

3.2.7.1.4 *[Table]* Kahn tear test results for 6013-T6 sheet.

3.2.7.1.5 *[Figure]* Range of crack-growth resistance curves (R-curves) for 6013-T6 sheet of thicknesses 0.063-in., 0.080-in., and 0.100-in.

3.3 Mechanical Properties at Various Temperatures

3.3.1 Tension.

3.3.2 Compression.

3.3.3 Impact.

3.3.4 Bending.

3.3.5 Torsion and Shear.

3.3.6 Bearing.

3.3.7 Stress Concentration.

3.3.7.1 Fracture toughness, see Figure 3.2.7.1.3.

3.3.8 Combined Properties.

3.4 Creep and Creep Rupture Properties

3.5 Fatigue Properties

The resistance to fatigue in the presence of a notch is superior to that of 6061-T6; for smooth specimens the fatigue strengths are about equal. The smooth specimen fatigue performance is about equal to 2024-T3 for lives greater than 10^5 cycles, but is inferior for shorter lives (Ref. 2). Fatigue crack-growth rates under constant amplitude in both L-T and T-L orientations are similar to 6061-T6 (Ref. 2).

3.5.1 Conventional Fatigue Properties.

3.5.1.1 *[Figure]* Comparison of smooth and notched specimens in S-N fatigue for 6013-T6 sheet of

various gauges.

3.5.1.2 *[Figure]* S-N fatigue curves for smooth specimens of 6013-T6 sheet of thicknesses 0.063-in., 0.080-in., and 0.100-in.

3.5.2 Fatigue Crack Propagation.

3.5.2.1 *[Figure]* Fatigue crack-growth rates of 6013-T6 sheet 0.063-in. thick.

3.5.2.2 *[Figure]* Fatigue crack-growth rates of 6013-T6 sheet from 0.063 to 0.249-in. thick in L-T orientation.

3.5.2.3 *[Figure]* Fatigue crack-growth rates of 6013-T6 sheet from 0.063 to 0.249-in. thick in T-L orientation.

3.5.2.4 *[Figure]* Fatigue crack-growth rates for 6013-T6 sheet tested at a stress ratio of 0.4.

3.5.2.5 *[Figure]* Fatigue crack-growth rates for 6013-T6 sheet tested at a stress ratio of 0.8.

3.5.2.6 *[Figure]* Fatigue crack-growth rates for 6013-T6 sheet tested at a stress ratio of 0.1.

3.6 Elastic Properties

3.6.1 Poisson's Ratio, 0.33 (Ref. 4).

3.6.2 Tensile Elastic Modulus.

10×10^6 psi (Ref. 10).

9.9×10^6 psi (Refs. 2, 4).

3.6.3 Compression Modulus.

10.1×10^6 psi (Refs. 2, 4).

3.6.3.1 *[Figure]* Compressive tangent modulus for 6013-T6 sheet (Ref. 2).

4 Fabrication

4.1 Forming

The alloy is formable as extrusions and as sheet (see remarks in Section 1.9).

4.1.1 *[Table]* Comparison of the formability of 6013, 2024, and 6061 in various tempers.

4.1.2 *[Table]* Bend radii for 6013 sheet in various tempers and thicknesses.

4.2 Machining and Grinding

4.2.1 The alloy in T6 condition is reported to have good chemical milling properties (Ref. 3).

4.3 Joining

4.3.1 This alloy is weldable by the GTA, MGA and resistance methods (Refs. 12 and 3). Filler wires of 4043 and 4063 are recommended. Fusion line cracking may be encountered when using Mg bearing fillers (e.g. 5000 series). Welability has been rated as A (Ref. 4) essentially equivalent to 6061. However recent information (Ref. 19) has indicated that in the T4 condition, weld cracking in fillet welds and in full penetration welds using 4043 filler is more pronounced in 6013 than in 6061. This relative increase in cracking may be associated with sensitivity to grain growth (See 1.9) . For sound welds the strengths are 4 to 6 percent higher than obtained for 6061.

4.3.1.1 *[Table]* Tensile properties of GTA sheet welds.

4.4 Surface Treatment

Anodizing response is claimed to be similar to 6061 and superior to 7075 (Ref 2).

Excellent chemical milling quality has been reported (Ref. 3).

Table 1.3.1 AMS specifications for 6013 sheet (Refs. 14, 15)

Alloy: 6013		
Form	Sheet	
Temper	T4	T6
AMS	4347A	4216

Table 1.4.1 AMS specified composition (Refs. 14, 15)

Alloy: 6013		
Form	Sheet	
	Composition, percent	
Element	Min	Max
Mg	0.8	1.0
Cu	0.6	1.1
Si	0.6	1.0
Mn	0.20	0.8
Fe	-	0.50
Zn	-	0.25
Cr	-	0.10
Ti	-	0.10
Other, each	-	0.05
Other, total		0.15

Table 1.5.1.1 AMS specified heat treatments for sheet (Ref. 16)

Alloy: 6013	
Form	**Sheet**
Solution Treat	1055F, 1/2 hr
Quench	< 1/8 in. A.C.
	> 1/8 in. W.Q.
Natural Age T4	R.T. 336 hr minimum
Artifical Age T6	375F 4 to 5 hrs

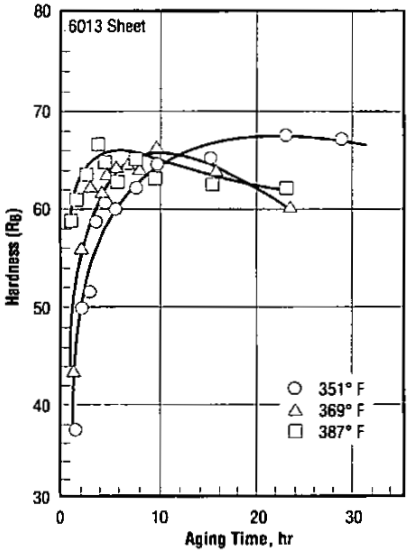


Fig. 1.5.1.2 Rockwell B hardness of 6013 sheet as a function of aging time at three different temperatures (Ref. 12)

Table 2.1.3.1 Thermal conductivity at room temperature

Alloy: 6013		
Form	**Sheet**	
Temper	**Thermal Conductivity (Btu/hr ft² deg F/in.)**	**Reference**
T4	1032	2
T6	1140	2
O	1250	10
T4	1070	10
T6	1160	10

Table 1.6.1 Hardness of 6013 sheet of O, T4, T6 and T62 tempers (Ref. 13)

Alloy: 6013			
Form	**Sheet**		
Thicknes	**0.063 in.**		
Temper	**Hardness (Rockwell**	**Standard Deviatio**	**No. of T**
T62	85.16	0.29	36
T6	82.38	0.37	45
T4	79.15	0.69	30
O	47.77	2.01	42

Table. 2.2.2.1 Electrical conductivity

Alloy: 6013			
Form	**Sheet**		
Temper	**IACS, (percent)**	**m(ohms/mm²)**	**Reference**
T4	38.3	22.2	2
T6	42.5	24.6	2
O	47	-	10
T4	40	-	10
T6	43	-	10

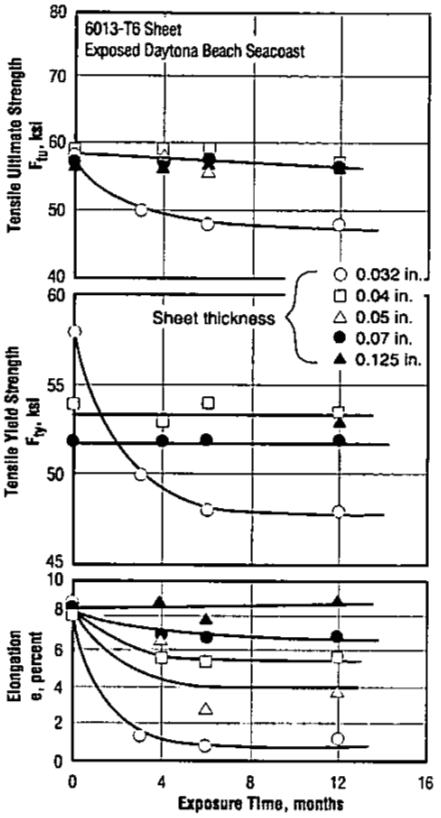


Fig. 2.3.1.1 Effect of seacoast exposure on retained tensile properties of 6013-T6 sheet of several thicknesses (Ref. 9)

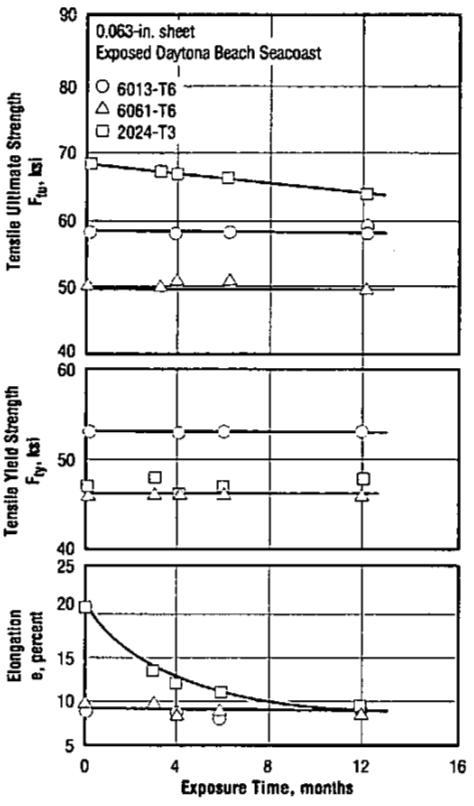


Fig. 2.3.1.2 Effect of seacoast exposure on retained tensile properties of 6013-T6, 6061-T6 and 2024-T3 sheet (Ref. 9)

Table 4.3.1.1 Tensile properties of GTA sheet welds (Ref. 18)

Alloy: 6013							
Form	**0.10-to 0.13-in. Sheet**						
Weld/H.T.	**T4 + Weld**	**T6 + Weld**	**T4 + Weld + T6 Age**	**T6 + Weld + T6 Age**	**T4 + Weld + ST WQ + T6 Age**	**T4 Weld + ST 36% Glycol Q + T6 Age**	**T4 + Weld + ST Mist Q + T6 Age**
As welded (a)							
F_{tu} (ksi)	37	36	37	38	55	54	50
F_{ty} (ksi)	26	26	31	35	48	47	41
e (percent)	4.8	3.2	2.5	2.6	10	10.7	10.3
Failure Location (b)	3HAZ	3HAZ	3HAZ	3HAZ	3HAZ	3HAZ	3HAZ
Weld Machined Flush							
F_{tu} (ksi)	33	36	37	36	41	47	43
F_{ty} (ksi)	23	24	29	30	38	42	38
e (percent)	3.5	4.7	3	2.9	5.7	3.2	2.8
Failure Location (b)	3W	1W/2HAZ	1W/2HAZ	1W/2HAZ	3W	3W	3Q

(a) GTA square butt, 2-pass welds with 4043 filler using 6061 parameters

(b) Number of specimens failed in weld/number failed in HAZ. There was no discernable difference between strengths of weld and HAZ failures but elongations were slightly lower for weld failures

References

1. "Alloy 6013 Sheet," Alcoa Technical Fact Sheet No. SPD-10-009 (undated).
2. "Alcoa Aluminum Alloy 6013," Alcoa Green Letter No. 225 (December 1987).
3. Kaneko, R. S.; Bakow, L.; Lee, E. W.; and Neu, C. E., "Aluminum 6013 Sheet Applications for New Navy Aircraft," Aeromat Conference (May 1990).
4. "Metallic Materials and Elements for Aerospace Vehicle Structures," *Military Handbook 5F*, pp. 3-229 to 3-231 (November 1, 1990).
5. Cieslak, S. J., Memorandum "re Alcoa Green Letter - Corrosion Resistance" (July 14, 1988).
6. "Tempers for Aluminum and Aluminum Alloy Products," Aluminum Association (August 1, 1989).
7. Zaiken, E., and Ritchie, R. O., "Effects of Microstructure on Fatigue Crack Propagation and Crack Closure Behavior in Aluminum Alloy 7150," *Materials Science and Engineering 70*, pp. 151-160 (1985).
8. Venkateswara Rao, K. T.; Yu, W.; and Ritchie, R. O., "On the Behavior of Small Fatigue Cracks in Commercial Aluminum-Lithium Alloys," *Eng. Fracture Mechanics*, Vol. 31, No. 4, pp. 623-635 (1988).
9. Letter K. R. Brown to H. Mindlin, Purdue University, CINDAS, "Corrosion Data on Alloy 6013," Kaiser Aluminum and Chemical Corp. (July 16, 1992).
10. "Alcoa 6013 Alloy," *Alloy Digest* (September 1987).
11. Letter K. R. Brown to H. Mindlin, Purdue University, CINDAS, "Mechanical and Corrosion Data on Alloy 6013," Kaiser Aluminum and Chemical Corp. (August 10, 1992).
12. Kaneko, R. S.; Bakow, L.; and Lee, E. W., "Aluminum Alloy 6013 Sheet for New Navy Aircraft," *Journal of Metals*, pp. 16-18 (May 1990).
13. Hardy, J. W., "Formability of Aluminum Alloy 6013 Sheet," Report MDC H5866, McDonnell Douglas Space Systems Co., Huntington Beach, CA (February 1990).
14. AMS 4216, Society of Automotive Engineers (July 1989).
15. AMS 4347A, Society of Automotive Engineers (April 1992).
16. AMS 2770E, Society of Automotive Engineers (January 1989).
17. Letter S. A. Jones to K. R. Brown, Kaiser Aluminum, Pleasanton, CA, "Comments on 6013 Data" (September 23, 1992).
18. Gutierrez, J. T.; Larson, B. F.; and Charles, J. F., "Fracture Mechanics, Forming and Weld Properties for 6013 Sheet." Report MDC, K0818, Douglas Aircraft Company, Long Beach, CA (December 1989).
19. Personal communication to W.F. Brown Jr. from J. Pengra: Lockheed Martin Skunk Works. Palmdale, CA.

	Al
7.6	Zn
2.5	Mg
1.5	Cu
0.15	Cr

7049

1 **GENERAL**

7049 and 7149 are wrought heat treated aluminum alloys which are used in the aerospace industry. In the T73 or T76 temper they have high strength and fracture toughness coupled with a high resistance to stress corrosion cracking in heavy sections.

In T73 temper, 7049 appears to have fatigue properties similar to 7075-T6 and 7079-T6 (1), and strength fracture toughness and stress corrosion properties similar to 7050-T73.

7149 is a high purity version of 7049. It has higher fracture toughness than 7049, but similar strength, fatigue, and corrosion properties (11, 12).

1.01 **Commercial Designation**

7049 (or 7149) -T73 and 7049-T7352 (forgings).
7049-T7351 (plate).
7049-T73511, 7049-T73510, 7049-T76511, and 7049-T76510 (extrusions).

1.02 **Alternate Designation**

UNS A97049.

1.03 **Specifications**

7049-T73 forgings: QQ-A-367 (28)
MIL-A-22771 (29)
AMS4111 (30).
7149-T73 forgings: AMS4320 (31).
7049-T73510 and -T73511 extrusions: AMS4157 (32).
7049-T76510 and -T76511 extrusions: AMS4159 (33).
7149-T73510 and -T73511 extrusions: AMS4343 (34).
7049-T7351 plate: AMS4200 (35).

1.04 **Composition**

Chemical compositions of 7049 and 7149, Table 1.04.

1.05 **Heat Treatment**

Both T73 and T76 tempers are solution heat treated and aged to different degrees past maximum strength, T6.

The product is usually stress relieved by stretching (final digit of temper designation = 1) or by compressing (final digit = 2).

The heat treatment procedure for forgings and extrusions that are not stress relieved by stretching or compression is given in MIL-6088. Users may obtain details from the producer of heat treatments for other products or for specific applications.

1.06 **Hardness**

(See also Figure 3.027232).

1.061 Typical hardness: 145 Brinell (500 kg load, 10 mm ball) (2) -T73
82 to 87 R_B (3) -T73
105 to 110 R_E (20) -T7351.

1.07 **Forms and Conditions Available**

7049 is currently available in die and hand forgings and heavy section extrusions up to 5 inch in thickness and in rolled plate form up to 4-1/4 inch in thickness. Other forms are subject to inquiry.

1.08 **Melting and Casting Practices**

1.09 **Special Considerations**

The plane strain fracture toughness of this alloy, like other high strength aluminum alloys, is sensitive to the content of the impurity elements iron and silicon. Reducing the content of these elements increases the fracture toughness with no change in tensile properties (see Tables 3.0214 and 3.027211) and no change in fatigue or corrosion behavior (11, 12).

As has been reported for other heat treated aluminum alloys (23), strength, hardness, and fracture toughness vary throughout the thickness of heavy sections of 7049 (see Figure 3.027232). Care should be taken that property comparisons are made at similar test sample locations, and that the data used are relevant to the section used in service.

2 **PHYSICAL AND CHEMICAL PROPERTIES**

2.01 **Thermal Properties**

2.011 Melting range.
2.012 Phase changes, alloy is subject to precipitation.
2.0121 Time-temperature-transformation diagrams.
2.013 Thermal conductivity: 89 Btu ft per (hr ft^2 F).
2.014 Thermal expansion, Figure 2.014.
2.015 Specific heat.
2.016 Thermal diffusivity.

2.02 **Other Physical Properties**

2.021 Density: 0.099 lb per $in.^3$ (6, 8), 2.74 gr per cm^3
0.102 lb per $in.^3$ (1), 2.82 gr per cm^3.
2.022 Electrical properties.
2.0221 Electrical conductivity, 38 percent minimum IACS (2).
20222 Electrical conductivity and yield strength of 7049-T7351 plate, Table 2.0222.
2.0223 Correlation of electrical conductivity and yield strength of 7049 Plate, Figure 2.0223 (7). (See also Table 3.0214.)
2.023 Magnetic properties, alloy is nonmagnetic.
2.024 Emissivity.
2.025 Damping capacity.

2.03 **Chemical Environments**

2.031 Corrosion performance of 7049 is similar to that of 7075, 7178, 7175, and 7050. Exfoliation resistance is good (3, 7, 13, 21).
2.0311 Results of accelerated exfoliation tests on 7049-T73 forgings, Table 2.0311.
2.032 Stress corrosion properties of this alloy in the T73 or T76 conditions are good (see data that follow). The slightly overaged T7X tempers are used in preference to T6 tempers because of their superior resistance to stress corrosion.
2.0321 Stress corrosion data from tests in industrial atmosphere, Table 2.0321.

	Al
7.6	Zn
2.5	Mg
1.5	Cu
0.15	Cr

7049

2.0322 Stress corrosion data from alternate immersion tests in artificial seawater, Table 2.0322.

2.0323 Percent survival of 7049-T7 die forgings versus ST yield strength when exposed to alternate immersion after 30 days and after 84 days, Figure 2.0323.

2.0324 Estimates of K_{Iscc} values for 7049-T73 forging in various media, Table 2.0324.

2.0325 K_{Iscc} estimates for 7049-T7351 plate in various media using samples with fatigue cracks, Table 2.0325.

2.0326 K_{Iscc} estimates for bolt-loaded DCB specimens of 7049-T7351 plate having pop-in precracks and tested under constant deflection conditions, Table 2.0326.

2.0327 Crack-growth rate versus initial stress intensity for 7049-T73 plate specimens exposed at Daytona Beach, Figure 2.0327.

2.0328 Crack growth in fatigue precracked DCB specimens of 3-inch 7049-T7351 plate in SL orientation under a constant load, Table 2.0328.

2.0329 Comparison of SCC results for 7049-T7351 plate based on selected exposure periods in several test media, Table 2.0329.

2.0330 Crack growth in fatigue precracked 1.25-inch 7049-T73 temper plates exposed to salt-chromate solution (7), Figure 2.0330.

2.0331 Crack growth in DCB specimen with pop-in precracks from 7049-T73 temper plates exposed at Daytona Beach (2), Figure 2.0331.

2.0332 Crack velocity versus K_i plot for 7049-T7351 plate at Daytona Beach, Figure 2.0332.

2.04 Nuclear Properties

3 MECHANICAL PROPERTIES

3.01 Specified Mechanical Properties

3.011 Aluminum Association mechanical property limits for T73 die forgings, Table 3.011.

3.012 Tentative minimum mechanical properties for die forgings and hand forgings, Table 3.012.

3.02 Mechanical Properties at Room Temperature

3.021 Tension.

3.0211 Tensile properties of 7049-T7351 plate from 1.25-inch to 4.25-inch thickness, Table 3.0211.

3.0212 Tensile properties of 7049-T73 hand forgings, Table 3.0212.

3.0213 Tensile properties of 7049-T73 die forgings, Table 3.0213.

3.0214 Tensile properties of 7049-T73511 and -T76511 extrusions of different chemical impurities, Table 3.0214.

3.0215 Tensile and other mechanical properties of 7049-T76 extrusions, Table 3.0215.

3.0216 Compression, shear, and bearing properties of 7049-T73 die forgings, Table 3.0216.

3.0217 Compression, shear, and bearing properties of 7049-T73 hand forgings, Table 3.0217 (see also Figure 3.06221).

3.0218 Compression and shear properties of 7049-T7351 plate, Table 3.0218.

3.0219 Effect of exposure at elevated temperature on room temperature tensile properties of forgings, Figure 3.0219.

3.022 Compression (see also Section 3.032).

3.0221 Stress-strain diagrams (see Section 3.032).

3.023 Impact.

3.0231 Charpy V-notch: 4.1 ft-lbs (8); 5.8 ft-lbs (longitudinal); 3.3 ft-lbs (transverse) (6); and see also Figure 3.0331 and Table 3.0215.

3.024 Bending.

3.025 Torsion and shear (see also Figure 3.0351 and Tables 3.0216, 3.0217, and 3.0218).

3.026 Bearing (see Figure 3.0361 and Tables 3.0216 and 3.0217).

3.027 Stress concentration.

3.0271 Typical notch tensile data (K_t = 3.0): Longitudinal = 103 ksi and transverse = 102 ksi (2).

3.0272 Fracture toughness.

3.02721 Extrusions.

3.027211 Fracture toughness of 7049-T73511 and -T76511 extrusions of different purity levels, Table 3.027211.

3.027212 Fracture toughness of 7049-T73 and -T76 extrusions of different dimensions, Table 3.027212.

3.02722 Forgings.

3.027221 Fracture toughness of die and hand forgings of 7049-T73, Table 3.027221.

3.027222 Fracture toughness of 7049-T73 hand forgings of different dimensions, Table 3.027222.

3.027223 Kahn tear test data for die forgings of 7049-T73, Table 3.027223.

3.02723 Plate.

3.027231 Fracture toughness of 7049-T7351 rolled plate of various thicknesses, Table 3.027231.

3.027232 Variation in hardness, fracture toughness, and tensile properties through the thickness of a 4.25-inch and a 2.5-inch thick rolled 7049-T7351 plate, Figure 3.027232.

3.03 Mechanical Properties at Various Temperatures

3.031 Tension.

3.0311 Stress-strain curves.

3.03111 Typical longitudinal stress-strain curves in tension for 5-inch forgings at room and elevated temperatures, Figure 3.03111.

3.03112 Typical transverse stress-strain curves in tension for 5-inch forgings at room and elevated temperatures, Figure 3.03112.

3.03113 Typical tensile stress-strain curves in longitudinal direction for 7049-T76 extrusions, Figure 3.03113.

3.03114 Typical tensile stress-strain curves in transverse direction for 7049-T76 extrusions, Figure 3.03114.

3.0312 Effect of exposure and test temperature on tensile properties of forgings, Figure 3.0312.

3.0313 Effect of temperature on tensile properties of 5-inch forgings, Figure 3.0313.

3.0314 Effect of temperature on the tensile properties and tensile modulus of 7049-T76 extrusions, Figure 3.0314.

3.0315 Tensile property data for the longitudinal direction for 7049-T73 extrusion and bar, and 7049-T76 extruded bar, Figure 3.0315.

3.0316 Tensile property data for the transverse direction for 7049-T73 bar and extrusion, and 7049-T76 extruded bar, Figure 3.0316.

3.0317 Tensile property data for the short transverse direction for 7049-T73 bar and extrusion, and 7049-T76 extruded bar, Figure 3.0317.

3.032	Compression. (See also Table 3.0215 for modulus data.)
3.0321	Stress-strain curves.
3.03211	Typical longitudinal stress-strain curves in compression for 5-inch forgings at room and elevated temperatures, Figure 3.03211.
3.03212	Typical transverse stress-strain curves in compression for 5-inch forgings at room and elevated temperatures, Figure 3.03212.
3.03213	Typical longitudinal compressive stress-strain curves for 7049-T76 extrusion, at room and elevated temperatures, Figure 3.03213.
3.03214	Typical transverse compressive stress-strain curves for 7049-T76 extrusion, at room and elevated temperatures, Figure 3.03214.
3.0322	Effect of exposure and test temperature on compressive yield strength of 5-inch forgings, Figure 3.0322.
3.0323	Effect of temperature on compressive yield strength of 5-inch forgings, Figure 3.0323.
3.0324	Effect of temperature on the compressive properties of 7049-T76 extrusion, Figure 3.0324.
3.033	Impact.
3.0331	Effect of temperature on Charpy V-notch impact energy, Figure 3.0331.
3.034	Bending.
3.035	Torsion and shear.
3.0351	Effect of exposure and test temperature on ultimate shear strength of forgings as determined with double shear test specimen, Figure 3.0351.
3.036	Bearing.
3.0361	Effect of exposure and test temperature on bearing properties of 5-inch forgings, Figure 3.0361.
3.037	Stress concentration.
3.0371	Notch properties.
3.038	Combined properties.
3.04	**Creep and Creep-Rupture Properties**
3.041	Creep-rupture curves for 5-inch forgings at 250, 300, and 500 F, Figure 3.041.
3.042	Creep curves for 5-inch forgings showing time for 0.2 percent plastic deformation, Figure 3.042.
3.043	Creep-rupture and creep deformation in transverse direction for 7049-T76 extrusions at various temperatures, Figure 3.043.
3.05	**Fatigue Properties**
3.051	Fatigue data for smooth and notched specimens from forgings at room and elevated temperatures, Table 3.051.
3.052	Axial load fatigue curves at room and elevated temperatures, Figure 3.052.
3.053	Axial load fatigue curves for smooth and notched specimens from 3-inch forgings at room temperature, Figure 3.053.
3.054	Axial load fatigue curve for notched specimens from forgings, Figure 3.054.
3.055	Axial load fatigue curves for notched specimens at room and elevated temperatures, Figure 3.055.
3.056	Notched and smooth fatigue data for 7049-T73511 extrusions of different purities, Figure 3.056.
3.057	Axial stress fatigue data for notched and smooth 7049-T73 integrally stiffened extrusions, Figure 3.057.
3.058	Notched axial stress fatigue data for a 7049-T73 extrusion, Figure 3.058.
3.059	Axial stress fatigue data for smooth and notched 7049-T73 extrusions at 250 F, Figure 3.059.
3.0510	Notched and smooth axial stress fatigue data for 7049-T73 and-T76 extrusions at 350 F, Figure 3.0510.
3.0511	Axial stress fatigue data for notched and smooth 7049-T73 integrally stiffened extrusions at 350 F, Figure 3.0511.
3.0512	Notched axial stress fatigue data for 7049-T76 extrusions at room and elevated temperatures, Figure 3.0512.
3.0513	Smooth axial stress fatigue data for 7049-T76 extrusions at various temperatures, Figure 3.0513.
3.0514	Unnotched axial stress fatigue data in the transverse direction for 7049-T7351 plate at various temperatures, Figure 3.0514.
3.0515	Notched axial stress fatigue data for 7049-T7351 plate at various temperatures, Figure 3.0515.
3.0516	Fatigue crack-growth data for 7049-T73 hand forging in different environments, Figure 3.0516.
3.0517	Effect of salt fog on the fatigue life of 7049-T73 forgings, Figure 3.0517.
3.0518	Fatigue crack-growth rate curves for 7149-T73511 and -T76511 extrusions in laboratory air and high humidity air, Figure 3.0518.
3.0519	Fatigue crack-growth rate curves for medium purity 7049-T73511 and -T76511 extrusions in laboratory air and high humidity air, Figure 3.0519.
3.0520	Fatigue crack-growth rate curves for low purity 7049-T73511 and -T76511 in laboratory air and high humidity air, Figure 3.0520.
3.06	**Elastic Properties**
3.061	Poisson's ratio.
3.062	Modulus of elasticity.
3.0621	Effect of temperature on modulus of elasticity, Figure 3.0621.
3.0622	Compression modulus.
3.06221	Effect of temperature on compression modulus, Figure 3.06221.
3.063	Modulus of rigidity.
3.064	Tangent modulus.
3.0641	Typical longitudinal curves in compression for 5-inch T73 forgings at room and elevated temperatures, Figure 3.0641.
3.0642	Typical transverse curves in compression for 5-inch T73 forgings at room and elevated temperatures, Figure 3.0642. (See also Figures 3.0643 and 3.0644.)
3.0643	Typical longitudinal tangent modulus curves in compression for T76 extrusions at room and elevated temperatures, Figure 3.0643.
3.0644	Typical transverse tangent modulus curves in compressions for T76 extrusions at room and elevated temperatures, Figure 3.0644.

	Al
7.6	Zn
2.5	Mg
1.5	Cu
0.15	Cr

7049

4 FABRICATION

4.01 Forming

Specific data on the fabrication characteristics of this alloy are not available at this time. Because of similarity in chemical composition, the formability is expected to be similar to 7075 and 7078 in comparable heat treat conditions.

	Al
7.6	Zn
2.5	Mg
1.5	Cu
0.15	Cr

7049

4.02 **Machining and Grinding**

For detailed information, refer to the Machinability Data Center, Metcut Research Associates, Inc., in Cincinnati, Ohio.

4.03 **Joining**

(See also 7075.)

4031 General. Weldability is limited because of crack sensitivity or loss in resistance to corrosion and loss of mechanical properties. Resistance spot welding can be done with special techniques that may require development (1).

4.04 **Surface Treatment**

REFERENCES

1 Military Standardization Handbook MIL-HDBK-5D, (June 1, 1983).

2 "7049-T73 Kaiser Aluminum's New Aluminum Alloy for Forgings," Kaiser Aluminum, DE-255 (January 1970).

3 Boeing Test Data on Alloy X7049-T73, Manufacturing Technology Division, Boeing Company, Seattle (December 1969).

4 Mixon, W. and Turley, R. V., "Evaluation of Aluminum Alloys 7049-T73 and 7175-T736 Die Forgings," Eng. Technical Report No. MDC-J0692, Douglas Aircraft Company (April 1970).

5 Deel, O. L. and Mindlin, H., "Engineering Data on New and Emerging Structural Materials," Battelle Memorial Institute, Technical Report AFML-TR-70-252 (October 1970).

6 Deel, O. L., "Engineering Data on New Aerospace Structural Materials," Prepared for Air Force Materials Laboratory by Battelle Columbus Laboratories, AFML-TR-75-97 (June 1975).

7 Dorward, R. C. and Hasse, K. R., "Flaw Growth of 7075, 7475, 7050, and 7049 Aluminum Plate in Stress Corrosion Environments," NASA NAS 8-30890, Kaiser Report CFT RR 76-32 (October 15, 1976).

8 Data Sheet, "Mechanical Property Data 7049 Aluminum-T73 Forgings," Prepared by Battelle Memorial Institute, Columbus Laboratories, issued by Air Force Materials Laboratory, Wright-Patterson AFB, Ohio (December 1969).

9 The Aluminum Association, "Tempers for Aluminum Alloy Products Registered with the Aluminum Association," Revised (June 15, 1970).

10 Jones, R. E., "Mechanical Properties of 7049-T73 and 7049-T76 Aluminum Alloy Extrusions at Several Temperatures," AFML-TR-72-2, Air Force Materials Laboratory, Wright-Patterson AFB, Ohio (February 1972).

11 Petrak, G. J., "Effects of Purity Level on the Mechanical Properties of 7000-Series Aluminum," Technical Report AFWAL-TR-80-4079, Air Force Materials Laboratory, Wright-Patterson AFB, Ohio (October 1980).

12 Van Orden, J. M., et al, "Effects of Purity on Fatigue and Fracture of 7XXX-T76511 Aluminum Extrusions," Journal of Aircraft, Vol. 16, No. 5, (May 1979) p 327-335.

13 Babilon, C. F., Wygonik, R. H., Nordmark, G. E., and Lifka, B. W., "Mechanical Properties, Fracture Toughness, Fatigue Crack Growth Rates and Corrosion Characteristics of High-Toughness Aluminum Alloy Forgings, Sheet and Plate," AFML-TR-73-83, Air Force Materials Laboratory, Wright-Patterson AFB, Ohio (April 1973).

14 Ferguson, R. R. and Berryman, R. C., "Fracture Mechanics Evaluation of B-1 Materials," AFML-TR-76-137, Air Force Materials Laboratory, Wright-Patterson AFB, Ohio (October 1976).

15 Battelle Memorial Institute, Columbus Laboratories, Final report on program for the static and fatigue evaluation of a 3-inch thick 7049-T73 aluminum forging prepared for Kaiser Aluminum and Chemical Corporation (August 1969).

16 Private Communication Between O. Deel, Battelle Memorial Institute, and L. J. Barker, Kaiser Aluminum and Chemical Corporation (December 1969).

17 L. J. Barker to Paul Ruff, Battelle Columbus Laboratories, Letter to Military Handbook 5 Committee enclosing mechanical property data for 7049-T735 plate (May 25, 1982).

18 Deel, O. L. and Mindlin, H., "Engineering Data on New Aerospace Structural Materials," Technical Report AFML-TR-72-196, Volume II, Air Force Materials Laboratory, Wright-Patterson AFB, Ohio (September 1972).

19 Person, N. L., "Fatigue Properties of Aluminum Alloy Extrusions – A Compilation of Data," Kaiser Aluminum and Chemical Corporation Research Report CFT RR 81-6 (November 1982).

20 Brown, K. R., Letter to H. Hucek, Battelle Columbus Laboratories, March 3, 1983, enclosing fracture toughness data on Kaiser 7049-T7351 rolled plate.

21 Dorward, R. C. and Hasse, K. R., "Flaw Growth of 7075, 7475, 7050, and 7049 Aluminum Plate in Stress Corrosion Environments: 2-Year Marine Atmosphere Results," NASA NAS 8-30890, Kaiser Report CFT RR 78-16 (June 22, 1978).

22 Humphries, T. S. and Nelson, E. E., "Seacoast Stress Corrosion Cracking of Aluminum Alloys," NASA TM 82393, George C. Marshall Space Flight Center, Alabama (January 1981).

23 Brown, K. R., "Factors Influencing the Fracture Toughness of High Strength Aluminum Alloys," Proceedings of ICSMA-6, Melbourne, Australia (August 1982) p 765.

24 Staley, J. T., "Comparison of Aluminum Alloys 7050, 7049, MA52 and 7175-T736 Die Forgings," AFML-TR-73-34, Air Force Materials Laboratory, Wright-Patterson AFB, Ohio (May 1973).

25 Data Sheets, "Mechanical Properties-7049-T73 Hand Forgings and Die Forgings," Kaiser Aluminum and Chemical Corporation (April 1970).

26 Registration Record of Aluminum Association Designations and Chemical Composition Limits for Wrought Aluminum and Wrought Aluminum Alloys," Aluminum Association, Inc., Washington, D. C. (March 1, 1980).

27 Pratt, W. M., "Material-Kaiser Aluminum Alloy X7049-T73, Effect of Elevated Temperature on Mechanical Properties," Report FGT-5541, General Dynamics, Fort Worth Division (December 1969).

28 Federal Specification – Aluminum Alloy Forgings, QQ-A-367 H (December 26, 1973 – amendments to January 21, 1981).

29 MIL-A-22771C Military Specification, Aluminum Alloy Forgings, Heat Treated (August 25, 1969).

30 AMS 4111A, "Aluminum Alloy Forgings, 7049-T73," Society of Automotive Engineers, Warrendale, Pa. (Revised October 15, 1980).

31 AMS 4320, "Aluminum Alloy Forgings, 7149-T73", Society of Automotive Engineers, Warrendale, Pa. (Issued July 1, 1981).

32 AMS 4157A, "Aluminum Alloy Extrusions, 7049-T73511," Society of Automotive Engineers, Warrendale, Pa. (Revised July 1, 1982).

33 AMS 4159A, "Aluminum Alloy Extrusions, 7049-T76511," Society of Automotive Engineers, Warrendale, Pa. (Revised July 1, 1982).

34 AMS 4343, "Aluminum Alloy Extrusions, 7149-T73511," Society of Automotive Engineers, Warrendale, Pa. (Issued January 15, 1980).

35 AMS 4200, "Aluminum Alloy Plate, 7049-T7351," Society of Automotive Engineers, Warrendale, Pa. (Issued January 15, 1978).

	Al
7.6	Zn
2.5	Mg
1.5	Cu
0.15	Cr

7049

	Al
7.6	Zn
2.5	Mg
1.5	Cu
0.15	Cr

7049

Alloy	7049 (2)	7049 (3, 4, 35)		7149 (3, 4, 31)
Composition	Percent Nominal	Percent Min	Max	Percent Max
Zn	7.6	7.2	8.2	8.2
Mg	2.5	2.0	2.9	2.9
Cu	1.5	1.2	1.9	1.9
Cr	0.15	0.10	0.22	0.22
Si	–	–	0.25	0.15
Fe	–	–	0.35	0.20
Ti	–	–	0.10	0.10
Mn	–	–	0.20	0.20
Others				
Each	–	–	0.05	0.05
Total	–	–	0.15	0.15
Al	Balance	Balance		Balance

TABLE 1.04. CHEMICAL COMPOSITIONS OF 7049 AND 7149 (2,3,4,31,35)

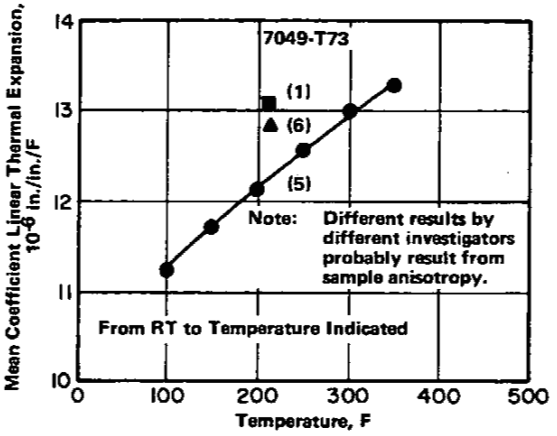


FIGURE 2.014. THERMAL EXPANSION (1,5,6)

Alloy	7049-T7351			
Form	Plate			
	Electrical Conductivity, percent IACS		Yield Strength, ksi	
Thickness, inch	Min Age	Typical Age	Min Age	Typical Age
1.25	40.8	42.5	71.5	67.0
3.00	40.1	41.7	69.8	65.3

TABLE 2.0222. ELECTRICAL CONDUCTIVITY AND YIELD STRENGTH OF 7049-T7351 PLATE (7)

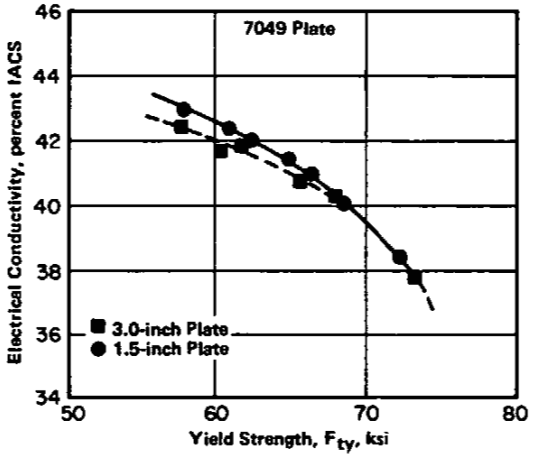


FIGURE 2.0223. CORRELATION OF ELECTRICAL CONDUCTIVITY AND YIELD STRENGTH OF 7049 PLATE (7)

Alloy	7049-T73	
Form	Forgings	
Sample Thickness or Dimensions, inch	Visual Rating(a)	
	EXCO(b)	Salt Spray(c)
Die Forgings		
≤1.000	P	–
≤1.000	P (T/2)	–
1.001 to 2.000	P	E-A
	E-A(T/2)	–
2.001 to 3.000	P	–
	P	–
1.001 to 2.000	P	–
2.001 to 3.000	P	–
4.001 to 5.000	P	–
Hand Forgings		
2 x 16	P	P
3 x 16	E-A	–
4 x 16	P	–
5 x 20	E-B	E-A

Note: All test specimens were located within 10 percent of the product thickness, except those noted to be T/2, mid-thickness.

(a) ASTM Method G34-72: P = pitting, and E = exfoliation; severity is denoted by the letter A, B, or C in increasing severity.

(b) Total immersion in 4N. NaCl + 0.5N. KNO_3 + 0.1N. HNO_3 solution for 48 hours.

(c) Total immersion in acidified salt solution for 1 week.

TABLE 2.0311. RESULTS OF ACCELERATED EXFOLIATION TESTS ON 7049-T73 FORGINGS (13)

Alloy	7049-T73		
Form	4.5-inch diam Die Forging		
Test	Stress Corrosion[a]		
Specimen	Battelle Type[b]		
Forging Number	Grain Direction	Stress, ksi	Days to Failure
1	ST	55	NF[c]
2	ST	55	NF
3	ST	55	NF
1	ST	45	NF
2	ST	45	NF
3	ST	45	NF
1	ST	35	NF
2	ST	35	NF
2	ST	35	NF

(a) Industrial atmosphere in Renton, Washington.
(b) Battelle tuning-fork type specimen – chromic acid anodized to minimize general corrosion.
(c) NF – no failure in 90 days.

TABLE 2.0321. STRESS CORROSION DATA FROM TESTS IN INDUSTRIAL ATMOSPHERE (3)

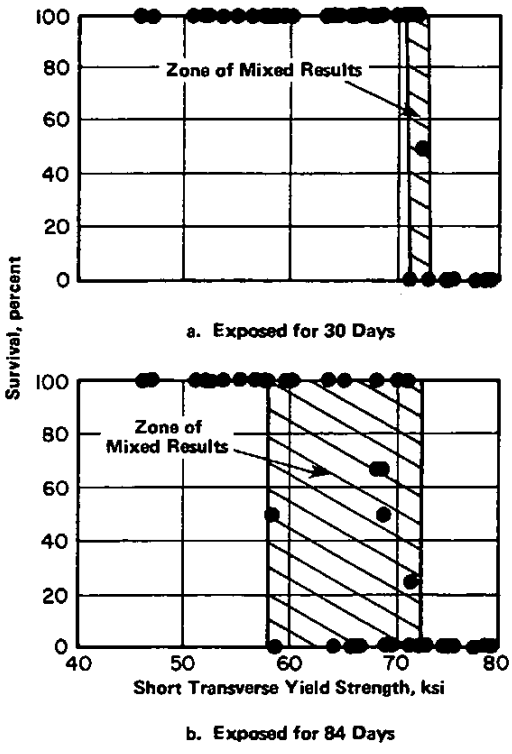


FIGURE 2.0323. PERCENT SURVIVAL OF 7049-T7X DIE FORGINGS VERSUS ST YIELD STRENGTH WHEN EXPOSED TO ALTERNATE IMMERSION AFTER 30 DAYS AND AFTER 84 DAYS (24)

Alloy	7049-T73			
Form	Forgings			
Test	Stress Corrosion[a]			
Sustained Stress,[a] ksi	Exposure Days[b]	F_{tu}, ksi (Residual)	F_{tu} (R)[c] / F_{tu}(O)	e, percent (Residual)
45	84 NF	69.7	0.90	3.3
45	84 NF	63.4	0.82	2.8
45	84 NF	65.2	0.85	2.2
45	84 NF	54.1	0.70	0.6
45	84 NF	64.9	0.84	1.9
40	84 NF	65.7	0.85	1.9
40	84 NF	65.8	0.85	0.0
40	84 NF	68.8	0.89	1.5

Note: Axial (constant load).

(a) Alternate immersion in substitute ocean water per ASTM D1141-52. Solution pH between 7.8 and 8.2. Cycle consisted of 10 minutes immersion and 50 minutes air dry each hour for 84 days or until failure.
(b) NF = No failure.
(c) Ratio of ultimate strength: R = Residual and O = Original.

TABLE 2.0322. STRESS CORROSION DATA FROM ALTERNATE IMMERSION TESTS IN ARTIFICIAL SEAWATER (4)

Alloy	7049-T73			
Form	3 x 4 x 48-inch Forged Block			
Direction	K_{Ic}, ksi$\sqrt{in.}$	Environment[a]	$\frac{K_{Iscc}}{K_{Ic}}$, percent	K_{Iscc}, ksi$\sqrt{in.}$
LT	38	STW	55	21.0
		SCS	73	27.6
		FCS	>75	>28.5
TL	23	STW	87	20.0
SL	23	STW	80	18.5

(a) STW (sump tank water) – see Code 3221, Table 2.0335, SCS (shop cleaning solvent) – aliphatic naphtha, and FCS (field cleaning solvent) – trisodium phosphate.
(b) Fatigue crack specimens treated in laboratory air.

TABLE 2.0324. ESTIMATES OF K_{Iscc} VALUES FOR 7049-T73 FORGING IN VARIOUS MEDIA (14)

Al
7.6 Zn
2.5 Mg
1.5 Cu
0.15 Cr

7049

	Al
7.6	Zn
2.5	Mg
1.5	Cu
0.15	Cr

7049

Alloy	7049-T7351				
Form	Plate				
Type of Tests	Constant Load				
Test Direction	LT	SL	SL		
Plate Thickness, inch	Yield Strength, ksi	K_{Ic}, ksi$\sqrt{in.}$	K_{Iscc}, ksi$\sqrt{in.}$(a)		
			Synthetic Seawater(b)	Salt-Chromate Solution(c)	Daytona Beach
3.0	65.1	25.1	23.2 (23.0)(d)	<23.2 (22.0)	– –
1.25	67.0	25.3	20.0 (21.5)	13.2 (<16.0)	19.1 (23.0)

(a) Stress intensity at which crack-growth rate decreased to 1 x 10^{-5} in./hr.
(b) Alternate immersion, 10 minutes in solution plus 50 minutes in air.
(c) Constant immersion in 0.6 M. NaCl + 0.02 M. $Na_2Cr_2O_7$ + 0.07 M. $NaC_2H_3O_2$ + $HC_2H_3O_2$ to pH = 4.
(d) Numbers in parentheses are K_{Iscc} estimates based on specimens containing pop-in precracks and tested under constant deflection conditions.

TABLE 2.0325. K_{Iscc} ESTIMATES FOR 7049-T7351 PLATE IN VARIOUS MEDIA USING SAMPLES WITH FATIGUE CRACKS (7)

Alloy	7049-T7351						
Form	Plate						
Plate Thickness, inch	LT Yield Strength, ksi	SL K_{Iscc}, ksi$\sqrt{in.}$(a)			TL K_{Iscc}, ksi$\sqrt{in.}$(a)		
		Daytona Beach	Synthetic Seawater(b)	Salt-Chromate Solution(c)	Daytona Beach	Synthetic Seawater(b)	Salt-Chromate Solution(c)
1.25	67	23	21.4	<15.9	26.8	26.4	26.4
3.00	65	23	23.0	21.8	26.4	25.9	>26.8

(a) Stress intensity at which crack-growth rate decreased to 1 x 10^{-5} in./hr.
(b) Alternate immersion, 10 minutes in solution plus 50 minutes in air.
(c) Constant immersion in 0.6 M. NaCl + 0.02 M. $Na_2Cr_2O_7$ + 0.07 M. $NaC_2H_3O_2$ + $HC_2H_3O_2$ to pH = 4.

TABLE 2.0326. K_{Iscc} ESTIMATES FOR BOLT-LOADED DCB SPECIMENS OF 7049-T7351 PLATE HAVING POP-IN PRECRACKS AND TESTED UNDER CONSTANT DEFLECTION CONDITIONS (7, 21)

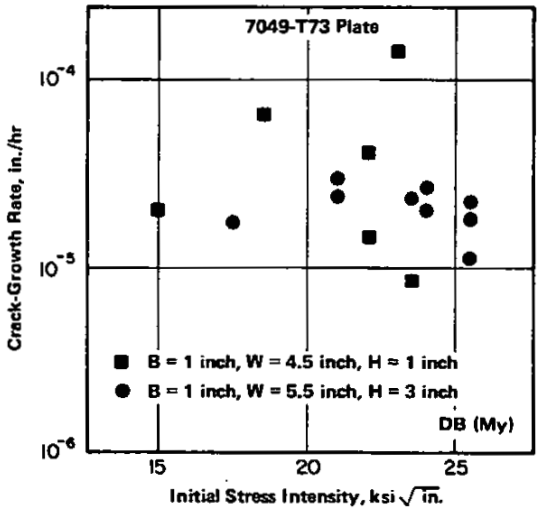


FIGURE 2.0327. CRACK-GROWTH RATE VERSUS INITIAL STRESS INTENSITY FOR 7049-T73 PLATE SPECIMENS EXPOSED AT DAYTONA BEACH (7)

Al	
7.6	Zn
2.5	Mg
1.5	Cu
0.15	Cr

7049

Alloy	7049-T7351					
Form	Plate					
Yield Strength(a), ksi	K_{Ic}, ksi$\sqrt{in.}$	Exposure Time, days	Stress Intensity,(b) ksi$\sqrt{in.}$	Crack Extension, inch	Average Crack Velocity, 10^{-8} in./sec	Measured Range of Velocity, 10^{-8} in./sec
Synthetic Seawater(c)						
65.1	25.1	61 90	24.6 to 25.1 23.3 to 23.7	0.0315 0.0197	0.59 0.24	0.51 to 0.55 0.16 to 0.59
Salt-Chromate Solution(d)						
65.1	25.1	90 67	24.5 to 27.1 22.4 to 24.2	0.150 0.098	1.93 1.69	0.98 to 1.65 0.67 to 1.81

(a) Test direction for yield strength only was LT.
(b) Initial applied stress intensity.
(c) Alternate immersion, 10 minutes in solution plus 50 minutes in air.
(d) See Table 2.0326.

TABLE 2.0328. CRACK GROWTH IN FATIGUE PRECRACKED DCB SPECIMENS FROM 3-INCH 7049-T7351 PLATE IN SL ORIENTATION UNDER A CONSTANT LOAD (7)

Alloy	7049-T7351							
Form	3-inch Plate							
Stress, percent F_{ty}(b)	Failure Ratio(a)							
	Kennedy Space Center Seacoast			Alternate Immersion in Salt Water(c)			Alternate Immersion in Seawater(c)	
	12 mo	24 mo	38 mo	0.3 mo	0.7 mo	3 mo	1 mo	3 mo
75	0/8	0/8	3/8	0/3	0/3	2/3	0/3	0/3
100	0/8	5/8	7/8	0/3	0/3	3/3	0/3	0/3

(a) Number of specimens failed/number of specimens exposed.
(b) Smooth round ST axial stress specimens.
(c) Ten minutes in solution plus 50 minutes in air.

TABLE 2.0329. COMPARISON OF SCC RESULTS FOR 7049-T7351 PLATE BASED ON SELECTED EXPOSURE PERIODS IN SEVERAL TEST MEDIA (22)

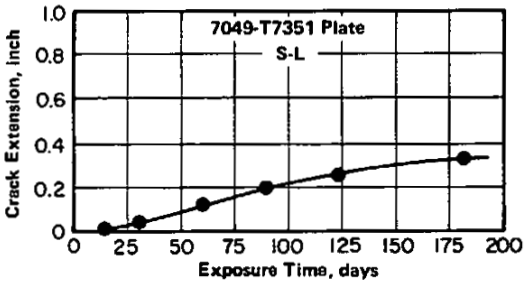


FIGURE 2.0330. CRACK GROWTH IN FATIGUE PRE-CRACKED 1.25-INCH 7049-T73 TEMPER PLATES EXPOSED TO SALT-CHROMATE SOLUTION (7)

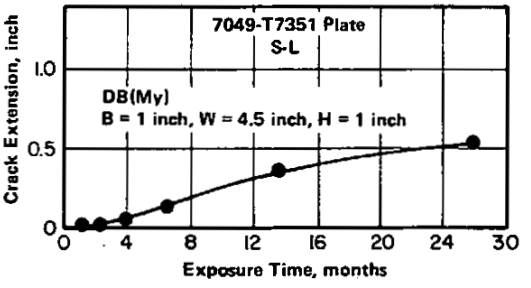


FIGURE 2.0331. CRACK GROWTH IN DCB SPECIMENS WITH POP-IN PRECRACK FROM T73 TEMPER PLATES EXPOSED AT DAYTONA BEACH (21)

	Al
7.6	Zn
2.5	Mg
1.5	Cu
0.15	Cr

7049

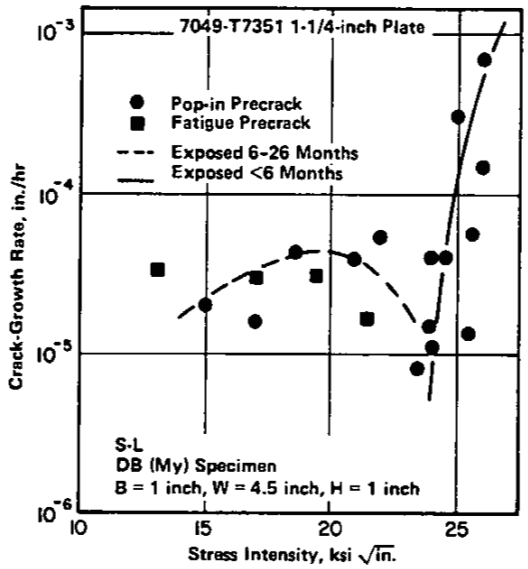


FIGURE 2.0332. CRACK VELOCITY VERSUS STRESS INTENSITY PLOT FOR 7049-T7351 PLATE AT DAYTONA BEACH (21)

Alloy	7049-T73					
Form	Die Forgings[a]					
	F_{tu}, ksi (Min)		F_{ty}, ksi (Min)		e, percent[b] (Min)	
Thickness, inch	A	B	A	B	A	B
Up thru 1.000	72.0	71.0	62.0	61.0	7	3
1.001 to 2.000	72.0	70.0	62.0	60.0	7	3
2.001 to 3.000	71.0	70.0	61.0	60.0	7	3
3.001 to 4.000	71.0	70.0	61.0	60.0	7	2
4.001 to 5.000	70.0	68.0	60.0	58.0	7	2

(a) A -- parallel to grain flow and B – not parallel to grain flow.
(b) 2 inch or 4D gage length.

TABLE 3.011. ALUMINUM ASSOCIATION MECHANICAL PROPERTY LIMITS FOR T73 DIE FORGINGS (9)

Alloy		7049-T73							
Form		Die Forgings[a]					Hand Forgings		
Thickness, inch		≤1.000	1.001 to 2.000	2.001 to 3.000	3.001 to 4.000	4.001 to 5.000	2.001 to 3.000	3.001 to 4.000	4.001 to 5.000
F_{tu}, ksi (Min)	L	72	72	71	71	70	71	69	67
	T	–	–	–	–	–	71	69	67
	ST	71	70	70	70	68	69	67	66
F_{ty}, ksi (Min)	L	62	62	61	61	60	61	59	56
	T	–	–	–	–	–	59	57	56
	ST	61	60	60	60	58	58	56	55
F_{cy}, ksi (Min)	L	64	64	63	63	62	61	59	57
	T	–	–	–	–	–	60	58	56
	ST	58	58	59	57	56	62	60	59
F_{su}, ksi (Min)		40	40	40	40	39	40	39	38
e, percent (Min)	L	7	7	7	7	7	9	8	7
	T	–	–	–	–	–	4	3	3
	ST	3	3	3	2	2	3	2	2

(a) For die forgings, the L and ST values are for the directions parallel (within ± 15 degrees) and not parallel (as close as possible to ST direction) respectively, to the forging flow lines.

TABLE 3.012. DESIGN MECHANICAL PROPERTIES FOR DIE FORGINGS AND HAND FORGINGS (1)

	Al
7.6	Zn
2.5	Mg
1.5	Cu
0.15	Cr

7049

Alloy	7049-T7351								
Form	Plate								
Thickness, inch	Source	F_{tu}, ksi			F_{ty}, ksi			e, percent		
		L	LT	ST	L	LT	ST	L	LT	ST
3.00	(6)	75.5	74.6	–	66.5	64.7	–	13.0	10.7	–
3.00	(7)	75.1	76.2	72.5	65.5	65.3	60.4	12.0	9.8	5.0
1.25	(7)	77.5	75.5	71.9	67.6	67.0	63.3	12.3	11.0	4.0
1.50 (1 lot)	(17)	79.4	76.7	75.8	70.3	67.4	63.3	12.5	11.5	8.0
2.00 (2 lots)	(17)	77.3	77.6	76.0	68.6	68.3	64.0	12.7	10.4	7.7
2.50 (1 lot)	(17)	74.2	74.9	71.5	63.7	64.0	59.3	12.5	10.5	7.0
3.50 (2 lots)	(17)	73.9	74.0	71.6	64.0	62.8	59.2	12.5	10.6	5.5
3.75 (1 lot)	(17)	76.9	77.4	75.1	69.1	67.1	63.8	13.0	10.0	6.4
4.00 (1 lot)	(17)	75.3	75.4	70.0	65.9	64.5	58.5	11.0	11.5	6.0
4.25 (2 lots)	(17)	71.4	71.6	68.4	60.7	59.7	56.8	11.9	11.0	4.5

TABLE 3.0211. TENSILE PROPERTIES OF 7049-T7351 PLATE FROM 1.25-INCH TO 4.25-INCH THICKNESS (6, 7, 17)

Alloy	7049-T73						
Form	Hand Forgings						
			Tensile				
Source	Size or Thickness, inch	Direction	F_{tu}, ksi	F_{ty},(a) ksi	e (in 4D), percent	RA, percent
(13)	2 x 16	L	76.4	68.8	11.0	30
		LT	75.1	67.0	10.5	24
		ST	70.6	62.4	3.1	4
(13)	3 x 16	L	74.2	65.4	13.0	34
		LT	75.2	66.2	11.5	27
		ST	72.2	62.3	7.5	12
(13)	11 x 16	L	80.0	72.8	12.5	31
		LT	76.4	68.5	9.5	17
		ST	75.5	67.5	7.9	16
(13)	5 x 20	L	70.3	60.1	13.5	31
		LT	68.4	58.1	12.0	23
		ST	68.1	59.1	6.0	6
(15)	3	L	73.8	64.6	13.2	–
		LT	76.8	68.7	10.8	–
		ST	73.8	67.4	8.0	–
(16)	5	L	72.9	64.2	8.8	–
		LT	74.9	66.5	11.0	–
		ST	70.9	61.9	6.0	–
(14)	3(b)	L	76	67.0	12.0	33
		LT	73	64.0	9.0	13
		ST	74	62.0	9.0	–

(a) The values at 0.2 percent offset.
(b) This 3-inch forging is T7352.

TABLE 3.0212. TENSILE PROPERTIES OF 7049-T73 HAND FORGINGS (13, 14, 15, 16)

	Al
7.6	Zn
2.5	Mg
1.5	Cu
0.15	Cr

7049

Alloy	7049-T73					
Form	Die Forgings					
Forging Size	Direction	Source	F_{tu}, ksi	F_{ty}, ksi	e, percent	RA, percent
≤1.000 inch	L	(13)	81.3	74.5	13.5	32.0
	ST		71.9	61.8	10.0	22.0
1.001 to 2.000 inch (Avg 4 Lots)	L	(13)	78.9	72.0	12.7	30.0
	ST		75.6	67.9	8.4	10.0
	L(a)	(4)	77.5	69.1	11.5	25.6
	T(a)	(4)	71.7	61.8	8.9	17.1
	ST(b)	(4)	76.9	68.7	9.0	17.7
2.001 to 3.000 inch (Avg 3 Lots)	L	(13)	79.0	71.5	12.5	30.0
	ST	(13)	74.0	65.3	7.7	11.0
4.001 to 5.000 inch	L	(13)	76.5	65.7	12.5	26.0
	ST	(13)	73.3	65.5	2.9	4.0
24 lb	L	(14)	77.0	68.0	13.0	31.0
24 lb	ST	(14)	74.0	67.0	6.0	16.0
24 lb	L	(14)	88.0	74.0	12.0	–
24 lb	T	(14)	77.0	70.0	6.0	–
24 lb	ST	(14)	74.0	69.0	4.0	–

(a) L and T samples from 4.5-inch thick section.
(b) ST samples from 1.3-inch thick section.

TABLE 3.0213. TENSILE PROPERTIES OF 7049-T73 DIE FORGINGS (4, 13, 14)

Alloy	7049-T73511 and -T76511									
Form	1.5 x 4.5-inch(a) Extruded Rectangles									
				T73511 (11)(b)				T76511 (12)			
Chemical Purity	Si, percent	Fe, percent	Direction	F_{tu}, ksi	F_{ty}, ksi	e, percent	RA, percent	F_{tu}, ksi	F_{ty}, ksi	e, percent	RA, percent
High(c)	0.08	0.09	L	83.9	76.7	13.3	35.6	83.3	74.6	12	31
			T	78.5	70.3	12.5	26.8	78.2	69.6	9	14
			ST	74.8	65.3	8.0	11.7	77.6	64.9	10	11
Medium	0.11	0.20	L	82.5	75.4	12.4	29.8	83.7	74.1	11	26
			T	76.5	69.2	10.5	18.2	79.8	71.4	11	17
			ST(d)	54.1	38.4	11.3	14.7	75.9	66.6	8	10
Low	0.16	0.37	L	80.0	73.1	11.6	27.1	81.7	73.3	10	22
			T	75.7	68.6	9.0	11.6	74.9	67.8	7	10
			ST	69.2	62.3	5.0	5.0	73.9	64.9	8	9

(a) Average of two or three specimens.
(b) Electrical conductivity (percent IACS): high–40.3; medium–40.5; and low–40.1.
(c) Equivalent of 7149.
(d) Anomalous T7351 result recognized, no explanation found.

TABLE 3.0214. TENSILE PROPERTIES OF 7049-T73511 AND -T76511 EXTRUSIONS OF DIFFERENT CHEMICAL IMPURITIES (11, 12)

Alloy	7049-T76					
Form	Extrusions					
	4 x 4 inch (18)			3-1/4 x 3-1/2 inch (10)		
Direction	L	T	ST	L	T	ST
F_{tu}, ksi	83.4	76.2	76.3	82.7	76.7	75.1
F_{ty}, ksi	75.9	67.4	67.7	75.5	68.6	65.8
e, percent	12.7	11.2	11.7	11.6	11.3	8.3
RA, percent	35.6	23.3	22.6	31.0	29.0	18.0
Modulus, 1000 ksi	10.7	9.9	10.4	–	–	–
F_{cy}, ksi	78.8	74.7	–	–	–	–
Compression Modulus, 1000 ksi	10.9	10.5	–	–	–	–
F_{su}, ksi	45.4	42.8	–	–	–	–
Charpy-V, ft-lbs	5.8	1.3	–	–	–	–

TABLE 3.0215. TENSILE AND OTHER MECHANICAL PROPERTIES OF 7049-T76 EXTRUSIONS (10, 18)

Alloy	7049-T73						
Form	Die Forgings						
Thickness Range, inch	Direction	F_{cy}, ksi	F_{su}, ksi	F_{bru}, ksi e/D=1.5	F_{bru}, ksi e/D=2.0	F_{bry}, ksi e/D=1.5	F_{bry}, ksi e/D=2.0
≤1.000	L	75.5	45.1	114.9	148.0	92.7	114.2
	ST	65.5	43.9	–	–	–	–
1.001 to 2.000	L	76.8	47.4	115.0	155.6	98.1	119.7
	ST	71.4	46.8	–	–	–	–
2.001 to 3.000	L	75.4	45.9	118.6	147.7	99.2	113.5
	ST	67.9	44.6	–	–	–	–
4.001 to 5.000	L	70.1	44.8	110.6	138.8	97.0	113.8
	ST	68.3	44.1	–	–	–	–

TABLE 3.0216. COMPRESSION, SHEAR, AND BEARING PROPERTIES OF 7049-T73 DIE FORGINGS (13)

	Al
7.6	Zn
2.5	Mg
1.5	Cu
0.15	Cr

7049

Alloy	7049-T73						
Form	Hand Forgings						
Size, inch	Direction	F_{cy}, ksi	F_{su}, ksi	F_{bru}, ksi e/D=1.5	F_{bru}, ksi e/D=2.0	F_{bry}, ksi e/D=1.5	F_{bry}, ksi e/D=2.0
2 x 16	L	75.5	45.3	103.1	133.8	95.1	108.0
	LT	70.2	45.7	106.4	137.7	100.3	113.4
	ST	71.9	43.5	–	–	–	–
3 x 16	L	66.5	44.8	118.0	153.0	101.4	118.2
	LT	67.0	42.3	107.0	139.1	88.2	105.8
	ST	65.4	43.2	–	–	–	–
4 x 16	L	66.5	44.8	108.5	150.0	91.8	116.3
	LT	69.8	43.6	112.2	145.8	98.4	118.8
	ST	73.4	44.2	–	–	–	–
5 x 20	L	62.6	42.6	98.1	139.9	86.2	107.5
	LT	62.1	40.7	100.3	126.8	86.4	105.5
	ST	61.3	41.2	–	–	–	–

TABLE 3.0217. COMPRESSION, SHEAR, AND BEARING PROPERTIES OF 7049-T73 HAND FORGINGS (13)

Alloy	7049-T7351						
Form	Plate						
Thickness, inch	Source	No of Tests	F_{cy}, ksi L	F_{cy}, ksi T	F_{cy}, ksi ST	F_{su}, ksi L	F_{su}, ksi T
1.50	(17)	1	72.5	73.9	75.9	42.9	41.8
2.00	(17)	2	71.3	75.8	75.5	45.2	44.7
2.50	(17)	1	65.0	70.3	70.3	43.8	44.0
3.50	(17)	1	65.0	69.9	72.2	43.3	43.2
3.75	(17)	1	64.4	69.6	68.4	43.7	43.4
4.00	(17)	1	65.5	68.4	68.9	44.1	43.4
4.25	(17)	2	61.4	66.0	66.9	42.8	42.4
3.00	(6)	3	64.1	69.2	–	46.1	45.4

TABLE 3.0218. COMPRESSION AND SHEAR PROPERTIES OF 7049-T7351 PLATE (6, 17)

	Al
7.6	Zn
2.5	Mg
1.5	Cu
0.15	Cr

7049

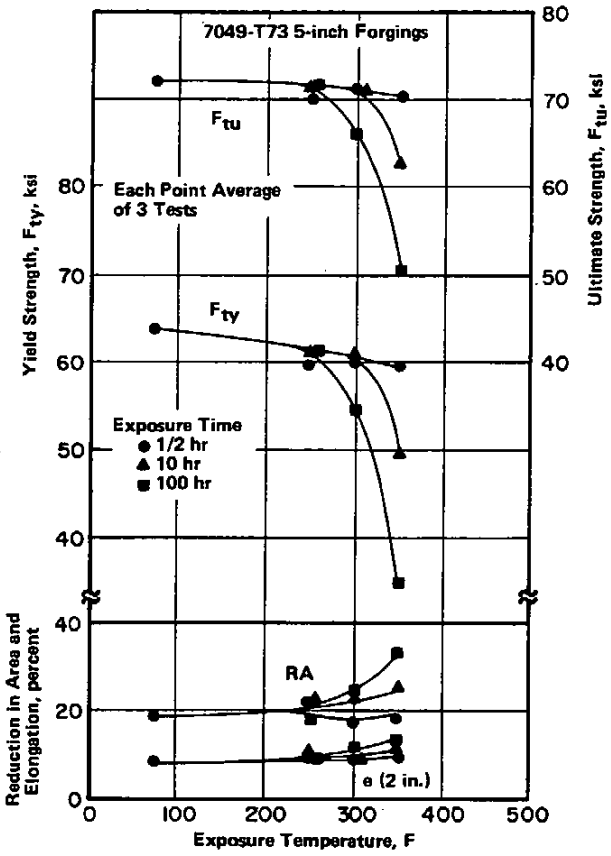


FIGURE 3.0219. EFFECT OF EXPOSURE AT ELEVATED TEMPERATURE ON ROOM TEMPERATURE TENSILE PROPERTIES OF FORGINGS (27)

Alloy	7049-T73511 and -T76511						
Form	Extrusion, 1.5 x 4.5 inch Rectangle						
				T73511		T76511	
Chemical Purity	Si, percent	Fe, percent	Direction	K_{Ic}, ksi$\sqrt{in.}$	F_{ty}, ksi	K_{Ic}, ksi$\sqrt{in.}$	F_{ty}, ksi
High[a]	0.08	0.09	LT	33.9	76.7	33.0	74.6
			TL	26.0	70.3	23.0	69.6
Medium	0.11	0.20	LT	29.7	75.4	29.0	74.1
			TL	22.1	69.2	21.0	71.4
Low	0.16	0.37	LT	23.8	73.1	23.0	73.3
			TL	18.1	68.6	17.0	67.8

(a) Equivalent of 7149 composition.

TABLE 3.027211. FRACTURE TOUGHNESS OF 7049-T73511 AND -T76511 EXTRUSIONS OF DIFFERENT PURITY LEVELS (11, 12)

Alloy	7049-T73 and -T76		
Form	Extrusions		
		K_{Ic}, ksi$\sqrt{in.}$ (Avg of Three Tests)		
Sample and Size, inch	Direction	Room Temp	0 F	-64 F
T73, Integrally Stiffened, 3 x 11-1/4 Section	LT	28.1	25.9	24.7
	TL	25.2	24.1	23.2
	ST	20.3	21.1	22.2(a)
T73, Bar, 3-1/4 x 3-1/2	LT	33.2	34.2	31.4
	TL	22.0	20.6	20.0
	ST	23.0	21.5	20.7(b)
T76, Bar, 3-1/4 x 3-1/2	LT	32.7	33.1	30.4
	TL	20.0	20.2	19.2(a)
	ST	20.9(a)	20.8	19.4

(a) Two tests only.
(b) One test only.

TABLE 3.027212. FRACTURE TOUGHNESS OF 7049-T73 AND -T76 EXTRUSIONS OF DIFFERENT DIMENSIONS (10)

Al
7.6 Zn
2.5 Mg
1.5 Cu
0.15 Cr

7049

Alloy	7049-T73			
Form	Forgings			
Size and Forging	Direction	K_{Ic} or K_Q, ksi$\sqrt{in.}$(a)	K_c, ksi$\sqrt{in.}$(b)	Test Specimen Thickness, inch
24 lb Die	LT	(26)	–	1.00
		28	–	1.00
24 lb Die	LT	(50)	–	1.50
		(37)	–	1.50
3 x 24 x 48-inch Hand	LT	(39), 39, 38	–	2.00
		(38), (37)	55, 51	1.25
	LT	(20), (26)	–	1.50
	SL	23	–	1.25
	LT	(39), (40)	83, 87	0.75

(a) K_Q values, which are invalid K_{Ic} data, are in parentheses.
(b) Plane stress K_c determined by 25 percent secant offset on ASTM E561 compact tension specimen.

TABLE 3.027221. FRACTURE TOUGHNESS OF DIE AND HAND FORGINGS OF 7049-T73 (14)

Alloy	7049-T73(a)				
Form	4.5-inch diam Die Forgings				
Orientation	Transverse to Grain Flow				
Tear Strength, ksi	Tear Strength / Yield Strength	Energy Required to Initiate / Propagate a Crack, in.-lb		Total Energy, in.-lb	Unit(b) Propagation Energy, in.-lb/in.^{2}
41.6	0.68	16.6	14.8	31.4	74.1

(a) Each value average of three tests; Kahn tear test specimen was employed.
(b) Unit propagation energy is a measurement of unstable crack growth. The higher values represent higher toughness.

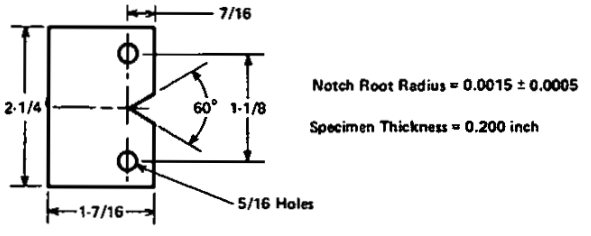


TABLE 3.027223. KAHN TEAR TEST DATA FOR DIE FORGINGS OF 7049-T73 (4)

Alloy	7049-T73	
Form	Hand Forgings	
Dimension, inch	Direction	K_{Ic}, ksi$\sqrt{in.}$(a) (or Meaningful K_Q per ASTM B645)
2 x 16	LT	27.2
	TL	18.9
	SL	16.6
3 x 16	LT	30.8
	TL	23.2
	SL	22.5
4 x 16	LT	32.8
	TL	21.0
	SL	20.8
5 x 20	LT	26.6
	TL	18.4(b)
	SL	19.8

(a) Average of two tests.
(b) One test only.

TABLE 3.027222. FRACTURE TOUGHNESS OF 7049-T73 HAND FORGINGS OF DIFFERENT DIMENSIONS (13)

	Al
7.6	Zn
2.5	Mg
1.5	Cu
0.15	Cr

7049

Alloy	7049-T7351			
Form	Plate			
Thickness, inch	Source	Fracture Toughness (K_{Ic}), ksi $\sqrt{in.}$		
		LT	TL	SL
1.25	(7)	35.8	28.4	25.3
1.50	(20)	39.7	31.2	–
2.50	(20)	40.6	33.9	28.2
3.00	(7)	30.1	24.7	25.1
3.00	(6)	34.0	28.1	–
4.00	(20)	43.2	32.4	30.2
4.25	(20)	40.2	35.9	31.3

TABLE 3.027231. FRACTURE TOUGHNESS OF 7049-T7351 ROLLED PLATE OF VARIOUS THICKNESSES (6, 7, 20)

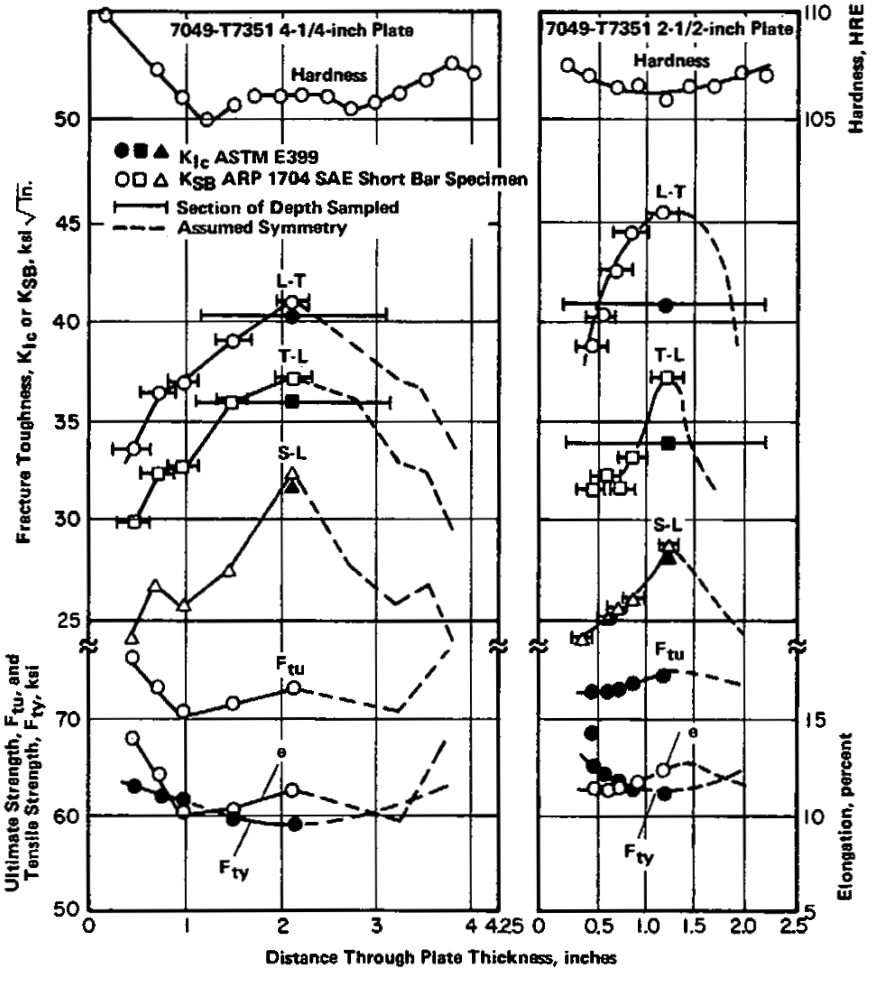


FIGURE 3.027232. VARIATION IN FRACTURE TOUGHNESS, HARDNESS, AND MECHANICAL PROPERTIES THROUGH THE THICKNESS OF 4.25-INCH AND 2.5-INCH THICK ROLLED 7049-T7351 PLATE (20)

	Al
7.6	Zn
2.5	Mg
1.5	Cu
0.15	Cr

7049

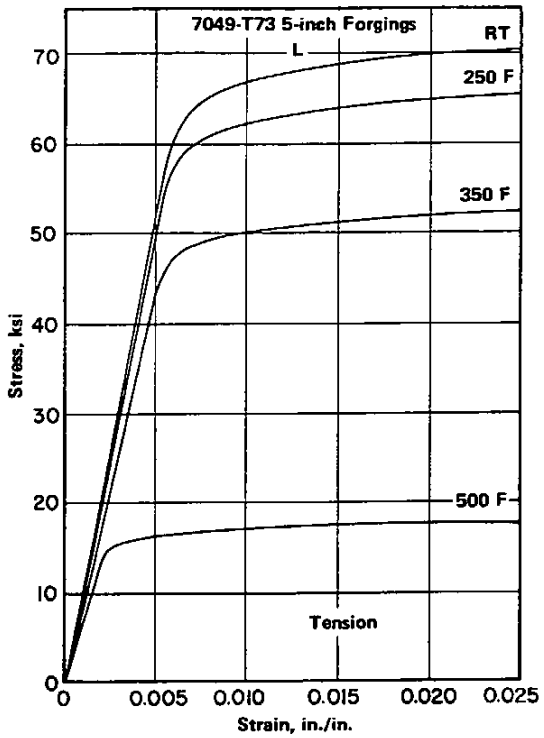


FIGURE 3.03111. TYPICAL LONGITUDINAL STRESS-STRAIN CURVES IN TENSION FOR 5-INCH FORGINGS AT ROOM AND ELEVATED TEMPERATURES (16)

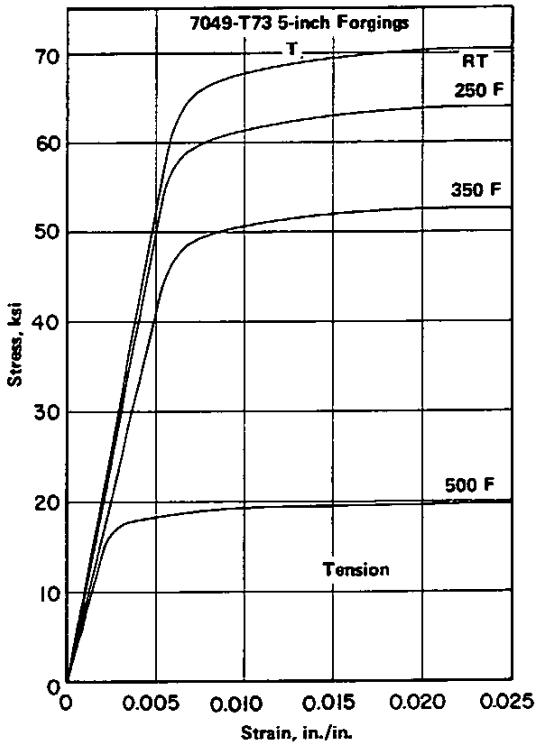


FIGURE 3.03112. TYPICAL TRANSVERSE STRESS-STRAIN CURVES IN TENSION FOR 5-INCH FORGINGS AT ROOM AND ELEVATED TEMPERATURES (16)

	Al
7.6	Zn
2.5	Mg
1.5	Cu
0.15	Cr

7049

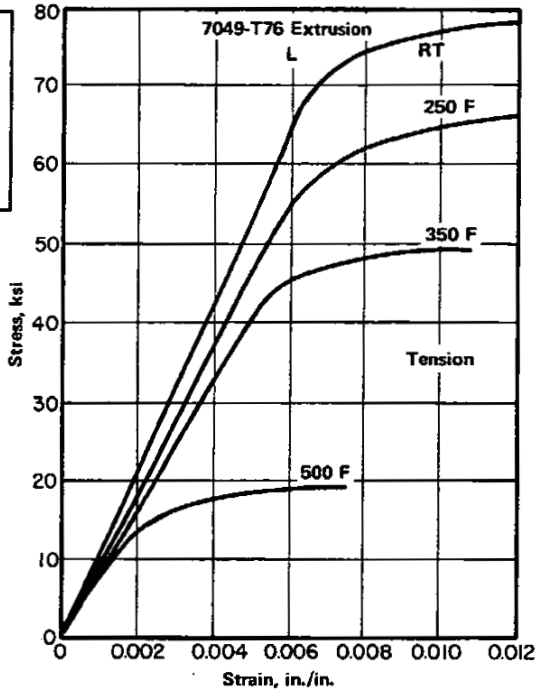


FIGURE 3.03113. TYPICAL TENSILE STRESS-STRAIN CURVES IN LONGITUDINAL DIRECTION FOR 7049-T76 EXTRUSIONS (18)

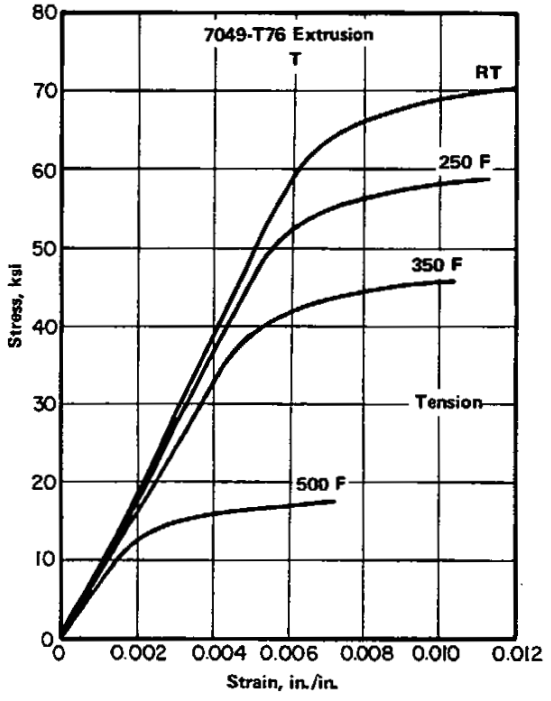


FIGURE 3.03114. TYPICAL TENSILE STRESS-STRAIN CURVES IN TRANSVERSE DIRECTION FOR 7049-T76 EXTRUSIONS (18)

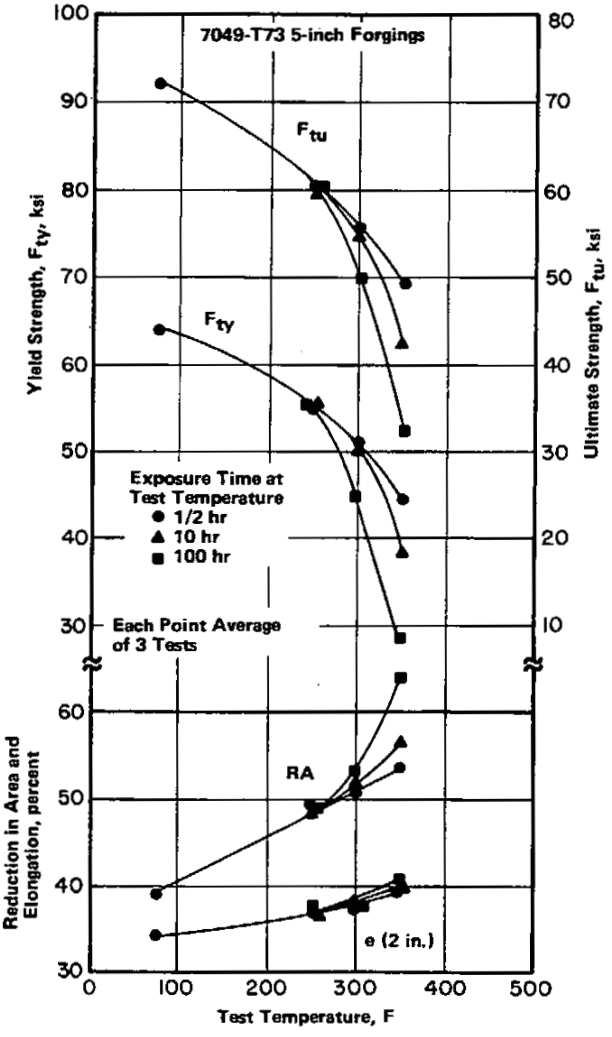


FIGURE 3.0312. EFFECT OF EXPOSURE AND TEST TEMPERATURE ON TENSILE PROPERTIES OF FORGINGS (27)

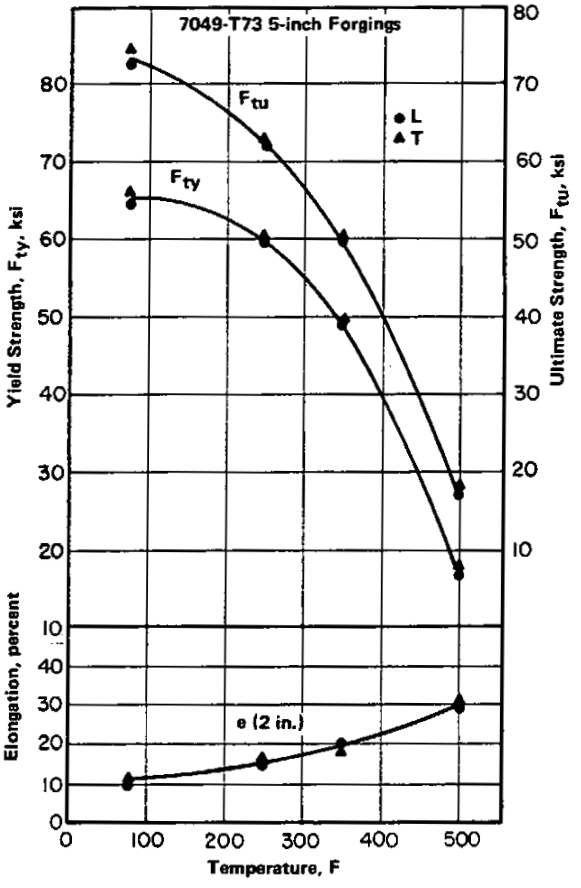
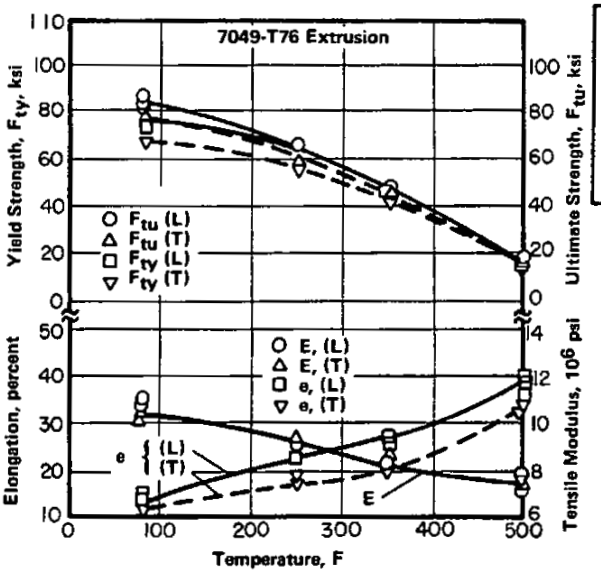


FIGURE 3.0313. EFFECT OF TEMPERATURE ON TENSILE PROPERTIES OF 5-INCH FORGINGS (8)



	Al
7.6	Zn
2.5	Mg
1.5	Cu
0.15	Cr

7049

FIGURE 3.0314. EFFECT OF TEMPERATURE ON THE TENSILE PROPERTIES AND TENSILE MODULUS OF 7049-T76 EXTRUSION (18)

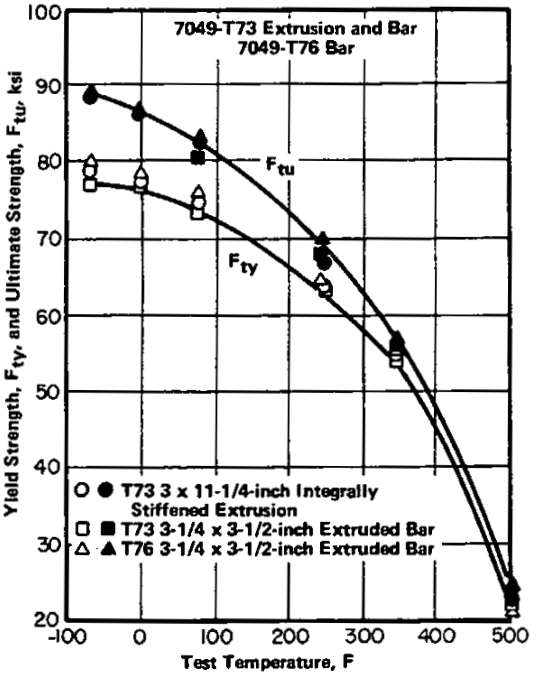


FIGURE 3.0315. TENSILE PROPERTY DATA FOR THE LONGITUDINAL DIRECTION FOR 7049-T73 BAR AND EXTRUSION AND 7049-T76 EXTRUDED BAR (10)

	Al
7.6	Zn
2.5	Mg
1.5	Cu
0.15	Cr

7049

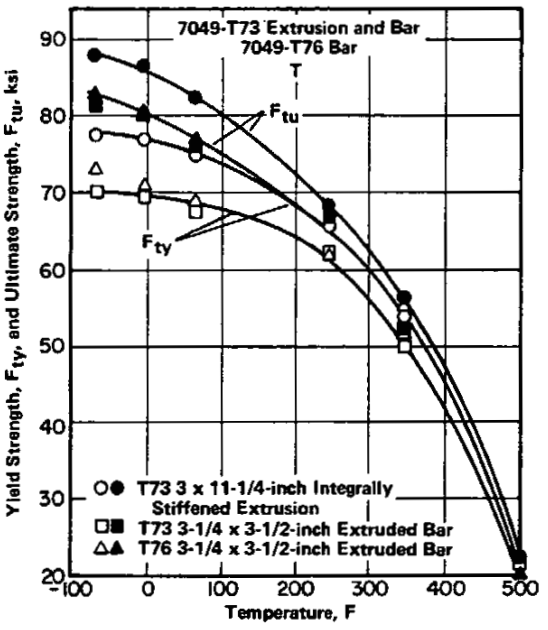


FIGURE 3.0316. TENSILE PROPERTY DATA FOR THE TRANSVERSE DIRECTION FOR 7049-T73 BAR AND EXTRUSION, AND 7049-T76 EXTRUDED BAR (10)

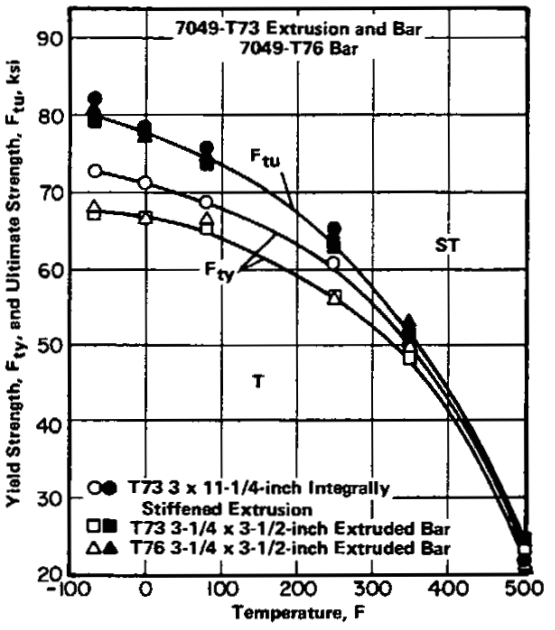


FIGURE 3.0317. TENSILE PROPERTY DATA IN THE SHORT TRANSVERSE DIRECTION FOR 7049-T73 BAR AND EXTRUSION, AND 7049-T76 EXTRUDED BAR (10)

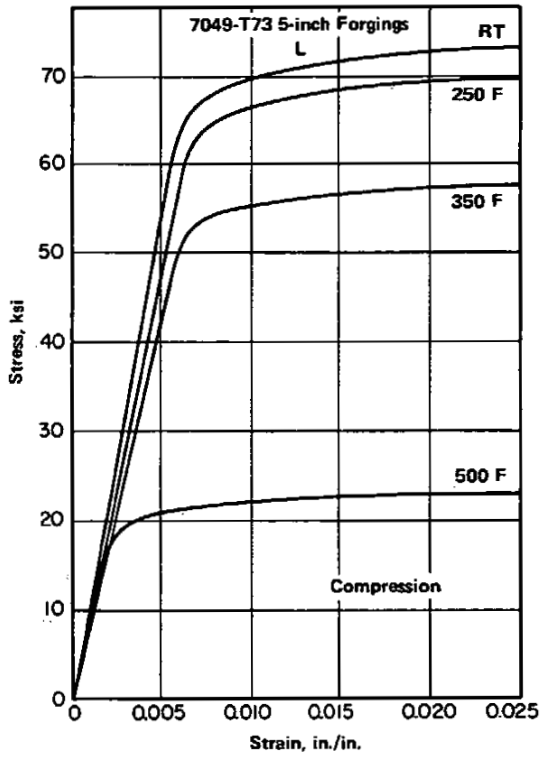


FIGURE 3.03211. TYPICAL LONGITUDINAL STRESS-STRAIN CURVES IN COMPRESSION FOR 5-INCH FORGINGS AT ROOM AND ELEVATED TEMPERATURES (16)

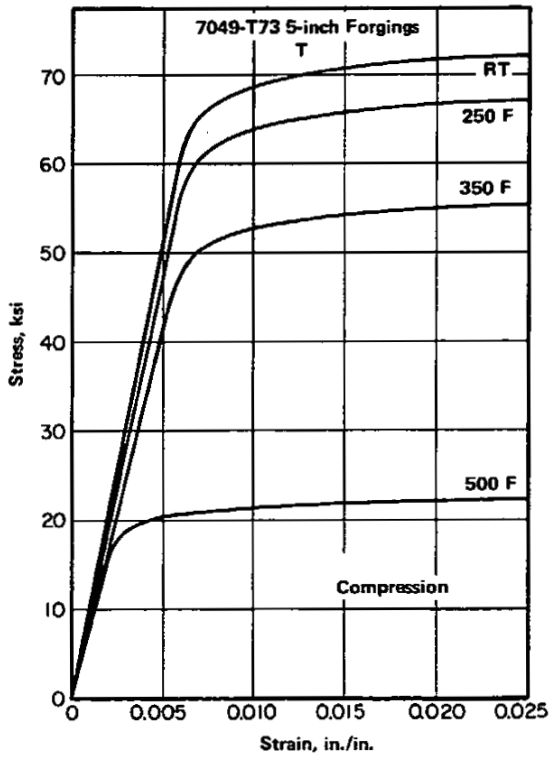


FIGURE 3.03212. TYPICAL TRANSVERSE STRESS-STRAIN CURVES IN COMPRESSION FOR 5-INCH FORGINGS AT ROOM AND ELEVATED TEMPERATURES (16)

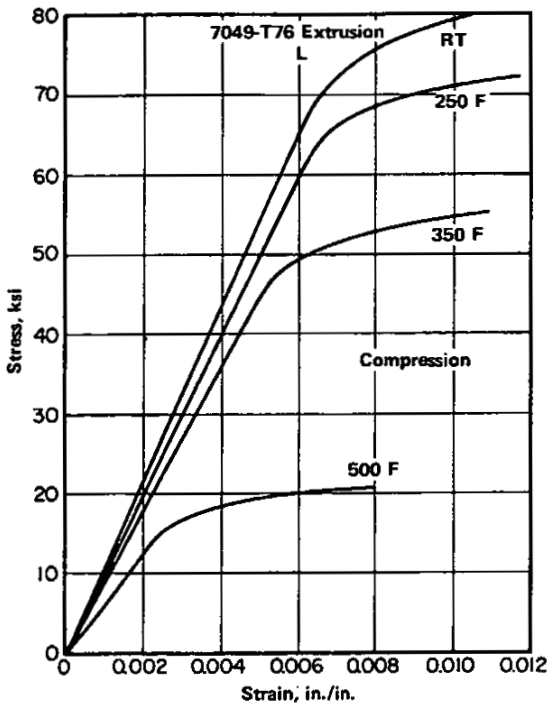


FIGURE 3.03213. TYPICAL LONGITUDINAL COMPRESSIVE STRESS-STRAIN CURVES FOR 7047-T76 EXTRUSION AT ROOM AND ELEVATED TEMPERATURES (18)

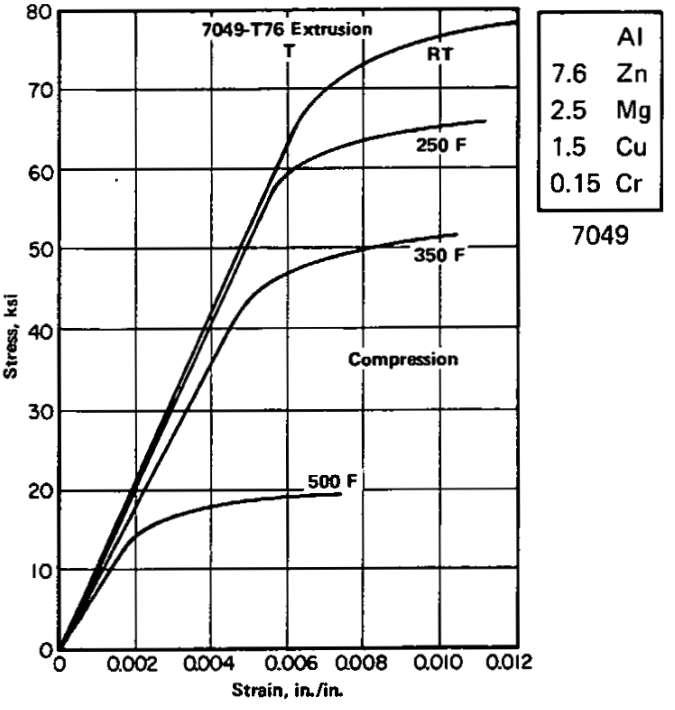


FIGURE 3.03214. TYPICAL TRANSVERSE COMPRESSIVE STRESS-STRAIN CURVES FOR 7049-T76 EXTRUSION AT ROOM AND ELEVATED TEMPERATURES (18)

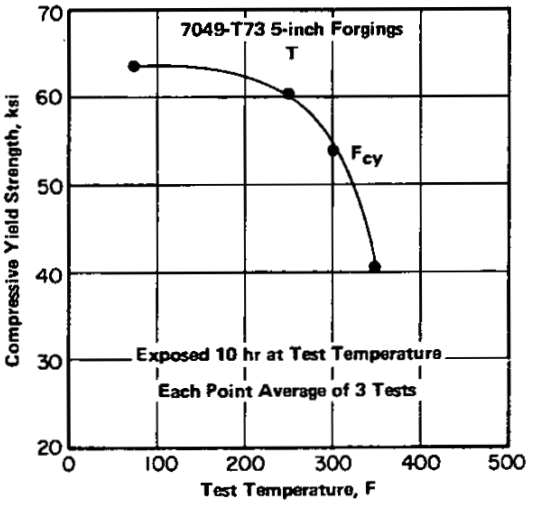


FIGURE 3.0322. EFFECT OF EXPOSURE AND TEST TEMPERATURE ON COMPRESSIVE YIELD STRENGTH OF 5-INCH FORGINGS (27)

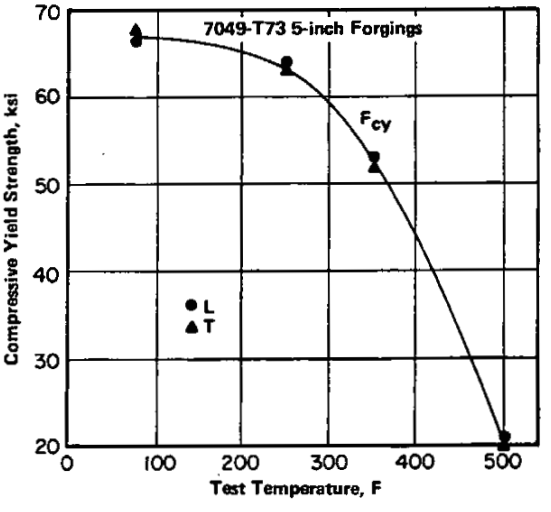


FIGURE 3.0323. EFFECT OF TEMPERATURE ON COMPRESSIVE YIELD STRENGTH OF 5-INCH FORGINGS (8)

	Al
7.6	Zn
2.5	Mg
1.5	Cu
0.15	Cr

7049

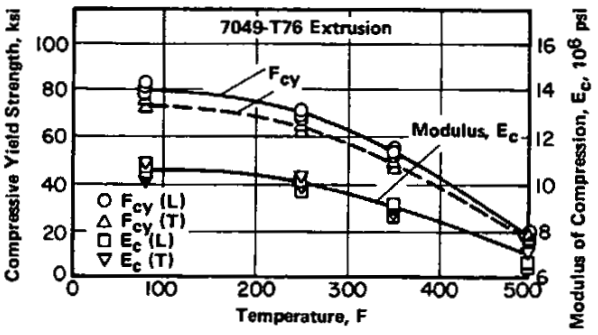


FIGURE 3.0324. EFFECT OF TEMPERATURE ON THE COMPRESSIVE PROPERTIES OF 7049-T76 EXTRUSION (18)

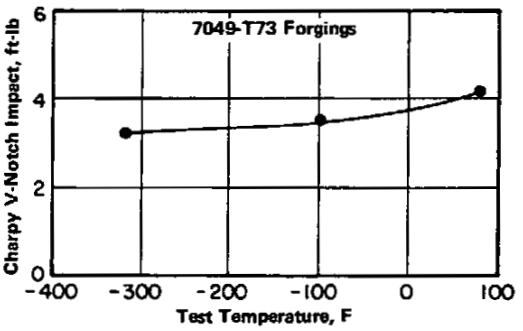


FIGURE 3.0331. EFFECT OF TEMPERATURE ON CHARPY V-NOTCH IMPACT ENERGY (8)

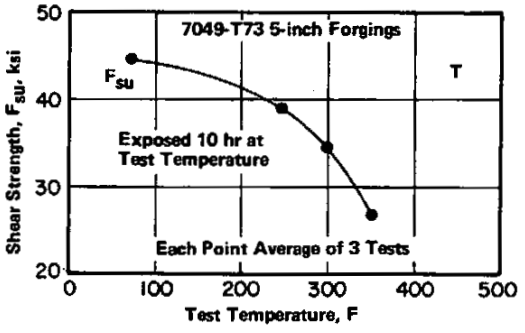


FIGURE 3.0351. EFFECT OF EXPOSURE AND TEST TEMPERATURE ON ULTIMATE SHEAR STRENGTH OF FORGINGS AS DETERMINED WITH DOUBLE SHEAR TEST SPECIMEN (27)

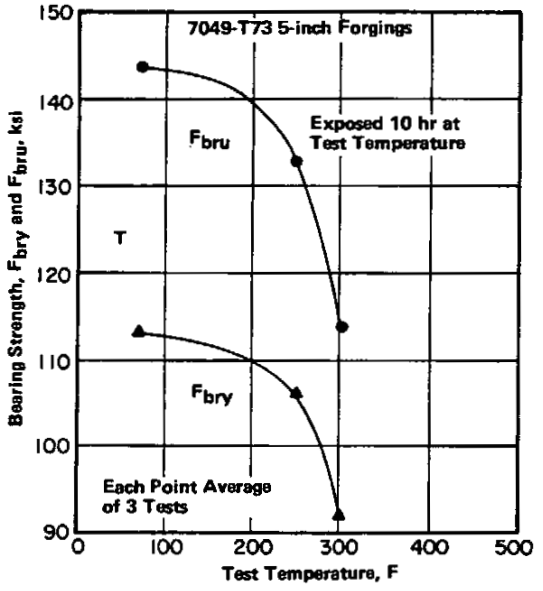


FIGURE 3.0361. EFFECT OF EXPOSURE AND TEST TEMPERATURE ON BEARING PROPERTIES OF 5-INCH FORGINGS (27)

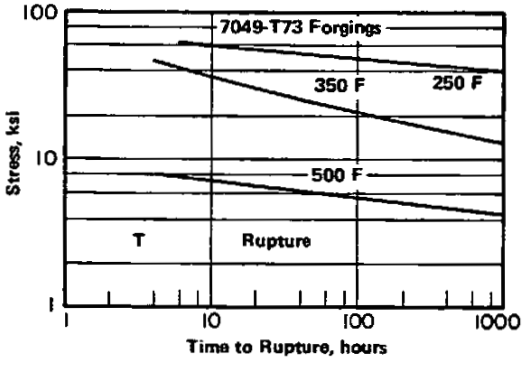


FIGURE 3.041. CREEP RUPTURE CURVES FOR 5-INCH FORGINGS AT 250, 350, AND 500 F (8)

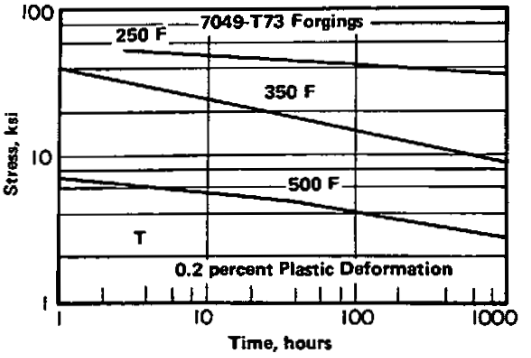


FIGURE 3.042. CREEP CURVES FOR 5-INCH FORGINGS SHOWING TIME FOR 0.2 PERCENT PLASTIC DEFORMATION (8)

	Al
7.6	Zn
2.5	Mg
1.5	Cu
0.15	Cr

7049

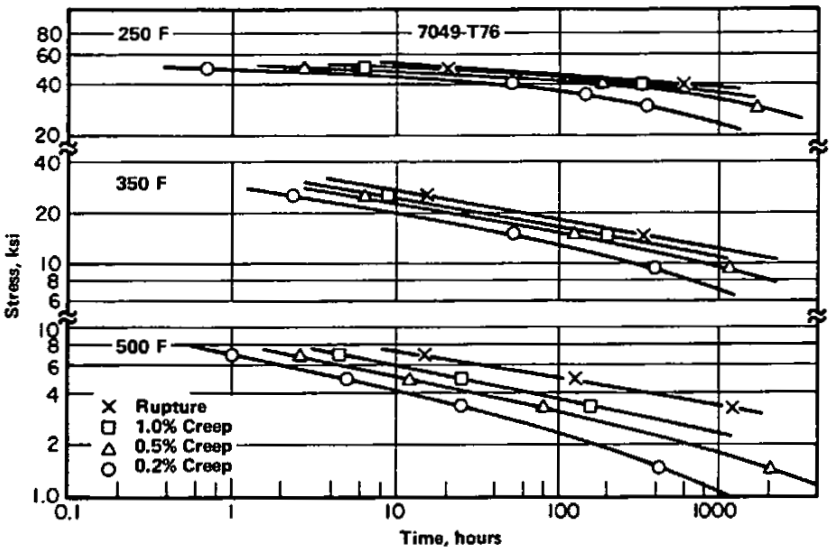


FIGURE 3.043. CREEP RUPTURE AND CREEP DEFORMATION IN TRANSVERSE DIRECTION FOR 7049-T76 EXTRUSIONS AT VARIOUS TEMPERATURES (18)

Alloy	7049-T73		
Form	5-inch Forgings		
Orientation	Transverse		
Test Temperature, F	RT	250	350
Test	Axial Fatigue Strength, ksi[a]		
Smooth, R = 0.1			
10^3 Cycles	73	71	70
10^5 Cycles	57	53	48
10^7 Cycles	46	40	38
Notched, R = 0.1 (K_t = 3.0)			
10^3 Cycles	50	50	50
10^5 Cycles	21	20	19
10^7 Cycles	16	13	11

(a) Stress for number of cycles indicated.

TABLE 3.051. FATIGUE DATA FOR SMOOTH AND NOTCHED SPECIMENS FROM FORGINGS AT ROOM AND ELEVATED TEMPERATURES (8)

	Al
7.6	Zn
2.5	Mg
1.5	Cu
0.15	Cr

7049

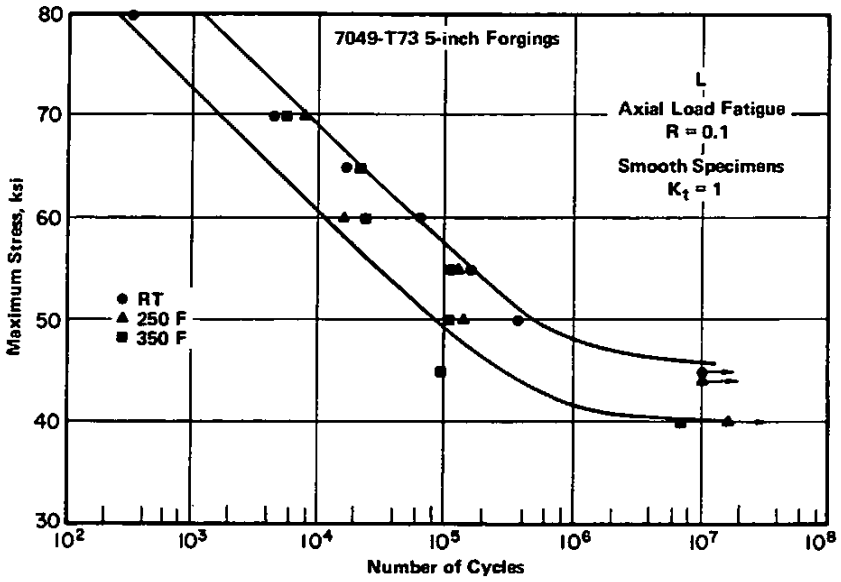


FIGURE 3.052. AXIAL LOAD FATIGUE CURVES AT ROOM AND ELEVATED TEMPERATURES (16)

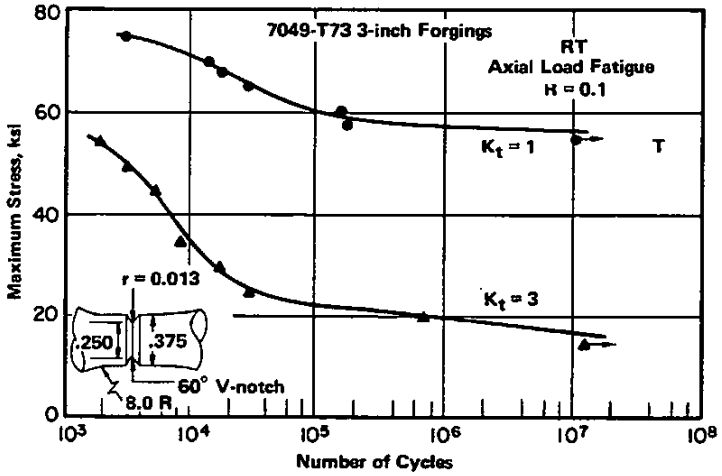


FIGURE 3.053. AXIAL LOAD FATIGUE CURVES FOR SMOOTH AND NOTCHED SPECIMENS FROM 3-INCH FORGINGS AT ROOM TEMPERATURE (15)

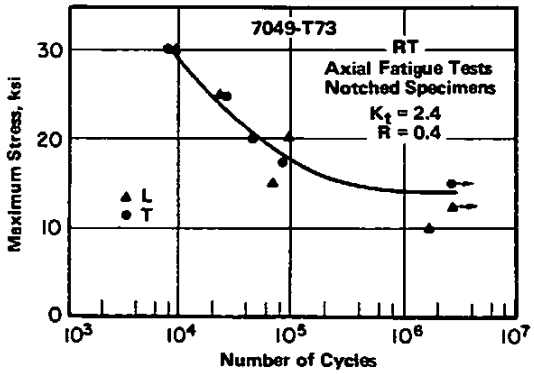


FIGURE 3.054. AXIAL LOAD FATIGUE CURVE FOR NOTCHED SPECIMENS FROM FORGINGS (4)

	Al
7.6	Zn
2.5	Mg
1.5	Cu
0.15	Cr

7049

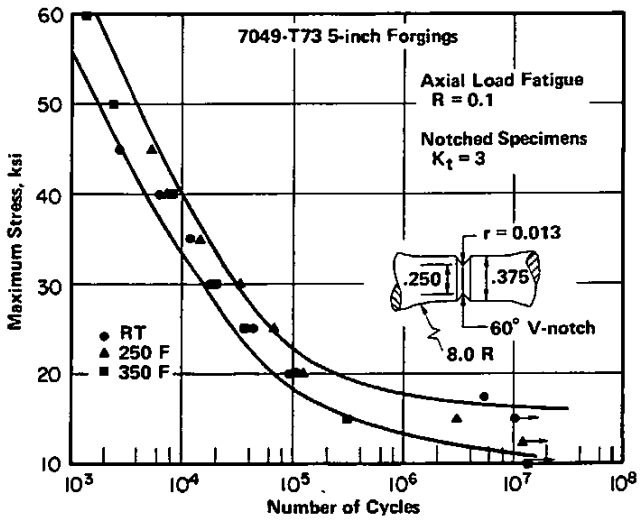


FIGURE 3.055. AXIAL LOAD FATIGUE CURVES FOR NOTCHED SPECIMENS AT ROOM AND ELEVATED TEMPERATURES (16)

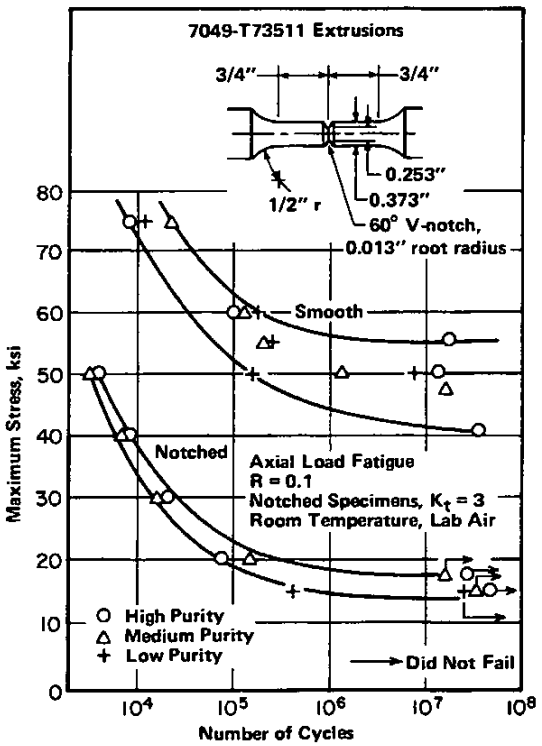


FIGURE 3.056. NOTCHED AND SMOOTH FATIGUE DATA FOR 7049-T73511 EXTRUSIONS OF DIFFERENT PURITIES (11)

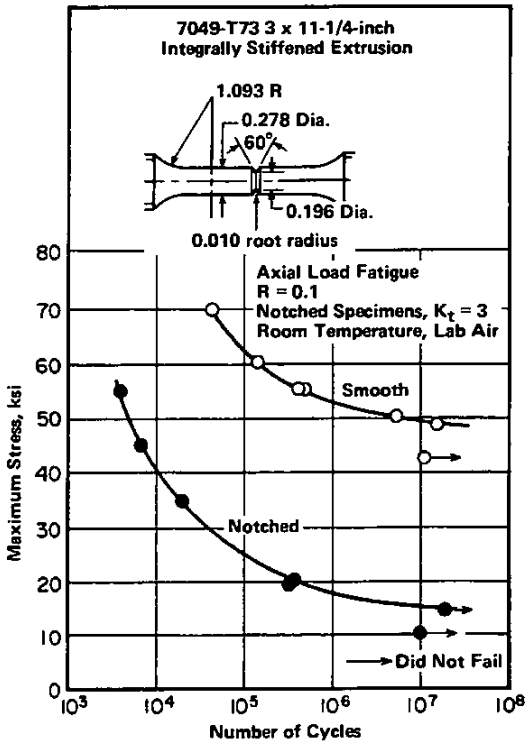


FIGURE 3.057. AXIAL STRESS FATIGUE DATA FOR NOTCHED AND SMOOTH 7049-T73 INTEGRALLY STIFFENED EXTRUSIONS (10)

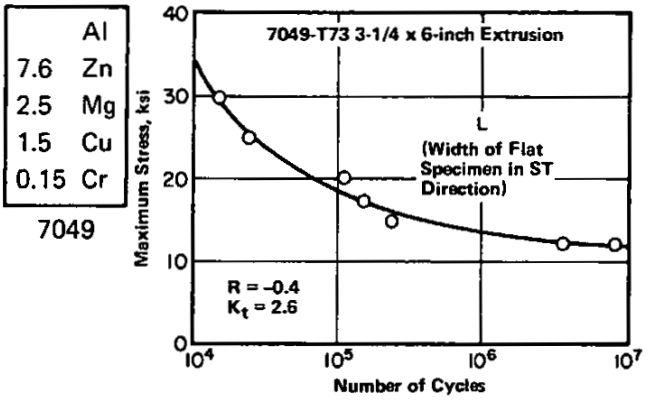


FIGURE 3.058. NOTCHED AXIAL STRESS FATIGUE DATA FOR A 7049-T73 EXTRUSION (19)

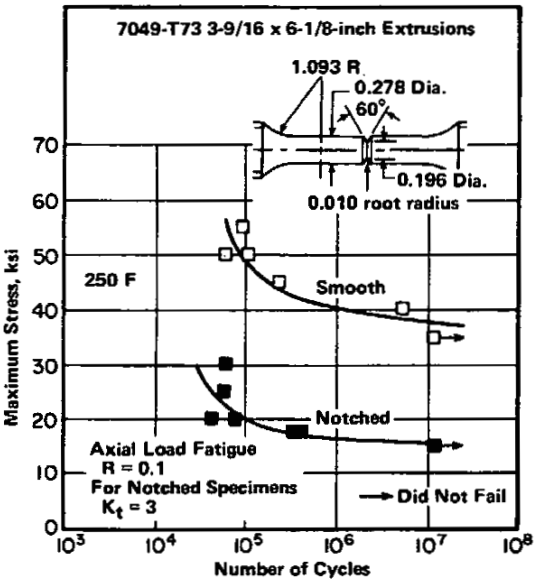


FIGURE 3.059. AXIAL STRESS FATIGUE DATA FOR SMOOTH AND NOTCHED 7049-T73 EXTRUSIONS AT 250 F (10)

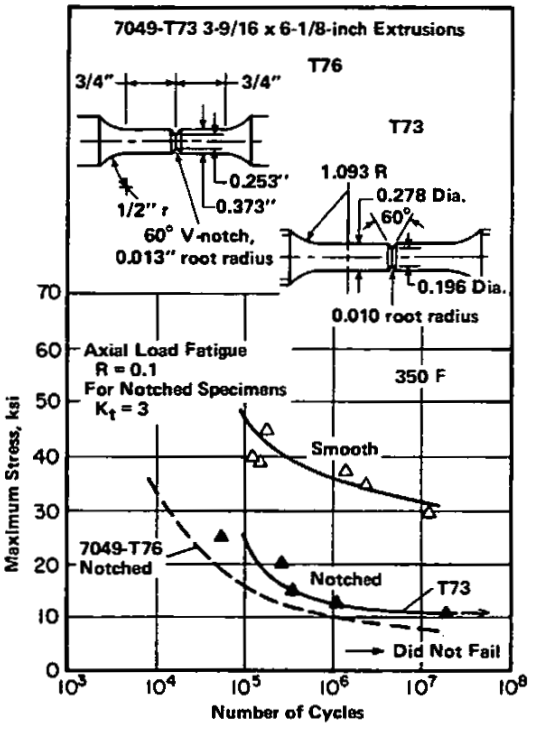


FIGURE 3.0510. NOTCHED AND SMOOTH AXIAL STRESS FATIGUE DATA FOR 7049-T73 AND T76 EXTRUSIONS AT 350 F (10,18)

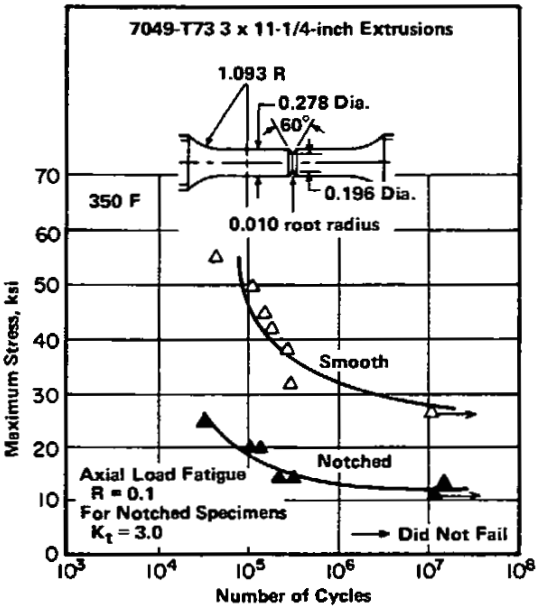


FIGURE 3.0511. AXIAL STRESS FATIGUE DATA FOR NOTCHED AND SMOOTH 7049-T73 INTEGRALLY STIFFENED EXTRUSIONS AT 350 F (10)

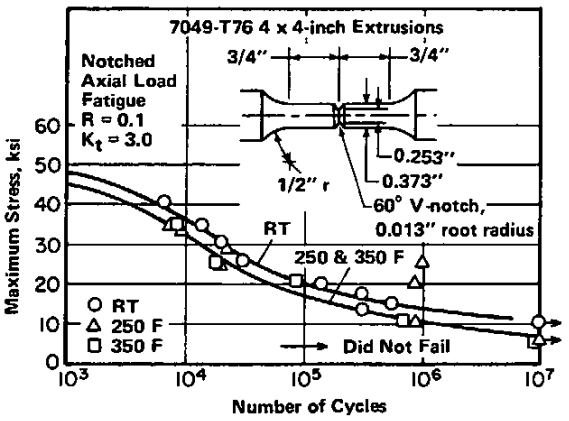


FIGURE 3.0512. NOTCHED AXIAL STRESS FATIGUE DATA FOR 7049-T76 EXTRUSIONS AT ROOM AND ELEVATED TEMPERATURES (18)

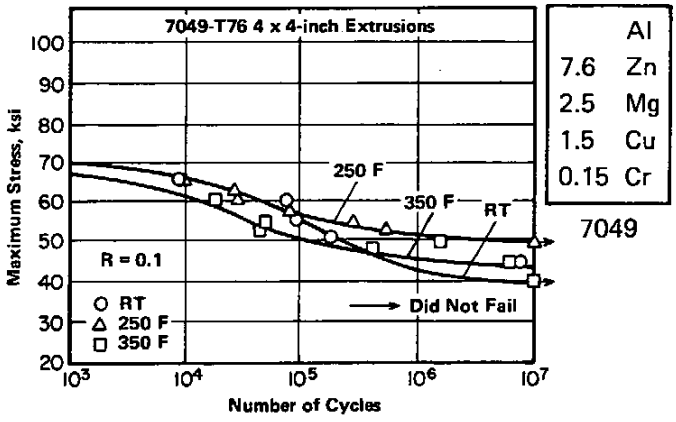


FIGURE 3.0513. SMOOTH AXIAL STRESS FATIGUE DATA FOR 7049-T76 EXTRUSIONS AT VARIOUS TEMPERATURES (18)

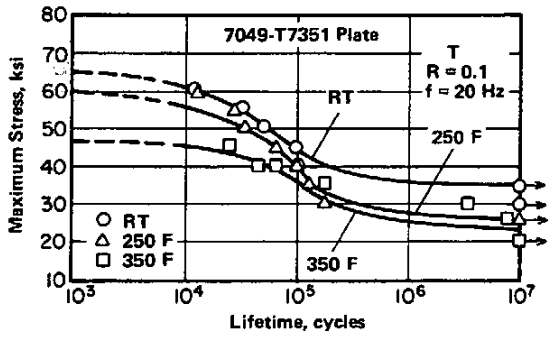


FIGURE 3.0514. UNNOTCHED AXIAL STRESS FATIGUE DATA IN THE TRANSVERSE DIRECTION FOR 7049-T7351 PLATE AT VARIOUS TEMPERATURES (18)

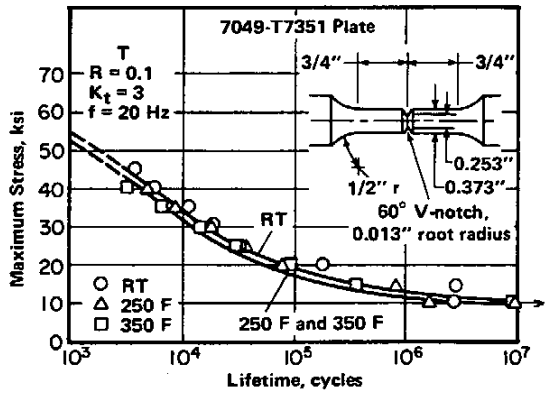


FIGURE 3.0515. NOTCHED AXIAL STRESS FATIGUE DATA FOR 7049-T7351 PLATE AT VARIOUS TEMPERATURES (18)

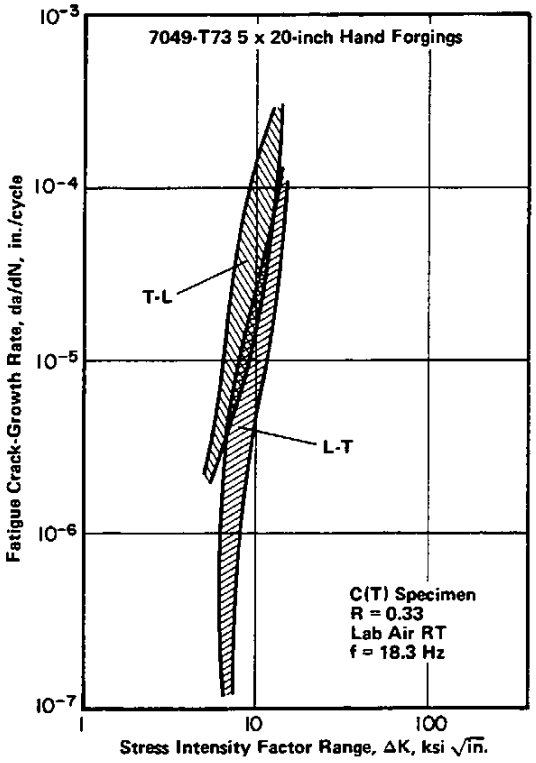


FIGURE 3.0516. FATIGUE CRACK-GROWTH DATA FOR 7049-T73 HAND FORGING IN DIFFERENT ENVIRONMENTS (13)

	Al
7.6	Zn
2.5	Mg
1.5	Cu
0.15	Cr

7049

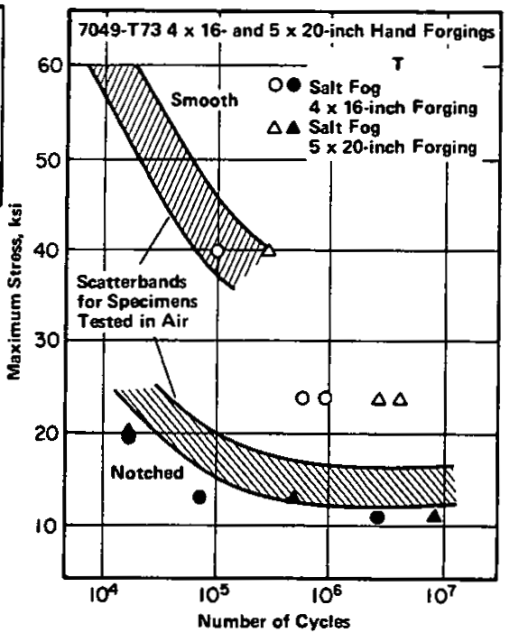


FIGURE 3.0517. EFFECT OF SALT FOG ON THE FATIGUE LIFE OF 7049-T73 FORGINGS (13)

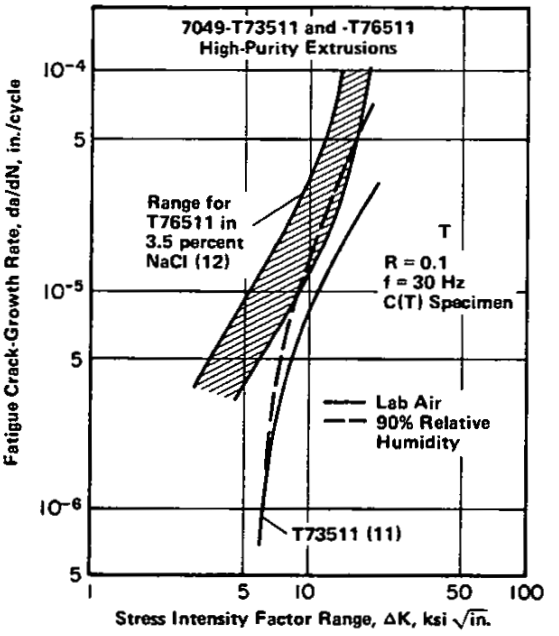


FIGURE 3.0518. FATIGUE CRACK-GROWTH RATE CURVES IN HIGH PURITY 7149-T73511 AND -T76511 EXTRUSIONS IN LABORATORY AIR AND HIGH HUMIDITY AIR (11,12)

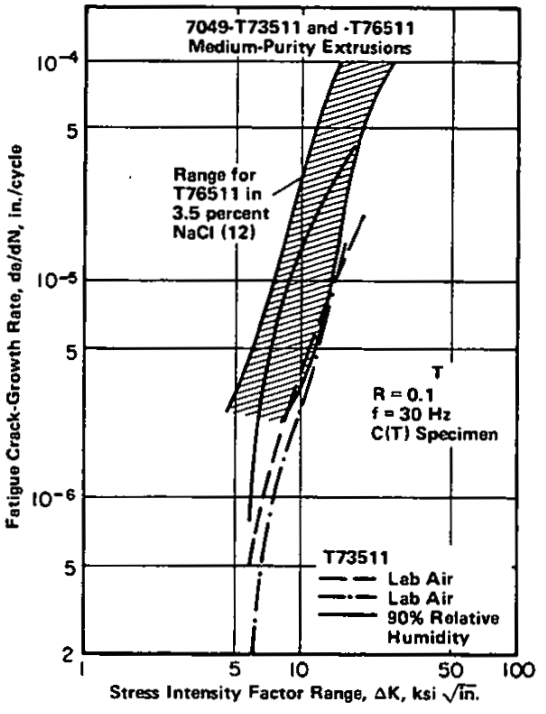


FIGURE 3.0519. FATIGUE CRACK-GROWTH RATE CURVES FOR MEDIUM PURITY 7049-T73511 AND -T76511 EXTRUSIONS IN LABORATORY AIR AND HIGH HUMIDITY AIR (11,12)

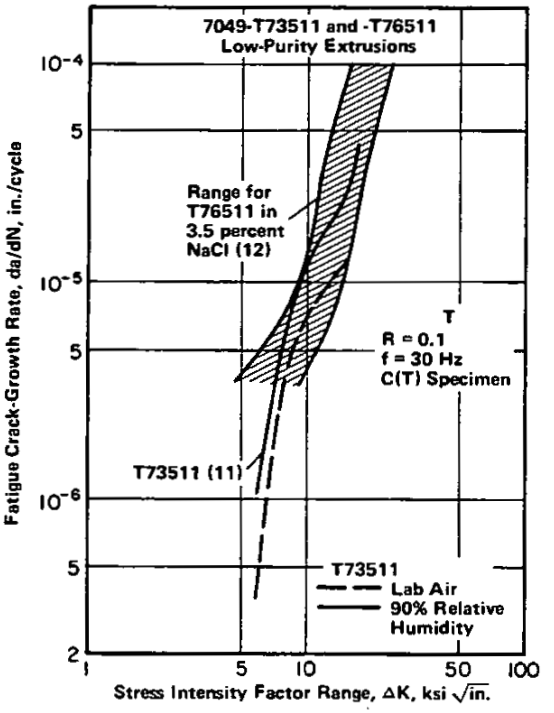


FIGURE 3.0520. FATIGUE CRACK-GROWTH RATE CURVES FOR LOW PURITY 7049-T73511 AND -T76511 IN LABORATORY AIR AND HIGH HUMIDITY AIR (11,12)

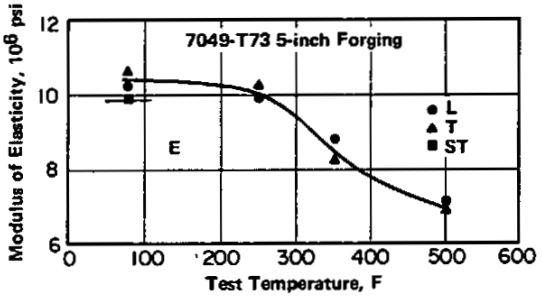


FIGURE 3.0621. EFFECT OF TEMPERATURE ON MODULUS OF ELASTICITY (8)

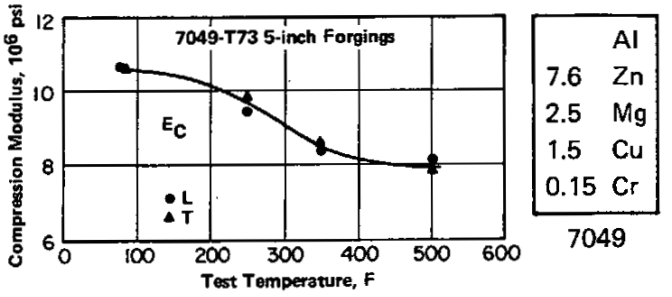


FIGURE 3.06221. EFFECT OF TEMPERATURE ON COMPRESSION MODULUS (8)

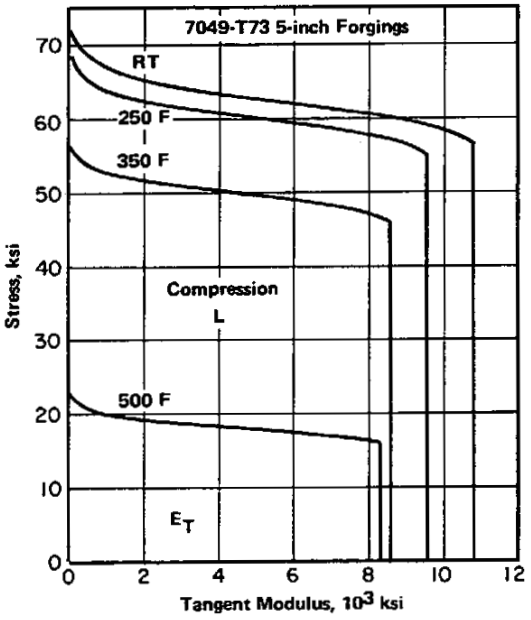


FIGURE 3.0641. TYPICAL TANGENT MODULUS CURVES IN COMPRESSION FOR 5-INCH FORGINGS AT ROOM AND ELEVATED TEMPERATURES (16)

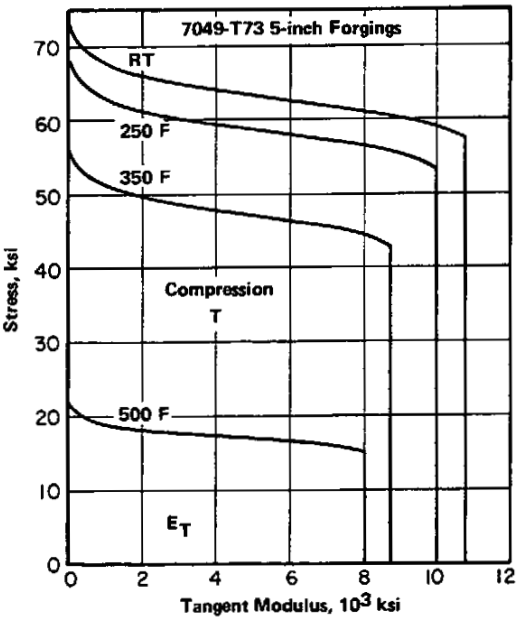


FIGURE 3.0642. TYPICAL TANGENT MODULUS CURVES IN COMPRESSION FOR 5-INCH FORGINGS AT ROOM AND ELEVATED TEMPERATURES (16)

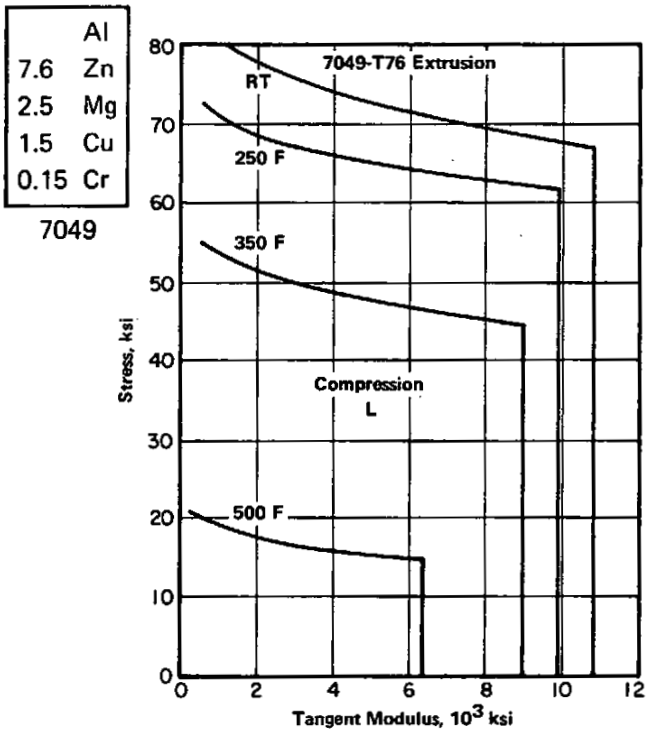


FIGURE 3.0643. TYPICAL LONGITUDINAL TANGENT MODULUS CURVES IN COMPRESSION FOR T76 EXTRUSIONS AT ROOM AND ELEVATED TEMPERATURES (18)

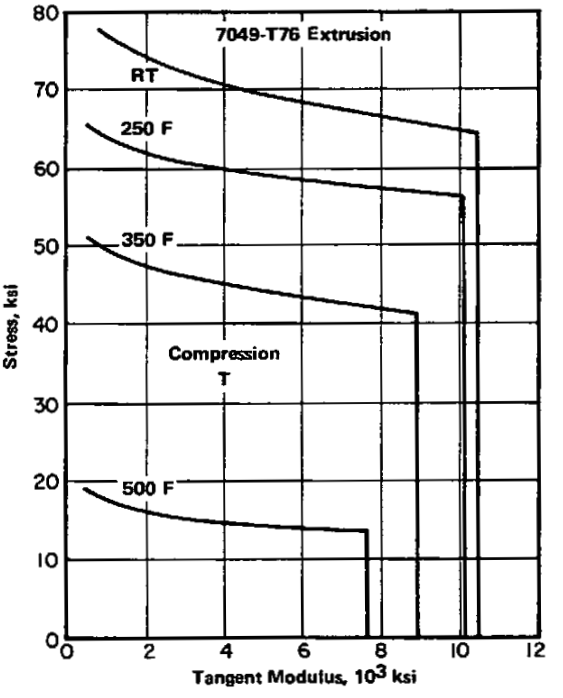


FIGURE 3.0644. TYPICAL TRANSVERSE TANGENT MODULUS CURVES IN COMPRESSION FOR T76 EXTRUSIONS AT ROOM AND ELEVATED TEMPERATURES (18)

	Al
6.2	Zn
2.25	Mg
2.3	Cu
0.12	Zr

7050 Al

1 **GENERAL**

Age-hardenable aluminum alloy 7050 has a good combination of strength, fracture toughness, and corrosion resistance in both thick and thin wrought sections. In relatively thick forgings, extrusions, and plate, it provides a combination of strength, stress-corrosion resistance, and toughness superior to that of 7075. In sheet and relatively thin extrusions, 7050 in the T76 type temper provides strength comparable to that of 7075-T6 with superior exfoliation resistance and fracture toughness. Its chemical composition differs from that of other Al-Zn-Mg-Cu alloys in two significant respects: one, it contains zirconium in place of chromium as a recrystallization and grain-control addition, and two, it has a copper-magnesium ratio greater than 0.8. The absence of chromium contributes to low quench sensitivity, and the relatively high copper content results in additional strengthening during second-step aging.

Alloy 7050 has close controls on its iron and silicon contents and is one of the newer high purity aluminum alloys which combine high strength with good fracture toughness.

7050 is generally available in three tempers: (a) T73 which provides the highest resistance to stress-corrosion cracking and the highest fracture toughness along with the lowest tensile strength; (b) T76 which provides the highest strength but stress corrosion resistance and fracture toughness inferior to that in the T73 temper; and (c) T74 (previously T736) which provides properties intermediate between the T73 and T76 tempers. 7050 should be considered for any aerospace applications requiring strength levels in the range provided by 7075-T6 and 7079-T6 alloys along with high resistance to stress corrosion and exfoliation and good toughness (4,8,11).

1.01 **Commercial Designation**

7050, ALCOA MA15.

1.02 **Alternate Designation**

SAE-ASTM UNS A97050.

1.03 **Specifications**

ASTM B 247.

1.031 AMS Specifications, Table 1.031.

1.04 **Composition**

1.041 AMS specified alloy composition, Table 1.041.

1.042 Producer's composition of cladding alloys for 7050, Table 1.042.

1.05 **Heat Treatment**

1.051 Solution treatment. Generally from 880 to 900 F followed by water quenching. Details concerning the temperature of the quench bath and soaking times are given in Tables 1.056 and 1.057. Plate is generally spray quenched and particular attention should be given to the proper operation of the spray equipment to avoid soft areas in the product. (See Code 3221, Section 1.09.)

Forgings are sometimes quenched in a mixture of water and polyalkylene glycol which exhibits inverse solubility in water. It is soluble at room temperature but when the temperature is raised above about 165 F a precipitate separates from the solution in the form of an organic polymer which will be deposited on the surface of a quenched part. Under these circumstances, cooling is somewhat slower than with a water quench but more uniform. Consequently, residual stresses and distortions are significantly reduced. For 7050 the following recommendations are given concerning glycol quenching (40): (a) maximum thickness of 3-inch, (b) mechanical agitation of the part or quench medium, (c) quench time of 2 min./in., (d) maximum glycol concentration of 12 percent, and (e) maximum quench temperature of 90 F.

1.052 Stress relief. Relief of quenching stresses for all products except die forgings, wire, rod, and rivets is accomplished by plastic deformation of 1 to 5 percent depending on the product form as shown in Table 1.056.

1.053 Aging. Some specifications (e.g., AMS 2770D) call for aging to be delayed several days at room temperature following quenching. However, for 7050, the magnitude of the delay time has an insignificant effect on the aged properties. For all products a double aging is employed. The aging conditions for all products except sheet are given in Tables 1.056 and 1.057 for the AMS and MIL specifications, respectively.

Producer's recommendations for aging are shown in Table 1.058. Note that there are variations between the producer's recommended aging treatments and those given by the AMS (compare Tables 1.056 and 1.058), with longer aging times being specified for some products by the AMS. While these differences are not large, longer aging will result in reduced tensile strength properties but increased resistance to stress corrosion. Stress relief by plastic deformation preceding aging will introduce a strength anisotropy and reduce peak strengths (37).

Sheet would normally be furnished in the T76 condition. AMS 2770D (39) gives the following aging treatment for this condition: 250 F, 6 to 8 hr + 350 F 3.5 to 4.5 hr. Attempts to change the temper condition (e.g., T6 to T7) by reaging require carefully controlled specially designed treatments for which no general rules have been established.

1.054 Annealing. The type of annealing treatment depends on the thermal and mechanical history of the material. Reannealing of the annealed temper 0 may be required following partial forming and can be accomplished by holding at 650 F for sufficient time to achieve uniform temperature. Rapid heating and minimum holding times will avoid grain coarsening. Annealing treatment for other temper conditions is as follows: 760 F, 2 to 3 hr + cooling to 450 F at a rate of 45 to 70 F/hr. For maximum microstructural stability and formability, an additional 2 to 6 hr at 450 F may be employed. When annealing thin gage clad products, time at maximum temperature must be minimized to avoid diffusion from the core to the cladding (37).

	Al
6.2	Zn
2.25	Mg
2.3	Cu
0.12	Zr

7050 Al

1.055 Special treatments. It is reported that a three- or four-step aging practice can be more "beneficial" than the two-step process for certain complex parts (37).

1.056 AMS specified heat treatments, Table 1.056.

1.057 Heat treatments for plate, extrusions, wire, rod, and rivets specified in MIL 6088F, Table 1.057.

1.058 Producer's recommended heat treatments, Table 1.058.

1.059 Cooling rate effects after solution treatment on the fully aged yield strength for 7000 series alloys, Figure 1.059.

1.0510 Dimensional stability of as-solution treated and quenched 7050, Figure 1.0510.

1.06 **Hardness**

AMS 4108A and AMS 4107A specify that hardness of forgings should be greater than 135 HRB (10-mm ball/500-kg load). However, this is not a requirement for acceptance if other properties are met.

1.07 **Forms and Conditions Available**

Forgings, plate, sheet, wire, rod, and rivets as shown in Tables 1.056 and 1.057.

1.08 **Melting and Casting Practice**

This alloy can be melted and alloyed in oil-fired, gas-fired, or electric furnaces and cast into ingots of any size for subsequent working.

1.09 **Special Considerations**

1.091 Type 7050 has relatively low quench sensitivity, which means that it does not need to be quenched as rapidly after solution treatment as other age-hardenable aluminum alloys. Slower quenching minimizes distortion and subsequent straightening operations without seriously affecting strength or corrosion resistance; however, some loss in toughness appears to occur in products quenched slowly (8).

1.0911 A comparison of the effects of the cooling rate after solution treatment of various aluminum alloys on the yield strength attained after aging to maximum strength is shown in Figure 1.059.

1.092 Electrical conductivity measurements are used as an indication of the effectiveness of the T74- and T73-type heat treatments for 7050 alloy. Electrical conductivity values above 40 percent IACS indicate that the proper metallurgical structure has been obtained to provide optimum corrosion resistance and toughness. Lower conductivity is indicative of lower corrosion resistance and toughness, but, possibly, higher strength (1,2,3).

1.093 Fatigue in aggressive environments. The conventional fatigue strength is considerably reduced at cyclic lives greater than about 10^5 cycles in the presence of a 3.5 percent salt fog (e.g., Figures 3.0516, 3.0517, and 3.05118). This effect in the high cycle life range is likely associated with pitting corrosion.

The effects of aggressive environments on fatigue crack-growth are complicated by differences in the applied cyclic load frequencies. While various frequencies have been used in investigations of 7050 products, the following general observations appear justified. Exposure to 3.5 percent salt fog moderately increases the crack-growth rates of T7452 hand forgings as compared with the rates obtained in dry air (Figure 3.0521). A more substantial deleterious effect is noted for salt fog in tests on 7050-T7651 extrusions (Figure 3.05210); larger effects are noted for -T6 sheet (Figure 3.05222). The same figures also show that moist air has an accelerating effect but to a smaller degree than salt fog. Tests on 7108-clad 7050-T6 sheet (Figures 3.05223 and 3.05224) yield essentially the same results for the effects of moist air and salt fog as that observed for the bare form. Tests on extrusions in the T7651 condition at 6 Hz show substantial increases in crack-growth rates in a 3.5 percent NaCl solution as compared with the growth rates in dry air (Figures 3.0512 and 3.0513) which appear to fade out at low K values. Sump water appears to have a more aggressive effect than moist air in tests on 7050-T7351 plate (Figure 3.0526). In the case of 7050-T7351 extrusions, the difference between the growth rates in moist air and in dry air is lost in the scatter (Figures 3.05217 to 3.05219).

Information on 7050-T7351 extrusions tested in dry air and in moist air at very low crack-growth rates (Figures 3.05214, 3.05216, and 3.05218) indicate that the threshold ΔK value at $R = 0.5$ is less than 2 ksi $\sqrt{in.}$ and less than 5 ksi $\sqrt{in.}$ for $R = 0.33$. These low growth rate tests corresponded to cyclic frequencies of 15 to 30 Hz. The value of about 4 ksi $\sqrt{in.}$ obtained for a 7050-T7351 extrusion (Figure 3.05216) agrees fairly well with the trend of the curves toward about this value for 7050-T7651 extrusions tested in dry air and in 3.5 percent NaCl solution (Figures 3.05212 and 3.05213). While none of this information can establish a K_{th} value, it is valuable in defining the lower limits of crack propagation in 7050 alloy.

1.094 Fatigue crack-growth in spectrum loading. It has been pointed out that microstructures producing high plane strain fracture toughness values do not always correspond to those which will provide the longest lives under certain types of spectrum (variable load amplitude) loading (42). The results obtained to date illustrate important aspects of the problem but are not yet sufficiently complete to permit design of a microstructure for any given spectrum.

The preliminary conclusions (42,43) may be summarized as follows:

(a) Overaging to T7 tempers coupled with increased copper content increases crack-growth resistance in constant amplitude loading and spectrum loading with either low level overloads, infrequently spaced high level overloads, or low nominal ΔK values.

(b) High purity (reduced intermetallic constituents) favors improved fatigue crack-growth resistance at high ΔK levels. However, for spectra with high overloads superimposed frequently on a base with a relatively low ΔK,

increasing the volume fraction of coarse intermetallics may be beneficial. The effect results from the formation of incipient cracks at particle locations introduced by the overloads. These cracks then tend to produce a branching of the fatigue crack at the lower ΔK levels. This branching is an energy absorbing process and tends to retard general crack growth in the spectrum.

(c) The effect of overaging on spectra with high overloads is to reduce the growth of the main crack during overloads and to decrease the amount of secondary cracks and, therefore, to reduce their effect on crack retardation at lower ΔK levels in the spectra.

1.095 Effect of high rate deformation in compression (shock hardening) on the tensile properties of 7050-T7451 (-T73651) plate, Table 1.095.

2 PHYSICAL AND CHEMICAL PROPERTIES

2.01 Thermal Properties

2.011 Melting range, 910 to 1165 F (8).

2.012 Phase changes.

2.0121 Time-temperature-transformation diagram.

2.0122 See 7175, Code 3219, Section 2.0122.

2.013 Thermal conductivity at room temperature (37):
T7651X: 89 Btu/ft/hr/ft^2/F
T7451X (T73651): 91 Btu/ft/hr/ft^2/F
T7351X: 93 Btu/ft/hr/ft^2/F.

2.014 Thermal expansion, Figure 2.014.

2.015 Specific heat.

2.016 Thermal diffusivity.

2.02 Other Physical Properties

2.021 Density, 0.102 lb/in.^{3} (8,11).

2.022 Electrical conductivity.

2.0221 Electrical conductivity of various forms and conditions, Table 2.0221

2.0222 AMS specified values for electrical conductivity of various forms and conditions, Table 2.0222.

2.023 Magnetic properties. Alloy 7050 is nonmagnetic.

2.024 Emittance.

2.025 Damping capacity.

2.03 Chemical Properties

(See also Section 4.04.)

2.031 General corrosion resistance. The higher copper content in 7050 as compared with that in 7075 or 7079 results in a slightly greater degree of general surface attack in aggressive environments. All products would be expected to exhibit pitting and a moderate degree of exfoliation when subjected to ASTM G 34-79 (EXCO Test). Results from this test have been reported by the producer and are shown in Table 3.014 for plate, forgings, and extrusions. The rating <EB places the alloy somewhere between superficial (EA) and moderate (EB) ratings for exfoliation resistance.

2.0311 Corrosion protection by cladding. Two cladding compositions (7072 and 7108) have been developed for 7050 (35,38) and are shown in Table 1.042. The 7108 has somewhat higher strength but is more difficult to produce. Both compositions have essentially the same corrosion resistance and give equal protection to the core. 7108-clad 0.180-inch thick sheet panels were exposed to salt-SO_2 fog for 4, 6, and 8 weeks (41). Conditions were as follows: 5 percent NaCl solution pH 6.5 to 7.2, cabinet temperature 95 F, SO_2 gas injection 1 hr every 5 hr at 25 cc/min. Stepped panels were machined to expose the core at the T/4 and T/2 planes and scribed panels were tested to determine the sacrificial protection afforded to the core by the cladding. After the stepped panels were exposed for 4 weeks, the cladding had been reduced by 50 percent from an original value of about 4.3 mils, and after 8 weeks no cladding remained. These stepped panel tests showed the cladding had corrosion resistance superior to the core. The scribed panels showed no core attack for an 1/8-inch wide scribe and only slight attack in a 1/4-inch wide scribe after 8 weeks of exposure.

	Al
6.2	Zn
2.25	Mg
2.3	Cu
0.12	Zr

7050 Al

2.032 Stress corrosion. The 7050 alloy and tempers offer higher combinations of strength and stress corrosion resistance than other aluminum alloy-temper systems, especially in thick products. The capabilities of 7050 for meeting the requirements of ASTM G 47-79 for determining susceptibility to stress corrosion are shown in Table 3.014 for plate, forgings, and extrusions. ASTM G 47 provides short transverse tests for small specimens stressed in tension and subjected to alternate immersion into a 3.5 percent NaCl solution with a 10-min. immersion period and a 50-min. dry time. The exposure time is 20 days for the 7000 series alloys unless cracking occurs sooner. The stresses shown in Table 3.014 should yield a 20-day minimum life. Qualitative stress corrosion ratings of 7050 and 7075 based on ASTM G 64-80 are shown in Table 2.034. (This table does not list the T73 temper for 7050 which presumably would be equal to the T73 temper of 7075.)

The producer (37) has conducted a very large number of long duration stress corrosion tests on 7050 plate, forgings, and extrusions in the T76, T74, and T73 (extrusions only) tempers. These include alternate immersion tests in 3.5 percent NaCl solution and marine and industrial exposures. While such tests do not establish lower stress bounds they are valuable for comparative purposes and for risk judgments.

Some examples of these types of tests in the ST direction have been included in this section. The results for 2-inch and 3-inch 7050-T7451 plate specimens subjected to alternate immersion into a 3.5 percent NaCl solution and into ASTM synthetic seawater are shown in Table 2.035. For the 2-inch plate, no failures were observed in 1,140 days for exposure to a stress of about 50 percent F_{ty} in the 3.5 percent NaCl solution. For the 3-inch plate, failures were observed in 54 days at a stress of about 66 percent F_{ty}. Interestingly, a similar exposure to synthetic seawater did not produce failure in 1,140 days at about 85 percent F_{ty} for either plate thickness. Table 2.036 indicates that a 4- to 6-inch 7050-T7351 plate subjected to alternate immersion into a 3.5 percent NaCl solution at 50 percent F_{ty} can

	Al
6.2	Zn
2.25	Mg
2.3	Cu
0.12	Zr

7050 Al

survive for at least 84 days. The results of alternate immersion tests on 7050-T7651 and -T7351 extrusions are given in Table 2.0311. They indicate that failures well under 84 days might be expected at 50 to 56 percent F_{ty} with the T7351 temper showing considerably better performance than the T7651 temper. The resistance to stress-corrosion cracking tends to decrease with the electrical conductivity as shown in Figure 2.0314.

Data on stress-corrosion cracking in fastner holes machined into 7050-T76 extruded bar are provided in Table 2.0317. The results apply to alternate immersion into a 3.5 percent NaCl solution at a gross stress of 34 percent F_{ty} and illustrate the sensitivity to interference fit with the smallest interference producing no cracks in 60 days of exposure.

Stress corrosion tests in marine environments on 7050-T7451 plate (Tables 2.035 and 2.037) indicate survival times in excess of 3 years when stressed to 50 percent F_{ty}. For 7050-T7651 extrusions, marine environment exposure at about 35 percent F_{ty} (Table 2.0312) produced failures in less than 3 months. Extrusions in the T7351 condition given similar exposures survived 6 months at 56 percent F_{ty}.

Stress corrosion tests in industrial atmospheres show less sensitivity to cracking than that observed in marine environments. This is illustrated by comparing the results obtained for 7050-T7651 extrusions (Table 2.0312) and 7050-T7351 extrusions (Table 2.0313) in these two environments. It will be noted that the T7351 temper is superior to the T7651 temper in the industrial atmospheres as might be expected from the additional aging given this condition.

2.033 Stress-corrosion crack velocity. Tests which permit the determination of crack velocity as a function of the stress intensity factor K provide additional information on stress-corrosion cracking resistance and under ideal circumstances can yield a value of stress intensity (K_{Iscc}) below which a crack would not grow under steady load in an aggressive environment. Under the best of circumstances, K_{Iscc} is difficult to determine and for many aluminum alloys the situation is further complicated by the presence of corrosion products which can wedge open the crack.

Crack velocity data for 7050 has been presented in several different ways. The most complete representation gives the velocity as a function of the instantaneous K (Figure 2.039). Two other forms are used which give less information but have the advantage of requiring less data analysis. Both report average velocities over a specified time period. The more complete of the two gives the initially applied K_I and the K_I at the end of the specified time period (Table 2.038), while the other gives only the initially applied K_I (Table 2.0316). None of the available data are sufficient to unambiguously establish a K_{Iscc} value for any of the forms and tempers of 7050.

The data for 7050-T7451 plate subjected to marine exposure (Figure 2.039) illustrate the scatter encountered in crack velocity measurements and the difficulty of establishing a K_{Iscc} even in the most complete representation. On the basis of these data, the K_{Iscc} of the 3-inch plate could be less than 5 ksi $\sqrt{in.}$ and that for the 1-1/4-inch plate could be less than 12 ksi $\sqrt{in.}$ The plateau velocity of the 1-1/4-inch plate is clearly lower than that of the 3-inch plate. Average crack velocities over 15 days in a 3.5 percent NaCl environment are shown for SL tests on 7050-T7351 plate in Table 2.038 for initially applied K values between 24 and 31 ksi $\sqrt{in.}$ With one exception, these velocities increase with increasing plate thickness. Average velocities over 202 days are shown in Table 2.0310 for 7050-T7451 plate tested in the SL orientation by alternate immersion into a 3.5 percent NaCl solution or by periodic moistening with this solution. There seems to be little difference in the velocities considering the scatter normally encountered in such tests. The table does indicate the substantial residual displacement due to corrosion product wedging.

Average crack velocities in 3.5 percent NaCl solution are given in Table 2.0316 for tests in the SL orientation of 7050-T7651 and -T7351 extrusions. The main conclusion from these data is that the T7351 temper has, as might be expected, lower crack velocities. Additional test results on 7050-T7651 and -T7351 extrusions are shown in Table 2.0315. Crack growth occurred in all specimens but the results indicate the superiority of the T7351 temper condition. While very long failure times characterize a K_i level of about 40 percent K_{Ic} for 7050-T7651 and 75 percent K_{Ic} for 7050-T7351, it is not possible to estimate K_{Iscc} values.

3 MECHANICAL PROPERTIES

3.01 Specified Mechanical Properties

3.011 AMS specified minimum tensile properties for 7050-T73651 (-T7451) die forgings, Table 3.011.

3.012 AMS specified tensile properties for 7050-T7651 plate and 7050-T76511, -T73511, and -T736511 (-T7451) extrusions, Table 3.012.

3.013 AMS specified minimum fracture toughness properties for 7050-T73651 (-T7451) plate, Table 3.013.

3.014 Producer's guaranteed minimum properties and capabilities for 7050 plate, forgings, and extrusions, Table 3.014.

3.015 Producer's proposed design mechanical properties for 7050-T7651 plate, Table 3.015.

3.016 Producer's proposed design mechanical properties for 7050-T7451 plate, Table 3.016.

3.017 Producer's tentative mechanical properties for bare and clad 7050-T76 sheet, Table 3.017.

3.02 Mechanical Properties at Room Temperature

3.021 Tension – stress-strain diagrams – tension properties.

3.0211 Tensile stress-strain curves for 7050-T7451 (-T73651) hand forgings, Figure 3.0211.

3.0212 Tensile stress-strain curves for 7050-T74 (-T736) die forgings, Figure 3.0212.

3.0213 Tensile stress-strain curves for 7050-T7451 (-T73651) plate, Figure 3.0213.

3.0214	Tensile stress-strain curves for 7050-T7351 plate, Figure 3.0214.
3.0215	Tensile stress-strain curves for 7050-T7651 extrusions of several thicknesses, Figure 3.0215.
3.0216	Tensile stress-strain curves for 7050-T7351 extrusions of several thicknesses, Figure 3.0216.
3.0217	Tensile stress-strain curves for 7050-T76 sheet, Figure 3.0217.
3.0218	Tensile properties of 7050-T7451 (-T73651) hand forgings of various sizes, Table 3.0218.
3.0219	Tensile properties of 7050-T74 (-T736) die forgings of various sizes, Table 3.0219.
3.02110	Tensile properties of 7050-T7351 plate of various thicknesses, Table 3.02110.
3.02111	Effects of exposures to elevated temperatures on tensile ultimate and yield strengths of 7050-T7451 (-T73651) plate, Figure 3.02111.
3.02112	Tensile properties of 7050-T7451 (-T73651) plate of various thicknesses, Table 3.02112.
3.02113	Tensile properties of 7050-T7651 extrusions of various thicknesses and cross sections, Table 3.02113.
3.02114	Tensile properties of 7050-T7351 extrusions of various thicknesses and cross sections, Table 3.02114.
3.02115	Effect of section thickness on tensile properties of 7050-T7651 extrusions of various cross sections, Table 3.02115.
3.02116	Tensile properties of various extruded shapes in the T76511 condition, Table 3.02116.
3.02117	Tensile properties of 7050-T76 sheet, Table 3.02117.
3.022	Compression – stress-strain diagrams – compression properties.
3.0221	Compressive stress-strain curves for 7050-T7452 (-T73652) hand forgings, Figure 3.0221.
3.0222	Compressive stress-strain curves for 7050-T74 (-T736) die forgings, Table 3.0222.
3.0223	Compressive stress-strain curves for 7050-T7351 plate, Figure 3.0223.
3.0224	Compressive stress-strain curves for 7050-T7451 (-T73651) plate, Figure 3.0224.
3.0225	Compressive stress-strain curves for 7050-T7651 extrusions of several thicknesses, Figure 3.0225.
3.0226	Compressive stress-strain curves for 7050-T76 sheet, Figure 3.0226.
3.0227	Compressive yield strength of 7050-T7452 (-T73652) hand forgings of various sizes, Table 3.0227.
3.0228	Compressive yield strength of 7050-T74 (-T736) die forgings of various thicknesses, Table 3.0228.
3.0229	Compressive yield strength of 7050-T7351 plate of various thicknesses, Table 3.0229.
3.02210	Compressive yield strength of 7050-T6 sheet and 7050-T7451 (-T73651) plate of various thicknesses, Table 3.02210.
3.02211	Compressive yield strength of 7050-T7651 extrusions of various thicknesses and cross sections, Table 3.02211.
3.02212	Compressive yield strength of 7050-T7351 extrusions of various thicknesses and cross sections, Table 3.02212.
3.023	Impact.
3.024	Bending.
3.025	Torsion and shear.
3.0251	Shear strength of 7050-T7452 (-T73652) hand forgings, Table 3.0251.
3.0252	Shear strength of 7050-T74 (-T736) die forgings, Table 3.0252.
3.0253	Shear strength of 7050-T6 sheet and 7050-T7451 (-T73651) plate, Table 3.0253.
3.0254	Shear strength of 7050-T7351 plate, Table 3.0254.
3.0255	Shear strength of 7050-T7651 extrusions, Table 3.0255.
3.0256	Shear strength of 7050-T7351 extrusions, Table 3.0256.
3.026	Bearing.
3.0261	Bearing properties of 7050-T7452 (-T73652) hand forgings, Table 3.0261.
3.0262	Bearing properties of 7050-T74 (-T736) die forgings, Table 3.0262.
3.0263	Bearing properties of 7050-T76 sheet and 7050-T7451 (-T73651) plate, Table 3.0263.
3.0264	Bearing properties of 7050-T651 extrusions, Table 3.0264.
3.0265	Bearing strength of 7050-T7651 extrusions, Table 3.0265.
3.0266	Bearing properties of 7050-T7351 extrusions, Table 3.0266.
3.027	Stress concentration.
3.0271	Notch properties.
3.0272	Fracture toughness.
3.02721	General. Static fracture in high strength aluminum alloys occurs primarily by a process of void nucleation and growth. Under these circumstances the fracture toughness is affected by the size and distribution of impurity particles. These particles are formed during ingot solidification by a combination of iron and silicon, and sometimes manganese, with aluminum and solute atoms. These particles do not contribute to the strength of the alloy and have been shown to fracture at very low average matrix strains resulting in void formation (39). The 7050 alloy is produced with close controls on iron and silicon and offers a considerable advantage in fracture toughness over 7075 with negligible sacrifice in strength. Fracture toughness of 7050 like other high strength aluminum alloys decreases with product thickness and is anisotropic being lower in the SL or ST directions (e.g., Table 3.02722, Figure 3.02724, and Table 3.02725). Special ingot processing techniques (intermediate thermal mechanical treatments) have been applied (30) in an attempt to improve the properties of 7050. These treatments (Table 3.02727) increased the yield strength but reduced the fracture toughness in comparison to the commercially produced product.
3.02722	Plane strain fracture toughness of plate, hand forgings, and die forgings, Table 3.02722.
3.02723	Plane strain fracture toughness values for crack initiation and arrest in 7050-T7451 (-T73651) plate for SL orientation, Table 3.02723.
3.02724	Effect of extrusion section thickness on plane strain fracture toughness, Figure 3.02724.
3.02725	Plane strain fracture toughness of various extruded shapes, Table 3.02725.
3.02726	Extrusion cross sections used for fracture toughness and crack-growth rate tests, Figure 3.02726.

	Al
6.2	Zn
2.25	Mg
2.3	Cu
0.12	Zr

7050 Al

	Al
6.2	Zn
2.25	Mg
2.3	Cu
0.12	Zr

7050 Al

3.02727 Plane strain fracture toughness of specially processed very high purity 7050 plate, Table 3.02727.

3.02728 Special processing schedules provided to 7050 very high purity plate, Table 3.02728.

3.028 Combined properties.

3.03 Mechanical Properties at Various Temperatures

3.031 Tension – stress-strain diagrams – tension properties.

3.0311 Tensile stress-strain curves for 7050-T7452 (-T73652) plate at room and elevated temperatures, Figure 3.0311.

3.0312 Tensile properties of 7050-T7451 (-T73651) plate in the temperature range -65 to 350 F, Figure 3.0312.

3.0313 Tensile properties of 7050-T7451 (-T73651) plate in the temperature range of 70 to 500 F, Figure 3.0313.

3.0314 Effects of elevated temperatures on tensile ultimate and yield strengths of 7050-T7451 (-T73651) plate after various exposure times at test temperature, Figure 3.0314.

3.0315 True stress as a function of strain rate for tests on a sheet at 900 F, Figure 3.0315.

3.032 Compression – stress-strain diagrams – compression properties.

3.0321 Compressive stress-strain curves for 7050-T7451 (-T73651) plate at room and elevated temperatures, Figure 3.0321.

3.0322 Effects of temperature on compressive yield strength of 7050-T7451 (-T73651) plate, Figure 3.0322.

3.033 Impact.

3.034 Bending.

3.035 Torsion and shear.

3.036 Bearing.

3.037 Stress concentration.

3.0371 Notch properties.

3.0372 Fracture toughness.

3.03721 Effects of low and elevated temperatures on plane-strain fracture toughness of 7050-T7451 (-T73651) plate, Figure 3.03721.

3.038 Combined properties.

3.04 Creep and Creep-Rupture Properties

3.041 Creep and creep-rupture curves for 7050-T7451 (-T73651) plate, Figure 3.041.

3.05 Fatigue Properties

3.051 Conventional fatigue properties.

3.0511 Low cycle fatigue results for 7050 plate subjected to different aging treatments, Figure 3.0511.

3.0512 Low cycle fatigue results for two processing treatments of very high purity 7050 plate, Figure 3.0512.

3.0513 Modified Goodman diagrams for longitudinal smooth and notch fatigue properties of 7050-T7452 (-T73652) hand forgings, Table 3.0513.

3.0514 Modified Goodman diagrams for long transverse smooth and notch fatigue properties of 7050-T7452 (-T73652) hand forgings, Figure 3.0514.

3.0515 Modified Goodman diagrams for short transverse smooth and notch fatigue properties of 7050-T7452 (-T73652) hand forgings, Figure 3.0515.

3.0516 S-N curves at R = 0 for smooth specimens from 7050-T7452 (-T73652) hand forgings tested in air and in salt fog, Figure 3.0516.

3.0517 S-N curves at R = 0 for smooth specimens from 7050-T7451 (-T73651) plate tested in air and in salt fog, Figure 3.0517.

3.0518 S-N bands at R = 0 for smooth, L, LT, and ST specimens from 7050-T7351 plate of various thicknesses, Figure 3.0518.

3.0519 S-N band at R = 0 for notched specimens from 7050-T7351 plate of various thicknesses, Figure 3.0519.

3.05110 Fatigue life at various temperatures of smooth and notched 7050-T7451 (-T73651) plate, Figure 3.05110.

3.05111 Modified Goodman diagrams for fatigue properties of smooth and notched 7050-T7451 (-T73651) plate, Figure 3.05111.

3.05112 S-N band at R = +0.1 for smooth specimens from 7050-T7651 and -T7351 extrusions of various thicknesses and cross sections, Figure 3.05112.

3.05113 S-N band at R = -1.0 for smooth specimens from 7050-T7651 and -T7351 extrusions of various thicknesses and cross sections, Figure 3.05113.

3.05114 S-N band at R = +0.1 for notched specimens from 7050-T7651 and -T7351 extrusions of various thicknesses and cross sections, Figure 3.05114.

3.05115 S-N band at R = -1.0 for notched specimens from 7050-T7651 and -T7351 extrusions of various thicknesses and cross sections, Figure 3.05115.

3.05116 Modified Goodman diagrams for smooth and notch fatigue properties of 7050-T76511 extrusions, Figure 3.05116.

3.05117 S-N band at R = +0.1 for smooth specimens from 7050-T7651 extrusions subjected to salt fog, Figure 3.05117.

3.05118 S-N curves at R = 0 for smooth specimens from 7050 extrusions in the T76511 condition tested in air and in salt fog, Figure 3.05118.

3.05119 S-N band at R = 0.1 for smooth and notched specimens of 7050-T7351 extrusions subjected to salt fog, Figure 3.05119.

3.05120 Modified Goodman diagrams for smooth and notch fatigue properties of 7050-T6 sheet, Figure 3.05120.

3.05121 S-N bands at several R ratios for smooth L and LT specimens from 7050-T6 clad sheet, Figure 3.05121.

3.05122 S-N bands at several R ratios for L and LT notched specimens from 7050-T6 clad sheet, Figure 3.05122.

3.052 Fatigue crack-growth rates.

3.0521 Fatigue crack-growth rates of 7050-T7452 (-T73652) hand forgings in TL and SL orientations in dry air, humid air, and salt fog, Figure 3.0521.

3.0522 Fatigue crack-growth rates of 7050-T7451 (-T73651) plate and 7050-T74 (-T736) die forgings in dry air and in 3.5 percent NaCl solution, Figure 3.0522.

3.0523 Fatigue crack-growth rates for 1-inch and 6-inch 7050-T7451 (-T73651) plate in TL and SL orientations in dry air and in salt fog, Figure 3.0523.

3.0524 Crack growth in 7050-T7451 (-T73651) plate subjected to a truncated transport flight spectrum, Table 3.0524.

3.0525 Fatigue crack-growth rates in dry air and in sump water for 2-inch and 4-inch 7050-T7351 plate tested in LT orientation, Figure 3.0525.

3.0526 Fatigue crack-growth rates in dry air, moist air, and in sump water for 2-inch 7050-T7351 plate tested in TL orientation, Figure 3.0526.

3.0527 Fatigue crack-growth rates in sump water for 4-inch 7050-T7351 plate tested in TL orientation, Figure 3.0527.

3.0528 Fatigue crack-growth rates in dry air, moist air, and in sump water for 4-inch 7050-T7351 plate tested in SL orientation, Figure 3.0528.

3.0529 Composition of synthetic sump tank water, Table 3.0529.

3.05210 Fatigue crack-growth rates in dry air, humid air, and in salt fog for 7050-T7651 extrusions tested in TL and SL orientations, Figure 3.05210.

3.05211 Fatigue crack-growth rates in dry air and in moist air for 7050-T7651 extrusion tested in LT and TL orientations, Figure 3.05211.

3.05212 Fatigue crack-growth rates for various extruded shapes of 7050-T76511 tested in TL orientation in dry air and in salt water, Figure 3.05212.

3.05213 Fatigue crack-growth rates for various extruded shapes of 7050-T76511 tested in LT orientation in dry air and in salt water, Figure 3.05213.

3.05214 Near threshold fatigue crack-growth rates at R = 0.5 in dry air and in moist air for TL specimens from 7050-T7351 C5A wing plank extrusion, Figure 3.05214.

3.05215 Fatigue crack-growth rates in dry air and in moist air for LT specimens from 7050-T7351 C5A wing plank extrusion, Figure 3.05215.

3.05216 Fatigue crack-growth rates in dry air and in moist air for 7050-T7351 extrusion tested in TL orientation, Figure 3.05216.

3.05217 Fatigue crack-growth rates in dry air and in moist air for 7050-T7351 extrusion tested in LT and TL orientations, Figure 3.05217.

3.05218 Near threshold fatigue crack-growth rates at R = 0.5 in dry air and in moist air for LT specimens from 7050-T7351 C5A wing plank extrusion, Figure 3.05218.

3.05219 Fatigue crack-growth rates in dry air and in moist air for TL specimens from 7050-T7351 C5A wing plank extrusion, Figure 3.05219.

3.05220 Fatigue crack-growth rates at R = 0.05 and R = 0.275 in dry argon for 7050-T6 sheet tested in LT orientation, Figure 3.05220.

3.05221 Fatigue crack-growth rates at R = 0.5 and R = 0.7 in dry argon for 7050-T6 sheet tested in LT orientation, Figure 3.05221.

3.05222 Fatigue crack-growth rates in dry air, humid air, and salt fog for 7050-T6 sheet tested in TL and LT orientations, Figure 3.05222.

3.05223 Fatigue crack-growth rates in dry air, moist air, and in 3.5 percent salt fog for clad 7050-T76 sheet tested in LT orientation, Figure 3.05223.

3.05224 Fatigue crack-growth rates in dry air, moist air, and in 3.5 percent salt fog for clad 7050-T76 sheet tested in TL orientation, Figure 3.05224.

3.06 Elastic Properties

3.061 Poisson's ratio, 0.33.

3.062 Modulus of elasticity.

3.0621 Static modulus of elasticity in tension and compression for various forms, Figure 3.0621.

3.0622 Effect of temperature on the static modulus of elasticity in tension and compression for 7050-T7451 (-T73651) plate, Figure 3.0622.

3.0623 Mean ($\bar{X}$) and standard deviation(s) of the tension and compression modulus for 7050-T7651 and -T7351 extrusions and 7050-T7351 plate, Table 3.0623.

3.063 Modulus of rigidity, 3.9 x 10^3 ksi.

3.064 Tangent modulus.

3.0641 Tensile tangent modulus for 7050-T7651 extrusions of several thicknesses, Figure 3.0641.

3.0642 Tensile tangent modulus for 7050-T7351 extrusions of various thicknesses, Figure 3.0642.

3.0643 Compressive tangent modulus for 7050-T7451 (-T73651) plate at various temperatures, Figure 3.0643.

3.0644 Compressive tangent modulus for 7050-T7351 plate, Figure 3.0644.

	Al
6.2	Zn
2.25	Mg
2.3	Cu
0.12	Zr

7050 Al

4 FABRICATION

4.01 Forming

The recommended minimum bend radii for 7050 are equal to or less than those required for 7075, depending on the material thickness and temper (e.g., the suggested minima for 0.5-inch 7050-0 and -T7451 plate are 3t and 6t, respectively) (37).

4.02 Machining and Grinding

Machinability is excellent in all forms and tempers. Chemical milling of 7050-T7451 is slightly slower than that for 7075-T651 with a slightly more uniform surface than that obtained in the 7075 alloy.

4.03 Joining

4.031 Welding. Weldability of 7050 is not good. Butt welds of 7050 plate have been made using standard (5356, 4043) and experimental filler alloys and the GMA and GTA processes. Most of the resulting welds contained cracks and porosity. Tensile tests across the welds showed approximately 50 percent joint efficiency and very low elongation of about 1.0 percent (8).

4.032 Brazing as a practical joining technique for the 7050 alloy is precluded by wetting problems and its relatively low melting range (8).

4.033 Fastening. 7050-T73 (E) rivets are an excellent replacement for 2024-T4 (DD) "ice box" rivets. They are slightly stronger and can be driven in the T73 condition. Design allowables for 7050-T73 style rivets in rivets joints have been developed. Threaded fasteners have been produced successfully and appear to be at least 15 percent stronger than 7075-T73. Additionally, they have superior toughness to 2024-T4 threaded fasteners as measured by resistance to twist-off.

4.04 Surface Treating

Procedures for cleaning, anodizing, conversion coating, and painting are similar to those used for 7075. However, it has been reported that deoxidizing and etching treatments used prior to anodizing or dye penetrant inspection resulted in

	Al
6.2	Zn
2.25	Mg
2.3	Cu
0.12	Zr

7050 Al

more intergranular attack in 7050-T7 tempers than in 7075-T7 tempers. The producer has developed procedures to avoid these problems should they arise (37).

REFERENCES

1 AMS 4050A (July 15, 1977).

2 AMS 4108 (January 1, 1977).

3 AMS 4107A (January 15, 1977).

4 Davies, R. E., Nordmark, G. E., and Walsh, J. D., "Design Mechanical Properties, Fracture Toughness, Fatigue Properties, Exfoliation and Stress-Corrosion Resistance of 7050 Sheet, Plate, Hand Forgings, Die Forgings and Extrusions", Report N00019-72-C-0512 to Naval Air Systems Command from Alcoa Laboratories (July 1975).

5 Sprowls, D. O., Walsh, J. D., and Coursens, J. W., "Evaluating Stress Corrosion Crack Propagation Rates in High Strength Aluminum Alloys with Bolt Loaded Precracked Double Cantilever Beam Specimens", Presented at Tri-Service Conference on Corrosion of Military Equipment, Dayton, Ohio (October 31, 1974).

6 Staley, J. T., "Resistance to Stress-Corrosion Cracking of Al-Zn-Mg-Cu Alloys Containing Zr or Mn", 1973 Westec Conference, Los Angeles, California (March 12-13, 1973).

7 Staley, J. T., "Further Development of Aluminum Alloy X7050", Final Report from Alcoa to Naval Air Systems Command, Contract N00019-71-C-0131 (May 8, 1972).

8 Mayer, L. W., "Alcoa Green Letter: Alcoa Alloy 7050" (April 1973).

9 Dill, H. D. and Rich, D. L., "Evaluation of Aluminum Plate Alloys 7075-T7351, X7050-T73651 and 2021-T81", Report MDC A1755, McDonnell Douglas Corporation (May 1972).

10 Jones, R. E., and Fudge, K. A., "Engineering Design Data for Aluminum Alloy 7050-T73651 Plate", AFML TR-73-269, University of Dayton Research Institute (November 1973).

11 Deel, O. L., Ruff, P. E., and Mindlin, H., "Engineering Data on New Aerospace Structural Materials", AFML-TR-73-114, Battelle's Columbus Laboratories (June 1973).

12 Rinnovatore, J. V., Lukens, K. F., and Corrie, J. D., "Aluminum Alloys with Improved Resistance to Exfoliation", Metals Engineering Quarterly, Vol. 13 (August 1973).

13 Staley, J. T., "Comparison of Aluminum Alloy 7050, 7049, MA52 and 7175-T736 Die Forgings", AFML-TR-73-34, Alcoa Laboratories (May 1973).

14 Figge, F. A., "Advanced Metallic Structure: Air Superiority Fighter Wing Design for Improved Cost, Weight, and Integrity. Volume III. Materials Test Program", Northrup Corporation, Prepared for Air Force Flight Dynamics Laboratory (June 1973).

15 Schra, L. and 't Hart, W.G.J., "Engineering Property Comparisons of 7050-T73651, 7010-T7651, and 7010-T73651 Aluminum Alloy Plate", Engineering Fracture Mechanics, Vol. 17, No. 6 (1983), p 493.

16 Doward, R. C. and Hasse, K. R., "Estimating Plane Strain Fracture Toughness of High Strength Aluminum Alloys from Crack Arrest Toughness", Journal of Testing and Evaluation, Vol. 5 (May 1977) p 174.

17 Hasse, K. R. and Doward, R. C., "Flaw Growth of 7075, 7475, 7050 and 7049 Aluminum Alloy Plate in Stress Corrosion Environments (Contract NAS 8-30890) 4-Year Marine Atmosphere Results", Research Report CFT-RR-81-15, Kaiser Aluminum Corporation Center for Technology (October 31, 1981).

18 Van Orden, J. M. and Pettit, D. E., "Corrosion Fatigue Crack Growth in 7050 Aluminum Alloy Extrusions", Journal of Aircraft, Vol. 13 (November 1976) p 873.

19 Staley, J. T., Jacoby, J. E., Davies, R. E., Nordmark, G. E., Walsh, J. D., and Rudolph, F. R., "Aluminum Alloy 7050 Extrusions", Alcoa Laboratories, AF Contract 33615-73-C-5015, AFML TR-76-129 (March 1977).

20 Brownhill, D. J., Davies, R. E., Nordmark, G. E., and Ponchel, B. M., "Exploratory Development for Design Data on Structural Aluminum Alloys in Representative Aircraft Environments", Alcoa Laboratories, AF Contract 33615-74-C-5089, AFML TR 77-102 (July 1977).

21 AMS 4201 (January 15, 1980).

22 AMS 4341 (April 15, 1978).

23 AMS 4340A (July 15, 1980).

24 AMS 4342 (April 15, 1978).

25 Personal communication between L. N. Mueller, Alcoa Technical Center, and W. F. Brown, Jr.

26 Kaneko, R. S. and Simenz, R. F., "Corrosion Thresholds for Interference Fit Fasteners and Cold Worked Holes", Stress Corrosion New Approaches, ASTM STP 610 (1976) p 252.

27 Neu, C. E., "Properties of Shock Hardened 7050 Aluminum Alloy", Naval Air Systems Command, Report No. NAOC 81251-60 (November 1981).

28 Ghosh, A. K. and Hamilton, C. H., "Deformation and Fracture in Al-Zn-Mg Alloys at Elevated Temperature", Strength of Metals and Alloys Proceedings of the 5th International Conference, Vol. 2, Aachen Federal Republic of Germany (August 27-31, 1979).

29 Brown, R. D. and Weertman, J., "Mean Stress Effects on Crack Propagation Rate and Crack Closure in 7050 T6 Aluminum Alloy", Engineering Fracture Mechanics, Vol. 10 (1978) p 757.

30 Sanders, R. E. and Starke, E. A., Jr., "The Effect of Intermediate Thermal Mechanical Treatments on Fatigue Properties of a 7050 Aluminum Alloy", Metallurgical Transactions A, Vol. 9A (August 1978) p 1087.

31 Humphries, T. S. and Nelson, E. E., "Seacoast Stress Corrosion Cracking of Aluminum Alloys", NASA TM-82393, MSFC (January 1981).

32 Hunsicker, H. Y., "Dimensional Change in Heat Treating Aluminum Alloys", Metallurgical Transaction A, Vol. 11A (May 1980) p 759.

33 Sanders, T. H. and Starke, E. A., Jr., "The Relationship of Microstructure to Monotonic and Cyclic Straining of Two Age Hardened Aluminum Alloys", Metallurgical Transaction A, Vol. 7A (September 1976) p 1407.

34 Van Orden, J. M., Krupp, W. E., Walden, E., and Ryder, J. T., "Effects of Purity on Fatigue and Fracture of 7XXX-T7651 Aluminum Extrusion, Journal of Aircraft, Vol. 16, No. 5 (May 1979) p 327.

35 Staley, J. T., "Heat Treatable Cladding for New Aluminum 7050 T76 Sheet", Composite Reliability, ASTM STP 580 (1975) p 621.

36 Heat Treatment of Aluminum Alloys, MIL H 6008F Amendment 1 (December 30, 1982).

37 Personal communication between L. N. Mueller, Alcoa Technical Center, and W. F. Brown, Jr. (1983).

38 Personal communication between E. Suphder, Alcoa Technical Center, and W. F. Brown, Jr. (1983).

39 Tanaka, J. P., Pampillo, C. A., and Low, J. R., Jr., "Fractographic Analysis of Low Energy Fracture of an Aluminum Alloy", ASTM STP 463, Edited by W. F. Brown, Jr. (1970) p 191.

40 Collins, J. F. and Maduell, C. E., "Polyalkylene Glycol Quenching of Aluminum Alloys", Materials Performance, Vol. 16 (July 1977) p 20.

41 Ketcham, S. J., "Corrosion Resistance of Clad 7050 Sheet", Proceedings of 1974 Triservice Corrosion of Military Equipment Conference, October 1974, Vol. 1, AFML TR-74-42, Vol. 1 (September 1975) p 515.

42 Bucci, R. J., Thakker, A. B., Sanders, T. H., Sawtell, R. R., and Staley, J. T., "Ranking 7XXX Aluminum Alloy Fatigue Crack Growth Resistance Under Constant Amplitude and Spectrum Loading", ASTM STP 714, Edited by Bryan and Potter (1980) p 41.

43 Staley, J. T., "Influence of Microstructure on Fatigue and Fracture of Aluminum Alloys", International Symposium on Fracture Mechanics, Vol. 55 (April 1979) p 277.

Al
6.2 Zn
2.25 Mg
2.3 Cu
0.12 Zr

7050 Al

Alloy	7050						
Form	Hand Forgings	Die Forgings	Plate		Extrusions		
Condition	Sol Treat + Age	Sol Treat + SR(a) + Age	Sol Treat + Age	Sol Treat + SR + Age	Sol Treat + SR + Age		
Temper	T736	T73652	T73651(b)	T7651	T73511	T76511	T736511(c)
AMS	4108A	4107A	4050A	4201	4341	4340A	4342
Source	3	2	1	21	22	23	24

(a) SR – stress relieved by plastic deformation (see Section 1.05).
(b) Alcoa T7451.
(c) Alcoa T74511.

TABLE 1.031. AMS SPECIFICATIONS (1-3, 21-24)

Alloy	7050	
	Percent	
Composition	Min	Max
Zn	5.7	6.7
Cu	2.0	2.6
Mg	1.9	2.6
Zr	0.08	0.15
Fe	–	0.15
Si	–	0.12
Mn	–	0.10
Ti	–	0.06
Cr	–	0.04
Other, Each	–	0.05
Other, Total	–	0.15
Al	Balance	

TABLE 1.041. AMS SPECIFIED ALLOY COMPOSITION (1-3, 21-24)

	Al
6.2	Zn
2.25	Mg
2.3	Cu
0.12	Zr

7050 Al

Alloy	7050			
Form	Cladding Alloys			
Designation	7072		7108	
	Percent			
Composition	Min	Max	Min	Max
Zn	0.8	1.3	4.5	5.5
Cu	–	0.10	–	0.05
Mg	–	0.10	0.7	1.4
Zn	–	–	0.12	0.25
Fe	–	(a)	–	0.10
Si	–	(a)	–	0.10
Mn	–	0.10	–	0.05
Ti	–	–	–	0.05
All Others(b)	–	0.15	–	0.10

(a) Composition of Fe and Si was 0.7 percent (maximum).
(b) Composition of any of "all other" elements was 0.05 percent (maximum).

TABLE 1.042. PRODUCER'S COMPOSITION OF CLADDING ALLOYS FOR 7050 (38)

Alloy	7050						
Form	Hand Forgings	Die Forgings	Plate		Extrusions		
Condition	T73652(a)	T736(b)	T73651(c)	T7651	T73511	T76511	T736511(d)
Solution Treat	880 to 900 F, 1 hr, Min WQ (140 to 160 F) +	880 to 900 F, 1 hr, Min WQ (140 to 160 F) +	(e)	(e)	880 to 890 F, 1/4 hr, Min WQ (<100 F) +	880 to 890 F, WQ (<100 F) +	880 to 890 F, WQ (<100 F) +
Stress(f) Relief	1 to 5 percent Compression +	0 +	1.5 to 3 percent Stretch	1.5 to 3 percent Stretch	1 to 3 percent Stretch +	1 to 3 percent Stretch +	1 to 3 percent Stretch +
Age	240 to 260 F, 24 hr + 340 to 360 F, 8 hr, AC	240 to 260 F, 24 hr + 340 to 360 F, 12 hr, AC	(e)	(e)	240 to 260 F, 1 to 24 hr + 340 to 360 F, 12 hr, AC	240 to 260 F, 3 to 24 hr + 340 to 360 F, 8 hr, AC	240 to 260 F, 1 to 24 hr + 340 to 360 F, 10 hr, AC
Source	3	2	1	21	23	22	24

(a) Alcoa T7452.
(b) Alcoa T74.
(c) Alcoa T7451.
(d) Alcoa T74511.
(e) See Table 1.057.
(f) Plastic strain.

TABLE 1.056. AMS SPECIFIED HEAT TREATMENTS (1-3, 21-24)

Alloy	7050				
Form	Plate		Extrusions		Wire, Rod, and Rivets
Condition	T7651	T7451(a)	T76510	T76511(b)	T73
Solution(c) Treat	880 to 900 F, WQ	880 to 900 F, WQ	880 to 900 F, WQ	880 to 900 F, WQ	880 to 900 F, WQ
Age(a)	+ 240 to 260 F, 3 to 6 hr, AC + 315 to 335 F, 12 to 15 hr, AC	+ 240 to 260 F, 3 to 6 hr, AC + 315 to 335 F, 24 to 30 hr	+ 240 to 260 F, 3 to 8 hr, AC + 315 to 335 F, 15 to 18 hr, AC	+ 240 to 260 F, 3 to 6 hr, AC + 315 to 335 F, 15 to 18 hr, AC	+ 245 to 255 F, 4 min., AC + 350 to 360 F, 8 hr

(a) Preceeding aging stress relief is applied by stretching to all products except wire, rod, and rivets.
(b) This temper designation indicates minor straightening follows stress relief.
(c) Soaking time at solution temperature depends on the method of heating and the thickness. (See MIL H6088F, Table 4.) Quench delay time depends on thickness. (See MIL H6088F, Table 6.)

TABLE 1.057. HEAT TREATMENTS FOR PLATE, EXTRUSIONS, WIRE, ROD, AND RIVETS SPECIFIED IN MIL 6088F (36)

Alloy	7050						
Solution Treatment	890 F, WQ, All Forms						
First Step Aging	To T7 Temper 250, 3 to 8 hr, All Forms						
Second Step(a) Aging at 350 F	Hand Forgings	Die Forgings	Plate(b)			Extrusions	Rivets
Temper	T7452	T74	T7651	T7451	T7351	T7651X	T73
Time, hr	6 to 8	6 to 12	3.4 to 7.3	6.8 to 8.6	(b)	4.3 to 5.1	(8 Min)

(a) Equivalent time of second step aging within the limits 300 to 360 F:

$t_T = t_{350} \exp\left(\frac{31390}{T + 460} - 39.42\right)$ where t_{350} is given in above Table and t_T is the time at another temperature.

(b) 330 F, 36 hr.

Note: Essentially equivalent to MIL 6088F.

TABLE 1.058. PRODUCER'S RECOMMENDED HEAT TREATMENTS (37)

Al
6.2 Zn
2.25 Mg
2.3 Cu
0.12 Zr

7050 Al

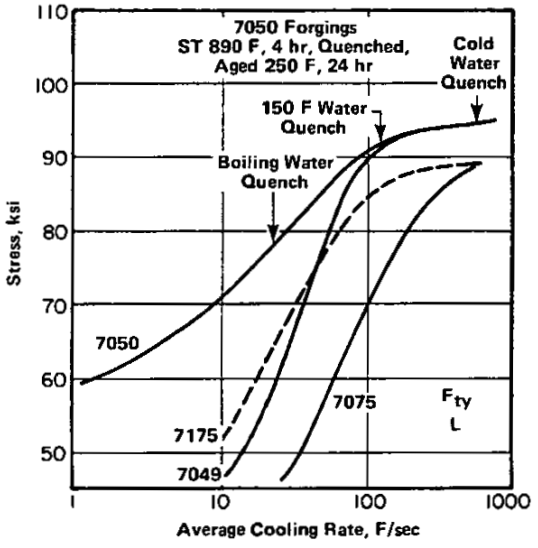


FIGURE 1.059. COOLING RATE EFFECTS AFTER SOLUTION TREATMENT ON FULLY AGED YIELD STRENGTH FOR 7000 SERIES ALLOYS (8,13)

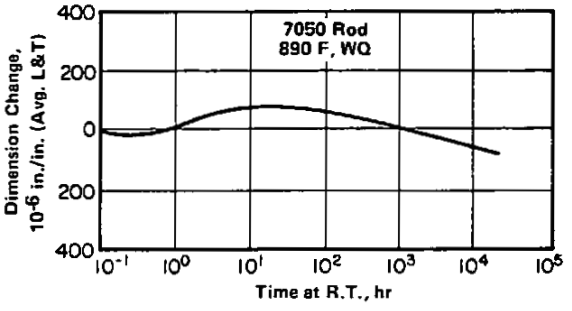


FIGURE 1.0510. DIMENSIONAL STABILITY OF AS-SOLUTION TREATED AND QUENCHED 7050 (32)

Alloy	7050							
Form	1/2-inch Plate							
Condition	7050-T7451							
Treatment	As Received		As Received + 250 F, 4 hr		250 F, 4 hr + Shock Hardened (Shock Velocity 5730 m/sec, 2 μsec Pulse, 9 percent Transient Strain)			
					As Shocked		Shocked + 250 F, 4 hr	
Direction	L	T	L	T	L	T	L	T
F_{tu}, ksi	75	75	76	75	73	69	74	76
F_{ty}, ksi	65	65	66	65	72	70	69	68
e (inch), percent	16	12	15	12	10	5	9	13
RA, percent	42	38	44	37	17	9.7	10	38

TABLE 1.095. EFFECT OF HIGH RATE DEFORMATION IN COMPRESSION (SHOCK HARDENING) ON THE TENSILE PROPERTIES OF 7050-T7451 (-T73651) (25)

	Al
6.2	Zn
2.25	Mg
2.3	Cu
0.12	Zr

7050 Al

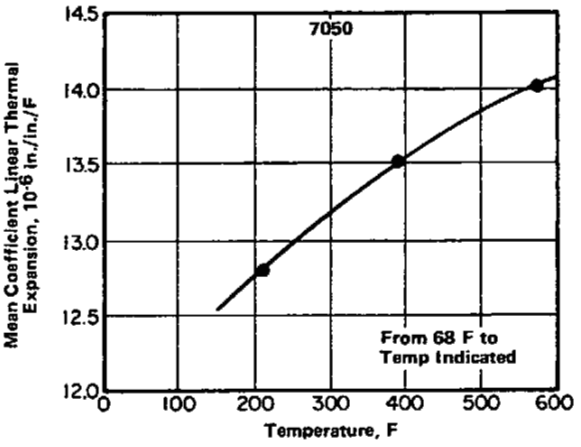


FIGURE 2.014. THERMAL EXPANSION (37)

Alloy	7050			
		Electrical Conductivity,		Electrical Resistivity, microhm-in.
Form	Condition	percent IACS	megohms/ in.^{3}	
Sheet	T76	38.3	0.563	1.78
Plate	T7451	41.4	0.607	1.65
Die Forgings	T736	41.4	0.607	1.65
Hand Forgings	T7452	42.2	0.621	1.61
Extrusions	T76511	39.4	0.580	1.73

TABLE 2.0221. ELECTRICAL CONDUCTIVITY OF VARIOUS FORMS AND CONDITIONS (4, 37)

Alloy	7050						
Form	Hand Forgings	Die Forgings	Plate		Extrusions		
AMS	4108	4107A	4050A	4201	4341	4340A	4342
Condition	T736	T73652(a)	T73651(b)	T7651	T73511	T76511	T736511
Electrical Conductivity, percent IACS	>40	>40	>40	>39	>40(c)	≥39(d)	>40

(a) Alcoa T7452.
(b) Alcoa T7451.
(c) 40 = IACS <41, F_{ty} (L) <69 ksi, IACS >41, and F_{ty} is not limited.
(d) AMS gives an unclear qualification to this value.

TABLE 2.0222. AMS SPECIFIED VALUES FOR ELECTRICAL CONDUCTIVITY OF VARIOUS FORMS AND CONDITIONS (1-3, 21-24)

Alloy and Temper	Test Direction	Rolled Plate	Rod and Bar	Extruded Shapes	Forgings
7050-T76	L	A	A	A	(1)
	LT	A	B	A	(1)
	ST	C	B	C	(1)
7050-T74	L	A	(1)	A	A
	LT	A	(1)	A	A
	ST	B	(1)	B	B
7075-T6	L	A	A	A	A
	LT	B(2)	D	B(2)	B(2)
	ST	D	D	D	D
7075-T76	L	A	(1)	A	(1)
	LT	A	(1)	A	(1)
	ST	C	(1)	C	(1)
7075-T73	L	A	A	A	A
	LT	A	A	A	A
	ST	A	A	A	A

Rating	Interpretation
A	Very high. No record of service problems and SCC not anticipated in general applications.
B	High. No record of service problems and SCC not anticipated at stresses of the magnitude caused by solution heat treatment. Precautions must be taken to avoid high sustained tensile stress exceeding 50 percent of the minimum specified yield strength produced by any combination of sources including heat treatment straightening, forming, fit-up, and sustained service loads.
C	Intermediate. SCC not anticipated if the total sustained tensile stress is less than 25 percent of the minimum specified yield strength. This rating is designed for the short transverse direction in improved products used primarily for high resistance to exfoliation corrosion in relatively thin structures where appreciable short transverse stresses are unlikely.
D	Low. SCC failures have occurred in service or would be anticipated if there is any sustained tensile stress in the designated test direction. This rating currently is designated only for the short transverse direction in certain materials.

Note: The stress levels mentioned above are not to be interpreted as "threshold" stresses, and are not recommended for design. Other documents, such as MIL-HDBK-5, MIL-STD-1568, NASC-SD-24, and MSFC-SPEC-522A should be consulted for design recommendations.

(1) Rating is not established because the product is not offered commercially.
(2) Rating is one class lower for thicker sections: extrusions, 1-inch (25 mm) and over; plate and forgings, 1.5-inch (40 mm) and over.

TABLE 2.034. ASTM G 64 CLASSIFICATION OF RESISTANCE TO STRESS-CORROSION CRACKING OF 7050 AND 7075 (37)

Alloy	7050-T7451 (ST Direction)															
Form	Plate															
Thickness	2-inch (F_{ty} = 61 ksi) 0.07 Fe, 0.06 Si									3-inch (F_{ty} = 59 ksi) 0.11 Fe, 0.06 Si						
Exposure[a]	Sea Coast[b]			AI[c] 3.5 percent NaCl			AI[d] Seawater			Sea Coast[b]			AI[c] 3.5 percent NaCl		AI[d] Seawater	
Stress, ksi	31	46	61	31	46	51	31	46	51	26	39	50	39	50	39	50
Number Exposed	8	8	8	3	3	3	3	3	3	8	8	8	3	3	3	3
Number Failed	0	0	2	0	2	3	0	0	0	0	1	0	2	3	0	0
Failure Time Range, days	–	–	840 to 1020	–	87	87	–	–	–	–	810	–	54 to 63	54 to 78	–	–

(a) Test discontinued after 1,140 days.
(b) 120 to 130 ft from MCAN high tide at Kennedy Space Center.
(c) Alternate immersion (AI) – Method 823 (Fed. Std. 1516) is essentially the same as ASTM G44.
(d) Alternate immersion in ASTM 0114-52 synthetic seawater using Method 823.

TABLE 2.035. RESULTS OF STRESS CORROSION TESTS FOR THE ST DIRECTION OF 7050-T7451 (-T73651) PLATE IN SEVERAL ENVIRONMENTS (31)

Al
6.2 Zn
2.25 Mg
2.3 Cu
0.12 Zr

7050 Al

	Al
6.2	Zn
2.25	Mg
2.3	Cu
0.12	Zr

7050 Al

Alloy	7050-T7351 (0.06 to 0.08 Fe, 0.03 to 0.06 Si)					
Form	Plate					
Exposure	Alternate Immersion 3.5 percent NaCl (ASTM G44-75)					
Thickness	ST Direction					
	4-inch (F_{ty} = 60 ksi)		5-inch (F_{ty} = 59 ksi)		6-inch (F_{ty} = 57 ksi)	
Stress, ksi	30 to 31	46	29 to 30	43 to 44	29	43
Number Exposed	6	6	6	6	6	6
Number Failed	0	0	0	1	0	1
Failure Time Range, days	–	–	–	84	–	64
Survival(a) Time, days	84	84	84	84	84	84

(a) Test discontinued at 84 days.

TABLE 2.036. RESULTS OF ALTERNATE IMMERSION TESTS IN 3.5 PERCENT NaCl SOLUTION ON SHORT TRANSVERSE SPECIMENS OF 7050-T7351 PLATE (20)

Alloy	7050-T7451							
Thickness	1.25-inch Plate				3-inch Plate			
Tensile Strengths	LT F_{tu} = 78 ksi, F_{ty} = 69 ksi				LT F_{tu} = 73 ksi, F_{ty} = 62 ksi			
Fracture Toughness	LT K_{Ic} = 29 ksi$\sqrt{in.}$, SL K_{Ic} = 24.3 ksi$\sqrt{in.}$				LT K_{Ic} = 24.8 ksi$\sqrt{in.}$, SL K_{Ic} = 25.4 ksi$\sqrt{in.}$			
Applied Stress, ksi ST Direction	25	35	45	55	25	35	45	55
Max Exposure(a) 54 months (1,620 days)	3/0	3/0	3/3 All in 9 months	3/3 3.4 months 5 months 11 months	3/0	3/0	3/0	3/1 19 months

(a) Number exposed/number failed in months indicated; specimens were 0.125-inch in diameter.

TABLE 2.037. STRESS CORROSION RESULTS FOR 7050-T7451 (-T73651) PLATE EXPOSED TO A MARINE ENVIRONMENT AT DAYTONA BEACH (17)

Alloy	7050-T7351			
Form	Plate SL Direction			
Thickness	2-inch	4-inch	6-inch (Lot 1)	6-inch (Lot 2)
Average Crack Velocity Over 15 days, 10^{-4} in./hr	1.19	2.4	0.29	4.5
K_I at 15 day, ksi$\sqrt{in.}$	28	25.5	25	20

Note: Bolt loaded double cantilever beam: B = 1-inch, 2H = 1-inch, W = 5-inch, 24 < K_{Ij} < 31 ksi$\sqrt{in.}$, 3.5 percent NaCl solution drops in notch, three times per day (Monday through Friday) once per day on Saturday and Sunday.

TABLE 2.038. AVERAGE CRACK VELOCITIES FOR VARIOUS THICKNESSES OF 7050-T7351 PLATE EXPOSED TO 3.5 PERCENT NaCl SOLUTION WITH CRACKS IN SL DIRECTION (20)

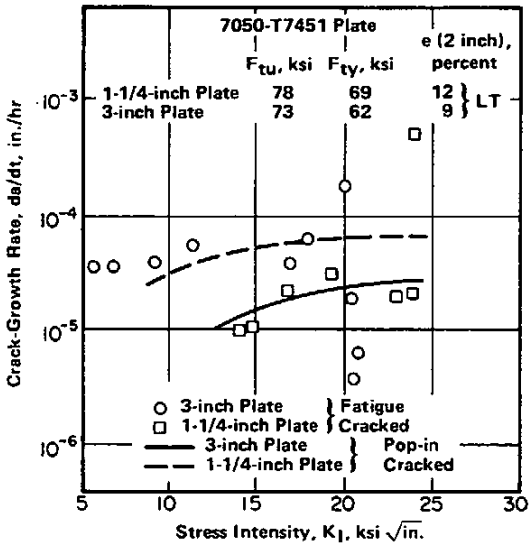


FIGURE 2.039. CRACK-GROWTH RATES IN SL ORIENTATION AS A FUNCTION OF STRESS INTENSITY FOR 7050-T7451 (-T73651) PLATE EXPOSED TO A MARINE ATMOSPHERE AT DAYTONA BEACH (17)

Al
6.2 Zn
2.25 Mg
2.3 Cu
0.12 Zr

7050 Al

Alloy	7050-T7451 (L and T F_{tu} = 75.4 ksi, F_{ty} = 66.8 ksi)					
Test Type[a]	Alternate Immersion[b] 3.5 percent NaCl (pH ~6) 1 hr in Solution + 11 hr Out (RT)			Periodic Moistening[b] Twice per Day with 3.5 percent NaCl (pH ~6) (RT)		
Location of Specimen	Surface	Center	Surface	Surface	Center	Surface
Crack Growth, inch	0.067	0.055	0.11	0.051	0.051	0.094
Mean da/dt[c], in./hr x 10^{-4}	0.14	0.12	0.23	0.10	0.10	0.19
Percent Residual Displacement[d]	24	24	27	25	23	27

(a) SL, DB (My) specimen, bolt loaded: 2H = 0.67-inch, W = 3.5-inch, A_o ~ 1.46-inch, fatigue cracked to K_i ~ 24 ksi$\sqrt{in}$.
(b) Total exposure 202 days.
(c) More than 202 days.
(d) Displacement after unloading due to corrosion product wedging.

TABLE 2.0310. CRACK GROWTH RESULTS FOR 7050-T7451 (-T73651) PLATE IN 3.5 PERCENT NaCl SOLUTION (15)

Alloy	7050					
Form	Extrusions (See Table 3.02113)					
Exposure	Alternate Immersion in 3.5 percent NaCl (ASTM G44-75)					
Condition	ST Direction					
	T7351 ($\bar{X}$ST F_{ty} = 62.8 ksi, S = 1.74 ksi)			T7651 ($\bar{X}$ST F_{ty} = 68.9 ksi, S = 1.84 ksi)		
Stress, ksi	52	45	35	35	25	15
Number Exposed	15	39	24	15	32	12
Number Failed	15	35	23	11	18	1
Failure Time Range, days	7 to 84	19 to 84	28 to 84	3 to 7	10 to 84	69
Survival Time, days[a]	–	84	84	84	84	84

(a) Test discontinued at 84 days.

TABLE 2.0311. RESULTS OF ALTERNATE IMMERSION TESTS IN 3.5 PERCENT NaCl SOLUTION ON SHORT TRANSVERSE SPECIMENS OF 7050-T7651 AND -T7351 EXTRUSIONS (19)

Alloy	7050			
Form	Extrusions (See Table 3.02113)			
Condition	T7651 ($\bar{X}$ST F_{ty} = 68.9 ksi, S = 1.84 ksi)[a]			
Exposure[b]	Sea Coast Atmosphere		Industrial Atmosphere	
Stress, ksi[c]	35	25	35	25
Number Exposed	15	23	15	24
Number Failed	13	5	2	1
Failure Time Range, days	75 to 401	75 to 231	1097	1140
Survival Time Range, days	681 to 1304	385 to 1304	705 to 1335	432 to 1335

(a) Based on F_{ty} of all shapes.
(b) Sea coast – Point Judith, R.I., and industrial – Alcoa Center, Pa.
(c) Tensile bars, 0.125-inch, stressed in constant strain fixtures in ST direction.

TABLE 2.0312. RESULTS OF STRESS CORROSION TESTS ON SHORT TRANSVERSE SPECIMENS OF 7050-T7651 EXTRUSIONS (19)

	Al
6.2	Zn
2.25	Mg
2.3	Cu
0.12	Zr

7050 Al

Alloy	7050					
Form	Extrusions (See Table 3.02113)					
Condition	T7351 ($\bar{X}$ST F_{ty} = 62.8 ksi, S = 1.74 ksi)(a)					
Exposure(b)	Sea Coast Atmosphere			Industrial Atmosphere		
Stress, ksi(c)	52	45	35	52	45	35
Number Exposed	18	33	24	18	30	27
Number Failed	9	7	1	2	0	0
Failure Time, Range, days	102 to 527	71 to 276	198	426 to 431	–	–
Survival Time Range, days	385 to 681	283 to 681	283 to 385	432 to 694	362 to 694	362 to 432

(a) Based on F_{ty} of all shapes.
(b) Sea coast – Point Judith, R.I., and industrial – Alcoa Center, Pa.
(c) Tensile bars, 0.125-inch, stressed in constant strain fixtures in ST direction.

TABLE 2.0313. RESULTS OF STRESS CORROSION TESTS ON SHORT TRANSVERSE SPECIMENS OF 7050-T7351 EXTRUSIONS (19)

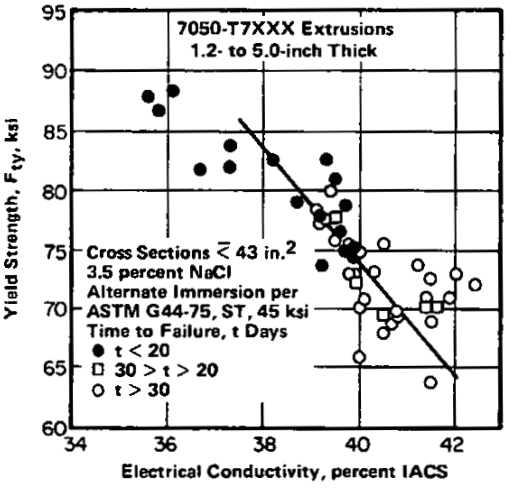


FIGURE 2.0314. STRESS CORROSION PERFORMANCE AS A FUNCTION OF ELECTRICAL CONDUCTIVITY FOR 7050 EXTRUSIONS STRESSED TO 45 PERCENT F_{ty} IN THE ST DIRECTION (19)

Alloy	7050								
Form	Extrusions								
Condition	T7651 ($\bar{X}$ST F_{ty} = 68.9 ksi, S = 1.84)						T7351 ($\bar{X}$ST F_{ty} = 62.8 ksi, S = 1.74)		
Section Size, inch	3 x 18		5 x 6-1/4				3 x 18		
K_{Ic}, ksi$\sqrt{in.}$	19		18				20		
K_i, percent K_{Ic}(a)	65	40	80	70	60	50	90	80	75
Test Time, hr(b)	566	>2304	120	540	822	2820	198	>2172	>3082
Crack Growth,(c) 10^{-4}-inch	1250	1160	770	2500	3030	3710	1370	670	1420
K_{If}, ksi$\sqrt{in.}$(c)	19	10	17	19	22	20	23	18	20

(a) Ring loaded C(T) specimens, SL orientation: B = 1-inch, W/B ~3; K_i based on load and crack mouth displacement.
(b) Time to failure on 0.3 M NaCl, pH = 4.
(c) Based on load and crack mouth displacement, monitored every 8 hr.

TABLE 2.0315. FAILURE TIMES OF C(T) SL SPECIMENS FROM 7050-T7651 AND -T7351 EXTRUSIONS SUBJECTED TO VARIOUS INITIAL STRESS INTENSITY (K_i) LEVELS IN A SALT-DICHROMATE SOLUTION (19)

Alloy	7050(a)			
Form	Extrusions SL Direction			
Condition	T7651		T7351	
Extrusion(b) Cross Section, in.^{2}	<43	61 to 66	<43	61 to 66
Initial K_i, ksi$\sqrt{in.}$	18 to 24	19 to 26	24 to 25	22 to 28
Average Crack Velocity, 10^{-4} in./hr				
in 15 days	6.6	6.6	4.4	3.4
in 30 days	4.7	5.5	2.56	2.4

(a) See note under Table 2.038 for specimen and exposure conditions.
(b) Various extruded shapes, 1.8- to 5-inch thickness.

TABLE 2.0316. AVERAGE CRACK VELOCITIES IN 3.5 PERCENT NaCl SOLUTION FOR VARIOUS EXTRUDED SHAPES OF 7050-T7651 AND -T7351 TESTED IN SL DIRECTION (19)

Al
6.2 Zn
2.25 Mg
2.3 Cu
0.12 Zr

7050 Al

Alloy	7050-T76		
Form	Extruded Bar		
Condition	3/16-inch Holes in ST Direction Without and With Interference Fit Fastners of Al and Ti		
Exposure	Alternate Immersion 3.5 percent NaCl, 10 min. Immersion + 50 min. Air at 34 percent F_{ty}		
Interference, inch	0.033 to 0.005	0.002	0.0005
Evidence for SCC in 60 Days	Cracks	Incipient Cracks	No Cracks

TABLE 2.0317. EFFECT OF INTERFERENCE FIT ON STRESS-CORROSION CRACKING OF FASTNER HOLES IN 7050-T76 EXTRUSION (26)

Alloy	7050-T73651 (-T7451)						
Form	Die Forgings						
Direction	L				T		
	Axis of Specimen <15° from Forging Flow Lines				Axis of Specimen >15° from Forging Flow Lines		
Thickness, t, inch	$t \leq 2$	$2 < t \leq 4$	$4 < t \leq 5$	$5 < t \leq 6$	$t \leq 2$	$2 < t \leq 4$	$4 < t \leq 6$
F_{tu}, ksi	72	71	70	70	68	67	66
F_{ty}, ksi	62	61	60	59	56	55	54
e (2-inch or 4D), percent	7	7	7	7	5	4	3

TABLE 3.011. AMS SPECIFIED MINIMUM TENSILE PROPERTIES FOR 7050-T73651 (-T7451) DIE FORGINGS (2)

Alloy	7050				
Form	Plate		Extrusions		
Condition	T7651		T76511	T73511	T736511 (T7451)
Thickness, inch	0.25 to 2.500		N/A	N/A	N/A
Direction	L	LT	L	L	L
F_{tu}, ksi	76	76	79	70	73
F_{ty}, ksi	66	66	69	60	63
e (2-inch or 4D), percent	8	6	7	8	7

TABLE 3.012. AMS SPECIFIED TENSILE PROPERTIES FOR 7050-T7651 PLATE (21) AND 7050-T76511, -T73511, AND T736511 (-T7451) EXTRUSIONS (22-24)

Alloy	7050-T73651 (-T7451)		
Form	2- to 6-inch Thick Plate		
Direction	LT	TL	SL
K_{Ic}, ksi$\sqrt{in.}$	24	22	20

TABLE 3.013. AMS SPECIFIED MINIMUM FRACTURE TOUGHNESS PROPERTIES FOR 7050-T73651 (-T7451) PLATE (1)

	Al
6.2	Zn
2.25	Mg
2.3	Cu
0.12	Zr

7050 Al

Alloy	7050													
Form	Condition	Thickness, inch	Direction	F_{tu} (Min), ksi	F_{ty}, ksi Min	F_{ty}, ksi Max	e (Min), percent	SCC[a] Stress, % F_{ty}	SCC[a] Stress, ksi	Exfoliation[b] Corrosion, EXCO	Exfoliation[b] Corrosion, Plane	K_{Ic} (Min), ksi$\sqrt{in.}$[c] L-T	K_{Ic} (Min), ksi$\sqrt{in.}$[c] T-L	K_{Ic} (Min), ksi$\sqrt{in.}$[c] S-L
Plate	T7651	0.250 to 1.000	LT	76.0	66.0	–	8	–	20	<EB	t/10	26	24	–
		1.001 to 1.500	LT	77.0	67.0	–	8	–	20	<EB	t/10	26	24	20
		1.501 to 2.000	LT	76.0	66.0	–	8	–	20	<EB	t/10	26	24	20
		2.001 to 3.000	LT	76.0	66.0	–	7	–	20	<EB	t/10	24	23	20
	T7451	0.250 to 2.000	LT	74.0	64.0	–	9	50	–	<EB	Any	29	25	–
		2.001 to 3.000	LT	73.0	63.0	–	8	50	–	<EB	Any	27	24	21
		3.001 to 4.000	LT	72.0	62.0	–	6	–	35	<EB	Any	26	23	21
		4.001 to 5.000	LT	71.0	61.0	–	5	–	35	<EB	Any	25	22	21
		5.001 to 6.000	LT	70.0	60.0	–	4	–	35	<EB	Any	24	22	21
Die Forgings	T74	Up to 2.000	(d)	72.0	62.0	72.0	7	50	–	–	–	–	–	–
		2.001 to 4.000	(d)	71.0	61.0	72.0	7	50	–	–	–	–	–	–
		4.001 to 5.000	(d)	70.0	60.0	72.0	7	50	–	–	–	–	–	–
		5.001 to 6.000	(d)	70.0	59.0	72.0	7	50	–	–	–	–	–	–
		0.700 to 0.350	–	–	–	–	–	–	–	–	–	27	19	19
		3.501 to 7.000	–	–	–	–	–	–	–	–	–	25	19	19
Hand Forgings	T7452	Up to 2.000	L	72.0	63.0	–	9	50	–	–	–	–	–	–
		2.001 to 3.000	L	72.0	62.0	–	9	50	–	–	–	–	–	–
		3.001 to 4.000	L	71.0	61.0	–	9	–	35	–	–	–	–	–
		4.001 to 5.000	L	70.0	60.0	–	9	–	35	–	–	–	–	–
		5.001 to 6.000	L	69.0	59.0	–	9	–	35	–	–	–	–	–
		6.001 to 7.000	L	68.0	58.0	–	9	–	35	–	–	–	–	–
		7.001 to 8.000	L	67.0	57.0	–	9	–	35	–	–	–	–	–
		0.700 to 0.350	–	–	–	–	–	–	–	–	–	27	17	16
		3.501 to 7.000	–	–	–	–	–	–	–	–	–	25	17	16
Extrusions	T7651X	0.250 to 5.000	L	79.0	69.0	–	7	25	–	<EB	t/1	–	–	–
	T7451X	0.250 to 3.000	L	73.0	63.0	–	7	50	–	<EB	Any	–	–	–
		3.001 to 5.000	L	73.0	63.0	–	7	–	35	<EB	Any	–	–	–
	T7351X	0.250 to 5.000	L	70.0	60.0	–	8	75	–	–	–	–	–	–
		0.250 to 5.000	L	70.0	60.0	69.0	8	75	–	–	–	–	–	–

(a) ASTM G47-79, 20-day survival.
(b) ASTM G34-79.
(c) ASTM E399 and B645. Lower thickness limit for a valid K_{Ic} is 0.5-inch (12.7 mm); S-L specimens require thickness of at least 1.2-inch (30.5 mm).
(d) Parallel to direction of grain flow.

TABLE 3.014. PRODUCER'S GUARANTEED MINIMUM PROPERTIES AND CAPABILITIES FOR 7050 PLATE, FORGINGS AND EXTRUSIONS (37)

	Al
6.2	Zn
2.25	Mg
2.3	Cu
0.12	Zr

7050 Al

Alloy		7050-T7651				
Form		Plate				
Thickness, t, inch		0.25 < t ⩽ 0.50	0.5 < t ⩽ 1.0	1.0 < t ⩽ 1.5	1.5 < t ⩽ 2.0	2.0 < t ⩽ 3.0
Basis(a)		S	S	A	A	S
F_{tu}, ksi	L	76	76	77	76	76
	LT	76	76	77	76	76
	ST	–	–	–	–	70
F_{ty}, ksi	L	66	66	67	66	66
	LT	66	66	67	66	66
	ST	–	–	–	–	60
F_{cy}, ksi	L	64	64	65	64	64
	LT	68	68	69	69	69
	ST	–	–	–	–	68
F_{su}, ksi		44	43	42	46	47
F_{bru}, ksi	e/D = 1.5	112	111	111	115	116
	e/D = 2.0	143	142	141	147	149
F_{bry}, ksi	e/D = 1.5	91	88	87	92	95
	e/D = 2.0	105	103	101	105	109
e, percent	L	9	9	9	9	8
	LT	8	8	8	8	7
	ST	–	–	–	–	1.5
E, 10^3 ksi		10.3				
E_c, 10^3 ksi		10.8				
G, 10^3 ksi		4.0				
Poission's Ratio		0.33				

(a) S = specification properties and A = statistical property values after MIL-HBBK-5.

TABLE 3.015. PRODUCER'S PROPOSED DESIGN MECHANICAL PROPERTIES FOR 7050-T7651 PLATE (37)

Alloy		7050-T7451 (-T73651)					
Form		Plate					
Thickness, t, inch		0.25 ⩽ t < 1.5	1.5 < t ⩽ 2.0	2.0 < t ⩽ 3.0	3.0 < t ⩽ 4.0	4.0 < t ⩽ 5.0	5.0 < t ⩽ 6.0
Basis(a)		A	A	A	A	A	A
F_{tu}, ksi	L	74	74	73	72	71	70
	LT	74	74	73	72	71	70
	ST	–	–	68	68	67	67
F_{ty}, ksi	L	64	64	63	62	61	60
	LT	64	64	63	62	61	60
	ST	–	–	59	58	57	57
F_{cy}, ksi	L	63	62	61	60	58	57
	LT	66	67	66	65	64	63
	ST	–	–	63	63	63	62
F_{su}, ksi		42	44	44	44	43	43
F_{bru}, ksi	e/D = 1.5	105	113	112	110	108	107
	e/D = 2.0	140	145	143	141	139	137
F_{bry}, ksi	e/D = 1.5	86	92	91	91	91	91
	e/D = 2.0	101	103	103	104	105	105
e, percent	L	10	10	9	9	9	8
	LT	9	9	8	6	5	4
	ST	–	–	2	2	2	2
E, 10^3 ksi		10.3					
E_c, 10^3 ksi		10.6					
G, 10^3 ksi		3.9					
Poisson's Ratio		0.33					

(a) A = statistical property values after MIL-HDBK-5.

TABLE 3.016. PRODUCER'S PROPOSED DESIGN MECHANICAL PROPERTIES FOR 7050-T7451 PLATE (25)

Al
6.2 Zn
2.25 Mg
2.3 Cu
0.12 Zr

7050 Al

Alloy		7050						
Form		Sheet			7108-Clad Sheet		7072-Clad Sheet	
Temper		T76			T76		T76	
Thickness, inch		0.040 to 0.089	0.090 to 0.187	0.188 to 0.249	0.040 to 0.089	0.090 to 0.249	0.040 to 0.089	0.090 to 0.249
F_{tu}, ksi	L	76	76	76	75	74	–	–
	LT	77	77	77	75	75	72	73
F_{ty}, ksi	L	67	67	67	65	65	–	–
	LT	67	67	67	65	65	61	62
F_{cy}, ksi	L	66	67	68	64	64	–	–
	LT	71	71	71	67	67	–	–
F_{su}, ksi		46	45	45	45	45	–	–
F_{bru}, ksi	e/D = 1.5	118	118	118	114	114	–	–
	e/D = 2.0	152	152	152	148	148	–	–
F_{bry}, ksi	e/D = 1.5	93	93	93	92	92	–	–
	e/D = 2.0	106	106	106	106	106	–	–
e, percent	L	–	–	–	–	–	–	–
	LT	7	7	7	7	7	7	7
E, 10^3 ksi		10.2			10.2		–	
E_c, 10^3 ksi		10.6			10.6		–	
G, 10^3 ksi		3.9			3.9		–	
Poisson's Ratio		0.33			0.33		–	

TABLE 3.017. PRODUCER'S TENTATIVE MECHANICAL PROPERTIES FOR BARE AND CLAD 7050-T76 SHEET (37)

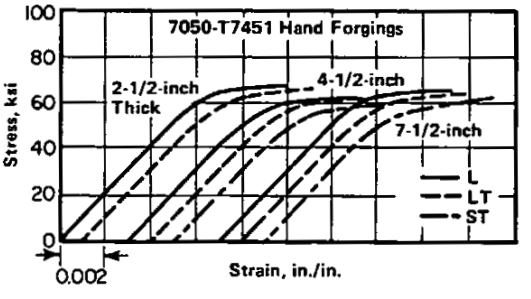


FIGURE 3.0211. TENSILE STRESS-STRAIN CURVES FOR 7050-T7451 (-T73651) HAND FORGINGS (4)

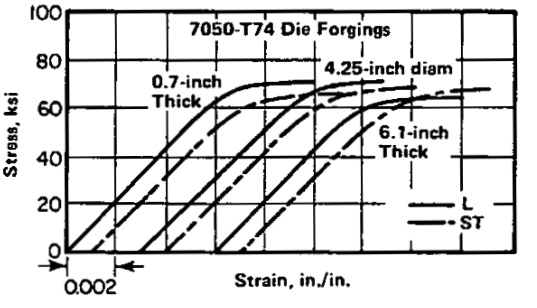


FIGURE 3.0212. TENSILE STRESS-STRAIN CURVES FOR 7050-T74 (-T736) DIE FORGINGS (4)

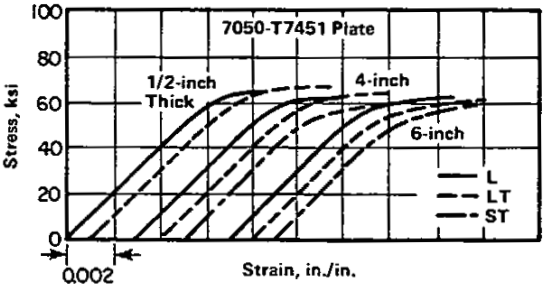


FIGURE 3.0213. TENSILE STRESS-STRAIN CURVES FOR 7050-T7451 (-T73651) PLATE (4)

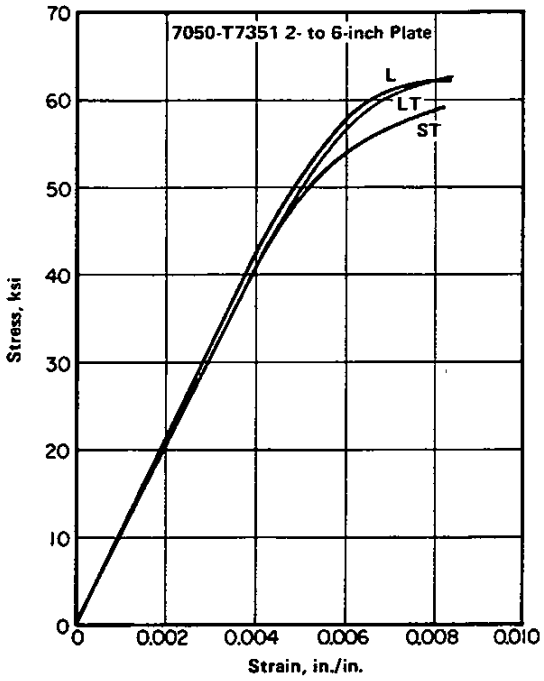
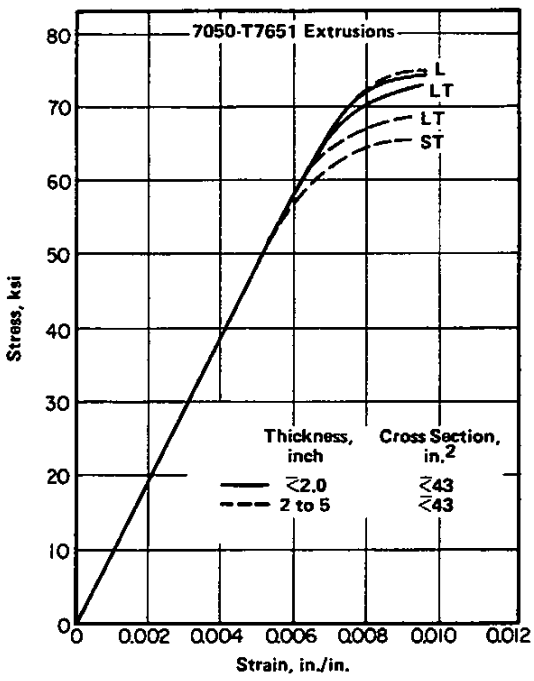


FIGURE 3.0214. TENSILE STRESS-STRAIN CURVES FOR 7050-T7351 PLATE (20)



	Al
6.2	Zn
2.25	Mg
2.3	Cu
0.12	Zr

7050 Al

FIGURE 3.0215. TENSILE STRESS-STRAIN CURVES FOR 7050-T7651 EXTRUSIONS OF SEVERAL THICKNESSES (19)

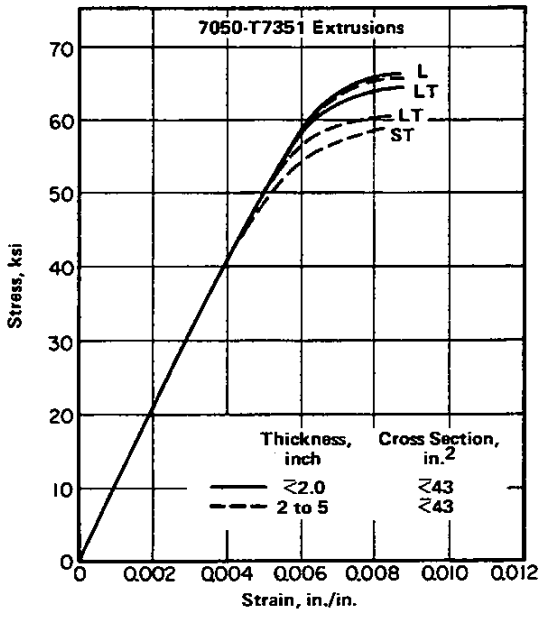


FIGURE 3.0216. TENSILE STRESS-STRAIN CURVES FOR 7050-T7351 EXTRUSIONS OF SEVERAL THICKNESSES (19)

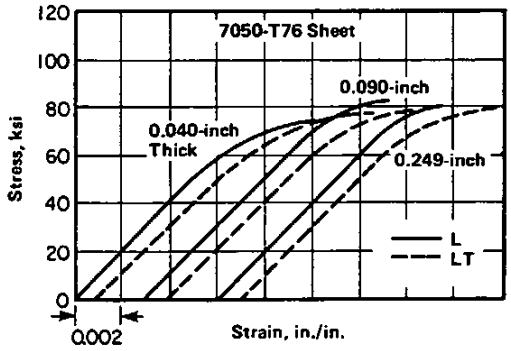


FIGURE 3.0217. TENSILE STRESS-STRAIN CURVES FOR 7050-T76 SHEET (4)

	Al
6.2	Zn
2.25	Mg
2.3	Cu
0.12	Zr

7050 Al

Alloy	7050-T7451			
Form	Hand Forgings			
Size, inch	Direction	F_{tu}, ksi	F_{ty}, ksi	e (2 inch), percent
2 x 8 x 72	L	79.3	72.6	9.5
	LT	78.0	71.3	6.5
	ST	78.7	67.6	4.7
2-1/2 x 22 x 60	L	76.7	67.3	10.5
	LT	75.9	65.5	13.0
	ST	74.3	61.3	10.0
3-1/2 x 14 x 72	L	71.6	61.1	13.5
	LT	70.1	60.2	8.8
	ST	67.9	56.5	4.3
4-1/2 x 22 x 84	L	72.6	62.6	12.5
	LT	70.6	59.8	10.0
	ST	70.6	59.2	7.5
5-1/2 x 22 x 60	L	73.3	64.4	11.5
	LT	71.6	64.4	6.0
	ST	70.4	59.6	4.8
7-1/2 x 22 x 42	L	72.2	61.4	13.2
	LT	71.0	60.8	5.5
	ST	70.2	58.0	5.5

TABLE 3.0218. TENSILE PROPERTIES OF 7050-T7451 (-T73651) HAND FORGINGS OF VARIOUS SIZES

Alloy	7050-T736			
Form	Die Forgings			
Thickness, inch	Direction	F_{tu}, ksi	F_{ty}, ksi	e (2 inch), percent
Up to 2.000	L	77.9	70.4	13.0
	ST	74.5	66.1	7.6
2.001 to 4.000	L	75.6	67.4	13.0
	LT	70.6	63.6	6.0
4.001 to 5.000	L	76.5	69.2	13.0
	ST	73.1	65.2	6.0
5.001 to 6.000	L	74.4	65.8	9.8
	ST	73.5	67.1	5.0

TABLE 3.0219. TENSILE PROPERTIES OF 7050-T74 (-T736) DIE FORGINGS OF VARIOUS SIZES (4)

Alloy	7050-T7351														
Form	Plate														
Thickness(a)	2-inch			3-inch			4-inch			5-inch			6-inch		
Direction	L	LT	ST	L	LT	ST	L	LT	ST	L	LT	ST	L	LT	ST
F_{tu}, ksi	71	72	69	73	74	72	73	74	72	72	73	70	70	72	68
F_{ty}, ksi	61	61	55	64	64	61	64	63	59	63	62	59	61	60	57
e (4D), percent	14	12	8	12	11	6.5	11	10	6.8	11	10	6.6	11	10	5.1
RA, percent	34	27	14	29	20	12	27	16	10	23	15	9	20	14	7

(a) Average of single tests on each plate from two lots.

TABLE 3.02110. TENSILE PROPERTIES OF 7050-T7351 PLATE OF VARIOUS THICKNESSES (20)

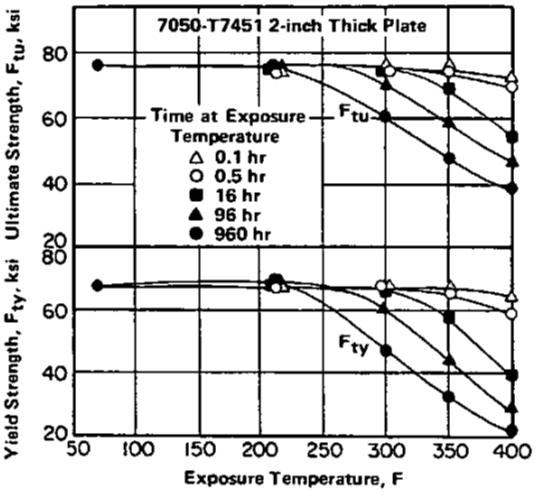


FIGURE 3.02111. EFFECTS OF EXPOSURES TO ELEVATED TEMPERATURES ON TENSILE ULTIMATE AND YIELD STRENGTHS OF 7050-T7451 (-T73651) PLATE (8)

Alloy	7050-T7451				
Form	Thickness, inch	Direction	F_{tu}, ksi	F_{ty}, ksi	e (2 inch), percent
Plate	0.250 to 2.000	L	76.3	66.9	13.8
		LT	76.3	66.7	12.8
Plate	4.000	L	73.0	64.4	11.5
		LT	74.5	63.8	10.5
		ST	71.4	60.3	6.8
Plate	6.000	L	71.4	62.6	9.2
		LT	71.8	60.5	6.8
		ST	68.2	58.1	4.2

Al
6.2 Zn
2.25 Mg
2.3 Cu
0.12 Zr

7050 Al

TABLE 3.02112. TENSILE PROPERTIES OF 7050-T7451 (-T73651) PLATE OF VARIOUS THICKNESSES (4)

Alloy	7050-T7651							
Form	Extrusions							
Thickness, inch	0.187 to 1.2(a)		1.5 to 2.9(b)			3.5 to 5.0(c)		
Direction	L	LT	L	LT	ST	L	LT	ST
F_{tu}, ksi	83	83	82	80	78	86	81	11
F_{ty}, ksi	75	74	75	73	68	78	72	5
e (4D), percent	13	12	13	10	6	77	70	3

(a)-Seven extrusions, 5 to 29 $in.^2$ cross section.
(b)-Five extrusions, 11 to 65 $in.^2$ cross section.
(c)- Three extrusions, 26 to 32 $in.^2$ cross section.

TABLE 3.02113. TENSILE PROPERTIES OF 7050-T7651 EXTRUSIONS OF VARIOUS THICKNESSES AND CROSS SECTIONS (19)

Alloy	7050-T7351							
Form	Extrusions							
Thickness, inch	0.67 to 1.2(a)		1.5 to 2.9(b)			3.5 to 5.0(c)		
Direction	L	LT	L	LT	ST	L	LT	ST
F_{tu}, ksi	78	77	76	76	74	80	74	75
F_{ty}, ksi	69	68	68	67	63	72	66	64
e (4D), percent	14	11	13	12	6.5	11	8	7.5

(a) Four extrusions, 14 to 29 $in.^2$ cross section.
(b) Nine extrusions, 11 to 65 $in.^2$ cross section.
(c) Two extrusions, 26 and 31 $in.^2$ cross sections.

TABLE 3.02114. TENSILE PROPERTIES OF 7050-T7351 EXTRUSIONS OF VARIOUS THICKNESSES AND CROSS SECTIONS (19)

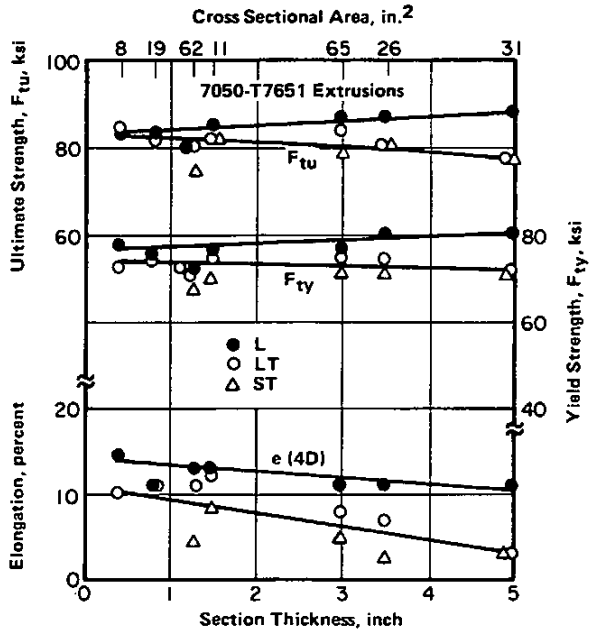


FIGURE 3.02115. EFFECT OF SECTION THICKNESS ON TENSILE PROPERTIES OF 7050-T7651 EXTRUSIONS OF VARIOUS CROSS SECTIONS (19)

	Al
6.2	Zn
2.25	Mg
2.3	Cu
0.12	Zr

7050 Al

Alloy	7050-T6511											
Form	Extrusions											
Direction	L				T				ST			
Extrusion[a]	W	Y	Z	S	W	Y	Z	S	W	Y	Z	S
F_{tu}, ksi	84	87	88	85	78	82	82	82	78	80	81	82
F_{ty}, ksi	71	79	82	78	76	75	75	75	69	73	71	71
e, percent	11	13	12	14	10	13	9	12	5	9	7	10

(a) See Figure 3.027.

TABLE 3.02116. TENSILE PROPERTIES OF VARIOUS EXTRUDED SHAPES IN THE T6511 CONDITION (18)

Alloy	7050-T76			
Form	Sheet			
Thickness, inch	Direction	F_{tu}, ksi	F_{ty}, ksi	e (2 inch), percent
0.040 to 0.249	L	82.1	76.5	10.7
	LT	82.5	76.3	10.9

TABLE 3.02117. TENSILE PROPERTIES OF 7050-T76 SHEET (4)

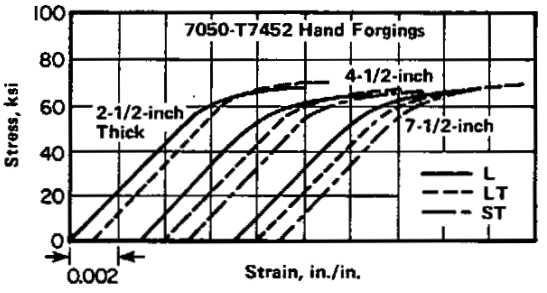


FIGURE 3.0221. COMPRESSIVE STRESS-STRAIN CURVES FOR 7050-T7452 (-T73652) HAND FORGINGS (4)

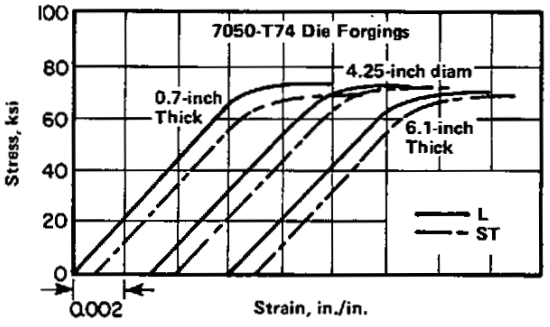


FIGURE 3.0222. COMPRESSIVE STRESS-STRAIN CURVES FOR 7050-T74 (-T736) DIE FORGINGS (4)

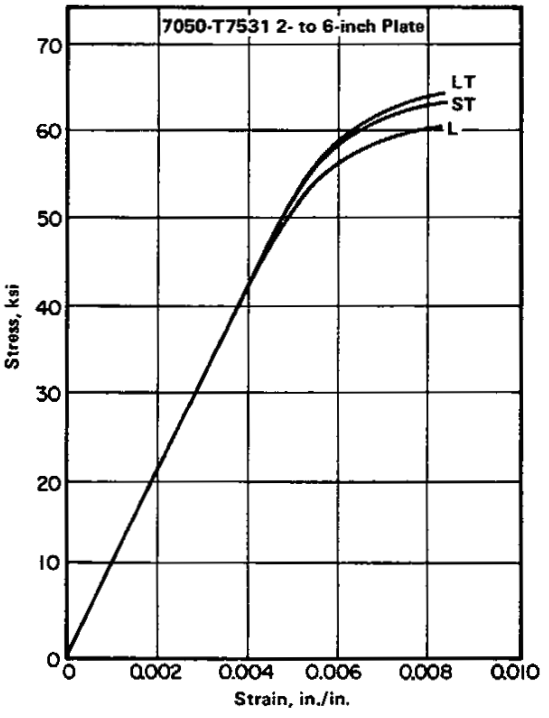


FIGURE 3.0223. COMPRESSIVE STRESS-STRAIN CURVES FOR 7050-T7351 PLATE (20)

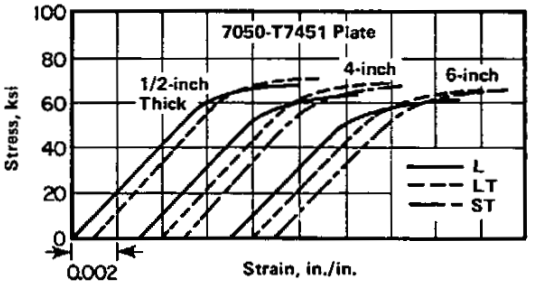


FIGURE 3.0224. COMPRESSIVE STRESS-STRAIN CURVES FOR 7050-T7451 (-T73651) PLATE (4)

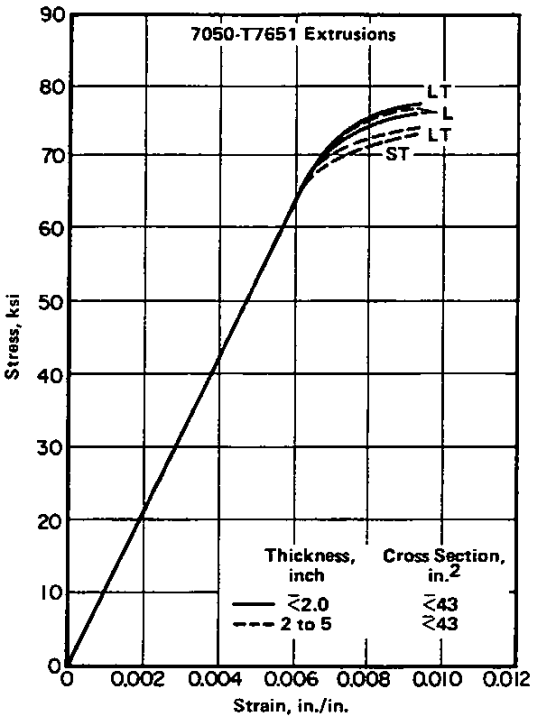


FIGURE 3.0225. COMPRESSIVE STRESS-STRAIN CURVES FOR 7050-T7651 EXTRUSIONS OF SEVERAL THICKNESSES (19)

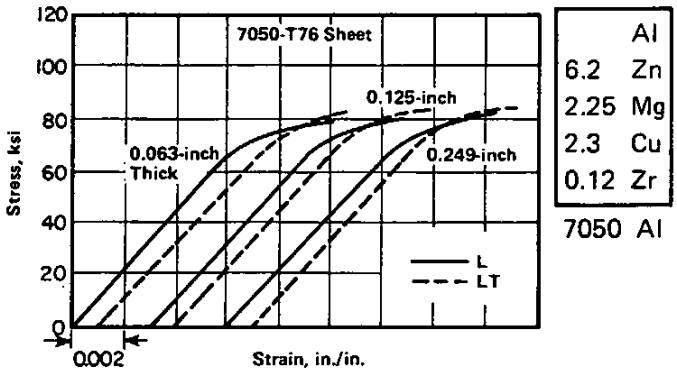


FIGURE 3.0226. COMPRESSIVE STRESS-STRAIN CURVES FOR 7050-T76 SHEET (4)

Alloy	7050-T74	
Form	Die Forgings	
Thickness, inch	Orientation	F_{cy}, ksi
Up to 2.000	L	74.5
	ST	69.8
2.000 to 4.000	L	72.8
	ST	67.8
4.000 to 5.000	L	72.7
	ST	68.1
5.001 to 6.000	L	71.8
	ST	67.9

TABLE 3.0228. COMPRESSIVE YIELD STRENGTH OF 7050-T74 (-T736) DIE FORGINGS OF VARIOUS THICKNESSES (4)

Alloy	7050-T7452	
Form	Hand Forgings	
Size, inch	Orientation	F_{cy}, ksi
2 x 8 x 72	L	77.0
	LT	76.4
	ST	79.2
2-1/2 x 22 x 60	L	67.2
	LT	69.0
	ST	68.5
3-1/2 x 14 x 72	L	64.9
	LT	65.1
	ST	63.7
4-1/2 x 22 x 84	L	64.0
	LT	67.2
	ST	63.3
5-1/2 x 22 x 60	L	66.8
	LT	67.0
	ST	66.3
7-1/2 x 22 x 42	L	64.0
	LT	66.0
	ST	65.4

TABLE 3.0227. COMPRESSIVE YIELD STRENGTH OF 7050-T7452 (-T73652) HAND FORGINGS OF VARIOUS SIZES (14)

Alloy	7050-T7351																	
Form	Plate																	
Thickness[a]	2-inch			3-inch			4-inch			5-inch			6-inch					
Direction	L	LT	ST	L	LT	ST	L	LT	ST	L	LT	ST	L	LT	ST			
F_{cy}, ksi	59	63	62	61	66	65	61	66	64	60	65	63	57	63	61			

(a) Average of single tests on each plate from two lots.

TABLE 3.0229. COMPRESSIVE YIELD STRENGTH OF 7050-T7351 PLATE OF VARIOUS THICKNESSES (20)

	Al
6.2	Zn
2.25	Mg
2.3	Cu
0.12	Zr

7050 Al

Alloy	7050									
Form	Sheet		Plate							
Condition	T6		T7451							
Thickness, inch	0.040 to 0.25		0.25 to 2.0		4.0			6.0		
Direction	L	LT	L	LT	L	LT	ST	L	LT	ST
F_{cy}, ksi	77	81	66	69	62	68	67	59	65	65

TABLE 3.02210. COMPRESSIVE YIELD STRENGTH OF 7050-T6 SHEET AND 7050-T7451 (-T73651) PLATE OF VARIOUS THICKNESSES (4)

Alloy	7050-T7651								
Form	Extrusions								
Thickness, inch	0.187 to 1.2(a)		1.5 to 2.9(b)			3.5 to 6.0(c)			
Direction	L	LT	L	LT	ST	L	LT	ST	
F_{cy}, ksi	77	78	75	77	78	83	78	76	

(a) Seven extrusions, 5 to 29 in.^{2} cross section.
(b) Five extrusions, 11 to 65 in.^{2} cross section.
(c) Three extrusions, 26 to 32 in.^{2} cross section.

TABLE 3.02211. COMPRESSIVE YIELD STRENGTH OF 7050-T7651 EXTRUSIONS OF VARIOUS THICKNESSES AND CROSS SECTIONS (19)

Alloy	7050-T7351								
Form	Extrusions								
Thickness, inch	0.67 to 1.2(a)		1.5 to 2.9(b)			3.5 to 5.0(c)			
Direction	L	LT	L	LT	ST	L	LT	ST	
F_{cy}, ksi	69	71	68	70	71	74	69	69	

(a) Four extrusions, 14 to 29 in.^{2} cross section.
(b) Nine extrusions, 11 to 65 in.^{2} cross section.
(c) Two extrusions, 26 and 31 in.^{2} cross sections.

TABLE 3.02212. COMPRESSIVE YIELD STRENGTH OF 7050-T7351 EXTRUSIONS OF VARIOUS THICKNESSES AND CROSS SECTIONS (19)

Alloy	7050-T7452	
Form	Hand Forgings	
Size, inch	Orientation	F_{su}, ksi
2 x 8 x 72	L	48.2
	LT	47.0
	ST	47.5
2-1/2 x 22 x 60	L	43.5
	LT	43.5
	ST	42.4
3-1/2 x 14 x 72	L	42.3
	LT	41.9
	ST	42.1
4-1/2 x 22 x 84	L	42.9
	LT	42.2
	ST	41.5
5-1/2 x 22 x 60	L	43.9
	LT	43.9
	ST	42.0
7-1/2 x 22 x 42	L	43.4
	LT	42.8
	ST	41.5

TABLE 3.0251. SHEAR STRENGTH OF 7050-T7452 (-T73652) HAND FORGINGS (4)

Alloy	7050-T74	
Form	Die Forgings	
Thickness, inch	Orientation	F_{su}, ksi
Up to 2.000	L	47.4
	ST	47.0
2.001 to 4.000	L	44.6
	ST	41.0
4.001 to 5.000	L	46.3
	ST	44.6
5.001 to 6.000	L	47.5
	ST	44.4

TABLE 3.0252. SHEAR STRENGTH OF 7050-T74 (-T736) DIE FORGINGS (4)

Alloy	7050									
Form	Sheet				Plate					
Condition	T6				T7451					
Thickness, inch	0.040 to 0.25		0.25 to 2.0		4.0			6.0		
Direction	L	LT	L	LT	L	LT	ST	L	LT	ST
F_{su}, ksi	50	52	46	46	46	46	43	46	46	42

TABLE 3.0253. SHEAR STRENGTH OF 7050-T6 SHEET AND 7050-T7451 (-T73651) PLATE (4)

Alloy	7050-T7351														
Form	Plate														
Thickness(a)	2-inch			3-inch			4-inch			5-inch			6-inch		
Direction	L	LT	ST	L	LT	ST	L	LT	ST	L	LT	ST	L	LT	ST
F_{su}, ksi	44	43	–	45	45	43	46	45	42	45	45	42	44	44	41

(a) Average of single tests on each plate from two lots.

TABLE 3.0254. SHEAR STRENGTH OF 7050-T7351 PLATE (20)

Al
6.2 Zn
2.25 Mg
2.3 Cu
0.12 Zr

7050 Al

Alloy	7050-T7651							
Form	Extrusions							
Thickness, inch	0.187 to 1.2(a)		1.5 to 2.7(b)			3.5 to 5.0(c)		
Direction	L	LT	L	LT	ST	L	LT	ST
F_{su}, ksi	48	47	48	46	41	48	47	42

(a) Seven extrusions, 5 to 29 $in.^2$ cross section.
(b) Five extrusions, 11 to 65 $in.^2$ cross section.
(c) Three extrusions, 26 to 32 $in.^2$ cross section.

TABLE 3.0255. SHEAR STRENGTH OF 7050-T7651 EXTRUSIONS (19)

Alloy	7050-T7351							
Form	Extrusions							
Thickness, inch	0.67 to 1.2(a)		1.5 to 2.9(b)			3.5 to 5.0(c)		
Direction	L	LT	L	LT	ST	L	LT	ST
F_{su}, ksi	45	44	45	44	40	43	43	42

(a) Four extrusions, 14 to 29 $in.^2$ cross section.
(b) Nine extrusions, 11 to 65 $in.^2$ cross section.
(c) Two extrusions, 26 and 31 $in.^2$ cross sections.

TABLE 3.0256. SHEAR STRENGTH OF 7050-T7351 EXTRUSIONS (19)

Alloy	7050-T7452					
Form	Hand Forgings					
		F_{bru}, ksi		F_{bry}, ksi		
Size, inch	Orientation	e/D = 1.5	e/D = 2.0	e/D = 1.5	e/D = 2.0	
2 x 8 x 72	L	114.4	154.5	99.1	120.0	
	LT	118.5	155.2	102.3	120.1	
2-1/2 x 22 x 60	L	105.8	139.0	92.8	111.8	
	LT	112.6	145.4	95.3	112.9	
3-1/2 x 14 x 72	L	99.7	136.4	91.1	107.7	
	LT	102.0	135.0	90.9	108.1	
4-1/2 x 22 x 84	L	99.0	133.5	90.4	106.6	
	LT	104.2	131.1	88.4	104.0	
5-1/2 x 22 x 60	L	104.2	132.9	92.8	108.2	
	LT	103.7	136.2	91.8	109.8	
7-1/2 x 22 x 42	L	102.2	135.4	87.2	100.8	
	LT	102.2	129.4	84.8	99.0	

TABLE 3.0261. BEARING PROPERTIES OF 7050-T7452 (-T73652) HAND FORGINGS (4)

	Al
6.2	Zn
2.25	Mg
2.3	Cu
0.12	Zr

7050 Al

Alloy	7050-T74				
Form	Die Forgings				
		F_{bru}, ksi		F_{bry}, ksi	
Thickness, inch	Orientation	e/D = 1.5	e/D = 2.0	e/D = 1.5	e/D = 2.0
Up to 2.000	L	114.0	147.8	97.7	114.6
2.001 to 4.000	L	101.4	137.3	88.4	106.9
4.001 to 5.000	L	109.7	145.1	96.4	110.0
5.001 to 6.000	L	106.1	138.4	95.1	111.0

TABLE 3.0262. BEARING PROPERTIES OF 7050-T74 (-T736) DIE FORGINGS (4)

Alloy	7050						
				F_{bru}, ksi		F_{bry}, ksi	
Form	Condition	Thickness, inch	Orientation	e/D = 1.5	e/D = 2.0	e/D = 1.5	e/D = 2.0
Sheet	T76	0.040 to 0.249	L	129.5	167.9	109.0	121.3
			LT	129.6	167.8	108.6	124.4
Plate	T7451	0.250 to 2.000	L	113.2	148.1	93.2	110.5
			LT	113.4	148.1	93.5	112.9
Plate	T7451	4.000	L	115.8	147.4	96.5	110.0
			LT	114.8	148.0	96.1	112.0
Plate	T7451	6.000	L	110.2	141.8	94.6	110.2
			LT	112.2	144.8	94.8	111.8

TABLE 3.0263. BEARING PROPERTIES OF 7050-T76 SHEET AND 7050-T7451 (-T73651) PLATE (4)

Alloy	7050-T7351									
Form	Plate									
Thickness(a)	2-inch		3-inch		4-inch		5-inch		6-inch	
Direction	L	LT	L	LT	L	LT	L	LT	L	LT
F_{bru}, ksi										
e/D = 1.5	–	110	113	113	112	113	110	111	109	111
e/D = 2.0	–	142	147	147	144	147	142	143	–	140
F_{bry}, ksi										
e/D = 1.5	–	93	93	94	94	94	91	90	89	92
e/D = 2.0	–	109	109	111	111	111	110	109	–	111

(a) Average of single tests on each plate from two lots.

TABLE 3.0264. BEARING PROPERTIES OF 7050-T7351 PLATE (20)

Alloy	7050-T7651											
Form	Extrusions											
e/D	1.5						2.0					
Thickness, inch	0.187 to 1.2(a)		1.5 to 2.9(b)		3.5 to 5.0(c)		0.187 to 1.2		1.5 to 2.0		3.5 to 5.0	
Direction	L	LT	L	LT	L	LT	L	LT	L	LT	L	LT
F_{bru}, ksi	124	125	124	123	123	115	159	160	159	159	157	152
F_{bry}, ksi	106	106	105	104	105	103	123	127	120	121	121	120

(a) Seven extrusions, 5 to 29 $in.^2$ cross section.
(b) Five extrusions, 11 to 65 $in.^2$ cross section.
(c) Three extrusions, 26 to 32 $in.^2$ cross section.

TABLE 3.0265. BEARING STRENGTH OF 7050-T7651 EXTRUSIONS (19)

Alloy	7050-T7351											
Form	Extrusions											
e/D	1.5						2.0					
Thickness, inch	0.67 to 1.6(a)		1.5 to 2.9(b)		3.5 to 5.0(c)		0.67 to 1.6(a)		1.5 to 2.9(b)		3.5 to 5.0(c)	
Direction	L	LT	L	LT	L	LT(d)	L	LT	L	LT	L	LT(c)
F_{bru}, ksi	115	115	116	116	111	112	150	149	150	150	145	145
F_{bry}, ksi	96	96	96	96	97	94	113	114	114	117	115	119

(a) Four extrusions.
(b) Nine extrusions.
(c) Two extrusions.
(d) One extrusion.

TABLE 3.0266. BEARING PROPERTIES OF 7050-T7351 EXTRUSIONS (19)

Al
6.2 Zn
2.25 Mg
2.3 Cu
0.12 Zr

7050 Al

Alloy	7050				
Form	Condition	Thickness, inch	K_{Ic}(a) L-T	T-L	S-L
Plate	T7451	1.000	33.1	28.7	–
		2.000	36.0	29.0	24.5
		4.000	31.8	26.8	24.9
		6.000	27.2	24.8	23.8
Hand Forgings	T7451	2-1/2 x 22 x 60	29.6	26.7	19.2
		3-1/2 x 22 x 84	30.2	22.6	21.2
		4-1/2 x 22 x 84	34.7	20.5	18.4
		5-1/2 x 22 x 60	32.2	20.3	19.4
		7-1/2 x 22 x 42	33.7	–	19.7
Die Forgings	T736	0.7	–	38.2	26.0
		1.25	–	35.4	24.2
		3.5	28.7	–	–
		4.25 diam	38.7	–	–
		5.5	29.5	–	19.7
		6.1	–	–	21.2

(a) Compact tension specimens in accordance with ASTM E399.

TABLE 3.02722. PLANE STRAIN FRACTURE TOUGHNESS OF PLATE, HAND FORGINGS, AND DIE FORGINGS (4)

Alloy	7050
Form	3-inch Plate
Condition	T7451 LT F_{ty} = 65 ksi
Crack Orientation	SL
K_{Ic}, ksi$\sqrt{in.}$	25.4 (Avg of Three Tests)
K_{Ia}, ksi$\sqrt{in.}$ 2H = 1-inch	25.6 (Avg of Seven Measurements)
K_{Ia}, ksi$\sqrt{in.}$ 2H = 3-inch	25.3 (Avg of Six Measurements)

Note:
SL C(T) specimen: B = 1.25-inch, mid-thickness.
SL DB (My) specimen: B = 1-inch and L = 5-inch with 10 percent side grooves.

TABLE 3.02723. PLANE STRAIN FRACTURE TOUGHNESS VALUES FOR CRACK INITIATION AND ARREST IN 7050-T7451 (-T73651) PLATE FOR SL ORIENTATION (16)

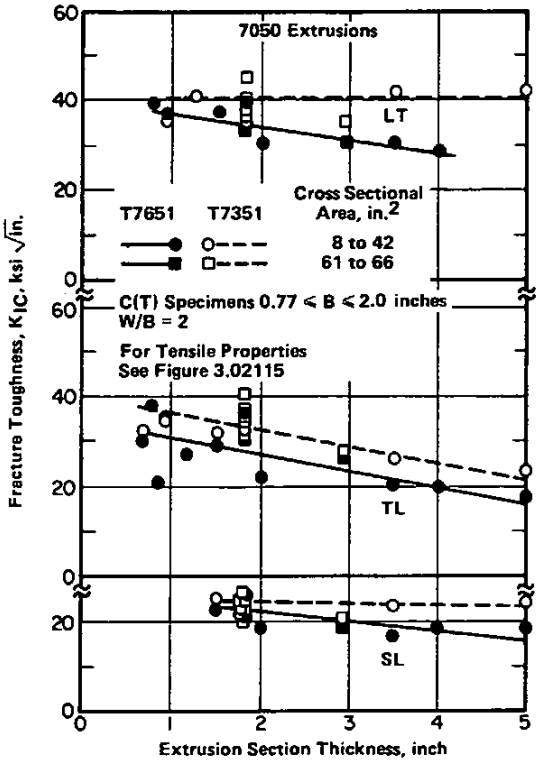


FIGURE 3.02724. EFFECT OF EXTRUSION SECTION THICKNESS ON PLANE STRAIN FRACTURE TOUGHNESS (19)

	Al
6.2	Zn
2.25	Mg
2.3	Cu
0.12	Zr

7050 Al

Alloy	7050-T76511												
Form	Extrusions												
Crack Orientation	LT				TL				SL				LS
Extrusion(a)	W	Y	Z	S	W	Y	Z	S	W	Y	Z	S	W
K_{Ic}, ksi$\sqrt{in.}$(b)	33	32	30	39	25	24	19	27	–	27	17	–	50

(a) See Figure 3.02726.
(b) K_{Ic} according to E399-72; C(T) specimens: B = 0.75 inch, W/B = 2.

TABLE 3.02725. PLANE STRAIN FRACTURE TOUGHNESS OF VARIOUS EXTRUDED SHAPES (18)

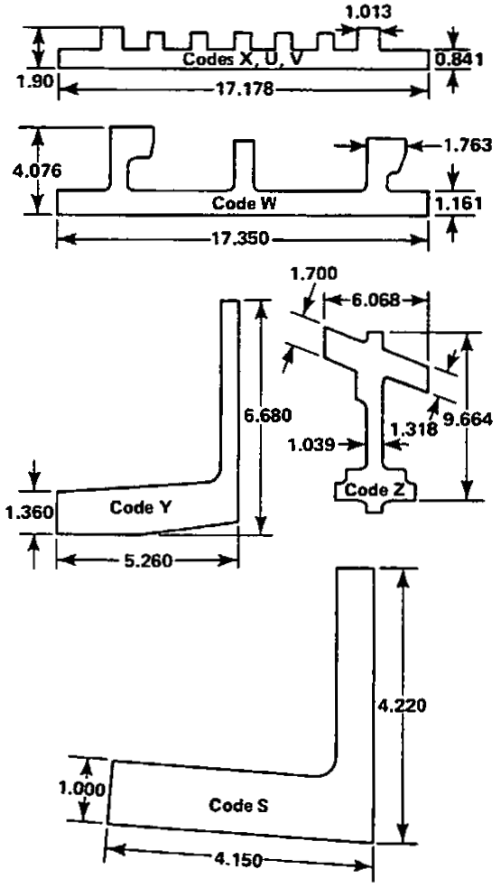


FIGURE 3.02726. EXTRUSION CROSS SECTIONS USED FOR FRACTURE TOUGHNESS AND CRACK-GROWTH RATE TESTS (18)

Alloy	7050 (0.02 Fe, 0.01 Si)		
Form	Plate		
Special Processing (See Table 3.02728)	CP(a)	AR(b)	AR + HR
F_{ty}, ksi	76	84	82
e, percent	11	11	10
K_{Ic}, ksi$\sqrt{in.}$			
LT	24	19	22
TL	26	19	23
Recrystallization, percent	45	94	68

(a) Commercial processing.
(b) As recrystallized.

TABLE 3.02727. PLANE STRAIN FRACTURE TOUGHNESS OF SPECIALLY PROCESSED VERY HIGH PURITY 7050 PLATE (30)

Alloy	7050 (0.02 Fe, 0.01 Si)
Processing Schedule	Procedure
AR(a) (1-inch Plate)	850 F, 48 hr, FC to 775 F, 5 hr, FC to 500 F, 4 hr, WQ + 81 percent HR at 274 F + 850 F, 48 hr, WQ
AR + HR(b)	ITMT + 40 percent HR at 800 F
CP(c) (1.5-inch Plate)	Hot Roll at 775 F, AC
T6X1(d)	ITMT or ITMT + AR or CP 890 F, 3 hr, WQ + 5 days at RT + 250 F, 4 hr + 335 F, 4 hr

(a) As recrystallized.
(b) Hot rolled.
(c) Commercial processing.
(d) Final treatment given to all material.

TABLE 3.02728. SPECIAL PROCESSING SCHEDULES PROVIDED TO 7050 VERY HIGH PURITY PLATE (30)

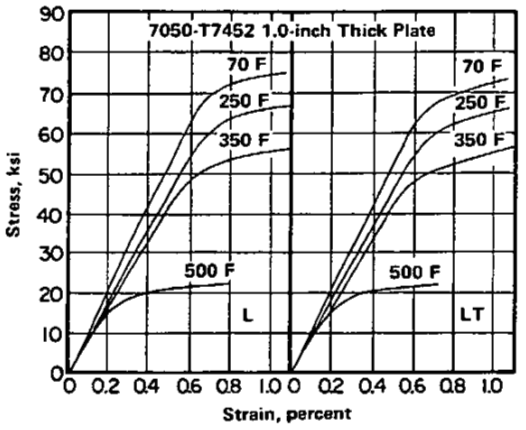


FIGURE 3.0311. TENSILE STRESS-STRAIN CURVES FOR 7050-T7452 (-T73652) PLATE AT ROOM AND ELEVATED TEMPERATURES (11)

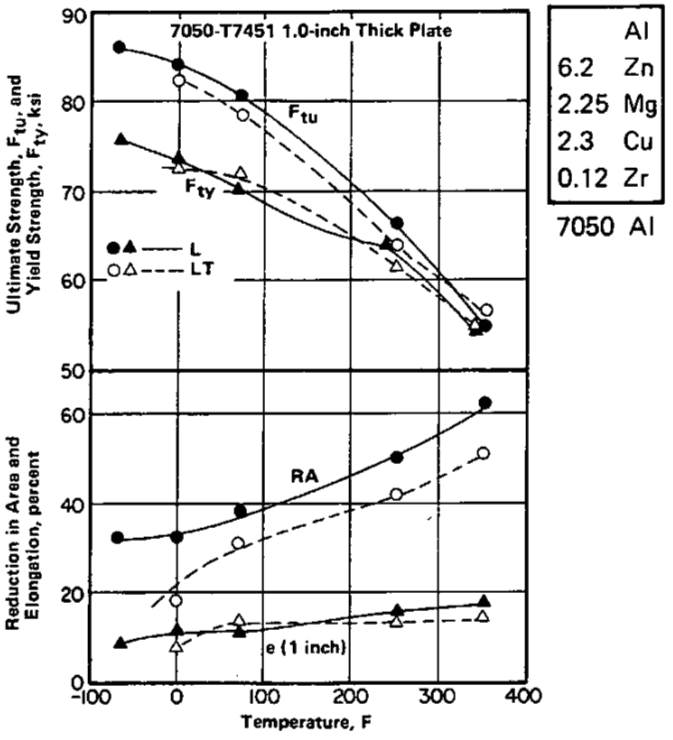


FIGURE 3.0312. TENSILE PROPERTIES OF 7050-T7451 (-T73651) PLATE IN THE TEMPERATURE RANGE -65 TO 350 F (10)

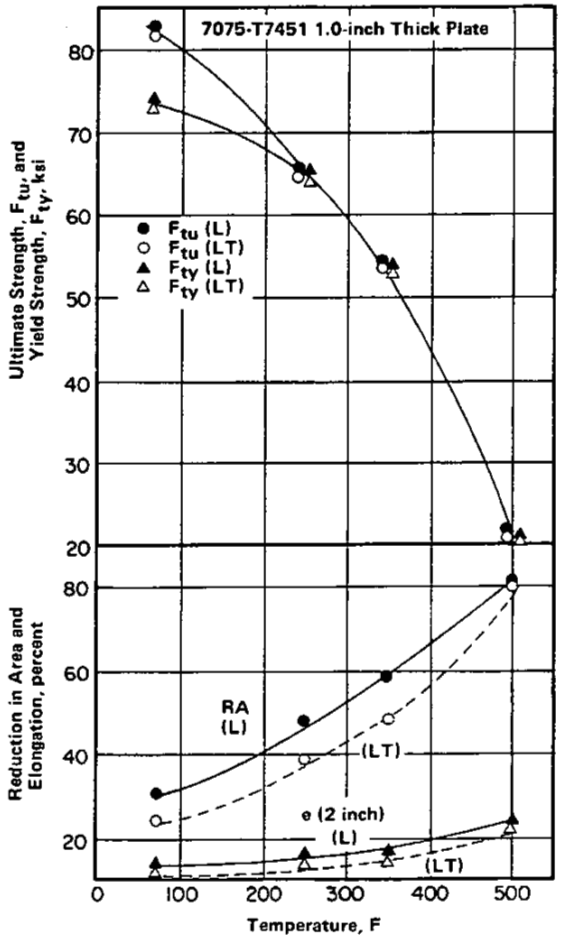


FIGURE 3.0313. TENSILE PROPERTIES OF 7050-T7451 (-T73651) PLATE IN THE TEMPERATURE RANGE OF 70 TO 500 F (11)

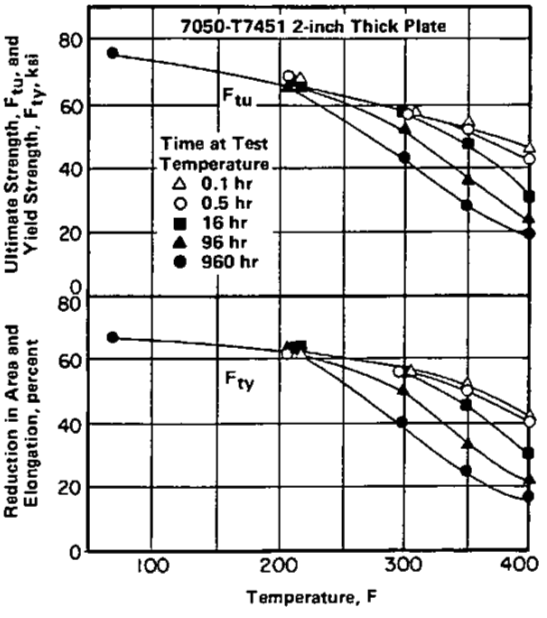


FIGURE 3.0314. EFFECTS OF ELEVATED TEMPERATURES ON TENSILE ULTIMATE AND YIELD STRENGTHS OF 7050-T7451 (-T73651) PLATE AFTER VARIOUS EXPOSURE TIMES AT TEST TEMPERATURE (8)

	Al
6.2	Zn
2.25	Mg
2.3	Cu
0.12	Zr

7050 Al

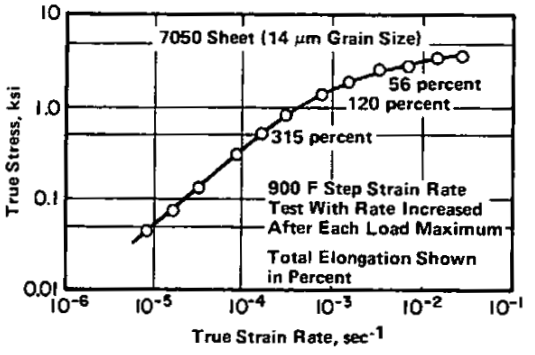


FIGURE 3.0315. TRUE STRESS AS A FUNCTION OF STRAIN RATE FOR TESTS ON A SHEET AT 900 F (28)

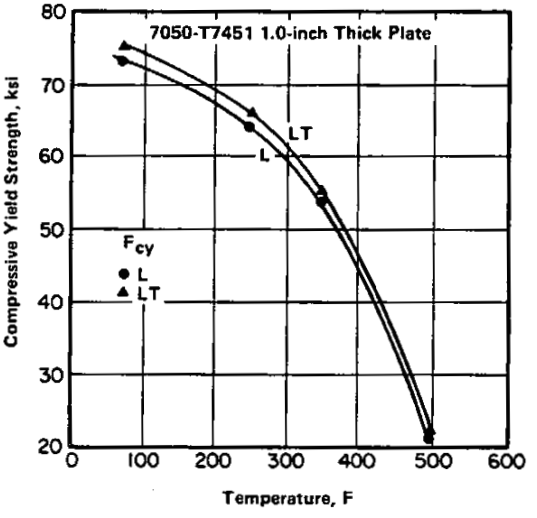


FIGURE 3.0322. EFFECTS OF TEMPERATURE ON COMPRESSIVE YIELD STRENGTH OF 7050-T7451 (-T73651) PLATE (11)

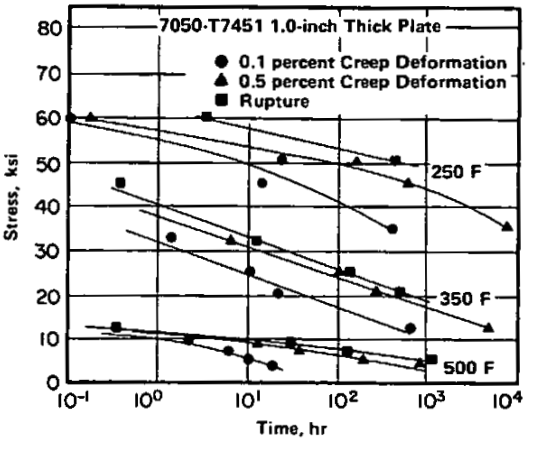


FIGURE 3.041. CREEP AND CREEP-RUPTURE CURVES FOR 7050-T7451 (-T73651) PLATE (11)

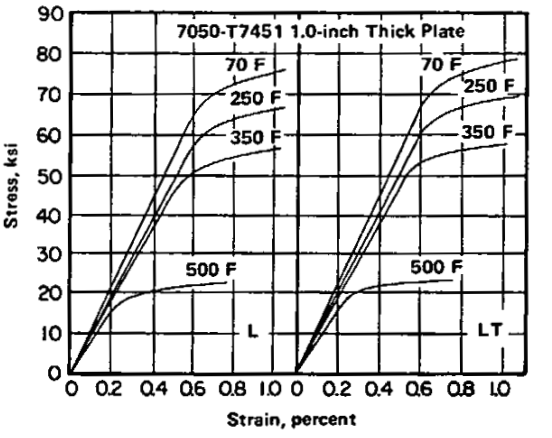


FIGURE 3.0321. COMPRESSIVE STRESS-STRAIN CURVES FOR 7050-T7451 (-T73651) PLATE AT ROOM AND ELEVATED TEMPERATURES (11)

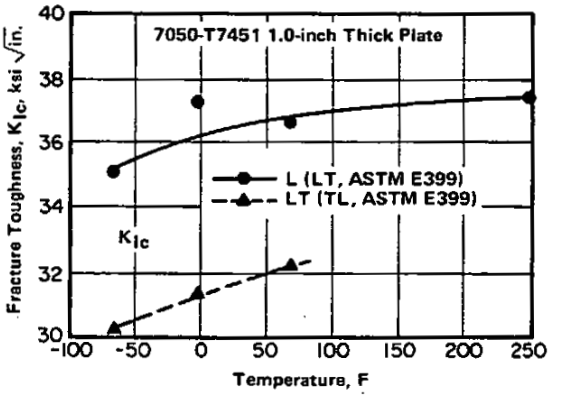


FIGURE 3.03721. EFFECTS OF LOW AND ELEVATED TEMPERATURES ON PLANE-STRAIN FRACTURE TOUGHNESS OF 7050-T7451 (-T73651) PLATE (10)

Note: K_{Ic} values determined with compact tension specimens in accordance with ASTM E399.

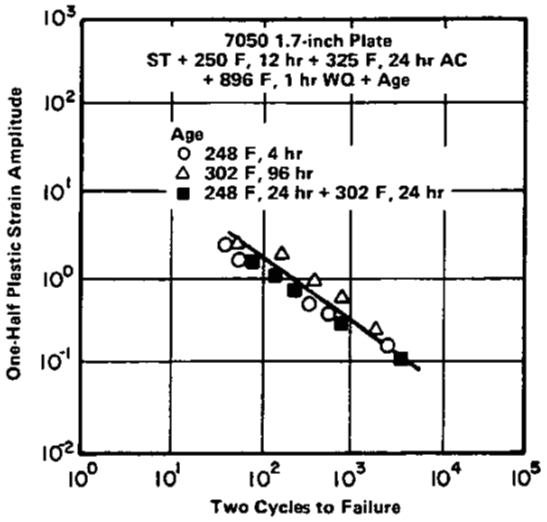
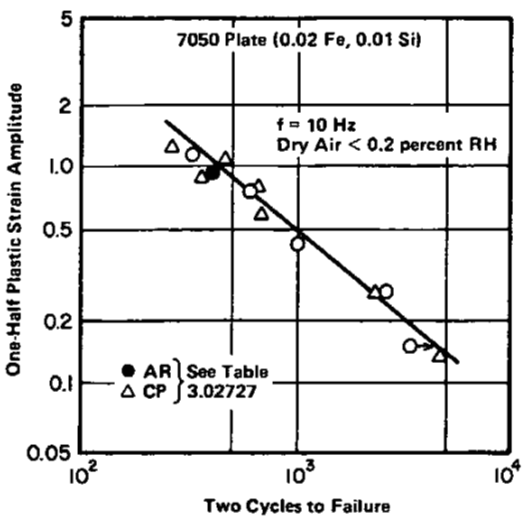


FIGURE 3.0511. LOW CYCLE FATIGUE RESULTS FOR 7050 PLATE SUBJECTED TO DIFFERENT AGING TREATMENTS (33)



	Al
6.2	Zn
2.25	Mg
2.3	Cu
0.12	Zr

7050 Al

FIGURE 3.0512. LOW CYCLE FATIGUE RESULTS FOR TWO PROCESSING TREATMENTS OF VERY HIGH PURITY 7050 PLATE (30)

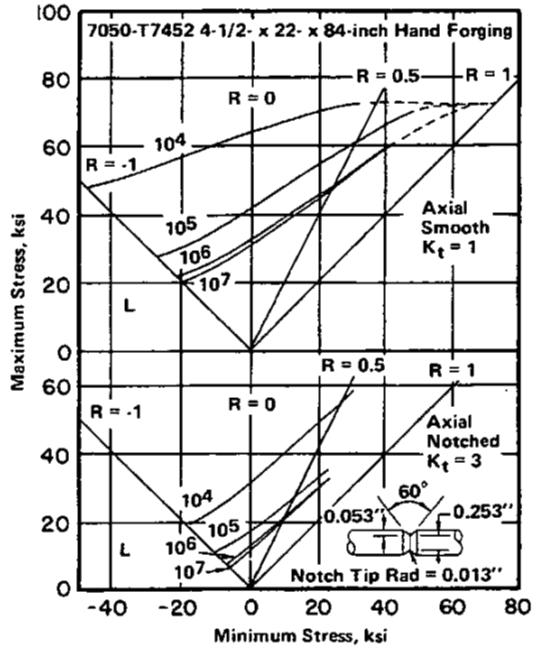


FIGURE 3.0513. MODIFIED GOODMAN DIAGRAMS FOR LONGITUDINAL SMOOTH AND NOTCH FATIGUE PROPERTIES OF 7050-T7452 (-T73652) HAND-FORGINGS (4)

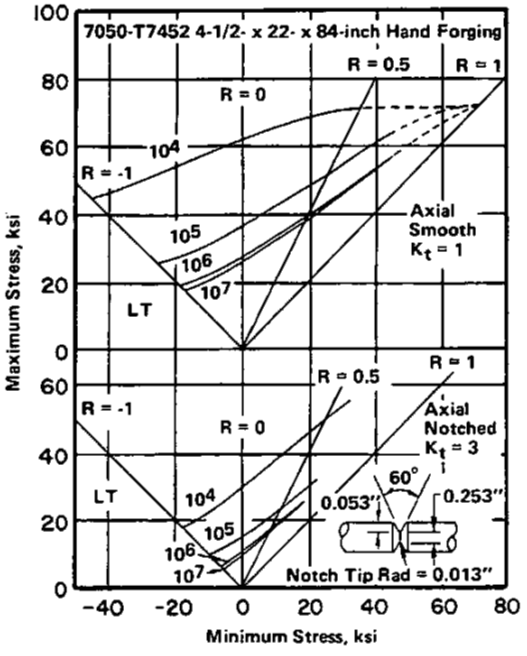


FIGURE 3.0514. MODIFIED GOODMAN DIAGRAMS FOR LONG-TRANSVERSE SMOOTH AND NOTCH FATIGUE PROPERTIES OF 7050-T7452 (-T73652) HAND-FORGINGS (4)

Al
6.2 Zn
2.25 Mg
2.3 Cu
0.12 Zr

7050 Al

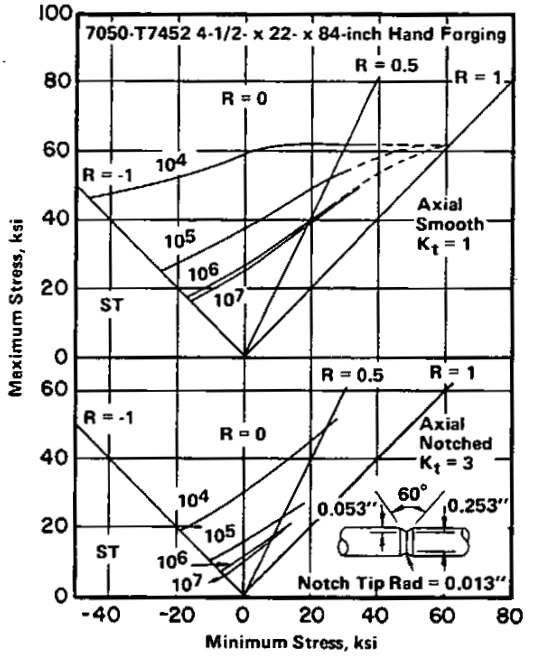


FIGURE 3.0515. MODIFIED GOODMAN DIAGRAMS FOR SHORT-TRANSVERSE SMOOTH AND NOTCH FATIGUE PROPERTIES OF 7050-T7452 (-T73652) HAND-FORGINGS (4)

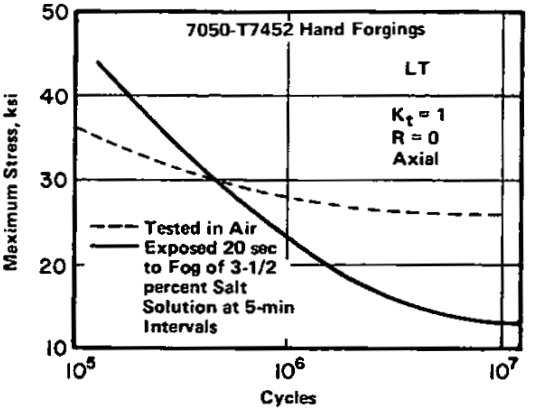


FIGURE 3.0516. S-N CURVES AT R = 0 FOR SMOOTH SPECIMENS FROM 7050-T7452 (-T73652) HAND FORGINGS TESTED IN AIR AND IN SALT FOG (4)

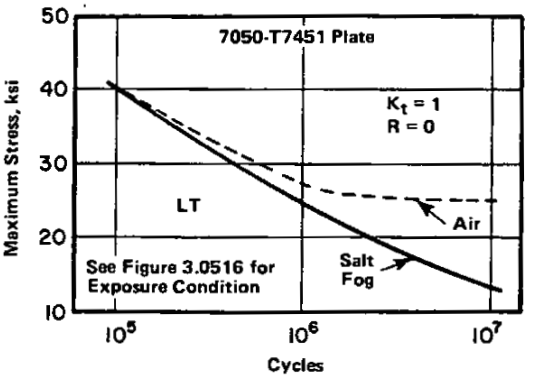


FIGURE 3.0517. S-N CURVES AT R = 0 FOR SMOOTH SPECIMENS FROM 7050-T7451 (-T73651) PLATE TESTED IN AIR AND IN SALT FOG (4)

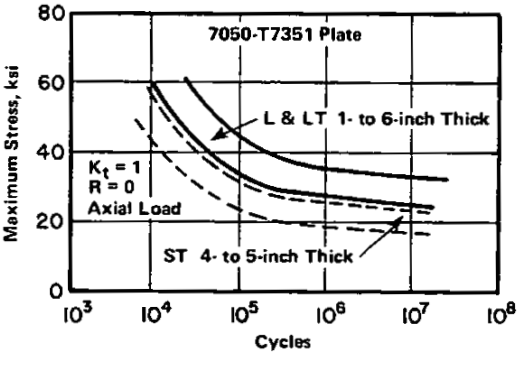


FIGURE 3.0518. S-N BANDS AT R = 0 FOR SMOOTH L, LT, AND ST SPECIMENS FROM 7050-T7351 PLATE OF VARIOUS THICKNESSES (20)

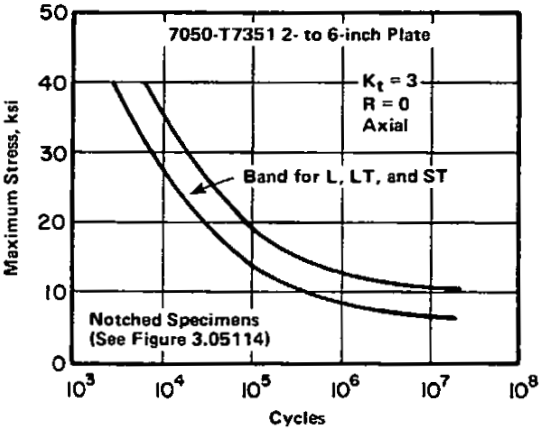


FIGURE 3.0519. S-N BAND AT R = 0 FOR NOTCHED SPECIMENS FROM 7050-T7351 PLATE OF VARIOUS THICKNESSES (20)

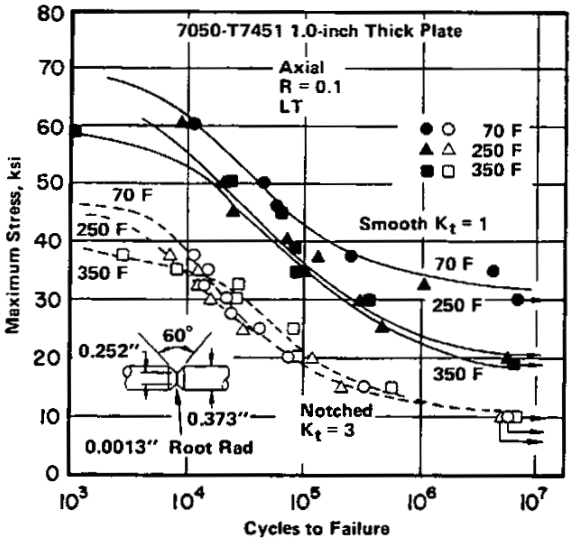


FIGURE 3.05110. FATIGUE LIFE AT VARIOUS TEMPERATURES OF SMOOTH AND NOTCHED 7050-T7451 (-T73651) PLATE (11)

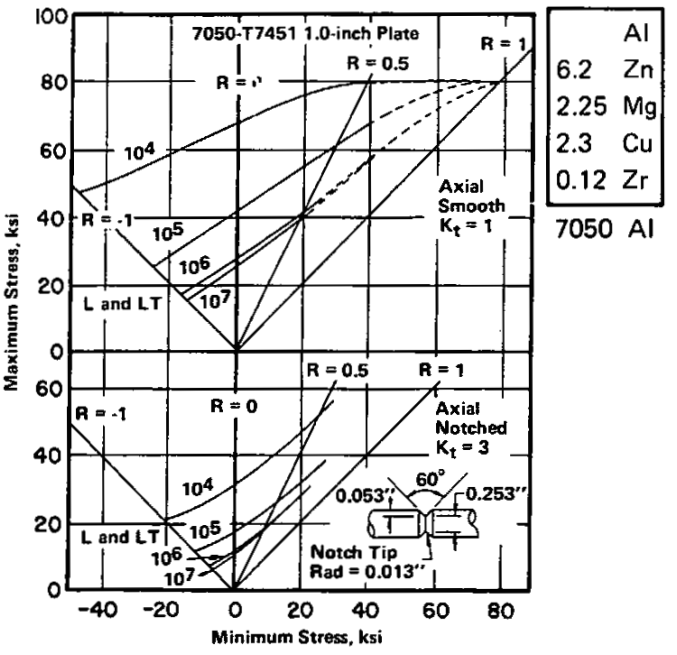


FIGURE 3.05111. MODIFIED GOODMAN DIAGRAMS FOR FATIGUE PROPERTIES OF SMOOTH AND NOTCHED 7050-T7451 (-T73651) PLATE (4)

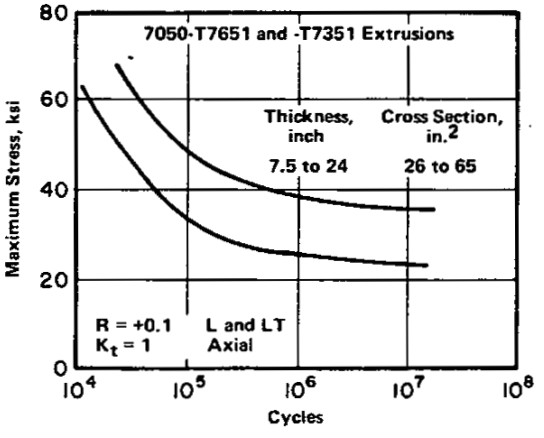


FIGURE 3.05112. S-N BAND AT R = +0.1 FOR SMOOTH SPECIMENS FROM 7050-T7651 AND -T7351 EXTRUSIONS OF VARIOUS THICKNESSES AND CROSS SECTIONS (19)

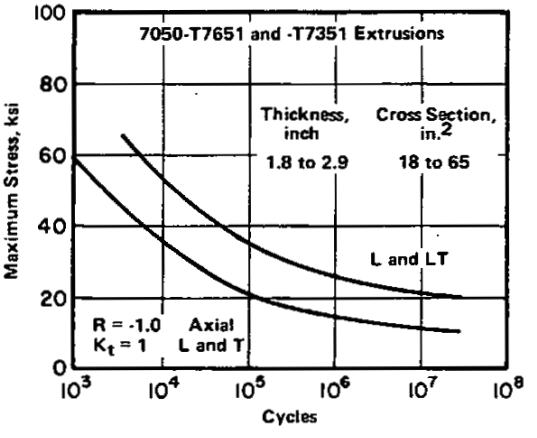


FIGURE 3.05113. S-N BAND AT R = -1.0 FOR SMOOTH SPECIMENS FROM 7050-T7651 AND -T7351 EXTRUSIONS OF VARIOUS THICKNESSES AND CROSS SECTIONS (19)

	Al
6.2	Zn
2.25	Mg
2.3	Cu
0.12	Zr

7050 Al

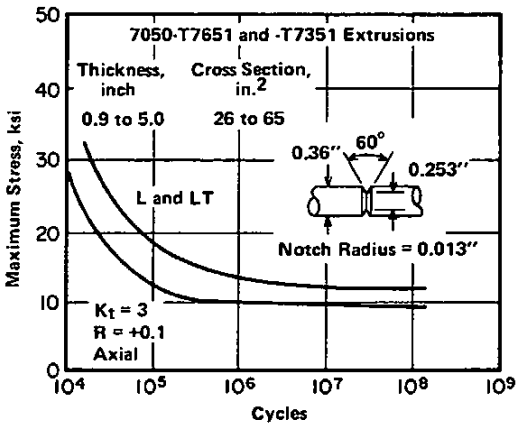


FIGURE 3.05114. S-N BAND AT R = +0.1 FOR NOTCHED SPECIMENS FROM 7050-T7651 AND -T7351 EXTRUSIONS OF VARIOUS THICKNESSES AND CROSS SECTIONS (19)

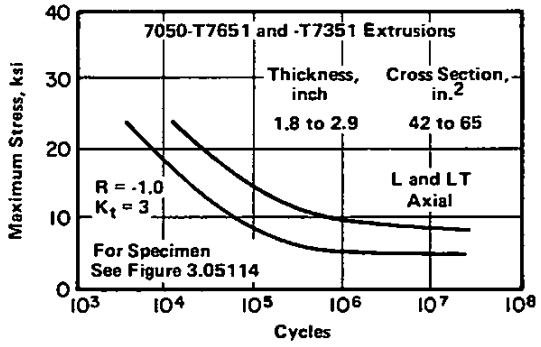


FIGURE 3.05115. S-N BAND AT R = -1.0 FOR NOTCHED SPECIMENS FROM 7050-T7651 AND -T7351 EXTRUSIONS OF VARIOUS THICKNESSES AND CROSS SECTIONS (19)

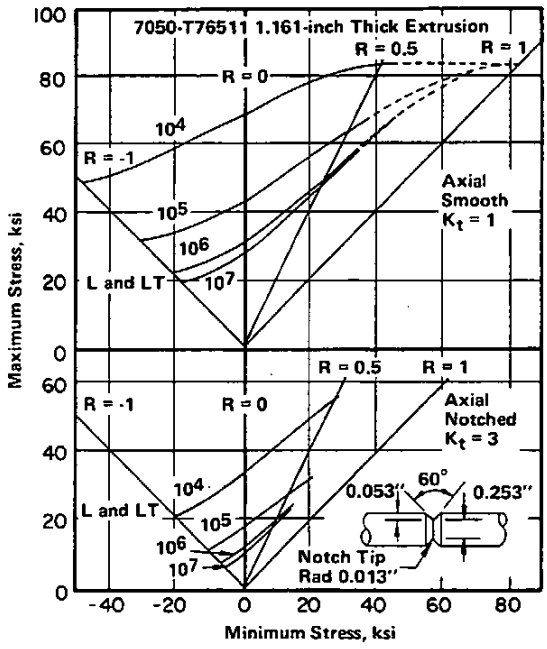


FIGURE 3.05116. MODIFIED GOODMAN DIAGRAMS FOR SMOOTH AND NOTCH FATIGUE PROPERTIES OF 7050-T76511 EXTRUSIONS (4)

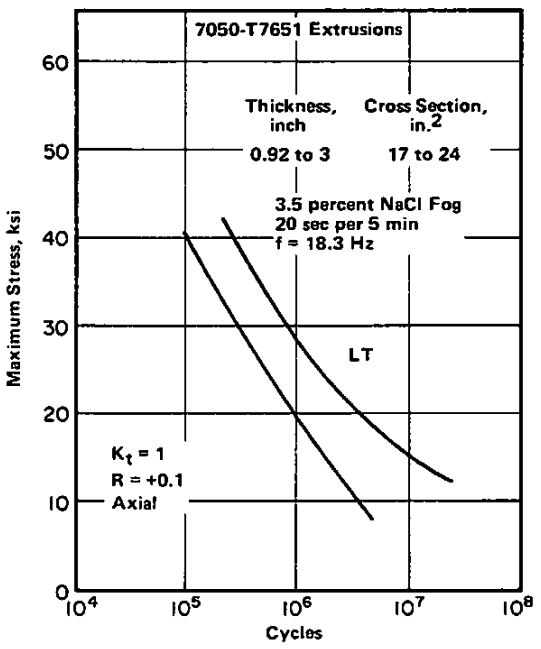


FIGURE 3.05117. S-N BAND AT R = +0.1 FOR SMOOTH SPECIMENS FROM 7050-T7651 EXTRUSIONS SUBJECTED TO SALT FOG (19)

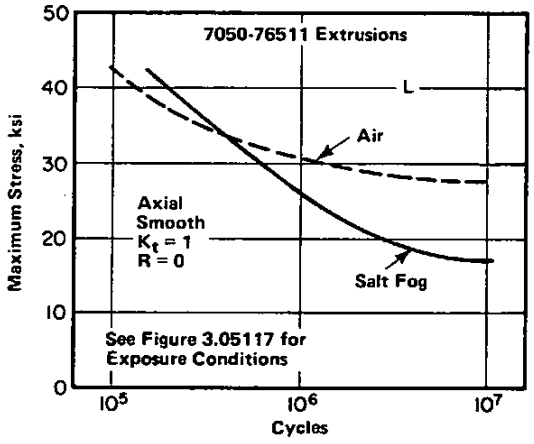


FIGURE 3.05118. S-N CURVES AT R = 0 FOR SMOOTH SPECIMENS FROM 7050 EXTRUSIONS IN T76511 CONDITION TESTED IN AIR AND IN SALT FOG (4)

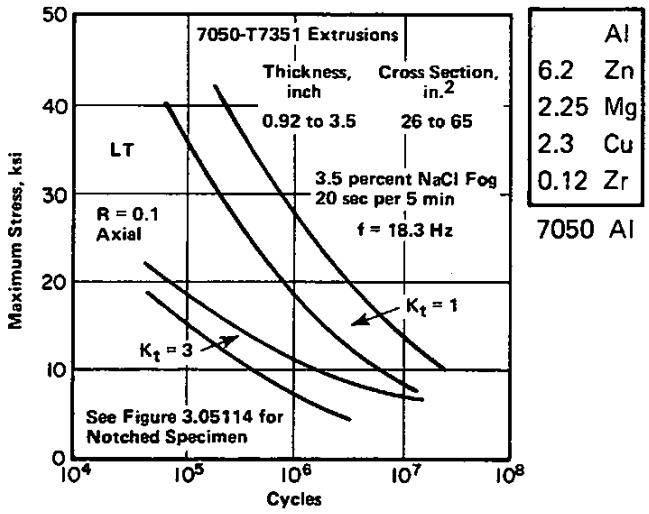


FIGURE 3.05119. S-N BAND AT R = 0.1 FOR SMOOTH AND NOTCHED SPECIMENS OF 7050-T7351 EXTRUSIONS SUBJECTED TO SALT FOG (19)

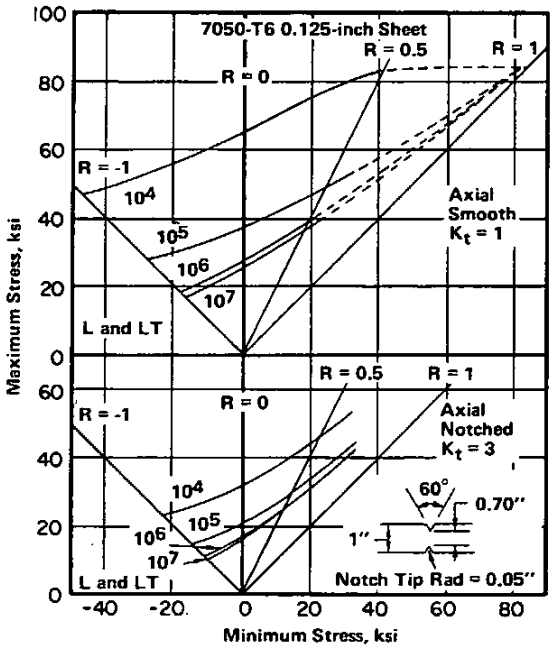


FIGURE 3.05120. MODIFIED GOODMAN DIAGRAMS FOR SMOOTH AND NOTCH FATIGUE PROPERTIES OF 7050-T6 SHEET (4)

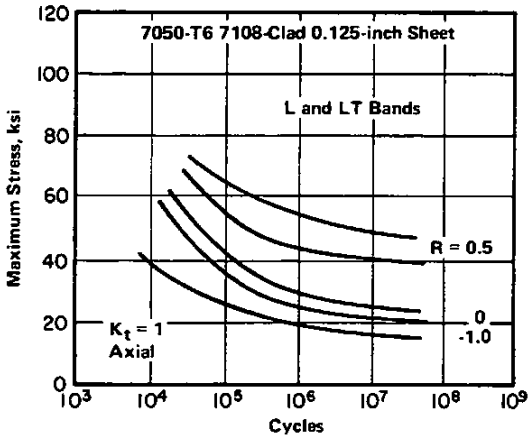


FIGURE 3.05121. S-N BANDS AT SEVERAL R RATIOS FOR SMOOTH L AND LT SPECIMENS FROM 7050-T6 CLAD SHEET (37)

	Al
6.2	Zn
2.25	Mg
2.3	Cu
0.12	Zr

7050 Al

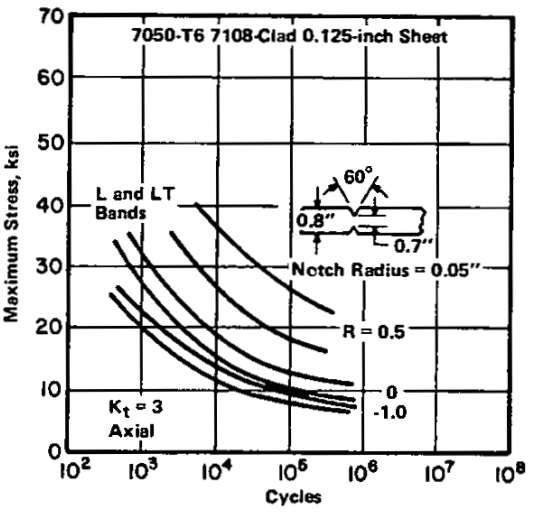


FIGURE 3.05122. S-N BANDS AT SEVERAL R RATIOS FOR L AND LT NOTCHED SPECIMENS FROM 7050-T6 CLAD SHEET (37)

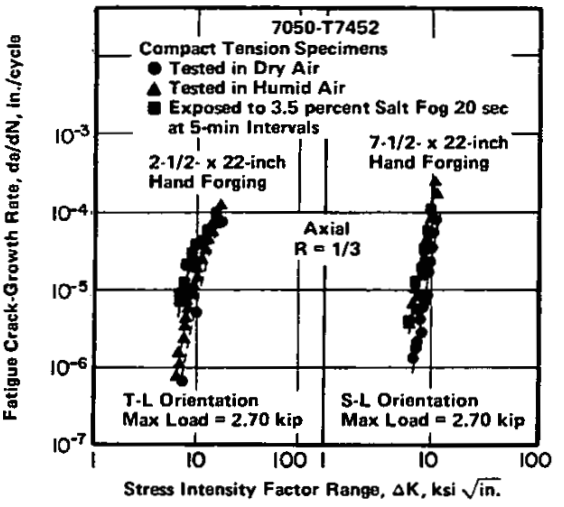


FIGURE 3.0521. FATIGUE CRACK-GROWTH RATES OF 7050-T7452 (-T73652) HAND FORGINGS IN TL AND SL ORIENTATIONS IN DRY AIR, HUMID AIR, AND SALT FOG (4)

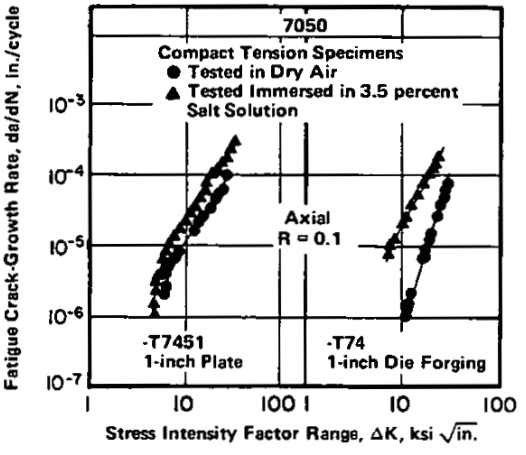


FIGURE 3.0522. FATIGUE CRACK-GROWTH RATES OF 7050-T7451 (-T73651) PLATE AND 7050-T74 (-T36) DIE FORGINGS IN DRY AIR AND IN 3.5 PERCENT NaCl SOLUTION (14)

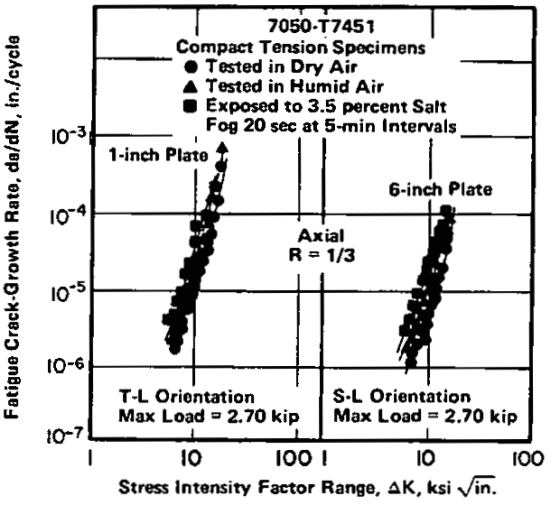


FIGURE 3.0523. FATIGUE CRACK-GROWTH RATES FOR 1-INCH AND 6-INCH 7050-T7451 (-T73651) PLATE IN TL AND SL ORIENTATIONS IN DRY AIR AND IN SALT FOG (4)

Alloy	7050		
Form	3.3-inch Plate		
Condition	T7451 L and T F_{tu} = 75.4 ksi, F_{ty} = 66.8 ksi		
Flights for[a] $0.32 < \Delta a < 1.18$-inch	Surface	Core	Surface
Thickness, inch			
0.079	5272	5405	4890
0.157	4358	3691	4341
0.354	3530	3712	3515
0.551	3275	3143	3385

(a) TWIST spectrum truncated: $\pm 1.3\ \sigma_{max}/\sigma_0$ gust levels occurring eight times per 4000 flights; σ_0 = 8 ksi is mean flight stress.
(b) LT, center cracked plate specimens, W = 4.33-inch.

TABLE 3.0524. CRACK GROWTH IN 7050-T7451 (-T73651) PLATE SUBJECTED TO A TRUNCATED TRANSPORT FLIGHT SPECTRUM (15)

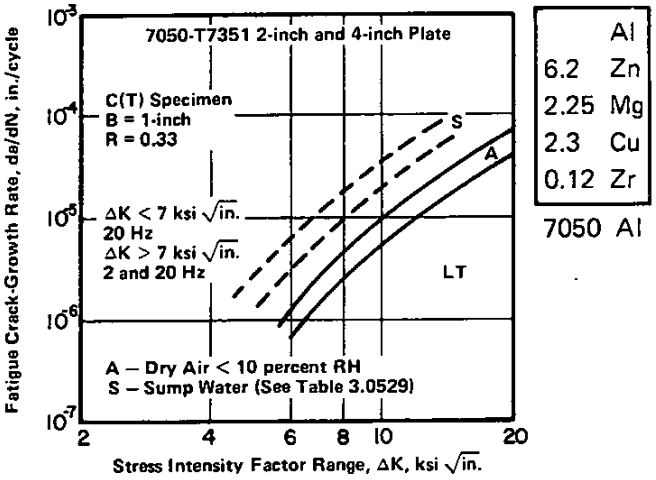


FIGURE 3.0525. FATIGUE CRACK-GROWTH RATES IN DRY AIR AND IN SUMP WATER FOR 2-INCH AND 4-INCH 7050-T7351 PLATE TESTED IN LT ORIENTATION (20)

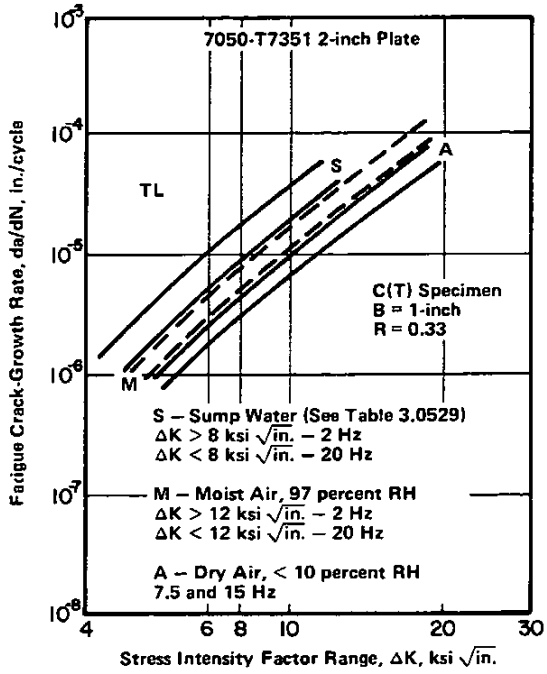


FIGURE 3.0526. FATIGUE CRACK-GROWTH RATES IN DRY AIR, MOIST AIR, AND IN SUMP WATER FOR 2-INCH 7050-T7351 PLATE TESTED IN TL ORIENTATION (20)

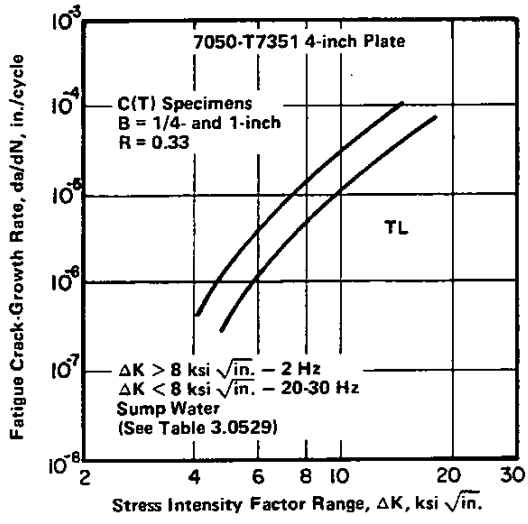


FIGURE 3.0527. FATIGUE CRACK-GROWTH RATES IN SUMP WATER FOR 4-INCH 7050-T7351 PLATE TESTED IN TL ORIENTATION (20)

	Al
6.2	Zn
2.25	Mg
2.3	Cu
0.12	Zr

7050 Al

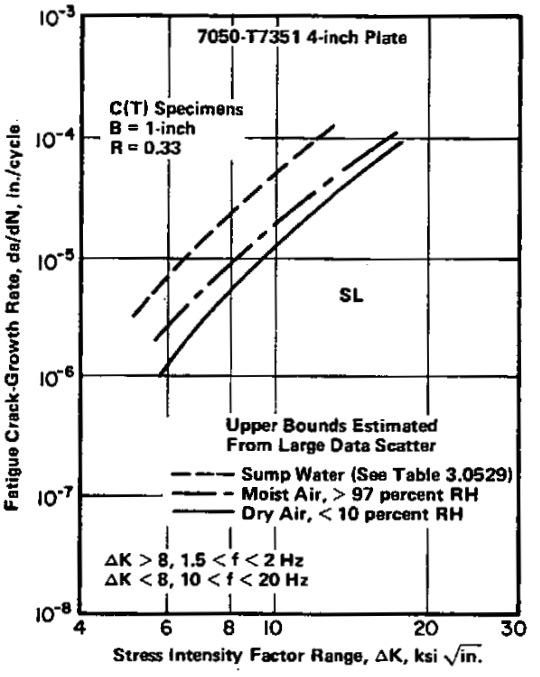


FIGURE 3.0528. FATIGUE CRACK-GROWTH RATES IN DRY AIR, MOIST AIR, AND IN SUMP WATER FOR 4-INCH 7050-T7351 PLATE TESTED IN SL ORIENTATION (20)

Sump Tank Water			
Composition	Salt, ppm	Metal Ion, ppm	Chloride, ppm
$CaCl_2$	15	18	32
$CdCl_2$	1000	490	310
$MgCl_2$	50	6	18
NaCl	100	20	30
$ZnCl_2$	10	4.7	5.2
$CrCl_3 \cdot 6H_2O$	1	0.2	0.3
$CrCl_3 \cdot 2H_2O$	1	0.4	0.4
$FeCl_3$	5	1.7	3.3
$MnCl_2 \cdot 4H_2O$	5	1.4	1.8
$NiCl_2 \cdot 6H_2O$	1	0.2	0.3
$PbCl_2$	1	0.7	0.3

TABLE 3.0529. COMPOSITION OF SYNTHETIC SUMP TANK WATER (20)

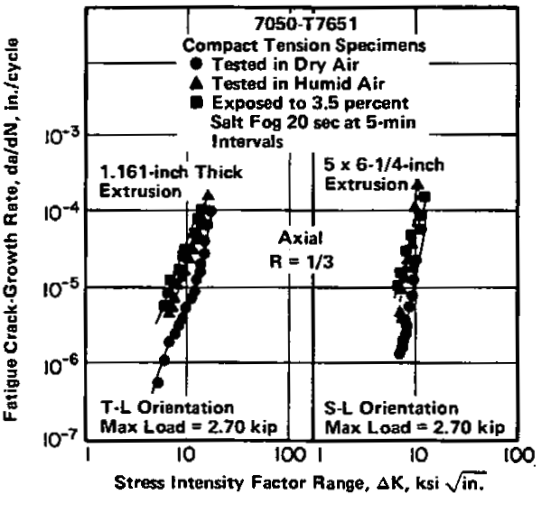


FIGURE 3.05210. FATIGUE CRACK-GROWTH RATES IN DRY AIR, HUMID AIR, AND IN SALT FOG FOR 7050-T7651 EXTRUSIONS TESTED IN TL AND SL ORIENTATIONS (4)

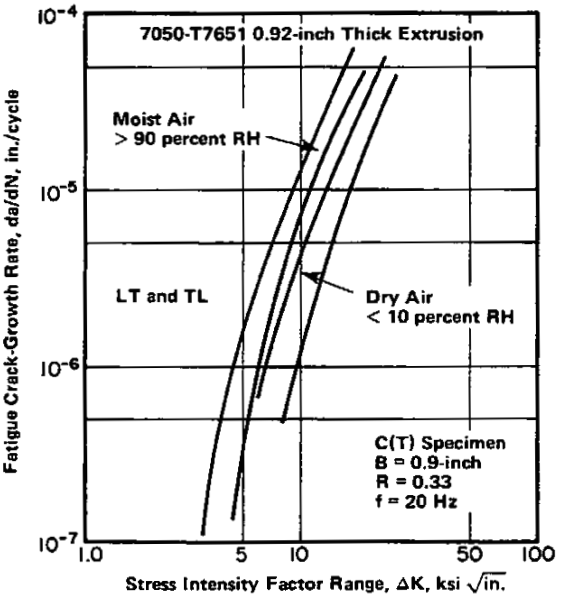


FIGURE 3.05211. FATIGUE CRACK-GROWTH RATES IN DRY AIR AND IN MOIST AIR FOR 7050-T7651 EXTRUSION TESTED IN LT AND TL ORIENTATIONS (19)

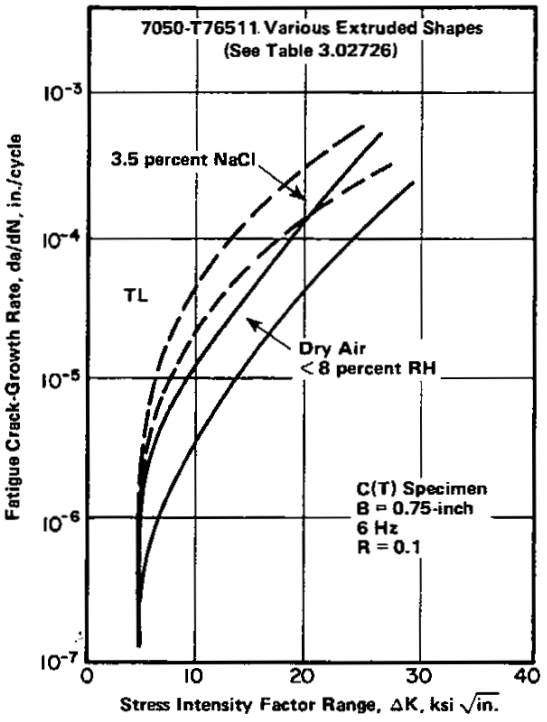


FIGURE 3.05212. FATIGUE CRACK-GROWTH RATES FOR VARIOUS EXTRUDED SHAPES OF 7050-T76511 TESTED IN TL ORIENTATION IN DRY AIR AND IN SALT WATER (18)

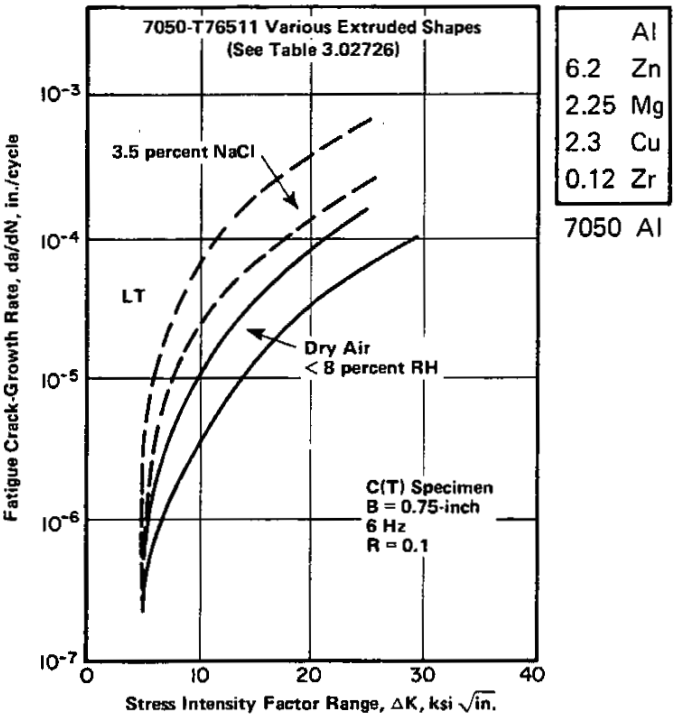


FIGURE 3.05213. FATIGUE CRACK-GROWTH RATES FOR VARIOUS EXTRUDED SHAPES OF 7050-T76511 TESTED IN LT ORIENTATION IN DRY AIR AND IN SALT WATER (18)

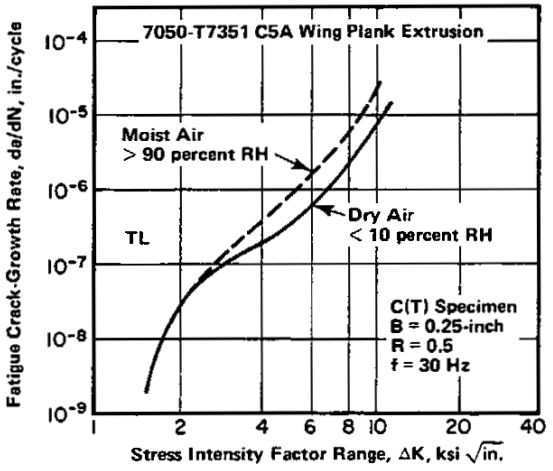


FIGURE 3.05214. NEAR THRESHOLD FATIGUE CRACK-GROWTH RATES AT R = 0.5 IN DRY AIR AND IN MOIST AIR FOR TL SPECIMENS FROM 7050-T7351 C5A WING PLANK EXTRUSION (19)

	Al
6.2	Zn
2.25	Mg
2.3	Cu
0.12	Zr

7050 Al

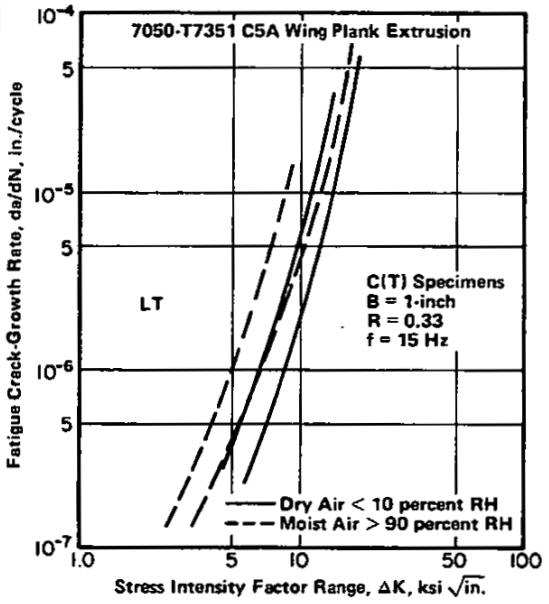


FIGURE 3.05215. FATIGUE CRACK-GROWTH RATES IN DRY AIR AND IN MOIST AIR FOR LT SPECIMENS FROM 7050-T7351 C5A WING PLANK EXTRUSION (19)

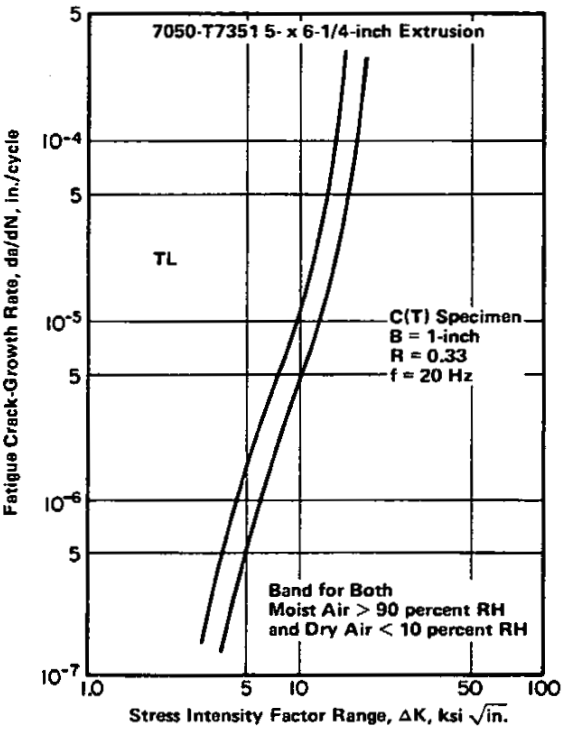


FIGURE 3.05216. FATIGUE CRACK-GROWTH RATES IN DRY AIR AND IN MOIST AIR FOR 7050-T7351 EXTRUSION TESTED IN TL ORIENTATION (19)

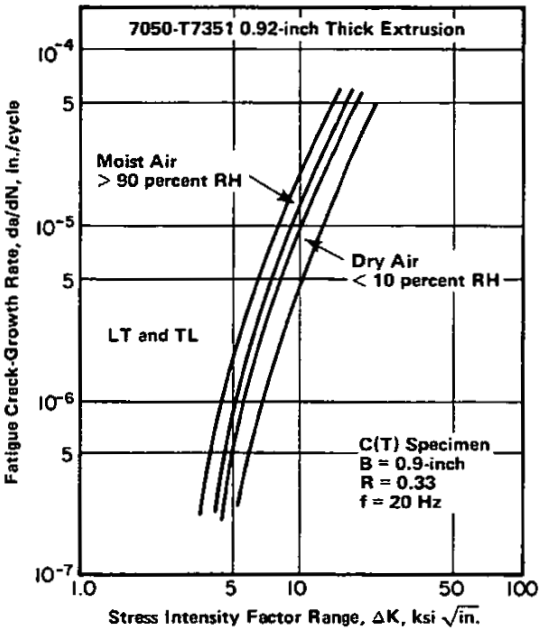


FIGURE 3.05217. FATIGUE CRACK-GROWTH RATES IN DRY AIR AND IN MOIST AIR FOR 7050-T7351 EXTRUSION TESTED IN LT AND TL ORIENTATIONS (19)

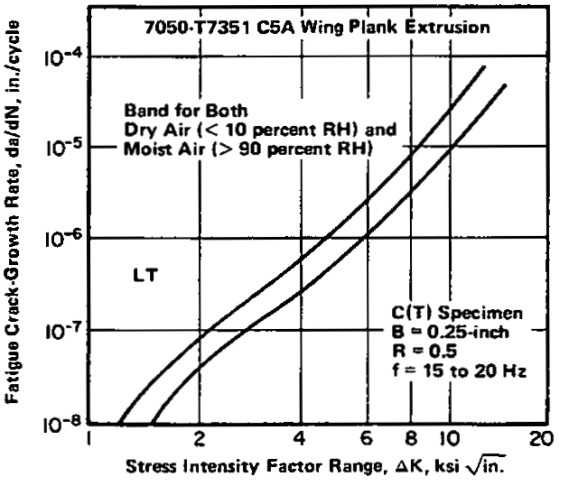


FIGURE 3.05218. NEAR THRESHOLD FATIGUE CRACK-GROWTH RATES AT R = 0.5 IN DRY AIR AND IN MOIST AIR FOR LT SPECIMENS FROM 7050-T7351 C5A WING PLANK EXTRUSION (19)

	Al
6.2	Zn
2.25	Mg
2.3	Cu
0.12	Zr

7050 Al

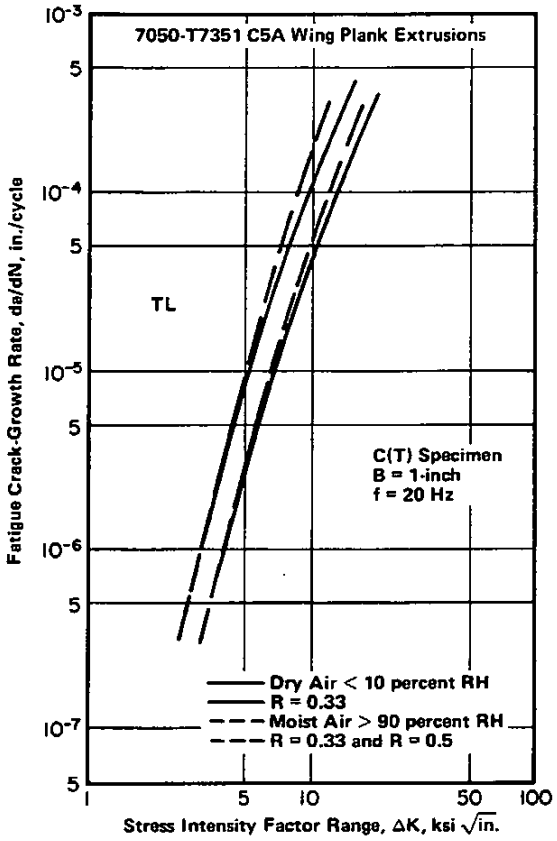


FIGURE 3.05219. FATIGUE CRACK-GROWTH RATES IN DRY AIR AND IN MOIST AIR FOR TL SPECIMENS FROM 7050-T7351 C5A WING PLANK EXTRUSION (19)

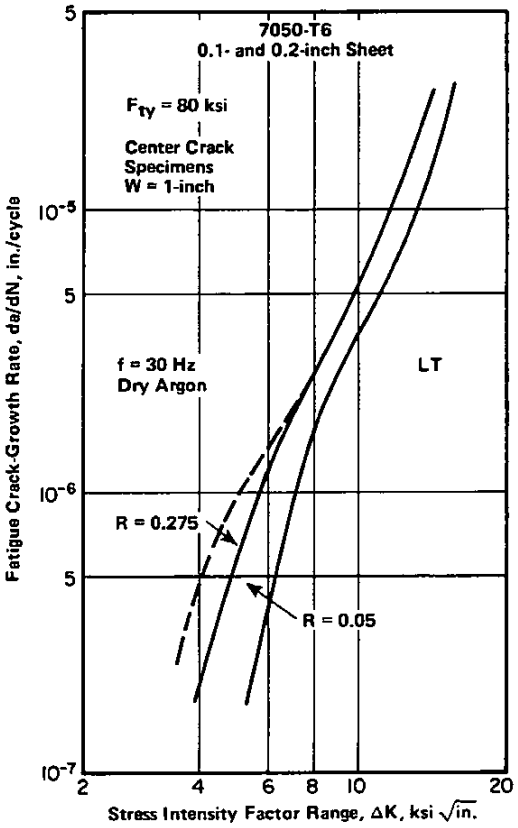


FIGURE 3.05220. FATIGUE CRACK-GROWTH RATES AT R = 0.05 AND R = 0.275 IN DRY ARGON FOR 7050-T6 SHEET TESTED IN LT ORIENTATION (29)

	Al
6.2	Zn
2.25	Mg
2.3	Cu
0.12	Zr

7050 Al

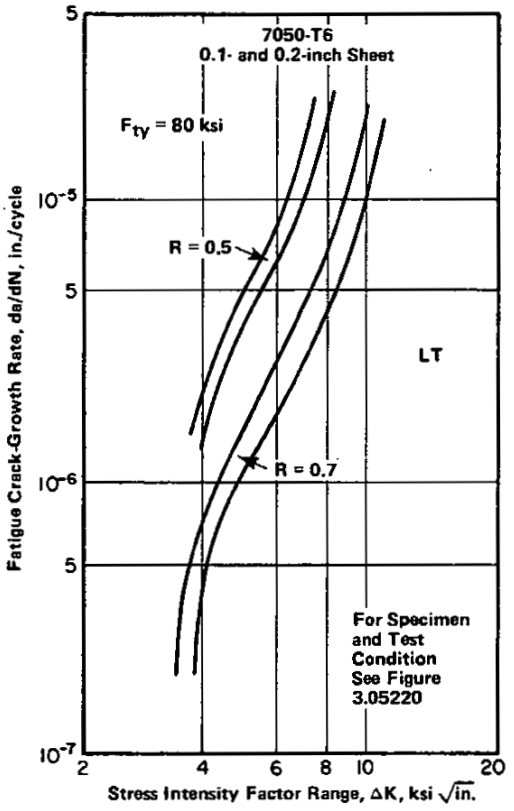


FIGURE 3.05221. FATIGUE CRACK-GROWTH RATES AT R = 0.5 AND R = 0.7 IN DRY ARGON FOR 7050-T6 SHEET TESTED IN LT ORIENTATION (29)

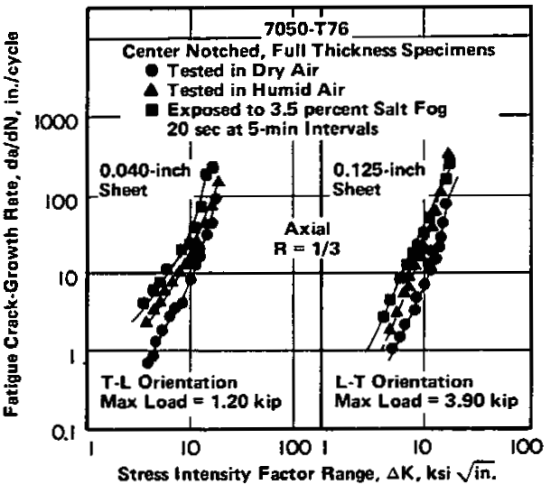


FIGURE 3.05222. FATIGUE CRACK-GROWTH RATES IN DRY AIR, HUMID AIR, AND SALT FOG FOR 7050-T76 SHEET TESTED IN TL AND LT ORIENTATIONS (4)

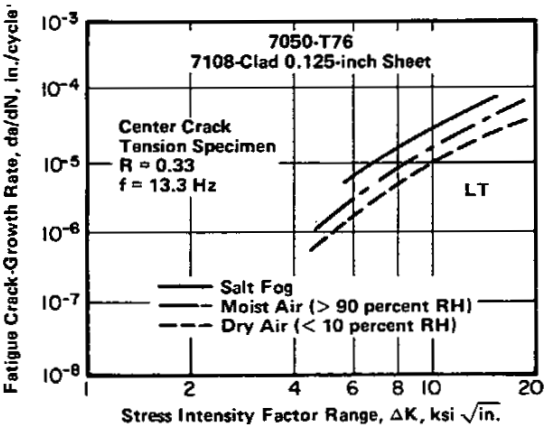


FIGURE 3.05223. FATIGUE CRACK-GROWTH RATES IN DRY AIR, MOIST AIR, AND IN 3.5 PERCENT SALT FOG FOR CLAD 7050-T76 SHEET TESTED IN LT ORIENTATION (37)

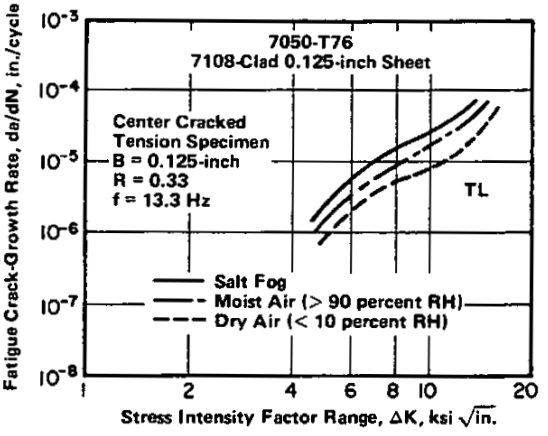


FIGURE 3.05224. FATIGUE CRACK-GROWTH RATES IN DRY AIR, MOIST AIR, AND IN 3.5 PERCENT SALT FOG FOR CLAD 7050-T76 SHEET TESTED IN TL ORIENTATION (37)

Alloy	7050		
Form	Condition	E, 10^3 ksi	E_c, 10^3 ksi
Sheet	T76	10.2	10.5
Plate	T7451	10.3	10.5
Hand Forgings	T7452	10.2	10.5
Die Forgings	T736	10.2	10.5

Note: Variations in specimen orientation (L, LT, and ST) have no significant effects on these values.

TABLE 3.0621. STATIC MODULUS OF ELASTICITY IN TENSION AND COMPRESSION FOR VARIOUS FORMS (4)

	Al
6.2	Zn
2.25	Mg
2.3	Cu
0.12	Zr

7050 Al

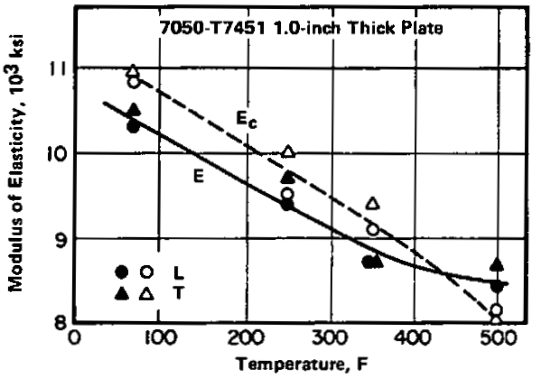


FIGURE 3.0622. EFFECT OF TEMPERATURE ON STATIC MODULUS OF ELASTICITY IN TENSION AND COMPRESSION FOR 7050-T7451 (-T73651) PLATE (11)

Alloy	7050								
Form	Extrusions						Plate		
Condition	T7651X			T7351X			T7351		
Direction	L	LT	ST	L	LT	ST	L	LT	ST
Number of Extrusions or Plates	7	7	3	7	7	2	5 Plates (2- to 6-inch)		
E, $\bar{X}$, 10^3 ksi	10.24	10.45	10.15	10.26	10.66	10.23	10.24	10.34	10.19
S, 10^3 ksi	0.155	0.166	–	0.0808	0.0423	–	0.021	0.048	0.04
E_c, $\bar{X}$, 10^3 ksi	10.73	11.03	10.83	10.66	11.02	10.66	10.54	–	–
S, 10^3 ksi	0.101	0.0711	–	0.0424	0.134	–	0.042	–	–

TABLE 3.0623. MEAN ($\bar{X}$) AND STANDARD DEVIATION(S) OF THE TENSION AND COMPRESSION MODULES FOR 7050-T7651 AND -T7351 EXTRUSIONS AND 7050-T7351 PLATE (19,20)

Al
6.2 Zn
2.25 Mg
2.3 Cu
0.12 Zr

7050 Al

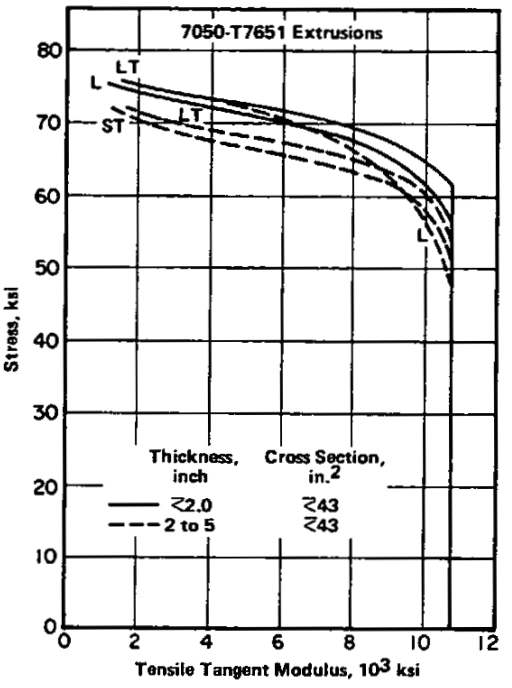


FIGURE 3.0641. TENSILE TANGENT MODULUS FOR 7050-T7651 EXTRUSIONS OF SEVERAL THICKNESSES (18)

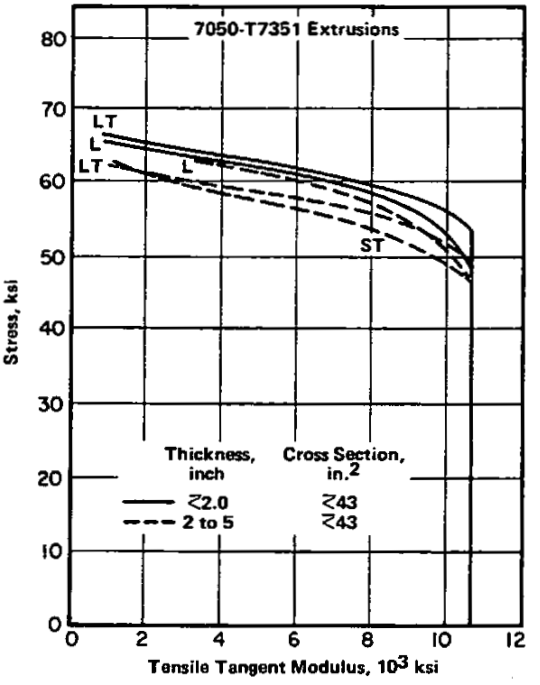


FIGURE 3.0642. TENSILE TANGENT MODULUS FOR 7050-T7351 EXTRUSIONS OF VARIOUS THICKNESSES (18)

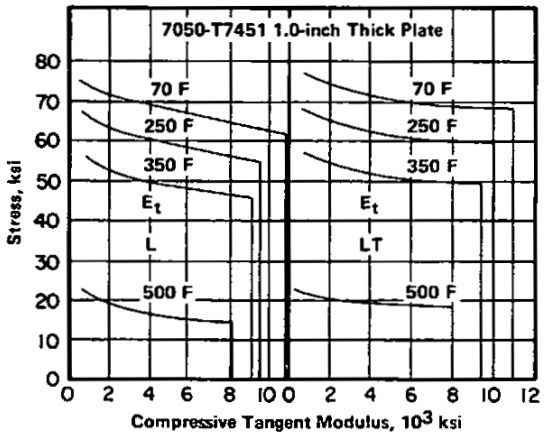


FIGURE 3.0643. COMPRESSIVE TANGENT MODULUS FOR 7050-T7451 (-T73651) PLATE AT VARIOUS TEMPERATURES (11)

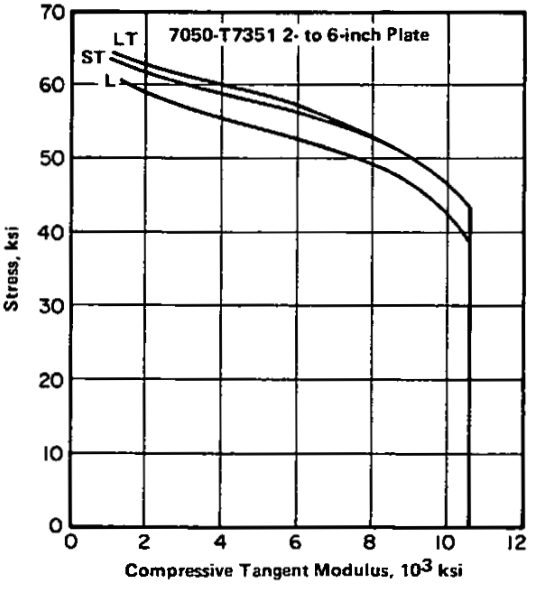


FIGURE 3.0644. COMPRESSIVE TANGENT MODULUS FOR 7050-T7351 PLATE (20)

NONFERROUS ALLOYS

	Al
5.5	Zn
2.5	Mg
1.6	Cu
0.3	Cr

CLAD 7075

1. GENERAL

In order to improve the corrosion resistance of 7075 sheet, strip and plate, these are clad with a low zinc alloy, 7072. This imparts to Clad 7075 a corrosion resistance equal to that of pure aluminum, although overheating impairs this protective covering. The cladding reduces the strength of 7075 by about 5 percent, but improves the formability to a slight extent. Therefore, only complementary and additional information to that presented for 7075 is given below. This information in turn also applies to bar, sheet, strip and plate of the unclad alloy with the exceptions noted below.

1.01 Commercial Designation. Clad 7075.

1.02 Alternate Designations. Alclad 7075, Clad 75 S, Alclad 75 S (all obsolete).

1.03 Specifications. Table 1.03.

TABLE 1.03

AMS	Form	Military
4039	Plate T651 Condition	
4046	Sheet, plate T6 Condition, Clad 1 side	
4047 B	Sheet, plate, roll tapered, T6 Condition	
4048 C	Sheet, plate, 0 Condition	
4049 C	Sheet, plate, T6 Condition	

1.04 Composition. Table 1.04.

TABLE 1.04

Source	AMS (1)(2)(3)(4)(5)			
	Core		Cladding*	
	Percent		Percent	
	Min	Max	Min	Max
Copper	1.2	2.0	-	0.10
Magnesium	2.1	2.9	-	0.10
Manganese	-	0.30	-	0.10
Iron	-	0.7	-	0.7
Silicon	-	0.50	-	
Zinc	5.1	6.1	0.8	1.3
Chromium	0.18	0.40	-	-
Titanium	-	0.20	-	-
Other impurities				
each	-	0.05	-	0.05
total	-	0.15	-	0.15
Aluminum	Balance		Balance	

* The nominal cladding thickness is between 4 and 1.5 percent of the total thickness on each side, depending on the total thickness of the product. Cladding thicknesses greater than 4 percent are obsolete.

1.05 Heat Treatment. Clad 7075 is heat treated under the same conditions as 7075, but the shortest heat treatment time, consistant with securing the required properties, should be used. Prolonged heating or repeated reheat treatments, which cause diffusion of alloying elements into the coating and impair the resistance to corrosion, should be avoided. See Clad 2024 also.

1.06 Hardenability. See 7075.

1.07 Forms and Conditions Available

1.071 Alloy is available in the full commercial range of sizes for sheet, strip and plate.

1.072 Alloy is available in the 0, T6 and T651 Conditions.

1.08 Melting and Casting Practice. See 2024 and Clad 2024.

1.09 Special Considerations

1.091 Effect of directionality on stress strain curves for sheet and plate, in T6 Condition. Fig. 1.091.

1.092 Prolonged heating or repeated reheat treatments cause diffusion of alloying elements into the coating and impair the resistance to corrosion. See Clad 2024.

2. PHYSICAL AND CHEMICAL PROPERTIES

2.01 Thermal Properties

2.013 Thermal conductivity. 75.1 Btu ft per (hr sq ft F).

2.014 Thermal expansion. 0 Condition, 12.9×10^{-6} in per in per F. T6 Condition, 13.1×10^{-6} in per in per F.

2.015 Specific heat. 0.23 Btu per (lb F).

2.02 Other Physical Properties

2.021 Density. 0.101 lb per cu in. 2.80 gr per cu cm.

3. MECHANICAL PROPERTIES

3.01 Specified Mechanical Properties

3.011 Design properties. See MIL-HDBK-5.

3.012 AMS specified mechanical properties for tapered sheet and plate, Table 3.012.

TABLE 3.012

Source	AMS (3)		
Alloy	Al-5.5Zn-2.5Mg-1.6Cu-0.3Cr		
Form	Tapered sheet and plate		
Condition	T6		
Thickness - in	0.040 to 0.187	0.188 to 0.499	0.500 to 1.000
F_{tu}, min -ksi	72	75	77
F_{ty}, min -ksi	62	64	66
e(2 in), min-percent	8	8	6

3.013 Aluminum Association specified mechanical properties for 0 Condition. Table 3.013

TABLE 3.013

Source	(6, p. 35)			
Alloy	Al-5.5Zn-2.5Mg-1.6Cu-0.3Cr*			
Condition	0			
Thickness - in	0.008 to 0.014	0.015** to 0.062	0.063 to 0.187	0.188 to 0.499
Clad Thickness Percent per side	4	4	2 1/2	1 1/2
F_{tu}, max - ksi	36	36	38	39
F_{ty}, max - ksi	20	20	20	21
e(2 in), min-percent	9	10	10	10

* For thickness of plate ≥ 0.500 inch properties are the same as core material, see 7075.

** 4 percent clad thickness for plate thickness over 0.063 in is obsolete and is only shown for information.

3.014 Aluminum Association specified mechanical properties for T6 and T651 Condition, Table 3.014.

TABLE 3.014

Source	(6, p. 35)				
Alloy	Al-5.5Zn-2.5Mg-1.6Cu-0.3Cr* (Clad)				
Form	Sheet and plate				
Condition	T6 and T651				
Thickness - in	0.008 to 0.011	0.012 to 0.039	0.040** to 0.499	0.063 to 0.187	0.188 to 0.499
Clad Thickness-%	4	4	4	2 1/2	1 1/2
F_{tu}, min-ksi	68	70	72	73	75
F_{ty}, min-ksi	58	60	62	63	64
e(2 in), min-percent	5	7	8	8	8

* For thickness of plate ≥ 0.500 inch properties are the same as core material, see 7075.

** 4 percent clad thickness for plate thickness over 0.053 in is obsolete and is only shown for information.

3.02 Mechanical Properties at Room Temperature. See 3.03 also.

3.021 Typical mechanical properties, Table 3.021.

	Al
5.5	Zn
2.5	Mg
1.6	Cu
0.3	Cr

CLAD 7075

TABLE 3.021

Source	(7, p. 26)	
Form	Wrought products	
Condition	0	T6
F_{tu}, typ - ksi	32	76
F_{ty}, typ - ksi	14	67
F_{su}, typ - ksi	22	46
e(2 in), typ - percent	17	11

3.03 Mechanical Properties at Various Temperatures

3.031 Short time tension properties

3.0311 Complete stress strain curves for sheet in 0 and T6 Conditions at room and elevated temperatures, Fig. 3.0311.

3.0312 Stress strain curves for sheet in T6 Condition at room and elevated temperatures, Fig. 3.0312.

3.0313 Effect of exposure and test temperature on tensile properties of sheet in T6 Condition, Fig. 3.0313.

3.032 Short time properties other than tension

3.0321 Stress strain curves in compression for sheet in T6 Condition at room and elevated temperatures, Fig. 3.0321.

3.0322 Effect of exposure and test temperature on compressive yield strength of sheet in T6 Condition, Fig. 3.0322.

3.0323 Effect of exposure and test temperature on bearing properties of sheet in T6 Condition, Fig. 3.0323.

3.0324 Effect of exposure and test temperature on shear strength of sheet in T6 Condition, Fig. 3.0324.

3.04 Creep and Creep Rupture Properties

3.041 Creep and creep rupture curves for sheet in T6 Condition at 300 F, Fig. 3.041

3.042 Short time total strain curves for sheet in T6 Condition at 300 to 600 F, Fig. 3.042.

3.043 Master curves for 0.5 percent total strain and creep rupture for sheet in T6 Condition, Fig. 3.043.

3.05 Fatigue Properties. Table 3.05 .

TABLE 3.05

Source	(8, p. 142)								
Form	Sheet								
Condition	T6								
Temp F	Method	Stress Ratio		Stress Concentration	Fatigue Strength - ksi at Cycles				
		A	R		10^5	10^6	10^7	10^8	$5x10^8$
RT	Rot beam	∞	-1	Smooth K = 1	29	20	15	13	12.5

3.06 Elastic Properties. See Clad 2024 also.

3.061 Tangent modulus curves in compression for sheet and plate in T6 Condition at room temperature, Fig. 3.061.

3.062 Tangent modulus curves in compression for sheet in T6 Condition at room and elevated temperatures, Fig. 3.062.

4. FABRICATION

4.01 Forming and Casting

4.011 Relationship of holding time to forming temperatures for sheet in T6 Condition, Fig. 4.011.

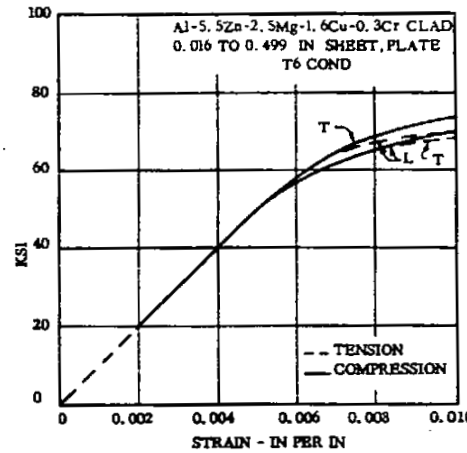


FIG. 1.091 EFFECT OF DIRECTIONALITY ON STRESS STRAIN CURVES FOR SHEET AND PLATE IN T6 CONDITION (9, p. 84)

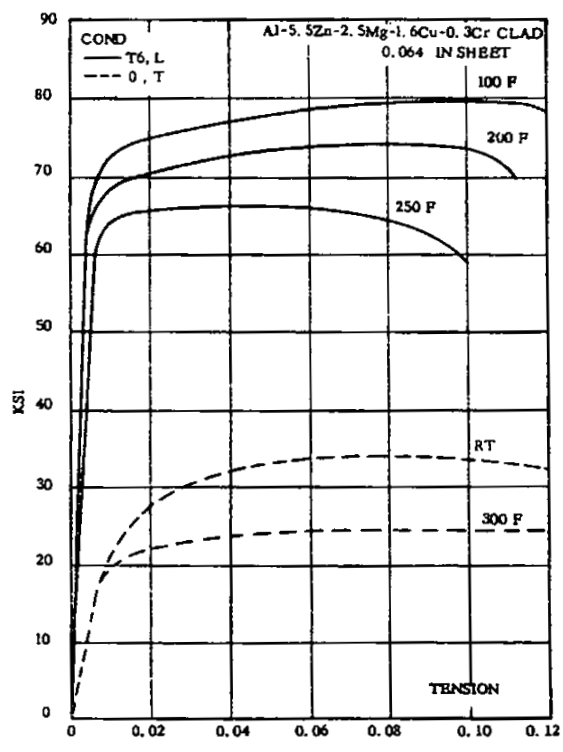


FIG. 3.0311 COMPLETE STRESS STRAIN CURVES FOR SHEET IN 0 AND T6 CONDITIONS AT ROOM AND ELEVATED TEMPERATURES (10, Fig. 19, 20)

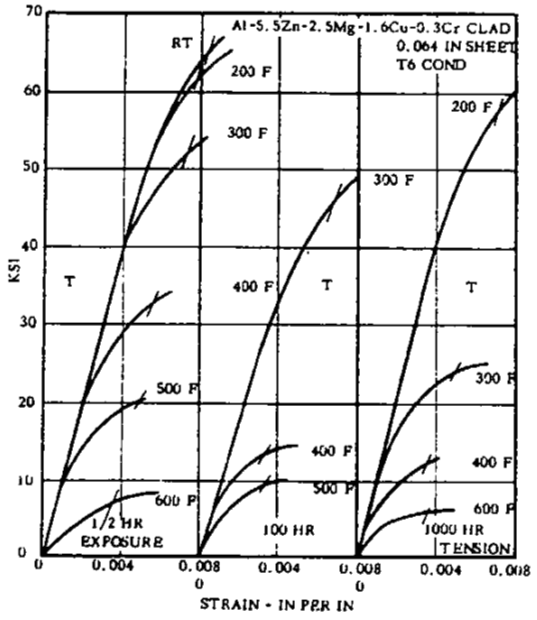
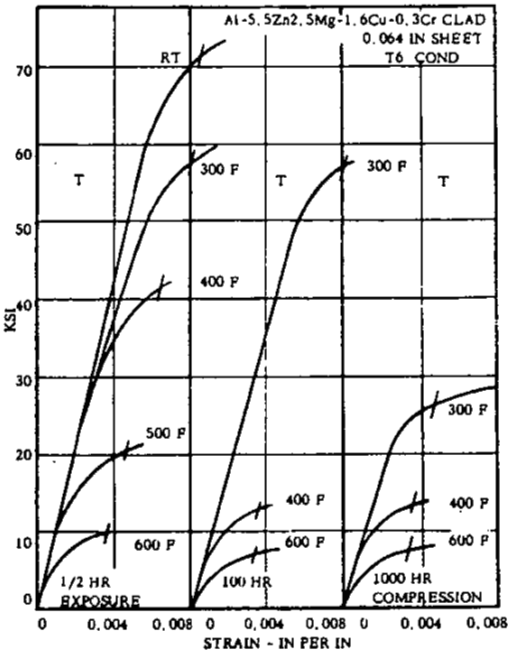


FIG. 3.0312 STRESS STRAIN CURVES FOR SHEET IN T6 CONDITION AT ROOM AND ELEVATED TEMPERATURES

(12, p. 169, 174)



	Al
5.5	Zn
2.5	Mg
1.6	Cu
0.3	Cr

CLAD 7075

FIG. 3.0321 STRESS STRAIN CURVES IN COMPRESSION FOR SHEET IN T6 CONDITION AT ROOM AND ELEVATED TEMPERATURES

(12, p. 175-180)

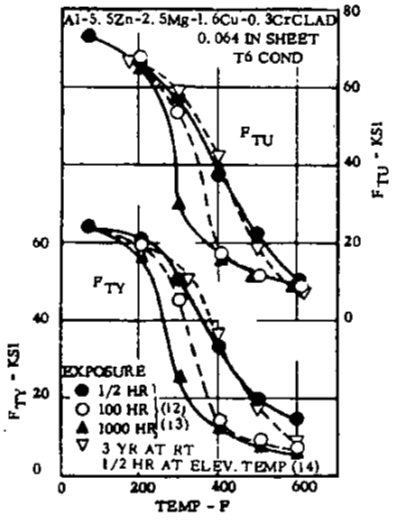


FIG. 3.0313 EFFECT OF EXPOSURE AND TEST TEMPERATURE ON TENSILE PROPERTIES OF SHEET IN T6 CONDITION

(12, p. 101)(13, p. 52)(14, p. 29, 30)

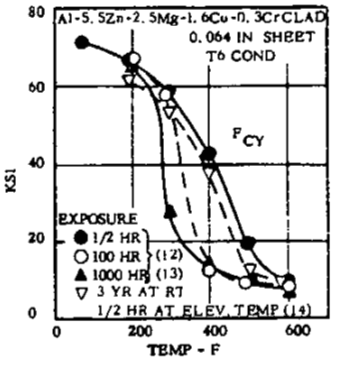


FIG. 3.0322 EFFECT OF EXPOSURE AND TEST TEMPERATURE ON COMPRESSIVE YIELD STRENGTH OF SHEET IN T6 CONDITION

(12, p. 102)(13, p. 52)(14, p. 27)

	Al
5.5	Zn
2.5	Mg
1.6	Cu
0.3	Cr

CLAD 7075

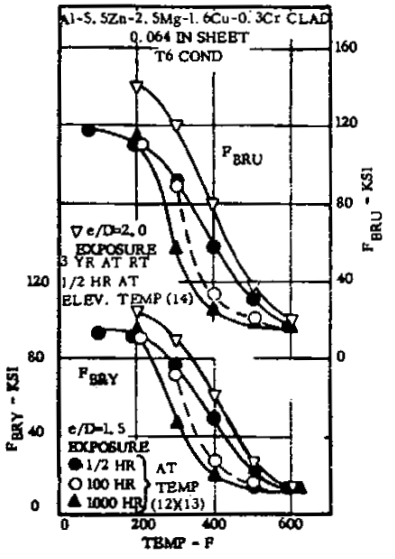


FIG. 3.0323 EFFECT OF EXPOSURE AND TEST TEMPERATURE ON BEARING PROPERTIES OF SHEET IN T6 CONDITION (12, p. 103)(13, p. 52)(14, p. 25)

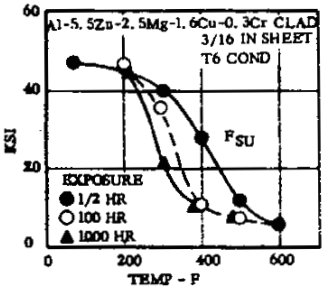


FIG. 3.0324 EFFECT OF EXPOSURE AND TEST TEMPERATURE ON SHEAR STRENGTH OF SHEET IN T6 CONDITION (12, p. 104)(13, p. 52)

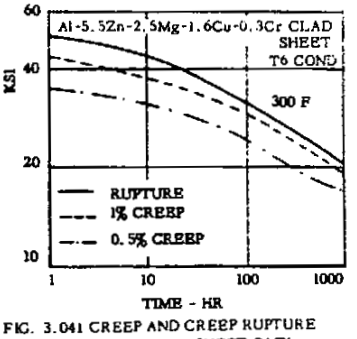


FIG. 3.041 CREEP AND CREEP RUPTURE CURVES FOR SHEET IN T6 CONDITION AT 300F (15, p. 5)

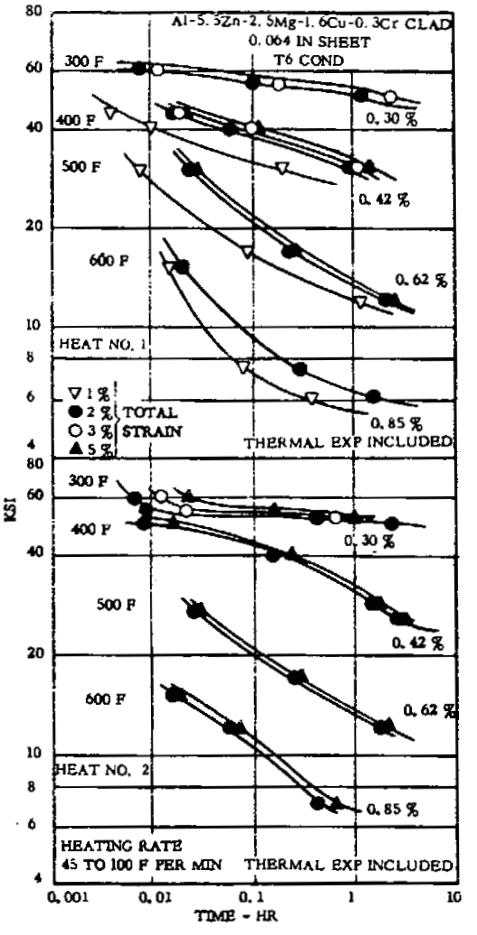


FIG. 3.042 SHORT TIME TOTAL STRAIN CURVES FOR SHEET IN T6 CONDITION AT 300 TO 600 F (16, p. 38-41)

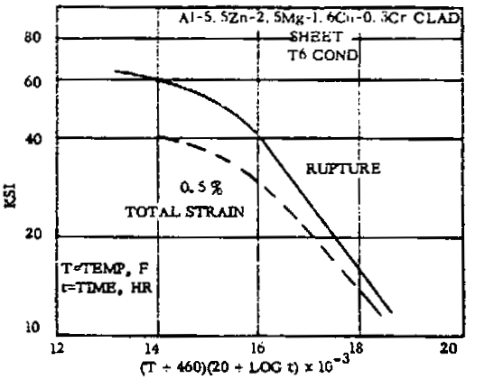


FIG. 3.043 MASTER CURVES FOR 0.5 PERCENT TOTAL STRAIN AND CREEP RUPTURE FOR SHEET IN T6 CONDITION (15, p. 8)

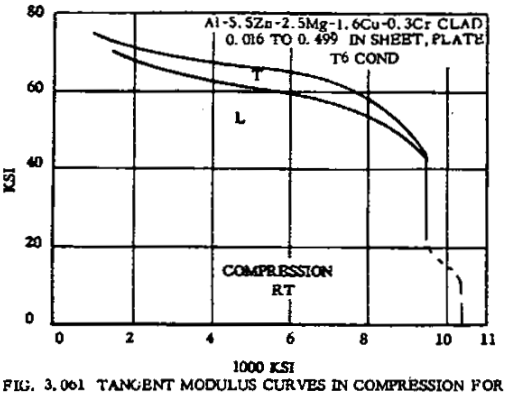


FIG. 3.061 TANGENT MODULUS CURVES IN COMPRESSION FOR SHEET AND PLATE IN T6 CONDITION AT ROOM TEMPERATURE (9, p. 84)

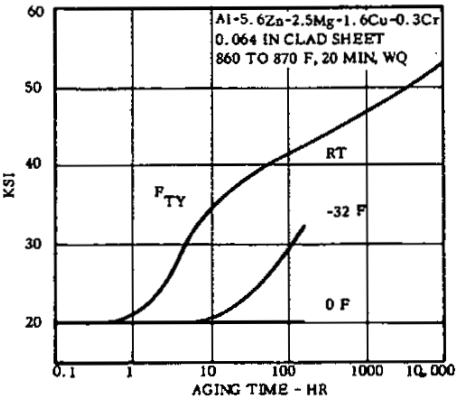


FIG. 4.011 RELATIONSHIP OF HOLDING TIME TO FORMING TEMPERATURES FOR SHEET IN T6 CONDITION (17)

	Al
5.5	Zn
2.5	Mg
1.6	Cu
0.3	Cr

CLAD 7075

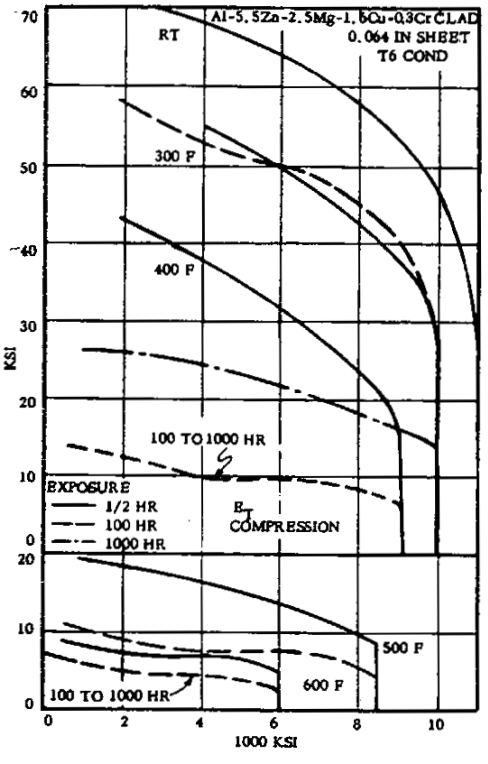


FIG. 3.062 TANGENT MODULUS CURVES IN COMPRESSION FOR SHEET IN T6 CONDITION AT ROOM AND ELEVATED TEMPERATURES (12, p. 185-189)

REFERENCES

1 AMS 4039, (April 30, 1960)
2 AMS 4046, (Jan. 15, 1961)
3 AMS 4057 B, (Jan. 15, 1957)
4 AMS 4048 C, (Aug. 15, 1958)
5 AMS 4049 C, (Aug. 15, 1958)
6 Aluminum Association, "Standards for Wrought Aluminum Mill Products", 4th Edition, (Aug. 1961)
7 Alcoa Aluminum Handbook, (1959)
8 Reynolds Metal Co., "The Aluminum Data Book, "(1958)
9 Department of Defense, "Strength of Metal Aircraft Elements," ANC-5, (March 1955)
10 Sachs, G., Espey, G., and Kasik, G. B., "Correlation of Information Available on the Fabrication of Aluminum Alloys, "Sect. IV, Pt. V, National Defense Research Committee, (Sept. 15, 1944)
11 Achbach, W. P., Favor, R. J. and Hyler, W. S., "Materials-Property-Design Criteria for Metals," Pt. VI, WADC TR 55-150, (Oct. 1957)
12 Doerr, D. D., "Determination of Physical Properties of Non-Ferrous Structural Sheet Materials at Elevated Temperatures", Pt. I, AF TR 6517, (Dec. 1951)
13 Miller, D. E., "Determination of Physical Properties of Ferrous and Non-Ferrous Structural Sheet Materials at Elevated Temperatures", Pt. 3, AF TR 6517, (June 1954)
14 Miller, D. E., "Determination of the Tensile, Compressive and Bearing Properties of Ferrous and Non-Ferrous Structural Sheet Materials at Elevated Temperatures", Pt. 5, AF TR 6517, (Dec. 1957)
15 Hyler, W. S. and Crover, H. J., "Materials-Property-Design Criteria for Metals, "Pt. 2, WADC TR 55-150, (Nov. 1955)
16 VanEcho, J. A., Gulloti, D. V., Bilster, J. R. and Simmons, W. F., "Short-Time Creep Properties of Structural Sheet Materials for Aircraft and Missiles", Pt. 4, AF TR 6731, (Jan. 1956)
17 Nock and Wooll, Iron Age, Vol. 159, (1947)

1 General

Aluminum alloy 7150 is a refinement of alloy 7050. The chemical composition of 7150 and 7050 are compatible, so an alloy can usually be defined either way. Composition limits for 7150 were adjusted to eliminate a small range of compositions which would produce mechanical properties at the lower end of the distribution, permitting a small increase in the allowable design strengths. Alloy 7150 has a marginally higher range of zinc content and a marginally lower range of copper and magnesium (Table 1.4.1). It should be noted, however, that as producers usually avoid the extremes of the composition ranges, 7150, as supplied to normal orders, will satisfy the requirements of 7050 as well. The more developed alloy, 7150, has been used as a vehicle for the introduction of improved tempers, e.g., T61511 and T7751, which have superior corrosion and other properties. In other tempers, the alloy has fatigue, stress corrosion, and exfoliation corrosion properties similar to 7050. It is the new tempers that have caused renewed interest in the alloy.

Its most conspicuous use is for wing plates on a majority of large commercial aircraft, where its relatively high compressive yield strength is an advantage; however, subject to specification legalities, it may be used technically anywhere that 7050 is used.

1.1 Commercial Designation

7150.

1.2 Alternate Designation

UNS No. A97150.

1.3 Specifications

1.3.1 *[Table]* AMS material specifications.

1.4 Composition

1.4.1 *[Table]* Aluminum Association registered chemical composition limits.

1.5 Heat Treatment

Heat treatments are generally proprietary to the producer. Solution heat treatments are similar to alloy 7050.

1.5.1 T Tempers. Peak aging treatments to T6 tempers are similar to 7050; however, the T6151, T61511, T7751, and T77511 aging treatments are not only proprietary, but also patented. The alloy may be produced in the same tempers as for alloy 7050. These include T6, T74, and T76 tempers (see Code 3222).

1.5.2 Annealing. Soak at 775F for 2 to 3 hours, cool at 50F per hour to 500F. The subsequent cooling rate is unimportant (Ref. 1).

1.6 Hardness

1.7 Forms and Conditions Available

Sheet, plate, extrusions, die and hand forgings.

1.8 Melting and Casting Practices

This alloy is supplied in the wrought form and is not recommended for foundry applications.

Al
6.4 Zn
2.4 Mg
2.2 Cu
0.12 Zr

1.9 Special Considerations

7150 has a high compressive yield strength (Ref. 4) which is particularly important in upper wing plates on large commercial aircraft.

This alloy is essentially similar to alloy 7050, and the majority of properties are closely similar or superior to 7050. It is recommended that data for 7050 in Code 3222 of this handbook be reviewed by the reader.

2 Physical Properties and Environmental Effects

2.1 Thermal Properties

2.1.1 Melting Range. The melting range is expected to be the same as for alloy 7050; i.e., 910 - 1165F (Ref. Code 3222).

2.1.2 Phase Changes. The alloy is subject to precipitation, but the solid matrix is always face centered cubic.

2.1.2.1 Time temperature transformation diagrams.

2.1.3 Thermal Conductivity at Room Temperature. The thermal conductivity of 7150 is expected to be the same as that for the appropriate temper of 7050; i.e.,

T7651, 89 Btu/ft/hr/ft^2/F

T7451, 91 Btu/ft/hr/ft^2/F

T7351, 93 Btu/ft/hr/ft^2/F

(Ref. Code 3222, Section 2.013)

2.1.4 Thermal Expansion (see Section 1.9).

2.1.5 Specific Heat.

2.1.6 Thermal Diffusivity.

2.2 Other Physical Properties

2.2.1 Density. 0.102 lb/cu in. (Ref.4).

2.2.2 Electrical Properties.

2.2.2.1 Electrical conductivity.

2.2.3 Magnetic Properties. Alloy is non-magnetic.

© 1993 by Purdue Research Foundation, West Lafayette, Indiana 47907. All Rights Reserved. U.S. Government License. This material may be used, duplicated or disclosed by United States Government agencies without the payment of any royalty.

2.3 Chemical Environments

2.3.1 General Corrosion. The corrosion performance of this alloy is markedly sensitive to the heat treatment condition. Overall, the corrosion resistance improves for T651, to T6151 or T61511, to T7751. The alloy is subject to exfoliation corrosion; however, the degree depends strongly on the product temper.

2.3.1.1 *[Table]* Exfoliation corrosion resistance of 7150 plate.

2.3.2 Stress Corrosion Resistance.

2.3.2.1 *[Table]* Stress corrosion resistance of 1.75-in. thick 7150-T7751 plate (Ref. 9).

2.3.2.2 *[Table]* Short transverse stress corrosion results for 1.75-in. thick 7150-T7751 plate (Ref. 9).

2.3.2.3 *[Table]* Stress corrosion test results on "C" ring specimens of 1.1-in. thick 7150-T77 plate (Ref. 11).

2.3.2.4 *[Figure]* Stress corrosion crack growth rates for a specimen of 1.1-in. thick 7150-T77 plate (Ref. 11).

2.4 Nuclear Properties

3 Mechanical Properties

3.1 Specified Mechanical Properties

3.1.1 *[Table]* Aluminum Association specified minimum tensile properties (Ref. 5).

3.1.2 *[Table]* Design mechanical properties of 7150-T6151 plate.

3.1.3 *[Table]* Minimum (S-Basis) design mechanical properties of 7150-T7751 plate.

3.1.4 *[Table]* Minimum (S-Basis) design mechanical properties of 7150-T61511 extrusions.

3.1.5 *[Table]* Minimum (S-Basis) design mechanical properties of 7150-T77511 extrusions.

3.2 Mechanical Properties at Room Temperature

3.2.1 Tension.

3.2.1.1 *[Figure]* Typical tensile stress-strain curves for 7150-T6151 plate.

3.2.1.2 *[Figure]* Typical tensile stress-strain curves for 7150-T61511 extrusion.

3.2.1.3 *[Figure]* Typical tensile stress-strain curves for 7150-T7751 plate.

3.2.1.4 *[Figure]* Typical tensile stress-strain curves for 7150-T77511 extrusion.

3.2.1.5 *[Table]* Producer guaranteed minimum long transverse mechanical properties of 7150-T6151 plate.

3.2.1.6 *[Table]* Mechanical properties and exfoliation rating in the longitudinal direction for various tempers of 7150 plate compared to alloys 7075 and 7050 (Ref. 3).

3.2.1.7 *[Table]* Tensile property variations through the thickness of 1-in. thick 7150-T6151 plate.

3.2.1.8 *[Table]* Tensile properties of 1-in. thick commercial 7150-T77 plate.

3.2.1.9 *[Table]* Tensile properties of 1.1-in. thick commercial 7150-T77 plate.

3.2.1.10 *[Table]* Tensile properties of 1.75-in. thick commercial 7150-T7751 plate.

3.2.2 Compression (see also 3.2.1.5 and 3.2.1.6 for F_{cy} data).

3.2.2.1 *[Figure]* Compressive stress-strain curves for 7150-T6151 plate.

3.2.2.2 *[Figure]* Compressive stress-strain curves for 7150-T61511 extrusion.

3.2.2.3 *[Figure]* Compressive stress-strain curves for 7150-T7751 plate.

3.2.2.4 *[Figure]* Compressive stress-strain curves for 7150-T77511 extrusion.

3.2.2.5 *[Figure]* Compressive tangent modulus curves for 7150-T6151 plate.

3.2.2.6 *[Figure]* Compressive tangent modulus curves for 7150-T61511 extrusion.

3.2.2.7 *[Figure]* Compressive tangent modulus curves for 7150-T7751 plate.

3.2.2.8 *[Figure]* Compressive tangent modulus curves for 7150-T77511 extrusion.

3.2.3 Impact.

3.2.4 Bending.

3.2.5 Torsion and Shear.

3.2.6 Bearing.

3.2.7 Stress Concentration.

3.2.7.1 Notch properties.

3.2.7.2 Fracture toughness.

3.2.7.2.1 *[Table]* Plane strain fracture toughness of 1-in. thick 7150-T6151 plate.

3.2.7.2.2 *[Table]* Plane strain fracture toughness of 1.75-in. thick 7150-T7751 plate.

3.2.7.2.3 *[Table]* Plane strain fracture toughness of 1.1-in. thick 7150-T7751 plate.

3.3 Mechanical Properties at Various Temperatures

3.3.1 Tension.

3.3.2 Compression.

3.3.3 Impact.

3.3.4 Bending.

3.3.5 Torsion and Shear.

3.3.6 Bearing.

3.3.7 Stress Concentration.

3.3.7.1 Fracture toughness.

3.3.8 Combined Properties.

3.4 Creep and Creep Rupture Properties

3.5 Fatigue Properties

3.5.1 Conventional High Cycle Fatigue Properties.

3.5.1.1 *[Figure]* Smooth and notched S-N fatigue data for 1.75-in. thick 7150-T7751 plate.

3.5.2 Low Cycle Fatigue.

3.5.2.1 *[Figure]* Low cycle fatigue behavior of 7150-T77 plate tested under strain control in longitudinal orientation.

3.5.2.2 *[Figure]* Low cycle fatigue behavior of 7150-T77 plate tested under strain control in transverse orientation.

3.5.2.3 *[Figure]* Cyclic stress response curves for a range of plastic strain amplitudes for 7150-T77 plate tested under strain control in longitudinal orientation.

3.5.2.4 *[Figure]* Cyclic stress response curves for a range of plastic strain amplitudes for 7150-T77 plate tested under strain control in transverse orientation.

3.5.3 Fatigue Crack Propagation.

3.5.3.1 *[Figure]* Fatigue crack growth data for 1.75-in. thick 7150-T7751 plate in L-T orientation.

3.5.3.2 *[Figure]* Fatigue crack growth data for 1.75-in. thick 7150-T7751 plate in T-L orientation.

3.5.3.3 *[Figure]* Fatigue crack growth rates at two stress ratios for 1-in. thick 7150 plate of various tempers.

3.5.3.4 *[Figure]* Fatigue crack growth rates for 1.1-in. thick 7150-T77 plate tested in high humidity air.

3.5.3.5 *[Figure]* Fatigue crack growth rates of 1-in. 7150 plate of various tempers. Small cracks and large cracks are compared.

3.5.3.6 Special considerations. The rates of growth of short cracks (i.e., those of sizes around 0.05 in. in length and which approach the dimensions of local microstructure or the local plastic region around the crack tip) are significant at stress intensity levels well below the fatigue threshold at which fatigue cracks are presumed dormant. These, in general, grow at rates much higher than "long" cracks (ca. 0.5 in. or greater). The use of "long" crack data to predict "short" crack behavior could lead to non-conservative predictions of structure life for this alloy and for many alloys of aluminum and other metals.

3.6 Elastic Properties

3.6.1 Poissons Ratio.

3.6.2 Tensile Elastic Modulus. Longitudinal - 68 GPa (9.86 x 10^6 psi), Transverse - 71 GPa (10.3 x 10^6 psi) (means of duplicate tests) (Ref. 10).

3.6.3 Compression Modulus.

4 Fabrication

4.1 Forming

4.2 Machining and Grinding

4.3 Joining

4.3.1 Weldability. Alloy 7150 is not weldable by conventional techniques.

4.4 Surface Treatment (see 1.9 and Code 3222, Section 4.4, of this handbook).

Table 1.3.1 AMS material specifications (Ref. 4)

Alloy: 7150			
AMS Specifications	**Form**	**Temper**	**Issue Date**
4306	Bare plate	T6151	October 1988
4252	Bare plate	T7751	October 1989
4307	Extrusion	T61511	October 1988
4345	Extrusion	T77511	October 1989

Table 1.4.1 Aluminum Association registered composition limits (Ref. 1)

Alloy: 7150			
Element		**Content (wt percent)**	
		Minimum	**Maximum**
Silicon		–	0.12
Iron		–	0.15
Copper		1.9	2.5
Manganese		–	0.10
Magnesium		2.0	2.7
Chromium		–	0.04
Zinc		5.9	6.9
Zirconium		0.08	0.15
Titanium		–	0.06
Others	Each	–	0.05
	Total	–	0.15

Table 2.3.1.1 Exfoliation corrosion resistance of 7150 plate (Ref. 3)

Alloy: 7150	
Form	1-in. Plate
Temper	**EXCO Rating**
T6151	EC
T7751	EB

Table 2.3.2.1 Stress corrosion resistance of 1.75-in. thick 7150-T7751 plate (Ref. 9)

Alloy: 7150-T7751		
Form	1.75-in. Plate	
Specimen	ST tensile bars, 0.16-in. diameter, 0.5-in. gage length	
Environment	Submerged 10 min./hr in 3.5 percent NaCl/H_2O, 50 min./hr in 30 percent RH air at 72F	
Test Stress (ksi)	**Exposure Time (hour)**	**Failure**
65	98	Yes
60	116	Yes
55	112	Yes
50	170	Yes
45	239	Yes
40	243	Yes
35	459	Yes
30	467	Yes
20	1198	No

Table 2.3.2.2 Short transverse stress corrosion results for 1.75-in. thick 7150-T7751 plate (Ref. 9)

Alloy: 7150-T7751	
Form	1.75-in. Plate
Specimen	C(T), B = 1 in., W = 2 in., dead weight loading[a]
Orientation	Short - Longitudinal
Environment	Constant immersion in distilled water with 3.5 percent NaCl, aerated at RT
Failure (hours)	**Applied Stress Intensity (ksi $\sqrt{in.}$)**
868	21.0
751	22.8
691	18.6

[a] Reference ASTM E 399.

Table 2.3.2.3 Stress corrosion test results on "C" ring specimens of 1.1-in. thick 7150-T7751 plate (Ref. 11)

Alloy: 7150-T7751	
Form	1.1-in. Plate
Specimen	"C" rings, 0.07-in. thick, screw loaded
Orientation	Short - Longitudinal
Environment	Alternate immersion in 3.5 percent NaCl/H_2O, 10 min., 50 min. in laboratory air at RT
Failure (hours)	**Applied Stress (ksi)**
21	70
24	50
504[a]	25
168	35

[a] Failure may have occurred earlier, but the crack was obscured by salt deposits.

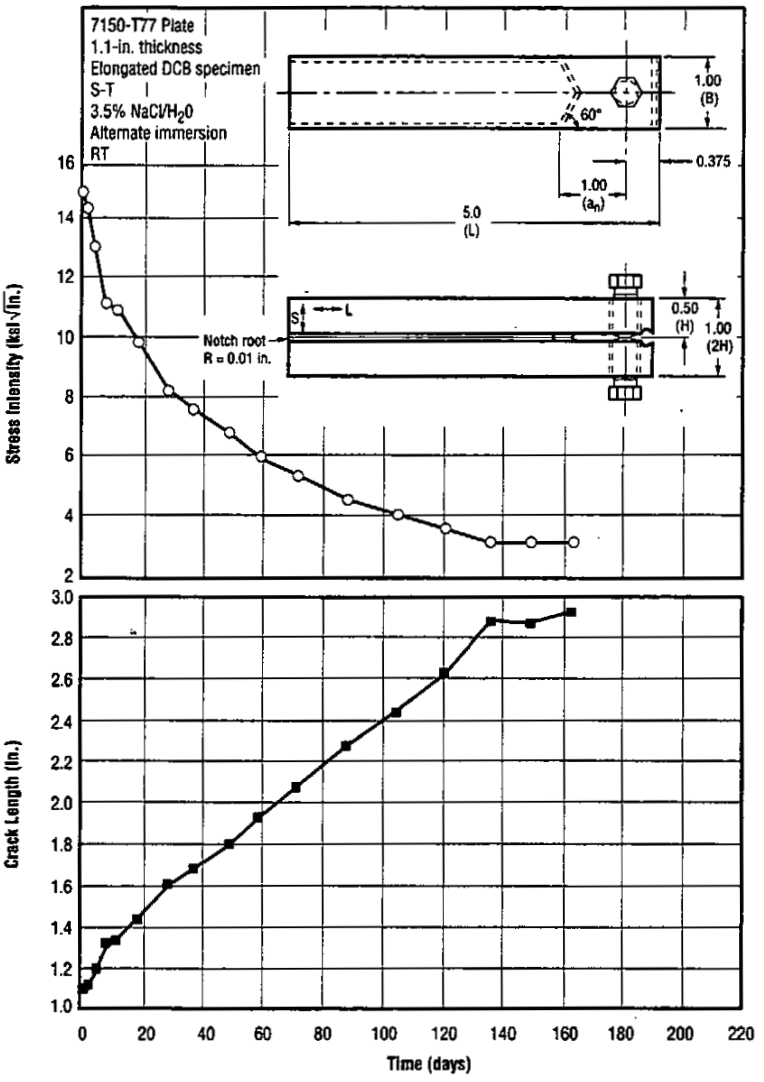


Fig. 2.3.2.4 Stress corrosion crack growth rates for a specimen of 1.1-in. thick 7150-T77 plate (Ref. 11)

Table 3.1.1 Aluminum Association registered minimum tensile properties (Ref. 5)

Alloy: 7150						
Form	**Temper**	**Thickness (in.)**	**Orientation**	**F_{tu} (ksi)**	**F_{ty} (ksi)**	**e (percent)**
Plate	T651	0.500 - 0.749	Longitudinal	83.0	78.0	8
			Transverse	84.0	77.0	8
		0.750 - 1.000	Longitudinal	84.0	78.0	8
			Transverse	84.0	78.0	8
		1.001 - 1.500	Longitudinal	84.0	78.0	8
			Transverse	84.0	77.0	8
Plate	T6151	0.750 - 1.000	Longitudinal	84.0	78.0	9
			Transverse	84.0	78.0	9
		1.001 - 1.500	Longitudinal	84.0	78.0	9
			Transverse	84.0	77.0	9
Extrusions	T6510 & T6511	0.250 - 0.749	Longitudinal	86.0	78.0	7
		0.750 - 2.00	Longitudinal	88.0	78.0	7
Extrusions	T61510 & T61511	0.249 max	Longitudinal	87.0	81.0	9
		0.250 - 0.499	Longitudinal	87.0	82.0	8
		0.500 - 0.749	Longitudinal	88.0	83.0	9
		0.750 - 2.000	Longitudinal	89.0	84.0	8
Plate	T7751	0.250 - 0.499	Longitudinal	80.0	74.0	8
			Transverse	80.0	74.0	8
		0.500 - 0.749	Longitudinal	83.0	77.0	8
			Transverse	83.0	76.0	8
		0.750 - 1.500	Longitudinal	84.0	78.0	8
			Transverse	84.0	77.0	8
		1.501 - 3.000	Longitudinal	82.0	76.0	7
			Transverse	82.0	75.0	6
Extrusions	T77511	0.240 max	Longitudinal	85.0	78.0	7
		0.250 - 0.499	Longitudinal	87.0	82.0	8
			Transverse	82.0	76.0	–
		0.500 - 0.749	Longitudinal	88.0	83.0	9
			Transverse	83.0	79.0	–
		0.750 - 2.000	Longitudinal	89.0	84.0	8
			Transverse	83.0	78.0	–

Table 3.1.2 Design mechanical properties of 7150-T6151 plate (Ref. 4)

Alloy: 7150-T6151					
Form		Plate			
Mechanical Properties		**Thickness (in.)**			
		0.750 - 1.000		**1.001 - 1.500**	
Basis[a]		**A**	**B**	**A**	**B**
F_{tu} (ksi)	Longitudinal	84[c]	87	84[d]	87
	Long Transverse	84	87	84[e]	86
F_{ty} (ksi)	Longitudinal	78[c]	81	78[d]	81
	Long Transverse	77	79	77	78
F_{cy} (ksi)	Longitudinal	77	80	75	77
	Long Transverse	81	83	80	82
F_{su} (ksi)		45	47	45	46
F_{bru} (ksi)[b]	e/D = 1.5	121	125	121	124
	e/D = 2.0	155	160	155	158
F_{bry} (ksi)[b]	e/D = 1.5	102	105	101	104
	e/D = 2.0	119	122	118	121
e, S-Basis (percent)	Longitudinal	9	–	9	–
	Long Transverse	9	–	9	–
E, 10^3 (ksi)		10.2			
E_c, 10^3 (ksi)		10.6			
G, 10^3 (ksi)		3.9			
μ		0.33			

[a] At least 99 percent (for A-Basis) and 90 percent (for B-Basis) of the population of values is expected to equal or exceed the mechanical property allowable, with a confidence of 95 percent.

[b] Bearing values are "dry pin" values.

[c] S-Basis - The A values are higher than specification minimum values as follows: $F_{tu}(L)$ = 85 ksi and $F_{ty}(L)$ = 79 ksi.

[d] S-Basis - The A values are higher than specification minimum values as follows: $F_{tu}(L)$ = 86 ksi and $F_{ty}(L)$ = 80 ksi.

[e] S-Basis - The A value is higher than specification minimum value as follows: $F_{tu}(LT)$ = 85 ksi.

Table 3.1.3 Minimum (S-Basis)[a] design mechanical properties of 7150-T7751 plate (Ref. 4)

Alloy: 7150-T7751					
Form		Plate			
Mechanical Properties		Thickness (in.)			
		0.250 - 0.499	0.500 - 0.749	0.750 - 1.500	1.501 - 3.000
F_{tu} (ksi)	Longitudinal	80	83	84	82
	Long Transverse	80	83	84	82
	Short Transverse	–	–	–	77
F_{ty} (ksi)	Longitudinal	74	77	78	76
	Long Transverse	74	76	77	75
	Short Transverse	–	–	–	67
F_{cy} (ksi)	Longitudinal	73	76	77	75
	Long Transverse	77	79	81	79
F_{su} (ksi)		46	47	48	47
F_{bru} (ksi)[b]	e/D = 1.5	119	124	125	122
	e/D = 2.0	154	160	162	158
F_{bry} (ksi)[b]	e/D = 1.5	102	105	106	104
	e/D = 2.0	117	120	121	118
e (percent)	Longitudinal	8	8	8	7
	Long Transverse	8	8	8	6
	Short Transverse	–	–	–	1
E, 10^3 (ksi)		10.3			
E_c, 10^3 (ksi)		10.7			
G, 10^3 (ksi)		3.9			
μ		0.33			

[a] S-Basis - Minimum value specified by the governing industry specification (e.g. AMS, ASTM, etc.) or federal or military standards for the material.

[b] Bearing values are "dry pin" values.

Table 3.1.4 Minimum (S-Basis)[a] design mechanical properties of 7150-T61511 extrusions (Ref. 4)

Alloy: 7150-T61511						
Form		Extrusions				
Mechanical Properties		**Thickness (in.)**				
		0.250 - 0.499	**0.500 - 0.749**	**0.750 - 0.999**	**1.000 - 1.499**	**1.500 - 2.000**
F_{tu} (ksi)	Longitudinal	87	88	89	89	89
	Long Transverse	80	79	79	77	74
F_{ty} (ksi)	Longitudinal	82	83	84	84	84
	Long Transverse	73	73	73	71	68
F_{cy} (ksi)	Longitudinal	80	81	82	83	84
	Long Transverse	80	80	80	78	75
F_{su} (ksi)		44	45	45	44	42
F_{bru} (ksi)[b]	e/D = 1.5	119	120	120	118	116
	e/D = 2.0	152	153	154	152	150
F_{bry} (ksi)[b]	e/D = 1.5	100	100	100	97	94
	e/D = 2.0	118	120	120	119	117
e (percent)	Longitudinal	8	9	8	8	8
E, 10^3 (ksi)		10.4				
E_c, 10^3 (ksi)		11.0				
G, 10^3 (ksi)		4.0				
μ		0.33				

[a] S-Basis - Minimum value specified by the governing industry specification (e.g. AMS, ASTM, etc.) or federal or military standards for the material.

[b] Bearing values are "dry pin" values.

Table 3.1.5 Minimum (S-Basis)[a] design mechanical properties of 7150-T77511 extrusions (Ref. 4)

Alloy: 7150-T77511					
Form		Extrusions			
Cross Sectional Area (in.^{2})		≤ 20			
Mechanical Properties		**Thickness (in.)**			
		≤ 0.249	**0.250 - 0.499**	**0.500 - 0.749**	**0.750 - 2.000**
F_{tu} (ksi)	Longitudinal	85	87	88	89
	Long Transverse	81	82	83	83
F_{ty} (ksi)	Longitudinal	78	82	83	84
	Long Transverse	74	76	79	78
F_{cy} (ksi)	Longitudinal	78	82	83	85
	Long Transverse	76	80	81	82
F_{su} (ksi)		44	45	46	46
F_{bru} (ksi)[b]	e/D = 1.5	122	124	125	123
	e/D = 2.0	158	161	162	159
F_{bry} (ksi)[b]	e/D = 1.5	100	105	106	108
	e/D = 2.0	118	124	125	127
e (percent)	Longitudinal	7	8	9	8
E, 10^3 (ksi)		10.4			
E_c, 10^3 (ksi)		10.9			
G, 10^3 (ksi)		4.0			
μ		0.33			

[a] S-Basis - Minimum value specified by the governing industry specification (e.g. AMS, ASTM, etc.) or federal or military standards for the material.

[b] Bearing values are "dry pin" values.

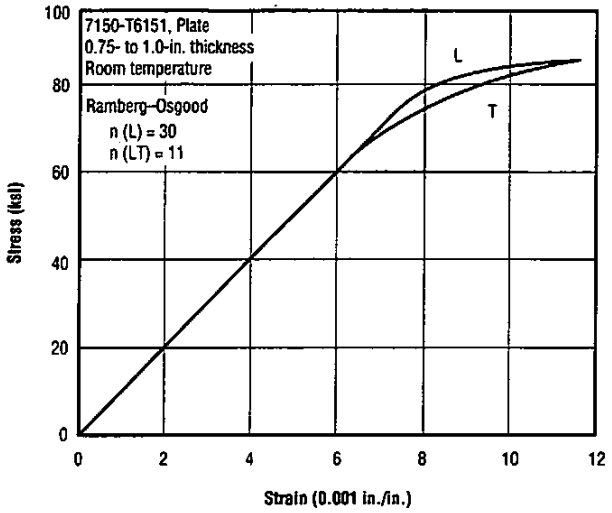


Fig. 3.2.1.1 Typical tensile stress-strain curves for 7150-T6151 plate (Ref. 4)

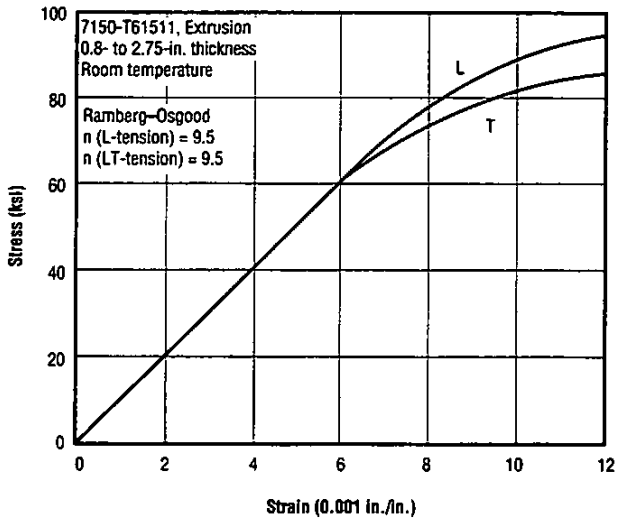


Fig. 3.2.1.2 Typical tensile stress-strain curves for 7150-T61511 extrusion (Ref. 4)

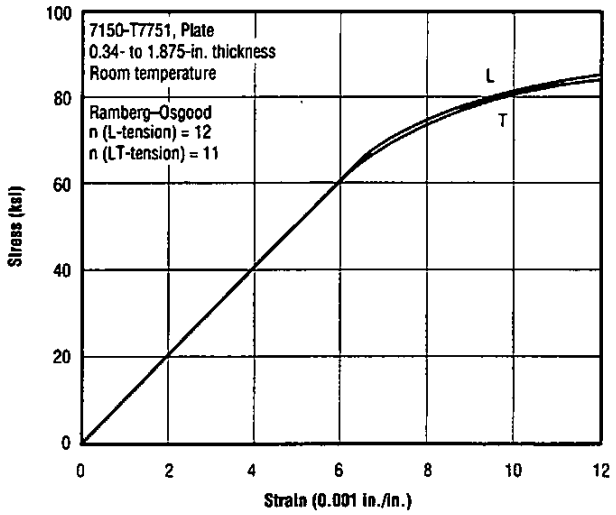


Fig. 3.2.1.3 Typical tensile stress-strain curves for 7150-T7751 plate (Ref. 4)

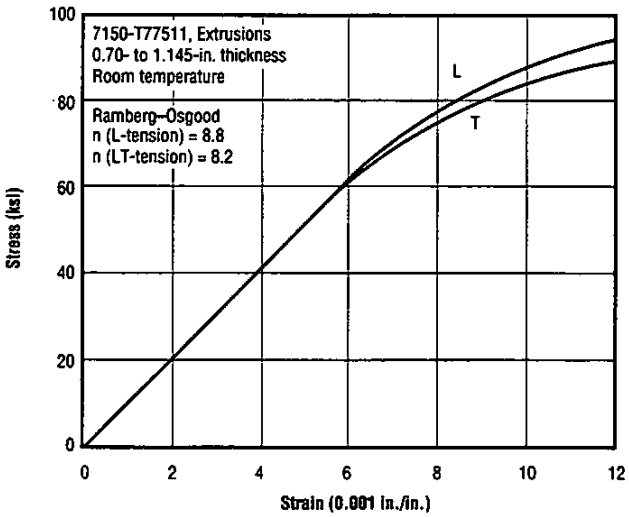


Fig. 3.2.1.4 Typical tensile stress-strain curves for 7150-T77511 extrusion (Ref. 4)

Table 3.2.1.5 Producer guaranteed minimum long transverse mechanical properties of 7150-T6151 plate (Ref. 2)

Alloy: 7150-T6151				
Form	Plate			
Thickness (in.)	F_{tu} (ksi)	F_{ty} (ksi)	F_{cy} (ksi)	e (percent)
0.750 - 1.000	84	78	77	9
1.001 - 1.500	84	77	77	9

Table 3.2.1.6 Mechanical properties and exfoliation rating in the longitudinal direction for various tempers of 7150 plate compared to alloys 7075 and 7050 (Ref. 3)

Alloy: 7150						
Form		1-in. Plate				
Alloy	Temper	F_{tu} (ksi)	F_{ty} (ksi)	F_{cy} (ksi)	e (percent)	EXCO Rating
7150	T7751	84	78	77	8	EB
7150	T6151	84	78	77	9	EC
7075	T651	76	69	66	6	ED
7075	T7651	70	59	59	6	EB
7050	T7651	76	66	65	6	EB
7050	T7451	74	64	63	10	EB

Table 3.2.1.7 Tensile property variations through the thickness of 1-in. thick 7150-T6151 plate (Ref. 6)

Alloy: 7150-T6151[a]				
Form	1-in. Plate			
Orientation	Longitudinal			
Location	**F_{tu} (ksi)**	**F_{ty} (ksi)**	**e (percent)**	**RA (percent)**
T/4	91	85	12	22
T/2	91	84	11	18
3T/4	92	84	12	18

Note: T/4 and 3T/4 refer to the quarter thickness and three quarter thickness of the plate, and T/2 to the mid thickness.

The diameters of the reduced sections of the tensile specimens were 0.5 in. at T/2, and 1/4 in. at T/4 and 3T/4.

[a] Identified as early notation, T6E189, in reference.

Table 3.2.1.8 Tensile properties of 1-in. thick commercial 7150-T77 plate (Ref. 10)

Alloy: 7150-T77		
Form	1-in. Plate[a]	
	Orientation	
	Longitudinal	**Transverse**
F_{ty} (ksi)	77.7	81.3
F_{tu} (ksi)	84.0	85.3
e, 1-in. (percent)	13.5	10.5
RA (percent)	22	15
True Strain to Fracture (percent)	0.25	0.17
True Fracture Stress (ksi)	92.1	91.3

[a] Tested at mid-thickness.

Table 3.2.1.9 Tensile properties of 1.1-in. thick commercial 7150-T77 plate (Ref. 11)

Alloy: 7150-T77		
Form	1.1-in. Plate[a]	
	Orientation	
	Longitudinal[b]	**Transverse[c]**
F_{ty} (ksi)	83.2	86.5
F_{tu} (ksi)	89.1	90.7
e, 1 in. (percent)	10.3	10.0
RA (percent)	32.3	26.4

[a] Tested at mid-thickness.

[b] Average of 3 specimens.

[c] Average of 2 specimens.

Table 3.2.1.10 Tensile properties of 1.75-in. thick commercial 7150-T7751 plate (Ref. 9)

Alloy: 7150-T7751			
Form	1.75-in. Plate[a]		
Orientation	**F_{ty} (ksi)[b]**	**F_{tu} (ksi)[b]**	**e, 1-in. (percent)[b]**
Longitudinal	82.6	86.4	8.9
Transverse	80.3	86.1	8.3
Short Transverse	74.7	82.6	7.4

[a] Tested at mid-plane.

[b] Averages of 3 specimens.

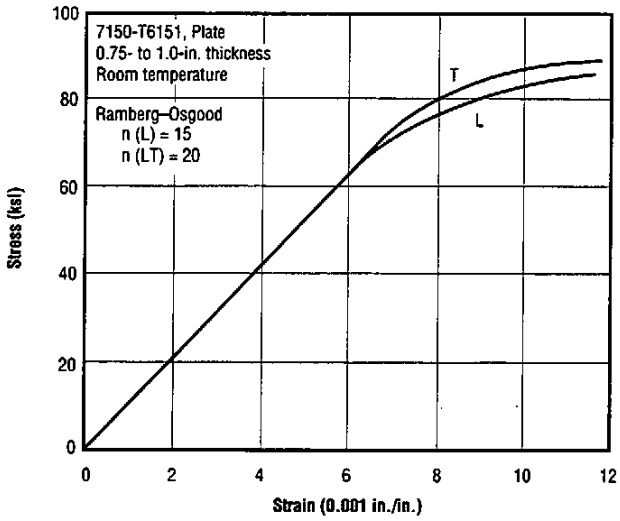


Fig. 3.2.2.1 Typical compressive stress-strain curves for 7150-T6151 plate (Ref. 4)

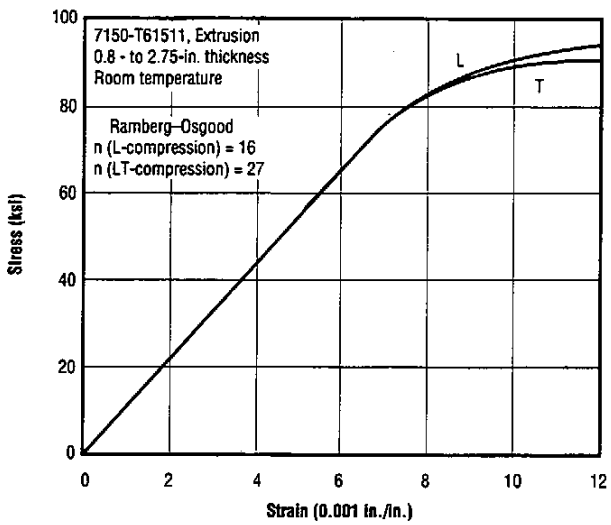


Fig. 3.2.2.2 Typical compressive stress-strain curves for 7150-T61511 extrusion (Ref. 4)

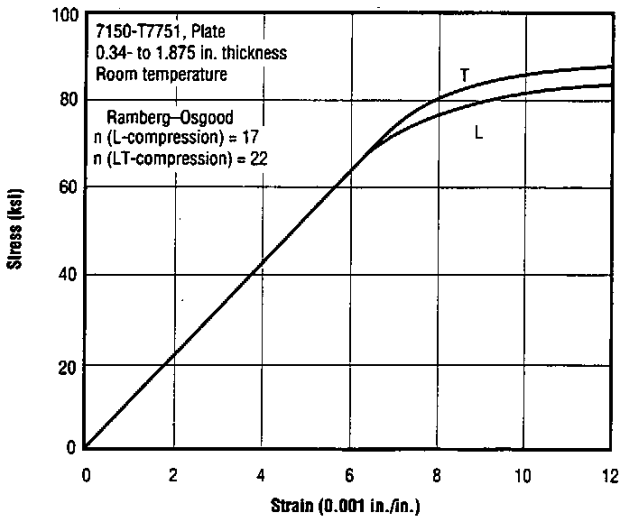


Fig. 3.2.2.3 Typical compressive stress-strain curves for 7150-T7751 plate (Ref. 4)

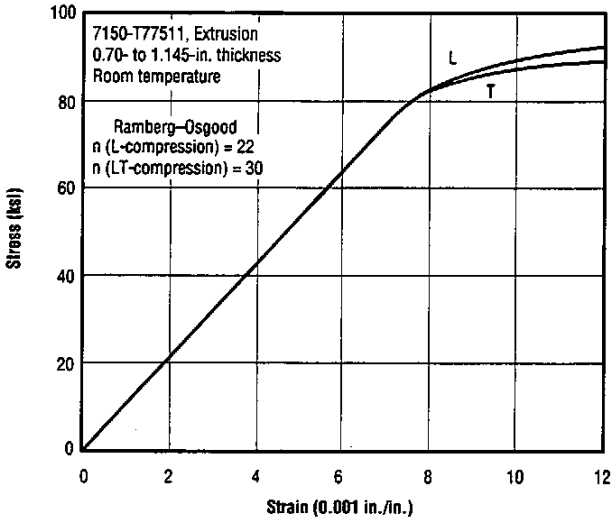


Fig. 3.2.2.4 Typical compressive stress-strain curves for 7150-T77511 extrusion (Ref. 4)

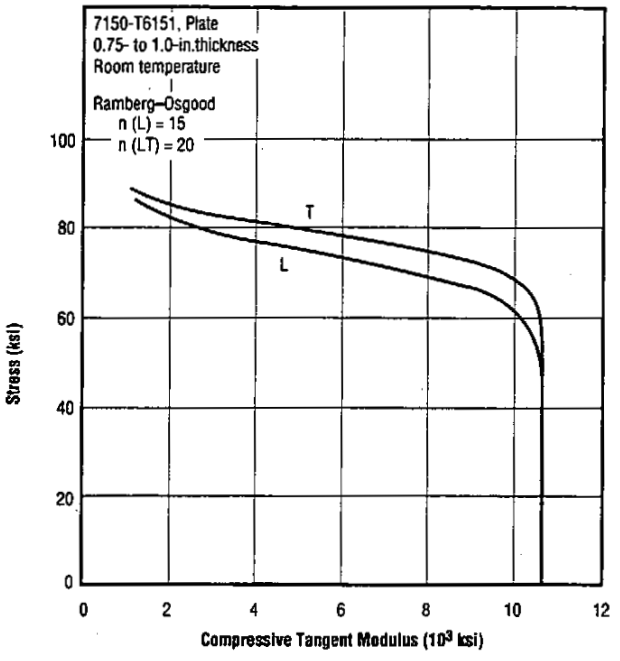


Fig. 3.2.2.5 Typical compressive tangent modulus curves for 7150-T6151 plate (Ref. 4)

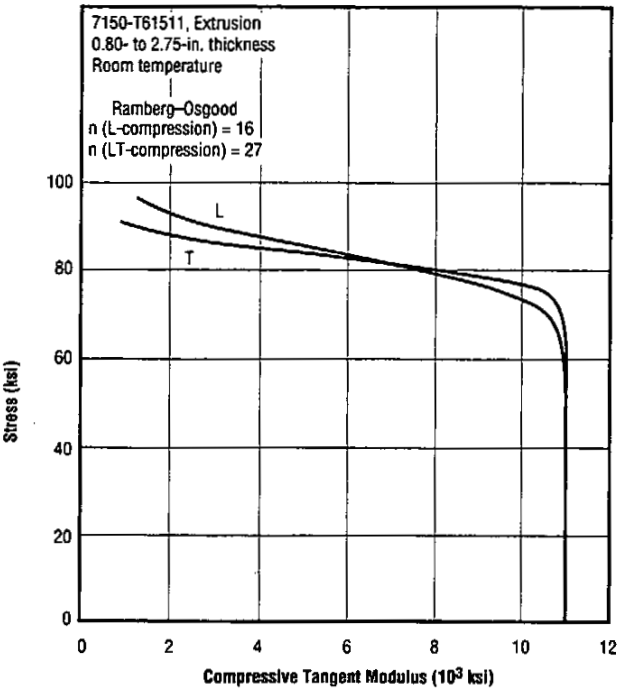


Fig. 3.2.2.6 Typical compressive tangent modulus curves for 7150-T61511 extrusion (Ref. 4)

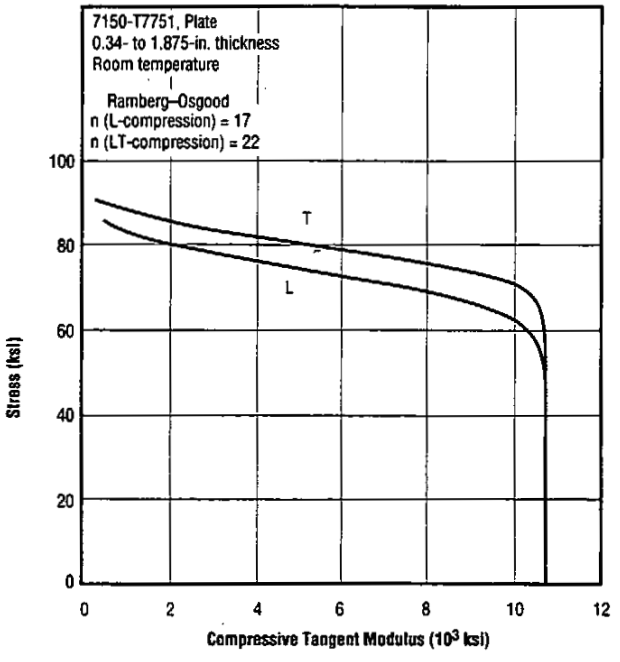


Fig. 3.2.2.7 Typical compressive tangent modulus curves for 7150-T7751 plate (Ref. 4)

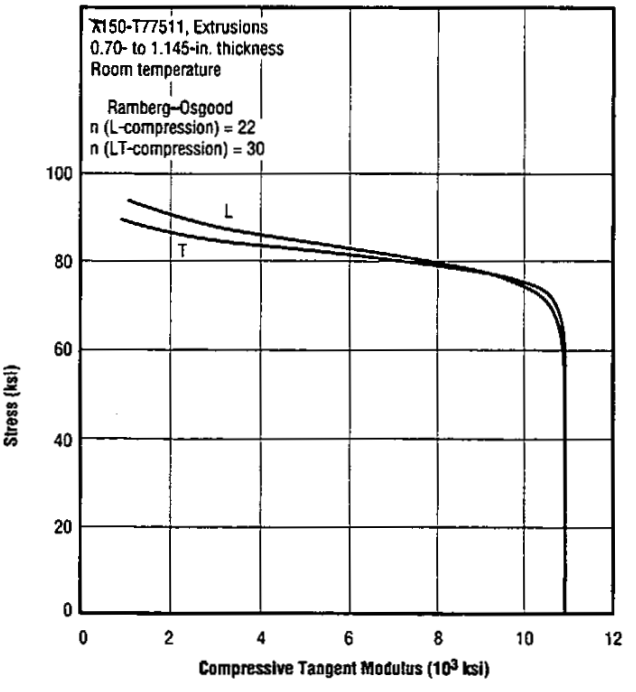


Fig. 3.2.2.8 Typical compressive tangent modulus curves for 7150-T77511 extrusion (Ref. 4)

Table 3.2.7.2.1 Plane strain fracture toughness of 1-in. thick 7150-T6151 plate (Ref. 6)

Alloy: 7150-T6151[a]	
Form	1-in. Plate
Orientation	L-T
Fracture Toughness, K_{Ic} (ksi $\sqrt{in.}$)[b]	
27	
29	

[a] Identified as early notation, T6E189, in reference.

[b] Tests valid according to ASTM E 399, average of 2 tests.

Table 3.2.7.2.2 Plane strain fracture toughness of 1.75-in. thick 7150-T7751 plate (Ref. 9)

Alloy: 7150-T7751	
Form	1.75-in. Plate
Specimen	C(T), B = 1 in., W = 2 in.[a]
Orientation	**Fracture Toughness, K_{Ic} (ksi $\sqrt{in.}$)[b]**
L-T	20.7
T-L	20.9
S-L	22.8

[a] Reference ASTM E 399.

[b] Average of 5 tests.

Table 3.2.7.2.3 Plane strain fracture toughness of 1.1-in. thick 7150-T7751 plate (Ref. 11)

Alloy: 7150-T7751	
Form	1.1-in. Plate
Specimen	C(T), B = 1 in.[a]
Orientation	**Fracture Toughness, K_{Ic} (ksi $\sqrt{in.}$)[b]**
L-T	23.8
T-L	22.0

[a] Reference ASTM E 399.

[b] Average of 3 tests.

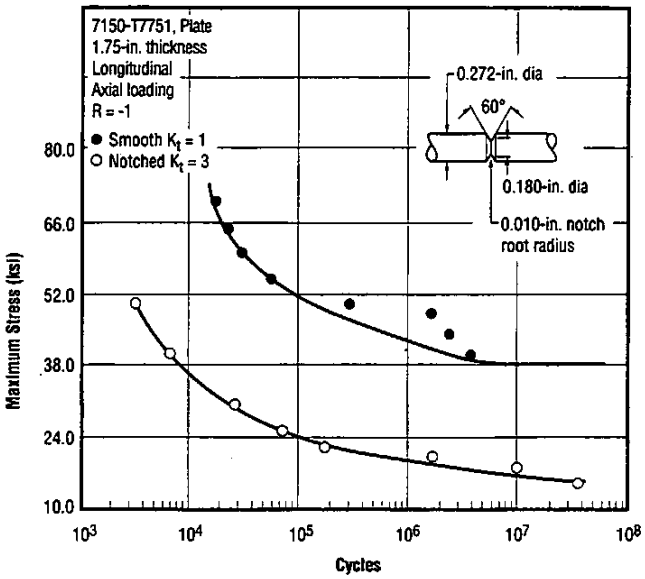


Fig. 3.5.1.1 Smooth and notched SN fatigue data for 1.75-in. thick 7150-T7751 plate (Ref. 9)

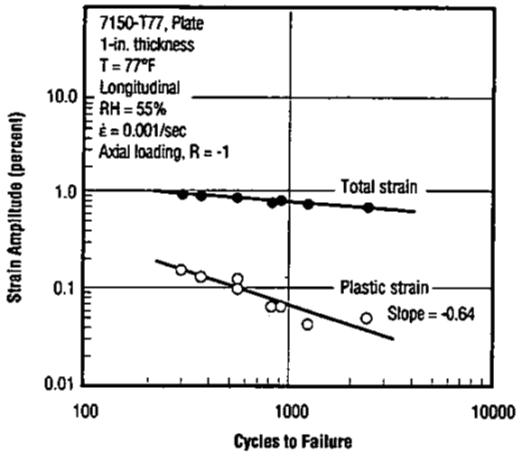


Fig. 3.5.2.1 Low cycle fatigue behavior of 7150-T77 plate tested under axial strain control in longitudinal orientation (Ref. 10)

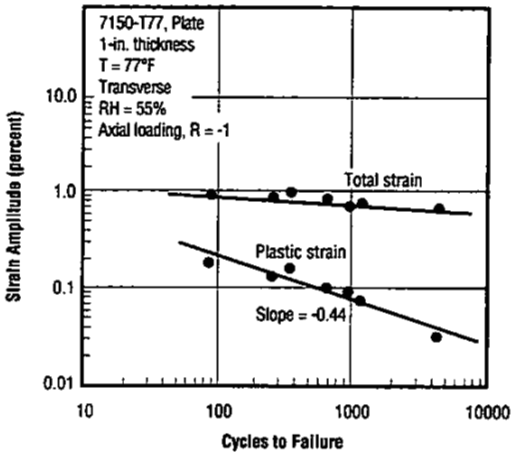


Fig. 3.5.2.2 Low cycle fatigue behavior of 7150-T77 plate tested under axial strain control in transverse orientation (Ref. 10)

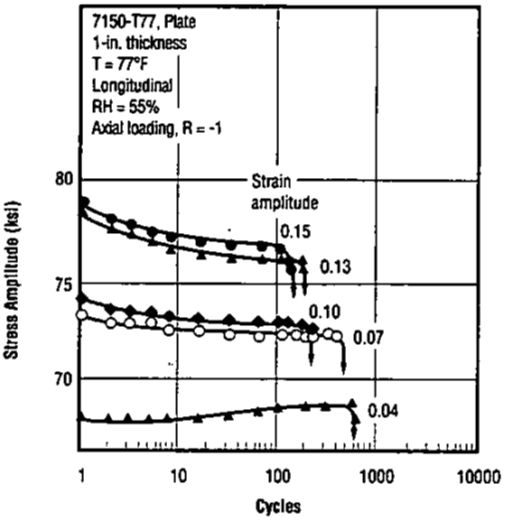


Fig. 3.5.2.3 Cyclic stress response curves for a range of plastic strain amplitudes for 7150-T77 plate tested under axial strain control in longitudinal orientation (Ref. 10)

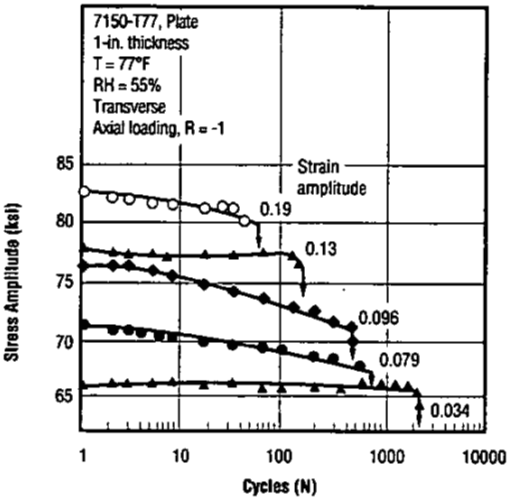


Fig. 3.5.2.4 Cyclic stress response curves for a range of plastic strain amplitudes for 7150-T77 plate tested under axial strain control in transverse orientation (Ref. 10)

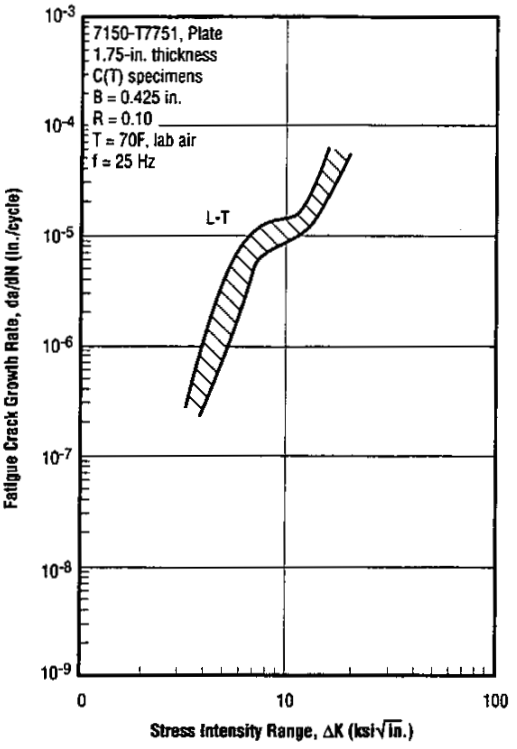


Fig. 3.5.3.1 Fatigue crack growth data for 1.75-in. thick 7150-T7751 plate in L-T orientation (Ref. 9)

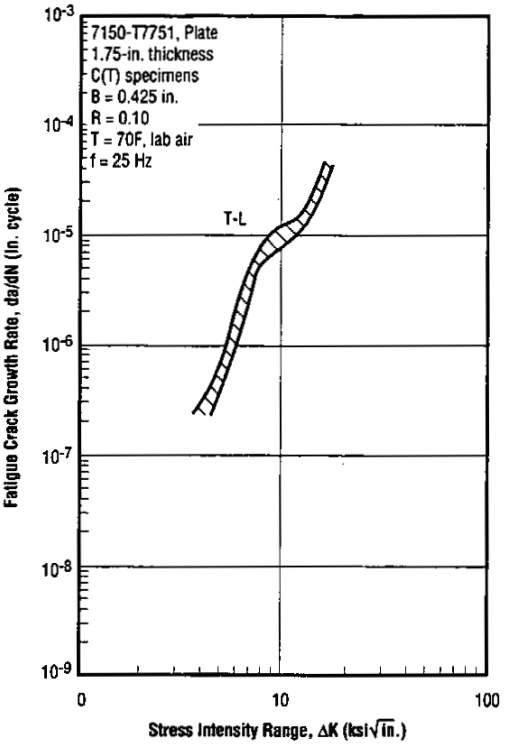


Fig. 3.5.3.2 Fatigue crack growth data for 1.75-in. thick 7150-T7751 plate in T-L orientation (Ref. 9)

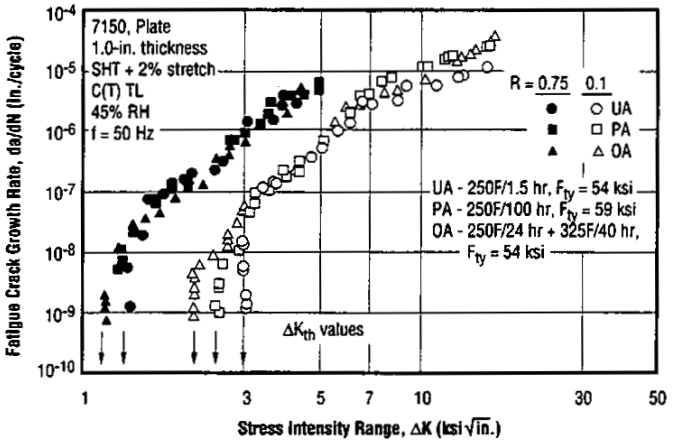


Fig. 3.5.3.3 Fatigue crack growth rates at two stress ratios for 1-in. plate of various tempers (Ref. 8)

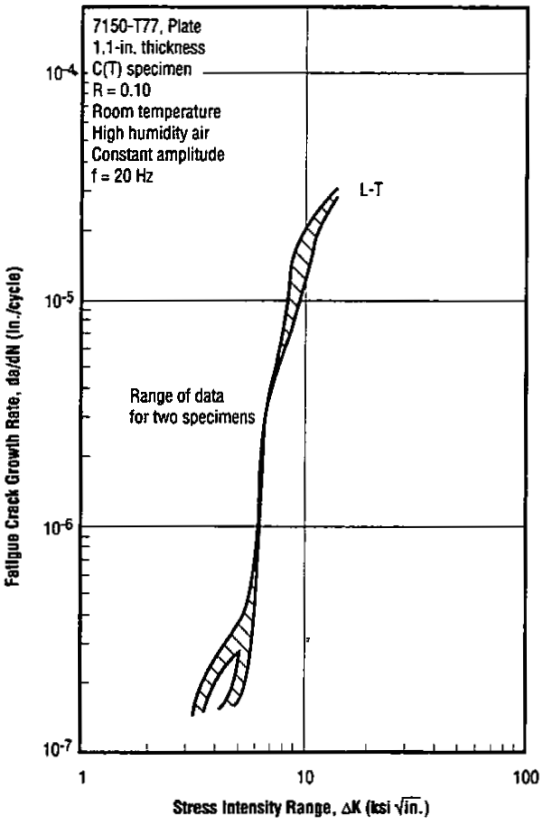


Fig. 3.5.3.4 Fatigue crack growth rates for 1.1-in. thick 7150-T77 plate tested in high humidity air (Ref. 11)

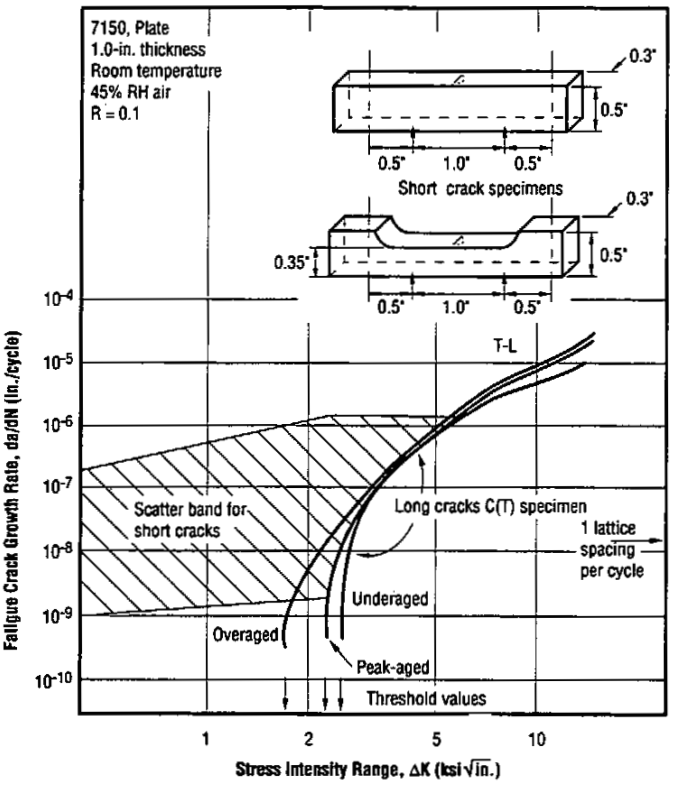


Fig. 3.5.3.5 Fatigue crack growth rates of 1.0 in. 7150 plate of various tempers. Small cracks and large cracks are compared (Ref. 8)

References

1. "Registration Record of International Alloy Designations and Chemical Composition Limits for Wrought Aluminum and Wrought Aluminum Alloys," Aluminum Association, Inc., Washington, DC (April 1991).
2. Alcoa Aerospace Technical Fact Sheet, "Alloy 7150-T6151 Plate," (February 1986).
3. Alcoa Aerospace Technical Fact Sheet, "New Alloy 7150-T7751," (September 1989).
4. "3.7.5, 7150 Alloy," *Military Handbook 5F*, p. 3-381 (November 1990).
5. "Tempers for Aluminum and Aluminum Alloy Products," Aluminum Association, Inc., Washington, DC (August 1989).
6. G. V. Scarich, and P. E. Bretz, "Fatigue Crack-Growth Resistance of Aluminum Alloys Under Spectrum Loading," Northrop Corporation, Aircraft Division, NOR 85-141 (December 1985).
7. E. Zaiken, and R. O. Ritchie, *Engineering Fracture Mechanics* Vol. 22, No. 1, pp. 35-48 (1985).
8. K. T. Venkateswara Rao; W. Yu; and R. O. Ritchie, "On the Behavior of Small Fatigue Cracks in Commercial Aluminum-Lithium Alloys," *Engineering Fracture Mechanics* Vol. 31, No. 4, pp. 623 (1988).
9. Patrick W. Ertel, "Mechanical Property Data on Aluminum Alloy 7150-T7751 Plate," Wright Research and Development Center, Wright Patterson AFB, OH 45433-6533. Interim Report No. WRDC-TR-90-4068 (August 1990).
10. T. S. Srivatsan, and David Lanning, Jr., "Cyclic Strain Resistance and Fracture Behavior of 7150 Aluminum Alloy," *Engineering Fracture Mechanics* Vol. 42, No. 5, pp. 877-892 (1992).
11. G. J. Petrak, *Air Force Materials Laboratory Evaluation Report*, No. MLS-88-17 (March 14, 1988).

This page is blank.

	Al
5.6	Zn
2.5	Mg
1.6	Cu
0.25	Cr
Low	Ti
	Mn
	Si

7175 Al

1 **GENERAL**

7175 is a wrought, heat treatable aluminum forging alloy produced by special techniques involving control of impurities, forging, and heat treating procedures. The alloy 7175 was developed to provide improvements in mechanical properties, fracture toughness, and stress-corrosion resistance when compared to 7075. It is available only in the form of die and hand forgings. Die forgings are available in the T66 and T74 tempers, while hand forgings are available in the T74 and T7452 tempers. The higher strength temper, T66, has longitudinal strength and fracture toughness approximately 15 percent higher than 7075-T6 but, like 7075-T6, its resistance to stress corrosion is relatively low. Die and hand forgings in the T74 condition develop static strengths about equal to those of 7075-T6 forgings, with fracture toughness and fatigue properties equal or superior to those of 7075-T73 forgings, plus high resistance to stress-corrosion cracking.

1.01 **Commercial Designations**

7175-T66 (die forgings)
7175-T74 (formerly T736) (die forgings)
7175-T74 (formerly T736) (hand forgings)
7175-T7452 (formerly T73652) (hand forgings).

1.02 **Alternate Designations**

UNS A97175.

1.03 **Specifications**

7175-T66 die forgings: AMS 4148A (19)
7175-T736 (T74) die forgings: AMS 4149A (20)
7175-T736 (T74) hand forgings: AMS 4149A (20)
7175-T73652 (T7452) hand forgings: AMS 4179A (21).

1.04 **Composition**

Chemical composition of 7175, Table 1.04.

1.05 **Heat Treatment**

1.051 The heat treatments for this alloy are proprietary to the producer, Alcoa (7). In general, the T66 temper indicates solution treatment followed by artificial aging. The T74 temper indicates solution treatment followed by stabilization (overaging). The T7452 temper indicates solution treatment, stress relieved by compressing to produce a permanent set of 1 to 5 percent, and precipitation heat treatment (21,22).

1.06 **Hardness**

1.061 Specified minimum hardness:
T66 die forgings, 140 Brinell (500-kg load, 10-mm ball) (19)
T74 die and hand forgings, 135 Brinell (500-kg load, 10-mm ball) (20)
T7452 hand forgings, 135 Brinell (500-kg load, 10-mm ball) (21).

1.062 Rockwell hardness of forgings, Table 1.062.

1.07 **Forms and Conditions Available**

Alloy 7175 is available as T66 and T74 die forgings and as T74 and T7452 hand forgings in section thicknesses up to 6 inches.

1.08 **Melting and Casting Practice**

The material can be melted and alloyed in oil-fired, gas-fired, or electric-induction furnaces and cast into ingot molds of any desired size for subsequent working into forging stock.

1.09 **Special Considerations**

1.091 Residual stresses are normally introduced into 7175-T66 and 7175-T74 forgings, as well as other aluminum forging alloys, in quenching from the solution heat treat temperature. A detailed study has shown that a 7175-T74 landing-gear cylinder forging had residual compressive stress on the outside surface from 9 to 15 ksi and on the inside surface from 6 to 12 ksi. These stresses are not believed to significantly influence resistance to stress corrosion, but they are sufficient to introduce distortion during machining, which must be taken into consideration in selecting and fabricating this alloy. Test programs are under way to evaluate stress relief treatments that will provide the optimum level of mechanical properties combined with acceptable levels of stress relief (2,3).

The forged properties are directional, the short-transverse mechanical properties and stress corrosion resistance being lower than those in the longitudinal and long-transverse directions.

2 **PHYSICAL AND CHEMICAL PROPERTIES**

2.01 **Thermal Properties**

2.011 Melting range, 893 to 1180 F (6).

2.012 Phase changes, alloy is subject to precipitation.

2.0121 Time-temperature-transformation diagrams.

2.0122 In the as-cast, annealed, or as-fabricated condition, the alpha matrix contains a coarse second phase of $MgZn_2$ which goes into solution during solution heat treatment. Artificial aging causes the formation first of Guinier-Preston Zones high in manganese and zinc and, subsequently, particularly at aging temperatures above 300 F, of finely divided precipitates of $MgZn_2$ and $MgZn_2Al_2$. With overaging (stabilization) copper also precipitates in finely divided form. The copper precipitate is believed to have a strongly favorable effect on resistance to stress corrosion (6,9).

2.013 Thermal conductivity:
76 Btu/ft/hr/ft²/F at 77 F for T66 temper
90 Btu/ft/hr/ft²/F at 77 F for T74 temper
90 Btu/ft/hr/ft²/F at 77 F for T7452 temper (16).

2.014 Thermal expansion:
12.5×10^{-6} in./in./F at 68 to 250 F (11)
12.9×10^{-6} in./in./F at 68 to 212 F (16).

2.015 Specific heat, 0.23 Btu/lb/F at 212 F (16).

2.016 Thermal diffusivity.

2.02 **Other Physical Properties**

2.021 Density, 0.101 lb/in.³ (11,16).

2.022 Electrical properties, Table 2.022.

2.023 Magnetic properties, nonmagnetic.

2.024 Emittance.

2.0241 Essentially the same as 7075 alloy in comparable tempers (10). (See 7075, Code 3207, Section 2.016.)

2.025 Damping capacity.

	Al
5.6	Zn
2.5	Mg
1.6	Cu
0.25	Cr
Low	Ti
	Mn
	Si

7175 Al

2.03 **Chemical Properties**

2.031 The alloy is subject to general corrosion in marine atmospheres (4).

2.032 Effects of specimen orientation, heat treatment, and stress on time to stress corrosion failure in alternate immersion tests in salt water, Table 2.032.

2.033 Effects of 84 days exposure to stress corrosion by alternate immersion in salt water on short-transverse residual strength and ductility of two forgings, Table 2.033.

2.034 Loss in long-transverse tensile strength as a result of various types of corrosion and stress corrosion exposures, Table 2.034.

2.035 Results of stress-corrosion tests on short-transverse specimens exposed to alternate 10-minute immersions in 3.5 percent sodium chloride solution and 50-minute drying periods, Figure 2.035.

2.036 Percent of short-transverse specimens, stressed at 42 ksi and 35 ksi, surviving alternate 10-minute immersions in 3.5 percent sodium chloride solution and 50-minute drying periods, Figure 2.036.

2.037 Crack-growth rate in precracked double cantilever beam specimens with stress applied in short-transverse direction; specimens were wet three times per day with 3.5 percent sodium chloride solution, Figure 2.037.

2.038 Stress-corrosion resistance of die forgings to 3.5 percent NaCl alternate immersion and to Federal Test Method 823, Figure 2.038.

2.0381 Results of stress-corrosion tests on die forgings in 3.5 percent NaCl alternate immersion, Figure 2.0381.

2.039 Results of stress corrosion tests on die forgings in an industrial atmosphere, Figure 2.039.

2.04 **Nuclear Properties**

(See 7075, Code 3207, Section 2.041.)

3 **MECHANICAL PROPERTIES**

3.01 **Specified Mechanical Properties**

3.011 AMS specified mechanical properties for T66 and T74 die forgings at room temperature, Table 3.011.

3.012 AMS specified mechanical properties for T74 and T7452 hand forgings at room temperature, Table 3.012.

3.013 Design mechanical properties for die forgings at room temperature, Table 3.013.

3.014 Design mechanical properties for hand forgings at room temperature, Table 3.014.

3.015 Specified mechanical properties for forgings at room temperature, Table 3.015.

3.02 **Mechanical Properties at Room Temperature**

3.021 Tension.

3.0211 Stress-strain diagrams. Typical stress-strain curves for die forgings and hand forgings at room temperature, Figure 3.0211.

3.0212 Tensile properties of forgings of various sizes, Table 3.0212.

3.0213 Tensile properties of Model 727 support elevator forging in two heat treated conditions, Table 3.0213.

3.0214 Tentative minimum tensile, fracture toughness, and stress-corrosion properties of T74 forgings, Table 3.0214.

3.022 Compression. (See also Tables 3.013, 3.014, and 3.015.)

3.0221 Stress-strain diagrams. (See Figure 3.0211.)

3.0222 Compressive yield strength of Model 727 support elevator forging in two heat treated conditions, Table 3.0222.

3.023 Impact.

3.0231 Charpy V-notch impact strength. (See Figure 3.0331.)

3.024 Bending.

3.025 Torsion and shear. (See also Tables 3.013, 3.014, and 3.015.)

3.0251 Longitudinal, T74 condition, F_{su} = 47.5 ksi (1); transverse, T74 condition, F_{su} = 49.2 ksi (1).

3.026 Bearing. (See Tables 3.013, 3.014, and 3.015.)

3.027 Stress concentration.

3.0271 Notch properties.

3.0272 Fracture toughness. (See also Table 3.0214.)

3.02721 Variations in plane strain fracture toughness with different heat treatments and specimen orientations, Table 3.02721.

3.02722 Fracture toughness of 7175-T66 die forgings, Table 3.02722.

3.02723 Fracture toughness of 7175-T74 die forgings, Table 3.02723.

3.02724 Fracture toughness of 7175-T74 and T7452 hand forgings, Table 3.02724.

3.028 Combined properties.

3.03 **Mechanical Properties at Various Temperatures**

3.031 Tension.

3.0311 Stress-strain diagrams.

3.03111 Tensile stress-strain curves at various temperatures, Figure 3.03111.

3.0312 Effect of temperature on tensile properties, Figure 3.0312.

3.0313 Effect of temperature on tensile properties of T74 die forgings, Figure 3.0313.

3.0314 Effect of test temperature on tensile properties of forged bar, Figure 3.0314.

3.032 Compression.

3.0321 Stress-strain diagrams.

3.03211 Compressive stress-strain curves at various temperatures, Figure 3.03211.

3.0322 Effect of temperature on compressive yield strength, Figure 3.0322.

3.033 Impact.

3.0331 Charpy V-notch impact properties at low temperatures, Figure 3.0331.

3.034 Bending.

3.035 Torsion and shear.

3.036 Bearing.

3.037 Stress concentration.

3.0371 Notch properties.

3.0372 Fracture toughness.

3.03721 Fracture toughness of forged bar at several temperatures, Table 3.03721.

3.038 Combined properties.

3.04 **Creep and Creep-Rupture Properties**

3.041 Creep and creep-rupture curves, Figure 3.041.

3.042 Minimum creep rate curves, Figure 3.042.

	Al
5.6	Zn
2.5	Mg
1.6	Cu
0.25	Cr
Low	Ti
	Mn
	Si

7175 Al

3.05 **Fatigue Properties**

3.051 Axial fatigue properties for forgings in T74 and T66 conditon, Figure 3.051.

3.052 Constant fatigue-life diagram for smooth, axially loaded, shot-peened specimens in T74 condition, Figure 3.052.

3.053 Constant fatigue-life diagram for notched, axially loaded specimens in T74 condition, Figure 3.053.

3.054 Axial fatigue properties at various temperatures for forgings in T74 condition, Figure 3.054.

3.055 Rotating beam fatigue properties for forgings in T74 and T66 conditions, Figure 3.055.

3.056 Fatigue crack-growth rates for T74 forgings at room temperature and elevated temperatures, Figure 3.056.

3.057 Fatigue crack-growth rates for T74 forgings at room temperature and at low temperatures, Figure 3.057.

3.06 **Elastic Properties**

3.061 Poisson's ratio, $\mu = 0.33$ (16).

3.062 Modulus of elasticity:
$E = 10.2 \times 10^3$ ksi
$E_c = 10.7 \times 10^3$ ksi (16).

3.0621 Effect of temperature on tensile modulus of elasticity, Figure 3.0621.

3.0622 Effect of temperature on compressive modulus of elasticity, Figure 3.0622.

3.0623 Compressive tangent modulus curves at various temperatures, Figure 3.0623.

3.0624 Typical compressive tangent modulus curves for T74 die forging and hand forgings at room temperature, Figure 3.0624.

3.063 Modulus of rigidity, $G = 3.9 \times 10^3$ ksi (3,16).

4 FABRICATION

4.01 **Forming**
(See 7075, Code 3207, Section 4.01.)

4.02 **Machining and Grinding**
Although detailed studies of the machining characteristics of 7175 have not been carried out, indications are that it has excellent machinability in both heat treated conditions similar to the 7075 alloy, which can be machined to excellent surface finish at high speeds and feeds while maintaining excellent tool life (13).

4.03 **Joining**
Welding. The weldability of 7175 alloy is comparable to that of 7075, which has a relatively low weldability rating (10). (See 7075, Code 3207, Sections 4.031 and 4.032.)

4.04 **Surface Treating**
Although little or no work on surface treating of 7175 has been done, it is expected that it will be susceptible to anodizing and to any other treatments applicable to 7075.

REFERENCES

1 AMS 4038A (1966).
2 AMS 4044C (1964).
3 AMS 4045C (1964).
4 AMS 4122D (1966).
5 AMS 4123C (1966).
6 AMS 4139F (1956).
7 AMS 4154G (1967).
8 AMS 4168A (1963).
9 AMS 4169B (1963).
10 AMS 4170 (1954).
11 Alcoa Aluminum Handbook (1962).
12 Aluminum Association, "Standards for Wrought Aluminum Mill Products" (September 1965).
13 ANC-5, "Strength of Metal Aircraft Elements" (March 1955).
14 Alcoa Research Laboratories, "Data Sheet" (September 9, 1957).
15 Howell, F. M. and Stickley, G. W., "Isochronous Stress-Strain Curves for Several Heat Treated Wrought Aluminum Alloys at 300 and 400 F", Alcoa Research Laboratories, Mechanical Testing Division (April 29, 1958).
16 MIL-HDBK-5c, Change Notice 1 (December 15, 1978).
17 The Aluminum Association, "Tempers for Aluminum Alloy Products Registered with the Aluminum Association", Revised June 15, 1970.
18 Aluminum Association Alloy Designations and Chemical Composition Limits for Wrought Aluminum Alloys, Revised February 1, 1971.
19 AMS 4148A, "Aluminum Alloy Die Forgings, 7175-T66", Society of Automotive Engineers, Warrendale, Pennsylvania, Revised July 1, 1981.
20 AMS 4149A, "Aluminum Alloy Forgings, 7175-T736", Society of Automotive Engineers, Warrendale, Pennsylvania, Revised October 1, 1981.
21 AMS 4179A, "Aluminum Alloy Hand Forgings, 7175-T73652", Society of Automotive Engineers, Warrendale, Pennsylvania, Revised July 1, 1981.
22 Aluminum Standards and Data, Seventh Edition, The Aluminum Association (June 1982).
23 Deel, O. L., "Collected Engineering Data Sheets" (Air Force Data Sheet Program), Prepared for Air Force Materials Laboratory by Battelle Columbus Division, AFML-TR-78-179 (December 1978).
24 Compilation of Fracture Mechanics Data From Alcoa, Contract No. F33615-73-C-5051, with Letter from R. H. Wygonik, Aluminum Company of America to J. E. Campbell, Battelle Columbus Division (June 1973).
25 Jones, R. E., "Fracture Toughness and Fatigue Crack Growth Properties of 7175-T736 Aluminum Alloy Forging at Several Temperatures", University of Dayton Research Institute, AFML-TR-72-1 (February 1972).
26 Lauchner, E. A., "Preventing Stress Corrosion Cracking in High Strength Aluminum Alloys", Metals Engineering Quarterly, Vol. 11, No. 2 (May 1971).
27 Speidel, M. O., "Stress Corrosion Cracking of Aluminum Alloys", *Metallurgical Transactions A*, Vol. 6A, No. 4, The Metallurgical Society of AIME and the American Society for Metals (April 1975).
28 Speidel, M. O. and Hyatt, M. V., "Stress Corrosion Cracking of High Strength Aluminum Alloys", Advances in Corrosion Science and Technology, Vol. 2, Edited by M. G. Fontana and R. Staehle, Plenum Press (1972).

	Al
5.6	Zn
2.5	Mg
1.6	Cu
0.25	Cr
Low	Ti
	Mn
	Si

7175 Al

29 Babilon, C. F., Wygonik, R. H., Nordmark, G. E., and Lifka, B. W., "Mechanical Properties, Fracture Toughness, Fatigue, Environmental Fatigue Crack Growth Rates, and Corrosion Characteristics of High Toughness Aluminum Alloy Forgings, Sheet and Plate", Aluminum Company of America, AFML-TR-73-83 (April 1973).

30 Staley, J. T., "Comparison of Aluminum Alloy 7050, 7049, MA52, and 7175-T736 Die Forgings", Alcoa Laboratories, AFML-TR-73-34 (May 1973).

Alloy	7175 Al		
	Percent	Percent	
Element	Nominal	Min	Max
Zn	5.6	5.1	6.1
Mg	2.5	2.1	2.9
Cu	1.6	1.2	2.0
Cr	0.23	0.18	0.28
Fe	–	–	0.20
Si	–	–	0.15
Mn	–	–	0.10
Ti	–	–	0.10
Others, Each	–	–	0.05
Total	–	–	0.15
Al	Balance	Balance	

TABLE 1.04. AMS CHEMICAL COMPOSITION OF 7175 Al (3,19,20,21)

Alloy	7175 Al	
Form	Forgings	
Condition	T66	T74
HRB	92	88
HRE	110	108

TABLE 1.062. ROCKWELL HARDNESS OF FORGINGS (3,5)

Alloy	7175 Al	
Form	Forgings	
Condition	T66	T74
Electrical Conductivity, percent IACS	29.8	38.7
megmhos/in.^{3}	0.440	0.570
Electrical Resistivity microhm, in.	2.28	1.76

TABLE 2.022. ELECTRICAL PROPERTIES (4,5,6)

	Al
5.6	Zn
2.5	Mg
1.6	Cu
0.25	Cr
Low	Ti
	Mn
	Si

7175 Al

Alloy	7175 Al					
Form	Forgings					
Condition	T66			T74		
Specimen Orientation	Stress (F_{ty}) ksi	Stress (F_{ty}) percent	Days to Stress Corrosive Failure[a]	Stress (F_{ty}) ksi	Stress (F_{ty}) percent	Days to Stress Corrosive Failure[a]
Longitudinal	21.0	25.0	NF[b]	55.5	75.0	NF[b]
	21.0	25.0	NF[b]	55.5	75.0	NF[b]
	42.0	50.0	NF[b]	55.5	75.0	NF[b]
	42.0	50.0	NF[b]	66.6	90.0	NF[b]
	63.0	75.0	NF[b]	66.6	90.0	NF[b]
	63.0	75.0	NF[b]	66.6	90.0	NF[b]
Long Transverse	19.75	25.0	NF	36.0	50.0	NF
	19.75	25.0	NF	36.0	50.0	>90
	19.75	25.0	7	36.0	50.0	NF
	29.63	37.5	7	54.0	75.0	NF
	29.63	37.5	NF	54.0	75.0	NF
	29.63	37.5	14.3	54.0	75.0	NF
	39.5	50.0	7	59.4	82.5	NF
	39.5	50.0	NF	59.4	82.5	NF
	39.5	50.0	1.3	59.4	82.5	NF
	59.25	75.0	1	64.8	90.0	NF
	59.25	75.0	2	64.8	90.0	NF
	59.25	75.0	1	64.8	90.0	NF
Short Transverse	8.75	12.5	NF	33.5	50.0	NF
	8.75	12.5	NF	33.5	50.0	NF
	8.75	12.5	NF	33.5	50.0	NF
	17.5	25.0	52.3	50.25	75.0	7
	17.5	25.0	14.3	50.25	75.0	8.25
	17.5	25.0	7	50.25	75.0	23
	35.0	50.0	2	60.3	90.0	1
	35.0	50.0	2	60.3	90.0	1.29
	35.0	50.0	2	60.3	90.0	1

(a) Alternate 10-minute immersions in 3.5 percent sodium chloride solution and 50-minute drying periods. Failure defined as the time at which the first crack was visually detected at 10X.

(b) NF means no failure in 105 days maximum test time.

TABLE 2.032. EFFECTS OF SPECIMEN ORIENTATION, HEAT TREATMENT, AND STRESS ON TIME TO STRESS CORROSION FAILURE IN ALTERNATE IMMERSION TESTS IN SALT WATER (4)

	Al
5.6	Zn
2.5	Mg
1.6	Cu
0.25	Cr
Low	Ti
	Mn
	Si

7175 Al

Alloy		7175Al		
Condition		T74		
Form		Forgings		
Specimen Orientation		Short Transverse		
Ultimate Tensile Strength, ksi	Elongation (1 in.), percent	Exposure Stress, ksi	Residual* F_{tu}, ksi	Residual*, Elongation (1 in.)
73.1	5.8	25.0	70.1	3.0
73.1	5.8	25.0	70.4	4.4
73.1	5.8	25.0	63.7	3.1
73.1	5.8	30.0	63.4	1.6
73.1	5.8	30.0	59.8	0.9
73.1	5.8	30.0	63.3	1.1
76.1	6.2	35.0	56.5	1.6
76.1	6.2	35.0	63.1	1.8
76.1	6.2	35.0	54.9	1.7
76.1	6.2	40.0	61.2	0.9
76.1	6.2	40.0	50.2	1.0
76.1	6.2	40.0	63.6	1.2

*After 84 days alternate 10-minute immersions in 3.5 percent sodium chloride solution and 50-minute drying periods at indicated exposure stresses.

TABLE 2.033. EFFECTS OF 84 DAYS EXPOSURE TO STRESS CORROSION BY ALTERNATE IMMERSION IN SALT WATER ON SHORT-TRANSVERSE RESIDUAL STRENGTH AND DUCTILITY OF TWO FORGINGS (5)

Alloy		7175Al		
Condition		T74		
Form		Forgings		
Specimen Orientation		Long Transverse		
Environment	Exposure Stress, ksi	Exposure Stress, percent of F_{ty}	Days Exposed	Loss in F_{tu}, percent
Marine Atmosphere (Kure Beach, NC 80-ft lot)	50.9	75	392	8
	33.8	50	392	5
	0	0	392	4
Alternate Immersion in 3 percent NaCl sol	50.9	75	61	12
	0	0	62	6
Alternate Immersion in 1N NaCl Sol + 0.3 percent H_2O_2	50.9	75	61	16
	0	0	61	5

Note: Each data point is an average of three tests. No specimens fractured in stress corrosion during exposure.

TABLE 2.034. LOSS IN LONG-TRANSVERSE TENSILE STRENGTH AS A RESULT OF VARIOUS TYPES OF CORROSION AND STRESS CORROSION EXPOSURES (12)

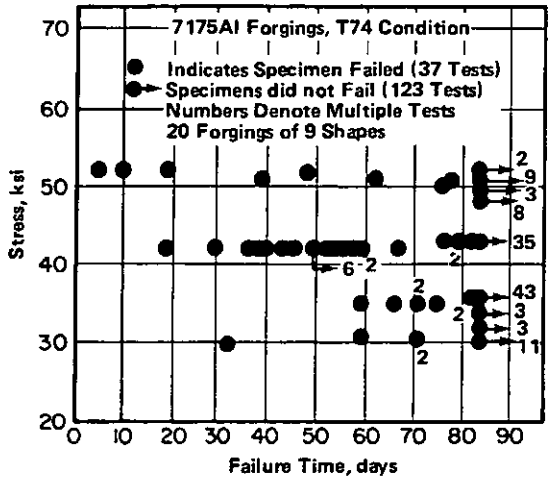


FIGURE 2.035. RESULTS OF STRESS-CORROSION TESTS ON SHORT-TRANSVERSE SPECIMENS EXPOSED TO ALTERNATE 10-MINUTE IMMERSIONS IN 3.5 PERCENT SODIUM CHLORIDE SOLUTION AND 50-MINUTE DRYING PERIODS (3)

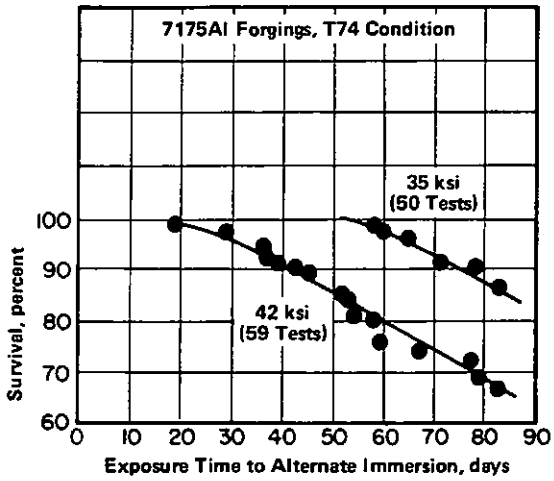


FIGURE 2.036. PERCENT OF SHORT-TRANSVERSE SPECIMENS, STRESSED AT 42 KSI AND 35 KSI, SURVIVING ALTERNATE 10-MINUTE IMMERSIONS IN 3.5 PERCENT SODIUM CHLORIDE SOLUTION AND 50-MINUTE DRYING PERIODS (3)

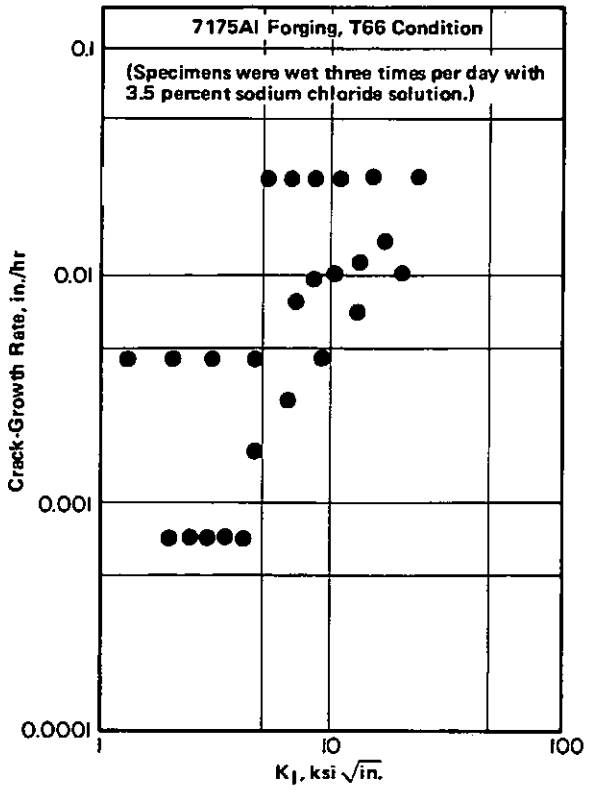


FIGURE 2.037. CRACK-GROWTH RATE IN PRECRACKED DOUBLE CANTILEVER BEAM SPECIMENS WITH STRESS APPLIED IN SHORT-TRANSVERSE DIRECTION (4,15)

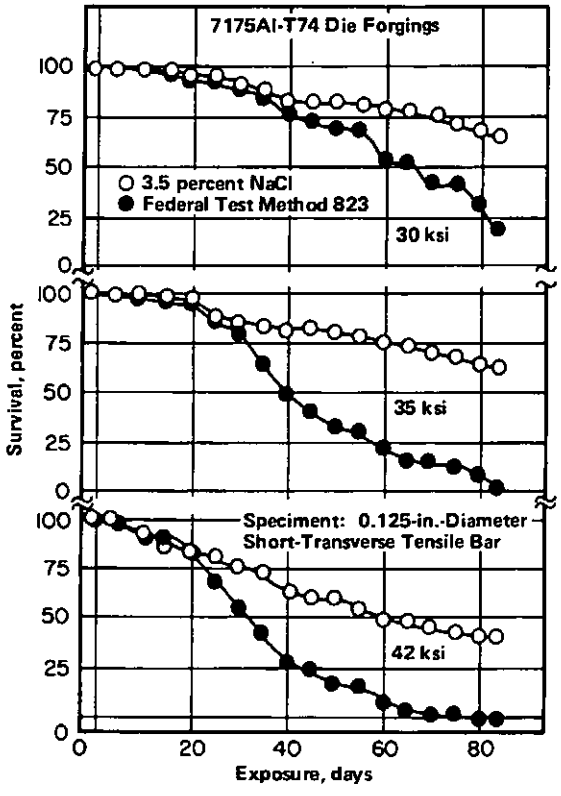


FIGURE 2.038. STRESS-CORROSION RESISTANCE OF DIE FORGINGS TO 3.5 PERCENT NaCl ALTERNATE IMMERSIONS AND TO FEDERAL TEST METHOD 823 (30)

	Al
5.6	Zn
2.5	Mg
1.6	Cu
0.25	Cr
Low	Ti
	Mn
	Si

7175 Al

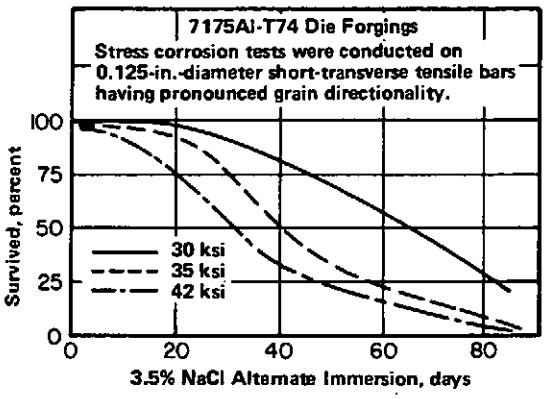


FIGURE 2.0381. RESULTS OF STRESS CORROSION-TESTS ON DIE FORGINGS IN 3.5 PERCENT NaCl ALTERNATE IMMERSION (30)

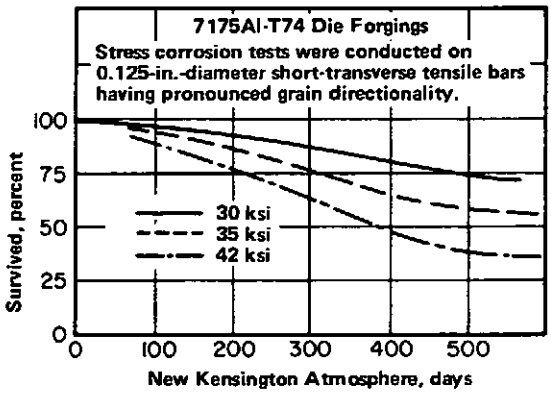


FIGURE 2.039. RESULTS OF STRESS-CORROSION TESTS ON DIE FORGING IN A INDUSTRIAL ATMOSPHERE (30)

Alloy		7175Al				
Specification		AMS 4148A	AMS 4149A			
Form		Die Forgings	Die Forgings			
Condition		T66	T74			
Thickness, in.		≤3.000	≤3.000	3.001-4.000	4.001-5.000	5.001-6.000
Ultimate Strength, ksi (Min)	L	86	76	73	70	68
	T	77	71	70	68	65
	A	77	71	70	68	65
Yield Strength, ksi (Min)	L	76	66	63	61	58
	T	66	62	60	58	55
	A	66	62	60	58	55
Elongation (2 in. or 4D), percent (Min)	L	7	7	7	7	7
	T	4	4	4	4	4
	A	4	4	4	4	4

L = Axis of specimen not more than 15° from parallel to forging flow lines.
T = Axis of specimen not more than 15° from perpendicular to forging flow lines.
A = Axis of specimen more than 15° from parallel and from vertical to flow lines.

TABLE 3.011. AMS SPECIFIED MECHANICAL PROPERTIES FOR T66 AND T74 DIE FORGINGS AT ROOM TEMPERATURE (19,20)

Alloy		7175Al									
Specification		AMS 4149A					AMS 4179A				
Condition		T74					T7452				
Form		Hand Forgings[a]					Hand Forgings[a]				
Thickness, in.		≤2.000	2.001-3.000	3.001-4.000	4.001-5.000	5.001-6.000	≤2.000	2.001-3.000	3.001-4.000	4.001-5.000	5.001-6.000
Ultimate Strength, ksi (Min)	L	73	73	71	68	65	71	71	68	65	63
	T	71	71	70	67	64	69	69	67	64	61
	ST	–	69	68	66	63	–	67	65	63	60
Yield Strength, ksi (Min)	L	63	63	61	57	54	61	61	57	54	51
	T	60	60	58	56	52	58	58	55	52	49
	ST	–	60	57	55	52	–	54	51	49	46
Elongation (2 in. or 4D), percent (Min)	L	9	9	9	8	8	9	9	9	8	8
	T	5	5	5	5	5	5	5	5	5	5
	ST	–	4	4	4	4	–	4	4	4	4

(a) Cross section not exceeding 156 $in.^2$.

TABLE 3.012. AMS SPECIFIED MECHANICAL PROPERTIES FOR T74 AND T7452 HAND FORGINGS AT ROOM TEMPERATURE (20,21)

	Al
5.6	Zn
2.5	Mg
1.6	Cu
0.25	Cr
Low	Ti
	Mn
	Si

7175 Al

Alloy		7175 Al	
Form		Die Forgings	
Specification		AMS 4148A	AMS 4149A
Condition		T66	T74
Thickness, in.		≤3.000	≤3.000
Ultimate Strength, ksi	L	86	76
	T(a)	77	71
Yield Strength, ksi	L	76	66
	T(a)	66	62
Compressive Yield Strength, ksi	L	–	67
	T(a)	–	63
Shear Strength, ksi		–	43
Ultimate Bearing Strength, ksi(b)			
e/D = 1.5		–	106
e/D = 2.0		–	140
Bearing Yield Strength, ksi(b)			
e/D = 1.5		–	86
e/D = 2.0		–	102
Elongation, percent	L	7	7
	T(a)	4	4

(a) T indicates grain direction not within ±15° of parallel to forging flow lines. F_{cy} (T) values are based upon short transverse test data.
(b) Bearing values are "dry pin" values.

TABLE 3.013. DESIGN MECHANICAL PROPERTIES FOR DIE FORGINGS AT ROOM TEMPERATURE (16)

Alloy		7175 Al							
Form		Hand Forgings							
Specification		AMS 4109(b)				AMS 4179			
Condition		T74				T7452			
Thickness, in.		≤3.000	3.001-4.000	4.001-5.000	5.001-6.000	≤3.000	3.001-4.000	4.001-5.000	5.001-6.000
Ultimate Strength, ksi	L	73	71	68	65	71	68	65	63
	LT	71	70	67	64	69	67	64	61
	ST	69	68	66	63	67	65	63	60
Yield Strength, ksi	L	63	61	57	54	61	57	54	51
	LT	60	58	56	52	58	55	52	49
	ST	60	57	55	52	54	51	49	46
Compressive Yield Strength, ksi	L	64	62	58	–	–	–	–	–
	LT	63	61	59	–	–	–	–	–
	ST	63	60	58	–	–	–	–	–
Shear Strength, ksi		42	41	39	–	–	–	–	–
Ultimate Bearing Strength, ksi(a)									
e/D = 1.5		103	101	97	–	–	–	–	–
e/D = 2.0		135	133	127	–	–	–	–	–
Bearing Yield Strength ksi(a)									
e/D = 1.5		84	81	78	–	–	–	–	–
e/D = 2.0		99	96	92	–	–	–	–	–
Elongation, percent	L	9	9	8	8	9	9	8	8
	LT	5	5	5	5	5	5	5	5
	ST	4	4	4	4	4	4	4	4

(a) Bearing values are "dry pin" values.
(b) The requirements of AMS 4109 are now embodied in AMS 4149A.

TABLE 3.014. DESIGN MECHANICAL PROPERTIES FOR HAND FORGINGS AT ROOM TEMPERATURE (16)

	Al
5.6	Zn
2.5	Mg
1.6	Cu
0.25	Cr
Low	Ti
	Mn
	Si

7175 Al

Alloy		7175Al	
Form		Forgings	
Size		Up 3 in. in Max Thickness	
Condition		T66	T74
Ultimate Strength, ksi (Min)	L	86	76
	ST	77	71
Yield Strength, ksi (Min)	L	76	66
	ST	66	62
Compressive Yield Strength, ksi (Min)	L	76	66
	ST	71	65
Shear Strength, ksi (Min)		47	42
Ultimate Bearing Strength, ksi (Min)			
e/D = 1.5		120	110
e/D = 2.0		150	141
Bearing Yield Strength, ksi (Min)			
e/D = 1.5		99	89
e/D = 2.0		110	99
Elongation (2 in.), percent (Min)	L	7	7
	ST	4	4

Note: For die forgings, the L and ST values for the directions parallel (within ±15°) and not parallel (as close as possible to the short-transverse direction), respectively, to the forging flow lines.

TABLE 3.015. SPECIFIED MECHANICAL PROPERTIES FOR FORGINGS AT ROOM TEMPERATURE (2,3,5)

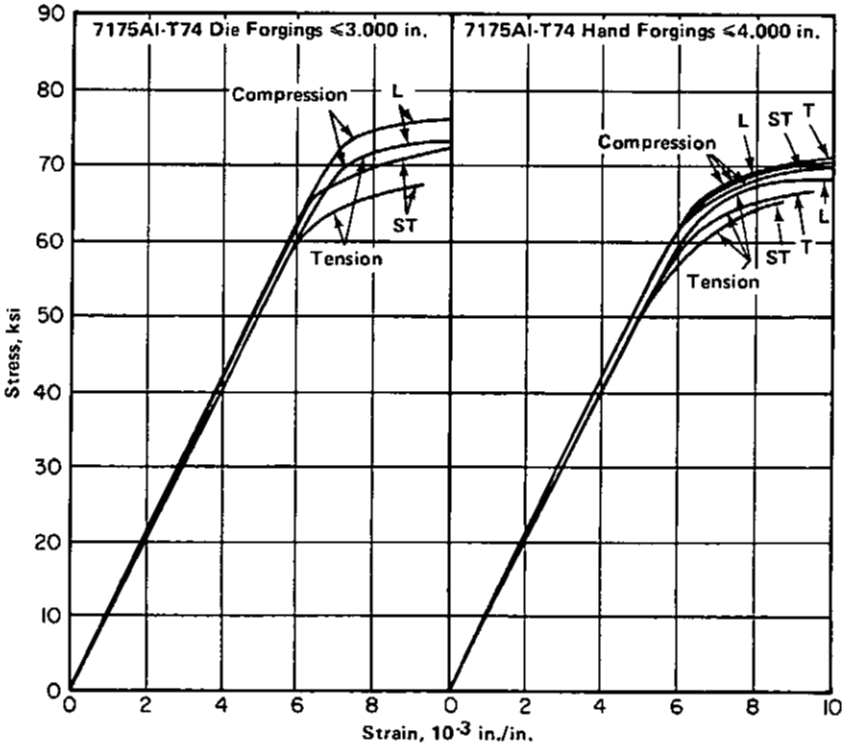


FIGURE 3.0211. TYPICAL STRESS-STRAIN CURVES FOR DIE FORGINGS AND HAND FORGINGS AT ROOM TEMPERATURE (29)

	Al
5.6	Zn
2.5	Mg
1.6	Cu
0.25	Cr
Low	Ti
	Mn
	Si

7175 Al

Alloy	7175Al					
Condition	T66			T74		
Property	Ultimate Strength, ksi	Yield Strength, ksi	Elongation (2 in.), percent	Ultimate Strength, ksi	Yield Strength, ksi	Elongation (2 in.), percent
Form	5- to 10-lb (Approx) Die Forgings					
Longitudinal	90.0	81.0	12.0	81.0	72.0	11.0
Form	38-lb Rib Forging					
Longitudinal	93.2	83.9	13.8	81.0	73.5	14.0
Transverse	81.7	70.4	11.0	74.4	65.7	11.5
Form	74-lb Spar Forging					
Longitudinal				79.6	72.8	13.8
Transverse				75.3	66.1	9.9
Form	96-lb Landing Gear Cylinder Forging					
Longitudinal				78.3	71.9	13.7
Transverse				75.3	67.5	9.0
Form	156-lb Spar Forging					
Longitudinal				80.1	72.6	12.8
Transverse				75.7	67.8	8.4
Form	620-lb Wing Spar Forging					
Longitudinal				79.4	71.9	13.9
Transverse				75.3	66.1	13.0

TABLE 3.0212. TENSILE PROPERTIES OF FORGING OF VARIOUS SIZES (3)

Alloy	7175Al							
Form	Model 727 Support Elevator Forgings							
Condition	T66				T74			
Specimen Condition	Ultimate Strength, ksi	Yield Strength, ksi	Elongation (2 in.), percent	Reduction in Area, percent	Ultimate Strength, ksi	Yield Strength, ksi	Elongation (2 in.), percent	Reduction in Area, percent
Longitudinal	93.0	83.9	11.0	14.4	80.1	73.8	12.8	35.9
Long Transverse	89.9	79.3	13.1	21.6	79.3	71.9	13.1	36.9
Short Transverse	84.0	70.2	9.7	14.8	76.5	66.8	8.9	16.4

TABLE 3.0213. TENSILE PROPERTIES OF MODEL 727 SUPPORT ELEVATOR FORGING IN TWO HEAT TREATED CONDITIONS (4)

Alloy		7175Al					
Condition		T74[b]					
Form		Forgings		Die Forgings			
Thickness, in.		≤3.000	≤3.000	≤3.000	3.001-4.000	4.001-5.000	5.001-6.000
Ultimate Strength, ksi	L	76	78	76	73	70	68
	T	71	–	71	70	68	65
	ST	–	–	–	–	–	–
Yield Strength, ksi	L	66	69	66	63	61	58
	T	62	–	62	60	58	55
Fracture Toughness K_{Ic}, ksi $\sqrt{in.}$	L	34	30-35	32-36	–	–	–
	T	31	–	32	–	–	–
	ST	–	19-26	23-33	–	–	–
Stress Corrosion Threshold Strength, ksi[a]	L	50	–	–	–	–	–
	T	50	–	–	–	–	–
	ST	35	≈25	35	–	–	–

(a) Highest sustained tensile stress at which a smooth test specimen will not fail in 3.5 percent NaCl alternate immersion test.

(b) Tentative minimum mechanical properties – applicable to parts with a maximum cross-section of 100 $in.^2$.

TABLE 3.0214. TENTATIVE MINIMUM TENSILE, FRACTURE TOUGHNESS AND STRESS-CORROSION PROPERTIES OF T74 FORGINGS (26,27,28)

	Al
5.6	Zn
2.5	Mg
1.6	Cu
0.25	Cr
Low	Ti
	Mn
	Si

7175 Al

Alloy	7175 Al	
Form	Model 727 Support Elevator Forging	
Condition	T66	T74
Specimen Orientation	Compressive Yield Strength, ksi	Ultimate Compressive Strength, ksi
Longitudinal	90.5	80.0
Long Transverse	84.2	75.4
Short Transverse	80.2	73.3

TABLE 3.0222. COMPRESSIVE YIELD STRENGTH OF MODEL 727 SUPPORT ELEVATOR FORGING IN TWO HEAT TREATED CONDITIONS (4)

Alloy	7175 Al	
Form	Forgings	
Condition	T66	T74
Specimen Orientation	K_{Ic}, ksi $\sqrt{in.}$	K_{Ic}, ksi $\sqrt{in.}$
Longitudinal	33.0	37.0
Long Transverse	24.4	31.5
Short Transverse	21.0	27.0

TABLE 3.02721. VARIATIONS IN PLANE STRAIN FRACTURE TOUGHNESS WITH DIFFERENT HEAT TREATMENTS AND SPECIMEN ORIENTATIONS (14)

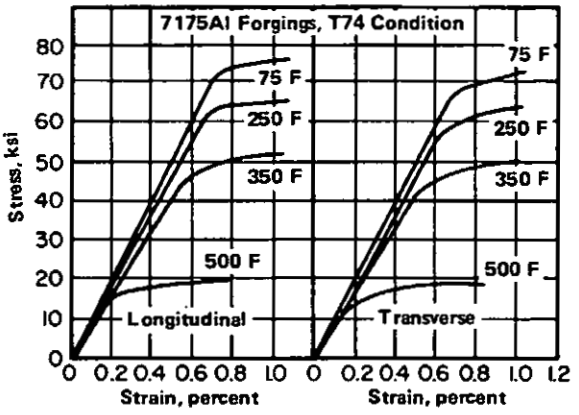


FIGURE 3.03111. TENSILE STRESS-STRAIN CURVES AT VARIOUS TEMPERATURES (1)

Alloy		7175 Al			
Form		Die Forgings			
Condition		T66			
Test		Plane Strain Fracture Toughness[a]			
Test Temperature, F	Yield Strength, ksi	Product Thickness, in.	Specimen Thickness, in.	Orientation[b]	K_{Ic}, ksi $\sqrt{in.}$
89	80.4	0.500	0.500	L-T	34.7
89	82.2	0.500	0.500	T-L	25.7
75	70.4	1.000	0.500	S-L	21.1
75	80.2	1.000	0.500	T-L	23.2
75	82.4	1.000	0.500	L-T	36.3
75	73.0	1.000	0.500	S-L	20.6

(a) Compact tension specimen. Test procedures as per ASTM E399.
(b) Specimen orientation as per ASTM E399.

TABLE 3.02722. FRACTURE TOUGHNESS OF 7175-T66 DIE FORGINGS (24)

	Al
5.6	Zn
2.5	Mg
1.6	Cu
0.25	Cr
Low	Ti
	Mn
	Si

7175 Al

Alloy		7175 Al			
Form		Die Forgings			
Condition		T74			
Test		Plane Strain Fracture Toughness[a]			
Test Temperature, F	Yield Strength, ksi	Product Thickness, in.	Specimen Thickness, in.	Orientation[b]	K_{Ic}, ksi $\sqrt{in.}$
84	70.6	0.500	0.500	L-T	27.3
89	67.1	0.500	0.500	S-L	27.1
84	66.3	0.750	0.500	S-L	27.5
82	66.3	1.000	0.500	S-L	26.0
75	65.7	1.000	0.500	S-L	25.5
75	73.0	1.000	0.500	T-L	31.5
82	76.9	1.500	0.500	L-T	31.5
82	67.9	1.500	0.499	S-L	24.1
82	65.2	1.500	0.750	S-L	26.0
78	68.0	2.000	0.750	L-T	27.4
80	66.7	2.000	0.750	S-L	24.1
81	63.8	2.500	0.750	S-L	28.2
83	66.3	3.000	0.750	S-L	26.5
84	66.3	2.000	1.000	L-T	34.7
82	73.8	2.750	1.000	T-L	24.6

(a) Compact tension specimen. Test procedures per ASTM E399.
(b) Specimen orientation as per ASTM E399.

TABLE 3.02723. FRACTURE TOUGHNESS OF 7175-T74 DIE FORGINGS (24)

Alloy		7175 Al				
Form		Hand Forgings				
Test		Plane Strain Fracture Toughness[a]				
Condition	Test Temperature, F	Yield Strength, ksi	Product Thickness, in.	Specimen Thickness, in.	Orientation[b]	K_{Ic}, ksi $\sqrt{in.}$
T74	82	66.4	2.000	0.749	S-L	26.3
	76	65.6	3.000	0.998	S-L	23.0
	76	65.7	3.000	0.998	T-L	25.4
	82	61.4	4.000	0.998	S-L	21.9
	82	59.9	4.000	1.000	T-L	27.0
	84	62.1	5.000	1.500	L-T	33.6
	84	70.0	5.000	1.500	T-L	28.2
T7452	82	62.9	3.750	2.000	L-T	39.8

(a) Compact tension specimen. Test procedures per ASTM E399.
(b) Specimen orientation per ASTM E399.

TABLE 3.02724. FRACTURE TOUGHNESS OF 7175-T74 AND T7452 HAND FORGINGS (24)

	Al
5.6	Zn
2.5	Mg
1.6	Cu
0.25	Cr
Low	Ti
	Mn
	Si

7175 Al

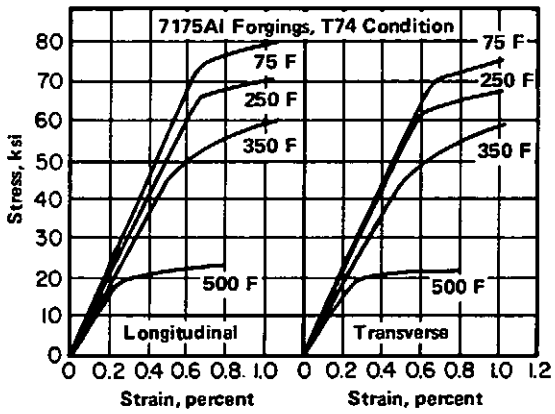


FIGURE 3.03211. COMPRESSIVE STRESS-STRAIN CURVES AT VARIOUS TEMPERATURES (1)

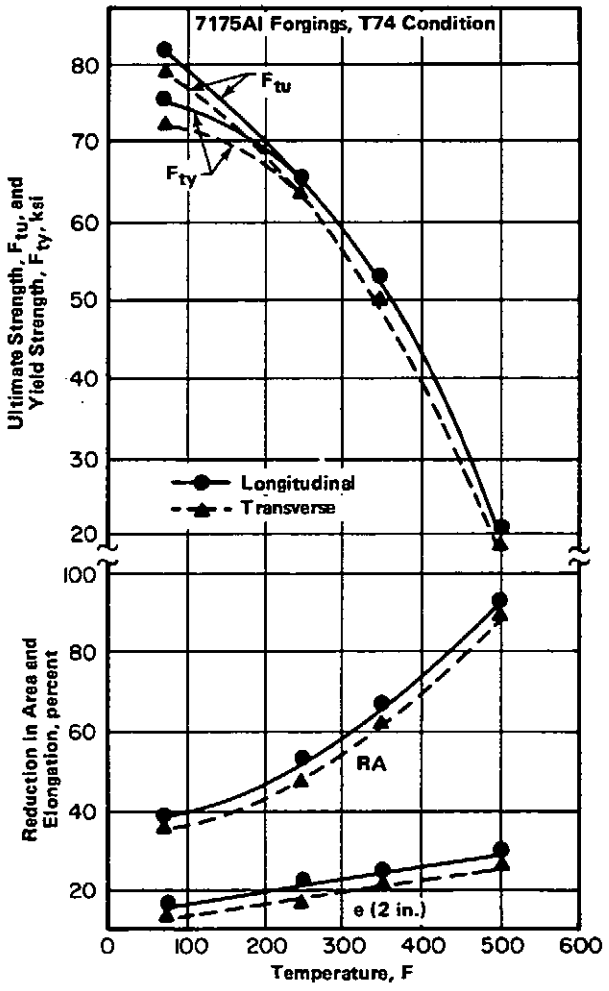


FIGURE 3.0312. EFFECT OF TEMPERATURE ON TENSILE PROPERTIES (1)

	Al
5.6	Zn
2.5	Mg
1.6	Cu
0.25	Cr
Low	Ti
	Mn
	Si

7175 Al

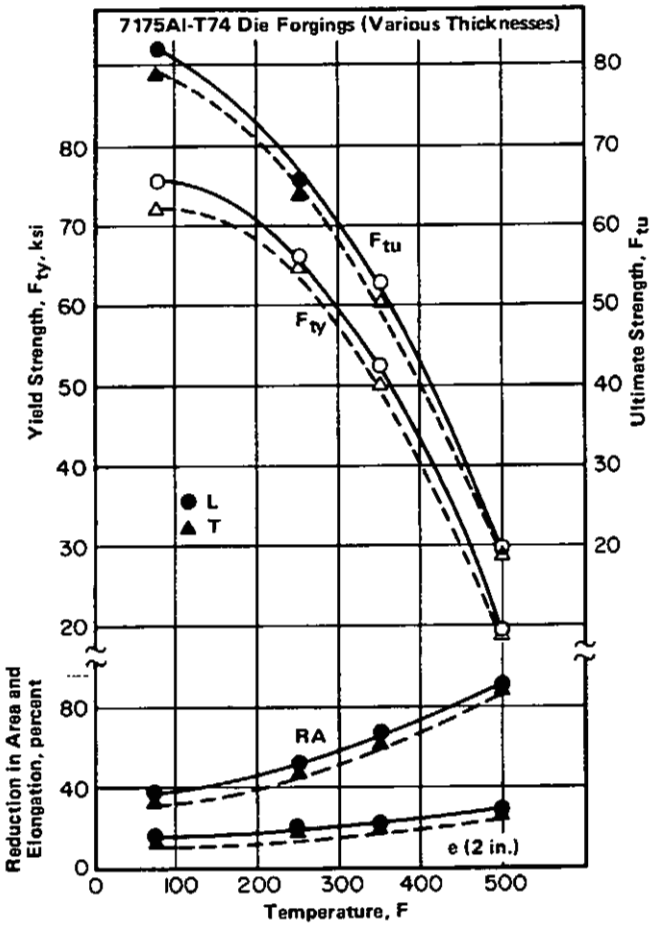


FIGURE 3.0313. EFFECT OF TEMPERATURE ON TENSILE PROPERTIES OF T74 DIE FORGINGS (23)

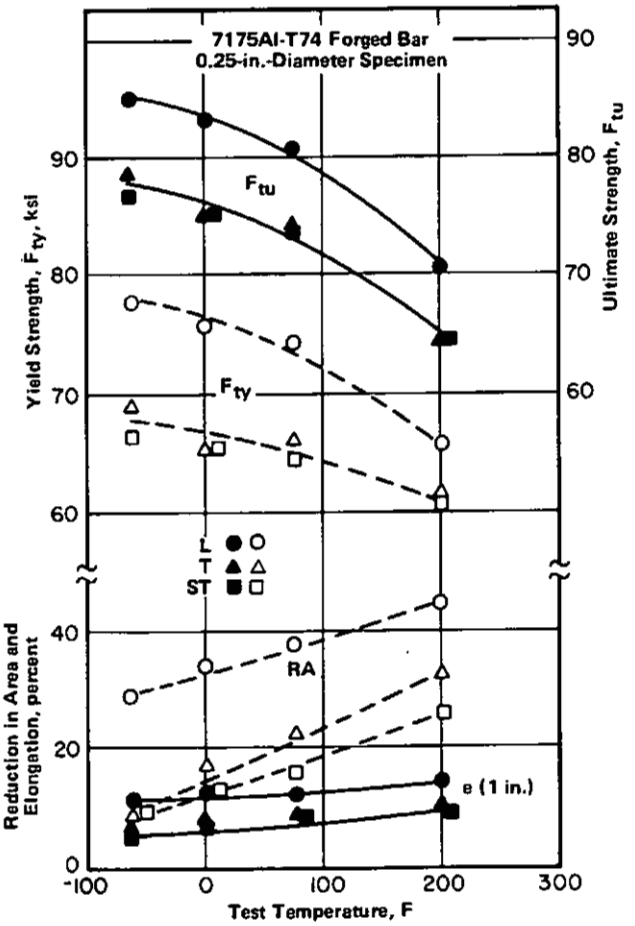


FIGURE 3.0314. EFFECT OF TEST TEMPERATURE ON TENSILE PROPERTIES OF FORGED BAR (25)

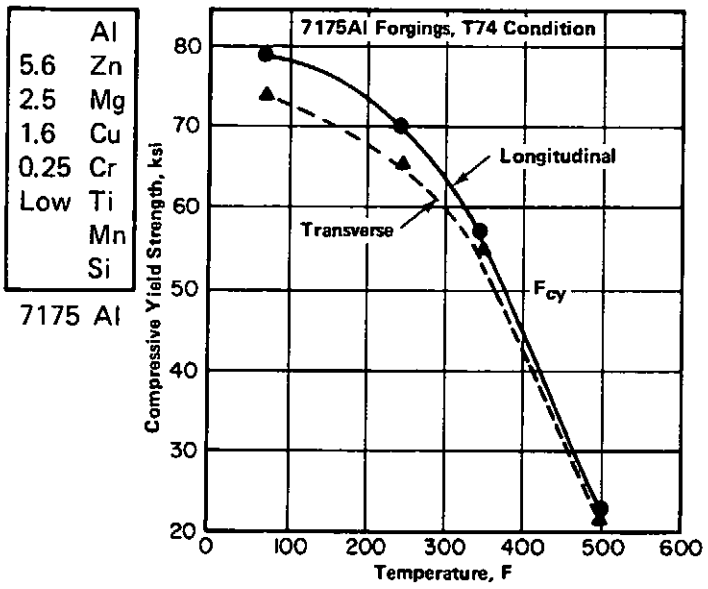


FIGURE 3.0322. EFFECT OF TEMPERATURE ON COMPRESSIVE YIELD STRENGTH (1)

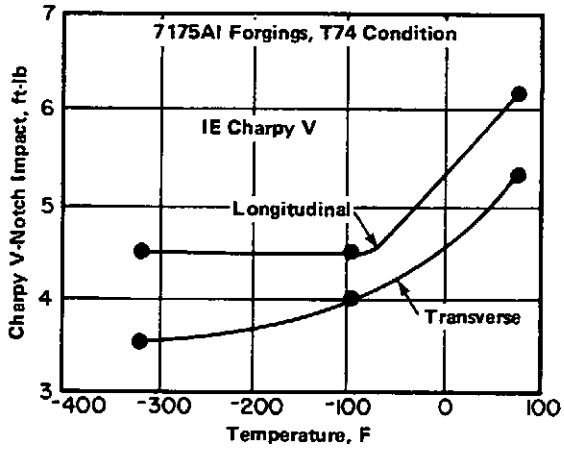


FIGURE 3.0331. CHARPY V-NOTCH IMPACT PROPERTIES AT LOW TEMPERATURES (1)

Alloy	7175Al		
Form	Forged Bar[a]		
Condition	T74		
Test	Plane Strain Fracture Toughness		
Test Temperature, F	Yield Strength, ksi	Orientation	K_{Ic},[b] ksi $\sqrt{in.}$
RT	66.3	T	22.7
RT	64.9	ST	31.9
-65	66.6	ST	26.3
0	65.9	ST	26.3
200	60.5	ST	34.1

(a) Average cross section of bar was 2.5 x 2.5 in.
(b) Compact tension specimens as per ASTM E399.

TABLE 3.03721. FRACTURE TOUGHNESS OF FORGED BAR AT SEVERAL TEMPERATURES (25)

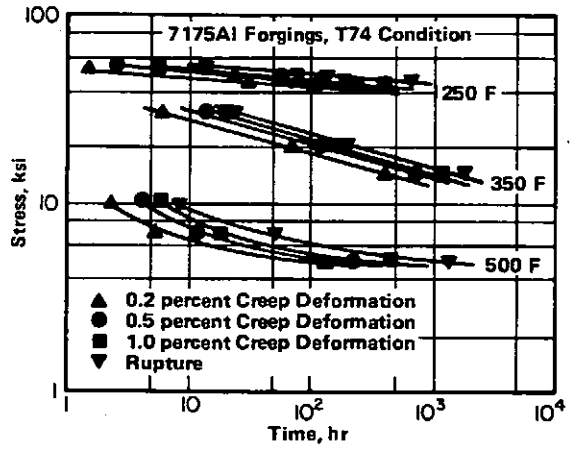


FIGURE 3.041. CREEP AND CREEP-RUPTURE CURVES (1)

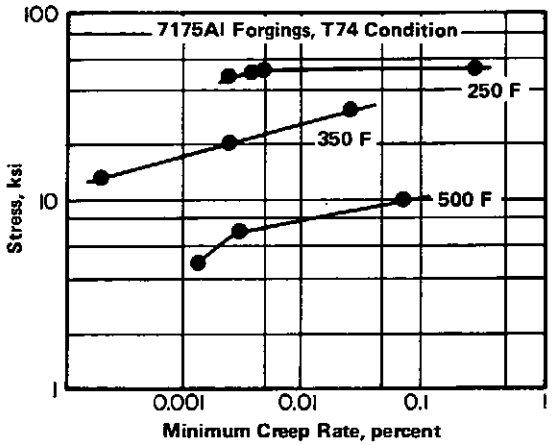


FIGURE 3.042. MINIMUM CREEP RATE CURVES (1)

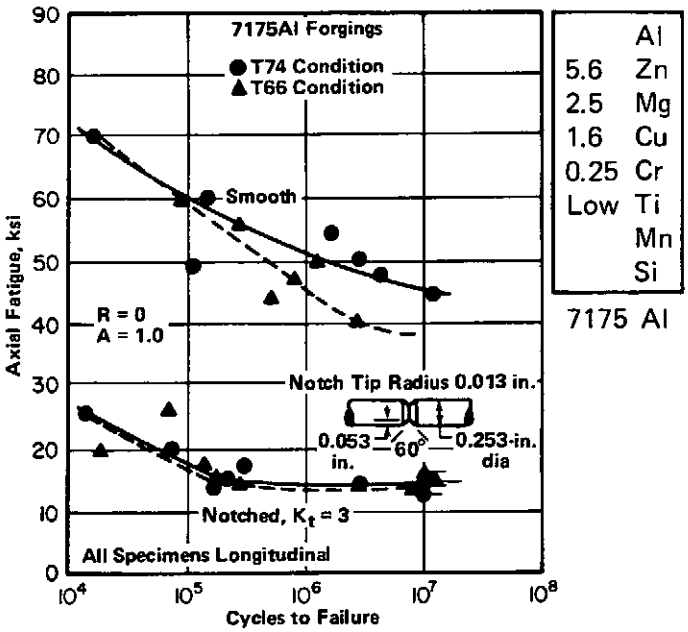


FIGURE 3.051. AXIAL FATIGUE PROPERTIES FOR FORGINGS IN T74 AND T66 CONDITION (3)

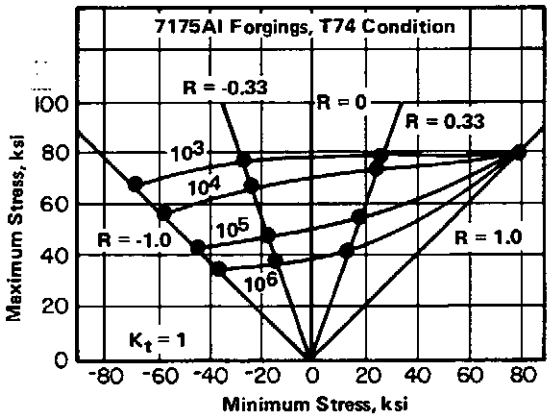


FIGURE 3.052. CONSTANT FATIGUE-LIFE DIAGRAM FOR SMOOTH, AXIALLY LOADED, SHOT-PEENED SPECIMENS IN T74 CONDITION (2)

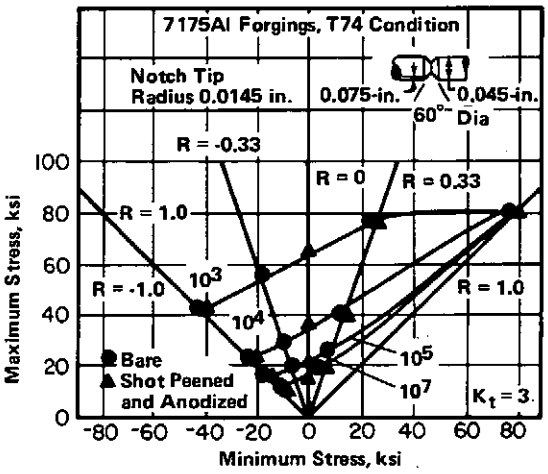


FIGURE 3.053. CONSTANT FATIGUE-LIFE DIAGRAM FOR NOTCHED, AXIALLY LOADED SPECIMENS IN T74 CONDITION (2)

	Al
5.6	Zn
2.5	Mg
1.6	Cu
0.25	Cr
Low	Ti
	Mn
	Si

7175 Al

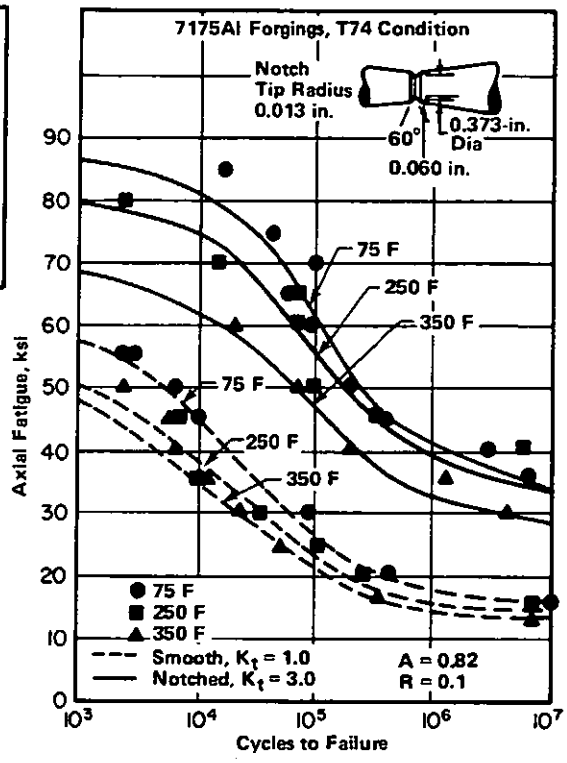


FIGURE 3.054. AXIAL FATIGUE PROPERTIES AT VARIOUS TEMPERATURES FOR FORGINGS IN T74 CONDITION (1)

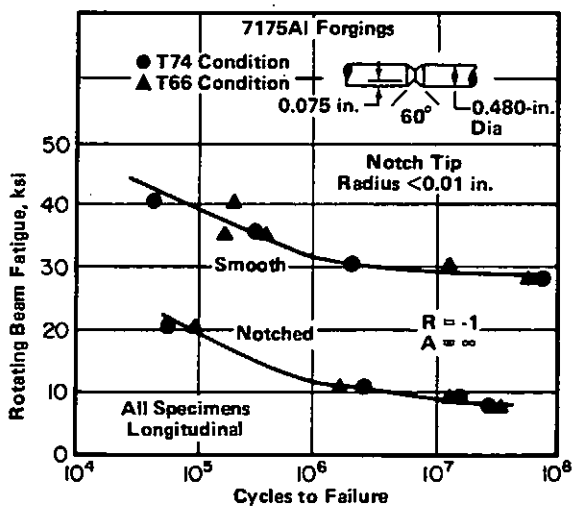


FIGURE 3.055. ROTATING BEAM FATIGUE PROPERTIES FOR FORGINGS IN T74 AND T66 CONDITIONS (3)

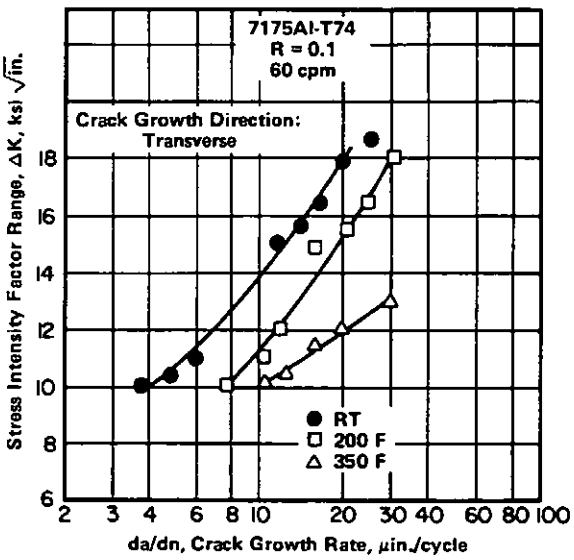


FIGURE 3.056. FATIGUE CRACK-GROWTH RATES FOR T74 FORGINGS AT ROOM TEMPERATURE AND ELEVATED TEMPERATURES (25)

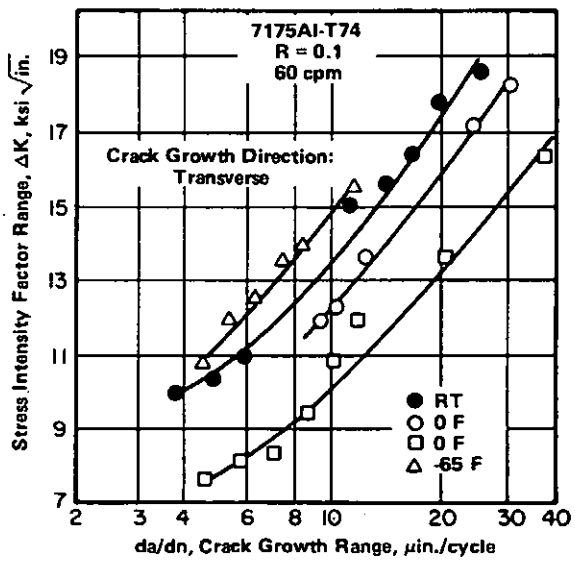


FIGURE 3.057. FATIGUE CRACK-GROWTH RATES FOR T74 FORGINGS AT ROOM TEMPERATURE AND AT LOW TEMPERATURES (25)

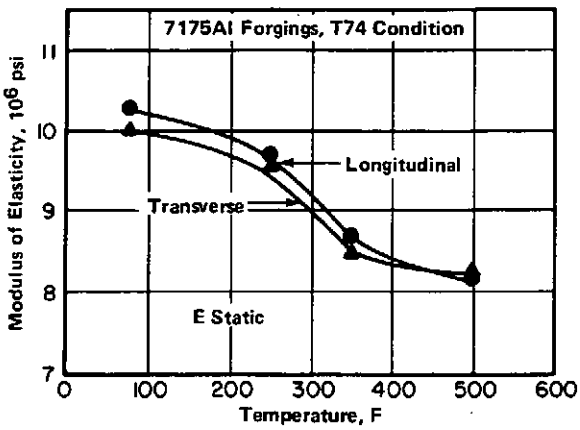


FIGURE 3.0621. EFFECT OF TEMPERATURE ON TENSILE MODULUS OF ELASTICITY (1)

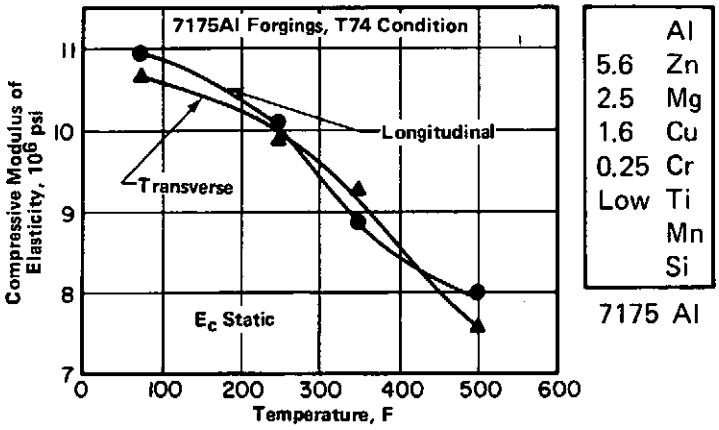


FIGURE 3.0622. EFFECT OF TEMPERATURE ON COMPRESSIVE MODULUS OF ELASTICITY (1)

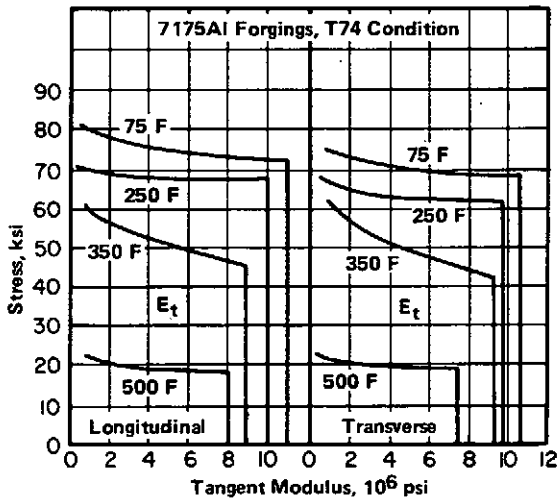


FIGURE 3.0623. COMPRESSIVE TANGENT MODULUS CURVES AT VARIOUS TEMPERATURES (1)

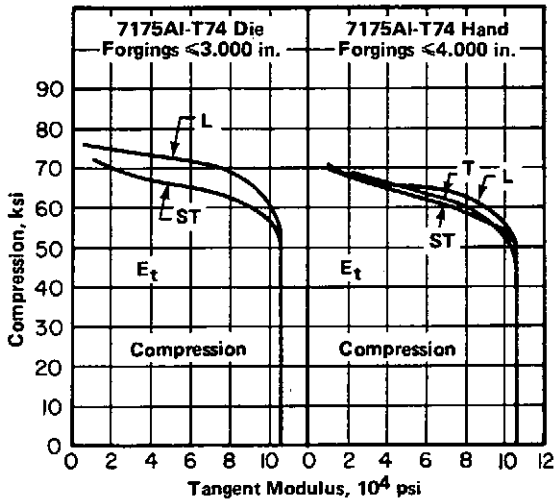


FIGURE 3.0624. TYPICAL COMPRESSIVE TANGENT MODULUS CURVES FOR T74 DIE FORGINGS AND HAND FORGINGS AT ROOM TEMPERATURE (29)

1 GENERAL

Aluminum alloy 7475 is primarily an aerospace alloy used in a heat treated condition. It is usually available as bare or clad sheet or as plate, but on occasions extrusions and forgings have been made for special applications in place of its sister alloys, 7075 and 7175.

Alloy 7475 is basically a high purity version of 7075, i.e., it contains lower iron and silicon, and has marginally lower upper limits on copper and magnesium. Special proprietary processing may sometimes be given to 7475. The limits on chemical composition reduce the amounts of second phase constituents, which result in higher fracture toughness at the same level of strength and corrosion resistance. In over-aged tempers, for example, T7x, 7475 is resistant to exfoliation and stress corrosion. Most aerospace applications are for components requiring high strength and toughness at temperatures up to 300 F.

1.01 Commercial Designation

7475 aluminum alloy.

1.02 Alternate Designation

UNS A97475.

1.03 Specifications

7475-T7351 plate: AMS 4202 (33)
7475-T651 plate: AMS 4090 (34)
7475-T7651 plate: AMS 4089 (35)
7475-T61 sheet: AMS 4084 (36)
7475-T761 sheet: AMS 4085 (37).

1.031 Explanation of temper designations. In the temper designations listed above, the first letter, "T", refers to a solution heat treated and aged condition, as distinct from work hardened, "H", or annealed, "O", or other conditions. The first digit which follows T, "6 or 7", refers to the degree of aging. Peak strength is designated by 6, whereas 7 indicates an over-aged temper in which some strength has been sacrificed for toughness, or corrosion or stress corrosion resistance. These tempers may be subdivided by a second digit, "6 or 3", in which case, T76 is usually stronger and is achieved with a shorter age than T73. The final temper digit, "1", indicates that the material has been stretched after solution heat treatment and before aging, to relieve residual stresses. In other products, "2" denotes stress relief by compression. Other intermediate digits refer to other processing steps that may be proprietary, and may differ from one supplier to another.

1.04 Composition

Aluminum Association composition limits, Table 1.04.

1.05 Heat Treatment

Details of the heat treatment should be obtained, when required, from the specific supplier of the material due to possible differences in fabrication history, and consequent differences in response to heat treatments.

1.06 Hardness

1.061 T61 sheet: R_B 89.
T761 sheet: R_B 85.
T7351 plate: R_B 76 to 85.
(See also Figure 3.02723.)

1.07 Forms and Conditions Available

Alloy 7475 is available as sheet (up to 0.25-inch thick) in both bare and clad forms, in either T61 or T761 tempers. It is also available in T7351, T7651, T76351, and T651 plate up to approximately 4 inches in thickness, and in extruded rods for the manufacture of cartridge cases. Producers and aerospace companies have also investigated the availability of 7475 structural forgings and extrusions; however, the data are not found in the open literature.

	Al
5.6	Zn
2.2	Mg
1.5	Cu
0.21	Cr
Low	Si
	Fe
	Mn
	Ti

7475 Al

There has been a considerable amount of successful development work on superplastic 7475 sheet, and it is likely that it will be available commercially in the near future. (See also Section 1.094.)

1.08 Melting and Casting Practices

1.081 The alloy can be melted and alloyed in oil-fired or electric-induction furnaces and cast into ingot molds of any desired shape for subsequent working into sheets, plates, or extrusions.

1.09 Special Considerations

1.091 The alloy loses both room and elevated temperature strength rapidly with increasing holding times at temperatures above 300 F (1).

1.092 The improved toughness and exfoliation resistance of this alloy over 7075 depends on maintaining the lower limits of silicon, iron, manganese, and titanium (3). (See Tables 3.02110 and 3.02725.)

1.093 As has been reported for other heat treated aluminum alloys in heavy sections, strength, hardness, and fracture toughness vary through the thickness. (See Figures 3.02722 and 3.02723.) Care should be taken so that property comparisons are made at similar test sample locations, and that the data used are relevant to the section used in service.

1.094 When fabricated by special (patented) practices, 7475 sheet can be superplastic at strain rates around 2×10^{-4} and temperatures around 950 F. Elongations of approximately 650 percent have been reported (24) in 7475 sheet suitable for forming (see Table 3.0215). Subsequent T6 properties of superplastically formed components were reported (25) to be satisfactory (see Figures 3.0216 and 3.0217), with only slight degradation due to cavitation. Fatigue properties of formed sheet are comparable to those of conventional sheet in the T6 temper (see Figure 3.05114).

2 PHYSICAL AND CHEMICAL PROPERTIES

2.01 Thermal Properties

2.011 Melting range, 890 to 1180 F (approximately).
2.012 Phase changes, none in the alpha phase.
2.0121 Time-temperature-transformation diagrams.

	Al
5.6	Zn
2.2	Mg
1.5	Cu
0.21	Cr
Low	Si
	Fe
	Mn
	Ti

7475 Al

2.0122 In the as-cast or annealed condition, the alpha matrix contains a coarse second phase of $MgZn_2$, which goes into solution during solution heat treatment. Artificial aging causes the formation first of Guinier-Preston zones high in zinc. Subsequently, particularly at aging temperatures above 300 F, finely divided precipitates of $MgZn_2$ and $MgZn_2Al_2$ appear. With overaging (stabilization), copper also precipitates in finely divided form. The low composition limits for silicon, iron, manganese, and titanium limit the formation of secondary insoluble phases to very small amounts. The smaller amounts of such secondary phases account for the good fracture toughness and corrosion resistance of this alloy (3, 7).

2.013 Thermal conductivity.

2.0131 The thermal conductivity, K, of this alloy is closely similar to that of 7075 in comparable tempers:
T61 and T651: 80 Btu/ft/hr/ft^2/F at 77 F
T761 and T7651: 90 Btu/ft/hr/ft^2/F at 77 F
T7351: 94 Btu/ft/hr/ft^2/F at 77 F.

2.014 Thermal expansion.

2.0141 Essentially the same as for 7075 in comparable tempers. Design value: 12.9×10^{-6} in. per in. per F in the range 68 to 212 F.

2.015 Specific heat.

2.0151 Essentially the same as for 7075 in comparable tempers:
T7351: 0.21 Btu/lb/F at 212 F
T61, T651, T761, and T7651: 0.23 Btu/lb/F at 212 F.

2.016 Thermal diffusivity.

2.02 Other Physical Properties

2.021 Density: 0.101 lb per in.^{3}.

2.022 Electrical properties, Table 2.022.

2.0221 Variation in electrical conductivity with tensile yield strength in 7475 plate, Figure 2.0221.

2.023 Magnetic properties, alloy is not magnetic.

2.024 Emissivity.

2.0241 Essentially the same as 7075 alloy in comparable tempers. (See 7075 Alloy, Code 3207, Section 2.016.)

2.03 Chemical Properties

2.031 The alloy is subject to general corrosion, similar to 7075 alloy (Code 3207), in marine and other corrosive atmospheres. In such environments, or where good surface appearance is a requirement, alclad material, anodizing, or painting is recommended (1).

2.032 In the T61 condition, the alloy is susceptible to stress corrosion cracking and the susceptibility is decreased significantly by over-aging to the T761 or T7351 condition. Susceptibility in the T61 condition is similar to 7075-T6 and in the T761 condition it is similar to 7075-T76 (1, 2). (See 7075, Code 3207, Sections 2.0311 through 2.0315.)

2.0321 Crack-growth rates for fatigue precracked specimens of 7475 plate exposed for 202 days to marine atmosphere at Daytona Beach, Florida, Figure 2.0321.

2.0322 Crack growth for fatigue precracked specimens of 7475 plate exposed for 202 days to marine atmosphere at Daytona Beach, Florida, Figure 2.0322.

2.0323 Crack growth for fatigue precracked specimens of 7475 plate immersed for 162 days in salt-chromate solution, Figure 2.0323.

2.0324 Estimated SL threshold stress intensity and K_{Iscc} for double cantilever beam specimens of 7475 plate, Table 2.0324.

2.0325 Stress corrosion behavior of superplastically strained 7475-T6 sheet, Table 2.0325.

2.033 7475 alloy is slightly susceptible to exfoliation corrosion in the T61 condition but highly resistant in the T761 condition. In a temper-for-temper comparison, the exfoliation resistance of 7475-T61 and T761 sheet is better than that of 7075-T6 and T76 sheet (1, 2, 3).

2.04 Nuclear Properties
(See 7075, Code 3207, Section 2.041.)

3 MECHANICAL PROPERTIES

3.01 Specified Mechanical Properties

3.011 AMS specified mechanical properties.

3.0111 AMS specified tensile properties for T7351 plate, Table 3.0111.

3.0112 AMS specified fracture toughness for T7351 plate, Table 3.0112.

3.0113 AMS specified tensile properties of T651 plate, Table 3.0113.

3.0114 AMS specified fracture toughness for T651 plate, Table 3.0114.

3.0115 AMS specified tensile properties for T7651 plate, Table 3.0115.

3.0116 AMS specified fracture toughness for T7651 plate, Table 3.0116.

3.0117 AMS specified tensile properties and fracture toughness for T651 sheet, Table 3.0117.

3.0118 AMS specified tensile properties and fracture toughness for T7651 sheet, Table 3.0118.

3.012 Design mechanical properties for 7475-T6 and -T76 sheet and plate, Table 3.012.

3.013 Design mechanical properties for 7475-T7351 plate, Table 3.013.

3.02 Mechanical Properties at Room Temperature

3.021 Tension.

3.0211 Stress-strain diagrams.

3.02111 Stress-strain curves for sheet in T61 condition, Figure 3.02111.

3.02112 Stress-strain curves for sheet in T761 condition, Figure 3.02112.

3.02113 Stress-strain curves for alclad sheet in T61 condition, Figure 3.02113.

3.02114 Stress-strain curves for alclad sheet in T761 condition, Figure 3.02114.

3.02115 Stress-strain curves for 1.5-inch plate in T7351 condition, Figure 3.02115.

3.02116 Stress-strain curves for 1.5-inch plate in T651 condition, Figure 3.02116.

3.0212 Typical tensile properties of bare and alclad sheet, Table 3.0212.

3.0213 Effect of exposure time at various elevated temperatures on the room temperature tensile properties of sheet in T61 condition, Figure 3.0213.

3.0214 Effect of exposure time at various elevated temperatures on the room temperature tensile properties of sheet in T761 condition, Figure 3.0214.

3.0215 Tensile elongation of superplastic 7475 sheet at various strain rates at 900 F and 960 F, Table 3.0215.

3.0216 Room temperature tensile properties of 7475-T6 sheet after uniaxial superplastic tensile deformation, Figure 3.0216.

3.0217	Room temperature properties of 7475-T6 sheet after superplastic plane strain tensile deformation, Figure 3.0217.
3.0218	Typical mechanical properties of 7475-T7351 plate, Table 3.0218.
3.0219	Mechanical properties of 7475-T651 plate, Table 3.0219.
3.02110	Effect of alloy purity on the mechanical properties of 7075/7475, Table 3.02110.
3.02111	Mechanical properties of 1.5-inch thick 7475 plate in various tempers, Table 3.02111.
3.022	Compression.
3.0221	Stress-strain diagrams.
3.02211	Compressive stress-strain curves for sheet in T61 condition, Figure 3.02211.
3.02212	Compressive stress-strain curves for sheet in T761 condition, Figure 3.02212.
3.02213	Compressive stress-strain curves for alclad sheet in T61 condition, Figure 3.02213.
3.02214	Compressive stress-strain curves for alclad sheet in T761 condition, Figure 3.02214.
3.02215	Typical compression stress-strain curves for 7475-T7351 plate, Figure 3.02215.
3.02216	Typical compression stress-strain curves for 7475-T7651 plate, Figure 3.02216.
3.02217	Typical compression stress-strain curves for 7475-T651 plate, Figure 3.02217.
3.0222	Compressive properties.
3.02221	Compressive yield strength of sheet, Table 3.02221.
3.02222	Compressive strength of T7475-T7351 plate of various thicknesses, Table 3.02222.
3.023	Impact.
3.0231	Room temperature Charpy V-notch results: 17.1 ft-lbs (longitudinal) and 5.9 ft-lbs (transverse). (Average of five specimens of T7351 plate 2-inch thick.) (14)
3.024	Bending.
3.025	Torsion and shear.
3.0251	Shear strength of sheet, Table 3.0251.
3.0252	Shear strength of plate, Table 3.0252.
3.026	Bearing.
3.0261	Bearing strength of sheet in various heat treated conditions, thicknesses, and orientations, Table 3.0261.
3.0262	Bearing properties of 7475-T7351 plate in various thicknesses, Table 3.0262.
3.027	Stress concentration.
3.0271	Notch properties.
3.02711	Residual strength (gross area stress at maximum load) of bare and alclad sheet as a function of original crack length, Figure 3.02711.
3.02712	Residual strength (gross area stress at maximum load) of sheet as a function of crack length at instability, Figure 3.02712.
3.02713	Fracture strength of center cracked panels of various widths in T761 condition, Table 3.02713.
3.02714	Fracture strength of center cracked specimens of various thicknesses in T61 condition, Table 3.02714.
3.02715	Plane stress fracture toughness K_c of 7475-T61 and -T761 sheet relative to tensile yield strength, Figure 3.02715.
3.02716	Correlations between notched tensile yield ratio (NYR) and K_{Ic} for 7075 and 7475 plate in T651, T7651, and T7351 tempers, Figure 3.02716.
3.0272	Fracture toughness. (See also Section 3.0.1.)
3.02721	Plane strain fracture toughness of 7475-T7351 plate of various thicknesses, Table 3.02721.
3.02722	Toughness variations through the thickness of 2-inch thick 7475-T7351 plate, Figure 3.02722.
3.02723	Toughness variations through the thickness of 2.75-inch thick 7475-T7351 plate, Figure 3.02723.
3.02724	Plane strain fracture toughness of 1.5-inch thick 7475-T7651 plate, Table 3.02724.
3.02725	Effect of alloy purity on the plane strain fracture toughness of 7075-T73511 and -T76511 extrusions, Table 3.02725.
3.02726	Plane strain fracture toughness K_{Ic} of 7475-T7351 plate produced from January 1976 to August 1978 by two U.S. producers, Table 3.02726.
3.028	Combined properties.

	Al
5.6	Zn
2.2	Mg
1.5	Cu
0.21	Cr
Low	Si
	Fe
	Mn
	Ti

7475 Al

3.03	Mechanical Properties at Various Temperatures
3.031	Tension.
3.0311	Stress-strain curves.
3.0312	Tensile properties.
3.03121	Sheet.
3.031211	Effect of low temperatures on tensile properties of sheet in T61 condition, Figure 3.031211.
3.031212	Effect of low temperatures on tensile properties of sheet in T761 condition, Figure 3.031212.
3.031213	Effect of elevated temperatures, after various holding times at temperature, on tensile properties of sheet in T61 condition, Figure 3.031213.
3.031214	Effect of elevated temperature, after various holding times at temperature, on tensile properties in T761 condition, Figure 3.031214.
3.031215	Tensile properties of longitudinal and transverse sheet specimens in T61 condition from -50 to 200 F, Figure 3.031215.
3.031216	Tensile properties of longitudinal and transverse sheet specimens in T761 condition from -50 to 200 F, Figure 3.031216.
3.03122	Plate.
3.031221	Tensile properties of longitudinal and transverse plate specimens in T7651 condition in the temperature range -65 F to +200 F, Figure 3.031221.
3.031222	Tensile properties of longitudinal and transverse plate specimens in T7351 condition at elevated temperatures, Figure 3.031222.
3.032	Compression.
3.0321	Stress-strain curves.
3.0322	Compressive yield strength and elastic modulus as a function of temperature, Figure 3.0322.
3.033	Impact.
3.034	Bending.
3.035	Torsion and shear.
3.036	Bearing.
3.037	Stress concentration.
3.0371	Notch properties.
3.0372	Fracture toughness.
3.03721	Plane strain fracture toughness as a function of temperature for T7651 plate, Figure 3.03721.
3.038	Combined properties.

3.04	Creep and Creep-Rupture Properties
3.041	Sheet.
3.0411	Creep and creep-rupture curves for T761 and T61 sheet at 75 F and 212 F, Figure 3.0411.
3.042	Plate.
3.0421	Creep-rupture and creep deformation curves for T7351 plate at 250 F, 350 F, and 500 F, Figure 3.0421.

	Al
5.6	Zn
2.2	Mg
1.5	Cu
0.21	Cr
Low	Si
	Fe
	Mn
	Ti

7475 Al

3.05 **Fatigue Properties**

3.051 Conventional fatigue properties.

3.0511 Constant fatigue life diagram for smooth axially loaded sheet specimens, Figure 3.0511.

3.0512 Constant fatigue life diagram for notched axially loaded sheet specimens, Figure 3.0512.

3.0513 Constant fatigue life diagram for smooth axially loaded alclad sheet specimens, Figure 3.0513.

3.0514 Constant fatigue life diagram for notched axially loaded alclad sheet specimens, Figure 3.0514.

3.0515 Axial fatigue life of smooth and notched specimens of 0.090-inch alclad sheet, Figure 3.0515.

3.0516 Axial fatigue life of smooth and notched specimens of 0.200-inch alclad sheet, Figure 3.0516.

3.0517 Axial fatigue life of smooth and notched specimens of 0.250-inch alclad sheet, Figure 3.0517.

3.0518 Axial fatigue life of smooth and notched longitudinal and transverse specimens of 1.5-inch thick 7475-T7651 plate, Figure 3.0518.

3.0519 Axial load fatigue lives of longitudinal and transverse smooth and notched specimens of 7475-T7351 and -T651 plate 1.5-inch thick, Figure 3.0519.

3.05110 Axial load fatigue lives of transverse smooth and notched specimens of 7475-T7351 and 7475-T651 plate 1.5-inch thick, Figure 3.05110.

3.05111 Axial stress fatigue life of 7475-T7351 plate in the transverse direction, Figure 3.05111.

3.05112 Axial stress fatigue life of notched specimens of 7475-T7351 plate in the transverse direction at elevated temperature, Figure 3.05112.

3.05113 Axial stress fatigue life of specimen of 1.5-inch thick 7475-T7651 plate, Figure 3.05113.

3.05114 Axial fatigue life of smooth specimens of 7475-T6 superplastically strained sheet, Figure 3.05114.

3.052 Fatigue crack-growth rates.

3.0521 Fatigue crack-growth rate of bare and alclad sheet, Figure 3.0521.

3.0522 Fatigue crack-growth rate of alclad sheet panels of various sizes at 75 F and -65 F, Figure 3.0522.

3.0523 Fatigue crack-growth rates for 0.125-inch thick specimen of 7475-T761 sheet in LT orientation–constant load tests, Figure 3.0523.

3.0524 Fatigue crack-growth rates for 0.125-inch thick specimen of 7475-T761 sheet in TL orientation–constant load tests, Figure 3.0524.

3.0525 Fatigue crack-growth rates for high and low copper content 7475-T7 plate, Figure 3.0525.

3.0526 Fatigue crack-growth rates for 1.5-inch thick specimen of 7475-T7651 plate in air and 3.5 percent salt water, Figure 3.0526.

3.0527 Fatigue crack-growth rates for 7475-T651 and -T7351 plate, Figure 3.0527.

3.0528 Fatigue crack-growth rates for 1.25-inch thick specimen of 7475-T73 plate, Figure 3.0528.

3.0529 Fatigue crack-growth rates for 7475-T7351 and -T651 plate in air and 3.5 percent NaCl solution, Figure 3.0529.

3.05210 Fatigue crack-growth rates for 7475-T7 in 0.25-inch thick plate containing a high (2.2 percent) copper content, Figure 3.05210.

3.05211 Fatigue crack-growth rates for 1.5-inch thick specimen of 7575-T7351 plate in air, Figure 3.05211.

3.06 **Elastic Properties**

3.061 Poisson's ratio.

3.062 Modulus of elasticity. (See also Tables 3.012, 3.013, 3.0215, and 3.02222 and Figures 3.031222 and 3.0322.)

3.0621 Tensile and compressive elastic modulii of 7475-T61 and -T761 sheet, Table 3.0621.

REFERENCES

1 Dickson, J. A., "Alcoa 467 Process X7475 Alloy", Alcoa Green Letter G. L. 216 5-70, Aluminum Company of America (May 1970).

2 Babilon, C. F., Wygonik, R. H., Nordmark, G. E., and Lifka, B. W., "Mechanical Properties, Fracture Toughness, Fatigue, Environmental Fatigue Crack Growth Rates, and Corrosion Characteristics of High-Toughness Aluminum Alloy Forgings, Sheet and Plate", Aluminum Company of America, Contract No. F33615-71-C-1571, Project No. 7381, Fourth Technical Management Report (February 15, 1972 – May 15, 1972).

3 Newcomer, R. E., "Improved Aluminum Alloys", McDonnell Aircraft Company, Report MDC A1666 (May 12, 1972).

4 Freed, C. N., Sullivan, A. M., and Stoop, J., "Comparison of Plane-Stress Fracture Toughness for Three Aluminum Sheet Alloys", Naval Research Laboratory, Report 7299 (August 11, 1971).

5 Wang, D. Y., "Plane Stress Fracture Toughness and Fatigue Crack Propagation of Aluminum Alloy Wide Panels", Douglas Aircraft Company, Douglas Paper 6054 (August 1972).

6 Turley, R. V., "Material Property Test Data for Aluminum Alloy X7475 and High Strength Clad Sheet Product", Preliminary release, Douglas Aircraft Company (July 26, 1972).

7 Van Horn, K. R., "Aluminum, Vol. 1", American Society for Metals (1967).

8 Aluminum Standards and Data, 3rd Edition, The Aluminum Association (January 1972).

9 Cervey, R. L., "Engineering Design Data for Aluminum Alloy 7475 in the T761 and T61 Condition", AFML-TR-72-173, University of Dayton Research Institute (September 1972).

10 Dorward, R. C., and Hasse, K. R., "Flaw Growth of 7075, 7475, 7050, and 7049 Aluminum Alloy Plate in Stress Corrosion Environments", Kaiser Aluminum & Chemical Corp., Center for Technology, Pleasanton, California, Research Report CFT-RR-76-32.

11 Babilon, C. F., Wygonik, R. H., Nordmark, G. E., and Lifka, B. W., "Mechanical Properties, Fracture Toughness, Fatigue, Environmental Fatigue Crack Growth Rates and Corrosion Characteristics of High Toughness Aluminum Alloy Forgings, Sheet and Plate", AFML-TR-73-83, Air Force Materials Laboratory, Wright Patterson Air Force Base, Ohio.

12 Brownhill, D. J., Davies, R. E., Nordmark, G. E., and Ponchel, B. M., "Exploratory Development for Efforts to Obtain Design Data on Structural Aluminum Alloys in Representative Aircraft Environments", Alcoa Technical Report, AFML Contract F33615-74-C-5089 (May 1976).

13 Humphries, T. S., and Nelson, E. E., "Seacoast Stress Corrosion of Cracking of Aluminum Alloys", Technical Memorandum, Materials and Processes Laboratory, Marshall Space Flight Center, National Aeronautics and Space Administration, Washington, D.C. (January 1981).

14 Deel, O. L., Ruff, P. E., and Mindlin, H., "Engineering Data on New Aerospace Structural Materials", Battelle Columbus Laboratories, AFML-TR-77-102, Air Force Materials Laboratory, Wright Patterson Air Force Base, Ohio (July 1977).

15 Brownhill, D. J., Davies, R. E., Nordmark, G. E., and Ponchel, B. M., "Exploratory Development for Design Data on Structural Aluminum Alloys in Representative Aircraft Environments", AFML-TR-77-102, Materials Laboratory, Wright Patterson Air Force Base, Ohio (July 1977).

16 Hall, L. R., Finger, R. W., and Spurr, W. F., "Corrosion Fatigue Crack Growth in Aircraft Structural Materials", AFML-TR-73-204, Air Force Materials Laboratory, Wright Patterson Air Force Base, Ohio (September 1973).

17 Cervay, R. R., "Aluminum Alloy 7475, T7651, Static and Dynamic Fracture Properties", AFML-TR-75-220 (also TR-75-20, April 1975), Air Force Wright Aeronautical Labs., Ohio (October 1975).

18 Hart, W.G.J.'t., Nederveen, A., Stoffels, E., and Tromp, J., "Fracture Toughness and Fatigue Properties of the New Aluminum Alloy 7475-T76", National Aerospace Laboratory, N.L.R., The Netherlands, N.L.R. TR 75168U.

19 Petrak, G. J., "Effect of Purity Levels on the Mechanical Properties of 7000 Series Aluminum", AFWAL-TR-80-4079, Air Force Materials Laboratory, Wright Patterson Air Force Base, Ohio (October 1980).

20 Van Orden, J. M., Krupp, W. E., Walden, E., and Ryder, J. T., "Effects of Purity on Fatigue and Fracture of 7xxx T6511 Aluminum Alloy Extrusions", Journal of Aircraft, Vol. 16, No. 5 (May 1979) p 327-335.

21 Bucci, R. J., "Selecting Aluminum Alloys to Resist Failure by Fracture Mechanisms", Engineering Fracture Mechanics, Vol. 12, No. 3 (1979) p 407-441.

22 Dorward, R. C., and Hasse, K. R., "Flaw Growth of 7075, 7475, 7050, and 7049 Aluminum Alloy Plate in Stress Corrosion Environments. Two Year Marine Atmosphere Results", Kaiser Aluminum & Chemical Corp., Center for Technology, Pleasanton, California, Research Report CFT-RR-78-16 (June 22, 1978).

23 Albrecht, J., and Lutjering, G., "Influence of Microstructure on Fatigue Crack Propagation Rate of Aluminum Alloys", European Space Agency Technical Translation, ESA TT 418, DLR-FB-77-07, Ruhr Universitat Bochum, West Germany (January 1978).

24 Hamilton, C. H., "Fine Grained Aluminum Superplasticity", Rockwell International Science Center, Thousand Oaks, California, Report No. SC 5187 .13 FR, ARSCD CR 8001 (February 1980).

25 Bampton, C. C., and Edington, J. W., "The Effect of Superplastic Deformation on the Subsequent Service Properties of Fine Grained 7475 Aluminum", Transactions ASME, Journal of Engineering Materials and Technology, Vol. 105 (January 1983) p 55-60.

26 Brown, K. R., "The Use of the Chevron Notched Short Bar Specimen for Plane Strain Fracture Toughness in Aluminum Alloys", ASTM Symposium on Chevron Notched Fracture Testing, Louisville, Kentucky, to appear in an ASTM STP (April 1983).

27 Staley, J. T., "Microstructure and Toughness of High Strength Aluminum Alloys", Properties Related to Fracture Toughness, ASTM STP 605, ASTM Materials (1976) p 71-103.

28 Military Handbook, 5c. Change Notice 3 (June 1981).

29 Cervay, R. R., "Static & Dynamic Fracture Properties for Aluminum Alloy 7475-T651 and T7351", AFML-TR-75-20, Air Force Materials Laboratory, Wright Patterson Air Force Base, Ohio (April 1975).

30 Mahoney, M. W., and Hamilton, C. W., "Superplastic Aluminum Evaluation", AFWAL TR-81-3051, Flight Dynamics Laboratory, Wright Patterson Air Force Base, Ohio (June 1981).

31 Kaufman, J. G., Sha, G. T., Kohm, R. F., and Bucci, R. J., "Notch Yield Ratios as a Quality Control Index for Plane Strain Fracture Toughness", Cracks and Fracture, ASTM STP 601, ASTM (1976) p 169-190.

32 Military Handbook, 5c. Change Notice 2 (December 1, 1979).

33 Aerospace Materials Specification AMS 4202 Revision A, Society of Automotive Engineers (July 1981).

34 Aerospace Materials Specification AMS 4090 Revision A, Society of Automotive Engineers (October 16, 1978).

35 Aerospace Materials Specification AMS 4089 Revision A, Society of Automotive Engineers (October 16, 1978).

36 Aerospace Materials Specification AMS 4084 Revision A, Society of Automotive Engineers (October 16, 1978).

37 Aerospace Materials Specification AMS 4085 Revision A, Society of Automotive Engineers (October 16, 1978).

38 Military Handbook, 5c. (September 15, 1976).

39 Brown, K. R., "Factors Affecting the Fracture Toughness of Aluminum Alloys", Proceedings of the ICSMA 6, Melbourne Australia (August 1982) p 765.

40 Bretz, P. E., Vasudevan, A. K., Bucci, R. J., and Malcolm, R. C., "Effect of Microstructure on 7xxx Aluminum Alloy Fatigue Crack Behavior", A.D. A112721, Alcoa/Dept. of the Navy (October 9, 1981).

	Al
5.6	Zn
2.2	Mg
1.5	Cu
0.21	Cr
Low	Si
	Fe
	Mn
	Ti

7475 Al

	Al
5.6	Zn
2.2	Mg
1.5	Cu
0.21	Cr
Low	Si
	Fe
	Mn
	Ti

7475 Al

Alloy	7475	
	Percent	
Composition	Min	Max
Si	–	0.10
Fe	–	0.12
Cu	1.2	1.9
Mn	–	0.06
Mg	1.9	2.6
Cr	0.18	0.25
Zn	5.2	6.2
Ti	–	0.06
Others		
Each	–	0.05
Total	–	0.15
Al	Remainder	

TABLE 1.04 ALUMINUM ASSOCIATION COMPOSITION LIMITS (1, 33-37)

Alloy	7475			
Form	Sheet		Plate	Extrusions
Temper	T61	T736	T7351	T73511
Electrical Conductivity, percent IACS	35.1	38.4	44.1	40.2
megaohms/in.^{3}	0.516	0.565	–	–
Electrical Resistivity, microohm/in.	1.94	1.77	–	–

TABLE 2.022. ELECTRICAL PROPERTIES (3,10,11,19)

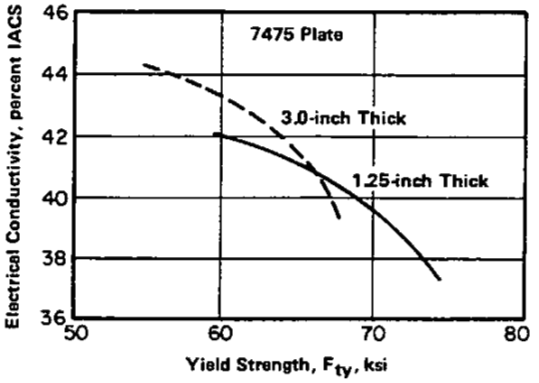


FIGURE 2.0221. VARIATION IN ELECTRICAL CONDUCTIVITY WITH TENSILE YIELD STRENGTH IN 7475 PLATE (10)

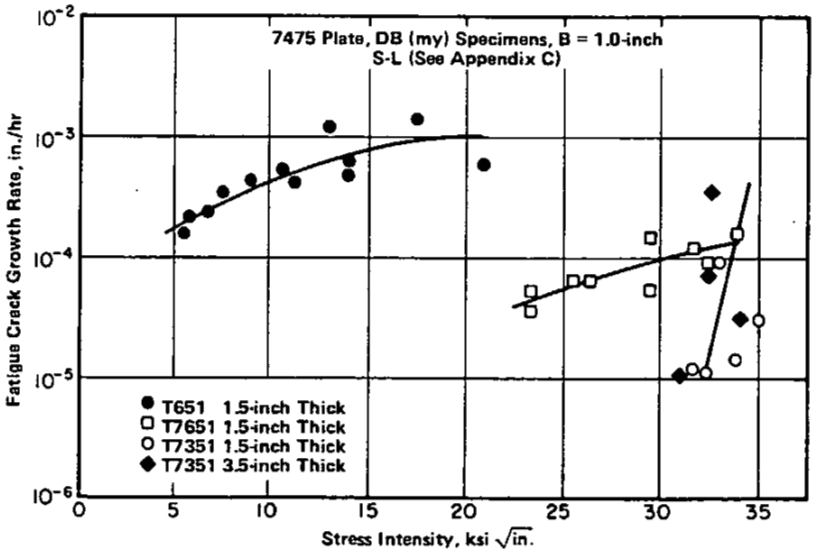


FIGURE 2.0321. CRACK-GROWTH RATES FOR FATIGUE PRECRACKED SPECIMENS OF 7475 PLATE EXPOSED FOR 202 DAYS TO MARINE ATMOSPHERE AT DAYTONA BEACH, FLORIDA (22)

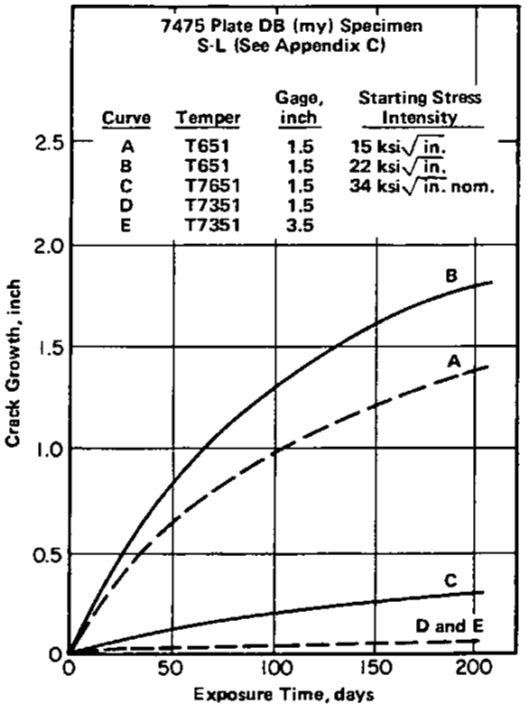


FIGURE 2.0322. CRACK GROWTH IN FATIGUE PRECRACKED SPECIMENS OF 7475 PLATE EXPOSED FOR 202 DAYS TO MARINE ATMOSPHERE AT DAYTONA BEACH, FLORIDA (22)

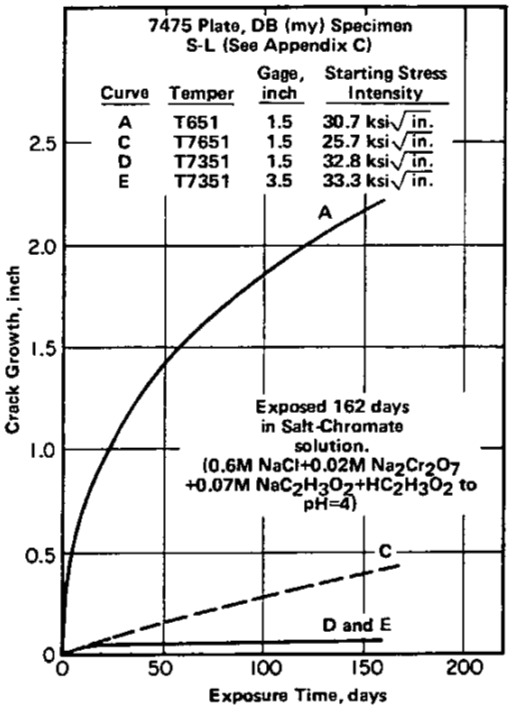


FIGURE 2.0323. CRACK GROWTH IN FATIGUE PRECRACKED SPECIMENS OF 7475 PLATE IMMERSED FOR 162 DAYS IN SALT-CHROMATE SOLUTION (22)

Al
5.6 Zn
2.2 Mg
1.5 Cu
0.21 Cr
Low Si
Fe
Mn
Ti

7475 Al

Alloy	7475		
Form	Plate		
Orientation	S-L		
		K_{Iscc}, ksi√in.(a)	
Thickness, inch	Temper	Salt-Chromate(b) Solution	Marine Atmosphere at Daytona Beach, 6 months
1.5	T651	<4	<5
1.5	T7651	<15	<22
1.5	T7351	~33	~32
3.5	T7351(c)	~30	~32

(a) At 4 x 10^{-9} in./sec crack-growth rate.
(b) See Figure 2.0323 for composition of salt-chromate solution.
(c) Nominal S-L K_{Ic} = 43.5 ksi√in. in laboratory air.

TABLE 2.0324. ESTIMATED S-L THRESHOLD STRESS INTENSITY, K_{Iscc}, FOR DOUBLE CANTILEVER BEAM SPECIMENS OF 7475 PLATE (22)

	Al
5.6	Zn
2.2	Mg
1.5	Cu
0.21	Cr
Low	Si
	Fe
	Mn
	Ti

7475 Al

Alloy	7475-T6				
Form	1.5-inch x 0.5-inch Superplastic Sheet(a)				
Test Material Treatment	Grain Diameter, μm		Sheet Thickness, inch	No. of Specimens Tested	Survived Exposure, percent
	L and LT	ST			
As Processed to Fine Grain Size + 1 hr at 961 F, + T6 Heat Treat	14.5	7.7	0.079	26	73
Same as Above	11.1	6.0	0.04	16	75
Same as Above + Slow Heat Up to Recrystallization Temperature	40.0	12.0	0.04	8	75
As Processed to Fine Grain Size, + Superplastic Uniaxial Strain, ($\bar{\epsilon}$ = 0.96, $\dot{\epsilon}$ = 2x10^{-4} sec^{-1}, Temp = 961 F) + T6 Heat Treatment	19.5	8.8	0.04	2	50
Same as Above with $\bar{\epsilon}$ = 1.28	20.4	9.2	0.04	2	100

(a) Specimen is bent elastically in a teflon jig to an outer fiber stress of 49.3 ksi, immersed in 3.5 percent NaCl solution for 10 minutes, immersed for 50 minutes in air. Humidity was not controlled and specimen was nonstandard.

TABLE 2.0325. STRESS CORROSION BEHAVIOR OF SUPERPLASTICALLY STRAINED 7475-T6 SHEET (31)

Alloy	7475-T7351			
Form	Plate			
Thickness, t, inch	Direction	F_{tu}, ksi	F_{ty}, ksi	e (2-inch), percent
0.25 < t < 1.500	L	68	57	10
	T	68	57	9
t = 1.500	L	68	57	10
	T	68	57	9
	ST	64	53	4
1.500 < t ≤ 2.000	L	67	55	10
	T	67	55	8
	ST	64	52	4
2.000 < t ≤ 2.500	L	66	54	10
	T	66	54	8
	ST	64	52	4
2.500 < t ≤ 3.000	L	65	53	10
	T	65	53	8
	ST	62	50	3
3.000 t ≤ 3.500	L	63	51	10
	T	63	51	8
	ST	61	48	3
3.500 < t ≤ 4.000	L	61	48	9
	T	61	48	7
	ST	59	46	3

TABLE 3.0111. AMS SPECIFIED TENSILE PROPERTIES FOR T7351 PLATE (33)

Alloy	7475-T7351	
Form	Plate	
Thickness, t, inch	Orientation	K_{Ic}, ksi $\sqrt{in.}$
$0.749 < t \leq 4.000$	L-T	38
$0.749 < t \leq 4.000$	T-L	32
$2.750 < t \leq 4.000$	S-L	25

TABLE 3.0112. AMS SPECIFIED FRACTURE TOUGHNESS FOR T7351 PLATE (33)

Alloy	7475-T651			
Form	Plate			
Thickness, t, inch	Direction	F_{tu}, ksi	F_{ty}, ksi	e (2-inch), percent
$0.250 \leq t \leq 0.499$	L	77	67	9
	LT	78	67	9
$0.499 < t \leq 1.000$	L	77	68	8
	LT	78	68	8
$1.000 < t \leq 1.500$	L	76	67	6
	LT	77	67	6

TABLE 3.0113. AMS SPECIFIED TENSILE PROPERTIES FOR T651 PLATE (34)

	Al
5.6	Zn
2.2	Mg
1.5	Cu
0.21	Cr
Low	Si
	Fe
	Mn
	Ti

7475 Al

Alloy	7475-T651
Form	Plate
Orientation	K_{Ic}, ksi $\sqrt{in.}$[a]
L-T	30
T-L	28

(a) Crack length is not less than 1.5 inch and specimen thickness is equal to plate thickness.

TABLE 3.0114. AMS SPECIFIED FRACTURE TOUGHNESS FOR T651 PLATE (34)

Alloy	7475-T7651			
Form	Plate			
Thickness, t, inch	Direction	F_{tu}, ksi	F_{ty}, ksi	e (2-inch), percent
$0.250 \leq t \leq 0.499$	L	70	60	9
	LT	71	60	9
$0.499 < t \leq 1.000$	L	69	59	8
	LT	70	59	8
$1.000 < t \leq 1.500$	L	69	59	6
	LT	70	59	6

TABLE 3.0115. AMS SPECIFIED TENSILE PROPERTIES FOR T7651 PLATE (35)

Alloy	7475-T7651
Form	Plate
Orientation	K_{Ic}, ksi $\sqrt{in.}$[a]
L-T	33
T-L	30

(a) Crack length is not less than 1.5 inch and specimen thickness is equal to plate thickness.

TABLE 3.0116. AMS SPECIFIED FRACTURE TOUGHNESS FOR T7651 PLATE (35)

Alloy	7475-T651			
Form	Sheet			
Thickness, t, inch	F_{tu}, ksi[a]	F_{ty}, ksi[a]	e (2-inch), percent[a]	K_Q, ksi $\sqrt{in.}$[b]
≥ 0.040	75	64	9	–
$0.040 \leq t \leq 0.125$	–	–	–	75
$0.125 < t \leq 0.249$	–	–	–	60

(a) Tensile test direction was not specified.
(b) K_Q was determined for L-T direction using M(T) specimen (W = 16 inch and B = sheet thickness) and procedure described in AMS 4084.

TABLE 3.0117. AMS SPECIFIED TENSILE PROPERTIES AND FRACTURE TOUGHNESS FOR T651 SHEET (36)

	Al
5.6	Zn
2.2	Mg
1.5	Cu
0.21	Cr
Low	Si
	Fe
	Mn
	Ti

7475 Al

Alloy	7475-T7651			
Form	Sheet			
Thickness, t, inch	F_{tu}, ksi(a)	F_{ty}, ksi(a)	e (2-inch), percent(a)	K_Q, ksi$\sqrt{in.}$(b)
$t \geq 0.040$	71	60	9	–
$0.040 \leq t \leq 0.125$	–	–	–	80
$0.125 < t \leq 0.249$	–	–	–	70

(a) Tensile test direction was not specified.
(b) K_Q was determined for L-T direction using M(T) specimen (W = 44 inch and B = sheet thickness) and procedure described in AMS 4085.

TABLE 3.0118. AMS SPECIFIED TENSILE PROPERTIES AND FRACTURE TOUGHNESS FOR T7651 SHEET (37)

Alloy	7475									
Form	Sheet	Plate			Sheet			Plate		
Condition	T61	T651			T761			T7651		
Thickness, in.	0.040-0.249	0.250-0.499	0.500-1.000	1.001-1.499	0.040-0.062	0.063-0.187	0.188-0.249	0.250-0.499	0.500-1.000	1.001-1.499
Basis	S	S	S	S	S	S	S	S	S	S
Mechanical properties:										
F_{tu}, ksi										
L	74	77	77	76	71	70	69	70	69	69
LT	75	78	78	77	71	71	71	71	70	70
F_{ty}, ksi										
L	65	67	68	67	61	60	60	60	59	59
LT	64	67	68	67	60	60	60	60	59	59
F_{cy}, ksi										
L	64	67	68	66	60	59	58	60	59	59
LT	68	70	71	70	63	63	63	63	62	62
F_{su}, ksi	45	44	43	40	43	42	41	41	39	37
F_{bru}*, ksi										
(e/D=1.5)	120	113	113	111	112	112	111	104	103	103
(e/D=2.0)	154	144	144	142	143	143	142	136	134	134
F_{bry}*, ksi										
(e/D=1.5)	97	91	93	91	90	90	90	82	81	81
(e/D=2.0)	110	106	107	106	104	104	104	97	95	95
e, percent										
LT	9	9	8	6	9	9	9	9	8	6
E, 10^3 ksi	10.0	10.2			10.0			10.2		
E_c, 10^3 ksi	10.5	10.6			10.5			10.6		
G, 10^3 ksi	3.8	3.9			3.8			3.9		
μ	0.33	0.33			0.33			0.33		

(a) Bearing values are "dry pin" values.

TABLE 3.012. DESIGN MECHANICAL PROPERTIES OF 7475-T6 AND -T76 SHEET AND PLATE (28)

Alloy	7475-T7351						
Form	Plate						
Thickness, in.	0.250-1.000	1.001-1.500	1.501-2.000	2.001-2.500	2.501-3.000	3.001-3.500	3.501 4.000
Basis	S	S	S	S	S	S	S
Mechanical properties:							
F_{tu}, ksi							
L	68	68	67	66	65	63	61
LT	68	68	67	66	65	63	61
ST	...	64[a]	64	64	62	61	59
F_{ty}, ksi							
L	57	57	55	54	53	51	48
LT	57	57	55	54	53	51	48
ST	...	53[a]	52	52	50	48	46
F_{cy}, ksi							
L	56	55	53	52	51	48	45
LT	59	59	57	55	54	52	49
ST	...	59[a]	57	56	55	53	50
F_{su}, ksi	39	39	40	40	40	39	37
F_{bru},[b] ksi							
(e/D = 1.5)	98	98	102	101	99	96	93
(e/D = 2.0)	127	127	132	130	128	124	120
F_{bry},[b] ksi							
(e/D = 1.5)	78	78	82	80	79	76	71
(e/D = 2.0)	93	93	95	93	92	88	83
e, percent							
L	10	10	10	10	10	10	9
LT	9	9	8	8	8	8	7
ST	...	4[a]	4	4	3	3	3
E, 10^3 ksi	10.3						
E_c, 10^3 ksi	10.6						
G, 10^3 ksi	3.9						
μ	0.33						

(a) Values applicable to 1.500 inch thickness only.
(b) Bearing values are "dry pin" values.

TABLE 3.013. DESIGN MECHANICAL PROPERTIES OF 7475-T7351 PLATE (32)

	Al
5.6	Zn
2.2	Mg
1.5	Cu
0.21	Cr
Low	Si
	Fe
	Mn
	Ti

7475 Al

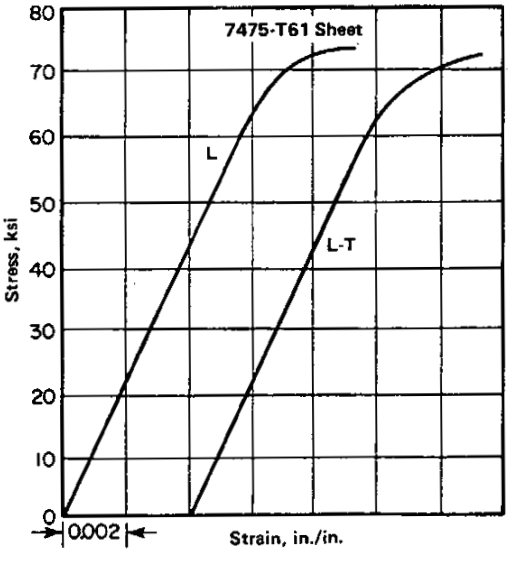


FIGURE 3.02111. STRESS-STRAIN CURVES FOR SHEET IN T61 CONDITION (1)

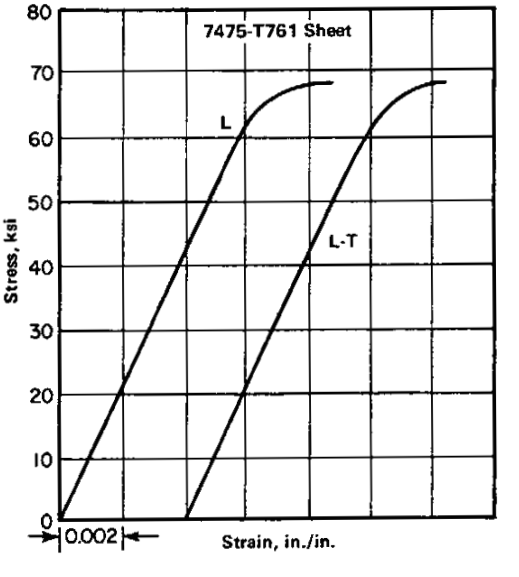


FIGURE 3.02112. STRESS-STRAIN CURVES FOR SHEET IN T761 CONDITION (1)

	Al
5.6	Zn
2.2	Mg
1.5	Cu
0.21	Cr
Low	Si
	Fe
	Mn
	Ti

7475 Al

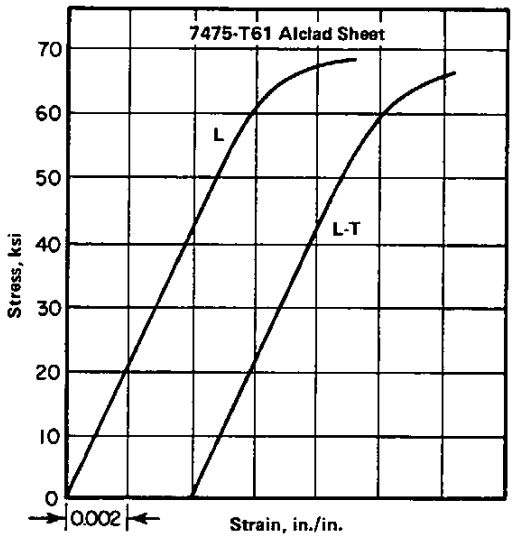


FIGURE 3.02113. STRESS-STRAIN CURVES FOR ALCLAD SHEET IN T61 CONDITION (1)

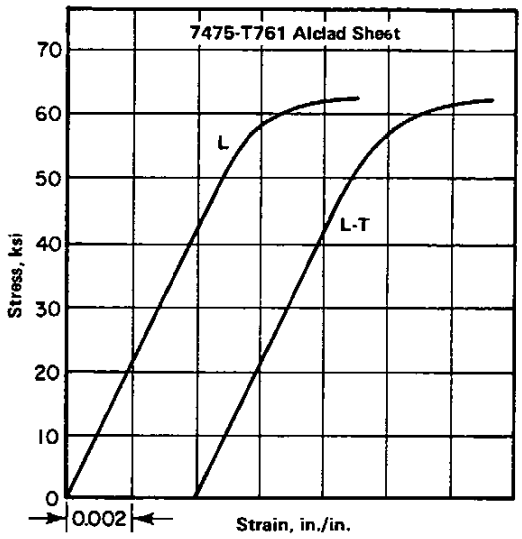


FIGURE 3.02114. STRESS-STRAIN CURVES FOR ALCLAD SHEET IN T761 CONDITION (1)

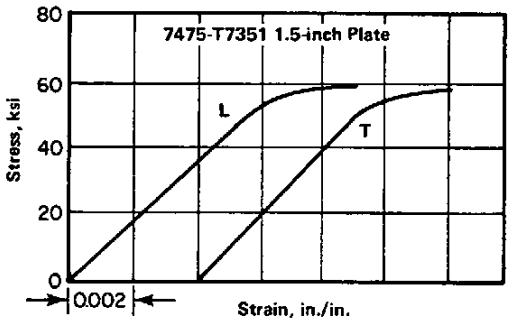


FIGURE 3.02115. STRESS-STRAIN CURVES FOR 1.5-INCH PLATE IN T7351 CONDITION (29)

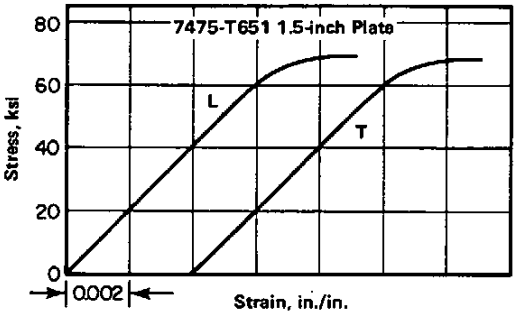


FIGURE 3.02116. STRESS-STRAIN CURVES FOR 1.5-INCH PLATE IN T651 CONDITION (29)

Alloy	7475							
Form	Bare Sheet						Alclad Sheet	
Condition	T61			T761			T61	T761
Thickness, inch	0.040	0.125	0.249	0.040	0.125	0.249	0.040-0.249	0.040-0.249
F_{tu}, ksi								
L	82.3	80.8	80.7	80.6	74.5	75.0	77.5	71.0
LT	80.6	81.3	82.0	78.6	75.6	76.2	77.5	–
F_{ty}, ksi								
L	76.6	75.6	76.4	74.0	66.6	67.4	72.5	61.0
LT	72.5	72.8	74.2	71.0	65.2	67.1	70.0	–
e (2-inch), percent								
L	10.8	12.2	13.2	10.8	12.0	13.8	12.5	12.0
LT	11.0	12.2	13.2	10.8	11.8	14.0	13.0	–

TABLE 3.0212. TYPICAL TENSILE PROPERTIES OF BARE AND ALCLAD SHEET (1,2,6)

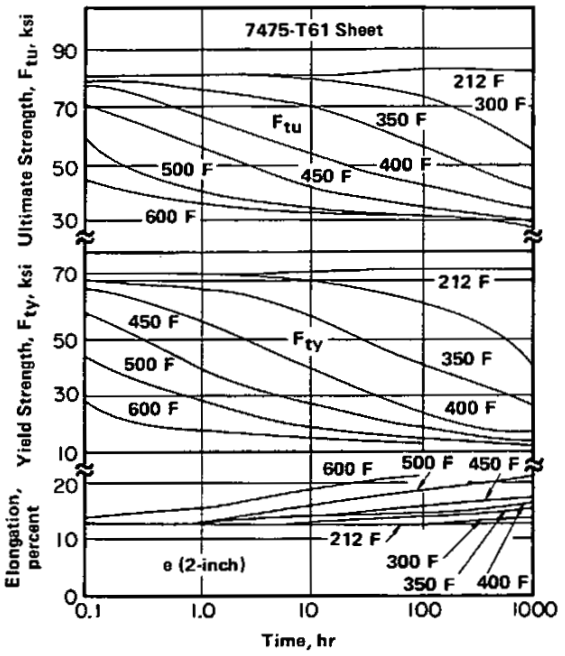


FIGURE 3.0213. EFFECT OF EXPOSURE TIME AT VARIOUS ELEVATED TEMPERATURES ON ROOM TEMPERATURE TENSILE PROPERTIES OF SHEET IN T61 CONDITION (1)

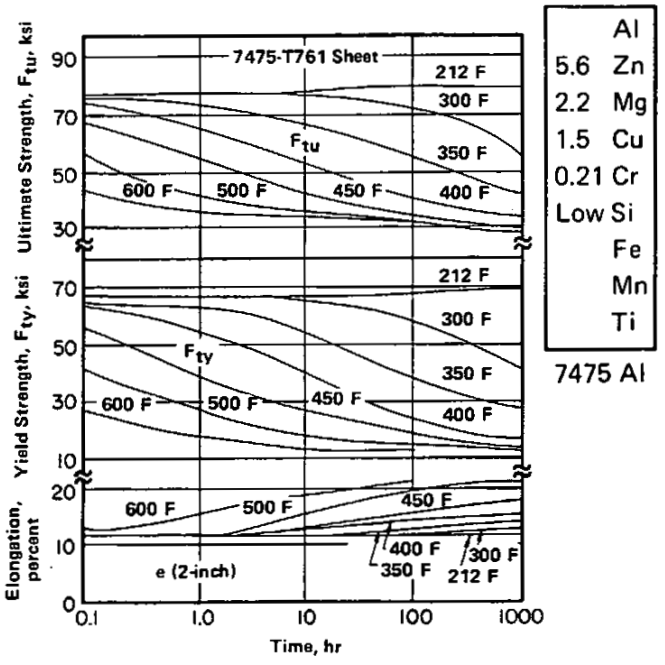


FIGURE 3.0214. EFFECT OF EXPOSURE TIME AT VARIOUS ELEVATED TEMPERATURES ON ROOM TEMPERATURE TENSILE PROPERTIES OF SHEET IN T761 CONDITION (1)

Alloy	7475-T6		
Form	Superplastic Sheet		
Orientation	Temp, F	Strain Rate, sec^{-1}	e, percent
L	900	10^{-2}	150
LT		10^{-2}	100
L		$5x10^{-3}$	125
LT		$5x10^{-3}$	200
L		10^{-3}	200
LT		10^{-3}	175
L		$2x10^{-4}$	306
LT		$2x10^{-4}$	200
L	960	10^{-2}	118
LT		10^{-2}	100
L		$5x10^{-3}$	200
LT		$5x10^{-3}$	175
L		10^{-3}	275
LT		10^{-3}	>450
L		$2x10^{-4}$	650
LT		$2x10^{-4}$	525
L		$5x10^{-5}$	425

TABLE 3.0215. TENSILE ELONGATION OF SUPERPLASTIC 7475 SHEET AT VARIOUS STRAIN RATES AT 900 F AND 960 F (24)

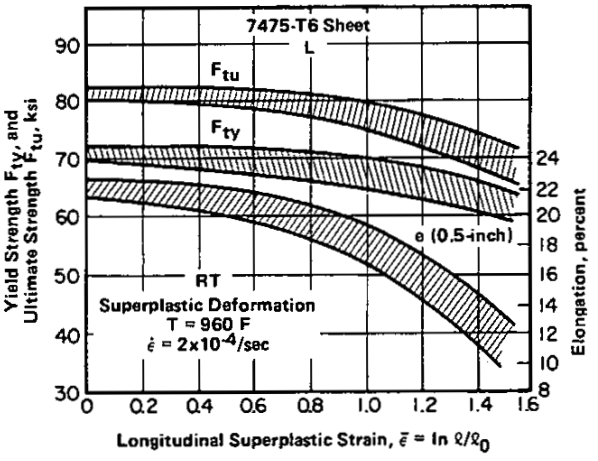


FIGURE 3.0216. ROOM TEMPERATURE TENSILE PROPERTIES OF 7475-T6 SHEET AFTER UNIAXIAL SUPERPLASTIC TENSILE DEFORMATION (25)

	Al
5.6	Zn
2.2	Mg
1.5	Cu
0.21	Cr
Low	Si
	Fe
	Mn
	Ti

7475 Al

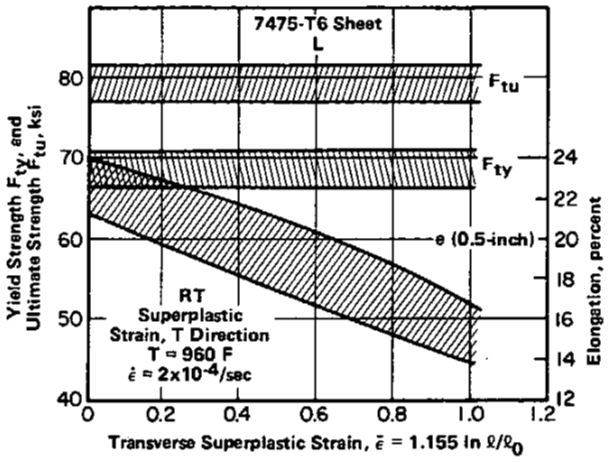


FIGURE 3.0217. ROOM TEMPERATURE PROPERTIES OF 7475-T6 SHEET AFTER SUPERPLASTIC PLANE STRAIN TENSILE DEFORMATION (25)

Alloy	7475-T7351						
Form	Plate						
Thickness, inch	Source	Direction	F_{tu}, ksi	F_{ty}, ksi	e (2-inch), percent	RA, percent	E, x 10^6 psi
0.5	15(d)	L	71.0	62.3	18	45	–
		T	73.4	63.8	14	29	–
0.75	15(d)	L	72.5	63.8	16	46	10.32
		T	73.2	63.7	14	37	10.41
1.25(a)	10	L	72.9	62.3	13	–	–
		T	71.9	61.0	11	–	–
		ST	65.7	58.1	4	–	–
1.5(a)	17	L	71.6	59.5	15	48	–
		T	70.0	58.9	17	52	–
1.75(b)	15(d)	L	72.6	61.8	15	41	–
		T	72.8	61.9	13	33	–
		ST	70.8	58.1	9	22	–
2.0(c)	14	L	72.1	62.9	18	48	10.2
		T	73.2	62.4	15	35	9.80
2.0	13	ST	71.0	59.0	14	–	–
2.25(b)	13	L	70.6	59.7	15	41	–
		T	71.6	60.2	12	28	–
		ST	69.7	57.2	8	18	–
2.75(b)	13	L	68.9	58.2	15	43	–
		T	70.4	58.8	12	26	–
		ST	68.5	54.8	10	19	–
3.0(a)	10	L	68.0	56.8	13	–	–
		T	68.2	55.8	10	–	–
		ST	65.2	52.9	5	–	–
3.0	13	ST	64.0	54.0	4.5	–	–
3.5(b)	15(d)	L	66.8	55.6	15	40	10.13(e)
		T	68.2	56.0	11	26	10.34(e)
		ST	67.6	54.2	9	16	10.23(e)
3.5(a)	10	T	68.1	57.0	14	–	–
4.0(b)	15(d)	L	64.0	52.6	15	41	–
		T	65.9	53.7	11	20	–
		ST	64.8	52.1	8	11	–

Note: Test locations in accordance with ASTM B557; test in accordance with ASTM E8.

(a) Average of triplicate specimens.
(b) Average of two lots.
(c) Average of duplicate specimens.
(d) Results are for "current practice" only, except for 4-inch plate from an earlier production practice.
(e) One lot.

TABLE 3.0218. TYPICAL MECHANICAL PROPERTIES OF 7475-T7351 PLATE (10,13,15,17)

Alloy	7475-T651					
Form	Plate					
Thickness, inch	Source	Direction	F_{tu}, ksi	F_{ty}, ksi	e, percent	RA, percent
1.5	17	L	78.7	70.9	16	37
		T	82.5	69.8	14	28
1.0	16	L	88.6	79.7	10	22
		T	84.9	75.7	11	26

TABLE 3.0219. MECHANICAL PROPERTIES OF 7475-T651 PLATE (17,16)

	Al
5.6	Zn
2.2	Mg
1.5	Cu
0.21	Cr
Low	Si
	Fe
	Mn
	Ti

7475 Al

Alloy			7075 (a)(7475) -T73511 and -T76511												
Form			1.5-inch x 4.5-inch Extrusions												
			F_{tu}, ksi			F_{ty}, ksi			e, percent			RA, percent			Conductivity, percent
Purity	Fe, percent	Si, percent	L	T	ST	L	T	ST	L	T	ST	L	T	ST	IACS
			T73511 (19)												
High	0.08	0.03	77.7	73.1	69.7	68.6	63.0	57.8	14.8	13.1	8.7	41.7	29.2	13.7	40.2
Medium	0.19	0.10	77.0	72.3	69.8	68.4	62.9	58.8	13.3	12.3	9.0	32.7	23.5	8.3	40.7
Low	0.26	0.14	73.9	70.2	67.0	65.3	60.9	57.2	12.7	11.7	6.5	31.9	20.8	8.0	40.0
			T76511 (20)												
High	0.08	0.03	82.5	76.6	75.7	73.1	66.6	62.5	11	10	9	23	16	14	
Medium	0.19	0.10	83.2	76.7	77.7	74.5	67.8	64.1	10	8	8	19	15	9	
Low	0.26	0.14	80.1	73.7	73.2	71.6	65.8	62.8	11	8	5	20	10	8	

(a) This high purity version is expected to behave similarly to 7475; results are included to show the effect of alloy purity.

TABLE 3.02110. EFFECT OF ALLOY PURITY ON THE MECHANICAL PROPERTIES OF 7075/7475 (19,20)

Alloy	7475-T6, -T76, -T73(a)		
Form	1.5-inch Thick Plate		
	Transverse		
Temper	F_{tu}, ksi	F_{ty}, ksi	e, percent
T6	82.6	78.9	13
T76	74.9	65.5	13
T73	67.3	56.0	14

(a) Production T6 plate, portions of which were aged in the laboratory to T76 and T73.

TABLE 3.02111. MECHANICAL PROPERTIES OF 1.5-INCH THICK 7475 PLATE IN VARIOUS TEMPERS (22)

	Al
5.6	Zn
2.2	Mg
1.5	Cu
0.21	Cr
Low	Si
	Fe
	Mn
	Ti

7475 Al

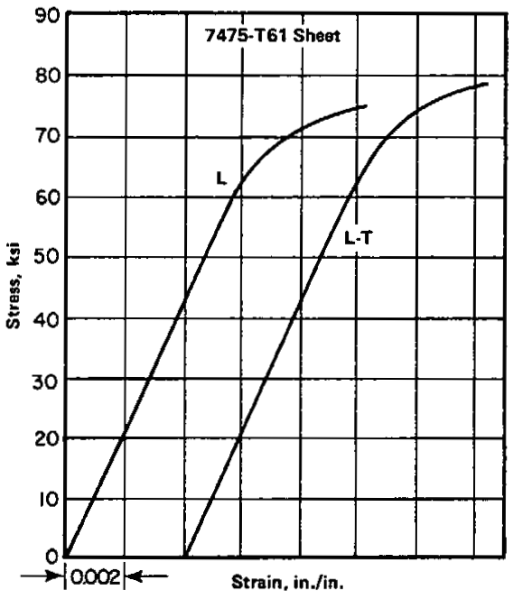


FIGURE 3.02211. COMPRESSIVE STRESS-STRAIN CURVES FOR SHEET IN T61 CONDITION (1)

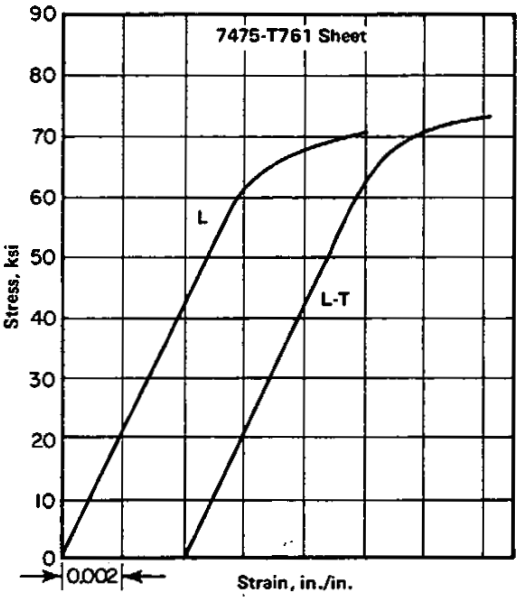


FIGURE 3.02212. COMPRESSIVE STRESS-STRAIN CURVES FOR SHEET IN T761 CONDITION (1)

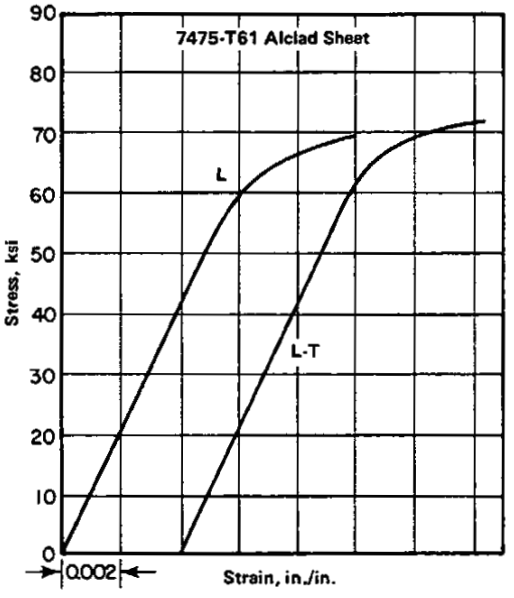


FIGURE 3.02213. COMPRESSIVE STRESS-STRAIN CURVES FOR ALCLAD SHEET IN T61 CONDITION (1)

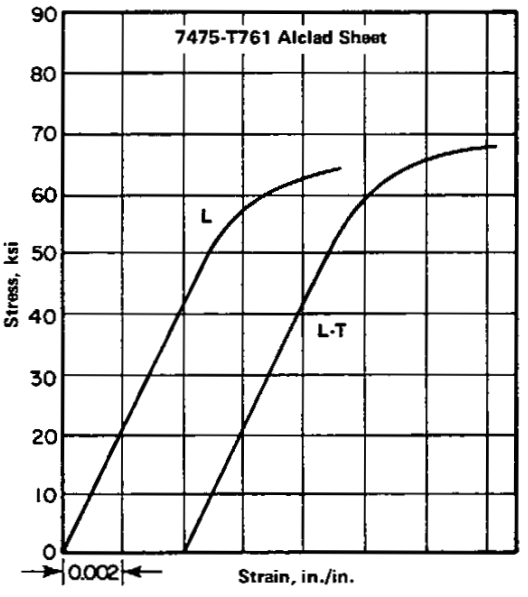


FIGURE 3.02114. COMPRESSIVE STRESS-STRAIN CURVES FOR ALCLAD SHEET IN T761 CONDITION (1)

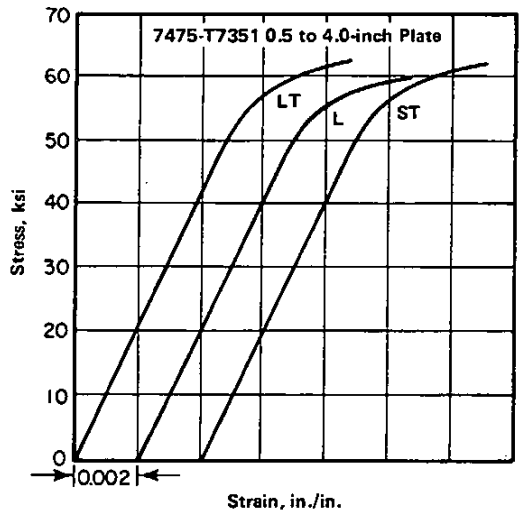


FIGURE 3.02215. TYPICAL COMPRESSION STRESS-STRAIN CURVES FOR 7475-T7351 PLATE (32)

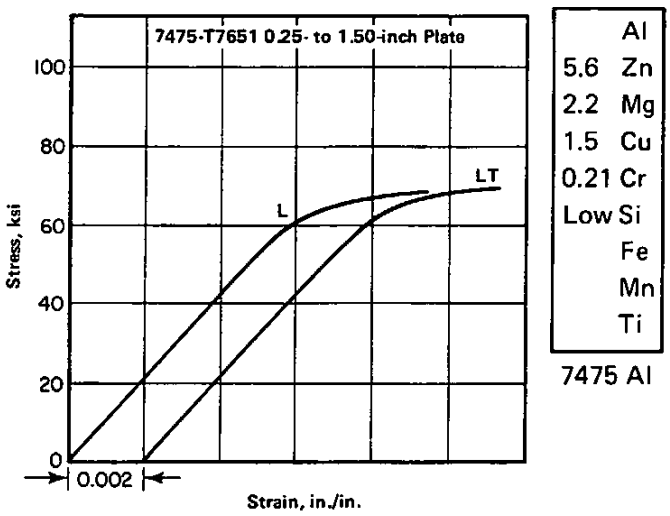


FIGURE 3.02216. TYPICAL COMPRESSION STRESS-STRAIN CURVES FOR 7475-T7651 PLATE (38)

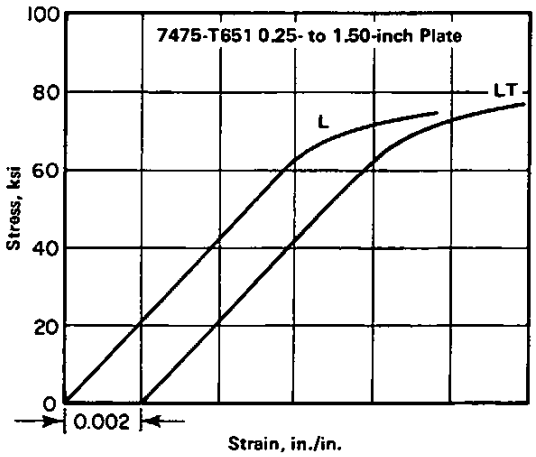


FIGURE 3.02217. TYPICAL COMPRESSION STRESS-STRAIN CURVES FOR 7475-T651 PLATE (38)

Alloy	7475-T61 and -T761	
Form	Sheet	
	T61	T761
Specimen Orientation	F_{cy}, ksi	F_{cy}, ksi
L	73.8	67.9
LT	77.6	70.8

TABLE 3.02221. COMPRESSIVE YIELD STRENGTH OF SHEET (2)

Alloy	7475-T7351		
Form	Plate		
Thickness, inch	Orientation	F_{cy}, ksi	Compressive Modulus, E_c, x 10^3 psi
0.50	L	62.3	–
	LT	66.6	–
0.75	L	63.4	10.69
	LT	66.6	10.81
3.50	L	53.8	10.48
	LT	58.3	10.80
	ST	58.8	10.60

TABLE 3.02222. COMPRESSIVE STRENGTH OF 7475-T7351 PLATE OF VARIOUS THICKNESSES (15)

	Al
5.6	Zn
2.2	Mg
1.5	Cu
0.21	Cr
Low	Si
	Fe
	Mn
	Ti

7475 Al

Alloy	7475-T61 and -T761	
Form	Sheet	
Specimen Orientation	T61 F_{su}, ksi	T761 F_{su}, ksi
L	51.8	48.2
LT	52.2	47.9

TABLE 3.0251. SHEAR STRENGTH OF SHEET (2)

Alloy	7475-T7351	
Form	Plate	
Thickness, inch	Orientation	F_{su}, ksi
0.50	L	43.9
	LT	43.6
0.75	L	42.6
	LT	42.1
3.50	L	42.5
	LT	41.8
	ST	37.5

TABLE 3.0252. SHEAR STRENGTH OF PLATE (15)

Alloy	7475-T61 and -T761					
Form	Sheet					
Condition	Thickness, inch	Specimen Orientation	F_{bru}, ksi e/D=1.5	F_{bru}, ksi e/D=2.0	F_{bry}, ksi e/D=1.5	F_{bry}, ksi e/D=2.0
T61	0.040	L	127.3	166.4	101.0	116.8
		LT	126.5	165.6	101.7	117.0
	0.125	L	133.3	164.8	114.3	130.4
		LT	132.9	165.6	114.2	130.8
	0.249	L	129.2	166.6	110.8	128.4
		LT	129.3	164.9	110.0	129.8
T761	0.040	L	123.8	161.0	95.8	113.8
		LT	123.4	165.6	98.6	114.5
	0.125	L	121.8	151.7	103.0	117.8
		LT	119.6	152.0	102.8	119.1
	0.249	L	119.1	151.3	100.2	116.0
		LT	118.6	151.6	99.0	118.7

TABLE 3.0261. BEARING PROPERTIES OF SHEET IN VARIOUS HEAT TREATED CONDITIONS, THICKNESSES, AND ORIENTATIONS (2)

Alloy	7475-T7351				
Form	Plate				
Thickness, inch	Orientation	F_{bru}, ksi e/D=1.5	F_{bru}, ksi e/D=2.0	F_{bry}, ksi e/D=1.5	F_{bry}, ksi e/D=2.0
0.50	L	112.6	145.7	91.1	114.8
	LT	114.3	143.7	95.2	112.5
0.75	L	107.7	140.3	88.5	108.3
	LT	108.2	138.3	89.6	104.2
3.50	L	105.9	139.6	84.3	100.4
	LT	109.2	136.7	90.8	101.5

TABLE 3.0262. BEARING PROPERTIES (FLATWISE) OF 7475-T7351 PLATE IN VARIOUS THICKNESSES (15)

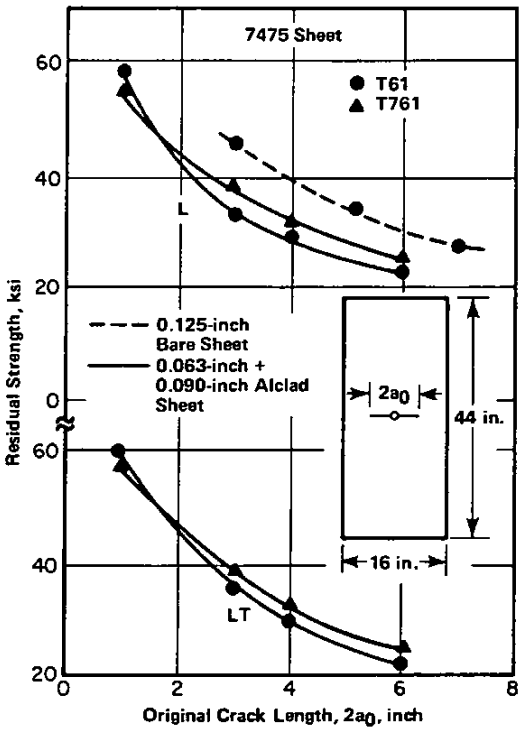


FIGURE 3.02711. RESIDUAL STRENGTH (GROSS AREA STRESS AT MAXIMUM LOAD) OF BARE AND ALCLAD SHEET AS A FUNCTION OF ORIGINAL CRACK LENGTH (1,3)

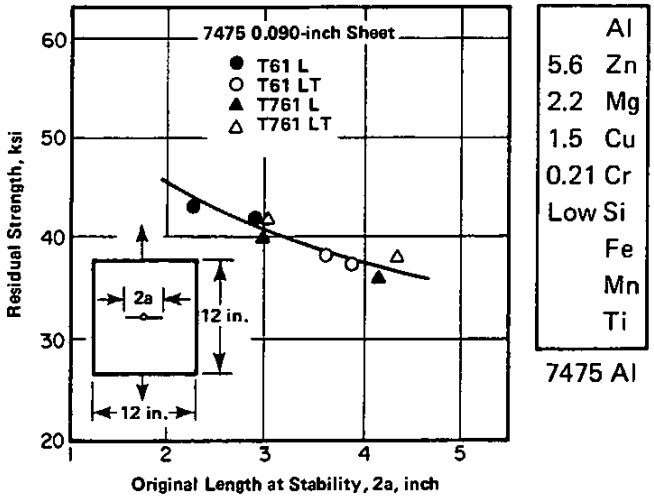


FIGURE 3.02712. RESIDUAL STRENGTH (GROSS AREA STRESS AT MAXIMUM LOAD) OF SHEET AS A FUNCTION OF CRACK LENGTH AT INSTABILITY (4)

Crack length at instability in this instance is the length of the crack, measured by a calibrated instrumented beam displacement gage, when the maximum load is reached. Beyond this point, crack growth accelerates, and fracture occurs with no increase in load.

Alloy		7475-T761				
Form		0.063-inch Alclad Sheet				
Orientation		Long Transverse				
F_{ty}, ksi	Panel Width (W), inch	Total Crack Length, inch: Initial ($2a_0$)	Total Crack Length, inch: Critical (2a)(a)	$\frac{2a_0}{W}$	Fracture Stress, ksi: Gross(b)	Fracture Stress, ksi: Net(c)
64	36	3.6	5.3	0.10	45.2	53.2
64	36	7.2	9.5	0.20	33.1	45.0
64	36	10.8	13.0	0.30	27.2	41.5
64	48	9.6	11.8	0.20	31.2	41.3
59	120	20.0	22.1	0.167	27.2	33.2
62	120	30.0	32.1	0.25	18.1	24.7

(a) Critical crack length is the length of the crack, measured optically to the nearest 0.1 inch, when the maximum load is reached. Beyond this point, crack growth accelerates and fracture occurs with no increase in load.
(b) Based on total uncracked cross sectional area of panel.
(c) Based on net cross sectional area of panel at section of critical crack.

TABLE 3.02713. FRACTURE STRENGTH OF CENTER CRACKED PANELS OF VARIOUS WIDTHS IN T761 CONDITION(5)

Alloy		7475-T61				
Form		Alclad Sheet				
Orientation		Long Transverse				
F_{ty}, ksi	Specimen, inch: Width (W)	Specimen, inch: Thickness	Original Crack Length ($2a_0$), inch	$\frac{2a_0}{W}$	Fracture Stress, ksi: Gross(a)	Fracture Stress, ksi: Net(b)
69.2	7.50	0.087	2.55	0.34	37.2	56.3
69.2	7.50	0.088	2.50	0.33	39.0	58.5
70.4	7.49	0.250	2.55	0.34	28.1	42.5
70.4	7.50	0.250	2.50	0.33	26.6	40.0
70.6	7.49	0.190	2.50	0.33	30.1	45.0
70.6	7.49	0.190	2.50	0.33	34.6	52.0

(a) Based on uncracked cross sectional area of specimen.
(b) Based on net cross sectional area of specimen at section of original crack.

TABLE 3.02714. FRACTURE STRENGTH OF CENTER CRACKED SPECIMENS OF VARIOUS THICKNESSES IN T61 CONDITION (6)

	Al
5.6	Zn
2.2	Mg
1.5	Cu
0.21	Cr
Low	Si
	Fe
	Mn
	Ti

7475 Al

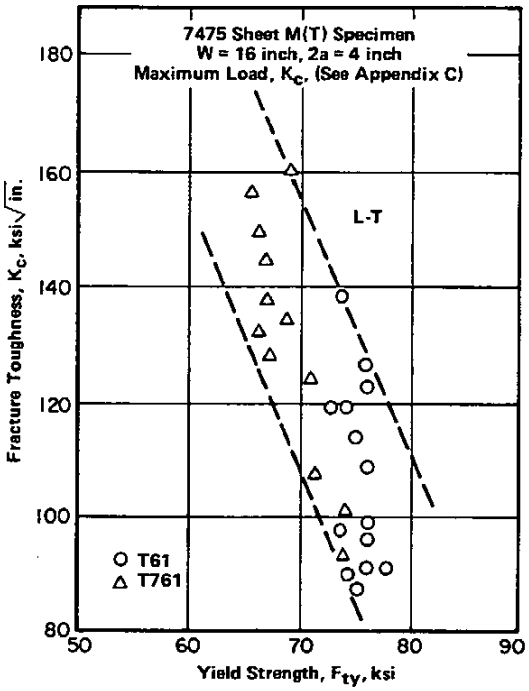


FIGURE 3.02715. PLANE STRESS FRACTURE TOUGHNESS K_C OF 7475-T61 AND -T761 SHEET RELATIVE TO TENSILE YIELD STRENGTH (23)

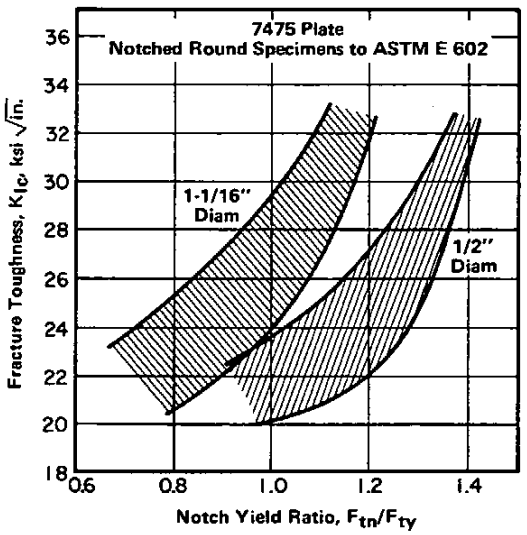


FIGURE 3.02716. CORRELATIONS BETWEEN NOTCHED TENSILE YIELD RATIO (NYR) AND K_{Ic} FOR 7075 AND 7475 PLATE IN T651, T7651, AND T7351 TEMPERS (31)

Alloy	7475-T7351			
Form	Plate			
Thickness, inch	Source	K_{Ic}, or meaningful K_Q[a], ksi$\sqrt{in.}$[b] L-T	T-L	S-L
1.5	10	38.0 (1.0)	28.8 (1.0)	24.3 (0.5)
	17	–	–	35.1 (0.5)
	30	–	–	38.5 (0.5)
1.75	15(c)	–	39.5 (1.75)	–
	26	47.5 (1.7)	–	–
2.0	39	52.7 (2.0)	40.5 (1.25)	–
2.25	15(c)	48.7 (2.25)	37.2 (2.25)	–
2.75	15(c)	48.4 (2.74)	37.7 (2.74)	33.3 (1.0)
	26	–	–	37.0 (1.0)
3.0	10	36.7 (1.25)	27.7 (1.25)	27.0 (1.0)
	26	44.8 (2.5)	34.2 (2.5)	32.6 (1.0)
3.5	15(c)	50.2 (3.0)	37.0 (3.0)	32.5 (1.25)
	26	49.0 (2.5)	33.7 (2.5)	33.4 (1.0)
4.0	15(c)	45.0 (3.0)	32.8 (2.0)	30.2 (1.5)

(a) According to ASTM B645.
(b) Figures in parentheses are the thickness of the ASTM E399 CT specimen, B (inch). See text section 1.093.
(c) Results are for "current practice" only, except for 4-inch plate from an earlier production practice.

TABLE 3.02721. PLANE STRAIN FRACTURE TOUGHNESS OF 7475-T7351 PLATE OF VARIOUS THICKNESSES (10,12,17,26,39)

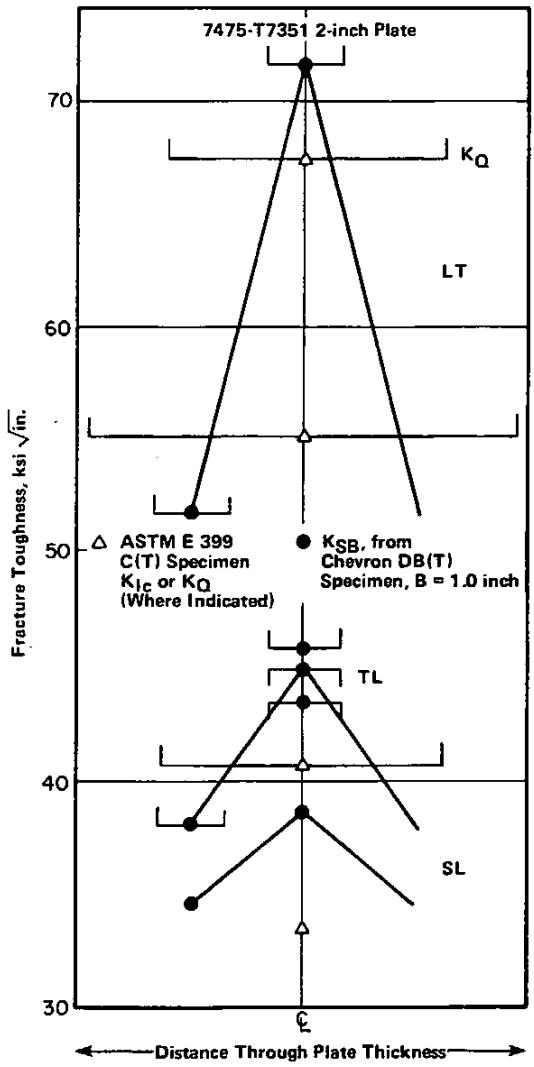


FIGURE 3.02722. TOUGHNESS VARIATIONS THROUGH THE THICKNESS OF 2-INCH THICK 7475-T7351 PLATE (26)

Length of horizontal bars denotes the thickness of material sampled by the toughness test specimen. According to AMS1704.

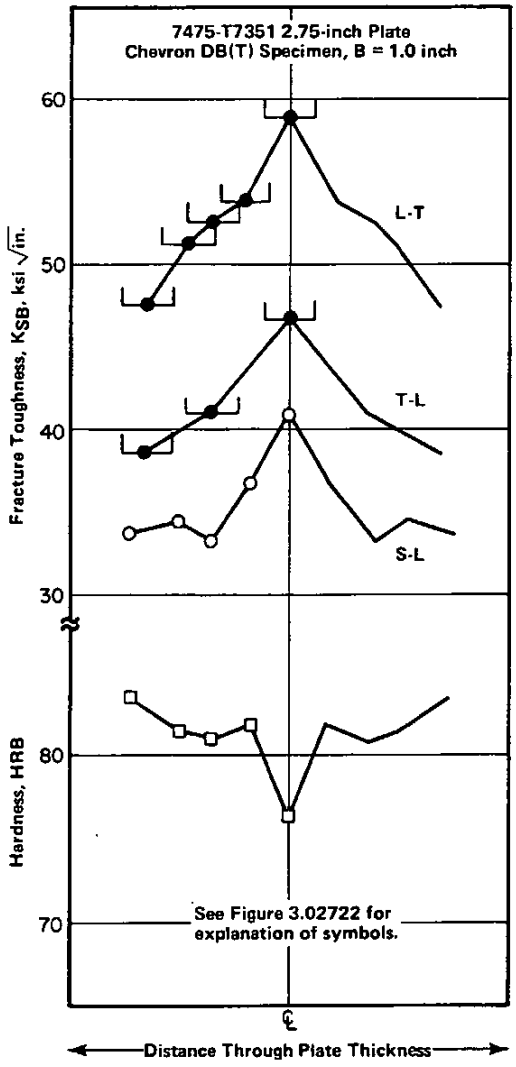


FIGURE 3.02723. TOUGHNESS VARIATIONS THROUGH THE THICKNESS OF 2.75-INCH THICK 7475-T7351 PLATE (39)

Al
5.6 Zn
2.2 Mg
1.5 Cu
0.21 Cr
Low Si
Fe
Mn
Ti

7475 Al

Alloy	7475-T7651
Form	1.5-inch Plate
Orientation	K_{Ic}, ksi √in.
L-T	49.2
T-L	44.2
S-L	38.3 (Invalid, K_Q)

TABLE 3.02724. PLANE STRAIN FRACTURE TOUGHNESS OF 1.5-INCH THICK 7475-T7651 PLATE (17)

Alloy	7075-T73511[a] and -T76511				
Form	1.5- x 4.5-inch Extrusions				
Purity	Fe, percent	Si, percent	Orientation	T73511 K_{Ic}, ksi √in.[b]	T76511 K_{Ic}, ksi √in.[b]
High	0.08	0.03	L-T	43.0	37.0
			T-L	30.0	26.0
Medium	0.19	0.10	L-T	30.6	35.0
			T-L	21.9	23.0
Low	0.26	0.14	L-T	27.3	26.0
			T-L	21.7	18.0

(a) These high purity samples are expected to behave similarly to 7475.
(b) Average of two tests.

TABLE 3.02725. EFFECT OF ALLOY PURITY ON THE PLANE STRAIN FRACTURE TOUGHNESS OF 7075-T73511 AND -T76511 EXTRUSIONS (19,20)

	Al
5.6	Zn
2.2	Mg
1.5	Cu
0.21	Cr
Low	Si
	Fe
	Mn
	Ti

7475 Al

Alloy	7475-T7351		
Form	1.75- to 4.0-inch Plate		
Orientation	L-T	T-L	S-L
Number of Tests	137	81	24
Average, K_{Ic}, ksi$\sqrt{in.}$	49.2	40.9	32.4
Standard Deviation, K_{Ic}, ksi$\sqrt{in.}$	4.5	3.9	1.4
Skewness Coefficient	+0.2	+0.8	-0.4
Actual Minimum Value, K_{Ic}, ksi$\sqrt{in.}$	39.5	34.9	28.0
A Value[a], K_{Ic}, ksi$\sqrt{in.}$	37.4-38.1	30.2-32.9	27.9-27.5
B Value, K_{Ic}, ksi$\sqrt{in.}$	42.5-42.6	34.8-35.3	29.8-29.7
C Value, K_{Ic}, ksi$\sqrt{in.}$	–	–	28.7
D Value, K_{Ic}, ksi$\sqrt{in.}$	–	–	30.3

(a) The lower limit is based on normal distribution and the upper limit is based on Pearson's Type III function (using skewness) – the upper limit is believed to be more realistic.

TABLE 3.02726. PLANE STRAIN FRACTURE TOUGHNESS, K_{Ic}, OF 7475-T7351 PLATE PRODUCED FROM JANUARY 1976 TO AUGUST 1978 BY TWO U.S. PRODUCERS (31)

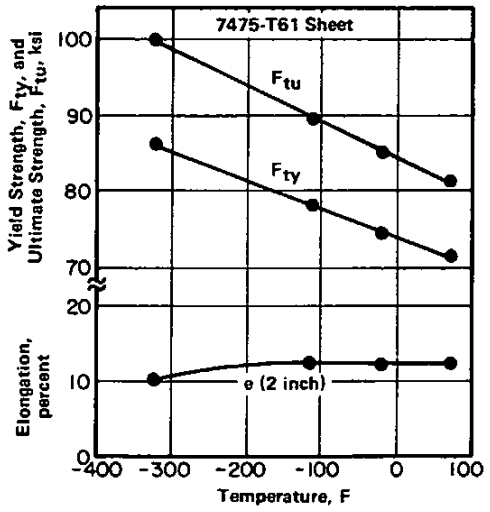


FIGURE 3.031211. EFFECT OF LOW TEMPERATURES ON TENSILE PROPERTIES OF SHEET IN T61 CONDITION (1)

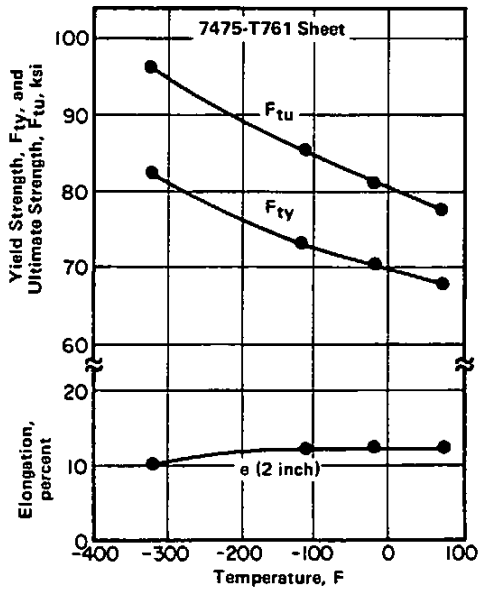


FIGURE 3.031212. EFFECT OF LOW TEMPERATURES ON TENSILE PROPERTIES OF SHEET IN T761 CONDITION (1)

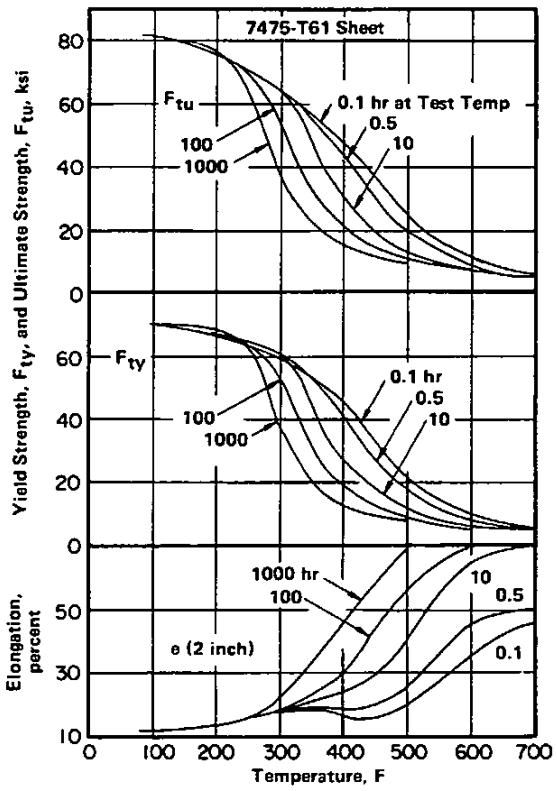


FIGURE 3.031213. EFFECT OF ELEVATED TEMPERATURES, AFTER VARIOUS HOLDING TIMES AT TEMPERATURE, ON TENSILE PROPERTIES OF SHEET IN T61 CONDITION (1)

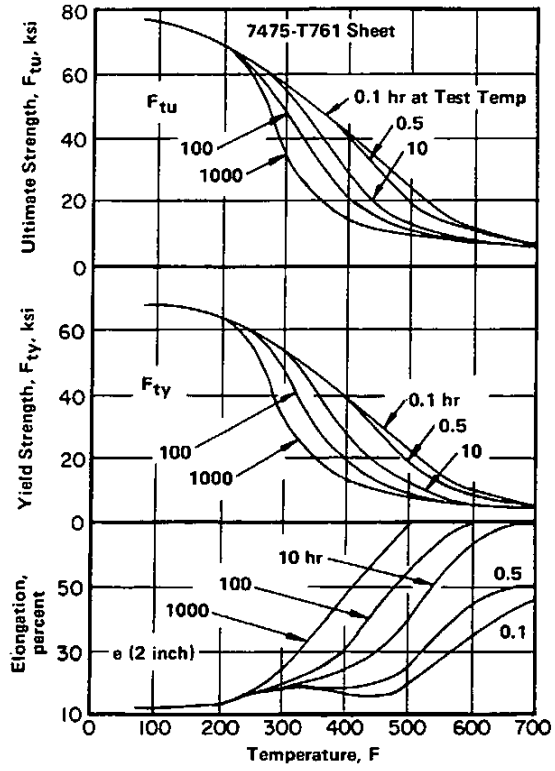


FIGURE 3.031214. EFFECT OF ELEVATED TEMPERATURES AFTER VARIOUS HOLDING TIMES AT TEMPERATURE, ON TENSILE PROPERTIES OF SHEET IN T761 CONDITION (1)

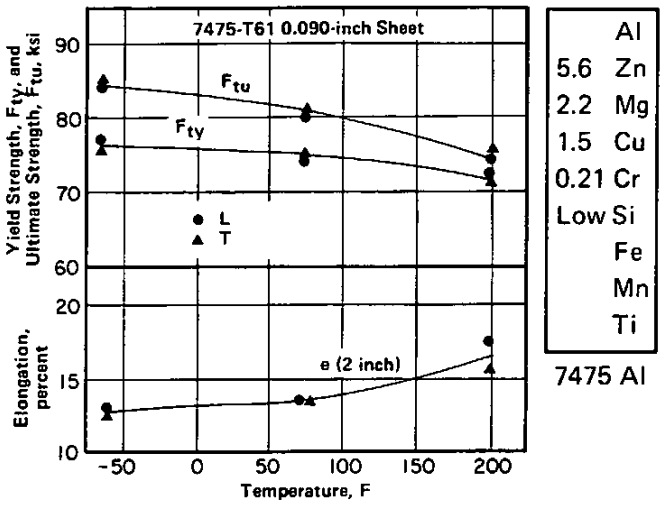


FIGURE 3.031215. TENSILE PROPERTIES OF LONGITUDINAL AND TRANSVERSE SHEET SPECIMENS IN T61 CONDITION FROM -50 TO 200 F (9)

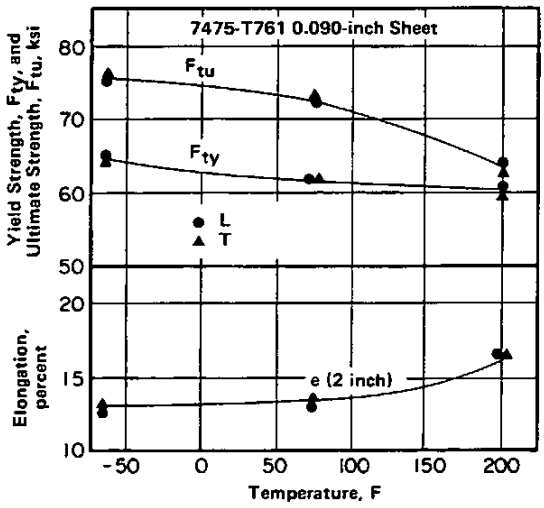


FIGURE 3.031216. TENSILE PROPERTIES OF LONGITUDINAL AND TRANSVERSE SHEET SPECIMENS IN T761 CONDITION FROM -50 TO 200 F (9)

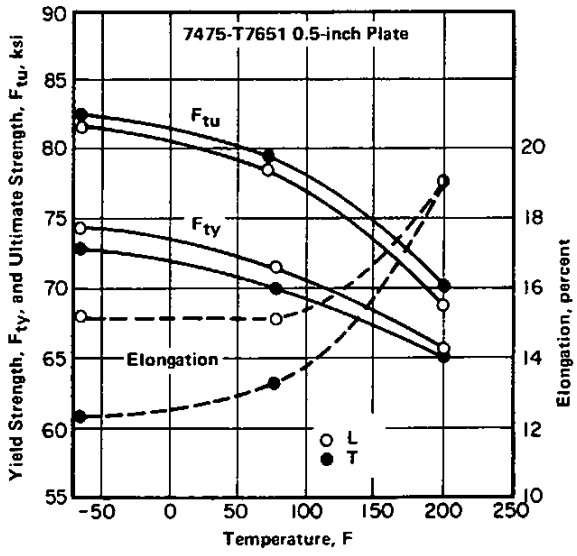


FIGURE 3.031221. TENSILE PROPERTIES OF LONGITUDINAL AND TRANSVERSE PLATE SPECIMENS IN T7651 CONDITION IN THE TEMPERATURE RANGE -65 F TO +200 F (29)

	Al
5.6	Zn
2.2	Mg
1.5	Cu
0.21	Cr
Low	Si
	Fe
	Mn
	Ti

7475 Al

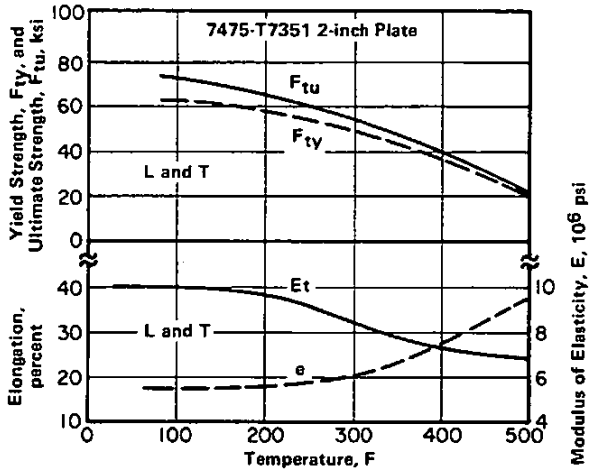


FIGURE 3.031222. TENSILE PROPERTIES OF LONGITUDINAL AND TRANSVERSE PLATE SPECIMENS IN T7351 CONDITION AT ELEVATED TEMPERATURES (14)

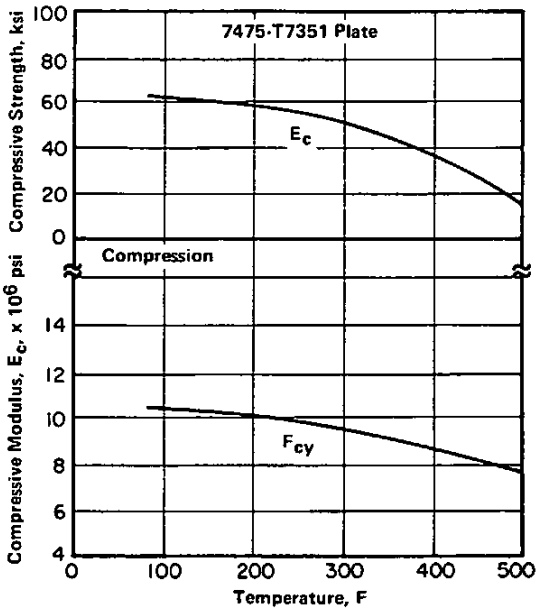


FIGURE 3.0322. COMPRESSIVE YIELD STRENGTH AND ELASTIC MODULUS AS A FUNCTION OF TEMPERATURE (14)

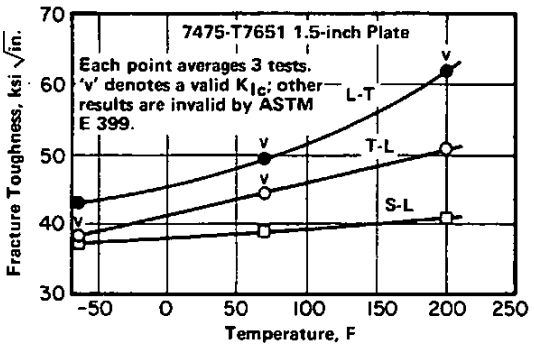


FIGURE 3.03721. PLANE STRAIN FRACTURE TOUGHNESS AS A FUNCTION OF TEMPERATURE FOR T7651 PLATE (29)

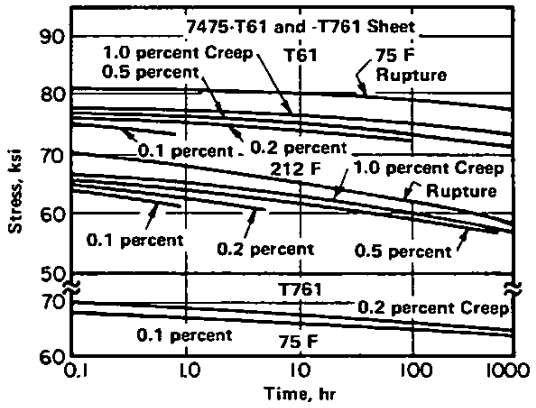


FIGURE 3.0411. CREEP AND CREEP-RUPTURE CURVES FOR T761 AND T61 SHEET AT 75 F AND 212 F (1)

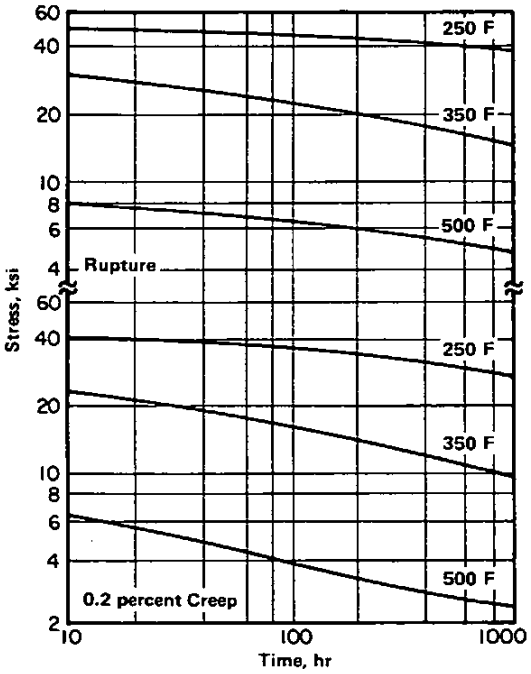


FIGURE 3.0421. CREEP-RUPTURE AND CREEP DEFORMATION CURVES FOR T7351 PLATE AT 250 F, 350 F, AND 500 F (14)

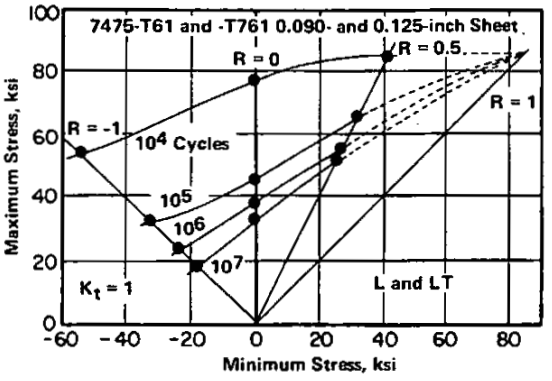
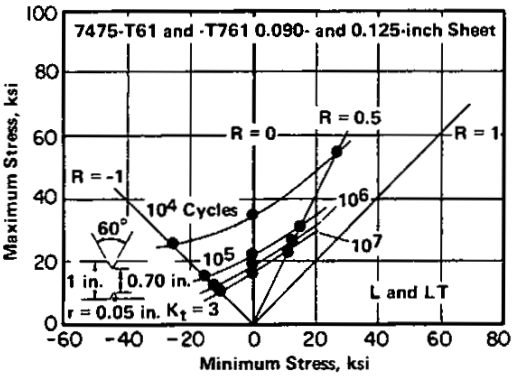


FIGURE 3.0511. CONSTANT FATIGUE LIFE DIAGRAM FOR SMOOTH, AXIALLY LOADED SHEET SPECIMENS (1)



	Al
5.6	Zn
2.2	Mg
1.5	Cu
0.21	Cr
Low	Si
	Fe
	Mn
	Ti

7475 Al

FIGURE 3.0512. CONSTANT FATIGUE LIFE DIAGRAM FOR NOTCHED, AXIALLY LOADED SHEET SPECIMENS (1)

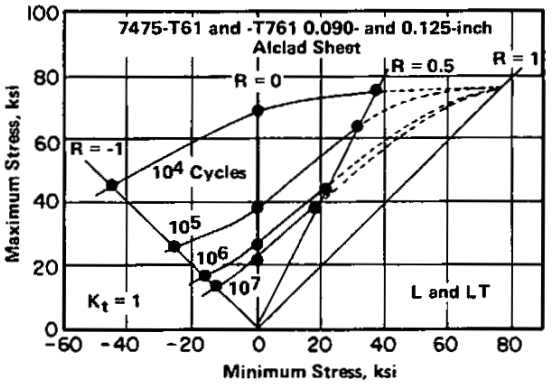


FIGURE 3.0513. CONSTANT FATIGUE LIFE DIAGRAM FOR SMOOTH, AXIALLY LOADED ALCLAD SHEET SPECIMENS (1)

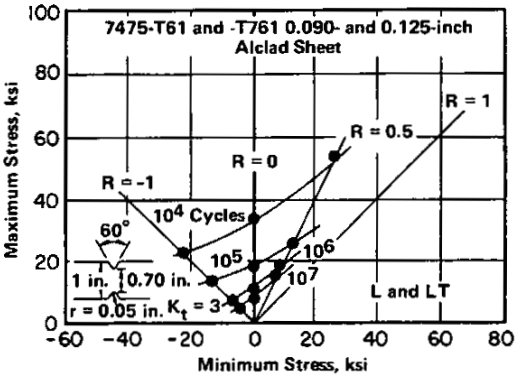


FIGURE 3.0514. CONSTANT FATIGUE LIFE DIAGRAM FOR NOTCHED, AXIALLY LOADED ALCLAD SHEET SPECIMENS (1)

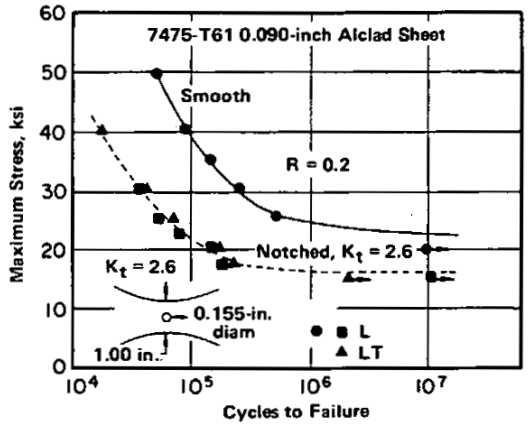


FIGURE 3.0515. AXIAL FATIGUE LIFE OF SMOOTH AND NOTCHED SPECIMENS OF 0.090-INCH ALCLAD SHEET (6)

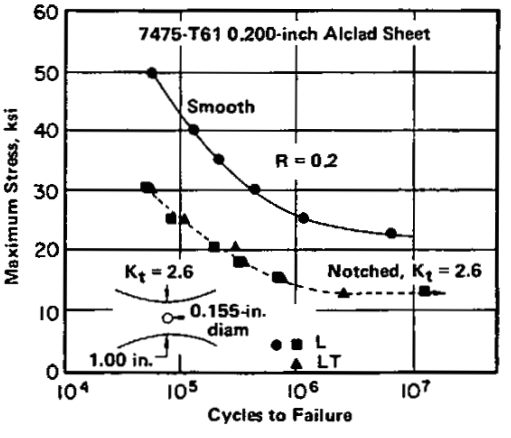


FIGURE 3.0516. AXIAL FATIGUE LIFE OF SMOOTH AND NOTCHED SPECIMENS OF 0.200-INCH ALCLAD SHEET (6)

	Al
5.6	Zn
2.2	Mg
1.5	Cu
0.21	Cr
Low	Si
	Fe
	Mn
	Ti

7475 Al

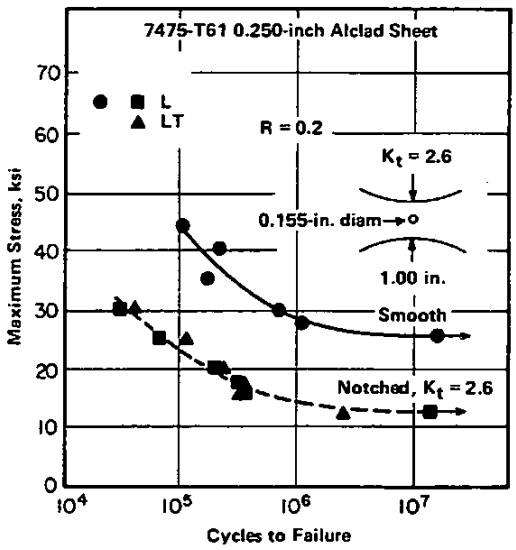


FIGURE 3.0517. AXIAL FATIGUE LIFE OF SMOOTH AND NOTCHED SPECIMENS OF 0.250-INCH ALCLAD SHEET (6)

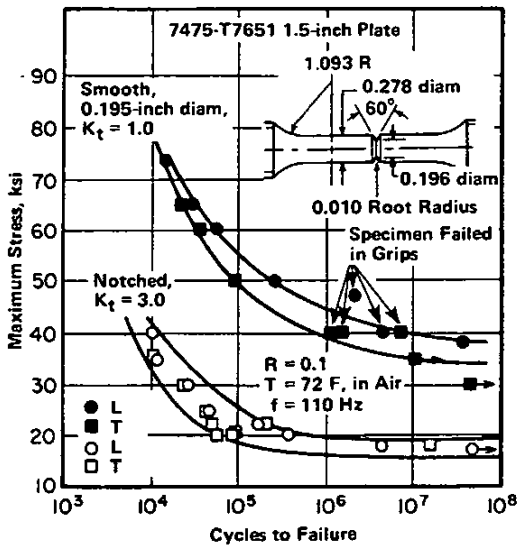


FIGURE 3.0518. AXIAL FATIGUE LIFE OF SMOOTH AND NOTCHED LONGITUDINAL AND TRANSVERSE SPECIMENS OF 1.5-INCH THICK 7475 T7651 PLATE (7)

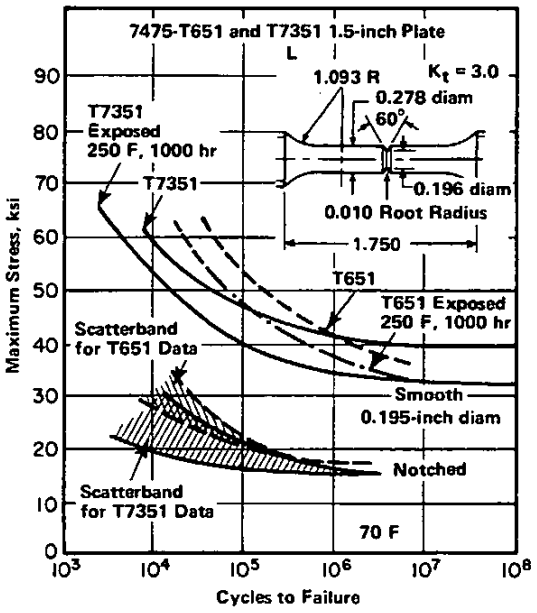


FIGURE 3.0519. AXIAL LOAD FATIGUE LIVES OF LONGITUDINAL AND TRANSVERSE SMOOTH AND NOTCHED SPECIMENS OF 7475-T7351 AND -T651 PLATE (29)

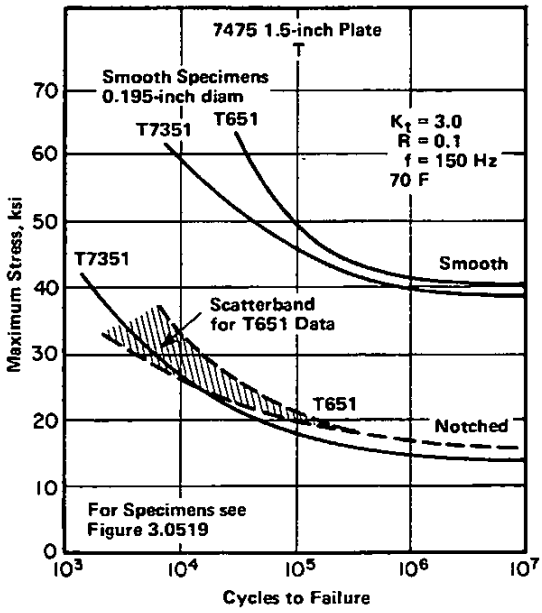


FIGURE 3.05110. AXIAL LOAD FATIGUE LIVES OF TRANSVERSE SMOOTH AND NOTCHED SPECIMENS OF 7475-T7351 AND 7475-T651 PLATE 1.5-INCH THICK (29)

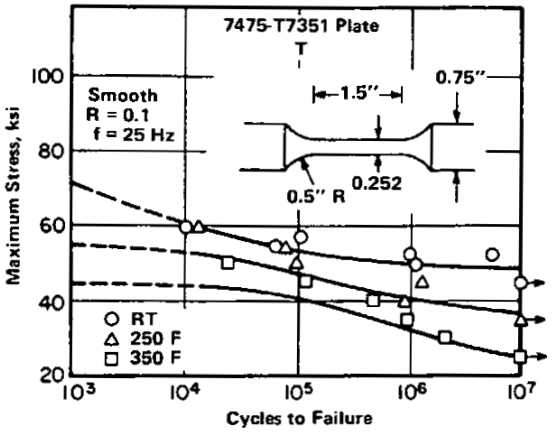


FIGURE 3.05111. AXIAL STRESS FATIGUE LIFE OF 7475-T7351 PLATE IN THE TRANSVERSE DIRECTION (14)

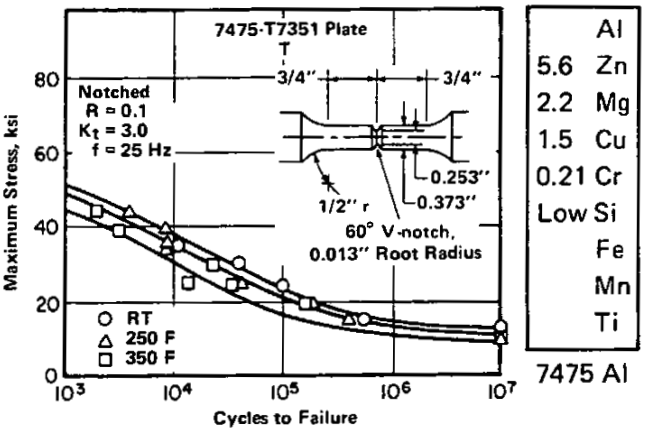


FIGURE 3.05112. AXIAL STRESS FATIGUE LIFE OF NOTCHED SPECIMENS OF 7475-T7351 PLATE IN THE TRANSVERSE DIRECTION AT ELEVATED TEMPERATURE (11)

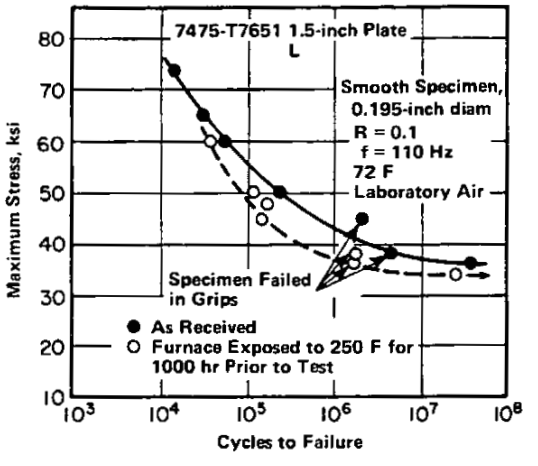


FIGURE 3.05113. AXIAL STRESS FATIGUE LIFE OF SPECIMEN 7475-T7651 PLATE (17)

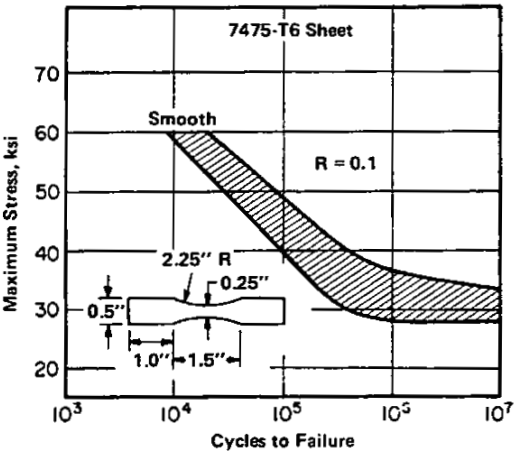


FIGURE 3.05114. AXIAL FATIGUE LIFE OF SMOOTH SPECIMENS OF 7475 T6 SUPERPLASTICALLY STRAINED SHEET (30)

	Al
5.6	Zn
2.2	Mg
1.5	Cu
0.21	Cr
Low	Si
	Fe
	Mn
	Ti

7475 Al

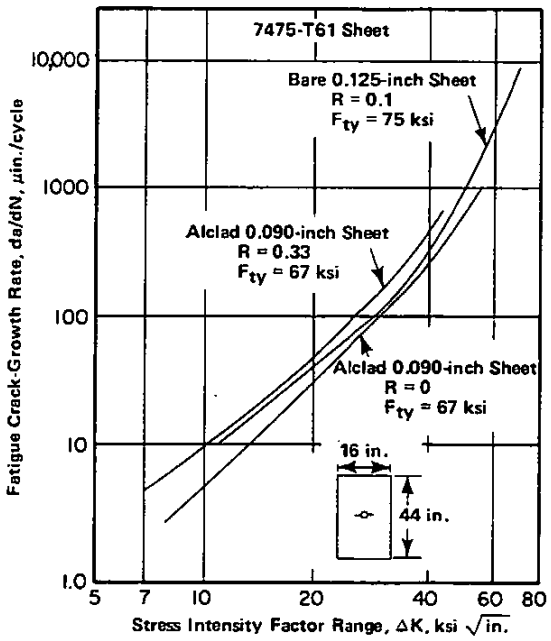


FIGURE 3.0521. FATIGUE CRACK-GROWTH RATE OF BARE AND ALCLAD SHEET (1,3)

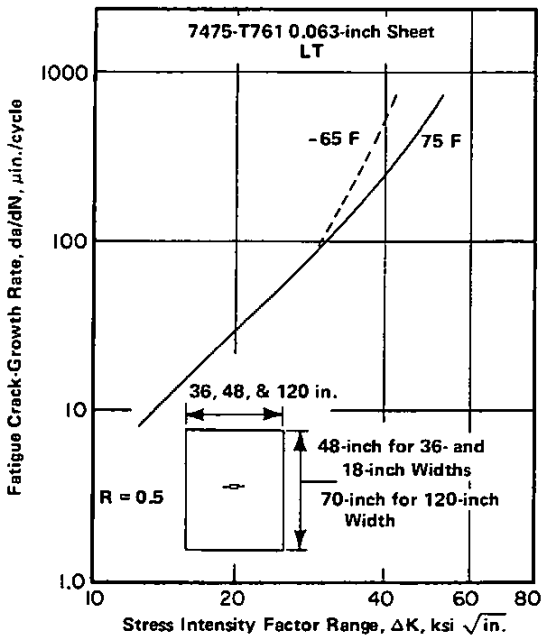


FIGURE 3.0522. FATIGUE CRACK-GROWTH RATE OF ALCLAD SHEET PANELS OF VARIOUS SIZES AT 75 F AND -65 F (5)

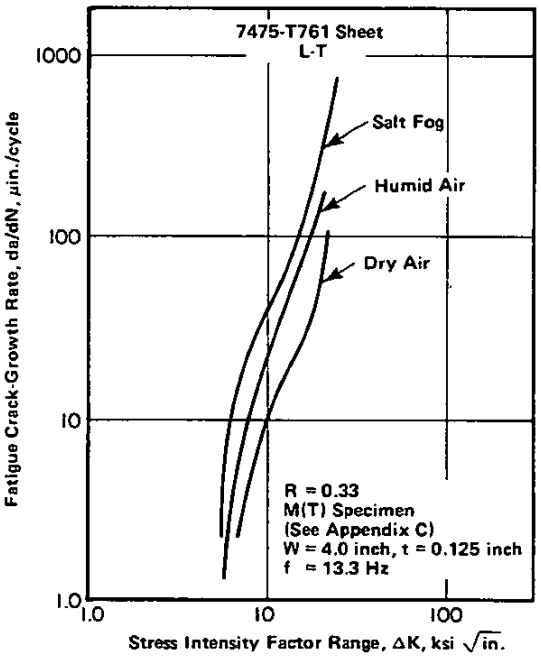


FIGURE 3.0523. FATIGUE CRACK-GROWTH RATES FOR 0.125-INCH THICK SPECIMENS OF 7475-T761 SHEET IN LT ORIENTATION – CONSTANT LOAD TESTS (11)

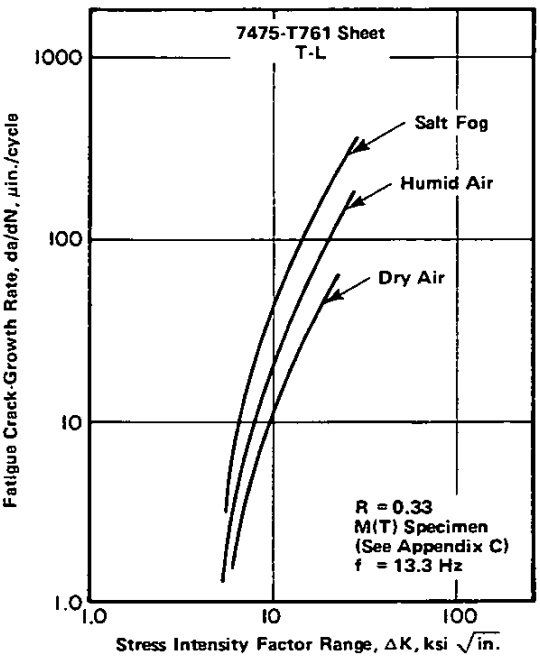


FIGURE 3.0524. FATIGUE CRACK-GROWTH RATES FOR 0.125-INCH THICK SPECIMENS OF 7475-T761 SHEET IN TL ORIENTATION – CONSTANT LOAD TESTS (11)

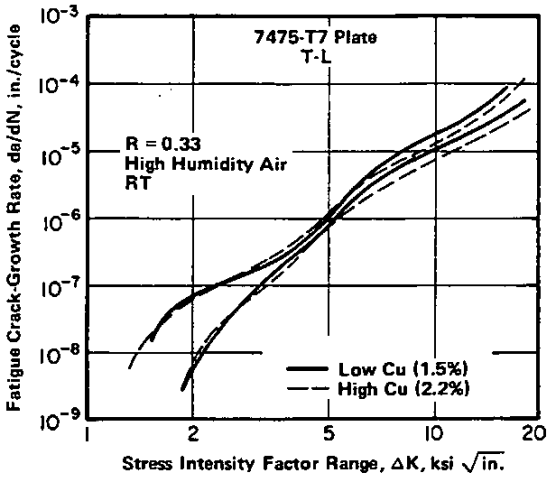


FIGURE 3.0525. FATIGUE CRACK-GROWTH RATES FOR HIGH AND LOW CONTENT COPPER 7475-T7 PLATE (40)

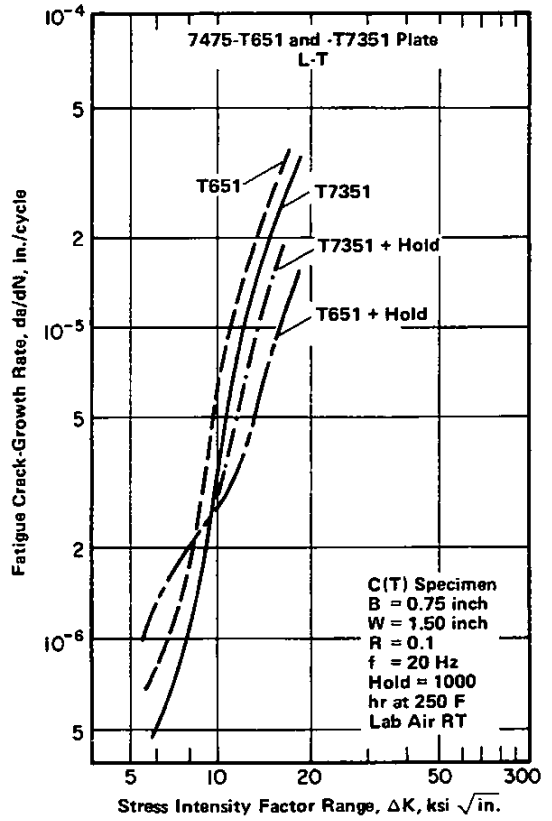


FIGURE 3.0527. FATIGUE CRACK-GROWTH RATES OF 7475-T651 AND -T7351 PLATE (29) (FIGURE 13 AND 14)

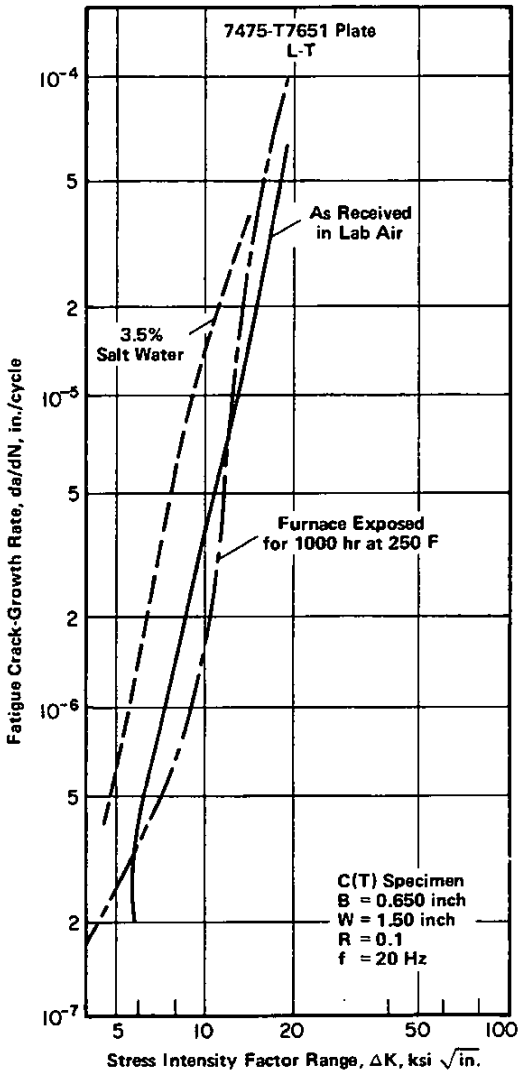


FIGURE 3.0526. FATIGUE CRACK-GROWTH RATES FOR 1.5-INCH THICK SPECIMENS OF 7475-T7651 PLATE IN AIR AND 3.5 PERCENT SALT WATER (17)

	Al
5.6	Zn
2.2	Mg
1.5	Cu
0.21	Cr
Low	Si
	Fe
	Mn
	Ti

7475 Al

	Al
5.6	Zn
2.2	Mg
1.5	Cu
0.21	Cr
Low	Si
	Fe
	Mn
	Ti

7475 Al

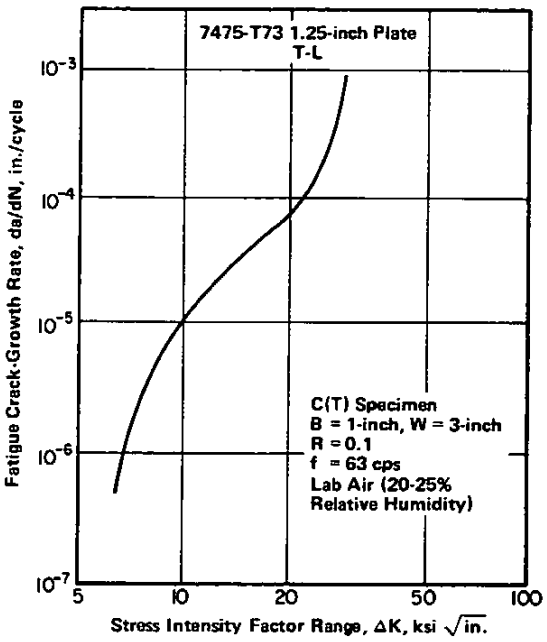


FIGURE 3.0528. FATIGUE CRACK-GROWTH RATES FOR 1.25-INCH THICK SPECIMENS OF 7475-T73 PLATE (10)

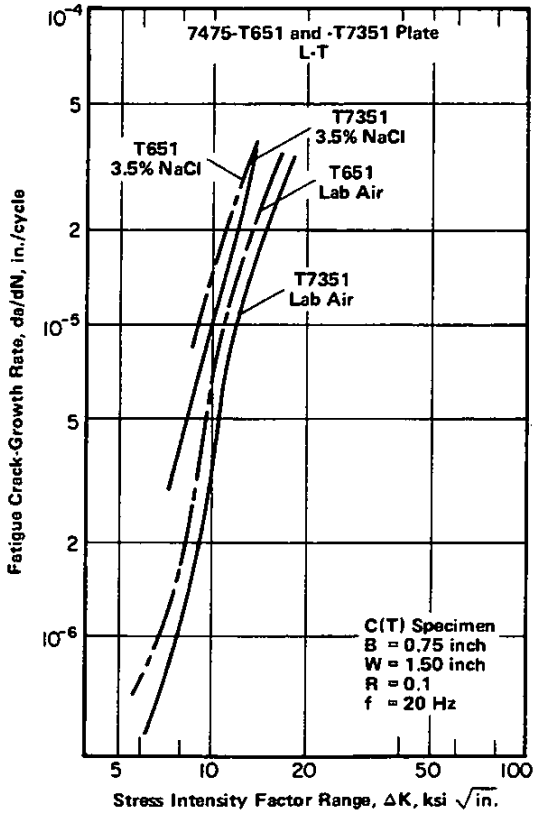


FIGURE 3.0529. FATIGUE CRACK-GROWTH RATES OF 7475-T7351 AND -T651 PLATE IN AIR AND 3.5 PERCENT NaCl SOLUTION (29)

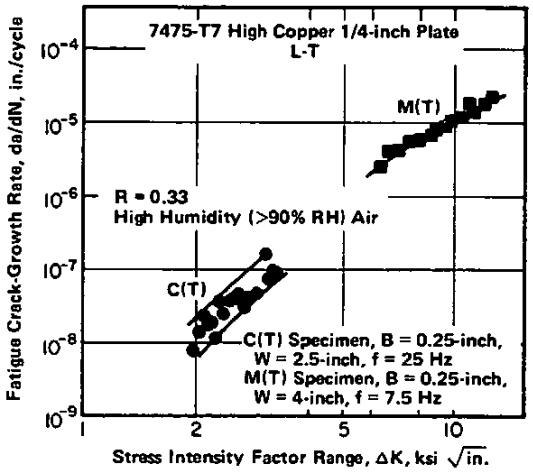


FIGURE 3.05210. FATIGUE CRACK-GROWTH RATES FOR 7475-T7 0.25-INCH THICK PLATE CONTAINING A HIGH (2.2 PERCENT) COPPER CONTENT (40)

	Al
5.6	Zn
2.2	Mg
1.5	Cu
0.21	Cr
Low	Si
	Fe
	Mn
	Ti

7475 Al

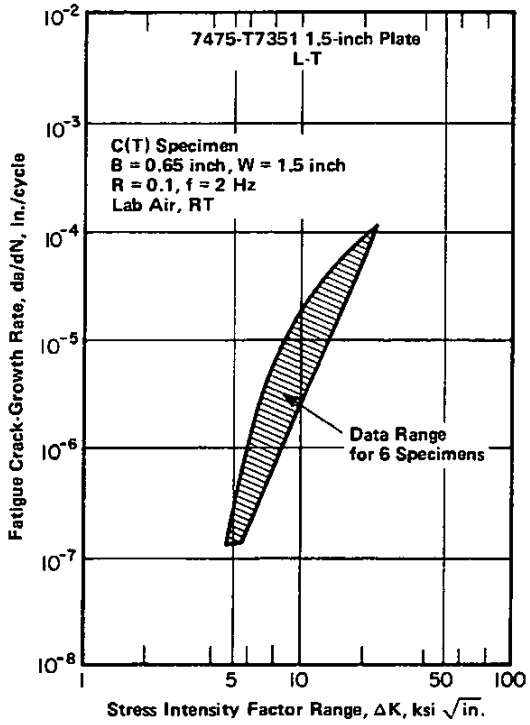


FIGURE 3.05211. FATIGUE CRACK-GROWTH FOR 1.5-INCH THICK SPECIMEN OF 7475-T7351 PLATE IN AIR (28)

Alloy	7475-T61 and -T761		
Form	Sheet		
		Modulus of Elasticity, E, x 10^6 psi	
Orientation	Stress	T61	T761
Longitudinal	Tensile	10.03	10.09
	Compressive	10.46	10.47
Transverse	Tensile	10.03	10.04
	Compressive	10.53	10.53

TABLE 3.0621. TENSILE AND COMPRESSIVE ELASTIC MODULII OF 7475-T61 AND -T761 SHEET (11)

1 General

The 8090/8091 alloys have undergone extensive development during the last seven years. Compared with conventional aluminum alloys they now offer a ten percent reduction in density coupled with a ten percent increase in stiffness. The 8090/8091 alloys are Li-Cu-Mg-Zr compositions, with 8091, the richer of the two, having the higher strength potential. The following development targets have been established for these alloys: 8090-T6 as a replacement for 2014-T6; 8090-T8 (damage tolerant temper) as a replacement for 2024-T3; and 8091-T8 as a replacement for 7075-T6. For the 8090 alloy these goals have generally been achieved, providing that "replacement" is not taken to mean direct substitution in all applications. The 8091 alloy has encountered production problems and is not yet available in commercial quantities. The Al-Li alloys do present special problems not commonly encountered in conventional aluminum alloys. These are associated with the presence of embrittling phases, crystallographic and mechanical anisotropy, and the possibility of liquid metal embrittlement associated with sodium and potassium impurities. There are several areas where additional investigations or further studies are needed, including (1) control of embrittling phases as they affect the toughness of large sections; (2) influence of sodium and potassium on fracture toughness and sustained-load crack growth and development of means to reduce the content of these elements; (3) a better understanding of the relationship between crystallographic and mechanical anisotropy and fracture control of critical structures; (4) the practical significance of stability problems at moderately elevated temperatures; and (5) development of optimum joining techniques.

Note: Sections of this chapter contain fracture toughness data which have not been derived from standardized tests; in some cases, these tests are not completely described. Such data have been designated as K_Q and are qualitatively useful for comparative purposes but only when obtained from the same test types.

1.1 Commercial Designations

8090, 8091, 8090-T7, 8090-T6, 8090-T81 (proposed).

1.2 Alternate Designations

Lital A (8090), Lital B (8091), and Lital C (8090-T81).

1.3 Specifications

1.3.1 *[Table]* Tentative mechanical properties for 8090 Aluminum Association Registration.

1.4 Composition

1.4.1 *[Table]* Composition of 8090 and 8091.

1.5 Heat Treatment

Al
2.5 Li
1.3 Cu
1.0 Mg

General for 8090 and 8091. Combinations of ingot processing and heat treatments are still under development. What follows represents current practice designed to optimize the combination of strength, fracture toughness, and stress corrosion resistance (Ref. 15). By controlling the amount of cold work during processing and increasing the heating rate during solution treatment, it is possible to produce either equiaxed or lamellar recrystallized grain structures. The recrystallized fraction increases with decreasing rolling temperatures and with increasing solution times (Figure 1.5.3.2). Recrystallized damage tolerant tempers are produced by proprietary processing, involving both cold work prior to solution treatment and followed by other special heat treatments. Damage tolerant material is generally underaged. The need for rapid cooling rates from the solution temperature limits the production of recrystallized material to sheet stock or equally thin sections. In general, rapid cooling from the solution temperature is beneficial in avoiding embrittling phases (Sections 1.9.1 and 2.1.2) and results in improved fracture energy (Table 1.5.3.1).

Temper designations given in this section reflect the changes in processing and heat treatment which are still not completely established and the differences between the U.S. Aluminum Association system and the system used in other countries. Where available, the actual processing and heat treatments are given.

1.5.2 Homogenization. For 8090 ingots, heat to 932F at 90F per hour, raise to 1022F at 36F per hour, and hold 24 hours, AC. For 8091 ingots, heat to 932F at 90F per hour, raise to 1022F at 18F per hour, and hold 24 hours, AC.

1.5.3 Solution Treat (ST). All forms: 986F (530C) in salt WQ; 1004F (940C) in air, WQ sometimes used for plate.

1.5.3.1 *[Table]* Effect of quench rate on the tensile properties and Charpy energy of 8090 as quenched, and stretched and aged.

1.5.3.2 *[Figure]* Recrystallized fractions as functions of rolling temperature and solution time.

1.5.3.3 *[Table]* Effect of quench rate and recovery treatments on the SL fracture toughness of 8090 naturally aged plate.

1.5.4 Natural Age (T4); ST followed by natural aging. After solution treatment, stability of the tensile properties is maintained for about 10 hours, after which natural aging takes place at a rather slow rate being complete in 100 to 1000 hours depending on processing subsequent to solution treatment (Figure 3.2.1.2).

T351 ST + 1.5 to 7 percent Stretch + Natural Age.

© 1992 by Purdue Research Foundation, West Lafayette, Indiana 47907.
All Rights Reserved.

1.5.5 Artificial Age. The heat treatments encountered at the time this chapter was prepared are summarized in Table 1.5.5.1. Deviations from these treatments and temper designations may appear in the future.

1.5.5.1 *[Table]* Summary of artifical aging treatments found in recent literature (June 1992).

1.5.6 Effects of Reaging. The SL fracture toughness of plate in the T8 condition can be improved by reaging (sometimes called a reversion or recovery treatment) using rapid heating and cooling from the reaging temperature (Ref. 21). Air cooling may be satisfactory for thin sections (Ref. 29). Substantial increases in fracture toughness of plate can be obtained by 5 minutes aging in salt at temperatures between 375 and 450F followed by cold water quenching (Figure 1.5.6.1). The toughness-changes with reaging appear to be time-temperature dependent, with aging times on the order of 5 to 10 min. producing the maximum toughness increase (Figure 1.5.6.2). The improvement in SL toughness is accompanied by moderate losses in F_{tu} and F_{ty} and increases in elongation and reduction of area (Figure 1.5.6.3). One explanation for the increase in toughness associated with reaging is a reduction in Li segration at grain boundaries which is responsible for the brittle intergranular fracture of the single-aged alloy (Ref. 21). The toughness improvement produced by reaging can be reversed by exposure to moderately elevated temperatures. This loss in toughness is time-temperature dependent (Figure 1.5.6.4) with substantial improvements due to reaging being retained at 140F for 2000 hours.

1.5.6.1 *[Figure]* Effect of reaging temperature on the SL fracture toughness of 8090-T8 plate.

1.5.6.2 *[Figure]* Effect of reaging temperature and time on the SL fracture toughness of 8090-T8 plate.

1.5.6.3 *[Figure]* Effect of reaging temperature on short-transverse tensile properties of 8090-T8 plate.

1.5.6.4 *[Figure]* Effect of temperature and time of re-embrittlement on SL fracture toughness of 8090-T8 plate given a reaging (toughening) treatment.

1.6 Hardness

1.6.1 *[Figure]* Variation of hardness with aging temperature and time for 8090 rod.

1.7 Forms and Conditions Available

Sheet and plate are readily available. Forgings and extrusions have been produced, but not in quantity.

1.8 Melting and Casting Practice, see Section 1.9

1.9 Special Considerations

1.9.1 Microstructure. A major factor which appears to limit the short-transverse tensile ductility and the fracture toughness for the SL and TL crack orientations, as well as the stress corrosion resistance, is the precipitation of the T_2 phase (Section 2.1.2) along high angle boundaries. The amount of this phase present is a function of the composition and the cooling rate from the solution temperature (Section 2.1.2.1). Its presence can be minimized by rapid cooling; however, for large forgings, the cooling rates under the best of circumstances may be so slow that substantial losses in fracture toughness are encountered (e.g., see Figure 3.3.7.1.1). It is probably impossible to completely avoid T_2 in rapidly quenched sections greater than one-inch thick (Ref. 4-18); however, its presence in small amounts does not preclude the development of satisfactory properties. Aging at low temperatures is beneficial in reducing the deleterious effects of the T_2 phase (Tables 2.3.2.2 and 3.2.1.6). For this reason, thick sections are advantageously aged at relatively low temperatures to minimize the presence of this phase. However, low aging temperatures require long aging times to develop satisfactory strength; and commercial practice is often a compromise (Ref. 4-18).

1.9.2 Directionality. Unrecrystallized structures are heavily layered with grains oriented in the direction of major hot working (e.g., the rolling direction). These structures possess both crystallographic and mechanical anisotropy which are more pronounced than observed in conventional aluminum alloys. The crystallographic anisotropy is evidenced by a minimum in tensile strength properties and a maximum in elongation at about 45 degrees to the rolling direction (e.g., see Figure 3.2.1.8 and Table 3.2.1.14). For sheet or other sections which are amenable to recrystallization treatment, the directionality can be reduced, but with some sacrifice in strength (Figure 3.2.1.9). However, recrystallized sheet can exhibit crack propagation at about 70 degrees to the rolling direction (Refs. 5-2, 5-5).

The mechanical anisotropy in heavy sections is evidenced by relatively low short-transverse elongation and fracture toughness (Tables 3.2.1.1.1 and 3.2.1.1.3). This directionality can be reduced by underaging (e.g., see Table 3.2.1.6).

1.9.3 Safety. Lithium is a highly reactive metal; hence, special precautions are required for melting, processing, machining, and scrap disposal (Ref. 17). Molten Al-Li alloys can explode violently when in contact with water. The reaction is more energetic than with pure aluminum (Figure 1.9.3.1). Dross and skimmings are also highly reactive in water, and large amounts of hydrogen gas are evolved. Heat treatment in salt baths may result in explosions if incipient melting occurs. When Al-Li alloys are heated above 500F, surface oxidation occurs and lithium oxide and hydroxide are formed. These products or the decomposition product, lithium carbonate, can be skin and eye irritants or, if inhaled as dust, can cause upper respiratory distress. The American Industrial Hygiene Association has recommended a Workplace Environmental Exposure Level of one milligram per

cubic meter of air for a one-minute ceiling limit for the particulates of lithium oxide and hydroxide. Scrap segregation is presently necessary because it is not known what effect small amounts of lithium may have on the properties of other aluminum alloys. See Ref. 17 for more detailed information and safety precautions.

1.9.3.1 *[Figure]* Energy released as a function of weight of metal for pure aluminum and Al-2.5 percent Li with water coolant.

1.9.4 Lithium Depletion. Solution treatment in air or in salt can result in a loss of lithium from the surface, which can result in a decrease in the strength of the aged alloy (Figure 3.2.1.3). This loss appears to be slightly less in the salt than in air. It has been shown that the surface lithium loss is associated with sub-surface voids (Figure 1.9.4.1). Even for long solution times, the damaged surface layers could be removed by machining 5 mil from the exposed surfaces. Thus, normal finishing operations should be sufficient, in most cases, to eliminate the effects of lithium loss. However, in the case of thin sheet, some reduction in design allowables may be necessary, particularly if multiple solution treatments are used.

1.9.4.1 *[Figure]* Depth of onset of subsurface porosity and microhardness gradient as a function of solution treatment time.

1.9.5 Hydrogen Embrittlement. The alloy can be hydrogen embrittled by cathodic charging (Ref. 4-22).

1.9.6 Liquid Metal Embrittlement. The presence of sodium and/or potassium in very small quantities (<10 ppm) can result in creep (sustained load) crack growth at stress intensity factors well below K_{Ic}. Somewhat larger quantities can substantially reduce the SL fracture toughness. In commercial Al-Li alloys sodium is the predominate contaminant and tends to form liquid phases associated with grain boundary inclusions. The result is liquid metal embrittlement with low energy intergranular fracture. The effect of sodium on sustained load crack growth in Al-Li alloys is similar to that observed with other types of aggressive environments. A threshold K value is observed below which cracks do not grow. Above this value the velocity increases rapidly at low K levels and then more slowly with increasing K to a plateau velocity as K approaches critical value (Figure 1.9.6.1).

In plate, considerably higher SL crack velocities are observed for sodium contents of 40 ppm than for 10 ppm (Ref. 18 and Figure 1.9.6.2). However, reducing the sodium content to 3-5 ppm apparently does not substantially change the creep-crack behavior (compare the 176F 10 ppm sodium data in Figure 1.9.6.2 with the 176F 3-to-5 ppm sodium data in Figure 1.9.6.1). As might be expected, the crack velocity at a given K level increases with increase in the exposure temperature (Figure 1.9.6.1). At K values of 5.5 ksi$\sqrt{in.}$ ($<K_Q/2$) crack velocities are approximately $3x10^{-3}$ in. per hour at 240F for the two commercial plates investigated (Figure 1.9.6.3). Extrapolation of the Arrhenius plot in this figure indicates a crack velocity of about $2x10^{-5}$ in. per hour at K = 5.5 ksi$\sqrt{in.}$ and 120F. The susceptibility of 8090 to creep crack growth is much higher than observed in conventional aluminum alloys (Figure 1.9.6.4).

The fracture toughness of plate is reduced by the presence of sodium, but reducing the sodium content below 10 ppm did not change the fracture toughness (compare the K_Q values in Figure 1.9.6.2 with those given in Table 1.9.6.5 for the naturally aged alloy).

Creep cracking has also been observed in 8090 sheet (Ref. 19). The damage mechanism appears to be similar to that in plate with crack velocities being strongly dependent on the temperature (Figure 1.9.6.6). Recrystallized sheet appears to exhibit much higher crack velocities at a given K level than unrecrystallized sheet whose behavior is similar to that of 2024Al (Figure 1.9.6.7). This may be due in part to the lower sodium content of the unrecrystallized sheet used in the referenced investigation.

While the results available to date are from one investigator and are limited in scope, they point to a potential problem that may limit the application of this alloy. A threshold K level below which creep cracking would be absent appears to be less than 4 ksi$\sqrt{in.}$, and growing cracks would be expected to accelerate rapidly. It does not appear that the deleterious influence of sodium and potassium can be eliminated by conventional melting or processing practices.

1.9.6.1 *[Figure]* Crack velocity as a function of K level for 8090 plate tested at elevated temperatures.

1.9.6.2 *[Figure]* Crack velocity as a function of K level for two experimental 8090 plates showing the effect of sodium content.

1.9.6.3 *[Figure]* Arrhenius plot of crack velocity in 8090 plate as a function of reciprocal of absolute temperature at a K level of 5.5 ksi$\sqrt{in.}$

1.9.6.4 *[Figure]* Crack velocity at 248F as a function of K level for 8090 and 2014-T851 plates.

1.9.6.5 *[Table]* Supplementary information for data derived from Refs. 21-24.

1.9.6.6 *[Figure]* Crack velocity as a function of K level at 176F and 248F for 8090 recrystallized sheet.

1.9.6.7 *[Figure]* Crack velocity as a function of K level at 248F for 8090 recrystallized and unrecrystallized sheet and for 2024-T3 sheet.

1.9.6.8 *[Figure]* Effect of sodium content in lithium on the short-transverse fracture toughness of stretched and aged 8090 plate.

1.9.7 Stability. Exposure at a moderate temperature (210F) for 100 hours can substantially reduce the fracture toughness of plate (Table 1.9.7.1). Recrystallized and unrecrystallized sheet show a small increase in room temperature tensile strength after exposure for 1000 hours in the temperature range between 200 and 300F. Exposure at higher temperatures results in a loss in retained strength which is somewhat less for the recrystallized sheet (Figure 1.9.7.2). The same sheet exposed for 1000 hours at moderately elevated temperatures (see Table 1.9.7.3) shows a substantial loss in toughness for 302F exposure. Exposure at 210F for long times (up to 1000 hours) produces a very small decrease in the fatigue crack growth threshold and higher crack propagation rates only at high ΔK value (Figure 3.5.2.18). Data available at the time this chapter was prepared do not define the time-temperature relation for this instability. However, recent data show that following very long times at room temperature there is a loss in fracture toughness of plate (Table 1.9.7.4). On the basis of these limited data it appears that plate which has been cold worked before aging is less susceptible than plate which is simply aged after solution treating.

Proprietary stabilizing treatments have been developed (Ref. 24) which have the potential of minimizing this effect. Structurally stabilized extrusions did not exhibit a decrease in Charpy V impact energies after 18,000 hours following final heat treatment (Table 1.9.7.5). Extrusions given several different aging treatments (Table 1.9.7.6) maintained reasonably good fracture toughness values after 3.3 years storage at ambient temperature. Hopefully, the present results will stimulate additional work to establish the nature of this stability problem as it relates to practical applications and to better define remedial treatments.

1.9.7.1 *[Table]* Effect of prolonged exposure at elevated temperature on tensile properties and fracture toughness of 8090 plate.

1.9.7.2 *[Figure]* Tensile strength of recrystallized (ReX) and unrecrystallized (UnReX) 8090 sheet at room temperature after 1000 hours exposure at elevated temperatures and at the exposure temperature after 1000 hours at that temperature.

1.9.7.3 *[Table]* Percent loss in room temperature fracture toughness of recrystallized and unrecrystallized 8090 sheet after 1000 hours exposure to moderately elevated temperatures.

1.9.7.4 *[Table]* Effect of long-time exposure at room temperature on the retained SL fracture toughness of 8090 plate.

1.9.7.5 *[Table]* Effect of long-time exposure on the room temperature tensile and impact properties of structurally stabilized 8090 extrusions.

1.9.7.6 *[Table]* Tensile yield strength and fracture toughness for structurally stabilized 8090 extrusion after 3.3 years at room temperature.

2 Physical and Environmental Effects

2.1 Thermal Properties

2.1.1 Melting Range: approximately 1100F.

2.1.2 Phase Changes. The alloy is hardened by precipitation of several complex phases of Al-Cu-Li-Zr. In the as-quenched condition (naturally aged T3), the phases are $\delta'(Al_2Li)$ and $\beta'(Al_3Zr)$ for both 8090 and 8091. In the artificially aged condition (T6), the phases in 8090 are δ', β', $T_1(Al_2CuLi)$, and $S(Al_2CuMg)$. In 8091-T8, the T_1 phase is not present (Ref. 6).

The β' phase is present as small coherent particles which are effective in retarding sub-grain boundary migration and coalescence. The phase can act as nuclei for precipitation of δ' and, while the resulting complex phase makes a contribution to the strength by inhibition of planar slip, its main strengthening effect is through the inhibition of recrystallization (Ref. 15).

The lath-like S phase is the major hardening phase in the artificially aged alloys and its precipitation is increased by cold work before aging. In the naturally aged alloy it is heterogeneous, being located primarily at the grain boundaries. A small amount of plastic deformation before aging results in a more uniform distribution of the S phase which is nucleated on the dislocations produced by the cold work. This homogeneous distribution contributes strongly to the strength. It has been shown that double aging (without stretching) will contribute to a more uniform distribution of the S phase (Ref. 5-6).

The Li-containing phases which precipitate in the grain boundaries can result in an adjacent lithium-depleted zone which contributes to grain boundary fractures. This depleted zone is more pronounced in the 8091 alloy.

A T_2, Al_6CuLi_3, icosahedral phase can also be present in these alloys in combination with magnesium as $Al_6Cu(MgLi)_3$. This quasi-crystalline phase forms along the grain boundaries and is particularly damaging to the fracture toughness and resistance to stress corrosion. It is present as a result of slow solidification but can be removed by homogenization treatments. It is also formed during slow cooling from the solution treatment. Its presence can be minimized by use of rapid quenching and its effects minimized by low aging temperatures (Refs. 4-18, 15).

2.1.2.1 Time-temperature transformation diagrams.

2.1.2.1.1 *[Figure]* Nucleation start curves for 8090 copper-lean alloy.

2.1.2.1.2 *[Figure]* Nucleation start curves for 8090 copper-rich alloy.

2.1.2.1.3 *[Figure]* Volume fractions of the T_2 phase for 8090 copper-lean alloy.

2.1.2.1.4 *[Figure]* Volume fractions of the T_2 phase for 8090 copper-rich alloy.

2.1.2.1.5 *[Figure]* Volume fractions of the S phase for 8090 copper-lean alloy.

2.1.2.1.6 *[Figure]* Volume fractions of the S phase for 8090 copper-rich alloy.

2.1.3 Thermal Conductivity: 50.26 Btu-ft/(hr-ft^2-F).

2.1.4 Thermal Expansion.

2.1.5 Specific Heat: 0.22 Btu/(lb F).

2.1.6 Thermal Diffusivity: 3.88 ft^2/hr.

2.2 Other Physical Properties

2.2.1 Density. For 8090: 0.0917 lb/in.^{3}. For 8091: 0.0921 lb/in.^{3}.

2.2.2 Electrical Properties.

2.2.3 Magnetic Properties.

2.2.4 Emittance.

2.2.5 Damping Capacity.

2.3 Chemical Environments

2.3.1 General Corrosion. There is a small database available for the general corrosion resistance of 8090 and none for 8091. Some data for the general corrosion resistance of 8090 are presented in Tables 2.3.1.1 and 2.3.1.2. Intergranular and exfoliation tests (Table 2.3.1.1) indicate that lower aging temperature produce better corrosion resistance in these test types. The results in salt spray (Table 2.3.1.2) are inconclusive regarding the effects of aging temperature or concerning a comparison of recrystallized with unrecrystallized sheet.

Corrosion rates are low in near neutral NaCl solutions (pH near 7) but increase rapidly as the solution becomes highly acidic or alkaline (Figure 2.3.1.3).

2.3.1.1 *[Table]* Intergranular and exfoliation test results on 8090-T351 extrusions given several aging treatments.

2.3.1.2 *[Table]* Stress-corrosion thresholds and exfoliation behavior for several heat treated conditions of 8090 sheet and one condition of plate.

2.3.1.3 *[Figure]* Corrosion rates of 8090-T851 partially recrystallized extrusions in NaCl solutions of 1<pH<13.

a. pH = 2, 4, 5, 7
b. pH = 1, 13

2.3.2 Stress Corrosion. Slow strain rate tests of unrecrystallized 8090 plate in 3.5 percent NaCl do not show any improvement associated with low aging temperatures (Table 2.3.2.1). Alternate immersion tests on 8090 forgings (Table 2.3.2.2) might be interpreted to indicate that better performance is associated with the low aging temperatures, but these data are from two test types and may not be strictly comparable. For recrystallized 8090 sheet, low aging temperatures appear to give inferior stress-corrosion thresholds compared with the more fully aged conditions (Table 2.3.1.2). The stress-corrosion threshold for unrecrystallized plate tested in the short-transverse direction is well below that for sheet (Table 2.3.1.2). There is little data that would establish a K threshold for stress-corrosion cracking. Tests on unrecrystallized plate in humid air (Figure 2.3.2.3) suggest a value of 12 ksi$\sqrt{\text{in.}}$ for that environment.

2.3.2.1 *[Table]* Stress corrosion of 8090-T8 plate in 0.5M NaCl at a slow strain rate.

2.3.2.2 *[Table]* Results of stress-corrosion tests of 8090 heavy forgings illustrating the possible beneficial effects of low temperature aging and possible deleterious effects of relatively high silicon.

2.3.2.3 *[Figure]* Stress-corrosion crack velocity in humid air for 8090-T651.

3 Mechanical Properties

3.1 Specified Mechanical Properties

3.1.1 *[Table]* Commercial specifications for 8090 hand forgings and sheet.

3.1.2 *[Table]* Commercial specifications for 8090 plate.

3.1.3 *[Table]* Producer's guaranteed tensile properties and fracture toughness for extrusions.

3.1.4 *[Table]* Producer's guaranteed tensile properties and fracture toughness for plate.

3.1.5 *[Table]* Producer's guaranteed tensile properties for sheet in the T6 and T8 tempers.

3.1.6 *[Table]* Producer's guaranteed tensile properties and fracture toughness for hand forgings.

3.2 Mechanical Properties at Room Temperature

3.2.1 Tension Stress-strain Diagrams and Tension Properties

3.2.1.1 *[Figure]* Monotonic and stabilized cyclic stress-strain curves for 8090-T8 plate.

3.2.1.2 *[Figure]* Effect of natural aging time and quench rate on tensile properties of 8090 and 8091 sheet.

3.2.1.3 *[Figure]* Effect of solution time on tensile yield and ultimate strength of 8090-T6 solution treated in air or a salt bath and effect of surface removal after solution treatment for 256 hours.

3.2.1.4 *[Figure]* Effect of aging time at 302F on tensile properties of recrystallized sheet.

3.2.1.5 *[Figure]* Effect of prestrain after aging on tensile properties of unrecrystallized (UR) or partially recrystallized (PR) sheet.

3.2.1.6 *[Table]* Effect of aging temperature and time on tensile properties and fracture toughness of 8090 forgings.

3.2.1.7 *[Figure]* Effect of amount of stretch and aging time on yield strength and elongation of 8090-T3 sheet.

3.2.1.8 *[Figure]* Tensile properties of unrecrystallized 8090 sheet as a function of angle to the rolling direction.

3.2.1.9 *[Figure]* Tensile properties of damage tolerant 8090 sheet as a function of angle to the rolling direction.

3.2.1.10 *[Table]* Comparison of two thermomechanical treatments illustrating the beneficial effects of increased stretching preceding aging coupled with low aging temperature for 8091 0.5-inch plate.

3.2.1.11 *[Table]* Comparison of two thermomechanical treatments illustrating the beneficial effects of increased stretching preceding aging coupled with lower aging temperature for 8091 1-inch plate.

3.2.1.12 *[Table]* Tensile properties and fracture toughness for naturally aged and artificially aged 8090 and 8091 plate.

3.2.1.13 *[Table]* Tensile properties of 8090-T6 forgings compared with those of sheet.

3.2.1.14 *[Table]* Tensile properties of 8090-T8 heavy plate at different thickness positions.

3.2.1.15 *[Table]* Comparison of tension and compression yield strengths for 8090 and 8091 in the T651 temper.

3.2.2 Compression Stress-strain Diagram and Compression Properties, see also Table 3.2.1.15.

3.2.3 Impact, see also Tables 1.5.3.1 and 1.9.7.5.

3.2.3.1 *[Figure]* Loss in Charpy V energy relative to as-quenched condition for isothermal aging of 8090 lean alloy.

3.2.3.2 *[Figure]* Loss in Charpy V energy relative to as-quenched condition for isothermal aging of 8090 rich alloy.

3.2.4 Bending.

3.2.5 Torsion and Shear, see Table 3.2.6.1.

3.2.6 Bearing.

3.2.6.1 *[Table]* Bearing and shear strengths of 8091-T8 and 8091-T877 plate.

3.2.7 Stress Concentration.

3.2.7.1 Notch properties, see Section 3.3.7.1.

3.2.7.2 Fracture toughness, see Sections 1.5.6, 1.9.6, and 1.9.7; Table 3.2.1.6 and Tables 3.2.1.10 to 3.2.1.13.

3.2.7.2.1 General. Fracture toughness information for 8090 and 8091 is available from a number of sources most of which do not use standardized test procedures and sometimes do not report details of the tests used to determine the reported values. Very few valid K_{Ic} values have been published. Most of the fracture toughness data in this chapter has been designated as K_Q even though the test procedure does not conform to any standard. For this reason caution should be used in comparing the values of K_Q. For sheet materials, K_c or K_{app} have been reported. These measurements of fracture toughness for sheet involve tests according to ASTM E 561 using center-cracked M(T) panels where the toughness values are based on maximum load and corresponding crack length (K_c), or the maximum load and the original crack length (K_{app}). Different investigators have used panels of considerably different width and in some cases no width is specified. The values of K_c and K_{app} will depend on the panel width (Table 3.2.7.2.3). For this reason meaningful comparisons of sheet fracture toughness values are not always possible.

The fracture toughness of unrecrystallized 8090 and 8091 is highly directional with the SL and ST orientations having relatively low toughness (e.g., Table 3.2.1.12). The fracture toughness in the TL orientation of unrecrystallized plate can be improved by increased stretching coupled with long-time aging at reduced temperatures (Tables 3.2.1.10 and 3.2.1.11). This treatment also improves the tensile properties. The SL and ST toughness in unrecrystallized

plate can be improved by very long-time aging at relatively low temperature (Table 3.2.1.6). Damage tolerant plate has reduced strength with substantially increased fracture toughness but still shows significantly lower values for the ST crack orientation (Table 3.1.4).

In the case of sheet, the highest fracture toughness values (K_c or K_{app}) are obtained with fine-grained, recrystallized material (Figure 3.2.7.2.4).

3.2.7.2.2 *[Figure]* Effect of aging temperature and time on the short-transverse (SL) toughness of 8090-T651 plate.

3.2.7.2.3 *[Table]* Effect of panel width on the K_c values obtained for 8090-T81 sheet.

3.2.7.2.4 *[Figure]* Effect of grain structure on fracture toughness (K_c and K_{app}) of 8090 sheet.

3.2.7.2.5 *[Figure]* Fracture toughness (K_c) as a function of aging time for stretched and unstretched 8090 sheet.

3.2.8 Combined Properties.

3.3 Mechanical Properties at Various Temperatures

3.3.1 Tension Stress-strain Diagrams and Tensile Properties.

3.3.1.1 *[Figure]* Effect of temperature on the tensile yield strength and elongation of 8090 plate.

3.3.1.2 *[Figure]* Effect of test temperature on tensile yield strength of extruded rod and sheet in the T6 condition.

3.3.1.3 *[Figure]* Effect of test temperature on tensile yield strength of 8090 sheet in T6 and T8 conditions.

3.3.1.4 *[Figure]* Effect of test temperature on the tensile yield strength of 8090-T6 extrusions subjected to short and long-time exposures at test temperature.

3.3.1.5 *[Figure]* Effect of low test temperatures on two 8090-T852 forging blocks of different sizes.

3.3.1.6 *[Figure]* Effect of low test temperatures on tensile strength of 8090 as-quenched plate.

3.3.1.7 *[Figure]* Effect of low test temperatures on tensile strain properties of 8090 as-quenched plate.

3.3.1.8 *[Figure]* Effect of low test temperatures on the strain hardening exponent of 8090 as-quenched plate.

3.3.1.9 *[Table]* Tensile properties and fracture toughness of 8090 plate at room temperature and -320F for two conditions of heat treatment.

3.3.2 Compression Stress-strain Diagrams and Compression Properties.

3.3.3 Impact.

3.3.4 Bending.

3.3.5 Torsion and Shear.

3.3.6 Bearing.

3.3.7 Stress Concentrations.

3.3.7.1 Notch properties.

3.3.7.1.1 *[Figure]* Effect of test temperature on sharp-notch strength ratio of two 8090-T852 forging blocks, the larger (Block A) of which exhibited grain boundary embrittlement due to the T_2 phase.

3.3.7.2 Fracture toughness.

3.3.7.2.1 *[Figure]* Effect of low test temperatures on SL fracture toughness of single- and double-aged plate.

3.4 Creep and Creep Rupture Properties

3.5 Fatigue Properties

3.5.1 Conventional Fatigue Properties. The conventional fatigue life of smooth specimens is increased by those factors which increase the tensile strength (e.g., see Figure 3.5.1.2). However, this effect appears to fade out as the test temperature increases (Figure 3.5.1.3). In the T651 condition heat treatment the smooth and notch fatigue strength of 8090 and 8091 appear to be essentially identical (Figures 3.5.1.4 and 3.5.1.5). In the presence of 3.5 percent NaCl the smooth fatigue life of 8090-T6 plate is greatly reduced as are the cycles to crack initiation (Figures 3.5.1.6 and 3.5.1.7).

3.5.1.1 *[Figure]* S-N scatter bands for 8090 at two yield strength levels.

3.5.1.2 *[Figure]* S-N scatter bands for two yield strength levels of 8090 tested at 184F.

3.5.1.3 *[Figure]* S-N scatter bands for two yield strength levels of 8090 tested at 305F.

3.5.1.4 *[Figure]* S-N scatter bands for axial-load fatigue of smooth specimens of 8090 and 8091 plate.

3.5.1.5 *[Figure]* S-N scatter bands for axial-load fatigue of notch specimens of 8090 and 8091 plate.

3.5.1.6 *[Figure]* S-N curves for 8090-T6 plate tested in air or in 3.5 percent NaCl.

3.5.1.7 *[Figure]* Fatigue crack initiation curves for 8090-T6 plate in air or 3.5 percent NaCl.

3.5.1.8 *[Figure]* S-N curves for an 8090-T6 forged compressor casing at RT and at 302F.

3.5.1.9 *[Figure]* Low-cycle fatigue behavior for extruded bar.

3.5.1.10 *[Figure]* Low-cycle fatigue strength for two 8090-T6 forgings.

3.5.1.11 *[Figure]* Low-cycle fatigue curve for 8090-T851.

3.5.2 Fatigue Crack Propagation. **Long crack** (equal or greater than the material thickness) fatigue propagation rates in unrecrystallized material are strongly influenced by the crystallographic texture and the mechanical anisotropy (poor short-transverse ductility) associated with elongated grains with weak boundaries. These structural features produce transgranular, tortuous crack paths for cracks oriented in the LT and TL directions. This behavior results in crack closure forces associated with fracture surface asperities. The closure forces lower fatigue crack propagation rates for the TL and LT crack orientations at low R ratios. At high R ratios the beneficial effects of crack closure are decreased and fatigue crack propagation rates and threshold values increase (Figure 3.5.2.7). If the crack closure effects are removed, threshold values are less than 1 ksi$\sqrt{\text{in.}}$ (Figure 3.5.2.17). Crack propagation rates for the 45-degree orientation are higher than the corresponding rates for the LT and TL orientations, presumably due to a more planar crack path (Figure 3.5.2.8). In the case of heavy plate, the grain size tends to increase toward the center resulting in lower TL crack propagation rates than at the surface (Figure 3.5.2.10).

Crack propagation in the ST and SL orientations proceeds largely by intergranular delamination and this results in increased propagation rates and lower threshold values as compared with the LT and TL orientations (Figure 3.5.2.9).

Aging treatments which increase the tensile strength tend to lower the threshold values (Figures 3.5.2.1, 3.5.2.2, and 3.5.2.6). However, these aging effects on the fatigue crack propagation rates are reduced at higher ΔK levels (Figures 3.5.2.1 and 3.5.2.2).

Only limited data are available for the influence of environment on the fatigue crack propagation rates. Rates for the LT, TL, and LS crack orientation are all increased substantially in the presence of 3.5 percent NaCl (Figures 3.5.2.16 and 3.5.2.19). The effects of under- and overaging observed for tests in air tend to disappear for tests in vacuum, indicating a possible strong influence of humidity (Figure 3.5.2.3).

Short cracks are grown in three- or four-point bending of smooth specimens with electropolished surfaces. Crack sizes are determined by replication. Such "naturally" occurring cracks initiate along slip bands in the vicinity of microstructural heterogeneities or from subgrain boundaries. Subsequent growth is crystallographic with arrests and changes in direction at grain boundaries (Refs. 10, 5-8). The shape of the developing crack is close to semicircular. As might be expected the propagation rates exhibit considerable scatter, since multiple paths may develop from an origin. Crack propagation rates are considerably higher than for long cracks particularly at low values of ΔK and when no threshold is observed (Figures 3.5.2.12 to 3.5.2.14). Crack closure is essentially absent during the early growth stage of small cracks; however, as the size increases, closure forces develop and the propagation rates approach those of long cracks (Figure 3.5.2.14). Apparently the effects of alloy composition and crack orientation are lost in the scatter associated with small crack growth (Figure 3.5.2.15). It should be noted that the use of linear elastic fracture mechanics to characterize the K values for cracks in the order of the grain size may not give values which can be compared with those for long cracks.

3.5.2.1 *[Figure]* Fatigue crack propagation rates for 8090-T3 and 8090-T8 plate.

3.5.2.2 *[Figure]* Fatigue crack propagation rates for 8091-T3 and 8091-T8 plate.

3.5.2.3 *[Figure]* Fatigue crack propagation rates for three aged conditions of 8090 extrusions tested in air or in vacuum.

3.5.2.4 *[Table]* Heat treatments used in producing the test material representing the fatigue crack propagation rates illustrated in Figures 3.5.2.5 and 3.5.2.6.

3.5.2.5 *[Figure]* Fatigue crack propagation rates for 8090 plate given several treatments.

3.5.2.6 *[Figure]* Fatigue crack propagation rates for 8091 plate given several treatments.

3.5.2.7 *[Figure]* Fatigue crack propagation rates at R = 0.1 and 0.7 for 8091 plate.

3.5.2.8 *[Figure]* Fatigue crack propagation rates for 8090 1.4-inch plate for several crack orientations at the plate center.

3.5.2.9 *[Figure]* Fatigue crack propagation rates for 8090 4-inch plate for several crack orientations at the plate center.

3.5.2.10 *[Figure]* Fatigue crack propagation rates for 8090 4-inch plate at various thickness positions for TL crack orientation.

3.5.2.11 *[Figure]* Effect of shot peening on crack growth rate of a notched 8090 plate.

3.5.2.12 *[Figure]* Fatigue crack propagation rates for short and long cracks in overaged 8090 extrusions.

3.5.2.13 *[Figure]* Fatigue crack propagation rates for short and long cracks in peak-aged (T8) 8090 extrusions.

3.5.2.14 *[Figure]* Fatigue crack propagation rates for long and short cracks in 8090-T3 plate.

3.5.2.15 *[Figure]* Scatter band for fatigue crack propagation rates of short cracks for several aluminium alloys.

3.5.2.16 *[Figure]* Fatigue crack propagation rates in air and in 3.5 percent NaCl for 8090-T6 plate tested in different crack orientations.

3.5.2.17 *[Figure]* Fatigue crack growth rates for 8090-T351 and -T8 plate. Data corrected for closure.

3.5.2.18 *[Figure]* Effect of exposure at 210F on fatigue crack growth rate of 8090-T8 plate.

3.5.2.19 *[Figure]* Fatigue crack growth rates for 8090-T8 plate in air and in 3.5 percent NaCl solution.

3.6 Elastic Properties

3.6.1 Poisson's Ratio.

3.6.2 Modulus of Elasticity. 8090: 11,528 ksi; 8091: 11,585 ksi (Ref. 1, Figure 2).

3.6.2.1 *[Figure]* Young's modulus as a function of angle from rolling direction for 8090-T3 sheet.

3.6.3 Modulus of Rigidity.

3.6.3.1 *[Figure]* Shear modulus as a function of angle from rolling direction for 8090-T3 sheet.

3.6.4 Tangent Modulus.

3.6.5 Secant Modulus.

4 Fabrication

4.1 Forming

4.1.1 Superplastic Forming. Both 8090 and 8091 can be superplastically formed and simultaneously solution treated. If the starting condition of the sheet is as-rolled, the flow stress will be high, poor finish may result, and cavitation may be encountered, particularly if coarse recrystallized grains are present. Several sheet processing routes have been proposed to develop properties that will optimize superplastic performance. These are reviewed in Ref. 4-14. The 8090 alloy shows little quench sensitivity and, in gages up to about 0.12 in., can be air quenched off the forming machine. In contrast, 8091 sheet may require water quenching to avoid reduction in strength properties (Ref. 4-14). Tests at various strain rates indicate that higher elongations may be obtained by constant velocity deformation than by constant strain rate deformation (Figure 4.1.1.1).

4.1.1.1 *[Figure]* Elongation as a function of strain rate for 8090 deformed at constant velocity or at constant strain rate.

4.1.2 Forging. A limited number of forgings have been produced from the 8090 alloy. Properties were reported in previous sections; however, no production details were provided. It would appear that the alloy can be successfully forged using conventional techniques. However, problems arise in heavy sections which may not cool rapidly enough to suppress precipitation, with resulting poor transverse properties and reduced fracture toughness (Section 1.9.1).

4.1.3 Extrusion. 8090 extrusions have been produced in various shapes with no reported special problems.

4.1.3.1 *[Figure]* Influence of extrusion conditions on back-end tensile yield strength of 4 x 1-in. flat bar.

4.2 Machining and Grinding

4.3 Joining

4.3.1 Welding.

4.3.1.1 General. Only limited data were available on welding of 8090 and 8091. Varestraint (1 percent augmented strain) and Houldcroft tests were performed on autogeneous GTA welds made on 8090, 2090, and several conventional aluminum alloys (Ref. 5-12). The results from both tests showed that the Al-Li alloys exhibited continuous networks of eutectic constituent along solidification grain boundaries, with little evidence of crack healing. Total crack length in the varestraint test was about 1.6 to 1.7 in. for the Al-Li alloys compared to 1-in. for 6061 and about 0.04 in. for 2219. In contrast, the Houldcroft test showed the Al-Li alloys to be superior to 6061. Clearly, additional work is needed.

Some results are available from tensile tests on GTA welded sheet using different fillers (Table 4.3.1.2). In the as-welded condition the best combination of strength and elongation was obtained using an Al-Mg(Zr) filler. Postweld aging improved the tensile yield and ultimate strengths of welds made with 8090 and Al-Mg fillers, with the 8090 filler weld being highest in strength. This heat treatment, however, produced strength values well below those expected for 8090-T6 sheet (F_{tu} = 68 ksi and F_{ty} = 54 ksi).

The surface of material to be welded should be cleaned by removing the layer of lithium oxide, which will adsorb moisture and result in weld porosity. In most cases a light machining will be sufficient.

4.3.1.2 *[Table]* Tensile properties of as-GTA-welded and post-heat-treated sheet specimens.

4.3.2 Fasteners. No data were available on the static or fatigue properties of fasteners. However, one investigation of the fatigue life of expanded fastener holes showed that cracks emanating from these holes advanced along planes included 50 to 60 degrees to the tensile axis (Ref. 5-11). This behavior is associated with crystallographic anisotropy and would probably also be observed in structures employing fasteners. Its significance to structural performance requires study.

4.4 Surface Treating

4.4.1 Anodizing. The sulphuric acid hard coat anodizing process has been successfully applied to 8090-T651 sheet. Dense adherent coatings were obtained up to 2 mil in thickness (Ref. 3-5).

Table 1.3.1 Tentative mechanical properties for 8090 Aluminum Association Registration (Ref. 29)

Alloy: 8090					
Form	**Plate (a)**				
Temper	**T7**				**T86**
Thickness (in.)	**0.250-1.500**	**1.501-2.000**	**2.001-3.000**	**3.001-4.000**	**0.250-1.250**
F_{tu} (ksi) (min)	65	63	62	60	60
F_{ty} (ksi) (min)	54	52	50	49	45
e (percent, 2 in.) (min)	3	3	3	2	5

(a) Plate stretched 5 to 7 1/2 percent before aging

Table 1.4.1 Composition of 8090 and 8091 (Ref. 1)

Alloy	8090		8091	
Composition	**Weight Percent**			
	Min	**Max**	**Min**	**Max**
Li	2.2	2.7	2.4	2.8
Cu	1.0	1.6	1.6	2.2
Mg	0.6	1.3	0.5	1.2
Zr	0.04	0.16	0.08	0.16
Fe	-	0.3	-	0.5
Si	-	0.2	-	0.3
Zn	-	0.25	-	0.25
Ti	-	0.1	-	0.1
Mn	-	0.1	-	0.1
Cr	-	0.1	-	0.1
Others, each	-	0.05	-	0.05
Total	-	0.15	-	0.15

Table 1.5.3.1 Effect of quench rate on the tensile properties and Charpy energy of 8090 as quenched, and stretched and aged (Ref. 16, Table 2 and Fig. 3)

Alloy: 8090									
Form	**1-inch T3 Plate**								
Quench	**1022F, 1 hour, Quench**								
Composition, weight percent	**2.28Li-0.86Cu-0.90Mg-0.13Zr-0.13Fe-0.06Si (Lean Alloy)**								
Quench Media	**Air Cool - 0.45F per sec**			**Polymer - 0.32F per sec**			**Water - 216F per sec**		
Age	**None**	**2 percent CW + 374F, 16 hr (a)**	**4 percent CW + 338F, 24 hr**	**None**	**2 percent CW + 374F, 16 hr**	**4 percent CW + 338F, 24 hr**	**None**	**2 percent CW + 374F, 16 hr**	**4 percent CV W + 338F, 24 hr**
F_{tu} (ksi)	60	65	67	57	70	70	54	71	70
F_{ty} (ksi)	34	58	58	33	60	60	30	62	60
e (percent)	6	8	6	17	8	7	18	8	8
Normalized Charpy V (a)	1	-	-	1.7	-	-	2.5	-	-
Composition, weight percent	**2.58Li-1.36Cu-0.89Mg-0.13Zr-0.17Fe-0.04Si (Rich Alloy)**								
F_{tu} (ksi)	65	70	79	65	76	75	62	78	75
F_{ty} (ksi)	39	60	64	41	65	65	38	67	65
e (percent)	6	5	5	11	7	5	16	8	7
Normalized Charpy V (b)	1	-	-	1.25	-	-	-	-	-

(a) 0.12-inch thick Charpy V-notch specimens with 0.001-inch notch root radius.
(b) Normalized to the as-quenched value for each composition.

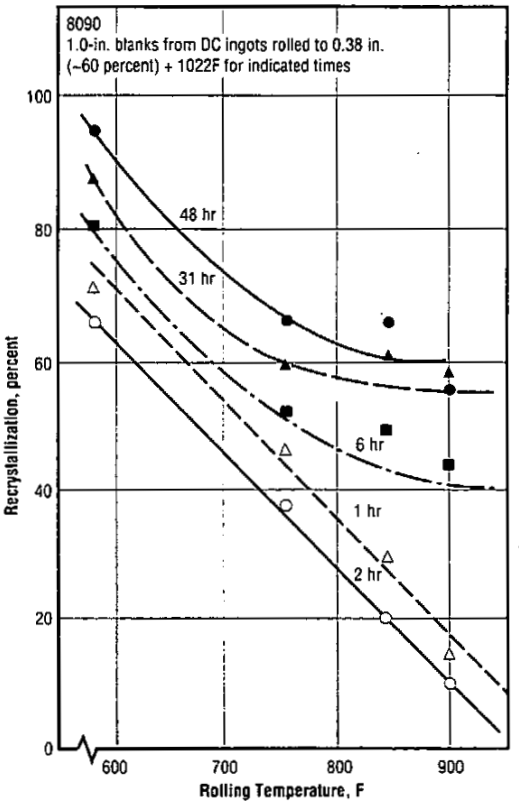


Fig. 1.5.3.2 Recrystallized fractions as functions of rolling temperature and solution time (Ref. 4-2, Fig. 2)

Table 1.5.3.3 Effect of quench rate and recovery treatments on the SL fracture toughness of 8090 naturally aged plate (Refs. 26, 28)

Alloy: 8090								
Form	**2-in. Plate ST 986F, Quench as Indicated**							
Age	**Natural 100 days**				**Natural + 410F, 10 min (b)**			
Quench (a)	**CW**	**HW**	**Oil**	**Air**	**CW**	**HW**	**Oil**	**Air**
K_Q (ksi $\sqrt{in.}$) (c)	23	9	8	6	31	19	15	9
Age	**338F, 32 hours**				**338F, 32 hours + 410F, 10 min**			
K_Q (ksi $\sqrt{in.}$) (c)	>35	-	-	14	>35	-	-	16

(a) CW - Cold Water; HW - Hot Water
(b) Recovery (reversion) treatment in salt
(c) 1-in. thick DCB specimens. See Table 1.9.6.5 for fracture toughness test method except these specimens were 1-in. thick

Table 1.5.5.1 Summary of artifical aging treatments found in recent literature (June 1992)

Alloy: 8090				
Temper	**Plate**	**Sheet**	**Forgings**	**Extrusions**
T6	538F (170C), 32 hours			
T8	Peakaged condition: ST + 2 to 4 percent stretch + 338F (170C), 32 to 40 hours. Also, 3 percent stretch 374F, 16 hours	(Also T81) Peakaged condition: ST + 1.5 to 2 percent stretch + 338F (170C), 32 to 40 hours	See Table 3.1.1 (Alloy producers furnished no recommendations)	ST + 410F (210C), 4 to 5 hours
T81	ST + 5 to 7 1/2 percent stretch, unspecified peakage (30)			
T651	2.5 to 4 percent stretch + 338F (170C), 16 hours			
T871	Damage tolerant underaged condition: ST + 6 to 7 percent stretch + 302F (150C), 12 hours	Damage tolerant underaged condition (my be recrystallized): ST + 1.5 to 2 percent stretch + 302F (150C), 24 hours		Damage tolerant underaged condition: ST + 1.5 to 3 percent stretch + 302F (150C), 12 hours
T8771	6 to 8 percent stretch, 338F, 32 hours			
T86	5 to 7 1/2 percent stretch, damage tolerant unspecified age (30)			

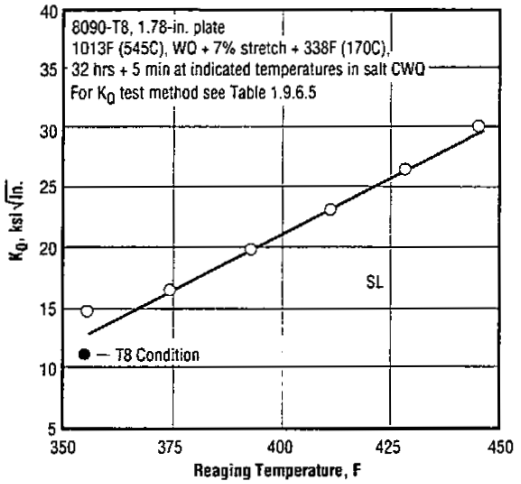


Fig. 1.5.6.1 Effect of reaging temperature on the SL fracture toughness of 8090-T8 plate (Ref. 21, Fig. 2)

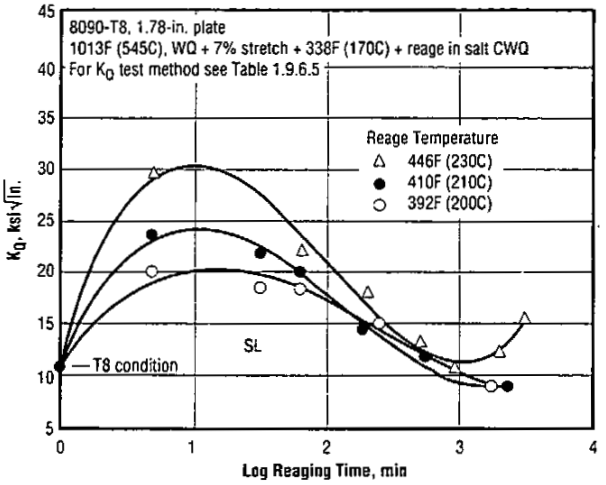


Fig. 1.5.6.2 Effect of reaging temperature and time on the SL fracture toughness of 8090-T8 plate (Ref. 21, Fig. 1)

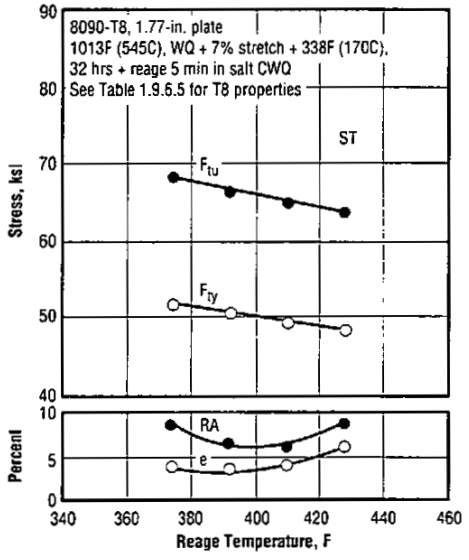


Fig. 1.5.6.3 Effect of reaging temperature on short-transverse tensile properties of 8090-T8 plate (Ref. 21, Table 2)

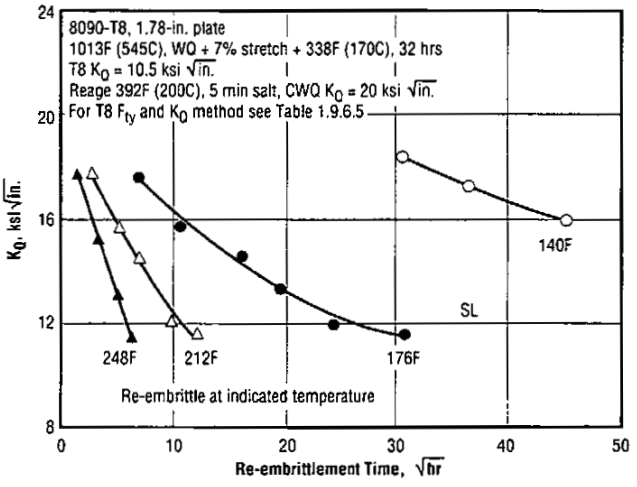


Fig. 1.5.6.4 Effect of temperature and time of re-embrittlement on SL fracture toughness of 8090-T8 plate given a reaging (toughening) treatment (Ref. 21, Fig. 4)

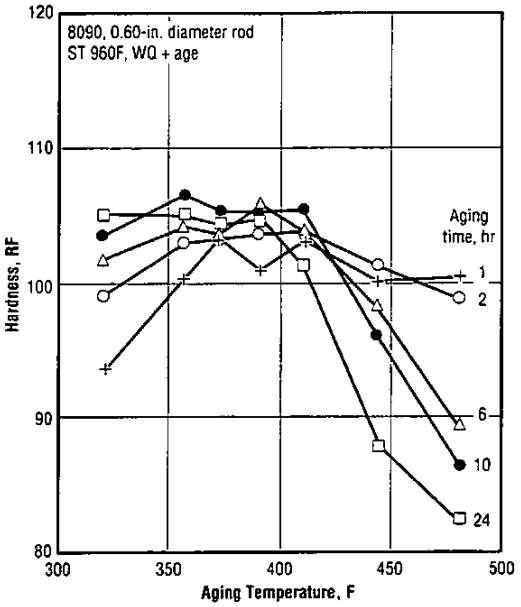


Fig. 1.6.1 Variation of hardness with aging temperature and time for 8090 rod (Ref. 5-1, Fig. 1)

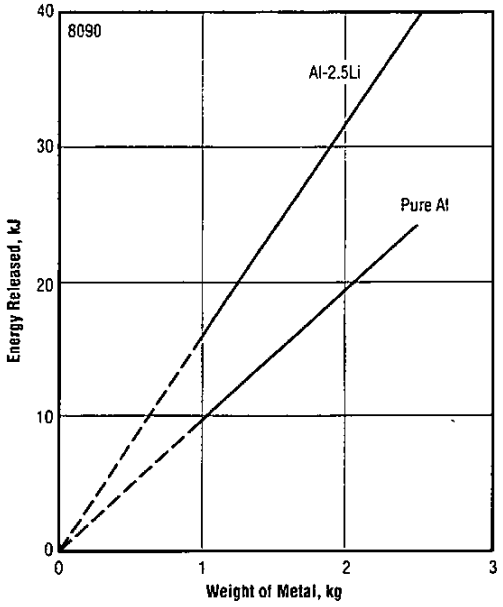


Fig. 1.9.3.1 Energy released as a function of weight of metal for pure aluminum and Al-2.5% Li with water coolant (Ref. 4-9, Fig. 2)

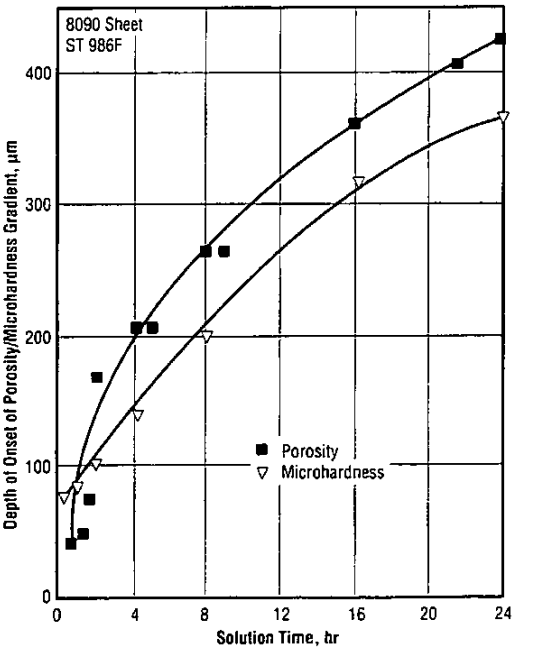


Fig. 1.9.4.1 Depth of onset of subsurface porosity and microhardness gradient as a function of solution treatment time (Ref. 4-8, Fig. 5)

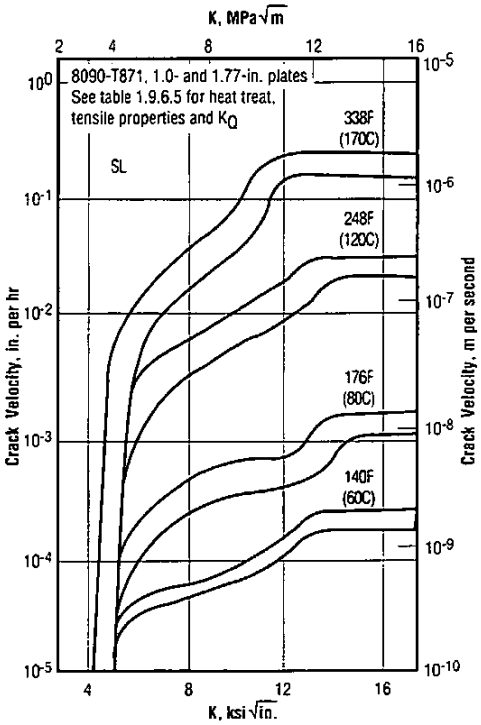


Fig. 1.9.6.1 Crack velocity as function of K level for 8090 plate tested at elevated temperatures (Ref. 22, Fig. 2)

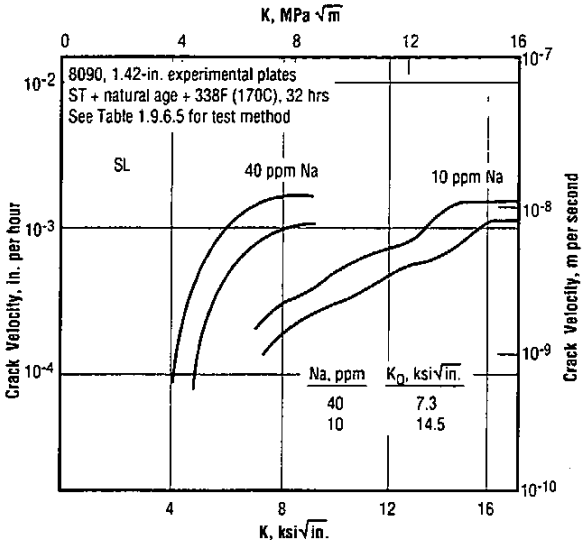


Fig. 1.9.6.2 Crack velocity as function of K level for two experimental 8090 plates showing the effect of sodium content (Ref. 22, Fig. 3)

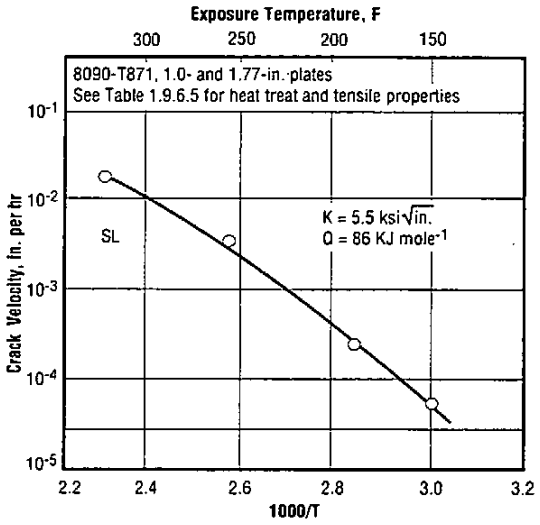


Fig. 1.9.6.3 Arrhenius plot of crack velocity in 8090 plate as a function of reciprocal of absolute temperature at a K level of 5.5 ksi√in. (Ref. 22, Fig. 5)

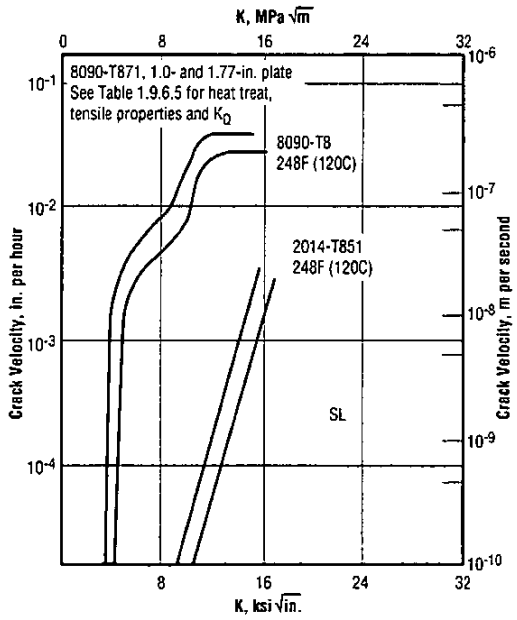


Fig. 1.9.6.4 Crack velocity at 248F as a function of K level for 8090 and 2014-T851 plates (Ref. 22, Fig. 4)

Table 1.9.6.5 Supplementary information for data derived from Refs. 21-24

Alloy	8090-T871 Unrecrystallized	8090-T3 Plate Unrecrystallized	8090-T81 Sheet Recrystallized	8090-T81 Sheet Unrecrystallized
Reference	23, Table 2	23, Table 6	26	26
Thickness (in.)	1.77 in.	1 in.	1/16 in.	1/16 in.
Na (ppm)	3	5	7	2
Heat Treat (a)	ST 1013F, CWQ + 7 percent Stretch + 338F, 32 hours	ST 1013F, CWQ + 2 percent Stretch + Natural Age, 1 year	ST + 302F, 24 hours	ST + 302F, 1 hour
F_{tu} (ksi)	69 (ST)	-	65 (all orientations)	61 (L), 52 (50 deg) (b)
F_{ty} (ksi)	54 (ST)	-	51 (L), 43 (60 to 70 deg) (b)	49 (L), 36 (50 deg) (b)
RA (percent)	4.3 (ST)	-	-	-
e (percent)	1.9 (ST)	-	-	-
Vickers (10kgf)	156	149	-	-
K_Q (ksi $\sqrt{in.}$)	10.5 (SL)	13 (SL)	-	-

Note: KQ & Crack Velocity Measurements All plate K_Q and crack velocity data in this Table and in Figs. 1.9.6.1-1.9.6.7 are from 25 mm square bolt-loaded cantilever-beam specimens precracked by bolt preload to produce pop-in. K_Q values reported represent 3 starts and stops of the crack following pop-in

(a) CWQ - cold water quench
(b) Deg. to load axis. L represents 0 deg.

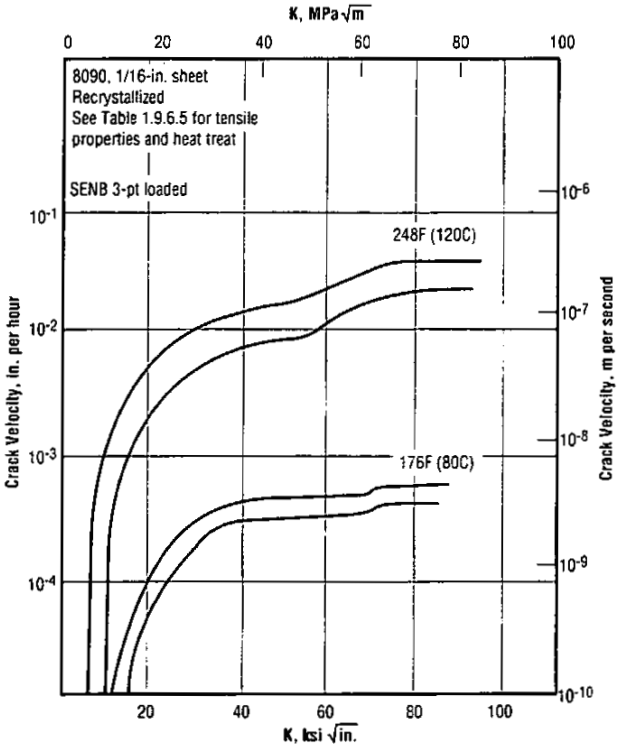


Fig. 1.9.6.6 Crack velocity as a function of K level at 176F and 248F for 8090 recrystallized sheet (Ref. 23, Fig. 2)

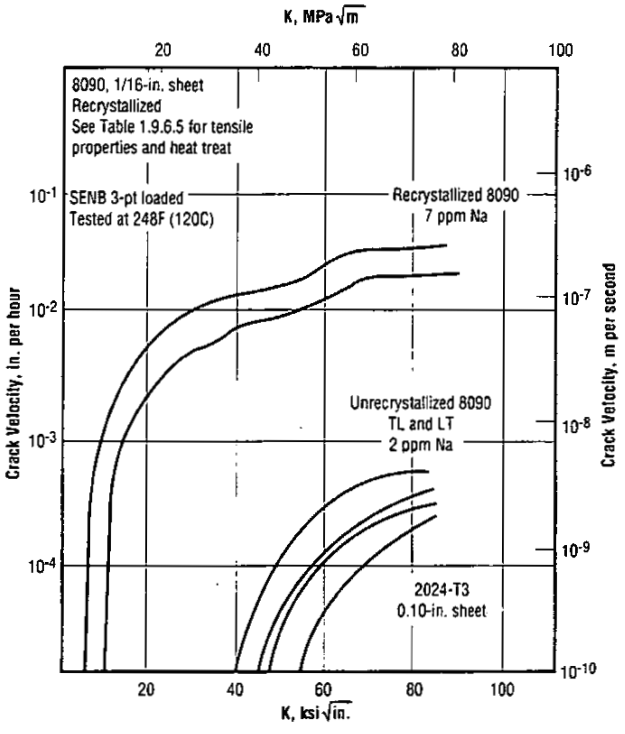


Fig. 1.9.6.7 Crack velocity as a function of K level at 248F for 8090 recrystallized and unrecrystallized sheet and for 2024-T3 sheet (Ref. 23, Fig. 1)

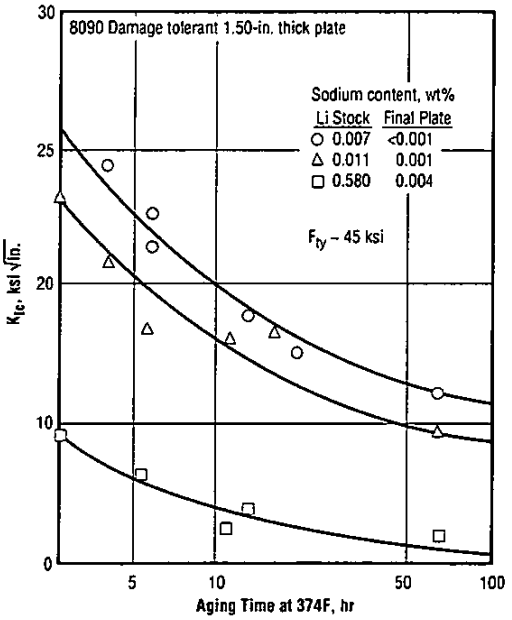


Fig. 1.9.6.8 Effect of sodium content in lithium on the short-transverse fracture toughness of stretched and aged 8090 plate (Ref. 13, Fig. 13)

Table 1.9.7.1 Effect of prolonged exposure at elevated temperature on tensile properties and fracture toughness of 8090 plate (Ref. 20, Table 1)

Alloy: 8090-T8			
Form	**4-in. Plate**		
Condition	**ST 986F, WQ + 1.5 to 3 percent Plastic Stretch + 338F, 32 hours**		
Location	**Specimens at mid-thickness**		
Exposure	**None**	**210F, 100 hours**	**210F, 1000 hours**
F F_{tu} (si)	75	75	76
F F_{ty} (si)	70	70	72
e (percent)	4.3	2.5	2
K K_{Ic} (si √in.) (a)	32 (b)	17	15

(a) Fracture toughness determined with 0.4-in. thick C(T) LT specimens
(b) Invalid value: insufficient thickness

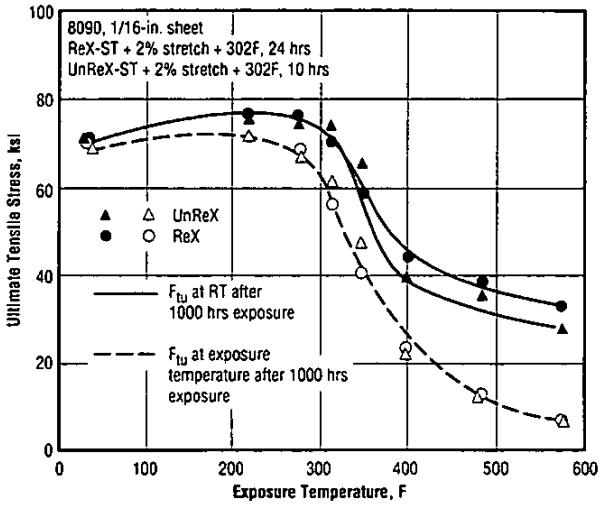


Fig. 1.9.7.2 Tensile strength of recrystallized (ReX) and unrecrystallized (UnReX) 8090 sheet at room temperature after 1000 hours exposure at elevated temperatures and at the exposure temperature after 1000 hours at that temperature (Refs. 27, 28)

Table 1.9.7.3 Percent loss in room temperature fracture toughness of recrystallized and unrecrystallized 8090 sheet after 1000 hours exposure to moderately elevated temperatures (Refs. 27, 28)

Alloy: 8090				
Form	**1/16-in. Sheet**			
Condition	**Recrystallized and Unrecrystallized**			
Heat Treatment	**See Fig. 1.9.7.2**			
1000 hr exposure temp (F)	32	75	150	302
Normalized I K_0(percent) (a)	100	100	80	53

(a) Normalized to 32F value. Toughness obtained from wide (78 in.) panel tests.

Table 1.9.7.4 Effect of long-time exposure at room temperature on the retained SL fracture toughness of 8090 plate (Refs. 26, 28)

Alloy: 8090									
Form	**Plate**								
Thickness (in.)	**1.77**			**1**			**1**		
Heat Treat	**-T8771**			**-T651**			**-T6**		
Exposure time (years) at RT	0	3	3.5	0	3	3.5	0	3	3.5
K_0 (ksi $\sqrt{in.}$) as exposed (SL) (a)	16	13	12	21	21	20	25	16	16
K_0 (ksi $\sqrt{in.}$) after 338F, 1 hour (SL)	-	-	16	-	-	21	-	-	27

(a) For fracture toughness test method see Table 1.9.6.5

Table 1.9.7.5 Effect of long-time exposure on the room temperature tensile and impact properties of structurally stabilized 8090 extrusions (Ref. 25)

Alloy: 8090								
Form	**Structurally Stabilized 2.5-in. x 0.54-in. Extrusion**							
Melt No.	**69**				**71**			
Locations	**Edge**		**Center**		**Edge**		**Center**	
RT Exposure (hours), at RT	280	18,000	280	18,000	280	18,000	280	18,000
F_{ty} (ksi)	74	69	61	61	77	77	68	66
Charpy V (LT) (ft-lbs)	10.9	11.1	8.2	8.4	10.7	10.2	7.5	7.5

Table 1.9.7.6 Tensile yield strength and fracture toughness for structurally stabilized 8090 extrusion after 3.3 years at room temperature (Ref. 25)

Alloy: 8090						
Form	**Structurally Stabilized 1.75-in. x 0.058-in. Extrusion**					
Exposure after Age	**3.3 years at RT**					
Location	**Center**			**Edge**		
Age Temperature (F) (a)	**250 16 hours**	**300 24 hours**	**350 24 hours**	**250 16 hours**	**300 24 hours**	**350 24 hours**
F_{ty} (ksi) L	40	49	55	47	56	62
K_{max} (ksi $\sqrt{in.}$) SL specimens (b)	54	50	16	-	-	29

(a) 980F + 4 percent stretch + age as indicated
(b) Chevron notch short bar tests. Toughness before exposure unknown

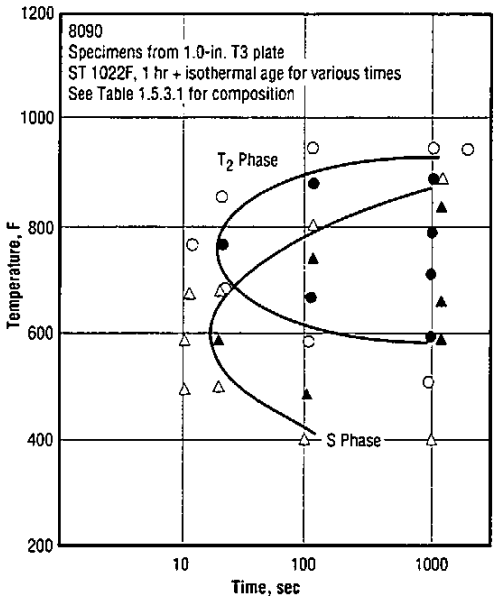


Fig. 2.1.2.1.1 Nucleation start curves for 8090 copper-lean alloy (Ref. 16, Fig. 6)

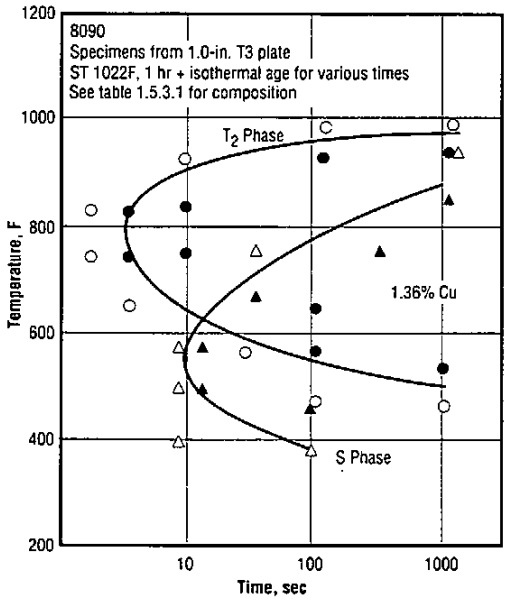


Fig. 2.1.2.1.2 Nucleation start curves for 8090 copper-rich alloy (Ref. 16, Fig. 5)

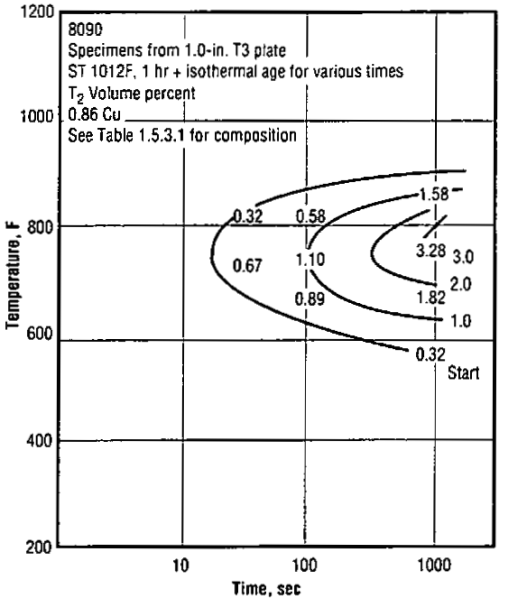


Fig. 2.1.2.1.3 Volume fractions of the T_2 phase for 8090 copper-lean alloy (Ref. 16, Fig. 6)

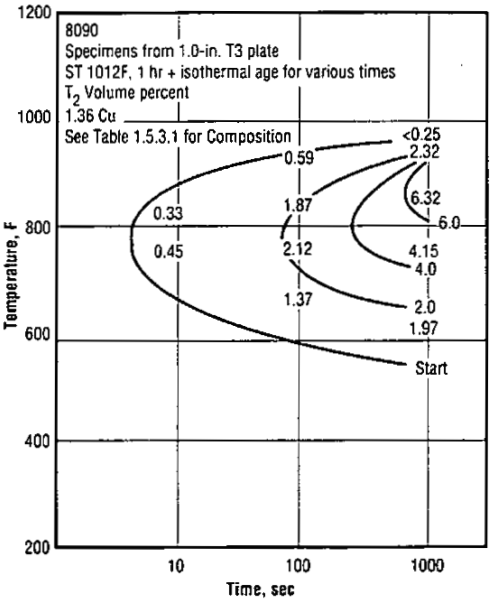


Fig. 2.1.2.1.4 Volume fractions of the T_2 phase for 8090 copper-rich alloy (Ref. 16, Fig. 6)

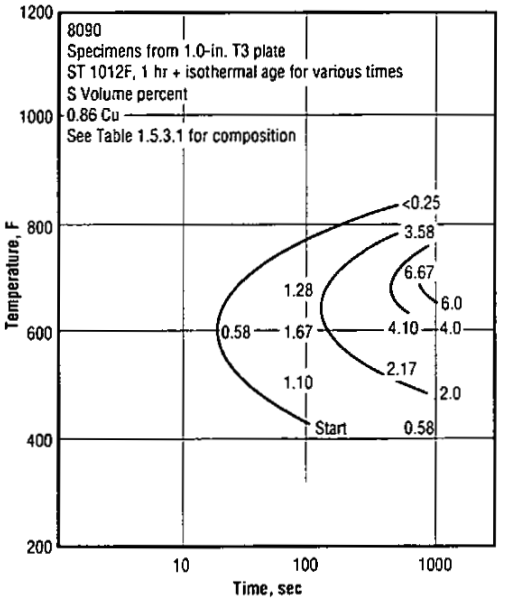


Fig. 2.1.2.1.5 Volume fractions of the S phase for 8090 copper-lean alloy (Ref. 16, Fig. 8)

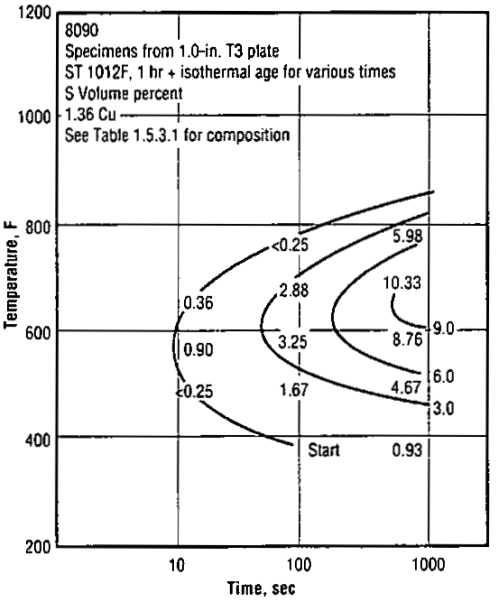


Fig. 2.1.2.1.6 Volume fractions of the S phase for 8090 copper-rich alloy (Ref. 16, Fig. 8)

Table 2.3.1.1 Intergranular and exfoliation test results on 8090-T351 extrusions given several aging treatments (Ref. 4-6, Table 4)

Alloy: 8090				
Form	**4-in. x 0.5-in. Extrusions**			
Test Method	**EXCO 48 hours, ASTM G 34**			
Heat Treat	**T351**	**T351 + 320F, 3 hours**	**T351 + 374F, 12 hours**	**T351 + 428F, 48 hours**
Test Result Surface	N	N	EA/EB	EA
Test Result Center (a)	EA	EA	EA/EB	EA/EB
Test Method	**MIL-H-6088 (b)**			
Test Result Surface	IG 0.001 in. (c)	Pits	IG 0.001 in.	N
Test Result Center	N	IG 0.001 in.	IG 0.001 in.	Pits

(a) Extrusion cut to expose the center plane to the corrodant
(b) NaCl, 1M + H_2O_2, 0.3 percent solution
(c) IG - Intergranular attack

Table 2.3.1.2 Stress-corrosion thresholds and exfoliation behavior for several heat treated conditions of 8090 sheet and one condition of plate (Refs. 27, 28)

Alloy: 8090				
Form	**Sheet**			
Condition	**Recrystallized**		**Unrecrystallized**	
Age Treatment	**SCC Threshold (ksi)**	**Salt Spray (a)**	**SCC Threshold (ksi)**	**Salt Spray (a)**
2-4 percent Stretch Natural Age	43.5	EA	-	P
2-4 percent Stretch 302F, 24 hours	25	EB/EC	-	-
2-4 percent Stretch 338F, 32 hours	43.5	EA	43.5	EA
No Stretch 338F, 32 hours	-	-	43.5	-
2-4 percent Stretch 338F, 8 hours	-	-	-	EC
Form	**2-in. Plate SL**			
6-8 percent Stretch 338F, 32 hours	-	-	22	-

(a) 14-day duration using acidified salt spray (ASTM G 85 Annex A1). Rating according to ASTM G 34

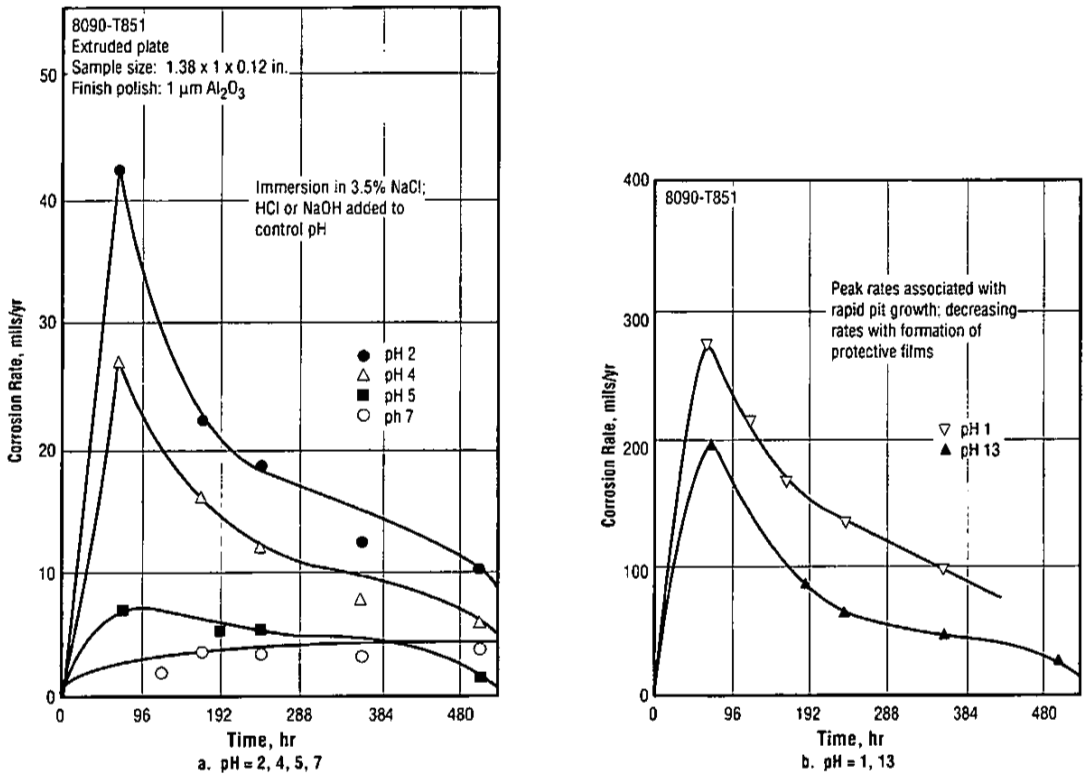


Fig. 2.3.1.3 Corrosion rates of 8090-T851 partially recrystallized extrusions in NaCl solutions of 1<pH<13 (Ref. 5-7, Fig. 5)

Table 2.3.2.1 Stress-corrosion of 8090-T8 plate in 0.5M NaCl at a slow strain rate (Ref. 5, Table 4)

Alloy: 8090						
Form and Condition	**1 in. Plate; ST + 6 percent Stretch + Age**					
Environment	**0.5M 3.5 percent NaCl at -700 mv (SCE); Strain Rate 10^{-6}/sec**					
Direction	**ST**			**L**		
Age	**338F, 4 hours**	**338F, 6 hours**	**377F, 4 hours**	**338F, 4 hours**	**338F, 6 hours**	**377F, 4 hours**
e (percent)						
Air	4.2	3.9	3.7	8.9	6.2	7.1
0.5M NaCl	0.4	0.2	0.5	1.1	1.1	1.3

Table 2.3.2.2 Results of stress-corrosion tests of 8090 heavy forgings illustrating the possible beneficial effects of low temperature aging and possible deleterious effects of relatively high silicon (Ref. 4-18, Table 3)

Alloy: 8090					
Form and Processing	**See Table 3.2.1.6**				
Environment	**Alternate Immersion in 3.5 percent NaCl, ASTM G 44**				
Direction	**Short Transverse**				
Condition	**Age 302F, 96 hours**				**Age 374F, 24 hours**
Specimen Type	**Tension**				**C-Ring**
Si Content	**0.08**		**0.11**		**0.08**
Applied Stress (ksi)	10 to 30	35 to 45	10	20 and 25	21 to 31
N/F (t) (a)	10/0	6/2 (4)	2/1 (9)	4/4 (5)	6/6 (13 to 31)

(a) N = no. tested; F = no. failed; (t) = days to failure

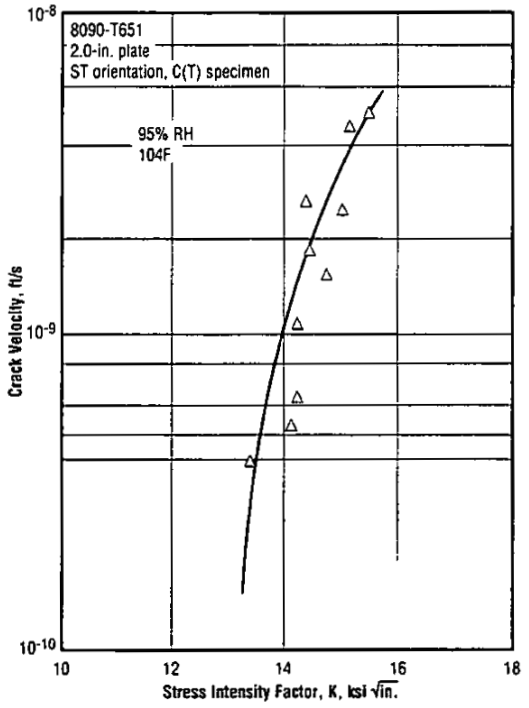


Fig. 2.3.2.3 Stress corrosion crack velocity in humid air for 8090-T651 (Ref. 3-1, Fig. 3)

Table 3.1.1 Commercial specifications for 8090 hand forgings and sheet (Refs. 7, 8)

Alloy: 8090-T8						
Heat Treat	**1013F, WQ (100F max) + CW (a) + 300F, 96 hours**					
Form	**Hand Forgings**			**Sheet**		
Thickness (in.) (b)	**2-3/8-17.499**			**0.040-0.249**	**0.024-0.249**	
Direction	**L**	**T**	**ST**	**T**	**T**	**T**
F_{tu} (ksi)	62	59	59	65	61	65
F_{ty} (ksi)	49	47	44	51	47	53
e (percent) (c)	5	2.5	2.5	4	4	4

(a) CW for forgings = 4 percent plastic compression; CW for sheet = 1.5 percent plastic stretch min
(b) Tensile requirements may be waived for thickness <2-3/8-in. D
(c) In 2 in. or 4D

Table 3.1.2 Commercial specifications for 8090 plate (Ref. 8)

Alloy	8090-T8				8090-T871 (a)	
Heat Treat	**ST 1013F, WQ (100F Max) + Stretch 1.5 percent Plastic Strain Min**				**Aging to be Approved**	
Direction	T	T	T	T	ST	ST
Thickness (in.)	**0.250-1.499**	**1.500-1.999**	**2.000-2.999**	**3.000-6.000**	**1.000-1.999**	**2.000-6.000**
F_{tu} (ksi)	65	65	63	63	61	60
F_{ty} (ksi)	55	53	50	50	49	48
e (percent) (b)	4	4	4	3	1.5	1.5

(a) Damage tolerant temper
(b) For T8 temper in 2 in. or 4D; for T871 temper, total autographic recorded strain

Table 3.1.3 Producer's guaranteed tensile properties and fracture toughness for extrusions (Ref. 1, Table 7)

Alloy: 8090				
Temper	**T8151 (a)**		**T8251**	
Direction	L	T	L	T
F_{tu} (ksi)	62	58	75	65
F_{ty} (ksi)	52	46	67	55
e (percent)	4	4	4	4
K_Q (ksi $\sqrt{in.}$) (b)	33	30	29	18

(a) Damage tolerant temper
(b) Method of measuring K_Q not defined

Table 3.1.4 Producer's guaranteed tensile properties and fracture toughness for plate (Ref. 1, Tables 3 and 4)

Alloy: 8090								
Form	**1.5- to 2.5-inch Plate**							
Temper	**T871**					**T81 (a)**		
Direction	**L**		**T**		**ST**	**L**	**T**	**ST**
Thickness Location (b)	**T/2**	**T/4**	**T/2**	**T/4**	**T/2**	**T/2**	**T/2**	**T/2**
F_{tu} (ksi)	72	64	69	65	62	61	61	54
F_{ty} (ksi)	62	63	60	55	49	51	46	38
e (percent)	4	4	4	4	2	5	5	2.5
K_Q (ksi $\sqrt{in.}$) (c)	27	-	24	24	15	35	30	18

(a) Damage tolerant temper
(b) T/2 = mid thickness; T/4 = quarter thickness
(c) Method of measuring K_Q not defined

Table 3.1.5 Producer's guaranteed tensile properties for sheet in the T6 and T8 tempers (Ref. 1, Table 6)

Alloy: 8090				
Form	Sheet			
Temper	T6		T8	
Direction	L	T	L	T
F_{tu} (ksi)	67	66.7	71	68
F_{ty} (ksi)	52	52	58	52
e (percent)	4	4	4	6

Table 3.1.6 Producer's guaranteed tensile properties and fracture toughness for hand forgings (Ref. 1, Table 8)

Alloy: 8090			
Form (a)	Hand Forgings >4-in. Section ST + Compress + Age		
Temper	T652		
Direction	L	T	ST
F_{tu} (ksi)	62	61	58
F_{ty} (ksi)	51	49	45
e (percent)	4	4	2
K_Q (ksi $\sqrt{in.}$) (b)	26	19	13

(a) No further details given
(b) Method of measuring K_Q not defined

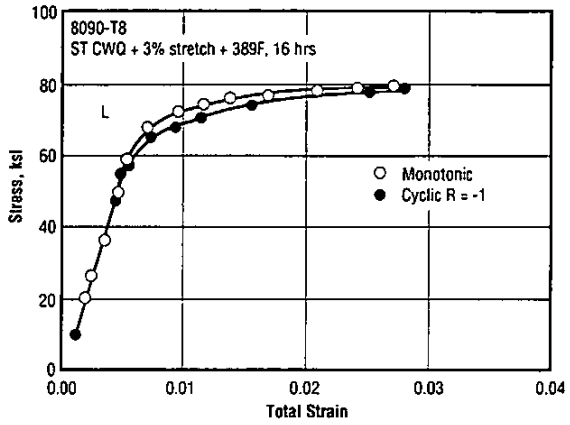


Fig. 3.2.1.1 Monotonic and stabilized cyclic stress-strain curves for 8090-T8 plate (Ref. 18, Fig. 4)

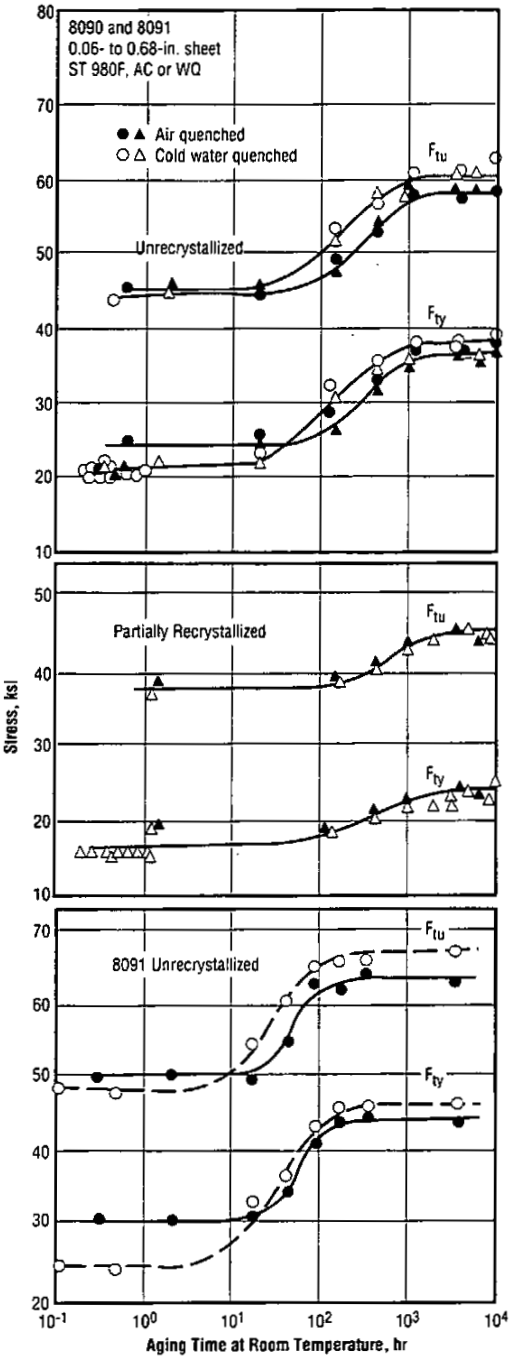


Fig. 3.2.1.2 Effect of natural aging time and quench rate on tensile properties of 8090 and 8091 sheet (Ref. 2, Fig. 1)

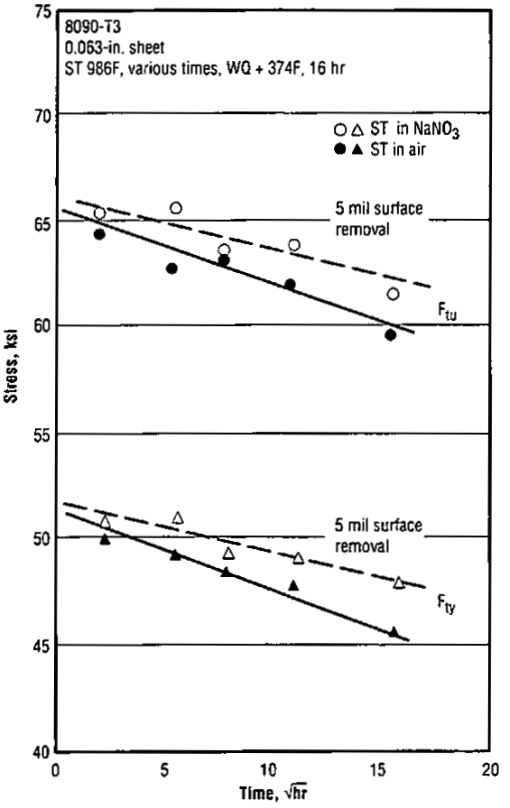


Fig. 3.2.1.3 Effect of solution time on tensile yield and ultimate strength of 8090-T6 solution treated in air or a salt bath and effect of surface removal after solution treatment for 256 hours (Ref. 9, Fig. 1, 3)

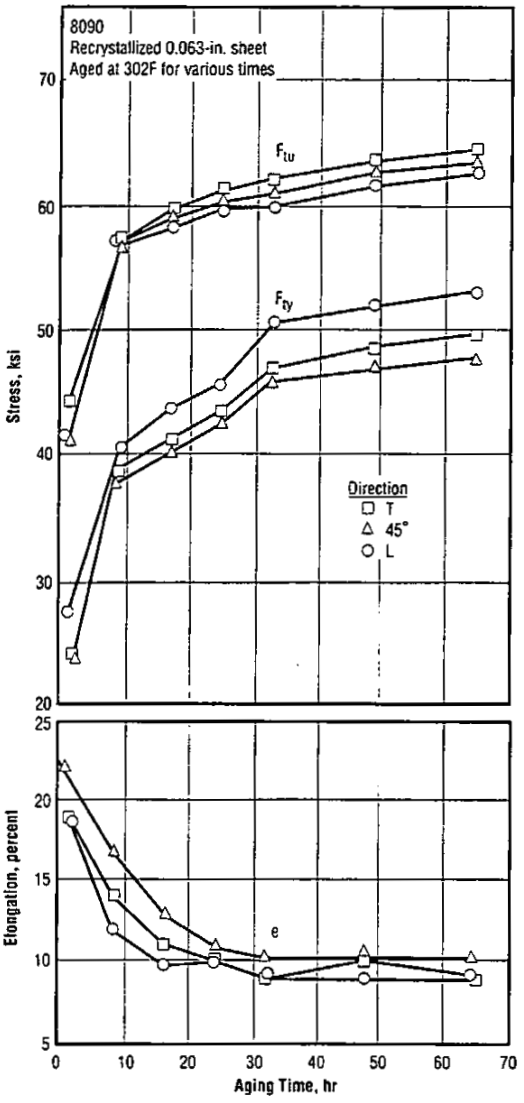


Fig. 3.2.1.4 Effect of aging time at 302F on tensile properties of recrystallized sheet (Ref. 5-2, Fig. 3)

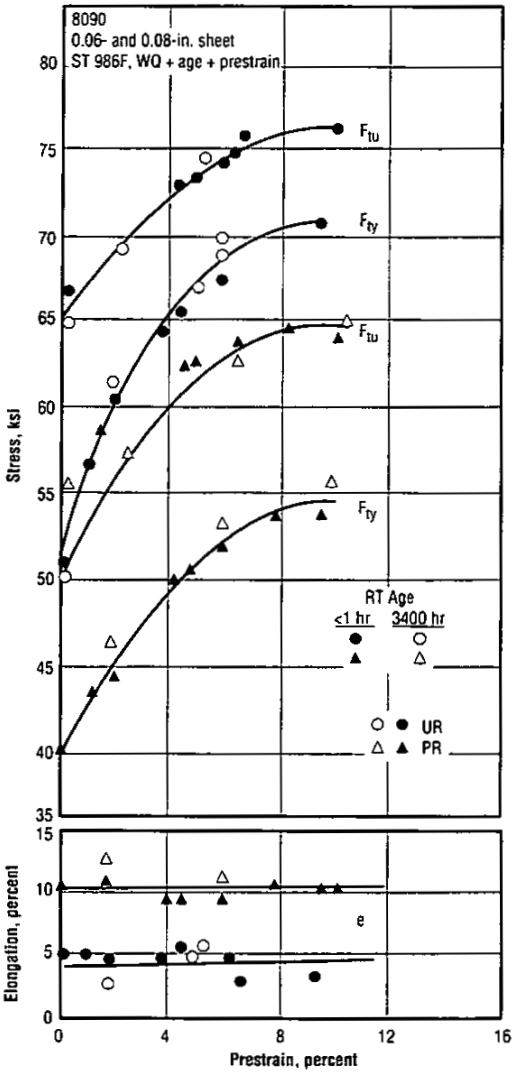


Fig. 3.2.1.5 Effect of prestrain after aging on tensile properties of unrecrystallized (UR) or partially recrystallized (PR) sheet (Ref. 2, Fig. 6)

Table 3.2.1.6 Effect of aging temperature and time on tensile properties and fracture toughness of 8090 forgings (Ref. 4-18, Table 1)

Alloy: 8090					
Form	**5 Forged Blocks Approx. 15.5 to 197 $in.^2$ in Cross Section and 5 to 18 in. in Length**				
Processing	**Direct Chill Cast Ingots, Stress Relieved + 1013F, 24 to 48 hours + Forging + 986F, 6 hours WQ + Compress 3 to 6 percent + Age**				
Direction	**ST Tensiles and ST or SL Fracture Toughness**				
Aging Temperature (F)	**302**			**338**	**374**
Aging Time (hr)	**24**	**48**	**96**	**16**	**16**
F_{tu} (ksi)	61	64	69	-	64
F_{ty} (ksi)	39	42	48	-	51
e (percent)	9	9	5	-	2.5
K_Q (ksi $\sqrt{in.}$)	-	-	21	17	9

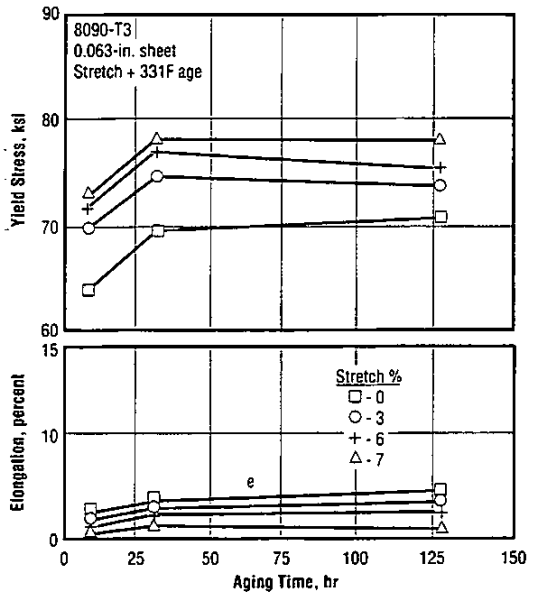


Fig. 3.2.1.7 Effect of amount of stretch and aging time on yield strength and elongation of 8090-T3 sheet (Ref. 4-13, Fig. 3)

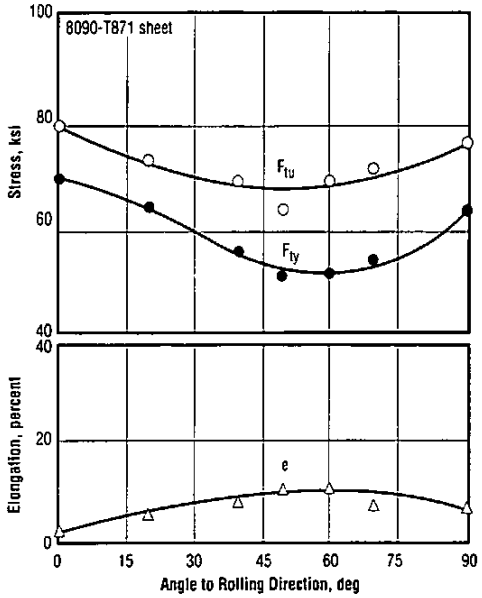


Fig. 3.2.1.8 Tensile properties of unrecrystallized 8090 sheet as a function of angle to the rolling direction (Ref. 1, Fig. 10)

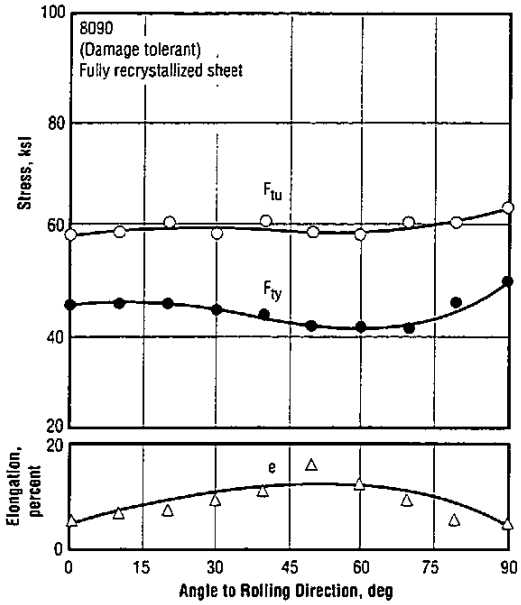


Fig. 3.2.1.9 Tensile properties of damage tolerant 8090 sheet as a function of angle to the rolling direction (Ref. 1, Fig. 8)

Table 3.2.1.10 Comparison of two thermomechanical treatments illustrating the beneficial effects of increased stretching preceding aging coupled with low aging temperature for 8091 0.5-inch plate (Ref. 4-11, Fig. 11)

Alloy: 8091				
Form	**0.5-inch Plate**			
Condition	**ST + 2 percent Stretch + 374F, 16 hours**		**ST + 7 percent Stretch + 338F, 32 hours**	
Direction	**L**	**T**	**L**	**T**
F_{tu} (ksi)	78	60	82	83
F_{ty} (ksi)	73	47	79	83
e (percent)	4	2.5	4	5
K_Q (ksi $\sqrt{in.}$)	-	14 (TL)	-	26 (TL)

Table 3.2.1.11 Comparison of two thermomechanical treatments illustrating the beneficial effects of increased stretching preceding aging coupled with lower aging temperatures for 8090 1-inch plate (Ref. 4-11, Fig. 9)

Alloy: 8090						
Form	**1-inch Plate**					
Condition	**ST + 2 percent Stretch + 374F, 16 hours**			**ST + 6 percent Stretch + 338F, 24 hours**		
Direction	**L**	**T**	**ST**	**L**	**T**	**ST**
F_{tu} (ksi)	73	70	67	79	75	71
F_{ty} (ksi)	63	58	48	70	61	54
e (percent)	5	5	3.2	5.5	7	3
K_Q (ksi $\sqrt{in.}$)	-	19 (TL)	9	-	24 (TL)	15

Table 3.2.1.12 Tensile properties and fracture toughness for naturally aged and artifically aged 8090 and 8091 plate (Ref. 6, Table 4)

Alloy: 8090 and 8091				
Form	**0.63-inch Plate**			
Alloy	**8090-T3**	**8090-T8**	**8091-T3**	**8091-T8**
Heat Treat (a)	**3 percent CW**	**3 percent CW + 374F, 16 hours**	**3 percent CW**	**3 percent CW + 374F, 16 hours**
F_{tu} (ksi)	51	76	60	84
F_{ty} (ksi)	33	70	45	78
e (percent)	17	6	11	6
K_{Ic} (ksi $\sqrt{in.}$)	16 SL	36 LT 13 SL	17 SL	20 LT 9 SL

(a) ST 986F, WQ + CW (stretch) + age

Table 3.2.1.13 Tensile properties of 8090-T6 forgings compared with those of sheet (Ref. 3-4, Table 2)

Alloy: 8090						
Heat Treat	**ST 1022F, 4 hours + 392F, 8 hours**					**See 1.5**
Form	**Bar, 2.5 in. x 1 in.**		**LP Compressor Half Casing**			**T6 Sheet**
Direction	**L**	**T**	**Axial**	**Circum**	**Radial**	**L (a)**
F_{tu} (ksi)	64	57	63	65	55	67
F_{ty} (ksi)	52	44	47	48	43	52
e (percent)	8	4	7	7	3	4
Fracture Mode (b)	IG + TG	IG + TG	TG	TG	IG	-

(a) Minimum guaranteed; see Table 3.1.5
(b) IG = intergranular; TG = transgranular shear

Table 3.2.1.14 Tensile properties of 8090-T8 heavy plate at different thickness positions (Ref. 5-3)

Alloy: 8090-T8										
Form	**Plate**									
Treatment	**1.2 and 2.4-in. Plates: ST 968F, WQ + 2.5 percent Stretch + 374F, 16 hours 4-in. Plate: ST 968F, WQ + 374F, 16 hours**									
Position	**Surface**			**Quarter**			**Center**			
Direction	**L**	**T**	**45**	**L**	**T**	**45**	**L**	**T**	**45**	**ST**
Thickness (in.)	**1.4**									
F_{tu} (ksi)	77	78	71	-	-	-	77	78	71	-
F_{ty} (ksi)	70	69	59	-	-	-	71	69	59	-
e (percent)	7	7	11	-	-	-	7	7	10	-
Thickness (in.)	**2.4**									
F_{tu} (ksi)	71	72	71	73	70	69	76	76	69	67
F_{ty} (ksi)	62	59	57	65	57	54	68	63	56	53
e (percent)	9	7	9	7	6	8	6	6	9	3
Thickness (in.)	**4**									
F_{tu} (ksi)	70	69		68	68		70	68	62	
F_{ty} (ksi)	59	55		58	52		60	55	48	
e (percent)	7	9		7	8		6	6	3	

Table 3.2.1.15 Comparison of tension and compression yield strengths for 8090 and 8091 in the T651 temper (Ref. 4-8, Fig. 13)

Alloy: 8090 and 8091				
Form	**1-inch Plate**			
Temper	**T651**		**T651**	
Alloy	**8090**		**8091**	
Direction	**L**	**T**	**L**	**T**
F_{tu} (ksi)	68	60	75	70
F_{cy} (ksi)	59	65	71	76

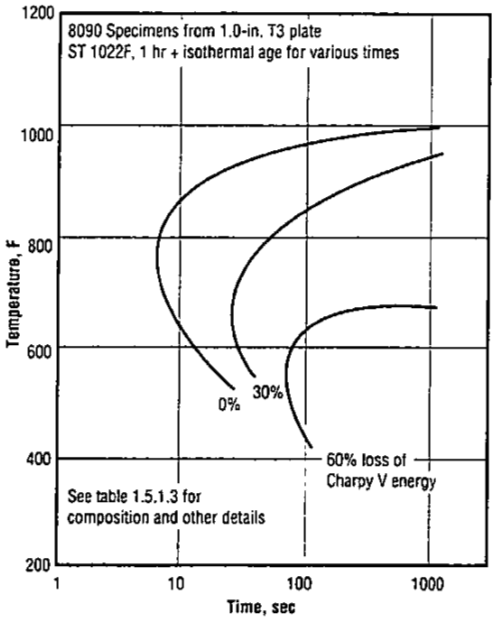


Fig. 3.2.3.1 Loss in Charpy V energy relative to as-quenched condition for isothermal aging of 8090 lean-alloy (Ref. 16, Fig. 9)

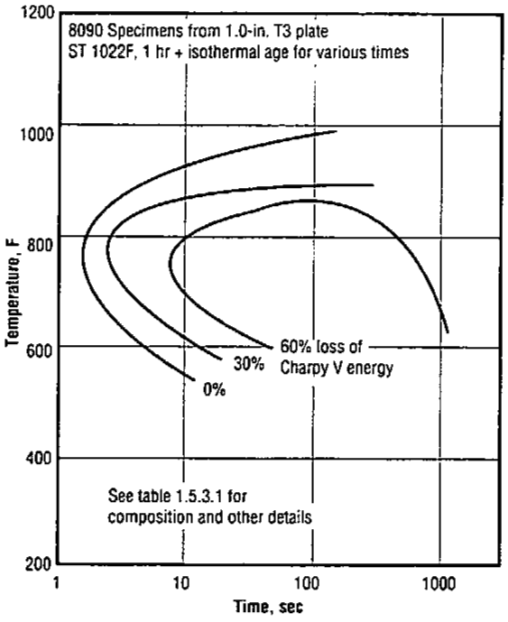


Fig. 3.2.3.2 Loss in Charpy V energy relative to as-quenched condition for isothermal aging of 8090 rich alloy (Ref. 16, Fig. 9)

Table 3.2.6.1 Bearing and shear strengths of 8091-T8 and 8091-T877 plate (Ref. 1, Tables 6 and 7)

Alloy: 8090 and 8091		
Alloy	**8090**	**8091**
Form	**Plate**	
Temper	**T877 (a)**	**T8**
	Shear	
F_{su} (ksi)	39	64
	Bearing	
F_{bu} (ksi)		
e/D = 1.5	102	-
e/D = 2	128	-
F_{by} (ksi)		
e/D = 1.5	86	-
e/D = 2	96	123

(a) Stretch 7 percent before aging

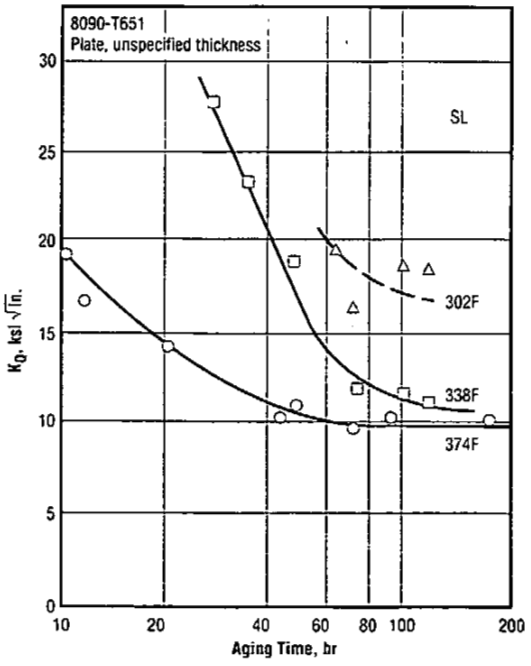


Fig. 3.2.7.2.2 The effect of aging temperature and time on the short transverse (SL) toughness of 8090-T651 plate (Ref. 13, Fig. 14)

Table 3.2.7.2.3 Effect of panel width on the K_c values obtained for 8090-T81 sheet (Ref. 5-5, Table 2 and Ref. 4-11, Fig. 4)

Alloy: 8090									
Form	0.06-inch Sheet								
Temper	T81 (Damage Tolerant)								
Reference	5-5						4-11		
Age	302F, 24 hours						302F, 12 hours		
Direction	L			T			T		
Panel Width (in.)	10	20	30	10	20	30	16	20	30
F_{ty} (ksi)	49	49	49	46	46	49	50	50	50
K_c (ksi $\sqrt{in.}$) (a)	104	127	149	86	101	-	137	145	159

(a) From R curves prepared according to E 561

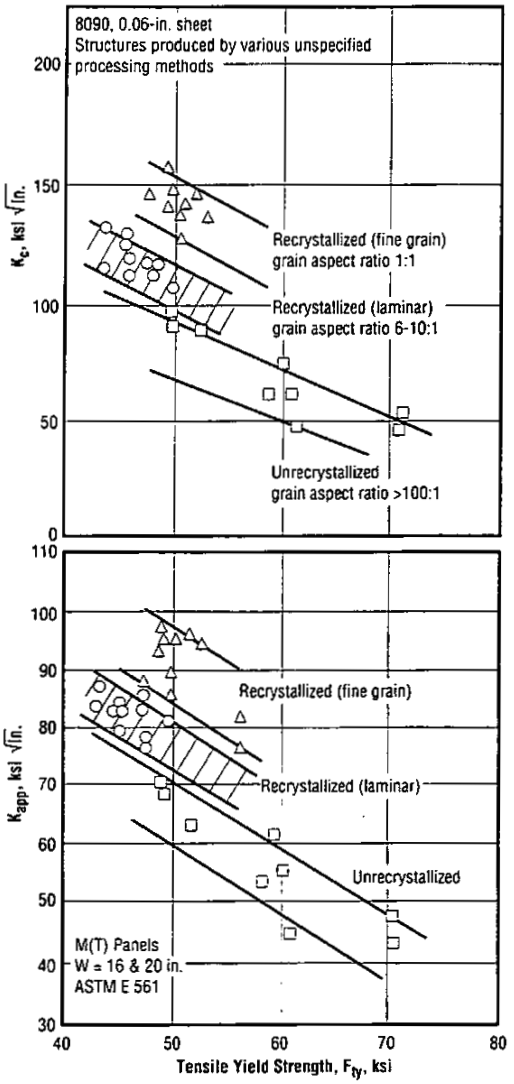


Fig. 3.2.7.2.4 Effect of grain structure on fracture toughness (K_c and K_{app}) of 8090 sheet (Ref. 4-11, Fig. 5)

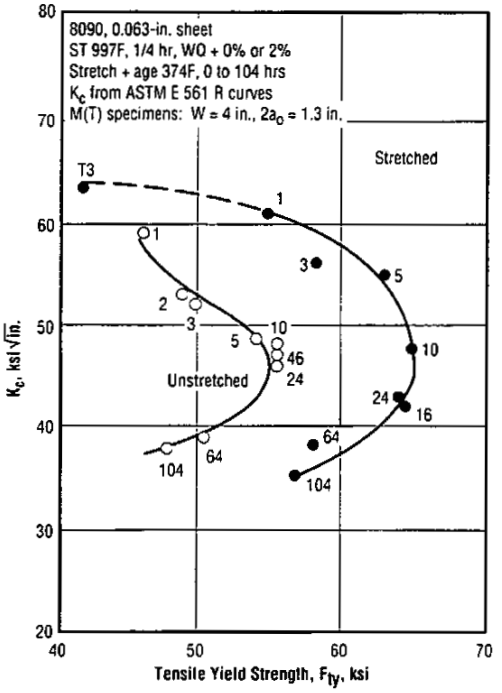


Fig. 3.2.7.2.5 Fracture toughness (K_c) as a function of aging time for stretched and unstretched 8090 sheet (Ref. 3-3, Fig. 8)

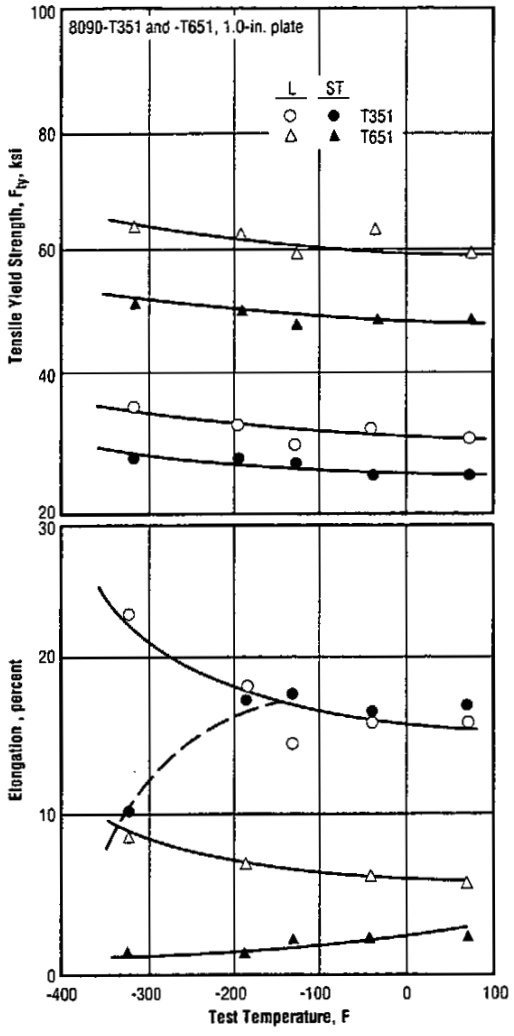


Fig. 3.3.1.1 Effect of temperature on the tensile yield strength and elongation of 8090 plate (Ref. 4-10, Table 1)

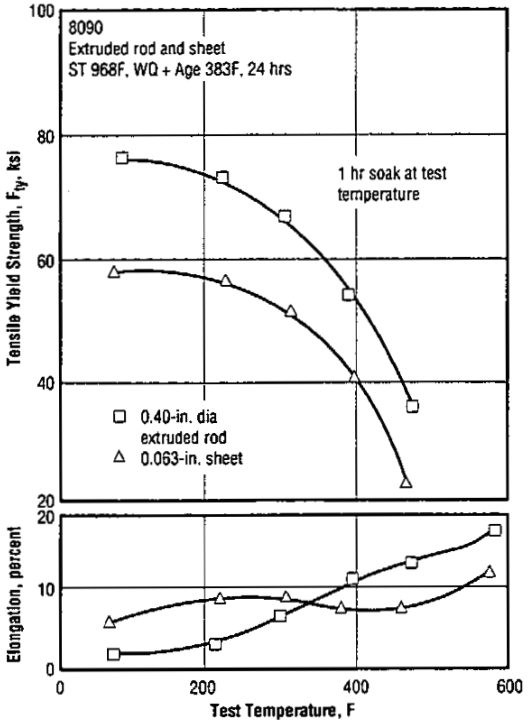


Fig. 3.3.1.2 Effect of test temperature on tensile yield strength of extruded rod and sheet in the T6 condition (Ref. 3-2, Fig. 4)

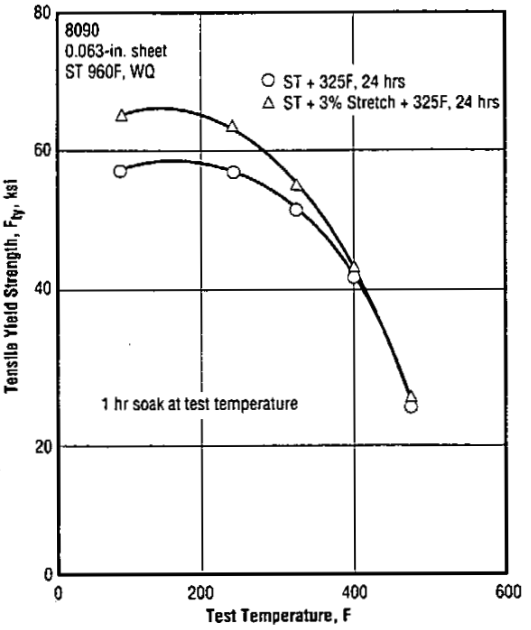


Fig. 3.3.1.3 Effect of test temperature on tensile yield strength of 8090 sheet in the T6 and T8 conditions (Ref. 3-2, Fig. 1)

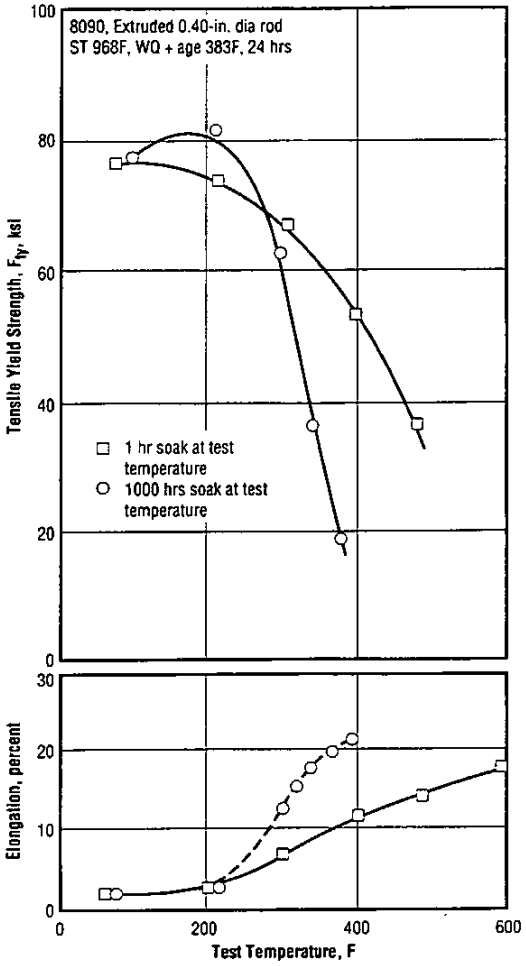


Fig. 3.3.1.4 Effect of test temperature on the tensile yield strength of 8090-T6 extrusions subjected to short and long time exposures at test temperature (Ref. 3-2, Fig. 5)

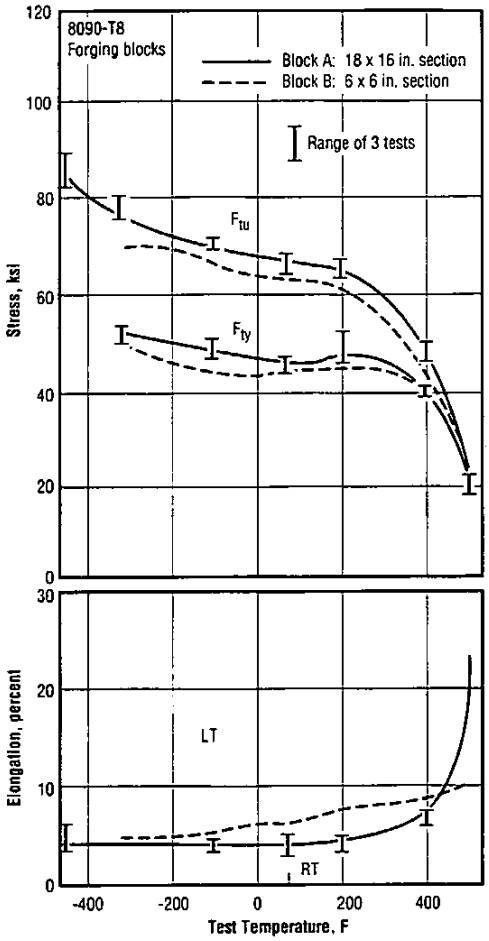


Fig. 3.3.1.5. Effect of low test temperatures on two 8090-T852 forging blocks of different size (Ref. 5-10, Fig. 2)

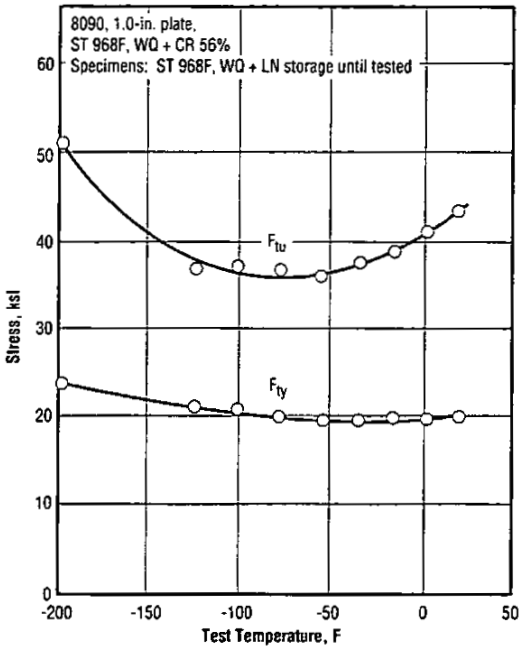


Fig. 3.3.1.6 Effect of low test temperatures on tensile strength of 8090 as-quenched plate (Ref. 5-9, Fig. 1)

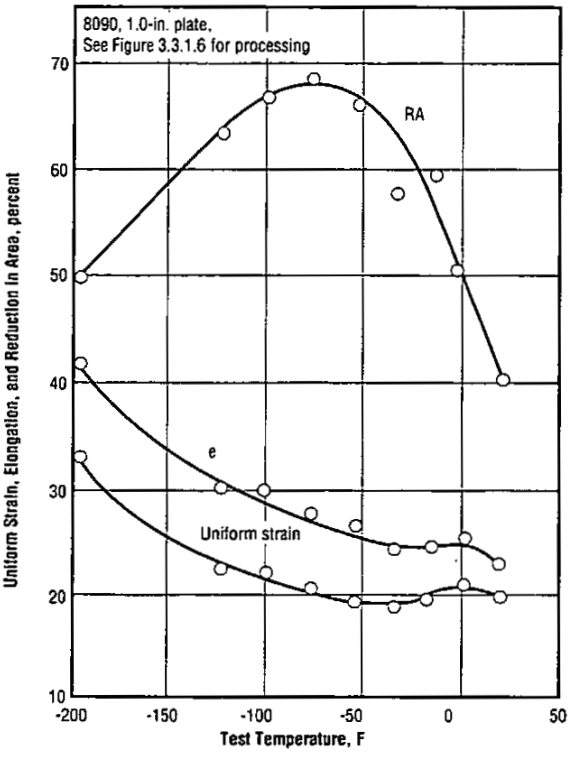


Fig. 3.3.1.7 Effect of low test temperatures on tensile strain properties of as-quenched 8090 plate (Ref. 5-9, Fig. 2)

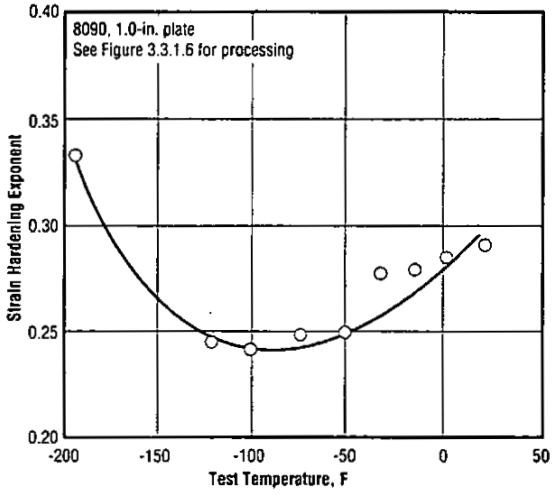


Fig. 3.3.1.8 Effect of low test temperatures on the strain hardening exponent of as-quenched 8090 plate (Ref. 5-9, Fig. 3)

Table 3.3.1.9 Tensile properties and fracture toughness of 8090 plate at room temperature and -320F for two conditions of heat treatment (Ref. 19, Table 2)

Alloy: 8090								
Form	**0.4- to 0.63-inch Plate**							
Heat Treatment	**ST + 3 percent Stretch + Natural Age**				**ST + 3 percent Stretch + 374F, 16 hours**			
Orientation	**LT**	**SL**	**LT**	**SL**	**LT**	**SL**	**LT**	**SL**
Test Temperature (F)	**RT**	**RT**	**-320**	**-320**	**RT**	**RT**	**-320**	**-320**
F_{tu} (ksi)	51		71		78		93	
F_{ty} (ksi)	32		37		70		75	
e (percent)	17		24		6		8	
K_{Ic} (ksi $\sqrt{in.}$)	24 (a)	15	18	15	33	12	35	11

(a) Invalid by ASTM E 399

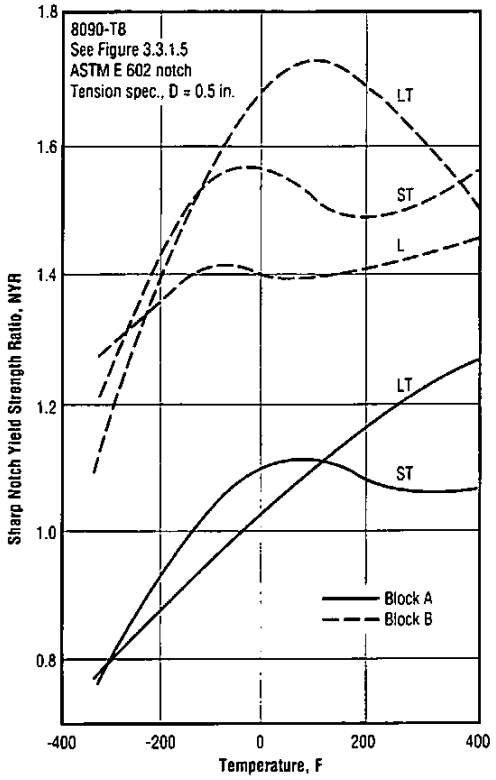


Fig. 3.3.7.1.1 Effect of test temperature on sharp-notch strength ratio of two 8090-T852 forging blocks, the larger (Block A) of which exhibited grain boundary embrittlement due to the T_2 phase (Ref. 5-10, Fig. 4)

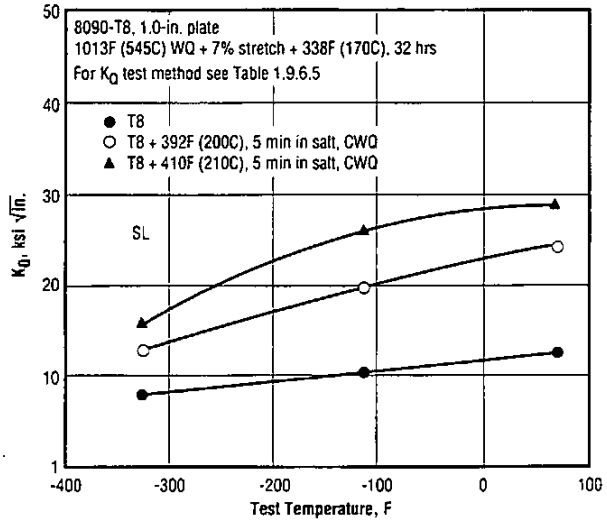


Fig. 3.3.7.2.1 Effect of low test temperatures on SL fracture toughness of single- and double-aged plate (Ref. 21 , Fig. 3)

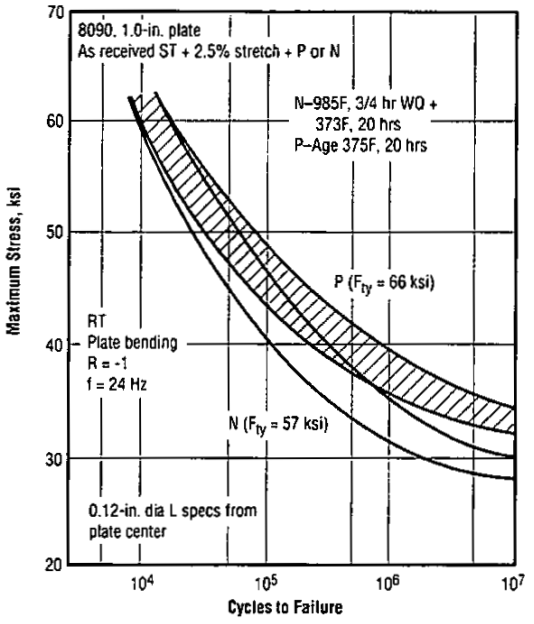


Fig. 3.5.1.1 S-N scatter bands for 8090 at two yield strength levels (Ref. 4-4, Fig. 3)

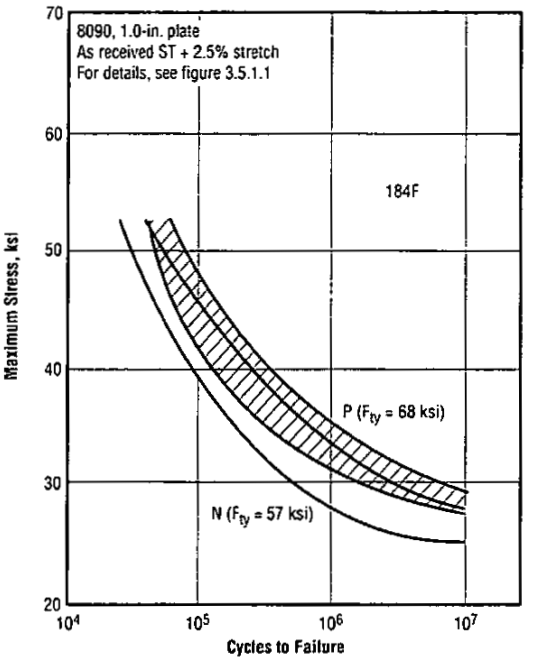


Fig. 3.5.1.2 S-N scatter bands for two yield strength levels of 8090 tested at 184F (Ref. 4-4, Fig. 3)

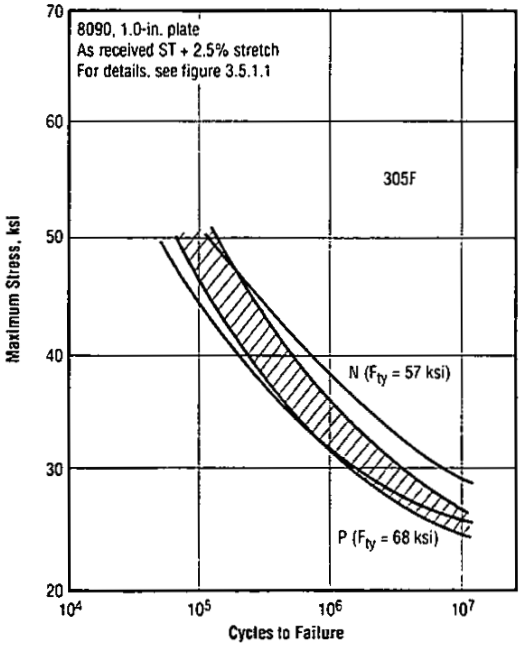


Fig. 3.5.1.3 S-N scatter bands for two yield strength levels of 8090 tested at 305F (Ref. 4-4, Fig. 3)

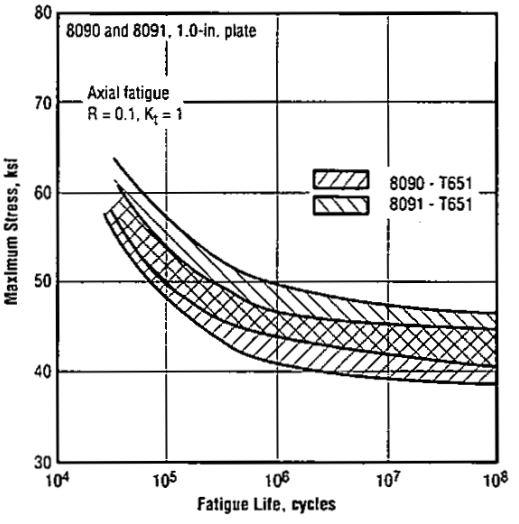


Fig. 3.5.1.4 S-N scatter bands for axial-load fatigue of smooth specimens of 8090 and 8091 plate (Ref. 13)

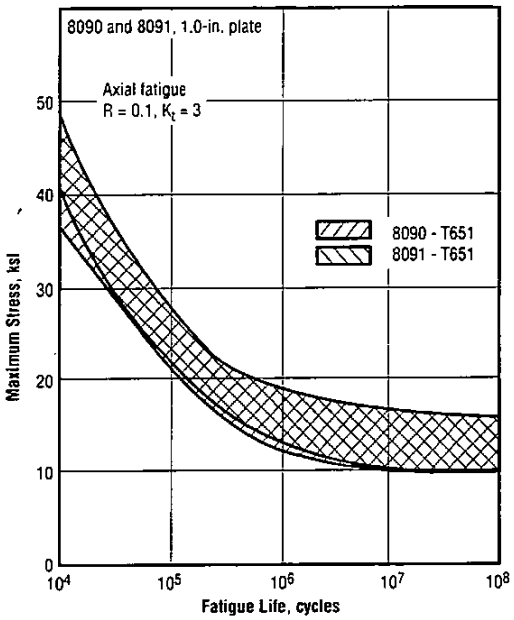


Fig. 3.5.1.5 S-N scatter bands for axial-load fatigue of notch specimens of 8090 and 8091 plate (Ref. 13)

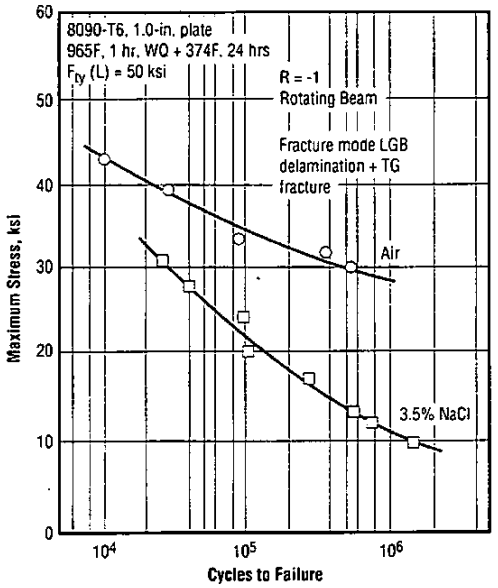


Fig. 3.5.1.6 S-N curves for 8090-T6 plate tested in air or in 3.5% NaCl (Ref. 4-7)

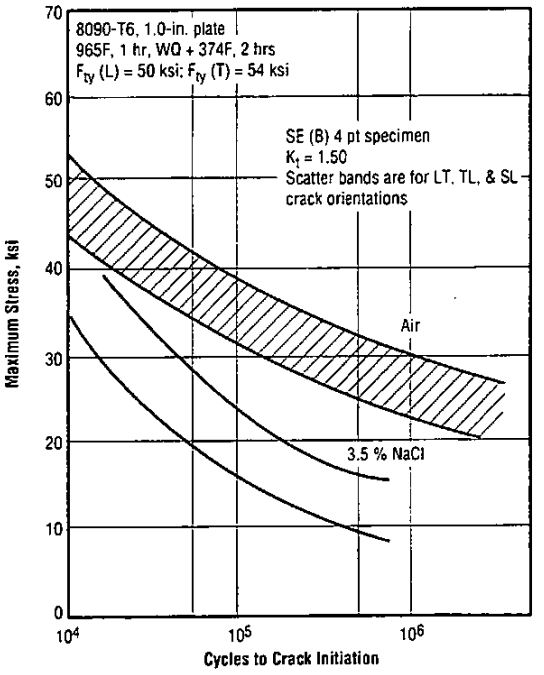


Fig. 3.5.1.7 Fatigue crack initiation curves for 8090-T6 plate in air or 3.5% NaCl (Ref. 4-7, Fig. 3)

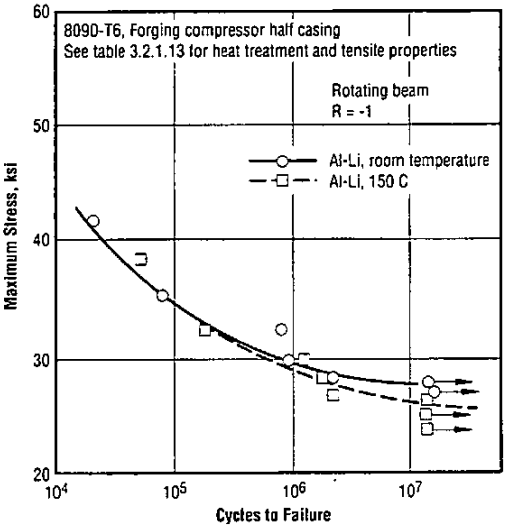


Fig. 3.5.1.8 S-N curves for an 8090-T6 forged compressor casing at RT and at 302F (Ref. 3-4, Fig. 11)

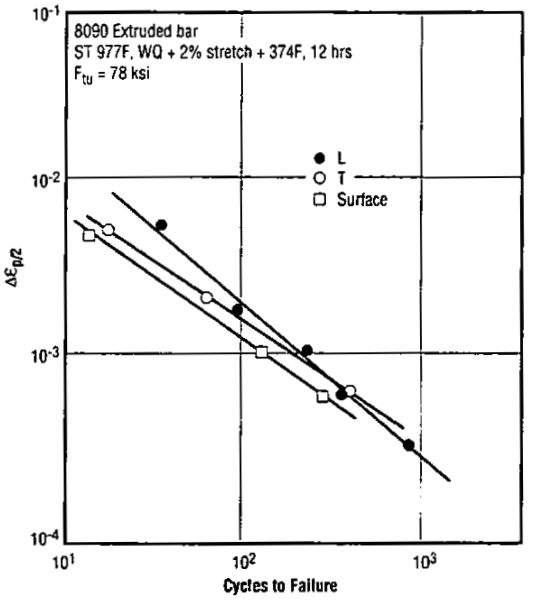


Fig. 3.5.1.9 Low-cycle fatigue behavior for extruded bar (Ref. 3, Fig. 4)

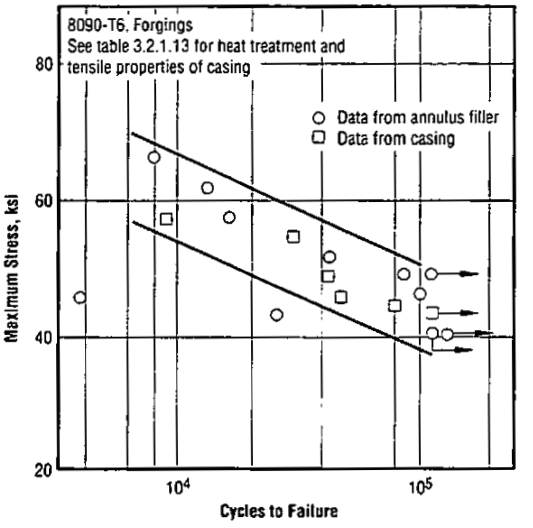


Fig. 3.5.1.10 Low-cycle fatigue strength for two 8090-T6 forgings (Ref. 3-4, Fig. 12)

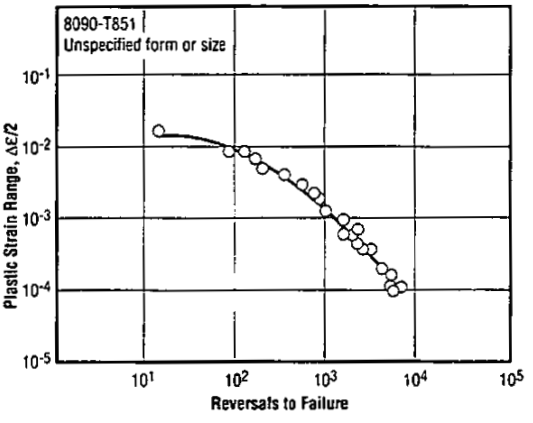


Fig. 3.5.1.11 Low-cycle fatigue curve for 8090-T851 (Ref. 18, Fig. 6)

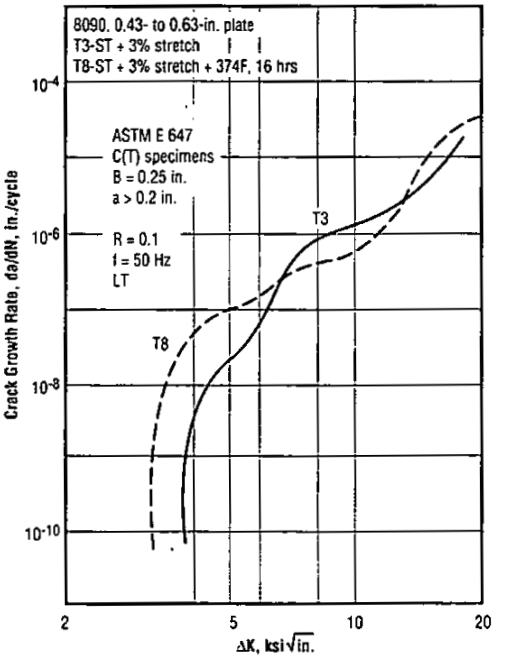


Fig. 3.5.2.1 Fatigue crack propagation rates for 8090-T3 and 8090-T8 plate (Ref. 10, Fig. 2a)

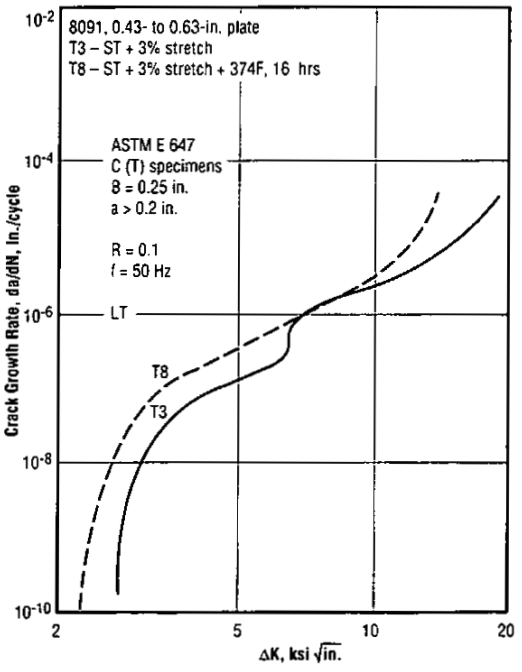


Fig. 3.5.2.2 Fatigue crack propagation rates for 8091-T3 and 8091-T3 plate (Ref. 10, Fig. 2b)

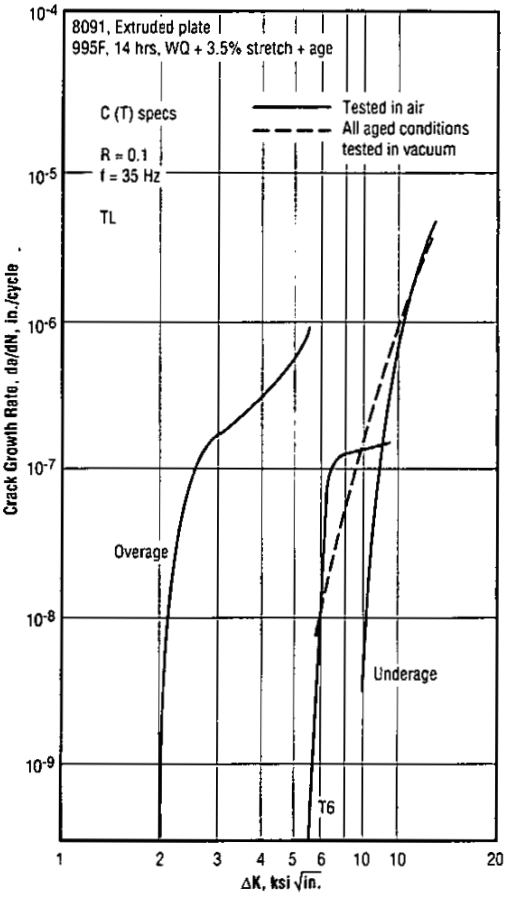


Fig. 3.5.2.3 Fatigue crack propagation rates for three aged conditions of 8090 extrusions tested in air or in vacuum (Ref. 4-5, Fig. 7)

Table 3.5.2.4 Heat treatments used in producing the test material representing the fatigue crack propagation rates illustrated in Figures 3.5.2.5 and 3.5.2.6 (Ref. 5-6, Tables 2 and 3)

Alloy: 8090 and 8091						
Form	**1.77-inch Plate**					
Treatment	**ST 1012F, WQ + 6 percent Stretch + 338F, 32 hours**		**Re ST, WQ + 338F, 100 hours**		**Re ST, WQ + RT, 24 hours + 338F, 48 hours**	
Designation	**(S)**		**(US)**		**(DA)**	
Alloy	**8090**	**8091**	**8090**	**8091**	**8090**	**8091**
F_{ty} (ksi)	69	67	59	59	52	59
Hardness (VHN)	159	164	149	159	149	158

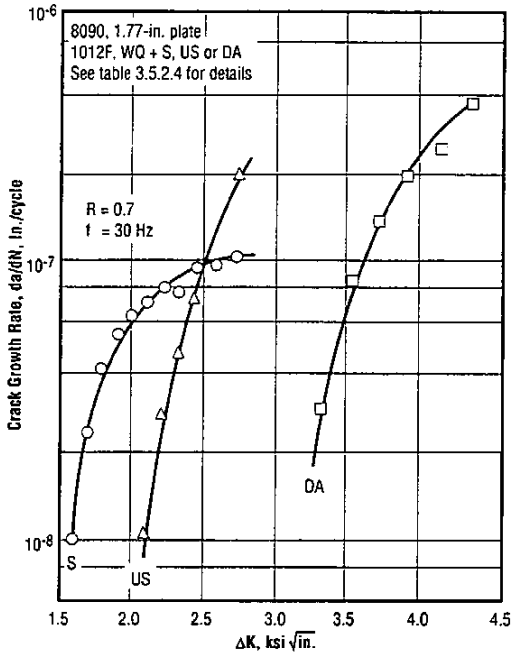


Fig. 3.5.2.5 Fatigue crack propagation rates for 8090 plate given several treatments (Ref. 5-6, Fig. 5)

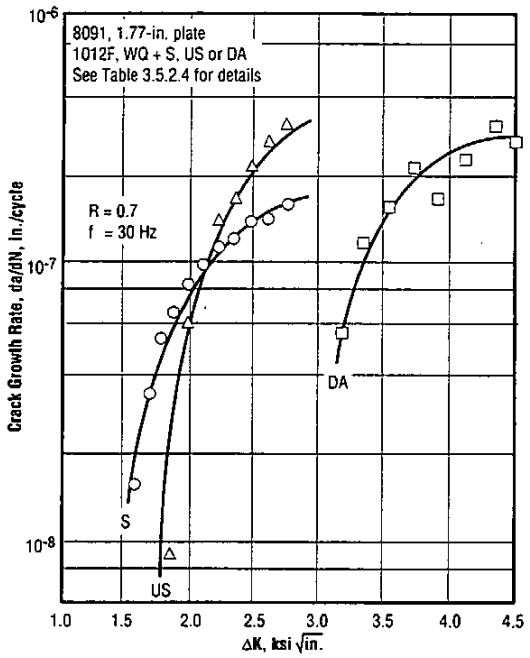


Fig. 3.5.2.6 Fatigue crack propagation rates for 8091 plate given several treatments (Ref. 5-6, Fig. 5)

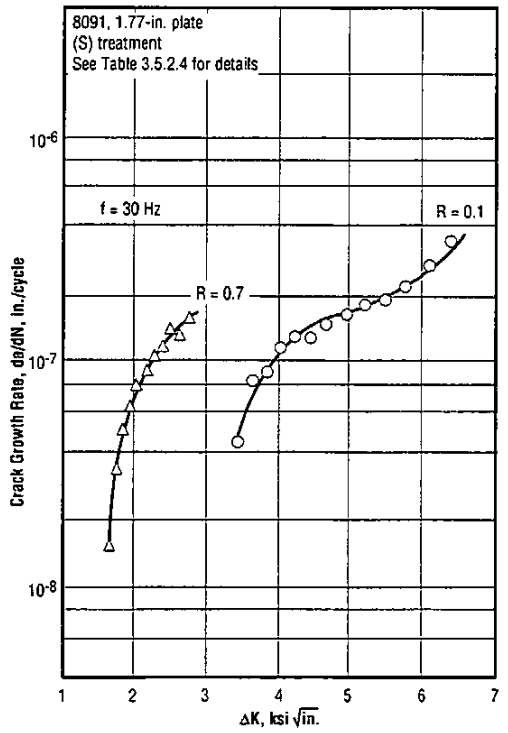


Fig. 3.5.2.7 Fatigue crack propagation rates at R = 0.1 and 0.7 for 8091 plate (Ref. 5-6, Fig. 5)

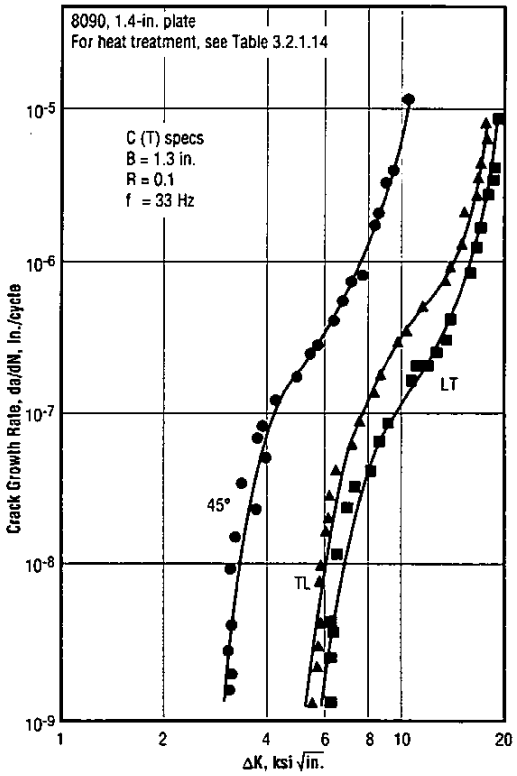


Fig. 3.5.2.8 Fatigue crack propagation rates for 8090 1.4-in. plate for several crack orientations at the plate center (Ref. 5-3, Fig. 6)

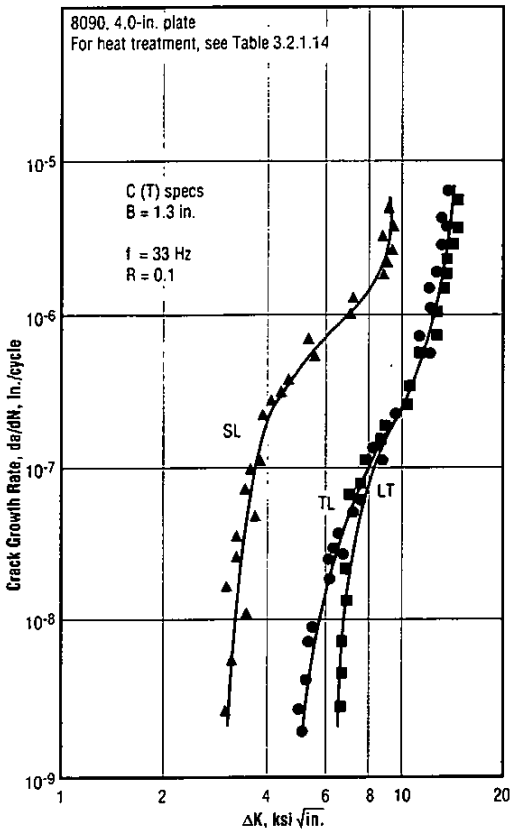


Fig. 3.5.2.9 Fatigue crack propagation rates for 8090 4-in. plate for several crack orientations at the plate center (Ref. 5-3, Fig. 8)

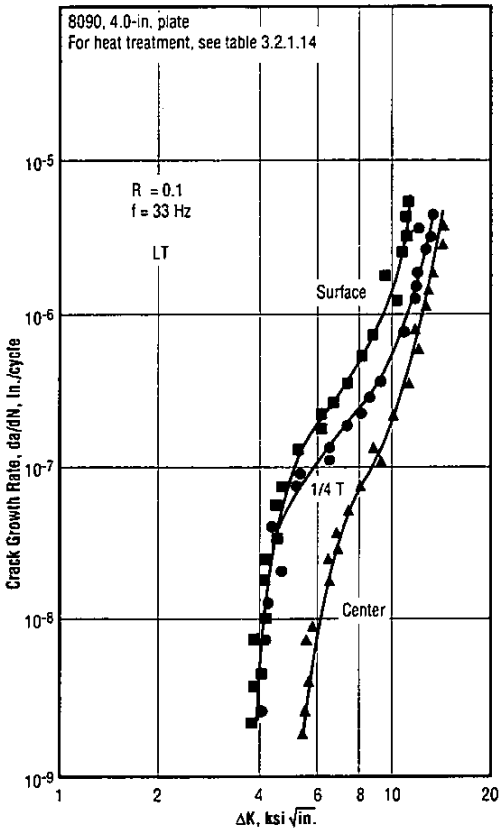


Fig. 3.5.2.10 Fatigue crack propagation rates for 8090 4-in. plate at various thickness positions for TL crack orientation (Ref. 5-3, Fig. 7)

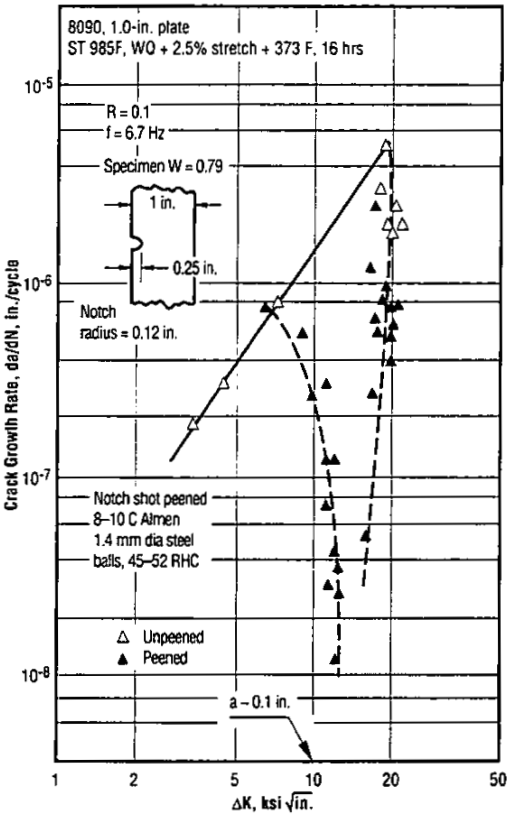


Fig. 3.5.2.11 Effect of shot peening on crack growth rate of a notched 8090 plate (Ref. 22, Fig. 5)

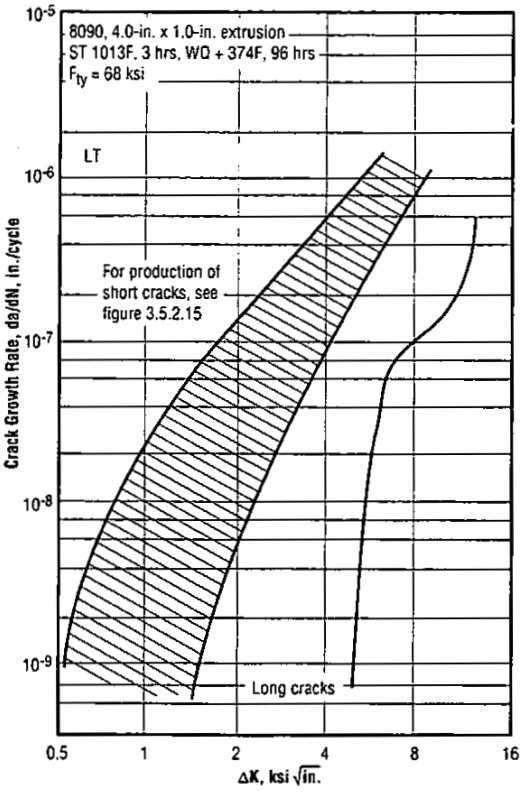


Fig. 3.5.2.12 Fatigue crack propagation rates for short and long cracks in overaged 8090 extrusions (Ref. 5-8, Fig. 2c)

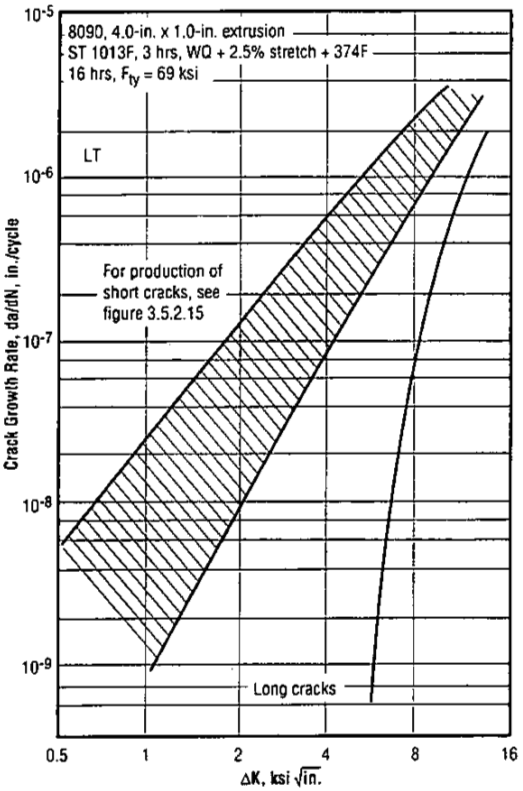


Fig. 3.5.2.13 Fatigue crack propagation rates for short and long cracks in peak-aged (T8) 8090 extrusions (Ref. 5-8, Fig. 2b)

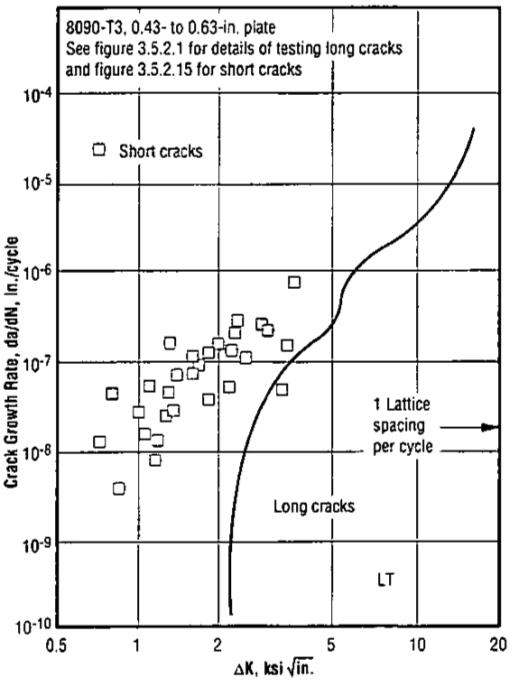


Fig. 3.5.2.14 Fatigue crack propagation rates for long and short cracks in 8090-T3 plate (Ref. 10, Fig. 5)

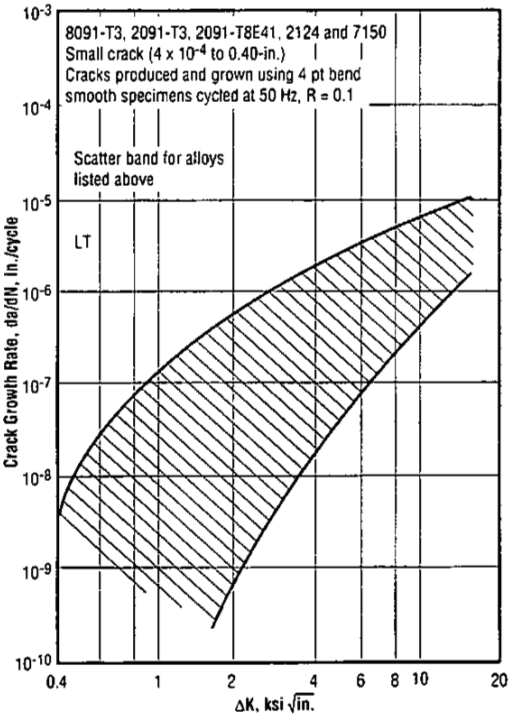


Fig. 3.5.2.15 Scatter band for fatigue crack propagation rates of short cracks for several aluminum alloys (Ref. 10, Fig. 7)

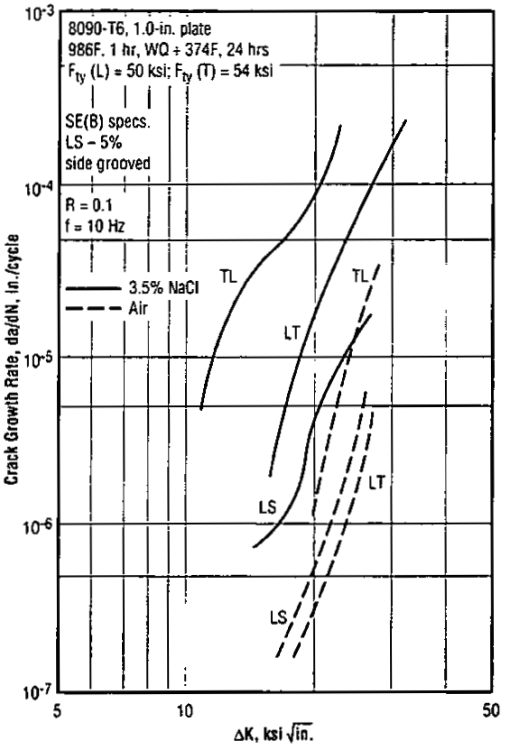


Fig. 3.5.2.16 Fatigue crack propagation rates in air and in 3.5% NaCl for 8090-T6 plate tested in different crack orientations (Ref. 4-7, Fig. 4)

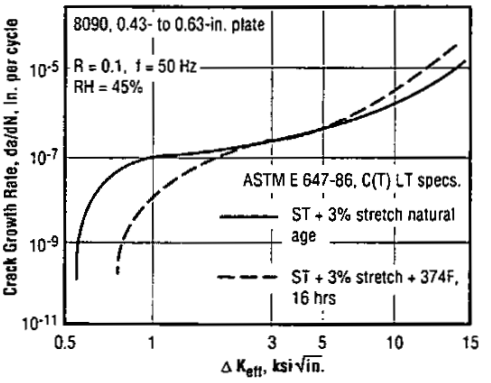


Fig. 3.5.2.17 Fatigue crack growth rates for 8090-T351 and -T8 plate. Data corrected for closure (Ref. 10, Fig. 9)

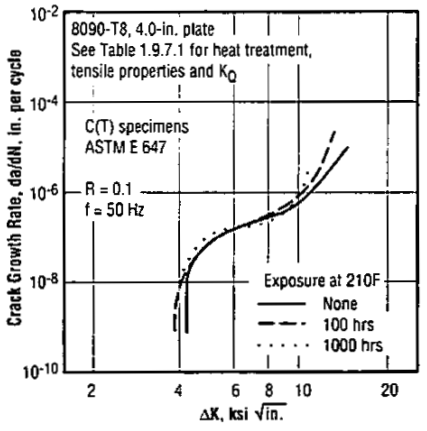


Fig. 3.5.2.18 Effect of exposure at 210F on fatigue crack growth rate of 8090-T8 plate (Ref. 20, Fig. 4)

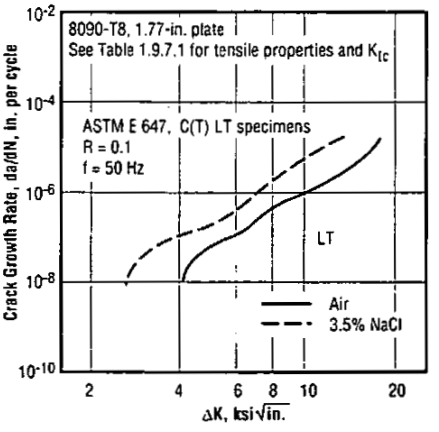


Fig. 3.5.2.19 Fatigue crack growth rates for 8090-T8 plate in air and in 3.5% NaCl solution (Ref. 18, Fig. 34)

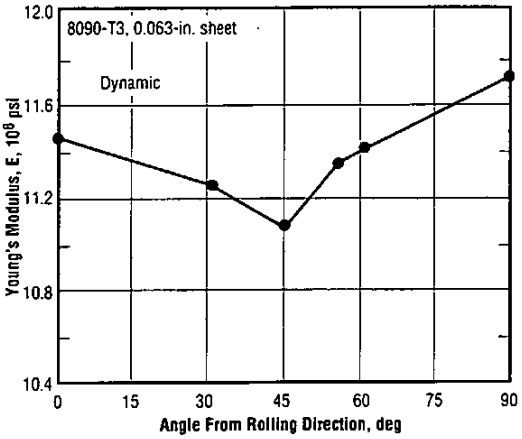


Fig. 3.6.2.1 Young's modulus as a function of angle from rolling direction for 8090-T3 sheet (Ref. 5-4, Fig. 2)

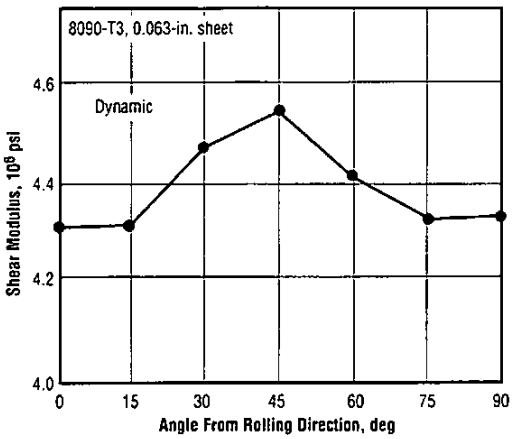


Fig. 3.6.3.1 Shear modulus as a function of angle from rolling direction for 8090-T3 sheet (Ref. 5-4, Fig. 3)

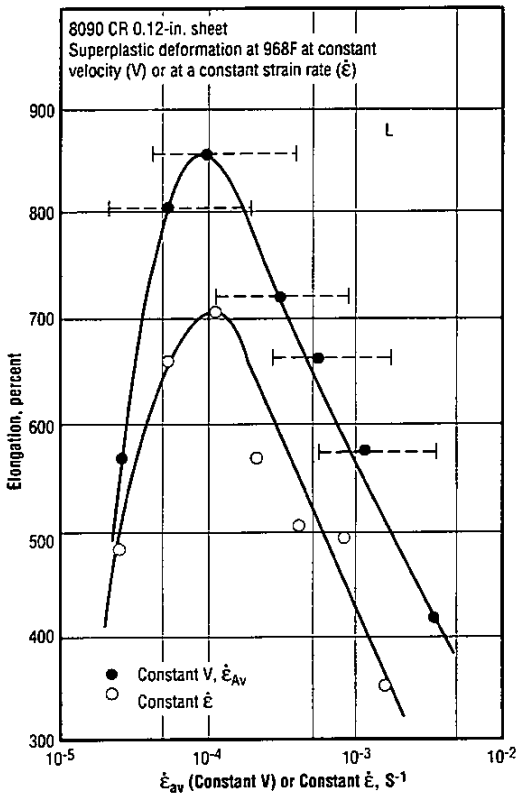


Fig. 4.1.1.1 Elongation as a function of strain rate for 8090 deformed at constant velocity or at constant strain rate (Ref. 4-15, Fig. 1)

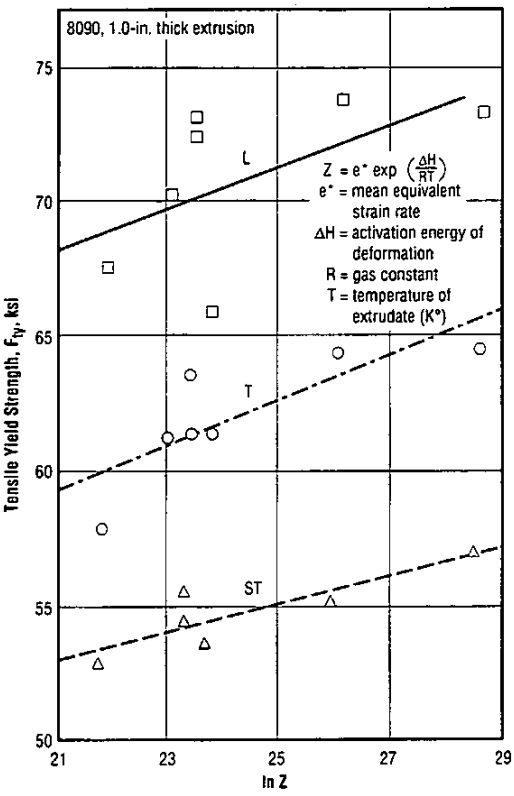


Fig. 4.1.3.1 Influence of extrusion conditions on back-end tensile yield strength of 4 x 1-in. flat bar (Ref. 4-19, Fig. 1)

Table 4.3.1.2 Tensile properties of as-GTA-welded and post-heat-treated sheet specimens (Ref. 4-2, Tables 3 and 4)

Alloy: 8090							
Form	**0.20-inch Sheet**						
Preweld Treatment	**986F, 12 hours + 374F, 16 hours (T6 Temper): F_{tu} = 73 ksi, F_{ty} = 63 ksi, e = 6 percent**						
Welding Conditions	**TIG Welds - 110 amps AC at 15 V Speed 0.04 to 0.16-inch/second Welds Transverse to Rolling Directions; Specimens Normal to Welds**						
Postweld Treatment	**None**					**374F, 16 hours**	
Filler	**Al**	**Al-5Si**	**Al-5Mg**	**Al-5Mg+(Zr)**	**8090**	**Al-5Mg**	**8090**
F_{tu} (ksi)	24	30	33	47	45	44	53
F_{ty} (ksi)	20	24	26	27	41	36	46
e (percent)	5	5	4	4	2	4	4
Fracture Path	TG (a)	Si (b)	TG	TG	IG	IG	IG

(a) TG = transgranular; IG = intergranular
(b) Si plates

References

1. LITAL Aluminum Lithium Alloys Update, Alcan Aerospace, Beachwood, OH (1988).
2. McDarmaid, D. S., "Effect of Natural Aging on the Tensile Properties of the Al-Li Alloy 8090, 8091, and 2091," *Materials Science and Engineering*, p. 193 (May 1988).
3. Khireddine, D.; Rahouadj, R.; and Clavel, M., *Acta Met.*, Vol. 37, No. 1, p. 191 (1989).
4. Mutoh, Y.; Fair, G. H.; Nobel, B.; and Waterhouse, R. B., "The Effect of Residual Stresses Induced by Shot-Peening on Fatigue Crack Propagation in Two High Strength Aluminum Alloys," *Fatigue and Fracture of Engineering Materials and Structures*, Vol. 10, No. 4, p. 261 (1987).
5. Lumsden, J. B., and Allen, A. T., "The Stress Corrosion Cracking Behavior of the Al-Li Alloy 8090," *Corrosion Science*, Vol. 44, No. 8, p. 527 (August 1988).
6. Venkateswara Rao, K. T., and Ritchie, R. O., "Mechanical Properties of Al-Li Alloys, Part 1 Fracture Toughness and Microstructure," *Materials Science and Technology*, Vol. 5, p. 882 (September 1989).
7. Material Specification for Aluminum-Lithium Alloy 8090, Hand Forgings, Lockheed Missiles and Space Co. (March 1990).
8. Material Specification for Aluminum-Lithium Alloy 8090, Sheet and Plate, ibid (January 1989).
9. Papazian, J. M.; Bott, G. C.; and Shaw, P., "Effects of Lithium Loss on Strength and Formability of Aluminum-Lithium Alloys 8090 and 8091," *Materials Science and Engineering*, p. 219 (October 1987).
10. Venkateswara Rao, K. T., and Ritchie, R. O., "Mechanical Properties of Al-Li Alloys, Part 2 Fatigue Crack Propagation," *Materials Science and Technology*, Vol. 5, p. 896 (September 1989).
11. Venkateswara Rao, K. T.; Yu, W.; and Ritchie, R. O., "Mechanisms of Fatigue Crack Propagation in Commercial Aluminum-Lithium Alloys," *Proceedings of the 1987 Aluminum-Lithium Symposium*, Los Angeles, CA, eds. Ramesh J. Kar, Suphal P. Agrawal, and William E. Quist, ASM International, OH, p. 173 (March 1987).
12. Grimes, R.; Miller, W. S.; and Reynolds, M. A., "The Status of Alcan's Aluminum-Lithium Programme," ibid, p. 41.
13. Peel, C. J.; McDarmaid, D. S.; and Evans, B., "Considerations of Critical Factors for the Design of Aerospace Structures Using Current and Future Aluminum-Lithium Alloys," ibid, p. 315.
14. Bretz, P. E., and Gilliland, R. G., "The Intensive Development Program That Produced Aluminum-Lithium Alloy," *Light Metal Age*, Vol. 45, p. 5 (April 1987).
15. Personal communication from P. O. Wakling, Alcan Inc., to W. F. Brown, Jr.
16. Colvin, G. N., and Starke, E. A., Jr., "Quench Sensitivity of the Al-Li-Cu-Mg Alloy 8090," *SAMPE Quarterly*, Vol. 19 (Reprint) (July 1988).
17. "The Safety, Health, and Recycling Aspects of Aluminum-Lithium Alloys (T4)," The Aluminum Association, Washington, DC.
18. Venkateswara Rao, K. T., and Ritchie, R. O., "Fatigue of Aluminum Lithium Alloys," *International Materials Reviews*, in press (1992).
19. Venkateswara Rao, K. T., and Ritchie, R. O., "Mechanisms Influencing the Cryogenic Fracture Toughness Behavior of Aluminum-Lithium Alloys," *Act. Metall. Mater.*, Vol. 38, No. 11, p. 2309.
20. McNulty, J. C., "The Effect of Prolonged Thermal Exposure on the Fatigue and Fracture Behavior of Aluminum-Lithium Alloys," Dept. of Materials Science and Engineering, University of California, Berkeley, CA.
21. Lynch, S. P., "Fracture of 8090 Aluminum-Lithium Plate I. Short Transverse Fracture Toughness," Aeronautical Research Laboratory, Defense Science and Technology Organization, Melbourne, Australia (1992).
22. Lynch, S. P., "Fracture of Aluminum-Lithium Alloy Plate II. Sustained Load Crack Growth in Dry Air at 50-200C," ibid.
23. Lynch, S. P., "Creep Crack Growth in 8090 Aluminum-Lithium Alloy Sheet," ibid.
24. Private communication from S. P. Lynch to W. F. Brown, Jr.
25. Data supplied to W. F. Brown, Jr. by Comalco Ltd., Melbourne, Australia.
26. Pitcher, P. D.; McDarmaid, D. S.; Peel, C. J.; and Hall, C., "Effect of Thermal Processing on the Fracture Toughness of 8090 Sheet and Plate," presented at the 6th Al-Li International Conference, Garmisch-Partenkirchen, Germany (October 7-11, 1991).
27. Peel, C. J., "Applications and Developments for Al-Li Alloys," ibid.
28. Private communication from C. J. Peel to W. F. Brown, Jr.
29. Alcoa registration (December 7, 1990).

3-0 The following references are all taken from the *Proceedings of the Third Aluminum-Lithium Conference, Aluminum-Lithium Alloys III,* University of Oxford, July 1985; eds. C. Baker, P. J. Gregson, S. J. Harris, and C. J. Peel; Publisher: Institute of Metals London (1986). The designation 3-n indicates the Third Conference and a reference within the Proceedings.

3-1 Holroyd, N. J.; Gary, A.; Scamans, G. M.; and Hermann, R., "Environment Sensitive Fracture of Al-Li-Cu-Mg Alloys," p. 310.

3-2 Pridham, M.; Noble, B.; and Harris, S. J., "Elevated Temperature Strength of Al-Li-Cu-Mg Alloys," p. 547.

3-3 White, J.; Miller, W. S.; Palmer, I. G.; Davis, R.; and Sanini, T. S., "Effect of Precipitation on Mechanical Properties of Al-Li-Cu-Mg-Zr Alloy," p. 530.

3-4 Doorbar, P. J.; Borradaile, J. B.; and Driver, D., "Evaluation of Aluminum-Lithium-Copper-Magnesium-Zirconium Alloy as a Forging Material," p. 486.

3-5 Stokes, K. R.; Moth, D. A.; and Sherwood, J. R., "Hard Anodizing and Marine Corrosion Characteristics of 8090 Al-Li-Cu-Mg-Zr Alloy," p. 296.

4-0 The following references are all taken from the *Proceedings of the Fourth International Aluminum-Lithium Conference,* Paris, France, June 1987; eds. G. Champier, B. Dubost, D. Mainnay, and L. Sabetay; Publisher: J. de Physique (September 1987). The designation 4-n indicates the Fourth Conference and a reference within the Proceedings.

4-1 Lepoac, P.; Nomine, A. M.; and Miannay, D., "Mechanical Properties of Electron Beam Welds in 8090 Alloy," p. C3-301.

4-2 Edwards, M. E., and Stoneham, V. E., "Fusion Welding of Al-Li-Cu-Mg (8090) Alloy," p. C3-293.

4-3 Webster, D., "The Effect of Low Melting Impurities on the Properties of Al-Li Alloys," p. C3-293.

4-4 Bischler, P. J. E., and Martin, J. W., "The Temperature Dependence of High Cycle Properties on an Al-Li-Cu-Mg Alloy," p. C3-761.

4-5 Tintillier, R.; Yang, H. S.; Ranganathan, N.; and Petit, J., "Near Threshold Fatigue Crack Growth in a 8090 Lithium Containing Alloy," p. C3-777.

4-6 Reboul, M., and Meyer, P., "Intergranular and Exfoliation Study of Al-Li-Cu-Mg-Zr Alloys," p. C3-881.

4-7 Haddleton, F. L.; Murphy, S.; and Griffin, T. J., "Fatigue and Corrosion Fatigue of 8090 Al-Li-Cu-Mg Alloy," p. C3-809.

4-8 Smith, A. F., "The Metallurgical Aspects of Aluminum-Lithium Alloys in Various Products Forms for Helicopter Structural Applications," p. C3-49.

4-9 Page, F. M.; Chamberlain, A. T.; and Grimes, R., "The Safety of Molten Aluminum-Lithium Alloys in the Presence of Coolants," p. C3-63.

4-10 Miller M. S.; White, J.; and Lloyd, D. J., "The Physical Metallurgy of Aluminum-Lithium-Copper-Magnesium-Zirconium Alloys 8090 and 8091," p. C3-139.

4-11 Miller, W. S.; White, J.; Reynolds, M. A.; McDarmaid, D. S.; and Starr, G. M., "Aluminum-Lithium-Copper-Magnesium-Zirconium Alloys With Strength and High Toughness-Solving the Perceived Dichotomy," p. C3-151.

4-12 Goncalves, M., and Sellars, C. M., "Static Recrystallization After Hot Working of Al-Li Alloys," p. C3-171.

4-13 Papazian, J. M.; Bott, C. G.; and Shaw, P., "Influence of Forming in the T3 Condition on the Properties of 2090-T8X, 2091-T8X, and 8090-T8X," p. C3-231.

4-14 Grimes, R.; Miller, W. S.; and Butler, R. G., "Development of Superplastic 8090 and 8091 Sheet," p. C3-239.

4-15 Ridley, N.; Livesey, D. W., and Pilling, J., "Optimization of Strain Rate Sensitivity During Superplastic Forming of Al-Li Alloy Lital A," p. C3-251.

4-16 Papazian, J. M.; Wagner, J. W.; and Rooney, W. D., "Porosity Development During Heat Treatment of Aluminum Lithium Alloys," p. C3-513.

4-17 Smith, A. F., "A Study of the Microstructure and Properties of Die Forgings in Aluminum-Lithium Alloys 2901 and 8090," p. C3-629.

4-18 Lewis, R. E.; Starke, E. A., Jr.; Coons, W. C.; Shiflet, G. J.; Willner, E.; Bjeletich, J. G.; Mills, C. H.; Harrington, R. M.; and Petrakiis, D. N., "Microstructure and Properties of Al-Li-Cu-Mg-Zr (8090) Alloy Heavy Section Forgings," p. C3-643.

4-19 Reynolds, M. A., and Creed, C., "The Development of 8090 and 8091 Alloy Extrusions," p. C3-195.

4-20 Xiao, Y., and Bompard, P., "Low Cycle Fatigue and Fatigue Crack Growth in Al-Li, Al-Li-Zr and 8090 Alloys," p. C3-737.

4-21 Damerval, C.; Raviart, J. L.; and Leclerc, G., "Influence of Processing Conditions on the Monotonic Properties of 8090 Alloy," p. C3-661.

4-22 Bensfeld, F.; Habashi, M.; Galland, J.; Fidelle, J. P.; Miannay, D.; and Rofidal, P., "Hydrogen Embrittlement in Al-Li-Cu-Mg Alloys," p. CS-587.

5-0 The following references are all taken from the *Proceedings of the Fifth International Aluminum-Lithium Conference*, Williamsburg, VA, March 1989;eds. T. H. Sanders, Jr., and E. A. Starke, Jr.; Materials and Component Engineering Publications, Birmingham, U.K. The designation 5-n indicates the Fifth Conference and a reference within the Proceedings.

5-1 Zhou, Z. O.; He Ji, X.; and Chen, C. O., "Fracture Mechanisms and Toughness of Al-Li-Cu-Mg-Zr Alloys," p. 879.

5-2 Gatenby, K. M.; Reynolds, M. A.; White, J.; and Palmer, I. G., "The Role of Microstructure in Controlling the Mechanical Properties of 8090 in Damage Tolerant Tempers," p. 909.

5-3 Harris, S. J.; Noble, B.; and Dodd, A., "The Effect of Texture on the Tensile and Fatigue Properties of 8090 Plate Alloys," p. 1061.

5-4 Rooney, W. D.; Papazian, J. M.; Balmuth, E. S.; Dacis, R. C.; and Adler, P. N., "Elastic Anisotropy in Al-Li Alloys," p. 799.

5-5 McDarmaid, D. S., and Peel, C. J., "Aspects of Damage Tolerance in 8090 Sheet," p. 003.

5-6 Peacock, H. D., and Martin, J. W., "The Effect of S Phase Distribution on Fatigue Crack Growth in Peak-Aged 8090 and 8091 Al-Li Alloys," p. 1013.

5-7 Srivatsan, T. S.; Bobecck, G. E.; Sudarshan, T. S.; and Molian, P. A., "Environmental Factors Affecting Localized Corrosion of Al-Li-Cu-Mg Alloys," p. 1237.

5-8 Birt, M. J., and Beevers, C. J., "The Fatigue Response of Aluminum-Lithium Alloy 8090," p. 983.

5-9 Welpman, K.; Lee, Y. T.; and Peters, M., "Low Temperature Behavior of 8090," p. 1513.

5-10 Wan, C. C.; Smallen, H.; and Carter, R. V., "Tensile Properties of 8090 Al-Li Alloy at Cryogenic Temperatures," p. 1533.

5-11 Hernman, R., and Reid, C. N., "Enhancing the Fatigue Life of Fastener Holes in Aluminum-Lithium Alloys," p. 1607.

5-12 Lippold, J. C., "Weldability of Commercial Aluminum-Lithium Alloys," p. 1365.

This page is blank.

1 GENERAL

This alloy has the highest strength of aluminum casting alloys coupled with relatively high toughness. Special attention must be given to casting methods to control hot tearing associated with relatively high shrinkage during solidification. The fully aged condition (-T6) should be avoided if integranular or stress corrosion may be a problem.

Weld repair of A201.0 castings is possible without cracking using carefully controlled techinques. B201 is an AMS designated aircraft quality grade with stronger quality assurance requirements, a reduced maximum on silver and iron content coupled with a slightly modified heat treatment.

Extensive investigations by Northrop (Ref. 9) showed that the properties obtained from cast plates could be used to sucessfully design large complex aerospace structures.

1.1 Commercial Designation - A201.0 (formerly KO-1)

1.2 Alternate Designations

1.2.1 *[Table]* Alternate designations.

1.3 Specifications

1.3.1 *[Table]* AMS specifications.

1.4 Composition

1.4.1 *[Table]* AMS and military specification compositions.

1.4.2 Effects of Alloying Elements. The addition of Ag to the base Al-Cu-Mg ternary (Ref. 18) has resulted in substantial increases in hardness and tensile strength. This modification of the aging response of Al-Cu-Mg casting by the addition of Ag is illustrated in Table 1.4.2.1 and Figure 1.4.2.2 which shows substantial increases in hardness and tensile strength are associated with the addition of a small amount of Ag.

As part of a program to establish the optimum foundry practices and design data for the cast Al-Cu-Mg-Ag alloy A201.0, Northrop (Ref. 6) attempted to systematically explore the influence of the major alloying elements (within the range of AMS 4223) and of the impurities Si and Fe on the tensile properties of sand and shell investment mold cast rectangular plates. These castings were produced using production equipment with procedures summarized in Table 1.4.2.3. The results were, in some cases, ambiguous and what follows presents the clearest examples. Increasing Mg resulted in increasing tensile and yield strengths of sand and investment castings and decreasing elongation (e.g., Figure 1.4.2.4). The tensile and yield strengths of both sand and investment castings increased with increasing Cu content but an unexpected increase in the elongation was obtained for the sand castings, Figure 1.4.2.5, while no effect on elongation was observed for the investment castings. As expected, additions of Ag produced substantial increases in the tensile strength properties coupled with a decrease in elongation for both types of castings (e.g., Figure 1.4.2.6). Iron contents above the maximum specified by AMS produced the expected decrease in tensile properties for the investment castings, Figure 1.4.2.7, but had only a small effect of the tensile and yield strength of the sand castings coupled with a large decrease in their elongation. Silicon compounds can promote eutectic melting during solution treatment (see Section 1.9.1). Increases above the 0.05 percent maximum silicon specified by AMS result in substantial reductions in the elongation of both types of castings, Figures 1.4.2.8 and 1.4.2.9, and increased tensile strength properties of sand castings, but Si had little effect on the tensile strength properties of investment castings.

Al
4.5 Cu
0.7 Ag
0.3 Mn
0.25 Mg
0.25 Ti

Northrop also investigated the properties of castings made from "out of AMS 4242 Specification" melts using rectangular sand cast plates with either Cu or Fe chills.

The in-specification and out-of-specification tensile properties and grain size are compared in Table 1.4.2.10. The largest effects are noted for the Cu-Ag-Mg increases where the tensile strengths are increased and the elongation drastically reduced. These effects are associated with substantial increases in the grain size. Increased Ti also reduces the elongation but to a much smaller extent. The Cu chill tended to reduce the grain size.

1.4.2.1 *[Table]* Maximum hardness and tensile strengths produced by aging at three temperatures for Al-Cu-Mg and Al-Cu-Mg-Ag alloy castings.

1.4.2.2 *[Figure]* Effect of silver addition on aging response of a Al-Cu-Mg casting.

1.4.2.3 *[Table]* Casting and heat treatment details for investment and sand cast plates used in the investigation of composition and other factors controlling the mechanical properties of A201.0 castings.

1.2.4.4 *[Figure]* Effect of magnesium content on the tensile properties of a sand composite cast plate.

1.4.2.5 *[Figure]* Effect of copper content on tensile properties of a sand composite cast plate.

This section produced with the support of NASA-Lewis Research Center.

© 1997 by Purdue Research Foundation, West Lafayette, Indiana 47907. All Rights Reserved. U.S. Government License. This material may be used, duplicated or disclosed by United States Government agencies without the payment of any royalty.

1.4.2.6 *[Figure]* Effect of silver content on the tensile properties of shell investment cast plates.

1.4.2.7 *[Figure]* Effect of iron content on the tensile properties of shell investment cast plates.

1.4.2.8 *[Figure]* Effect of silicon content on the tensile properties of shell investment cast plates.

1.4.2.9 *[Figure]* Effect of silicon content on the tensile properties of sand composite cast plates.

1.4.2.10 *[Table]* Effect of out of specification composition and mold cooling rate on tensile properties and grain size of sand composite cast plates.

1.5 Heat Treatment

General. The heat treatment consists of a solution phase designed to put the major alloying elements into solid solution in the aluminum matrix without encountering eutectic melting (see 1.9.1). Step solution treatments are given by AMS (see Table 1.5.6) to minimize eutectic melting. Room temperature aging produces the -T4 condition and some foundries prefer to age at room temperature up to 24 hrs. prior to artificial aging. A stabilized condition, -T43, is produced by aging at 310F for 1 to 2 hrs. A fully aged condition, -T6, is produced by aging at 310F for 20 hrs. Both the -T43 and the -T6 conditions are highly susceptible to intergranular and stress corrosion (see 2.3.2). The optimum condition (-T7) is an overage at 370F for 5 hrs.

Solution Treatment. Solution heat treatment times from 6 to 18 hrs. at 985F, Figures 1.5.1 and 1.5.2, had little effect on the tensile properties of sand and shell investment mold castings produced according to the processes outlined in Table 1.4.2.3. Generally, a water quench is used from the solution temperature. Quench water temperature up to 212F appears to have only a slight effect (e.g., Figure 1.5.3) on the tensile properties. (Refs. 6, 12) Quench delay time at room temperature up to 5 days had no significant effect on the tensile properties of sand or shell investment castings. (Ref. 6)

Aging. The tensile properties appear to be insensitive to the aging time between 3 to 7 hrs. at 370F for sand, Figure 1.5.4, and investment mold castings, Figure 1.5.5.

1.5.1 *[Figure]* Effect of solution heat treatment time on the tensile properties of shell investment cast plates.

1.5.2 *[Figure]* Effect of solution heat treatment time on the tensile properties of sand composite cast plates.

1.5.3 *[Figure]* Effect of quench water temperature on tensile properties of a shell investment cast plates.

1.5.4 *[Figure]* Effect of aging time at 370F on tensile properties of sand composite cast plates.

1.5.5 *[Figure]* Effect of aging time at 370F on tensile properties of a shell investment cast plates.

1.5.6 *[Table]* AMS and MIL Specification heat treatments.

1.6 Hardness (See Tables 1.4.2.1, 3.1.1, 3.2.1.5 and Figure 1.4.2.2)

1.7 Forms and Conditions Available. Investment and Sand Castings and Welding Wire

1.8 Melting and Casting Practice

1.8.1 General. The mechanical properties of a casting are complex functions of many variables including the mold design, placement of chills, gating and rising, grain refining techniques, melting crucible type and treatment, grain refinement additions and pouring temperature. In the case of castings for use in critical applications, all of these factors and the elimination of impurities are of prime concern. During the period from 1977 to 1984, the Air Force sponsored several programs to establish the techniques for producing high strength aluminum castings of complex design. Much of what follows is taken from the Northrop program to produce optimum properties in several alloys including A201.0. Information applicable to A201.0 concerning melting practice, degassing, holding time prior to degassing, mold design (for sand casting) and pouring temperature can be found in Code 3109 (Section 1.08) on A357, an Al-Si-Mg alloy.

In the Northrop program for establishing AMS specifications and design mechanical properties, use was made of a step plate sand casting shown in Figure 1.8.1.1. In other phases of the Nortrhrup program, specimens were removed from uniform thickness cast plates. Where available, the form of the casting is indicated on the Tables and Figures.

1.8.1.1 *[Figure]* Sand composite mold cast step plates for the Northrop investigation of manufacturing processes on design allowables.

1.8.1.2 *[Table]* Foundry practice in producing step plates.

1.8 2 Grain Refinement. While dendrite arm spacing (DAS) is important in controlling the mechanical properties of Al-Si-Mg alloys, this type of control is not possible in Al-Cu-Mg alloys, where dendrites are not discernible. In general, mechanical properties increase with a decrease in the grain size (e.g., Figure 1.8.2.1). Fine grain size minimizes the detrimental effects of grain boundary segregation of brittle phases which contribute to low energy grain boundary fractures. Grain size will decrease with increased cooling rate in a casting. However, control by this method is limited due to casting section size, microsegregation adjacent to chill faces, and mold-design factors necessary to prevent hot tearing (Ref. 12). The preferred method of grain size control is by inoculation with nucleating agents. A 5%Ti-1%B master alloy is the preferred inoculating agent. Upon cooling, crystals of $TiAl_3$ are nucleated on

the stable TiB_2 particles. The $TiAl_3$ has a crystal structure close to that of pure Al and is effective in nucleating the growth of dendrites from the melt. (Ref. 12) The effect of the inoculation requires a conditioning period in which the TiB_2 particles become dispersed. As holding time increases, the particles tend to coalesce — resulting in grain size increases as shown in Figure 1.8.2.2. Relatively short holding times between 1 and 10 minutes are recommended with additions of 0.01% and 0.02% Ti using the T-B master alloy. (Ref. 12) However, considerable variation may be found among foundries. Generally, the melt is stirred immediately after the addition of the grain refining agent. As mentioned above, it is generally observed that the mechanical properties improve with a decrease in grain size. The expected behavior is observed in sand mold cast rectangular plates, Figure 1.8.2.1. However, this is not always the case and essentially no effect is observed in similar shaped investment cast plates, Figure 1.8.2.3. A lack of grain size effect was also found when the average grain size of the material producing the data shown in Table 3.2.1.3 was decreased from 0.0032 in. to 0.0011 in. (Ref. 9) These exceptions to the improvement of mechanical properties with decrease in grain size may be associated with the use of relatively simple castings resulting in a minimum of segregation

1.8.2.1 *[Figure]* Effect of grain size on the tensile properties of a sand cast composite plate.

1.8.2.2 *[Figure]* Effect of holding time and titanium content on grain size of melt inoculated with 5%Ti - 1%B.

1.8.2.3 *[Figure]* Tensile properties of shell investment cast plate at various grain sizes.

1.9 Special Considerations

1.9.1 Eutectic Melting. In the process of solidification, dendrites of Al became progressively enriched in alloying elements rejecting low temperature melting solute into interdendritic spaces. This solute eventually reaches eutectic composition and is trapped between dendrite arms or in the grain boundaries. A summary of possible phases which can form during the solidification of A201.0 are shown in Table 1.9.1.1. The lowest melting phases are $CuMgAl_2$ with a melting point of 945F and $(CuFeMg)_3Si_2$ Al_{15} with a melting point of 986F. It has been recommended (Ref. 12) that a step solution heat treatment be used to diffuse these phases into the matrix. This is accomplished by short times at temperatures between about 900 and 960F followed by longer times at a higher temperature. This high temperature should be limited to that which will not produce grain growth and generally does not exceed 990F. A two step solution treatment is in the AMS Specifications (see Table 1.5.6) and two and three step treatments were used in some portions of the Northrop program (see Table 1.8.1.2). The necessity for its use probably depends on the tendency of a particular casting design to promote segregation.

1.9.1.1 *[Table]* Possible grain boundary phases present in castings.

1.9.2 Shrinkage. A201.0 alloy is more prone to shrinkage during solidification than the Al-Si-Mg alloys A356.0 and A357.0. This shrinkage can cause hot tearing in casting regions involving pronounced changes in section size which inhibit contraction of the solidifying alloy. Hot tears may be open fissures or in some cases may be filled with a low melting eutectic. Regions containing hot tears possess poor mechanical properties because either the fissures act like cracks or tears filled with eutectic are brittle regions. Hot tears generally communicate with the surface and can be found by NDI techniques. If the fissures are filled with eutectic, X-ray examination may reveal Cu-rich regions associated with the fissures. Careful mold design and proper grain refinement, resulting in a small grain size, can eliminate hot tears. (Ref. 12) Hot isostatic pressing can close the fissures if they are empty. As shown in Table 1.9.2.1, A201.0 did not exhibit any significant decrease in tensile strength but a considerable loss in elongation occurred when shrinkage increased from radiographic grade AB to CD

1.9.2.1 *[Table]* Effect of casting defects on the tensile properties of shell investment and sand composite mold castings.

1.9.3 Porosity. Porosity results from the entrapment of gas and, depending on its severity, can cause substantial loss of gross deformation capacity which results in decreased ultimate tensile strength and elongation (see Table 1.9.3.1). Notch fatigue strength is substantially reduced by porosity (compare Figures 3.5.1.4 and 3.5.1.10). However, the fracture toughness (Table 1.9.3.1) is not affected by the same amount of porosity. This is probably due to the fact that the round pores do not act as crack extensions.

1.9.3.1 *[Table]* Effect of round gas porosity on the tensile properties and fracture toughness of defective step plates compared with grade B plates.

1.9.4 Dross. Dross generally results from the entrapment of material lighter than the melt, such as aluminum oxide, introduced by excessive agitation. Depending on its shape and concentration, substantial reduction in gross deformation capacity can result, as shown in Table 1.9.2.1, by the loss in ultimate tensile strength and elongation.

1.9.5 HIP. Hot isostatic pressing (HIP) has been shown to be effective in improving the mechanical properties of castings having poor radiographic quality associated with internal defects. Castings with porosity of Grade C were subjected to several HIP schedules as shown in

Table 1.9.5.1. The as-cast material had very poor properties — breaking before reaching the yield strain. A schedule of 950F/10 ksi/6 hr and 980F/10 ksi/6 hr produced some improvement in tensile ultimate strength but no significant improvement in ductility. Increasing the time from 6 to 12 hr at 950F/10ksi resulted in substantial improvement in all tensile properties. The best results were produced by the highest pressure of 15 ksi at 950F/6 hr; this material was reported as having a radiographic grade of A. It should be noted that elongation values shown for material breaking before the 0.2 percent offset are probably produced by the inability to match the halves of the broken specimens for elongation measurements.

1.9.5.1 *[Table]* Effect of hot isostatic pressing on specimens removed from rejected turbofan rim.

1.9.6 Squeeze Casting. This process applies a pressure of from 16 to 30 ksi to the solidifying metal in the mold. The purpose of this pressurized casting method is to minimize shrinkage and gas porosity. Squeeze-cast A201.0 is reported to have an absence of grain boundary intermetallics in the fully heat treated condition. Squeeze casting is claimed to be responsible for tensile strength and elongation values superior to that of conventionally cast A201.0 alloy.

1.9.6.1 *[Table]* Tensile properties of squeeze cast and permanent mold castings.

2 Physical Properties and Environmental Effects

2.1 Thermal Properties

2.1.1 Melting Range. 1300 to 1400F.

2.1.2 Phase Changes. The phase changes responsible for the age hardening of A201.0 and other Al-Cu-Mg alloys are extremely complex and not completely defined. A useful summary of the proposed mechanisms is found in Ref. 15 which is concerned with effects of Si on the hardening process. The generally accepted sequence, as proposed by Mondolfo (Ref. 14), is as follows: Saturated solid solution →GP + GPB →Intermediate Phases→$CuAl_2$ (θ) + $CuMgAl_2$, where, GP represents Guinier-Preston Cu zones and GPB represents Guinier-Preston Bagariatskij Cu/Mg zones. The intermetallic compounds, $CuAl_2$ and $CuMgAl_2$, are the equilibrium phases. The primary strengthening is associated with the GP and GPB zone formations and the intermediate phases. Nucleation and some formation of these strengthening phases occurs during room temperature aging. The effects of Ag as a minor alloying addition results in the precipitation of an Ω phase (Refs. 14, 15) which has the same structure and composition of the θ phase but different orientation relationship to the matrix. This phase is reported to have greater thermal stability and contributes significantly to the age hardening.

2.1.3 Thermal Conductivity. 70 Btu/ft/hr/F. (Ref. 17)

2.1.4 Thermal Expansion

2.1.4.1 *[Figure]* Thermal Expansion.

2.1.5 Specific Heat. 0.22 Btu/lb/deg F.

2.1.6 Thermal Diffusivity.

2.2 Other Physical Properties

2.2.1 Density. 0.101 lb/$in.^3$.

2.2.2 Electrical Properties.

2.2.3 Magnetic Properties.

2.2.4 Emmitance.

2.2.5 Damping Capacity.

2.3 Chemical Environments

2.3.1 General Corrosion.

2.3.2 Stress Corrosion.

General. Data reported in Ref. 11 show the -T4 (not aged) condition to be resistant to both intergranular and stress corrosion. Artificial aging at 300 to 330F produces conditions highly susceptible to both intergranular and stress corrosion. Overaging at 360 to 370F (-T7) resulted in conditions which showed no corrosion under the test conditions reported. This type of information has discouraged the use of the -T6 (fully aged) condition.

2.3.2.1 *[Table]* Integranular and stress corrosion behavior as a function of aging temperature and time.

2.4 Nuclear Environments

3 Mechanical Properties

3.1 Specified Mechanical Properties

3.1.1 *[Table]* AMS specified mechanical properties.

3.1.2 *[Table]* Tensile properties specified in MIL-A-21180D.

3.2 Mechanical Properties at Room Temperature

3.2.1 Tension Stress-strain Diagrams and Tensile Properties.

3.2.1.1 *[Figure]* Cyclic stress-strain curve for specimens from sand composite cast plate.

3.2.1.2 *[Table]* Tensile and compression properties of specimens removed from sand cast mold step plates.

3.2.1.3 *[Table]* Smooth and notch tensile results for specimens from sand composite cast plates from three foundries.

3.2.1.4 *[Table]* Tensile properties of sand cast bars aged to the -T6 and -T7 conditions.

3.2.1.5 *[Table]* Tensile and compressive strength, elastic modulus and Vickers hardness of three types of castings providing different cooling rates.

3.2.1.6 *[Figure]* Effect of exposure time at elevated temperatures on room temperature tensile properties of -T7 sand cast test bars.

3.2.2 Compression Stress-strain Diagrams and Compression Properties.

3.2.2.1 Compressive strength. (see Table 3.2.1.2.)

3.2.3 Impact.

3.2.4 Bending.

3.2.5 Torsion and Shear.

3.2.5.1 *[Table]* Shear strength of specimens removed from sand cast mold step plates.

3.2.6 Bearing.

3.2.6.1 *[Table]* Bearing strength of specimens removed from sand cast mold step plates.

3.2.7 Stress Concentration.

3.2.7.1 Notch Properties.

3.2.7.1.1 Sharp notch tensile strength. (see Table 3.2.1.3)

3.2.7.2 Fracture Toughness. There is a very limited data base for valid plane strain fracture roughness values. The K_{Ic} range, Table 3.2.7.2.1, is between about 23 to 33 ksi$\sqrt{in.}$ and appears to increase with decreasing tensile strength. The presence of substantial amounts of porosity did not reduce the plane strain fracture toughness. (see Table 1.9.3.1)

3.2.7.2.1 *[Table]* Plane strain fracture toughness of separately sand cast blocks.

3.2.8 Combined Loading.

3.3 Mechanical Properties at Various Temperatures

3.3.1 Tension Stress-strain Diagrams and Tensile Properties.

3.3.1.1 *[Figure]* Effect of test temperature on tensile properties of specimens from sand mold step plates from Foundry A.

3.3.1.2 *[Figure]* Effect of test temperature on tensile properties of specimens from sand mold step plates from Foundry B.

3.3.1.3 *[Figure]* Effect of exposure time and test temperature on -T7 sand cast bars tested at the exposure temperature.

3.3.2 Compression Stress-strain Diagrams and Compression Properties.

3.3.3 Impact.

3.3.4 Bending.

3.3.5 Torsion and Shear.

3.3.6 Bearing.

3.3.7 Stress Concentration.

3.3.7.1 Notch properties.

3.3.7.2 Fracture toughness.

3.3.8 Combined Loading.

3.4 Creep and Creep Rupture Properties

3.4.1 *[Figure]* Time for 0.25 percent total creep at several elevated temperatures for -T7 sand cast test bars.

3.4.2 *[Figure]* Time for 0.5 percent total creep at several elevated temperatures for -T7 sand cast test bars.

3.4.3 *[Figure]* Time for 1.0 percent total creep at several elevated temperatures for -T7 sand cast test bars.

3.4.4 *[Figure]* Rupture time at several elevated temperatures for -T7 sand cast test bars.

3.5 Fatigue Properties

3.5.1 Conventional High Cycle Fatigue.

3.5.1.1 *[Figure]* Rotating bending fatigue strength at room temperature and 400F for -T7 sand cast test bars.

3.5.1.2 *[Figure]* Effect of HIP processing on the fatigue strength of axially loaded specimens from a rejected turbofan rim.

3.5.1.3 *[Figure]* Fatigue strength of axially loaded specimens from sand cast plates from three foundries.

3.5.1.4 *[Figure]* Fatigue strength of axially loaded notched specimens from designated areas of sand cast step plates.

3.5.1.5 *[Figure]* Fatigue strength of axially loaded notched specimens from sand cast plates from three foundries.

3.5.1.6 *[Figure]* Fatigue strength (R = -1.0) of axially loaded -T6 notched (K_t = 3) specimens from individually cast test bars.

3.5.1.7 *[Figure]* Fatigue strength (R = 0.2) of axially loaded -T6 notched (K_t = 3) specimens from individually cast test bars.

3.5.1.8 *[Figure]* Fatigue strength (R = -1.0) of axially loaded -T7 notched (K_t = 3) specimens from individually cast test bars.

3.5.1.9 *[Figure]* Fatigue strength (R = 0.2) of axially loaded -T7 notched (K_t = 3) specimens from individually cast test bars.

3.5.1.10 *[Figure]* Fatigue strength of axially loaded notched (K_t = 3) specimens from sand cast step plates containing porosity.

3.5.2 Low Cycle Fatigue.

3.5.2.1 *[Figure]* Strain vs life data for specimens from sand cast plate from three foundries.

3.5.3 Fatigue Crack Propagation.

3.5.3.1 *[Figure]* Fatigue crack growth rates for specimens removed from sand cast step plates from two foundries.

3.5.3.2 *[Figure]* Fatigue crack growth rates for sand cast plates from three foundries.

3.6 Elastic Properties

3.6.1 Poisson's Ratio.

3.6.2 Modulus of Elasticity. The available data do not definitely establish a modulus for the different temper conditions of A201. Internal defects in cast material can alter the modulus and may account for some of the variation reported. Values are reported in Table 3.2.1.5 for various tempers and casting conditions. A value of 10,300 ksi appears reasonable for the -T7 condition.

3.6.3 Modulus of Rigidity.

3.6.4 Tangent Modulus.

3.6.5 Secant Modulus.

4 Fabrication

4.1 Forming

4.2 Machining and Grinding

No special problems arise in machining of A201.0 which machines easily.

4.3 Joining

4.3.1 Welding. Very limited data are available on welding and no general rules can be given at this time.

Repair welding is often used on castings and a review of the methods and precautions is given in Ref.19. This reference points out that A201.0 is rather difficult to weld without cracking. This problem is probably associated with the alloy's relative high shrinkage during solidification (see Table 1.9.2.1). GTA welding data have been reported (Ref. 6) using AMS 4233 composition wire. These welds were made in such a way as to simulate weld repairs of castings. Thus, the weld metal did not constitute the entire test section. Tensile and fracture toughness values for parent metal and welded specimens were essentially equal, as shown in Table 4.3.1.2, indicating the absense of cracking problems.

4.3.1.1 *[Figure]* Location of specimens in the designated areas of welded step plates.

4.3.1.2 *[Table]* Welding conditions used to produce welds in step plates.

4.3.1.3 *[Table]* Effect of GTA welding on the average tensile properties and fracture toughness of sand cast step plates.

4.4 Surface Treating

4.4.1 Small surface irregularities are easily removed by light machining. Electroplating and anodizing impart good finishes.

Table 1.2.1 Alternate designations

Alloy	UNS
A201.0-T4	A12010
A201.0-T7	A02010
B201.0-T7	A02010
201.0	A02010
SAE 382	—

Table 1.3.1 AMS Specifications (Refs. 1-4)

Alloy	AMS	Form
A201.0-T4	4223C[1]	Castings Solution Heat Treated and Naturally Aged
A201.0-T7	4229C[2]	High Strength Castings Solution Heat Treated and Overaged
B201.0-T7	4242[3]	Sand Composite Castings Solution Heat Treated and Overaged Aircraft Structural Quality
201	4233[4]	Weld Wire

Table 1.4.1 AMS and military specification compositions (Refs. 1-4, 8)

Alloy	A201.0		B201.0	
Form	See Table 1.3.1			
Source	AMS 4223[1], 4229[2], 4233[4] and MIL-A-28110D[8]		AMS 4242[3]	
Elements	Minimum	Maximum	Minimum	Maximum
Copper	4.0	5.0	4.0	5.0
Silver	0.40	1.0	0.40	0.80
Manganese	0.20	0.40	0.20	0.50
Magnesium	0.15	0.35	0.20	0.30
Titanium	0.15	0.35	0.15	0.35
Iron	—	0.10	—	0.05
Silicon	—	0.05	—	0.05
Other, each	—	0.03[a]	—	0.05
Other, total	—	0.10	—	0.15
Aluminum	Remainder		Remainder	

[a] AMS 4233 gives Beryllium = 0.0008 max.

Table 1.4.2.1 Maximum hardness and tensile strengths produced by aging at three temperatures for Al-Cu-Mg and Al-Cu-Mg-Ag alloy castings (Ref. 13, Table 1)

Alloy	A201.0					
Form	Castings					
Melting Practice	High Purity Stock, degas with Chlorine, no grain refiners, chill cast in iron molds to give ingots 9.4 x 4.3 x 1.1 inch					
Homogenize (F/hr)	932/24					
Solution Treat (F)	968					
Composition	Al - 4Cu - 0.25Mg			Al - 4.4Cu - 0.27Mg - 0.71Ag		
Age (F/hr)	266/480	338/7.2	446/1.2	266/480	338/7.2	446/1.2
Vickers Hardness	116	105	85	153	140	120
F_{tu} (ksi)		45	39		51	38
F_{ty} (ksi)		38	24		51	38

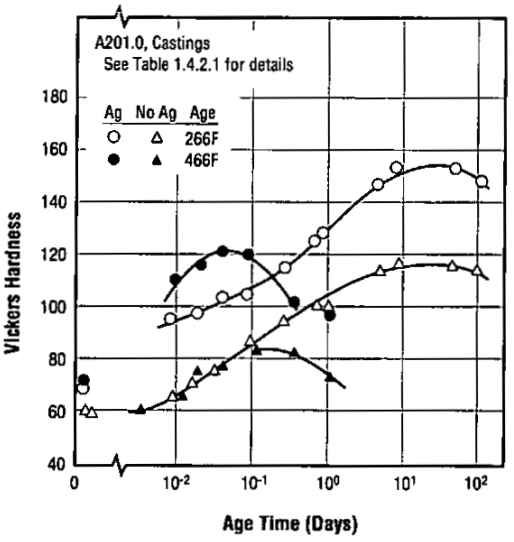


Figure 1.4.2.2 Effect of silver addition on aging response of a Al-Cu-Mg casting (Ref. 13, Fig. 1)

Table 1.4.2.3 Casting and heat treatment details for investment and sand cast plates used in investigation of composition and other factors controlling the mechanical properties of A201.0 castings (Ref. 6, pp. 32-39)

A201.0-T7	
Shell investment[a] Plates 3 x 10 x 3/16-in. thick	Sand Composite[a] Plates 3 x 10 x 3/4-in. thick
Six refractory coatings applied to wax pattern	Cope and drag sand mold with chills in cope and drag
Dewaxed with 100 psi steam	300-lb melt degassed with 90% Nitrogen + 10% Chlorine
Shell cured at 1200F 4 hr	Poured at 1375F into mold at RT
80-lb melt, grain refined with 5% Ti - 1% B at 1300F	Clean-up by rough grinding
Degassed 95% Nitrogen + 5% Freon 12	ST 975F 2 hr + 985F 18 hr, 40F, WQ
Poured at 1300F at 3-1/2 psi	Age RT 12-14 hr + 370F 5 hr
Clean with high velocity water	
ST 965F 2 hr + 990F 16 hr, WQ + straighten	
Age RT 12 hr + 370F 5 hr	

[a] Radiographic Grade B or better for heat treatment and composition studies; special plates were produced for effects of dross, shrinkage and porosity.

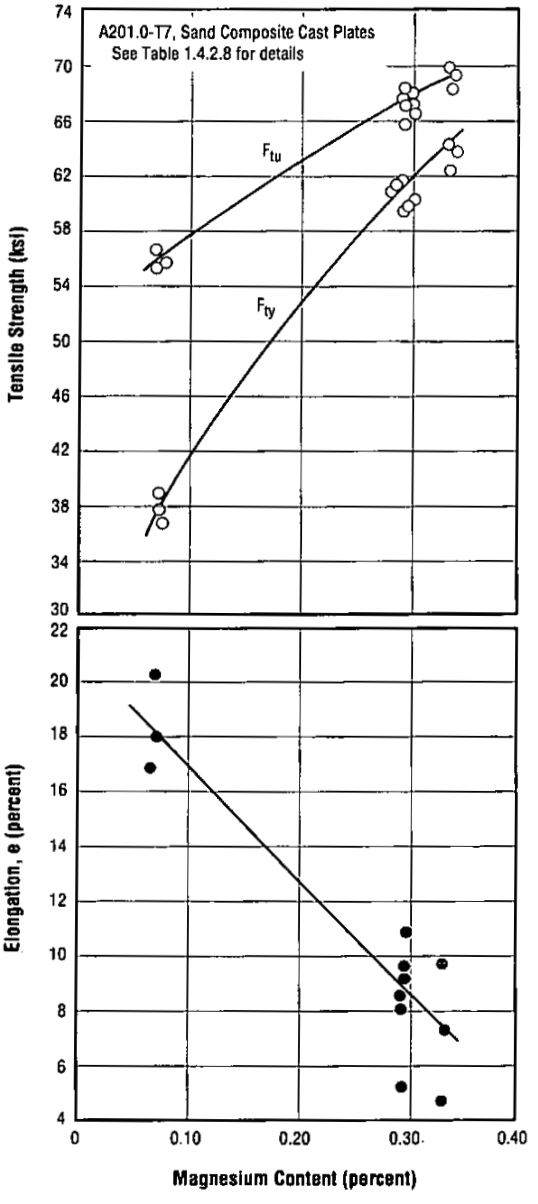


Figure 1.4.2.4 Effect of magnesium content on tensile properties of a sand composite cast plate (Ref. 13, Fig. 52)

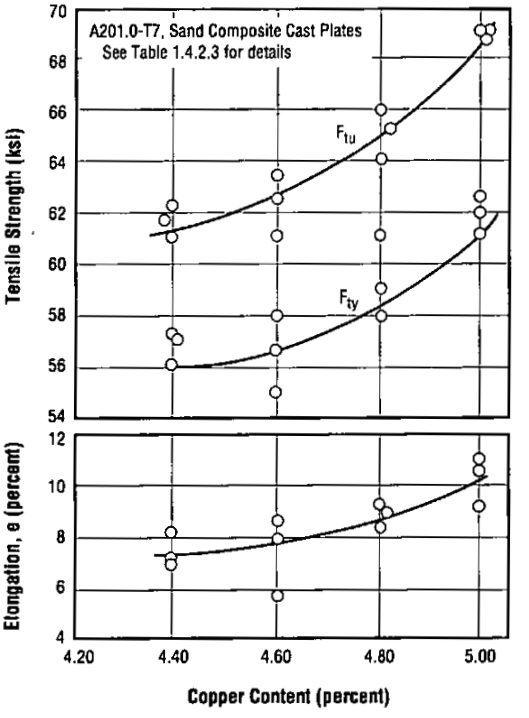


Figure 1.4.2.5 Effect of copper content on tensile properties of a sand composite cast plate (Ref. 6, Fig. 54)

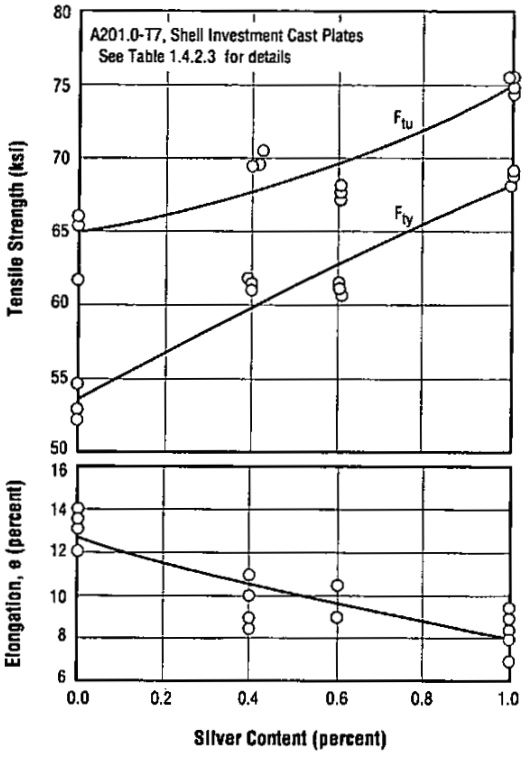


Figure 1.4.2.6 Effect of silver content on tensile properties of shell investment cast plates (Ref. 6, Fig. 56)

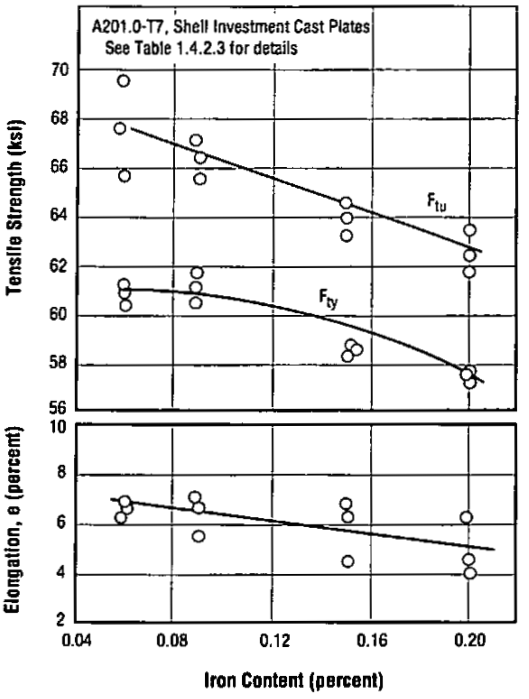


Figure 1.4.2.7 Effect of iron content on tensile properties of shell investment cast plates (Ref. 6, Fig. 58)

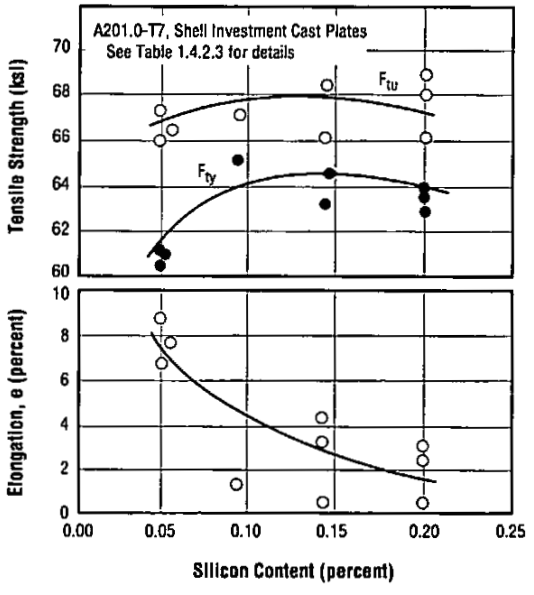


Figure 1.4.2.8 Effect of silicon content on tensile properties of shell investment cast plates (Ref. 6, Fig. 61)

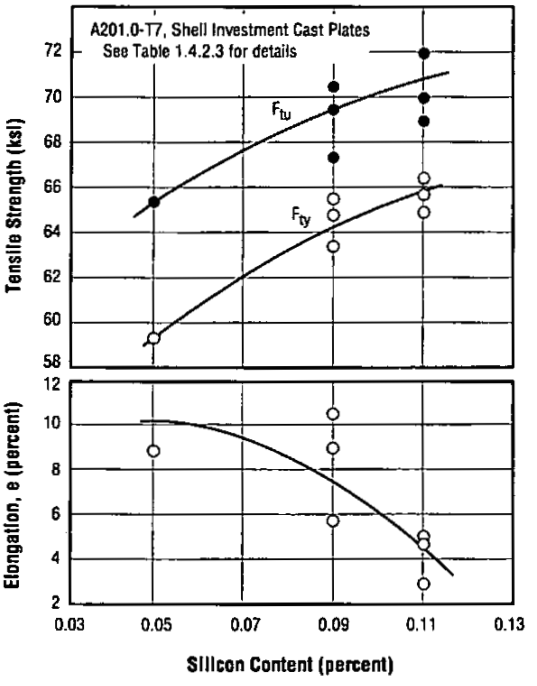


Figure 1.4.2.9 Effect of silicon content on tensile properties of sand composite cast plates (Ref. 13, Fig. 62)

Table 1.4.2.10 Effect of out-of-specification composition and mold cooling rate on tensile properties and grain size of sand composite cast plates (Ref. 9, Tables 33-36)

Alloy	A201.0-T7					
Form	0.75-in. Thick x 6-in. x 12-in. Cast Plates					
Heat Treat	ST 940F 2 hr + 960F 2 hr + 980F 16 hr + Age 360F 8 hr					
HIP	950F, 15 ksi, 3 hr					
Composition	AMS 4242 (See Table 1.4.1)		Outside AMS 4242			
			0.052 Ti		5.25Cu - 1.45Ag - 0.43Mg	
Pour Temperature/ Chill Material	1450F/Fe	1350F/Cu	1450F/Fe	1350F/Cu	1450F/Fe	1350F/Cu
F_{tu} (ksi)	65	67	69	69	74	77
F_{ty} (ksi)	60	60	64	64	73	72
e (percent)	6.3	9.4	3.0	3.2	1.4	5.7
Grain Size (10^{-4} in) at chill at edge	42 52	38 39	47 56	47 47	90 75	70 65

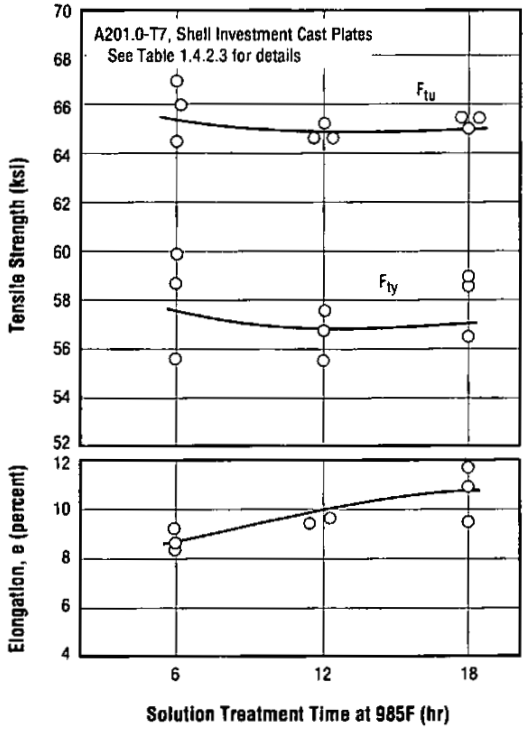


Figure 1.5.1 Effect of solution heat treatment time on tensile properties of shell investment cast plates (Ref. 6, Fig. 63)

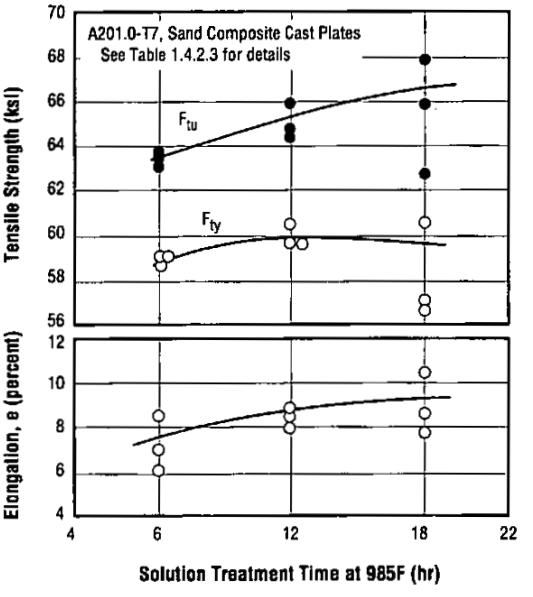


Figure 1.5.2 Effect of solution heat treatment time on tensile properties of sand composite cast plates (Ref. 6, Fig. 64)

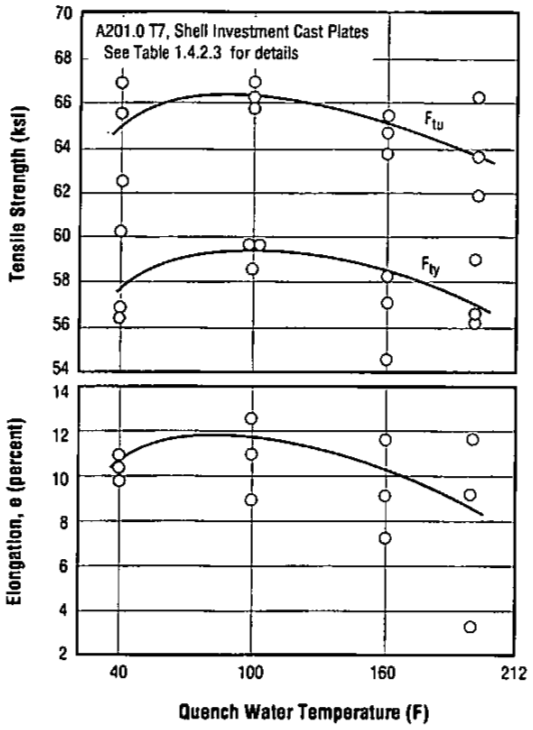


Figure 1.5.3 Effect of quench water temperature on tensile properties of shell investment cast plates (Ref. 6, Fig. 65)

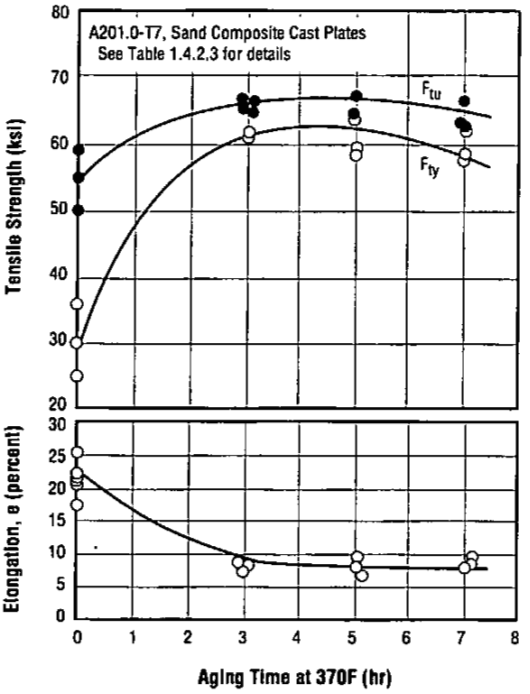


Figure 1.5.4 Effect of aging time at 370F on tensile properties of sand composite cast plates (Ref. 6, Fig. 70)

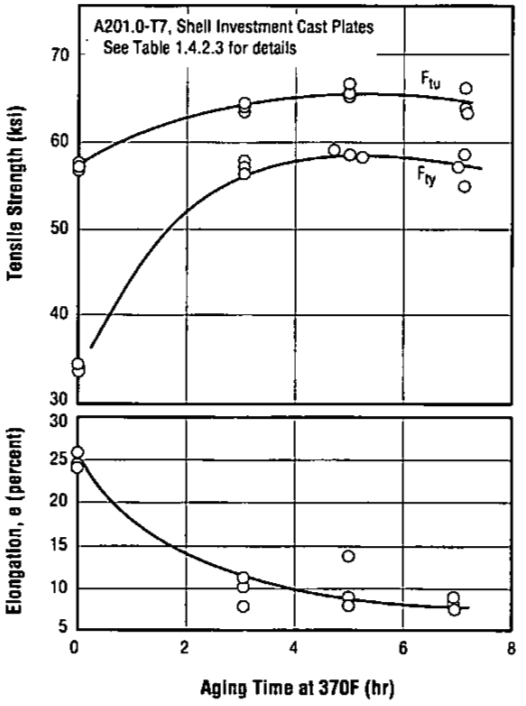


Figure 1.5.5 Effect of aging time at 370F on tensile properties of shell investment cast plates (Ref. 6, Fig. 69)

Table 1.5.6 AMS and MIL-Specification heat treatments (Refs. 1-3, 8)

Alloy	A201.0		B201.0	A201.0
Specification	AMS4223[1]	AMS 4229[2]	AMS 4242[3]	MIL-A-21180D[8]
Solution Treat	Heavy-wall castings 3/4-to 2-in. wall thickness 900 to 920F 2 hr + 980 to 990F 12 hr, quench	Heavy-wall castings as in 4223	All castings 945 to 965F 2 hr minimum + 970 to 990F 14 hr minimum	All castings 945 to 965F 2 hr minimum + 965 to 985F 8 to 24 hr[a]
	Thin-wall castings 940 to 960F, 2 hr + 980 to 990F 8 hr, quench	Thin-wall castings as in 4223	—	—
Age	RT 72 hr minimum	360 to 380F 5 hr	365 to 375F 5 hr minimum	360 to 380F 5 hr

[a] Soaking time varies with section thickness and grain size of the casting. Quench into a water bath at RT to 190F or into an aqueous solution of polyalkylene glycol.

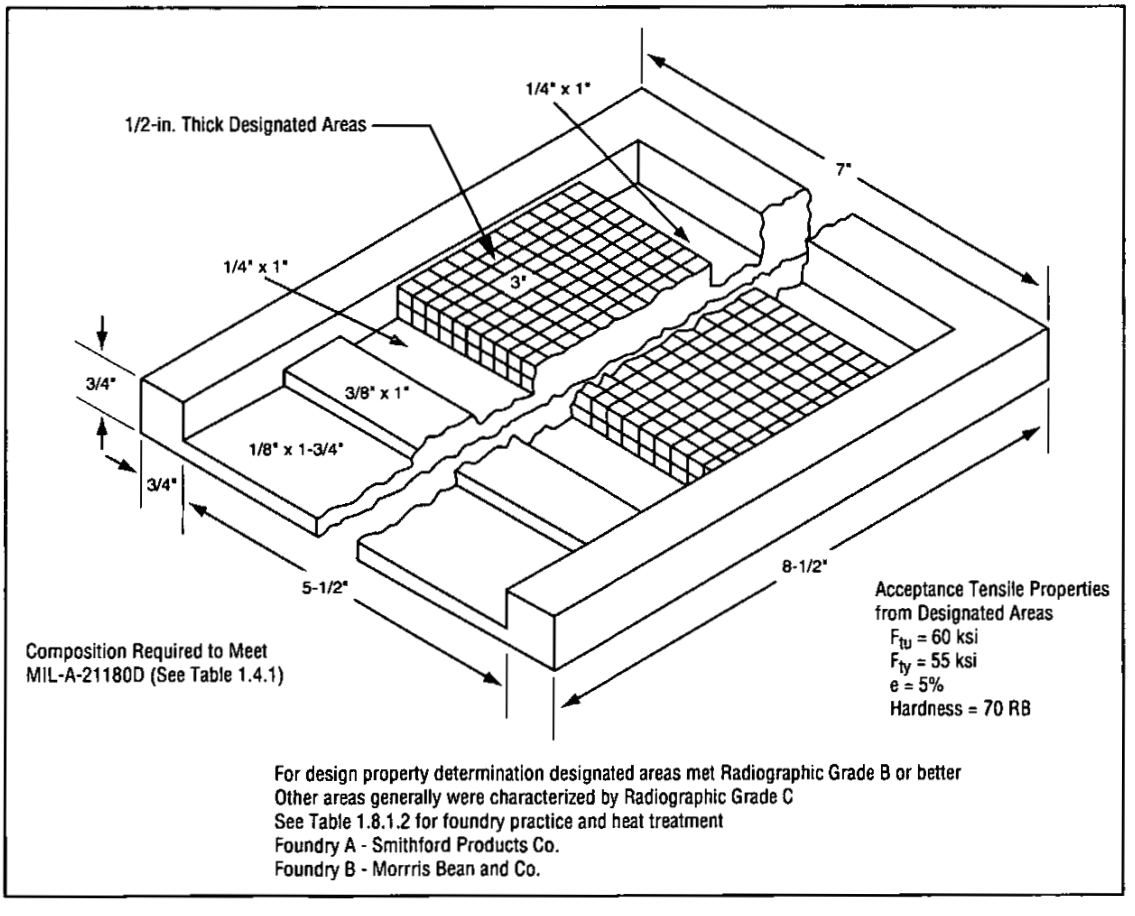


Figure 1.8.1.1 Sand composite mold cast step plates for Northrop Investigation of Manufacturing Processes on Design Allowables. (Ref. 6)

Table 1.8.1.2 Foundry practice in producing step plates (Ref. 6, p. 155 and Appendix E)

Alloy	A201.0	
Target Composition	4.5Cu, 0.50 - 1.0Ag, 0.25 - 0.35Mg otherwise as MIL-A-28110D	
Form	Sand Composite Mold Cast Step Plates	
Foundry	A	B
Degas	$N_2 + Cl_2$	Argon + Freon
Grain Size Control	5%Ti - 1%B pour within 30 minutes	Ti - B to give 0.02% Ti stir, wait 10 minutes, pour
Pouring Temperature (F)	1300	1400
Solution Treat (F/hr)	940/1	920/2
	960/1	950/2
	980/12	960/2
		980/18
Age (F/hr)	RT/12-24 + 370/5	RT/12 + 370/5

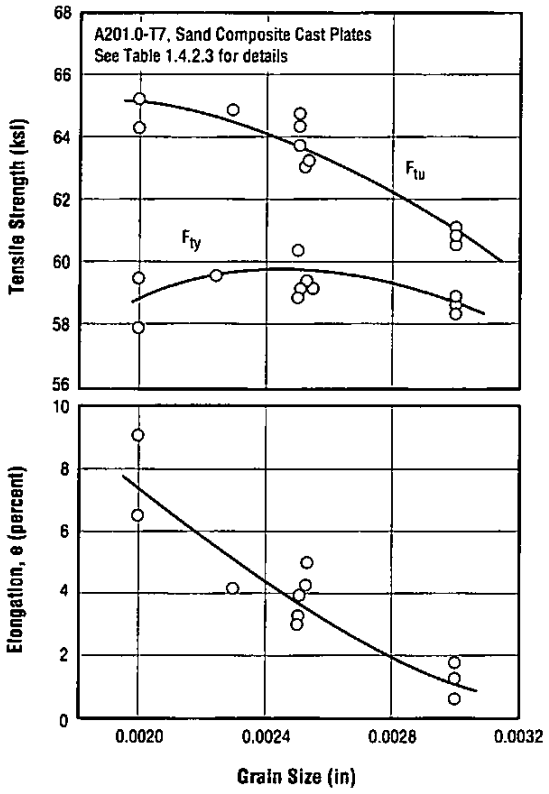


Figure 1.8.2.1 Effect of grain size on the tensile properties of a sand composite cast plate (Ref. 6, Fig. 75)

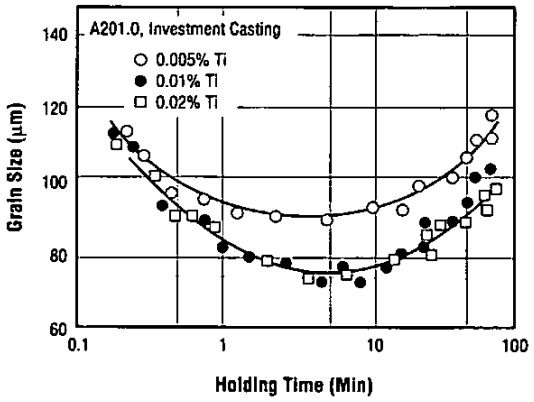


Figure 1.8.2.2 Effect on holding time and titanium content on grain size of melt inoculated with 5%Ti - 1%B (Ref. 12, Fig. F)

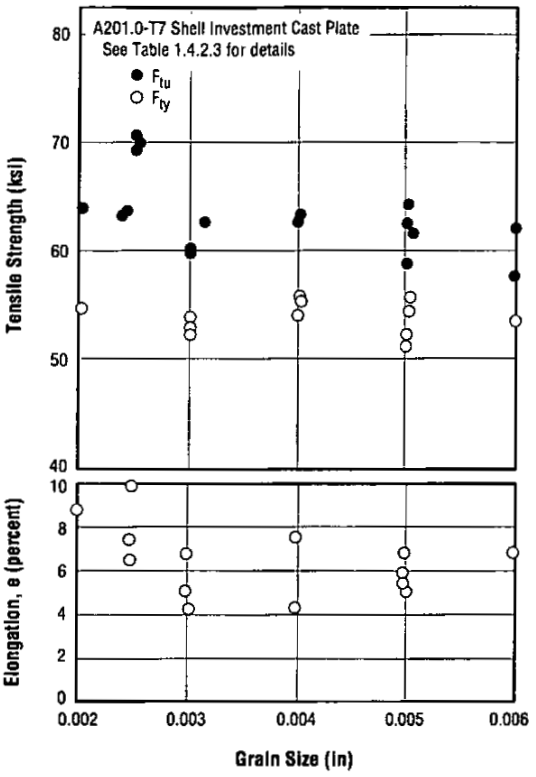


Figure 1.8.2.3 Tensile properties of shell investment cast plate at various grain sizes (Ref. 6, Fig. 74)

Table 1.9.1.1 Possible grain boundary phases present in castings (Ref. 12, Appendix B)

Alloy	A201.0
Form	Casting
Grain Boundary Phase	Melting Temperature (F)
$CuAl_2$	1096
$CuMgAl_2$	945
Ag_2Al	1340
$Cu_2Mn_3Al_{20}$	1141
$(CuFeMn)Al_6$	1209
$(CuFeMn)_3Si_2Al_{15}$	986
$FeSiAl_5$	1132
Mg_2Si	1103
$(FeMn)Al_6$	1213
$TiAl_3$	2338

Table 1.9.2.1 Effect of casting defects on the tensile properties of shell investment and sand composite mold castings (Ref. 6, Figs. 76, 77)

Alloy	A201.0-T7			
Condition[a]	For Casting and Heat Treat Details, See Table 1.4.2.3			
Form	Shell Investment		Sand Composite	
Defect Type	Shrinkage		Dross	
Radiographic Grade	AB	CD	B	D
F_{tu} (ksi) range	59.5 – 61.0	56.0 – 56.4	65.2 – 68.0	54.3 – 57.9
F_{ty} (ksi) range	51.6 – 53.0	51.2 – 51.8	57.6 – 60.2	51.4 – 53.5
e (percent) range	6.2 – 7.2	3.3 – 3.9	6.5 – 9.4	0.7 – 2.0

[a] Specially cast plates with defects.

Table 1.9.3.1 Effect of round gas porosity on the tensile properties and fracture toughness of defective step plates compared with Grade B plates (Ref. 6, pp. 267, 269)

Alloy	A201.0-T7	
Condition	Step Plates, See Figure 1.8.1.1	
Radiographic Grade	D[a]	B[b]
F_{tu} (ksi) Average Minimum Maximum n[c]	 58.2 56.7 69.3 4	 64
F_{ty} (ksi) Average Minimum Maximum n	 56.1 54.9 57.2 4	 56.1
e (percent) Average Minimum Maximum n	 1 1 1 4	 5.6
K_{Ic} (ksi $\sqrt{in.}$) Average[d] Minimum Maximum	 24.4 23.4 25.3	 24

[a] Round gas porosity No. 5 and 6.

[b] Average - specimens from designated areas.

[c] n = number of specimens.

[d] Round gas porosity No. 6.

Table 1.9.5.1 Effect of hot isostatic pressing on specimens removed from rejected turbofan rim (Ref. 7, Tables 6, 7)

Alloy	A201.0				
Form	Turbofan Engine Front Frame Rim				
Condition	HIP + 940F 2 hr + 970F 2 hr + 980F 6 hr, WQ + RT, 12 hr + 370F 5 hr, AC				
Grade	Porosity Radiographic Grade C Before HIP				
HIP Cycle	None	950F/10 ksi/6 hr	950F/10 ksi/12 hr	950F/15 ksi/6 hr	980F/10 ksi/6 hr
F_{tu} (ksi)					
n[a]	6	6	13	7	6
Mean	28.3	30.1	57.1	66.5	37.7
Sdev[b]	9.8	11.37	8.57	2.99	8.07
F_{ty} (ksi)					
n[a]	6	6	13	7	6
Mean	(c)	(c)	49.3	49.7	(c)
Sdev[b]			5.5	3.00	
RA (percent)					
n[a]	6	6	13	7	6
Mean	1.3	1.52	10.3	14	1.8
Sdev[b]	0.23	0.75	5.66	3.97	0.612
e (percent)					
n[a]	6	6	7	7	6
Mean	1.7	1.5	9.8	9.8	1.6
Sdev[b]	0.321	0.505	2.14	2.14	0.271

[a] n = number of tests.

[b] Standard deviation.

[c] Specimens failed before 0.2 percent strain.

Table 1.9.6.1 Tensile properties of squeeze cast and permanent mold castings (Ref. 20, Table 2)

Alloy	A201.0-T6	
Form	Castings[a]	
Composition	Within AMS 4223	
Cast Process	Squeeze 22 ksi	Permanent Mold
F_{tu} (ksi)	72	65
F_{ty} (ksi)	65	55
e (percent)	12.1	8
Grain Size (in.)	0.004	—

[a] Details concerning the mold design and size not given.

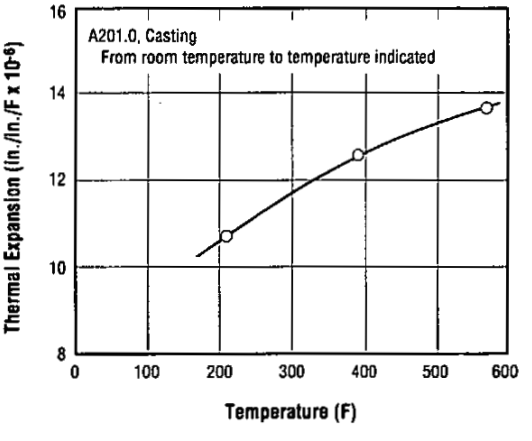


Figure 2.1.4 Thermal expansion (Ref. 17)

Table 2.3.2.1 Intergranular and stress corrosion behavior as a function of aging temperature and time (Ref. 11, Fig. 16)

Alloy	A201.0						
Composition	4.85Cu, 0.72Ag, 0.28Mg, 0.30Mg						
Form	Green Sand Cast Bars						
Condition	ST[a] + Age						
Age Temperature (F)	0	300	320	310(-T6)	330	360	370(-T7)
Age Time (hr)		1	2	20	10 - 32	12	5
Intergranular[b] Penetration (mils)	0	5	20	12.5	10	0	0
SCC Failure Time[c]	> 30 days	< 24 hr	< 24 hr	5 days	< 30 days	> 30 days	> 30 days

[a] Not given.

[b] Immersion for 6 hours at 86F in 57g NaCl + 10 mil 30% H_2O_2 in 1 liter distilled water.

[c] Alternate immersion at 75% F_{ty} in 3.5% NaCl solution 50 minutes + 10 minutes out.

Table 3.1.1 AMS Specified mechanical properties (Refs. 1-3)

Alloy	A201.0-T4			A201.0-T7			B201.0-T7[a]		
AMS[b]	4223(1)			4229(2)			4242(3)		
Specimens Location	Designated Areas	Other Areas	Separately Cast	Designated Areas	Other Areas	Separately Cast	Designated Areas	Other Areas	Integrally Attached Coupons
F_{tu} (ksi) min.	50	35	50	60	56	60	60	56	62
F_{ty} (ksi) min.	30	25	30	50	48	50	50	48	55
e (percent) min.	12	5	12	3	1.5	3	3	2	5
Hardness - BHN 10/500 10/1000	80 - 110 85 - 115			110 - 145 115 - 150					

[a] Specimens cut from designated area of a casting or from an attached coupon shall show no evidence of stress corrosion cracking when tested at 37.5 ksi for 30 days in accordance with ASTM G 44.

[b] AMS 4223 and 4229 also call out requirements for stress corrosion resistance but these are not specific as in AMS 4242.

Table 3.1.2 Tensile properties specified in MIL-A-21180D (Ref. 8)

Alloy	A201.0			
Condition	-T7			
Specimen Location	Designated Areas		Any Area	
Strength Class	1	2	10	11
F_{tu} (ksi)	60	60	60	56
F_{ty} (ksi)	50	50	56	48
e (percent)	3	5	3	1.5

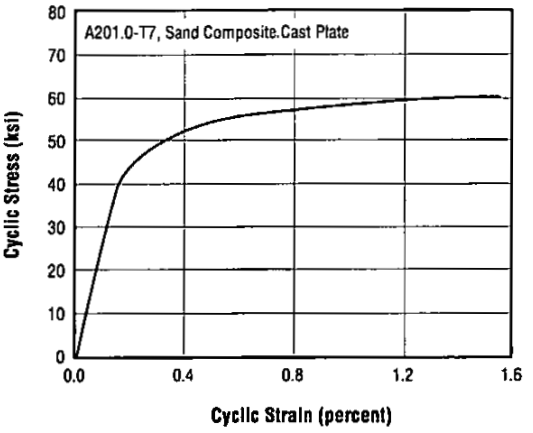


Figure 3.2.1.1 Cyclic stress-strain curve for specimen from sand composite cast plate (Ref. 9, Fig. 89)

Table 3.2.1.2 Tensile and compression properties of specimens removed from sand cast mold step plates (Ref. 6, pp. 226, 235)

Alloy	A201.0			
Form	Sand Mold Cast Step Plates, See Figure 1.8.1.1			
Condition	For Heat Treatment, See Table 1.8.1.2			
Foundry	A		B	
Step Plate Location	Designated Area	Areas Not Designated	Designated Area	Areas Not Designated
F_{tu} (ksi)				
Average	64.0	60.5	65.8	65.4
Minimum	59.9	55.4	62.8	62.9
Maximum	69.0	66.6	69.6	67.6
n [a]	51	32	52	33
F_{ty} (ksi)				
Average	58	55.3	60.2	61.2
Minimum	53.7	50.7	56.2	67.7
Maximum	62.7	58.7	63.4	63.5
n	51	32	52	33
e (percent)				
Average	6	4	6	3
Minimum	2	3	2	1
Maximum	11	8	9	9
n	51	32	52	33
F_{cy} (ksi)				
Average	64.7	55.3	64.2	68.9
Minimum	63.4	57.0	62.0	61.6
Maximum	65.5	54.5	64.2	63.9
n	5	5	5	5

[a] Number of tests.

Table 3.2.1.3 Smooth and notch tensile results for specimens from sand composite cast plates from three foundries (Ref. 9, Tables D1-D3)

Alloy	A201.0		
Composition	AMS 4242		
Form	16 x 6 x 1.25-in. Thick Cast Plates from Three Foundries Each Foundry used Metal Chills in Somewhat Different Rigging		
Grain Size	0.0032 in.		
HIP	950F, 15 ksi, 3 hr		
Supplier	Foundry A	Foundry B	Foundry C
Number of Tests	8	10	8
Solution Treat	940F 2 hr + 960F 2 hr + 980F 16 hr, RT WQ	940F 2 hr + 950F 2 hr + 980F 16 hr, RT WQ	920F 2 hr + 950F 2 hr + 970F 2 hr + 980F 16 hr, RT WQ
Age	380F 5 hr	360F 8 hr	RT 24 hr + 360F 8 hr
F_{tu} (ksi) Average Minimum Maximum	 66 65 67	 70 68 73	 67 64 70
F_{ty} (ksi) Average Minimum Maximum	 57 54 58	 63 60 66	 60 58 62
e (percent) Average Minimum Maximum	 9 8 11	 8 7 9	 8 7 10
NYS/F_{ty}[a] Average Minimum Maximum	 1.59 1.5 1.65	 1.32 1.27 1.38	 1.5 1.43 1.57

[a] ASTM E 602 0.5-inch diameter specimen.

Table 3.2.1.4 Tensile properties sand cast bars aged to the -T6 and -T7 conditions (Ref. 5, Table 1)

Alloy	A201.0	
Form	Green Sand Cast Bars	
Composition	As AMS 4223 except 0.16 - 0.35Mg	
Solution Treat	970F 2 hr + 985F 20 hr, WQ	
Age	310F 20 hr, -T6	370F 5 hr, -T7
F_{tu} (ksi) Average Minimum Maximum n[a]	 67.9 66.3 69.4 6	 65.7 65.3 66.0 3
F_{ty} (ksi) Average Minimum Maximum n	 58.4 55.7 67.7 6	 62.7 63.1 62.6 3
e (percent) Average Minimum Maximum n	 8.1 7 10.5 6	 2.7 2 4 3

[a] Number of bars tested.

Table 3.2.1.5 Tensile and compressive strength, elastic modulus and Vickers hardness for three types of castings providing different cooling rates (Ref. 16, Tables A1-A3)

Alloy	A201.0								
Composition	Within AMS 4223								
Solution Treat	955F 2 hr + 385F 14 hr, WQ + RT 24 hr								
Cast Form [a]	Permanent Mold			Sand Cast			Insulated		
Temper [b]	-T43	-T6	-T7	-T43	-T6	-T7	-T43	-T6	-T7
F_{tu} (ksi)	59	65	63	52	57	56	40	52	51
F_{ty} (ksi)	36	58	57	35	52	54	33	51	50
e (percent)	21	7	6	8	1	1.7	7	2	0.8
RA (percent)	21	11	8	10	3.4	1.7	6	1.8	1.3
F_{cy} (ksi)	39	63	62	58	58	59	35	35	55
E-Tension (1000 ksi)	9.25	10.8	11.2	8.0	9.4	9.1	8	9.5	8.4
E-Compression (1000 ksi)	9.94	10.6	10	10	8.2	10.3	10	9.1	10.4
Vickers Hardness	135	153	145	133	152	150	128	148	128

a Casting details not given.

b -T43 = Age 310F 1/2 hour, AC
-T6 = Age 310F 20 hours, AC
-T7 = Age 370F 5 hours, AC.

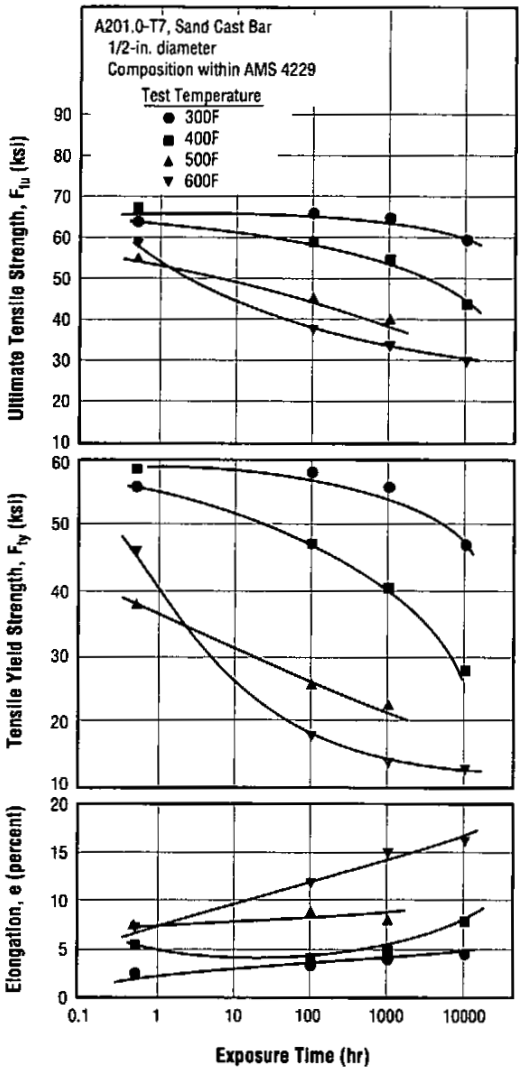


Figure 3.2.1.6 Effect of exposure time at elevated temperature on room temperature tensile properties of -T7 sand cast test bars (Ref. 10, Table 4)

Table 3.2.5.1 Shear strength of specimens removed from sand cast mold step plates (Ref. 6, p. 235)

Alloy	A201.0			
Form	See Figure 1.8.1.1			
Condition	See Table 1.8.1.2			
Foundry	A		B	
Step Plate Location	Designated Area	Areas Not Designated	Designated Area	Areas Not Designated
F_{su} (ksi)				
Average	41.0	38.8	40.2	39.4
Minimum	40.1	37.2	40.1	38.7
Maximum	41.3	39.9	41.3	39.9
n [a]	5	5	5	5

[a] Number of tests.

Table 3.2.6.1 Bearing strength of specimens removed from sand cast mold step plates (Ref. 6, p. 235)

Alloy	201			
Form	See Figure 1.8.1.1			
Condition	See Table 1.8.1.2			
Foundry	A		B	
Step Plate Location	Designated Area	Areas Not Designated	Designated Area	Areas Not Designated
e/D	1.5			
F_{bru} (ksi)				
Average	99.5	107.4	110.0	108.4
Minimum	93.2	106.1	110.2	107.2
Maximum	103.6	108.7	111.4	109.9
n[a]	6	5	5	5
F_{bry} (ksi)				
Average	88.7	87.8	98.7	90.4
Minimum	86.6	87.1	91.3	89.1
Maximum	90.1	88.2	98.8	92.8
n	5	5	5	5
e/D	2			
F_{bru} (ksi)				
Average	136.9	127.5	142.4	129.7
Minimum	136.1	125.5	139.1	105.3
Maximum	139.6	129.7	145.5	136.5
n	5	5	5	5
F_{bry} (ksi)				
Average	111.1	87.8	112.6	104.4
Minimum	103.8	87.1	106.1	102.0
Maximum	131.4	88.3	115.4	105.5
n	5	5	4	5

[a] Number of tests.

Table 3.2.7.2.1 Plane strain fracture toughness of separately sand cast blocks (Ref. 6, p. 247)

Alloy	A201.0-T7	
Condition	Separately Sand Cast Blocks	
Foundry	A	B
F_{tu} (ksi)		
Average	61.3	58
Minimum	59.4	54.8
Maximum	63.2	60.1
n[a]	2	3
K_{Ic} (ksi $\sqrt{in.}$)		
Average	24.1	32.2
Minimum	23.2	30.7
Maximum	24.9	33.2
n	2	3

[a] Number of tests.

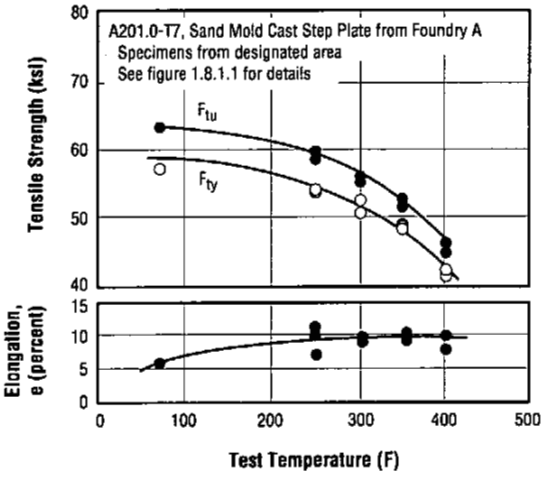


Figure 3.3.1.1 Effect of test temperature on tensile properties of specimens from sand mold step plates from Foundry A (Ref. 6, Table 47)

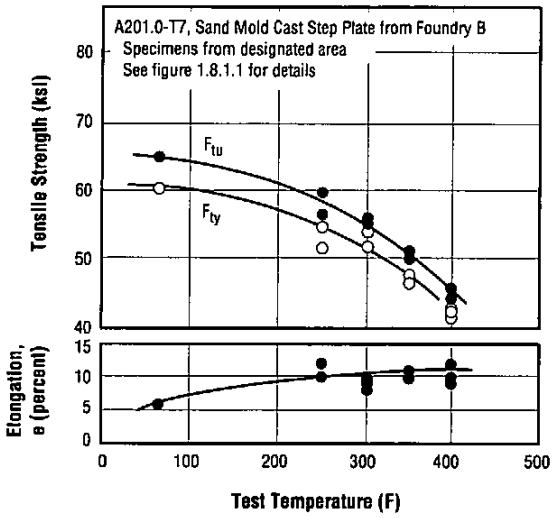


Figure 3.3.1.2 Effect of test temperature on tensile properties of specimens from sand mold step plates from Foundry B (Ref. 6, Table 48)

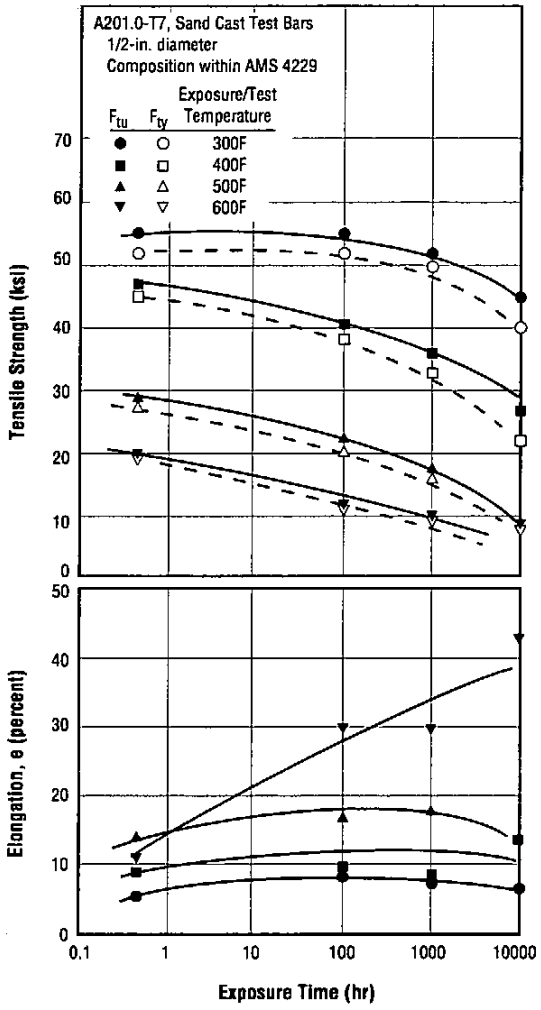


Figure 3.3.1.3 Effect of exposure time and test temperature on -T7 sand cast test bars tested at the exposure temperature (Ref. 10, Table 3)

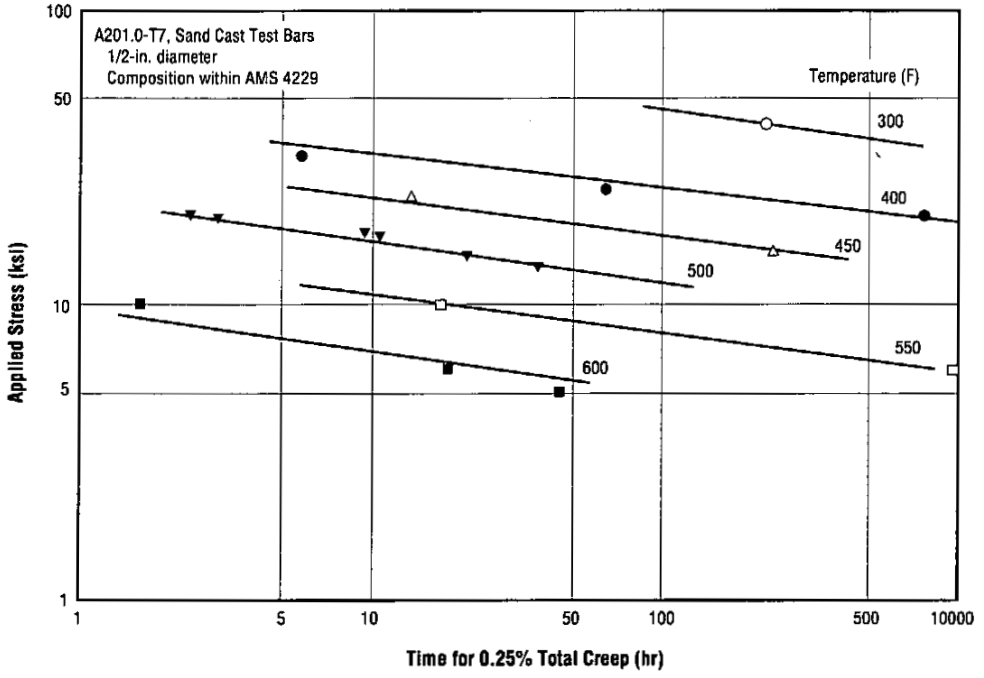


Figure 3.4.1 Time for 0.25 percent total creep at several elevated temperatures for -T7 sand cast test bars (Ref. 10, Fig. 5)

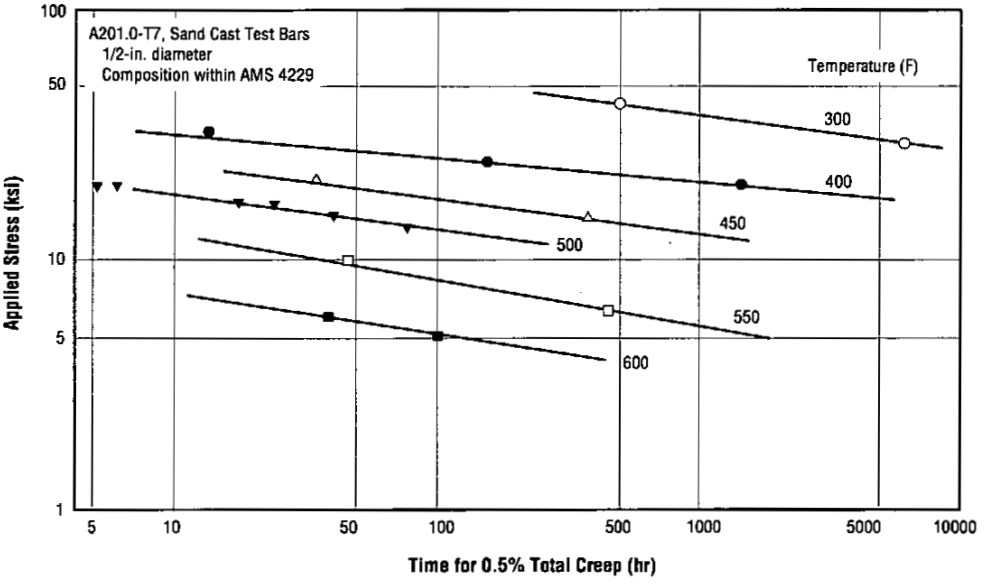


Figure 3.4.2 Time for 0.5 percent total creep at several elevated temperatures for -T7 sand cast test bars (Ref. 10, Fig. 4)

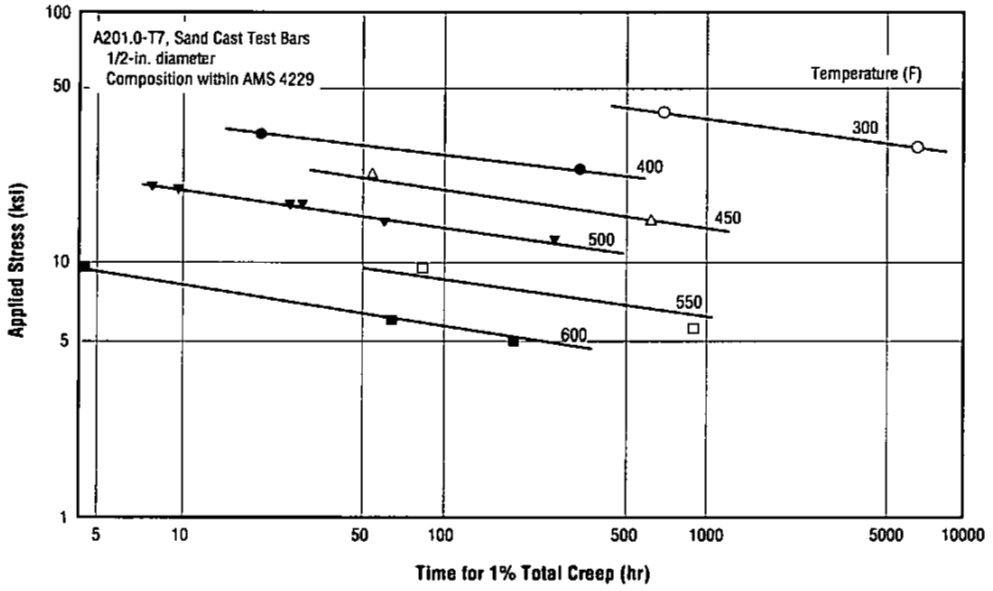


Figure 3.4.3 Time for 1.0 percent total creep at several elevated temperatures for -T7 sand cast test bars (Ref. 10, Fig. 3)

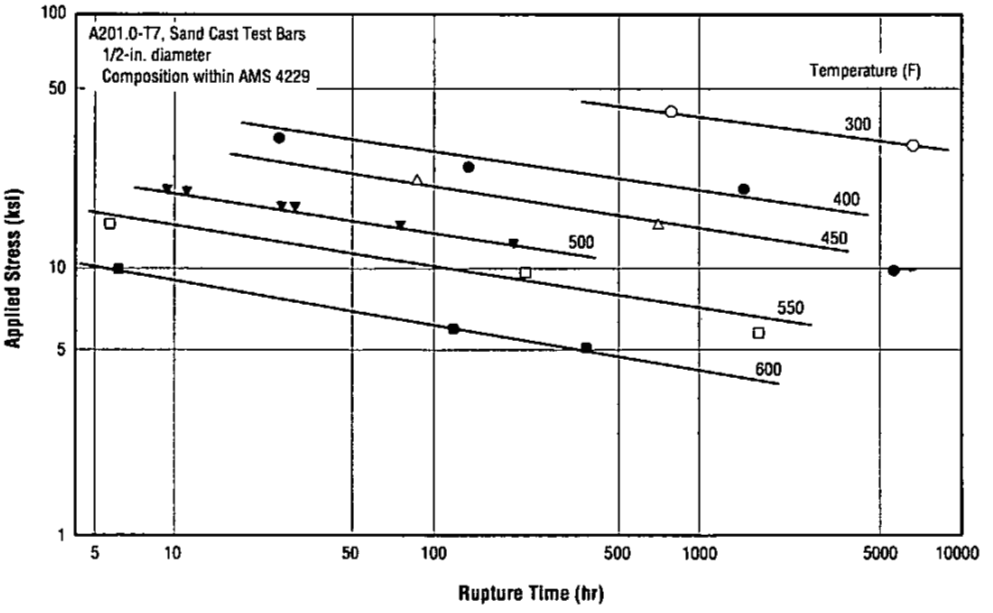


Figure 3.4.4 Rupture time at several elevated temperatures for sand cast test bars (Ref. 10, Fig. 1)

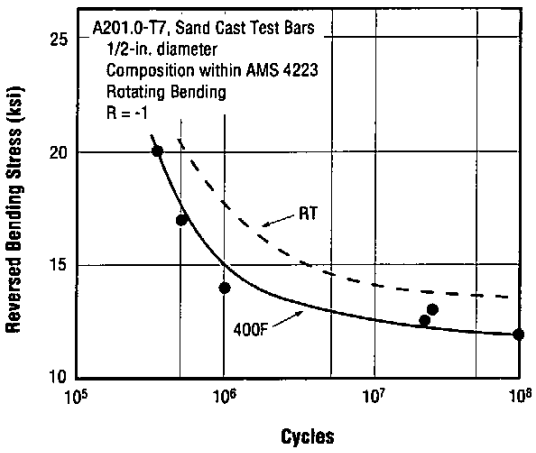


Figure 3.5.1.1 Rotating bending fatigue strength at room temperature and 400F for -T7 sand cast test bars (Ref. 10, Fig. 6)

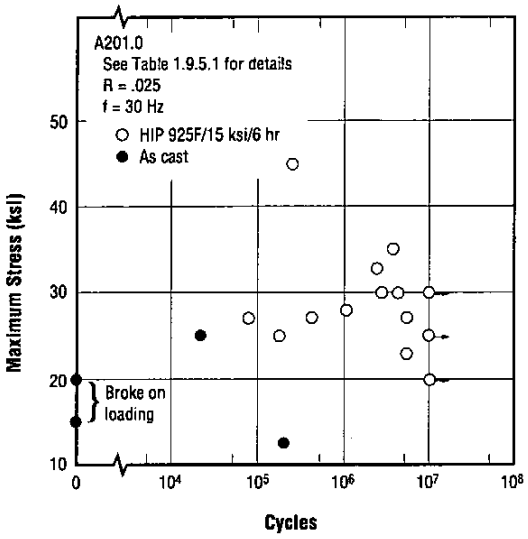


Figure 3.5.1.2 Effect of HIP processing on the fatigue strength of axially loaded specimens from a rejected turbofan rim (Ref. 7, Table 8)

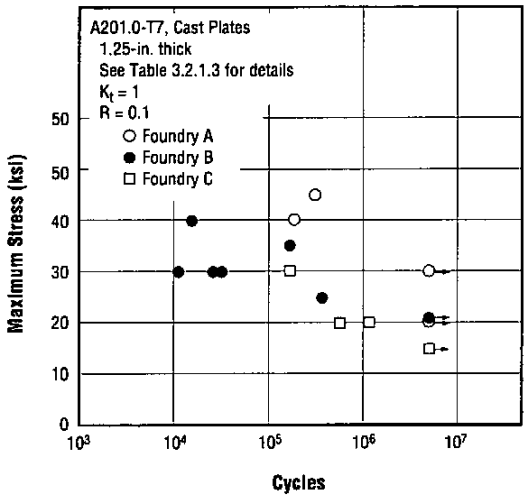


Figure 3.5.1.3 Fatigue strength of axially loaded specimens from sand cast plates from three foundries (Ref. 9, Table 8)

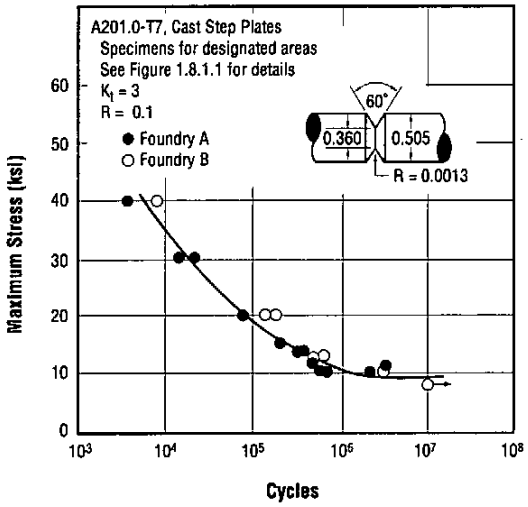


Figure 3.5.1.4 Fatigue strength of axially loaded notched specimens from designated areas of sand cast step plates (Ref. 6, Fig. 108)

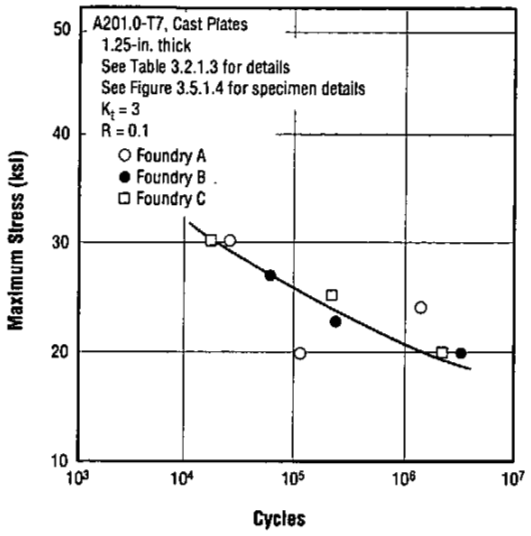


Figure 3.5.1.5 Fatigue strength of axially loaded notch specimens from sand cast plates from three foundries (Ref. 9, Table D5)

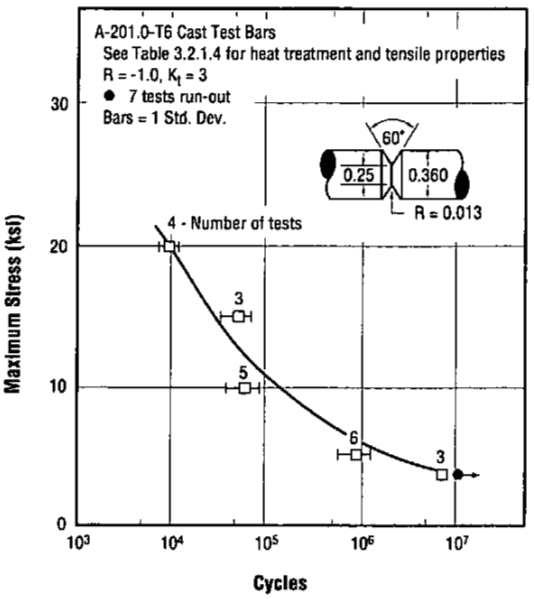


Figure 3.5.1.6 Fatigue strength (R = -1.0) of axially loaded -T6 notched (K_t = 3) specimens from individually cast test bars (Ref. 5, Table A2)

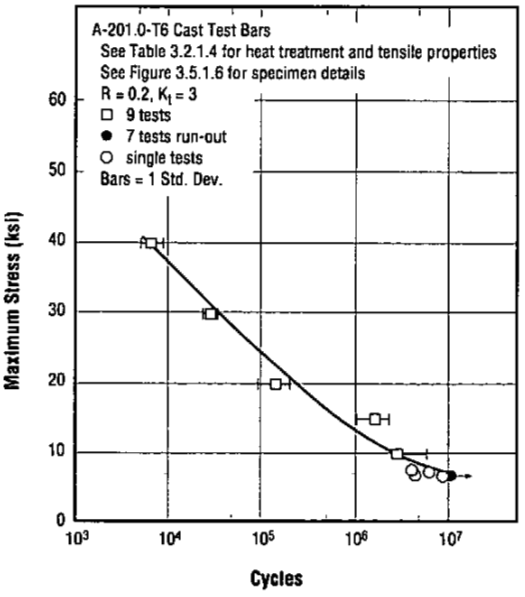


Figure 3.5.1.7 Fatigue strength (R = 0.2) of axially loaded -T6 notched (K_t = 3) specimens from individually cast test bars (Ref. 5, Table A1)

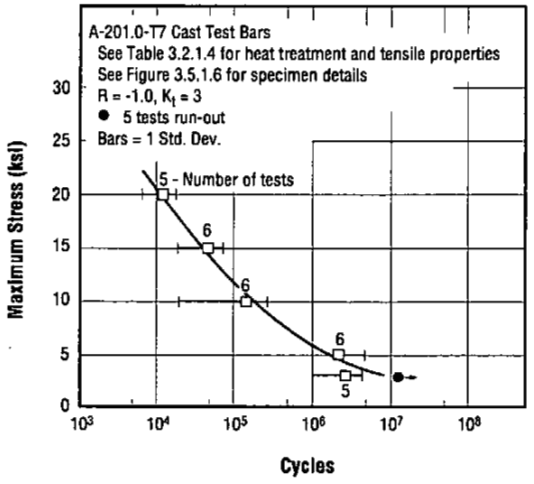


Figure 3.5.1.8 Fatigue strength (R = -1.0) of axially loaded -T7 notched (K_t = 3) specimens from individually cast test bars (Ref. 5, Table A6)

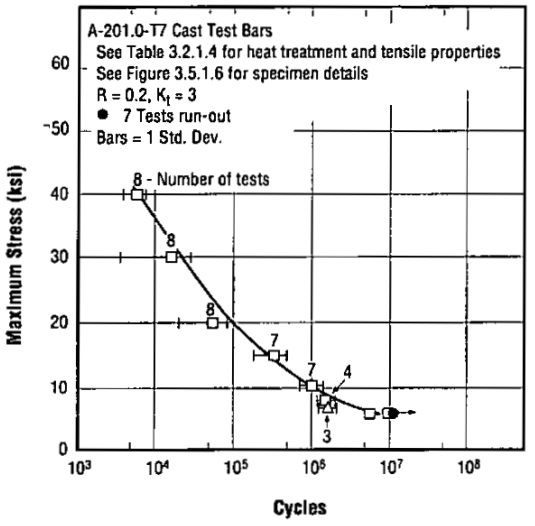


Figure 3.5.1.9 Fatigue strength (R = 0.2) of axially loaded -T7 notched (K_t = 3) specimens from individually cast test bars (Ref. 5, Table A4)

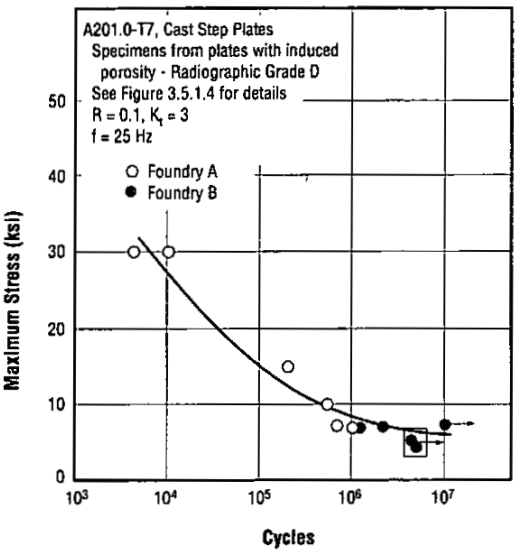


Figure 3.5.1.10 Fatigue strength of axially loaded notched (K_t = 3) specimens from sand cast step plates containing porosity (Ref. 6, Fig. 119)

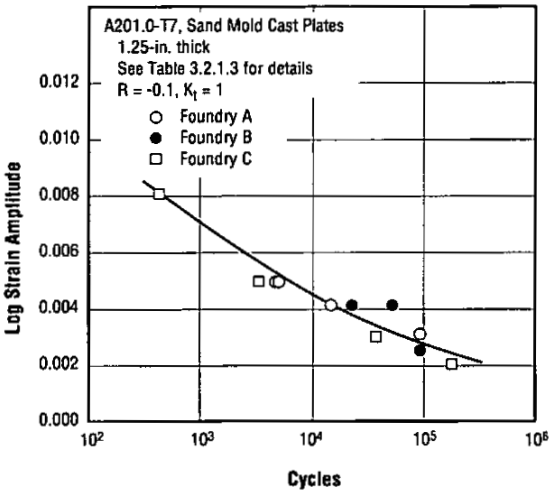


Figure 3.5.2.1 Strain vs life data for specimens from sand cast plate from three foundries (Ref. 9, Table D6)

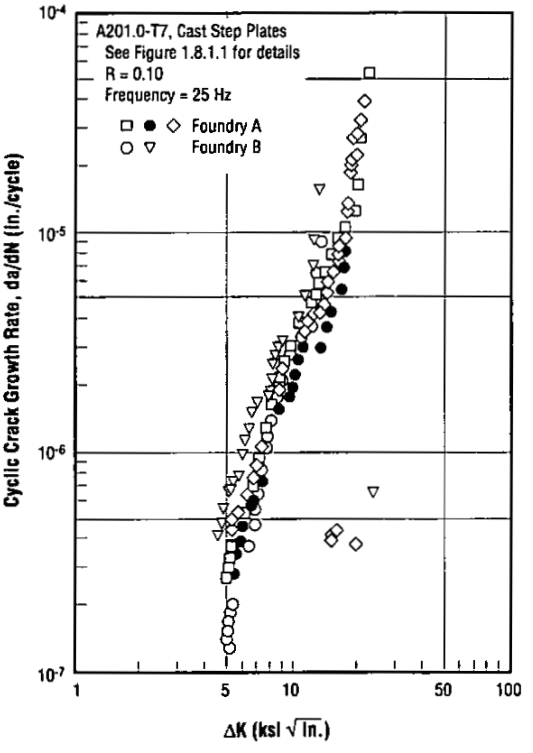


Figure 3.5.3.1 Fatigue crack growth rates for specimens removed from sand cast step plates from two foundries (Ref. 6, Fig. 109)

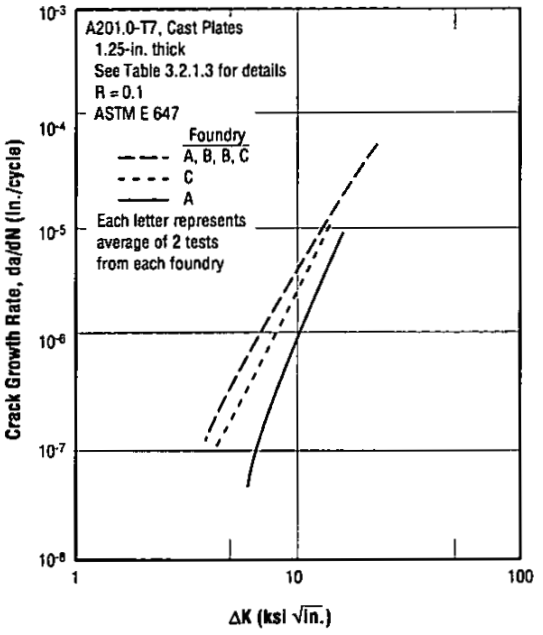


Figure 3.5.3.2 Fatigue crack growth rates for sand cast plates from three foundries (Ref. 9, Tables D1-D6)

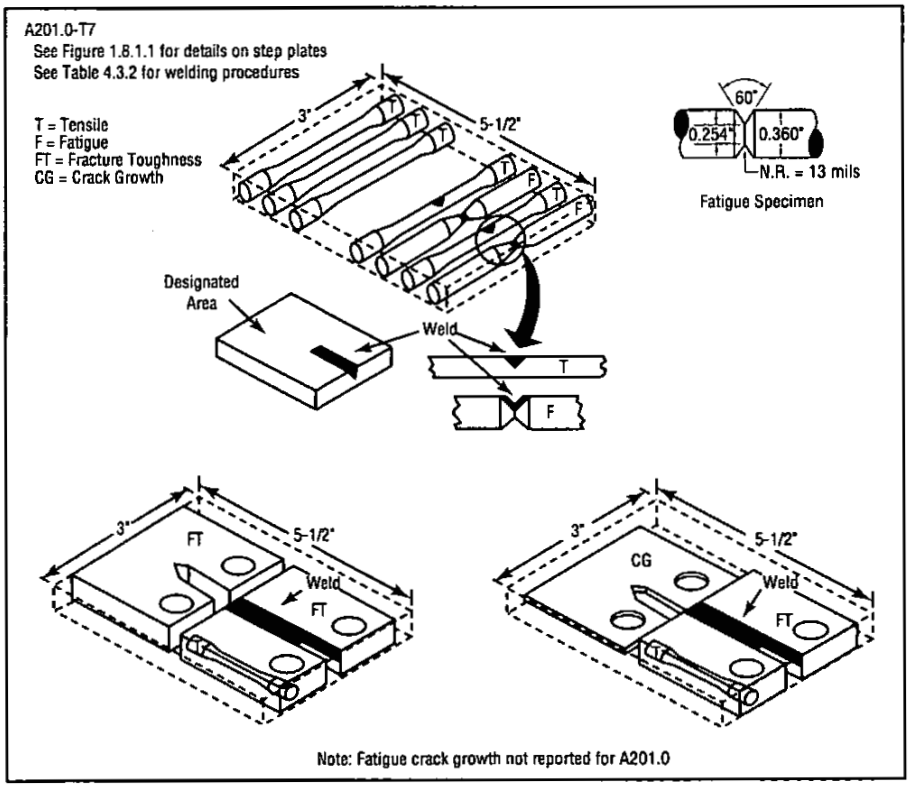


Figure 4.3.1.1 Location of specimens in the designated areas of welded step plates (Ref. 6, Fig. 110)

Table 4.3.1.2 Conditions used to produce welds in step plates (Ref. 6, pp. 251-252)

Alloy	A201.0
Condition	-T7
Coupon Location	Designated Areas of Step Plates (See Figure 4.3.1.1)
Weld Preperation	60° V-groove 0.25-in. deep with 3/32-in. radius, cleaned with 47% HNO_3 + 3% HF + 50% water + deionized water rinse + air dry
Filler Metal	0.094-inch diameter wire with AMS 4233 composition
Welds	4 pass GTA direct current, straight polarity, 100% He shielding, current 130-150 amps, voltage 18-22 v

Table 4.3.1.3 Effect of GTA welding on the average tensile properties and fracture toughness of sand cast step plates (Ref. 6, pp. 256-258)

Alloy	A201.0			
Form	Specimens from Welded Designated Areas of Step Plates See Figure 4.3.1.1 for Weld Locations and Table 4.3.1.2 for Welding Conditions			
Step Plate Source	Foundry A		Foundry B	
Specimen Location	Parent Metal	Weld	Parent Metal	Weld
F_{tu} (ksi)	64	66	66	66
F_{ty} (ksi)	58	59	60	60
e (percent)	5.6	5.3	5.6	5.6
K_Q (ksi $\sqrt{in}$)	27	37	29	—

REFERENCES

1. AMS 4223C, Society of Automotive Engineers (March 1996).
2. AMS 4229C, Society of Automotive Engineers (January 1990).
3. AMS 4242, Society of Automotive Engineers (July 1986).
4. AMS 4233, Society of Automotive Engineers (October 1986).
5. K.J. Oswalt, "Comparsion of the Fatigue Behavior of High Strength Cast Aluminum Alloys 201 and A357," Northrop Corporation, Hawthrone, CA (December 1, 1971).
6. K.J. Oswalt and Y. Lii, "Manufacturing Methods for Process Effects on Aluminum Castings Allowables," Northrop Corporation, Aircraft Division, Final Report for Period April 1980 to July 1984, AFML-TR-4117 (March 1986).
7. S.J. Vonk, G.S. Hoppin and K.W. Benn, "Hot Isostatic Pressing of Aluminum Alloy Castings," Garrett Turbine Engine Co., Phoenix AZ, Naval Air Systems Command, Contract N00019-79-0649, Final Report (June 15, 1991).
8. Military Specification, "Aluminum Alloy Castings, High Strength," MIL-A-21180D (December 14, 1991).
9. M.W. Ozelton, S.J. Mocarski and P.G. Porter, "Durability and Damage Tolerance of Aluminum Castings," Northrop Corp., Aircraft Division, Final Report for Period Sept. 1985 to June 1991, WL-TR-91-4111 (June 1991).
10. C.M. Tyler, F.R. Mollard and W.S. Peterson, "Alloy 201 (KO-1) Aluminum Casting Alloy with Excellent High Temperature Properties," TMS Paper Selection, Metallurgical Society of AIME, Paper No. F71-3.
11. M.S. Misra and K.J. Oswalt, "Corrosion Behavior of Al-Cu-Ag (201) Alloy," *Metals Engineering Quarterly*, p. 39 (May 1976).
12. Steve Kennerknecht, "Metallurgical Aspects of Quality Control in the Production of Premium Quality Aluminum Investment Castings for the Aerospace Industry," AGARD (CP 325) (1982).
13. J.A. Taylor, B.A. Parker and J. Pollmear, "Precipitation in Al-Cu-Mg-Ag Casting Alloy," *Metal Science*, p. 478 (October 1978).
14. S. Abis, P. Mengucci and G. Riontino, "A Study of the High Temperature Ageing of Al-Mg-Cu-Ag Alloy 201," *Philosopical Magazine*, B, Vol. 67, No. 4, p. 465 (1993).
15. ibid., "Influence of Si Additions on the Aging Process of an Al-Cu-Mg-Ag Alloy," ibid., Vol. 70, No. 5, p. 851 (1994).
16. "Mechanical Properties of Premium Aluminum Casting Alloys with Various Cooling Rates," The Olin Corporation, New Haven, CT (January 1973).
17. Alloy Digest, "Aluminum Alloy 201.0 (July 1995).
18. I.J. Polmear, " The Effects of Small Additions of Silver on the Aging of Some Aluminum Alloys," Trans. Met. Soc., AIME, Vol. 230, p. 1331 (1950).
19. T.J. Bosworth, "Repair Welding Aluminum Castings," *Modern Casting*, p. 19 (April 1984).
20. J. Summers, A. Bloyce, and G.A. Chadwick, "Squeeze Castings of Aluminum Alloys," Hi Tech Materials R&D, Conference: Advanced Aluminum and Magnesium Alloys, The Netherlands, June 1990 (Published by ASM Intl., 1990).

1 General

Aluminum Alloy A357.0 is a premium Mg_2Si casting alloy developed for applications in the aerospace industry. It is normally produced to a standard specification as A357.0 and to a more carefully controlled specification as D357.0. The latter variety requires control of the dendrite arm spacing (DAS), tighter composition limits on impurities, radiographic requirements and in some cases requirements on fracture toughness and fatigue properties. Mechanical properties of F_{tu} = 50 ksi, F_{ty} = 40 ksi, and e = 5 percent can be obtained in properly engineered castings of this alloy. Large complex castings having thin and thick intersecting sections have been produced from A357.0 and D357.0. These castings have passed the same qualification tests applied to similar built-up wrought aluminum structures. Such cast parts, if put into production, can be cost efficient as compared to similar built-up wrought parts. It should be emphasized that castings for critical applications should be produced by foundries qualified for the production of premium castings. The important features for such qualification and the expected performance have been established by several Air Force programs that form the principal basis for this section.

It should be noted that the AMS Specifications for D357.0 were written after the major Air Force Programs were completed and, strictly speaking, it is not possible to directly connect the data in this section with these new Specifications. However, where the composition and mechanical properties conform to the AMS Specification for D357.0, the data are designated as D357.0; otherwise the data are designated as A357.0.

1.1 Commercial Designations

Cast A357.0, Cast D357.0

1.2 Alternate Designations - See Table 1.4.2

1.3 Specifications

AMS 4219C, AMS 4249, AMS 4241A, AMS 4246B, MIL-A-21180D, and ASTM B 108.

1.4 Composition

1.4.1 General. Magnesium and silicon are the major alloying elements with Mg_2Si being the primary hardening agent during aging. Tensile strength increases and ductility decreases with increasing amounts of magnesium, as shown in Figure 1.4.3.1. However, increases in magnesium content above about 0.6 percent have little effect on the tensile properties. The only other elements intentionally added are beryllium and titanium. They do not contribute significantly to the strength but have indirect beneficial effects. Thus, beryllium tends to reduce the oxidation of magnesium during melting, and to scavenge iron, which tends to form a brittle, intermetallic, Fe-Si phase that reduces ductility. Titanium is a grain refiner providing a fine dispersion of TiAl particles in the melt which act as nuclei for the primary aluminum dendrites. As will be discussed later, attempts are often made to control the eutectic microstructure through the additions of modifiers such as sodium or strontium. (See 1.8.5)

	Al
7.0	Si
0.6	Mg
0.15	Ti
0.05	Be

1.4.2 *[Table]* AMS and ASTM composition for A357.0 and D357.0.

1.4.3 Effect of element contents on tensile properties.

1.4.3.1 *[Figure]* Effect of magnesium content on the tensile properties of shell investment castings.

1.4.3.2 *[Figure]* Effects of iron, beryllium, and magnesium contents on tensile and fracture properties of plates cast in permanent molds.

Beryllium offsets to some extent the negative effects of increasing iron content.

1.4.3.3 *[Table]* Average tensile, notch yield strength ratio, and percent porosity for specimens cut from cast blocks produced with two chill rates and aged at two temperatures.

The faster Cu chill resulted in higher elongation, somewhat higher NTS/F_{ty} ratio, and less porosity. Age treatment significantly affected only the NTS/F_{ty} ratio for the slower Fe chill.

1.4.3.4 *[Figure]* Relative effects of silicon content on tensile properties of D357.0-T6 sand-castings.

Increasing Si content significantly decreases elongation, while causing only minor relative reduction in other tensile properties.

1.4.3.5 *[Figure]* Relative effects of magnesium content on tensile properties of D357.0-T6 sand-castings.

Within the specification range, increasing Mg content reduces elongation, but has little relative effect on other tensile properties.

1.4.3.6 *[Figure]* Relative effects of the combined titanium, manganese, and beryllium contents on tensile properties of D357.0-T6 sand-castings.

Increasing the content of these three elements reduces elongation and has little relative effect on other tensile properties.

This section produced with the support of NASA-Lewis Research Center.

© 1997 by Purdue Research Foundation, West Lafayette, Indiana 47907. All Rights Reserved. U.S. Government License. This material may be used, duplicated or disclosed by United States Government agencies without the payment of any royalty.

1.5 Heat Treatment

1.5.1 The heat treatment for both A357.0 and D357.0 is given in the applicable AMS specifications as 1000F to 1020F solution treatment with the solution time, quenching media and aging temperature being selected to produce the specified properties. The following heat treatment may be used as a guide: Solution treat 1000F to 1020F, 12 to 15 hours, followed by quenching in water with 15 percent ethylene glycol, and aging at 315 to 325F for 4 to 12 hours to produce the T6 condition. Quench delay time does not appear to be important.

Attempts to improve the properties of A357.0 by hot isostatic pressing of the as-poured castings were not successful. The cooling rates from the isostatic press are so slow that the alloy had to be solution heat treated following pressing. The process was able to close porosity but was not able to produce significant improvement over that obtained by the best normal foundry practice without hot isostatic pressing. (Ref. 25)

1.5.2 While the tensile properties decrease with increasing quench-water temperature (see Figure 1.5.6), a cold-water quench increases residual stress gradients and distortion in thin sections. These problems are minimized by quenching in warm water [e.g., 160F (Ref. 10)] or by the use of a water + glycol quench. Generally, the water is at room temperature and 15 to 25 percent ethylene glycol is added. It is common practice to delay aging for 16 hours following quenching. This delay tends to increase the elongation with only a slight decrease in tensile strength (Ref. 30). This effect may be inferred from Figure 1.5.9.

1.5.3 Straightening must be performed in the solution-treated condition.

1.5.4 *[Figure]* Effect of solution-treatment time on tensile properties of shell investment castings.

1.5.5 *[Figure]* Effect of solution-treatment time on tensile properties of sand-castings.

1.5.6 *[Figure]* Effect of quench-water temperature on tensile properties of shell investment castings.

1.5.7 *[Figure]* Effect of quench-water temperature on tensile properties of sand-castings.

1.5.8 *[Figure]* Effect of delay time between solution treatment and quench for shell investment castings.

1.5.9 *[Figure]* Effect of delay time between solution treatment and quench for sand-castings.

1.5.10 *[Figure]* Effect of aging time on tensile properties of investment castings.

1.5.11 *[Figure]* Effect of aging time on tensile properties of sand-castings.

1.6 Hardness

(See Figures 2.2.2.1, 2.2.2.2 and Table 3.1.1)

1.7 Forms and Conditions Available

Castings

1.8 Melting and Casting Practice

1.8.1 General. The mechanical properties of a casting are complex functions of the melting and pouring techniques, mold and core making, chilling and insulation, and the gating and risering methods. There are no general rules which may be applied to all types of castings and for critical applications a carefully planned development phase is essential. During a period from 1977 to 1984 the Air Force sponsored development programs at Northrop, General Dynamics, and Boeing. The goal of these programs was to develop cost-effective manufacturing methods and design specifications for the production of large, complex castings suitable for use in high-performance aircraft. The alloy A357.0-T6 was featured in these programs. The program at Northrop was concentrated on establishing an optimum composition for a premium A357.0 casting alloy (later designated as D357.0) and the development of design mechanical properties. The General Dynamics program demonstrated the successful production of an F-16 vertical-tail understructure. The Boeing "CAST" program was concerned with details of the casting process and the production of a large, thin-walled casting for the nose gear support bulkhead for the YC-14 airplane. The summary of foundry practices in Sections 1.8.3 and 1.8.4 is primarily taken from this program.

For assessment of mechanical properties, the following types of castings were used:

Northrop - Shell investment and composite, sand-cast, uniform-thickness plates (Tables 3.2.1.4 and 3.2.1.5) and stepped-plate, composite sand-castings with a designated area representing the maximum thickness which could be examined to insure detection of Grade B soundness (Figure 1.8.1.1).

General Dynamics - Separately cast sections of the vertical-tail understructure for the F-16 (Table 3.2.1.6) and the full casting (Table 3.2.1.7).

Boeing - Separately cast sections of the full-scale bulkhead shown in Figures 1.8.1.2 and 1.8.1.3.

1.8.1.1 *[Figure]* Sand-mold, stepped-plate configuration used in the Northrop Program to determine design property data for sand-cast A357.0-T6 from two suppliers. A (Magnesium Alloy Products) and B (Teledyne Cast Products). Two integral tensile coupons attached to optional locations.

1.8.1.2 *[Figure]* Large, thin-walled, composite sand-cast nose-gear support bulkhead for the YC-14 airplane. Ten identical castings were each produced by the Boeing and the Hitchcock Foundries using Boeing-developed manufacturing plans and tooling.

1.8.1.3 *[Figure]* Nose landing-gear support bulkhead casting showing locations of specimens removed from five sections of the casting (each section heat treated separately).

1.8.2 Fluidity. Good fluidity is especially important in the production of complex, thin-walled castings in order to avoid cold shuts and shrinkage defects. The double spiral fluidity test (Figure 1.8.2.1) was used to evaluate the effects of mold, sand, mold coatings, and alloy composition (Ref. 10). AFS 53, 70, and 140 silica sands were investigated with a sodium silicate - CO_2 binder. In addition, tests were made using zircon and chromite sand. Best results were obtained with AFS 70 sand. The effects of amorphous carbon and hexachlorethane mold coatings were investigated with the configuration shown in Figure 1.8.2.1, using AFS 70 mold sand and a pouring temperature of 1400F. The best results were obtained with amorphous carbon, which produced a 40 percent increase in fluidity compared with uncoated molds. Variations of silicon, magnesium, and beryllium within the composition limits of the alloy did not affect the fluidity.

1.8.2.1 *[Figure]* Double spiral fluidity test casting.

1.8.3 Holding temperature. The charge of molten metal is held until degassing and mold preparation are complete. Holding temperatures from 1250 to 1450F were investigated for holding times from essentially 0 to 24 hours. Charges were melted in 350-pound-capacity, silicon carbide crucibles with a minimum amount of surface exposed to the atmosphere (Ref. 5). Results showed that neither temperature nor holding time within the ranges investigated had a significant effect on silicon, magnesium, or beryllium contents of the melt, but that the amount of hydrogen in the melt increased with holding temperature and slightly with holding time. Based on these results, the holding temperature prior to degassing is suggested to be in the range between 1250 and 1325F.

1.8.4 Degassing. Hydrogen is the only gas having measurable solubility in aluminum. As shown in Figure 1.8.4.1, the solubility decreases rapidly as the melt cools to the solid state. This decrease in solubility results in trapped hydrogen gas in the form of porosity in the casting. The source of hydrogen is the reaction between molten aluminum and water. Water may be introduced into the melt in various ways including the products of fuel combustion, mold coatings, moisture absorbed or chemically combined with fluxes (the reaction products of fluxing with chlorine are highly hygroscopic), moisture adsorbed on the surface of the charge components or tools and moisture in the air.

The amount of hydrogen in the melt can be determined accurately by use of the Telegas analyzer (Ref. 11). This instrument is not generally suitable for use in a production environment and a so-called "vacuum-freeze" test is widely used. In this test a small sample of the melt is slowly solidified under a vacuum of about 5 mm of Hg, and watched carefully for the appearance of bubbles. Bubble formation is strongly resisted by the surface tension of the melt, but is greatly enhanced by the presence of minute inclusions. The presence of inclusions complicates the interpretation of the vacuum freeze test as an indicator of hydrogen content. However, the absence of bubbles coupled with the absence of porosity in the sectioned sample does indicate low hydrogen content. Boeing recommended that the hydrogen content of A357.0 not exceed 0.15 ml/100 gm within 2 hours of pouring (Ref. 10).

Boeing investigated three methods of degassing, namely the introduction of nitrogen gas, hexachlorethane, and a gaseous mixture of 90 to 95 percent nitrogen plus 10 percent chlorine. Degassing temperatures ranged from 1250 to 1400F, with times up to 2 hours. Satisfactory results were obtained (Figure 1.8.4.2) using either nitrogen with a carefully controlled flow rate or with a mixture of nitrogen and chlorine gas, with this mixture providing the most rapid degasification. Hexachlorethane was added in the form of tablets at a melt temperature of 1300 to 1350F. This chemical reacts with aluminum to produce a bubbling reaction. The effect of 2- to 4-ounce additions to a 350-pound melt was found to be unsatisfactory in that an increase in hydrogen content was observed (Ref. 5). The effect of a dried NaCl/KCl overflux was evaluated for the prevention of hydrogen absorption and removal of oxides. The hydrogen content increased due to the hygroscopic nature of the flux. Boeing points out that when using chlorine as a degassing agent, all degassing tools should be preheated prior to immersion in the melt. Omission of this precaution may result in an explosion. Degassing with the nitrogen-plus-chlorine mixture at 1250 and 1300F did not produce a loss of alloy constituents but at 1400F there was a loss of magnesium and beryllium.

1.8.4.1 *[Figure]* Solubility of hydrogen in solid and molten aluminum as a function of temperature.

1.8.4.2 *[Figure]* Effect of degassing time and temperature on hydrogen content.

1.8.5 Eutectic modifiers. The interdendritic phases consist primarily of silicon and the binary eutectic, Al + Si, which together constitute about 90 percent of the interdendritic particle area. Other interdendritic phases include the ternary eutectic (Al + Si + Mg_2Si) and complex compounds of Al-Fe-Si-X (Ref. 21). Ideally, the interdendritic structure should be finely divided and spheriodal. Acicular forms tend to reduce the alloy ductility. The interdendritic morphology is controlled in part by the phosphorus content with acicular silicon particles being associated with increasing phosphorus (Ref. 27). The phosphorus may be

effectively removed by the addition of sodium or strontium. These elements form compounds with magnesium, and these compounds combine with the phosphorus. The result is a fibrous eutectic. However, the use of these modifiers is not without problems. Sodium has a much higher reactivity than strontium at molten aluminum temperatures and tends to burn off. Boeing (Ref. 5) found that the addition of sodium tended to produce bubbles and increased the hydrogen content. Degassing following the introduction of sodium reduced the sodium level below that required for eutectic modification.

The addition of strontium did not produce a visible reaction, but the melt hydrogen content increased and degassing depleted the strontium content. Considering the problems associated with sodium and strontium additions, Boeing chose not to use modifiers but depended on controlled solidification rates to produce a satisfactory microstructure. However, strontium is a frequently used modifier and antimony also has been used (Ref. 26). It has the advantage of being unaffected by holding time, degassing, or remelting. However, it produces a lamellar eutectic microstructure which is somewhat inferior to the fibrous type.

1.8.5.1 *[Figure]* Effect of strontium content on the ratio of notched tensile strength to tensile yield strength of D357.0-T6 sand-castings.

1.8.6 Pouring temperature. Pouring temperature for large thin-walled castings is very critical. If the temperature is too high, a coarse grain structure will result along with porosity, shrinkage, and oxide formation. If the temperature is too low, misruns, cold shuts, and shrinkage can be encountered. The pouring temperature for aluminum castings is usually between 1325 and 1450F. In the Boeing program, pouring temperature was investigated over the range from 1350 to 1450F using the test-plate configuration shown in Figure 1.8.6.1. The highest values of F_{tu}, F_{ty}, and e were obtained for those specimens nearest the chill, and poured at 1350F.

1.8.6.1 *[Figure]* Test plate configuration incorporating a chill.

1.8.7 Mold and core making. In general, molds and cores should be strong enough to permit handling and to resist deterioration by the molten metal, have good permeability to evolved gases, hold dimensional tolerances, and provide good shake-out capability. Sand types and binder combinations were investigated in the Boeing program (Ref. 5). Round-grain silica sands were found to be superior to the angular, olivine types in terms of flowability during molding and in terms of casting surface finish. AFS 70 silica sand was compared with olivine sand using a synthetic resin binder. Results showed a pronounced superiority for the silica sand in terms of tensile and compressive strength as a function of storage time and in terms of permeability. In addition to the synthetic resin binder, similar tests were also conducted with silica sand using sodium silicate cured with CO_2, sodium silicate no-bake, and oil-urethane no-bake systems. While silica sand bonded with sodium silicate systems displayed good mold properties, the strengths obtained decreased after relatively short (20 hours) storage time. Poorest performance was obtained using the synthetic resin binders. On balance, the best performance in terms of strength after prolonged storage, was obtained with no-bake, oil-urethane binders (e.g., Linocure). However, the bonding reaction of this system is extremely temperature sensitive and sand temperature must be above 65F.

1.8.8 Parting agents. Parting agents are used to prevent the mold sand from sticking to the pattern or the mold section interfaces. Parting agents are often recommended by the manufacturer of the binders. In the Boeing program, all parting agents were spray or brush applied. With the Linocure binder system, Ashland L 16 provided fine detail pickup and was otherwise satisfactory. (Ref. 5)

1.8.9 Mold leveling. When using molds with multiple flasks for large castings, leveling can be critical. Boeing (Ref. 5) found that for castings such as shown in Figure 1.8.1.2, leveling with a telescope was far more accurate than using a bubble level.

1.8.10 Insulation materials. Materials such as plaster, ceramic, and fibrous material are commonly used to insulate risers and in some cases thin sections to improve the fluidity of the molten metal in order to avoid cold shuts or misruns. Typically, aluminum castings will display a decrease in volume of about 6.5 percent during solidification. This shrinkage is controlled by proper placement of insulated risers. Investigations during the Boeing program (Ref. 5) showed that plaster, even when followed by long drying, outgassed when contacted by molten metal. The optimum material for riser insulation appeared to be a paper-fiber-glass composite, and for insulation of thin sections, a ceramic-foam block.

1.8.11 Chill size and location. The purpose of chills in a mold is to promote directional solidification and a desirable microstructure. In the Boeing program (Ref. 5), chill materials were investigated using the configuration shown in Figure 1.8.6.1. Iron, aluminum, copper, and graphite were compared in their effects on tensile properties for specimens taken 1, 4, 8, and 11 inches from the chilled end. Chill size and shape were also investigated using aluminum. Substantial increases in tensile strength and elongation were obtained using any of the chill materials, as compared with values obtained without a chill (e.g., Figure 1.8.11.1). As might be expected, the largest increase in properties occurred nearest the chilled end. For a given volume of chill material, copper produced the highest tensile strength and elongation. Chill shape for equal volume did not exhibit a significant effect. The tensile yield strength was little affected by the presence of chills. The results indicated that the mass of the chill should be equal to

one to two times the mass of the metal being chilled. Copper chills are expensive, and a combination of copper and aluminum chills can be used to reduce costs. Copper chills might be used in sections greater than 1-inch thick, while aluminum chills could be used in lighter sections. The location and size of chills will, of course, depend on the casting configuration. In large thin-walled castings which incorporate complex gating systems and numerous risers, chills must be used extensively to control proper metal solidification.

1.8.11.1 *[Figure]* Effect of various chill metals and distance from the chill for sand-castings (derived from Ref. 5, Figures 55, 56).

1.8.11.2 *[Figure]* Configuration of fatigue test specimen used to measure the effects of chill rates and aging processes on high-cycle fatigue life.

1.8.11.3 *[Figure]* Effect of chill rates and aging processes on tension-tension fatigue life of notched specimens of D357.0 alloy at 20 ksi maximum stress.

Little effect of aging process was found, but the faster solidification rate with Cu chills almost doubled average fatigue life, compared to the slower solidification rate with Fe chills. This improvement appears to be at least partially the result of lower porosity with the faster solidification, as noted on the figure.

1.8.11.4 *[Figure]* Effect of porosity resulting from different chill rates and aging processes on tension-tension fatigue life of notched specimens of D357.0 alloy at 20 ksi maximum stress.

Porosity alone has a minor effect on fatigue life at levels below 0.04 percent. Above 0.04 percent, average fatigue life decreases significantly with increasing porosity

1.8.11.5 *[Figure]* Effect of magnesium content on tension-tension fatigue life of notched specimens of D357.0 alloy at 20 ksi maximum stress, with different chill rates and aging processes.

Increasing Mg content from 0.45 to 0.55 percent dramatically increases fatigue life when coupled with faster solidification rates. At the slower solidification rate some fatigue life increase is also seen. These results confirm the expected strengthening benefits of additional eutectic.

1.8.12 Gating and risering. Boeing (Ref. 5) used complex, thin-walled castings of several designs to investigate optimum gating and risering techniques. Horizontal gating is most commonly used because it produces low metal turbulence, but large thin-walled castings present problems of nonuniform directional solidification and mold sag if cast in the horizontal position. When castings are made in the vertical position, directional solidification is enhanced because metal is gated into the casting only when it is required to fill space. Solidification is then controlled by proper use of chills. In contrast, horizontal castings are usually filled from the bottom of the mold cavity and then into the risers, with the result that all metal must pass through the casting before solidification can begin. This gives rise to nonuniform directional solidification and associated reduced mechanical properties. The disadvantage of a vertical gating system is a large sprue height, which if not properly accounted for in the sprue design can give rise to turbulence.

An unpressurized gating system should be employed where the cross section of the sprue base is less than the sum of the total areas of the runner and ingates. Such a system produces slow, non-turbulent metal flow. Using a metal flow rate of 7 pounds per second, Boeing investigated various gating ratios and concluded that, for large thin-walled vertical castings, a ratio of 1:6:8 should be used where the numbers represent the gross area of sprue, downrunner, and ingate, respectively. As shown in Figure 1.8.12.1, a cascading sprue was used to take advantage of maintaining hydrostatic head with minimum turbulence. To ensure adequate filling in the cascade system, the base area of the upper sprues should be approximately 50 percent greater than lower sprues. All sprues should be tapered to prevent entrapment of air. While conical shape is generally used, Boeing (Ref. 5) found that metal turbulence was reduced by a tapered rectangular design.

Basic features of the pouring well, runner, and ingate are shown in Figure 1.8.12.2. The pouring well is located under the base of the sprue and has as its purpose reduction in the flowing metal velocity. The optimum shape of the well was found to be cylindrical with a flat bottom. Runners should have a square cross section in order to minimize the metal surface area exposed to its walls. There should be a generous radius at the transition from the runner to the ingate in order to reduce turbulence. Ingates should be at the top of the runner so that molten metal fills the runner before it enters the mold and any dross that has formed will rise to the surface and adhere to the sand.

Risers must be designed to permit the solidifying metal to be fed continuously by a reservoir of molten metal from the risers. For thin-walled castings, a large number of closely spaced risers are necessary. The distance from the riser to a chill will influence the mechanical properties, with short distances being desired to increase solidification rates.

1.8.12.1 *[Figure]* Cascading sprue designed to combine good hydrostatic head with minimum turbulence.

1.8.12.2 *[Figure]* Basic features of pouring well, runner, and ingate.

1.8.13 A series of casting trials at a given foundry is typically required to optimize composition, heat treatment, and casting parameters before the required properties of premium castings are obtained. In a research study

conducted by the Aluminum Division Research Committee 2C of the American Foundrymen's Society (Ref. 40), a first set of castings failed to meet strength goals, but was followed by a second set in which yield strength, for example, increased by 30 percent.

1.8.13.1 *[Figure]* Improvement in tensile yield strength from the first to the second set of sand-castings.

1.9 Special Considerations (See also Section 1.8)

1.9.1 Effect of dendrite refinement. The mechanical properties of Al-Si-Mg alloys as well as many other casting alloys are influenced by the dendrite cell size or by a related and, recently, a more widely used measurement, the secondary dendrite arm spacing (DAS). The logarithm of DAS has been shown to be a linearly increasing function of the logarithm of solidification time for a variety of casting alloys (Ref. 22). The smaller the DAS the higher the F_{tu} and the elongation (Ref. 23). This points to the importance of using properly designed chills in the casting of critical parts. The value of F_{ty} is essentially unaffected by DAS. A correlation between DAS and the tensile properties of cast A357.0 is relatively easy to establish for simple cast shapes by examination of the microstructure in a region near the fracture of extracted tensile coupons. Some examples are shown in Figures 1.9.1.1 and 1.9.1.2 for specimens taken from shell investment or composite sand-cast blocks. Two methods of measuring DAS are described in DAE ARP 1947 (Ref. 33): a preferred method, and an alternate method yielding a particle intercept distance (PID) which is less accurate. A surface replication technique for DAS determinations on a cast part has been described (Ref. 29) and is incorporated in the DAS ARP.

If a linear relation is assumed between the DAS and F_{tu} it is possible to specify a maximum DAS value for a casting by determination of the DAS and F_{tu} from two attached tensile coupons having a minimum difference in DAS of 0.001 inch (Ref. 33). Presumably the procedure will ensure that the portion of the casting examined will meet some minimum value of F_{tu}. However, the relationship between DAS and the tensile properties is apparently difficult to determine. In some cases, a linear relation may best describe the data, as, for example, in Figure 1.9.1.3 while in other cases the relation does not appear to be linear (e.g., Figure 1.9.1.1), or the scatter is so large that the relationship is obscured as illustrated in Figures 1.9.1.6 to 1.9.1.11 for specimens cut from large, thin-walled castings. If the DAS is averaged over selected ranges (see Figure 1.9.1.12), the scatter is reduced, but this is a subjective procedure. While there is good evidence for the dependence of F_{tu} and elongation on DAS, the determination of useful relations obviously requires considerable experience in making the measurements and in interpretation of the data.

1.9.1.1 *[Figure]* Effect of dendrite arm spacing on tensile properties of shell investment cast plates.

1.9.1.2 *[Figure]* Effect of dendrite arm spacing on tensile properties of sand-cast plates.

1.9.1.3 *[Figure]* Effect of dendrite arm spacing on tensile strength of specimens from development sand-castings.

1.9.1.4 *[Figure]* Effect of dendrite arm spacing on tensile yield strength of specimens from development sand-castings.

1.9.1.5 *[Figure]* Effect of dendrite arm spacing on tensile elongation of specimens from development sand-castings.

1.9.1.6 *[Figure]* Effect of dendrite arm spacing on tensile strength of specimens with Grade A soundness taken from sand-cast bulkheads.

1.9.1.7 *[Figure]* Effect of dendrite arm spacing on tensile yield strength of specimens with Grade A soundness taken from sand-cast bulkheads.

1.9.1.8 *[Figure]* Effect of dendrite arm spacing on tensile elongation of specimens with Grade A soundness taken from sand-cast bulkheads.

1.9.1.9 *[Figure]* Effect of dendrite arm spacing on tensile strength of specimens with Grades B and C soundness taken from sand-cast bulkheads.

1.9.1.10 *[Figure]* Effect of dendrite arm spacing on tensile yield strength of specimens with Grades B and C soundness taken from sand-cast bulkheads.

1.9.1.11 *[Figure]* Effect of dendrite arm spacing on tensile elongation of specimens with Grades B and C soundness taken from sand-cast bulkheads.

1.9.1.12 *[Figure]* Effect of dendrite arm spacing and radiographic soundness on tensile properties of development castings.

Note that the data shown represent the average of four selected DAS ranges. This subjective procedure greatly reduces the scatter in the original data.

1.9.2 Effect of impurities. The major impurity in A357.0 is iron, which has the effect of capturing a sufficient amount of magnesium in complex compounds with silicon and minor impurities to degrade the strength and to substantially reduce the elongation. The iron compounds tend to form acicular inclusions in the interdendritic structure, which probably accounts for the loss in ductility. The addition of beryllium tends to reduce the number of iron-bearing compounds and to favorably modify their morphology, off-setting to some extent the negative effects of increased iron content (Figure 1.4.3.2) (Ref. 35). However, beryllium requires special handling techniques and some foundries hesitate to use it. Recently, it has been shown (Ref. 21) that the beryllium can be eliminated, insofar as its effect on

F_{ty} is concerned. However, this reference does not give data on F_{tu} or elongation. The reduction of iron to levels below about 0.1 percent would require extreme caution in avoiding contamination from crucibles, tools, and scrap. Phosphorus has a deleterious effect, as discussed in Section 1.8.5. Other elements are generally so low in concentration that they are of no concern in premium quality castings.

1.9.3 Radiographic quality. The most frequent radiographic indications of discontinuities that are cause for rejection in aircraft castings are dross (less dense material), shrinkage sponge, and porosity (Ref. 12). Radiographs are graded as quality levels A, B, C, or D in accordance with MIL-C-6021. These quality levels are based on ASTM E 155 Reference Radiographs which provide examples of increasing severity of a given type of seven discontinuities from least detectable (No. 1) to the most severe (No. 8). For example, quality Grade B, according to MIL-C-6021, permits gas holes not exceeding those on Reference Radiograph No. 1. It should be noted that for practical purposes, industrial radiography is insensitive to discontinuities that are less than 1 percent of the part thickness. For this reason, it is not possible to qualify castings to Grade B in thicknesses over 1/2 inch. The Aluminum Association (Ref. 34) has published quality level standards for general commercial application which are less stringent than those in MIL-C-6021. For example, their highest quality level (AA) specifies Reference Radiograph No. 2 for gas holes.

For aircraft applications in critical areas, Grade B minimum is generally specified. As indicated in Tables 1.9.3.1 and 1.9.3.2 there is a substantial degradation in tensile properties of A357.0-T6 in going from Grade B to Grades C or D. High-cycle fatigue life is also substantially reduced, as shown in Figures 3.5.1.5 and 3.5.1.10. The presence of microshrinkage increases the spread of fatigue-crack propagation rates as indicated by comparison of Figures 3.5.1.9 and 3.5.1.10.

1.9.3.1 *[Table]* Effect of dross and gas porosity on tensile properties of shell investment and sand-cast plates.

1.9.3.2 *[Table]* Effect of excessive gas and shrinkage porosity on the tensile properties of sand-castings.

1.9.4 Ultrasonic inspection. Ultrasonic inspection appears useful in the detection of small amounts of dispersed gas or shrinkage porosity in castings up to 4 inches thick (Ref. 6). However, reference standards must be developed from radiographic information on material not more than 3/4-inch thick (limit of ASTM Reference Radiographs).

1.9.5 Microporosity. Reduction in tensile properties of Al-Si-Mg casting alloys has been attributed to microporosity associated with the reduction in volume during solidification (Ref. 28). This porosity may be below the threshold but can be revealed by a process using fluorescent-dye-penetrant. The casting surface is chem-milled and a plastic replica is made of the area to be examined. Using the fluorescent-dye-penetrant on the replica reveals the microporosity as small spots. It is suggested that the density of spots (number per unit area) and the size of the spots can be related to the mechanical properties of the casting (Ref. 28).

2 Physical Properties and Environmental Effects

2.1 Thermal Properties

2.1.1 Melting range: 1035 to 1135F.

2.1.2 Phase changes.

2.1.3 Thermal conductivity.

2.1.4 Thermal expansion.

68 to 212F, 11.9 in./in./F

68 to 392F, 12.5

68 to 572F, 12.9

2.1.5 Specific heat.

2.1.6 Thermal diffusivity.

2.2 Other Physical Properties

2.2.1 Density, 0.097 lb/in^3.

2.2.2 Electrical properties.

2.2.2.1 *[Figure]* Effect of aging time on the electrical conductivity and hardness of shell investment castings.

2.2.2.2 *[Figure]* Effect of aging time on the electrical conductivity and hardness of sand-castings.

2.2.2.3 Electrical resistivity, 1.71 microhm-inch.

2.2.3 Magnetic properties. Alloy is not ferromagnetic.

2.2.4 Emittance.

2.2.5 Damping capacity.

2.3 Chemical Environments

2.3.1 See Alloy 6061 (Code 3206) in this handbook.

2.4 Nuclear Environments

3 Mechanical Properties

3.1 Specified Mechanical Properties

3.1.1 *[Table]* AMS and ASTM specifications for mechanical properties and microstructure.

3.1.2 *[Table]* Military specification mechanical properties.

3.2 Mechanical Properties at Room Temperature

3.2.1 Tension – stress-strain diagrams – tension properties.

3.2.1.1 *[Figure]* Stress-strain curves for sand-cast plate.

3.2.1.2 *[Table]* Tensile, compressive, shear, and bearing properties for specimens removed from designated areas of Northrop sand-cast stepped plates from Suppliers A and B.

3.2.1.3 *[Table]* Tensile, compressive, shear, and bearing properties for specimens removed from nondesignated areas of Northrop sand-cast stepped plates from Supplier B.

3.2.1.4 *[Table]* Tensile properties and hardness of investment cast test plates.

Note that the tensile properties in this table are not always the same as those shown in related Figures 1.4.3.1, 1.5.4, 1.5.6, 1.5.8, and 1.5.10, for the nominal foundry practices and heat treatments listed here. Reasons for these discrepancies are not given in the reference. Therefore, data on each of these figures should only be used to define trends with respect to the specific independent variable in that figure.

3.2.1.5 *[Table]* Tensile properties and hardness of sand-cast test plates.

Note that the tensile properties in this table are not always the same as those shown in related Figures 1.5.5, 1.5.7, 1.5.9, and 1.5.11, for the nominal foundry practices and heat treatments listed here. Reasons for these discrepancies are not given in the reference. Therefore, data on each of these figures should only be used to define trends with respect to the specific independent variable in that figure.

3.2.1.6 *[Table]* Tensile properties of specimens removed from webs and flanges of a development casting for the F-16 vertical tail understructure.

3.2.1.7 *[Table]* Tensile properties of composite sand-cast F-16 vertical tail understructure cast at Alcoa.

3.2.1.8 *[Table]* Average tensile properties of specimens removed from two full-scale bulkheads from the Boeing Foundry.

3.2.1.9 *[Table]* Average tensile properties of specimens removed from two full-scale bulkheads from the Hitchcock Foundry.

3.2.1.10 *[Figure]* Effect of holding time at 212 or 400F on tensile properties at room temperature

3.2.1.11 *[Figure]* Configuration of double-ligament tensile (DLT) specimen in test rig used to measure anisotropy in mechanical properties of cylindrical sand-castings.

3.2.1.12 *[Table]* Effect on tensile properties of specimen orientation with respect to axis of sand-cast cylinders.

Only ultimate strength and elongation in the tangential orientation are significantly affected.

3.2.1.13 *[Table]* Smooth tensile, notch tensile and fatigue toughness properties of specimens from sand composite cast plates from three suppliers and from F5 wing pylons.

3.2.1.14 *[Table]* Smooth tensile and fracture toughness properties of specimens from sand composite cast plates with intentional defects.

3.2.2 Compression – stress-strain diagrams – compression properties (See Tables 3.2.1.2 and 3.2.1.3).

3.2.2.1 *[Figure]* Compressive stress-strain curve for sand-cast plate.

3.2.3 Impact.

3.2.4 Bending.

3.2.5 Torsion and shear (see Tables 3.2.1.2 and 3.2.1.3).

3.2.6 Bearing (see Tables 3.2.1.2 and 3.2.1.3).

3.2.7 Stress concentration.

3.2.7.1 Notch properties.

3.2.7.2 Fracture toughness (see also Tables 3.2.1.13, 3.2.1.14 and 4.3.1.2).

3.2.7.2.1 General. Attempts to measure the plane-strain fracture toughness, K_{Ic}, in accordance with ASTM E 399 have met with little success. Frequently specimens removed from a casting are of insufficient thickness to measure a valid K_{Ic}. This, per se, is not a basic problem if the specimen represents essentially the full thickness of the section being examined. In fact, this is a good finding and indicates that fracture of the part will probably not be controlled by plane-strain fracture. However, in most cases where the thickness is sufficient, valid values of K_{Ic} cannot be obtained because of excess fatigue-crack front curvature. (e.g., see Tables 3.2.7.2.2 and 3.2.7.2.3). In these examples, the primary cause of invalid values was crack front curvature. The excessive crack front curvature in castings is due to a combination of residual stresses associated with quenching from the solution temperature and to the nonuniform microstructure, which is generally finer at the surface due to a more rapid solidification rate. Various remedies for this curvature problem have been suggested including lateral compression and

side grooving. Side grooving will probably help, but removes part of the material in the casting. However, if the material removed does have a superior microstructure to that remaining, it may be speculated that the side-grooved specimen will yield underestimates of the true fracture resistance of the actual part.

A few valid values of K_{Ic} have been reported (see Table 3.2.7.2.2) which vary from about 16 to 19 ksi $\sqrt{in}$. It is not clear whether or not the casting from which these specimens were taken represent D357.0 as presently defined in the AMS specification. Values as low as 13 ksi $\sqrt{in}$. have been suggested for design (Ref. 13). In light of more recent K_Q values (e.g., Table 3.2.7.2.4) such a design value seems rather low. K_Q values obtained from intentionally defective step plates with severe sponge shrinkage (Table 3.2.7.2.6) show no significant difference from plates having radiographic Grade B or better. Tests at -65F on the same type of specimens as represented in Table 3.2.7.2.2 did not reveal any difference between K_Q at -65 or at room temperature. This behavior would be expected for most aluminum alloys.

3.2.7.2.2 *[Table]* Results of tests on ASTM E 399 compact specimens removed from separately sand-cast blocks.

3.2.7.2.3 *[Table]* Results of tests on ASTM E 399 compact specimens removed from separately sand-cast bulkhead lugs.

3.2.7.2.4 *[Table]* Results of tests on ASTM E 399 compact specimens removed from separately sand-cast blocks and from designated areas of stepped plates.

3.2.7.2.5 *[Table]* Results of tests on ASTM E 399 compact specimens removed from full-scale F-16 vertical tail understructure.

3.2.7.2.6 *[Table]* Fracture toughness of specimens removed from intentionally produced defective step plates.

3.2.8 Combined properties

3.3 Mechanical Properties at Various Temperatures

3.3.1 Tension – stress-strain diagrams – tension properties.

3.3.1.1 *[Figure]* Effect of test temperature and holding time on tensile properties.

3.3.1.2 *[Figure]* Effect of elevated test temperature on tensile properties of sand-castings.

3.3.2 Compression – stress-strain diagrams – compression properties.

3.3.3 Impact.

3.3.4 Bending.

3.3.5 Torsion and shear.

3.3.6 Bearing.

3.3.7 Stress concentration.

3.3.7.1 Fracture toughness.

3.3.8 Combined properties.

3.4 Creep and Creep Rupture Properties

3.4.1 *[Figure]* Creep and creep rupture at 350F.

3.5 Fatigue Properties

3.5.1 Conventional high-cycle fatigue.

3.5.1.1 *[Figure]* S-N curves for axial fatigue of separately sand-cast test specimens.

3.5.1.2 *[Figure]* S-N curves for smooth and notched specimens.

3.5.1.3 *[Figure]* S-N curves at elevated temperature for specimens removed from sand-cast stepped plates.

3.5.1.4 *[Figure]* S-N curves for notched specimens from sand-castings.

3.5.1.5 *[Figure]* Effect of sponge shrinkage (Grade C) and round gas porosity (Grade D) on notched fatigue properties of sand-castings.

3.5.1.6 *[Table]* Smooth and notched fatigue properties of separately sand-cast specimens and specimens removed from cast bulkhead.

3.5.1.7 *[Figure]* S-N curves for smooth specimens from composite sand-cast plates from three suppliers and specimens from F5 wing pylon.

Maximum stresses for materials from Foundries B and C are significantly lower than for Foundry A material for the same high-cycle fatigue lives. Referring to the tensile properties in Table 3.2.1.13, only the lower NTS/F_{ty} ratios of Foundries B and C material correlate with these fatigue results. Good correlation was found between the fatigue lives of specimens from full-scale F5 wind pylon castings and those of plate castings, both from Foundry A.

3.5.1.8 *[Figure]* S-N curves for notched specimens from composite sand-cast plates from three suppliers.

Little difference between foundries is seen in fatigue lives with stress concentrations.

3.5.1.9 *[Figure]* Effect of gas porosity on S-N curves for smooth specimens from composite sand-cast plates.

Metal was not de-gassed in order to introduce the porosity. Grades B and C porosities averaged 1.1 and 1.7 percent, respectively, with bubble aspect ratios of approximately 2. Grade D porosity was not reported. For a fatigue life of 10^7 cycles, Grade B porosity reduced maximum stress about 30 percent, compared to the baseline material without porosity, while reductions for Grades C and D materials were about 60 percent.

3.5.1.10 *[Figure]* Effect of shrinkage porosity on S-N curves for smooth specimens from composite sand-cast plates.

Shrinkage porosity levels were approximately the same as gas porosity levels, but were non-spherical. Effects on Grade B material fatigue resistance were somewhat more detrimental than gas porosity (see Figure 3.5.1.9). Reductions in the fatigue lives of Grade C material were approximately the same from shrinkage porosity as from gas porosity.

3.5.1.11 *[Figure]* Effect of dross on S-N curves for smooth specimens from composite sand-cast plates.

Grades B and C dross porosity at 1.6 to 0.6 percent levels, respectively, reduced high-cycle fatigue lives as much as Grade C gas and shrinkage porosity at slightly higher levels.

3.5.2 Low-cycle-fatigue.

3.5.2.1 *[Figure]* Strain-fatigue life curve for smooth specimens from composite sand-cast plates from three suppliers.

Unlike fatigue resulting from stress-cycling (see Figure 3.5.1.7), strain-cycle fatigue data from the three foundries are indistinguishable. While not reported in the reference, this probably is the result of a cyclic strain softening behavior, in which maximum stress decreases with continued strain cycling, but maximum strain increases with continued stress cycling. Correlation of the fatigue lives for two R ratios (-1 and 0.1) on the basis of maximum strain is reasonable.

3.5.3 Fatigue-crack propagation.

3.5.3.1 *[Figure]* Fatigue-crack growth rates for specimens removed from designated areas in sand-cast stepped plates.

3.5.3.2 *[Figure]* Fatigue-crack growth rates at 250 and 400F for specimens removed from designated areas in sand-cast stepped plates.

3.5.3.3 *[Figure]* Scatter bands of fatigue-crack growth rates for specimens removed from a cast bulkhead.

3.5.3.4 *[Figure]* Scatter band of fatigue-crack growth rates for specimens removed from a cast bulkhead in shear web areas exhibiting microshrinkage.

3.5.3.5 *[Table]* Measures of the variability in cycles required to grow a crack from an initial to a final value (derived from tests on seven s pecimens).

3.5.3.6 *[Figure]* Fatigue-crack growth rates in lab air and in high humidity for specimens removed from full-scale F-16 vertical tail substructure.

3.5.3.7 *[Figure]* Fatigue-crack growth rates at several R-ratios for specimens removed from full-scale F-16 vertical tail substructure.

3.5.3.8 *[Figure]* Fatigue-crack growth rates for specimens removed from full-scale F-16 vertical tail substructure.

3.5.3.9 *[Figure]* Scatter bands of fatigue-crack growth rates for specimens from composite sand-cast plates from three suppliers, for water- and glycol-quenched conditions.

Crack growth is slower for glycol-quenched material, but with greater scatter. Differences between materials from different suppliers were not significant.

3.5.3.10 *[Figure]* Scatter band of fatigue-crack growth rates for specimens cut from a F5 aircraft wing pylon, compared with plate specimen growth rates.

Growth rates for full-scale pylon casting specimens were in excellent agreement with those from plate casting specimens.

3.5.3.11 *[Figure]* Effects of gas porosity on fatigue-crack growth rates of specimens from cast plates.

3.5.3.12 *[Figure]* Effects of gas porosity or dross on fatigue-crack growth rates of specimens from cast plates.

3.6 Elastic Properties

3.6.1 Poisson's ratio.

3.6.2 Modulus of elasticity.

3.6.2.1 *[Figure]* Effect of temperature on tensile modulus of elasticity.

3.6.3 Modulus of rigidity.

3.6.4 Tangent modulus.

3.6.5 Secant modulus.

4 Fabrication

4.1 Forming

4.2 Machining and Grinding

4.3 Joining

4.3.1 Welding.

4.3.1.1 General. The alloy may be welded in any temper. However, where joining of sections is done by welding it is advisable to do this in the as-cast (F) or annealed condition (T2) where the ductility is high and then to heat treat the assembly to the T6 condition (Ref. 37). This sequence results in stress relief. Repair welding of castings containing localized areas of shrinkage, porosity, or dross can be accomplished using wire conforming to AMS 4246B. Repair welds may be made in fully heated casting if the reduction in mechanical properties is not detrimental to the performance, as in an area where the stresses are low (Ref. 38). If cracking occurs during repair welding the entire casting should be annealed before further repair is attempted.

Simulated weld repairs were made in the Northrop programs. In one case (Ref. 12) the welds were made in grooves cut into designated areas of the step plates with no intentional defects and specimens were abstracted from these plates such that the gauge sections contained substantial amounts of the weld material (see Figure 4.3.1.2). In another case (Ref. 41) the weld grooves were machined into 16 x 16 x 1.25-in. cast plates containing intentional defects. In both cases the plates were heat treated to the T6 condition after welding. Tensile tests on weld-containing specimens from plates with no intentional defects (Table 4.3.1.3) show properties essentially equal to the unwelded metal. Fracture toughness data based on K_Q also indicate no difference between welded and unwelded specimens. On the other hand, differences are observed in the notch fatigue strength (Figure 4.3.1.5), with the welded specimens having shorter lives in the range above about 10^5 cycles. Fatigue-crack growth rates (Figure 4.3.1.6) for welded specimens scatter considerably but appear to be higher than those for unwelded specimens.

4.3.1.2 *[Figure]* V-grooved (60-degree V, 0.25-inch deep with 3/32-inch radius) weld specimens from Northrop stepped plates.

Welding procedure reported as "normal" to fill the groove.

4.3.1.3 *[Table]* Effect of weld repairs on tensile properties and fracture toughness of specimens from stepped plate sand-castings.

4.3.1.4 *[Figure]* Effect of weld repairs on fatigue strength of smooth specimens from composite sand-cast stepped plates, compared with the effects of gas porosity alone.

4.3.1.5 *[Figure]* Effect of weld repairs on fatigue strength of notched specimens from stepped plate sand-castings.

4.3.1.6 *[Figure]* Effect of weld repairs on fatigue-crack growth rates of specimens from sand-cast plates with Grade B gas porosity.

4.3.2 Bonding.

4.3.2.1 The effect of the as-cast surface finish of A357.0-T6 adherends on the relative strengths of bond joints was investigated using single-shear lap tests and comparing the cast specimen results with comparable results for machined 2024-T3 adherends (Ref. 36). Surface preparation and bonding procedures were the same for both the A357.0-T6 and 2024-T3 alloys. Two adhesive systems, dry and wet environments, and several test temperatures were included in the test program. Ratios of the lap-bond strength of the as-cast adherends to that of the machined adherends varied from 0.65 to 1.24.

4.3.2.2 *[Table]* Single-shear lap bond strength of as-cast A357.0-T6 adherends with two adhesive systems.

4.3.2.3 *[Table]* Surface preparation and bonding procedures for fabrication of lap joint test specimens.

Table 1.4.2 AMS and ASTM composition for A357.0 and D357.0

Alloy	357.0, A357.0 and D357.0											
Specification	AMS 4219C, MIL-A-11180D, ASTM B 686		AMS 4249		AMS 4241A		AMS 4246B		ASTM B 108		ASTM B 108	
Reference	1, 45, 46		2		43		44		45		45	
Designation[c]	A357.0-T61		D357.0-T6		D357.0-T6		357		A357.0		357.0	
UNS	A13570		A43570		A43570		A03570		A13570		A03570	
Grade/Type	Aircraft Quality		Damage Tolerant[a] Aircraft Quality		DAS Controlled[b] Aircraft Quality		Weld Wire		Permanent Mold Castings		Permanent Mold Castings	
Composition	Minimum	Maximum	Minimum	Maximum	Minimum	Maximum	Minimum	Maximum	Minimum	Maximum	Minimum	Maximum
Si	6.5	7.5	6.5	7.5	6.5	7.5	6.5	7.5	6.5	7.5	6.5	7.5
Mg	0.40	0.7	0.55	0.6	0.55	0.6+	0.45	0.6	0.4	0.7	0.45	0.6
Ti	0.04	0.20	0.10	0.20	0.10	0.20	—	0.20	0.04	0.2	—	0.2
Be	0.04	0.07	0.04	0.07	0.04	0.07	—	0.15	—	—	—	—
Fe	—	0.20	—	0.12	—	0.12	—	0.05	—	0.2	—	0.15
Cu	—	0.20	—	—	—	—	—	0.05	—	0.2	—	0.05
Mn	—	0.10	—	0.10	—	0.10	—	0.03	—	0.1	—	0.03
Zn	—	0.10	—	—	—	—	—	0.05	—	0.1	—	0.05
Other, each	—	0.05	—	0.05	—	0.05	—	0.05	—	0.05	—	0.05
Other, total	—	0.15	—	0.15	—	0.15	—	0.15	—	0.15	—	0.15

[a] Requires fatigue and fracture toughness and DAS ≤ 0.002 inch.

[b] DAS measurements are used to arrive at the specified mechanical properties.

[c] Designations established by the Aluminum Association and adopted by AMS.

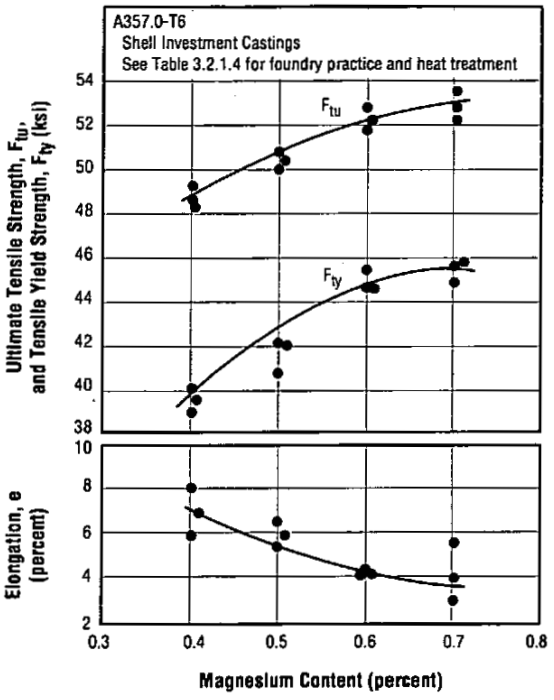


Figure 1.4.3.1 Effect of magnesium content on the tensile properties of shell investment castings (Ref. 12)

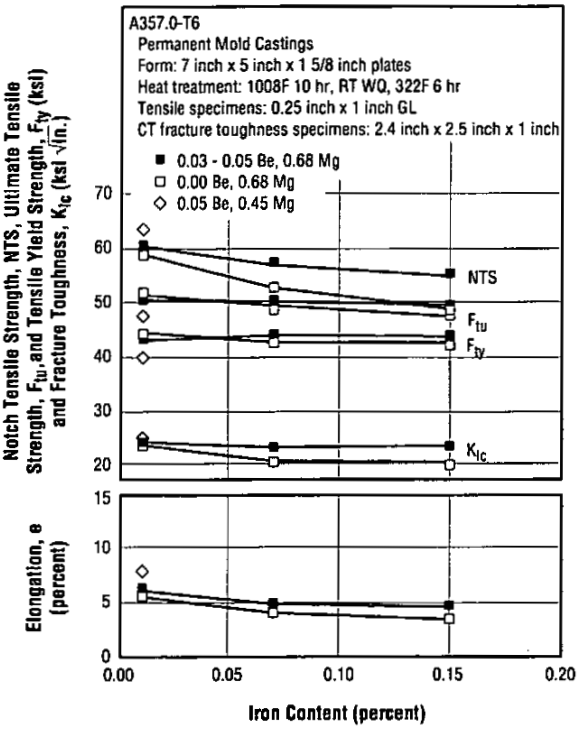


Figure 1.4.3.2 Effects of iron, beryllium, and magnesium contents on tensile and fracture properties of plates cast in permanent molds (Ref. 35)

Table 1.4.3.3 Average tensile, notch yield strength ratio, and percent porosity for specimens cut from cast blocks produced with two chill rates and aged at two temperatures (Ref. 41)

Alloy	D357.0-T6			
Composition	AMS 4219C (except Mg 0.55-0.6) Eight variations within specification limits			
Form	6 inch x 12 inch x 0.75 inch Sand Castings			
Si Modifier	Sr			
Mold and Pour Conditions	Slow Cool: Fe chill + 1440F pour temperature Average DAS = 2.0 mils DAS range = 1.4 - 2.7 mils Fast Cool: Cu chill + 1380F pour temperature Average DAS = 2.3 mils DAS range = 1.5 - 2.9 mils			
Solution Treat	1010F 16 hr, RT, WQ			
Age	315F 12 hr or 335F 6 hr			
Radiographic Quality	Grade B or better			
Test Replications	1 per composition/age/chill combination			
Average Properties	Fe chill		Cu chill	
	315F 12 hr	335F 6 hr	315F 12 hr	335F 6 hr
F_{tu} (ksi)	50	51	52	53
F_{ty} (ksi)	42	44	42	45
e (percent)	4.3	3.8	6.4	6.0
NTS/F_{ty} [a]	1.21	1.15	1.28	1.20
Porosity (percent)	0.047	0.024	0.007	0.015

[a] Notch tensile, ASTM E 602, 0.5-inch diameter specimen.

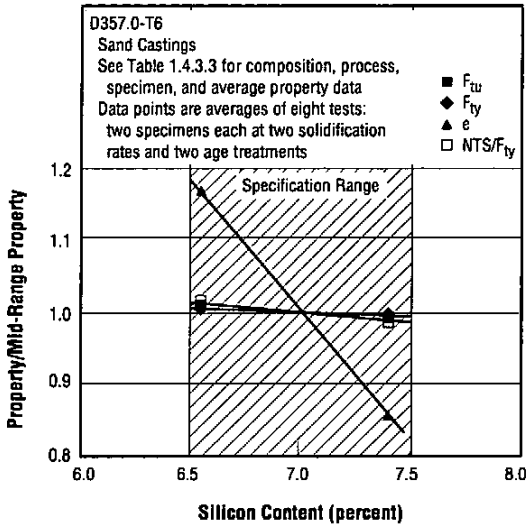


Figure 1.4.3.4 Relative effects of silicon content on tensile properties of D357.0-T6 sand castings (Ref. 41)

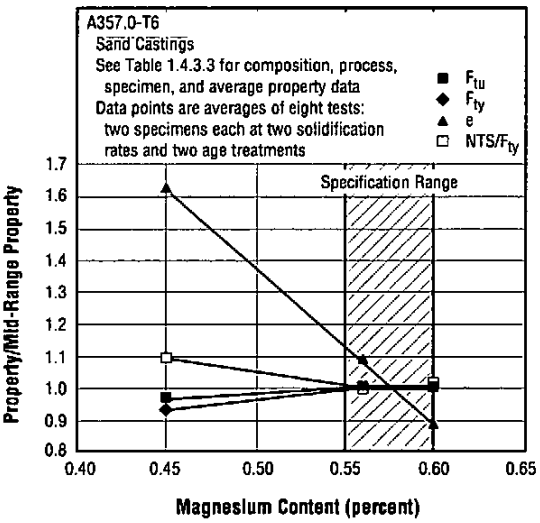


Figure 1.4.3.5 Relative effects of magnesium content on tensile properties of D357.0-T6 sand castings (Ref. 41)

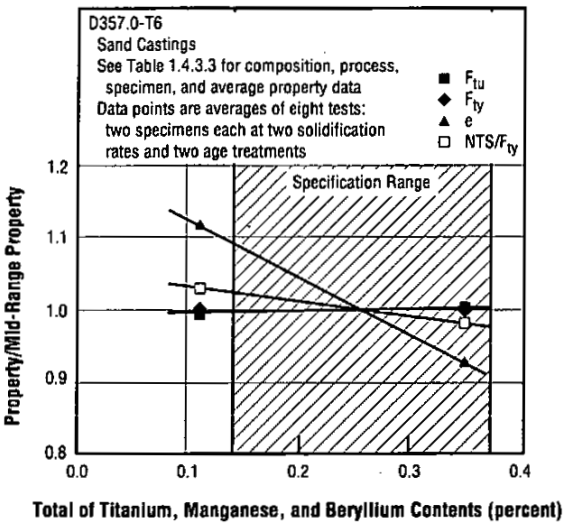


Figure 1.4.3.6 Relative effects of the combined titanium, manganese, and beryllium contents on tensile properties of D357.0-T6 sand castings (Ref. 41)

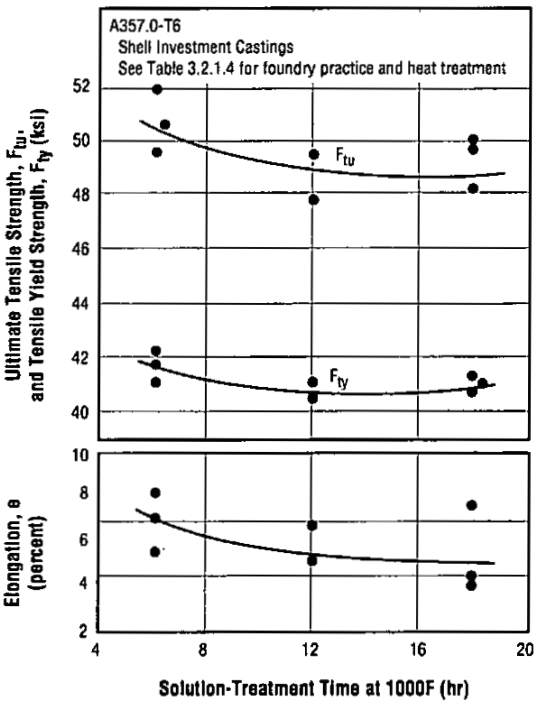


Figure 1.5.4 Effect of solution-treatment time on tensile properties of shell investment castings (Ref. 12)

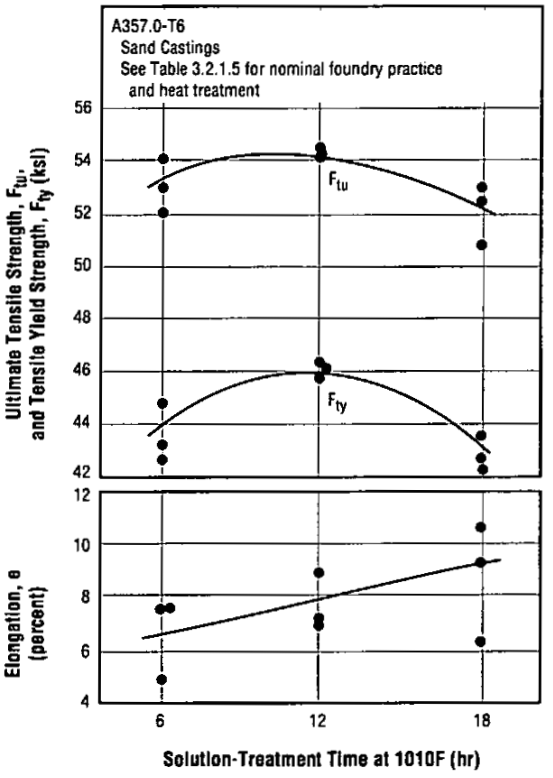


Figure 1.5.5 Effect of solution-treatment time on tensile properties of sand castings (Ref. 12)

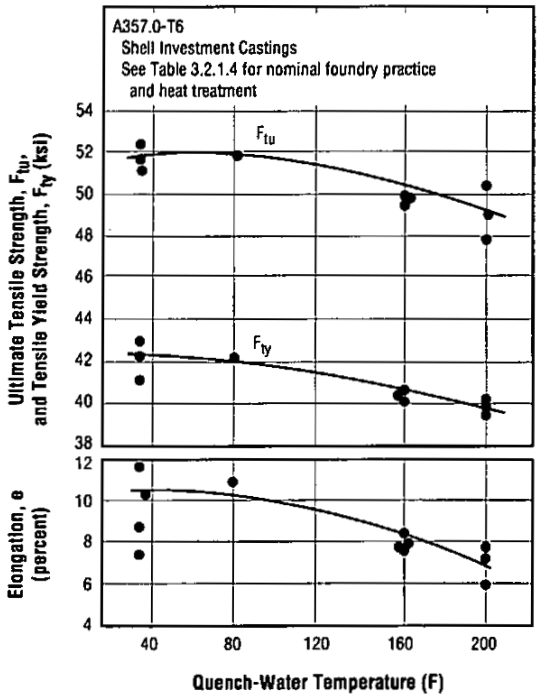


Figure 1.5.6 Effect of quench-water temperature on tensile properties of shell investment castings (Ref. 12)

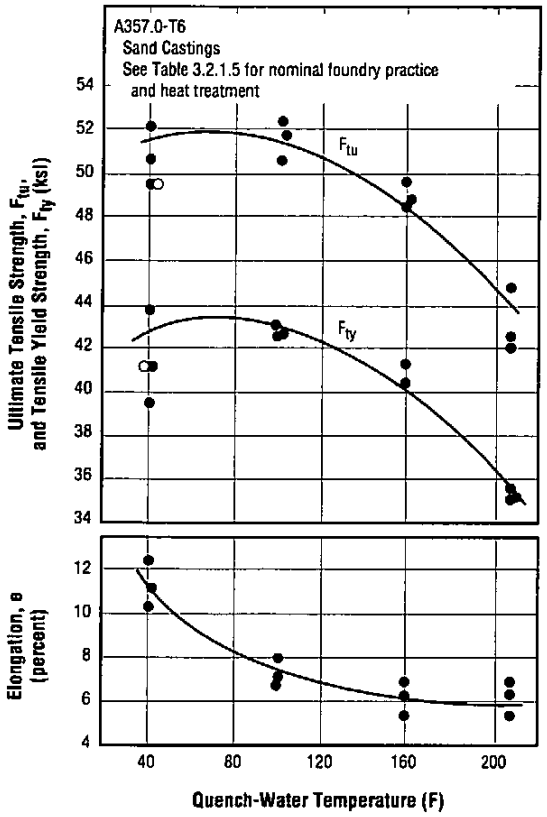


Figure 1.5.7 Effect of quench-water temperature on tensile properties of sand castings (Ref. 12)

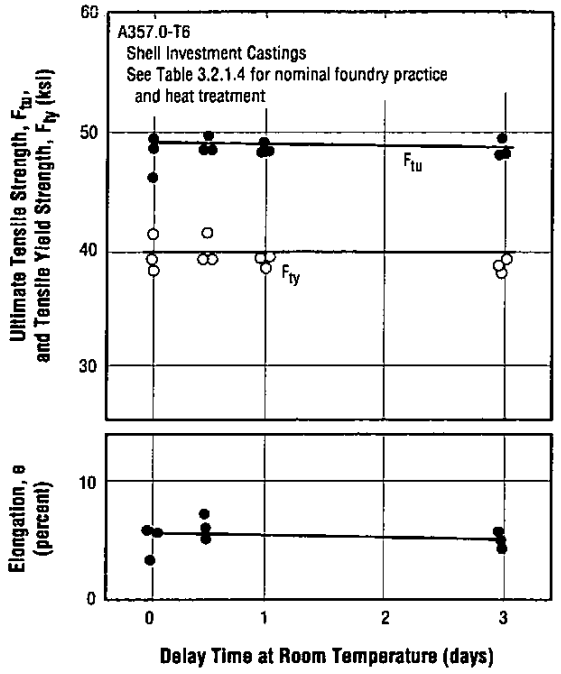


Figure 1.5.8 Effect of delay time between solution treatment and quench for shell investment castings (Ref. 12)

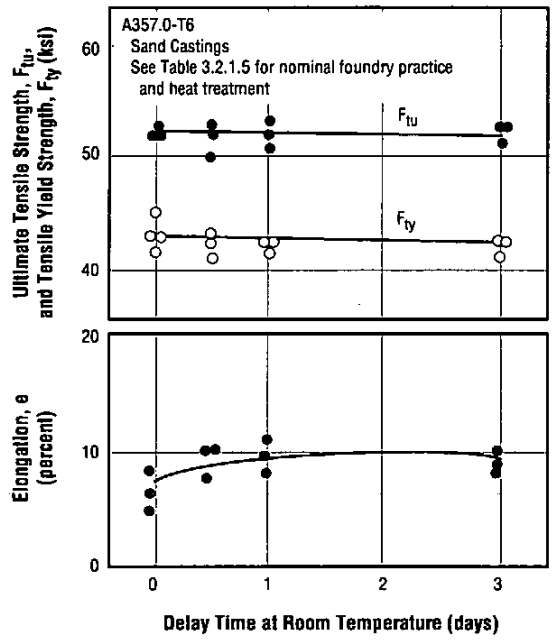


Figure 1.5.9 Effect of delay time between solution treatment and quench for sand castings (Ref. 12)

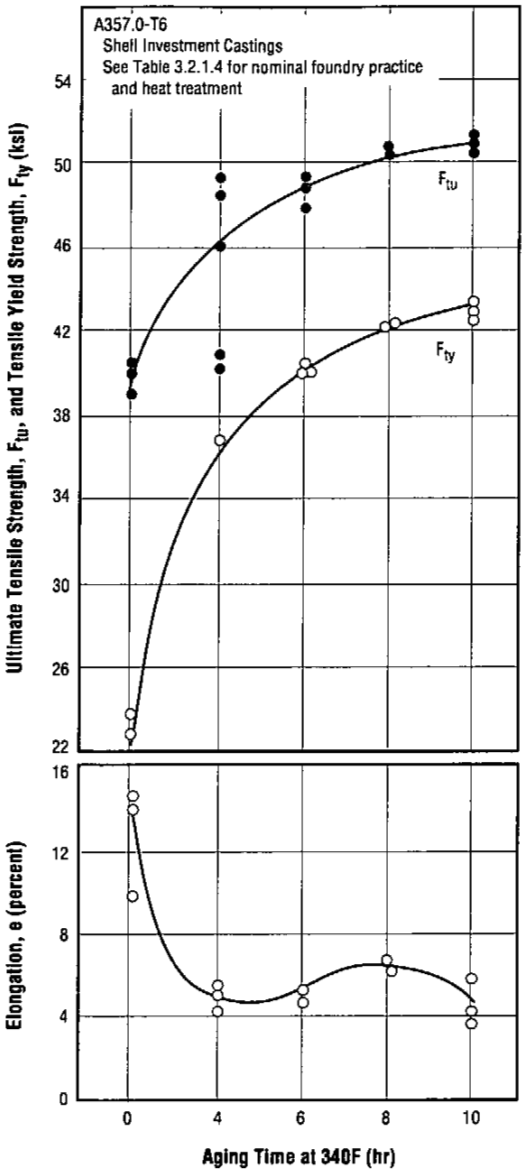


Figure 1.5.10 Effect of aging time on tensile properties of investment castings (Ref. 12)

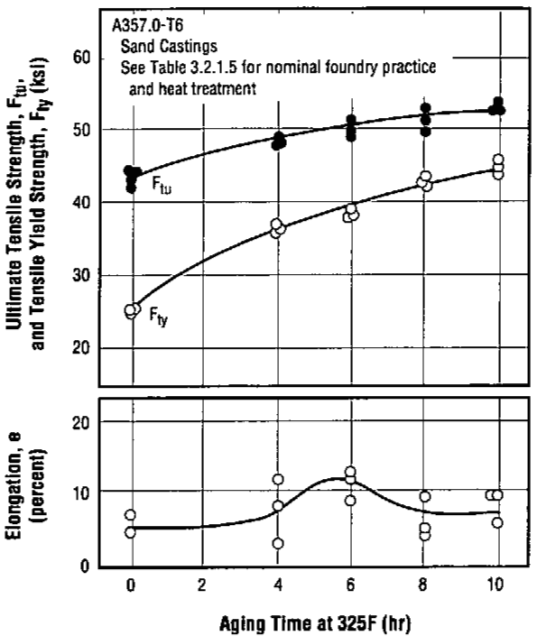


Figure 1.5.11 Effect of aging time on tensile properties of sand castings (Ref. 12)

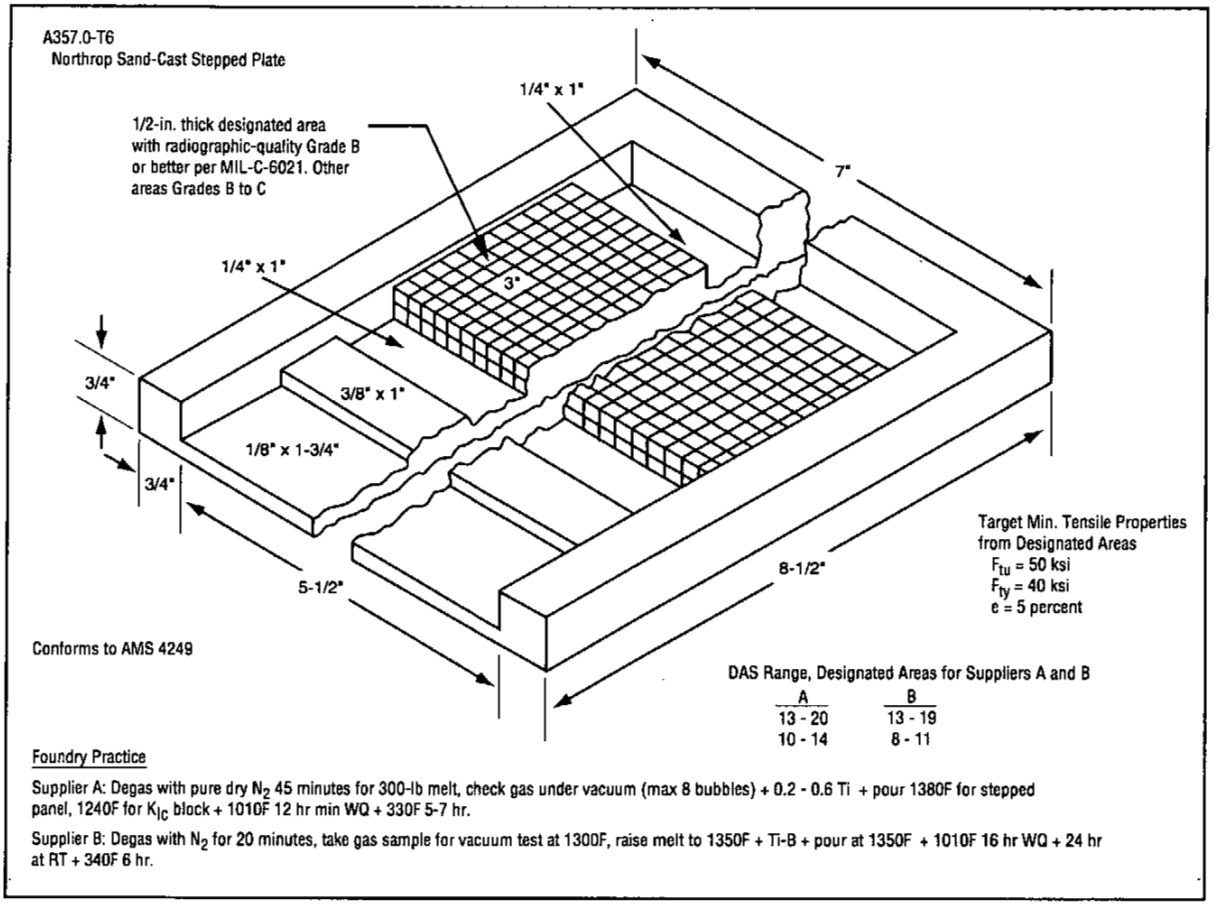


Figure 1.8.1.1 Sand-mold stepped-plates configuration used in the Northrop program to determine design property data for sand-cast A357.0-T6 from two suppliers: A (Magnesium Alloy Products) and B (Teledyne Cast Products). Two integal tensile coupons attached at optional locations. (Ref. 12)

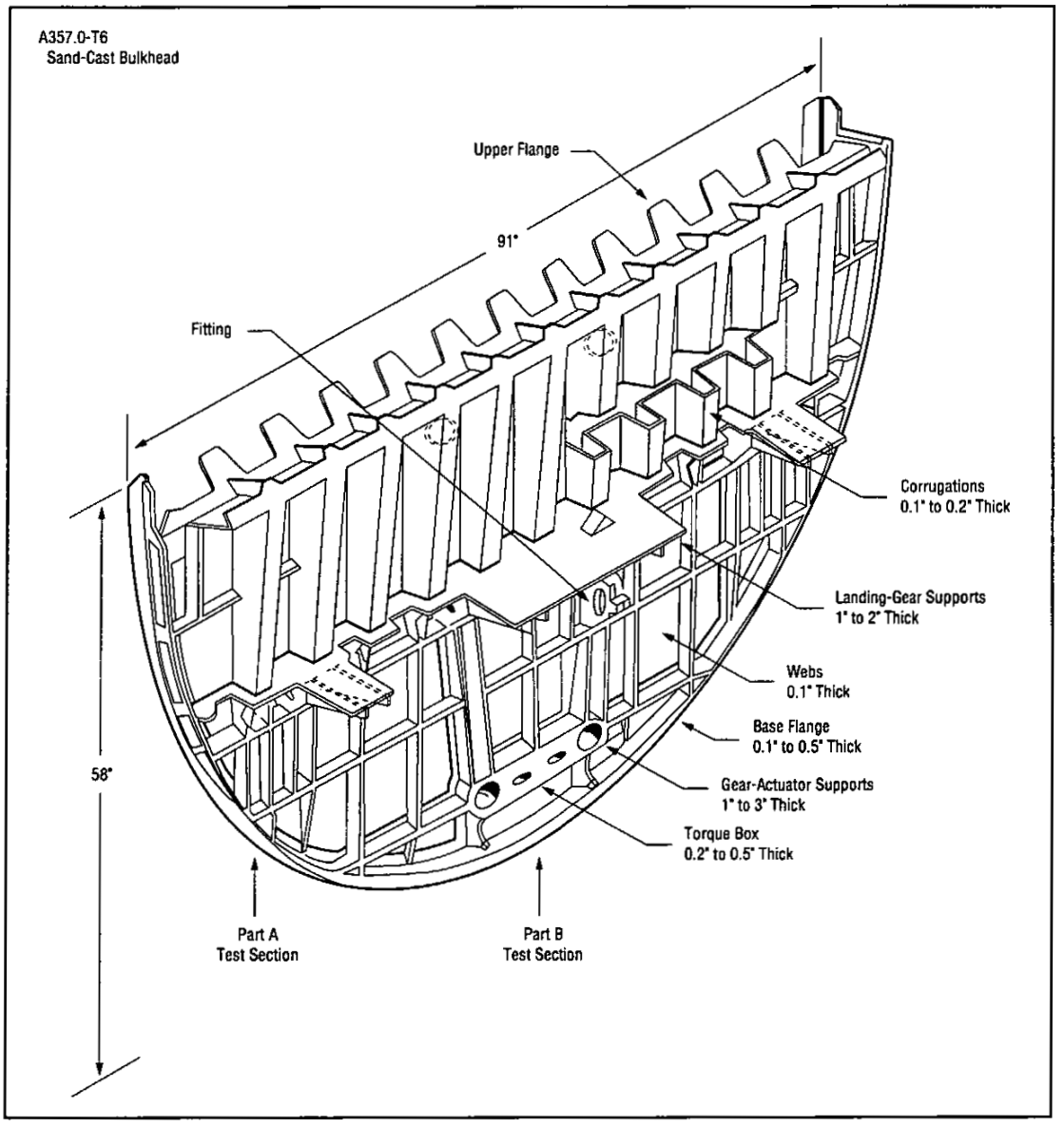


Figure 1.8.1.2 Large, thin-walled, composite sand-cast nose-gear support bulkhead for the YC-14 airplane. Ten identical castings were each produced by the Boeing and the Hitchcock Foundries using Boeing-developed manufacturing plans and tooling (Ref. 10)

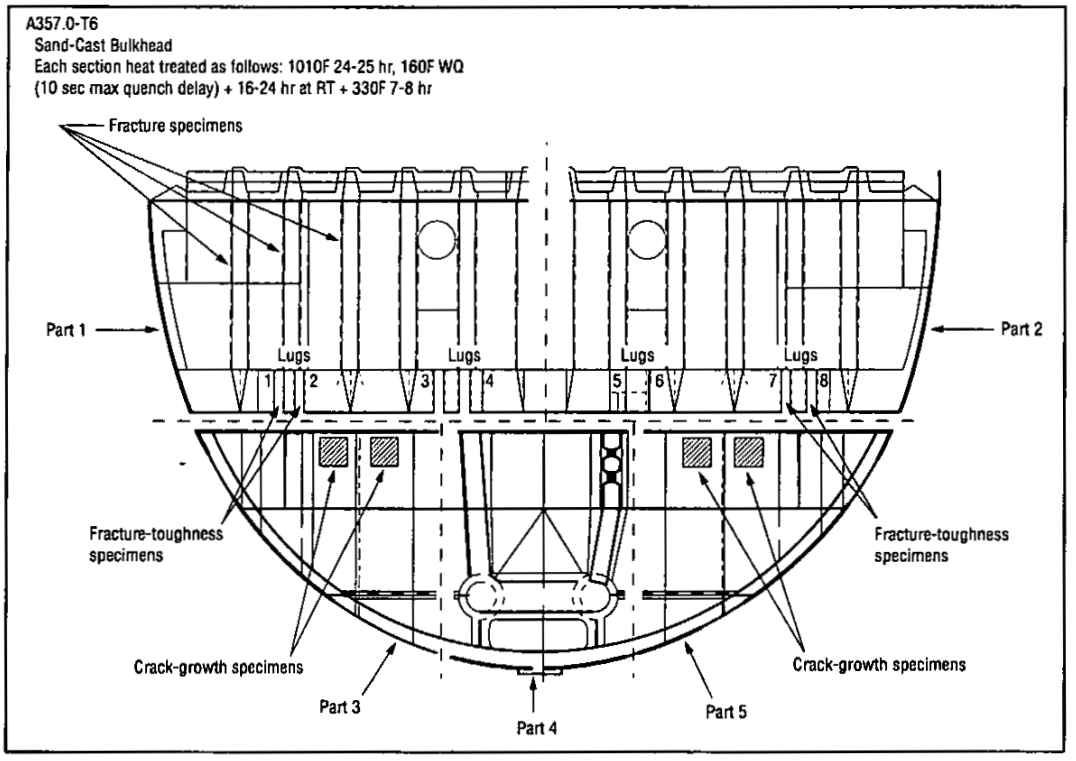


Figure 1.8.1.3 Nose landing-gear support bulkhead casting showing locations of specimens removed from five sections of the casting (Each section heat treated separately) (Ref. 7)

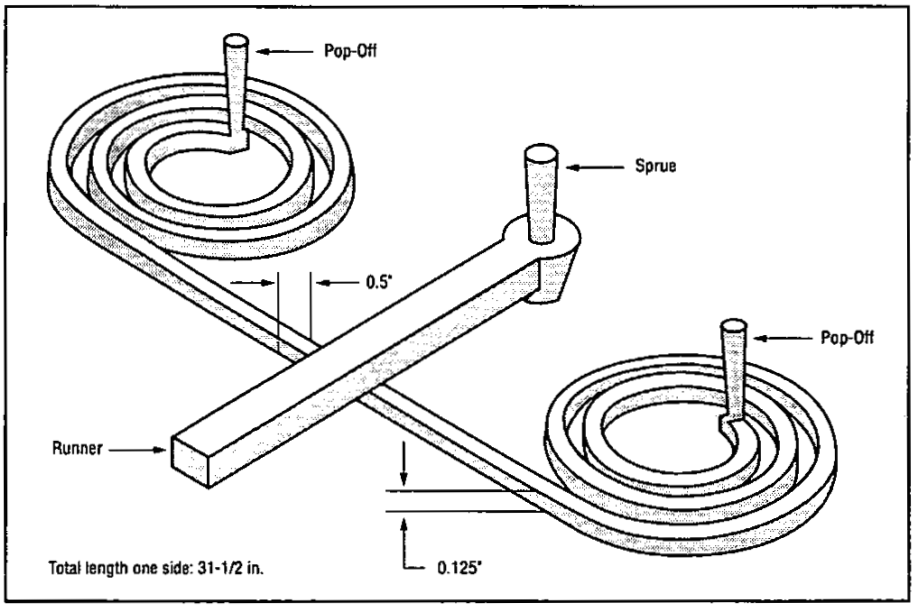


Figure 1.8.2.1 Double spiral fluidity test casting (Ref. 10)

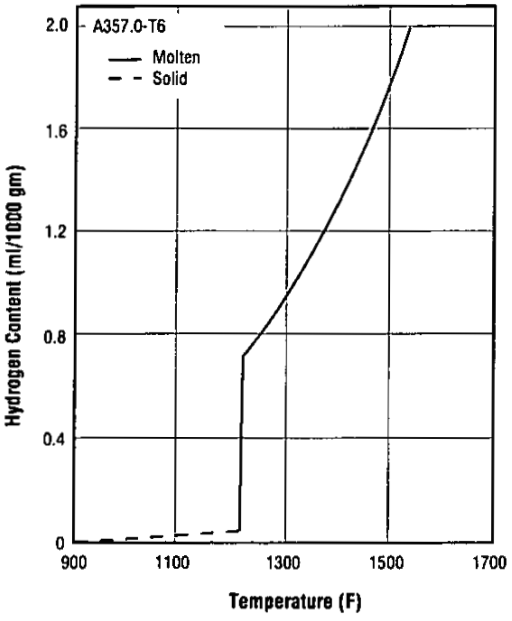


Figure 1.8.4.1 Solubility of hydrogen in solid and molten aluminum as a function of temperature (Ref. 10)

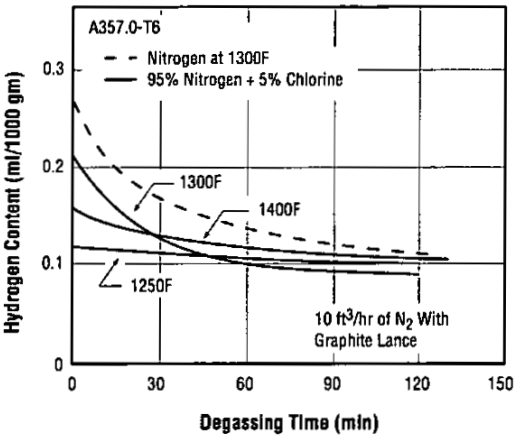


Figure 1.8.4.2 Effect of degassing time and temperature on hydrogen content (Ref. 5)

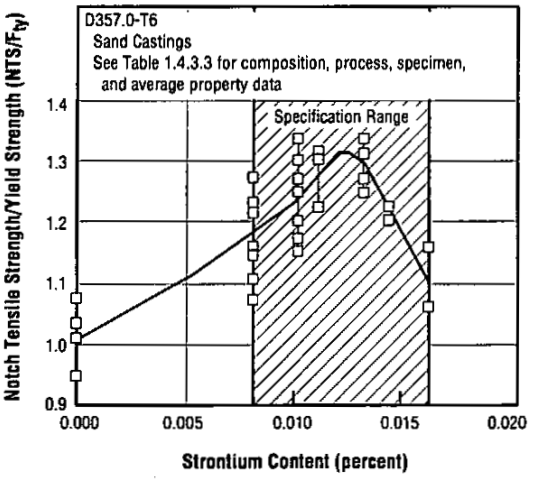


Figure 1.8.5.1 Effect of strontium content on the ratio of notched tensile strength to tensile yield strength of D357.0-T6 sand castings (Ref. 41)

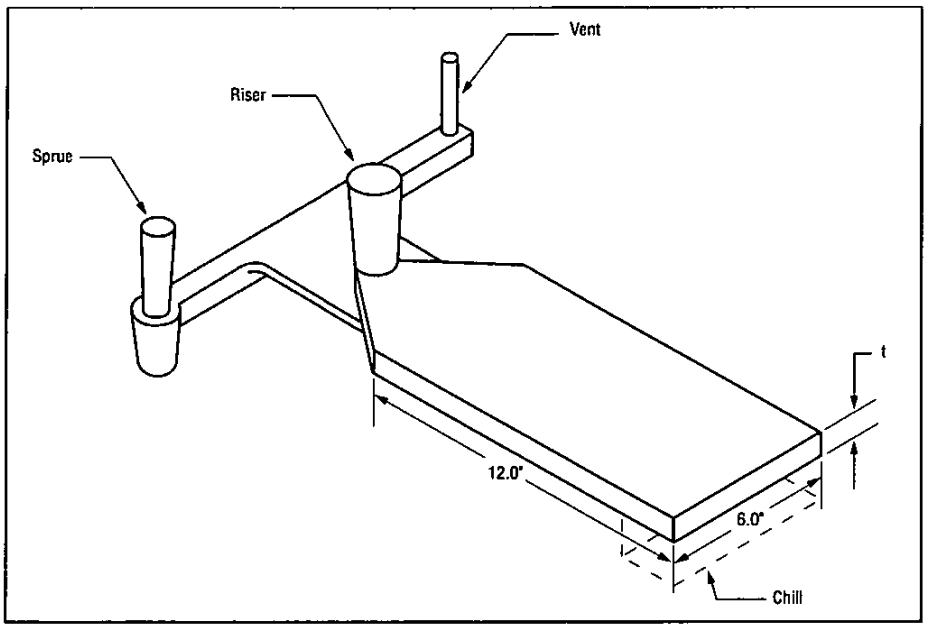


Figure 1.8.6.1 Test plate configuration incorporating a chill (Ref. 5)

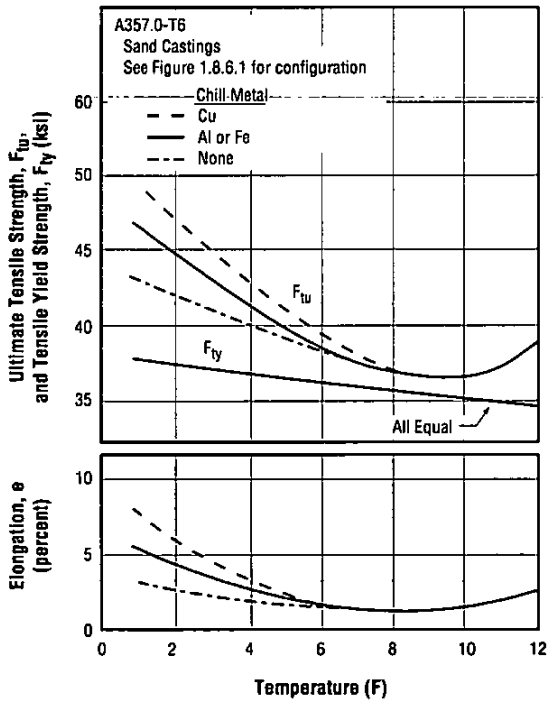


Figure 1.8.11.1 Effect of various chill metals and distance from the chill for sand castings (Ref. 5, Figures 55, 56)

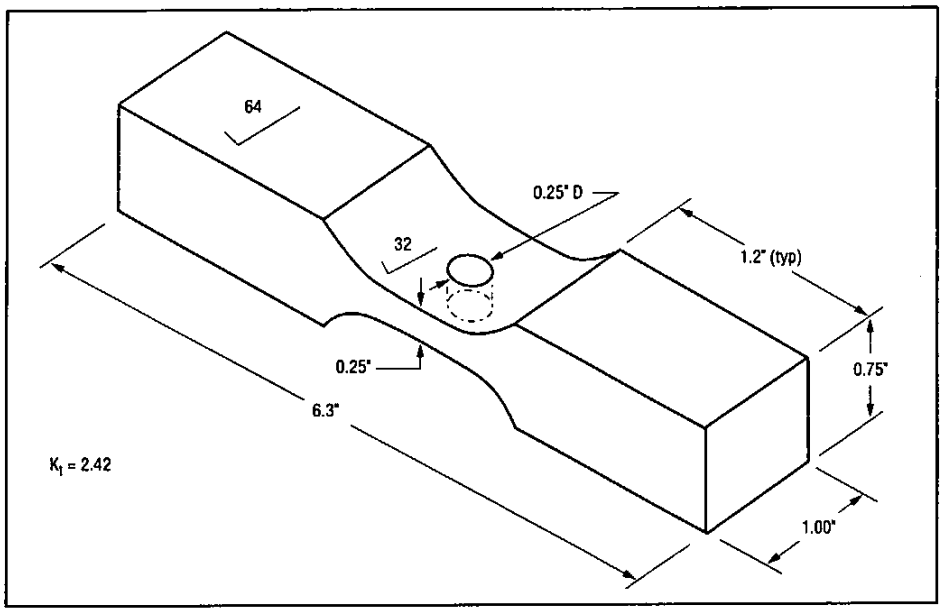


Figure 1.8.11.2 Configuration of fatigue test specimen used to measure the effects of chill rates and aging processes on high-cycle fatigue life (Ref. 41)

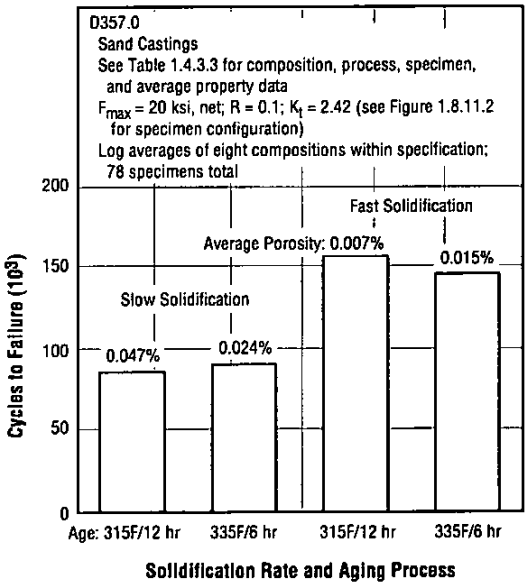


Figure 1.8.11.3 Effect of chill rates and aging proceses on tension-tension fatigue life of notched specimens of D357.0 alloy at 20 ksi maximum stress (Ref. 41)

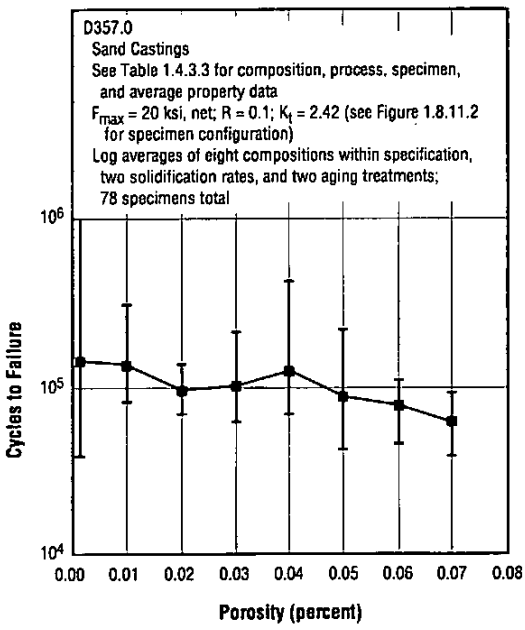


Figure 1.8.11.4 Effect of porosity from different chill rates and aging processes on tension-tension fatigue life of notched specimens of D357.0 alloy at 20 ksi maximum stress (Ref. 41)

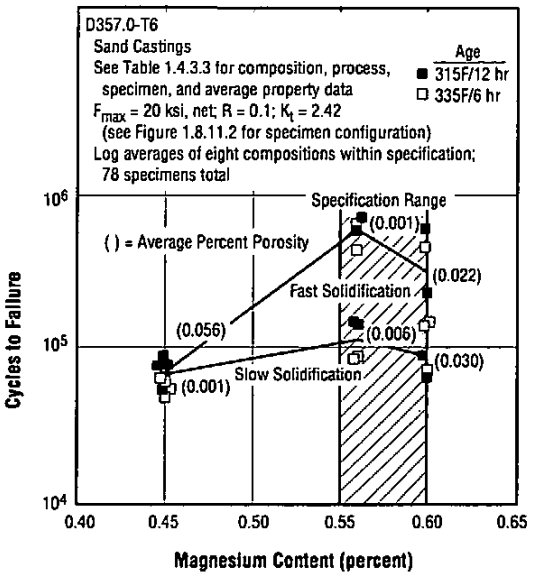


Figure 1.8.11.5 Effect of magnesium content on tension-tension fatigue life of notched specimens of D357.0 alloy at 20 ksi maximum stress, with different chill rates and aging processes (Ref. 41)

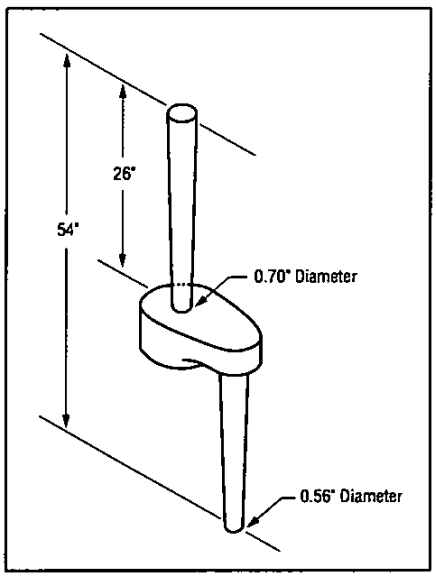


Figure 1.8.12.1 Cascading sprue designed to combine good hydrostatic head with minimum turbulence (Ref. 5)

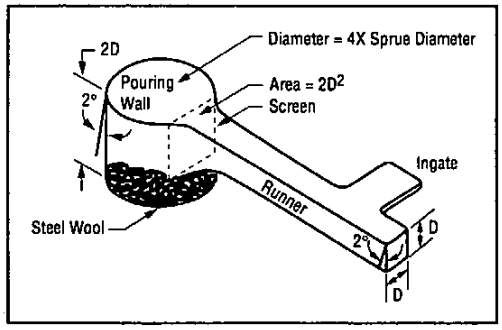


Figure 1.8.12.2 Basic features of pouring well, runner, and ingate (Ref. 5)

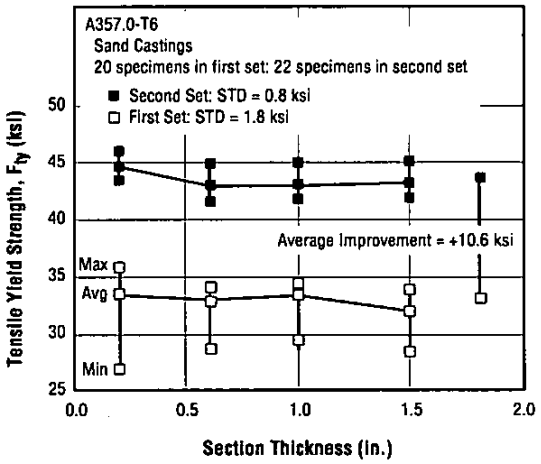


Figure 1.8.13.1 Improvement in tensile yield strength from the first to the second set of sand castings (Ref. 40)

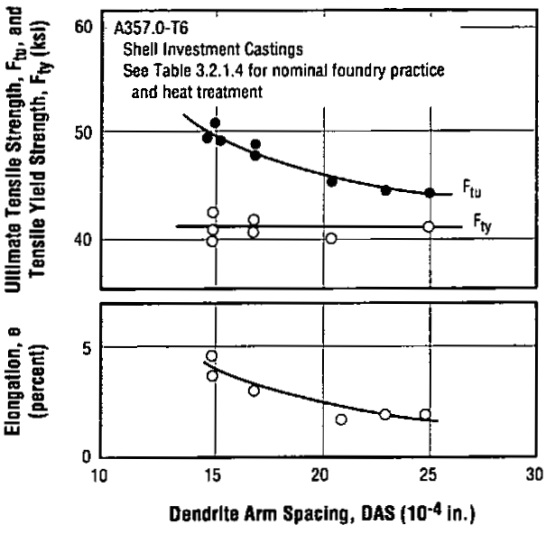


Figure 1.9.1.1 Effect of dendrite arm spacing on tensile properties of shell investment cast plates (Ref. 12)

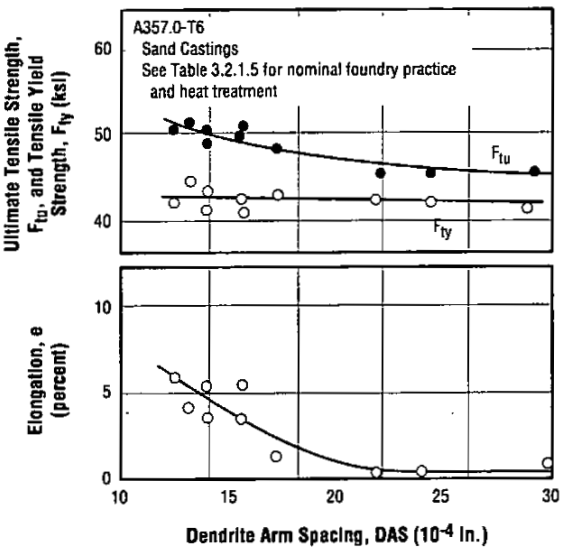


Figure 1.9.1.2 Effect of dendrite arm spacing on tensile properties of sand-cast plates (Ref. 12)

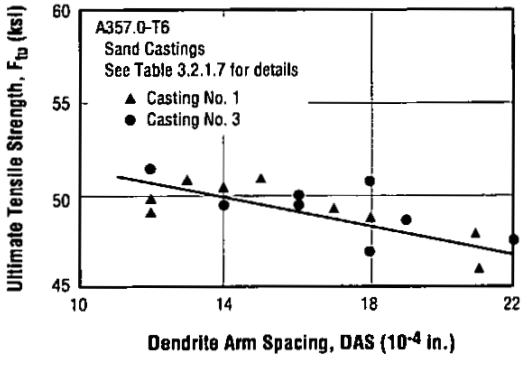


Figure 1.9.1.3 Effect of dendrite arm spacing on tensile strength of specimens from development sand castings (Ref. 13)

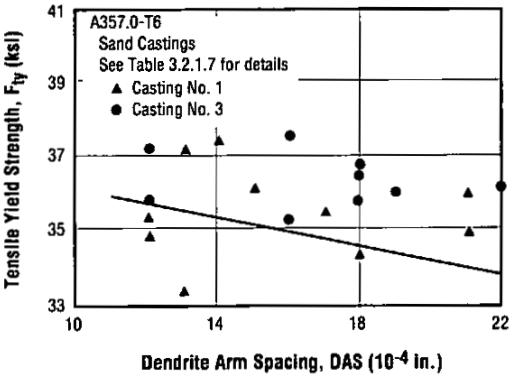


Figure 1.9.1.4 Effect of dendrite arm spacing on tensile yield strength of specimens from development sand castings (Ref. 13)

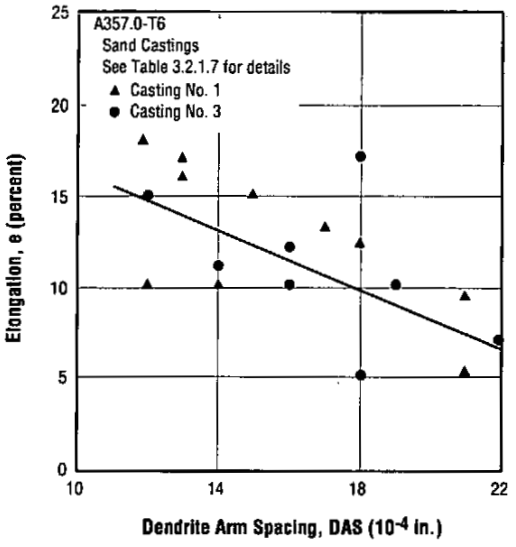


Figure 1.9.1.5 Effect of dendrite arm spacing on tensile elongation of specimens from development sand castings (Ref. 13)

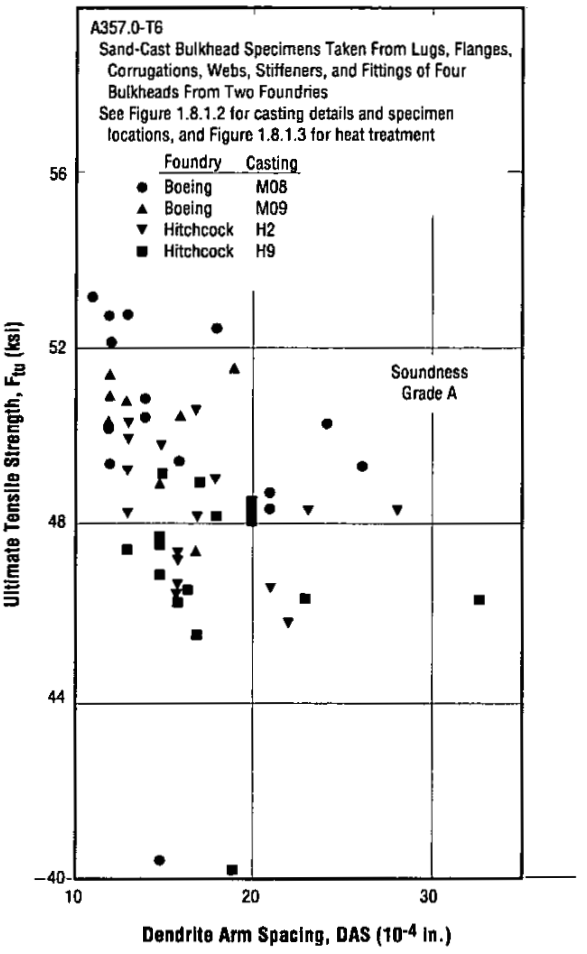


Figure 1.9.1.6 Effect of dendrite arm spacing on tensile strength of specimens with Grade A soundness taken from sand-cast bulkheads (Ref. 10)

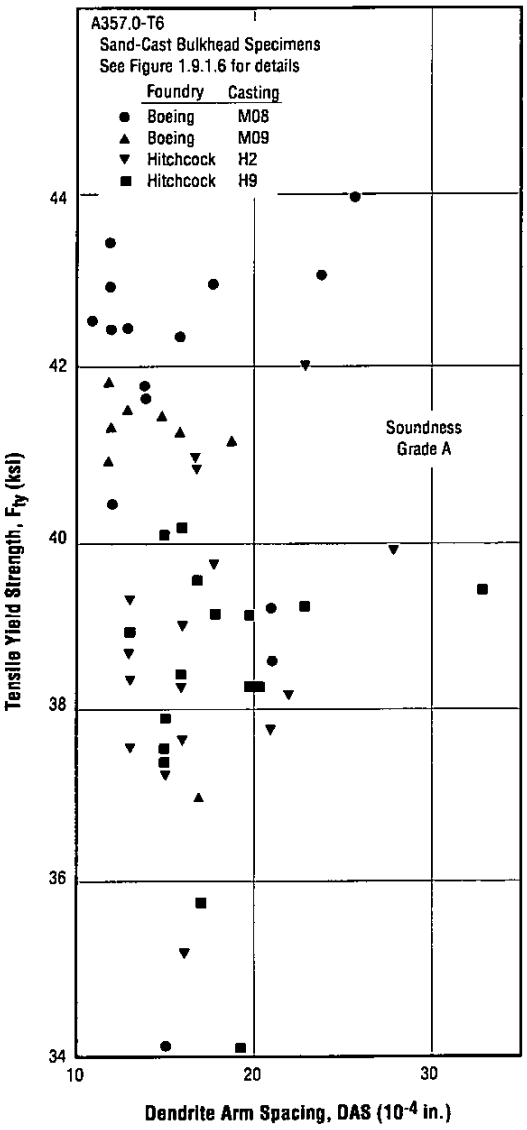


Figure 1.9.1.7 Effect of dendrite arm spacing on tensile yield strength of specimens with Grade A soundness taken from sand-cast bulkheads (Ref. 10)

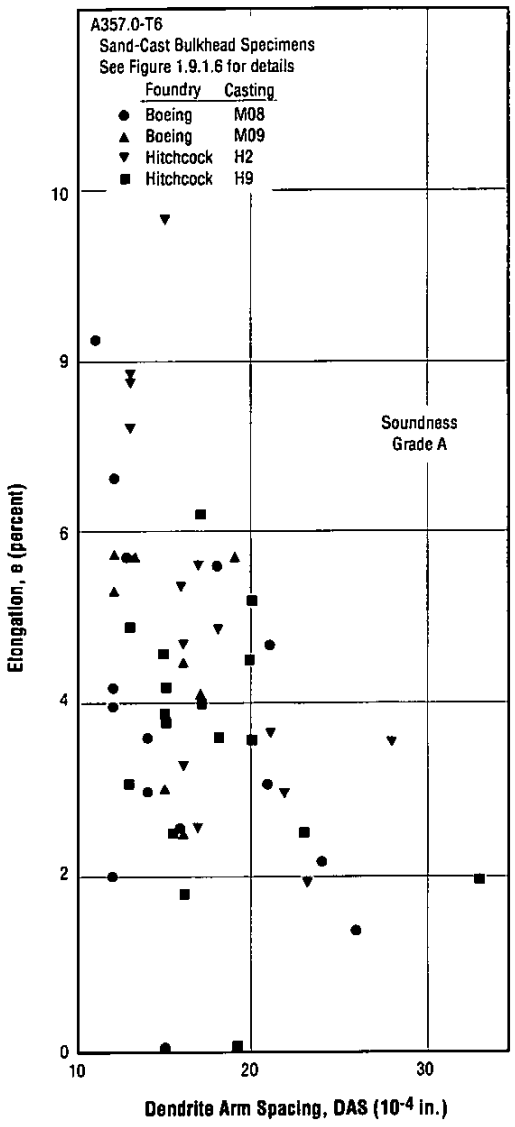


Figure 1.9.1.8 Effect of dendrite arm spacing on tensile elongation of specimens with Grade A soundness taken from sand-cast bulkheads (Ref. 10)

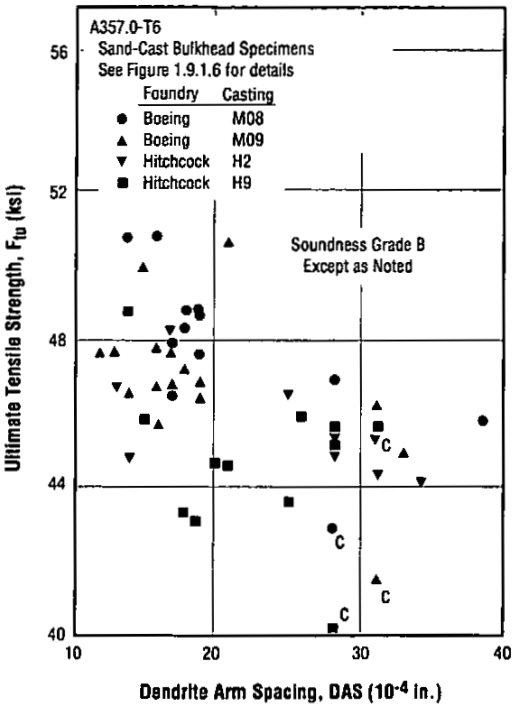


Figure 1.9.1.9 Effect of dendrite arm spacing on tensile strength of specimens with Grades B and C soundness taken from sand-cast bulkheads (Ref. 10)

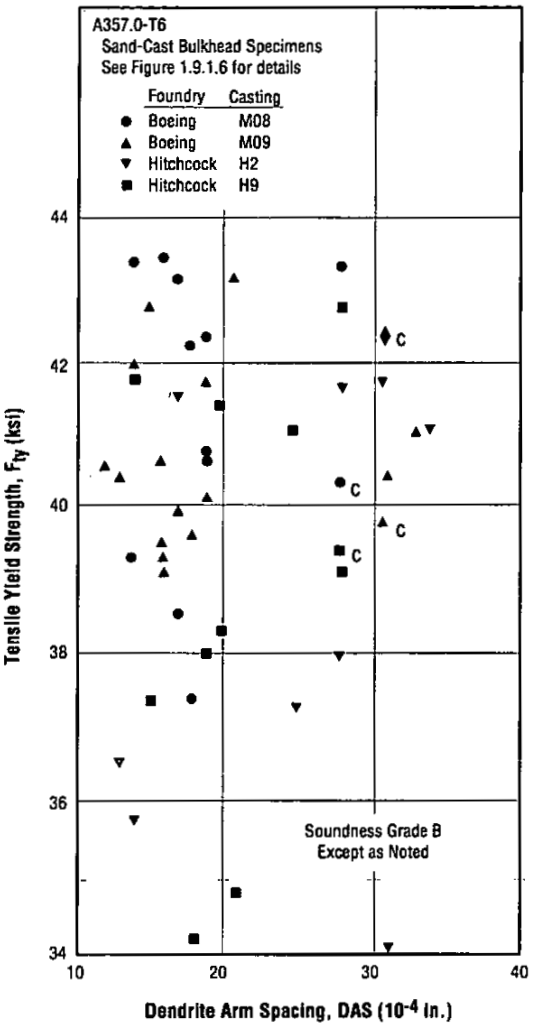


Figure 1.9.1.10 Effect of dendrite arm spacing on tensile yield strength of specimens with Grades B and C soundness taken from sand-cast bulkheads (Ref. 10)

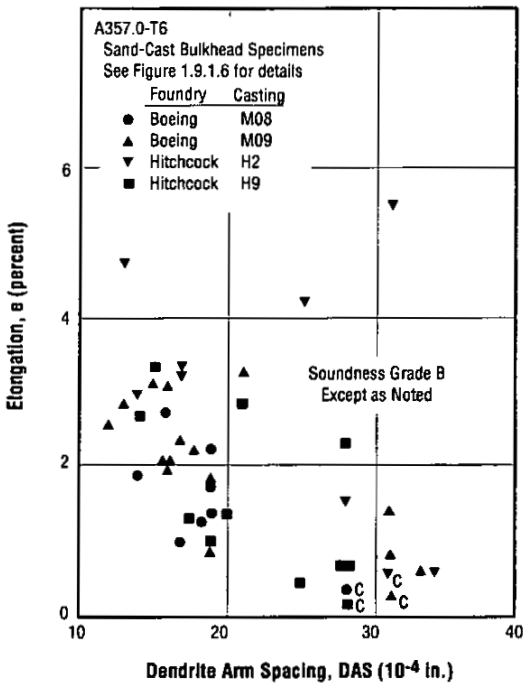


Figure 1.9.1.11 Effect of dendrite arm spacing on tensile elongation of specimens with Grades B and C soundness taken from sand-cast bulkheads (Ref. 10)

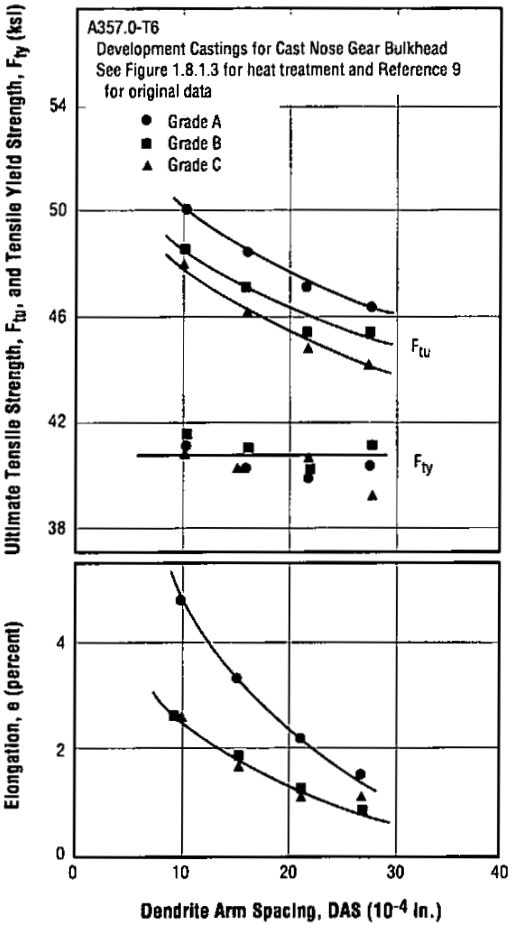


Figure 1.9.1.12 Effect of dendrite arm spacing and radiographic soundness on tensile properties of development castings (Ref. 16)

Note: The data shown represent the average of four selected DAS ranges. This subjective procedure greatly reduces the scatter in the original data.

Table 1.9.3.1 Effect of dross and gas porosity on tensile properties of shell investment and sand-cast plates (Ref. 12)

Alloy	A357.0-T6					
Form	Shell Investment Cast				Sand Casting	
Foundry Practice and Heat Treatment	See Table 3.2.1.4				See Table 3.2.1.5	
Type of Discontinuity	Dross		Gas Porosity		Dross	
Radiographic Grade[a]	A – B	C – D	A – B	C – D	A – B	C – D
F_{tu} (ksi)	49 – 51	42	49 – 51	33 – 38	51 – 53	31 – 47
F_{ty} (ksi)	40 – 42	40	40 – 42	31 – 38	43 – 45	30 – 42
e (percent)	4 – 5	0.5	4 – 5	0.5 – 2	6 – 9	0.2

[a] According to MIL-C-6021.

Table 1.9.3.2 Effect of excessive gas and shrinkage porosity on the tensile properties of sand castings (Ref. 12)

Alloy		A357.0-T6			
Form		Specially Cast Plates to Produce Low Quality Sand Casting			
Grade		D	C – D		B or Better[a]
Type of Discontinuity		Sponge Shrinkage	Round Gas Porosity		
ASTM Plate[b]		No. 4	No. 4	No. 7	
No. of Tests		3	3	2	106
F_{tu} (ksi)	Average	43.8	42.8	47.2	54.3
	Range	40.7 – 46.4	45.4 – 48.8	46.7 – 47.7	—
F_{ty} (ksi)	Average	41.3	42.3	41.3	45.8
	Range	39.7 – 42.2	41.8	42.7	—
e (percent)	Average	1.8	3	3	5.5
	Range	1 - 2	2 - 4	3 - 3	—

[a] See Table 3.2.1.2.

[b] ASTM E 155 Reference Radiographs.

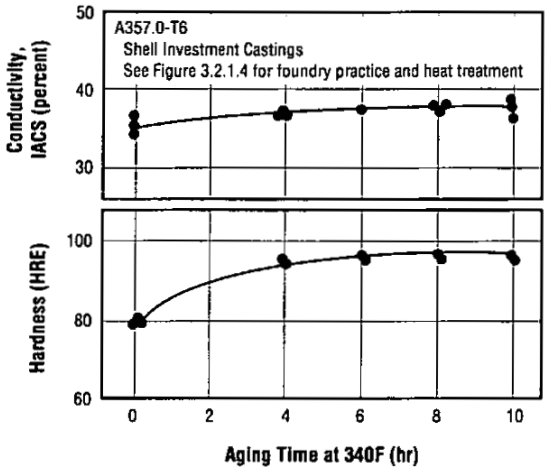


Figure 2.2.2.1 Effect of aging time on the electrical conductivity and hardness of shell investment castings (Ref. 12)

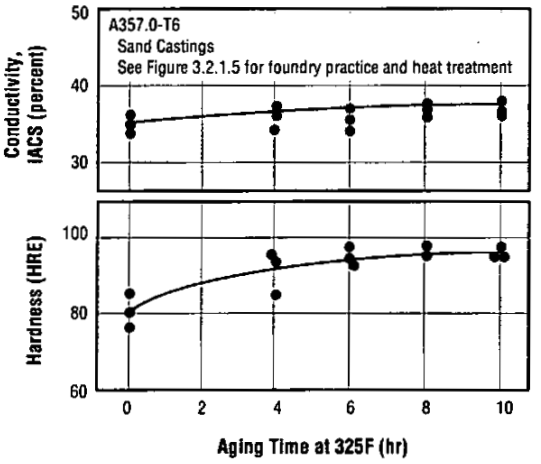


Figure 2.2.2.2 Effect of aging time on the electrical conductivity and hardness of sand castings (Ref. 12)

Table 3.1.1 AMS and ASTM specifications for mechanical properties and microstructure

Alloy	A357.0 and D357.0							
Specification[g]	AMS 4219	AMS 4219C	AMS 4249 and 4241A[c]		ASTM B 108		ASTM B 686	
Specimen Location	Any Area	Separately or Integrally Cast	Designated Area	Other Area	Separately Cast[f]	Designated Area[f]	Any Area	Designated Area
F_{tu} (ksi)	38	41	50	45	45	46	41	45
F_{ty} (ksi)	30	32	40	36	36	36	31	35
e (percent)	2	3	3	2	3	3	3	3
Hardness Brinell[d] 10 to 500kg 10 to 1000 Kg	85 to 115 85 to 120	85 to 115 85 to 120	90	90				

Special Requirements for AMS 4249[a,e]	
K_{Ic} (ksi $\sqrt{in.}$) ASTM E 1304	21
Fatigue Life[b] (cycles)	
Spec. Dia. = 0.5 in.	Log Avg. 85,000 Min. 46,000
Spec. Dia. = 0.375 in.	Log Avg. 78,000 Min. 42,000
Spec. Dia. = 0.25 in.	Log Avg. 88,000 Min. 36,000

[a] Each casting shall have at least two tensile and two fracture toughness coupons. One coupon to remain attached and used only if re-heat treatment is required.

[b] Three fatigue specimens (ASTM E 466) are to be tested from integrally cast coupons or from specimens cut from castings. Testing conditions are K_t = 1, Maximum Stress = 40 ksi, R = 0.1 and Frequency from 10 to 20 Hz. Specimens cut from castings may have gauge diameters of 0.5, 0.375 or 0.25 inches.

[c] The tensile properties shown above for AMS 4241A are associated with procedures for determining the dendrite arm spacing (DAS) from integrally cast chilled and unchilled specimens. These results are then used to determine the DAS necessary to achieve the specified properties. For details concerning DAS requirements reference should be made to AMS 4241A and its related documents.

[d] Casting should not be rejected on basis of hardness if tensile properties are met.

[e] Designated areas of castings shall have a DAS < 0.002 inch determined in accordance with ARP1947.

[f] Applies to castings with maximum section thickness of 2 inches.

[g] For references see Table 1.4.2.

Table 3.1.2 Military specification mechanical properties (Ref. 45)

Alloy	A357.0-T6 and D357.0-T6				
Source	MIL-A-21180D				
Specimen Location	Designated Areas		Any Area		
Strength Class	1	2	10	11	12
F_{tu} (ksi)	45	50	38	41	45
F_{ty} (ksi)	35	40	28	31	35
e (percent)	3	5	5	3	3

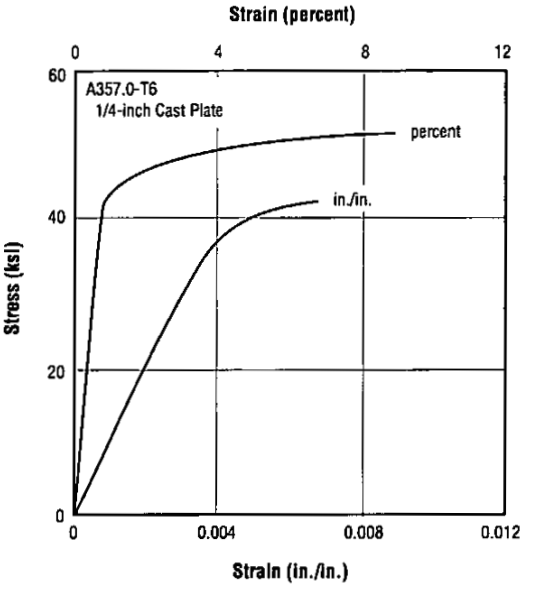


Figure 3.2.1.1 Stress-strain curves for sand-cast plate (Ref. 30)

Table 3.2.1.2 Tensile, compressive, shear, and bearing properties for specimens removed from designated areas of Northrop sand-cast stepped plates from Suppliers A and B (Ref. 12)

Alloy	A357.0-T6								
Condition	Specimens Taken From Northrop Sand-Cast Stepped Plates From Suppliers A and B (See Figure 1.8.1.1)								
Plate Area	Designated Areas (Radiographic Quality B or Better)[a]								
Property	F_{tu} (ksi)	F_{ty} (ksi)	e (percent)	F_{cy} (ksi)	F_{su} (ksi)	F_{bru}, 1.5 e/d (ksi)	F_{bry}, 1.5 e/d (ksi)	F_{bru}, 2.0 e/d (ksi)	F_{bry}, 2.0 e/d (ksi)
Number of Tests	106	106	106	106	10	10	10	10	10
Average	54.3	45.8	5.5	47.2	34.4	92.9	74.3	117.3	84.7
Standard Deviation	1.35	1.41	b	N/A	N/A	N/A	N/A	N/A	N/A
Low Value	51.7	42.2	2	44.1	33.7	90.6	69.4	107.5	82

[a] Includes designated and nondesignated areas from Supplier A since both areas had radiographic quality of B or better.

[b] Distribution not normal.

Note: N/A = not applicable (sample size too small for design purposes).

Table 3.2.1.3 Tensile, compressive, shear, and bearing properties for specimens removed from nondesignated areas of Northrop sand-cast stepped plates from Supplier B (Ref. 12)

Alloy	A357.0-T6								
Condition	Specimens Taken From Northrop Sand-Cast Stepped Plates From Supplier B (See Figure 1.8.1.1)								
Plate Area	Nondesignated Areas (Radiographic Quality B to C)								
Property	F_{tu} (ksi)	F_{ty} (ksi)	e (percent)	F_{cy} (ksi)	F_{su} (ksi)	F_{bru}, 1.5 e/d (ksi)	F_{bry}, 1.5 e/d (ksi)	F_{bru}, 2.0 e/d (ksi)	F_{bry}, 2.0 e/d (ksi)
Number of Tests	32	32	32	5	5	5	5	5	5
Average	50.5	43.7	3	45.6	33.8	92.4	74.8	116.4	82.6
Low Value	44.8	40.8	1	44.1	33.0	90.7	71.0	113.3	83.9

Table 3.2.1.4 Tensile properties and hardness of investment cast test plates (Ref. 12)

Alloy	A357.0-T6			
Form	3-inch x 10-inch x 3/16-inch Thick Shell Investment Casting			
Foundry Practice	300 lb Melt at 1300F + 1.4 lb (5% Ti + 1% B) Grain Refiner + (95% N + 5% Feron 12) Degas + 1300F Pressurized (3-1/2 psia) Pour + High-Pressure H_2O Clean			
Heat Treat	1000F 12 hr, WQ + 12 hr at RT + 340F 6 hr			
Tensile Properties	F_{tu} (ksi)	F_{ty} (ksi)	e (percent)	Hardness, RE
n = 10: $\bar{x}$	48.4	40.3	5.8	94
σ	0.88	0.60	1.08	1.43

Comments: Plate surface DAS range: 1.2 - 1.6 mils
Plate radiographic quality: Grade B (min)
One specimen per plate
10 plates, average Mg 0.51%, Fe 0.10 - 0.13%

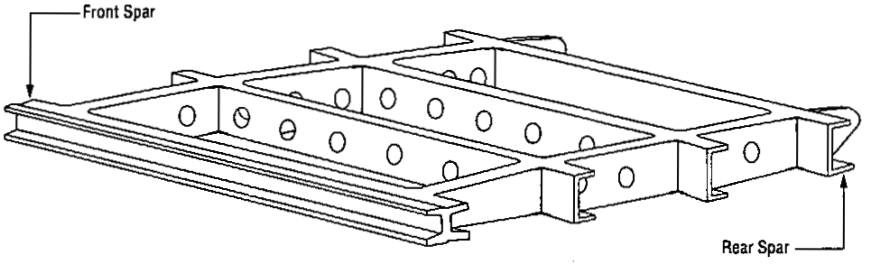
Table 3.2.1.5 Tensile properties and hardness of sand-cast test plates (Ref. 12)

Alloy	A357.0-T6			
Form	3-inch x 10-inch x 3/16-inch Thick Shell-Cast Plates			
Foundry Practice	AFS Bank Sand With 0.8 percent Pepset Binder, Chills in Both Cope and Drag, Two Risers, Steel Wool and Screens in Well of Sprue, 1000-lb Melt at 1300F + (90% N + 10% Cl), Degas + 1375F, Pour			
Heat Treat	1010F 18 hr, 40F WQ (7-11 sec Q Delay) + 12-24 hr at RT + 325F 8 hr			
Tensile Properties	F_{tu} (ksi)	F_{ty} (ksi)	e (percent)	Hardness, RE
n = 9: $\bar{x}$	48.8	41.1	5.5	96
σ	0.89	1.02	0.90	0.87

Comments: Plate surface DAS range: 0.9 - 1.2 mils
Plate radiographic quality: Grade B (min)
One specimen per plate
9 plates, Mg 0.58 - 0.59%, Fe 0.08 - 0.12%

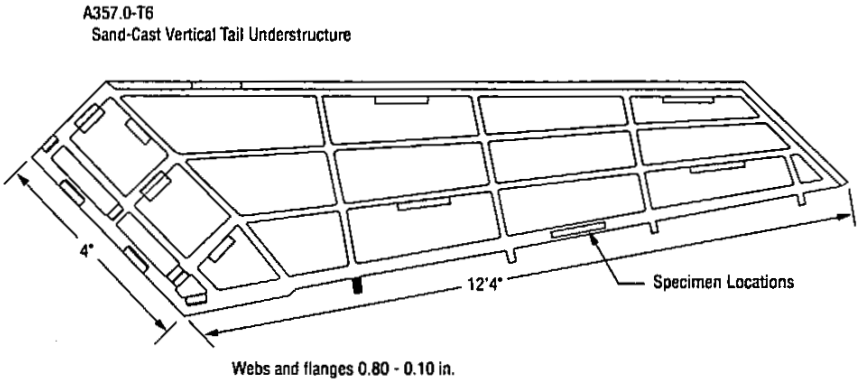
Table 3.2.1.6 Tensile properties of specimens removed from webs and flanges of a development casting for the F-16 vertical tailunderstructure (Ref. 13)

A357.0-T6
Development Sand Casting
See Table 3.2.1.7 for heat treatment



Casting		No. 2	No. 3
Number of Tests		20	20
F_{tu} (ksi)	Average	50.8	51.0
	Range	45.4 – 53.6	47.8 – 53.5
F_{ty} (ksi)	Average	39.4	39.2
	Range	36.8 – 42.3	36.7 – 43.3
e (percent)	Average	9.6	10.7
	Range	5 – 17	7 – 15

Table 3.2.1.7 Tensile properties of composite sand-cast F-16 vertical tail understructure cast at Alcoa (Ref. 13)



Foundry Practice	Melt in Two 500-lb Silicon Carbide Crucibles at 1300F, Degas with 90% N_2 + 10% Cl_2 for 20 min, Vacuum Gas Check (2 - 5 mm Hg With No Bubbles Permitted).Raise Melt to 1440F and Add 5% Ti + 1% B as Grain Refiner. Pour at 1440F. Solution Treat 1010F 15 hr, Quench in 15% Ucon A + Water, Hold 16 hr at RT, Age 310F 6 hr					
Casting Number	2	3	5	6	7	8
Number of Specimens	25	26	29	32	9	8
F_{tu} (ksi) Mean	50.8	50.8	49.0	48.7	51.4	52.2
Std Dev	1.86	1.55	2.38	3.50	0.95	0.74
F_{ty} (ksi) Mean	39.2	40.3	38.6	39.2	38.1	40.6
Std Dev	1.31	3.53	1.27	1.83	0.85	0.65
e (percent) Mean	9.5	10.1	9.3	7.3	13.5	11.1
Std Dev	2.71	2.40	3.32	4.06	1.93	2.23
Results From All Six Castings						
F_{tu} (ksi) Average 49.9 Range 42.3[a] – 53.6	F_{ty} (ksi) Average 39.0 Range 35.5 – 43.3		e (percent) Average 9.4 Range 2[a] – 17.0			

[a] Specimen not machined all over.

Table 3.2.1.8 Average tensile properties of specimens removed from two full-scale bulkheads from the Boeing Foundry (Ref. 10)

Alloy	A357.0-T6					
Foundry	Boeing					
Casting	M08			M09		
Location[a]	F_{tu} (ksi)	F_{ty} (ksi)	e (percent)	F_{tu} (ksi)	F_{ty} (ksi)	e (percent)
Lugs	52.6	42.6	6.1	51	41.1	5.4
Upper Flange	48.2	39.5	3.1	46.9	38.5	2.7
Corrugations	49.1	40.6	2.0	47.4	39.8	3.0
Webs and Stiffeners	49.7	42.7	2.1	46.7	40.8	1.7
Fitting	50.3	43.0	2.2	50.5	41.2	4.5
Periphery Flange	45.0	41.9	0.6	44.8	40.9	1.0

[a] For locations and heat treatments, see Figure 1.8.1.3.

Table 3.2.1.9 Average tensile properties of specimens removed from two full-scale bulkheads from the Hitchcock Foundry (Ref. 10)

Alloy	A357.0-T6					
Foundry	Hitchcock					
Casting	H2			H9		
Location[a]	F_{tu} (ksi)	F_{ty} (ksi)	e (percent)	F_{tu} (ksi)	F_{ty} (ksi)	e (percent)
Lugs	49.4	38.1	7.7	48.1	38.1	5.1
Upper Flange	45.3	34.5	4.7	44.4	34.9	2.7
Corrugations	47.0	38.6	3.7	45.5	38.5	2.1
Webs and Stiffeners	46.8	39.1	2.8	45.9	39.1	2.3
Fitting	48.4	39.9	3.6	46.4	39.4	2.0
Periphery Flange	44.8	41.8	0.6	42.6	41.2	0.4

[a] For locations and heat treatments, see Figure 1.8.1.3.

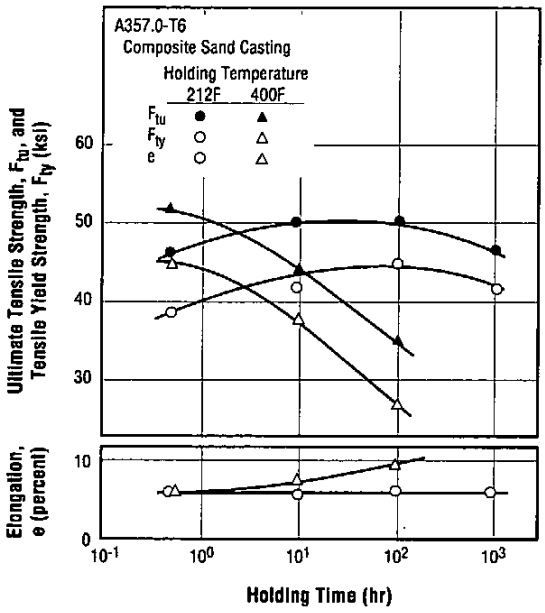


Figure 3.2.1.10 Effect of holding time at 212 or 400F on tensile properties at room temperature (Ref. 19)

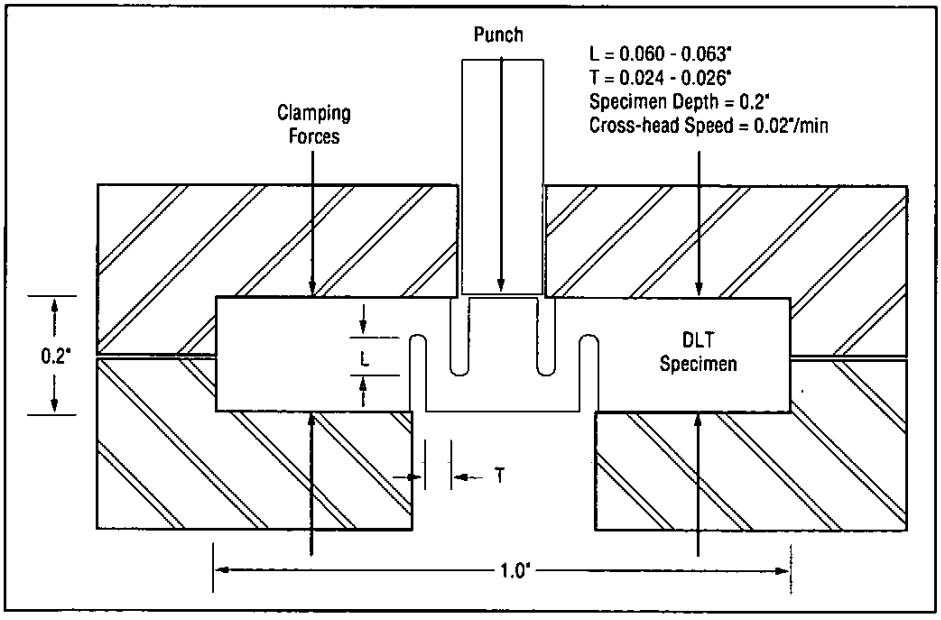


Figure 3.2.1.11 Configuration of double ligament tensile (DLT) specimen in test rig used to measure anisotropy in mechanical properties of cylindrical sand castings (Ref. 42)

Table 3.2.1.12 Effect on tensile properties of specimen orientation with respect to axis of sand-cast cylinders (Ref. 42)

Alloy	A357.0-T6		
Form	Sand-Cast Cylinders 6-inch outside diameter, 1-inch inside diameter		
Composition	7.0 Si, 0.08 Fe, 0.20 Cu, 0.55 Mg, 0.10 Zn, 0.05 Be		
Specimen Geometry	DLT (See Figure 3.2.1.11 for details)		
Test Conditions	RT, Laboratory Air, 55% R.H		
Ligament Orientation With Respect to Axis of Cylinder[a]	F_{ty} (ksi)	F_{tu} (ksi)	e (percent)
Longitudinal	42.9	54.6	8.9
Radial	41.3	55.0	9.6
Tangential	42.4	50.1	8.0

[a] Average of four tests per orientation.

Table 3.2.1.13 Smooth tensile, notch tensile and fracture toughness properties of specimens from sand composite cast plates from three suppliers and from F5 wing pylons (Ref. 41)

Alloy	D357.0-T6							
Composition	AMS 4241 plus Si modifier (either Sr or Na)							
Form	16 x 6 x 1.25-in. cast plates from three foundries, each using metal chills in somewhat different rigging						F5 wing pylon 65 lb; 5' long	
Supplier	Foundry A		Foundry B		Foundry C		Alcoa	
Si Modifier	Na		Sr		Na		See below	
Solution Treat	1015F 15 hr RT WQ or RT GQ[a]		1010F 24 hr RT WQ or RT GQ		1010F 19 hr RT WQ or 1010F 16 hr, RT GQ		1010F 15 hr RT WQ	
Age	335F 6 hr		315F 13 hr		RT 24 hr, 335F 6 hr		325F 5.5 hr	
Properties	Water Quench	Glycol Quench	Water Quench	Glycol Quench	Water Quench[b]	Glycol Quench[b]	Na mod.	Sr mod.
F_{tu}[c] (ksi)								
Average	54	53	52	49	54	51	52	53
Minimum	51	51	50	48	53	50	49	49
Maximum	55	55	53	50	55	52	53	53
F_{ty} (ksi)								
Average	45	43	45	42	47	44	42	41
Minimum	44	42	44	41	46	43	39	39
Maximum	47	44	46	43	48	44	44	43
e (percent)								
Average	5.9	6.6	4.5	3.4	5.4	4.9	6.8	10.2
Minimum	3.5	5.5	3.0	2.5	3.9	4.6	3.5	8.0
Maximum	8.5	9.0	5.6	4.3	8.2	5.2	8.6	11.7
NTS/F_{ty}[d]								
Average	1.40	1.33	1.36	1.38	1.12	1.01	1.44	1.49
Minimum	1.23	1.30	1.30	1.35	0.97	0.98	1.44	1.49
Maximum	1.51	1.36	1.45	1.41	1.36	1.07	1.44	1.49
K_{Ic}[e] (ksi $\sqrt{in.}$)								
Average		21		22		22		

[a] 25 percent glycol solution.

[b] Second batch of cast plates; first batch rejected for low elongation.

[c] ASTM B 557 specimen.

[d] ASTM E 602 0.5-inch D specimen.

[e] ASTM B 647 compact tension specimen.

Table 3.2.1.14 Smooth tensile and fracture toughness properties of specimens from sand composite cast plates with intentional defects (Ref. 41)

Alloy	D357.0-T6								
Composition	AMS 4241 plus Si modifier (Na)								
Form	16 x 6 x 1.25-in. Cast Plates								
Supplier	Alcoa								
Si Modifier	Na								
Solution Treat	1015F 15 hr, RT WQ or RT GQ[a]								
Age	335F 6 hr								
Properties	Baseline[b]	Gas Porosity			Shrinkage Porosity		Foreign Material		Weld Repair[e]
	Grade A/B	Grade B	Grade C	Grade D	Grade B	Grade C	Grade B	Grade C	Grade A/B
F_{tu}[c] (ksi)									
Average	54	51	50	49	51	51	54	53	55
Minimum	53	47	49	48	50	50	51	49	54
Maximum	55	52	53	49	53	51	55	53	56
F_{ty} (ksi)									
Average	48	45	46	44	46	46	46	41	47
Minimum	47	42	44	44	44	45	45	39	46
Maximum	48	46	48	45	48	46	48	43	48
e (percent)									
Average	3.9	3.3	2.7	1.5	2.7	2.9	4.6	10.2	5.1
Minimum	1.1	2.1	1.5	1.3	1.5	2.2	3.1	8.0	3.5
Maximum	5.0	4.3	7.9	1.7	7.9	3.9	7.5	11.7	8.0
K_{Ic}[d] (ksi $\sqrt{in.}$)									
Average		21	22		20	23			

[a] 25 percent glycol solution.

[b] No intentional defects.

[c] ASTM B 557 specimen.

[d] ASTM E 602 compact tension specimen.

[e] See Section 4.3.1.1 for description of tests.

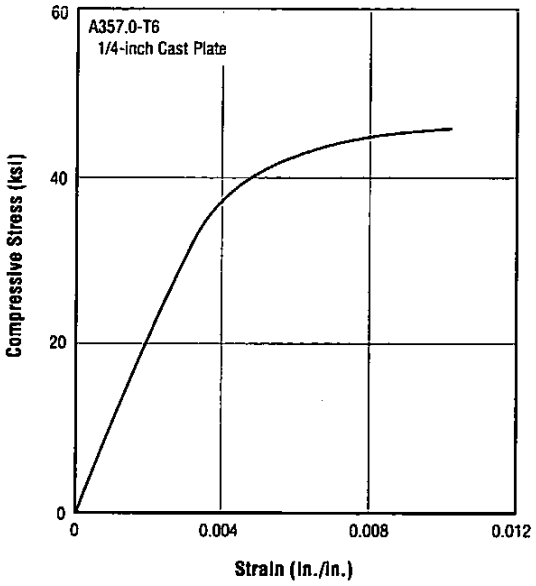


Figure 3.2.2.1 Compressive stress-strain curve for sand-cast plate (Ref. 30)

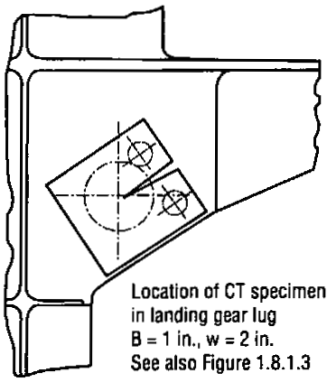
Table 3.2.7.2.2 Results of tests on ASTM E 399 compact specimens removed from separately sand-cast blocks (Ref. 31)

Alloy	A357.0-T6											
Form	0.690 - 0.750-inch Thick CT Specimens From Separately Cast Blocks (See Figure 1.8.1.3 for Heat Treatment)											
F_{ty} (ksi)	41	41	40	42	42	41	41	36	42	42	38	38
K_Q[a] (ksi $\sqrt{in.}$)	20.5	11.6	17.5	14.3	—	13.5	—	17.2	—	20.8	—	19.9
K_{Ic}[b] (ksi $\sqrt{in.}$)	—	—	—	—	16.6	—	16	—	19.4	—	18.2	—

[a] Values not valid due to excessive crack front curvature.

[b] Values valid according to ASTM E 399-78.

Table 3.2.7.2.3 Results of tests on ASTM E 399 compact specimens removed from sand-cast bulkhead lugs (Ref. 7)



Supplier A	Supplier B
K_Q[a] (ksi $\sqrt{in.}$)	K_Q[a] (ksi $\sqrt{in.}$)
24.4	21.6
20.5	20.8
20.6	19.7
20.0	20.6
21.4	18.3 } [b]
21.6	18.7 } [b]
	13.9 } [b]

[a] No valid K_{Ic} values due to crack curvature.

[b] Excessive microshrinkage.

Table 3.2.7.2.4 Results of tests on ASTM E 399 compact specimens removed from separately sand-cast blocks and from designated areas of stepped plates (Ref. 12)

Alloy	A357.0-T6		
Foundry Practice and Heat Treatment	See Table 3.2.1.5		See Figure 1.8.1.1
Form	Separately Cast Block		Stepped Plates Designated Areas
Supplier	A	B	A
F_{tu} (ksi)	51.4	52.3	55
F_{ty} (ksi)	43.3	45.9	47.2
e (percent)	6	5	7.7
Specimen Thickness (in.)	0.8	0.8	0.5
K_Q[a] (ksi $\sqrt{in.}$) Range	25.7 - 26.7	25.5 - 26.6	18.5 - 25.2

[a] No valid E 399 values due to insufficient thickness or excess crack curvature.

Table 3.2.7.2.5 Results of tests on ASTM E 399 compact specimens removed from full-scale F-16 vertical tail understructure (Ref. 13)

Alloy	A357.0-T6	
Form	CT Specimens From Full-Scale F-16 Vertical Tail Understructure (See Table 3.2.1.7)	
Specimen No.	Thickness (in)	K_Q[a] (ksi $\sqrt{in.}$)
2	0.295	23.1
5	0.154	25.8
7	0.293	22.7
10	0.248	30.1

[a] Insufficient thickness according to ASTM E 399.

Table 3.2.7.2.6 Fracture toughness of specimens removed from intentionally produced defective step plates (Ref. 12)

Alloy	D357.0
Castings	Step Plates (See Figure 1.8.1.1)
Radiographic Grade	Worse than D
Discontinuity Type	Sponge Shrinkage Nos. 6 and 7
Specimen	0.5-in thick CT
K_Q (ksi $\sqrt{in.}$)	
Minimum	22.5
Maximum	25.1
Average	23.0
Number of Tests	3

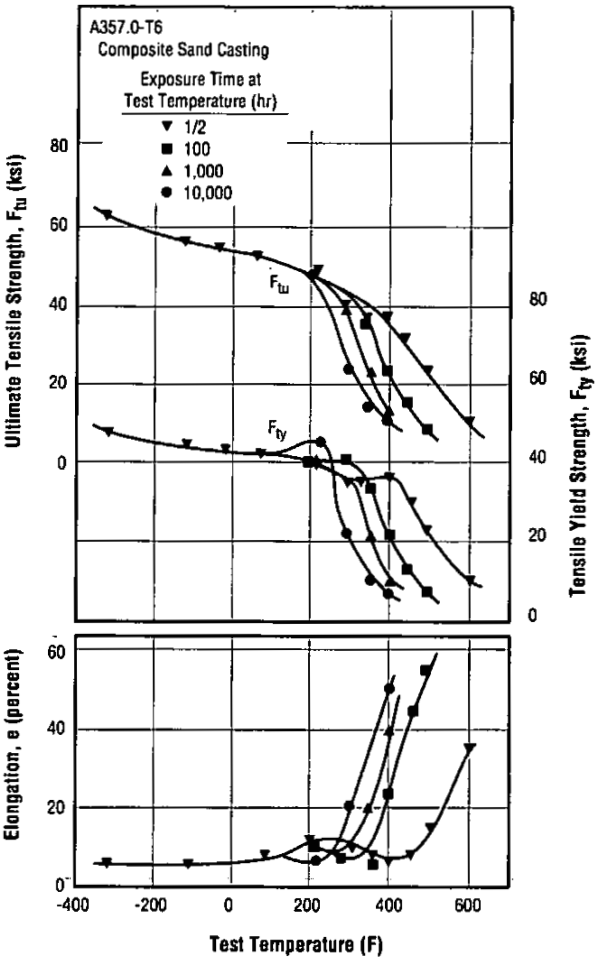


Figure 3.3.1.1 Effect of test temperature and holding time on tensile properties (Ref. 19)

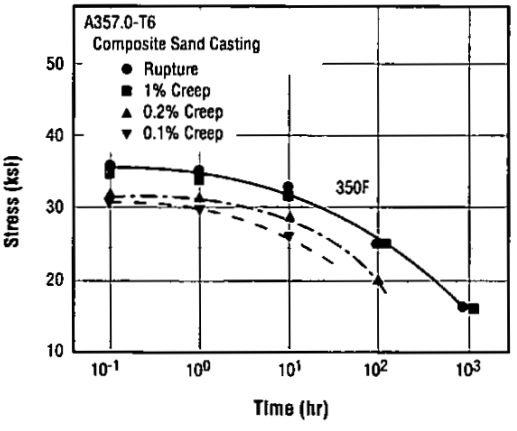


Figure 3.4.1 Creep and creep rupture at 350F (Ref. 19)

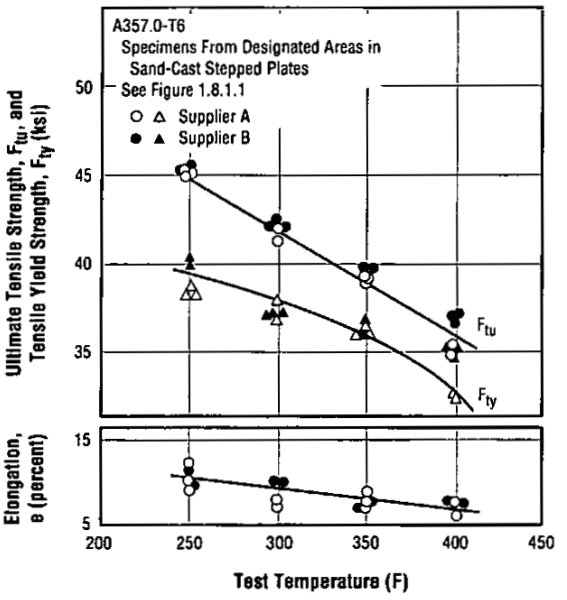


Figure 3.3.1.2 Effect of elevated test temperature on tensile properties of sand castings (Ref. 12)

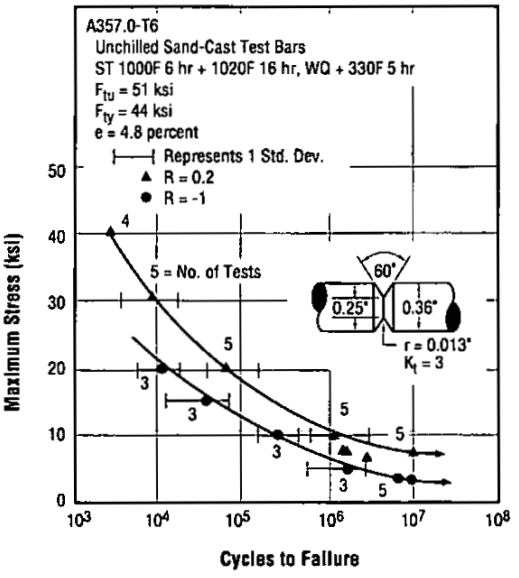


Figure 3.5.1.1 S-N curves for axial fatigue of separately sand-cast test specimens (Ref. 17)

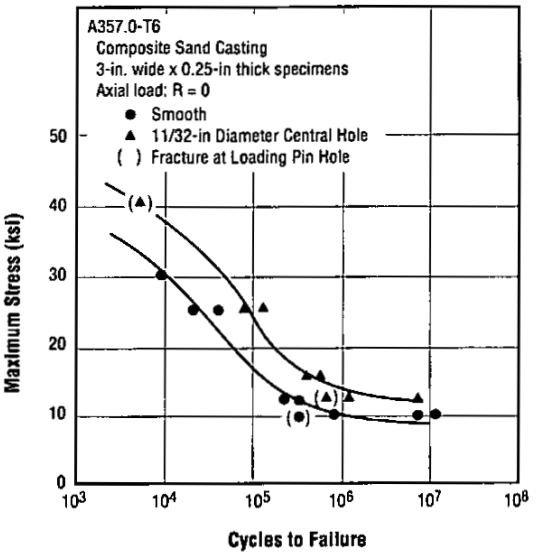


Figure 3.5.1.2 S-N curves for smooth and notched specimens (Ref. 19)

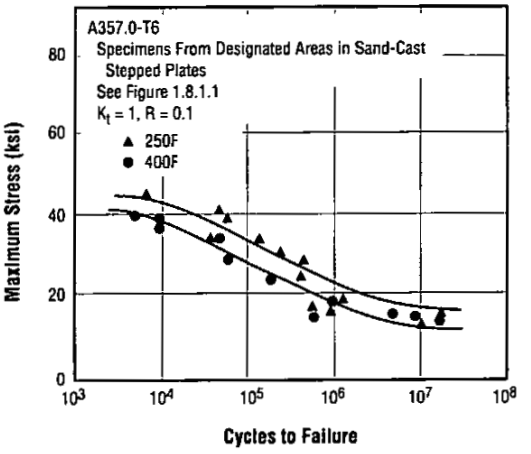


Figure 3.5.1.3 S-N curves at elevated tempertures for specimens removed from sand-cast stepped plates (Ref. 32)

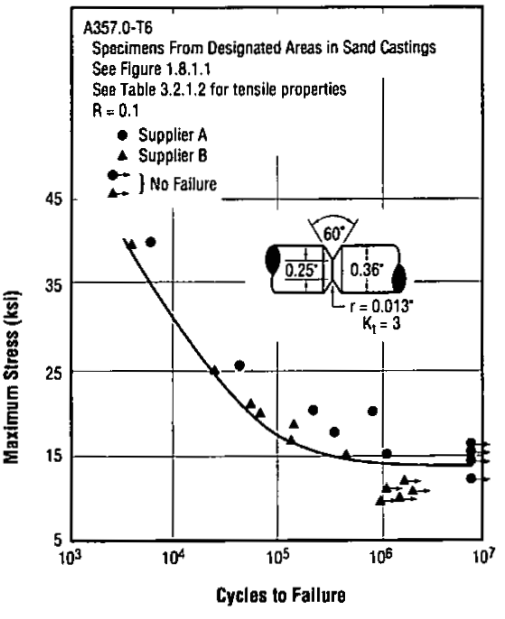


Figure 3.5.1.4 S-N curves for notched specimens from sand-castings (Ref. 12)

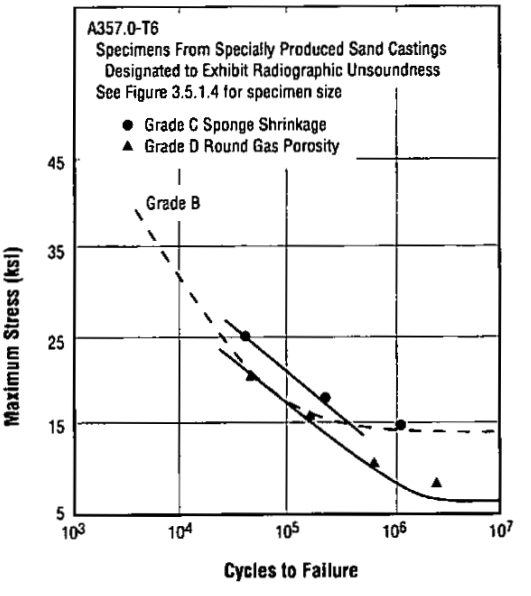


Figure 3.5.1.5 Effect of sponge shrinkage (Grade C) and round gas porosity (Grade D) on notched fatigue properties of sand castings (Ref. 12)

Table 3.5.1.6 Smooth and notched fatigue properties of separately sand-cast specimens and specimens removed from cast bulkhead (Refs. 4, 7)

Alloy	A357.0-T6 Sand-Cast		
Condition	Separately Cast Specimens (4)		Specimens From Bulkhead Corrugations (7)
Specimen Type[a]	Smooth	$K_t = 3$	$K_t = 3$
Number of Tests	20	16	10
Maximum Stress (ksi), R = 0.06	18	16	18
Range of Cycles to Failure (10^3)	75 - 380	58 - 180	30 - 103
Weibull Characteristic Life (10^3 cycles)	220	98	—
95 percent Reliability With 95 percent Confidence (Weibull) Cycles to Failure (10^3)	56	26	—

[a] Specimens approximately 1-1/8 inch wide by 1/8 inch thick. $K_t = 3$; specimens had 3/16-inch diameter hole.

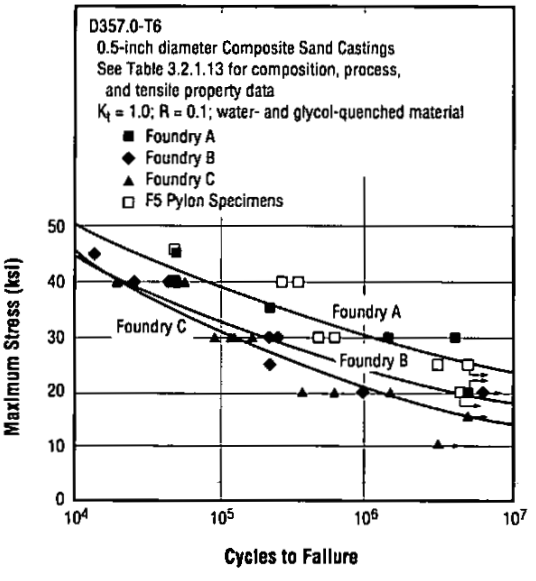


Figure 3.5.1.7 S-N curves for smooth specimens from composite sand-cast plates from three suppliers and from designated areas of four F5 wing pylons (Ref. 41)

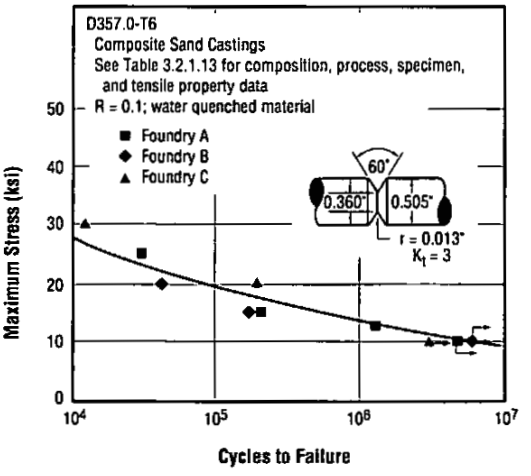


Figure 3.5.1.8 S-N curves for notched specimens from composite sand-cast plates from three suppliers (Ref. 41)

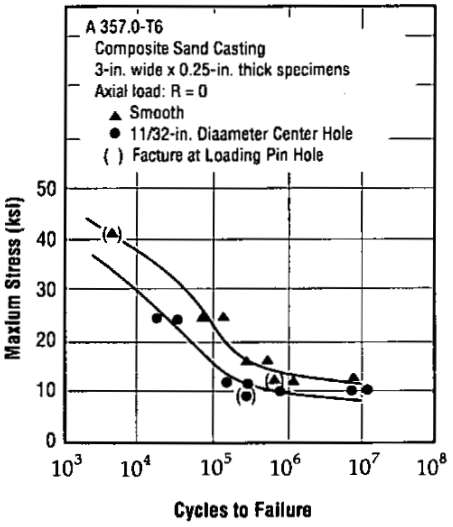


Figure 3.5.1.2 S-N curves for smooth and notched specimens (Ref. 19).

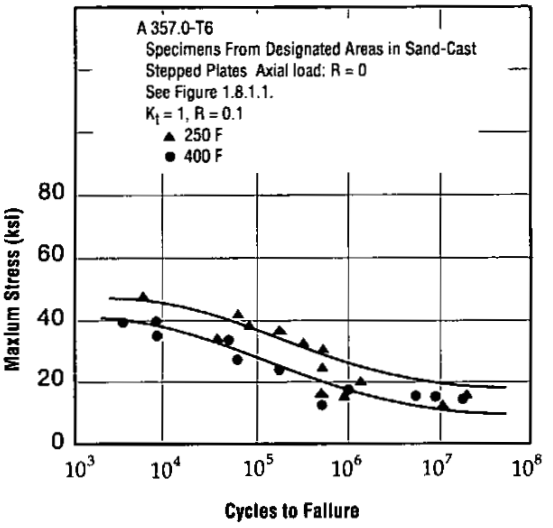


Figure 3.5.1.3 S-N curves at elevated temperatures for speciment removed from sand-cast stepped plates (Ref. 32)

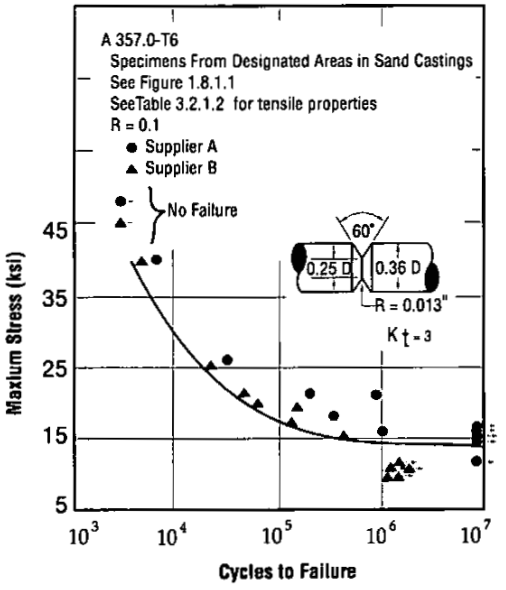


Figure 3.5.1.4 S-N curves for notched specimens from sand-castings (Ref. 12)

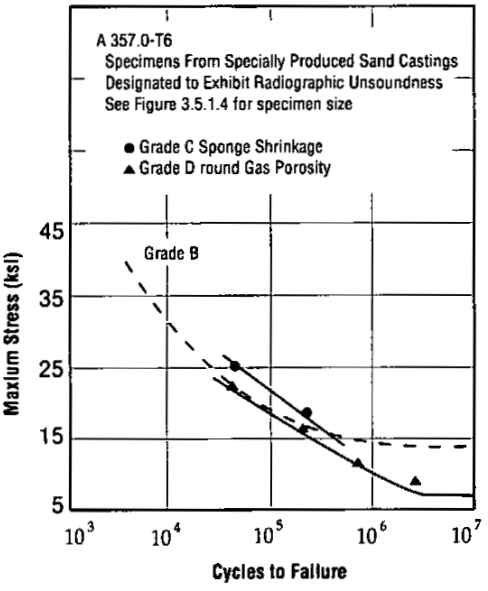


Figure 3.5.1.5 Effect of sponge shrinkage (Grade C) and round gas porosity (Grade D) on notched fatiguw properties of send castings (Ref. 12)

Table 3.5.1.6. Smooth and notched fatigue properties of separately sand-cast specimens and specimens removed from cast bulkhead (Refs. 4, 7)

Alloy	A357.0-T6 Sand-Cast		
Condition	Separately Cast Specimens (4)		Specimens from Bulkhead Corrugation (7)
Specimen Type[a]	Smooth	$K_t = 3$	$K_t = 3$
Number of Tests	20	16	10
Maximum Stress (ksi), R = 0.06	18	16	18
Range of Cycles to Failure (10^3)	75-380	58-180	30-103
Weibull Chaaracteristic Life (10^3 cycles)	220	98	–
95 percent reliability with 95 percent confidence (Weibull Cycles to Failure (10^3)	56	26	–

[a] Specimens approximaately 1-1/8 inch wide by 1/8 inch thick $K_t = 3$; specimens had 3/16-inch diameter hole.

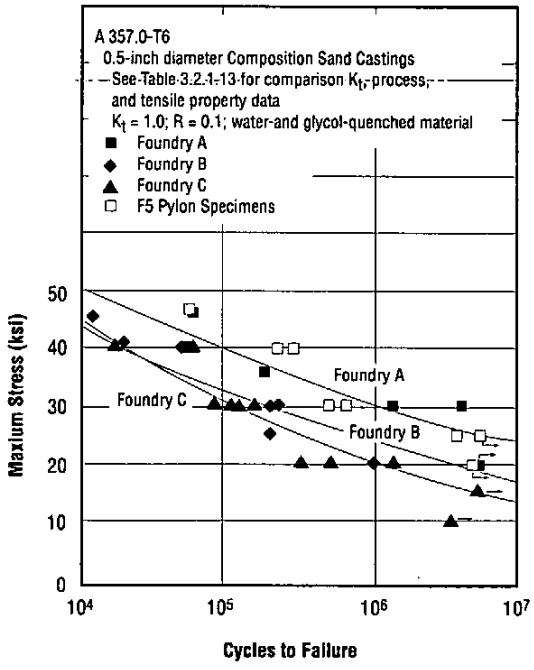


Figure 3.5.1.7 S-N curves for smooth specimens from composite sand-cast plates from three suppliers and from designated areas of four F5 wing Pylons (Ref. 41)

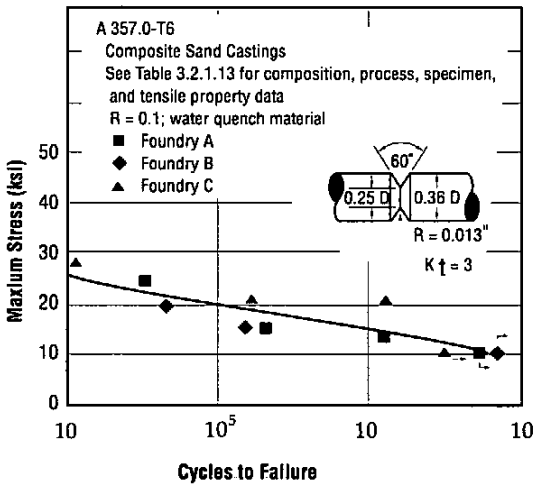


Figure 3.5.1.8 S-N curves for notched specimens from composite sand-cast plates from three suppliers (Ref. 41)

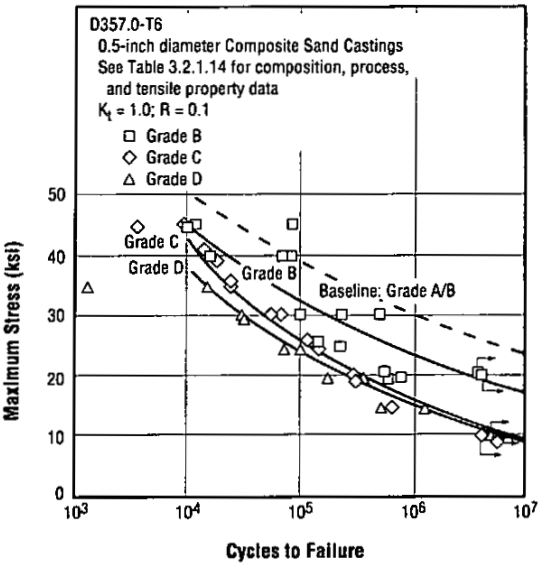


Figure 3.5.1.9 Effect of gas porosity on S-N curves for smooth specimens from composite sand-cast plates (Ref. 41)

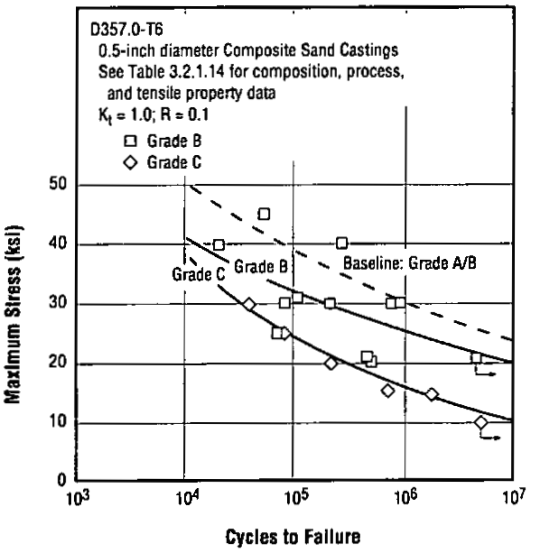


Figure 3.5.1.10 Effect of shrinkage porosity on S-N curves for smooth specimens from composite sand-cast plates (Ref. 41)

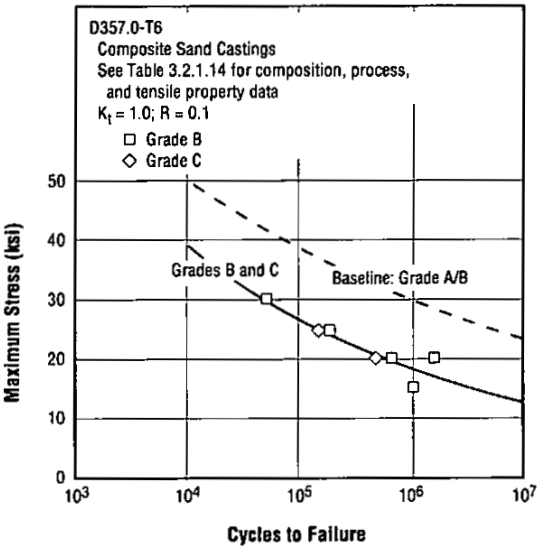


Figure 3.5.1.11 Effect of dross on S-N curves for smooth specimens from composite sand-cast plates (Ref. 41)

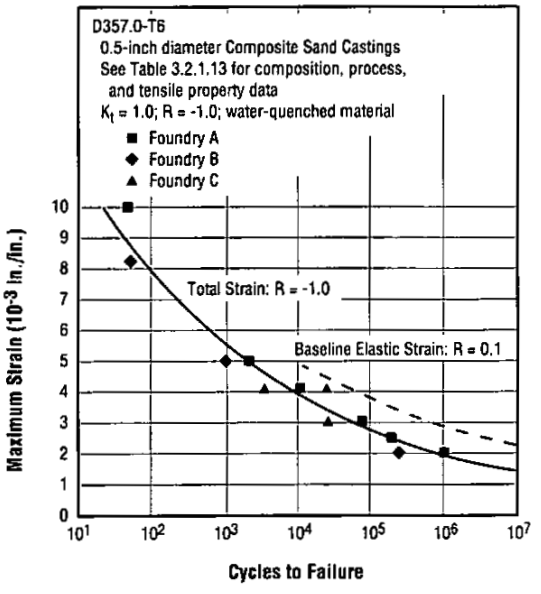


Figure 3.5.2.1 Strain-fatigue life curve for smooth specimens from composite sand-cast plates from three suppliers (Ref. 41)

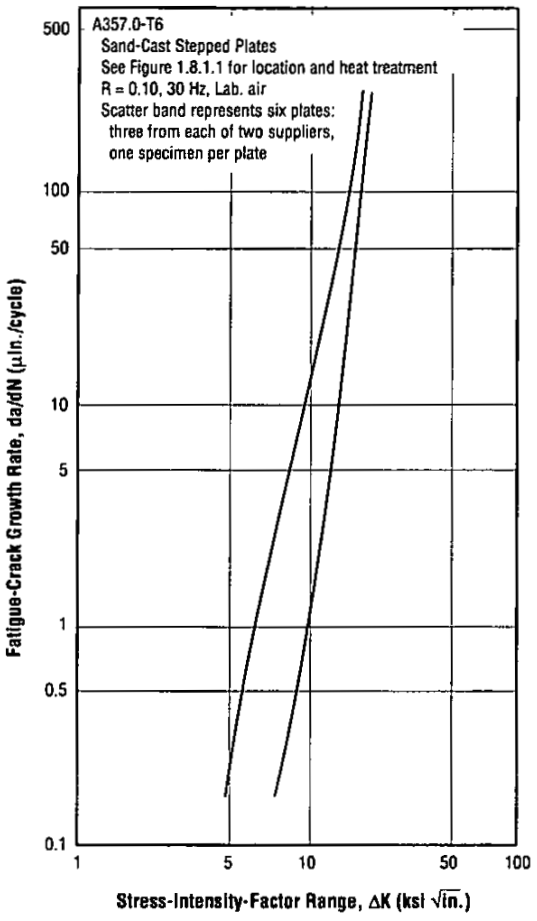


Figure 3.5.3.1 Fatigue-crack growth rates for specimens removed from designated areas in sand-cast stepped plates (Ref. 12)

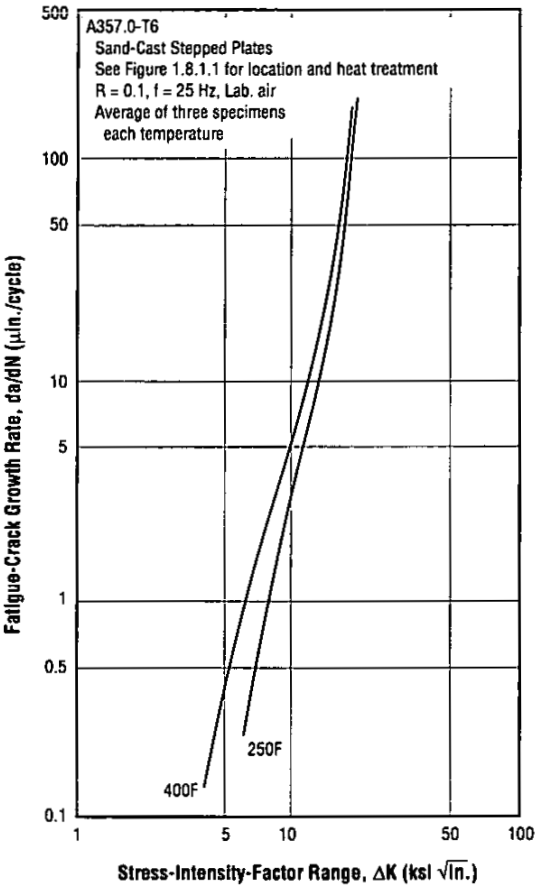


Figure 3.5.3.2 Fatigue-crack growth rates at 250 and 400F for specimens removed from designated areas in sand-cast stepped plates (Ref. 12)

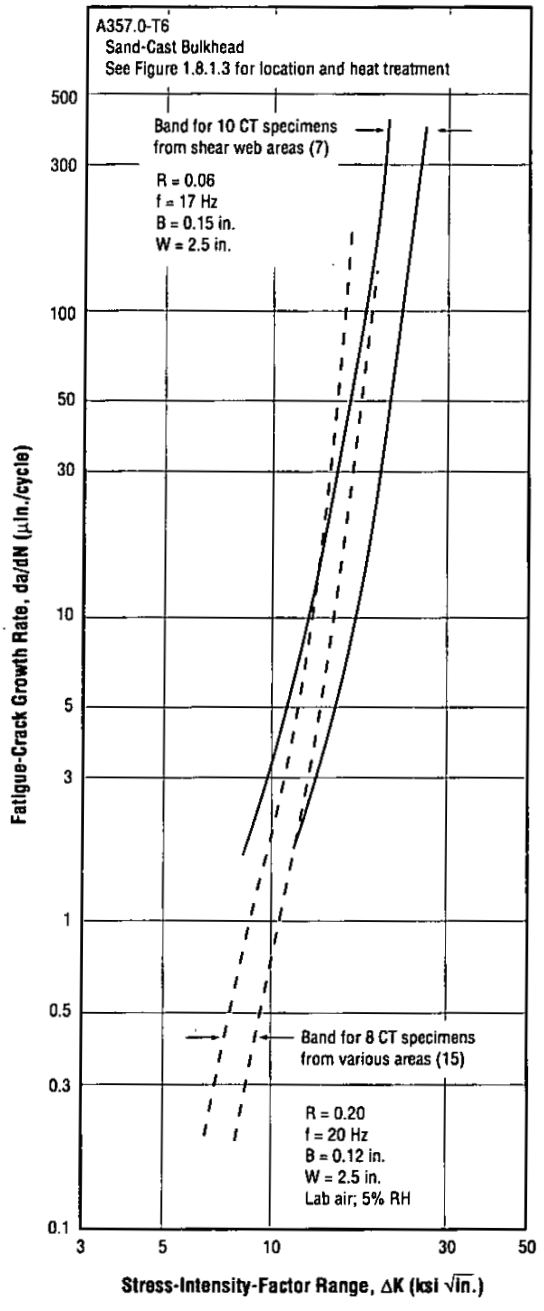


Figure 3.5.3.3 Scatter bands of fatigue-crack growth rates for specimens removed from a cast bulkhead (Refs. 7, 15)

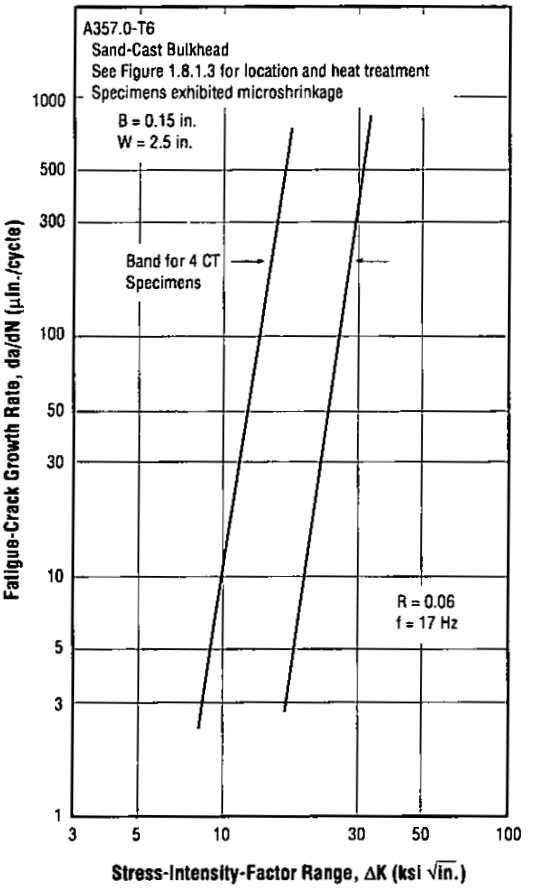


Figure 3.5.3.4 Scatter band of fatigue-crack growth rates for specimens removed from a cast bulkhead in shear web areas exhibiting microshrinkage (Ref. 7)

Table 3.5.3.5 Measures of the variability in cycles required to grow a crack from an initial to a final value (derived from tests on seven specimens) (Ref. 15)

Alloy	A357.0-T6			
Form	Cast Full-Scale Bulkheads (see Figure 1.8.1.3 for details)[a]			
Test Condition	a_f Constant			
a_i (in.)	a_f (in.)	Mean Life (kcycles)	Std Dev of Life	C.O.V.[b]
0.688	1.302	828.2	143.0	0.18
0.749	—	595.3	95.9	0.16
0.841	—	303.6	69.8	0.23
0.933	—	131.2	26.7	0.20
1.026	—	46.83	4.3	0.09
1.118	—	12.75	3.4	0.26
1.120	1.302	2.2	1.26	0.57
Test Condition	$(a_i - a_f)$ Constant			
0.688	0.749	232.9	56.3	0.24
0.749	0.841	290.5	55.2	0.19
0.841	0.933	173.3	45.4	0.26
0.933	1.026	84.38	23.6	0.28
1.026	1.118	34.04	4.55	0.13
1.118	1.210	10.54	2.4	0.23
1.120	1.302	2.21	1.3	0.57

[a] Average tensile properties from specimens cut from fatigue-crack growth CT specimens: F_{tu} = 49.9 ksi, F_{ty} = 43.5 ksi, e = 4.3 percent.

[b] Coefficient of variation.

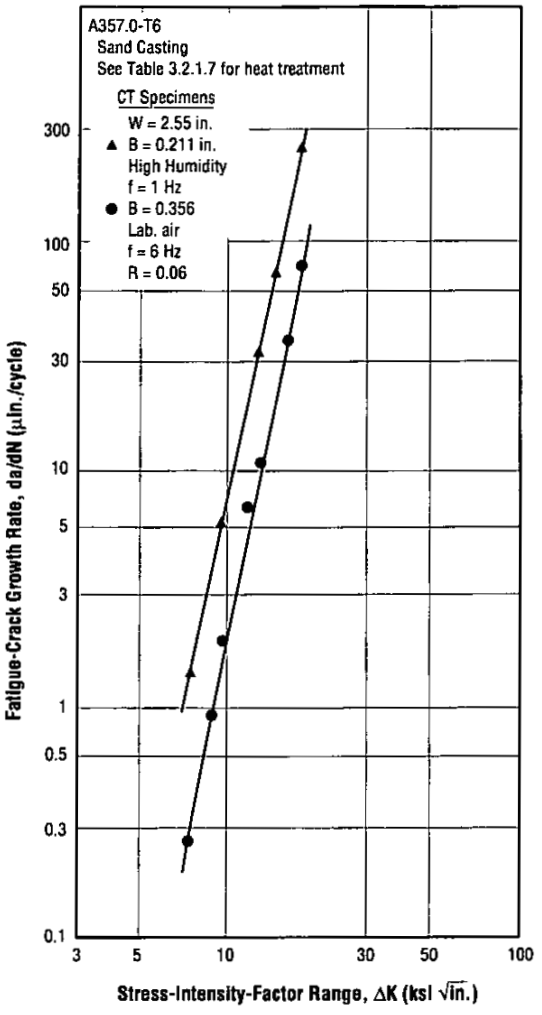


Figure 3.5.3.6 Fatigue-crack growth rates in lab air and in high humidity for specimens removed from full-scale F-16 vertical tail substructure (Ref. 13)

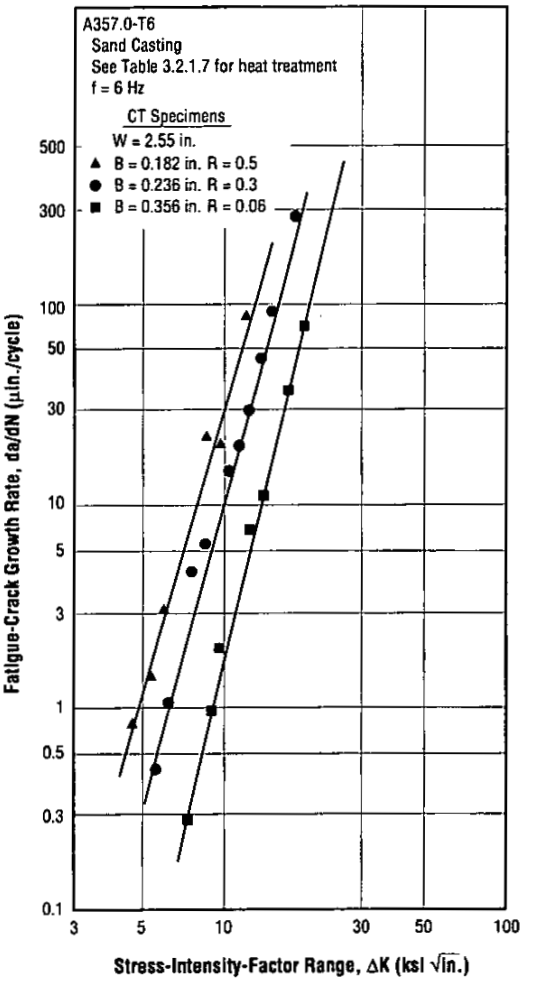


Figure 3.5.3.7 Fatigue-crack growth rates at several R-ratios for specimens removed from full-scale F-16 vertical tail substructure (Ref. 13)

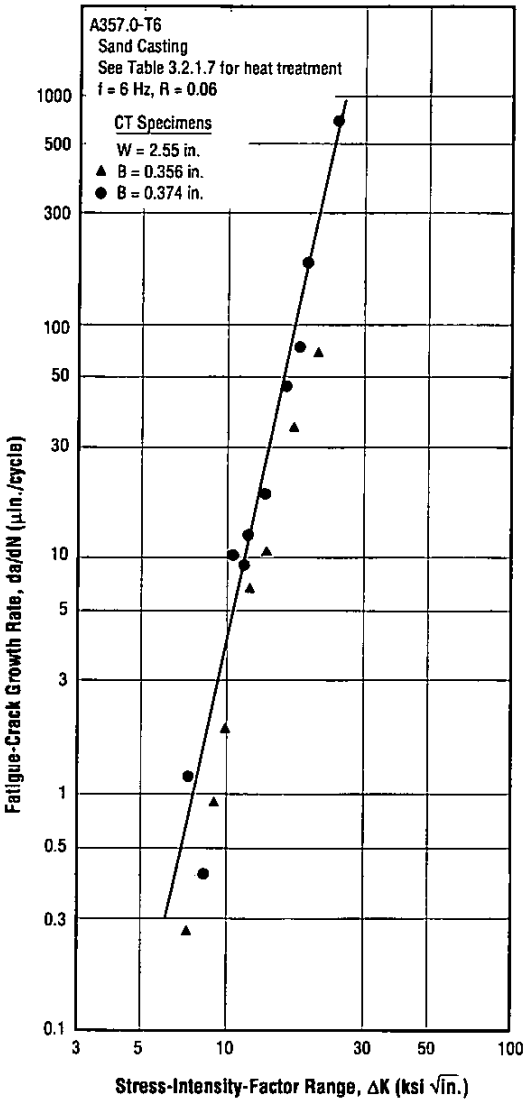


Figure 3.5.3.8 Fatigue-crack growth rates for specimens removed from full-scale F-16 vertical tail substructure (Ref. 13)

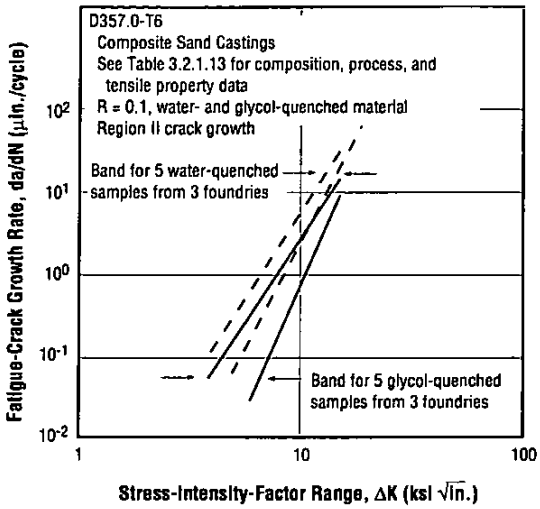


Figure 3.5.3.9 Scatter bands of fatigue-crack growth rates for specimens from composite sand-cast plates from three suppliers, for water- and glycol-quenched conditions (Ref. 41)

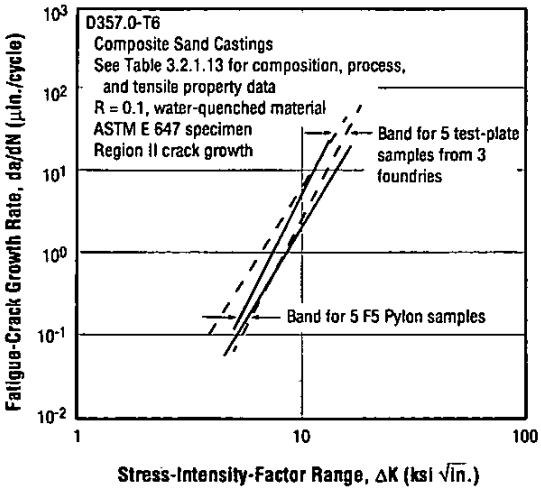


Figure 3.5.3.10 Scatter bands of fatigue-crack growth rates for specimens cut from a F5 aircraft wing pylon, compared with plate specimen growth rates (Ref. 41)

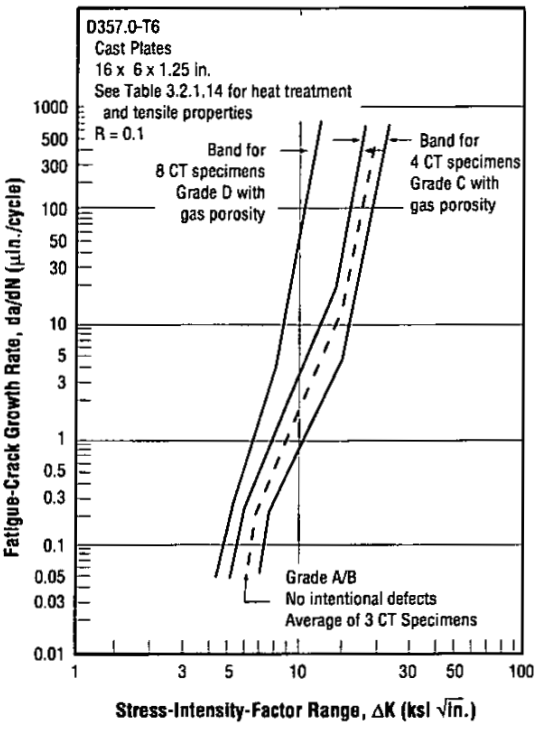


Figure 3.5.3.11 Effects of gas porosity on fatigue-crack growth rates of specimens from cast plates (Ref. 41)

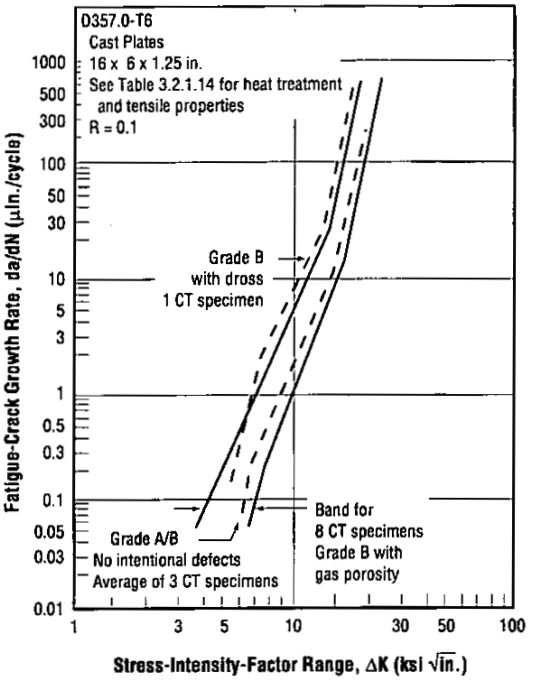


Figure 3.5.3.12 Effects of gas porosity or dross on fatigue-crack growth rates of specimens from cast plates (Ref. 41)

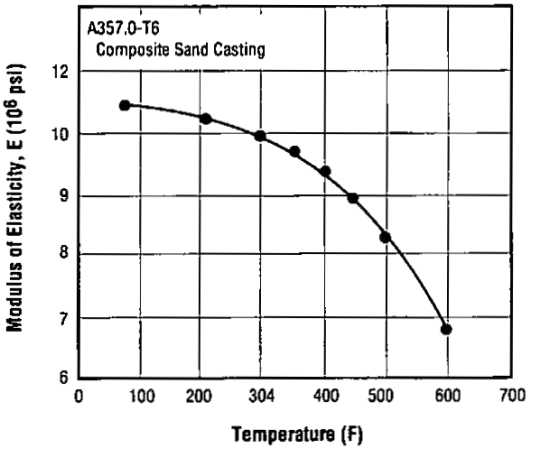


Figure 3.6.2.1 Effect of temperature on tensile modulus of elasticity (Ref. 20)

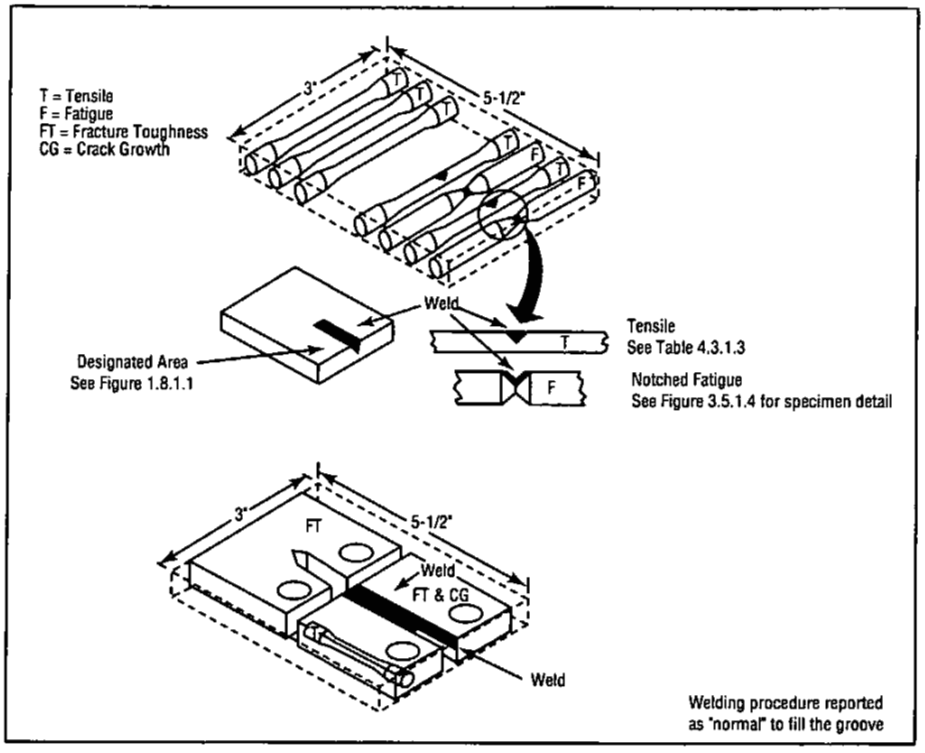


Figure 4.3.1.2 V-grooved (60-degree V, 0.25-inch deep with 3/32-inch radius) weld specimens from Northrop stepped plates (Ref. 12)

Table 4.3.1.3 Effect of weld repairs on tensile properties and fracture toughness of specimens from stepped plate sand castings (Ref. 12)

Alloy	A357.0-T6 Sand Castings							
Condition	V-Grooved Welds in Designated Areas of Northrop Stepped Plates (See Figure 4.3.1.2 for Configuration)							
Test Type	Tensile						Fracture Toughness[b]	
Welded	Yes			No			Yes	No
	F_{tu} (ksi)	F_{ty} (ksi)	e (percent)	F_{tu} (ksi)	F_{ty} (ksi)	e (percent)	K_Q (ksi $\sqrt{in.}$)	K_Q (ksi $\sqrt{in.}$)
Average	55.5	46.0	7.7	55.0	47.2	7.7	24.2	21.5
Range[a]	54.4 - 56.4	45.0 - 47.5	5.0 - 9.0	—	—	—	22.8 - 27.4	18.5 - 25.2

[a] Six tensile and three fracture toughness specimens per condition.

[b] Compact specimens approximately 0.5 inch thick; insufficient to yield valid ASTM E 399 values.

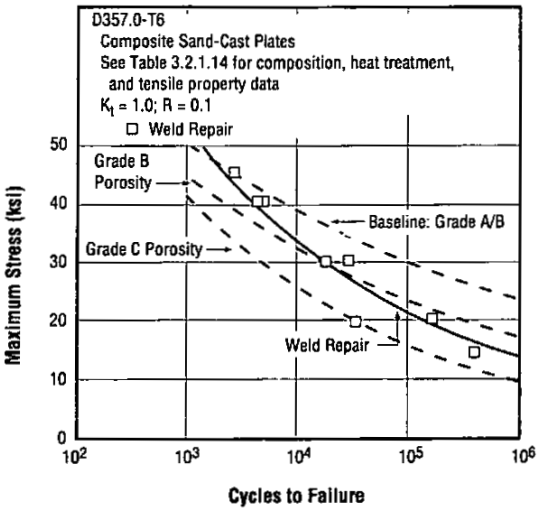


Figure 4.3.1.4 Effect of weld repairs on fatigue strength of smooth specimens from composite sand-cast stepped plates, compared with effects of gas porosity alone (Ref. 41)

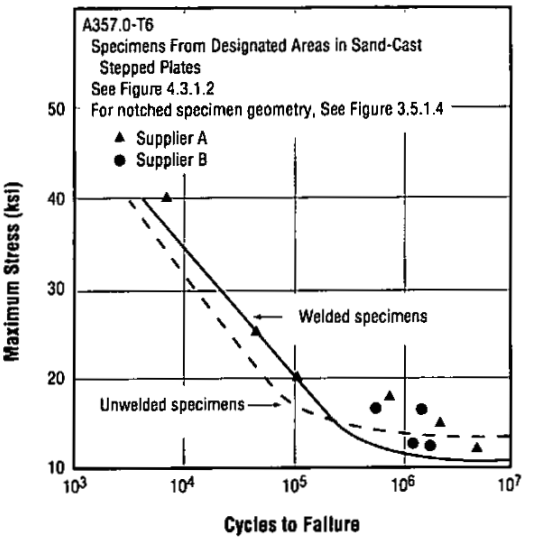


Figure 4.3.1.5 Effect of weld repairs on fatigue strength of notched specimens from stepped plate composite sand castings (Ref. 12)

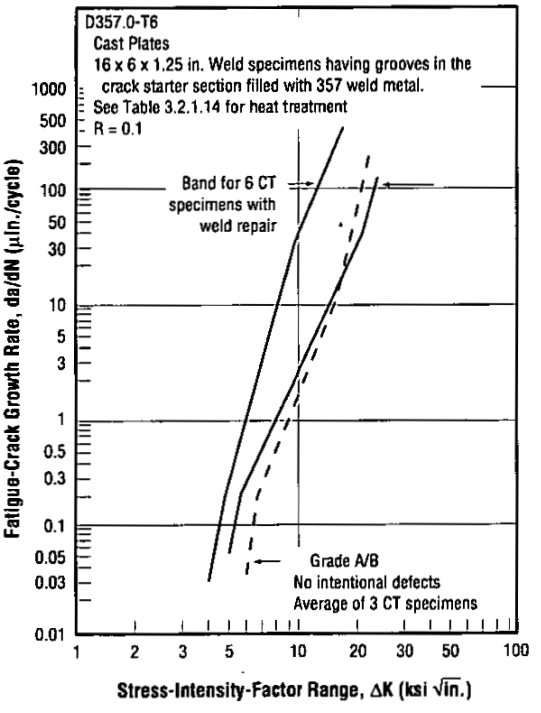


Figure 4.3.1.6 Effect of weld repair on fatigue-crack growth rates of specimens from sand-cast plates with Grade B porosity (Ref. 41)

Table 4.3.2.2 Single-shear lap bond strength of as-cast A357.0-T6 adherends with two adhesive systems (Ref. 36)

Alloy	A357.0-T6			
Form	Station 170 Bulkhead of YC-14 Fuselage			
Specimen Geometry	Flat Strips 0.12-in. Thick by 0.475-in. Wide			
Bond Surface Condition	As-received Rough Cast			
Bonding Procedure	See Table 4.3.2.3 for details			
Adhesive System (Cure Temperature)	Test Condition	Aging Condition	Single-shear Lap Bond Strength[a] (psi)	Fraction of 2024-T3 Lap Bond Strength[b]
Hysol EA 9628H (250F)	RT	Dry	5,690	0.87
		Wet[c]	5,430	0.85
	180F	Dry	4,090	0.89
		Wet	3,350	0.79
American Cyanamid FM 300 (350F)	RT	Dry	4,300	0.98
		Wet	4,730	0.99
	300F	Dry	1,660	0.65
		Wet	1,780	0.73
	350F	Dry	570	1.24
		Wet	320	0.74

[a] Average of 5 replications.

[b] ASTM D 1002 procedure; machined surfaces; same bonding; average of 5 replications.

[c] 2 weeks exposure to 100% RH at 120F.

Table 4.3.2.3 Surface preparation and bonding procedures for fabrication of lap joint test specimens (Ref. 36)

1. Solvent wipe with acetone.
2. Vapor degrease 10 minutes in trichloroethane.
3. Alkaline wash 10 minutes at 155F.[a]
4. Rinse 10 minutes in continuous flow tap water.
5. Etch 10 minutes in optimized FPL at 155F.[b]
6. Rinse 10 minutes in agitated continuous flow tap water.
7. Anodize 20 minutes in 9 - 12 percent phosphoric acid solution at 15 volts.[c]
8. Rinse 10 minutes in continuous flow tap water.
9. Dry 10 minutes with heat gun or oven at 150F.
10. Prime with American Cyanamid BR-127 approx. 0.0002 inch thick.
11. Air dry 10 minutes at RT; oven dry 60 minutes at 250F.
12. Hand-layup bond joint with binder clips for pressure.
13. Oven cure at required temperature.

[a] 1 gallon tap water, 170 gm Turco 4215, 7 ml Turco 4215 additive.

[b] 11 l tap water, 417 gm sodium dichromate, 2 l sulfuric acid, 26 gm shredded 2024-T3 Al.

[c] per ASTM D 3933; 1 l tap water, 69 ml phosphoric acid, 85 percent or 84.5 ml phosphoric acid, 75 percent.

REFERENCES

1. AMS 4241A, Aluminum Alloy Castings, Society of Automotive Engineers (July 1, 1992).
2. AMS 4249, Aluminum Alloy Castings, Society of Automotive Engineers (July 1, 1992).
3. Goehler, D.D., "Cast Aluminum Structures Technology (CAST)," AFFDL TR 77-36, Contract F33615-76-C-3111, The Boeing Co. (May 1977).
4. Goehler, D.D., "Cast Aluminum Structures Technology, Phase III (CAST)," AFFDL TR 78-7, Contract F33615-76-C-3111, The Boeing Co. (May 1978).
5. Christner R.G., and Goehler, D.D., "Cast Aluminum Structures Technology, Phase II," AFFDL TR 78-62, Contract F33615-76-C-3111, The Boeing Co. (May 1978).
6. McField, R.C., Logan, A., Faber, J.W., and Southworth, H.L., "Cast Aluminum Structures Technology (CAST) - Fabrication of Demonstration Articles and Production Hardware (Phase IV)," AFFDL TR 79-302, Contract F33615-76-C-3111, The Boeing Co. (March 1979).
7. Gunther, C.K., "Cast Aluminum Structures Technology (CAST) - Structural Test and Evaluation (Phase V) - Part II: Fatigue and Fracture Properties of Cast Aluminum Bulkheads," AFFDL TR 80-3021, Pt. II, Contract F33615-76-C-3111, The Boeing Co. (March 1979).
8. Gunther, C.K., "Cast Aluminum Structures Technology (CAST) - Structural Test and Evaluation (Phase V) - Part I: Full Scale Test," AFFDL TR 80-3021, Pt. I, Contract F33615-76-C-3111, The Boeing Co. (March 1979).
9. McLellan, D.L, "Cast Aluminum Structures Technology (CAST) - Structural Test and Evaluation (Phase V) - Part III: Static Properties Allowables," AFFDL TR 80-3021, Contract F33615-76-C-3111, The Boeing Co. (March 1979).
10. Faber, J.W., "Cast Aluminum Structures Technology (CAST) - Structural Test and Evaluation (Phase VI) - Summary Technical Report," AFFDL TR 80-3020, Contract F33615-76-C-3111, The Boeing Co. (March 1979).
11. Brondyke, K.J., and McCormick, T.F., "Melting, Remelting, Degassing/Fluxing and Handling," *Aluminum, Vol. III, Fabrication and Finishing*, K.R. Van Horn, Editor, ASM, Cleveland, OH (1967).
12. Oswalt, K.J., and Lii, Y., "Manufacturing Methods for Process Effects on Aluminum Casting Alowables," AFWAL TR 84-4117, Contract F33615-79-C-5116, Northrop Corp. (March 1985).
13. Doyle, C.E., et al., "Cast Aluminum Aircraft Structure," Vols I and II, AFWAL TR 84-4070, Contract F33615-79-C-5001, General Dynamics, Fort Worth, TX (June 1984).
14. Oswalt, K.J., and Misra, M.S., "Dendrite Arm Spacing (DAS): A Nondestructive Test to Evaluate Tensile Properties of Premium Quality Aluminum Alloy (Al-Si-Mg) Castings," *AFS International Cast Metals Journal*, Vol. 6, p. 23 (1981).
15. Tirpak, J.D., "The Variability of Fatigue-Crack Growth Life in Aluminum Casting Alloy A357-T6," AFWAL TR-86-4115 (July 1986).
16. McLellan, D.L., "Tensile Properties of A357-T6 Aluminum Castings," *Journal of Testing and Evaluation*, Vol. 8, p. 170 (July 1980).
17. Oswalt, K.J., "A Comparison of the Fatigue Behavior of High Strength Cast Aluminum Alloys 201 and A357," Northrop Corp., Aircraft Division, NOR 71-229 (December 1, 1971).
18. Alcoa Product Manual, "Premium Castings," Alcoa, Premium Castings Division, Corona, CA (1972).
19. Alcoa Premium Castings Division, Corona, CA (1969).
20. Private communication from A.F. Maloit, Pasadena, CA to W.F. Brown, Jr., Bay Village, OH.
21. Granger, D.A., Kersker, M.M., and Sawtell, R.R., "Effect of Beryllium on the Properties of A357.0 Castings," *AFS Transactions*, Vol. 92 (1984).

22. Bardes, B.P., and Flemings, M.C., "Dendrite Arm Spacing and Solidification Time in an Al-Cu Alloy," *AFS Transactions*, Vol. 74, p. 406 (1966).

23. Spear, R.E., and Gardner, G.R., "Dendrite Cell Size," *AFS Transactions*, Vol. 71, p. 209 (1963).

24. McLellan, D.L., and Tuttle, M.M., "Manufacturing Methodology Improvement for Aluminum Casting Ductility," AFWL TR-82-4135, Contract F33615-80C-3209, Boeing Military Airplane Co., (December 1982).

25. Kutchera, R.E., Schweikert, W.H., and Bailey, P.G., "Manufacturing Methods for Process Effects on Aluminum Casting Allowables," AFWAL TR 80-4176, Contract F33615-76-C-5076, General Electric Co., Aircraft Engine Business Group (June 1981).

26. Nagel, G., and Portalier, R., "Structural Modification of Aluminum-Silicon Alloys by Antimony Treatment," *AFS International Cast Metals Journal*, Vol. 5, No. 4, p. 2 (December 1980).

27. Kennerknecht, S., "Metallurgical Aspects of Quality Control in the Production of Premium Quality Aluminum Investment Casting for the Aerospace Industry," *AGARD Conference Proceedings No. 325, Advanced Castings Technology*, 54th Meeting of the AGARD Structures and Materials Panel in Brussels, Belgium (April 1982).

28. Stein, D., "Quantitative Nondestructive Tensile Testing of A356/A357 Aluminum Alloy Castings," Hughes Helicopters, Paper presented at *AFS 84th Casting Congress*, St. Louis, MO (April 1980).

29. Faber, J.W., "Metallographic Analysis Techniques Used During the Cast Aluminum Structures Technology (CAST) Program," *12th National SAMPE Technical Conference*, p. 768 (October 1980).

30. Development: Premium Alloy Castings of Alloy A357.0-T6, Alcoa, Pittsburgh, PA (1971).

31. Gunther, C.K., "Cast Aluminum Primary Aircraft Structure," Boeing Military Aircraft Co., p. 323 (December 1979).

32. Tirpak, J.D., "Elevated Temperature Properties of Cast Aluminum Alloys A201-T7 and A357-T6," AFWAL TR-85-4114 (November 1985).

33. SAE ARP 1947, "Dendrite Arm Spacing of Structural Aircraft Quality D357 Aluminum Alloy Castings, Determination and Acceptance of" (October 1, 1985).

34. "Standards for Aluminum Sand and Permanent Mold Castings," The Aluminum Association, Washington, D.C.

35. Tan, Y.-H., Lee, S.-L., and Lin, Y.-L., "Effects of Beryllium and Iron Content on Plane-Strain Fracture Toughness in A357 Alloys," *Metallurgical and Materials Trans. A*, Vol. 26A, pp. 2937-2945 (November 1995).

36. Kuhbander, R.J., Caldwell, S.J., and Fiscus, S.E., "Cast Aluminum Bonding Study," AFWAL TR-88-4065 (May 1988).

37. Bosworth, T.J., "Repair Welding Aluminum Castings, Part 2," *Modern Casting*, Vol. 74:4, pp. 19-22 (April 1984).

38. Anon., "Alcotec Alloy R-A357.0 Al-Si-Mg-Be Filler Wire for Sand and Permanent Mold Castings," *Alloy Digest* (September 1992).

39. Marsh, L.E., and Reinemann, G., "Premium Quality Aluminum Castings Theory, Practice, and Assurances," *Transactions of the American Foundrymen's Society*, Vol. 87, pp. 413-422 (1979).

40. Zinkham, R.E., "A New Quality Assurance Tool for Aluminum Castings, Including A Study of A357 Fracture Toughness," *Transactions of the American Foundryman's Society*, Vol. 97, pp. 959-968 (May 1989).

41. Ozelton, M.W., Mocarski, S.J., and Porter, P.G., "Durability and Damage Tolerance of Aluminum Castings," WL-TR-91-4111, Contract F33615-85-C-5015, Northrop Corp. (October 1991).

42. Srivatsan, T.S., Meyers, C.W., and Berry, J., "A Method for Determining the Tensile Properties and Anisotropy of Aluminum Alloys," *Journal of Testing and Evaluation*, Vol. 15:4, pp. 196-204 (July 1987).

43. AMS 4241A, Aluminum Alloy Castings, Society of Automotive Engineers (July 1, 1992).

44. AMS 4245B, Aluminum Alloy Welding Wire, Society of Automotive Engineers (July 1996).

45. Military Specification MIL-A-21180D, Aluminum Alloy Castings - High Strength Amendment 1 (December 14, 1991).

46. ASTM B 108 Aluminum Alloy Permanent Mold Castings, ASTM Annual Book of Standards, Vol. 02.02 (1995).

47. ASTM B 108 Aluminum Alloy Castings - High Strength, ASTM Annual Book of Standards, Vol. 02.02 (1995).